DEVELOPMENT OF A CONVERGENT FRAGMENT COUPLING STRATEGY TOWARD GRAYANANE DITERPENOIDS: ENANTIOSELECTIVE SYNTHESIS OF (+)-AURICULATOL A

Thesis by

Jordan Kenji Thompson

In Partial Fulfillment of the Requirements

for the Degree of

Doctor of Philosophy

CALIFORNIA INSTITUTE OF TECHNOLOGY

Pasadena, California

2026

(Defended June 27th, 2025)

© 2026

Jordan Kenji Thompson

ORCID: 0009-0007-6395-7087

All Rights Reserved

To the spirit of science, discovery, and the pursuit of knowledge

ACKNOWLEDGEMENTS

As I reflect on the last five years, I am filled with gratitude for the experience of conducting research at Caltech. This campus has been a vibrant, inspiring home where ideas flourished. The friendships formed within this program have been integral to the experience, and I will always cherish the memories we created while developing exciting new chemical reactions and pushing the boundaries of our field. Every breakthrough, challenge, and late-night discussion has shaped me into the scientist I am today. I leave Caltech with a full heart, immensely thankful for the people, the science, and the unforgettable spirit of discovery that defined these years.

I am profoundly grateful to Professor Sarah Reisman for her exceptional mentorship and unwavering dedication to my growth as a researcher. I thank her for welcoming me into her group and for believing in me throughout the years, even when I doubted myself. Her leadership, which has been full of fervor, creativity, and intellectual rigor, has shaped the way I approach science and inspired me to pursue bold, meaningful questions. She has instilled in me a deep curiosity and a focused intensity for developing chemical reactions, lessons I will carry with me throughout my career. Thanks to her guidance, I leave the group ready to tackle complex synthetic challenges, explore new scientific frontiers, and contribute thoughtfully to medicinal chemistry at Bristol Myers Squibb.

I am sincerely grateful to my thesis committee, composed of Professor Brian Stoltz (chair), Professor Greg Fu, and Professor Jonas Peters, for their guidance and support throughout my PhD. Their insights during my proposition's exam challenged me to think more critically and deeply about chemistry. I am especially thankful for their continued

investment in my growth over the years.

I've been incredibly fortunate to work alongside the outstanding research staff at Caltech, especially Dr. Scott Virgil, whose tireless work running the 3CS facility—and somehow always being in two places at once—has supported students across campus with unmatched dedication. Scott's presence in our group meetings and his enthusiasm for tackling tough chemistry have made him an invaluable part of our community. I'm also deeply thankful to Dr. David Vander Velde, whose deep expertise and generosity have shaped much of my understanding of NMR spectroscopy.

Thank you to Tomomi Kano and Beth Marshall for their help scheduling and keeping Schlinger running and the administrative support of Anya Janowski, Alison Kinard, Rebecca Fox, Joe Drew, Alison Ross, Greg Rolette, and Armando Villasenor.

I am deeply grateful to all the past and present members of the Reisman group who have made these years so memorable, collaborative, and enriching. When I first joined, Skyler Mendoza welcomed me with warmth and set an incredible example of how to thrive as productive chemists during a busy time. I am thankful to Yujia Tao, whose brilliance and dedication made her a scientific role model to work next to, and to Conner Farley, who laid the essential foundation for the auriculatol project, welcomed me into the group, and made me feel a part of the team. Dave Charboneau's energy and guidance, especially in connecting our work to inorganic chemistry, brought a valuable perspective to every project. I have cherished the friendship and deep scientific conversations with Alex Shimozono, as well as the kindness and support of senior group members like Ray Turro, Sara Dibrell, Karli Holman, Travis DeLano, and Jeff Kerkovius. Thank you to Sven Richter for the fun times playing badminton (while also discussing chemistry on our way to

practice together), and to Simon Cooper for the many shared adventures, including yoga classes, exploring Los Angeles, and learning more organic synthesis from you. Thank you to Philip Boehm, who always encouraged me to keep going and brought such a genuine friendship and enthusiasm for scientific discovery. Yasuki Soda showed me what it truly means to be a focused and productive scientist, and I am very glad we worked next to each other. Thank you to Shawn Teh for all your contributions to the project in his 6-month research stay and putting together a wonderful master's thesis. It was incredible to see how much you were able to achieve in this short time. I feel lucky to have found wonderful friends in Andrea Stegner and Ally Stanko. I would sincerely like to thank Kala Youngblood for her partnership and dedication on the auriculatol project; you're positivity during the project's most challenging times carried us through. Thank you to Olivia Morales for the scientific conversations, shared chemical usage, and late night chats. Thank you to Will Chen, Nathan Friede, and Chung Shin for their expertise and guidance in reaction development (and maintenance of the glovebox). I feel especially fortunate to have formed close friendships with Stanna Dorn, who cultivated an enriching environment, and Gino Occhialini, who helped me with DFT and brainstormed creative strategies for end-game strategies in the auriculatol synthesis. To my cohort, Emily Chen and Cedric Lozano, there is no one else I would have rather gone through the past five years with, and your friendship and support have made the experience so much better. I would like to thank Garry Zhang for his inquisitiveness, enthusiasm, and genuine excitement to learn organic synthesis. Mentoring you has been one of the most fulfilling parts of my graduate experience, and it has been a joy to watch you grow and develop as a scientist, from a high school student to a Caltech admit, freshman student, and beyond.

Prior to joining Caltech, I am deeply indebted to my scientific mentors who propelled my early development during my undergraduate studies at UC Berkeley. First and foremost, thank you to Professor Tom Maimone for welcoming me into his group and for his steady support, even after I left Berkeley. Thank you for supporting our published work, along with your constant encouragement and sharpness. I would like to express my sincerest gratitude to Danny Thach for his pivotal roles in my early development. Danny generously took the time to teach me most of the knowledge I had upon starting at Caltech, always encouraging me to learn and to keep running reactions with curiosity and perseverance. He connected me to other research colleagues, encouraged me to enroll in graduate-level synthesis courses, and stayed patient through my learning, and I am so happy we have stayed in touch post-Berkeley. I am also deeply thankful to my supportive lab colleagues during the pre-COVID Berkeley days — including Andrew Musacchio, Mikiko Okumura, Ken Esguerra, Bingqi Tong, Claire Harmange-Magnani, Karl Haelsig, Rachel Rosen, Vasil Vasilev, Andre Sanchez, Lukas Spessert, Beth Zhang, Danny Huang, among others — whose camaraderie and encouragement were essential to my growth. Thank you to Stephen Harwood for all his advice over the years. I am also grateful to Professor Richmond Sarpong, Professor Dean Toste, Professor John Hartwig, and Professor Anne Baranger for their invaluable support during coursework and their thoughtful guidance through the graduate school application process. Their mentorship laid the foundation for my growth as a scientist.

Finally, I want to express my deepest gratitude to my beautiful family. To my parents, Michele and Jim Thompson, thank you for raising me with endless love, patience, and strength. You have always put me and my brothers first, making countless sacrifices

to support our education, dreams, and happiness. The life lessons that you have taught me, especially during life's toughest moments, has carried me further than I ever thought possible. To my brothers, Justin and Jack, thank you for your kindness, humor, and steady presence in my life. Growing up with you has been one of life's greatest joys, and your support has meant everything to me. To my nephew JJ Thompson, uncles and aunts, Ryan and Yen Oshima, Tracy and Will Womack, and to my cousin Miranda Mead, thank you for the warmth, encouragement, and love throughout this journey. Lastly, I would like to thank my grandparents, Bernie and June Oshima and David and Jean Thompson, for their love and support. Your encouragement has been a consistent source of strength. You have taught me so much about how to live a full, meaningful, and enriching life.

ABSTRACT

Total synthesis is a cornerstone of organic chemistry, serving not only as a demonstration of synthetic strategy and innovation but also as a gateway to accessing biologically active natural products that are often scarce or inaccessible from natural sources. Among such natural products, the grayanane diterpenoids represent a structurally complex and medicinally intriguing family of compounds. These molecules, first identified as the active agents in "mad honey," have a rich history of traditional use and a modern resurgence in medicinal interest due to their activity as sodium channel modulators, carbonic anhydrase inhibitors, and potential analgesics. Grayanotoxin III, in particular, exhibits great pain-relieving properties, positioning it and its analogs as compelling targets for chemical synthesis. Despite their early isolation and full structural elucidation by the early 1960s, the grayananes remain difficult to access in the realm of total synthesis, a testament to their dense stereochemical architecture and unusual [5-7-6-5] fused tetracyclic core. This work explores synthetic strategies toward the construction of these challenging natural products, with the aim of enabling broader access to their biological potential and deepening our understanding of chemical tools to use in their synthesis.

This work introduces complex bond-forming strategies and methods development, with a particular emphasis on nickel catalysis to advance the total synthesis of grayanane diterpenoids. A convergent approach was designed to maximize efficiency at each stage, beginning with the development of a model system to rapidly evaluate γ-functionalization strategies of butenolides or masked butenolide equivalents using siloxyfuran intermediates as a polarity reversal tactic. Key advances include the synthesis of a 5,5-fused butenolide fragment and the discovery and optimization of a unique vinylogous Mukaiyama aldol

reaction. Early studies on the diastereoselective 1,4-reduction of butenolides and the development of a nickel-catalyzed α-enolate arylation reaction are highlighted. Subsequent chapters explore the construction of the 3.2.1 bicycle through a range of innovative transformations, including a Snider radical cascade, palladium-catalyzed decarboxylative Tsuji-Stoltz allylation, and a nickel-catalyzed intramolecular carbonyl 1,2-addition. The result of these efforts is a rapid fragment coupling strategy that enables access to the pentacyclic core of auriculatol A through the use of a nickel catalyzed α-enolate alkenylation reaction using a unique olefin-supported nickel catalyst. In addition to discovering that low-valent olefin-supported nickel catalysts are privileged for α-enolate arylation and alkenylation, an unexpected 6-membered ring-containing side product was isolated in these reactions, which could have unique mechanistic implications in the area of dehydrogenative catalysis. To follow, detailed investigations into late-stage olefin functionalization and hydrogenation ultimately culminate in the first synthesis of (+)-auriculatol A along with its epimer (+)-9-*epi*-auriculatol A. Collectively, these studies offer a blueprint for future synthetic approaches to the broader grayanane diterpenoid family and stand as a hallmark achievement for the synthesis of grayanane natural products containing an embedded **e** ring in an uncommon pentacyclic scaffold.

PUBLISHED CONTENT AND CONTRIBUTIONS

Portions of the work described herein were disclosed in the following publication:

Thompson, J. K.; Youngblood, K. C.; Teh, S. Y. H.; Farley, C. M.; Zhang, Z.; Virgil, S. C.; Reisman, S. E. *J. Am. Chem. Soc.* **2025**, *147*, 42170–42174. DOI: 10.1021/jacs.5c17269, Copyright © 2025 Journal of the American Chemical Society. This article is available online at: https://pubs.acs.org/doi/10.1021/jacs.5c17269.

TABLE OF CONTENTS

CHAPTER 1 ***1***

Introduction to the grayanane diterpenoids

1.1 INTRODUCTION 1

1.2 BACKGROUND ON THE GRAYANANE DITERPENOIDS 1

1.2.1 Grayanane diterpenoid discovery and biological activity 1

1.2.2 Prior art: synthetic access to the grayanotoxins 4

1.2.3 Prior art: access to the principinol skeleton 5

1.2.4 Prior art: divergent access to the grayanotoxin and principinol frameworks 8

1.2.5 Summary of approaches 10

1.2.6 Other grayanane synthesis attempts 11

1.2.7 Biosynthesis of the grayanane diterpenoids 11

1.2.8 Introduction to auriculatol A 13

1.3 CONCLUDING REMARKS 14

1.4 NOTES AND REFERENCES 15

CHAPTER 2 ***20***

Vinylogous Mukaiyama Aldol and α-enolate arylation model studies

2.1 INTRODUCTION 20

2.2 A NOTE ON MODEL SYSTEMS 21

2.3 MODEL SYSTEM ROUTE DESIGN 21

2.3.1 Retrosynthetic analysis 21

2.3.2 Aldehyde synthesis 23

2.3.3 Butenolide synthesis 24

2.3.4 Final optimization of the butenolide route 27

2.3.5 Investigation of direct γ-functionalization methods 31

2.4 THE VINYLOGOUS MUKAIYAMA ALDOL REACTION 32

2.4.1 Siloxyfuran formation 32

2.4.2 Hit identification and reaction optimization 33

2.4.3 Stereochemical analysis 36

2.5 A-ENOLATE ARYLATION SUBSTRATE SYNTHESIS 39

2.5.1 Secondary alcohol protection 39

2.5.2 Chemoselective butenolide reduction 39

2.6 Ni-CATALYZED INTRAMOLECULAR A-ENOLATE ARYLATION 41

2.6.1 Buchwald's intermolecular α-enolate arylation of lactones 41

2.6.2 Phosphine ligand modifications 42

2.6.3 Other ligands 47

2.6.4 Final control studies 52

2.7 CONCLUDING REMARKS 52

2.8 EXPERIMENTAL SECTION 54

2.9 NOTES AND REFERENCES 98

APPENDIX 2 ***105***

Supporting Information Relevant to Chapter 2

A2.1 SPECTRA RELEVANT TO CHAPTER 2 106

A2.2 CRYSTALLOGRAPHIC DATA RELEVANT TO CHAPTER 2 180

A2.2.1 Enolate arylation product **57** 180

CHAPTER 3 ***200***

Late stage **d** ring installation on the α-enolate arylation product

3.1 INTRODUCTION 200

3.2 EXPLORATION OF LATE-STAGE ARENE REDUCTION 201

3.2.1 Birch Reduction with liquid ammonia 201

3.2.2 Ammonia-free Birch Reduction strategies 209

3.3 ATTEMPT AT D-RING INSTALLATION 211

3.3.1 Hydrolysis and β–γ isomerization 211

3.3.2 Photochemical allene [2+2] 212

3.3.3 Exploration of Dowd-Beckwith 213

3.5 CONCLUDING REMARKS 216

3.6 EXPERIMENTAL SECTION 217

3.7 NOTES AND REFERENCES 226

APPENDIX 3 ***230***

Spectra Relevant to Chapter 3

CHAPTER 4 ***257***

3.2.1 bicycle synthesis

4.1 INTRODUCTION 257

4.2 VERSATILE 3.2.1 BICYCLE SYNTHESIS THROUGH THE SNIDER RADICAL CASCADE 258

4.2.1 A transform-based approach for 3.2.1 bicyclic aldehyde synthesis: use of the Snider Radical Cascade 258

4.2.2 Synthesis of the Snider Radical Cascade substrate 261

4.2.3 Studies to affect the Snider Radical Cascade 262

4.2.4 Advancement to the key fragment (**107A**) 263

4.2.5 Further derivatization of the key fragment (**107A**) 265

4.2.6 Strategies to shorten the key fragment (**107B**) synthesis 266

4.3 ASYMMETRIC 3.2.1 BICYCLE SYNTHESIS THROUGH RADICAL INTERMEDIATES 271

4.3.1 Chiral induction through the use of a chiral auxiliary

4.3.2 Chiral atom-transfer reactions 273

4.3.3 Asymmetric radical cascade from chiral enamine 279

4.4 ASYMMETRIC STRATEGIES THROUGH CYCLOHEXANONE SUBSTRATES 285

4.4.1 Early studies from cyclohexanone substrates 285

4.4.2 Tsuji-Stoltz Allylation as a method for quaternary stereocenter formation 289

4.4.3 Strategies for ring closure 293

4.4.4 Nickel-catalyzed carbonyl 1,2-addition 297

4.4.5 Advancement to the asymmetric key fragment (**107B**) 306

4.4.6 Other avenues for more expedient 3.2.1 bicycle synthesis: use of a Michael-Aldol cascade 308

4.5 CONCLUDING REMARKS 311

4.6 EXPERIMENTAL SECTION 312

4.7 NOTES AND REFERENCES 378

APPENDIX 4 ***392***

Spectra Relevant to Chapter 4

CHAPTER 5 ***500***

Development of a vinylogous Mukaiyama Aldol fragment coupling reaction and intramolecular Ni-catalyzed α-enolate alkenylation

5.1 INTRODUCTION 500

5.2 CONVERGENT FRAGMENT COUPLING: OPTIMIZATION OF THE VINYLOGOUS MUKAIYAMA ALDOL ADDITION 501

5.2.1 Early optimization of enol triflate substrate (**107A**) VMAR 501

5.2.2 Investigation of Br substrate (**107B**) 506

5.3 Ni-CATALYZED A-ENOLATE ALKENYLATION 510

5.3.1 Synthesis of OTf and Br substrates 510

5.3.2 Initial experimentation on the key intramolecular cross-coupling: use of phosphine ligands 511

5.3.3 Discovery of electron-deficient olefin (EDO) ligands for the intramolecular α-enolate alkenylation 518

5.3.4 Assessing the necessity of reaction components and scalability of the Ni-catalyzed α-enolate alkenylation 529

5.4 CONCLUDING REMARKS 530

5.5 EXPERIMENTAL SECTION 531

5.6 NOTES AND REFERENCES 547

APPENDIX 5 ***557***

Supporting Information Relevant to Chapter 5

CHAPTER 6 ***609***

End Game

6.1 INTRODUCTION 609

6.2 PREFUNCTIONALIZED *EXO*-OLEFIN STRATEGIES 610

6.2.1 Mukaiyama hydration of the *exo*-olefin 610

6.2.2 Elaboration of hydrated products 614

6.2.3 Synthesis of new hydrogenation substrates 617

6.3 SELECTIVE FUNCTIONALIZATION STRATEGIES 619

6.3.1 Elaboration of substrate **105** 619

6.3.2 Completion of the synthesis of (+)-auriculatol A 623

6.4 CONCLUDING REMARKS 624

6.5 EXPERIMENTAL SECTION 625

6.6 NOTES AND REFERENCES 662

APPENDIX 6 ***667***

Spectra Relevant to Chapter 6

ABOUT THE AUTHOR ***783***

LIST OF ABBREVIATIONS

$[\alpha]_D$	angle of optical rotation of plane-polarized light
Ac	acetyl
acac	acetylacetonate
aq.	aqueous
atm	atmosphere(s)
bpy	2,2'-bipyridine
Bn	benzyl
bp	boiling point
br	broad
Bu	butyl
*i*Bu	*iso*-butyl
*n*Bu	*norm*-butyl
*t*Bu	*tert*-butyl
c	concentration of sample for measurement of optical rotation
^{13}C	carbon-13 isotope
° C	degrees Celcius
calcd	calculated
cis	on the same side
cm^{-1}	wavenumber(s)
CO	carbon monoxide
COD	1,5-cyclooctadiene

conv.	conversion
COSY	homonuclear correlation spectroscopy
Δ	heat or difference
δ	chemical shift in ppm
d	doublet
D	deuterium
DA	Diels–Alder
dba	dibenzylideneacetone
DBU	1,8-diazabicyclo[5.4.0]undec-7-ene
DCC	*N,N′*-dicyclohexylcarbodiimide
DCE	1,2-dichloroethane
DCM	dichloromethane
DDQ	2,3-dichloro-5,6-dicyano-1,4-benzoquinone
DIBAL	diisobutylaluminum hydride
diglyme	bis(2-methoxyethyl) ether
DMA	*N,N*-dimethylacetamide
DMAP	4-(dimethylamino)pyridine
DME	1,2-dimethoxyethane
DMF	*N*,*N*-dimethylformamide
DMPU	1,3-dimethyl-3,4,5,6-tetrahydro-2(1H)-pyrimidinone
DMSO	dimethylsulfoxide
dppf	1,1'-bis(diphenylphosphino)ferrocene
dr	diastereomeric ratio

dtbbpy	4,4′-di-tert-butyl-2,2′-dipyridyl
ee	enantiomeric excess
E	*trans* (entgegen) olefin geometry
EDC	*N*-(3-dimethylaminopropyl)-*N*'-ethylcarbodiimide hydrochloride
e.g.	for example (Latin: *exempli gratia*)
ent	enantiomer of
epi	epimeric
equiv.	equivalent(s)
ESI	electrospray ionization
Et	ethyl
et al.	and others (Latin: *et alii*)
FD	field desorption
FI	field ionization
FTIR	fourier transform infrared spectroscopy
g	gram(s)
glyme	dimethoxyethane
h	hour(s)
^{1}H	proton
[H]	reduction
HFIP	hexafluoroisopropanol
HMBC	heteronuclear multiple-bond correlation spectroscopy
HMDS	hexamethyldisilazide
HMPA	hexamethylphosphoramide

$h\upsilon$	irradiation with light
HPLC	high performance liquid chromatography
HRMS	high resolution mass spectrometry
HSQC	heteronuclear single quantum coherence spectroscopy
Hz	hertz
i.e.	that is (Latin: *id est*)
in situ	in the reaction mixture
iso	isomeric
J	coupling constant in Hz
k	rate constant
kcal	kilocalorie(s)
L	liter
l	levorotatory
LCMS	liquid chromatography–mass spectrometry
LDA	lithium diisopropylamide
m	multiplet or meter(s)
M	molar or molecular ion
μ	micro
Me	methyl
MeOH	methanol
MeCN	acetonitrile
mg	milligram(s)
MHz	megahertz

min	minute(s)
mL	milliliter(s)
mol	mole(s)
MOM	methoxymethyl
Ms	methanesulfonyl (mesyl)
m/z	mass-to-charge ratio
NBS	*N*-bromosuccinimide
nm	nanometer(s)
nM	nanomolar
NMO	*N*-methylmorpholine *N*-oxide
NMR	nuclear magnetic resonance
nOe	nuclear Overhauser effect
NOESY	nuclear Overhauser enhancement spectroscopy
o	*ortho*
[O]	oxidation
OMe	methoxy
p	*para*
PCC	pyridinium chlorochromate
Ph	phenyl
pH	hydrogen ion concentration in aqueous solution
PhH	benzene
PhMe	toluene
pin	pinacol

pK_a	acid dissociation constant
pm	picometer(s)
PMB	*para*-methoxybenzyl
ppm	parts per million
PPTS	pyridinium *para*-toluenesulfonate
Pr	propyl
*i*Pr	isopropyl
*n*Pr	propyl or *norm*-propyl
psi	pounds per square inch
pyr	pyridine
q	quartet
quant.	quantitative
R	generic group
R	rectus
RCM	ring-closing metathesis
ref	reference
R_f	retention factor
rr	regioisomeric ratio
rt	room temperature
sat.	saturated
s	singlet or seconds
SAR	structure-activity relationship
SFC	supercritical fluid chromatography

t	triplet
TBACl	tetra-*n*-butylammonium chloride
TBAF	tetra-*n*-butylammonium fluoride
TBAI	tetra-*n*-butylammonium iodide
TBS	*tert*-butyldimethylsilyl
Tf	trifluoromethanesulfonyl
TFA	trifluoroacetic acid
THF	tetrahydrofuran
TLC	thin layer chromatography
TMS	trimethylsilyl
TOF	time-of-flight
Tol	tolyl
trans	on the opposite side
Ts	*para*-toluenesulfonyl (tosyl)
TS	transition state
UV	ultraviolet
vide infra	see below
vide supra	see above
w/v	weight per volume
VMAR	vinylogous Mukaiyama aldol reaction
X	anionic ligand or halide
xs	excess
Z	*cis* (zusammen) olefin geometry

Chapter 1

Introduction to the grayanane diterpenoids[1]

1.1 INTRODUCTION

The initial discovery of the grayanane diterpenoids is described, followed by a thorough analysis of past work in grayanane diterpenoid total synthesis. This chapter concludes in an introduction to auriculatol A as an intriguing target for total synthesis.

1.2 BACKGROUND ON THE GRAYANANE DITERPENOIDS

1.2.1 Grayanane diterpenoid discovery and biological activity

The grayanane diterpenoids are a class of biologically active natural products that were first discovered as the active ingredients in "mad honey".[1] Upon ingestion of "mad honey", one may experience a variety of symptoms: dizziness, weakness, nausea, and in some cases, vomiting. Although Mad Honey Disease remains one of the most common food intoxications in Turkey and Japan for both humans and livestock, it is rarely lethal.

Rather, in small doses, it has been used as a homeopathic medicine for the treatment of gastric pains, bowel disorders, and hypertension.[1] Furthermore, it is believed to be a sexual stimulant.[1] While grayanotoxins I, II, III, and IV (**1**-**4**) have all been shown to exist in mad honey, grayanotoxin III (**2**) is the principal constituent in *rhododendron* and, in some studies, has been shown to possess greater pain-relieving properties than morphine (Scheme 1.1).[2]

Scheme 1.1. *Initial discovery of the grayanane diterpenoids.*

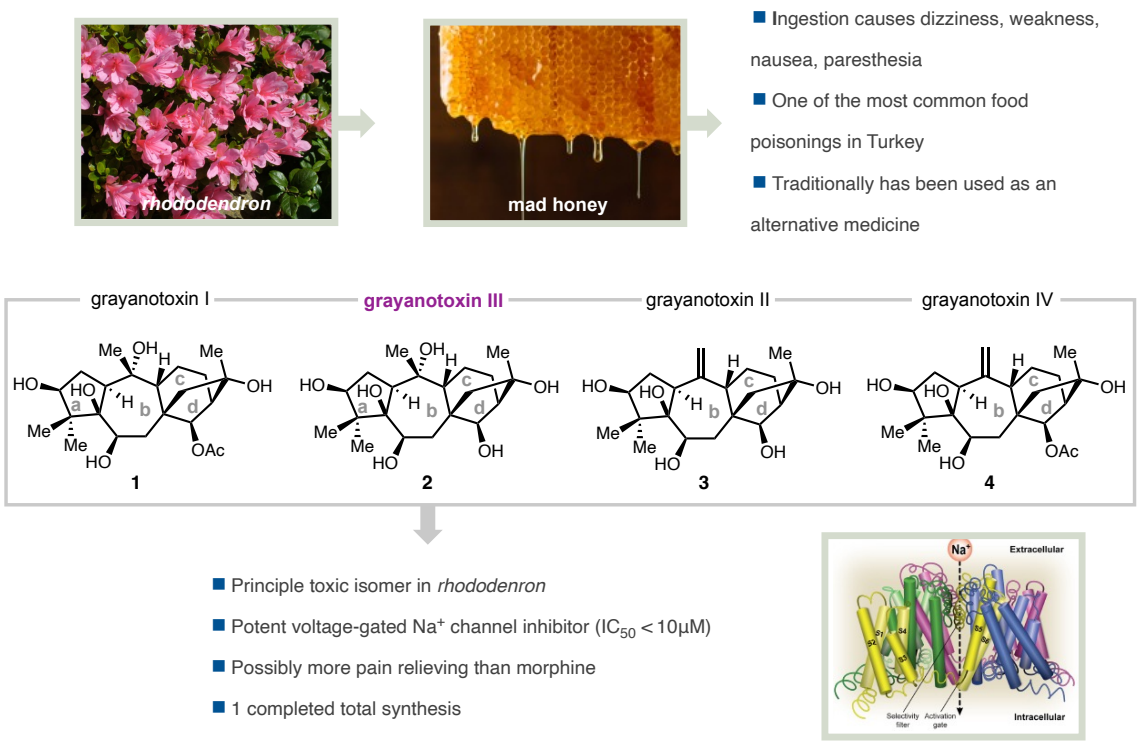

Many grayananes are neurotoxins, interfering with the transmission of the action potential by blocking sodium channels in cell membranes. These compounds prevent inactivation of neurons, which keeps them in a state of depolarization, during which entry of calcium into the cells may be facilitated. More recently, honey extracts from the endemic plant in the Black Sea region, *Rhododendron ponticum*, have shown micromolar inhibitory

potency as carbonic anhydrase inhibitors, specifically the human (h) isomers hCA I and hCA II.[3] The World Health Organization (WHO) has outlined compounds that target these inhibitors as essential medicines.[4] Additionally, compounds of this class have been shown to exhibit promising bioactivity against several other human diseases, including HIV (Scheme 1.2).[5]

Scheme 1.2. *About the grayanane diterpenoids.*

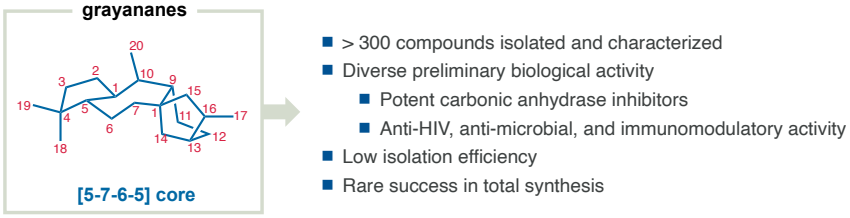

Since their initial discovery, more than 300 members of this class have been isolated and characterized.[7] Common to all grayanane diterpenoids is a tetracyclic fused [5-7-6-5] ring skeleton decorated with hydroxyl groups around their perimeter. Despite their promising biological studies, isolation yields are incredibly low. In one study, the concentration of grayanotoxins in several *rhododendron* species was found to be approximately 10 mg / 100 g of plant leaves or 0.01% w/w.[8] Some species, however, have been shown to contain 0.2% grayanotoxin I, such as *Rhododendron catawibiense* or *Rhododendron ponticum*.[8] Overall, these targets are rare in total synthesis despite full characterization of grayanane structure dating back to the early 1960's.[9] The structural and stereochemical complexity of grayanane diterpenoids may be the primary reason for their synthetic elusiveness.

1.2.2 Prior art: synthetic access to the grayanotoxins

Despite isolation of grayanotoxin I dating back to 1912 (earliest report) by German phytochemist, Otto Tunmann, many early studies were executed by Japanese researchers.[10] Shikiro Miyajima and Sankichi Takei isolated grayanotoxins I–III from 1934 to 1936, and the full characterization of their structures was assigned in 1961 and 1962 by groups of researchers at Nagoya University, Kyoto University, and Tokyo University.[10]

Over a decade later, in 1976, Matsumoto and coworkers achieved a landmark total synthesis of (±)-grayanotoxin II in relay fashion.[11] Utilization of dienone rearrangement, reminiscent of studies on the santonin rearrangement,[12] afforded intermediate cyclopropyl-oxyallylcation **6** (Scheme 1.3). Nucleophilic attack from acetate delivered **7**, which was elaborated to (±)–grayanotoxin II (**2**) in a total synthetic sequence of greater than 40 steps. This was undoubtedly a pivotal achievement for the total synthesis community but left room for further improvement considering the steps to elaborate the unfunctionalized **c** and **d** rings.

Scheme 1.3. *Matsumoto's utilization of the dienone rearrangement to form the* ***a*** *and* ***b*** *rings of grayanotoxin II.*

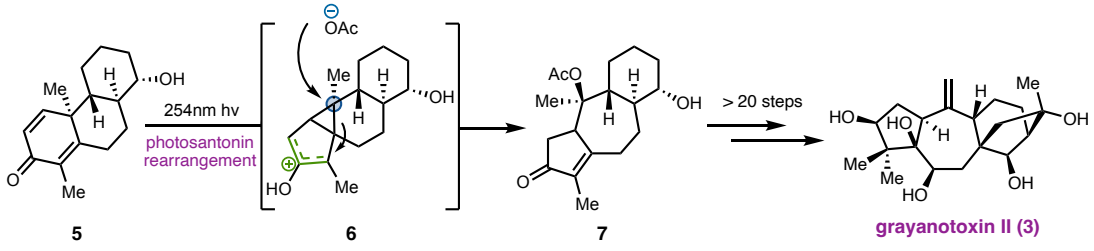

In 1994, Shirahama and coworkers used reductive couplings to access (−)-grayanotoxin III (**2**).[13] Nucleophilic opening of epoxide **9** with **8** formed **10**. A SmI_2-mediated reductive cyclization set two stereocenters with excellent stereocontrol to afford

11 in 79% yield (Scheme 1.4). Pinacol coupling formed the **b** ring in **13**, which was elaborated to the natural product (**3**). The use of a pre-functionalized **c** and **d** ring accounted for a longest linear sequence of 28 steps, drastically reducing step count compared to Matsumoto's efforts. Furthermore, the synthesis was asymmetric, with fragment **8** originating from the chiral pool and **9** through Sharpless asymmetric epoxidation.

Scheme 1.4. *Shirahama's use of reductive couplings to assemble the* ***a*** *and* ***b*** *rings.*

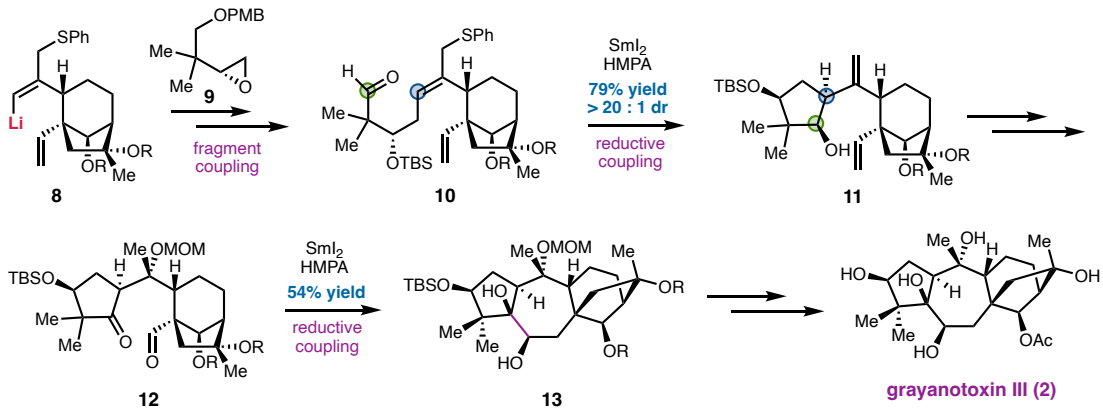

1.2.3 Prior art: access to the principinol skeleton

Recently, there has been a surge in interest from the total synthesis realm in providing synthetic access to the principinol framework. This has likely been elicited by the recency in isolation and characterization of these novel targets.[14] Structurally, some principinols differ only slightly from the grayanotoxins. Principinol D and F, for example, are simply the C1 epimer of grayanotoxin III and II, respectively (Scheme 1.5). On the contrary, principinol C contains a C6 ketone rather than a C5-C6 diol and is the C9-C10 epimer when compared to grayanotoxin III. The dissimilarity of principinol C to other grayanane natural products has large implications when trying to contextualize the biosynthesis of these compounds. It brings into question the biochemical mechanism for formation of these natural products, which will be discussed later in this chapter.

Scheme 1.5. *Structure of principinols C-F.*

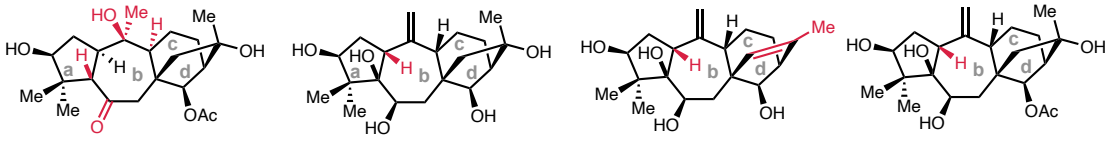

principinol C (**14**) principinol D (**15**) principinol E (**16**) principinol F (**17**)

In 2018, Newhouse and others disclosed an elegant synthesis of (−)-principinol D.[15] Functionalized 3.2.1 bicycle **19** was synthesized in 8 steps and coupled with building block **18** via a 1,2 addition/protection sequence (Scheme 1.6). Selective olefin oxidative cleavage was achieved in 3 steps to form **21**, setting the stage for Giese addition of the ketyl radical formed from SmI_2 reduction of the pendant aldehyde to furnish **22** in 63% yield. Functional group manipulations and installation of the C10 terminal alkene formed (−)-principinol D in 18 steps longest linear sequence, establishing a high standard for other synthetic groups publishing in this area. The use of convergent fragment coupling strategy with two stereochemically rich, functionalized substrates is impressive and enabled rapid formation of molecular complexity. While construction of **18** was originally enantioenriched through Corey–Bakshi–Shibata (CBS) reduction, fragment **19** is racemic, providing low yield in the 1,2-addition step due to formation of 4 diastereomers. For this reason, further development in the domain of asymmetric 3.2.1 bicycle fragment synthesis could improve synthetic efforts toward these natural products.

Scheme 1.6. *Convergent fragment coupling synthesis by Newhouse.*

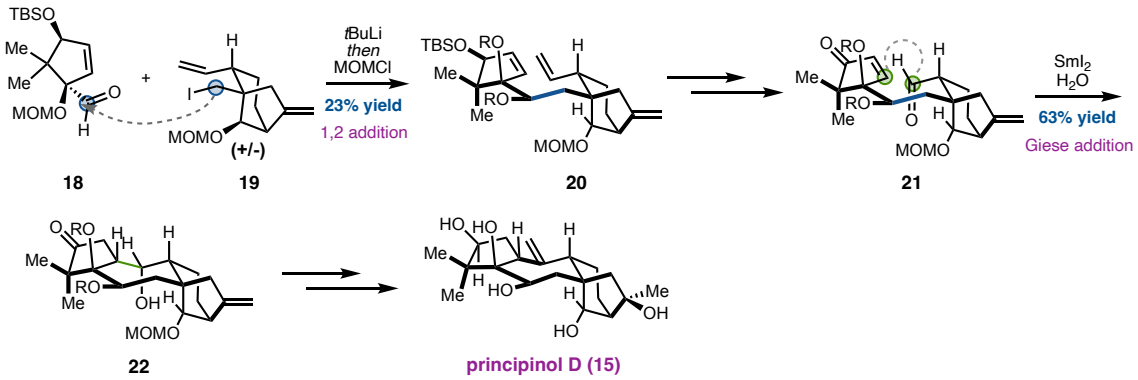

In 2022, the Jia group disclosed an expedient synthesis of (−)-principipol C in 21 steps.[16] Central to their strategy was a unique Pauson–Khand reaction to construct the 7,5-bicyclic ring system. This work contrasts nicely with strategies from Matsumoto and Shirahama. Indeed, use of prefunctionalized building blocks reduced the subsequent functional group manipulations required later in the synthesis. 3.2.1 bicycle **28** was prepared in 97% *ee* through the use of an asymmetric conjugate addition of **24**, catalyzed by copper/Taddol-derived monodentate phosphonite system (**25**), followed by quenching of the resultant enolate with Mander's reagent (Scheme 1.7).[17] Installation of a propargyl group proceeded smoothly, and the alkyne could be coupled to the alpha position of the ketone through a Mn-mediated reductive cyclization (**28**). Elaboration to **29** enabled investigation of the key step. In the optimized condition, the Pauson–Khand reaction occurred in 45% yield to form **30**, which could be elaborated to the natural product. The use of the Pauson–Khand reaction represents a remarkably powerful disconnection, furnishing three carbon-carbon bonds in a single step.

Scheme 1.7. *Pauson–Khand forms the core of (–)-principinol C.*

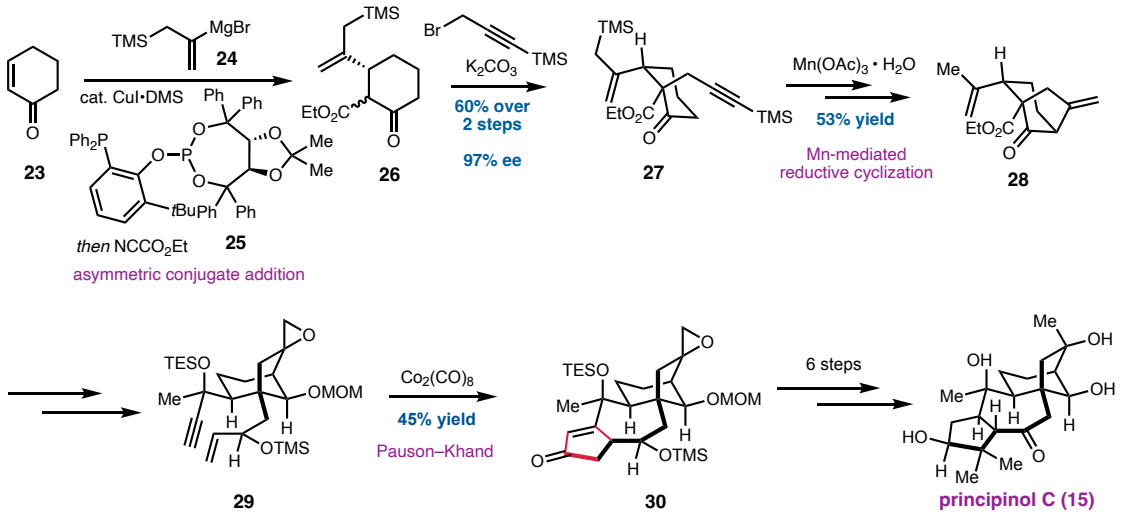

1.2.4 Prior art: divergent access to the grayanotoxin and principinol frameworks

Luo *et al.* published the shortest synthetic sequence to any grayanane, (−)-grayanotoxin III (**2**), in 18 steps.[18] Their strategy utilized convergent fragment coupling of **31** and **32** through sequential diastereoselective Mukaiyama Aldol with a squaramide catalyst (**33**) followed by Sakurai Allylation to form **34** in the same pot (Scheme 1.8). Following vinylation, diene **35** was cyclized in a Prins-type manner to an acid-generated bridgehead carbocation to access **36**. Taken together, three Lewis acid-mediated cyclizations efficiently constructed a minimally-oxidized core of the molecule (**36**), impressively, in just 8 steps. Notably, however, synthetic efforts to rearrange the **c** and **d** rings were necessary, as the correct connectivity of the **c** and **d** rings had not been established. Because the synthetic strategy relied on late-stage oxidation, synthetic access to a variety of grayanane skeletons was achieved. Namely, by judicious choice of oxidation sequences, the syntheses of (−)-grayanotoxin III (**2**), (+)-principinol E (**17**), and (−)-

rhodomollein XX (not pictured) could be achieved. This work represents one of two papers detailing divergent synthetic access to grayanotoxin and principinol cores to date.

Scheme 1.8. *Luo's rapid and divergent synthesis of grayanane diterpenoids.*

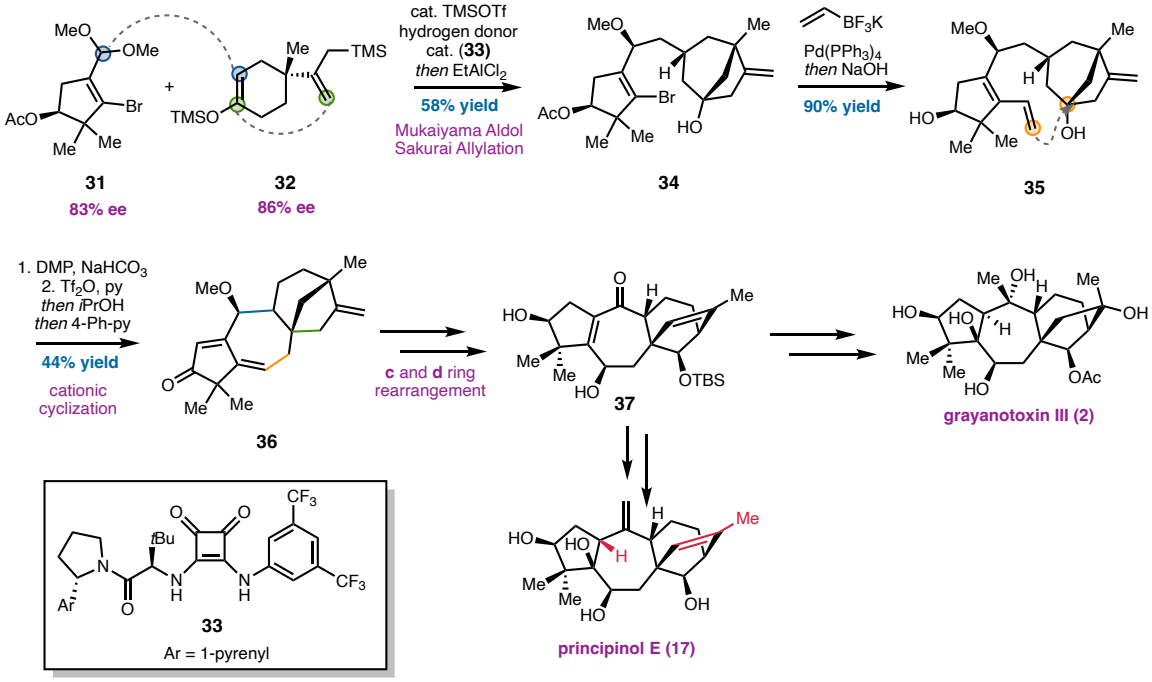

An elegant divergent synthesis of a plethora of grayanane natural products was disclosed by Ding and coworkers.[19] Utilization of a more advanced photosantonin rearrangement than the early report from Matsumoto enabled synthetic access to the grayanotoxin skeleton.[20] The substrate for their photosantonin rearrangement was assembled through an oxidative dearomatization induced (ODI) [5+2] cycloaddition, a strategy that is similar to previous disclosures from this group in their synthetic studies towards (−)-rhodomollanol A.[21] With synthetic access to **39**, functional group manipulations enabled the succinct synthesis of (−)-principinol D (**15**) in 19 steps (Scheme 1.9). Brilliantly, treatment of intermediate **39** with PPTS enabled a grob fragmentation/carbonyl cascade to epimerize the C1 stereochemistry and enable the

synthesis of several grayanotoxin natural products in addition to the principinols. Overall, this paper disclosed the synthesis of nine grayanane natural products, namely grayanotoxin II (**3**), grayanotoxin III (**2**), rhodojaponin III (not pictured), grayanotoxin XV (not pictured), principinol D (**15**), iso-grayanotoxin II (not pictured), 1,5-seco-grayanotoxin-$D^{1,10}$-ene (not pictured), and leucothols B and D (not pictured). Key to their synthetic strategy is the judicious use of the ODI [5+2] and photosantonin rearrangement to rapidly build molecular complexity. Computational studies reveal the mechanism for the unique Grob fragmentation/carbonyl-ene sequence, while judicious choice of oxidation reactions and rearrangements of the established 5,7,6,5 skeleton enable divergent access to a myriad of natural products.

Scheme 1.9. *Ding's divergent approach to the grayanane and principinol frameworks.*

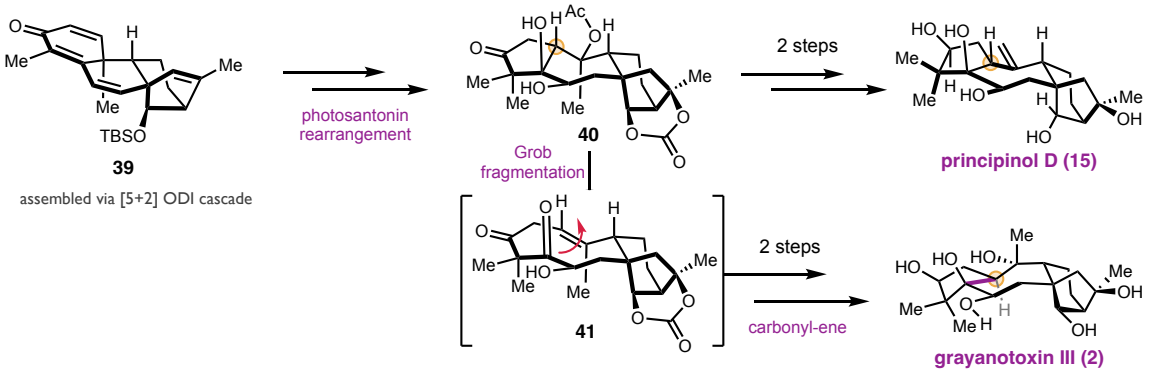

1.2.5 Summary of approaches

An excellent chemical review of syntheses prior to 2022 is available online.[22] Therein, a table and schematic containing brief advantages and disadvantages are described (Table 1.1) in addition to a nice overview schematic (Scheme 1.10).

Table 1.1. *Summary of approaches prior to 2022.*

synthesis	number of steps	overall yield	advantages	drawbacks
Matsumoto (1976)	> 40	<0.0005%	–	many steps, racemic
Shirahama (1994)	38	0.05%	enantioselective	many steps
Newhouse (2019)	19	0.4%	convergent, few steps	limited to C1 epimers of the general structure
Ding (2019	22—23	1.2—1.4%	few steps, highest yielding	limited to C1—C5 dehydrogenated grayananes
Luo (2022)	18—19	0.01—0.05%	few steps, flexible	lower yields
Jia (2022)	22	0.5%	few steps, modular	not convergent

Scheme 1.10. *Overview of synthetic strategies.*

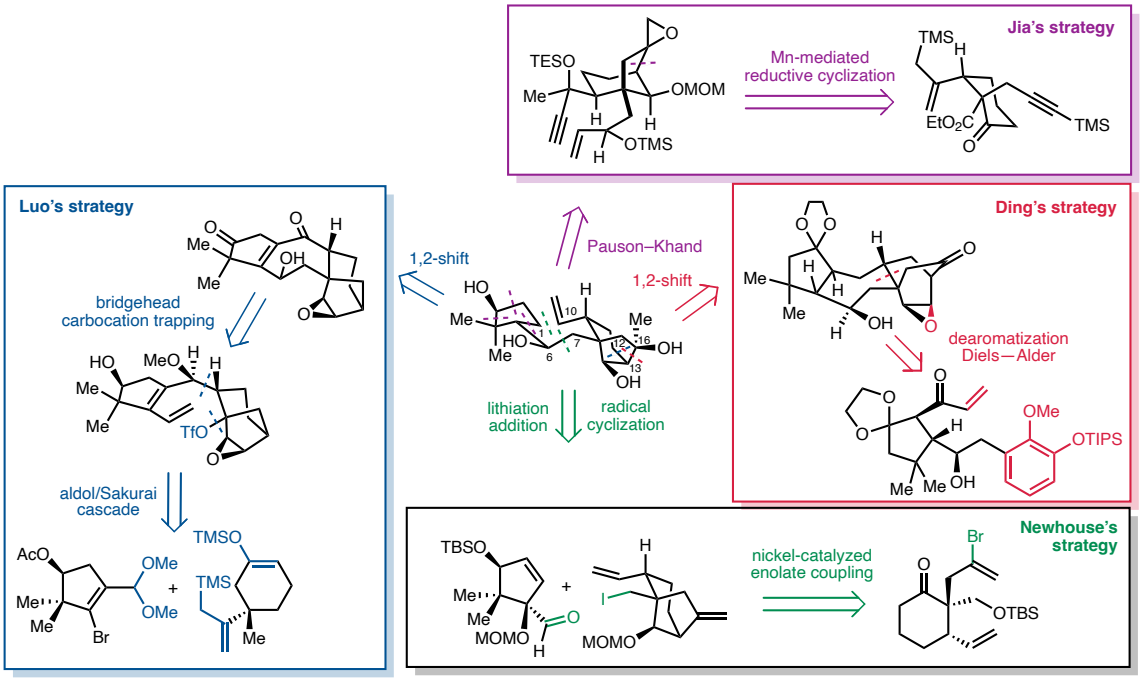

1.2.6 Other grayanane synthesis attempts

There have been many attempts in the literature towards grayanane natural products that have contributed significantly to provide foundational studies towards these targets. An in-depth discussion of these works can be found online.[23]

1.2.7 Biosynthesis of the grayanane diterpenoids

Generally, the biosynthesis of complex diterpenes is thought to occur through two phases: 1) a cyclization phase and 2) an oxidation phase.[24] Specifically, the grayananes are

thought to arise from polyene cyclization of geranylgeranyl diphosphate (**42**), catalyzed by copalyl diphosphate synthase and *ent*-kaurene synthase to access the *ent*-kaurene (**43**) (Scheme 1.11). Internal bond migration of the kaurene skeleton, and a series of oxidations furnish the grayanotoxin framework (**44**). Interestingly, the grayananes are very closely related to the gibberellanes, a classic target for synthetic organic chemists, and only differ in the direction of bond migration from the kaurane skeleton (not pictured). Oxidation of the *ent*-kaurene affords the *ent*-kauranoids (**45**), and there has been a unified synthetic strategy disclosed for these targets from the Reisman group in the past.[25] An L-serine-mediated oxidation and C7-C10 bond formation allow access to the napelline type diterpenoid alkaloids (DAs) (**46**). An alternative polyene cyclization can generate the *ent*-atisane structure (**47**), and an analogous oxidation/C7-C10 bond formation furnishes the denutatine-type DAs (**48**). Wagner-Meerwein and oxidation events bioenzymatically form the aconitine-type DAs, which also have been successful targets from the Reisman group (not pictured).[26]

Scheme 1.11. *Biosynthesis of representative diterpenoids.*

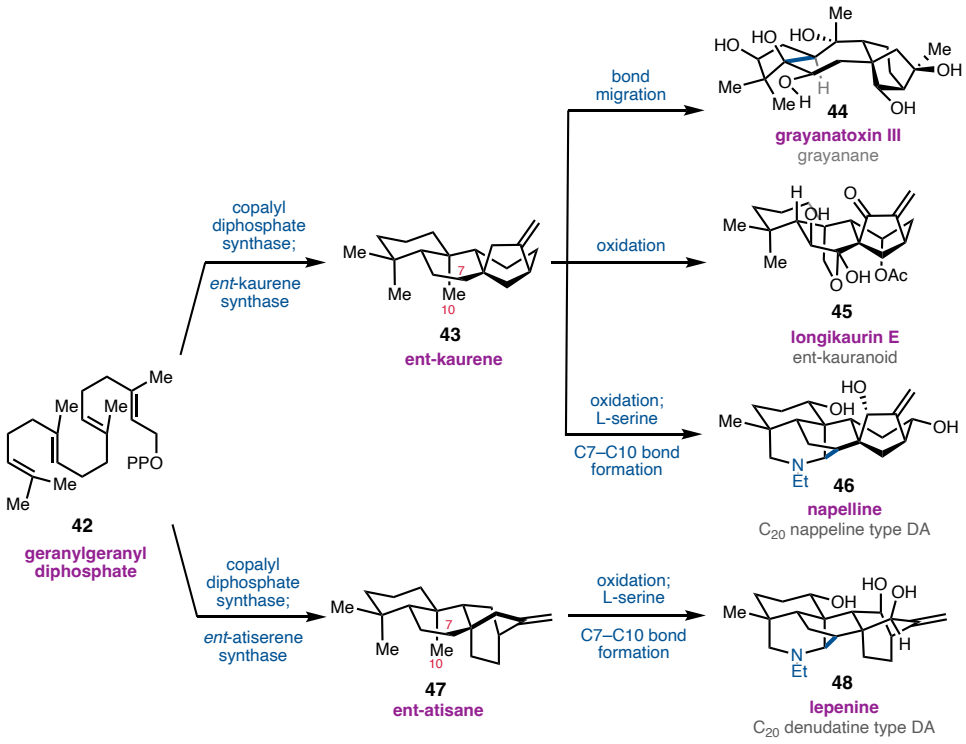

1.2.8 Introduction to auriculatol A

In 2019, a new pentacyclic grayanane diterpenoid, auriculatol A (**49**), was isolated and structurally characterized from *Rhododendron auriculatum* (Scheme 1.12).[27] 14 mg was isolated from > 50 kg of *rhododendron* leaves. Similar isolation yields were disclosed in this report for the newly discovered auriculatol B (**50**), auriculatol C (**51**), and 19-Hydroxy-3-*epi*-auriculatol B (**52**). The compounds, along with grayanotoxins I (**1**) and IV (**3**), were tested for analgesic activities in a writhing test induced by HOAc. It was found that some of these grayanane diterpenoids exhibited significant analgesic activities, with inhibition rates > 50% at doses of 0.2 and 0.04 mg/kg, exhibiting greater analgesic potency than morphine.

Structurally, auriculatol A is the first 5,20-epoxygrayanane diterpenoid containing a 7-oxabicyclo[4.2.1]-nonane motif (the **e** ring in **49**) and a *trans/cis/cis/cis*-fused 5/5/7/6/5 pentacyclic ring structure (Scheme 1.12). The rarity of this motif points to a way to conduct structure-activity relationship (SAR) studies with respect to the more common grayanotoxin and principinol scaffolds. Moreover, the development of a robust and modular approach to access this novel grayanane framework remains underdeveloped.

Scheme 1.12. *Structure of auriculatol A and other new grayananes isolated from Rhododendron auriculatum.*

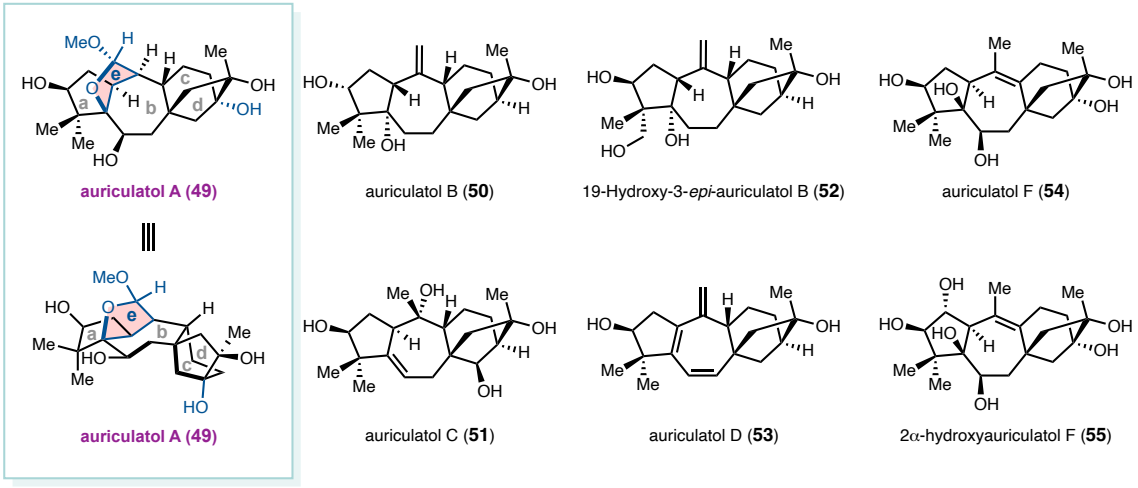

1.3 CONCLUDING REMARKS

In conclusion, this chapter has provided an analysis of completed grayanane syntheses up to January 2024. While there have been many syntheses, representing a variety of strategies for assembly of these complex targets, they can be subdivided into three main groups: 1) synthesis of the grayanotoxin framework 2) synthesis of the principinol framework and 3) divergent access to both the grayanotoxins and principinols. The benefits and limitations of these approaches were discussed in detail. Typical step

counts of recent syntheses were in the realm of 18-25 steps and 0.4-1.4% overall yield. The biosynthesis of the grayananes and related congeners like the ent-kauranoids and diterpenoid alkaloids were introduced. Finally, auriculatol A was introduced and discussed.

1.4 NOTES AND REFERENCES

(1) (a) Koca, A. F.; Koca, I. Poisoning by mad honey: A brief review. *Food Chem. Toxicol.* **2007**, *45*, 1315−1318. (b) Gunduz, A.; Turedi, S.; Russell, R. M.; Ayaz, F. A. Clinical review of grayanotoxin/mad honey poisoning past and present. *Clin. Toxicol.* **2008**, *46*, 437−442. (c) Jansen, S. A.; Kleerekooper, I.; Hofman, Z. L.; Kappen, I. F. P.; Stary-Weinzinger, A.; van der Heyen, M. A. G. Grayanotoxin poisoning: 'Mad Honey Disease' and beyond. *Cardiovasc. Toxicol.* **2012**, *12*, 208−215.

(2) Sun, N.; Zheng, G.; He, M.; Feng, Y.; Liu, J.; Wang, M.; Zhang, H.; Zhou, J.; Yao, G. Grayanane diterpenoids from the leaves of *Rhododendron auriculatum* and their analgesic activities. *J. Nat. Prod.* **2019**, *82*, 1849−1860.

(3) Durdagi, S.; Scozzafava, G.; Vullo, D.; Sahin, H.; Kolayli, S.; Supuran, C. T. The Coumarin-Binding Site in Carbonic Anhydrase Accommodates Structurally Diverse Inhibitors: The Antiepileptic Lacosamide As an Example and Lead Molecule for Novel Classes of Carbonic Anhydrase Inhibitors. *J. Enzyme Inhib. Med. Chem.* **2014**, *29*, 469–475.

(4) *WHO model list of essential medicines - 22nd list, 2021.* https://www.who.int/publications/i/item/WHO-MHP-HPS-EL-2021.02 (accessed 2022-01-28).

(5) Li, Y.; Liu, Y. B.; Yu, S. S. Grayanoids from the Ericaceae family: structures,

biological activities and mechanism of action. *Phytochem. Rev.* **2013**, *12*, 305−325.

(6) (a) Zhong, G. H.; Hu, M. Y.; Wei, X. Y.; Weng, Q. F.; Xie, J. J.; Liu, J. X.; Wang, W. X. Grayanane diterpenoids from the flowers of *Rhododendron molle* with cytotoxic activity against a *Spodoptera frugiperda* cell line. *J. Nat. Prod.* **2005,** *68,* 924–926. (b) Zhou, J.; Liu, T.; Zhang, H.; Zheng, G.; Qiu, Y.; Deng, M.; Zhang, C.; Yao, G. Anti-inflammatory grayanane diterpenoids from the leaves of *Rhododendron molle*. *J. Nat. Prod.* **2018**, *81*, 151–161. (c) Zhu, Y. X.; Zhang, Z. X.; Yan, H. M.; Lu, D.; Zhang, H. P.; Li, L.; Liu, Y.; Li, Y. B. Antinociceptive diterpenoids from the leaves and twigs of *Rhododendron decorum*. *J. Nat. Prod.* **2018***, 81,* 1183–1192. (d) Niu, C. S.; Li, Y.; Liu, Y. B.; Ma, S. G.; Liu, F.; Cui, L.; Yu, H. B.; Wang, X. J.; Qu, J.; Yu, S. S. Grayanane diterpenoids with diverse bioactivities from the roots of *Pieris formosa. Tetrahedron.* **2018**, *74*, 375–382. (e) Popescu, R.; Kopp, B. The genus Rhododendron: an ethnopharmacological and toxicological review. *J. Ethnopharmacol.* **2013**, *147*, 42–62. (f) Cheng, X. A.; Xie, J. J.; Hu, M. Y.; Zhang, Y. B.; Huang, J. F. Induction of intracellular Ca^{2+} and pH changes in Sf9 insect cells by rhodojaponin-III, a natural botanic insecticide isolated from *Rhododendron molle*. *Molecules*. **2011**, *16*, 3179–3196. (g) Takahashi, H.; Hirata, S.; Minami, H.; Fukuyama, Y. Triterpene and flavanone glycoside from *Rhododendron simsii*. *Phytochemistry.* **2001**, *56*, 875–879.

(7) (a) Qiang, Y.; Zhou, B.; Gao, K. Chemical constituents of plants from the genus *Rhododendron*. *Chem. Biodivers.* **2011**, *8*, 792–815. (b) Li, C. H.; Yan, X. T.; Zhang, A. L.; Gao, J. M. Structural diversity and biological activity of the genus *Pieris* terpenoids. *J. Agric. Food Chem.* **2017**, *65*, 9934–9949. (c) Li, Y.; Liu, Y. B.; Yu, S. S. Grayanoids from the Ericaceae family: structures, biological activities and mechanism of action. *Phytochem.*

Rev. **2013**, *12*, 305–325.

(8) Dierks, F.; Lechtenberg, M.; Hensel, A. Isolation of grayanotoxin I from *Rhododendron* species and quantification by densitometry. *Planta Medica*, **2013**, *79,* 14.

(9) (a) Kakisawa, H.; Kurono, M.; Takahashi, S.; Hirata, Y. Structure of grayanotoxin-I and III. *Tetrahedron Lett.* **1961**, *2*, 59–67. (b) Kojima, T.; Nakanishi, K. The full stereochemistry of the grayanotoxin and a novel rearrangement. *Tetrahedron Lett.* **1964**, *21*, 1329–1336. (c) Kakisawa, H.; Kozima, T.; Yanai, M.; Nakanishi, K. Stereochemistry of grayanotoxins*. Tetrahedron.* **1965**, *21*, 3091–3104.

(10) (a) Iwasa, J.; Kumazawa, Z.; Nakajima, M. Studies on the Active Principles of *Leucothoe grayana* MAX: Part VIII. The Structure of Grayanotoxin-II. *Agr. Biol. Chem.* **1961**, *25*, 793–797. (b) Kakisawa, H.; Yanai, M.; Kozima, T.; Nakanishi, K. The Stereochemistry of the Grayanotoxins. *Tetrahedron Lett.* **1962**, *6*, 215–219.

(11) Fisch, M. H.; Richards, J. H. The Mechanism of Photoconversion of Santonin. *J. Am. Chem. Soc.* **1963**, *85*, 3029–3030.

(12) (a) Hamanaka, N.; Matsumoto, T. Partial Synthesis of Grayanotoxin. *Tetrahedron Lett.* **1972**, *13*, 3087−3090. (b) Gasa, S.; Hamanaka, N.; Matsunaga, S.; Okuno, T.; Takeda, N.; Matsumoto, T. Relay Total Synthesis of Grayanatoxin II. *Tetrahedron Lett.* **1976**, *17*, 553−556.

(13) Kan, T.; Hosokawa, S.; Nara, S.; Oikawa, M.; Ito, S.; Matsuda, F.; Shirahama, H. Total Synthesis of (−)-Grayanotoxin III. *J. Org. Chem*. **1994**, *59*, 5532−5534.

(14) Liu, C.; Lei, C.; Zhong, Y.; Gao, L.; Li, J.; Yu, M.; Li, J.; Hou, A. Novel grayanane diterpenoids from *Rhododendron principis*. *Tetrahedron.* **2014**, *70,* 4317–4322.

(15) Turlik, A.; Chen, Y.; Scruse, A. C.; Newhouse, T. R. Convergent Total Synthesis

of Principinol D, a Rearranged Kaurane Diterpenoid. *J. Am. Chem. Soc.* **2019**, *141*, 8088-8092.

(16) Ma, T.; Cheng, H.; Pitchakuntla, M.; Ma, W.; Jia, Y. Total Synthesis of (−)-Principinol C. *J. Am. Chem. Soc.* **2022**, *144*, 20196–20200.

(17) Guo, J.; Li, B.; Ma, W.; Pitchakuntla, M.; Jia, Y. Total Synthesis of (−)-Glaucocalyxin A. *Angew. Chem. Int. Ed.* **2020**, *59*, 35, 15195–15198.

(18) Kong, L.; Yu, H.; Deng, M.; Wu, F.; Jiang, Z.; Luo, T. Enantioselective Total Syntheses of Grayanane Diterpenoids: (–)-Grayanotoxin III, (+)–Principinol E, and (–)-Rhodomollein XX. *J. Am. Chem. Soc.* **2022**, *144*, 5268–5273.

(19) Zhu, A.; Lyu, Y.; Xia, Q.; Wu, Y.; Tang, D.; He, C.; Zheng, G.; Feng, Y.; Wang, Y.; Yao, G.; Ding, H. Divergent Synthetic Approach to Grayanane Diterpenoids. *J. Am. Chem. Soc.* **2023**, *145*, 15, 8540–8549.

(20) (a) Shiozake, M.; Mori, K.; Matsui, M.; Hiraoka, T. Photochemical synthesis of compounds with grayanotoxin skeleton. *Tetrahedron Lett.* **1972,** *13*, 657–660. (b) Trommsdorff, H. Ueber santonin. *Ann. Chem. Pharm.* **1834**, *11*, 190–207. (c) Barton, D. H. R.; De Mayo, P.; Shafiq, M. Photochemical transformations. Part I. Some preliminary investigations. *J. Am. Chem. Soc*. **1957**, *79,* 929–935.

(21) Gao, J.; Rao, P.; Xu, K.; Wang, S.; Wu, Y.; He, C.; Ding, H. Total Synthesis of (−)-Rhodomoollanol A. *J. Am. Chem. Soc.* **2020**, *142*, 10, 4592–4597.

(22) Fay, N.; Blieck, R.; Kouklovsky, C.; de la Torre, A. Total synthesis of grayanane natural products. *Beilstein J. Org. Chem*. **2022**, *18*, 1707–1719.

(23) (a) Kan, T.; Matsuda, F.; Yanagiya, M.; Shirahama, H. Stereocontrolled construction of B-ring of graynotoxins via samarium(II) iodide promoted pinacol coupling

cyclization. *Synlett*. **1991**, 391–392. (b) Paquette, L. A.; Borelly, S. Studies directed toward the total synthesis of kalmanol. An approach to construction of the C/D diquinane substructure. *J. Org. Chem.* **1995**, *60*, 6912–6921. (c) Borelly, S.; Paquette, L. Studies directed to the synthesis of unusual cardiotoxic agent kalmonol. Enantioselective construction of the advanced tetracyclic 7-oxy-5,6-dideoxy congener. *J. Am. Chem. Soc.* **1996**, *118*, 727–740. (d) Chow, S.; Kreß, C.; Albæk, N.; Jessen, C.; Williams, C. M. Determining a synthetic approach to pierisformaside C. *Org*. *Lett.* **2011**, *13*, 5286–5289.

(24) Cherney, E. C.; Baran, P. S. Terpenoid-Alkaloids: Their Biosynthetic Twist of Fate and Total Synthesis. *Isr. J. of Chem.* **2011**, *51*, 3-4, 391–405.

(25) Yeoman, J. T. S., Mak, V. W.; Reisman, S. E. A Unified Strategy to *ent*-Kauranoid Natural Products: Total Syntheses of (−)-Trichorabdal A and (−)-Longikaurin E. *J. Am. Chem. Soc.* **2013**, *135*, 32, 11764–11767.

(26) Wong, A. R.; Fastuca, N. J.; Mak, V. W.; Kerkovius, J. K.; Stevenson, S. M.; Reisman, S. E. Total Syntheses of the C_{19} Diterpenoid Alkaloids (−)-Talatisamine, (−)-Liljestrandisine, and (−)-Liljestrandinine by a Fragment Coupling Approach. *ACS Cent. Sci.* **2021**, *7*, 8, 1311–1316.

(27) Sun, N.; Zheng, G.; He, M.; Feng, Y.; Liu, J.; Wang, M.; Zhang, H.; Zhou, J.; Yao, G. Grayanane diterpenoids from the leaves of *Rhododendron auriculatum* and their analgesic activities. *J Nat Prod*. **2019**, *82*, 1849–1858.

Chapter 2

Vinylogous Mukaiayama Aldol and α-enolate arylation model studies[†]

2.1 INTRODUCTION

This chapter discusses a model system that rapidly tested strategies for γ-functionalization of butenolides. This includes the synthesis of a key, 5-5-fused butenolide fragment in addition to the initial discovery and optimization of a unique vinylogous Mukaiyama Aldol reaction. Early application of 1,4-reduction of butenolides to lactones is discussed. Concepts in the development of a Ni-catalyzed α-enolate arylation reaction are also explored in detail. This chapter provides a model system for the synthesis of auriculatol A, and with Chapter 3, could provide a nice entry to the synthesis of auriculatol A itself or other grayanane ditepenoid natural products more generally.

[†] Portions of this chapter were adapted from the following communication: Thompson, J. K.; Youngblood, K. C.; Teh, S. Y. H.; Farley, C. M.; Zhang, Z.; Virgil, S. C.; Reisman, S. E. *J. Am. Chem. Soc.* **2025**, *147*, 42170–42174. J.K.T. was supported by the NSF GRFP (DGE-1745301). S.E.R. acknowledges fellowship support by the NIH (R35GM118191). The research presented in this chapter was completed in collaboration with Dr. Conner Farley, a former postdoctoral researcher in the Reisman group.

2.2 A NOTE ON MODEL SYSTEMS

The use of a model system is appealing in many aspects, as it provides quick synthetic access to test preliminary hypotheses. In troubleshooting difficult reactivity on simpler systems, model systems may provide insight into the challenges of certain strategies, decrease long-term synthetic burden, and provide a platform to learn reactivity trends before abandoning the development of novel strategies on challenging substrates. However, the results obtained from model systems are not always generalizable, model systems may require optimizations themselves, and model system substrate synthesis is not always trivial. A good model system, nevertheless, takes these considerations into account, often through an in-depth cost-benefit analysis, and is modular, allowing changes in approach as challenges arise.

2.3 MODEL SYSTEM ROUTE DESIGN

2.3.1 Retrosynthetic analysis

We envisioned that the model system route could aid in the development of a vinylogous Mukaiyama aldol addition on an *aryl* aldehyde followed by a Ni-catalyzed α-enolate *arylation* reaction – which could then be parlayed into the development of a vinylogous Mukaiyama aldol addition on a *3.2.1 bicyclic* aldehyde and an α-enolate *alkenylation* reaction. Retrosynthetically from auriculatol A (**49**), disconnection of the **d** ring could provide enone **56**, which could be accessed from Birch Reduction of **57**. Utilizing the intramolecular α-enolate arylation transform, **58** was targeted as a key precursor. It was thought that **58** could be accessed from conjugate reduction of butenolide

59, which could be formed using various γ-functionalization methods. Perhaps the simplest transformation would be the vinylogous aldol reaction, conjoining two fragments **60** and **61** and allowing access to **59**. We hoped to leverage the reactivity of the butenolide as a polarity reversal tactic. While there are reactions known to functionalize butenolides at the γ-position, there are few reports to form fully substituted centers in aldehyde couplings (typically couplings are done with Michael acceptors).[1] Furthermore, past reports do not contain such a hindered site for reactivity of the nucleophile at the γ-center and are often left unsubstituted (Scheme 2.1B). In some cases, α-alkylation has been reported to dominate over the desired vinylogous reactivity.[2] In anticipation of these challenges, concise syntheses of building blocks **60** and **61** were targeted.

***Scheme 2.1. A**. Second generation retrosynthetic analysis **B**. Key challenge: a hindered site for reactivity.*

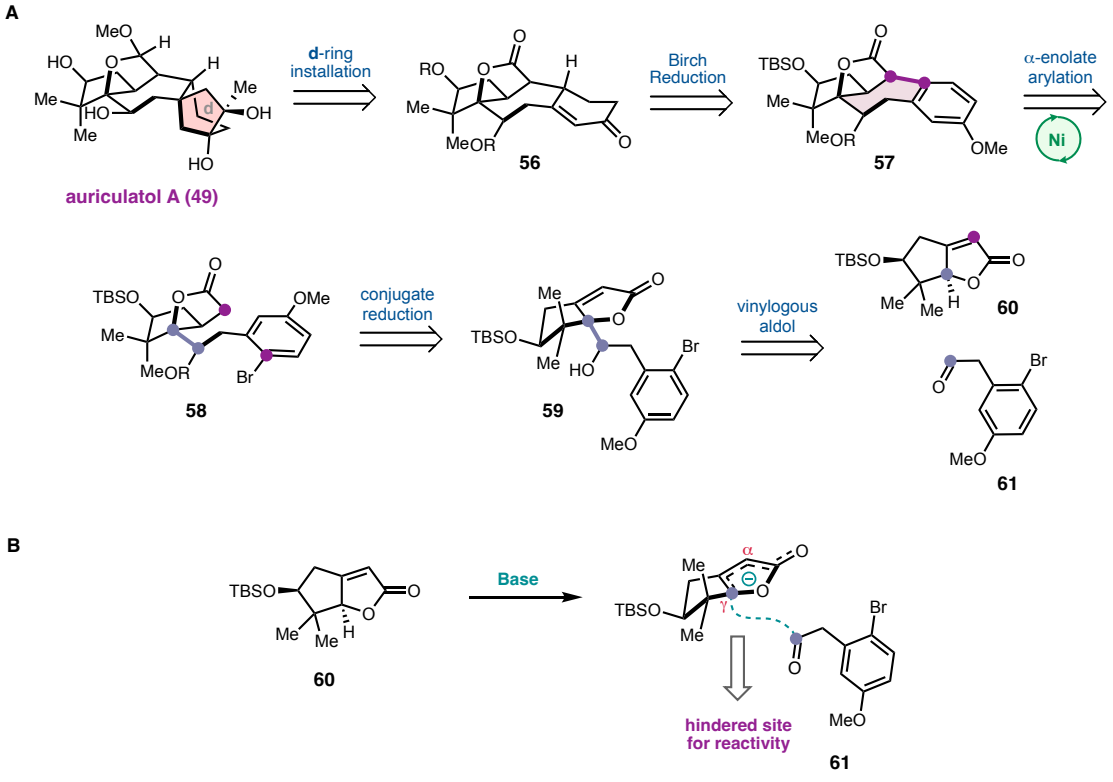

2.3.2 Aldehyde synthesis

Target aldehyde **61** was envisioned to be accessed from commercially available 2-bromo-5-methoxybenzaldehyde (**62**). Treatment with methylene triphenylphosphorane afforded **63** in 50% yield. Consistent with literature precedent, hydroboration of **63** provided **64** in modest yield due to competing formation of the Markovnikov product.[3] From **64**, **61** could be formed by DMP oxidation in 79% yield.[4]

Scheme 2.2. *Original synthesis of fragment* ***61***.

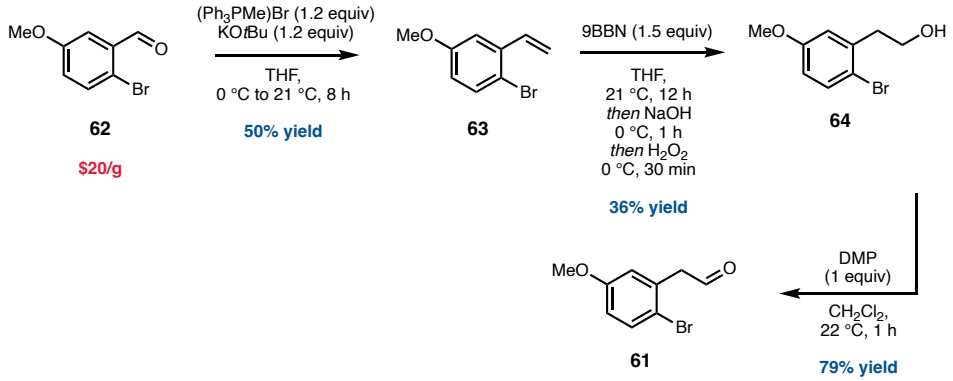

Given the low yield in the hydroboration of styrene **63**, it was found that 3-methoxybenzeneethanol (**65**) could be purchased for $15/g, undergo selective para-bromination[5] and the same oxidation with DMP, and provide **61** in 77% yield over two steps (Scheme 2.3).

Scheme 2.3. *Improved synthesis of* ***61***.

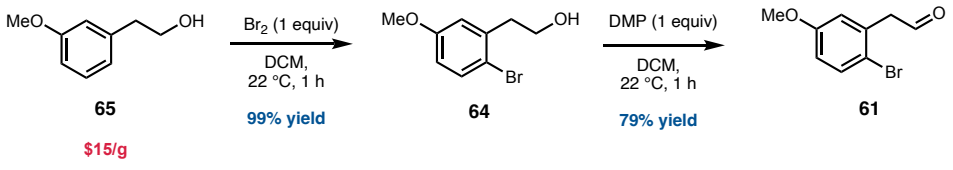

2.3.3 Butenolide synthesis

To access butenolide **60**, it was envisioned that direct cyclization of **66** would offer a straightforward, direct approach (Scheme 2.4). Alcohol **66** could be formed *via* reduction of enone **67**, which could be formed from aldol condensation with ethyl glyoxylate (**68**), tracing back to known ketone **69**. Ketone **69** could arise from a known protection reaction of **70**, allowing for a known CBS reduction of **63**. This would necessitate the use of 2,2-dimethyl-1,3-cyclopentadione (**71**) as the starting material for this fragment.

Scheme 2.4. *Butenolide synthesis: the original synthetic plan.*

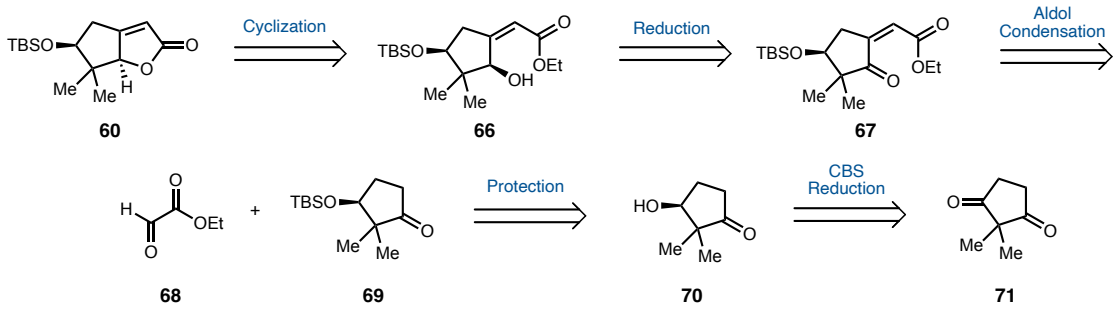

In practice, the plan in Scheme 2.4 was more difficult to implement than expected. Although the CBS reduction and protection sequence formed the desired product, in our hands, it did not occur in the same yield or *ee* as reported (Scheme 2.5A).[6,7] One significant, unanticipated challenge was achieving high yields in the aldol condensation protocol. Utilizing conditions from Vashchenko,[8] the direct condensation of **69** with ethyl glyoxylate (**68**) did not occur under a variety of thermodynamic aldol reaction conditions (Scheme 2.5B). Attempts using kinetic bases such as LHMDS or LDA and treatment with **68** resulted in unconsumed starting material and poor yields of **72** (Scheme 2.5C). Mukaiyama aldol conditions[9] from silyl enol ether **73** provided **72** in 33% yield with high recovery of **69** (Scheme 2.5D).

Scheme 2.5. A. *CBS reduction/protection of* ***71****.* ***B.*** *Failed aldol condensation results.* ***C.*** *Difficulties inducing the Aldol reaction.* ***D.*** *Low-yielding Mukaiyama Aldol.*

A

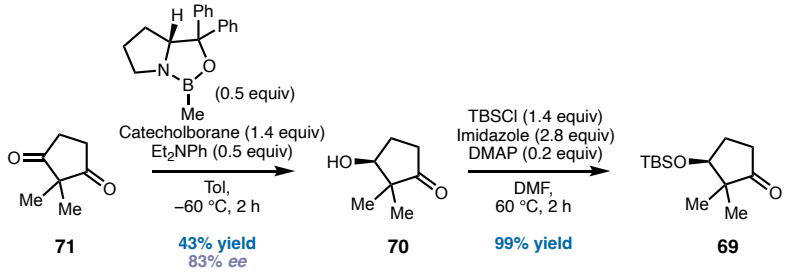

B

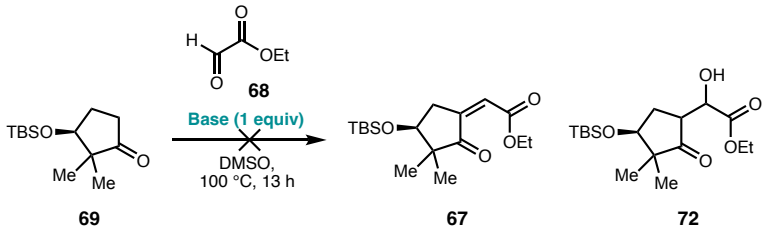

entry	base	conversion	result
1	NaOMe	< 5%	sm, trace **72**
2	NaOEt	< 5%	sm, trace **72**
3	NaOH[a]	< 9%	sm, trace **72**
4	KOH[a]	< 5%	sm, trace **72**
5	KO*t*Bu	< 5%	sm, trace **67**

[a]0.3 eq of base was used

C

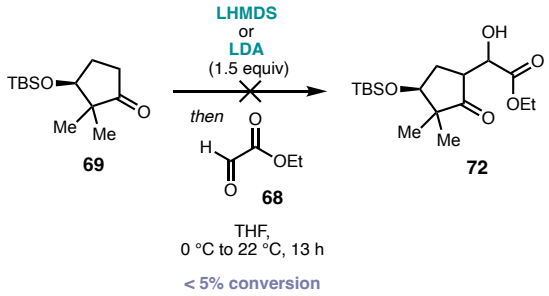

D

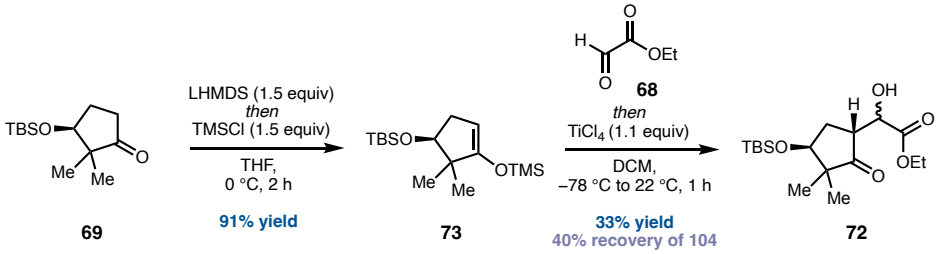

A one-step protocol involving DABCO as a base[10] afforded alcohol **72** in 24% yield (Scheme 2.6). Elimination with Burgess reagent proceeded in 59% yield (**67**). Unfortunately, the direct cyclization of **67** proved troublesome. Upon treatment with $NaBH_4$, for example, no cyclization was observed (not shown). However, hydrogenation with H_2 and Pd/C proceeded smoothly, forming **74** in 75% yield as a 20:1 mixture of diastereomers, from which ketone reduction with $NaBH_4$ occurred with concomitant lactonization to form **75** in 91% yield. From there, a two-step protocol involving α-selenylation and H_2O_2-mediated elimination afforded target butenolide **60** in 65% yield over two steps.

Scheme 2.6. *Second-generation route to butenolide* ***60****.*

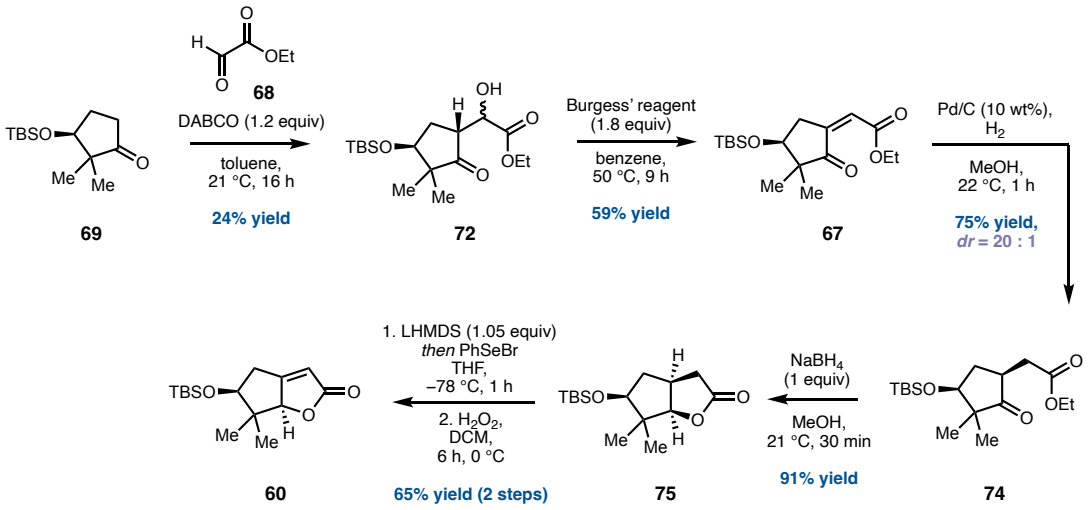

While this route served to test ideas with regards to fragment coupling reactions, it did not provide enough material for extensive front-line investigation. Instead, a higher yielding route was desired. To this end, **69** was oxidized to enone **76** with 3 equivalents of IBX and NMO.[6] Luche Reduction converted **76** to **77**, which set the stage for a Ueno Stork Cyclization[11] to access **78** (Scheme 2.7). The bromoketal **78** could then be converted to the lactone **75** via Jones oxidation,[12] albeit in low yield. A two-step desaturation protocol

consisting of α-selenylation to form **80** and Grieco-type elimination provided **60** in 65% yield over two steps. Starting with 10 g of **71**, more than 1 g of butenolide **60** could be synthesized.

Scheme 2.7. *Third-generation route to butenolide* ***60***.

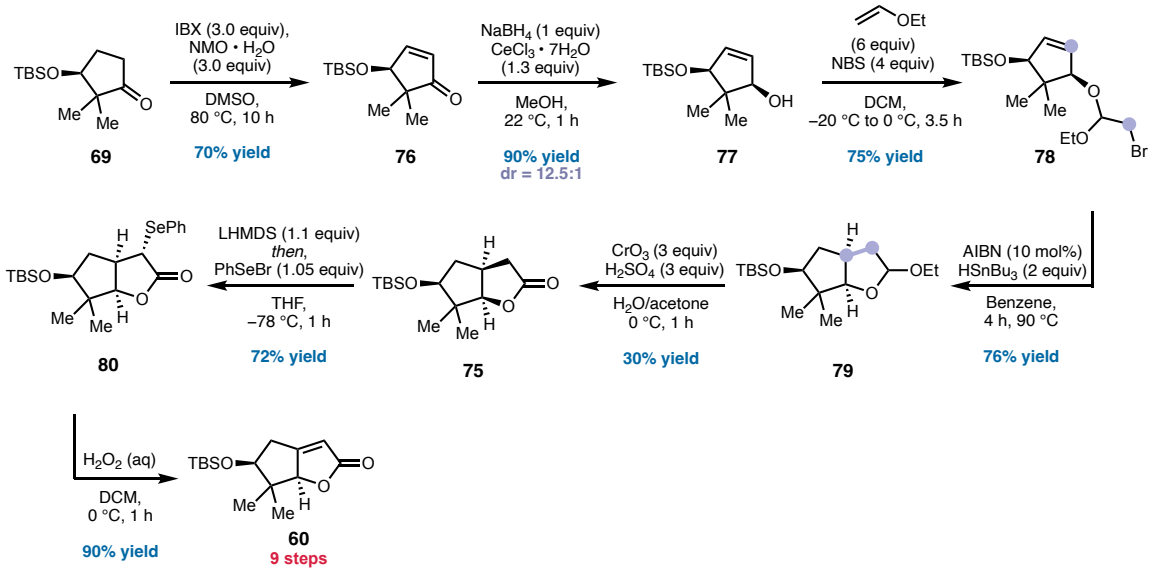

2.3.4 Final optimization of the butenolide route

While allowing gram-scale access to butenolide **60**, the third-generation route could be improved. The route used superstoichiometric quantities of tributyltinhydride, chromium(III) trioxide, and totaled 9 steps, with 3% overall yield. Significant improvements reducing step-count and minimizing toxic, reactive reagents could be made.

One of the major challenges was the CBS reduction. This reaction required close monitoring of an internal temperature of −60 °C and could only comfortably be scaled-up to 20 g. Furthermore, the use of catecholborane on this scale was prohibitively expensive. Noyori hydrogenation could provide higher yields and *ee*'s of the target secondary alcohol (**70**). Indeed, building off work done by Metz,[14] Baudoin's protocol for Noyori Transfer Hydrogenation[15] provided 85% yield and > 99% *ee*, as determined by supercritical fluid

chromatography (SFC) analysis of the benzoylated alcohol **81** (Scheme 2.8).

Scheme 2.8. *Noyori Transfer Hydrogenation of **71**.*

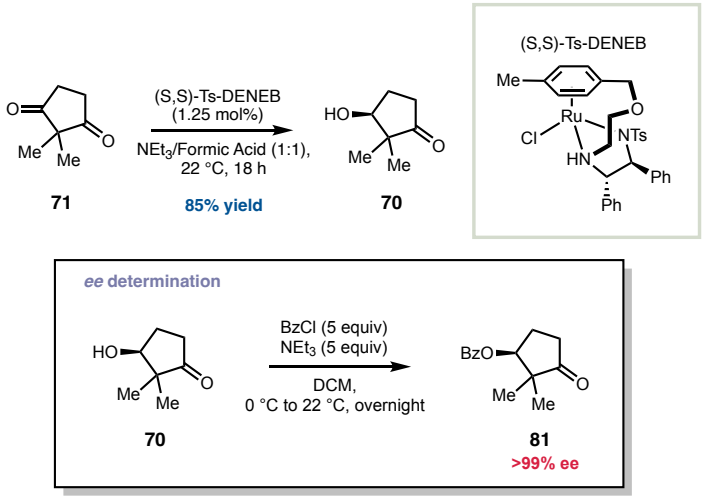

With higher yields of enantiopure material, we turned to shortening the route and minimizing toxic reagents. In our analysis of current and past routes, it became clear that most strategies utilized oxidation/reduction steps to facilitate C-C and C-O forming events. It was recognized that ester **82** was in the same oxidation level as butenolide **60** (Scheme 2.9B). Thus, it was envisioned that a direct cyclization and isomerization of **82** could provide access to **60**. Taken together, we believed that strategies testing the direct cyclization of **82** could provide direct formation of butenolide **60**.

Scheme 2.9. *New ideas for rapid butenolide synthesis.*

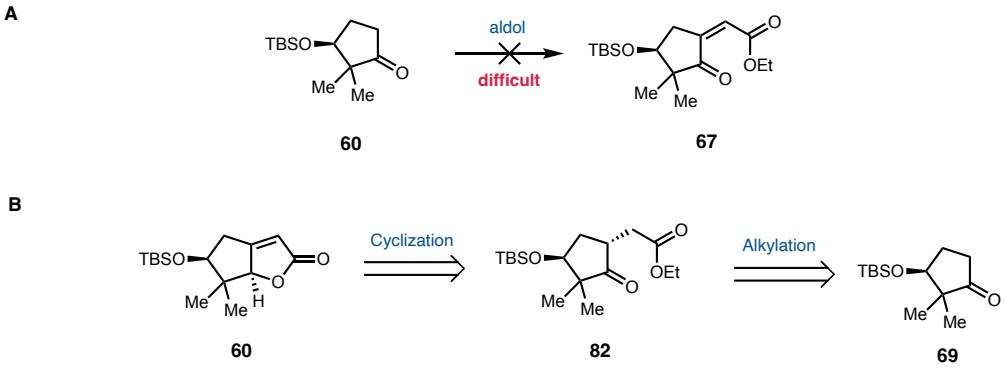

In order to access **82**, silyl enol ether **73** could be cyclopropanated to yield **83** (Scheme 2.10A). Upon acid-mediated fragmentation,[17] **82** could be formed in good yield. **82** was then investigated for direct cyclization. Acid-mediated cyclizations inspired by Paul Knorr furan synthesis[18] primarily resulted in no reaction, likely due to an electronic mismatch for cyclization, while treatment with larger equivalencies or heat led to TBS-deprotection (not shown). Reduction of **82** was also explored. Treatment with sodium borohydride, zinc borohydride, and SmI_2 were all ineffective, giving rise to secondary alcohol **84**, which could not be cyclized to butenolide **60**. As a result, cyclization from the acid was tested (Scheme 2.10B). Following saponification of **82** to form **85**, treatment with NaOAc in boiling Ac_2O proceeded to form undesired spirocycle **86**. A plausible mechanism involves intramolecular acylation of the enol tautomer of ketone in **85**. Gratifyingly, treatment of acid **85** with $SOCl_2$ resulted in formation of chlorolactone **87** (Scheme 2.10C). A plausible mechanism consistent with prior work involves ketone acylation of the acid chloride followed by trapping with chloride.[20] The direct elimination of chloride was more challenging than other systems in the literature, where weak bases such as pyridine or triethylamine were sufficient. Opting for gold-induced chloride elimination conditions from Chida,[51] silyl ether cleavage was observed (not shown). Moving to stronger bases, it was found that the elimination could be accomplished using lithium hexamethyldisilazide (LHMDS) in 71% yield (Scheme 2.11D). The respective sodium and potassium bases led to diminished yields (not shown).

Scheme 2.10. A. *Reductive approach to* ***60****.* ***B.*** *Unexpected spirolactonization side reaction.* ***C.*** *Promising chlorolactone formation* ***D.*** *Fruitful elimination conditions.*

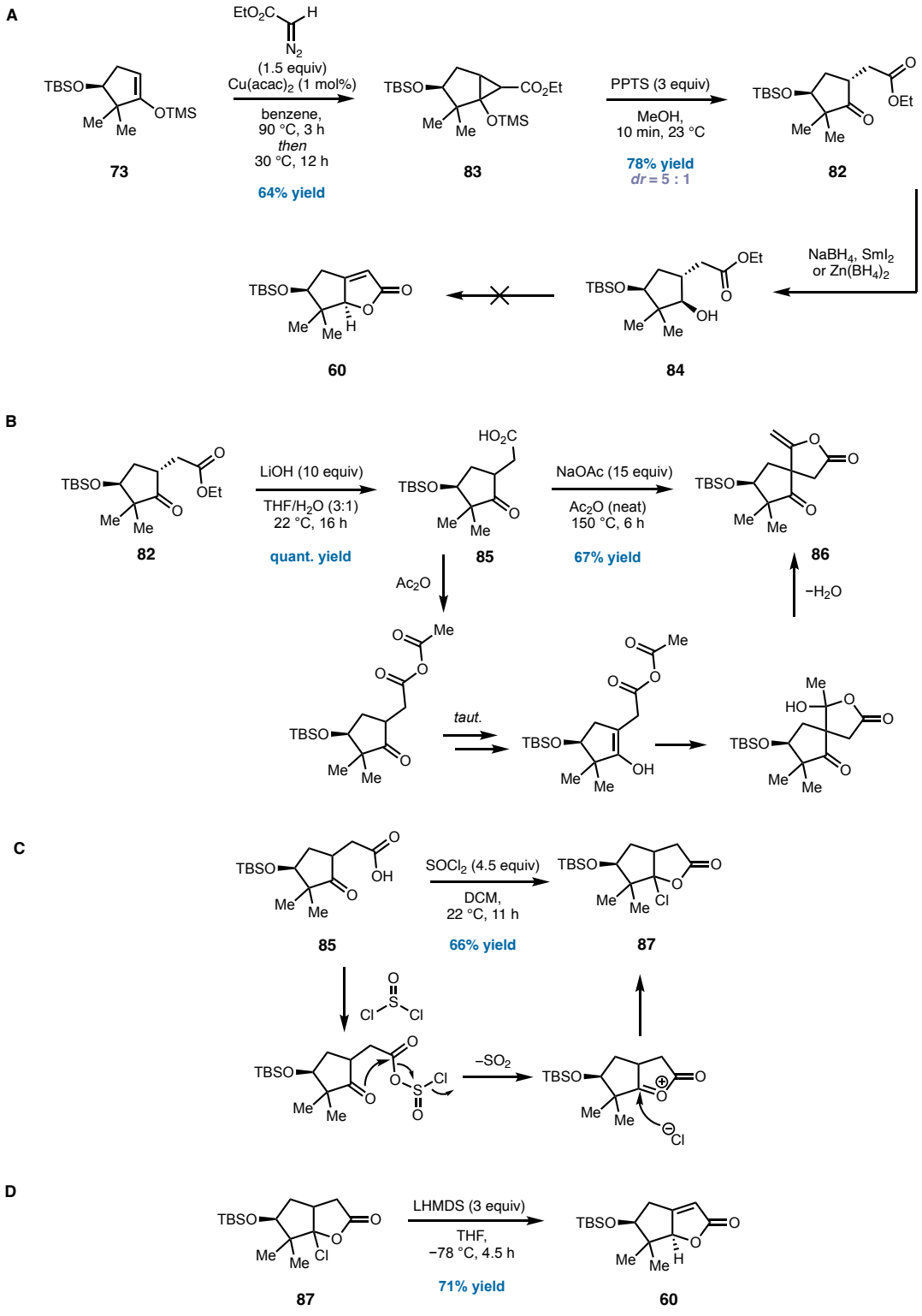

The final optimized route to **60** is depicted in Scheme 2.10 below. The cycloproponation of the silyl enol ether in Scheme 2.10A could be avoided using a simple alkylation procedure with ethyl bromoacetate, shortening the synthesis by 3 steps (Scheme 2.11). This 6-step synthesis enabled multi-gram scale synthesis of butenolide fragment **60**.

Scheme 2.11. *Optimized route to butenolide* ***60****.*

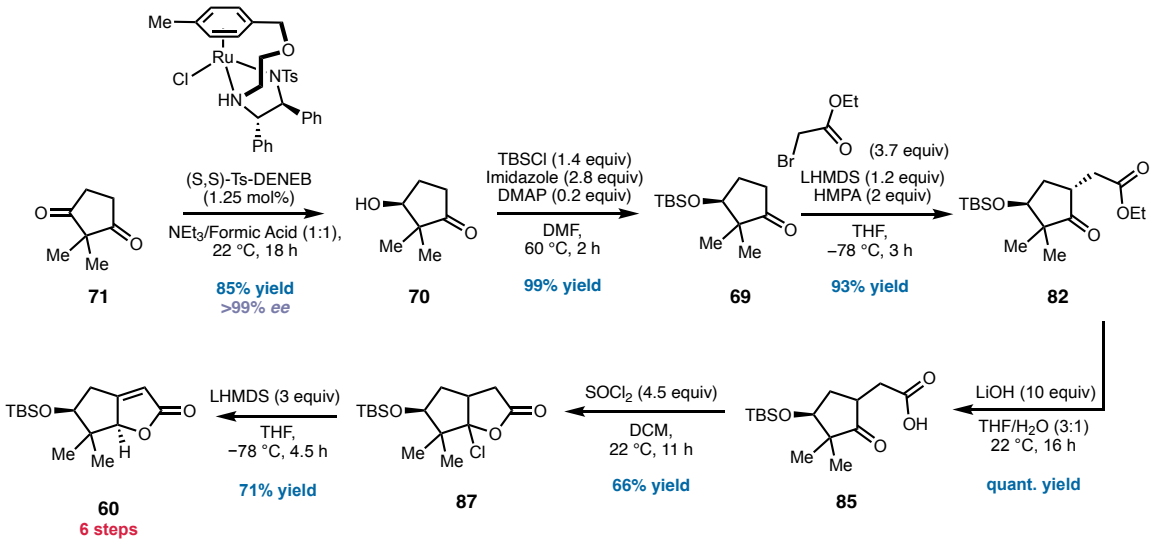

2.3.5 Investigation of direct γ-functionalization methods

Upon optimization of the butenolide synthesis, exploration of γ-functionalization methods could commence. Work by Shenvi and coworkers detailed a unique, butenolide heterodimerization enabled by electronic complementarity.[21] Adapting Shenvi's procedure, deprotonation of **60** with strong bases such as LDA and treatment with aldehyde **61** only led to a complex mixture with no detectible heterocoupling products formed by LCMS analysis (Scheme 2.12). We did, however, detect products corresponding to butenolide dimerization. Treatment of the lithium enolate of **60** and use of ZnI_2 as an additive also led to no desired product, detection of dimerization masses in crude LCMS samples, and formation of a complex mixture. From these results, it became clear that the

lithium enolate of butenolide **60** engages too quickly in undesired side-reactions, even at cryogenic temperatures. A new strategy would be necessary for testing the coupling of fragments **60** and **61**, given that they were now in hand.

Scheme 2.12. *Attempt at direct vinylogous aldol addition.*

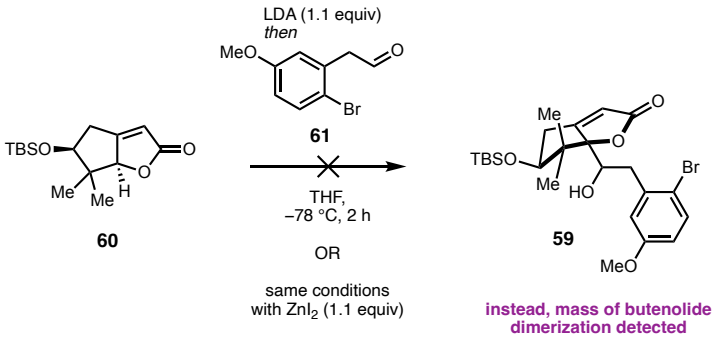

2.4 THE VINYLOGOUS MUKAIYAMA ALDOL REACTION

2.4.1 Siloxyfuran formation

The literature contains better precedent for γ-functionalization of siloxyfurans rather than directly from butenolides. Classified as a type of vinylogous Mukaiyama Aldol reaction, siloxyfuran addition to aldehydes is well-studied and documented on relatively simple substrates.[1,22] Siloxyfurans are thought to contain larger HOMO-coefficients at the γ-position rather than the α-position and engage in a variety of γ-functionalization reactions.[1,23] While they are unique in reactivity when compared to lithium enolates of butenolides, some studies have also been able to tune the degree of α- to γ-selectivity depending on the Lewis acid invoked.[24] Whereas Shirahama's seminal synthesis formed the C5-C6 bond using an intramolecular pinacol coupling, the respective intermolecular coupling remains underdeveloped. We hoped to leverage the use of the siloxyfuran as a

polarity reversal tactic.

When synthesizing siloxyfuran **88**, the methods of Newton and coworkers were helpful.[25] Upon a brief base screen, it was revealed that use of NEt_3 in Et_2O provided 99% yield of **88** (Scheme 2.13). Key to the success of this reaction was the use of vigorous stirring and quality of TBSOTf. During the purification of the siloxyfuran, expeditious purification through phosphate-buffered silica is required. Depending on the level of HOTf present in the TBSOTf or length of the column used for purification, some acid-mediated hydrolysis back to the butenolide starting material (**60**) may be observed, resulting in yields generally ranging from 80-99%.

Scheme 2.13. *Silylation of butenolide (**60**) to the corresponding siloxyfuran (**88**).*

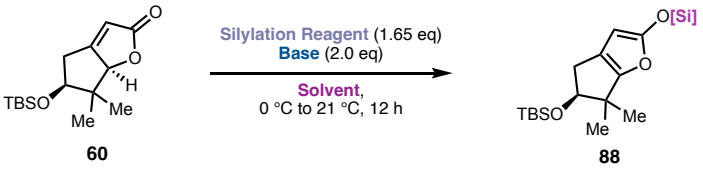

60 **88**

silylation reagent	base	solvent	result
TMSCl	NEt_3	CH_2Cl_2	< 5% conversion
TESOTf	NEt_3	CH_2Cl_2	< 5% conversion
TBSOTf	$EtN(iPr)_2$	Et_2O	50% conversion
TBSOTf	LHMDS	Et_2O	50% yield, full conversion
TBSOTf	NEt_3	Et_2O	**99% yield**

2.4.2 Hit identification and reaction optimization

Unfortunately, treatment of a stirring solution of siloxyfuran **88** and aldehyde **61** with canonical Lewis acids for this transformation led to substrate decomposition (Scheme 2.14, entries 1-3). Indeed, the siloxyfuran fragment **88** is more hindered than reported substrates for this reaction. Rarely do substrates contain substitution at the 5-position of

the furan. The presence of a bulky, all-carbon center in proximity to the desired position for reactivity also deems substrate **88** considerably more challenging. Nevertheless, screening a broad array of Lewis acids revealed a small amount of γ-functionalized product **59** isolated from a reaction utilizing $ZnBr_2$. When compared to $ZnCl_2$, ZnI_2, and $Zn(OTf)_2$, $ZnBr_2$ was the highest yielding (Scheme 2.14, entries 3-6). Switching to THF as solvent considerably increased the yield, likely due to the increased solubility of $ZnBr_2$ in THF and the coordinating ability of THF when compared to CH_2Cl_2. At a reaction time of 7 h, the vinylogous Mukaiyama Aldol reaction formed 52% yield of the desired product, and the reaction was completed on 2.5 gram scale to afford greater than 2 grams of desired product (Scheme 2.14, entry 7). The reactivity was unique with ZnX_2 salts. To date, no other Lewis acids attempted promoted the desired coupling reaction.

Scheme 2.14. *Vinylogous Mukaiyama aldol reaction optimization.*

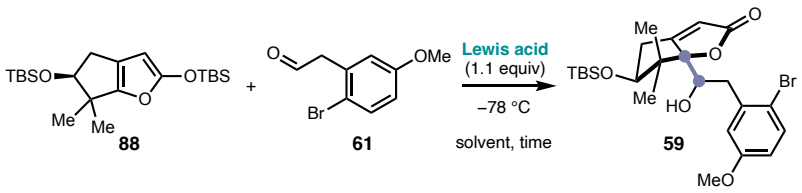

entry	Lewis acid	time	solvent	yield (%)	*dr*
1	$BF_3{\cdot}OEt_2$	2 h	CH_2Cl_2	–	–
2	TMSOTf	2 h	CH_2Cl_2	–	–
3	$SnCl_4$	2 h	CH_2Cl_2	–	–
4	$ZnCl_2$	2 h	CH_2Cl_2	11	5:1
5	$ZnBr_2$	2 h	CH_2Cl_2	14	5:1
6	ZnI_2	2 h	CH_2Cl_2	12	5:1
7	$Zn(OTf)_2$	2 h	CH_2Cl_2	–	–
8	$ZnBr_2$	2 h	THF	40	5:1
9	$ZnBr_2$	7 h	THF	52	8:1

One notable consideration throughout the optimization of this reaction was the diastereoselectivity. Throughout the optimization of this process, it became clear that the diastereoselectivity of the reaction was quite high at the fully substituted center (C5,

Scheme 2.15). Other diastereomers at the C5 have not been observed in this reaction (alkylation from the *si* face of the siloxyfuran). On the contrary, the diastereoselectivity of the secondary alcohol (C6) seemed to possess a temperature dependence. At higher temperatures, the diastereoselectivity decreased to the point where it was 1:1 at room temperatures, while at cryogenic temperatures, the diastereoselectivity was as high as 8:1 (Scheme 2.15).

Scheme 2.15. *Temperature dependence of the vinylogous Mukaiyama aldol reaction.*

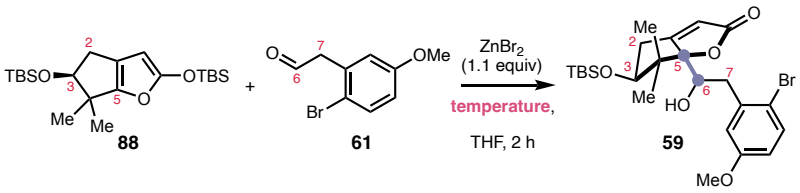

entry	temperature	diastereoselectivity	yield (%)
1	–78 °C	5:1	40
2	0 °C	3:1	34
3	22 °C	1:1	26
4 *	–78 °C	8:1	52

* reaction was run for 7 h instead of 2 h

NOESY analysis of the major diastereomer revealed a strong correlation between the hydrogen at C6 and C3, indicating they were in close proximity in the lowest energy conformation of the compound (Scheme 2.16A). Branching out from the key C6 center, strong NOESY correlations between the OH hydrogen and C2 were observed. This suggested that the reaction formed the wrong stereochemistry required for auriculatol A (**49**, Scheme 2.15B). These results were confirmed by crystallization of a downstream compound.

Scheme 2.16. A. *NOESY analysis of* ***59****.* ***B.*** *Necessary epimerization of C6.*

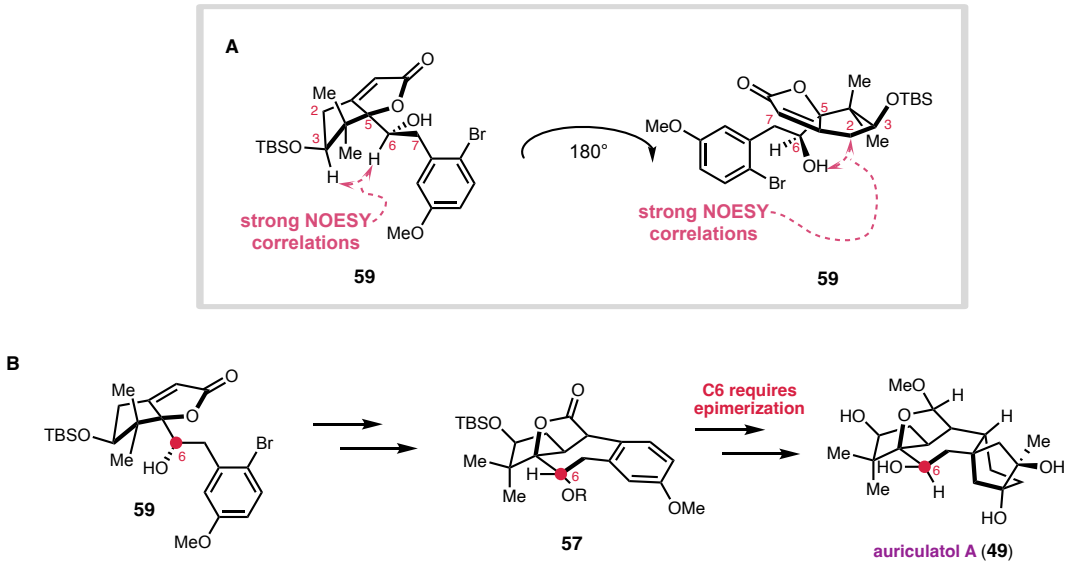

2.4.3 Stereochemical analysis

Several mechanisms could be operative for this vinylogous Mukaiyama aldol reaction. A brief discussion of possible mechanisms is provided: it is possible that the siloxyfuran engages in a hetero-Diels–Alder (DA) reaction, followed by fragmentation to the observed product. Indeed, this is a precedented process for Lewis acid catalyzed DA reactions with aldehydes (Scheme 2.17A); although, this process is not documented for siloxyfuran dienes.[26] In some hetero-DA papers, the "Mukaiyama aldol pathway" and the "hetero-DA pathway" have been tuned based on the identity of the Lewis acid.[27] The next possibility is that the reaction proceeds through a closed transition state in a Cram-chelation model (Scheme 2.17B).[29] Through activation of both the siloxyfuran and aldehyde, they may be brought in close proximity by $ZnBr_2$. If a Cram-chelation model is in effect, Zn^{2+} would likely bind the Lewis basic oxygen that is a part of the 5-membered furan rather than the silyl-protected oxygen. This is due to the fact that silyl ethers are often thought to be too large for chelation models when compared to Bn or alkyl ethers, and Felkin–Ahn

selectivity has been shown to dominate.[30] Though, there are exceptions to these rules,[31] and a chelation model cannot be definitively ruled out. As drawn in Scheme 2.17B, there is a gauche interaction between the R group and the gem-dimethyl group in this model, which may deem this model unlikely. The third option, and perhaps most convincing, is an open transition state (TS) (Scheme 2.17C). This is what is suggested in prior reports of these types of reactions.[1,22] Binding of the aldehyde to the Lewis acid lowers the LUMO, allowing engagement with the siloxyfuran in the key C-C bond-forming step.[26]

Scheme 2.17. *Mechanisms for the vinylogous Mukaiyama aldol addition.*

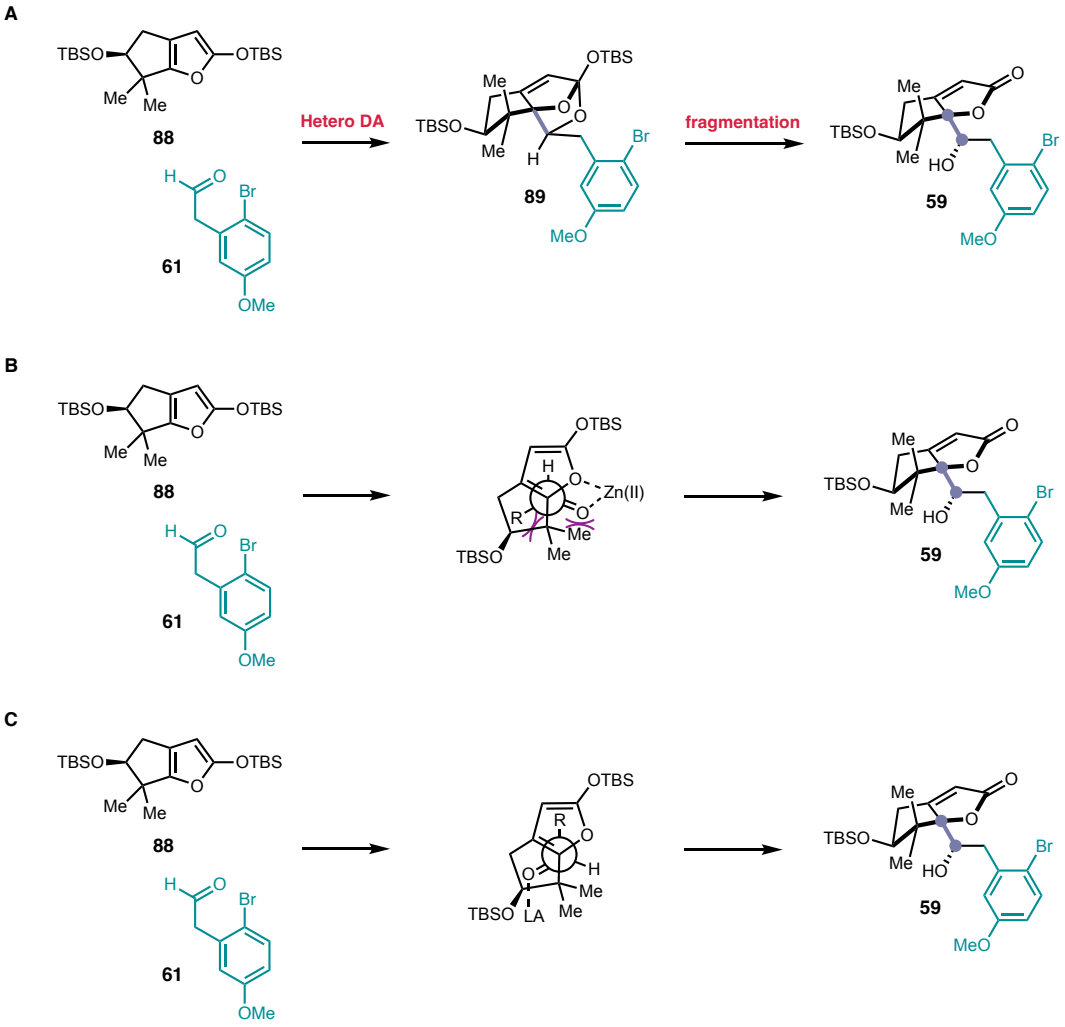

Given that the reaction likely proceeds through an open transition state, we can construct a model to justify the observed diastereoselectivity. Approach of the aldehyde from the *re* face of the siloxyfuran may be due to the bulkiness of the *beta* OTBS ether. In the favored transition state, the hydrogen is closest to the bulkiest part of the siloxyfuran: the gem-dimethyl group. Due to sterics, it is believed the Lewis acid should chelate the face of the aldehyde opposite to the R group. We believe two transition states are possible for the disfavored transition state. In disfavored transition state 1, we suggest a gauche interaction between the bound Lewis acid and the OTBS group of the siloxyfuran. In a second interpretation, the hydrogen is kept pointed towards the bulky, gem-dimethyl group (disfavored transition state 2). In this case, it is believed that steric clash between the OTBS group and the LA group would be present.

Scheme 2.18. *Vinylogous Mukaiyama aldol transition state analysis: the favored transition state and two possible disfavored transition states.*

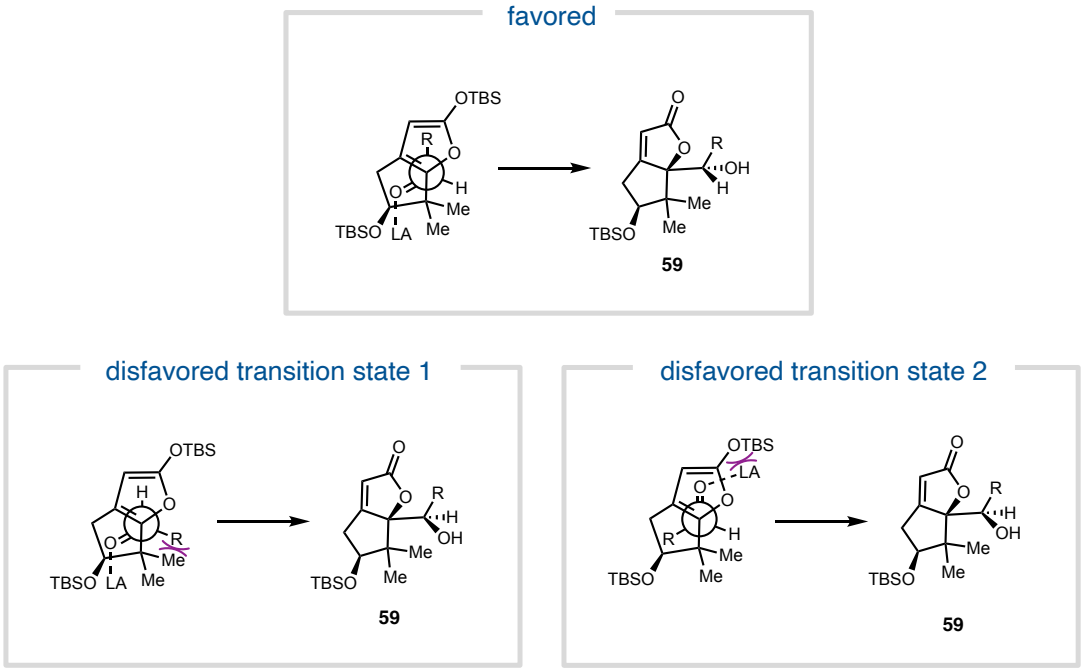

2.5 A-ENOLATE ARYLATION SUBSTRATE SYNTHESIS

2.5.1 Secondary alcohol protection

Elaboration of product **59** was challenging. Unsurprisingly, treatment of **59** with strong base led to a retro-aldol reaction and isolation of a mixture of butenolide **60** with aldehyde **61** (Scheme 2.19, entries 1-3). Surprisingly, use of a variety of protecting group conditions were unsuccessful, even ones that avoided the use of strong bases (Scheme 2.19, entries 4-6). This is likely attributed to the steric hindrance of the secondary alcohol. In its lowest energy conformation, the alcohol likely sits buried underneath the butenolide. After some screening, it became clear that protection as the MOM ether provided optimal yields of **90** (Scheme 2.19, entry 7).

Scheme 2.19. *Difficult secondary alcohol protection.*

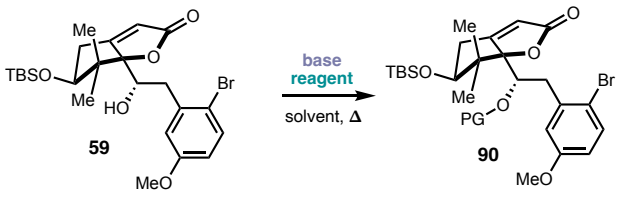

entry	base	reagent	solvent	result
1	NaH	BnBr	THF	retro-aldol
2	NaO*t*Bu	BnBr	THF	retro-aldol
3	LDA	BnBr	THF	retro-aldol
4	Imidazole	TBSCl, DMAP	DMF	NR
5	NEt_3	TBSOTf	CH_2Cl_2	NR
6	Pyridine	TBSOTf	CH_2Cl_2	NR
7	EtN*i*Pr_2	MOMCl	DCE	86% yield

2.5.2 Chemoselective butenolide reduction

Conjugate reduction of **90** was originally developed using a NEt_3-$NaBH_4$ mixture,[32] but this reaction was difficult to scale-up (Scheme 2.20, entry 1). Moving onto conditions employing stoichiometric NiH ($NiCl_2$ + $NaBH_4$),[33] though these conditions led to higher

yields and could be scaled up, they suffered from irreproducible yields due to competitive protodebromination (Scheme 2.20, entry 2). Eventually, conjugate reduction was improved using Buchwald's catalytic CuH system,[34] which delivered high yields of the product lactone **58** in excellent diastereoselectivity (*dr* > 20:1). Formation of the more cis-lactone over the trans-lactone is likely more energetically accessible. It is also possible that the TBS ether aids in blocking the *re* face of the butenolide on approach of CuH. Importantly, Stryker's reagent[35] did not react in this system (not shown).

Scheme 2.20. *Conjugate reduction of butenolide* ***90***.

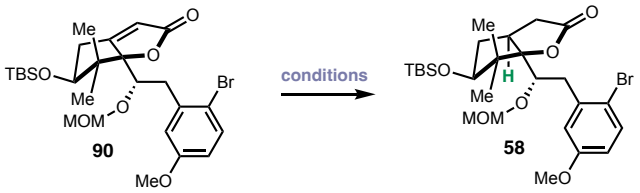

entry	conditions	result
1 *	NEt_3 (6 equiv), $NaBH_4$ (3 equiv) THF, 0 °C to 21 °C, 1 h	49% yield *dr* > 20 : 1
2 **	$NiCl_2 \cdot 6H_2O$ (1.5 equiv), $NaBH_4$ (1.1 equiv) THF/MeOH, –50 °C to 0 °C, 1 h	73% yield *dr* > 20 : 1
3	$CuCl_2 \cdot 2H_2O$ (5 mol%), (R)-tol-BINAP (5 mol%), PMHS (6 equiv), NaO*t*Bu (1.2 equiv), *t*BuOH (12 equiv) THF/DCM (3:1), 21 °C, 24 h	**85% yield** *dr* > 20 : 1

* difficulty scaling

** difficulty yielding reproducable results

Crystallization of product **58** could be completed by the slow evaporation of toluene. These data indicated that the NOESY analysis in Scheme 2.16A was correct in assigning the C5 and C6 stereochemistry from the vinylogous Mukaiyama aldol step. With rapid access to butyrolactone **58**, future studies could focus on exploring the intramolecular α-enolate arylation.

Scheme 2.21. *Crystallization of* ***58****.*

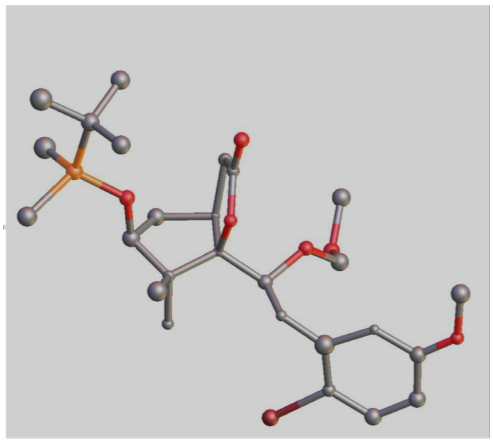

2.6 Ni-CATALYZED INTRAMOLECULAR A-ENOLATE ARYLATION

2.6.1 Buchwald's intermolecular α-enolate arylation of lactones

Turning to the literature, we became interested in Buchwald's disclosure of an intermolecular α-enolate arylation of lactones catalyzed by Ni-BINAP.[36] These conditions used low loadings of $Ni(COD)_2$ preligated with BINAP as the active catalyst species. The lactone enolate was generated from sodium hexamethyldisilazide (NaHMDS), while catalytic quantities of $ZnBr_2$ were used to facilitate faster catalytic turnover. The reaction was compatible with both aryl chlorides and aryl bromides, albeit aryl chlorides seemed to be more general and higher yielding. Different ZnX_2 salts were shown to boost the rate of reaction in catalytic quantities but hinder conversion in stoichiometric loadings. A variety of electron donating and electron withdrawing aryl halides were explored, with excellent yield and enantioselectivity.

Scheme 2.22. *Buchwald's α-enolate arylation of lactones.*

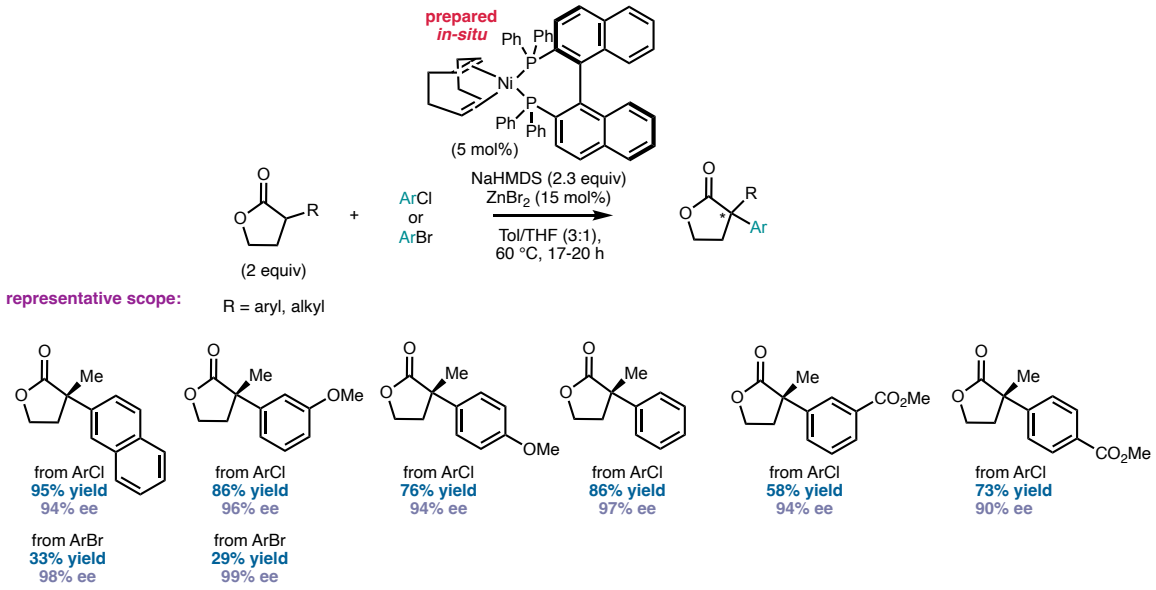

2.6.2 Phosphine ligand modifications

In an initial attempt to modify Buchwald's conditions for an intramolecular reaction instead of an intermolecular reaction, the catalyst loading was changed to 10 mol% and the base loading was reduced to 1.3 equivalents. Under these conditions using (BINAP)Ni(COD), trace quantities of the desired arylation product were isolated with the remaining mass balance accounted for in recovered starting material (Scheme 2.23, entry 1). It was hypothesized that different monodentate phosphines could free up coordination sites on Ni and promote catalyst turnover, as many monodentate phosphines have proven to be competent ligands in the enolate arylation of ketones.[37] While conversion was low with the alkyl phosphine *t*BuDavePhos, the conversion was better for RuPhos and DavePhos. On small scale, the yield for the DavePhos reaction exceeded 75% (Scheme 2.23, entry 4).

Scheme 2.23. *Initial exploration of Ni-catalyzed α-enolate arylation chemistry.*

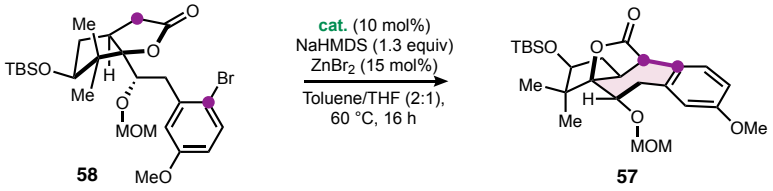

entry	cat.	starting material (%)	desired (%)
1	(COD)Ni(BINAP)	76	3
2	(COD)Ni(*t*BuDavePhos)$_2$	74	2
3	(COD)Ni(RuPhos)$_2$	31	8
4*	(COD)Ni(DavePhos)$_2$	0	79

* not reproducible or scalable

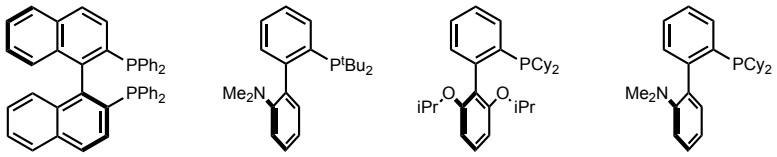

rac-BINAP ^{t}BuDavePhos RuPhos DavePhos

Upon scaling up this process, the selectivity of the reaction flipped to favor a new, unknown product in 51% yield, with only 2% desired product formation. In the ^{1}H NMR of the new product (**91**), the presence of two methylene peaks corresponding to C10 obviated that α-functionalization had not occurred. **91** contained a C10 singlet that did not engage in splitting with the methine C-H at C1. It was initially thought that the species observed was protodebromination; however when **91** was compared to a previous isolation of protodebromination, the spectra did not match. LCMS analysis confirmed that **91** possessed the same mass as compound **57**. This suggested that the unknown structure was the β-arylated product. In further support of this hypothesis, analysis of the HMBC data of **57** showed correlations between C20 and C11 but none present in the HMBC of compound **91** (Scheme 2.24).

Scheme 2.24. *Scale-up reveals a change in selectivity for β-arylation.*

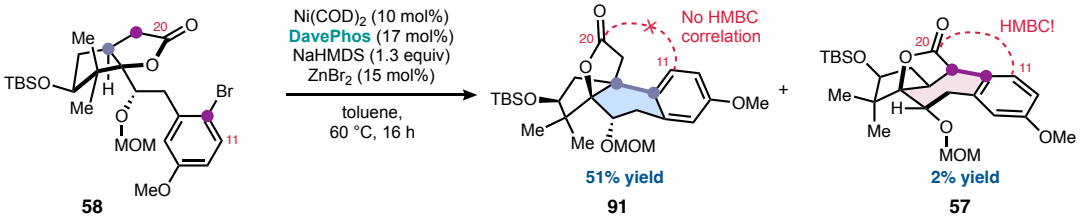

Ultimately, the structure of **57** was confirmed via X-ray crystallography (Scheme 2.25). In this structure, the newly formed C9-C11 bond and the structure of the 5-5-7-6 tetracyclic structure could be verified in addition to the presence of the TBS ether, MOM ether, and methoxy-arene.

Scheme 2.25. *Crystal structure of **57**.*

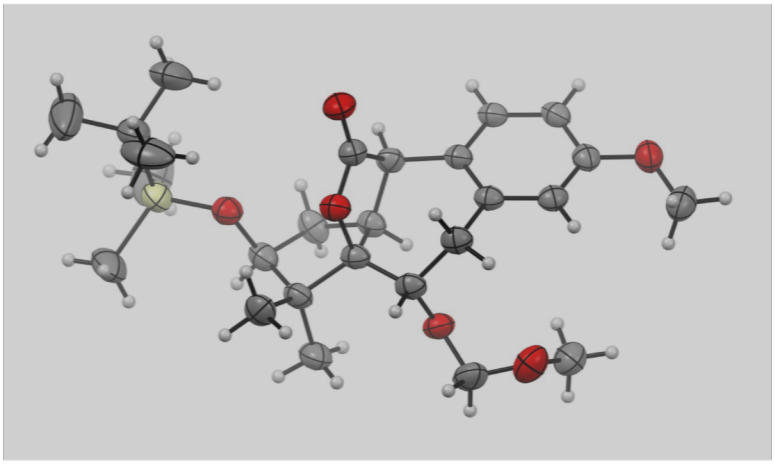

Surprised by the finding that scaling up of the conditions employing DavePhos as ligand led to β-arylation, we speculated the mechanism of the product's formation. Starting with the productive pathway, product **57** could arise from oxidative addition into the aryl bromide, transmetallation from the Na or Zn enolate, and reductive elimination (Scheme 2.26A). In the undesired pathway, we thought that deviation in the mechanism could occur from the "key intermediate". Instead of direct reductive elimination, β-hydride elimination

could install desaturation. Migratory insertion and reductive elimination could furnish **91** (Scheme 2.26B).

Scheme 2.26. A. *Productive catalysis mechanism.* ***B.*** *Posited mechanism for side-product formation.*

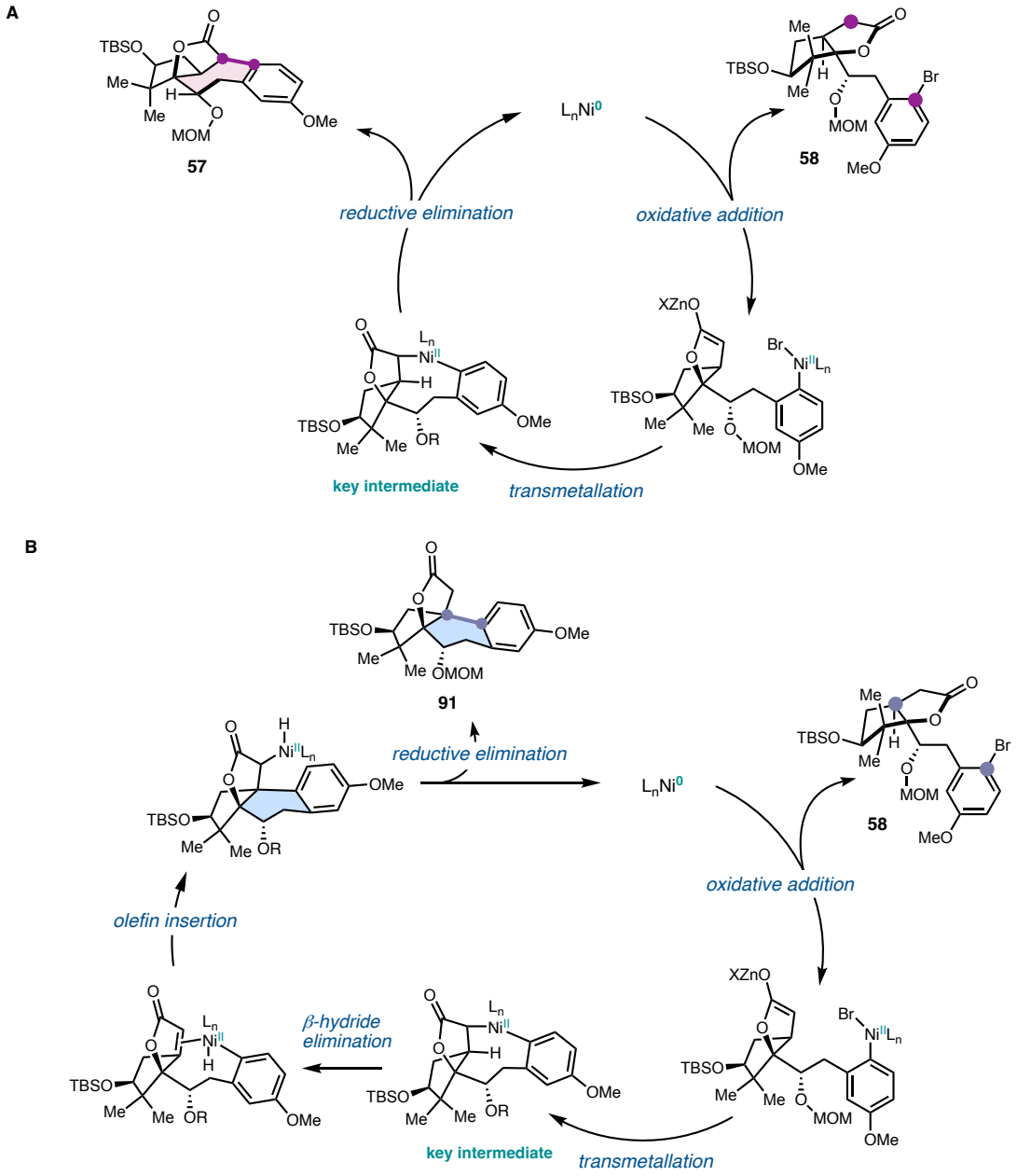

Given the proposed mechanism, it was hypothesized that use of bidentate phosphine ligands could disfavor β-hydride elimination by occupying the requisite

coordination site required for the β-hydride elimination pathway; tuning the steric and/or electronic properties of the ligand could increase conversion and limit the formation of **91**. It was ultimately found that using rigorously anhydrous toluene and THF, as prepared by Williams & Lawton,[38] was necessary for high conversions. Under conditions utilizing rigorously anhydrous solvents, many bidentate ligands proved to be competent at forming **57** in great yields (Scheme 2.27).

Scheme 2.27. *Bidentate phosphines as ligands for nickel-catalyzed intramolecular α-enolate arylation.*

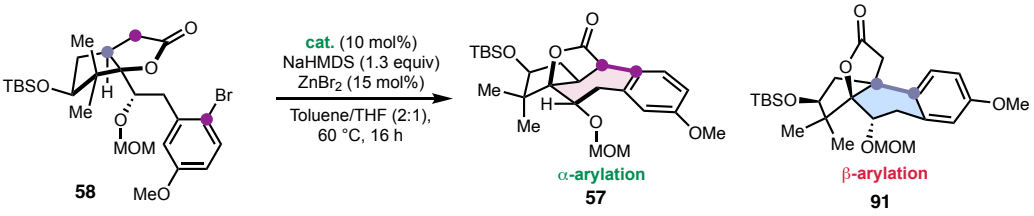

entry	cat.	starting material (%)	α-arylation (%)	β-arylation (%)
1	(COD)Ni(Me-DuPhos)	99	0	0
2	(COD)Ni(DCPE)	75	1	0
3	(COD)Ni(DCPB)	41	25	3
4	(COD)Ni(N-XantPhos)	13	53	17
5	(COD)Ni(DPPF)	12	57	8
6	(COD)Ni(*t*BuXantPhos)	12	63	5
7	(COD)Ni(DPPE)	12	73	8
8	(COD)Ni(XantPhos)	10	77	11
9	(COD)Ni(DPPP)	0	77	10
10	(COD)Ni(DPPP)*	5	77	10

* 200 mg scale

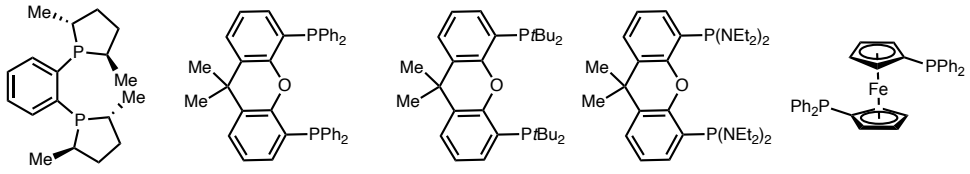

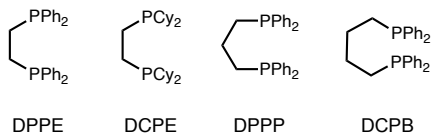

These data proved that the nickel catalysis and specifically the inhibition of the β-hydride elimination pathway was robust and could be conducted reproducibly for a wide variety of ligands – granted the caveat that use of specialty, anhydrous solvents was necessary, and the reaction itself was sensitive to quality of the glovebox atmosphere. The reaction was successfully scaled up to 200 mg scale using DPPP in a pressure flask without a drop in reaction yield, achieving an 11-step synthesis (LLS) of key tetracycle **57**.

Future investigation into the role of the DavePhos ligand in achieving good yields of β-arylation could be conducted. One explanation could be that the Lewis basic amine on DavePhos offers stabilizing dative interactions that facilitates in phosphine decoordination to a 16 e^- Ni complex, capable of β-hydride elimination over reductive elimination from the "key intermediate". Although this is speculative, it is reminiscent of work from the Newhouse group in the realm of carbonyl dehydrogenation and oxidative cycloalkenylations of ketones[39,40] and could be leveraged as a complimentary approach to β-arylated products. More studies are required to test the generalizability of the reaction and the mapping of chemical space when targeting β-arylation over α-arylation – these were to be considered outside of the scope of this work – and could be of interest in future work.

2.6.3 Other ligands

A control reaction to test the background reactivity of $Ni(COD)_2$ in the absence of phosphine ligand revealed the desired product was isolated in good yield; this result was both reproducible and scalable (Scheme 2.28).

Scheme 2.28. *Phosphine leave-out experiment.*

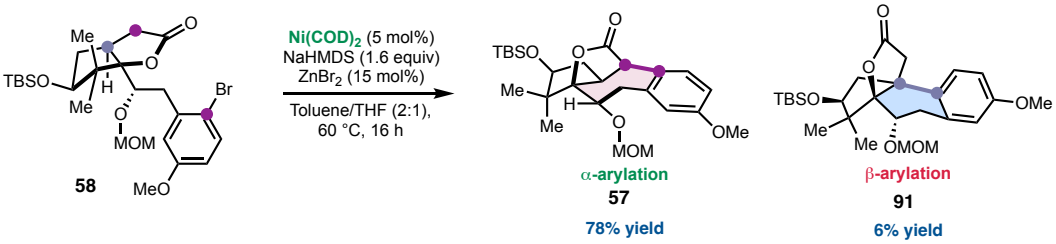

Generally, a combination of factors including cone angle, bite angle, and stereoelectronic properties may enhance a ligand's efficiency in catalysis. These attributes have been intensely documented in the literature.[41,42] What was surprising is that olefin ligands are electron-deficient when compared to phosphine ligands. At the time, it was believed that oxidative addition would not be energetically accessible without strongly σ-donating ligands; it was, perhaps naively assumed that the background reactivity of unligated $Ni(COD)_2$ would not effect the outcome of the reaction.

This result opened possibility to explore catalysts broader in scope, ligated by olefins, containing different electron counts, and possessing different stereoelectronic properties. Many Ni(0) catalysts and precatalysts have been recently reported in the literature, including Mongomery's original report of NHC-ligated Ni(0) catalysts for C-C and C-N bond formation[43] and Cornella's Ni(0) stillbene (stb) catalysts[44] (Scheme 2.29). Doyle's air-stable commercially available TMEDA-ligated Ni(II) catalyst capable of *in-situ* reduction to Ni(0) simply by heating[45] and Engle's commercially available nickel precatalysts[46,47] were also great options to explore. If the reaction did not require phosphine ligands, then the realm of possible opportunities for innovation could be expanded. Use of different precatalysts with or without phosphine ligands had the potential to catalyze the reaction. A simple leave-out experiment had far-reaching implications.

Scheme 2.29. *Some recently reported Ni(0) precatalysts.*

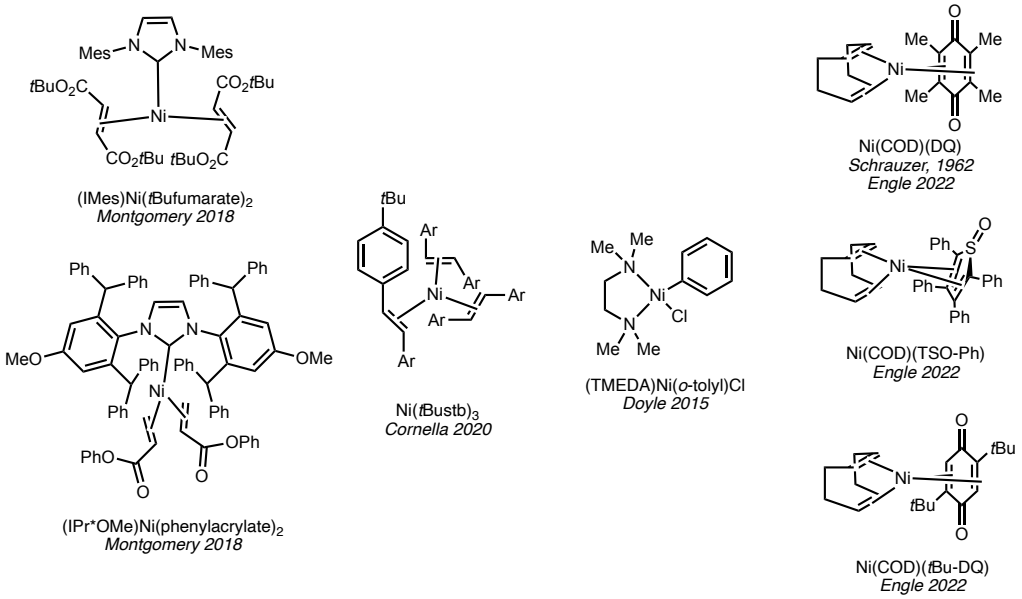

To fully understand the high yielding result without phosphine ligand, a variety of different ligands and precatalysts were tested to probe the reactivity. Up until this point, all reactions were setup the way Buchwald had described.[36] $Ni(COD)_2$ was preligated with phosphine ligand before being added to a solution of ArCl or ArBr, $ZnBr_2$, and the lactone enolate. We wondered if the preligation was necessary, and if the procedure involving addition of all solids to the starting material, followed by solvent at the end, would work. Changing the order of addition and using 1,3-Bis(dicyclohexylphosphino)propane (DCPP) as ligand in slight excess (1.5 equivs. with respect to $Ni(COD)_2$), indeed, no reaction was observed (Scheme 2.30, entry 1). With this new method for reaction setup, most nickel catalysts and precatalysts were inactive (Scheme 2.30, entries 2-6). In the literature, it has been shown that addition of electron-deficient olefins could help with catalyst stability and faster reductive elimination.[48,49] Use of phenyl acrylate, 4-CF_3 styrene, dimethylfumarate, and benzonitrile all led to no reaction (Scheme 2.30, entries 7-10); although, it is unclear if the electron-deficient olefin was able to ligate to nickel given that the reaction was setup

by adding all components and then solvent last. The only-phosphine ligated complex that seemed to work with the new order of addition was $Ni(PPh_3)_4$ in 24% yield (Scheme 2.30, entry 11).

Scheme 2.30. *New order of addition with no phosphine preligation to Ni(COD)₂.*

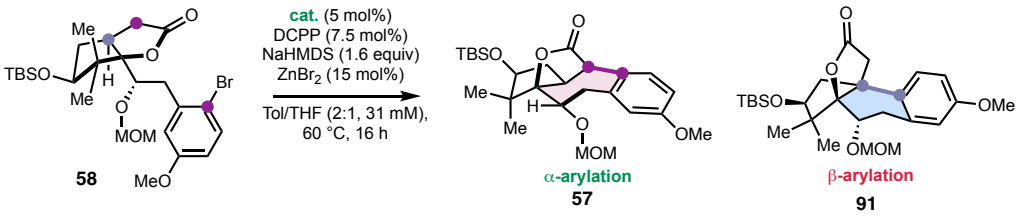

entry	cat.	additive (12 mol%)	starting material (%)	α-arylation (%)	β-arylation (%)
1	Ni(COD)DQ	-	42	-	-
2	(COD)Ni(TSO-Ph)	-	81	-	-
3	(IMes)Ni(*t*Bufumarate)$_2$	-	69	-	-
4	(IPr*OMe)Ni(phenyl acrylate)$_2$	-	55	-	-
5	(TMEDA)Ni(o-tolyl)Cl	-	62	-	4
6	Ni($^{t\text{Bu}}$stb)^3	-	23	-	-
7	Ni(COD)$_2$	phenyl acrylate	40	-	-
8	Ni(COD)$_2$	4-CF_3 styrene	60	-	-
9	Ni(COD)$_2$	dimethylfumarate	60	-	-
10	Ni(COD)$_2$	benzonitrile	62	7	-
11	Ni(PPh$_3$)$_4$	-	40	24	4

The data in Scheme 2.30 are in stark contrast to the experimental results obtained without phosphine ligand (Scheme 2.31). The reaction underwent higher conversions with many different catalysts. Although (COD)Ni(TSO-Ph) and (IPr*OMe)Ni(phenylacrylate)$_2$ only led to trace yields, use of Cornella's *t*Bu stillbene catalyst led to 12% yield, with minimal β-arylation (Scheme 2.31, entries 1-3). Compared to the (TSO-Ph)Ni(COD), use of (COD)Ni(*t*Bu-DQ) led to an increase in yield to 30% (Scheme 2.31, entry 4). Doyle's Ni(II) precatalyst led to a 44% yield of α-arylation (Scheme 2.31, entry 5). Both Ni(COD)$_2$ and Ni(COD)DQ catalyze the intramolecular α-enolate arylation in high yields (Scheme 2.31, entries 6-7). In the case of Ni(COD)DQ, we believe the use of the more electron-deficient duroquinone ligand with respect to cyclooctadiene promotes faster reductive

elimination, prohibiting β-hydride elimination and therefore the formation of the β-arylated product.

Scheme 2.31. *Got ligand? Phosphine-ligand free Ni(0) catalysts for α-enolate arylation.*

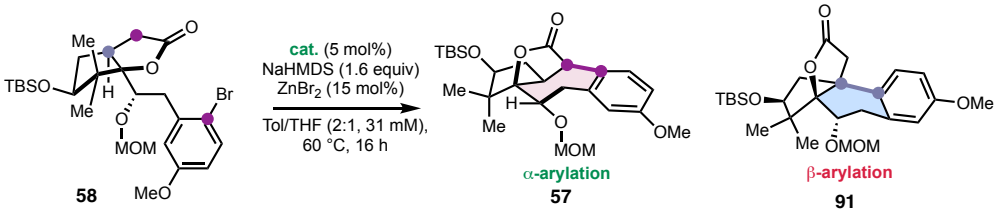

entry	cat.	starting material (%)	α-arylation (%)	β-arylation (%)
1	(COD)Ni(TSO-Ph)	77	2	0
2	(IPr*OMe)Ni(phenyl acrylate)$_2$	85	4	0
3	Ni($^{t\text{Bu}}$stb)^3	40	12	1
4	(COD)Ni(*t*Bu-DQ)	52	30	0
5	(TMEDA)Ni(o-tolyl)Cl	32	44	6
6	Ni(COD)$_2$	0	**78**	6
7	Ni(COD)DQ	0	**80**	0

These data suggest that Ni(COD)$_2$ had been catalyzing the reaction when phosphine ligands were used (Scheme 2.27) given that Ni(COD)$_2$ and the bidentate phosphine were used in a 1:1 ratio. This is evident when thinking about the equilibrium of Ni(COD)$_2$ with phosphines, as studied by Mori.[50] Using PPh$_3$, full exchange with COD was only observed after heating for prolonged periods at 80 °C. In our method for phosphine ligation to Ni(COD)$_2$, the equilibrium may lie slightly to the left, leaving phosphine ligand-free Ni(COD)$_2$ to catalyze the reaction while phosphine-ligated catalyst is inert. These conclusions are speculations and have not been confirmed.

2.6.4 Final control studies

Some control experiments elucidated what elements of the reaction were required (Scheme 2.32). Indeed, $ZnBr_2$ and heat were required for the reaction, which exhibited sluggish reaction profiles and recovery of starting material (Scheme 2.32, entries 2-3). The reactions were scalable and could be setup in the glovebox or using Schlenk technique (Scheme 2.32, entries 4 & 6).

Scheme 2.32. *Control studies in the phosphine-ligand free Ni-catalyzed α-enolate arylation.*

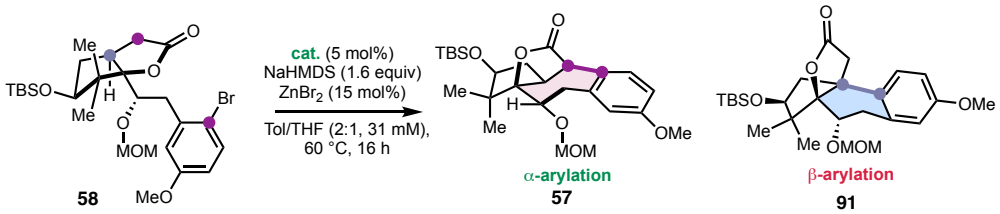

entry	cat.	scale	deviation	α-arylation (%)	β-arylation (%)
1	$Ni(COD)_2$	5 mg	—	78	6
2	$Ni(COD)_2$	5 mg	No $ZnBr_2$	5	1
3	$Ni(COD)_2$	5 mg	21 °C	3	1
4	$Ni(COD)_2$	25 mg	scale	78	8
5	Ni(COD)DQ	5 mg	—	80	0
6	Ni(COD)DQ	25 mg	scale	79	0

2.7 CONCLUDING REMARKS

This chapter introduces a model system used towards the synthesis of auriculatol A – first through explanation of the retrosynthetic logic and second through the forward synthesis of key butenolide building block **60** and aldehyde **61**. While the aldehyde fragment, **61**, was straightforward, synthetic access to **60** was far more challenging. Strategies attempted to form **72** through aldol condensation chemistry from compound **69** and Mukaiyama aldol reactions from **73**. While these were unsuccessful strategies, use of a Ueno-Stock bromoacetal **79** was applied in the development of a 9-step butenolide

fragment **60** synthesis. Later, a 6-step synthesis of **60** was developed, which utilized a Noyori transfer hydrogenation reaction and chlorinative cyclization-elimination sequence. Central to this strategy was thinking about direct cyclization approaches from compound **82** rather than superfluous oxidative or reductive chemistry.

Upon access to both model system fragments, the vinylogous Mukaiyama aldol addition reaction was developed. Key to this development was the use of Zn(II) Lewis acids and specifically the use of $ZnBr_2$. At cryogenic temperatures, the reaction could be conducted on gram-scales, providing synthetic access to gram-quantities of aldol product. Stereochemical analysis and transition-state analysis were described in detail. It is likely that the reaction proceeds through an open transition-state. The development of a Ni-catalyzed α-enolate arylation reaction was also explored in detail. Originally, adapting conditions from Buchwald's intermolecular α-enolate arylation of lactones employing bidentate phosphines as ligands, and later, use of olefin ligands. Specifically, the development of an Ni-catalyzed α-enolate arylation reaction to form the central 7-membered ring in auriculatol A was discovered using Ni(COD)dppp, $Ni(COD)_2$, and Ni(COD)DQ catalyst systems, ranging in yields from 77–80%. Taken together, this chapter provides a compelling demonstration of a model system for the synthesis of auriculatol A entry point for other grayanane ditepenoid natural products.

2.8 EXPERIMENTAL SECTION

Preparation of 1-bromo-4-methoxy-2-vinylbenzene (63):

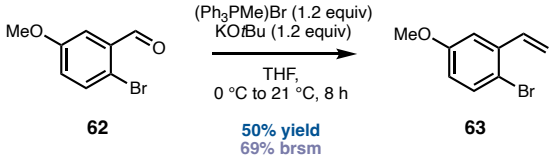

Styrene **63** was prepared according to the procedure described by Phumjan *et. al.*[52] KOtBu (6.8 g, 60.4 mmol, 1.3 equiv) was added to a stirred solution of CH_3PPh_3Br (21.6 g, 60.4 mmol, 1.3 equiv) in dry THF (10 mL/mmol) at −78°C under a N_2 atmosphere. The reaction was warmed to room temperature slowly, stirred for 30 minutes, cooled to −78 °C again, and charged with the corresponding benzaldehyde **62** (10.0 g, 46.4 mmol, 1.0 equiv) in THF. The reaction was stirred at −78 °C, warmed to room temperature, stirred for 3 hours, and quenched with H_2O. The aq. layer was extracted with EtOAc (3 x 100 mL), and the organic phase was dried over anhydrous Na_2SO_4, concentrated, and purified by column chromatography on silica (3% EtOAc/hexane) to obtain 1-bromo-4-methoxy-2-vinylbenzene (**63**) (4.9 g, 50% yield). Characterization data is consistent with that reported in the literature.[52]

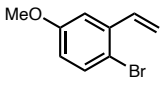

63

^{1}H NMR (500 MHz, $CDCl_3$) δ 7.43 (d, *J* = 9.8 Hz, 1H), 7.08 (d, *J* = 3.2 Hz, 1H), 7.02 (dd, *J* = 17.6, 11.3 Hz, 1H), 6.71 (dd, *J* = 8.7, 3.1 Hz, 1H), 5.69 (d, *J* = 17.3 Hz, 1H), 5.37 (dd, *J* = 10.9, 1.2 Hz, 1H), 3.82 (s, 3H).

Preparation of 2-bromo-5-methoxybenzeneethanol (64):

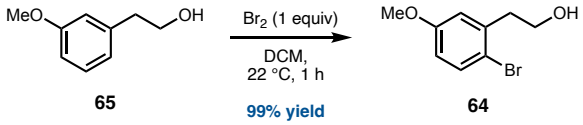

65 64

2-(3-Methoxyphenyl)ethanol (**65**) (4.92 g, 32.3 mmol, 1 equiv.) was dissolved in 323 mL of CH_2Cl_2 and cooled to 0 °C. To the solution was added dropwise bromine (1.66 mL, 32.3 mmol, 1 equiv.). After stirring for 5 h at 0 °C, an NMR aliquot was taken for analysis to ensure complete conversion. Following NMR aliquot, the reaction was quenched with 10% sodium metabisulfite (300 mL), extracted with CH_2Cl_2 (3 × 100 mL). The combined organic extracts were washed with brine (250 mL) and dried over anhydrous Na_2SO_4 and evaporated in vacuo to give the crude residue. The crude residue was columned using a gradient column 30-40% EtOAc/hexanes to provide 2-bromo-5-methoxybenzeneethanol (**64**) (7.47 g, 99%). The characterization of this compound is consistent with that reported in the literature.[5]

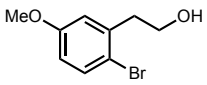

64

^{1}H NMR (500 MHz, $CDCl_3$) δ 7.23 (d, *J* = 7.9 Hz, 1H), 6.83 (d, *J* = 7.1 Hz, 1H), 6.79 (d, *J* = 6.5 Hz, 2H), 3.87 (t, *J* = 6.5 Hz, 2H), 3.81 (s, 3H), 2.86 (t, *J* = 6.5 Hz, 2H).

Preparation of aldehyde 61.

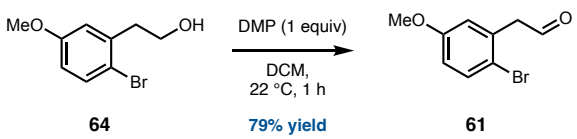

64 61

Dess-Martin periodinane (10.3g, 24.2 mmol, 1 equiv) was added to a three neck round bottom flask containing 225 mL CH_2Cl_2 under N_2 atmosphere. The resulting solution was

stirred for 3 minutes. The starting material (5.60 g, 24.2 mmol) was added to the resulting solution, and it was stirred for 1 hour. The reaction mixture was subjected to vacuum filtration over silica gel. The filtrate was collected, evaporated, and reduced under negative pressure to afford the product aldehyde as a yellowish-green oil (4.4 g, 79% yield).

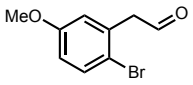

61

TLC (20% EtOAc/Hexanes): R_f 0.37 (yellow then grey with *p*-anisaldehyde, $KMnO_4$).

^{1}H NMR ($CDCl_3$, 400 MHz): δ 9.74 (t, *J* = 1.8 Hz, 1H), 7.49 (d, *J* = 8.7 Hz, 1H), 6.80 – 6.71 (m, 2H), 3.82 (d, *J* = 1.8 Hz, 2H), 3.79 (s, 3H).

^{13}C NMR (101 MHz, $CDCl_3$) δ 198.39, 159.31, 133.71, 128.47, 117.48, 115.41, 115.07, 55.65, 50.82.

FTIR (Neat, NaCl, thin film): 3428, 2938, 2905, 2936, 1723, 1595, 1475, 1314, 1242, 1162, 1054, 1025, 814 cm^{-1}.

HRMS (ESI): calc'd for $[M+H]^+$ 227.9780, found 227.9788.

Preparation of 2,2-dimethylcyclopenta-1,3-dione (71).

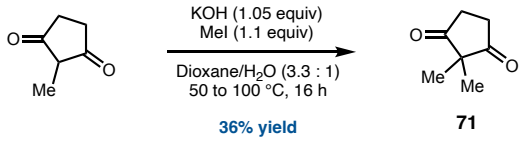

71

A 2 L round bottom flask was charged with 2-methylcyclopentane-1,3-dione (75.0 g, 669 mmol, 1.0 equiv), 731 mL of a 3:1 mixture of 1,4-dioxane/H_2O (562 mL 1,4-dioxane, 169 mL H_2O, 0.915 M), and a magnetic stir bar. The resulting suspension was stirred at room temperature for 15 min. KOH (39.4 g, 1.05 equiv) was added, stirred for 2 min, then iodomethane (104 g, 45.8 mL, 736 mmol, 1.1 equiv) was added. A small amount of water

and dioxane (<50 mL) were used to rinse the KOH that stuck to the sides of the neck of the flask down. The flask was fitted with a reflux condenser, and a Keck clamp was fitted to secure the reflux condenser. The mixture was heated from 50 °C to 100 °C and stirred for 15 h. After cooling to room temperature, the crude reaction mixture was poured into 200 mL of H_2O and then extracted with Et_2O (8 x 300 mL). The combined organic layers were washed with brine, dried with Na_2SO_4, filtered, and concentrated under reduced pressure. The residue was purified by column chromatography (30% EtOAc in hexanes) and then recrystallized from hot hexanes upon cooling to 0 °C to provide 2,2-dimethylcyclopentane-1,3-dione as a white crystalline solid (32.7 g, 36% yield).

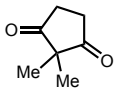

71

TLC (50% EtOAc/Hexanes): R_f 0.58 (*p*-anisaldehyde, $KMnO_4$).

^{1}H NMR ($CDCl_3$, 300 MHz): δ 2.80 (s, 4H), 1.15 (s, 6H).

^{13}C NMR (101 MHz, $CDCl_3$) δ 216.49, 52.77, 34.82, 20.38.

FTIR (CH_2Cl_2, NaCl, thin film): 2976, 1722, 1398, 1282, 1082, 792 cm^{-1}.

HRMS (ESI): calc'd for $[M+H]^+$ 126.06753, found 126.06750.

Melting Point: 42-44 °C

Preparation of (+)-3-hydroxy-2,2-dimethylcyclopentan-1-one (70) via Corey-Bakshi-Shibata Reduction (not recommended).

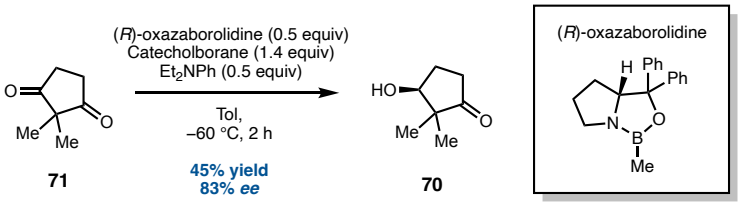

A dried 1L flask was charged 2,2-dimethylcyclopentanedione **71** (20 g, 159 mmol, 1.00 equiv) and (*R*)-oxazaborolidine 22.0 g, 79.3 mmol, 0.50 equiv) and evacuated and backfilled with nitrogen. Toluene (500 mL) was added in, followed by $PhNEt_2$ (12.6 mL, 79.3 mmol, 0.50 equiv). In order to dissolve of the (*R*)-oxazaborolidine, the reaction mixture was heated to 50 °C for 20 min. Then, the reaction mixture was cooled to –60 °C with a chloroform/dry ice bath. A solution of catecholborane (24.9 g, 208 mmol) as a 4 M solution in toluene was added with syringe pump over 2 h. The solution was prepared by taking 30 g of catecholborane (d = 1.12, so 26.8 mL = 250.2 mmol) and dissolving it in 35.7 mL of toluene. The reaction was stirred for 30 min at the same temperature and then quenched with MeOH (60 mL). The mixture was allowed to warm to room temperature and diluted with Et_2O (400 mL). Then, saturated aq. $NaHCO_3$ (200 mL) and 3 M NaOH aqueous solution (200 mL) were added to the flask. The mixture was stirred vigorously for 1 h. Vigorous stirring is very important to ensure decomposition of the leftover oxazaborolidine ligand. The mixture was loaded into a separatory funnel and the layers were separated. The aqueous phase was extracted with Et_2O (3 x 250 mL). The combined organic layers were washed with H_2O (400 mL), 0.5 M HCl aqueous solution (160 mL), and brine and dried over Na_2SO_4. Then, the solvent was removed *in vacuo*. The resulting solution was loaded onto a 2 L column, which was filled 1/3 with silica and subjected to a gradient 20 to 25% EtOAc/Hex and held at 25% until it all is eluted. Rotatory evaporation afforded **70** as a clear oil (9.10 g, 45% yield). Derivatization by benzoylation of the resultant secondary alcohol showed that the compound was formed in 83% enantiomeric excess by supercritical fluid chromatography (S3C1 05MIN10, see below).

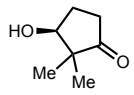

70

TLC (15% EtOAc/Hexanes): R_f 0.10 (*p*-anisaldehyde, $KMnO_4$).

^{1}H NMR ($CDCl_3$, 400 MHz): δ 4.07 – 4.02 (m, 1H), 2.51 – 2.41 (m, 1H), 2.31 – 2.19 (m, 2H), 1.96 – 1.86 (m, 1H), 1.03 (s, 6H).

^{13}C NMR (101 MHz, $CDCl_3$) δ 221.23, 78.35, 50.18, 34.27, 27.84, 22.29, 16.93.

FTIR (Neat, NaCl, thin film): 3444, 2967, 1467, 1459, 1406, 1382, 1288, 1105, 1079, 1062, 990, 968, 888 cm^{-1}.

HRMS (ESI): calc'd for $[M+H]^+$ 128.08318, found 128.08294.

$[\alpha]_D^{23}$: +9.3 (c 1.0 in $CHCl_3$)

Preparation of (+)-3-hydroxy-2,2-dimethylcyclopentan-1-one (70) via Noyori Transfer Hydrogenation (recommended).

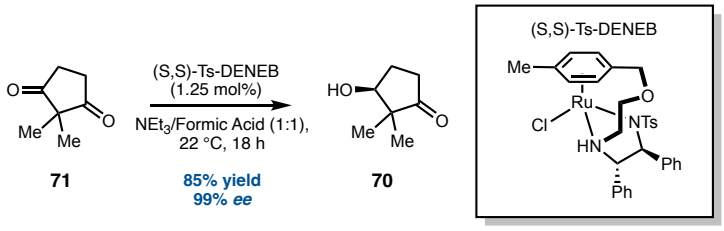

To a flame-dried 250 mL flask was added freshly distilled triethylamine (29.3 mL). Distilled formic acid (30 mL) acid was slowly added dropwise at 0 °C. In a nitrogen filled glovebox, a second flame-dried 250 mL round bottom flask was charged with 2,2-dimethyl-1,3-cyclopentadione **71** (15.0 g, 119 mmol, 1.0 equiv.) and (S,S)-Ts-DENEB (966 mg, 1.49 mmol, 1.25 mol%). A Teflon coated stir bar was then added in, and the flask was sealed with a rubber septum. The flask was removed from the glovebox. The viscous

solution of formic acid and triethylamine was transferred to the reaction flask via cannulation for a final concentration of 2 M. The reaction was stirred for a total of 18 h then quenched by addition of water (200 mL) and extracted with EtOAc (3 x 250 mL). The combined organic phases were washed with saturated aqueous sodium bicarbonate (200 mL) and brine (200 mL). The organic layers were dried over Na_2SO_4, filtered and then concentrated under reduced pressure. The crude material was purified via flash column chromatography (SiO_2, 40% to 50% EtOAc/Hexanes gradient) to afford **70** as a colorless oil (13.0 g, 85% yield). Spectral data were in agreement with literature values.[53] Enantioselectivity was measured in the subsequent step following benzoyl protection as 99% *ee*. A racemic standard of (±)-**70** was prepared using previously reported methods.[54]

Experimental note: Formic acid (40 mL) was freshly distilled over boric anhydride (20 g) prior to use.

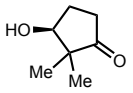

70

TLC (15% EtOAc/Hexanes): R_f 0.10 (*p*-anisaldehyde, $KMnO_4$).

^{1}H NMR ($CDCl_3$, 400 MHz): δ 4.07 – 4.02 (m, 1H), 2.51 – 2.41 (m, 1H), 2.31 – 2.19 (m, 2H), 1.96 – 1.86 (m, 1H), 1.03 (s, 6H).

^{13}C NMR (101 MHz, $CDCl_3$) δ 221.23, 78.35, 50.18, 34.27, 27.84, 22.29, 16.93.

FTIR (Neat, NaCl, thin film): 3444, 2967, 1467, 1459, 1406, 1382, 1288, 1105, 1079, 1062, 990, 968, 888 cm^{-1}.

HRMS (ESI): calc'd $C_7H_{11}O_2$ for $[M+H]^+$ 128.08318, found 128.08294.

$[\alpha]_D^{23}$: +9.3 (c 1.0 in $CHCl_3$)

Preparation of (*S*)-2,2-dimethyl-3-oxocyclopentyl benzoate (81).

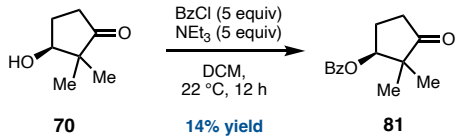

70 **14% yield** **81**

To (+)-3-hydroxy-2,2-dimethylcyclopentan-1-one (**70**) (5 mg, 39 umol) in dichloromethane (150 uL, 260 mM) was added triethylamine (27 uL, 195 umol, 5 equiv) at 0 °C. Then, benzoyl chloride (23 uL, 195 umol, 5 equiv) was added, and the reaction was warmed to room temperature over 2 hours. After stirring for 10 more hours, sodium bicarbonate (300 uL) was added, and the reaction was extracted with Et_2O (3 x 150 uL). The crude mixture was purified by preparatory TLC (20% EtOAc in Hex) to provide **81** (14% yield). The enantiomeric excess was determined to be 99% by chiral SFC (IC3, 2.5 mL/min, 5% IPA in CO_2, λ = 245 nm): t_R (major) = 2.76 min, t_R (minor) = 3.02 min.

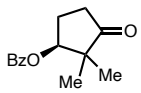

81

TLC (20% EtOAc/Hexanes): R_f 0.44 (UV, *p*-anisaldehyde).

^{1}H NMR ($CDCl_3$, 400 MHz): δ 8.01 (dd, J = 8.4, 1.4 Hz, 2H), 7.61 – 7.55 (m, 1H), 7.45 (t, J = 7.6 Hz, 2H), 5.41 – 5.34 (m, 1H), 2.56 – 2.36 (m, 3H), 2.16 – 2.05 (m, 1H), 1.14 (d, J = 3.8 Hz, 6H).

^{13}C NMR (101 MHz, $CDCl_3$) δ 219.82, 165.95, 133.39, 129.73, 128.64, 80.48, 49.55, 34.30, 25.63, 22.78, 17.90.

FTIR (Neat, NaCl, thin film): 2947, 2921, 1744, 1720, 1272, 1110 cm^{-1}.

HRMS (ESI): calc'd for $C_{14}H_{19}O_2$ $[M+H]^+$ 233.1172, found 233.1170.

SFC Method: S3C1 05MIN10

$[\alpha]_D^{23}$: +10.1 (c 1.0 in $CHCl_3$)

SFC data for racemate 81:

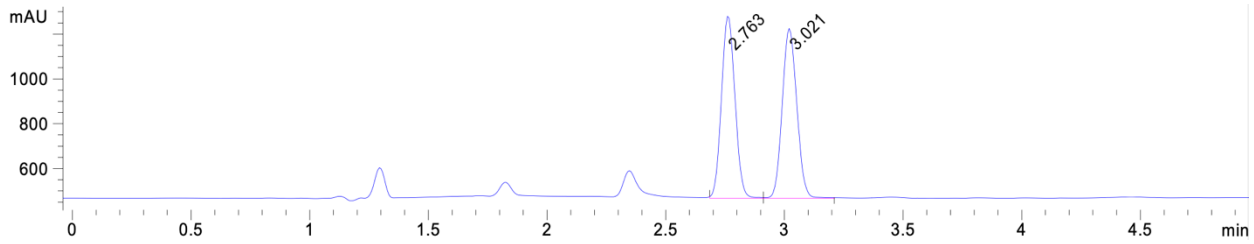

Peak #	RetTime [min]	Type	Width [min]	Area [mAU*s]	Height [mAU]	Area %
1	2.763	BV	0.0628	3229.34106	805.49390	49.9434
2	3.021	VB	0.0703	3236.65771	750.57135	50.0566

SFC data for enantioenriched 81:

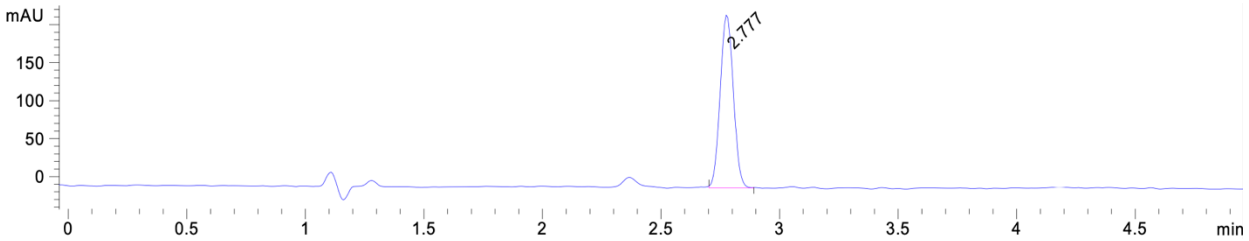

Peak #	RetTime [min]	Type	Width [min]	Area [mAU*s]	Height [mAU]	Area %
1	2.777	BB	0.0615	877.90887	225.10263	100.0000

Preparation of (+)-3-((*tert*-butyldimethylsilyl)oxy)-2,2-dimethylcyclopentan-1-one (69).

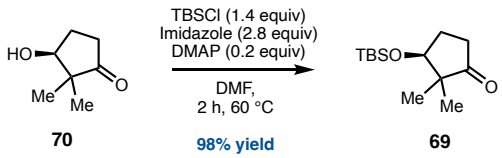

A 250 mL round bottom flask was charged with (+)-3-hydroxy-2,2-dimethylcyclopentan-1-one **70** (9.1 g, 71.0 mmol, 1.0 equiv), DMF (47.3 mL, 1.5 M), and a magnetic stir bar. To this solution, Imidazole (13.5 g, 199 mmol, 2.8 equiv), DMAP (1.73

g, 14.2 mmol, 0.2 equiv), and TBSCl (15.0 g, 99.4 mmol, 1.4 equiv) were sequentially added. The flask was fitted with a reflux condenser and stirred at 60 °C for 2 h. After cooling to room temperature, the crude reaction mixture was charged with ammonium chloride (200 mL). The mixture was extracted with a 1:1 solution of Et_2O in hexanes (200 mL x 3), then hexanes (100 mL x 2). The organic layers were washed with brine (200 mL), dried with Na_2SO_4, filtered, and concentrated under reduced pressure. The residue was purified via flash column chromatography (SiO_2, 0 to 5% EtOAc/Hexanes gradient) to afford **69** (16.9 g, 98% yield).

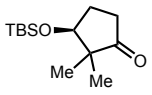

69

TLC (15% EtOAc/Hexanes): R_f 0.52 (*p*-anisaldehyde, $KMnO_4$).

^{1}H NMR ($CDCl_3$, 400 MHz): δ 3.95 (t, *J* = 5.2 Hz, 1H), 2.48 – 2.39 (m, 1H), 2.24 – 2.07 (m, 2H), 1.87 – 1.79 (m, 1H), 0.99 (s, 3H), 0.97 (s, 3H), 0.89 (s, 9H), 0.08 (s, 3H), 0.06 (s, 3H).

^{13}C NMR ($CDCl_3$, 101 MHz): δ 221.65, 78.75, 50.52, 34.38, 28.53, 25.86, 22.24, 18.18, 17.65, -4.41, -4.81.

FTIR (Neat, NaCl, thin film): 2958, 2930, 2958, 2887, 2857, 1744, 1470, 1383, 1254, 1085, 878, 776 cm^{-1}.

HRMS (ESI): calc'd for $C_{13}H_{27}O_2Si$ $[M+H]^+$ 242.16966, found 242.16954.

$[\alpha]_D^{23}$: + 28.0 (c 1.0 in $CHCl_3$)

Preparation of (+)-3-((*tert*-butyldimethylsilyl)oxy)-2,2-dimethylcyclopenten-1-one (76).

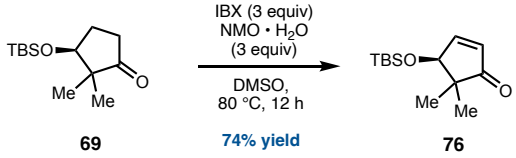

69 **76**

TBS Ketone **69** (16.9 g, 69.7 mmol) was dissolved in DMSO (700 mL, 0.1 M). IBX (see preparation of IBX procedure below, 58.6 g, 209 mmol, 3.0 equiv) was added, followed by NMO • H_2O (24.5, 209 mmol, 3.0 equiv). The reaction apparatus was heated to 80 °C. After 12 hours, the reaction was cooled to 0 °C and ½ sat. aq. $NaHCO_3$ (500 mL) was added, at first dropwise (be careful, as a large amount of bubbling was observed). 300 mL of EtOAc was added, then the reaction mixture was loaded into a 2 L separatory funnel, and the organic phase was separated out. The resulting aqueous layer was extracted with EtOAc (300 mL x 4). The combined organic layers were washed with sat. aq. NaHCO3 (500 mL), then washed with brine (500 mL), dried over anhydrous Na_2SO4, filtered, and concentrated under reduced pressure by rotary evaporation. Column chromatography with 10% EtOAc in hexanes afforded (+)-3-((*tert*-butyldimethylsilyl)oxy)-2,2-dimethylcyclopenten-1-one **76** (12.4 g, 74%) as a pale-yellow oil along with 5% starting material, which was carried forward to the next step.

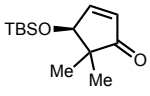

76

TLC (15% EtOAc/Hexanes): R_f 0.53 (*p*-anisaldehyde, $KMnO_4$, UV).

^{1}H NMR ($CDCl_3$, 400 MHz): δ 7.30 (dd, *J* = 5.6, 2.3 Hz, 1H), 6.13 (d, *J* = 6.6 Hz, 1H), 4.50 (s, 1H), 2.35 (s, 1H), 1.12 (s, 3H), 1.00 (s, 3H), 0.92 (s, 9H), 0.13 (d, *J* = 4.8 Hz, 6H).

^{13}C NMR ($CDCl_3$, 101 MHz): δ 212.02, 161.66, 131.92, 80.12, 49.00, 25.90, 22.65, 21.16, 18.31, -4.51, -4.61.

FTIR (Neat, NaCl, thin film): 2956, 2858, 1716, 1464, 1255, 1113, 877, 777 cm^{-1}.

HRMS (ESI): calc'd for $[M+H]^+$ 241.1619, found 241.1621.

Preparation of IBX:

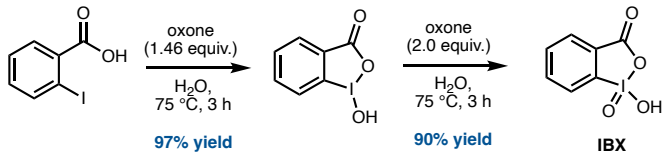

Procedure was adapted from Frigerio and coworkers.[45]

A two-liter three-necked round bottom flask equipped with a mechanical stirrer was charged with deionized water (975 mL), oxone (271 g, 442 mmol, 1.46 equiv.), and 2-iodobenzoic acid (75 g, 302 mmol, 1.0 equiv.). The reaction was heated to 75 °C over 30 min and vigorously stirred for 3 h. The reaction was cooled to 0 °C and stirred for 1 h 30 min under mild agitation. The crude reaction mixture was filtered and the solid was washed with ice-cold water (6 x 150 mL) and acetone (2 x 150 mL) to afford 63.2 g of di-oxidized product (97%) and then put directly into the next step. NMR ($DMSO-d_6$) revealed that the di-oxidized product was formed. The di-oxidized product (63.2 g, 239 mmol, 1 equiv.) was added into a 2L and setup to a mechanical stirrer. To the RBF was added deionized water (772 mL, 310 mM), and oxone (147 g, 479 mmol, 2 equiv.). The reaction was heated to 75 °C over 30 min and vigorously stirred for 3 h. The reaction was cooled to 0 °C and stirred for 1 h 30 min under mild agitation. The crude reaction mixture was filtrated and the solid was washed with ice-cold water (6 x 150 mL) and acetone (2 x 150 mL) to afford 60.0 g (90% yield) of IBX. Full characterization data is consistent with that in the literature.[45]

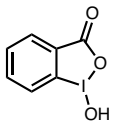

dioxidized product

^{1}H NMR (500 MHz, DMSO) δ 8.03 (s, 1H), 8.00 (dd, *J* = 7.5, 1.5 Hz, 1H), 7.95 (ddd, *J* = 8.5, 7.2, 1.5 Hz, 1H), 7.83 (dd, *J* = 8.1, 1.0 Hz, 1H), 7.69 (td, *J* = 7.3, 1.0 Hz, 1H).

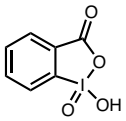

IBX

^{1}H NMR (500 MHz, DMSO) δ 8.13 (d, *J* = 7.9 Hz, 1H), 8.05 – 7.96 (m, 2H), 7.83 (t, *J* = 7.3 Hz, 1H).

Preparation of silyl enol ether 73.

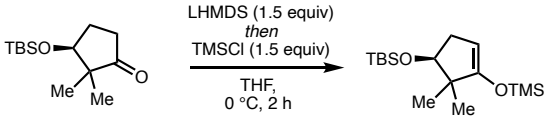

69 **73**

To a stirred solution of LHMDS (1 M in THF, 12.4 mL, 12.4 mmol) in THF (33 mL) was added dropwise **69** (2 g, 8.25 mmol) in THF (8 mL) at −78 ºC under N_2, and the reaction mixture was stirred for 1 h at –78 ºC. To the mixture was added dropwise TMSCl (1.6 mL, 12.6 mmol) at 0 ºC, and the mixture was stirred for 1 h at the same temperature. The reaction mixture was quenched with cooled sat. $NaHCO_3$ aqueous solution and extracted with hexanes (3 x 50 mL). The combined organic layers were washed with brine, dried over $MgSO_4$, and concentrated in vacuo. Column chromatography in pure hexanes yielded **73** (118 mg, 91% yield) of a clear oil.

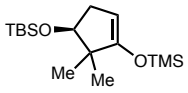

73

TLC: (100% Hexanes): R_f 0.38 (*p*-anisaldehyde).

^{1}H NMR (CDCl$_3$, 400 MHz): δ 4.33 (dd, J = 3.0, 1.9 Hz, 1H), 3.88 (t, J = 7.2 Hz, 1H), 2.32 (ddd, J = 14.2, 7.4, 3.0 Hz, 1H), 2.04 (ddd, J = 14.2, 7.1, 1.9 Hz, 1H), 0.94 (s, 3H), 0.89 (d, J = 3.6 Hz, 12H), 0.19 (s, 9H), 0.04 (d, J = 3.2 Hz, 6H).

^{13}C NMR (CDCl$_3$, 101 MHz: δ 159.52, 95.64, 79.30, 46.13, 35.49, 25.99, 24.24, 18.61, 18.25, 0.22, -4.29, -4.73.

FTIR (Neat, NaCl, thin film): 2957, 2857, 1637, 1253, 1104, 893, 841 cm^{-1}.

HRMS (ESI): N/A, does not ionize (Silyl enol ether hydrolyzes on HRMS column).

Preparation of ketoester 72.

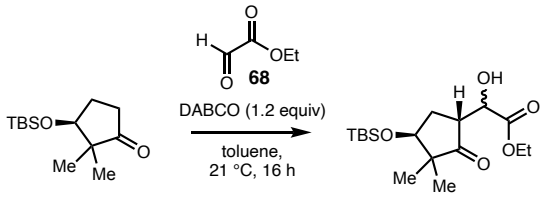

69 **72**

Cyclopentanone (**69**) (10.3 g, 42.5 mmol) was added to a flame dried single neck round bottom flask (100 mL) followed by anhydrous toluene (21.2 mL, 0.2 mM) at room temperature. To this mixture DABCO (572 mg, 5.1 mmol, 1.2 equiv) was added slowly over 10 minutes at room temperature, followed by ethyl glyoxylate (**68**, 50% solution in toluene, 842 uL, 1 equiv) dropwise. Then, the reaction was stirred for 24 h at room temperature and neutralized with aqueous 2N HCl. The aqueous phase was extracted with EtOAc (3 x 20 mL), and the combined organic layers were dried over anhydrous Na_2SO_4,

filtered, and concentrated under reduced pressure. The resulting crude product was purified by silica gel column chromatography (SiO_2, 15% EtOAc/hexane) to afford ethyl 2-hydroxy-2-(2-oxocyclopentyl)acetate (**72**) (2.0 g, 24% , a mixture of two diastereomers) as a colorless liquid.

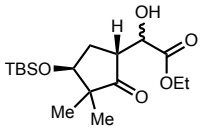

72

^{1}H NMR (300 MHz, $CDCl_3$) δ 4.72 (s, 1H), 4.37 – 4.11 (m, 6H), 4.00 – 3.93 (m, 2H), 3.28 – 3.03 (m, 2H), 2.97 – 2.69 (m, 1H), 2.37 – 2.13 (m, 1H), 2.11 – 1.64 (m, 3H), 1.37 – 1.23 (m, 9H), 1.05 (d, J = 2.9 Hz, 3H), 0.96 – 0.94 (m, 6H), 0.88 (d, J = 1.2 Hz, 9H), 0.07 (d, J = 4.0 Hz, 6H).

FTIR (Neat, NaCl, thin film): 3221, 2927, 1615, 1006 cm^{-1}.

HRMS (ESI): calc'd for $[M+H]^+$ 345.2092, found 345.2091.

Preparation of alkene 67.

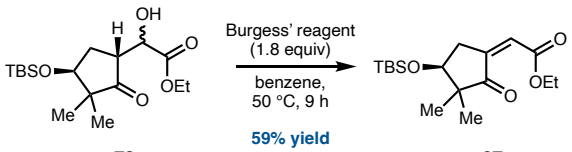

72 **67**

The diastereomeric mixture of ketoesters **72** (13.2 g, 22.1 mmol, 1.0 equiv.) was dissolved in benzene (220 mL, 0.10 M) in a flask equipped with a reflux condenser. Burgess reagent (9.48 g, 39.8 mmol, 1.8 equiv.) was added to the obtained solution. The mixture was heated to 50 °C. After 9 hours, the solution was allowed to cool to room temperature and NH_4Cl (sat. aq. 150 mL) was added. The layers were separated, and the aqueous layer was extracted with benzene (2 × 100 mL). The organic layers were combined, dried over

$MgSO_4$ and concentrated. The crude product was purified by flash column chromatography (SiO_2, 10% EtOAc/hexanes) to afford 59% yield (4.3 g) of **67** as a single diastereomer.

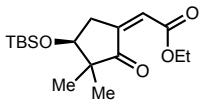

67

^{1}H NMR (300 MHz, $CDCl_3$) δ 6.60 (t, *J* = 2.9 Hz, 1H), 4.24 (s, 2H), 4.04 – 3.94 (m, 1H), 3.29 (ddd, *J* = 19.3, 6.0, 2.9 Hz, 1H), 2.93 (ddd, *J* = 19.4, 5.2, 3.0 Hz, 1H), 1.30 (s, 3H), 1.05 (s, 6H), 0.87 (s, 9H), 0.08 (d, *J* = 4.5 Hz, 6H).

FTIR (Neat, NaCl, thin film): 2934, 1667, 1215, 1210, 1157, 953, 931, 815 cm^{-1}.

HRMS (ESI): calc'd for $[M+H]^+$ 327.1986, found 327.1999.

Preparation of ketoester 74.

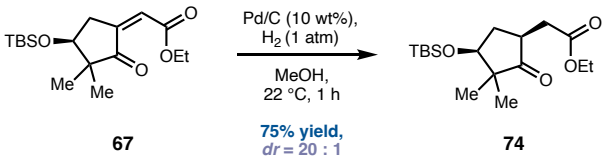

67 **74**

The enone (236 mg, 723 umol) was dissolved in MeOH (29 mL) to make a total concentration of 0.025 M, and Pd/C was added in (7.69 mg, 10 wt%). The flask was purged and backfilled 3x with N_2 and then 3x with H_2. The resulting was stirred for 1 h, and the reaction was done by TLC analysis. The reaction was worked up by filtration through celite, and the activated Pd/C that was collected on celite was disposed of in segregated waste and kept over water. The product was purified with 10% EtOAc/hexanes to afford 125 mg of product, corresponding to a 53% yield. NOESY determined it to be the cis diastereomer (> 20 : 1).

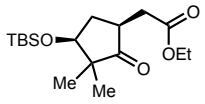

74

^{1}H NMR (400 MHz, $CDCl_3$) δ 4.15 (q, *J* = 7.1 Hz, 2H), 4.00 – 3.90 (m, 1H), 2.82 (dd, *J* = 16.4, 4.2 Hz, 1H), 2.36 (dd, *J* = 16.4, 9.4 Hz, 2H), 1.26 (t, *J* = 7.1 Hz, 3H), 1.05 (s, 3H), 0.94 (s, 3H), 0.89 (s, 9H), 0.07 (d, *J* = 4.1 Hz, 6H).

^{13}C NMR (101 MHz, $CDCl_3$) δ 172.35, 60.81, 50.21, 42.82, 35.46, 35.13, 25.87, 22.75, 18.16, 17.89, 14.36, -4.30, -4.79.

FTIR (Neat, NaCl, thin film): 2930, 2848, 1616, 1314, 1278, 1109, 896, 756 cm^{-1}.

HRMS (ESI): calc'd for $[M+H]^+$ 329.2143, found 329.2151.

Preparation of allylic alcohol 77.

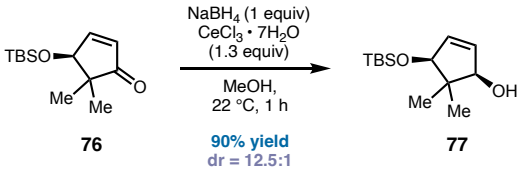

76 **90% yield** **dr = 12.5:1** **77**

(+)-3-((*tert*-butyldimethylsilyl)oxy)-2,2-dimethylcyclopenten-1-one (**76**) (12.4 g, 51.6 mmol) was dissolved in 507 mL of methanol (0.1 M) and $CeCl_3 \bullet H_2O$ (25.2 g, 67.6 mmol, 1.3 equiv) was added in. The reaction was stirred vigorously until all the $CeCl_3$ was dissolved (20 minutes). It was cooled to 0 °C with an ice bath. Then, at 0 °C, sodium borohydride (1.95 g, 51.6 mmol, 1 equiv) was added in *very* slowly (CAUTION: a lot of bubbling was observed). The solution was warmed to room temperature and stirred for 1 h and then quenched with saturated aqueous NH_4Cl (300 mL). Again, be careful when quenching sodium borohydride, as some bubbling was observed. Add aq. NH_4Cl slowly. The organic phase was partitioned with the aqueous phase in a separatory funnel, and the

resultant mixture was extracted with $CHCl_3$ (3 x 300mL). The combined extracts were dried over Na_2SO_4, filtered, and concentrated. Flash chromatography (20% EtOAc in hexanes) provided (+)-3-((*tert*-butyldimethylsilyl)oxy)-2,2-dimethyl-cyclopenten-1-ol (**77**) as a white solid (11.3 g, 90% yield) as a 10 : 1 mixture of cis : trans products. The diastereoselectivity is dependent on the addition rate of the $NaBH_4$, where slow addition maintaining an internal temperature of 0 °C delivers the product in >10:1 *dr*.

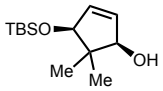

77

TLC (20% EtOAc/Hexanes): R_f 0.5 (*p*-anisaldehyde, $KMnO_4$).

^{1}H NMR ($CDCl_3$, 400 MHz): δ 5.95 (ddd, *J* = 5.9, 2.1, 0.9 Hz, 1H), 5.86 (ddd, *J* = 5.9, 2.1, 1.1 Hz, 1H), 4.08 (s, 1H), 4.00 (s, 1H), 1.01 (s, 3H), 0.96 (s, 3H), 0.89 (s, 9H), 0.07 (d, *J* = 3.7 Hz, 6H).

^{13}C NMR ($CDCl_3$, 101 MHz): δ 136.46, 135.30, 83.09, 82.78, 47.22, 26.33, 25.98, 18.27, 17.04, -4.35, -4.70.

FTIR (Neat, NaCl, thin film): 3375, 2930, 2858, 1464, 1361, 1254, 1076, 887, 775 cm^{-1}.

HRMS (ESI): calc'd for $[M+H]^+$ 243.1775, found 243.1178.

Preparation of Ueno-Stork bromoacetal 78.

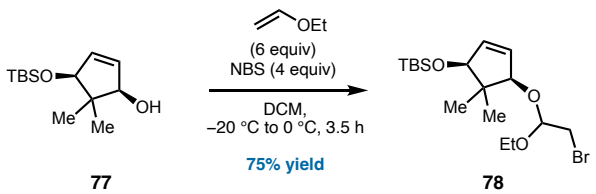

77 **78**

A 50 mL round bottom flask was charged with (±)-3-((tert-butyldimethylsilyl)oxy)-2,2-dimethyl-cyclopenten-1-ol **77** (1.0 g, 4.12 mmol, 1.0 equiv.) and CH_2Cl_2 (33.3 mL). The

resulting solution was cooled to —20 °C and *N*-bromosuccinamide (2.94 g, 16.5 mmol, 4.0 equiv.) was added directly followed by dropwise addition of ethyl vinyl ether (2.37 mL, 24.7 mmol, 6.0 equiv.). The reaction was stirred for 30 min at −20 °C and 3 h at 0 °C. The reaction mixture was cooled to −20 °C and *N*-bromosuccinamide (1.47 g, 8.25 mmol, 2.0 equiv.) was added directly followed by dropwise addition of ethyl vinyl ether (1.16 mL, 12.4 mmol, 3.0 equiv.). The reaction was stirred for 30 min at —20 °C and 3 h at 0 °C. The reaction was quenched by the addition of sat. aq. $Na_2S_2O_3$ (40 mL) at 0 °C and warmed to 21 °C. The phases were separated and the aq. phase was extracted with CH_2Cl_2 (3x 70 mL). The combined organic layers were washed with brine, dried over anhydrous sodium sulfate, and then concentrated in vacuo. The crude product was flushed through a flash chromatography column with phosphate buffered silica (pH = 7) (5-10% EtOAc in hexanes) to afford a yellow oil **78**, which was carried forward to the next step without any further purification.

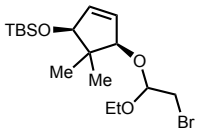

78

TLC (10% EtOAc/Hexanes): R_f 0.66 (p-anisaldehyde stains green).

^{1}H NMR ($CDCl_3$, 400 MHz): δ = 5.95 – 5.47 (m, 1H), 4.85 – 4.55 (m, 1H), 4.10 (dq, J = 3.3, 1.7 Hz, 1H), 4.05 (dq, J = 8.3, 1.7 Hz, 1H), 3.69 – 3.51 (m, 1H), 3.41 – 3.28 (m, 1H), 1.17 (td, J = 7.0, 3.0 Hz, 2H), 1.08 (d, J = 6.2 Hz, 2H), 0.84 (s, 4H), -0.00 (s, 2H).

^{13}C NMR (101 MHz, $CDCl_3$) δ 136.03, 135.92, 132.10, 131.33, 102.55, 101.12, 88.11, 86.70, 82.43, 82.40, 61.93, 61.28, 50.16, 49.68, 32.29, 32.05, 25.76, 18.32, 16.71, 16.68, 15.36, 15.33, -4.39, -4.67.

FTIR (Neat, NaCl, thin film): 2954, 2928, 2855, 1463, 1363, 1250, 1118, 1052, 893, 859, 838, 813, 777 cm^{-1}.

Preparation of ethyl acetal 79.

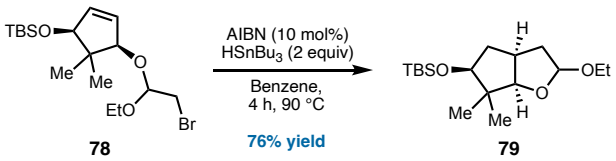

A flame-dried 100 mL three necked round-bottom flask was charged with the yellow oil **78** (1.43 g, 3.63 mmol, 1.0 equiv.) and benzene (32.9 mL). The reaction solution was degassed using N_2 for at least 15 min. To the degassed solution was added n-Bu_3SnH (2.11 g, 7.24 mmol, 2.0 equiv.) and 2,2'-azobisisobutyronitrile (3.64 mL 0.2 M in toluene, 119 mg, 724 µmol, 0.2 equiv.) and a reflux condenser was attached under a N_2 stream. The reaction mixture was heated to 90 °C and stirred for 10 h. After cooling to room temperature, the crude reaction mixture was concentrated in vacuo and directly purified with flash column chromatography (0 → 5% EtOAc in hexanes). The residue was resubjected under the identical condition to give cyclized product **79** as a colorless oil (546 mg, 1.74 mmol, 48% yield over two steps).

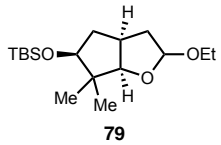

TLC (10% EtOAc/Hexanes): Rf 0.53 and 0.48 (p-anisaldehyde stains green).

^{1}H NMR (CDCl3, 400 MHz): δ = 5.45 – 4.98 (m, 1H), 4.06 (d, J = 8.0 Hz, 1H), 3.70 (dt, J = 9.7, 7.1 Hz, 1H), 3.66 (q, J = 5.5 Hz, 1H), 2.87 – 2.69 (m, 1H), 2.12 – 2.06 (m, 3H),

1.85 (ddd, J = 12.6, 7.7, 4.9 Hz, 1H), 1.42 (dt, J = 13.4, 4.6 Hz, 1H), 1.18 (t, J = 7.1 Hz, 4H), 0.95 (s, 4H), 0.90 (s, 4H), 0.88 (s, 10H), 0.02 (d, J = 2.1 Hz, 7H).

^{13}C NMR (101 MHz, $CDCl_3$) δ 106.53, 92.70, 81.25, 63.59, 44.94, 38.74, 38.31, 37.23, 28.06, 25.96, 17.64, 15.24, -4.28, -4.82.

FTIR (Neat, NaCl, thin film): 2991, 2857, 1744, 1721, 1464, 1382, 1360, 1255, 1125, 877, 836, 775 cm^{-1}.

HRMS (FD): m/z: calc. for $C_{17}H_{34}O_3Si$ $[M]^{\cdot+}$ 314.22772, found 314.22956.

Preparation of lactone 75 (recommended).

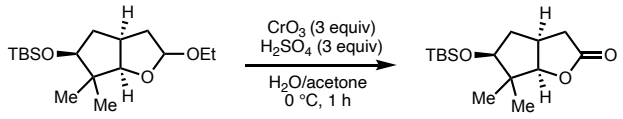

79 **75**

CrO_3 (5.48 g, 54.8 mmol, 3 equiv) was added into a 250 mL RBF equipped with a magnetic stir bar and water (69 mL) was added. H_2SO_4 (1.0 mL) was then added dropwise and with caution. In a separate 1L round bottom flask, the starting material (5.75 g, 18.3 mmol) was dissolved in acetone (183 mL) and cooled to 0 °C using an ice bath. To the starting material was then added the Jones reagent via syringe transfer dropwise, and the reaction was stirred under N_2 atmosphere for 15 min at 0 °C. After completion, as determined by TLC, the reaction was quenched with *i*PrOH and neutralized with saturated $NaHCO_3$ by dropwise addition at 0 °C. CAUTION: Add the $NaHCO_3$ slowly, as evolution of gas and bubbling was observed for 5 minutes. The mixture was extracted with Et_2O (250 mL x 3), washed with brine, and the organic layers were dried over Na_2SO_4 and concentrated in vacuo. The resulting product was purified by flash chromatography with 15 to 20% EtOAc/Hex,

isolating **75** as a white solid (1.65 g, 6.2 mmol, 30%). Segregate chromium waste, which is contained in the aq. layers, and tag appropriately.

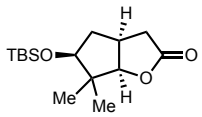

75

TLC (20% EtOAc/Hexanes): R_f 0.27 (blue with *p*-anisaldehyde, $KMnO_4$).

^{1}H NMR ($CDCl_3$, 400 MHz): δ 4.42 (dd, *J* = 7.4, 1.0 Hz, 1H), 3.73 (dt, *J* = 4.3, 1.3 Hz, 1H), 3.03 (ddddd, *J* = 11.3, 9.4, 7.4, 3.4, 2.0 Hz, 1H), 2.90 – 2.74 (m, 1H), 2.49 – 2.37 (m, 1H), 2.28 (ddd, *J* = 13.9, 9.5, 4.3 Hz, 1H), 1.59 (dt, *J* = 14.1, 1.8 Hz, 1H), 1.13 (s, 3H), 0.88 (s, 9H), 0.87 (s, 3H), 0.04 (d, *J* = 1.5 Hz, 6H).

^{13}C NMR ($CDCl_3$, 101 MHz): δ 177.67, 92.07, 81.58, 47.58, 41.42, 37.91, 35.74, 25.84, 25.11, 18.91, 18.18, -4.63, -4.99.

FTIR (Neat, NaCl, thin film): 2949, 2927, 2856, 1768, 1471, 1359, 1254, 1179, 1086, 1038, 833, 770 cm^{-1}.

HRMS (ESI): calc'd for $[M+H]^+$ 285.18805, found 285.18673.

Preparation of lactone 75 (not recommended).

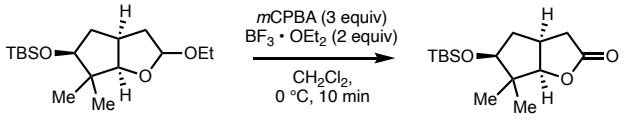

79 **75**

To a solution of ethyl ketal starting material (5.5 g, 17.6 mmol) and *m*CPBA (13.0 g, 52.8 mmol, 3 equiv) in CH_2Cl_2 at 0 °C was added BF_3 • Et_2O (4.35 mL, 35.2 mmol, 2 equiv). The solution was stirred for 15 min, then quenched with saturated aqueous thiosulfate. The aqueous layer was extracted with Et_2O (3 x 250 mL). The combined organic layer was

washed with sodium bicarbonate five times and brine, dried over $MgSO_4$, and concentrated. The residue was purified with flash column chromatography (10 to 15% EtOAc in hexanes) to afford the lactone product **75** (1.3 g, 5.6 mmol, 27% yield) as a white solid.

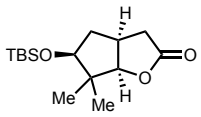

75

TLC (20% EtOAc/Hexanes): R_f 0.27 (blue with *p*-anisaldehyde, $KMnO_4$).

^{1}H NMR ($CDCl_3$, 400 MHz): δ 4.42 (dd, *J* = 7.4, 1.0 Hz, 1H), 3.73 (dt, *J* = 4.3, 1.3 Hz, 1H), 3.03 (ddddd, *J* = 11.3, 9.4, 7.4, 3.4, 2.0 Hz, 1H), 2.90 – 2.74 (m, 1H), 2.49 – 2.37 (m, 1H), 2.28 (ddd, *J* = 13.9, 9.5, 4.3 Hz, 1H), 1.59 (dt, *J* = 14.1, 1.8 Hz, 1H), 1.13 (s, 3H), 0.88 (s, 9H), 0.87 (s, 3H), 0.04 (d, *J* = 1.5 Hz, 6H).

^{13}C NMR ($CDCl_3$, 101 MHz): δ 177.67, 92.07, 81.58, 47.58, 41.42, 37.91, 35.74, 25.84, 25.11, 18.91, 18.18, -4.63, -4.99.

FTIR (Neat, NaCl, thin film): 2949, 2927, 2856, 1768, 1471, 1359, 1254, 1179, 1086, 1038, 833, 770 cm^{-1}.

HRMS (ESI): calc'd for $[M+H]^+$ 285.18805, found 285.18673.

Preparation of α-selenate 80.

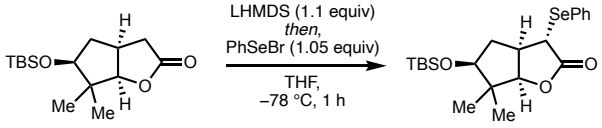

75 **80**

An oven dried 250 mL round-bottom flask was charged with LHMDS in THF (12.1 mL, titrated to be 0.83 M, 10.1 mmol) and cooled to −78 °C using a dry ice-acetone bath. Lactone starting material (2.60 g, 9.14 mmol, 1 equiv) was added dropwise as a 0.5 M

solution in THF to the solution of base at −78 °C and stirred for 25 min. Then, to a separate oven dried 200 mL flask, PhSeBr (2.26 g, 9.60 mmol, 1.05 equiv) was weighed out, and added as a 0.5 M solution to the stirring solution of enolate. The reaction was stirred at −78 °C for 25 more min. Ammonium chloride (50 mL) was then added, and the solution was warmed to room temperature. The flasks contents were then transferred to a 1L separatory funnel, extracted 3x with ether (3 x 100 mL), and washed with brine. The organic layer was dried with sodium sulfate, filtered, and concentrated down. The crude oil was purified via flash chromatography 0% EtOAc/Hex for one column volume, 2.5% EtOAc/Hex for two column volumes (gets off the orange impurity), then 5% EtOAc/Hex until the product is fully eluted to afford the α-selenylated product as a yellow oil (2.9 g, 6.7 mmol, 72% yield).

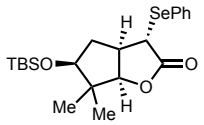

80

TLC (20% EtOAc/Hexanes): R_f 0.52 (blue with *p*-anisaldehyde, $KMnO_4$, UV).

^{1}H NMR ($CDCl_3$, 400 MHz): δ 7.69 – 7.64 (m, 2H), 7.40 – 7.29 (m, 3H), 3.88 (dd, *J* = 7.1, 1.0 Hz, 1H), 3.75 (d, *J* = 2.9 Hz, 1H), 3.67 (dt, *J* = 4.2, 1.2 Hz, 1H), 3.08 (ddt, *J* = 9.8, 7.2, 2.4 Hz, 1H), 2.30 (ddd, *J* = 14.3, 9.9, 4.2 Hz, 1H), 1.66 (dt, *J* = 14.3, 1.6 Hz, 1H), 1.06 (s, 3H), 0.85 (s, 9H), 0.75 (s, 3H), 0.01 (d, *J* = 2.6 Hz, 6H).

^{13}C NMR ($CDCl_3$, 101 MHz): δ 176.49, 136.03, 129.47, 129.17, 127.10, 90.49, 81.21, 47.51, 45.72, 45.45, 41.50, 25.83, 24.76, 18.90, 18.16, -4.67, -5.02.

FTIR (Neat, NaCl, thin film): 2954, 2929, 2856, 1765, 1472, 1256, 1169, 1089, 1058, 1003, 835, 775, 740 cm^{-1}.

HRMS (ESI): calc'd for $[M+H]^+$ 440.12804, found 440.12879.

Preparation of butenolide 60.

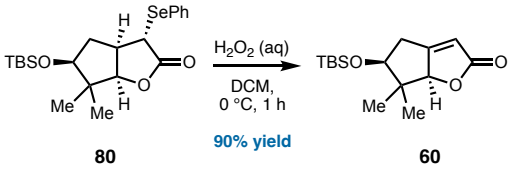

80 **60**

The α-selenylated lactone (2.98 g, 6.78 mmol, 1 equiv) was dissolved in DCM (93 mL) and charged with a large magnetic stir bar. H_2O_2 (6.93 mL, 30% solution in H_2O, 10 equiv) via direct injection was then added and the reaction was stirred vigorously (1000 rpm) for 3 h with a large stir bar. The reaction was monitored by TLC, as it may take longer. At the baseline there are some spots that appear by TLC, but they are not in enough quantity to observe in the NMR. I think the bright pink one at the baseline is selenoxide from the Greico-elimination. It was worked up by addition of sodium bicarbonate (100 mL), extraction with DCM (3 x 100 mL), washing with brine, drying with Na_2SO_4, and concentration *in vacuo*. Column chromatography of the crude mixture, loading the column by dissolving and rinsing with a minimal amount of toluene, was achieved with a gradient column: 12% EtOAc/Hex to get off the starting material (usually a very small amount <5%) then 15% EtOAc/Hex to isolate the product as a white solid (1.6 g, 90% yield).

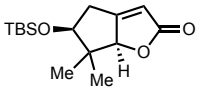

60

TLC (20% EtOAc/Hexanes): R_f 0.27 (grey with *p*-anisaldehyde, UV, $KMnO_4$).

^{1}H NMR ($CDCl_3$, 400 MHz): δ 5.75 (q, J = 2.1 Hz, 1H), 4.67 – 4.65 (m, 1H), 4.14 (dd, J = 9.1, 7.4 Hz, 1H), 2.96 (ddd, J = 18.7, 9.5, 2.2 Hz, 1H), 2.31 (ddt, J = 18.7, 7.3, 1.7 Hz, 1H), 1.23 (s, 3H), 0.90 (s, 9H), 0.61 (s, 3H), 0.07 (d, J = 4.9 Hz, 6H).

^{13}C NMR ($CDCl_3$, 101 MHz): δ 175.42, 173.32, 113.11, 90.78, 79.05, 45.02, 32.89, 25.88, 24.61, 18.10, 11.65, -4.46, -4.92.

FTIR (Neat, NaCl, thin film): 2954, 1774, 1130, 880 cm^{-1}.

HRMS (ESI): calc'd for $[M+H]^+$ 283.1723, found 283.1736.

$[\alpha]_D^{23}$: +190.9 (c 1.0 in $CHCl_3$)

Melting Point: 72-74 °C

Preparation of γ-keto ester 82.

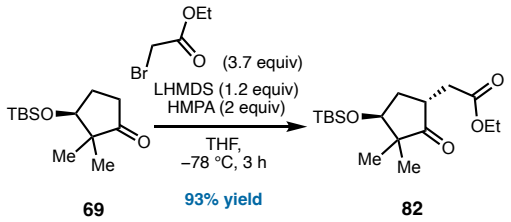

A 100 mL, oven dried flask with a magnetic stir bar was flame dried under vacuum. Then, it was cooled to 22 °C and 80 mL of THF was added. The solution was cooled to −78 °C and LHMDS solution (1M) was added in (1.2 equiv). It was stirred for 1 min before the starting material as a 1M solution was added in dropwise to maintain temp. below −75 °C, followed by HMPA (2 equiv, neat, also added in dropwise to maintain temp. below −75 °C). The mixture was stirred for 45 minutes at −78 °C before it was charged with freshly distilled ethyl bromoacetate (distilled over CaH_2) at that temperature dropwise. The solution was stirred for 10 minutes at −78 °C then removed from the bath to warm it up to room temperature. It was stirred 2 h at room temperature. Then, ammonium chloride (100

mL) was added in, followed by extracting with ethyl acetate three times (3 x 100 mL). Then, Na_2SO_4 was added in, and the mixture was filtered, concentrated, and NMR'd. The crude mixture was columned 0-10% EtOAc/Hex gradient to afford mixed fractions containing ethyl bromoacetate which could be purified via heating on full high vacuum at 75 °C for 8 hours to afford 6.3 g as a pure pale yellow oil, corresponding to a 93% yield.

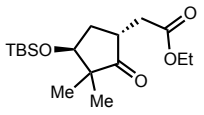

82

TLC: (10% EtOAc/Hexanes): R_f 0.34 (*p*-anisaldehyde).

^{1}H NMR ($CDCl_3$, 400 MHz): δ 4.22 – 4.06 (m, 2H), 4.00 (dd, J = 4.4, 2.5 Hz, 1H), 2.95 – 2.83 (m, 1H), 2.74 (dd, J = 16.5, 4.4 Hz, 1H), 2.41 (dd, J = 16.5, 8.4 Hz, 1H), 2.15 (ddd, J = 13.2, 8.9, 2.6 Hz, 1H), 1.93 (ddd, J = 13.2, 10.6, 4.4 Hz, 1H), 1.25 (t, J = 7.1 Hz, 3H), 1.04 (s, 3H), 0.98 (s, 3H), 0.88 (s, 9H), 0.07 (d, J = 10.1 Hz, 6H).

^{13}C NMR (CDCl3, 101 MHz): δ 221.61, 172.12, 77.09 60.75, 51.02, 41.85, 35.38, 34.90, 25.88, 23.13, 18.90, 18.21, 14.35, -4.54, -4.84.

FTIR (Neat, NaCl, thin film): 2930, 2857, 1753, 1464, 1361, 1178, 1039, 937, 775 cm^{-1}.

HRMS (ESI): calc'd for $C_{17}H_{33}O_4Si$ $[M+H]^+$ 329.2143, found 329.2154.

$[\alpha]_D^{23}$: +23.2 (c 1.0 in $CHCl_3$)

Preparation of γ-keto acid 85.

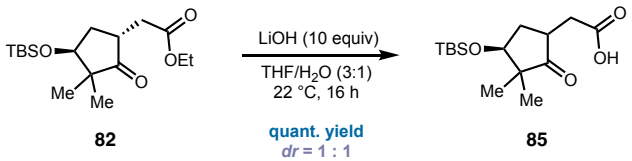

82 **85**

A 250 mL round bottom flask was charged with **82** (5.10 g, 15.5 mmol), THF (57 mL),

water (57 mL), and a magnetic stir bar. To the flask was cooled to 0 °C, then solid LiOH (3.71 g, 10 equiv) was added slowly at 0 °C. The stirring solution was warmed to room temperature and stirred for 7 hours. The reaction was quenched with 1M HCl dropwise until a pH of 3 was reached. The solution was extracted with ethyl acetate (3 x 30 mL), then dried with sodium sulfate, filtered and concentrated under vacuum. The acid was telescoped into the next step without any further purification, and a yield over two steps was reported.

Experimental note: It is important to not acidify the crude solition past a pH of 3 to prevent TBS deprotection.

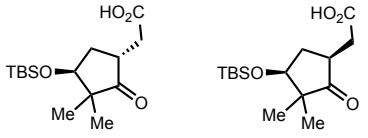

85

TLC: (40% EtOAc/Hexanes): R_f 0.10 (*p*-anisaldehyde).

^{1}H NMR ($CDCl_3$, 400 MHz): δ 4.00 (dd, J = 4.4, 2.4 Hz, 1H), 3.95 (dd, J = 7.7, 5.7 Hz, 1H), 3.00 – 2.82 (m, 2H), 2.78 (dd, J = 16.9, 4.8 Hz, 1H), 2.68 – 2.58 (m, 1H), 2.50 – 2.39 (m, 2H), 2.17 (ddd, J = 13.2, 8.9, 2.5 Hz, 1H), 1.94 (ddd, J = 13.2, 10.8, 4.4 Hz, 1H), 1.63 (ddd, J = 12.8, 9.7, 7.7 Hz, 2H), 1.05 (d, J = 2.8 Hz, 6H), 0.98 (s, 3H), 0.94 (s, 3H), 0.89 (d, J = 4.8 Hz, 18H), 0.17 – 0.01 (m, 12H).

^{13}C NMR (101 MHz, $CDCl_3$) δ 221.96, 220.69, 176.70, 176.50, 51.09, 50.31, 42.43, 41.59, 35.38, 35.16, 34.50, 30.11, 25.87, 23.20, 22.74, 18.21, 18.15, 17.91, -4.29, -4.55, -4.80, -4.85.

FTIR (Neat, NaCl, thin film): 3200, 2955, 2857, 1740, 1715, 1253, 1113, 1077, 834, 776 cm^{-1}.

HRMS (ESI): calc'd for $C_{15}H_{29}O_4Si$ $[M+H]^+$ 301.1830, found 301.1830.

$[\alpha]_D^{23}$: +17.7 (c 1.0 in $CHCl_3$)

Preparation of chlorolactone 87.

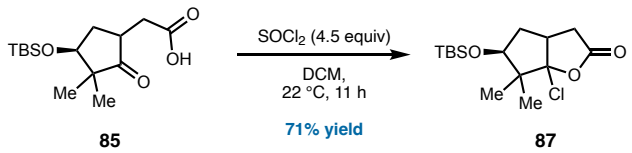

85 **87**

An oven dried 500 mL round bottom flask was charged with carboxylic acid **85** (4.66 g, 15.5 mmol), DCM (155 mL,100 mM), and a magnetic stir bar. Thionyl chloride (5.09 mL, 4.5 equiv, 69.8 mmol) was added to the reaction flask and stirred at room temperature for 11 hours. The thionyl chloride and DCM were removed via vacuum distillation, heating from 40 °C to 80 °C. The resulting crude oil was purified via flash column chromatography (SiO_2, 1% to 7% EtOAc/Hexanes). The volatiles were concentrated under reduced pressure to afford an inconsequential mixture of diastereomers **87** (1:1) obtained as a pale yellow amorphous and sticky solid (3.5 g, 71% yield over 2 steps). Analytically pure samples of both diastereomers were obtained and representative spectrum of the mixture as used in the next step is also provided.

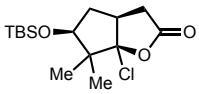

87A

TLC: (10% EtOAc/Hexanes): R_f 0.42 (*p*-anisaldehyde, brown).

^{1}H NMR ($CDCl_3$, 400 MHz): δ 2.60 (dddd, J = 14.2, 10.3, 4.9, 1.0 Hz, 1H), 2.43 (dd, J = 17.6, 1.1 Hz, 1H), 1.50 – 1.42 (m, 1H), 1.19 (s, 3H), 1.06 (s, 3H), 0.86 (s, 9H), 0.03 (d, J = 8.0 Hz, 6H).

^{13}C NMR (CDCl3, 101 MHz): δ 174.42, 115.66, 80.59, 52.71, 46.69, 40.62, 37.11, 25.73, 25.61, 18.09, 17.15, -4.72, -5.03.

FTIR (Neat, NaCl, thin film): 2950, 1806, 1471, 1251, 1158, 1042, 885, 779 cm^{-1}.

HRMS (ESI): calc'd for $C_{15}H_{27}O_3Si$ $[M-Cl]^+$ 283.1724, found 283.1726.

$[\alpha]_D^{22}$: +43.5 (c 1.0 in $CHCl_3$)

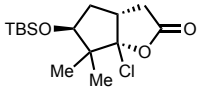

87B

TLC: (10% EtOAc/Hexanes): R_f 0.40 (*p*-anisaldehyde, brown).

^{1}H NMR (CDCl$_3$, 400 MHz): δ 3.87 (dd, *J* = 9.0, 8.3 Hz, 1H), 3.17 – 2.97 (m, 2H), 2.39 (d, *J* = 17.4 Hz, 1H), 2.16 – 1.97 (m, 1H), 1.65 (ddd, *J* = 13.9, 8.2, 3.1 Hz, 1H), 1.13 (s, 3H), 1.01 (s, 3H), 0.88 (s, 9H), 0.02 (d, *J* = 10.8 Hz, 6H).

^{13}C NMR (CDCl3, 101 MHz): δ 174.98, 114.05, 76.22, 50.84, 44.15, 38.21, 35.68, 25.83, 18.98, 18.39, 18.06, -4.38, -4.82.

FTIR (Neat, NaCl, thin film): 2856, 1806, 1471, 1206, 1128, 1025, 859 cm^{-1}.

HRMS (ESI): calc'd for $C_{15}H_{27}O_3Si$ $[M-Cl]^+$ 283.1724, found 283.1726.

$[\alpha]_D^{23}$: +22.2 (c 1.0 in $CHCl_3$).

Preparation of butenolide 60.

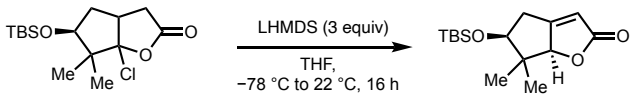

87 **60**

A flame-dried 200 mL RBF equipped with a magnetic stir bar and placed under N_2. The flask was charged with LHMDS (22.6 mL, 22.6 mmol, 3 equiv, 1 M in THF), followed

by THF (7 mL), and cooled to –78 °C. The chloro-lactone **87** was added dropwise as a solution in THF (2.4 g, 7.53 mmol, 1 equiv, 7 mL). The reaction was stirred at –78 °C for 4 hours then warmed to room temperature and stirred for 12 h. The reaction was quenched by addition of sat. aq. sodium bicarbonate (50 mL), the layers separated and the aqueous later extracted with Et_2O (3 x 50 mL). The combined organic layers were dried with Na_2SO_4, filtered and concentrated under reduced pressure. The resulting crude mixture was purified via flash column chromatography (SiO_2, 0% to 10% EtOAc/Hexanes) affording the pure butenolide **60** as a white solid (1.5 g, 71% yield).

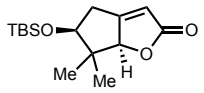

60

TLC (20% EtOAc/Hexanes): R_f 0.27 (grey with *p*-anisaldehyde, UV, $KMnO_4$).

^{1}H NMR ($CDCl_3$, 400 MHz): δ 5.75 (q, J = 2.1 Hz, 1H), 4.67 – 4.65 (m, 1H), 4.14 (dd, J = 9.1, 7.4 Hz, 1H), 2.96 (ddd, J = 18.7, 9.5, 2.2 Hz, 1H), 2.31 (ddt, J = 18.7, 7.3, 1.7 Hz, 1H), 1.23 (s, 3H), 0.90 (s, 9H), 0.61 (s, 3H), 0.07 (d, J = 4.9 Hz, 6H).

^{13}C NMR ($CDCl_3$, 101 MHz): δ 175.42, 173.32, 113.11, 90.78, 79.05, 45.02, 32.89, 25.88, 24.61, 18.10, 11.65, -4.46, -4.92.

FTIR (Neat, NaCl, thin film): 2954, 1774, 1130, 880 cm^{-1}.

HRMS (ESI): calc'd for $C_{15}H_{27}O_3Si$ $[M+H]^+$ 283.1723, found 283.1736.

$[\alpha]_D^{23}$: +195.9 (c 1.0 in $CHCl_3$)

Melting Point: 72-74 °C

Preparation of cyclopropane 83.

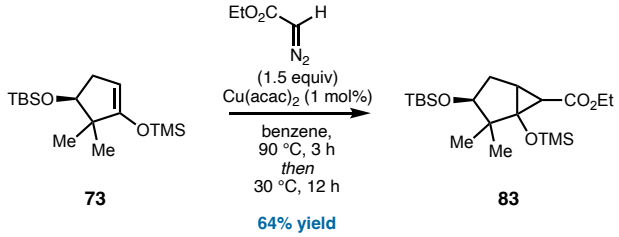

In an N_2-filled glovebox was weighed out $Cu(acac)_2$ (0.5 mg, 2.07 umol, 1 mol%), and it was dispensed into a vial containing neat starting material (65.0 mg, 207 umol, 1 equiv) and a magnetic stir bar. Then, a solution of ethyl diazoacetate in 132 uL of benzene was made, and it was added to a stirring solution of starting material and $Cu(acac)_2$ at 90 °C over 3 hours. After the addition, the reaction was stirred at 30 °C overnight. The next morning, the reaction was concentrated and filtered through a pad of silica. NMR reveals a ratio of 1.7 : 1 product to starting material. Column chromatography, eluting with 10% EA/hex provides 53.0 mg of product, corresponding to a 64% yield as a inconsequential mixture of diastereomers that could be converged to a single diastereomer in the next step.

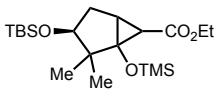

83

^{1}H NMR (500 MHz, $CDCl_3$) δ 4.18 – 4.04 (m, 4H), 3.67 – 3.62 (m, 1H), 3.25 (dd, *J* = 9.1, 7.0 Hz, 1H), 2.18 – 2.13 (m, 2H), 1.90 – 1.80 (m, 3H), 1.81 – 1.65 (m, 2H), 1.62 (d, *J* = 3.8 Hz, 1H), 1.32 – 1.26 (m, 6H), 1.06 (d, *J* = 1.4 Hz, 3H), 1.03 (s, 3H), 0.97 (s, 6H), 0.88 (d, *J* = 1.7 Hz, 18H), 0.19 – 0.15 (m, 18H).

^{13}C NMR (101 MHz, $CDCl_3$) δ 170.89, 170.54, 78.64, 76.50, 76.40, 75.70, 73.21, 60.66, 60.49, 46.08, 45.65, 33.26, 32.29, 31.80, 30.40, 28.69, 26.62, 25.98, 25.95, 25.88, 22.25, 21.60, 19.31, 18.22, 18.14, 14.54, 14.39, 1.68, 1.41, -4.32, -4.86.

FTIR (Neat, NaCl, thin film): 2920, 2861, 1697, 1478, 1373, 1152, 1052, 942, 756 cm^{-1}.

HRMS (ESI): calc'd for $[M+H]^+$ 401.2538, found 401.2543.

Preparation of γ-keto ester 82.

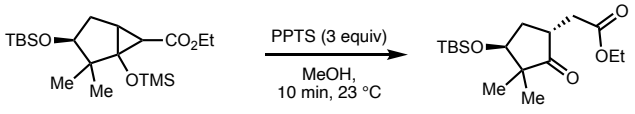

83 **82**

To a solution of starting material (25 mg, 62.4 umol) in EtOH (750 uL) was added solid PPTS (47.0 mg, 187 umol) at room temperature. The reaction was stirred 10 minutes and monitored by TLC. The reaction was worked up by addition of saturated aqueous sodium bicarbonate. Then, the mixture was extracted 3 times with ether (3 x 1 mL). The organic phases were dried with Na_2SO_4 and filtered, then concentrated. Crude NMR reveals a clean NMR spectrum of product that can be columned. Column conditions include a pipet column eluting with 0, 1, then 2% EtOAc/Hex.

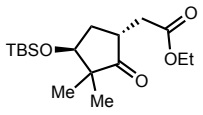

82

TLC: (10% EtOAc/Hexanes): R_f 0.34 (*p*-anisaldehyde).

^{1}H NMR ($CDCl_3$, 400 MHz): δ 4.22 – 4.06 (m, 2H), 4.00 (dd, J = 4.4, 2.5 Hz, 1H), 2.95 – 2.83 (m, 1H), 2.74 (dd, J = 16.5, 4.4 Hz, 1H), 2.41 (dd, J = 16.5, 8.4 Hz, 1H), 2.15 (ddd, J = 13.2, 8.9, 2.6 Hz, 1H), 1.93 (ddd, J = 13.2, 10.6, 4.4 Hz, 1H), 1.25 (t, J = 7.1 Hz, 3H), 1.04 (s, 3H), 0.98 (s, 3H), 0.88 (s, 9H), 0.07 (d, J = 10.1 Hz, 6H).

^{13}C NMR (CDCl3, 101 MHz): δ 221.61, 172.12, 77.09 60.75, 51.02, 41.85, 35.38, 34.90, 25.88, 23.13, 18.90, 18.21, 14.35, -4.54, -4.84.

FTIR (Neat, NaCl, thin film): 2930, 2857, 1753, 1464, 1361, 1178, 1039, 937, 775 cm^{-1}.

HRMS (ESI): calc'd for $[M+H]^+$ 329.2143, found 329.2154.

Preparation of secondary alcohol 84.

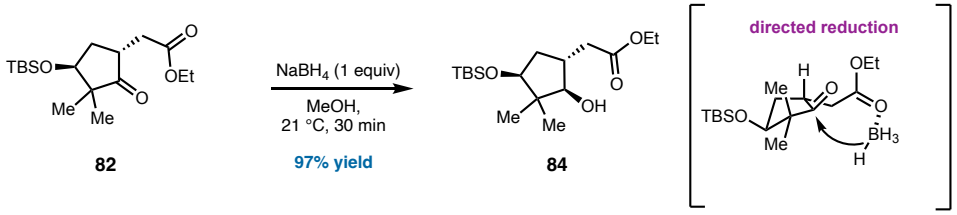

The starting material **82** (20 mg, 60.9 umol) in a 1-dram vial was diluted with squirt-bottle MeOH (500 uL, 122 mM), and it was cooled to 0 °C. $NaBH_4$ (2.30 mg, 60.9 umol, 1 equiv) was added in slowly, and the reaction was stirred for 10 minutes, upon which TLC indicated full conversion of starting material. The reaction was worked up by addition of saturated aq. NH_4Cl (500 uL), and the resulting aqueous phase was extracted with diethyl ether (3 x 500 uL). The product was purified by preparatory thin layer chromatography (prep. TLC) in 50% EA/hex to isolate 19.5 mg of product, corresponding to 97% yield.

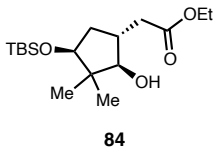

84

TLC: (20% EtOAc/Hexanes): R_f 0.34 (*p*-anisaldehyde).

^{1}H NMR ($CDCl_3$, 400 MHz): δ 4.14 (q, *J* = 7.2 Hz, 2H), 3.66 (t, *J* = 7.2 Hz, 1H), 3.34 – 3.25 (m, 1H), 2.62 (d, *J* = 6.0 Hz, 1H), 2.51 (dd, *J* = 15.9, 8.1 Hz, 1H), 2.41 (dd, *J* = 15.9, 6.8 Hz, 1H), 2.34 – 2.25 (m, 1H), 1.89 (ddd, *J* = 13.6, 11.0, 6.9 Hz, 1H), 1.55 – 1.49 (m, 1H), 1.25 (d, *J* = 7.1 Hz, 3H), 0.96 (s, 3H), 0.88 (d, *J* = 4.5 Hz, 12H), 0.02 (d, *J* = 5.1 Hz, 6H).

^{13}C NMR (CDCl3, 101 MHz): δ 173.93, 83.98, 78.01, 60.77, 46.09, 40.07, 39.87, 37.26, 25.93, 25.20, 18.15, 14.94, 14.35, -4.36, -4.83.

FTIR (Neat, NaCl, thin film): 3474, 2958, 2932, 1736, 1464, 1255, 1076, 856 cm^{-1}.

HRMS (ESI): calc'd for $[M+Na]^+$ 353.2118, found 353.2125.

Preparation of spirocycle 86.

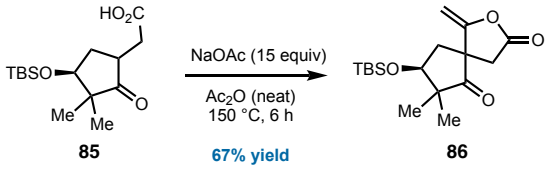

To the starting material (5 mg, 16.6 umol) in an oven-dried 1-dram vial was added in sodium acetate solid (20.5 mg, 250 umol, 15 equiv). Then, acetic anhydride (380 uL, 44 mM) was added in, and the reaction was stirred at 150 °C for 6 hours. The reaction was worked up by cooling to 0 °C and adding 0.5 mL of EtOAc. The mixture was concentrated, then filtered through a pad of cotton. Purification with preparatory TLC (15% EA/hex) allows for isolation of 3.6 mg of product **86** (67% yield). The stereochemistry of the spirocycle is not known but hypothesized to contain beta stereochemistry.

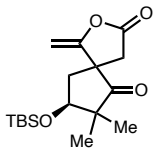

86

^{1}H NMR (400 MHz, CDCl$_3$) δ 4.86 – 4.79 (m, 1H), 4.24 – 4.18 (m, 1H), 4.11 – 4.05 (m, 1H), 2.88 (dd, *J* = 18.1, 1.5 Hz, 1H), 2.69 – 2.56 (m, 2H), 2.18 – 2.10 (m, 1H), 1.11 (dd, *J* = 13.6, 1.3 Hz, 6H), 0.93 – 0.84 (m, 9H), 0.10 (dd, *J* = 5.0, 1.3 Hz, 6H).

^{13}C NMR (101 MHz, CDCl$_3$) δ 217.89, 172.04, 159.60, 88.85, 53.66, 51.89, 42.34, 41.57,

25.88, 22.95, 18.99, 18.17, -4.45, -4.88.

FTIR (Neat, NaCl, thin film): 2951, 2852, 1713, 1479, 1360, 1134, 1026, 934, 721 cm^{-1}.

HRMS (ESI): calc'd for $[M+H]^+$ 325.1830, found 325.1823.

Preparation of TBS siloxyfuran 88.

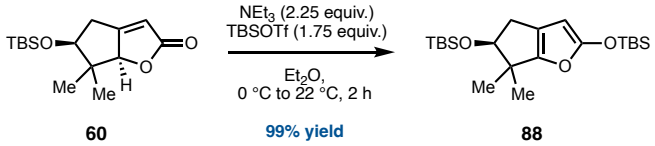

A flame-dried 50 mL RBF was charged with butenolide **60** (250 mg, 885 umol, 1.0 equiv.), a magnetic stir bar, and placed under nitrogen. To the starting material was added dry Et_2O (17.7 mL) and freshly distilled NEt_3 (278 uL, 1.99 mmol, 2.25 equiv.). It was stirred at room temperature until all butenolide starting material was dissolved. The reaction was cooled to 0 °C and TBSOTf (356 uL, 1.55 umol, 1.75 equiv.) was added dropwise. The reaction was stirred for 0 °C for 30 min then warmed to room temperature and stirred for 90 min. After stirring for 2 hours total, the reaction mixture was loaded directly on a phosphate-buffered silica plug (10 g of buffered silica) prewet with hexanes and the crude material was loaded onto the plug with Et_2O. The crude material was filtered through the silica plug with hexanes (3 x 50 mL). The eluent was reduced *in vacuo* and the residue was redissolved in MeCN (10 mL) and pentane (10 mL). The pentane layer was separated out, and the resulting ACN layer was extracted with pentane (2 x 10 mL). The combined pentane phases were reduced *in vacuo*. The residue was put on high vac for 12 h to afford **88** as a yellow oil (317 mg, 90% yield).

Experimental Note: the purity of TBSOTf is important, impurities such as TfOH will reduce the yield of this reaction. The phosphate buffered silica was prepared according to

literature procedures.[25]

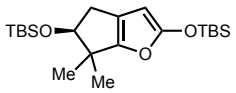

88

TLC: N/A (unstable to silica)

^{1}H NMR ($CDCl_3$, 400 MHz): ^{1}H NMR (400 MHz, $CDCl_3$) δ 4.96 (s, 1H), 4.24 (t, *J* = 6.9 Hz, 1H), 2.72 (dd, *J* = 14.1, 7.1 Hz, 1H), 2.31 (dd, *J* = 14.1, 6.7 Hz, 1H), 1.19 (s, 3H), 1.00 (s, 3H), 0.96 (s, 9H), 0.91 (s, 9H), 0.22 (s, 6H), 0.08 (s, 6H).

^{13}C NMR ($CDCl_3$, 101 MHz): δ 158.14, 151.21, 117.77, 83.58, 82.65, 42.97, 34.05, 25.96, 25.66, 25.22, 20.41, 18.27, 18.24, -4.35, -4.69, -4.71, -4.75.

FTIR (Neat, NaCl, thin film): 2956, 2930, 2859, 1585, 1471, 1361, 1255, 1101, 866, 787 cm^{-1}.

HRMS (ESI): calc'd for $C_{21}H_{41}O_3Si_2$ $[M+H]^+$ 396.25105, found 396.25179.

$[\alpha]_D^{22}$: +38.4 (c 1.0 in $CHCl_3$)

Preparation of aldol product 59.

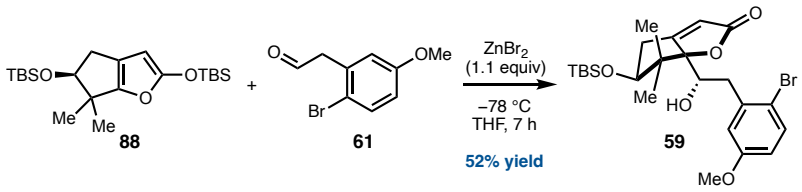

Before attempting this reaction, troubleshoot on small scale. The way **88** is purified is important. Follow the procedure for preparation of **88** above exactly.

A stirring solution of siloxyfuran starting material **88** (3.3 g, 8.29 mmol, 1 equiv) and aldehyde **61** (2.1 g, 9.29 mmol, 1.12 equiv) in THF (33 mL, 0.25 M) at −78 °C was

subjected to $ZnBr_2$ (2.1 g, 9.29 mmol, 3M solution in THF) via rapid injection. The resulting solution was stirred for 6.5 h then quenched at that temperature with NH_4Cl (50 mL) and extracted 3x with EtOAc (50 mL). The solution was dried with Na_2SO_4, filtered, and concentrated. Flash chromatography with 12% EtOAc in hexanes afforded the product **59** (2.2 g, 52% yield) as an 8:1 mixture of diastereomers and recovered butenolide **60** (702 mg, 30% yield. The product is a thick, gooey yellow-green oil that can be high vac'd into a foam and then crushed with a spatula into a nice yellow crystalline solid.

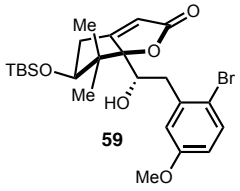

59

TLC (15% EtOAc/Hexanes): R_f 0.10 (*p*-anisaldehyde, stains brown).

^{1}H NMR ($CDCl_3$, 400 MHz): δ 7.45 (d, *J* = 8.8 Hz, 1H), 6.75 – 6.73 (m, 1H), 6.69 (dd, *J* = 8.7, 3.1 Hz, 1H), 5.91 – 5.89 (m, 1H), 4.67 (dd, *J* = 10.0, 4.8 Hz, 1H), 4.34 (dt, J = 10.8, 3.1 Hz, 1H), 3.78 (s, 3H), 3.18 – 3.08 (m, 2H), 2.58 (dd, *J* = 13.6, 10.5 Hz, 1H), 2.29 (dd, *J* = 16.6, 4.8 Hz, 1H), 1.64 (d, *J* = 3.8 Hz, 1H), 1.26 (s, 3H), 0.89 (s, 9H), 0.78 (s, 3H), 0.04 (s, 6H).

^{13}C NMR ($CDCl_3$, 101 MHz): δ 176.23, 174.36, 159.26, 137.84, 133.97, 117.61, 115.49, 115.11, 114.65, 97.10, 79.94, 71.23, 55.68, 47.41, 38.47, 35.09, 25.89, 20.59, 18.15, 16.19, 5.46, -4.47, -4.92.

FTIR (Neat, NaCl, thin film): 3449, 2954, 2929, 2892, 2856, 1746, 1651, 1595, 1572, 1471, 1444, 1416, 1389, 1290, 1252, 1193, 1164, 1132, 1091, 1049, 1006, 870, 838, 734 cm^{-1}.

HRMS (ESI): calc'd for $[M+H]^+$ 510.14316, found 510.14169.

Preparation of MOM-protected compound 90.

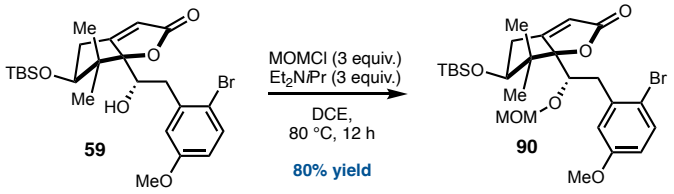

To a three-neck oven-dried 50 mL RBF was added the starting alcohol **59** (2.2 g, 4.3 mmol, 1 equiv) and 1,2-dichloroethane (21.5 mL, 0.2 M). The flask was fitted with a reflux condenser, cooled to 0 °C and charged with DIPEA (2.25 mL, 12.9 mmol, 3 equiv) and MOMCl (0.98 mL, 12.9 mmol, 3 equiv). The mixture was stirred for 12 h at 80 ºC. After cooling the reaction to room temperature, the reaction mixture was quenched with sat. $NaHCO_3$ aqueous solution and extracted with CH_2Cl_2 (3 x 25 mL). The combined organic layers were washed with brine, dried over $MgSO_4$, and concentrated in vacuo. After silica gel chromatography with 15% EtOAc in hexanes, the product **90** was isolated as a greenish-yellow, thick oil (1.9 g, 80% yield).

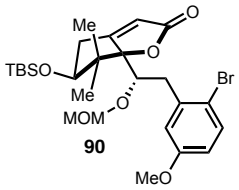

TLC (30% EtOAc/Hexanes): R_f 0.56 (*p*-anisaldehyde, stains brown).

^{1}H NMR ($CDCl_3$, 400 MHz): δ 7.39 (d, *J* = 8.8 Hz, 1H), 6.81 (d, *J* = 3.1 Hz, 1H), 6.67 (dd, *J* = 8.8, 3.1 Hz, 1H), 5.83 (dd, *J* = 2.4, 1.2 Hz, 1H), 4.51 (dd, *J* = 9.9, 5.7 Hz, 1H), 4.17 (dd, *J* = 10.4, 2.7 Hz, 1H), 4.01 (d, *J* = 6.8 Hz, 1H), 3.86 (d, *J* = 6.8 Hz, 1H), 3.77 (s, 3H), 3.23 (dd, *J* = 13.8, 2.7 Hz, 1H), 3.09 (ddd, *J* = 9.9, 9.9, 2.4 Hz, 1H), 3.08 (s, 3H), 2.97 (dd, *J* = 14.0, 10.4 Hz, 1H), 2.31 (ddd, *J* = 17.9, 5.7, 1.2 Hz, 1H), 1.36 (s, 3H), 0.90 (s, 9H), 0.78 (s, 3H), 0.07 (d, *J* = 3.9 Hz, 6H).

^{13}C NMR ($CDCl_3$, 101 MHz): δ 175.86, 174.66, 158.95, 138.72, 133.31, 118.50, 115.07, 114.73, 114.62, 97.97, 97.67, 79.50, 77.59, 56.57, 55.65, 47.20, 38.80, 33.81, 25.81, 21.88, 18.08, 16.32, -4.45, -4.99.

FTIR (Neat, NaCl, thin film): 2954, 2856, 1757, 1472, 1254, 1094, 1021, 869, 778 cm^{-1}.

HRMS (ESI): calc'd for $[M+H]^+$ 555.1699, found 555.1772.

Preparation of lactone 58.

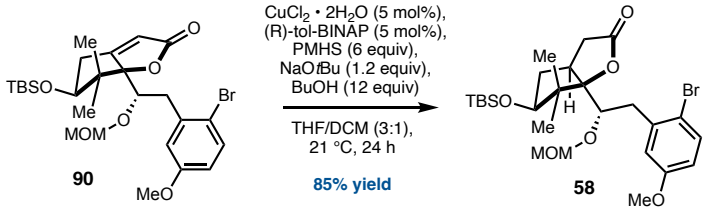

In the glovebox in a 25 mL oven-dried round bottom flask was added a magnetic stir bar and all solid reagents: $CuCl_2$ • $2H_2O$ (4.60 mg, 27.0 umol, 5 mol%), (*R*)-Tol-BINAP (18.3 mg, 27.0 umol, 5 mol%), and NaO*t*Bu (62.3 mg, 648 umol, 1.2 equiv). The round bottom flask was capped, taped, and pumped out of the glovebox. Following attachment to an N_2 inlet, 9 mL of SPS THF was added, and the reaction was stirred for 5 min. Then, PMHS (effective mass per hydride = 60 g/mol; d = 1.006, 190 uL, 6 equiv) was added dropwise, and the reaction was stirred for 5 more minutes. The starting material **58** (300 mg) as a solution in 3 mL of DCM and *t*BuOH (207 uL, 2.16 mmol, 4 equiv) was added in last, and the reaction was monitored by TLC. Upon completion as determined by TLC, the reaction was stirred for 2 hours before saturated aqueous NH_4Cl (10 mL) was added in dropwise. The ammonium chloride mixture was stirred vigorously to ensure mixing of layers for 15 minutes (bubbling was observed). Then, the solution was loaded into a 60 mL separatory funnel and extracted with EtOAc (3 x 10 mL). The combined organics were dried over

Na_2SO_4, filtered, and concentrated *in vacuo*. The resulting residue was purified by flash chromatography on silica gel eluting with 7.5% EtOAc in hexanes to give the product **58** as a white crystalline solid as a single diastereomer (256 mg, 85% yield).

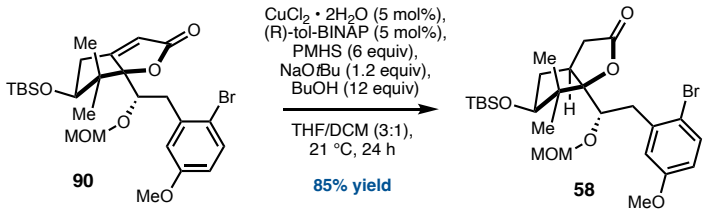

TLC (30% EtOAc/Hexanes): R_f 0.52 (*p*-anisaldehyde, stains brown)

^{1}H NMR ($CDCl_3$, 400 MHz): δ 7.37 (d, *J* = 8.8 Hz, 1H), 6.81 (d, *J* = 3.1 Hz, 1H), 6.67 (dd, *J* = 8.8, 3.1 Hz, 1H), 4.08 – 3.97 (m, 2H), 3.77 (s, 1H), 3.76 (s, 3H), 3.71 (d, *J* = 6.9 Hz, 1H), 3.21 – 2.94 (m, 2H), 2.41 – 2.28 (m, 2H), 1.57 (s, 2H), 1.50 (d, *J* = 14.2 Hz, 1H), 1.26 (s, 3H), 1.25 (s, 1H), 1.15 (s, 3H), 0.91 (s, 8H), 0.91 (d, *J* = 5.9 Hz, 1H), 0.06 (d, *J* = 4.7 Hz, 6H).

^{13}C NMR ($CDCl_3$, 101 MHz): δ 178.18, 159.04, 138.57, 133.09, 118.48, 115.14, 114.96, 100.20, 98.38, 86.10, 80.19, 56.96, 55.72, 48.96, 41.93, 40.40, 40.15, 38.71, 25.88, 23.48, 19.92, 18.25, -4.57, -4.97.

FTIR (Neat, NaCl, thin film): 2928, 2855, 1770, 1594, 1472, 1230, 1090, 1044, 835, 774 cm^{-1}.

HRMS (ESI): calc'd for $[M+H]^+$ 557.1856, found 557.1940.

Preparation of α-enolate arylation product 57.

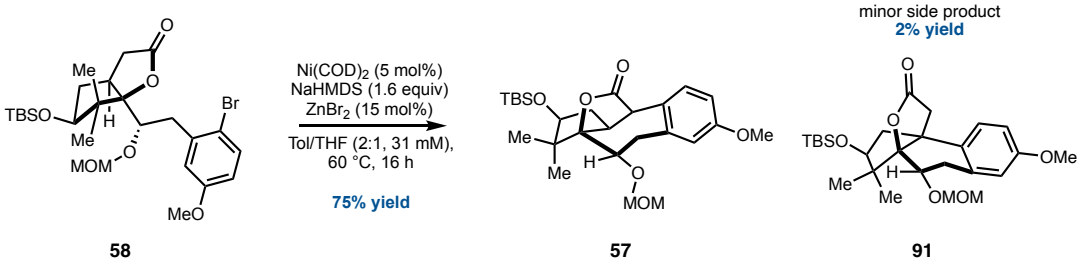

Reagents were purchased from STREM chemicals. Solvents were taken from the SPS and cannula'd into oven-dried schlenk flasks and stored over dried molecular sieves. The solvent was then degassed via freeze-pump thaw three times and pumped into the glovebox for use. NaHMDS and $ZnBr_2$ were stored in the glovebox at room temperature. $Ni(COD)_2$ was stored in the glovebox fridge at −30 °C.

In the glovebox, 15.0 mg of starting material (26.9 umol) along with a magnetic stir bar and 440 uL of toluene were added to a 2-dram vial. A stock solution of $Ni(COD)_2$ was prepared by dissolving 3.7 mg of $Ni(COD)_2$ in 1.4 mL of toluene. $ZnBr_2$ stock solution was prepared by taking 9.1 mg and dissolving it in 2.9 mL of THF. NaHMDS (7.9 mg, 43.0 umol, 1.6 equiv) was added directly to the vial of the starting material and toluene, followed by the $ZnBr_2$ stock solution (290 uL, 910 ug, 15 mol%) in THF and lastly the $Ni(COD)_2$ stock solution (140 uL, 370 ug, 5 mol%) in toluene. The reaction was then put on a stir plate for 16 hours at 60 °C. Upon completion, the reaction was removed from the hot plate and allowed to cool to room temperature. TLC in 2% ether/DCM shows basically only product in the reaction mixture. The mixture was quenched with a saturated aqueous NH_4Cl (1 mL) solution and extracted with Et_2O (3 × 1 mL). Then, 0.1 mL of technazene stock solution in ethyl acetate was added. The technazene stock solution was prepared fresh every time by weighing out 5 mg of technazene into a 1-dram vial, adding 0.5 mL of ethyl

acetate, and syringing out 0.1 mL. The combined extract was dried over Na_2SO_4, filtered, and dried under reduced pressure. Column chromatography in 0 to 5% ether/DCM affords a 10 mg mixture of desired product (75% yield) and undesired 6-membered "Heck-type" product (2% yield).

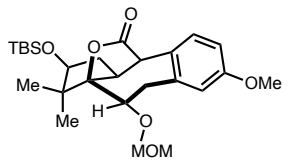

57

TLC (5% Ether/DCM): R_f 0.64 (*p*-anisaldehyde, stains blue).

^{1}H NMR ($CDCl_3$, 400 MHz): δ 7.07 (d, *J* = 8.2 Hz, 1H), 6.74 – 6.68 (m, 2H), 4.71 (d, *J* = 6.9 Hz, 1H), 4.15 (d, *J* = 6.9 Hz, 1H), 4.15 (dd, *J* = 4.6, 2.0 Hz, 1H), 3.77 (s, 3H), 3.72 (dd, *J* = 5.9, 2.8 Hz, 1H), 3.53 (s, 1H), 3.30i (s, 3H), 3.27 – 3.22 (m, 1H), 3.13 (dd, *J* = 16.4, 4.6 Hz, 1H), 2.98 (dd, *J* = 10.6, 5.5 Hz, 1H), 2.52 (ddd, *J* = 14.3, 10.6, 5.9 Hz, 1H), 1.53 (ddd, *J* = 14.4, 5.5, 2.8 Hz, 1H), 1.15 (s, 3H), 0.95 (s, 3H), 0.91 (s, 9H), 0.05 (d, *J* = 1.8 Hz, 6H).

^{13}C NMR ($CDCl_3$, 101 MHz): δ 175.81, 158.71, 137.00, 130.69, 130.57, 119.38, 111.69, 98.07, 97.44, 82.16, 56.91, 56.30, 55.36, 50.01, 43.87, 39.56, 36.72, 25.88, 23.96, 18.82, 18.14, -4.48, -4.91.

FTIR (Neat, NaCl, thin film): 3417, 2928, 2855, 1774, 1470, 1257, 1095, 1045 835 cm^{-1}.

HRMS (ESI): calc'd for $[M+H]^+$ 477.2594, found 477.2671.

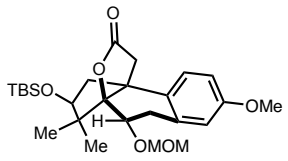

91

TLC (5% Ether/DCM): R_f 0.62 (*p*-anisaldehyde, stains blue).

^{1}H NMR (400 MHz, $CDCl_3$): δ 6.98 (d, *J* = 8.6 Hz, 1H), 6.80 (dd, *J* = 8.6, 2.7 Hz, 1H), 6.56 (d, *J* = 2.7 Hz, 1H), 4.84 (d, *J* = 6.7 Hz, 1H), 4.74 (d, *J* = 6.7 Hz, 1H), 4.13 (dd, *J* = 11.5, 6.2 Hz, 1H), 3.78 (s, 3H), 3.74 (dd, *J* = 4.6, 1.5 Hz, 1H), 3.42 (s, 3H), 3.18 – 3.08 (m, 2H), 3.02 (dd, *J* = 16.7, 6.3 Hz, 1H), 2.91 (dd, *J* = 18.1, 0.9 Hz, 1H), 2.35 (ddd, *J* = 14.1, 4.6, 1.0 Hz, 1H), 2.15 (dd, *J* = 14.0, 1.5 Hz, 1H), 1.32 (s, 3H), 1.16 (s, 3H), 0.92 (s, 9H), 0.06 (s, 6H).

^{13}C NMR (101 MHz, $CDCl_3$): δ 175.32, 157.85, 136.66, 131.85, 128.33, 114.45, 112.77, 97.60, 96.70, 83.32, 80.55, 77.23, 55.75, 55.29, 52.54, 52.25, 52.09, 49.19, 34.56, 25.80, 23.49, 21.10, 18.22, -4.77, -5.01.

FTIR (Neat, NaCl, thin film): 3423, 2932, 2856, 1774, 1412, 1313, 1011, 1045 845 cm^{-1}.

HRMS (ESI): calc'd for $[M+H]^+$ 477.2594, found 477.2695.

2.9 NOTES AND REFERENCES

(1) Casiraghi, G.; Battistini, L.; Claudio, C.; Rassu, G.; Zanardi, F. The Vinylogous Aldol and Related Addition Reactions: Ten Years of Progress. *Chem. Rev.* **2011**, *111*, 3076–3154.

(2) Adamkiewicz, A.; Weglarz, I.; Butkiewicz, A.; Woyciechowska, M.; Mlynarski, J. Lewis Acid-Catalyzed Stereoselective α-Addition of Chiral Aldehydes to Cyclic Dienol Silanes: Aqueous Synthesis of Chiral Butenolides. *Adv. Synth. Catal.* **2020**, *362*, 667–678.

(3) Wu, T.; Kang, X.; Bai, H.; Xiong, W.; Xu, G.; Tang, W. Enantioselective Construction of Spiro Quaternary Carbon Stereocenters via Pd-Catalyzed Intramolecular α-Arylation. *Org. Lett.* **2020**, *22*, 4602–4607.

(4) Kapadia, N.; Harding, W. Facile Synthesis of 4,5,6a,7-tetrahydrodibenzo[de,g]chromene Heterocycles and Their Transformation to Phenanthrene Alkaloids. *Tetrahedron*, **2013**, *69*, 8914–8920.

(5) Shishido, Y.; Wakabayashi, H.; Koike, H.; Ueno, N.; Nukui, S.; Yamagishi, T.; Murata, Y.; Naganeo, F.; Mizutani, M.; Shimada, K.; Fujiwara, Y.; Sakakibara, A.; Suga, O.; Kusano, R.; Ueda, S.; Kanai, Y.; Tsuchiya, M.; Satake, K. Discovery and Stereoselective Synthesis of the Novel Isochroman Neurokinin-1 Receptor Antagonist 'CJ-17,493'. *Bioorg. Med. Chem.* **2008**, *16*, 7193–7205.

(6) Turlik, A.; Chen, Y.; Scruse, A. C.; Newhouse, T. R. Convergent Total Synthesis of Principinol D, a Rearranged Kaurane Diterpenoid. *J. Am. Chem. Soc.* **2019**, *141*, 8088–8092.

(7) Kong, L.; Yu, H.; Deng, M.; Wu, F.; Jiang, Z.; Luo, T. Enantioselective Total Syntheses of Grayanane Diterpenoids: (–)-Grayanotoxin III, (+)–Principinol E, and (–)-

Rhodomollein XX. *J. Am. Chem. Soc.* **2022**, *144*, 5268–5273.

(8) Vashchenko, V.; Kutulya, L.; Krivoshey, A. Simple and Effective Protocol for Claisen–Schmidt Condensation of Hindered Cyclic Ketones with Aromatic Aldehydes. *Synthesis*, **2007**, *14*, 2125–2134.

(9) Mukaiyama, T.; Banno, K.; Narasaka, K. New Cross-Aldol Reactions. Reactions of Silyl Enol Ethers with Carbonyl Compounds Activated by Titanium Tetrachloride. *J. Am. Chem. Soc.* **1974**, *96*, 24, 7503–7509.

(10) Pesciaioli, F.; Righi, P.; Mazzanti, A.; Gianelli, C.; Mancinelli, M.; Bartoli, G.; Bencivenni, G. *Cinchona* Alkaloid-Catalyzed Enantioselective Direct Aldol Reaction of *N*-Boc-Oxindoles with Polymeric Ethyl Glyoxylate. *Adv. Synth. Catal.* **2011**, *353*, 2953–2959.

(11) Salom–Roig, X. J.; Dénès, F.; Renaud, P. Radical Cyclization of Haloacetals: The Ueno–Stork Reaction. *Synthesis* **2004**, *12*, 1903–1928.

(12) Stork, G.; Mook Jr., R.; Biller, S. A.; Rychnovsky, S. D. Free-Radical Cyclization of Bromo Acetals. Use in the Construction of Bicyclic Acetals and Lactones. *J. Am. Chem. Soc.* **1983**, *105*, 11, 3741–3742.

(13) Peng, Y.; Xiao, J.; Xu, X.; Duan, S.; Ren, L.; Shao, Y.; Wang, Y. Stereospecific Synthesis of Tetrahydronaphtho[2,3-*b*]furans Enabled by a Nickel-Promoted Tandem Reductive Cyclization. *Org. Lett.* **2016***, 18*, 19, 5170–5173.

(14) Kreutziger, J.; Jäger, A.; Metz, P. Asymmetric Transfer Hydrogenation of Prochiral Cyclic 1,3-Diketones. *Arkivoc* **2023**, (v), 43–53.

(15) Vyhivskyi, O.; Baudoin, O. Total Synthesis of the Diterpenes (+)-Randainin D and (+)-Barekoxide via Photoredox-Catalyzed Deoxygenative Allylation. *J. Am. Chem. Soc.*

2024, *146*, 16, 11486–11492.

(16) Li, C.; Tu, S.; Wen, S.; Li, S.; Chang, J.; Shao, F.; Lei, X. Total Synthesis of the G2/M DNA Damage Checkpoint Inhibitor Psilostachyin C. *J. Org. Chem.* **2011**, *76*, 3566–3570.

(17) Davies, L., Antoulinakis, E. G. (2001). Intermolecular Metal-Catalyzed Carbenoid Cyclopropanations. *Organic Reactions*, 1–326.

(18) Stauffer, F.; Neier, R. Synthesis of Tri- and Tetrasubstituted Furans Catalyzed by Trifluoroacetic Acid. *Org. Lett.* **2000**, *23*, 3535–3537.

(19) De Clercq, P.; Vandewalle, M. Total Synthesis of (±)-Damsin. *J. Org. Chem.* **1977**, *42*, 3447–3450.

(20) Knollmüller, M.; Gärtner, P.; Ferencic, M.; Noe, C. R.; Mereiter, K. An Improved Method for the *endo*-Fusion of Five-Membered Ring Lactones to the Bornane Ring System. *Eur. J. Org. Chem.* **1998**, 2507–2511.

(21) Huffman, B. J.; Chen, S.; Schwarz, J. L.; Plata, R. E.; Chin, E. N.; Lairson, L. L.; Houk, K. N.; Shenvi, R. A. Electronic Complementarity Permits Hindered Butenolide Heterodimerization and Discovery of Novel cGAS/STING Pathway Antagonists. *Nat. Chem.* **2020**, *12*, 310–317.

(22) Casiraghi, G.; Zanardi, F. The Vinylogous Aldol Reaction: A Valuable, Yet Understated Carbon–Carbon Bond-Forming Maneuver. *Chem. Rev.* **2000**, *100*, 1929–1972.

(23) Qin, T.; Johnson, R. P.; Porco Jr., J. A. Vinylogous Addition of Siloxyfuran to Benzopyryliums: A Concise Approach to the Tetrahydroxanthone Natural Products. *J. Am. Chem. Soc.* **2011**, *133*, 1714–1717.

(24) Jefford, C. W.; Jaggi, D.; Boukouvales, J. Diastereoselectivity in the Directed Aldol Condensation of 2-Trimethylsiloxyfurans with Aldehydes. A Stereodivergent Route to *Threo* and *Erythro* γ-Hydroxy-γ-Lactones. *Tetrahedron Lett.* **1987**, *28*, 4037–4040.

(25) Dissanayake, I.; Hart, J. D.; Becroft, E. C.; Sumby, C. J.; Newton, C. G. Bisketene Equivalents as Diels–Alder Dienes. *J. Am. Chem. Soc.* **2020**, *142*, 31, 13328–13333.

(26) Dustin, Covell. Catalytic, Enantioselective Hetero-Diels–Alder Reactions of Aldehydes. *UIUC library,* **2006**, *accessed via*: https://chemistry.illinois.edu/system/files/inline-files/05CovellChem535Abstract.pdf

(27) Danishefsky, S. J., DeNinno, M. P. Totally Synthetic Routes to the Higher Monosaccharides. *Angew. Chem. Int. Ed.* **1987**, *26*, 15–23.

(28) Parsaee, F.; Senarathna, M. C.; Kannangara, P. B.; Alexander, S. N.; Arche, P. D. E.; Welin, E. R. Radical Philicity and its Role in Selective Organic Transformations. *Nat. Chem. Rev.* **2021**, *5*, 486–499.

(29) Mengel, A.; Reiser, O. Around and Beyond Cram's Rule. *Chem. Rev.* **1999**, *99*, 1191–1223.

(30) Guillarme, S.; Plé, K.; Banchet, A.; Liard, A.; Haudrechy, A. Alkynylation of Chiral Aldehydes: Alkoxy-, Amino-, and Thio-Substituted Aldehydes. *Chem. Rev.* **2006**, *106*, 2355–2403.

(31) Stanton, G. R.; Johnson, C. N.; Walsh, P. J. Overriding Felkin Control: A General Method for Highly Diastereoselective Chelation-Controlled Additions to a-Silyloxy Aldehydes. *J. Am. Chem. Soc.* **2010**, *132*, 4399–4408.

(32) Bidar, M.; Tokmajyan, G.; Nasiri, F.; Avetisyan, A. Chemoselective Reduction of Unsaturated γ- and δ-Lactones by Sodium Borohydride in the Presence of Triethylamine

in THF, *Arkivoc* **2011**, (ix), 422–428.

(33) Yang, H.; Li, B.; Cai, X.; Qi, H.; Luo, Y.; Zhang, G. Chiral Decalins: Preparation from Oleanolic Acid and Application in the Synthesis of (−)-9-*epi*-Ambrox. *J. Nat. Prod.* **2006**, *69*, 11, 1531–1538.

(34) Rainka, M. P.; Milne, J. E.; Buchwald, S. L. Dynamic Kinetic Resolution of α,β-Unsaturated Lactones through Asymmetric Copper-Catalyzed Conjugate Reduction: Application to the Total Synthesis of Eupomatilone-3. *Angew. Chem. Int. Ed.* **2005**, *44*, 6177–6180.

(35) Deutsch, C.; Krause, N. CuH-Catalyzed Reactions. *Chem. Rev.* **2008**, *108*, 2916–2927.

(36) Spielvogel, D. J.; Buchwald, S. L. Nickel-BINAP Catalyzed Enantioselective α-Arylation of α-Substituted γ-Butyrolactones. *J. Am. Chem. Soc.* **2002**, *124*, 3500–3501.

(37) Tamaru, Y., Ed. *Modern Organonickel Chemistry*; Wiley-VCH Verlag GmbH & Co. KGaA, **2005**.

(38) Williams, B. G.; Lawton, M. Drying of Organic Solvents: Quantitative Evaluation of the Efficiency of Several Desiccants. *J. Org. Chem.* **2010**, *75*, 8351–8354.

(39) Huang, D.; Szewczyk, S. M.; Zhang, P.; Newhouse, T. R. Allyl-Nickel Catalysis Enables Carbonyl Dehydrogenation and Oxidative Cycloalkenylation of Ketones. *J. Am. Chem. Soc.* **2019**, *141*, 5669–5674.

(40) Huang, D.; Newhouse, T. R. Dehydrogenative Pd and Ni Catalysis for Total Synthesis. *Acc. Chem. Res.* **2021**, *54*, 1118–1130.

(41) Clevenger, A. L.; Stolley, R. M.; Aderibigbe, J.; Louie, J. Trends in the Usage of Bidentate Phosphines as Ligands in Nickel Catalysis. *Chem. Rev.* **2020**, *120*, 6124–6196.

(42) Hartwig, J. F. *Organotransition Metal Chemistry: From Bonding to Catalysis*. University Science Books: 2010.

(43) Nett, A. J.; Cañellas, S.; Higuchi, Y.; Robo, M. T.; Kochkodan, J. M.; Haynes II, M. T.; Kampf, J. W.; Montgomery, J. Stable, Well-Defined Nickel(0) Catalysts for Catalytic C–C and C–N Bond Formation. *ACS Catal.,* **2018**, *8*, 7, 6606–6611.

(44) Nattmann, L.; Cornella, J. Ni($^{4\text{-}t\text{Bu}}$stb)$_3$: A Robust 16-Electron Ni(0) Olefin Complex for Catalysis. *Organometallics*, **2020**, *39*, 18, 3295–3300.

(45) Shields, J. D.; Gray, E. E.; Doyle, A. G. A Modular, Air-Stable Nickel Precatalyst. *Org. Lett.* **2015**, 17, 2166−2169.

(46) Tran, V. T.; Kim, N., Rubel, C. Z.; Wu, X.; Kang, T.; Jankins, T. C.; Li, Z.; Joannou, M. V.; Ayers, A.; Gembicky, M.; Bailey, J.; Sturgell, E. J.; Sanchez, B. B.; Chen, J. S.; Lin, S.; Eastgate, M. D.; Wisniewski, S. R.; Engle, K. M. Structurally Diverse Bench-Stable Nickel(0) Pre-Catalysts: A Practical Toolkit for In Situ Ligation Protocols. *Angew. Chem. Int. Ed.* **2022**, *61*, 9, e202211794.

(47) G. N. Schrauzer, H. Thyret, Z. *Naturforsch*. *B* **1962**, *17*, 73–76.

(48) Ge, S.; Hartwig, J. F. Nickel-Catalyzed Asymmetric α-Arylation and Heteroarylation of Ketones with Chloroarenes: Effect of Halide on Selectivity, Oxidation State, and Room-Temperature Reactions. *J. Am. Chem. Soc.* **2011**, *133*, 41, 16330–16333.

(49) Huang, C.; Doyle, A. G. Electron-Deficient Olefin Ligands Enable Generation of Quaternary Carbons by Ni-Catalyzed Cross-Coupling. *J. Am. Chem. Soc.* **2015**, *137*, 5638–5641.

(50) Noda, N.; Yamaoka, S.; Ogi, U.; Horie, M.; Okano, K.; Mori, A. A Ni^0(COD)(DQ) complex as a catalyst precursor for oligothiophene and polythiophene synthesis. *Org.*

Biomol. Chem., **2024**, *22*, 2574–2579.

(51) Soda, Y.; Sugiyama, Y.; Yoritate, M.; Tajima, H.; Shibuya, K.; Ogihara, C.; Oishi, T.; Sato, T.; Chida, N. Unified Total Synthesis of Pentacyclic Stemoamide-type Alkaloids. *Org. Lett.* **2020**, *22*, 7502–7507.

(52) Phumjan, T.; Songthammawat, P.; Jongcharoenkamol, K.; Batsomboon, P.; Ruchirawat, S.; Ploypradith, P. Substituted 9-Anthraldehydes from Dibenzocycloheptanol Epoxides via Acid-Catalyzed Epoxide Opening/Semipinacol Rearrangement. *J. Org. Chem.* **2021**, *86*, 13322–13349.

(53) Shimizu, M.; Yamada, S.; Fujita, Y.; Kobayashi, F. Highly Stereocontrolled Reduction of 1,3-cyclopentadiones using Oxazaborolidine BH_3. *Tetrahedron* **2000**, 11, 3883–3886

(54) Budny, M.; Włodarczyk, J.; Muzioł, T.; Bosiak, M. J.; Wolan, A. Stereoselective Synthesis of Two Potential Metabolites of *cis*-metconazole. *Tetrahedron Letters*. **2017**, 58, 4285–4288.

Appendix 2

Supporting Information Relevant to Chapter 2:

Vinylogous Mukaiayama Aldol and α-enolate arylation model studies

Parameter	Value
Data File Name	/ Volumes/ nmrdata/ jkthomps/ vnmrsys/ data/ JKT-1-163-1/ PROTON01.fid/ fid
Title	PROTON01
Origin	Varian
Solvent	cdcl3
Temperature	3.0
Pulse Sequence	s2pul
Experiment	1D
Number of Scans	8
Receiver Gain	60
Relaxation Delay	1.0000
Pulse Width	5.6500
Acquisition Time	3.0000
Acquisition Date	2021-07-22T12:10:51
Spectrometer Frequency	499.59
Spectral Width	8000.0
Nucleus	1H
Acquired Size	24000
Spectral Size	65536

63

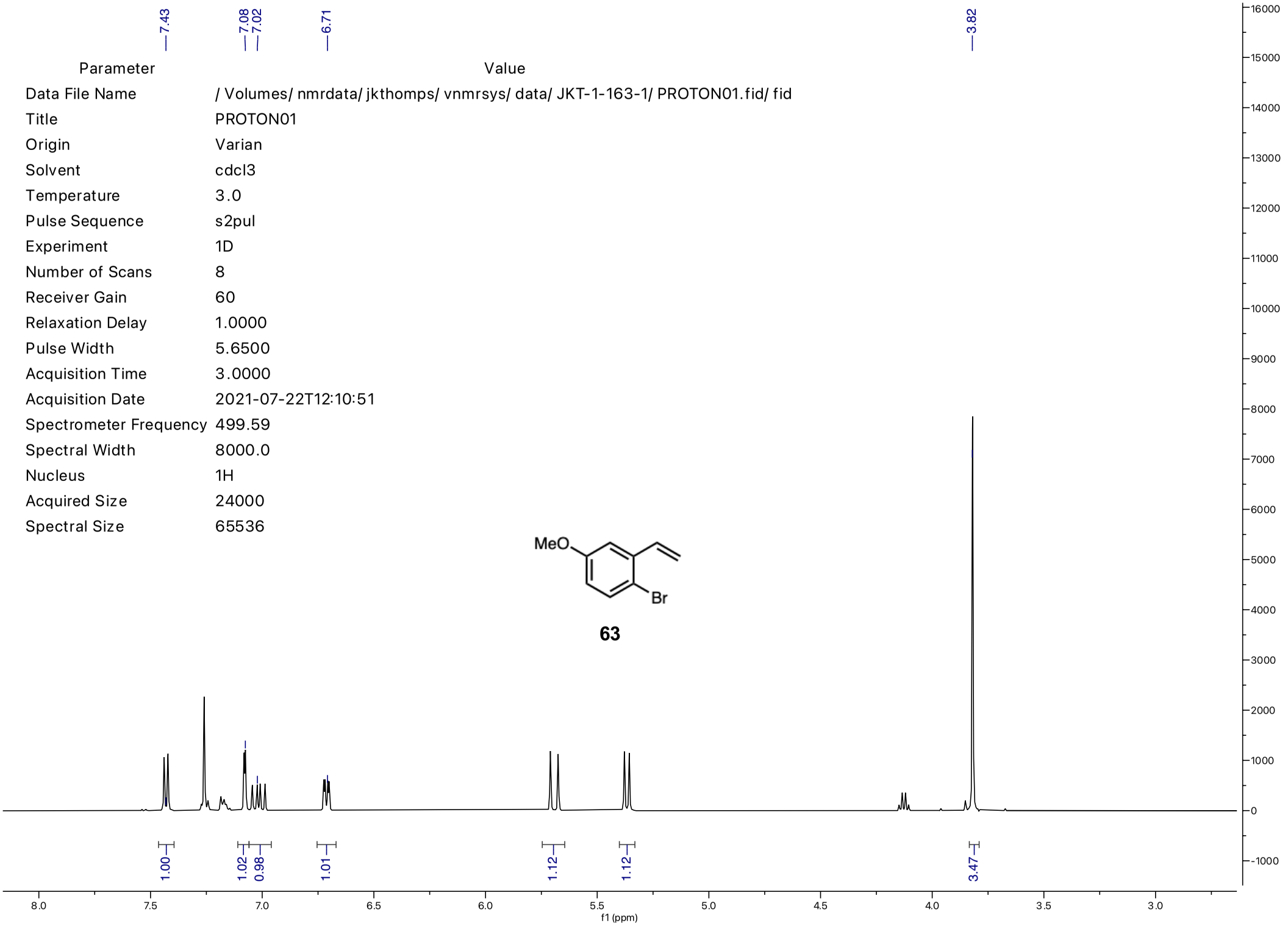

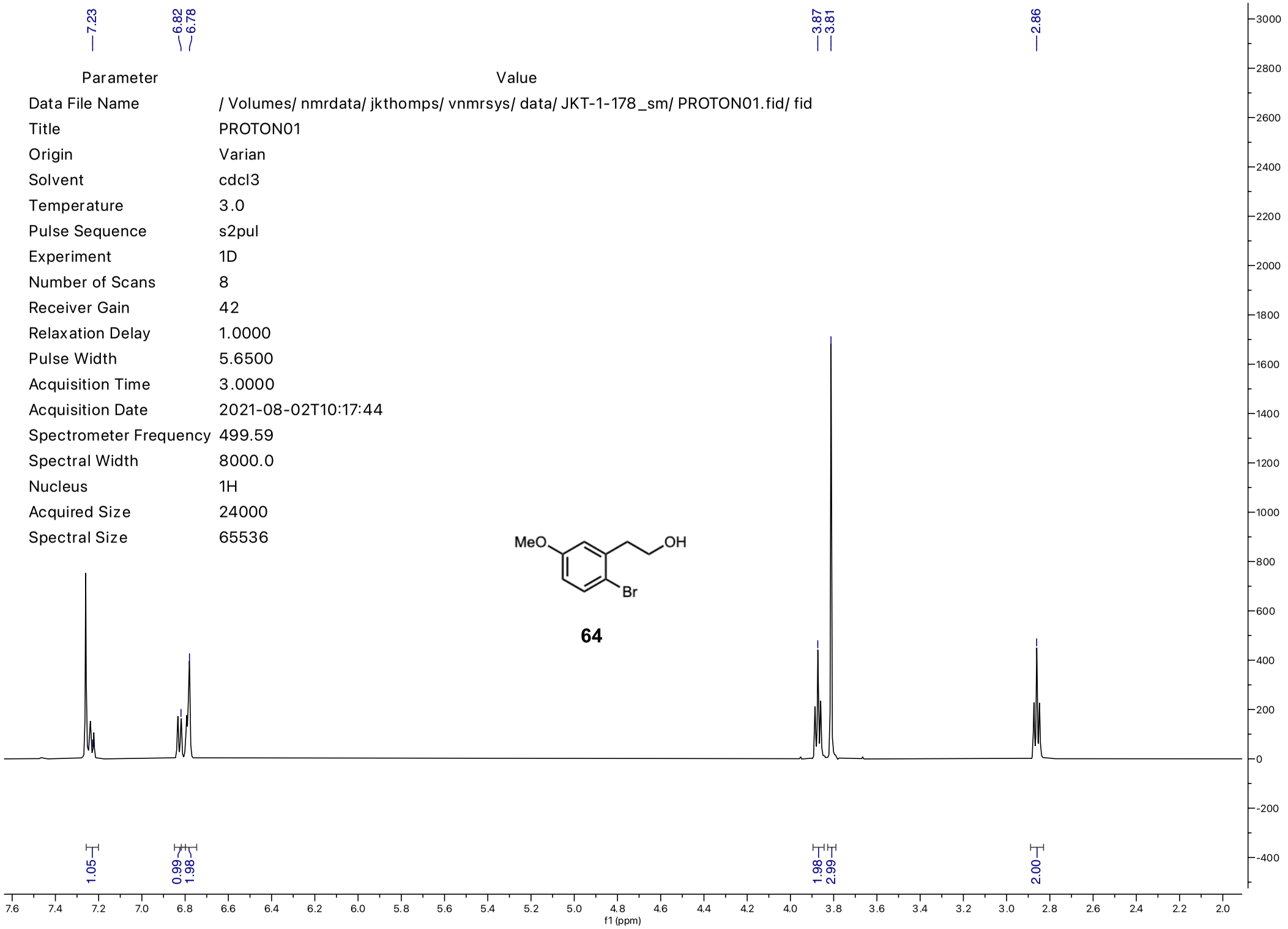
7.23
6.82
6.78
3.87
3.81
2.86
Parameter Value
Data File Name / Volumes/ nmrdata/ jkthomps/ vnmrsys/ data/ JKT-1-178_sm/ PROTON01.fid/ fid
Title PROTON01
Origin Varian
Solvent cdcl3
Temperature 3.0
Pulse Sequence s2pul
Experiment 1D
Number of Scans 8
Receiver Gain 42
Relaxation Delay 1.0000
Pulse Width 5.6500
Acquisition Time 3.0000
Acquisition Date 2021-08-02T10:17:44
Spectrometer Frequency 499.59
Spectral Width 8000.0
Nucleus 1H
Acquired Size 24000
Spectral Size 65536
MeO
OH
Br
64
1.05
0.99
1.98
1.98
2.99
2.00
f1 (ppm)

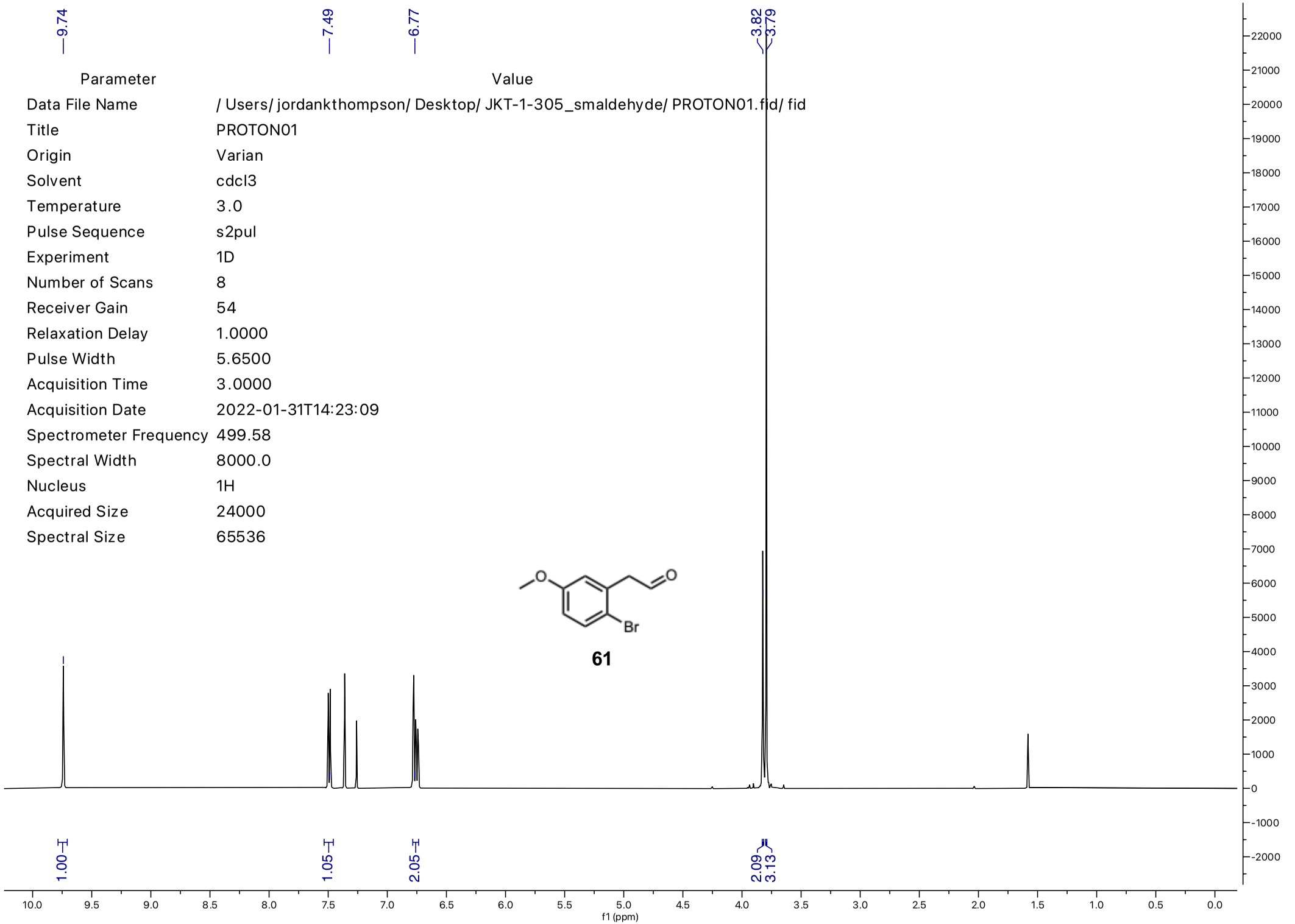
9.74
7.49
6.77
3.82
3.79
Parameter
Value
Data File Name
/ Users/ jordankthompson/ Desktop/ JKT-1-305_smaldehyde/ PROTON01.fid/ fid
Title
PROTON01
Origin
Varian
Solvent
cdcl3
Temperature
3.0
Pulse Sequence
s2pul
Experiment
1D
Number of Scans
8
Receiver Gain
54
Relaxation Delay
1.0000
Pulse Width
5.6500
Acquisition Time
3.0000
Acquisition Date
2022-01-31T14:23:09
Spectrometer Frequency
499.58
Spectral Width
8000.0
Nucleus
1H
Acquired Size
24000
Spectral Size
65536
O
O
Br
61
1.00
1.05
2.05
2.09
3.13
f1 (ppm)

198.39
159.31
133.71
128.47
117.48
115.41
115.07
55.65
50.82

Parameter	Value
Data File Name	/ Volumes/ nmrdata/ jkthomps/ nmr/ JKT-1-305_smaldehyde/ 2/ fid
Title	JKT-1-305_smaldehyde.2.fid
Origin	Bruker BioSpin GmbH
Solvent	CDCl3
Temperature	297.1
Pulse Sequence	zgpg30
Experiment	1D
Number of Scans	512
Receiver Gain	72.0
Relaxation Delay	1.0000
Pulse Width	10.0000
Acquisition Time	1.1622
Acquisition Date	2022-01-31T18:04:56
Spectrometer Frequency	100.62
Spectral Width	28195.5
Nucleus	13C
Acquired Size	32768
Spectral Size	65536

61

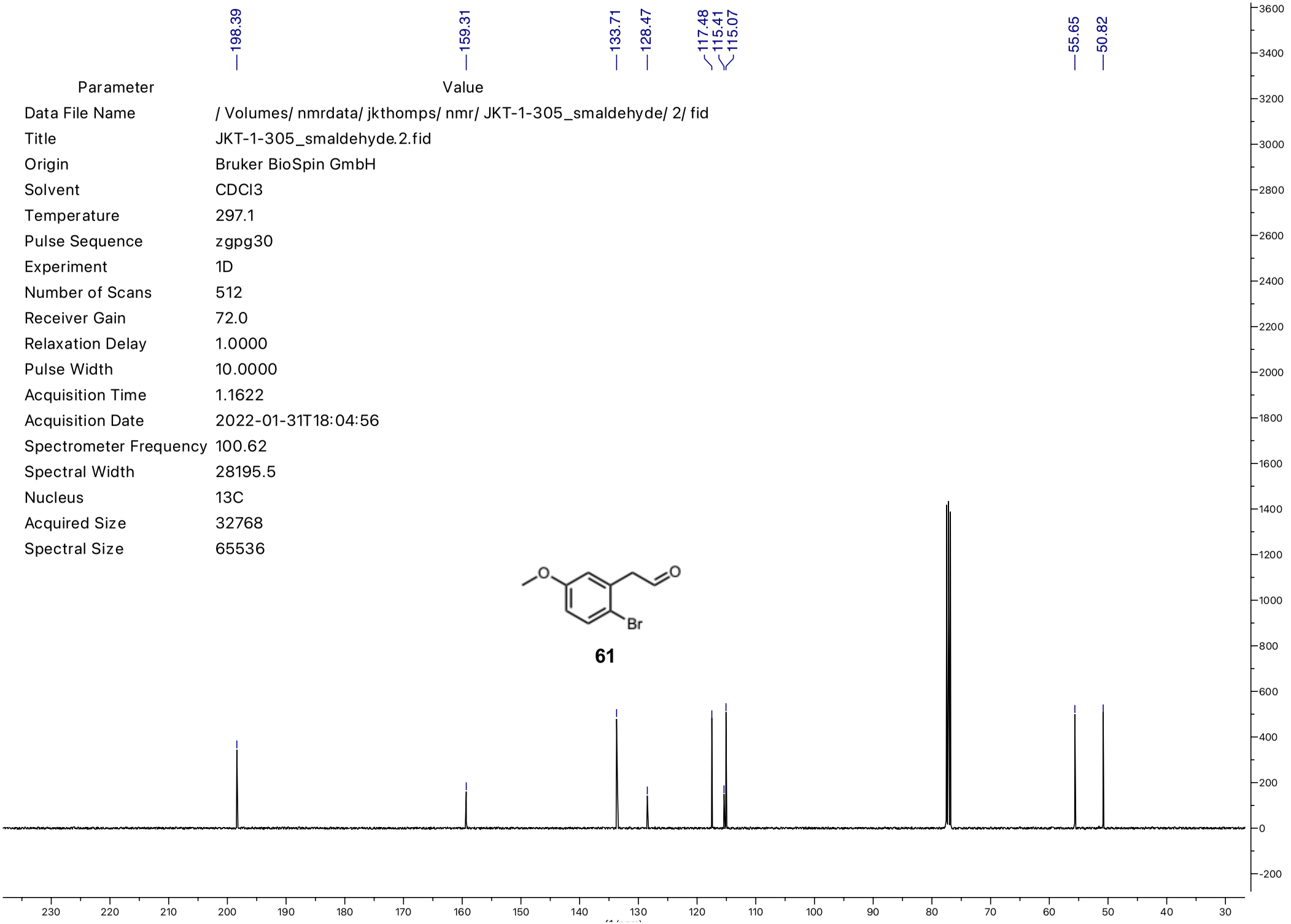

Parameter	Value
Data File Name	/ Volumes/ nmrdata/ jkthomps/ nmr/ JKT-1-characterization-1/ 1/ fid
Title	JKT-1-characterization-1.1.fid
Origin	Bruker BioSpin GmbH
Solvent	CDCl3
Temperature	297.2
Pulse Sequence	zg30
Experiment	1D
Number of Scans	16
Receiver Gain	142.8
Relaxation Delay	1.0000
Pulse Width	12.5000
Acquisition Time	4.0894
Acquisition Date	2021-12-22T10:22:26
Spectrometer Frequency	400.13
Spectral Width	8012.8
Nucleus	1H
Acquired Size	32768
Spectral Size	65536

71

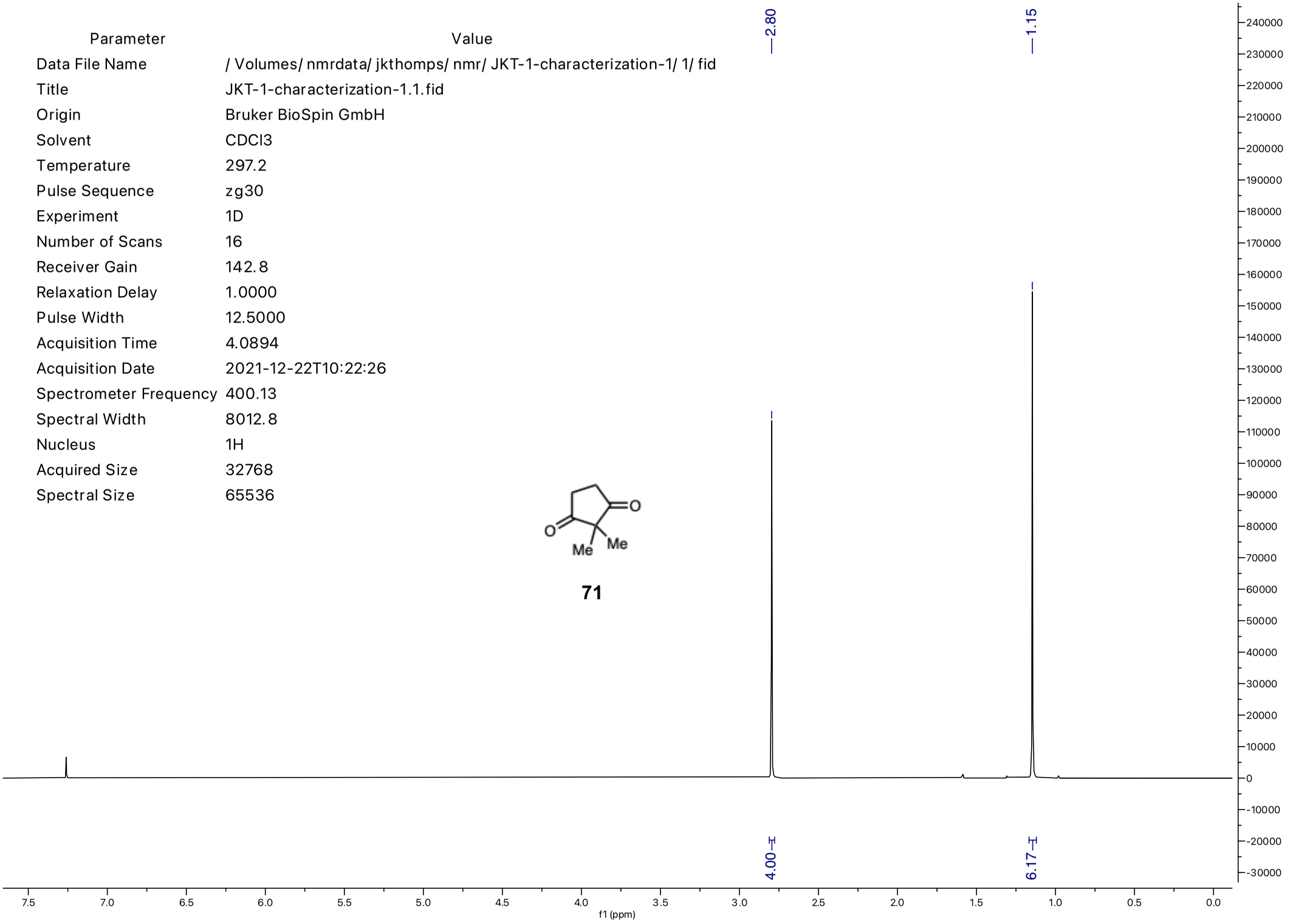

Parameter	Value
Data File Name	/ Volumes/ nmrdata/ jkthomps/ nmr/ JKT-1-characterization-1/ 2/ fid
Title	JKT-1-characterization-1.2.fid
Origin	Bruker BioSpin GmbH
Solvent	CDCl3
Temperature	297.2
Pulse Sequence	zgpg30
Experiment	1D
Number of Scans	512
Receiver Gain	38.0
Relaxation Delay	1.0000
Pulse Width	10.0000
Acquisition Time	1.3631
Acquisition Date	2021-12-22T10:44:26
Spectrometer Frequency	100.62
Spectral Width	24038.5
Nucleus	13C
Acquired Size	32768
Spectral Size	65536

71

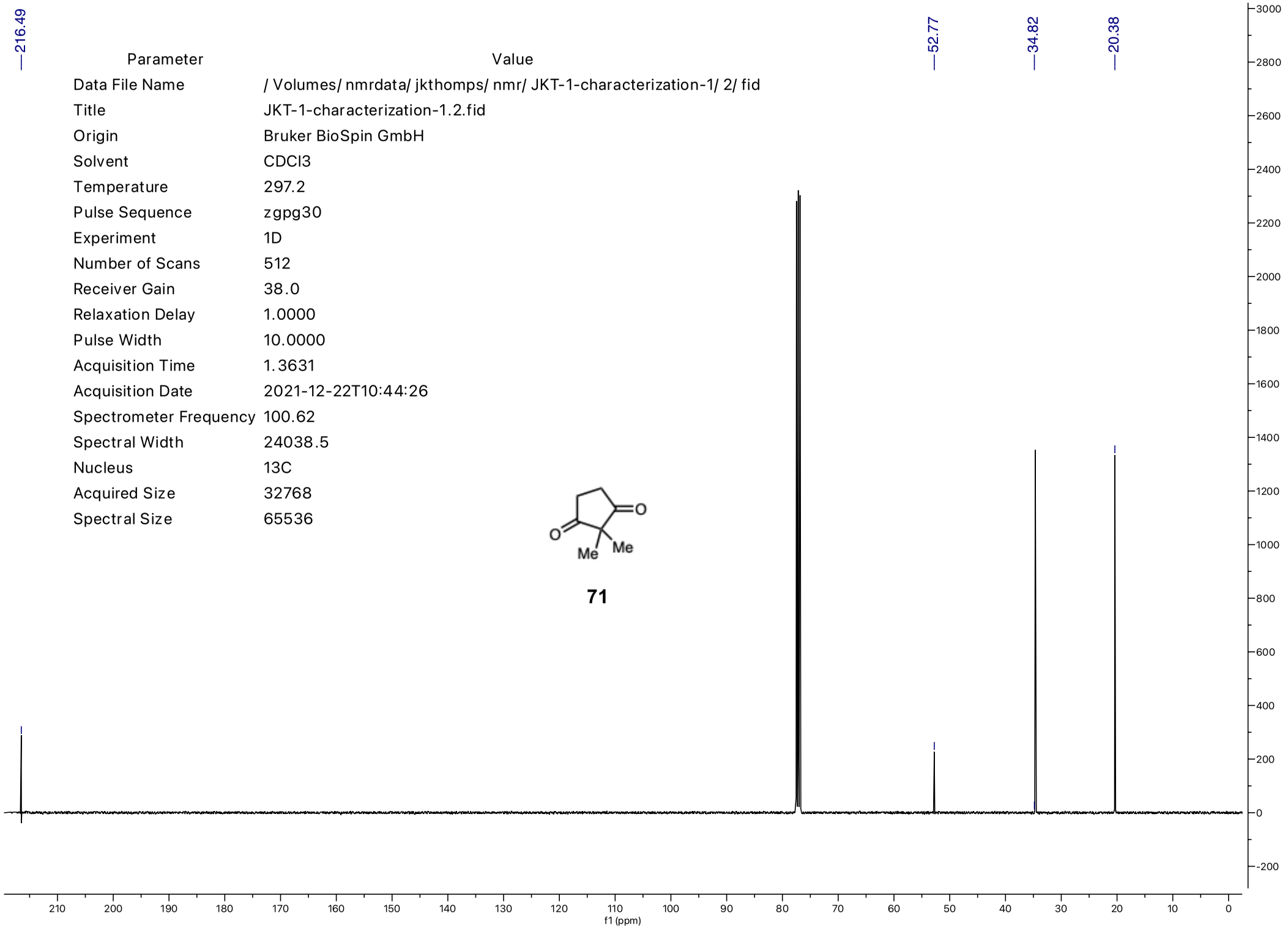

Parameter	Value
Data File Name	/ Users/ jordankthompson/ Desktop/ JKT-5-224_sm/ PROTON01.fid/ fid
Title	PROTON01
Origin	Varian
Solvent	cdcl3
Temperature	25.0
Pulse Sequence	s2pul
Experiment	1D
Number of Scans	8
Receiver Gain	48
Relaxation Delay	1.0000
Pulse Width	5.6500
Acquisition Time	3.0000
Acquisition Date	2024-01-22T11:59:49
Spectrometer Frequency	499.55
Spectral Width	8000.0
Nucleus	1H
Acquired Size	24000
Spectral Size	65536

70

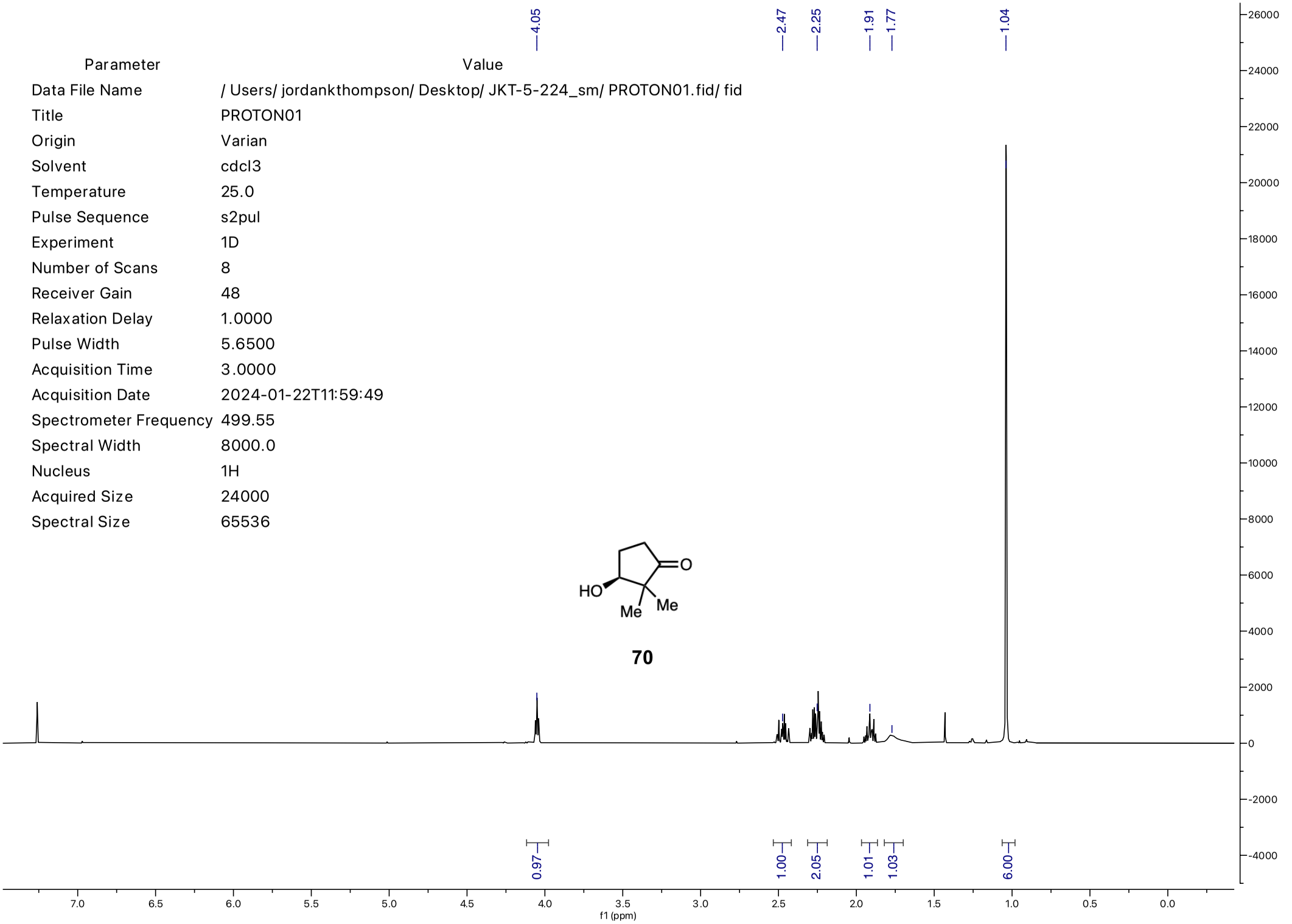

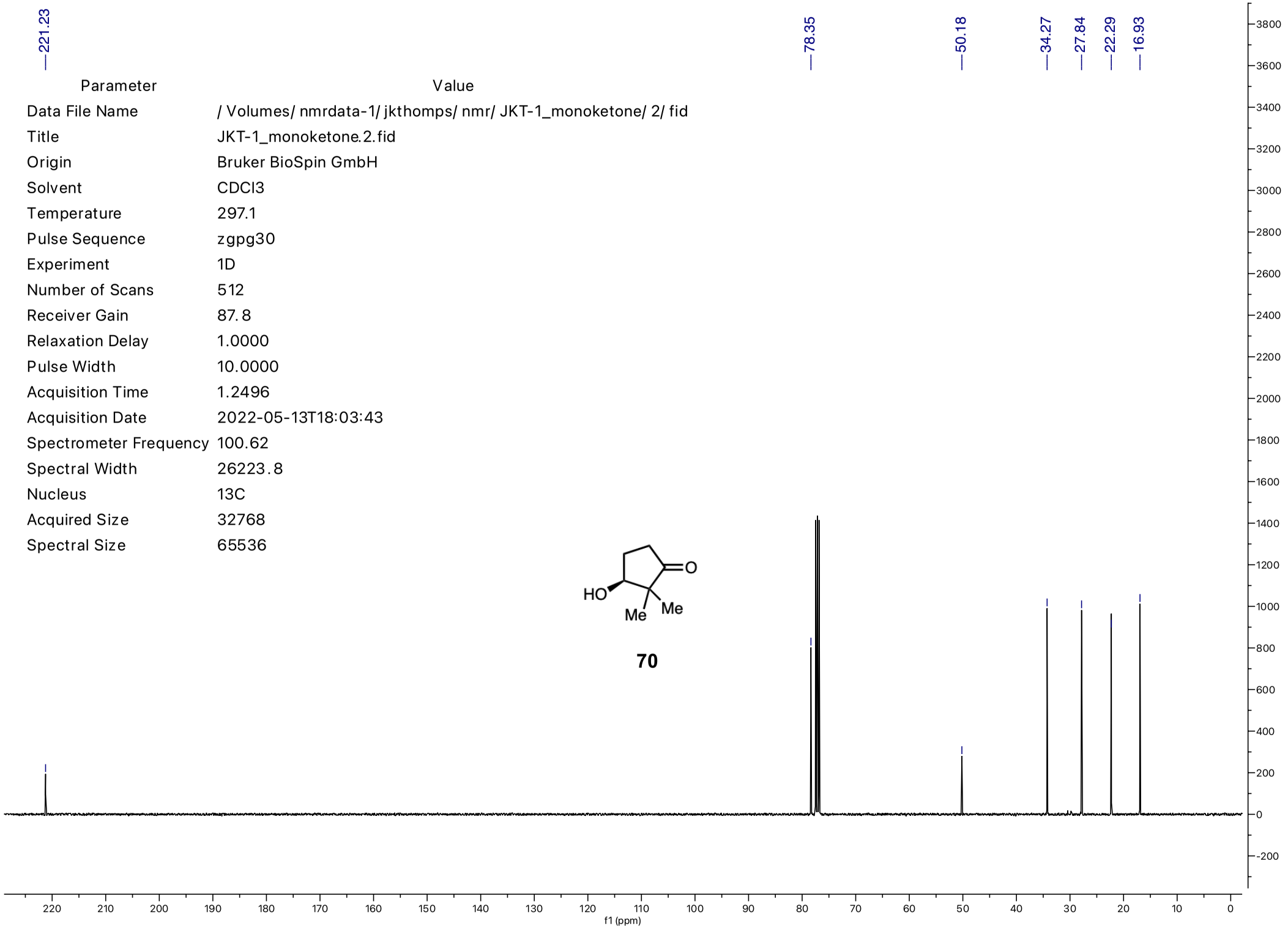

Parameter	Value
Data File Name	/ Volumes/ nmrdata-1/ jkthomps/ nmr/ JKT-1_monoketone/ 2/ fid
Title	JKT-1_monoketone.2.fid
Origin	Bruker BioSpin GmbH
Solvent	CDCl3
Temperature	297.1
Pulse Sequence	zgpg30
Experiment	1D
Number of Scans	512
Receiver Gain	87.8
Relaxation Delay	1.0000
Pulse Width	10.0000
Acquisition Time	1.2496
Acquisition Date	2022-05-13T18:03:43
Spectrometer Frequency	100.62
Spectral Width	26223.8
Nucleus	13C
Acquired Size	32768
Spectral Size	65536

70

Parameter	Value
Data File Name	/ Users/ jordankthompson/ Desktop/ JKT-6-13_sm/ PROTON01.fid/ fid
Title	PROTON01
Origin	Varian
Solvent	cdcl3
Temperature	25.0
Pulse Sequence	s2pul
Experiment	1D
Number of Scans	8
Receiver Gain	54
Relaxation Delay	1.0000
Pulse Width	5.6500
Acquisition Time	3.0000
Acquisition Date	2024-03-07T14:09:59
Spectrometer Frequency	499.55
Spectral Width	8000.0
Nucleus	1H
Acquired Size	24000
Spectral Size	65536

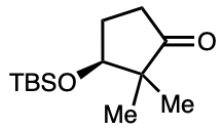

69

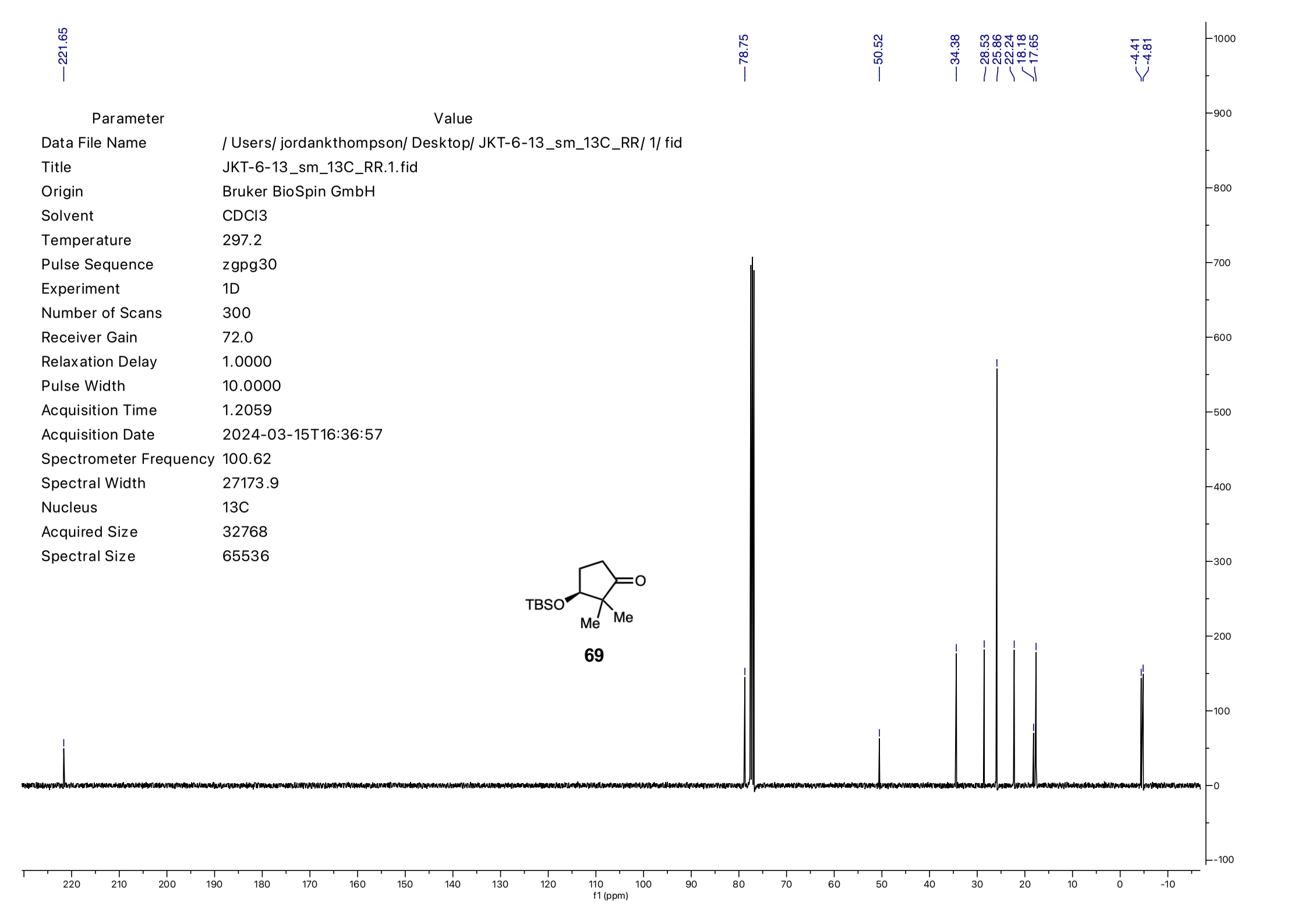
221.65
78.75
50.52
34.38
28.53
25.86
22.24
18.18
17.65
-4.41
-4.81
Parameter Value
Data File Name / Users/ jordankthompson/ Desktop/ JKT-6-13_sm_13C_RR/ 1/ fid
Title JKT-6-13_sm_13C_RR.1.fid
Origin Bruker BioSpin GmbH
Solvent CDCl3
Temperature 297.2
Pulse Sequence zgpg30
Experiment 1D
Number of Scans 300
Receiver Gain 72.0
Relaxation Delay 1.0000
Pulse Width 10.0000
Acquisition Time 1.2059
Acquisition Date 2024-03-15T16:36:57
Spectrometer Frequency 100.62
Spectral Width 27173.9
Nucleus 13C
Acquired Size 32768
Spectral Size 65536
TBSO
O
Me
Me
69
f1 (ppm)

Parameter	Value
Data File Name	/ Users/ jordankthompson/ Desktop/ CMF_1_136_columnSpotA/ PROTON01.fid/ fid
Title	PROTON01
Origin	Varian
Solvent	cdcl3
Temperature	25.0
Pulse Sequence	s2pul
Experiment	1D
Number of Scans	8
Receiver Gain	34
Relaxation Delay	1.0000
Pulse Width	5.1000
Acquisition Time	2.4999
Acquisition Date	2021-04-15T13:15:19
Spectrometer Frequency	300.09
Spectral Width	4796.2
Nucleus	1H
Acquired Size	11990
Spectral Size	65536

67

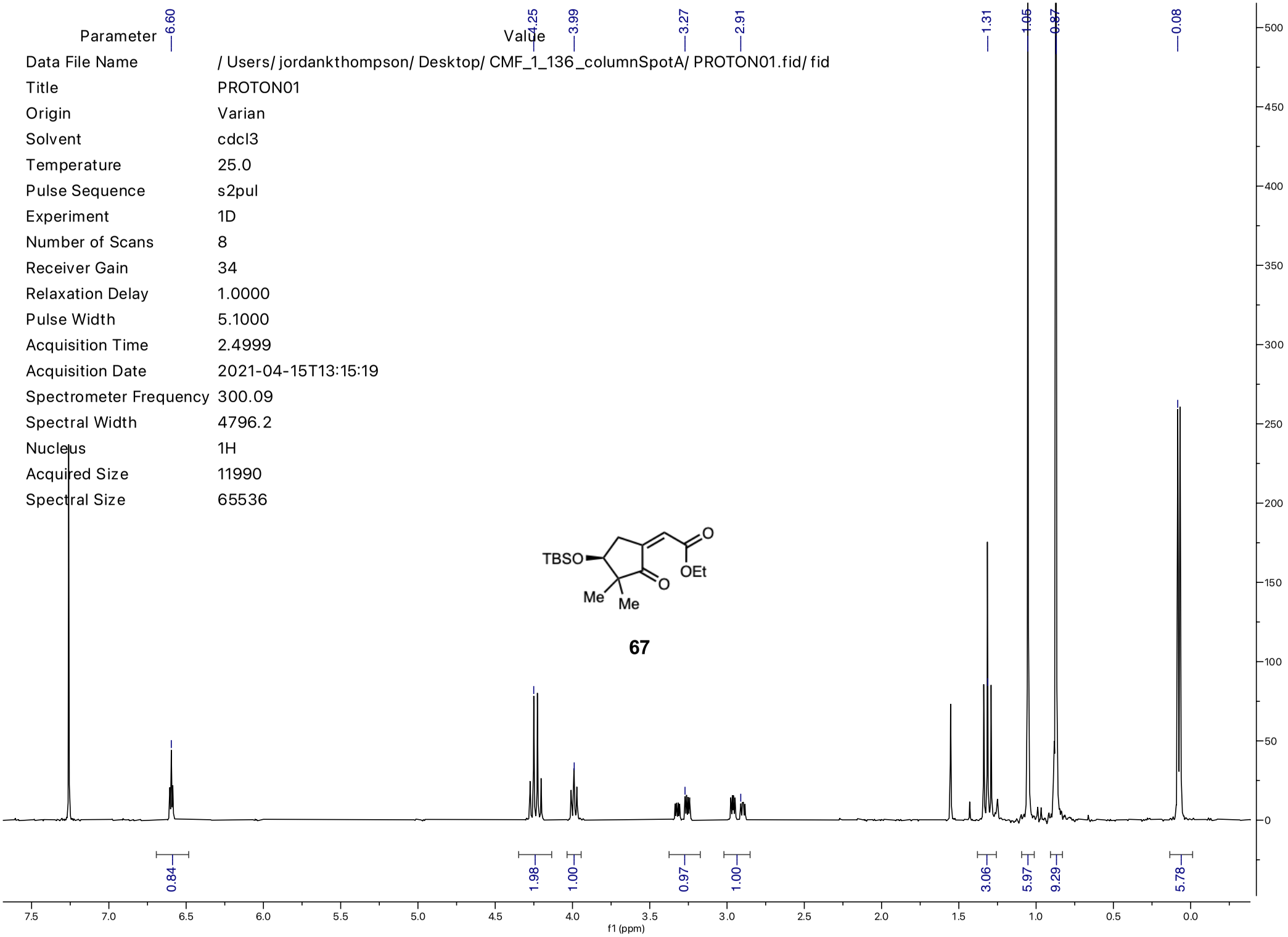

Parameter	Value
Data File Name	/ Users/ jordankthompson/ Downloads/ fid
Title	Downloads
Origin	Varian
Solvent	cdcl3
Temperature	25.0
Pulse Sequence	s2pul
Experiment	1D
Number of Scans	8
Receiver Gain	30
Relaxation Delay	1.0000
Pulse Width	5.1000
Acquisition Time	2.4999
Acquisition Date	2021-04-14T16:34:15
Spectrometer Frequency	300.09
Spectral Width	4796.2
Nucleus	1H
Acquired Size	11990
Spectral Size	65536

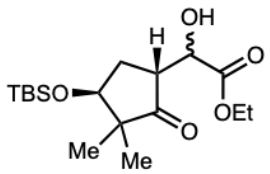

72

Parameter	Value
Data File Name	/ Volumes/ nmrdata/ jkthomps/ nmr/ JKT-6_13_pure/ 1/ fid
Title	JKT-6_13_pure.1.fid
Origin	Bruker BioSpin GmbH
Solvent	CDCl3
Temperature	297.1
Pulse Sequence	zg30
Experiment	1D
Number of Scans	16
Receiver Gain	78.7
Relaxation Delay	1.0000
Pulse Width	12.5000
Acquisition Time	4.0894
Acquisition Date	2024-03-07T20:13:25
Spectrometer Frequency	400.13
Spectral Width	8012.8
Nucleus	1H
Acquired Size	32768
Spectral Size	65536

73

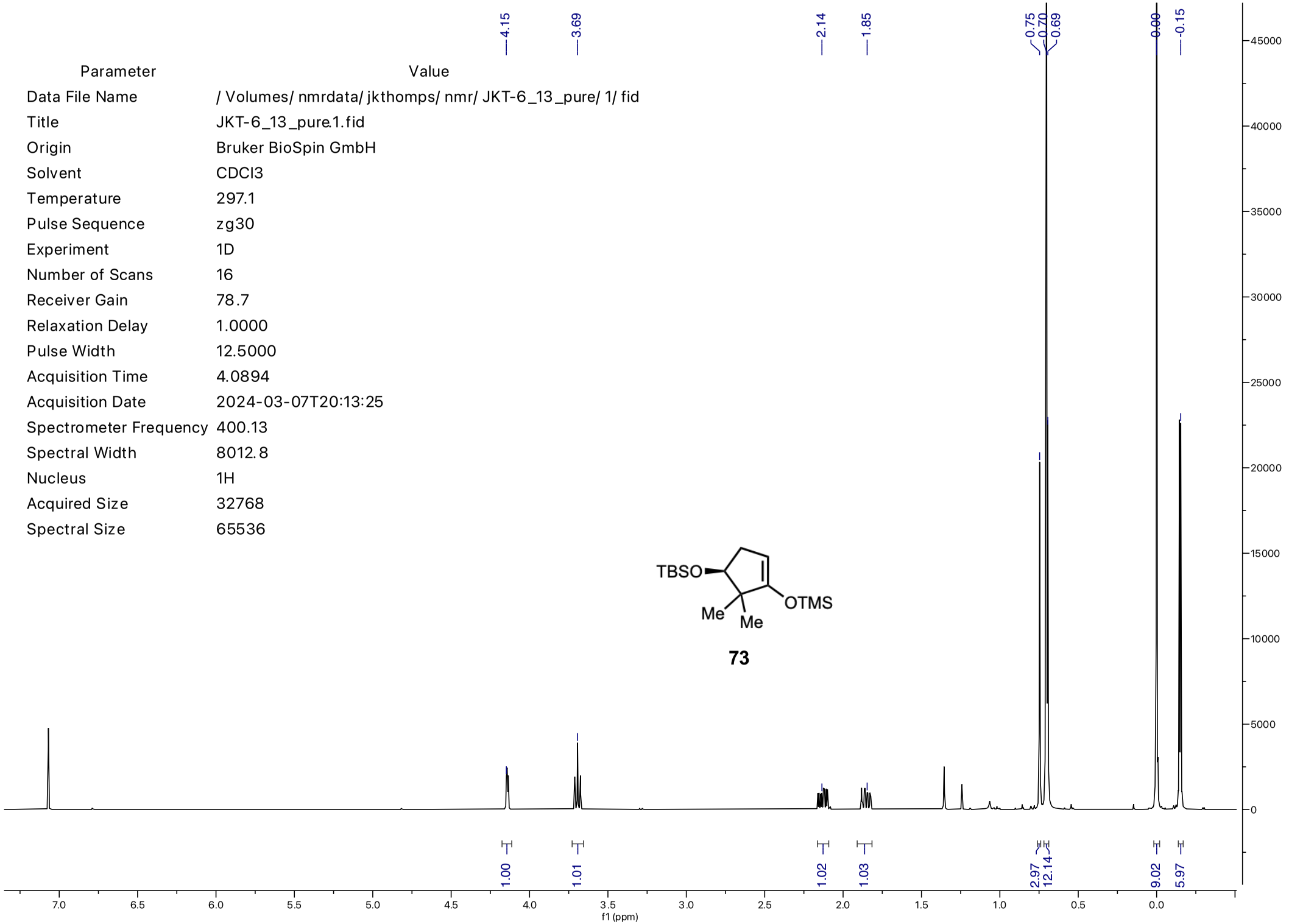

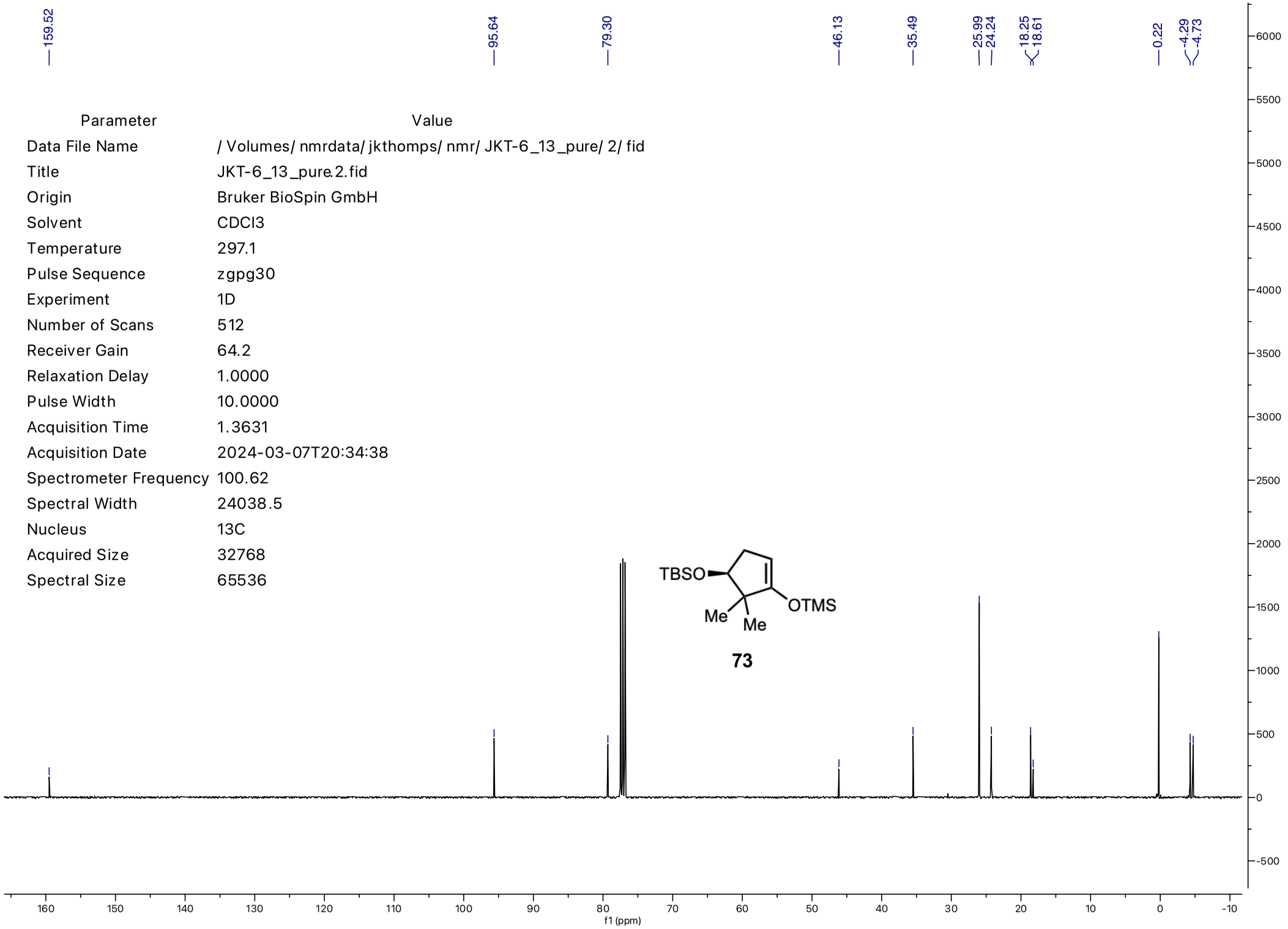

Parameter	Value
Data File Name	/ Volumes/ nmrdata/ jkthomps/ nmr/ JKT-6_13_pure/ 2/ fid
Title	JKT-6_13_pure.2.fid
Origin	Bruker BioSpin GmbH
Solvent	CDCl3
Temperature	297.1
Pulse Sequence	zgpg30
Experiment	1D
Number of Scans	512
Receiver Gain	64.2
Relaxation Delay	1.0000
Pulse Width	10.0000
Acquisition Time	1.3631
Acquisition Date	2024-03-07T20:34:38
Spectrometer Frequency	100.62
Spectral Width	24038.5
Nucleus	13C
Acquired Size	32768
Spectral Size	65536

73

Parameter	Value
Data File Name	/ Users/ jordankthompson/ Desktop/ CMF_1_137 _spotA/ 1/ fid
Title	CMF_1_137 _spotA.1.fid
Origin	Bruker BioSpin GmbH
Solvent	CDCl3
Temperature	297.1
Pulse Sequence	zg30
Experiment	1D
Number of Scans	16
Receiver Gain	156.2
Relaxation Delay	1.0000
Pulse Width	12.5000
Acquisition Time	4.0894
Acquisition Date	2021-04-15T19:31:47
Spectrometer Frequency	400.13
Spectral Width	8012.8
Nucleus	1H
Acquired Size	32768
Spectral Size	65536

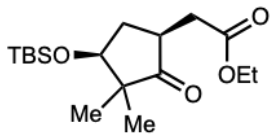

74

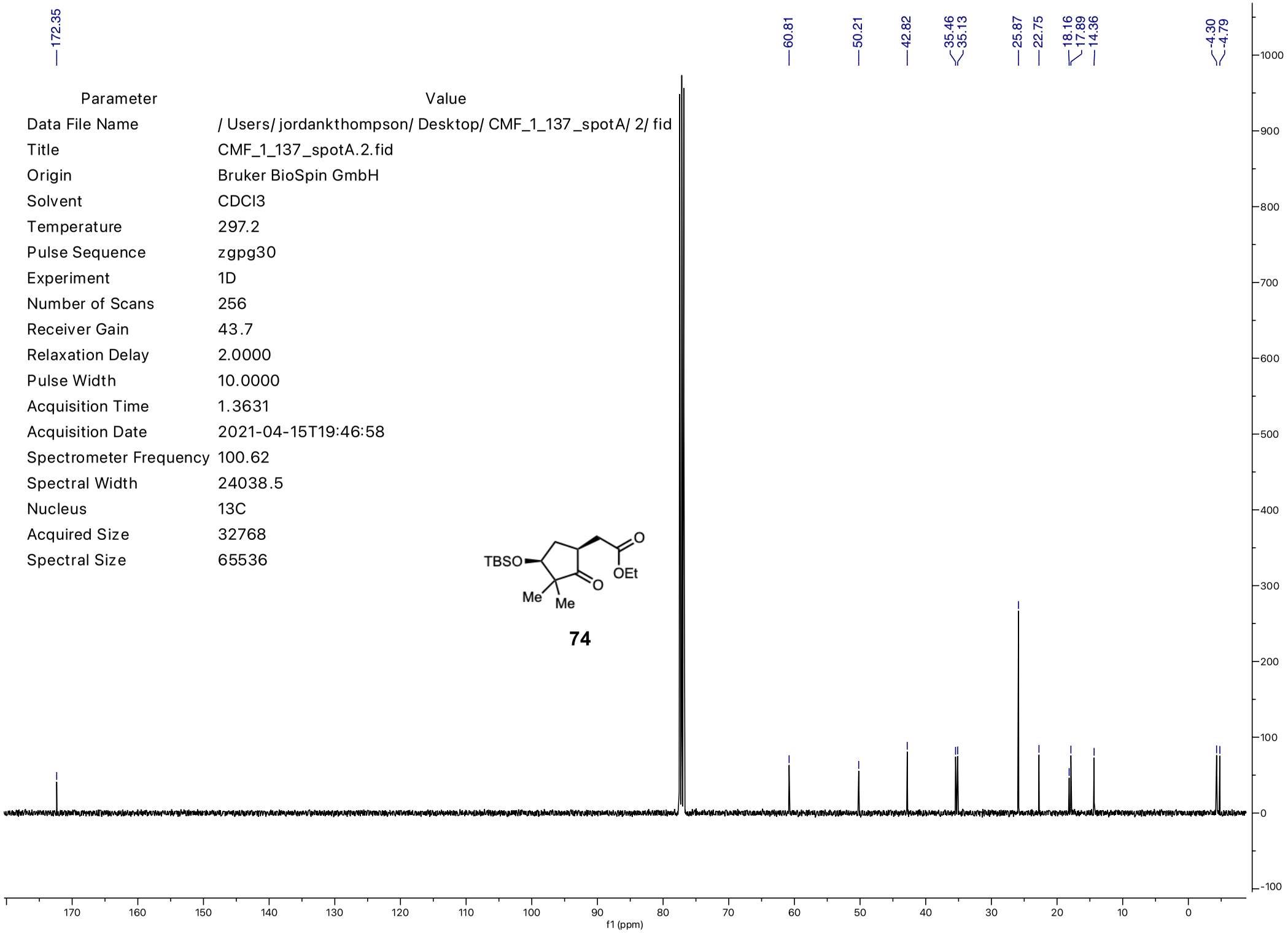
172.35
60.81
50.21
42.82
35.46
35.13
25.87
22.75
18.16
17.89
14.36
-4.30
-4.79
Parameter Value
Data File Name / Users/ jordankthompson/ Desktop/ CMF_1_137_spotA/ 2/ fid
Title CMF_1_137_spotA.2.fid
Origin Bruker BioSpin GmbH
Solvent CDCl3
Temperature 297.2
Pulse Sequence zgpg30
Experiment 1D
Number of Scans 256
Receiver Gain 43.7
Relaxation Delay 2.0000
Pulse Width 10.0000
Acquisition Time 1.3631
Acquisition Date 2021-04-15T19:46:58
Spectrometer Frequency 100.62
Spectral Width 24038.5
Nucleus 13C
Acquired Size 32768
Spectral Size 65536
TBSO
O
OEt
O
Me
Me
74
f1 (ppm)

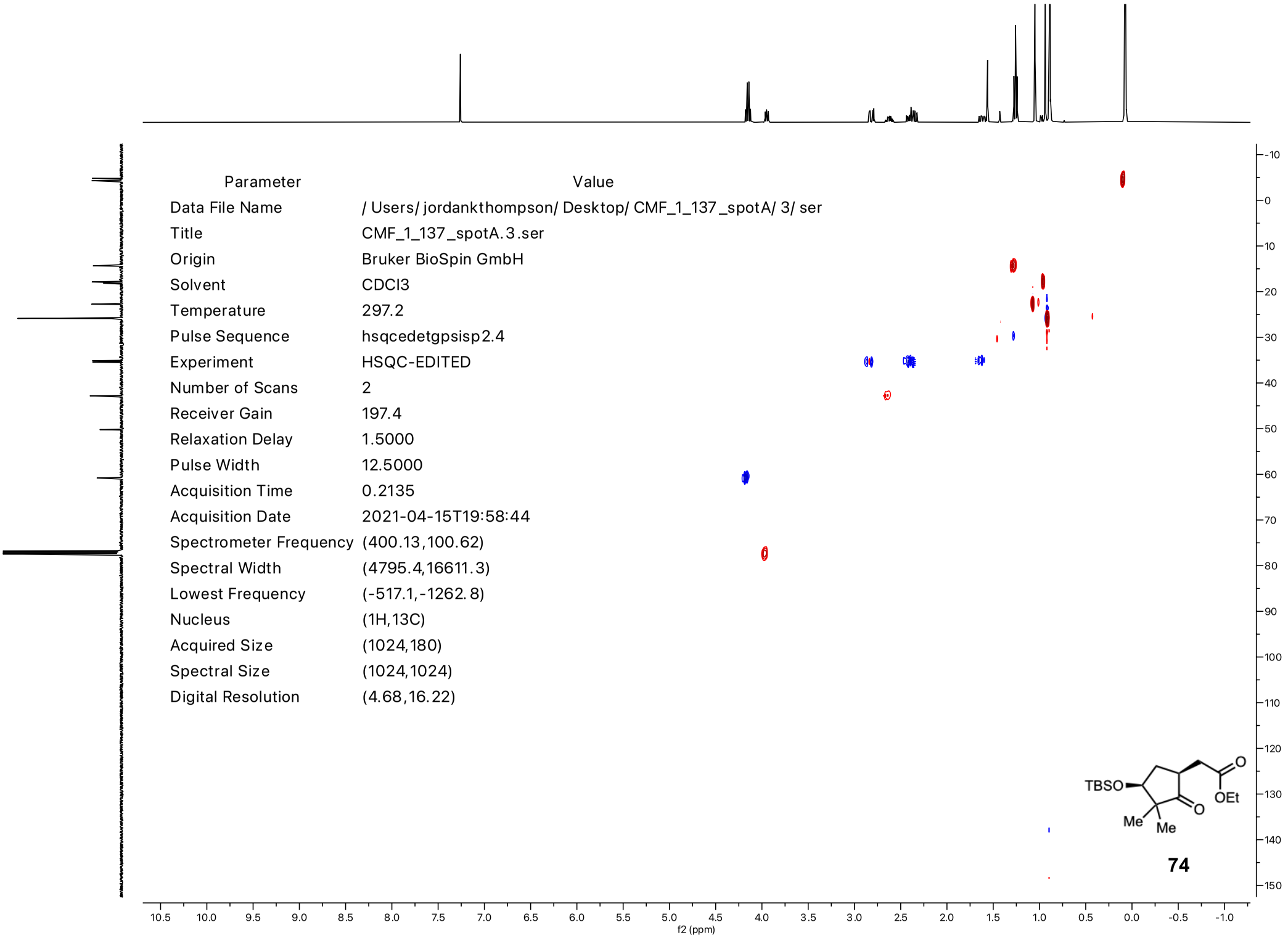
Parameter Value
Data File Name / Users/ jordankthompson/ Desktop/ CMF_1_137_spotA/ 3/ ser
Title CMF_1_137_spotA.3.ser
Origin Bruker BioSpin GmbH
Solvent CDCl3
Temperature 297.2
Pulse Sequence hsqcedetgpsisp2.4
Experiment HSQC-EDITED
Number of Scans 2
Receiver Gain 197.4
Relaxation Delay 1.5000
Pulse Width 12.5000
Acquisition Time 0.2135
Acquisition Date 2021-04-15T19:58:44
Spectrometer Frequency (400.13,100.62)
Spectral Width (4795.4,16611.3)
Lowest Frequency (-517.1,-1262.8)
Nucleus (1H,13C)
Acquired Size (1024,180)
Spectral Size (1024,1024)
Digital Resolution (4.68,16.22)
TBSO
OEt
O
O
Me
Me
74
f2 (ppm)
f1 (ppm)

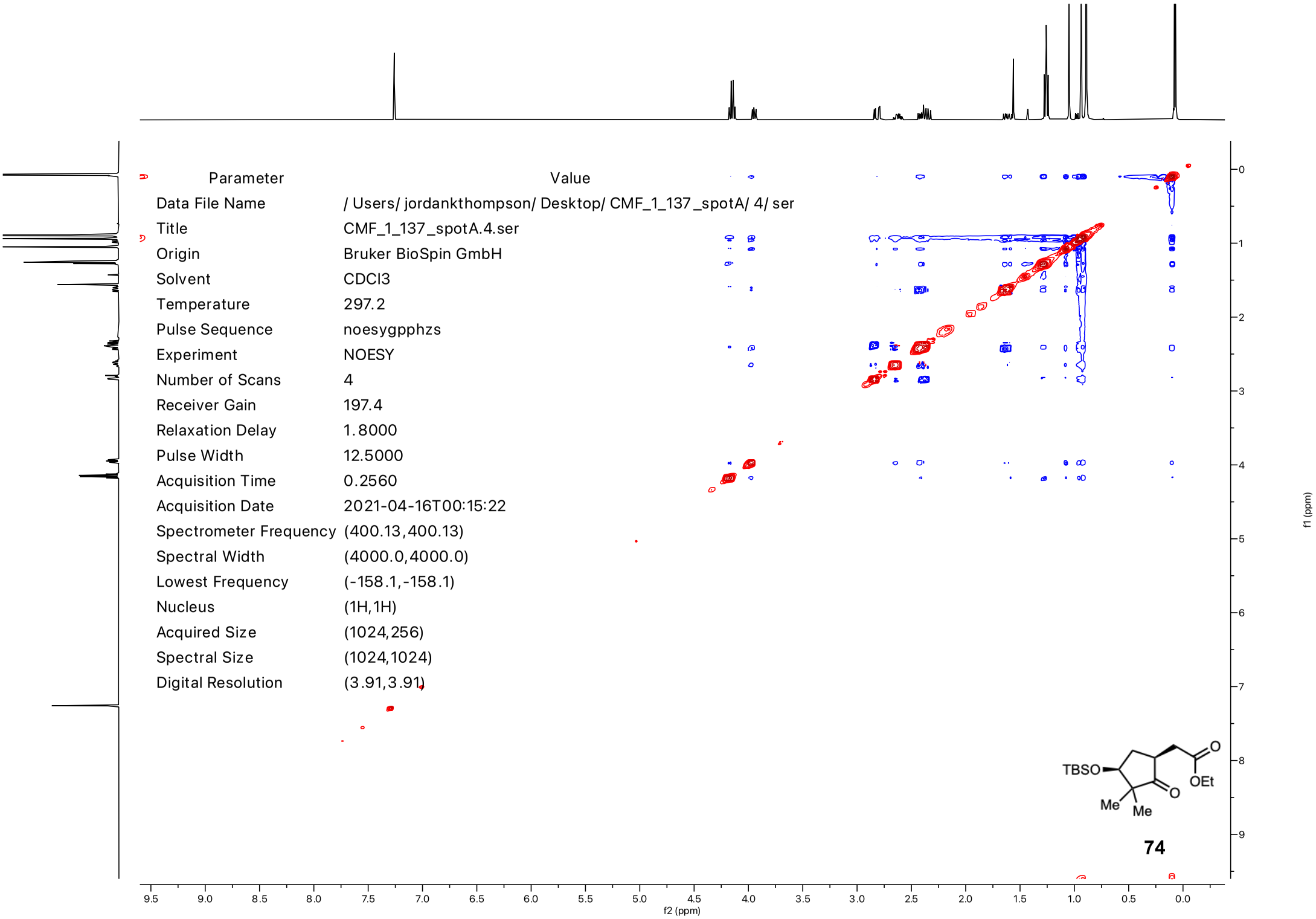
Parameter Value
Data File Name / Users/ jordankthompson/ Desktop/ CMF_1_137_spotA/ 4/ ser
Title CMF_1_137_spotA.4.ser
Origin Bruker BioSpin GmbH
Solvent CDCl3
Temperature 297.2
Pulse Sequence noesygpphzs
Experiment NOESY
Number of Scans 4
Receiver Gain 197.4
Relaxation Delay 1.8000
Pulse Width 12.5000
Acquisition Time 0.2560
Acquisition Date 2021-04-16T00:15:22
Spectrometer Frequency (400.13,400.13)
Spectral Width (4000.0,4000.0)
Lowest Frequency (-158.1,-158.1)
Nucleus (1H,1H)
Acquired Size (1024,256)
Spectral Size (1024,1024)
Digital Resolution (3.91,3.91)
TBSO
OEt
O
O
Me
Me
74
f2 (ppm)
f1 (ppm)

Parameter	Value
Data File Name	/ Users/ jordankthompson/ Desktop/ CMF_1_137_COSY/ 2/ ser
Title	CMF_1_137_COSY.2.ser
Origin	Bruker BioSpin GmbH
Solvent	CDCl3
Temperature	297.1
Pulse Sequence	cosygpppqf
Experiment	COSY
Number of Scans	1
Receiver Gain	64.2
Relaxation Delay	1.9205
Pulse Width	12.5000
Acquisition Time	0.2765
Acquisition Date	2021-04-16T14:51:22
Spectrometer Frequency	(400.13,400.13)
Spectral Width	(3703.7,3703.7)
Lowest Frequency	(-460.9,-460.9)
Nucleus	(1H,1H)
Acquired Size	(1024,128)
Spectral Size	(1024,1024)
Digital Resolution	(3.62,3.62)

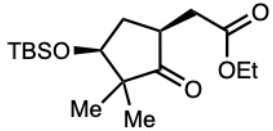

74

f2 (ppm)

f1 (ppm)

Parameter	Value
Data File Name	/ Volumes/ nmrdata/ jkthomps/ nmr/ JKT-1-297-3_washed/ 3/ fid
Title	JKT-1-297-3_washed.3.fid
Origin	Bruker BioSpin GmbH
Solvent	CDCl3
Temperature	297.1
Pulse Sequence	zg30
Experiment	1D
Number of Scans	16
Receiver Gain	197.4
Relaxation Delay	1.0000
Pulse Width	12.5000
Acquisition Time	4.0894
Acquisition Date	2022-01-25T21:51:45
Spectrometer Frequency	400.13
Spectral Width	8012.8
Nucleus	1H
Acquired Size	32768
Spectral Size	65536

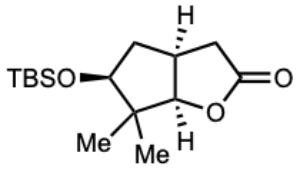

75

Parameter	Value
Data File Name	/ Volumes/ nmrdata/ jkthomps/ nmr/ JKT-1-297-3_washed/ 2/ fid
Title	JKT-1-297-3_washed.2.fid
Origin	Bruker BioSpin GmbH
Solvent	CDCl3
Temperature	297.2
Pulse Sequence	zgpg30
Experiment	1D
Number of Scans	512
Receiver Gain	64.2
Relaxation Delay	1.0000
Pulse Width	10.0000
Acquisition Time	1.3631
Acquisition Date	2022-01-25T08:44:08
Spectrometer Frequency	100.62
Spectral Width	24038.5
Nucleus	13C
Acquired Size	32768
Spectral Size	65536

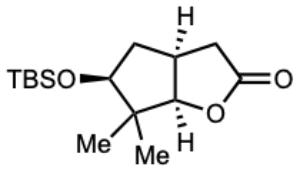

75

Parameter	Value
Data File Name	/ Volumes/ nmrdata/ jkthomps/ nmr/ JKT-4-Compound5/ 3/ fid
Title	JKT-4-Compound5.3.fid
Origin	Bruker BioSpin GmbH
Solvent	CDCl3
Temperature	297.1
Pulse Sequence	zg30
Experiment	1D
Number of Scans	16
Receiver Gain	176.8
Relaxation Delay	1.0000
Pulse Width	12.5000
Acquisition Time	4.0894
Acquisition Date	2023-08-26T14:16:05
Spectrometer Frequency	400.13
Spectral Width	8012.8
Nucleus	1H
Acquired Size	32768
Spectral Size	65536

60

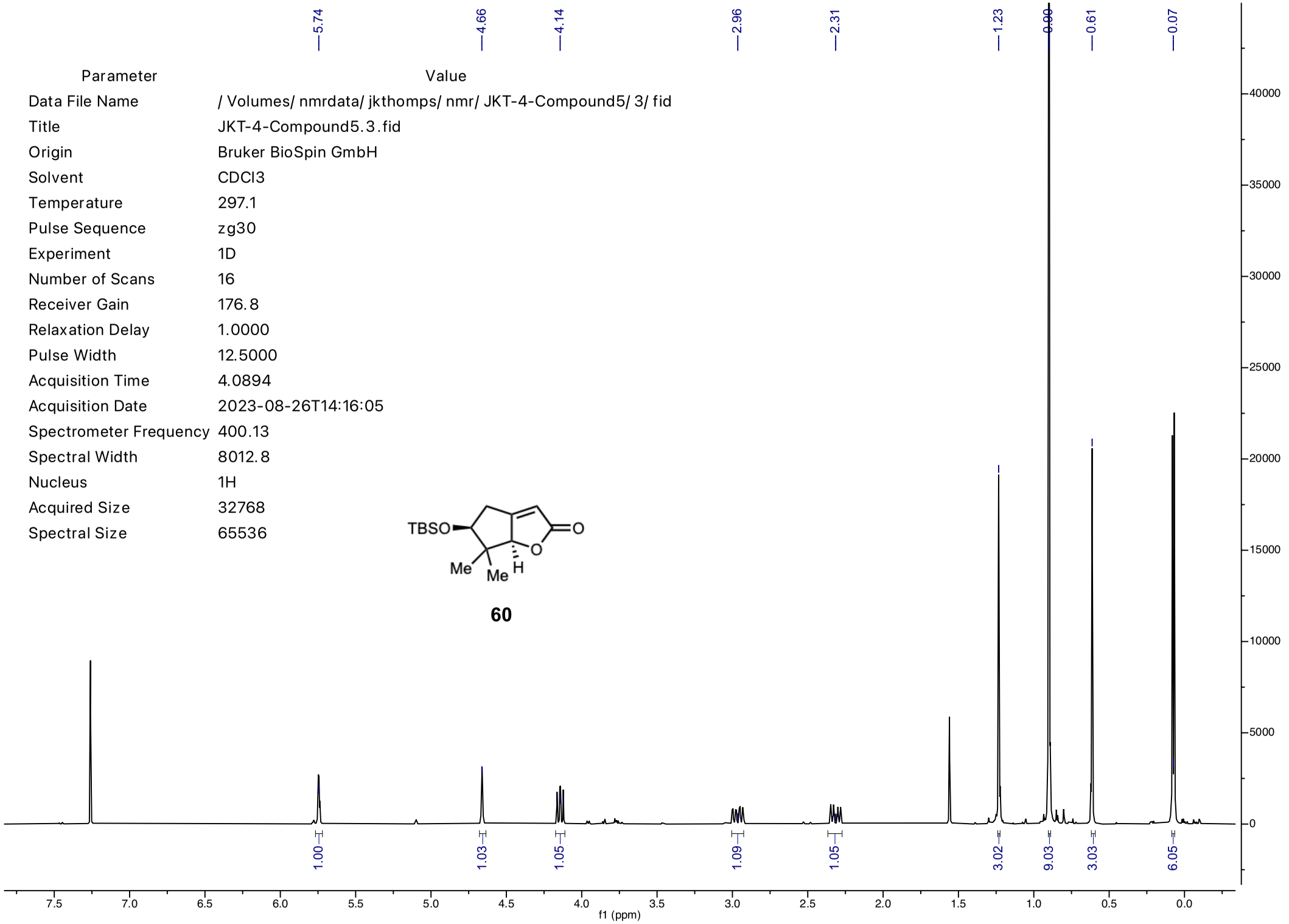

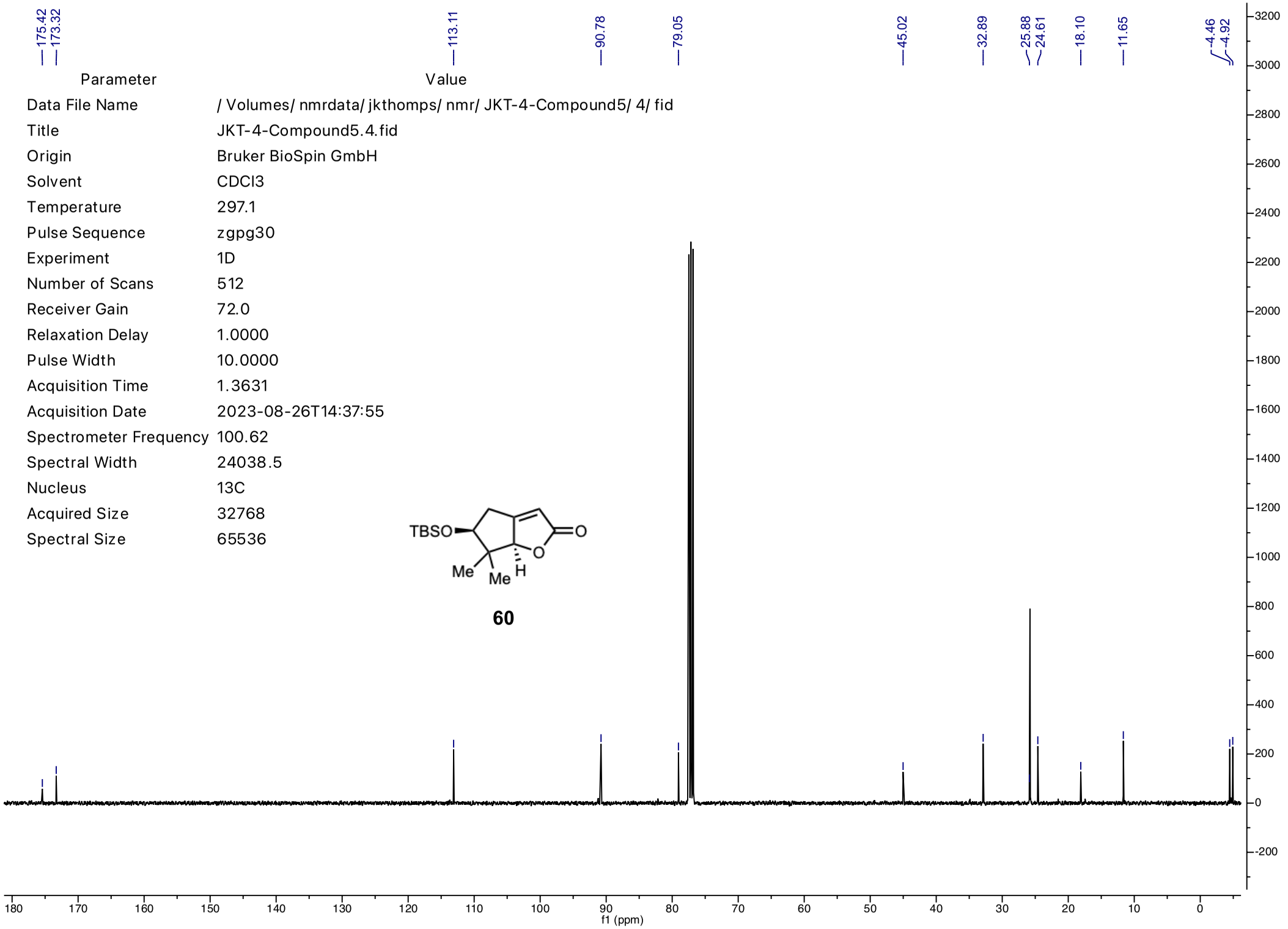
175.42
173.32
113.11
90.78
79.05
45.02
32.89
25.88
24.61
18.10
11.65
4.46
4.92
Parameter
Value
Data File Name / Volumes/ nmrdata/ jkthomps/ nmr/ JKT-4-Compound5/ 4/ fid
Title JKT-4-Compound5.4.fid
Origin Bruker BioSpin GmbH
Solvent CDCl3
Temperature 297.1
Pulse Sequence zgpg30
Experiment 1D
Number of Scans 512
Receiver Gain 72.0
Relaxation Delay 1.0000
Pulse Width 10.0000
Acquisition Time 1.3631
Acquisition Date 2023-08-26T14:37:55
Spectrometer Frequency 100.62
Spectral Width 24038.5
Nucleus 13C
Acquired Size 32768
Spectral Size 65536
TBSO
O
O
Me
Me
H
60
f1 (ppm)

Parameter	Value
Data File Name	/ Users/ jordankthompson/ Desktop/ JKT-4-203_pure/ 1/ fid
Title	JKT-4-203_pure.1.fid
Origin	Bruker BioSpin GmbH
Solvent	CDCl3
Temperature	297.1
Pulse Sequence	zg30
Experiment	1D
Number of Scans	16
Receiver Gain	72.0
Relaxation Delay	1.0000
Pulse Width	12.5000
Acquisition Time	4.0894
Acquisition Date	2023-07-08T01:38:51
Spectrometer Frequency	400.13
Spectral Width	8012.8
Nucleus	1H
Acquired Size	32768
Spectral Size	65536

77

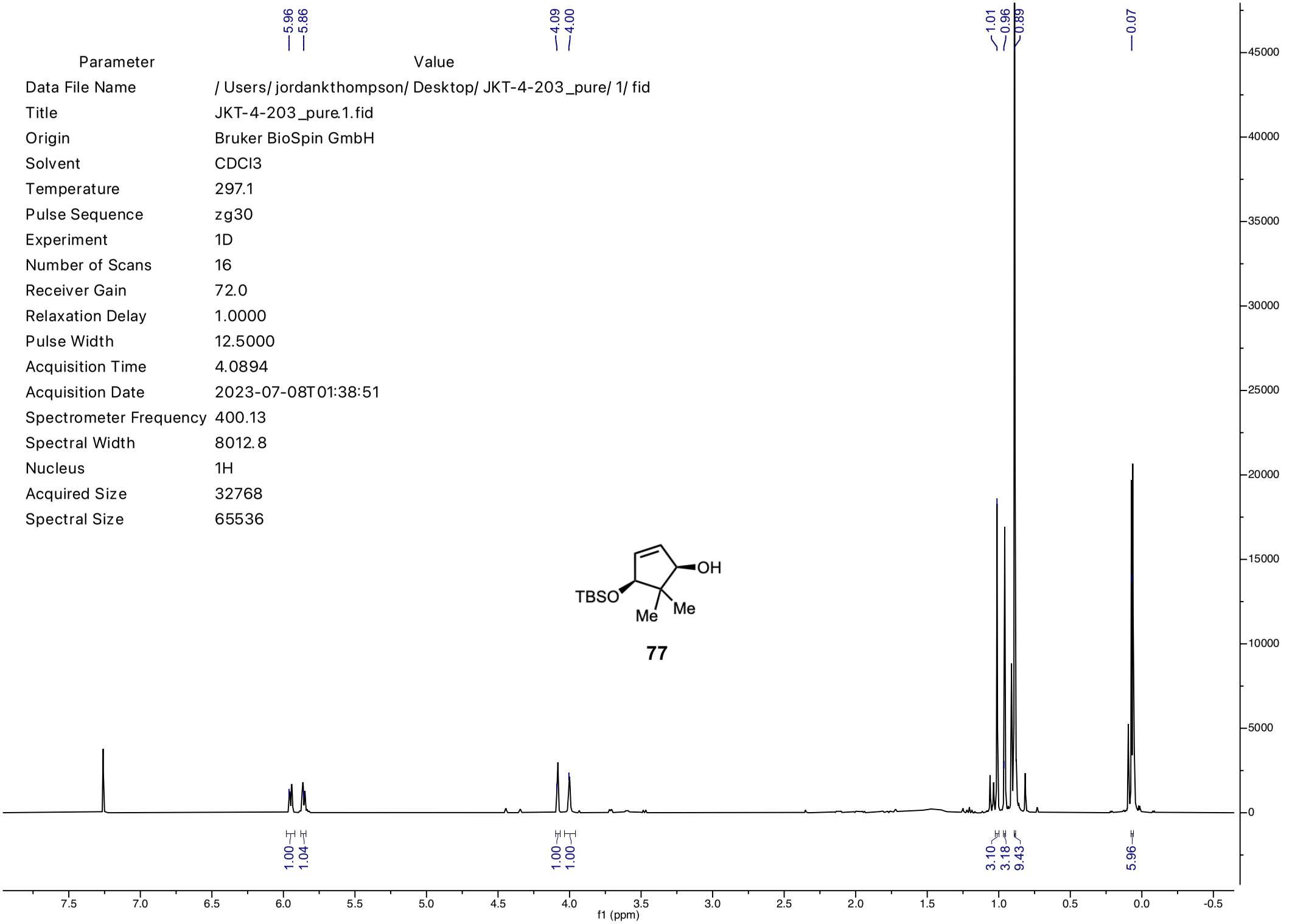

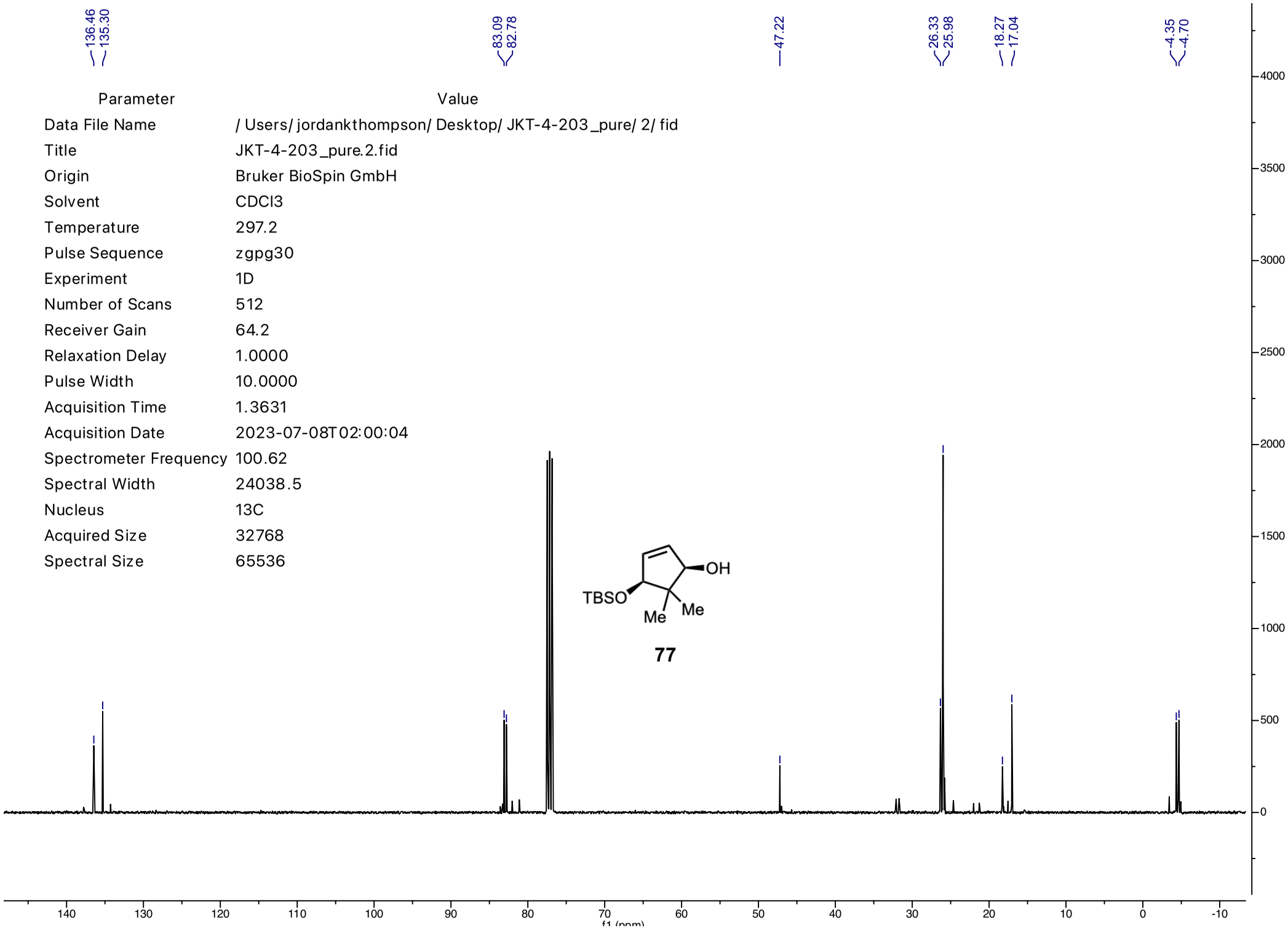

Parameter	Value
Data File Name	/ Users/ jordankthompson/ Desktop/ JKT-4-203_pure/ 2/ fid
Title	JKT-4-203_pure.2.fid
Origin	Bruker BioSpin GmbH
Solvent	CDCl3
Temperature	297.2
Pulse Sequence	zgpg30
Experiment	1D
Number of Scans	512
Receiver Gain	64.2
Relaxation Delay	1.0000
Pulse Width	10.0000
Acquisition Time	1.3631
Acquisition Date	2023-07-08T02:00:04
Spectrometer Frequency	100.62
Spectral Width	24038.5
Nucleus	13C
Acquired Size	32768
Spectral Size	65536

77

Parameter	Value
Data File Name	/ Users/ shawnteh/ Desktop/ ST-BrAcetal-1-h/ 1/ fid
Title	ST-BrAcetal-1-h.1.fid
Origin	Bruker BioSpin GmbH
Solvent	CDCl3
Temperature	297.1
Pulse Sequence	zg30
Experiment	1D
Number of Scans	16
Receiver Gain	197.4
Relaxation Delay	1.0000
Pulse Width	12.5000
Acquisition Time	4.0894
Acquisition Date	2024-05-17T15:14:13
Spectrometer Frequency	400.13
Spectral Width	8012.8
Nucleus	1H
Acquired Size	32768
Spectral Size	65536

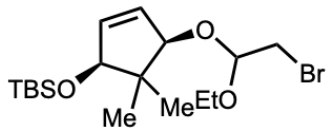

78

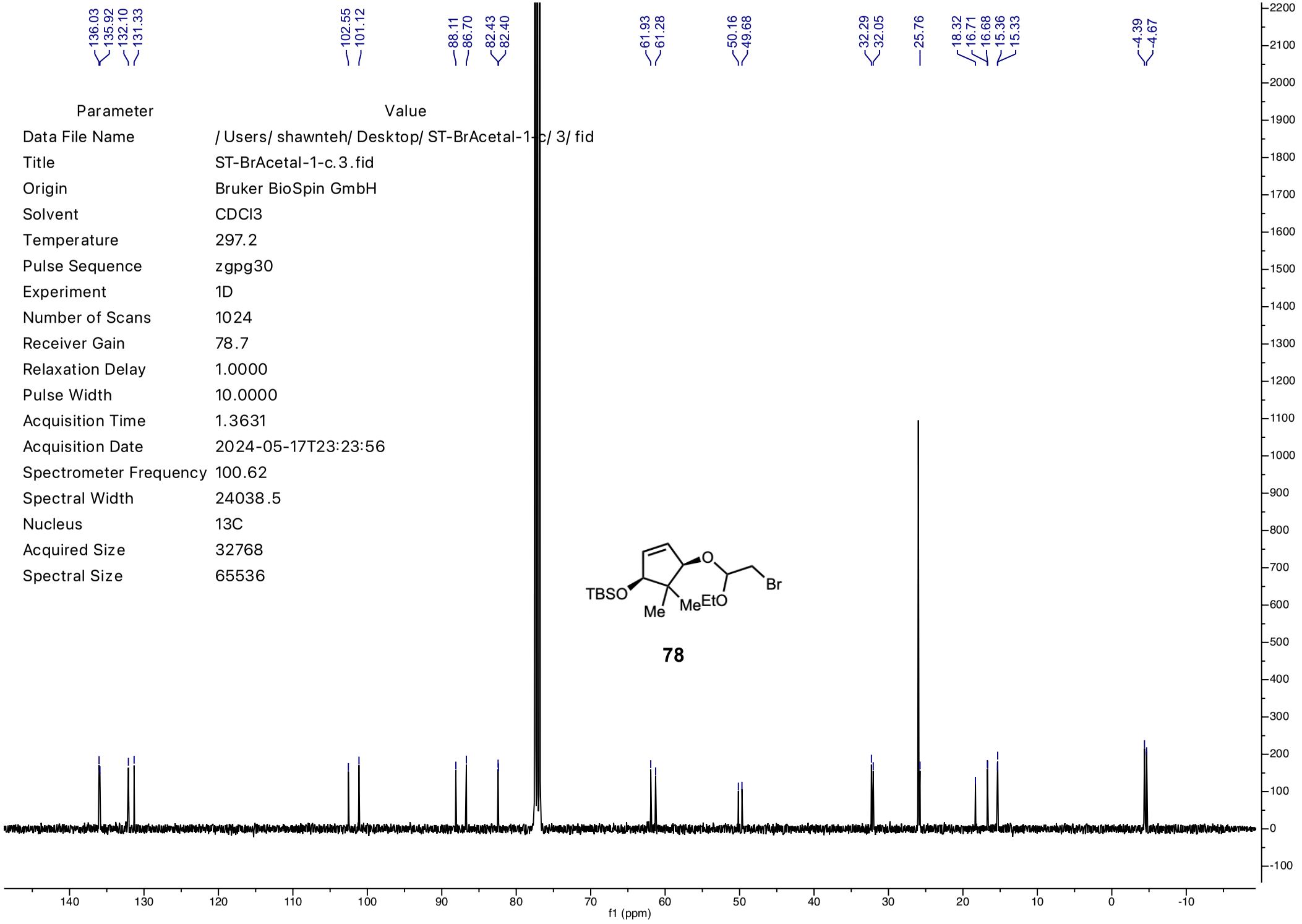
136.03
135.92
132.10
131.33
102.55
101.12
88.11
86.70
82.43
82.40
61.93
61.28
50.16
49.68
32.29
32.05
25.76
18.32
16.71
16.68
15.36
15.33
-4.39
-4.67
Parameter
Value
Data File Name
/ Users/ shawnteh/ Desktop/ ST-BrAcetal-1-c/ 3/ fid
Title
ST-BrAcetal-1-c.3.fid
Origin
Bruker BioSpin GmbH
Solvent
CDCl3
Temperature
297.2
Pulse Sequence
zgpg30
Experiment
1D
Number of Scans
1024
Receiver Gain
78.7
Relaxation Delay
1.0000
Pulse Width
10.0000
Acquisition Time
1.3631
Acquisition Date
2024-05-17T23:23:56
Spectrometer Frequency
100.62
Spectral Width
24038.5
Nucleus
13C
Acquired Size
32768
Spectral Size
65536
TBSO
Me
Me
EtO
O
Br
78
f1 (ppm)

Parameter	Value
Data File Name	/ Volumes/ nmrdata/ kyoungbl/ vnmrsys/ data/ KCY-2-ST-sp3_20240412_01/ KCY-2-ST-sp3-PROTON_01.fid/ fid
Title	KCY-2-ST-sp3-PROTON_01
Origin	Varian
Solvent	cdcl3
Temperature	25.0
Pulse Sequence	s2pul
Experiment	1D
Number of Scans	8
Receiver Gain	38
Relaxation Delay	1.0000
Pulse Width	2.6500
Acquisition Time	1.7080
Acquisition Date	2024-04-12T17:17:30
Spectrometer Frequency	599.56
Spectral Width	9592.3
Nucleus	1H
Acquired Size	16384
Spectral Size	65536

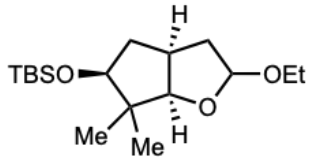

79

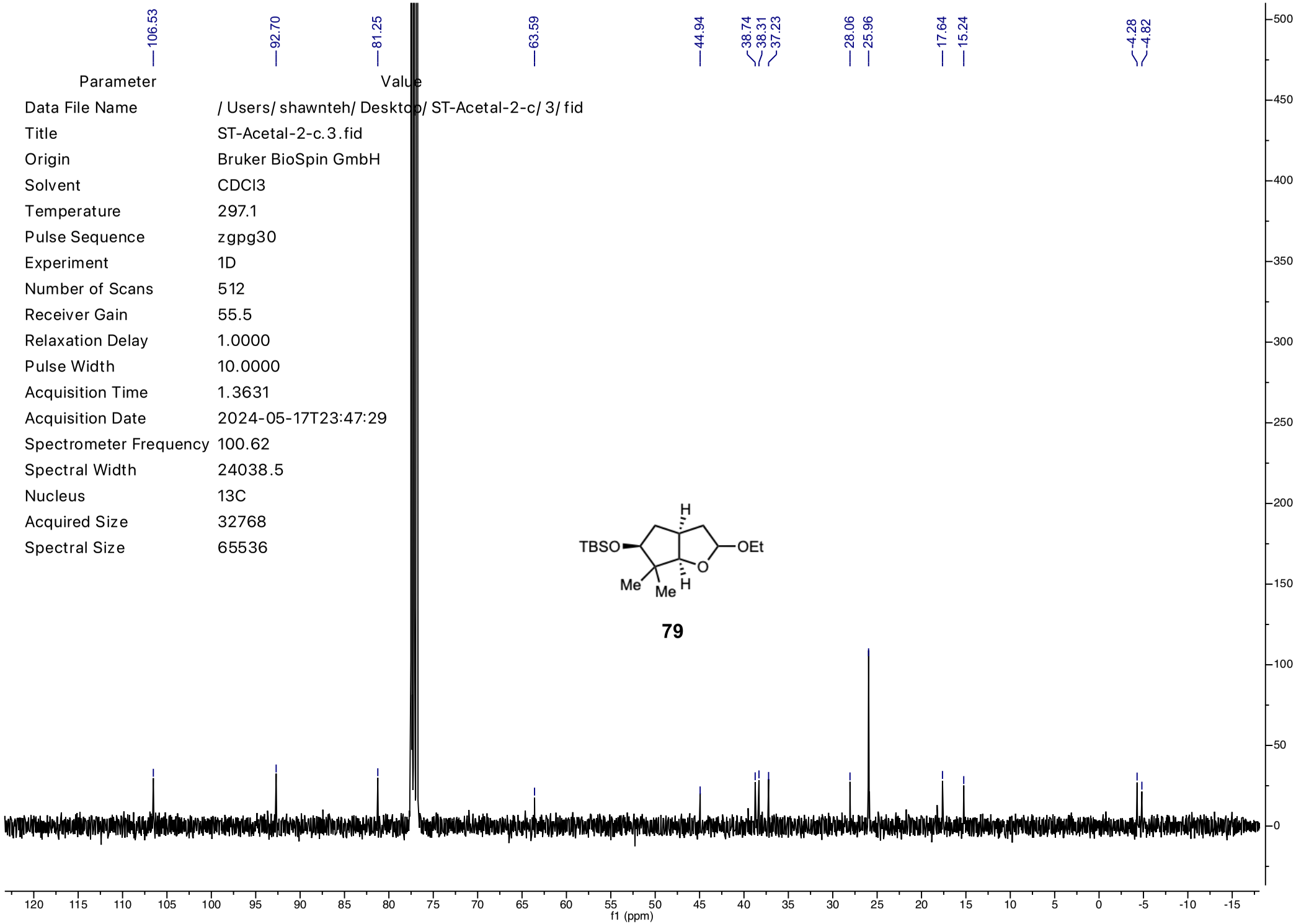
106.53
92.70
81.25
63.59
44.94
38.74
38.31
37.23
28.06
25.96
17.64
15.24
-4.28
-4.82
Parameter Value
Data File Name / Users/ shawnteh/ Desktop/ ST-Acetal-2-c/ 3/ fid
Title ST-Acetal-2-c.3.fid
Origin Bruker BioSpin GmbH
Solvent CDCl3
Temperature 297.1
Pulse Sequence zgpg30
Experiment 1D
Number of Scans 512
Receiver Gain 55.5
Relaxation Delay 1.0000
Pulse Width 10.0000
Acquisition Time 1.3631
Acquisition Date 2024-05-17T23:47:29
Spectrometer Frequency 100.62
Spectral Width 24038.5
Nucleus 13C
Acquired Size 32768
Spectral Size 65536
TBSO
OEt
H
O
Me
Me
H
79
f1 (ppm)

Parameter	Value
Data File Name	/ Volumes/ nmrdata/ jkthomps/ nmr/ JKT-1-298_pure/ 3/ fid
Title	JKT-1-298_pure.3.fid
Origin	Bruker BioSpin GmbH
Solvent	CDCl3
Temperature	297.2
Pulse Sequence	zg30
Experiment	1D
Number of Scans	16
Receiver Gain	78.7
Relaxation Delay	1.0000
Pulse Width	12.5000
Acquisition Time	4.0894
Acquisition Date	2022-01-25T21:27:06
Spectrometer Frequency	400.13
Spectral Width	8012.8
Nucleus	1H
Acquired Size	32768
Spectral Size	65536

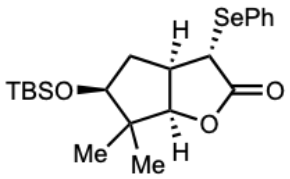

80

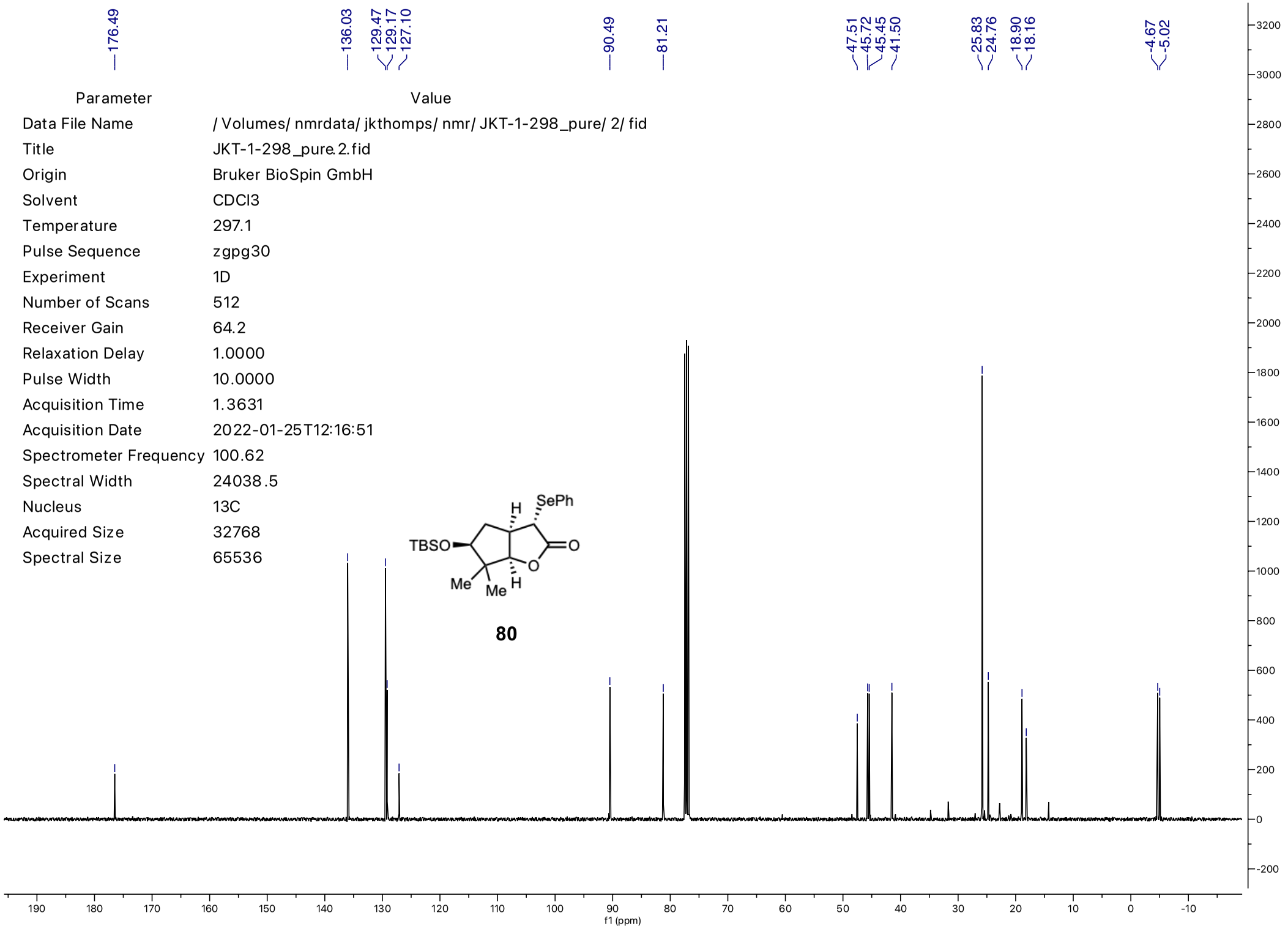
176.49
136.03
129.47
129.17
127.10
90.49
81.21
47.51
45.72
45.45
41.50
25.83
24.76
18.90
18.16
-4.67
-5.02
Parameter
Value
Data File Name
/ Volumes/ nmrdata/ jkthomps/ nmr/ JKT-1-298_pure/ 2/ fid
Title
JKT-1-298_pure.2.fid
Origin
Bruker BioSpin GmbH
Solvent
CDCl3
Temperature
297.1
Pulse Sequence
zgpg30
Experiment
1D
Number of Scans
512
Receiver Gain
64.2
Relaxation Delay
1.0000
Pulse Width
10.0000
Acquisition Time
1.3631
Acquisition Date
2022-01-25T12:16:51
Spectrometer Frequency
100.62
Spectral Width
24038.5
Nucleus
13C
Acquired Size
32768
Spectral Size
65536
H
SePh
TBSO
O
O
Me
Me
H
80
f1 (ppm)

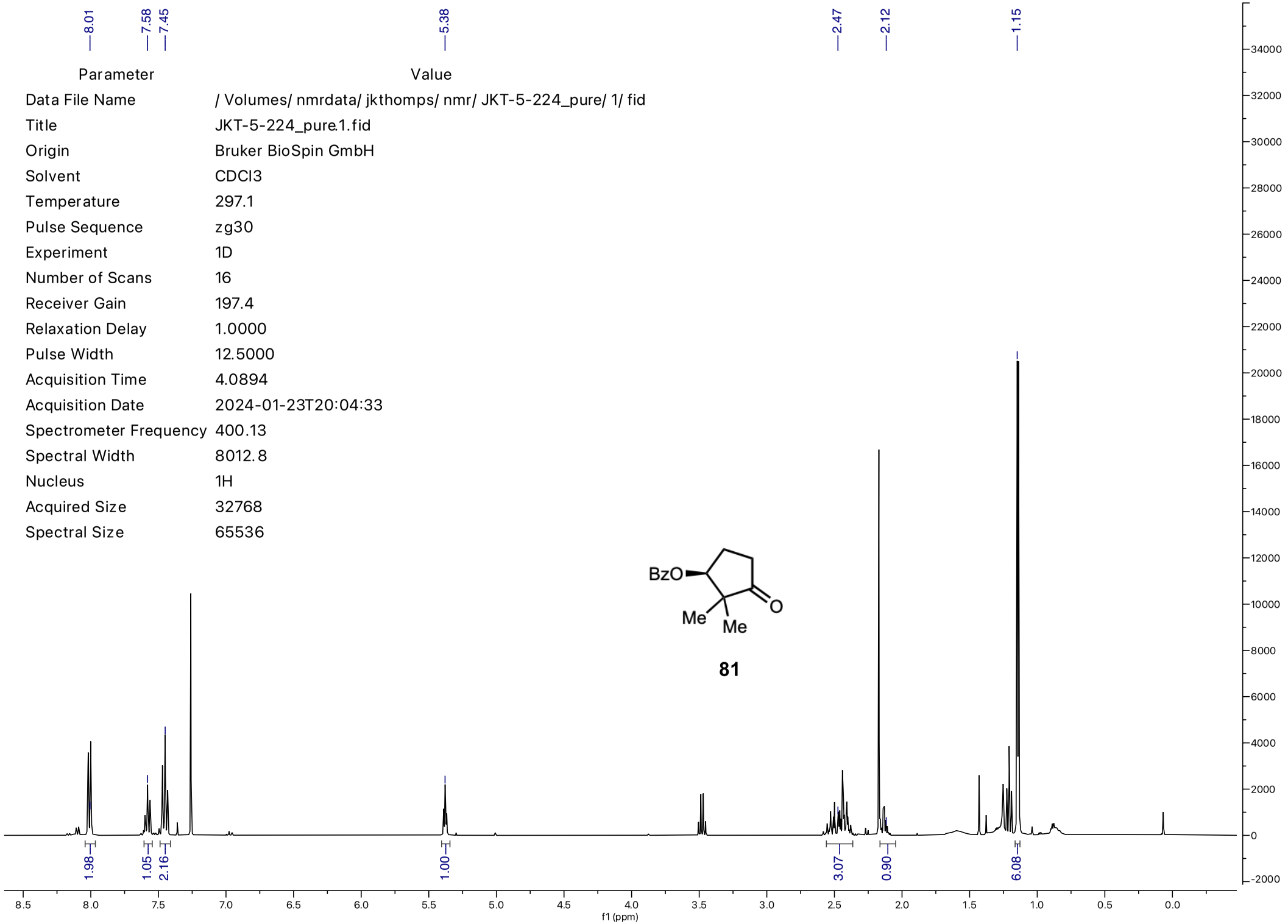
8.01
7.58
7.45
5.38
2.47
2.12
1.15
Parameter
Value
Data File Name / Volumes/ nmrdata/ jkthomps/ nmr/ JKT-5-224_pure/ 1/ fid
Title JKT-5-224_pure.1.fid
Origin Bruker BioSpin GmbH
Solvent CDCl3
Temperature 297.1
Pulse Sequence zg30
Experiment 1D
Number of Scans 16
Receiver Gain 197.4
Relaxation Delay 1.0000
Pulse Width 12.5000
Acquisition Time 4.0894
Acquisition Date 2024-01-23T20:04:33
Spectrometer Frequency 400.13
Spectral Width 8012.8
Nucleus 1H
Acquired Size 32768
Spectral Size 65536
BzO
O
Me
Me
81
1.98
1.05
2.16
1.00
3.07
0.90
6.08
f1 (ppm)

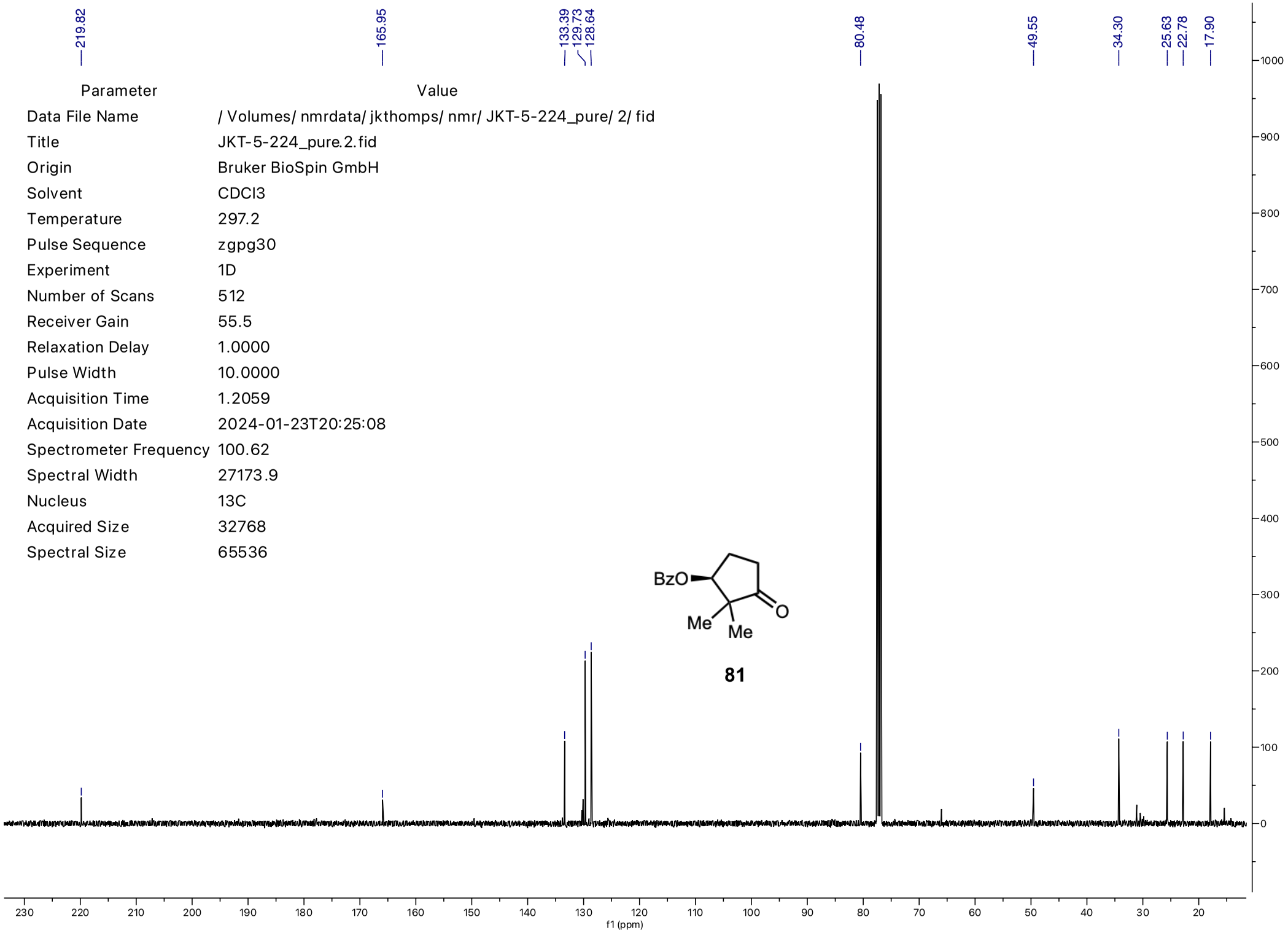
219.82
165.95
133.39
129.73
128.64
80.48
49.55
34.30
25.63
22.78
17.90
Parameter Value
Data File Name / Volumes/ nmrdata/ jkthomps/ nmr/ JKT-5-224_pure/ 2/ fid
Title JKT-5-224_pure.2.fid
Origin Bruker BioSpin GmbH
Solvent CDCl3
Temperature 297.2
Pulse Sequence zgpg30
Experiment 1D
Number of Scans 512
Receiver Gain 55.5
Relaxation Delay 1.0000
Pulse Width 10.0000
Acquisition Time 1.2059
Acquisition Date 2024-01-23T20:25:08
Spectrometer Frequency 100.62
Spectral Width 27173.9
Nucleus 13C
Acquired Size 32768
Spectral Size 65536
BzO
O
Me
Me
81
f1 (ppm)

Parameter	Value
Data File Name	/ Volumes/ nmrdata/ jkthomps/ nmr/ JKT-6-24-1/ 3/ fid
Title	JKT-6-24-1.3.fid
Origin	Bruker BioSpin GmbH
Solvent	CDCl3
Temperature	297.2
Pulse Sequence	zg30
Experiment	1D
Number of Scans	16
Receiver Gain	197.4
Relaxation Delay	1.0000
Pulse Width	12.5000
Acquisition Time	4.0894
Acquisition Date	2024-03-15T18:22:03
Spectrometer Frequency	400.13
Spectral Width	8012.8
Nucleus	1H
Acquired Size	32768
Spectral Size	65536

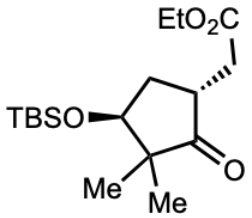

82

Parameter	Value
Data File Name	/ Volumes/ nmrdata/ jkthomps/ nmr/ JKT-6-24-1/ 2/ fid
Title	JKT-6-24-1.2.fid
Origin	Bruker BioSpin GmbH
Solvent	CDCl3
Temperature	297.1
Pulse Sequence	zgpg30
Experiment	1D
Number of Scans	700
Receiver Gain	64.2
Relaxation Delay	1.0000
Pulse Width	10.0000
Acquisition Time	1.3631
Acquisition Date	2024-03-15T18:50:51
Spectrometer Frequency	100.62
Spectral Width	24038.5
Nucleus	13C
Acquired Size	32768
Spectral Size	65536

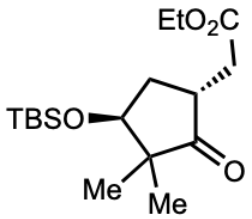

82

Parameter	Value
Data File Name	/ Users/ jordankthompson/ Desktop/ JKT-6-14-1_nextweek/ PROTON01.fid/ fid
Title	PROTON01
Origin	Varian
Solvent	cdcl3
Temperature	25.0
Pulse Sequence	s2pul
Experiment	1D
Number of Scans	8
Receiver Gain	48.0
Relaxation Delay	1.0000
Pulse Width	5.6500
Acquisition Time	3.0000
Acquisition Date	2024-03-15T11:01:23
Spectrometer Frequency	499.55
Spectral Width	8000.0
Nucleus	1H
Acquired Size	24000
Spectral Size	65536

83

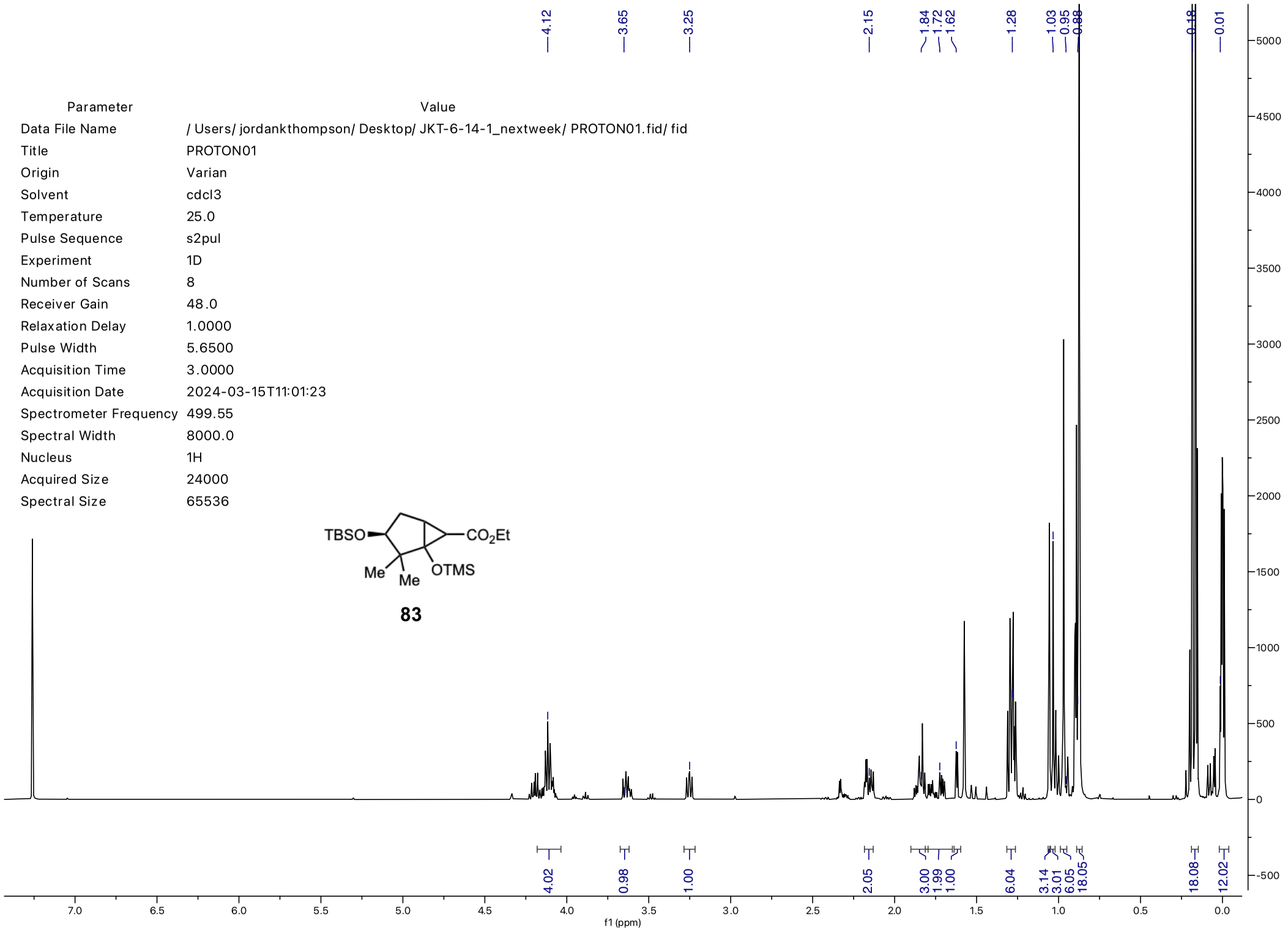

Parameter	Value
Data File Name	/ Volumes/ nmrdata-1/ data/ florence/ backup_nas/ jkthomps/ nmr/ JKT-6-14-1_13C/ 1/ fid
Title	JKT-6-14-1_13C.1.fid
Origin	Bruker BioSpin GmbH
Solvent	CDCl3
Temperature	297.1
Pulse Sequence	zgpg30
Experiment	1D
Number of Scans	750
Receiver Gain	72.0
Relaxation Delay	1.0000
Pulse Width	10.0000
Acquisition Time	1.2496
Acquisition Date	2024-03-15T15:27:50
Spectrometer Frequency	100.62
Spectral Width	26223.8
Nucleus	13C
Acquired Size	32768
Spectral Size	65536

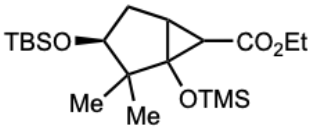

83

Parameter	Value
Data File Name	/ Volumes/ nmrdata/ jkthomps/ nmr/ JKT-6-59-1/ 1/ fid
Title	JKT-6-59-1.1.fid
Origin	Bruker BioSpin GmbH
Solvent	CDCl3
Temperature	297.1
Pulse Sequence	zg30
Experiment	1D
Number of Scans	16
Receiver Gain	112.8
Relaxation Delay	1.0000
Pulse Width	12.5000
Acquisition Time	4.0894
Acquisition Date	2024-04-05T07:51:36
Spectrometer Frequency	400.13
Spectral Width	8012.8
Nucleus	1H
Acquired Size	32768
Spectral Size	65536

84

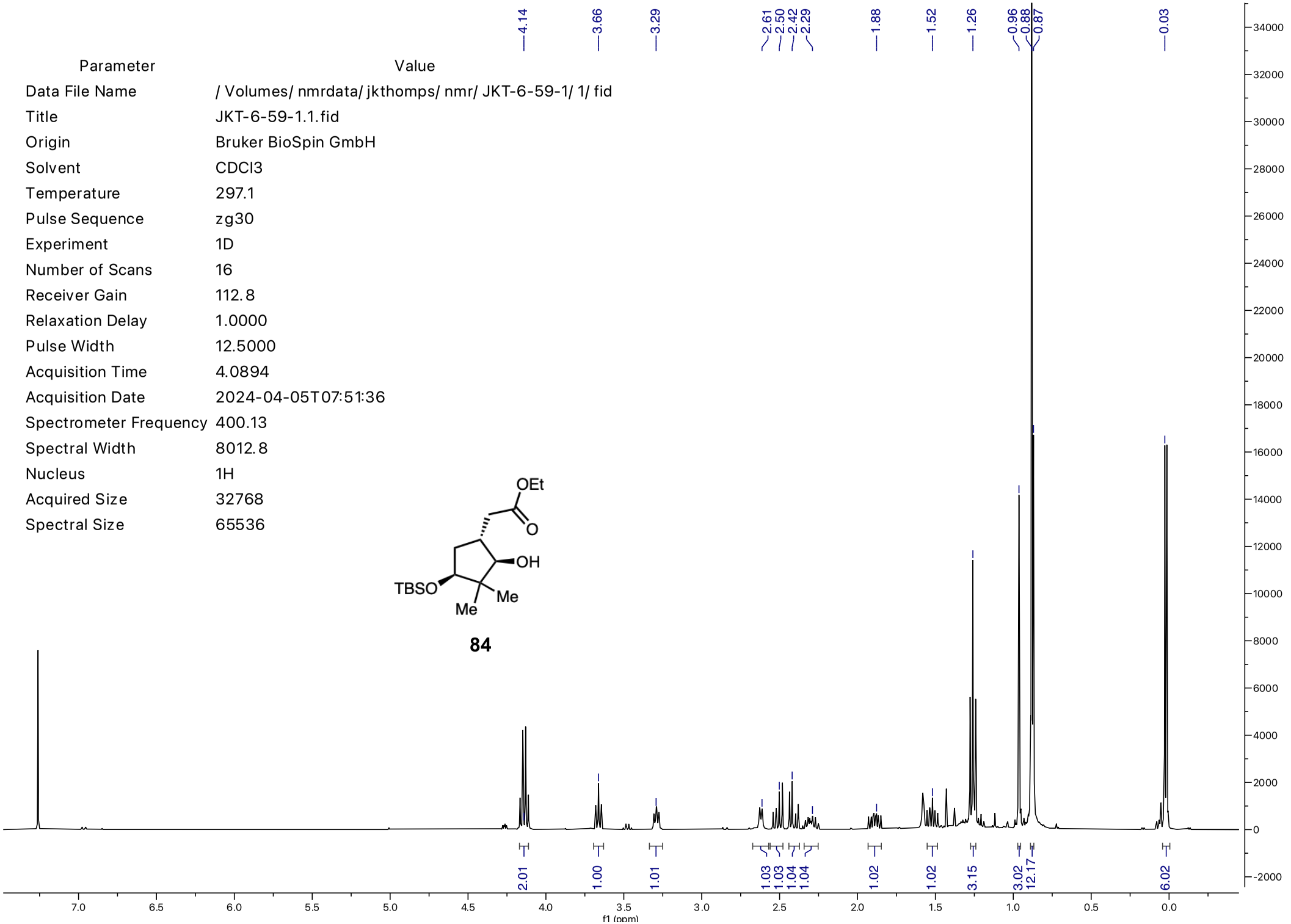

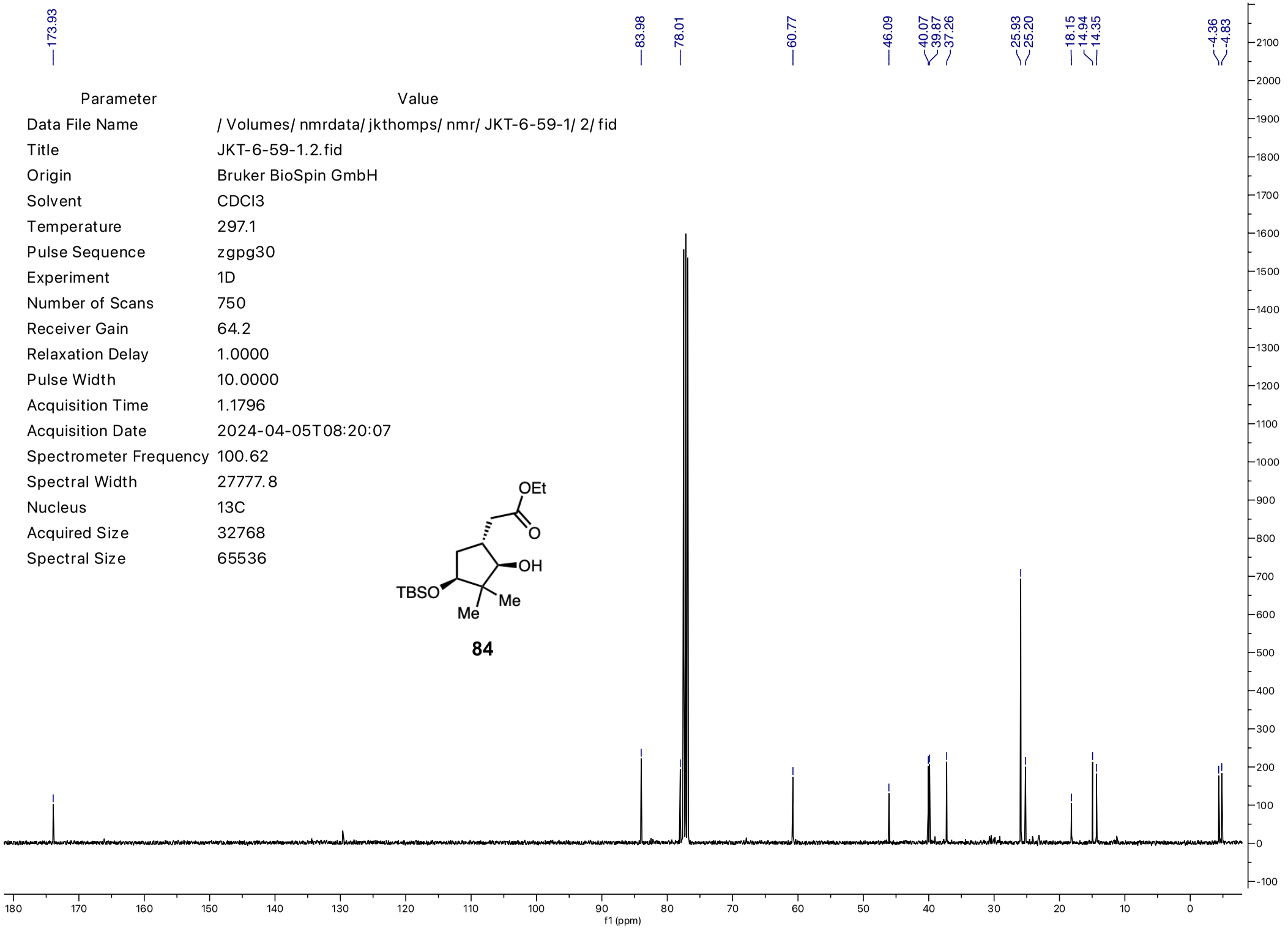

Parameter	Value
Data File Name	/ Volumes/ nmrdata/ jkthomps/ nmr/ JKT-6-59-1/ 2/ fid
Title	JKT-6-59-1.2.fid
Origin	Bruker BioSpin GmbH
Solvent	CDCl3
Temperature	297.1
Pulse Sequence	zgpg30
Experiment	1D
Number of Scans	750
Receiver Gain	64.2
Relaxation Delay	1.0000
Pulse Width	10.0000
Acquisition Time	1.1796
Acquisition Date	2024-04-05T08:20:07
Spectrometer Frequency	100.62
Spectral Width	27777.8
Nucleus	13C
Acquired Size	32768
Spectral Size	65536

84

Parameter	Value
Data File Name	/ Users/ jordankthompson/ Desktop/ JKT-6-268_pure2/ 1/ fid
Title	JKT-6-268_pure2.1.fid
Origin	Bruker BioSpin GmbH
Solvent	CDCl3
Temperature	297.2
Pulse Sequence	zg30
Experiment	1D
Number of Scans	16
Receiver Gain	176.8
Relaxation Delay	1.0000
Pulse Width	12.5000
Acquisition Time	4.0894
Acquisition Date	2024-12-05T10:07:02
Spectrometer Frequency	400.13
Spectral Width	8012.8
Nucleus	1H
Acquired Size	32768
Spectral Size	65536

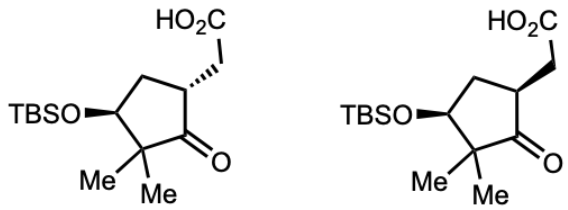

85

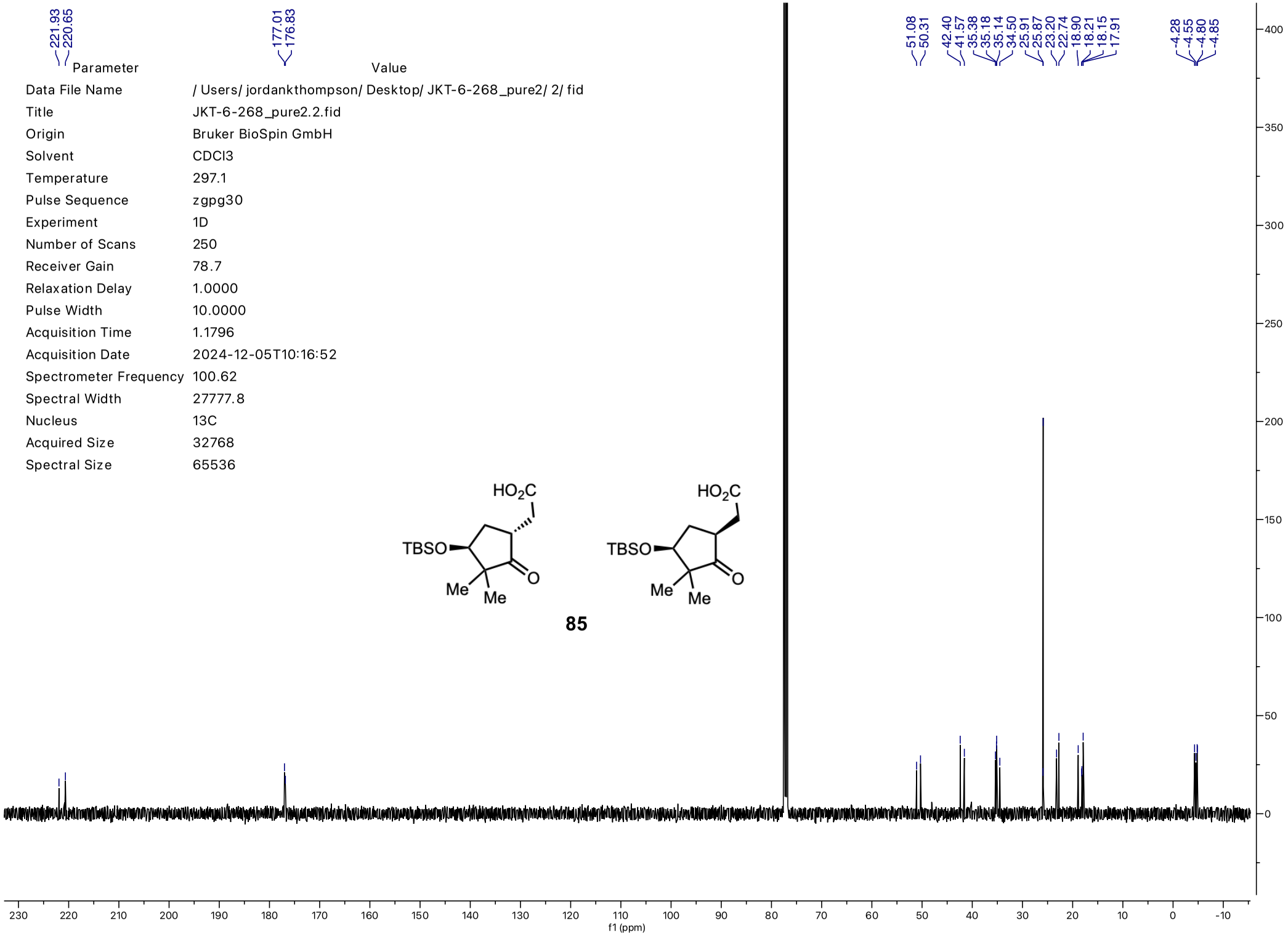
221.93
220.65
177.01
176.83
51.08
50.31
42.40
41.57
35.38
35.18
35.14
34.50
25.91
25.87
23.20
22.74
18.90
18.21
18.15
17.91
-4.28
-4.55
-4.80
-4.85
Parameter
Value
Data File Name / Users/ jordankthompson/ Desktop/ JKT-6-268_pure2/ 2/ fid
Title JKT-6-268_pure2.2.fid
Origin Bruker BioSpin GmbH
Solvent CDCl3
Temperature 297.1
Pulse Sequence zgpg30
Experiment 1D
Number of Scans 250
Receiver Gain 78.7
Relaxation Delay 1.0000
Pulse Width 10.0000
Acquisition Time 1.1796
Acquisition Date 2024-12-05T10:16:52
Spectrometer Frequency 100.62
Spectral Width 27777.8
Nucleus 13C
Acquired Size 32768
Spectral Size 65536
HO2C
TBSO
Me
Me
O
85
f1 (ppm)

Parameter	Value
Data File Name	/ Volumes/ nmrdata/ jkthomps/ nmr/ JKT-6-30_pure/ 1/ fid
Title	JKT-6-30_pure.1.fid
Origin	Bruker BioSpin GmbH
Solvent	CDCl3
Temperature	297.1
Pulse Sequence	zg30
Experiment	1D
Number of Scans	16
Receiver Gain	197.4
Relaxation Delay	1.0000
Pulse Width	12.5000
Acquisition Time	4.0894
Acquisition Date	2024-03-25T23:59:45
Spectrometer Frequency	400.13
Spectral Width	8012.8
Nucleus	1H
Acquired Size	32768
Spectral Size	65536

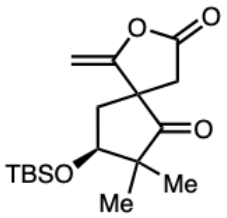

86

Parameter	Value
Data File Name	/ Volumes/ nmrdata/ jkthomps/ nmr/ JKT-6-30_pure/ 2/ fid
Title	JKT-6-30_pure.2.fid
Origin	Bruker BioSpin GmbH
Solvent	CDCl3
Temperature	297.2
Pulse Sequence	zgpg30
Experiment	1D
Number of Scans	1024
Receiver Gain	72.0
Relaxation Delay	1.0000
Pulse Width	10.0000
Acquisition Time	1.1796
Acquisition Date	2024-03-26T00:38:30
Spectrometer Frequency	100.62
Spectral Width	27777.8
Nucleus	13C
Acquired Size	32768
Spectral Size	65536

86

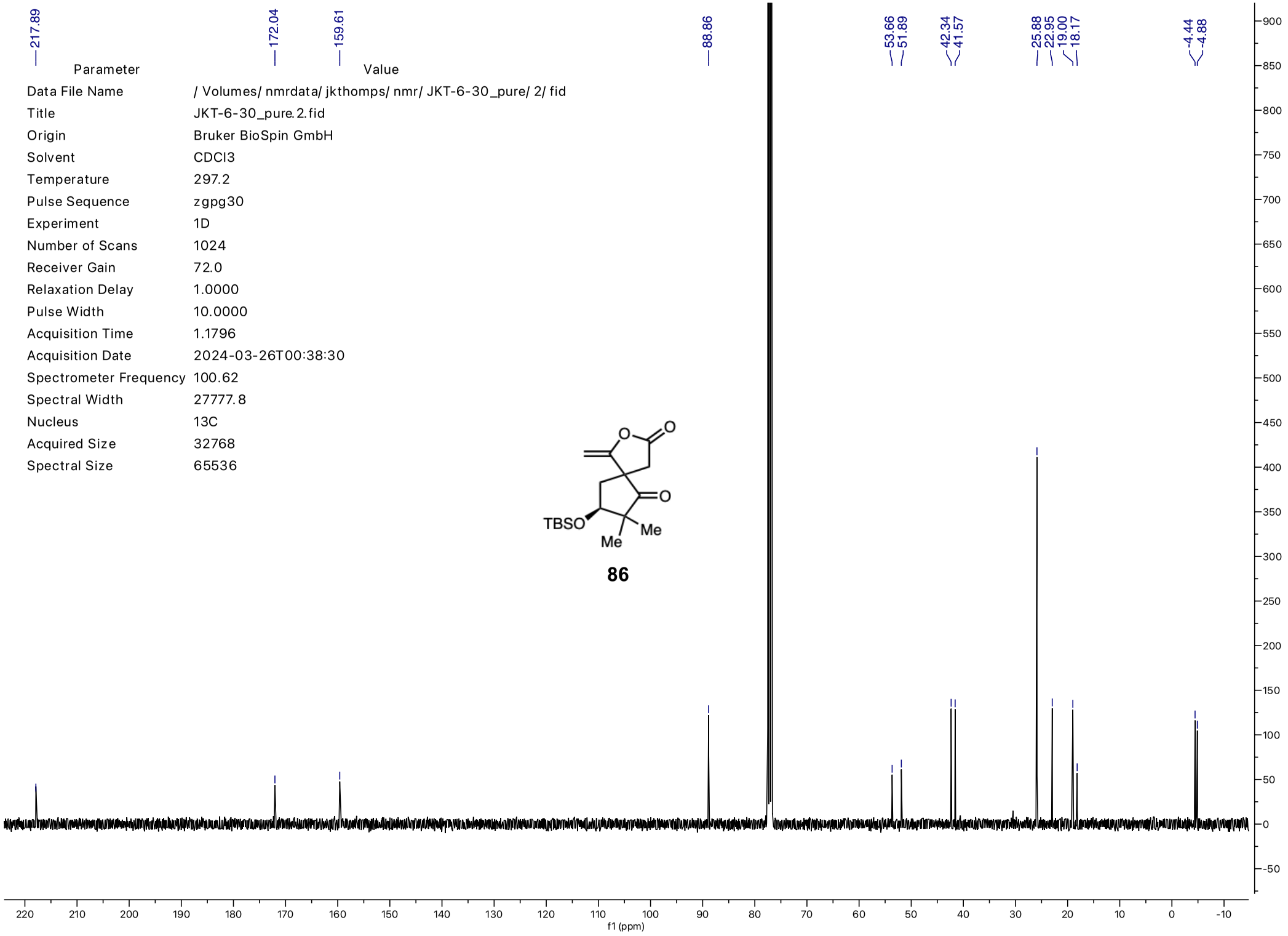

Parameter	Value
Data File Name	/ Volumes/ nmrdata/ jkthomps/ nmr/ JKT-6-30_pure/ 3/ ser
Title	JKT-6-30_pure.3.ser
Origin	Bruker BioSpin GmbH
Solvent	CDCl3
Temperature	297.1
Pulse Sequence	cosygpppqf
Experiment	COSY
Number of Scans	2
Receiver Gain	176.8
Relaxation Delay	1.9185
Pulse Width	12.5000
Acquisition Time	0.2785
Acquisition Date	2024-03-26T00:49:03
Spectrometer Frequency	(400.13,400.13)
Spectral Width	(3676.5,3676.5)
Lowest Frequency	(-384.9,-378.6)
Nucleus	(1H,1H)
Acquired Size	(1024,128)
Spectral Size	(1024,1024)
Digital Resolution	(3.59,3.59)

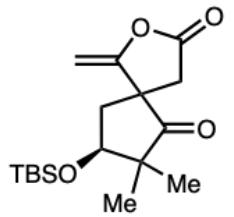

86

f2 (ppm)

f1 (ppm)

Parameter	Value
Data File Name	/ Volumes/ nmrdata/ jkthomps/ nmr/ JKT-6-30_pure/ 4/ ser
Title	JKT-6-30_pure.4.ser
Origin	Bruker BioSpin GmbH
Solvent	CDCl3
Temperature	297.1
Pulse Sequence	hsqcedetgpsisp2.4
Experiment	HSQC-EDITED
Number of Scans	4
Receiver Gain	197.4
Relaxation Delay	1.5000
Pulse Width	12.5000
Acquisition Time	0.2135
Acquisition Date	2024-03-26T01:11:13
Spectrometer Frequency	(400.13,100.62)
Spectral Width	(4795.4,16611.3)
Lowest Frequency	(-518.5,-1262.8)
Nucleus	(1H,13C)
Acquired Size	(1024,180)
Spectral Size	(1024,1024)
Digital Resolution	(4.68,16.22)

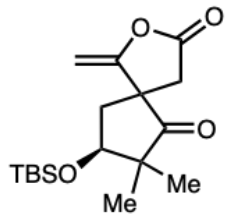

86

f2 (ppm)

f1 (ppm)

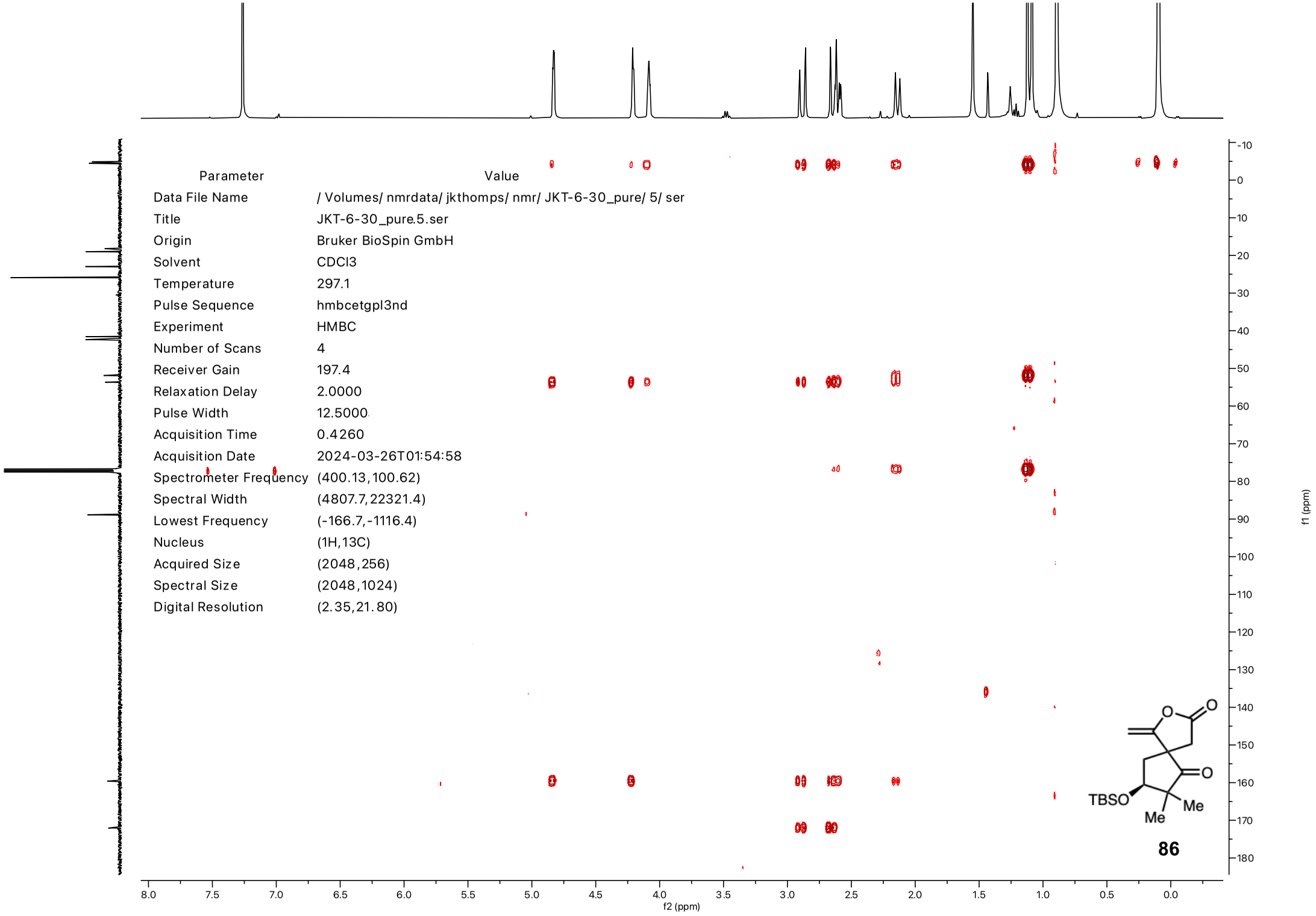
Parameter Value
Data File Name / Volumes/ nmrdata/ jkthomps/ nmr/ JKT-6-30_pure/ 5/ ser
Title JKT-6-30_pure.5.ser
Origin Bruker BioSpin GmbH
Solvent CDCl3
Temperature 297.1
Pulse Sequence hmbcetgpl3nd
Experiment HMBC
Number of Scans 4
Receiver Gain 197.4
Relaxation Delay 2.0000
Pulse Width 12.5000
Acquisition Time 0.4260
Acquisition Date 2024-03-26T01:54:58
Spectrometer Frequency (400.13,100.62)
Spectral Width (4807.7,22321.4)
Lowest Frequency (-166.7,-1116.4)
Nucleus (1H,13C)
Acquired Size (2048,256)
Spectral Size (2048,1024)
Digital Resolution (2.35,21.80)
f2 (ppm)
f1 (ppm)
TBSO
Me
Me
86

Parameter	Value
Data File Name	/ Users/ jordankthompson/ Desktop/ JKT-6-269_pure_RR/ 1/ fid
Title	JKT-6-269_pure_RR.1.fid
Origin	Bruker BioSpin GmbH
Solvent	CDCl3
Temperature	297.2
Pulse Sequence	zg30
Experiment	1D
Number of Scans	16
Receiver Gain	50.3
Relaxation Delay	1.0000
Pulse Width	12.5000
Acquisition Time	4.0894
Acquisition Date	2024-12-06T14:55:30
Spectrometer Frequency	400.13
Spectral Width	8012.8
Nucleus	1H
Acquired Size	32768
Spectral Size	65536

87

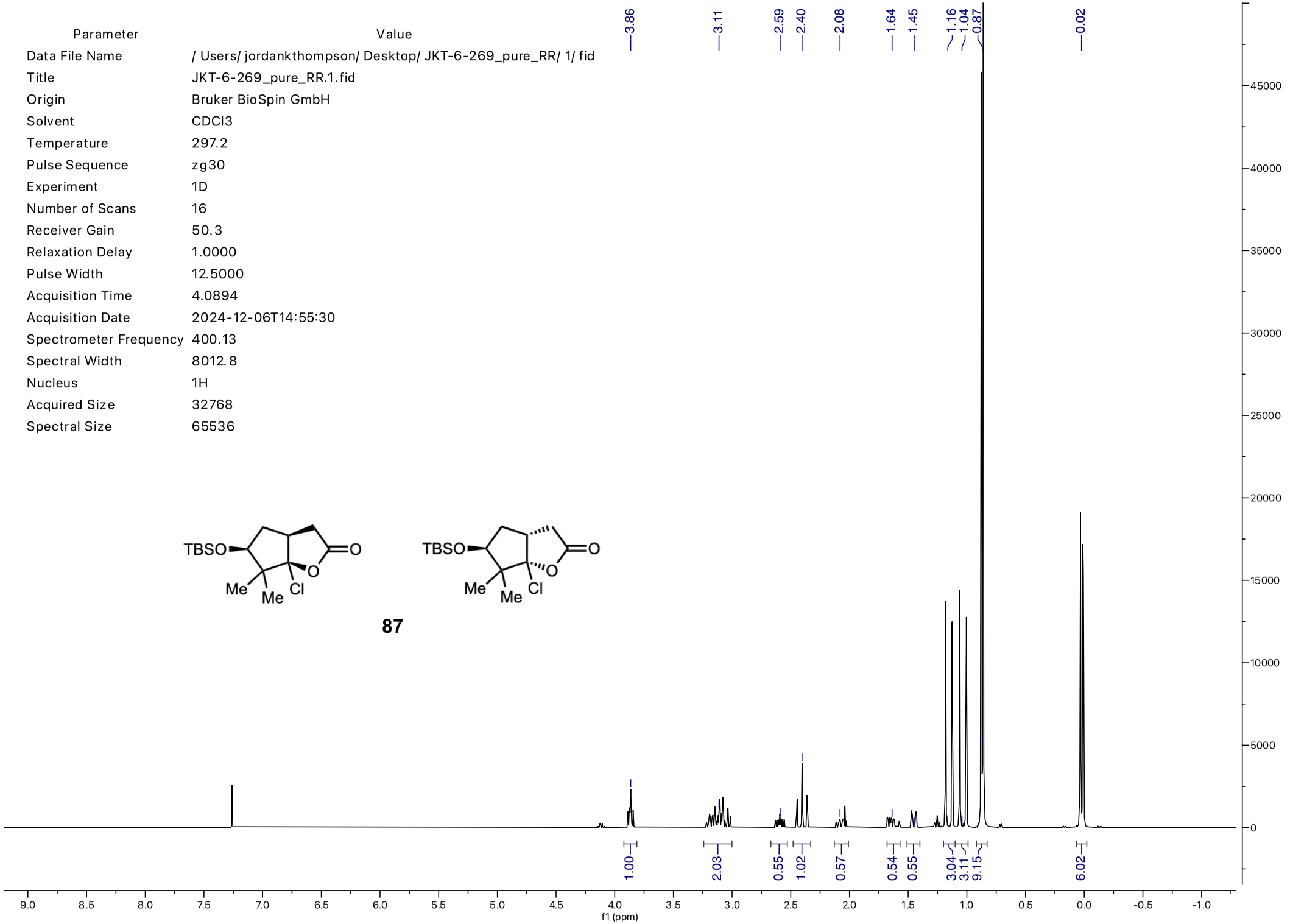

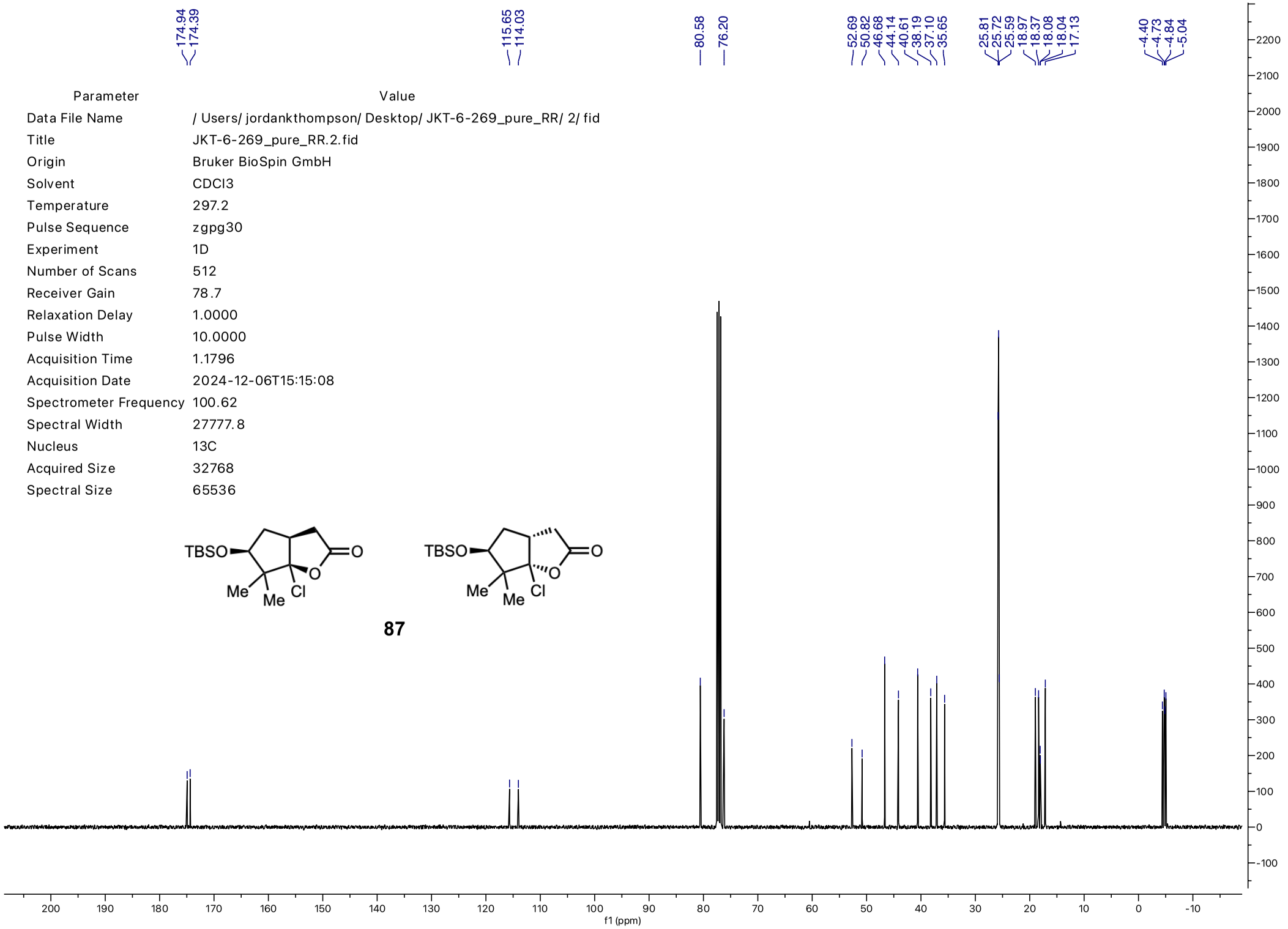

Parameter	Value
Data File Name	/ Users/ jordankthompson/ Desktop/ JKT-6-269_pure_RR/ 2/ fid
Title	JKT-6-269_pure_RR.2.fid
Origin	Bruker BioSpin GmbH
Solvent	CDCl3
Temperature	297.2
Pulse Sequence	zgpg30
Experiment	1D
Number of Scans	512
Receiver Gain	78.7
Relaxation Delay	1.0000
Pulse Width	10.0000
Acquisition Time	1.1796
Acquisition Date	2024-12-06T15:15:08
Spectrometer Frequency	100.62
Spectral Width	27777.8
Nucleus	13C
Acquired Size	32768
Spectral Size	65536

87

Parameter	Value
Data File Name	/ Volumes/ nmrdata/ jkthomps/ nmr/ JKT-6-42-2/ 1/ fid
Title	JKT-6-42-2.1.fid
Origin	Bruker BioSpin GmbH
Solvent	CDCl3
Temperature	297.2
Pulse Sequence	zg30
Experiment	1D
Number of Scans	16
Receiver Gain	197.4
Relaxation Delay	1.0000
Pulse Width	12.5000
Acquisition Time	4.0894
Acquisition Date	2024-03-30T09:31:33
Spectrometer Frequency	400.13
Spectral Width	8012.8
Nucleus	1H
Acquired Size	32768
Spectral Size	65536

87A

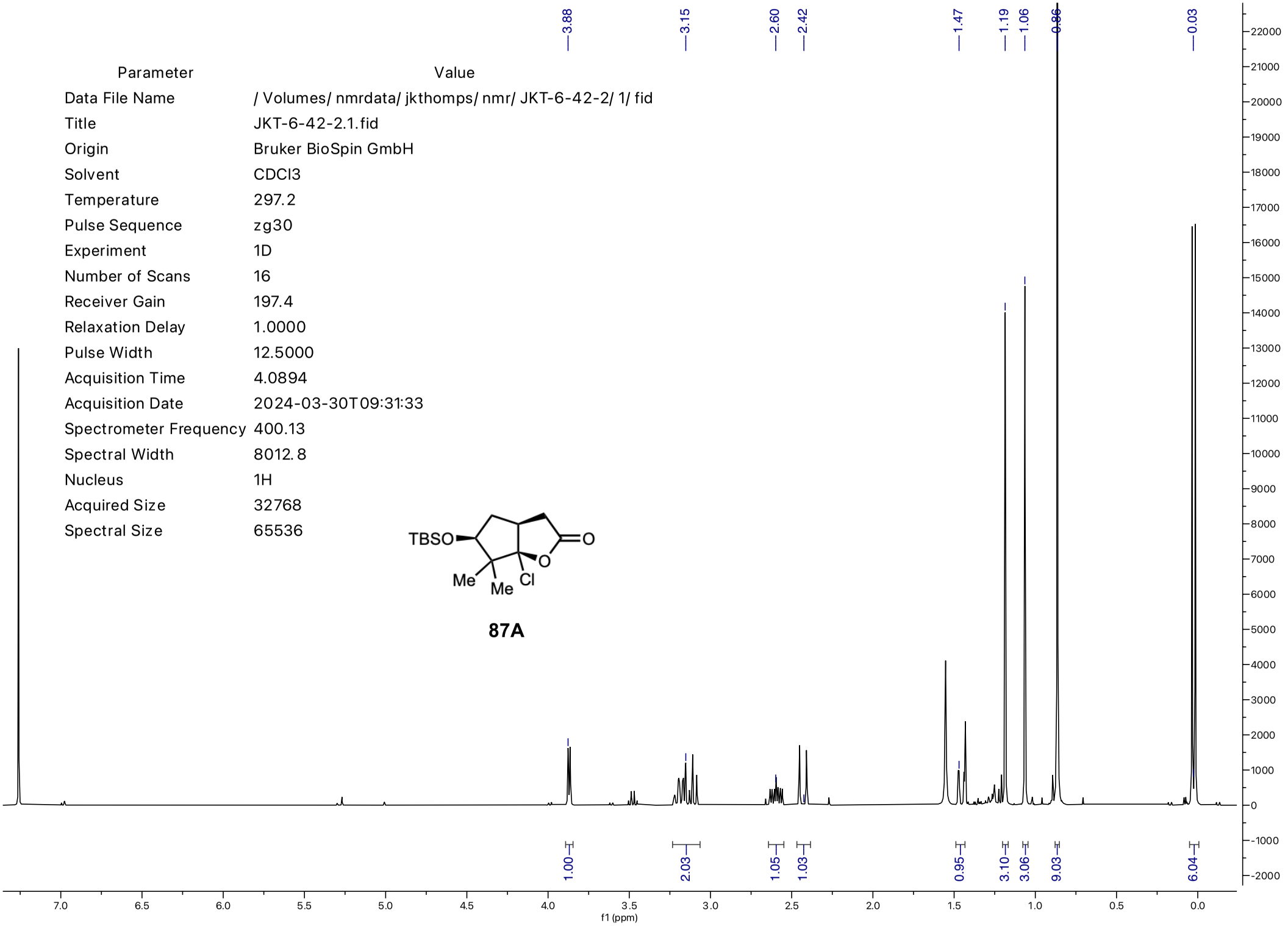

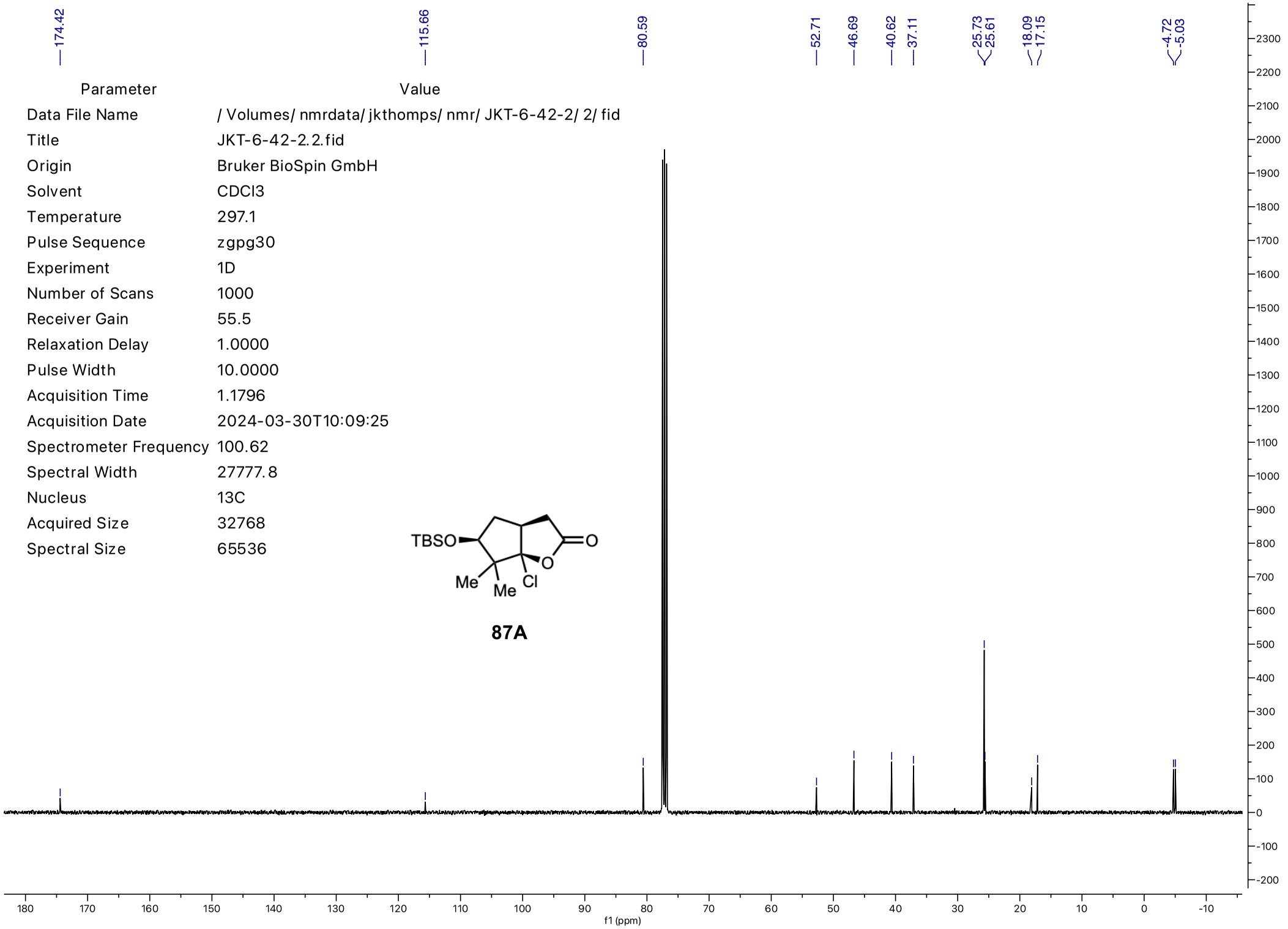
174.42
115.66
80.59
52.71
46.69
40.62
37.11
25.73
25.61
18.09
17.15
-4.72
-5.03
Parameter
Value
Data File Name
/ Volumes/ nmrdata/ jkthomps/ nmr/ JKT-6-42-2/ 2/ fid
Title
JKT-6-42-2.2.fid
Origin
Bruker BioSpin GmbH
Solvent
CDCl3
Temperature
297.1
Pulse Sequence
zgpg30
Experiment
1D
Number of Scans
1000
Receiver Gain
55.5
Relaxation Delay
1.0000
Pulse Width
10.0000
Acquisition Time
1.1796
Acquisition Date
2024-03-30T10:09:25
Spectrometer Frequency
100.62
Spectral Width
27777.8
Nucleus
13C
Acquired Size
32768
Spectral Size
65536
TBSO
O
O
Me
Me
Cl
87A
f1 (ppm)

Parameter	Value
Data File Name	/ Volumes/ nmrdata/ jkthomps/ nmr/ JKT-6-42-1/ 1/ fid
Title	JKT-6-42-1.1.fid
Origin	Bruker BioSpin GmbH
Solvent	CDCl3
Temperature	297.1
Pulse Sequence	zg30
Experiment	1D
Number of Scans	16
Receiver Gain	197.4
Relaxation Delay	1.0000
Pulse Width	12.5000
Acquisition Time	4.0894
Acquisition Date	2024-03-30T10:17:06
Spectrometer Frequency	400.13
Spectral Width	8012.8
Nucleus	1H
Acquired Size	32768
Spectral Size	65536

87B

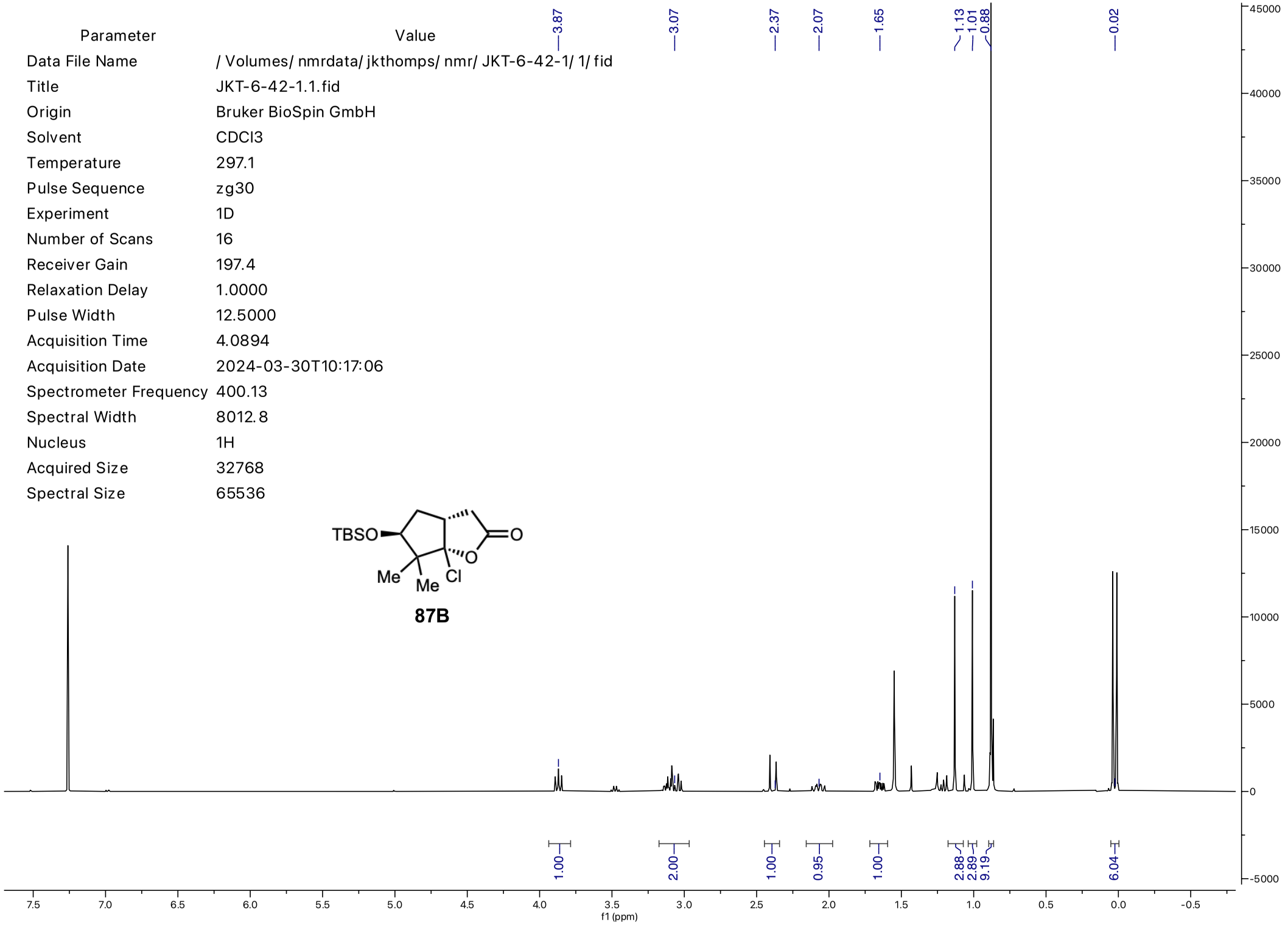

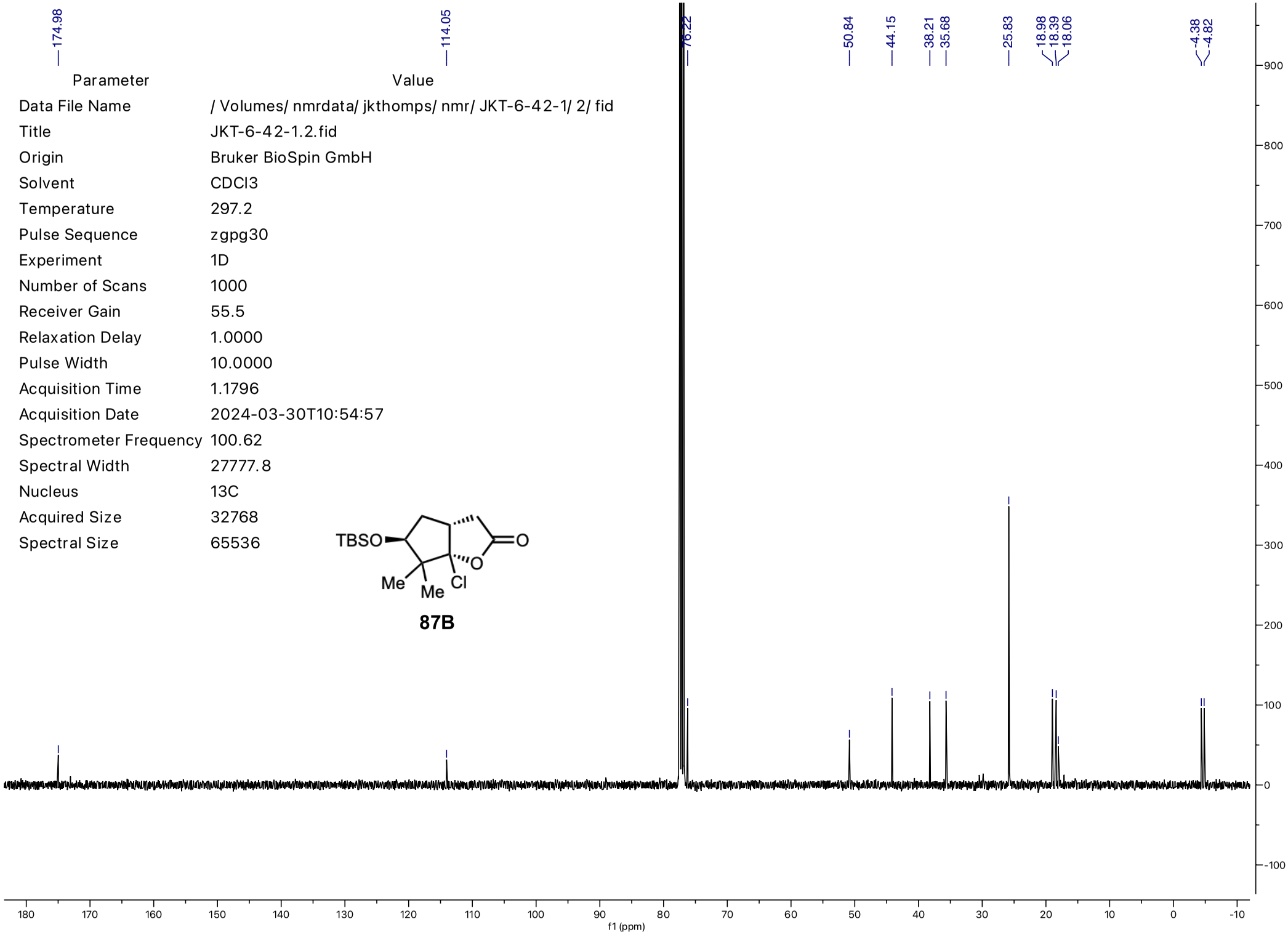

Parameter	Value
Data File Name	/ Volumes/ nmrdata/ jkthomps/ nmr/ JKT-6-42-1/ 2/ fid
Title	JKT-6-42-1.2.fid
Origin	Bruker BioSpin GmbH
Solvent	CDCl3
Temperature	297.2
Pulse Sequence	zgpg30
Experiment	1D
Number of Scans	1000
Receiver Gain	55.5
Relaxation Delay	1.0000
Pulse Width	10.0000
Acquisition Time	1.1796
Acquisition Date	2024-03-30T10:54:57
Spectrometer Frequency	100.62
Spectral Width	27777.8
Nucleus	13C
Acquired Size	32768
Spectral Size	65536

87B

Parameter	Value
Data File Name	/ Volumes/ nmrdata/ jkthomps/ nmr/ JKT-1-304_pure/ 1/ fid
Title	JKT-1-304_pure.1.fid
Origin	Bruker BioSpin GmbH
Solvent	CDCl3
Temperature	297.2
Pulse Sequence	zg30
Experiment	1D
Number of Scans	16
Receiver Gain	112.8
Relaxation Delay	1.0000
Pulse Width	12.5000
Acquisition Time	4.0894
Acquisition Date	2022-01-31T14:46:01
Spectrometer Frequency	400.13
Spectral Width	8012.8
Nucleus	1H
Acquired Size	32768
Spectral Size	65536

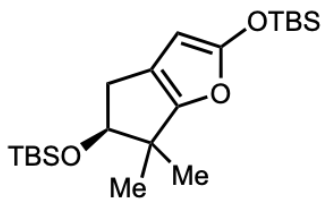

88

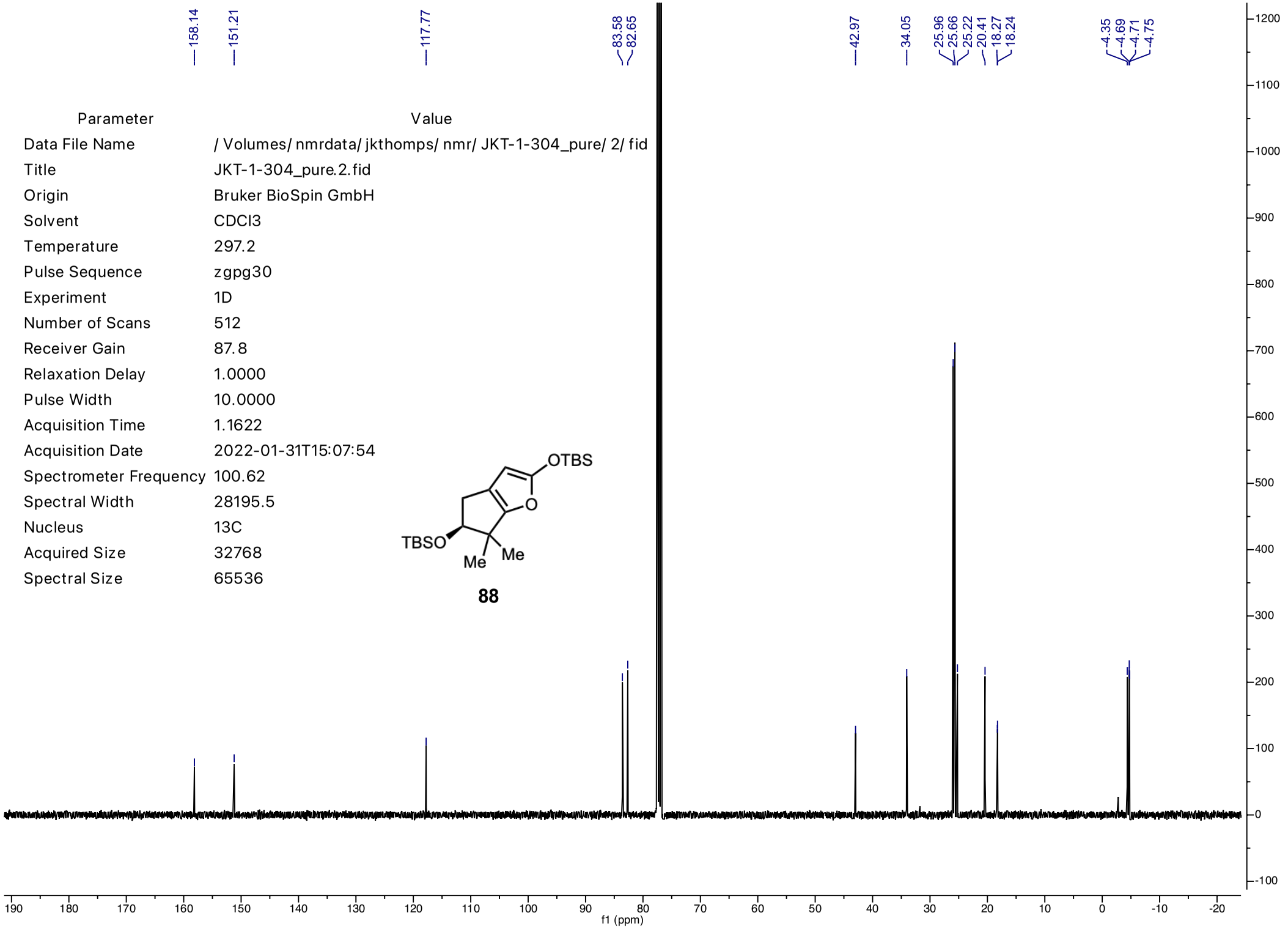

Parameter	Value
Data File Name	/ Volumes/ nmrdata/ jkthomps/ nmr/ JKT-1-304_pure/ 2/ fid
Title	JKT-1-304_pure.2.fid
Origin	Bruker BioSpin GmbH
Solvent	CDCl3
Temperature	297.2
Pulse Sequence	zgpg30
Experiment	1D
Number of Scans	512
Receiver Gain	87.8
Relaxation Delay	1.0000
Pulse Width	10.0000
Acquisition Time	1.1622
Acquisition Date	2022-01-31T15:07:54
Spectrometer Frequency	100.62
Spectral Width	28195.5
Nucleus	13C
Acquired Size	32768
Spectral Size	65536

88

Parameter	Value
Data File Name	/ Volumes/ nmrdata/ jkthomps/ nmr/ JKT-1-181-5/ 1/ fid
Title	JKT-1-181-5.1.fid
Origin	Bruker BioSpin GmbH
Solvent	CDCl3
Temperature	297.2
Pulse Sequence	zg30
Experiment	1D
Number of Scans	16
Receiver Gain	197.4
Relaxation Delay	1.0000
Pulse Width	12.5000
Acquisition Time	4.0894
Acquisition Date	2021-08-05T13:57:57
Spectrometer Frequency	400.13
Spectral Width	8012.8
Nucleus	1H
Acquired Size	32768
Spectral Size	65536

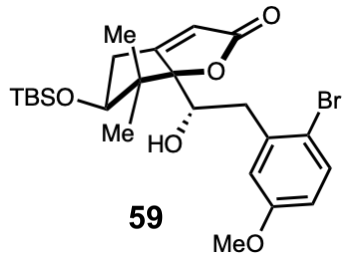

59

Parameter	Value
Data File Name	/ Volumes/ nmrdata/ jkthomps/ nmr/ JKT-1-characterization-4/ 6/ fid
Title	JKT-1-characterization-4.6.fid
Origin	Bruker BioSpin GmbH
Solvent	CDCl3
Temperature	297.1
Pulse Sequence	zgpg30
Experiment	1D
Number of Scans	512
Receiver Gain	55.5
Relaxation Delay	1.0000
Pulse Width	10.0000
Acquisition Time	1.3631
Acquisition Date	2021-12-22T14:01:33
Spectrometer Frequency	100.62
Spectral Width	24038.5
Nucleus	13C
Acquired Size	32768
Spectral Size	65536

59

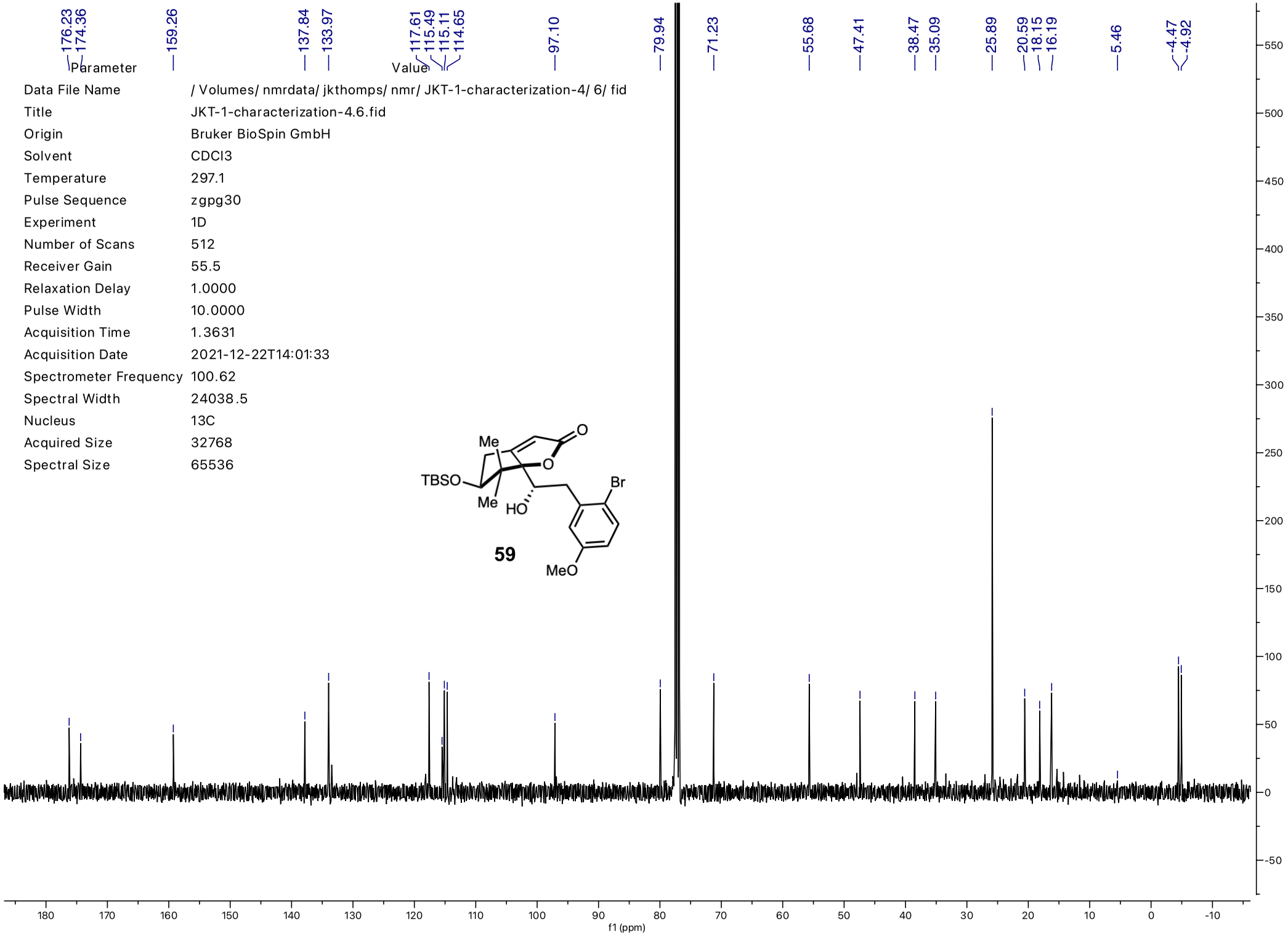

Parameter	Value
Data File Name	/ Volumes/ nmrdata/ jkthomps/ nmr/ JKT-1-characterization-4/ 6/ fid
Title	JKT-1-characterization-4.6.fid
Origin	Bruker BioSpin GmbH
Solvent	CDCl3
Temperature	297.1
Pulse Sequence	zgpg30
Experiment	1D
Number of Scans	512
Receiver Gain	55.5
Relaxation Delay	1.0000
Pulse Width	10.0000
Acquisition Time	1.3631
Acquisition Date	2021-12-22T14:01:33
Spectrometer Frequency	100.62
Spectral Width	24038.5
Nucleus	13C
Acquired Size	32768
Spectral Size	65536

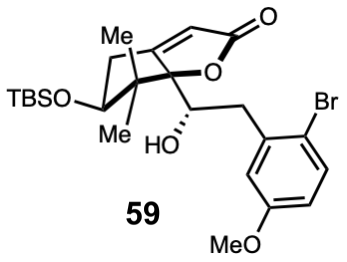

59

f2 (ppm)

f1 (ppm)

Parameter	Value
Data File Name	/ Users/ jordankthompson/ Desktop/ JKT-5-246_sm_pure/ 1/ fid
Title	JKT-5-246_sm_pure.1.fid
Origin	Bruker BioSpin GmbH
Solvent	CDCl3
Temperature	297.2
Pulse Sequence	zg30
Experiment	1D
Number of Scans	16
Receiver Gain	30.3
Relaxation Delay	1.0000
Pulse Width	12.5000
Acquisition Time	4.0894
Acquisition Date	2024-02-06T15:41:27
Spectrometer Frequency	400.13
Spectral Width	8012.8
Nucleus	1H
Acquired Size	32768
Spectral Size	65536

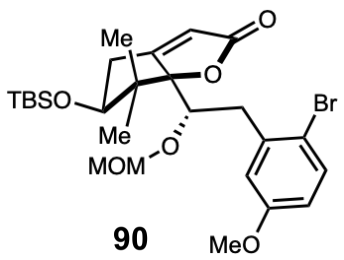

90

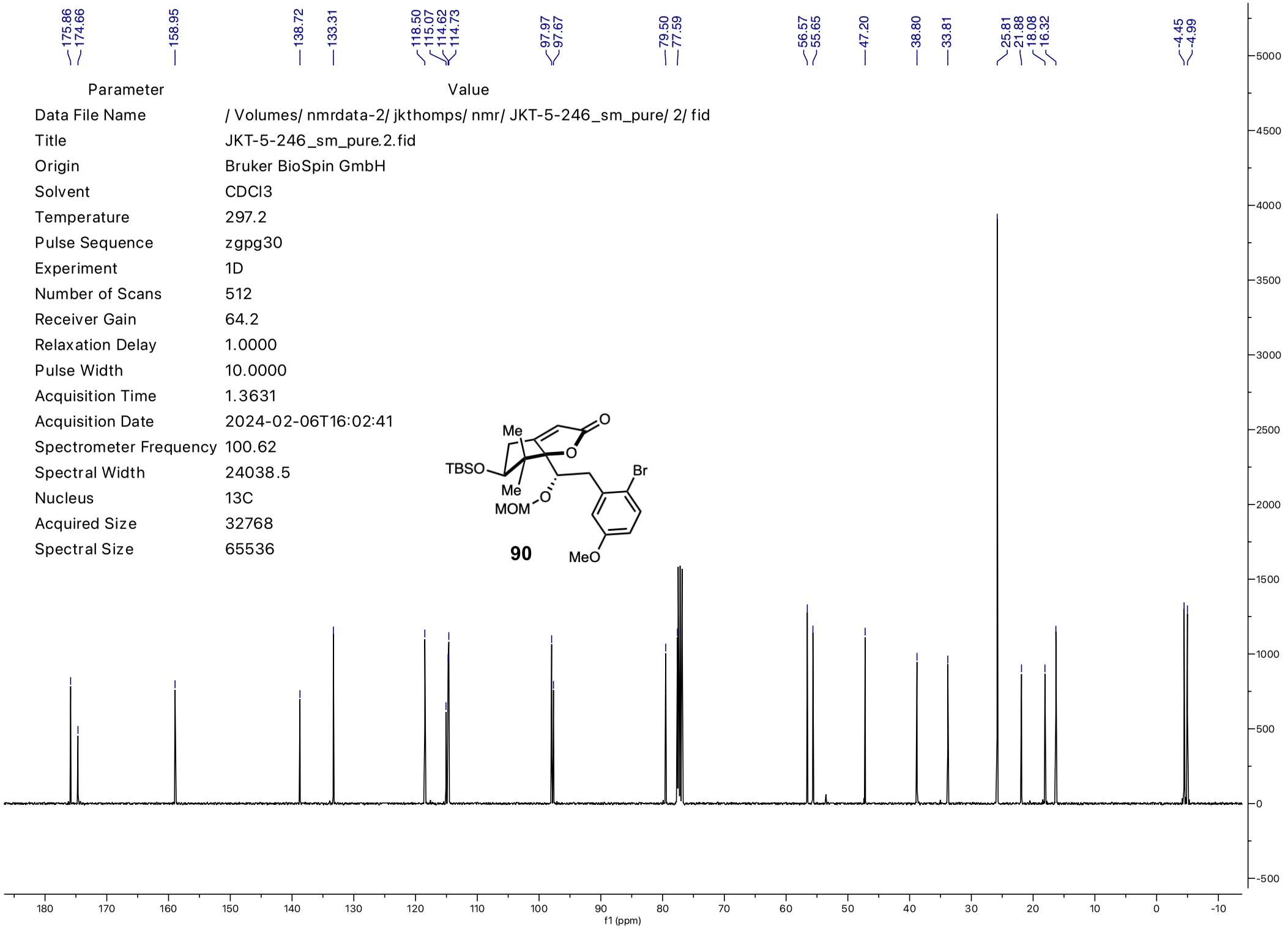
175.86
174.66
158.95
138.72
133.31
118.50
115.07
114.62
114.73
97.97
97.67
79.50
77.59
56.57
55.65
47.20
38.80
33.81
25.81
21.88
18.08
16.32
-4.45
-4.99
Parameter
Value
Data File Name
/ Volumes/ nmrdata-2/ jkthomps/ nmr/ JKT-5-246_sm_pure/ 2/ fid
Title
JKT-5-246_sm_pure.2.fid
Origin
Bruker BioSpin GmbH
Solvent
CDCl3
Temperature
297.2
Pulse Sequence
zgpg30
Experiment
1D
Number of Scans
512
Receiver Gain
64.2
Relaxation Delay
1.0000
Pulse Width
10.0000
Acquisition Time
1.3631
Acquisition Date
2024-02-06T16:02:41
Spectrometer Frequency
100.62
Spectral Width
24038.5
Nucleus
13C
Acquired Size
32768
Spectral Size
65536
Me
O
O
TBSO
Br
Me
MOM
O
MeO
90
5000
4500
4000
3500
3000
2500
2000
1500
1000
500
0
-500
180
170
160
150
140
130
120
110
100
90
80
70
60
50
40
30
20
10
0
-10
f1 (ppm)

Parameter	Value
Data File Name	/ Volumes/ nmrdata-2/ jkthomps/ nmr/ JKT-5-246_sm_pure/ 3/ ser
Title	JKT-5-246_sm_pure.3.ser
Origin	Bruker BioSpin GmbH
Solvent	CDCl3
Temperature	297.2
Pulse Sequence	cosygpppqf
Experiment	COSY
Number of Scans	1
Receiver Gain	10.8
Relaxation Delay	1.9308
Pulse Width	12.5000
Acquisition Time	0.2662
Acquisition Date	2024-02-06T16:08:25
Spectrometer Frequency	(400.13,400.13)
Spectral Width	(3846.2,3846.2)
Lowest Frequency	(-478.5,-452.6)
Nucleus	(1H,1H)
Acquired Size	(1024,128)
Spectral Size	(1024,1024)
Digital Resolution	(3.76,3.76)

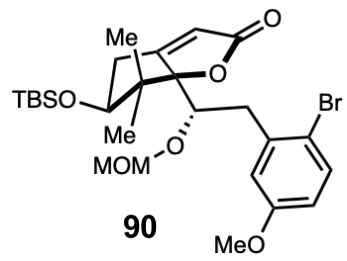

90

f2 (ppm)

f1 (ppm)

Parameter	Value
Data File Name	/ Volumes/ nmrdata/ jkthomps/ nmr/ JKT-1-compound11_1H/ 1/ fid
Title	JKT-1-compound11_1H.1.fid
Origin	Bruker BioSpin GmbH
Solvent	CDCl3
Temperature	297.1
Pulse Sequence	zg30
Experiment	1D
Number of Scans	16
Receiver Gain	156.2
Relaxation Delay	1.0000
Pulse Width	12.5000
Acquisition Time	4.0894
Acquisition Date	2022-05-07T15:43:45
Spectrometer Frequency	400.13
Spectral Width	8012.8
Nucleus	1H
Acquired Size	32768
Spectral Size	65536

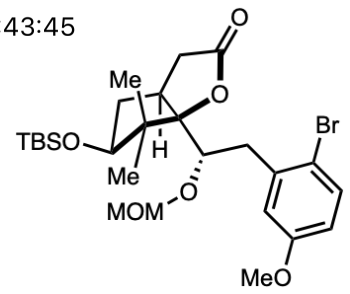

58

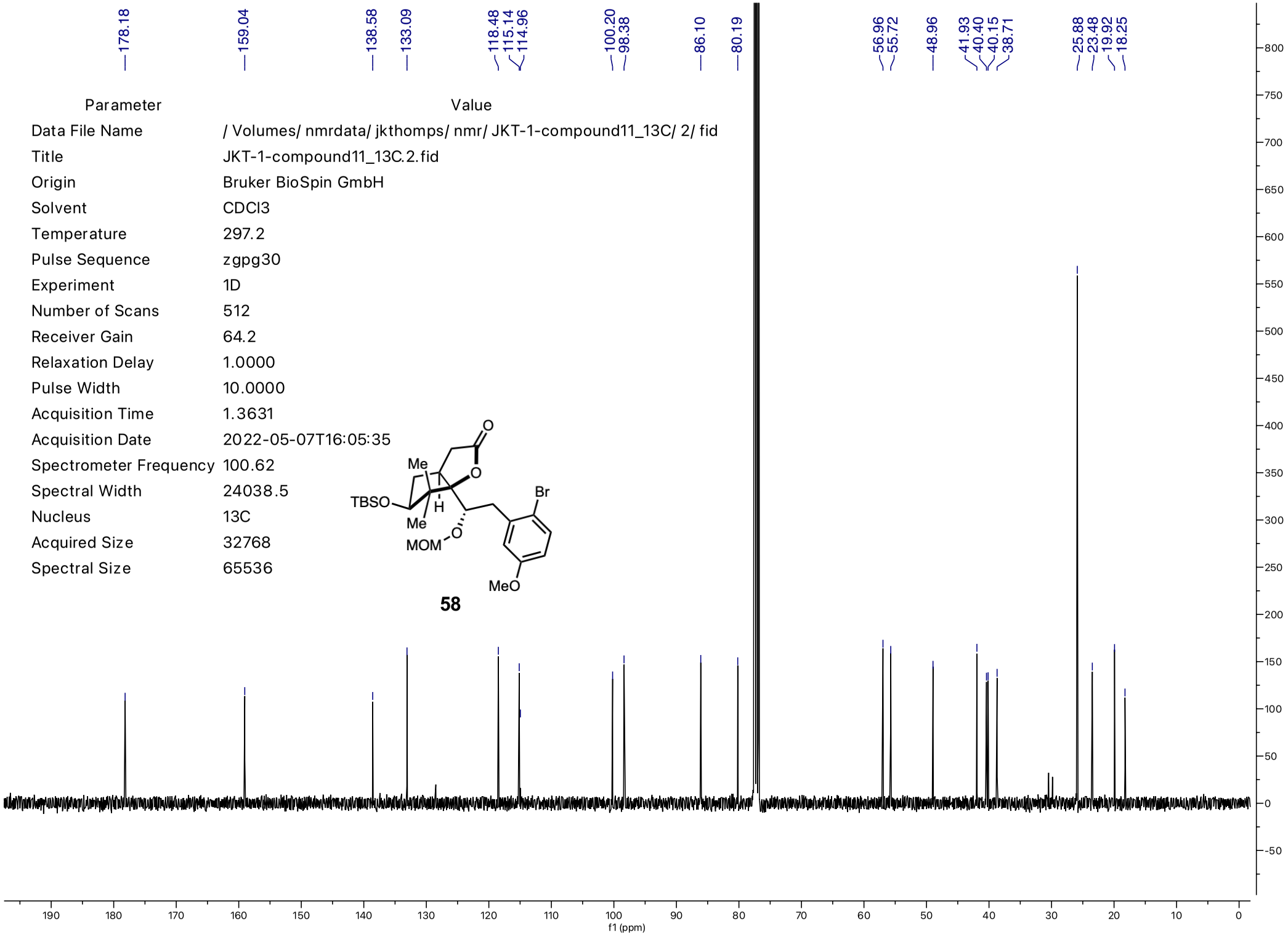
178.18
159.04
138.58
133.09
118.48
115.14
114.96
100.20
98.38
86.10
80.19
56.96
55.72
48.96
41.93
40.40
40.15
38.71
25.88
23.48
19.92
18.25
Parameter
Value
Data File Name
/ Volumes/ nmrdata/ jkthomps/ nmr/ JKT-1-compound11_13C/ 2/ fid
Title
JKT-1-compound11_13C.2.fid
Origin
Bruker BioSpin GmbH
Solvent
CDCl3
Temperature
297.2
Pulse Sequence
zgpg30
Experiment
1D
Number of Scans
512
Receiver Gain
64.2
Relaxation Delay
1.0000
Pulse Width
10.0000
Acquisition Time
1.3631
Acquisition Date
2022-05-07T16:05:35
Spectrometer Frequency
100.62
Spectral Width
24038.5
Nucleus
13C
Acquired Size
32768
Spectral Size
65536
O
Me
O
TBSO
H
Br
Me
MOM
O
MeO
58
800
750
700
650
600
550
500
450
400
350
300
250
200
150
100
50
0
-50
190
180
170
160
150
140
130
120
110
100
90
80
70
60
50
40
30
20
10
0
f1 (ppm)

Parameter	Value
Data File Name	/ Users/ jordankthompson/ Desktop/ JKT-1-268-1/ PROTON01.fid/ fid
Title	PROTON01
Origin	Varian
Solvent	cdcl3
Temperature	3.0
Pulse Sequence	s2pul
Experiment	1D
Number of Scans	8
Receiver Gain	52
Relaxation Delay	1.0000
Pulse Width	5.6500
Acquisition Time	3.0000
Acquisition Date	2021-12-08T14:14:10
Spectrometer Frequency	499.58
Spectral Width	8000.0
Nucleus	1H
Acquired Size	24000
Spectral Size	65536

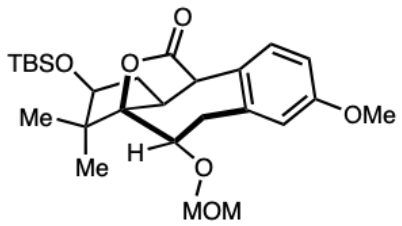

57

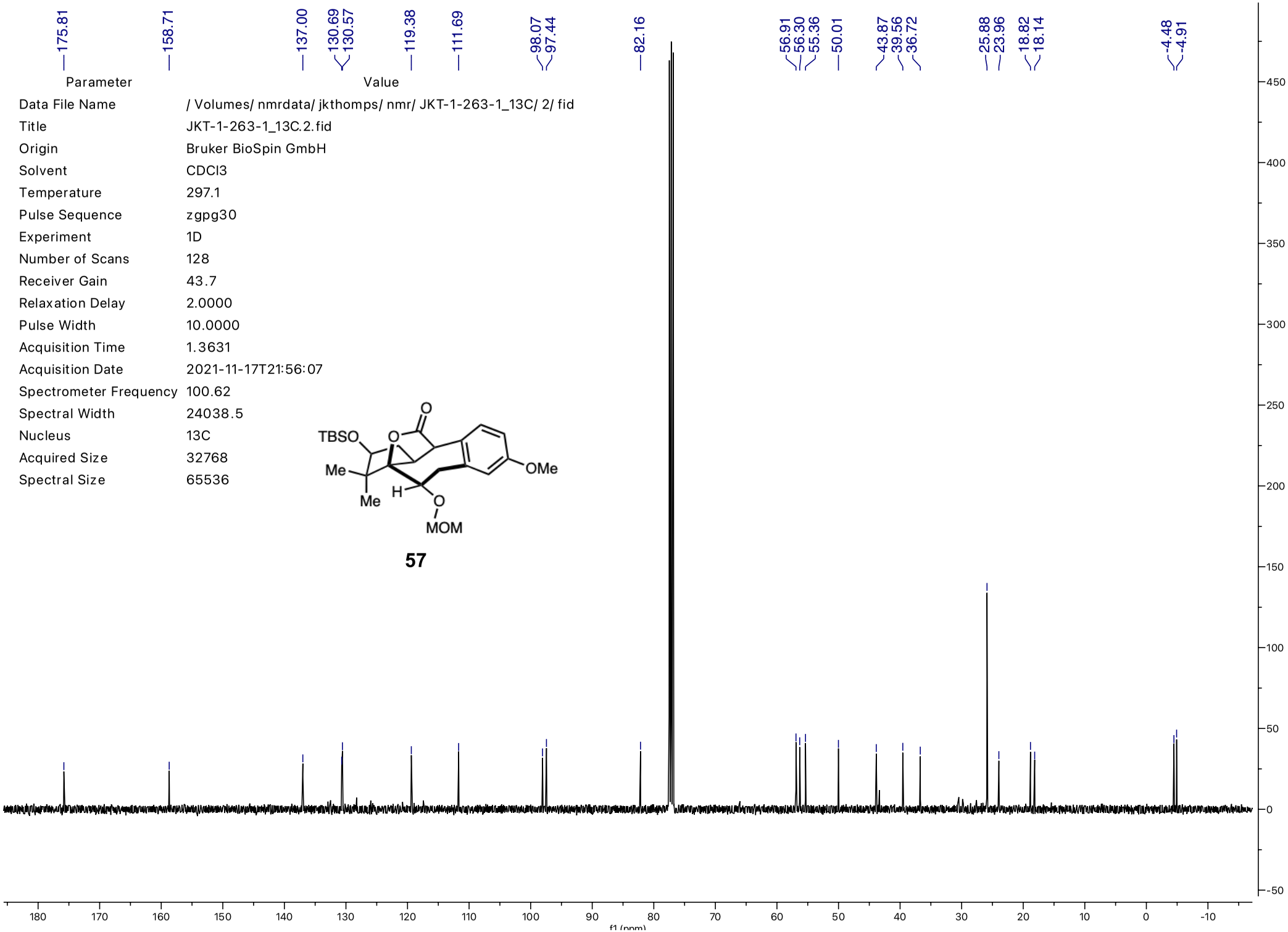

Parameter	Value
Data File Name	/ Volumes/ nmrdata/ jkthomps/ nmr/ JKT-1-263-1_13C/ 2/ fid
Title	JKT-1-263-1_13C.2.fid
Origin	Bruker BioSpin GmbH
Solvent	CDCl3
Temperature	297.1
Pulse Sequence	zgpg30
Experiment	1D
Number of Scans	128
Receiver Gain	43.7
Relaxation Delay	2.0000
Pulse Width	10.0000
Acquisition Time	1.3631
Acquisition Date	2021-11-17T21:56:07
Spectrometer Frequency	100.62
Spectral Width	24038.5
Nucleus	13C
Acquired Size	32768
Spectral Size	65536

57

Parameter	Value
Data File Name	/ Volumes/ nmrdata/ jkthomps/ nmr/ JKT-1-263-1_COSY/ 3/ ser
Title	JKT-1-263-1_COSY.3.ser
Origin	Bruker BioSpin GmbH
Solvent	CDCl3
Temperature	297.1
Pulse Sequence	cosygpppqf
Experiment	COSY
Number of Scans	2
Receiver Gain	64.2
Relaxation Delay	1.9349
Pulse Width	12.5000
Acquisition Time	0.2621
Acquisition Date	2021-11-17T22:06:35
Spectrometer Frequency	(400.13,400.13)
Spectral Width	(3906.3,3906.3)
Lowest Frequency	(-473.4,-481.0)
Nucleus	(1H,1H)
Acquired Size	(1024,128)
Spectral Size	(1024,1024)
Digital Resolution	(3.81,3.81)

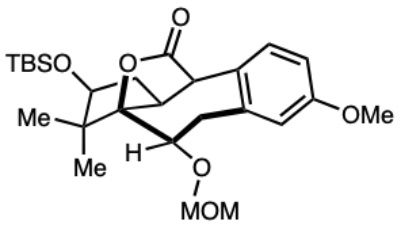

57

f2 (ppm)

f1 (ppm)

Parameter	Value
Data File Name	/ Volumes/ nmrdata/ jkthomps/ nmr/ JKT-1-263-1_HMBC/ 7/ ser
Title	JKT-1-263-1_HMBC.7.ser
Origin	Bruker BioSpin GmbH
Solvent	CDCl3
Temperature	297.2
Pulse Sequence	hmbcetgpl3nd
Experiment	HMBC
Number of Scans	4
Receiver Gain	197.4
Relaxation Delay	2.0000
Pulse Width	12.5000
Acquisition Time	0.4260
Acquisition Date	2021-11-18T12:05:12
Spectrometer Frequency	(400.13,100.62)
Spectral Width	(4807.7,22321.4)
Lowest Frequency	(-172.3,-1116.4)
Nucleus	(1H,13C)
Acquired Size	(2048,256)
Spectral Size	(2048,1024)
Digital Resolution	(2.35,21.80)

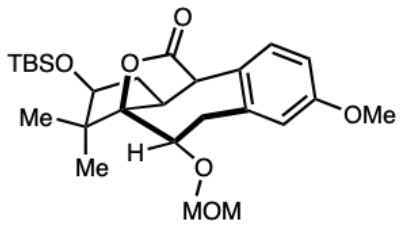

57

f2 (ppm)

f1 (ppm)

Parameter	Value
Data File Name	/ Volumes/ nmrdata/ jkthomps/ nmr/ JKT-1-263-1_HSQC/ 4/ ser
Title	JKT-1-263-1_HSQC.4.ser
Origin	Bruker BioSpin GmbH
Solvent	CDCl3
Temperature	297.2
Pulse Sequence	hsqcedetgpsisp2.4
Experiment	HSQC-EDITED
Number of Scans	2
Receiver Gain	197.4
Relaxation Delay	1.5000
Pulse Width	12.5000
Acquisition Time	0.2135
Acquisition Date	2021-11-17T22:18:16
Spectrometer Frequency	(400.13, 100.62)
Spectral Width	(4795.4, 16611.3)
Lowest Frequency	(-526.7, -1262.8)
Nucleus	(1H, 13C)
Acquired Size	(1024, 180)
Spectral Size	(1024, 1024)
Digital Resolution	(4.68, 16.22)

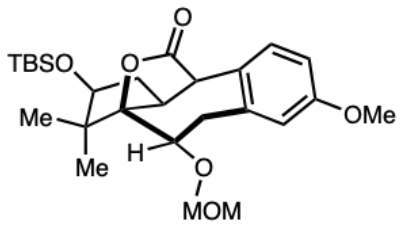

57

f2 (ppm)

f1 (ppm)

Parameter	Value
Data File Name	/ Volumes/ nmrdata/ jkthomps/ nmr/ JKT-1-263-1_NOESY/ 9/ ser
Title	JKT-1-263-1_NOESY.9.ser
Origin	Bruker BioSpin GmbH
Solvent	CDCl3
Temperature	297.2
Pulse Sequence	noesygpphzs
Experiment	NOESY
Number of Scans	4
Receiver Gain	64.2
Relaxation Delay	1.8000
Pulse Width	12.5000
Acquisition Time	0.2560
Acquisition Date	2021-11-17T23:03:50
Spectrometer Frequency	(400.13, 400.13)
Spectral Width	(4000.0, 4000.0)
Lowest Frequency	(-165.0, -165.9)
Nucleus	(1H, 1H)
Acquired Size	(1024, 256)
Spectral Size	(1024, 1024)
Digital Resolution	(3.91, 3.91)

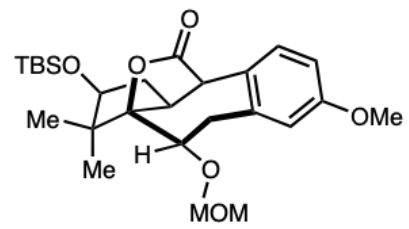

57

f2 (ppm)

f1 (ppm)

Parameter	Value
Data File Name	/ Volumes/ nmrdata/ jkthomps/ nmr/ JKT-1-263-2-3/ 1/ fid
Title	JKT-1-263-2-3.1.fid
Origin	Bruker BioSpin GmbH
Solvent	CDCl3
Temperature	297.1
Pulse Sequence	zg30
Experiment	1D
Number of Scans	16
Receiver Gain	176.8
Relaxation Delay	1.0000
Pulse Width	12.5000
Acquisition Time	4.0894
Acquisition Date	2021-11-18T00:44:30
Spectrometer Frequency	400.13
Spectral Width	8012.8
Nucleus	1H
Acquired Size	32768
Spectral Size	65536

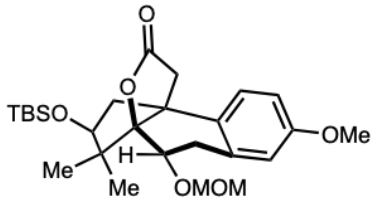

91

Parameter	Value
Data File Name	/ Volumes/ nmrdata/ jkthomps/ nmr/ JKT-1-263-2-3_/ 2/ fid
Title	JKT-1-263-2-3_.2.fid
Origin	Bruker BioSpin GmbH
Solvent	CDCl3
Temperature	297.2
Pulse Sequence	zgpg30
Experiment	1D
Number of Scans	512
Receiver Gain	43.7
Relaxation Delay	1.0000
Pulse Width	10.0000
Acquisition Time	1.3631
Acquisition Date	2021-11-18T12:31:30
Spectrometer Frequency	100.62
Spectral Width	24038.5
Nucleus	13C
Acquired Size	32768
Spectral Size	65536

91

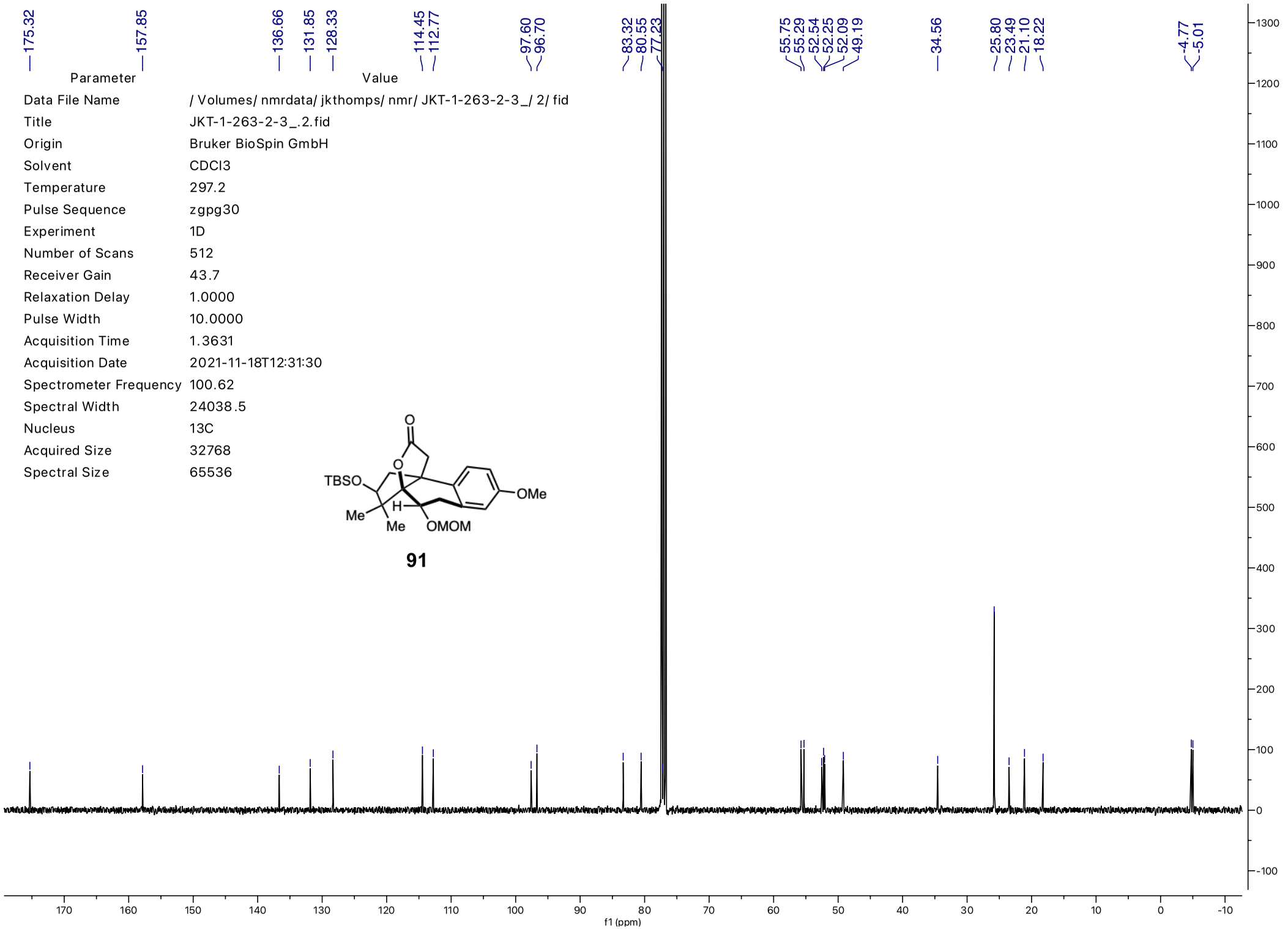

Parameter	Value
Data File Name	/ Volumes/ nmrdata/ jkthomps/ nmr/ JKT-1-263-2-3_/ 3/ ser
Title	JKT-1-263-2-3_.3.ser
Origin	Bruker BioSpin GmbH
Solvent	CDCl3
Temperature	297.1
Pulse Sequence	hsqcedetgpsisp2.4
Experiment	HSQC-EDITED
Number of Scans	2
Receiver Gain	197.4
Relaxation Delay	1.5000
Pulse Width	12.5000
Acquisition Time	0.2135
Acquisition Date	2021-11-18T12:43:16
Spectrometer Frequency	(400.13,100.62)
Spectral Width	(4795.4,16611.3)
Lowest Frequency	(-553.0,-1262.8)
Nucleus	(1H,13C)
Acquired Size	(1024,180)
Spectral Size	(1024,1024)
Digital Resolution	(4.68,16.22)

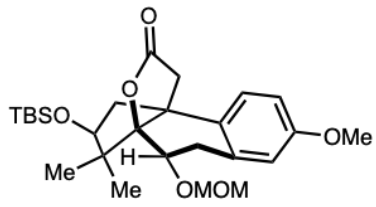

91

f2 (ppm)

f1 (ppm)

Parameter	Value
Data File Name	/ Volumes/ nmrdata/ jkthomps/ nmr/ JKT-1-263-2-3_/ 4/ ser
Title	JKT-1-263-2-3_.4.ser
Origin	Bruker BioSpin GmbH
Solvent	CDCl3
Temperature	297.2
Pulse Sequence	hmbcetgpl3nd
Experiment	HMBC
Number of Scans	4
Receiver Gain	197.4
Relaxation Delay	2.0000
Pulse Width	12.5000
Acquisition Time	0.4260
Acquisition Date	2021-11-18T21:59:03
Spectrometer Frequency	(400.13,100.62)
Spectral Width	(4807.7,22321.4)
Lowest Frequency	(-196.9,-1116.4)
Nucleus	(1H,13C)
Acquired Size	(2048,256)
Spectral Size	(2048,1024)
Digital Resolution	(2.35,21.80)

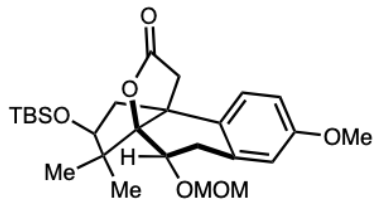

91

f2 (ppm)

f1 (ppm)

Parameter	Value
Data File Name	/ Volumes/ nmrdata/ jkthomps/ nmr/ JKT-1-263-2-3_COSY/ 3/ ser
Title	JKT-1-263-2-3_COSY.3.ser
Origin	Bruker BioSpin GmbH
Solvent	CDCl3
Temperature	297.1
Pulse Sequence	cosygpppqf
Experiment	COSY
Number of Scans	1
Receiver Gain	112.8
Relaxation Delay	1.9062
Pulse Width	12.5000
Acquisition Time	0.2908
Acquisition Date	2021-11-18T00:50:11
Spectrometer Frequency	(400.13,400.13)
Spectral Width	(3521.1,3521.1)
Lowest Frequency	(-389.4,-389.4)
Nucleus	(1H,1H)
Acquired Size	(1024,128)
Spectral Size	(1024,1024)
Digital Resolution	(3.44,3.44)

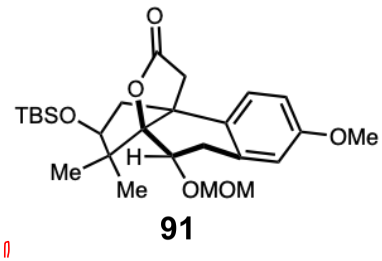

91

f2 (ppm)

f1 (ppm)

Parameter	Value
Data File Name	/ Volumes/ nmrdata/ jkthomps/ nmr/ JKT-1-263-2-3_NOESY/ 4/ ser
Title	JKT-1-263-2-3_NOESY.4.ser
Origin	Bruker BioSpin GmbH
Solvent	CDCl3
Temperature	297.1
Pulse Sequence	noesygpphzs
Experiment	NOESY
Number of Scans	4
Receiver Gain	197.4
Relaxation Delay	1.8000
Pulse Width	12.5000
Acquisition Time	0.2560
Acquisition Date	2021-11-18T01:35:56
Spectrometer Frequency	(400.13,400.13)
Spectral Width	(4000.0,4000.0)
Lowest Frequency	(-196.8,-189.1)
Nucleus	(1H,1H)
Acquired Size	(1024,256)
Spectral Size	(1024,1024)
Digital Resolution	(3.91,3.91)

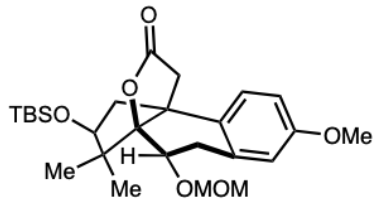

91

f2 (ppm)

f1 (ppm)

A2.2 CRYSTALLOGRAPHIC DATA RELEVANT TO CHAPTER 2

A2.2.1 Enolate arylation product 57

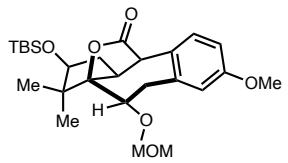

57

Table A2.1. *Crystal data and structure refinement for V22068.*

Identification code	V22068	
Empirical formula	C26 H40 O6 Si	
Formula weight	476.67	
Temperature	200(2) K	
Wavelength	1.54178 Å	
Crystal system	Monoclinic	
Space group	$P2_1/c$	
Unit cell dimensions	a = 20.0766(16) Å	a= 90°.
	b = 9.3852(11) Å	b= 94.599(9)°.
	c = 14.149(2) Å	g = 90°.
Volume	2657.3(5) $Å^3$	
Z	4	
Density (calculated)	1.191 Mg/m^3	
Absorption coefficient	1.077 mm^{-1}	
F(000)	1032	
Crystal size	0.300 x 0.300 x 0.150 mm^3	
Theta range for data collection	4.419 to 74.585°.	
Index ranges	-25<=h<=25, -11<=k<=11, -17<=l<=17	
Reflections collected	63428	
Independent reflections	5421 [R(int) = 0.0660]	

Completeness to theta = 67.679°	100.0 %
Absorption correction	Semi-empirical from equivalents
Max. and min. transmission	0.7538 and 0.5818
Refinement method	Full-matrix least-squares on F^2
Data / restraints / parameters	5421 / 431 / 376
Goodness-of-fit on F^2	1.026
Final R indices [I>2sigma(I)]	R1 = 0.0414, wR2 = 0.1024
R indices (all data)	R1 = 0.0540, wR2 = 0.1129
Extinction coefficient	n/a
Largest diff. peak and hole	0.268 and -0.272 e.$Å^{-3}$

Table A2.2. *Atomic coordinates (x 10^4) and equivalent isotropic displacement parameters ($Å^2$x 10^3) for V22068. U(eq) is defined as one third of the trace of the orthogonalized U^{ij} tensor.*

	x	y	z	U(eq)
O(1)	6995(1)	5679(1)	2646(1)	42(1)
C(1)	6980(1)	4476(2)	3164(1)	40(1)
O(2)	6816(1)	3354(1)	2812(1)	54(1)
C(2)	7188(1)	4803(1)	4197(1)	38(1)
C(3)	7573(1)	6204(2)	4138(1)	38(1)
C(4)	8321(1)	6072(2)	3970(1)	50(1)
C(5)	8396(1)	6572(2)	2950(1)	44(1)
O(3)	8377(1)	5377(1)	2329(1)	46(1)
Si(1)	9029(1)	4802(1)	1828(1)	53(1)
C(21)	9707(3)	4331(11)	2740(6)	120(3)
C(22)	9324(2)	6204(4)	1032(3)	95(1)

C(23)	8717(2)	3216(3)	1130(2)	70(1)
C(24)	9249(4)	2615(9)	525(6)	151(4)
C(25)	8477(2)	2049(3)	1754(3)	92(1(26)
	8090(3)	3739(6)	492(4)	96(2)
Si(1A)	8928(1)	4111(3)	2163(2)	50(1)
C(21A)	8669(5)	2452(8)	2742(7)	88(3)
C(22A)	9777(8)	4660(20)	2703(16)	87(5)
C(23A)	8921(3)	3848(8)	866(5)	60(2)
C(24A)	9430(9)	2612(17)	699(12)	85(5)
C(25A)	8260(7)	3394(18)	406(14)	124(6)
C(26A)	9168(4)	5184(9)	386(6)	81(2)
C(6)	7802(1)	7591(2)	2715(1)	44(1)
C(16)	7627(1)	7770(2)	1649(1)	55(1)
C(17)	7998(1)	9045(2)	3150(1)	62(1)
C(7)	7234(1)	6890(1)	3233(1)	38(1)
C(8)	6610(1)	7767(2)	3410(1)	42(1)
O(4)	6803(1)	8798(1)	4124(1)	46(1)
C(18)	6422(1)	10071(2)	4085(1)	63(1)
O(5)	5846(1)	9997(1)	4564(1)	65(1)
C(19)	5972(1)	10028(2)	5561(1)	65(1)
C(9)	6020(1)	6868(2)	3690(1)	42(1)
C(10)	6105(1)	6022(1)	4607(1)	37(1)
C(11)	5642(1)	6256(2)	5275(1)	39(1)
C(12)	5647(1)	5448(2)	6098(1)	40(1)
O(6)	5220(1)	5651(1)	6796(1)	51(1)
C(20)	4784(1)	6847(2)	6709(1)	58(1)
C(13)	6105(1)	4354(2)	6251(1)	41(1)
C(14)	6576(1)	4134(2)	5605(1)	39(1)
C(15)	6596(1)	4971(1)	4793(1)	36(1)

Table A2.3. *Bond lengths [Å] and angles [°] for V22068.*

O(1)-C(1)	1.3472(17)
O(1)-C(7)	1.4663(16)
C(1)-O(2)	1.1989(17)
C(1)-C(2)	1.5196(19)
C(2)-C(15)	1.5180(19)
C(2)-C(3)	1.5312(19)
C(2)-H(2)	1.0000
C(3)-C(7)	1.5416(18)
C(3)-C(4)	1.544(2)
C(3)-H(3)	1.0000
C(4)-C(5)	1.536(2)
C(4)-H(4A)	0.9900
C(4)-H(4B)	0.9900
C(5)-O(3)	1.4234(18)
C(5)-C(6)	1.544(2)
C(5)-H(5)	1.0000
O(3)-Si(1)	1.6299(13)
O(3)-Si(1A)	1.654(2)
Si(1)-C(21)	1.853(7)
Si(1)-C(22)	1.859(3)
Si(1)-C(23)	1.866(3)
C(21)-H(21A)	0.9800
C(21)-H(21B)	0.9800
C(21)-H(21C)	0.9800
C(22)-H(22A)	0.9800
C(22)-H(22B)	0.9800
C(22)-H(22C)	0.9800
C(23)-C(25)	1.509(4)

C(23)-C(24)	1.528(6)
C(23)-C(26)	1.568(6)
C(24)-H(24A)	0.9800
C(24)-H(24B)	0.9800
C(24)-H(24C)	0.9800
C(25)-H(25A)	0.9800
C(25)-H(25B)	0.9800
C(25)-H(25C)	0.9800
C(26)-H(26A)	0.9800
C(26)-H(26B)	0.9800
C(26)-H(26C)	0.9800
Si(1A)-C(23A)	1.850(7)
Si(1A)-C(21A)	1.854(7)
Si(1A)-C(22A)	1.882(11)
C(21A)-H(21D)	0.9800
C(21A)-H(21E)	0.9800
C(21A)-H(21F)	0.9800
C(22A)-H(22D)	0.9800
C(22A)-H(22E)	0.9800
C(22A)-H(22F)	0.9800
C(23A)-C(25A)	1.492(11)
C(23A)-C(26A)	1.528(9)
C(23A)-C(24A)	1.577(11)
C(24A)-H(24D)	0.9800
C(24A)-H(24E)	0.9800
C(24A)-H(24F)	0.9800
C(25A)-H(25D)	0.9800
C(25A)-H(25E)	0.9800
C(25A)-H(25F)	0.9800
C(26A)-H(26D)	0.9800

C(26A)-H(26E)	0.9800
C(26A)-H(26F)	0.9800
C(6)-C(16)	1.530(2)
C(6)-C(17)	1.536(2)
C(6)-C(7)	1.549(2)
C(16)-H(16A)	0.9800
C(16)-H(16B)	0.9800
C(16)-H(16C)	0.9800
C(17)-H(17A)	0.9800
C(17)-H(17B)	0.9800
C(17)-H(17C)	0.9800
C(7)-C(8)	1.536(2)
C(8)-O(4)	1.4299(17)
C(8)-C(9)	1.533(2)
C(8)-H(8)	1.0000
O(4)-C(18)	1.4171(19)
C(18)-O(5)	1.388(2)
C(18)-H(18A)	0.9900
C(18)-H(18B)	0.9900
O(5)-C(19)	1.413(2)
C(19)-H(19A)	0.9800
C(19)-H(19B)	0.9800
C(19)-H(19C)	0.9800
C(9)-C(10)	1.5195(19)
C(9)-H(9A)	0.9900
C(9)-H(9B)	0.9900
C(10)-C(11)	1.395(2)
C(10)-C(15)	1.405(2)
C(11)-C(12)	1.389(2)
C(11)-H(11)	0.9500

C(12)-O(6)	1.3715(18)
C(12)-C(13)	1.384(2)
O(6)-C(20)	1.423(2)
C(20)-H(20A)	0.9800
C(20)-H(20B)	0.9800
C(20)-H(20C)	0.9800
C(13)-C(14)	1.382(2)
C(13)-H(13)	0.9500
C(14)-C(15)	1.3959(19)
C(14)-H(14)	0.9500

C(1)-O(1)-C(7)	111.26(10)
O(2)-C(1)-O(1)	121.81(13)
O(2)-C(1)-C(2)	128.45(13)
O(1)-C(1)-C(2)	109.74(11)
C(15)-C(2)-C(1)	112.88(12)
C(15)-C(2)-C(3)	111.22(11)
C(1)-C(2)-C(3)	102.78(11)
C(15)-C(2)-H(2)	109.9
C(1)-C(2)-H(2)	109.9
C(3)-C(2)-H(2)	109.9
C(2)-C(3)-C(7)	102.34(10)
C(2)-C(3)-C(4)	116.18(13)
C(7)-C(3)-C(4)	105.99(11)
C(2)-C(3)-H(3)	110.6
C(7)-C(3)-H(3)	110.6
C(4)-C(3)-H(3)	110.6
C(5)-C(4)-C(3)	106.82(12)
C(5)-C(4)-H(4A)	110.4
C(3)-C(4)-H(4A)	110.4

C(5)-C(4)-H(4B)	110.4
C(3)-C(4)-H(4B)	110.4
H(4A)-C(4)-H(4B)	108.6
O(3)-C(5)-C(4)	109.88(12)
O(3)-C(5)-C(6)	111.89(12)
C(4)-C(5)-C(6)	105.05(12)
O(3)-C(5)-H(5)	110.0
C(4)-C(5)-H(5)	110.0
C(6)-C(5)-H(5)	110.0
C(5)-O(3)-Si(1)	123.16(10)
C(5)-O(3)-Si(1A)	131.95(11)
O(3)-Si(1)-C(21)	110.3(3)
O(3)-Si(1)-C(22)	109.57(14)
C(21)-Si(1)-C(22)	109.8(4)
O(3)-Si(1)-C(23)	104.32(11)
C(21)-Si(1)-C(23)	112.0(3)
C(22)-Si(1)-C(23)	110.71(15)
Si(1)-C(21)-H(21A)	109.5
Si(1)-C(21)-H(21B)	109.5
H(21A)-C(21)-H(21B)	109.5
Si(1)-C(21)-H(21C)	109.5
H(21A)-C(21)-H(21C)	109.5
H(21B)-C(21)-H(21C)	109.5
Si(1)-C(22)-H(22A)	109.5
Si(1)-C(22)-H(22B)	109.5
H(22A)-C(22)-H(22B)	109.5
Si(1)-C(22)-H(22C)	109.5
H(22A)-C(22)-H(22C)	109.5
H(22B)-C(22)-H(22C)	109.5
C(25)-C(23)-C(24)	109.3(4)

C(25)-C(23)-C(26)	106.5(3)
C(24)-C(23)-C(26)	110.9(5)
C(25)-C(23)-Si(1)	112.3(2)
C(24)-C(23)-Si(1)	111.8(4)
C(26)-C(23)-Si(1)	105.9(3)
C(23)-C(24)-H(24A)	109.5
C(23)-C(24)-H(24B)	109.5
H(24A)-C(24)-H(24B)	109.5
C(23)-C(24)-H(24C)	109.5
H(24A)-C(24)-H(24C)	109.5
H(24B)-C(24)-H(24C)	109.5
C(23)-C(25)-H(25A)	109.5
C(23)-C(25)-H(25B)	109.5
H(25A)-C(25)-H(25B)	109.5
C(23)-C(25)-H(25C)	109.5
H(25A)-C(25)-H(25C)	109.5
H(25B)-C(25)-H(25C)	109.5
C(23)-C(26)-H(26A)	109.5
C(23)-C(26)-H(26B)	109.5
H(26A)-C(26)-H(26B)	109.5
C(23)-C(26)-H(26C)	109.5
H(26A)-C(26)-H(26C)	109.5
H(26B)-C(26)-H(26C)	109.5
O(3)-Si(1A)-C(23A)	106.5(2)
O(3)-Si(1A)-C(21A)	109.0(3)
C(23A)-Si(1A)-C(21A)	110.2(4)
O(3)-Si(1A)-C(22A)	109.9(7)
C(23A)-Si(1A)-C(22A)	112.0(8)
C(21A)-Si(1A)-C(22A)	109.2(7)
Si(1A)-C(21A)-H(21D)	109.5

Si(1A)-C(21A)-H(21E)	109.5
H(21D)-C(21A)-H(21E)	109.5
Si(1A)-C(21A)-H(21F)	109.5
H(21D)-C(21A)-H(21F)	109.5
H(21E)-C(21A)-H(21F)	109.5
Si(1A)-C(22A)-H(22D)	109.5
Si(1A)-C(22A)-H(22E)	109.5
H(22D)-C(22A)-H(22E)	109.5
Si(1A)-C(22A)-H(22F)	109.5
H(22D)-C(22A)-H(22F)	109.5
H(22E)-C(22A)-H(22F)	109.5
C(25A)-C(23A)-C(26A)	110.4(10)
C(25A)-C(23A)-C(24A)	106.8(10)
C(26A)-C(23A)-C(24A)	107.4(9)
C(25A)-C(23A)-Si(1A)	114.1(9)
C(26A)-C(23A)-Si(1A)	110.7(5)
C(24A)-C(23A)-Si(1A)	107.0(7)
C(23A)-C(24A)-H(24D)	109.5
C(23A)-C(24A)-H(24E)	109.5
H(24D)-C(24A)-H(24E)	109.5
C(23A)-C(24A)-H(24F)	109.5
H(24D)-C(24A)-H(24F)	109.5
H(24E)-C(24A)-H(24F)	109.5
C(23A)-C(25A)-H(25D)	109.5
C(23A)-C(25A)-H(25E)	109.5
H(25D)-C(25A)-H(25E)	109.5
C(23A)-C(25A)-H(25F)	109.5
H(25D)-C(25A)-H(25F)	109.5
H(25E)-C(25A)-H(25F)	109.5
C(23A)-C(26A)-H(26D)	109.5

C(23A)-C(26A)-H(26E)	109.5
H(26D)-C(26A)-H(26E)	109.5
C(23A)-C(26A)-H(26F)	109.5
H(26D)-C(26A)-H(26F)	109.5
H(26E)-C(26A)-H(26F)	109.5
C(16)-C(6)-C(17)	109.22(13)
C(16)-C(6)-C(5)	113.13(13)
C(17)-C(6)-C(5)	107.13(14)
C(16)-C(6)-C(7)	113.18(13)
C(17)-C(6)-C(7)	111.24(13)
C(5)-C(6)-C(7)	102.68(11)
C(6)-C(16)-H(16A)	109.5
C(6)-C(16)-H(16B)	109.5
H(16A)-C(16)-H(16B)	109.5
C(6)-C(16)-H(16C)	109.5
H(16A)-C(16)-H(16C)	109.5
H(16B)-C(16)-H(16C)	109.5
C(6)-C(17)-H(17A)	109.5
C(6)-C(17)-H(17B)	109.5
H(17A)-C(17)-H(17B)	109.5
C(6)-C(17)-H(17C)	109.5
H(17A)-C(17)-H(17C)	109.5
H(17B)-C(17)-H(17C)	109.5
O(1)-C(7)-C(8)	105.86(11)
O(1)-C(7)-C(3)	104.40(10)
C(8)-C(7)-C(3)	113.58(11)
O(1)-C(7)-C(6)	106.30(11)
C(8)-C(7)-C(6)	119.33(12)
C(3)-C(7)-C(6)	106.17(11)
O(4)-C(8)-C(9)	111.08(12)

O(4)-C(8)-C(7)	107.45(11)
C(9)-C(8)-C(7)	113.90(12)
O(4)-C(8)-H(8)	108.1
C(9)-C(8)-H(8)	108.1
C(7)-C(8)-H(8)	108.1
C(18)-O(4)-C(8)	115.40(13)
O(5)-C(18)-O(4)	113.99(14)
O(5)-C(18)-H(18A)	108.8
O(4)-C(18)-H(18A)	108.8
O(5)-C(18)-H(18B)	108.8
O(4)-C(18)-H(18B)	108.8
H(18A)-C(18)-H(18B)	107.6
C(18)-O(5)-C(19)	113.34(15)
O(5)-C(19)-H(19A)	109.5
O(5)-C(19)-H(19B)	109.5
H(19A)-C(19)-H(19B)	109.5
O(5)-C(19)-H(19C)	109.5
H(19A)-C(19)-H(19C)	109.5
H(19B)-C(19)-H(19C)	109.5
C(10)-C(9)-C(8)	118.20(11)
C(10)-C(9)-H(9A)	107.8
C(8)-C(9)-H(9A)	107.8
C(10)-C(9)-H(9B)	107.8
C(8)-C(9)-H(9B)	107.8
H(9A)-C(9)-H(9B)	107.1
C(11)-C(10)-C(15)	118.73(12)
C(11)-C(10)-C(9)	117.42(12)
C(15)-C(10)-C(9)	123.75(13)
C(12)-C(11)-C(10)	121.39(13)
C(12)-C(11)-H(11)	119.3

C(10)-C(11)-H(11)	119.3
O(6)-C(12)-C(13)	115.89(13)
O(6)-C(12)-C(11)	124.36(14)
C(13)-C(12)-C(11)	119.75(13)
C(12)-O(6)-C(20)	117.55(13)
O(6)-C(20)-H(20A)	109.5
O(6)-C(20)-H(20B)	109.5
H(20A)-C(20)-H(20B)	109.5
O(6)-C(20)-H(20C)	109.5
H(20A)-C(20)-H(20C)	109.5
H(20B)-C(20)-H(20C)	109.5
C(14)-C(13)-C(12)	119.30(13)
C(14)-C(13)-H(13)	120.4
C(12)-C(13)-H(13)	120.4
C(13)-C(14)-C(15)	121.81(13)
C(13)-C(14)-H(14)	119.1
C(15)-C(14)-H(14)	119.1
C(14)-C(15)-C(10)	118.84(13)
C(14)-C(15)-C(2)	118.32(12)
C(10)-C(15)-C(2)	122.57(12)

Symmetry transformations used to generate equivalent atoms:

Table 4. *Anisotropic displacement parameters ($Å^2 x\ 10^3$) for V22068. The anisotropic displacement factor exponent takes the form: $-2p^2[\ h^2\ a^{*2}U^{11} + \ldots + 2\ h\ k\ a^*\ b^*\ U^{12}]$*

	U^{11}	U^{22}	U^{33}	U^{23}	U^{13}	U^{12}
O(1)	54(1)	38(1)	32(1)	-1(1)	-3(1)	-5(1)
C(1)	43(1)	35(1)	42(1)	-1(1)	5(1)	-1(1)
O(2)	64(1)	39(1)	58(1)	-12(1)	10(1)	-8(1)
C(2)	44(1)	33(1)	37(1)	6(1)	2(1)	3(1)
C(3)	46(1)	38(1)	30(1)	3(1)	-1(1)	-4(1)
C(4)	46(1)	63(1)	39(1)	7(1)	-1(1)	-6(1)
C(5)	50(1)	44(1)	39(1)	2(1)	4(1)	-11(1)
O(3)	49(1)	42(1)	47(1)	-1(1)	3(1)	-5(1)
Si(1)	51(1)	51(1)	59(1)	-2(1)	13(1)	-9(1)
C(21)	63(3)	167(8)	129(5)	-24(5)	-2(3)	30(4)
C(22)	126(3)	70(2)	97(2)	-17(2)	58(2)	-47(2)
C(23)	94(2)	44(2)	78(2)	-7(1)	36(2)	-16(1)
C(24)	166(6)	113(5)	193(8)	-85(5)	123(6)	-63(4)
C(25)	104(2)	48(2)	128(3)	18(2)	31(2)	-11(2)
C(26)	157(4)	61(3)	66(2)	-4(2)	-22(2)	-45(3)
Si(1A)	58(1)	35(1)	55(1)	7(1)	1(1)	-3(1)
C(21A)	124(7)	48(4)	95(6)	27(4)	25(6)	-1(4)
C(22A)	56(7)	86(7)	112(11)	19(6)	-42(7)	6(5)
C(23A)	58(4)	53(4)	73(4)	-3(3)	17(3)	-2(3)
C(24A)	104(9)	75(8)	77(6)	-2(6)	23(6)	29(8)
C(25A)	111(7)	90(10)	160(13)	-72(8)	-56(8)	21(6)
C(26A)	82(5)	92(6)	70(5)	24(4)	21(4)	11(4)
C(6)	60(1)	36(1)	36(1)	4(1)	8(1)	-7(1)

C(16)	76(1)	53(1)	37(1)	12(1)	10(1)	7(1)
C(17)	82(1)	43(1)	62(1)	-4(1)	22(1)	-18(1)
C(7)	51(1)	32(1)	30(1)	1(1)	-1(1)	-4(1)
C(8)	56(1)	36(1)	33(1)	6(1)	-2(1)	2(1)
O(4)	59(1)	33(1)	47(1)	-1(1)	4(1)	2(1)
C(18)	94(1)	39(1)	57(1)	9(1)	16(1)	15(1)
O(5)	64(1)	65(1)	64(1)	-7(1)	-1(1)	18(1)
C(19)	81(1)	56(1)	60(1)	-12(1)	15(1)	-4(1)
C(9)	46(1)	40(1)	39(1)	4(1)	-4(1)	3(1)
C(10)	42(1)	32(1)	36(1)	0(1)	-2(1)	-4(1)
C(11)	40(1)	35(1)	42(1)	-3(1)	-2(1)	-3(1)
C(12)	42(1)	40(1)	39(1)	-5(1)	5(1)	-9(1)
O(6)	52(1)	56(1)	48(1)	-4(1)	14(1)	-4(1)
C(20)	50(1)	62(1)	64(1)	-14(1)	12(1)	0(1)
C(13)	51(1)	37(1)	36(1)	3(1)	4(1)	-10(1)
C(14)	48(1)	30(1)	40(1)	3(1)	2(1)	-3(1)
C(15)	43(1)	30(1)	36(1)	2(1)	1(1)	-3(1)

Table A2.5. *Hydrogen coordinates (x 10^4) and isotropic displacement parameters ($Å^2$x 10^3) for V22068.*

	x	y	z	U(eq)
H(2)	7492	4039	4472	46
H(3)	7512	6813	4704	46
H(4A)	8594	6674	4427	59
H(4B)	8470	5071	4052	59
H(5)	8827	7097	2920	53

H(21A)	9812	5156	3149	181
H(21B)	10106	4050	2429	181
H(21C)	9562	3536	3124	181
H(22A)	9003	6303	475	142
H(22B)	9761	5935	827	142
H(22C)	9361	7113	1373	142
H(24A)	9663	2450	925	227
H(24B)	9333	3298	24	227
H(24C)	9091	1714	238	227
H(25A)	8337	1224	1362	138
H(25B)	8098	2396	2083	138
H(25C)	8840	1768	2220	138
H(26A)	7931	2971	61	145
H(26B)	8212	4568	121	145
H(26C)	7735	4005	894	145
H(21D)	8761	2538	3431	132
H(21E)	8918	1644	2511	132
H(21F)	8189	2299	2592	132
H(22D)	10108	3944	2557	131
H(22E)	9766	4742	3392	131
H(22F)	9898	5584	2442	131
H(24D)	9608	2736	80	127
H(24E)	9202	1691	717	127
H(24F)	9799	2640	1198	127
H(25D)	8316	3063	-240	186
H(25E)	7950	4202	382	186
H(25F)	8080	2617	773	186
H(26D)	9098	5077	-304	121
H(26E)	9645	5317	568	121
H(26F)	8919	6015	586	121

H(16A)	7228	8371	1543	83
H(16B)	7538	6833	1359	83
H(16C)	8002	8220	1361	83
H(17A)	8407	9384	2889	92
H(17B)	8077	8948	3840	92
H(17C)	7637	9729	3000	92
H(8)	6466	8289	2812	50
H(18A)	6705	10856	4358	75
H(18B)	6296	10307	3413	75
H(19A)	6231	9183	5770	98
H(19B)	5547	10032	5857	98
H(19C)	6226	10888	5748	98
H(9A)	5633	7514	3731	51
H(9B)	5902	6190	3168	51
H(11)	5316	6984	5164	47
H(20A)	5048	7722	6678	87
H(20B)	4518	6889	7259	87
H(20C)	4486	6756	6128	87
H(13)	6096	3762	6794	50
H(14)	6894	3391	5717	47

Table A2.6. *Torsion angles [°] for V22068.*

C(7)-O(1)-C(1)-O(2)	-177.96(14)
C(7)-O(1)-C(1)-C(2)	2.62(16)
O(2)-C(1)-C(2)-C(15)	-80.38(19)
O(1)-C(1)-C(2)-C(15)	98.99(13)
O(2)-C(1)-C(2)-C(3)	159.72(15)
O(1)-C(1)-C(2)-C(3)	-20.91(15)

C(15)-C(2)-C(3)-C(7)	-91.73(13)
C(1)-C(2)-C(3)-C(7)	29.31(14)
C(15)-C(2)-C(3)-C(4)	153.33(12)
C(1)-C(2)-C(3)-C(4)	-85.63(13)
C(2)-C(3)-C(4)-C(5)	108.60(14)
C(7)-C(3)-C(4)-C(5)	-4.26(16)
C(3)-C(4)-C(5)-O(3)	-95.21(15)
C(3)-C(4)-C(5)-C(6)	25.31(16)
C(4)-C(5)-O(3)-Si(1)	-109.59(13)
C(6)-C(5)-O(3)-Si(1)	134.12(12)
C(4)-C(5)-O(3)-Si(1A)	-73.7(2)
C(6)-C(5)-O(3)-Si(1A)	170.00(17)
C(5)-O(3)-Si(1)-C(21)	58.2(4)
C(5)-O(3)-Si(1)-C(22)	-62.82(17)
C(5)-O(3)-Si(1)-C(23)	178.62(14)
O(3)-Si(1)-C(23)-C(25)	-62.6(3)
C(21)-Si(1)-C(23)-C(25)	56.7(4)
C(22)-Si(1)-C(23)-C(25)	179.6(3)
O(3)-Si(1)-C(23)-C(24)	174.2(4)
C(21)-Si(1)-C(23)-C(24)	-66.5(6)
C(22)-Si(1)-C(23)-C(24)	56.5(5)
O(3)-Si(1)-C(23)-C(26)	53.3(3)
C(21)-Si(1)-C(23)-C(26)	172.6(4)
C(22)-Si(1)-C(23)-C(26)	-64.5(3)
C(5)-O(3)-Si(1A)-C(23A)	-137.5(3)
C(5)-O(3)-Si(1A)-C(21A)	103.6(4)
C(5)-O(3)-Si(1A)-C(22A)	-15.9(8)
O(3)-Si(1A)-C(23A)-C(25A)	-60.5(9)
C(21A)-Si(1A)-C(23A)-C(25A)	57.6(9)
C(22A)-Si(1A)-C(23A)-C(25A)	179.3(11)

O(3)-Si(1A)-C(23A)-C(26A)	64.8(5)
C(21A)-Si(1A)-C(23A)-C(26A)	-177.1(6)
C(22A)-Si(1A)-C(23A)-C(26A)	-55.4(9)
O(3)-Si(1A)-C(23A)-C(24A)	-178.4(8)
C(21A)-Si(1A)-C(23A)-C(24A)	-60.3(9)
C(22A)-Si(1A)-C(23A)-C(24A)	61.4(11)
O(3)-C(5)-C(6)-C(16)	-39.17(17)
C(4)-C(5)-C(6)-C(16)	-158.35(13)
O(3)-C(5)-C(6)-C(17)	-159.58(12)
C(4)-C(5)-C(6)-C(17)	81.24(14)
O(3)-C(5)-C(6)-C(7)	83.17(13)
C(4)-C(5)-C(6)-C(7)	-36.01(14)
C(1)-O(1)-C(7)-C(8)	-103.38(12)
C(1)-O(1)-C(7)-C(3)	16.77(15)
C(1)-O(1)-C(7)-C(6)	128.77(12)
C(2)-C(3)-C(7)-O(1)	-28.44(14)
C(4)-C(3)-C(7)-O(1)	93.73(13)
C(2)-C(3)-C(7)-C(8)	86.39(13)
C(4)-C(3)-C(7)-C(8)	-151.44(12)
C(2)-C(3)-C(7)-C(6)	-140.53(11)
C(4)-C(3)-C(7)-C(6)	-18.37(15)
C(16)-C(6)-C(7)-O(1)	45.12(16)
C(17)-C(6)-C(7)-O(1)	168.53(13)
C(5)-C(6)-C(7)-O(1)	-77.18(12)
C(16)-C(6)-C(7)-C(8)	-74.27(16)
C(17)-C(6)-C(7)-C(8)	49.14(17)
C(5)-C(6)-C(7)-C(8)	163.42(12)
C(16)-C(6)-C(7)-C(3)	155.89(13)
C(17)-C(6)-C(7)-C(3)	-80.70(15)
C(5)-C(6)-C(7)-C(3)	33.59(14)

O(1)-C(7)-C(8)-O(4)	169.05(10)
C(3)-C(7)-C(8)-O(4)	55.08(14)
C(6)-C(7)-C(8)-O(4)	-71.34(14)
O(1)-C(7)-C(8)-C(9)	45.57(14)
C(3)-C(7)-C(8)-C(9)	-68.40(15)
C(6)-C(7)-C(8)-C(9)	165.18(12)
C(9)-C(8)-O(4)-C(18)	-82.78(15)
C(7)-C(8)-O(4)-C(18)	152.02(13)
C(8)-O(4)-C(18)-O(5)	86.43(18)
O(4)-C(18)-O(5)-C(19)	73.7(2)
O(4)-C(8)-C(9)-C(10)	-58.82(17)
C(7)-C(8)-C(9)-C(10)	62.67(17)
C(8)-C(9)-C(10)-C(11)	124.43(14)
C(8)-C(9)-C(10)-C(15)	-59.31(19)
C(15)-C(10)-C(11)-C(12)	-1.9(2)
C(9)-C(10)-C(11)-C(12)	174.59(12)
C(10)-C(11)-C(12)-O(6)	177.88(13)
C(10)-C(11)-C(12)-C(13)	-2.1(2)
C(13)-C(12)-O(6)-C(20)	174.21(13)
C(11)-C(12)-O(6)-C(20)	-5.8(2)
O(6)-C(12)-C(13)-C(14)	-176.47(12)
C(11)-C(12)-C(13)-C(14)	3.5(2)
C(12)-C(13)-C(14)-C(15)	-1.0(2)
C(13)-C(14)-C(15)-C(10)	-3.0(2)
C(13)-C(14)-C(15)-C(2)	171.18(13)
C(11)-C(10)-C(15)-C(14)	4.36(19)
C(9)-C(10)-C(15)-C(14)	-171.86(13)
C(11)-C(10)-C(15)-C(2)	-169.58(12)
C(9)-C(10)-C(15)-C(2)	14.2(2)
C(1)-C(2)-C(15)-C(14)	125.46(13)

C(3)-C(2)-C(15)-C(14)	-119.62(13)
C(1)-C(2)-C(15)-C(10)	-60.57(17)
C(3)-C(2)-C(15)-C(10)	54.35(17)

Symmetry transformations used to generate equivalent atoms:

Chapter 3

*Late stage **d** ring installation on the α-enolate arylation product*[†]

3.1 INTRODUCTION

Herein are the efforts that were undertaken to elaborate the α-enolate arylation product. The major challenges include the installation of the **d** ring and formation of the e-ring, along with some functional group interconversions necessary for completion of the target. Optimization of a Birch reduction protocol, photochemical allene [2+2], and skeletal rearrangement to form the desired 3.2.1 bicycle are discussed.

Taken together, this chapter summarizes failed attempts to install the d-ring. Birch reduction yields were low, and material throughput greatly hampered further exploration. In order for the route to be viable for future studies, further exploration of dearomative strategies and development of the skeletal rearrangement (Dowd-Beckwith ring expansion)

[†] J.K.T. was supported by the NSF GRFP (DGE-1745301). S.E.R. acknowledges fellowship support by the NIH (R35GM118191).

are required. Key, positive results garnered from this chapter include the ease at which β–γ isomerization and photochemical allene 2+2 cycloaddition occur, with excellent yield and adequate diastereoselectivity. The synthesis of **57** is relatively short (just 11 steps longest-linear sequence) and may be amenable to further exploration in the future.

3.2 EXPLORATION OF LATE-STAGE ARENE REDUCTION

3.2.1 Birch Reduction with liquid ammonia

Synthetic access to **57** enabled exploration of chemistry to elaborate the tetracycle and conduct studies on late-stage **d** ring installation. Indeed, the original synthetic plan from the enolate arylation product used the Birch reduction as a way of mapping out downstream chemistry and the viability of late-stage **d** ring installation. Following β-γ isomerization and hydrolysis of the methoxy group, enone **56** was envisioned to be accessible (Scheme 3.1). Such a proposal seemed straightforward in planning but very difficult in practice.

Scheme 3.1. *Future plans in elaborating the tetracycle.*

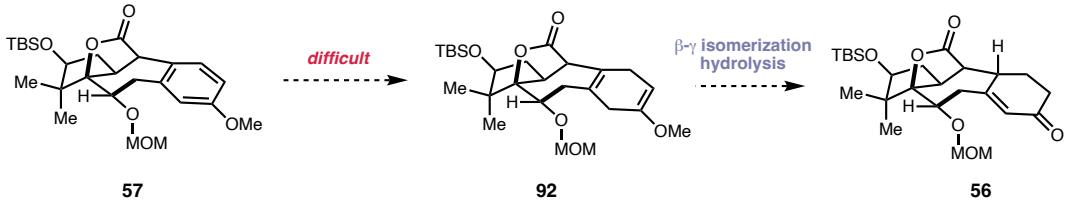

57 **92** **56**

Initial synthetic studies on the Birch reduction investigated the identity of the metal reductant and led to no product formation; lactone reduction was primarily observed (Scheme 3.2). Surveying the literature, it became clear that dissolving metal conditions are often used to reduce lactones to the lactol[1,2] or the diol[3-5]. It seemed from preliminary observation that the electron-rich arene was more difficult to reduce than the lactone.

Scheme 3.2. *Initial attempts to induce Birch reduction of **57**.*

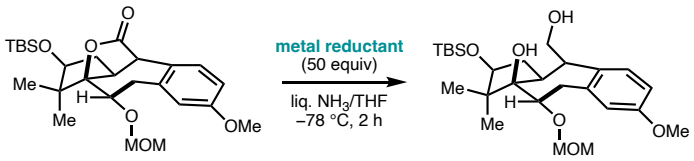

57 **93**

metal reductant	result
Li^0	32% yield
Na^0	65% yield
K^0	47% yield

Two main questions were put forth to investigate: *1) could use of more equivalents of metal reductant reduce the lactone and methoxyarene in a single step and 2) could the lactone be converted to a substrate that would not undergo Birch reduction?*

For the case of *1)*, it was found that, indeed, while use of higher equivalents of metal reductant formed diol **93**, the yield remained low (Scheme 3.3). The main difference in protocol for these experiments included the use of the Rabideau modification. The Rabideau modification uses alcohol additives as a component of the dissolving metal conditions rather than use in quenching the reaction. In order to accommodate alcohol additives under the reaction conditions, higher loadings of metal reductants (typically > 150 equiv) are required. These conditions are believed to help reduce electron-rich substrates due to protonation of the radical anion intermediate in the Birch reduction mechanism, which more easily accepts a second electron.[6] This could fundamentally change the mechanism of the process when compared to the conditions as shown in Scheme 3.2, which do not include an alcohol additive. Na^0 was used in this optimization rather than Li^0 or K^0, as an overall messier reaction profile of overreduction products was observed

with other metals. Furthermore, this observation is consistent with the findings of similar electron-rich systems in the literature.[7]

A dependence of product distribution on alcohol additive was found (Scheme 3.3). More hindered alcohol additives, such as *i*PrOH and *t*BuOH led to less arene reduction and higher yields of **93** (Scheme 3.3, entries 1-2). Interestingly, use of less hindered additives such as *s*BuOH and EtOH led to mixtures of lactol **94** and the desired product **95** (Scheme 3.3, entries 3-4). EtOH, being the least hindered alcohol additive in the series, led to 30% yield of the product (Scheme 3.3, entry 4). Surprisingly, MeOH as an additive led to no observed quantity of product (not shown). Taken together, these data suggest an interplay between the sterics of the alcohol additive and the ease of methoxy arene reduction.

Scheme 3.3. *Product distribution depends on the identity of the alcohol additive.*

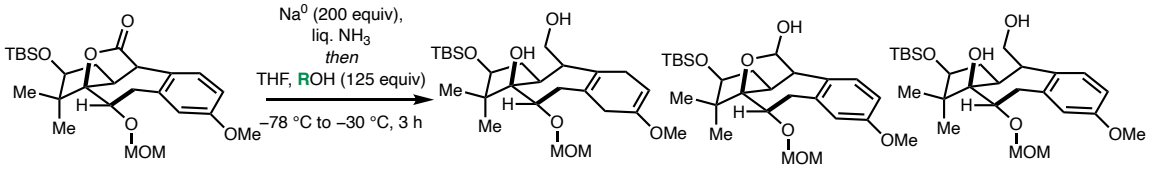

57 **95** **94** **93**

entry	ROH	**95** (%)	**94** (%)	**93** (%)	**57** (%)
1	*i*PrOH	12	—	30	3
2	*t*BuOH	15	—	33	6
3	*s*BuOH	21	27	—	5
4	EtOH	30	15	—	2

In order to investigate if the lactone moiety could be converted to a functional group that would not undergo Birch reduction, several steps were explored. It was noticed that auriculatol A's e-ring is comprised of a methyl acetal. If the installation of the methyl acetal in auriculatol could be accomplished from substrate **57**, the Birch reduction in the presence of the methyl acetal might be tolerated,[7] and the yield could be increased in the stepwise process. As a result, **96** was targeted (Scheme 3.4). In theory, lactol **94** should be formed

relatively easily by using diisobutylaluminum hydride (DIBAL), which could form a stable Al-*ate* complex at cryogenic temperatures. The lactol (**94**) could be methylated directly or converted to the methyl acetal in acidic methanol to produce **96**.

Scheme 3.4. *New synthetic plan: methyl acetal formation prior to Birch reduction.*

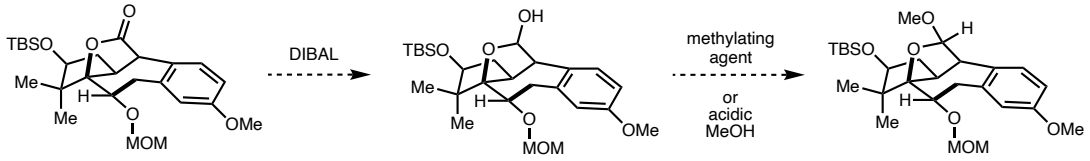

57 **94** **96**

In practice, monoreduction of **57** to **94** was more difficult than envisioned. In the presence of less than one equivalent of DIBAL, even at cryogenic temperatures, no evidence of **94** was observed (Scheme 3.5, entry 1). Instead, a 1:1 mixture of **57** and **93** was isolated, indicating that the Al-*ate* complex formed upon monoreduction of **57** likely had collapsed to the open-chain aldehyde form. More facile reduction of the aldehyde by another equivalent of DIBAL would form diol **93**. It's possible that the ring strain of the fused a-b-e scaffold makes ring-opening more energetically accessible.

Reductive ring-opening was observed under several other reaction conditions, including Buchwald's Ti-hydride[8], super hydride, and tritertbutoxylithium aluminum hydride (Scheme 3.5, entry 2, 3, & 5). Inspired by the work of Motoyama, use of Pd/C/Cu(acac)$_2$ system for silyl acetal formation led to no reaction (Scheme 3.5, entry 4).[9] In line with this, conditions for iridium-catalyzed silylation of esters led to no reaction, even at elevated temperatures (Scheme 3.5, entries 8-9).[10] It is reported that for sugar lactol synthesis, use of triethoxylithium aluminum hydride was uniquely effective.[11] Unfortunately, in our hands, no reaction was observed (Scheme 3.5, entry 7). The only conditions that gave appreciable quantities of lactol were dissolving metal reduction;

specifically, using a THF/EtOH solvent combination provided 32% yield of the target lactol **94**, along with 35% of the diol **93** (Scheme 3.5, entry 10). Although **94** was isolated as a single diastereomer, further NOESY analysis is required to assign the product's stereochemistry.

Scheme 3.5. *Reduction of **57**; attempts to generate intermediate lactol **94**.*

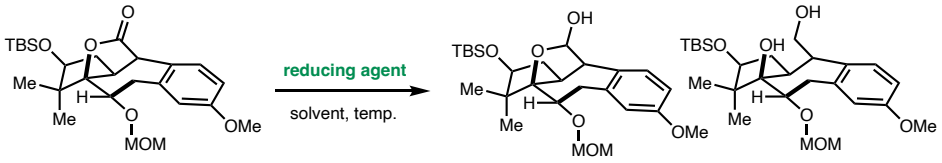

57 **94** **93**

entry	reducing agent	solvent	temperature (°C)	products observed	yield **167** (%)
1	DIBAL (0.8 equiv)	Et_2O	–78	**57**, **93**	-
2	Cp_2TiF_2/PMHS	THF	40	**57, 93**	-
3	super hydride	CH_2Cl_2	0	**57**, **93**	-
4	Pd/C/Cu(acac)$_2$, TMDS	THF	0 to 22	**57**	-
5	LiAlH(O*t*Bu)$_3$	THF	0	**57**, **93**	-
6	LiAlH(O*t*Bu)$_3$	THF	50	**93**	-
7	LiAlH(OEt)$_3$	THF	0	**57**	-
8	[Ir(COE)Cl]$_2$, H_2SiEt_2	CH_2Cl_2	21	**57**	-
9	[Ir(COE)Cl]$_2$, H_2SiEt_2	CH_2Cl_2	50	**57**	-
10	Na^0, NH_3 (*l*)	EtOH/THF	–78	**94**, **57**	32

Because of the low yield of the monoreduction of the lactol, only two conditions were attempted to methylate it. Both gave primarily starting material, as shown in Scheme 3.6. If this were to be attempted in the future, use of *p*TsOH in MeOH would likely lead to the desired methyl acetal; however, careful monitoring of equivalents, temperature, and time should be taken in order to ensure there is no competitive silyl ether cleavage.

Scheme 3.6. *Efforts to methylate lactol **94**.*

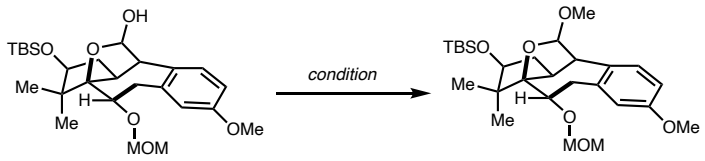

94 **97**

condition	result
NaH, MeI	rsm
PPTS, MeOH	rsm
PTsOH • H_2O, MeOH	decomp.

It was also thought that a one-step methylation-reduction protocol could be accomplished, allowing direct access to **97** from **57**. To this end, trimethyloxonium tetrafluoroborate and MeOTf were used as reagents thought to be electrophilic enough for lactone methylation in the presence of weak borohydride sources like sodium cyanoborohydride. For the case of trimethyloxonium tetrafluoroborate, strong precedent of the formation of zwitterion **99** was observed by mixing one equivalent of trimethyloxonium tetrafluoroborate with δ-butyrolactone **98** in dichloromethane at room temperature overnight (Scheme 3.7).[12]

Scheme 3.7. *Trimethyloxonium tetrafluoroborate as a lactone methylation reagent.*

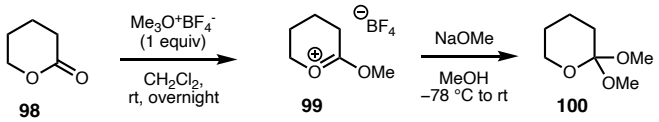

98 **99** **100**

Unfortunately, on **57**, use of trimethyloxonium led to silyl ether cleavage (**101**), and in larger equivalents, decomposition of starting material (Scheme 3.8A). Use of MeOTf led to lactone opening and isolation of methyl ester **102** (Scheme 3.8B). Unfortunately, perhaps unsurprisingly, any attempts to elaborate methyl ester **102** led to substrate reclosure and isolation of **57**. As a testament to this, **102** would close when left overnight

in an NMR tube containing deuterated chloroform. Conformationally, **102** displays strong NOESY correlations between the α-proton of the ester and the methylene between the arene and the MOM ether, indicating a change in conformation when compared to **57**. This is likely a strain-releasing process and perhaps the reason for formation of this unique compound.

Scheme 3.8. A. *Trimethyloxonium tetrafluoroborate leads to silyl ether cleavage and decomposition* ***B.*** *MeOTf provides methyl ester* ***102***.

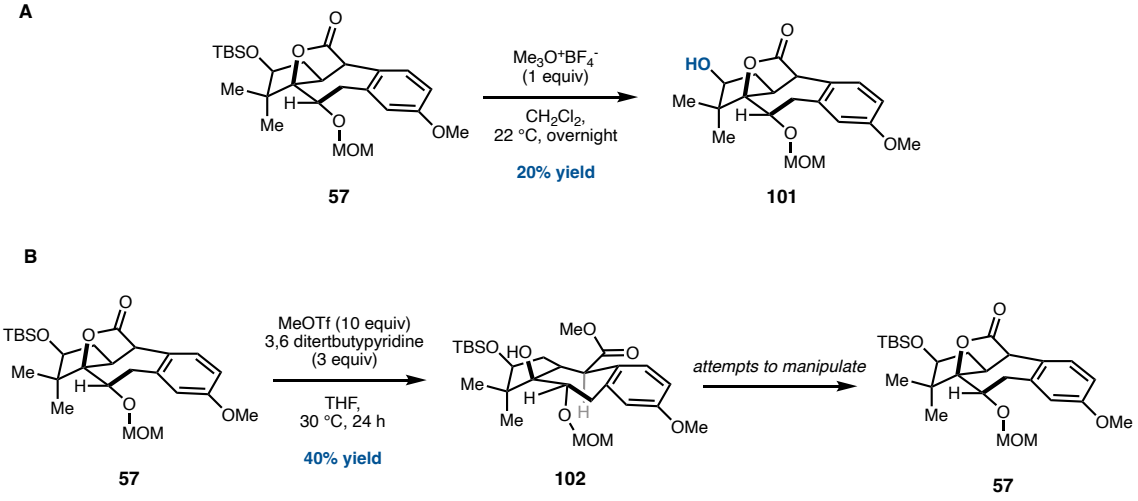

Given the interesting result that the lactone in **57** could be opened using MeOTf, the possibility to induce nucleophilic lactone opening through other means was explored. Quickly, it became clear that the use of MeOTf as an electrophilic lactone methylation source was unique. A variety of nucleophiles explored did not add in to the lactone (Scheme 3.8, entries 1-7). Presumably, this was indication that, while there may be some addition into the lactone, the equilibrium heavily favors ring closure to the starting material. Acidic conditions ultimately led to silyl ether cleavage (Scheme 3.9, entries 8-10).

Scheme 3.9. *Investigation of nucleophilic opening of **57**.*

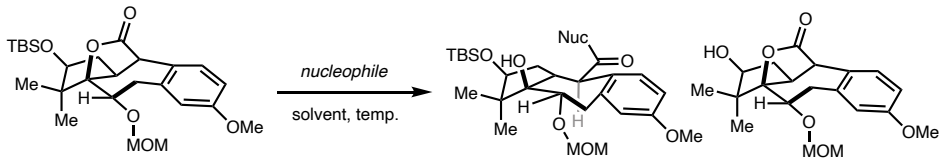

57 **102** **101**

entry	*nucleophile*	solvent	temperature (°C)	result
1	LiOH	THF	110 °C	no reaction
2	NaOH	THF	110 °C	no reaction
3	KOH	THF	110 °C	no reaction
4	LiOMe	MeOH	40 °C	no reaction
5	NaOMe	MeOH	40 °C	no reaction
6	NH_3	MeOH	40 °C	no reaction
7	1,3 dithiane	THF	0 °C	no reaction
8	MeOH, HCl	MeOH/H_2O	40 °C	**101**
9	NaOH, HCl	MeOH/H_2O	40 °C	**101**
10	KOH, HCl	MeOH/H_2O	40 °C	**101**

Due to the shortcomings of the approaches explored to convert the lactone to a different functionality, it was thought that the diol **93** could be a competent substrate in the Birch reduction. Carboxylic acids, for example, have been shown to be competent functionalities in Birch reductions.[13] Furthermore, the use of benzoic acid, for example, as a Birch reduction substrate is common. Unfortunately, using canonical Birch reduction conditions, product yields were even lower than the direct reduction from lactone **57**, providing product **95** in a mere 7% yield for the case of Li^0 (Scheme 3.10). No improvement was seen when using Na^0 instead of Li^0. These data necessitated the exploration of other means for methoxy-arene reduction. Indeed, when surveying the literature, a variety of protocols that do not use liquid ammonia are reported that could offer select advantages over traditional liquid ammonia-containing conditions.

***Scheme 3.10. 93** as a Birch reduction substrate.*

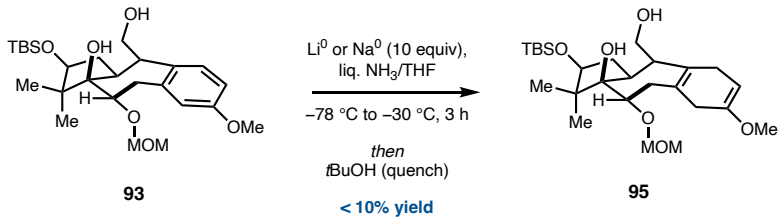

3.2.2 Ammonia-free Birch Reduction strategies

In 2021, Koide and coworkers disclosed a scalable Birch reduction protocol without the use of liquid ammonia (Scheme 3.11).[14] Instead, their method used ethylenediamine as an economical, safe replacement for liquid ammonia. Indeed, the use of ammonia-free Birch reduction strategies has been an exciting area of development in the past few decades. In 2002, Donohoe demonstrated the ability of di-*tert*-butylbiphenyl/Li^0 at reducing heteroaromatic compounds and some electron-deficient aromatics.[15] Then, in 2018, An disclosed the Birch reduction of arenes and heteroarenes using a Na^0 disperson/15-crown-6 mixture in an *i*PrOH/THF mixture.[16] Electrochemical and photochemical Birch reduction methodologies have also been developed. For the former, Baran developed an electrochemical reduction of electron-rich arenes using tri(pyrrolidine-1-yl)phosphine oxide as an overcharge protectant and 1,3-dimethylurea as a water-soluble proton source using sacrificial magnesium or aluminum electrodes.[17] The latter involves two key precedents from König and Miyake that use blue LED's and an iridium photocatalyst and organophotocatalyst, respectively.[18,19]

Scheme 3.11. *New, ammonia-free strategies for Birch reduction.*

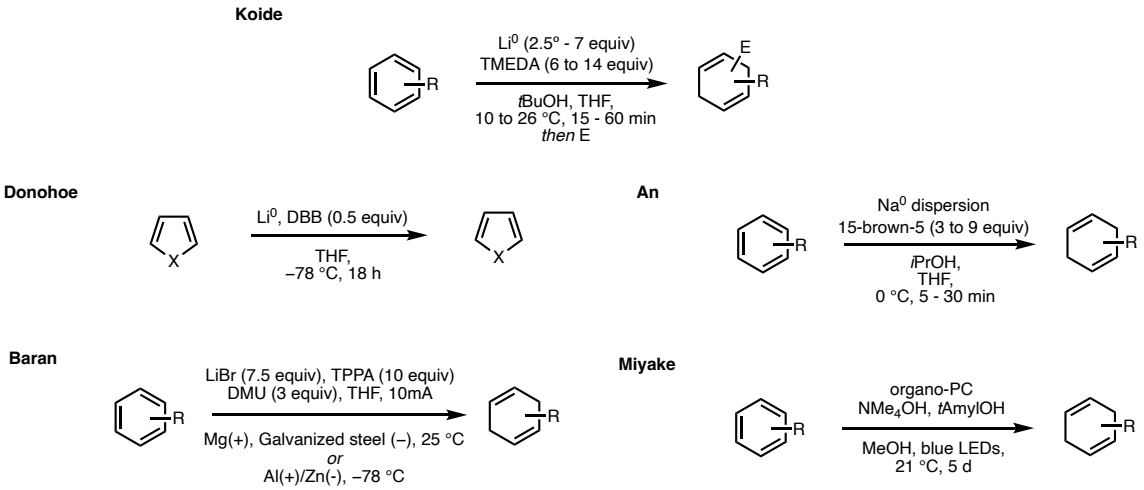

Under Koide's conditions, the reaction profiles were far worse than the dissolving metal conditions. Even after multiple attempts, varying the amount of metal reductant, additive, solvent, and temperature, reaction yields were consistently less than 10% (Scheme 3.12, entry 1). Within the reaction mixture contained a myriad of reduction products, including overreduction to saturated cyclohexane-containing products and even products corresponding to loss of the methoxy group. Donoe, Baran, and Miyake's conditions led to no reaction, likely due to the fact that electron rich arenes are thought to be less-easily reduced than other electron poor arenes (Scheme 3.12, entries 2, 4, & 5). An's conditions led to diol (**93**) formation, and no further reduction was observed (Scheme 3.12, entry 3).

Scheme 3.12. *Slim promise for alternative ammonia-free Birch reduction protocols.*

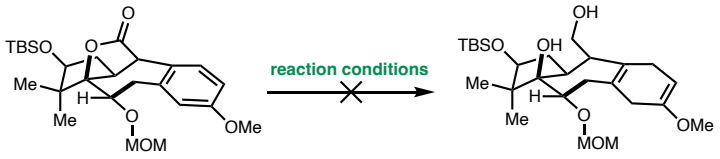

57 **95**

entry	reaction conditions	result
1	Koide	< 10% yield **95** in all cases, complex mixture
2	Donohoe	no reaction
3	An	formation of diol **93** (42% isolated yield)
4	Baran	no reaction
5	Miyake	no reaction

3.3 ATTEMPT AT D-RING INSTALLATION

3.3.1 Hydrolysis and β-γ isomerization

While the prospect of further optimization of the Birch reduction protocol seemed dreary, the result from Scheme 3.3, entry 4 gave ~30% yield of product **95**, and this result was repeatable and scalable. Given the fact that material throughput at the time allowed for more than 200 mg of the α-enolate arylation product, the yield was acceptable to further test some downstream chemistry. The first step necessitated the use of acid-mediated hydrolysis and β-γ isomerization. Fortunately, simple treatment of product **95** with 1 equivalent of 1M HCl led to the desired enone **103**. When conducted at 0 °C, the diastereoselectivity of this process formed from γ-protonation favored the desired diastereomer. This was confirmed by NOESY, which indicated strong coupling between the γ-proton and the methylene hydrogens α to the primary alcohol.

Scheme 3.13. *Hydrolysis β–γ isomerization goes as planned.*

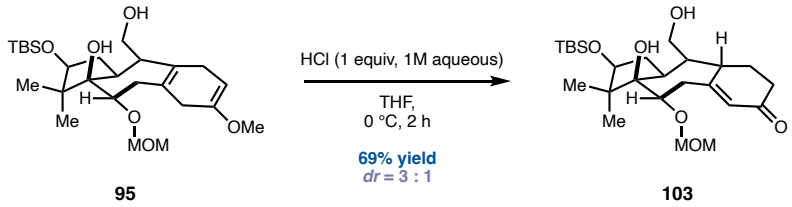

3.3.2 *Photochemical allene [2+2]*

One strategy envisioned for end-game of this route entailed precedent from Nagaoka and coworkers.[18] Following photochemical allene [2+2], the intermediate cyclobutane could be ring-expanded by ketyl radical formation and Dowd-Beckwith fragmentation. Theoretically, the allene [2+2] should proceed with good regioselectivity. The frontier molecular orbitals should align for secondary orbital overlap between the σ* C=O and the HOMO of the allene.[19,20] It is also possible the process goes through a stepwise mechanism.[21] In this case, starting from the triplet allene diradical, Giese addition to the enone forms a stabilized allylic and enolic radical that can recombine. Radical addition from the allene occurs at the terminal position to form the more stable, secondary, allylic radical, and the Giese addition occurs at the β-position of the enone due to a match in polarity. Regardless of the mechanism, in practice this result was confirmed experimentally, not only with good regioselectivity but also with good diastereoselectivity. Using an adaption from Corey's protocol,[22] **104** was isolated in 72% yield as a single diastereomer, as determined by strong NOESY correlations between the allylic methylene protons on the cyclobutane, the methine proton α to the cyclobutane, and the methylene α to the primary alcohol (Scheme 3.14).

Scheme 3.14. *[2+2] allene cycloaddition.*

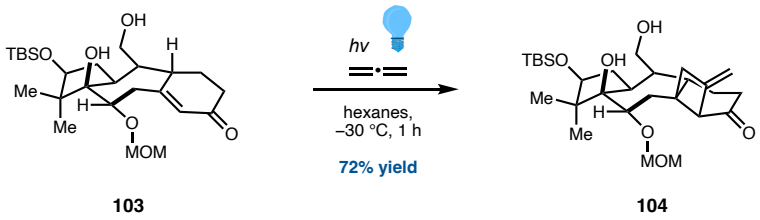

103 **104**

3.3.3 *Exploration of Dowd–Beckwith ring expansion*

Excited by the isolation of product **104**, attention was turned to the subsequent ring expansion. Nagaoka's work involves three different conditions that were optimized to allow adaption to various substrates for the skeletal rearrangement. The first condition (condition A) uses SmI_2 (3 equiv), HMPA (12 equiv), and *t*BuOH (1 equiv) in THF at room temperature, while the second condition (condition B) involves SmI_2 (3 equiv), LiCl (6 equiv), and *t*BuOH (1 equiv) in THF at refluxing temperature. The third condition (condition C) uses SmI_2 (4 equiv), TBABr (8 equiv) and HMPA (16 equiv) at refluxing temperature. The substrate scope contained a variety of substrates, delivering unique 3.2.1 bicycle-containing compounds in moderate to good yields (Scheme 3.15). Notably, substrates could bear ester functionalities, protected amines, aromatics, protected alcohols, and in some cases, free alcohols (although these substrates did not require *t*BuOH as an additive). Mechanistic studies were conducted to validate anion formation at the 1-bridge of the 3.2.1 bicycle by use of deuterated methanol as an additive in the rearrangement (96% deuterium incorporation).

Scheme 3.15. *Nagaoka's SmI_2-mediated skeletal rearrangement.*[18]

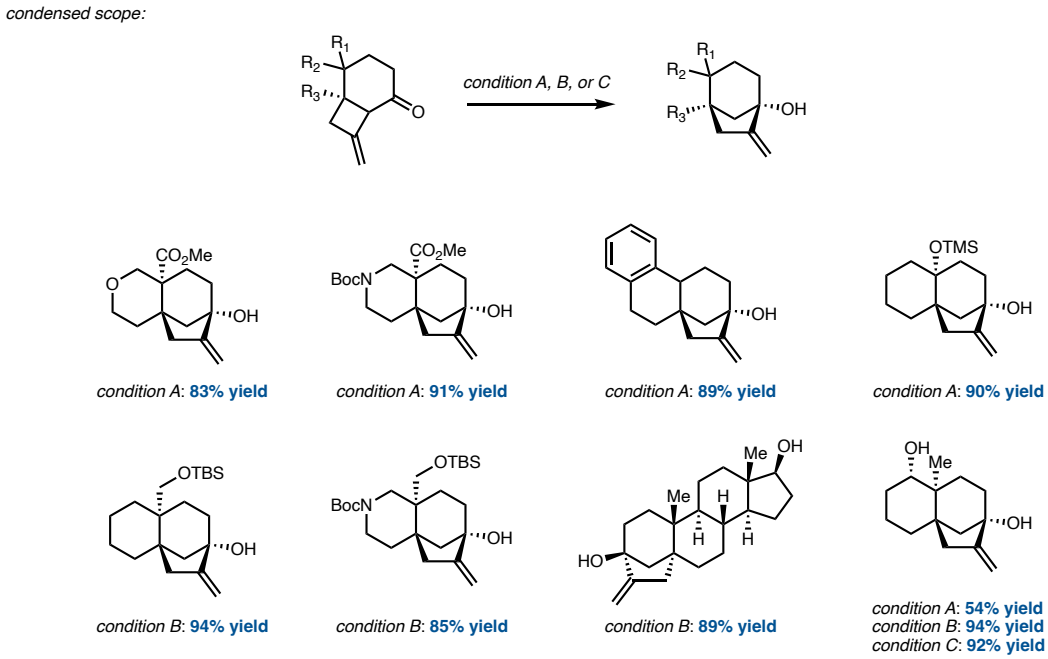

In our hands, employing Nagaoka's conditions led to no observed reaction, even with HMPA or LiCl as additives (Scheme 3.16). While this was disappointing, material throughput at the Birch reduction stage remained prohibitively low. This severely hindered further investigation.

Scheme 3.16. *Attempts at Dowd-Beckwith ring expansion.*

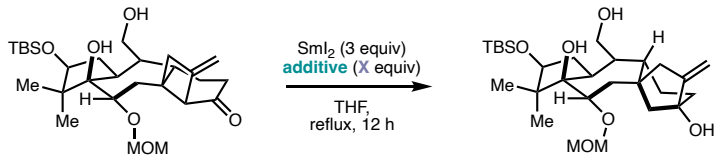

104

entry	additive	X	*t*BuOH (1 equiv) added?	result
1	HMPA	12	yes	no reaction
2	LiCl	6	yes	no reaction
3	HMPA	12	no	no reaction
4	LiCl	6	no	no reaction

Later, it was revealed from a publication from Dai and coworkers that higher

loadings of SmI_2 may have been necessary to achieve the desired reactivity (Scheme 3.17).[23] In this report, 10 equivalents of SmI_2 along with 20 equivalents and 40 equivalents of TBAB and HMPA as additives, respectively, were required for optimal yield of the rearrangement. The density of functional groups in the molecule that could intervene or chelate with SmI_2 first before coordination to the ketone SET to the desired ketyl radical are notable reasons why the desired rearrangement may not have occurred. For the case of substrate **104**, it is clear that the diol motif may have been problematic. In future attempts, it would be necessary to try higher loadings of SmI_2, HMPA, and use of TBAB as an additive.

Scheme 3.17. *Precedent for SmI_2 skeletal rearrangement from Dai and coworkers.*

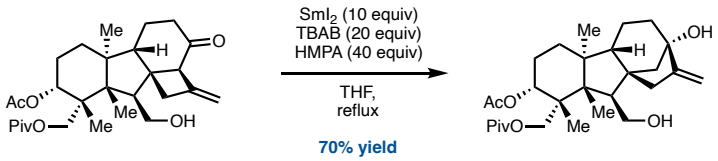

Given the difficulty in forming the d-ring using the methoxyarene reduction strategy, an interest in a new route developed. Using what was uncovered in Chapter 1 and 2 surrounding γ-functionalization of siloxyfurans and α-enolate arylation chemistry, establishing a route that brought in the eastern 3.2.1 bicycle already intact could offer some advantages. The obvious advantage is that the Birch reduction would be avoided, which would greatly advance material throughput and avoid the need for exhaustive reduction of the lactone to the diol. Secondly is that such a route would be more convergent. Convergency may increase synthetic efficiency in certain contexts.[23,24] At a fundamental level, convergent synthesis may allow for maximization of complexity-building steps compared to divergent synthesis, where the complexity-building steps are limited to one

fragment. This is what would be undertaken for the new, ambitious plan. Following some functional group interconversions, an α-enolate alkenylation could form the bond to deliver the key pentacycle (Scheme 3.18). The potential route would use a similar vinylogous Mukaiyama aldol on a more complex aldehyde fragment, bearing the 3.2.1 bicycle already intact. This would not only be in line with some of the research goals of the Reisman group, but potentially offer some benefits in circumventing the Birch reduction. While there are some notable challenges in developing this chemistry, this idea for a new route was pursued in full and discussed in detail in Chapter 4 & 5.

Scheme 3.18. *Revised, convergent route circumvents the use of the Birch reduction.*

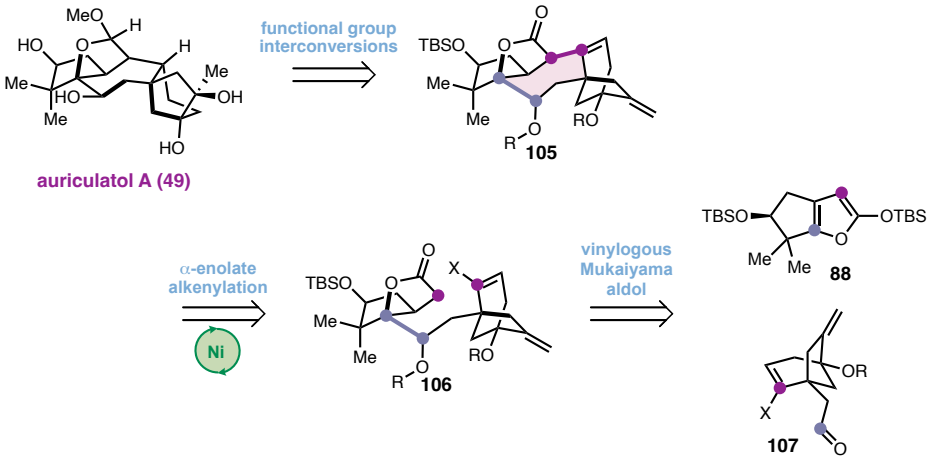

3.4 CONCLUDING REMARKS

This chapter summarizes efforts to elaborate α-enolate arylation products to end-game stages of the synthesis. Unfortunately, in many areas, these efforts were cumbersome due to a difficult Birch reduction step that often led to intractable mixtures of products possessing products from overreduction. Furthermore, attempts to convert the lactone functional group to the methyl acetal were not promising. The only condition that was found to form monoreduced lactone (lactol) was dissolving metal conditions, as shown in

Scheme 3.4, entry 10 – the low yield due to competitive formation of the overreduced diol.

Despite difficulty in achieving Birch reduction of the methoxyarene, the subsequent hydrolysis/β–γ isomerization step and 2+2 allene cycloaddition were incredibly efficient and provided high diastereoselectivity of the desired product in high yield. From α-enolate arylation product **57**, **104** could be formed in 3 steps in 15% yield as a single diastereomer, with the major costly step to yield being the Birch reduction. Nevertheless, while this was good for exploration of the 2+2 cycloaddition, material throughput limited the exhaustive exploration of the key skeletal rearrangement (Dowd-Beckwith ring expansion of cyclobutane **104**). Preliminary efforts were not fruitful but could be conducted more in-depth in the future, such as adaption of Dai's condition that employ 10 equivalents of SmI_2, 20 equivalents of TBAB, and 40 equivalents of HMPA in refluxing THF.

A new route was drawn up to avoid the use of a Birch reduction, as shown in Scheme 3.17. The main challenges would be the application of the α-enolate alkenylation and vinylogous Mukaiyama aldol to a more complex reaction than the chemistry developed in Chapter 1 & 2. A more in-depth exploration of the route can be found in subsequent Chapters 4 & 5.

3.5 EXPERIMENTAL SECTION

Preparation of diol 93:

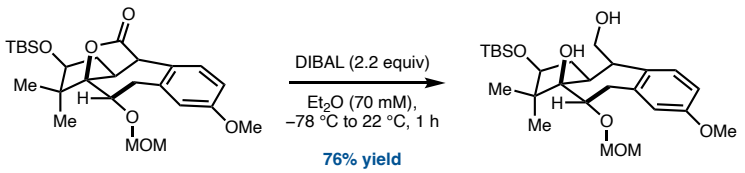

57 **93**

An oven-dried 1-dram vial was charged with starting material **57** (7 mg, 15 umol, 1.0

equiv), a magnetic stir bar, and the vial was put under N_2 atmosphere. Dry Et_2O was added (210 uL) to make a total concentration of 70 mM. Then, the vial was cooled to −78 °C and stirred for one minute. DIBAL (1 M solution in toluene, 17 uL, 1.2 equiv.) was added in using a microsyringe, and the reaction was stirred for 50 min at −78 °C, then rapidly warmed to room temperature, where it was stirred for 10 minutes. The reaction was quenched by addition of a saturated aqueous solution of Rochelle's salt (0.3 mL), stirred for 1 h, then extracted with dichloromethane three times (3 x 0.3 mL). The organic layer was dried with sodium sulfate, filtered, and concentrated to afford the product as a yellow oil, which was analytically pure without any further purification (5.3 mg, 76% yield).

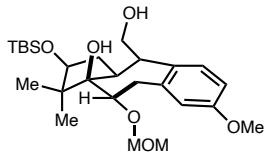

93

TLC (20% EtOAc/Hexanes): R_f 0.32 (*p*-anisaldehyde).

^{1}H NMR (400 MHz, $CDCl_3$): δ 7.04 (d, *J* = 8.2 Hz, 1H), 6.70 (d, *J* = 2.7 Hz, 1H), 6.65 (ddd, *J* = 8.2, 2.7, 0.7 Hz, 1H), 5.66 (dd, *J* = 8.9, 0.8 Hz, 1H), 5.37 (d, *J* = 8.8 Hz, 1H), 4.65 (q, *J* = 6.8 Hz, 2H), 3.97 (dd, *J* = 4.7, 1.9 Hz, 1H), 3.88 (d, *J* = 6.7 Hz, 1H), 3.76 (s, 3H), 3.34 (d, *J* = 17.1 Hz, 2H), 3.26 (d, *J* = 0.6 Hz, 3H), 2.99 – 2.86 (m, 2H), 2.69 (ddd, *J* = 15.3, 12.2, 6.8 Hz, 1H), 1.94 (dd, *J* = 15.4, 3.9 Hz, 1H), 1.19 (s, 3H), 0.94 (s, 9H), 0.90 (s, 4H), 0.13 (d, *J* = 3.5 Hz, 6H).

^{13}C NMR (101 MHz, $CDCl_3$): δ 158.07, 137.38, 134.31, 130.40, 119.14, 110.94, 106.20, 100.70, 97.27, 85.04, 63.40, 56.82, 55.31, 51.75, 44.77, 39.88, 37.24, 30.47, 26.00, 19.00, 18.48, -4.58, -4.94.

FTIR (NaCl, thin film): 3440, 2963, 1467, 1387, 1291, 1079, 1061, 990, 807 cm^{-1}.

HRMS (ESI): calc'd for $[M+H]^+$ 481.2980, found 281.2980.

Preparation of Birch-reduced compound 95:

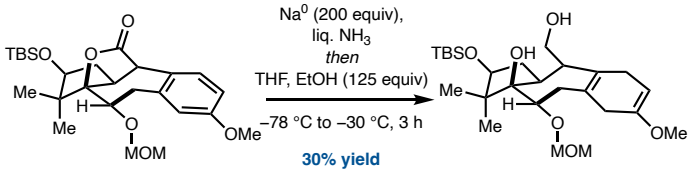

57 **95**

A 10 mL round-bottom flask was flame dried with a glass stir bar and then the flask was added to a dry ice/acetone bath (–78 °C). An ammonia balloon was stuck through the rubber septa and ammonia (about 5 mL) was condensed in by pulling slight vacuum and removing the vacuum inlet. Solid sodium (183 mg, 200 equiv.) was added to the reaction flask, and the reaction mixture was stirred for 5 min at –78 °C. Then, via syringe pump, a solution of starting material **57** (19 mg, 40 umol, 1.0 equiv.) and ethanol (280 uL, 125 equiv) in 2 mL of THF was added. The reaction was allowed to warm to −10 °C over 3 h. Upon cooling the reaction mixture to –78 °C to lower the internal pressure, solid NH_4Cl (20 mg) was added slowly, followed by EtOAc (5 mL). The cold bath was removed from the reaction apparatus, and the mixture was allowed to warm to ambient temperature overnight under a stream of nitrogen. EtOAc (5 mL) was added, and the mixture was poured into H_2O (5 mL). The extracts were separated, and the aqueous extract was further extracted with EtOAc (2 x 5 mL). The combined organic extracts were washed with brine (2 x 5 mL), dried with $MgSO_4$, filtered through cotton, and concentrated in vacuo. The crude was loaded onto a pipet column, eluting with 5 to 10% EtOAc/Hexanes to provide **95** as a clear oil (5.8 mg, 30% yield).

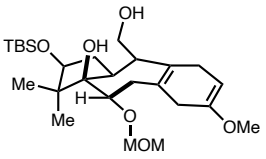

95

TLC (20% EtOAc/Hexanes): R_f 0.35 (*p*-anisaldehyde).

^{1}H NMR (400 MHz, $CDCl_3$): δ 5.63 (d, *J* = 8.9 Hz, 1H), 5.29 (d, *J* = 7.9 Hz, 1H), 4.65 – 4.60 (m, 2H), 4.57 – 4.55 (m, 1H), 3.85 (d, *J* = 6.7 Hz, 1H), 3.79 (dd, *J* = 4.3, 2.1 Hz, 1H), 3.52 (s, 3H), 3.34 (s, 3H), 2.93 (ddd, *J* = 15.8, 10.1, 4.4 Hz, 3H), 2.70 – 2.64 (m, 3H), 2.54 (s, 1H), 2.11 (dd, *J* = 16.3, 4.3 Hz, 1H), 1.81 (dd, *J* = 15.4, 3.9 Hz, 1H), 1.14 (s, 3H), 0.92 (s, 9H), 0.90 (d, *J* = 0.9 Hz, 3H), 0.11 (d, *J* = 5.2 Hz, 6H).

^{13}C NMR (101 MHz, $CDCl_3$): δ 152.78, 132.31, 123.74, 106.14, 100.85, 97.22, 90.54, 85.09, 66.02, 61.18, 56.53, 53.92, 51.62, 43.10, 39.82, 37.03, 35.02, 34.58, 30.47, 29.86, 25.99, 25.77, 19.00, 18.45, 15.43, -4.60, -4.97.

FTIR (NaCl, thin film): 3445, 2973, 1472, 1387, 1341, 1079, 990, 807 cm^{-1}.

HRMS (ESI): calc'd for $[M+H]^+$ 483.3136, found 481.3129.

Preparation of lactol 94:

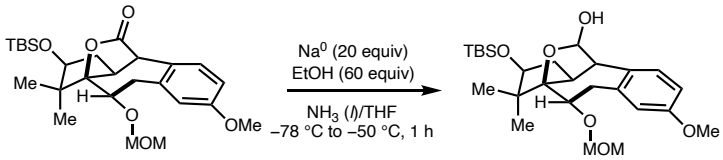

57 **94**

Ammonia (2.1 mL) was condensed using a cold finger into an oven-dried 10 mL round-bottom flask equipped with a glass magnetic stir bar. Freshly cut sodium wire (19 mg, 839 umol, 20 equiv) was added in, and the resulting blue solution was stirred for 15 minutes at −78 °C. A solution of starting material **57** (20 mg, 42 umol) in 0.5 mL of THF and 140 uL

of EtOH (60 equiv.) was added in using a syringe pump at a rate of 3.9 mL per hour. Following 1 h and after monitoring by TLC carefully, the solutions blue color faded, and the reaction could be quenched by allowing the ammonia to boil off under a stream of nitrogen for 15 minutes, addition of saturated aqueous NH_4Cl (1 mL), extracting the aq. layer with EtOAc (3 x 1 mL), washing with brine, drying with sodium sulfate, filtering, and concentrating. Preparatory TLC in 30% EtOAc allows for isolation of a clear oil **94** (6.4 mg, 32% yield) along with 36% yield of the diol **93** (overreduction).

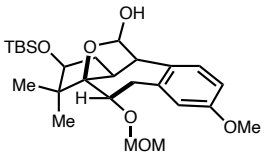

94

TLC (20% EtOAc/Hexanes): R_f 0.36 (*p*-anisaldehyde).

^{1}H NMR (400 MHz, $CDCl_3$): δ 7.08 (d, *J* = 8.2 Hz, 1H), 6.64 (d, *J* = 2.7 Hz, 1H), 6.58 (dd, *J* = 8.2, 2.7 Hz, 1H), 5.19 (s, 1H), 4.66 (qd, *J* = 6.7, 2.8 Hz, 2H), 4.17 (d, *J* = 15.3 Hz, 1H), 3.85 – 3.79 (m, 1H), 3.73 (s, 3H), 3.71 – 3.66 (m, 1H), 3.60 (s, 1H), 3.30 (s, 3H), 2.92 (dd, *J* = 15.6, 4.2 Hz, 1H), 2.70 (dd, *J* = 11.5, 5.6 Hz, 1H), 2.38 – 2.26 (m, 1H), 2.13 (ddd, *J* = 14.6, 5.7, 2.8 Hz, 1H), 0.84 (s, 9H), 0.80 (s, 3H), 0.42 (s, 3H), 0.11 (d, *J* = 2.7 Hz, 6H).

FTIR (NaCl, thin film): 3461, 2929, 1469, 1244, 1167, 1088, 1061, 919, 800 cm^{-1}.

HRMS: calc'd for $[M+H]^+$ 479.2823, found 479.2834.

Preparation of alcohol 101:

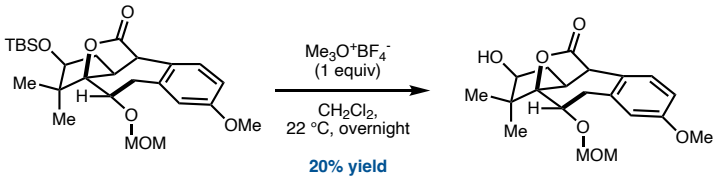

57 **101**

To the starting material **57** (4.9 mg, 10 umol, 1 equiv) in an oven-dried vial equipped with a magnetic stir bar was added 200 uL of CH_2Cl_2 to make a total concentration of 50 mM. Then, solid trimethyloxonium tetrafluoroborate (1.5 mg, 10 umol, 1 equiv) was added in, the vessel was capped, and the reaction was stirred overnight. The next day, preparatory TLC in 50% EtOAc/Hexanes delivered the product **101** as a clear oil (1 mg, 20% yield).

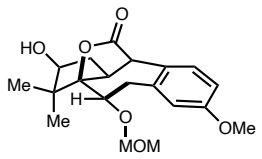

101

TLC (50% EtOAc/Hexanes): R_f 0.21 (*p*-anisaldehyde).

^{1}H NMR (400 MHz, $CDCl_3$): δ 7.13 – 7.07 (m, 1H), 6.75 – 6.69 (m, 2H), 4.74 – 4.66 (m, 2H), 4.20 (dd, *J* = 4.6, 2.1 Hz, 1H), 3.77 (s, 4H), 3.62 (s, 1H), 3.29 (s, 3H), 3.21 (ddt, *J* = 16.5, 2.0, 1.0 Hz, 1H), 3.14 (dd, *J* = 16.5, 4.6 Hz, 1H), 3.03 (dd, *J* = 11.1, 4.8 Hz, 1H), 2.73 (ddd, *J* = 15.3, 11.1, 6.7 Hz, 1H), 1.96 (d, *J* = 8.2 Hz, 1H), 1.63 (ddd, *J* = 15.4, 4.9, 1.6 Hz, 1H), 1.24 (s, 3H), 0.97 (s, 3H).

^{13}C NMR (101 MHz, $CDCl_3$): δ 176.10, 158.95, 136.82, 130.88, 129.63, 119.21, 111.86, 99.30, 97.31, 82.52, 57.01, 56.68, 55.39, 49.93, 43.86, 39.52, 36.20, 24.21, 17.75.

HRMS: calc'd for $[M+H]^+$ 363.1802, found 363.1802.

Preparation of ester 102:

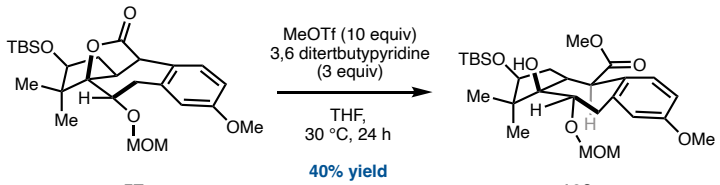

57 **102**

To the starting material **57** (10 mg, 21 umol, 1 equiv.) in an oven-dried 1-dram vial

equipped with a magnetic stir bar was added 2,6-di-*tert*-butylpyridine (14 uL, 3 equiv.) followed by MeOTf (7 uL, 3 equiv). The reaction was put on a hot plate at 30 °C. The reaction was stirred for one day before it was worked up by addition of methanol (50 uL). The solvent was removed *in vacuo* and preparatory TLC in 20% EtOAc/Hexanes provided the product as a clear oil (4.3 mg, 40% yield).

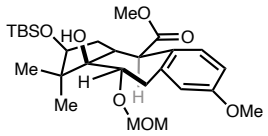

102

TLC (20% EtOAc/Hexanes): R_f 0.40 (*p*-anisaldehyde).

^{1}H NMR (400 MHz, $CDCl_3$): δ 6.92 (d, *J* = 8.3 Hz, 1H), 6.75 (d, *J* = 2.7 Hz, 1H), 6.63 (dd, *J* = 8.2, 2.7 Hz, 1H), 4.75 (d, *J* = 6.7 Hz, 1H), 4.58 – 4.53 (m, 2H), 3.92 (d, *J* = 6.2 Hz, 1H), 3.76 (s, 4H), 3.68 (dd, *J* = 4.6, 1.5 Hz, 2H), 3.60 (s, 3H), 3.33 (s, 3H), 2.88 (dd, *J* = 15.1, 6.5 Hz, 1H), 2.82 (td, *J* = 8.0, 4.0 Hz, 1H), 2.70 – 2.62 (m, 1H), 2.52 (ddd, *J* = 14.7, 11.5, 6.3 Hz, 1H), 1.05 (s, 3H), 0.95 (s, 3H), 0.94 (s, 9H), 0.13 (d, *J* = 25.8 Hz, 6H).

^{13}C NMR (101 MHz, $CDCl_3$): δ 174.35, 158.42, 140.30, 131.86, 130.70, 119.23, 110.43, 95.95, 85.00, 83.05, 75.37, 57.12, 55.24, 51.92, 51.49, 50.48, 43.78, 36.03, 34.85, 30.46, 29.85, 26.00, 24.89, 18.25, 17.59, -4.50, -5.04.

HRMS: calc'd for $[M+H]^+$ 509.2929, found 509.2939.

Preparation of enone 103:

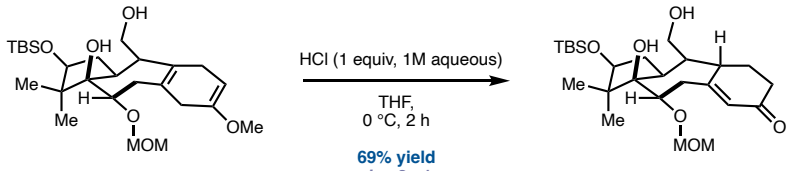

95 **103**

Aqueous hydrochloric acid solution (1 M, 1.00 equiv) was added to a solution of starting material (2.6 mg, 5.4 umol) in THF (975 uL, 5.5 mM) at 0 °C. The reaction was stirred vigorously for 2 h at 0 °C then quenched with saturated sodium bicarbonate (300 uL). The solution was extracted with Et_2O (3 x 0.5 mL), dried with sodium sulfate, filtered, and concentrated down. Preparatory TLC in 40% EtOAc/Hex afforded product as a yellow oil (1.7 mg, 69% yield) as a 3:1 mixture of diastereomers favoring the desired (**103**, as determined by NOESY analysis).

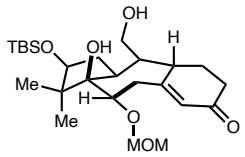

103

TLC (40% EtOAc/Hexanes): R_f 0.33 (*p*-anisaldehyde).

^{1}H NMR (400 MHz, $CDCl_3$): δ 5.94 (d, *J* = 2.5 Hz, 1H), 5.85 (d, *J* = 9.3 Hz, 1H), 5.34 (d, *J* = 9.3 Hz, 1H), 4.68 – 4.62 (m, 2H), 3.86 (d, *J* = 6.4 Hz, 1H), 3.82 (dd, *J* = 4.7, 2.2 Hz, 1H), 3.40 (s, 3H), 2.71 – 2.53 (m, 5H), 2.52 – 2.45 (m, 1H), 2.43 – 2.34 (m, 1H), 2.31 (s, 1H), 2.11 – 2.01 (m, 1H), 1.95 – 1.87 (m, 1H), 1.76 (dd, *J* = 15.1, 3.2 Hz, 1H), 1.15 (s, 3H), 0.95 (s, 3H), 0.92 (s, 9H), 0.12 (d, *J* = 5.2 Hz, 6H).

^{13}C NMR (101 MHz, $CDCl_3$): δ 198.84, 161.70, 132.75, 107.80, 100.02, 97.47, 85.53, 77.23, 61.85, 57.22, 51.17, 42.90, 40.73, 40.30, 37.66, 37.58, 31.00, 26.03, 25.82, 19.31, 18.35, -4.74, -5.13.

FTIR (NaCl, thin film): 3380, 2954, 1490, 1222, 1081, 997, 887 cm^{-1}.

HRMS: calc'd for $[M+H]^+$ 469.2980, found 469.2993.

Preparation of cyclobutane 104:

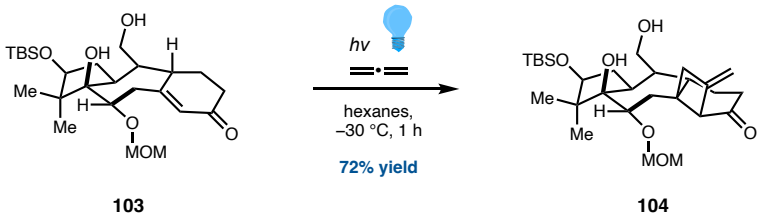

103 **104**

A solution of starting material **103** (1.7 mg, 3.6 umol, 1 equiv.) in hexanes (1.0 mL, 3.6 mM) was prepared in a quartz tube, and a stir bar was added in. Allene gas was bubbled through the solution at −30 °C, and noticeable change in volume indicated that allene had condensed. As bubbling continued, the solution was irradiated with UVC light in a photobox, put in place in order to shield from UV radiation exposure. After 10 minutes, the allene gas line was closed, and the reaction was further irradiated for 1 h at −30 °C. After 1 h, the solvent and allene were evaporated under a stream of nitrogen, and the product was analytically pure following high-vac, delivering the product **104** (1.3 mg, 72% yield) as a single diastereomer (as determined by NOESY analysis).

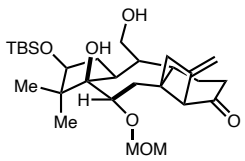

104

TLC (20% EtOAc/Hexanes): R_f 0.51 (*p*-anisaldehyde).

^{1}H NMR (400 MHz, $CDCl_3$): δ 5.98 (s, 1H), 5.20 (s, 1H), 4.91 (s, 1H), 4.86 (s, 1H), 4.66 (s, 2H), 4.14 (s, 1H), 3.80 (s, 1H), 3.75 (s, 1H), 3.43 (s, 3H), 2.77 (s, 1H), 2.60 (s, 2H), 2.42 (s, 5H), 2.13 (s, 1H), 1.97 (s, 1H), 1.93 (s, 1H), 1.84 (s, 1H), 1.76 (s, 1H), 1.10 (s, 3H), 0.91 (s, 12H), 0.10 (s, 6H).

^{13}C NMR (101 MHz, $CDCl_3$): δ 209.60, 141.99, 110.37, 109.23, 100.24, 98.22, 85.76,

78.78, 62.78, 58.65, 57.11, 51.29, 47.80, 43.52, 41.66, 39.86, 39.66, 39.60, 33.82, 27.74, 26.51, 25.81, 19.51, 18.33, -4.75, -5.13.

3.6 NOTES AND REFERENCES

(1) Holton, R. A.; Kennedy, R. M. Stereocontrol of the Metal-Ammonia Reduction: Formation of Either Cis- or Trans-Fused Decalones from a Common Intermediate. *Tetrahedron Lett.* **1987**, *28*, 3, 303–306.

(2) Janini, T. E.; Sampson, P. Cyclopropanation/Reduction of a 3,4-Disubstituted 2(5H)-Furanone: A Model for C-8 Methylation at the Taxane BC Ring Juncture. *J. Org. Chem.* **1997**, *62*, 5069–5073.

(3) Chakraborti, A. K.; Saha, B.; Ray, C.; Ghatak, U. R. Alkali Metal-Liquid Ammonia Reduction of γ-lactones to Diols and Cyclic Hemiacetals: Stereochemical Influence by the Neighbouring Group on the Nature of the Products. *Tetrahedron* **1987**, *43*, 19, 4433–4437.

(4) Jeong, B. S.; Choi, N. S.; Ahn, S. K.; Bae, H.; Kim, H. S.; Kim, D. Total Synthesis and Antiangiogenic Activity of Cyclopentane Analogues of Fumagillol. *Bioorg. Med. Chem. Lett.* **2005**, *15*, 3580–3583.

(5) Ho, G. M.; Zulueta, M. M. L.; Hung, S. C. Stereoselective One-Pot Synthesis of Polypropionates. *Nat. Commun.* **2017**, *8*, 15293.

(6) Murthy, A. R.; Sundar, N. S.; Rao, G. S. R. S. Studies in Metal-Ammonia Reduction–5: Reduction and Reductive Methylation of Some Naphthoic Acids. *Tetrahedron*. **1982**, *38*, 2831–2836.

(7) Roosen, P. C.; Karns, A. S.; Ellis, B. D.; Vanderwal, C. D. Evolution of a Short and Stereocontrolled Synthesis of (+)-7,20-Diisocyanoadociane. *J. Org. Chem.* **2022**, *87*,

1398–1420.

(8) Verdaguer, X.; Hansen, M. C.; Berk, S. C.; Buchwald, S. L. Titanocene-Catalyzed Reduction of Lactones to Lactols. *J. Org. Chem.* **1997**, *62*, 8522–8528.

(9) Hosokawa, S.; Toya, M.; Noda, A.; Morita, M.; Ogawa, T.; Motoyama, Y. Catalytic Silane-Reduction of Carboxylic Esters and Lactones: Selective Synthetic Methods to Aldehydes, Lactols, and Ethers via Silyl Acetal Intermediates. *ChemistrySelect,* **2018**, *3*, 2958–2961.

(10) Cheng, C.; Brookhart, M. Efficient Reduction of Esters to Aldehydes through Iridium-Catalyzed Hydrosilylation. *Angew. Chem. Int. Ed.* **2012**, *51*, 9422–9424.

(11) Gonzalez, C.; Kavoosi, S.; Sanchez, A.; Wnuk, S. F. Reduction of Sugar Lactones to Hemiacetals with Lithium Triethylborohydride. *Carbohydrate Research*, **2016**, *432*, 17–22.

(12) Deslongchamps, P.; Lessard, J.; Nadeau, Y. The Products of Hydrolysis of Cyclic Orthoesters as a Function of pH and the Theory of Stereoelectronic Control. *Can. J. Chem.* **1985**, *63*, 2485–2492.

(13) House, H. O.; Strickland, R. C.; Zaiko, E. J. Perhydroindan Derivatives. 17. Application of the Reduction-Methylation Sequence to 7-Methoxyhexahydrofluorene Derivatives. *J. Org. Chem.* **1976**, *41*, 2401–2408

(14) Burrows, J.; Kamo, S.; Koide, K. Scalable Birch Reduction with Lithium and Ethylenediamine in Tetrahydrofuran. *Science*. **2021**, *374*, 741–746.

(15) Donohoe, T. J.; House, D. Ammonia Free Partial Reduction of Aromatic Compounds Using Lithium Di-*tert*-Butylbiphenyl (LiDBB). *J. Org. Chem.* **2002**, *67*, 5015–5018.

(16) Lei, P.; Ding, Y.; Zhang, X.; Adijiang, A.; Li, H.; Ling, Y.; An, J. A Practical and Chemoselective Ammonia-Free Birch Reduction. *Org. Lett.* **2018**, *20*, 3439–3442.

(17) Peters, B. K.; Rodriguez, K. X.; Reisberg, S. H.; Beil, S. B.; Hickey, D. P.; Kawamata, Y.; Collins, M.; Starr, J.; Chen, L.; Udyavara, S.; Klunder, K.; Gorey, T. J.; Anderson, S. L.; Neurock, M.; Minteer, S. D.; Baran, P. S. Scalable and Safe Synthetic Organic Electroreduction Inspired by Li-ion Battery Chemistry. *Science.* **2019**, *363*, 838–845.

(18) Takatori, K.; Ota, S.; Tendo, K.; Matsunaga, K.; Nagasawa, K.; Watanabe, S.; Kishida, A.; Kogen, H.; Nagaoka, H. Synthesis of Methylenebicyclo[3.2.1]octanol by a Sm(II)-Induced 1,2-Rearrangement Reaction with Ring Expansion of Methylenebicyclo[4.2.0]octanone. *Org. Lett.* **2017**, *19*, 3763–3766.

(19) Hou, S. Y.; Yan, B. C.; Sun, H. D.; Puno, P. T. Recent Advances in the Application of [2+2] Cycloaddition in the Chemical Synthesis of Cyclobutane-Containing Natural Products. *Na. Prod. and Bioprospect.* **2024**, *14*, https://doi.org/10.1007/s13659-024-00457-9.

(20) McVeigh, M. S.; Sorrentino, J. P.; Hands, A. T.; Garg, N. K. Access to Complex Scaffolds Through [2+2] Cycloadditions of Strained Cyclic Allenes. *J. Am. Chem. Soc.* **2024**, *146*, 15420–15427.

(21) Alcaide, B.; Almendros, P.; Aragoncillo, C. Exploiting [2+2] Cycloaddition Chemistry: Achievements with Allenes. *Chem. Soc. Rev.* **2010**, *39*, 783–816.

(22) Corey, E. J.; Liu, K. Enantioselective Total Synthesis of the Potent Anti-HIV Agent Neotripterifordin. Reassignment of Stereochemistry at C(16). *J. Am. Chem. Soc.* **1997**, *119*, 9929–9930.

(23) Hsu, I. T.; Tomanik, M.; Herzon, S. B. Metric-Based Analysis of Convergence in Complex Molecule Synthesis. *Acc. Chem. Res.* **2021**, *54*, 903–916.

(24) Kerkovious, J. K.; Wong, A. R.; Mak, V. W.; Reisman, S. E. A Convergent Fragment Coupling Strategy to Access Quaternary Stereogenic Centers. *Chem. Sci.* **2023**, *14*, 4397–4400.

Appendix 3

Spectra Relevant to Chapter 3:

*Late stage **d** ring installation on the a-enolate arylation product*

Parameter	Value
Data File Name	/Volumes/nmrdata/jkthomps/nmr/JKT-1-274_proton/1/fid
Title	JKT-1-274_proton.1.fid
Origin	Bruker BioSpin GmbH
Solvent	CDCl3
Temperature	297.2
Pulse Sequence	zg30
Experiment	1D
Number of Scans	16
Receiver Gain	197.4
Relaxation Delay	1.0000
Pulse Width	12.5000
Acquisition Time	4.0894
Acquisition Date	2021-12-19T12:29:51
Spectrometer Frequency	400.13
Spectral Width	8012.8
Nucleus	1H
Acquired Size	32768
Spectral Size	65536

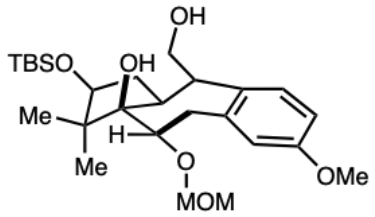

93

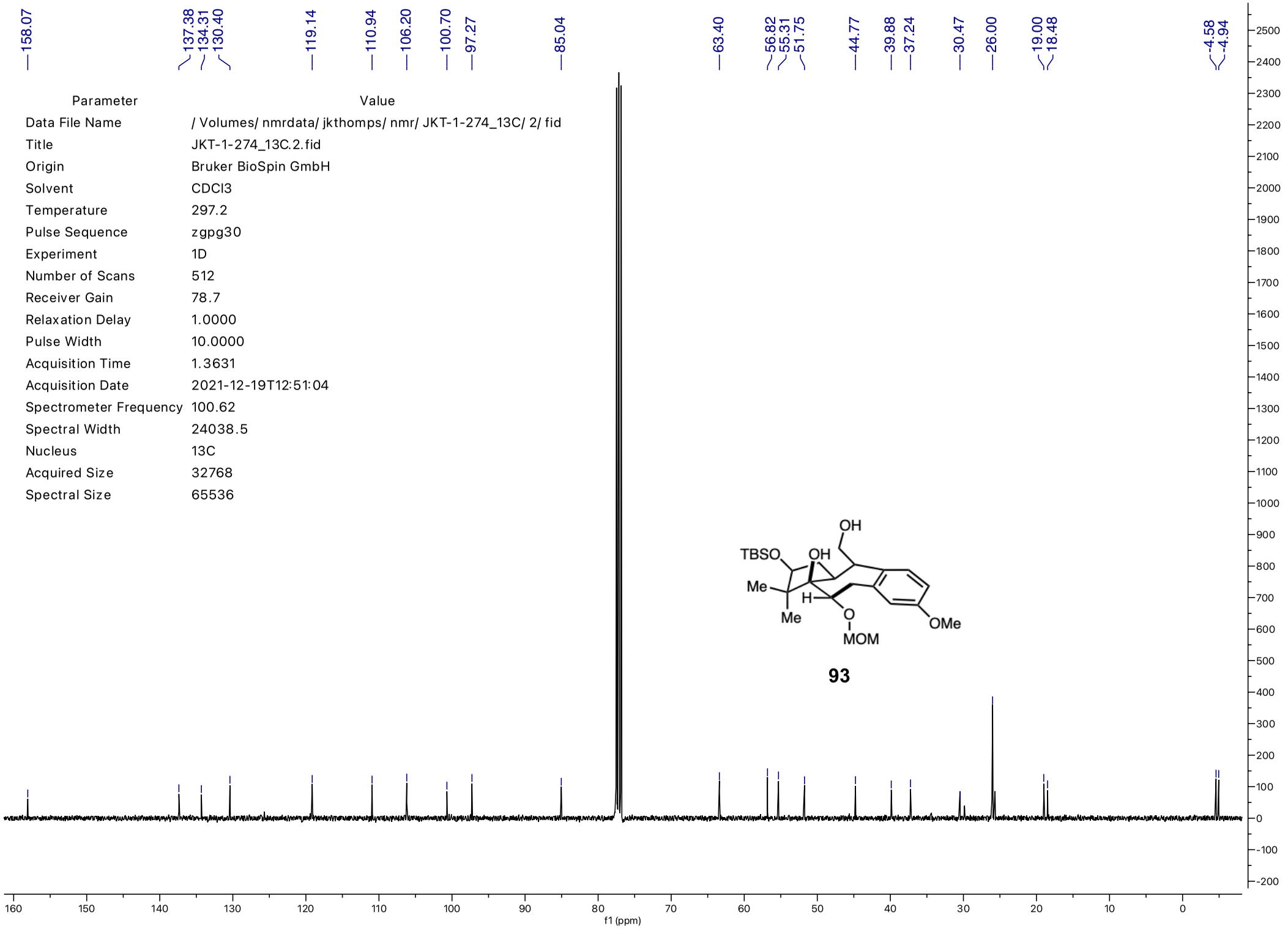
158.07
137.38
134.31
130.40
119.14
110.94
106.20
100.70
97.27
85.04
63.40
56.82
55.31
51.75
44.77
39.88
37.24
30.47
26.00
19.00
18.48
-4.58
-4.94
Parameter Value
Data File Name / Volumes/ nmrdata/ jkthomps/ nmr/ JKT-1-274_13C/ 2/ fid
Title JKT-1-274_13C.2.fid
Origin Bruker BioSpin GmbH
Solvent CDCl3
Temperature 297.2
Pulse Sequence zgpg30
Experiment 1D
Number of Scans 512
Receiver Gain 78.7
Relaxation Delay 1.0000
Pulse Width 10.0000
Acquisition Time 1.3631
Acquisition Date 2021-12-19T12:51:04
Spectrometer Frequency 100.62
Spectral Width 24038.5
Nucleus 13C
Acquired Size 32768
Spectral Size 65536
OH
TBSO
OH
Me
H
Me
O
MOM
OMe
93
f1 (ppm)

Parameter	Value
Data File Name	/ Volumes/ nmrdata/ jkthomps/ nmr/ JKT-1-274_HSQC/ 3/ ser
Title	JKT-1-274_HSQC.3.ser
Origin	Bruker BioSpin GmbH
Solvent	CDCl3
Temperature	297.1
Pulse Sequence	hsqcedetgpsisp2.4
Experiment	HSQC-EDITED
Number of Scans	2
Receiver Gain	197.4
Relaxation Delay	1.5000
Pulse Width	12.5000
Acquisition Time	0.2135
Acquisition Date	2021-12-19T13:02:49
Spectrometer Frequency	(400.13,100.62)
Spectral Width	(4795.4,16611.3)
Lowest Frequency	(-574.0,-1262.8)
Nucleus	(1H,13C)
Acquired Size	(1024,180)
Spectral Size	(1024,1024)
Digital Resolution	(4.68,16.22)

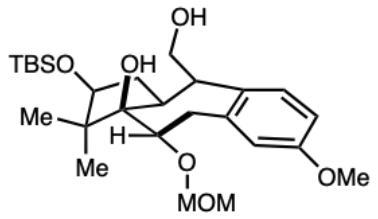

93

f2 (ppm)

f1 (ppm)

Parameter	Value
Data File Name	/ Volumes/ nmrdata/ jkthomps/ nmr/ JKT-1-274_NOESY/ 4/ ser
Title	JKT-1-274_NOESY.4.ser
Origin	Bruker BioSpin GmbH
Solvent	CDCl3
Temperature	297.1
Pulse Sequence	noesygpphzs
Experiment	NOESY
Number of Scans	3
Receiver Gain	197.4
Relaxation Delay	1.8000
Pulse Width	12.5000
Acquisition Time	0.2560
Acquisition Date	2021-12-19T13:37:30
Spectrometer Frequency	(400.13,400.13)
Spectral Width	(4000.0,4000.0)
Lowest Frequency	(-223.4,-218.6)
Nucleus	(1H,1H)
Acquired Size	(1024,256)
Spectral Size	(1024,1024)
Digital Resolution	(3.91,3.91)

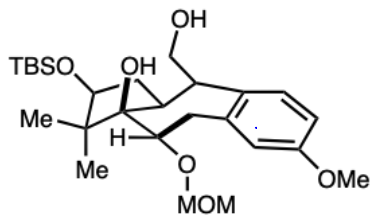

93

f2 (ppm)

f1 (ppm)

Parameter	Value
Data File Name	/ Volumes/ nmrdata/ jkthomps/ nmr/ JKT-1-325-5-1_3D/ 1/ fid
Title	JKT-1-325-5-1_3D.1.fid
Origin	Bruker BioSpin GmbH
Solvent	CDCl3
Temperature	297.1
Pulse Sequence	zg30
Experiment	1D
Number of Scans	16
Receiver Gain	197.4
Relaxation Delay	1.0000
Pulse Width	12.5000
Acquisition Time	4.0894
Acquisition Date	2022-02-21T22:28:18
Spectrometer Frequency	400.13
Spectral Width	8012.8
Nucleus	1H
Acquired Size	32768
Spectral Size	65536

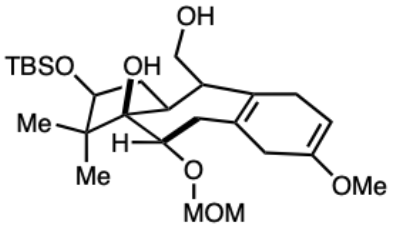

95

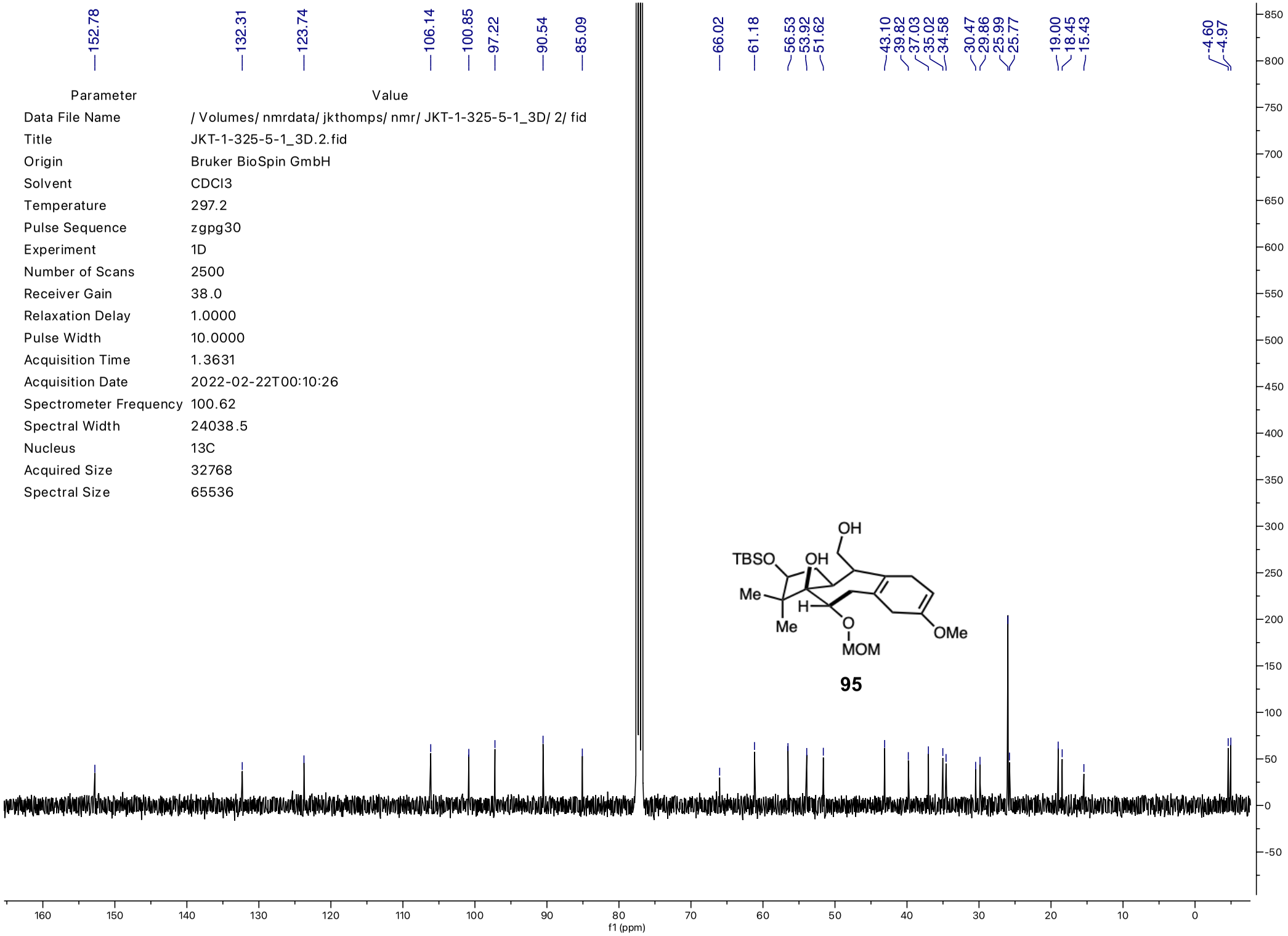
152.78
132.31
123.74
106.14
100.85
97.22
90.54
85.09
66.02
61.18
56.53
53.92
51.62
43.10
39.82
37.03
35.02
34.58
30.47
29.86
25.99
25.77
19.00
18.45
15.43
-4.60
-4.97
Parameter Value
Data File Name / Volumes/ nmrdata/ jkthomps/ nmr/ JKT-1-325-5-1_3D/ 2/ fid
Title JKT-1-325-5-1_3D.2.fid
Origin Bruker BioSpin GmbH
Solvent CDCl3
Temperature 297.2
Pulse Sequence zgpg30
Experiment 1D
Number of Scans 2500
Receiver Gain 38.0
Relaxation Delay 1.0000
Pulse Width 10.0000
Acquisition Time 1.3631
Acquisition Date 2022-02-22T00:10:26
Spectrometer Frequency 100.62
Spectral Width 24038.5
Nucleus 13C
Acquired Size 32768
Spectral Size 65536
OH
TBSO
OH
Me
H
Me
O
MOM
OMe
95
850
800
750
700
650
600
550
500
450
400
350
300
250
200
150
100
50
0
-50
160
150
140
130
120
110
100
90
80
70
60
50
40
30
20
10
0
f1 (ppm)

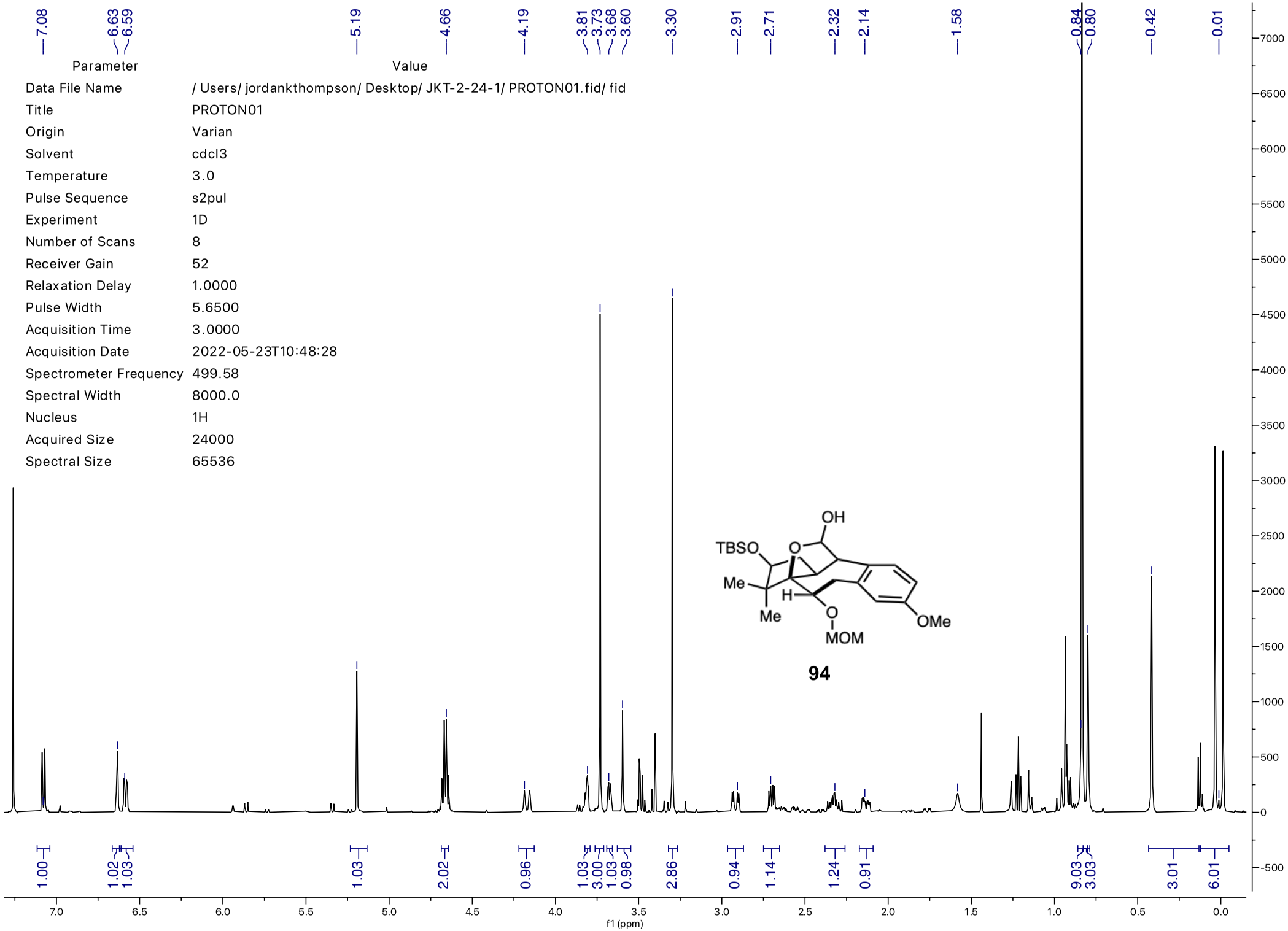
7.08
6.63
6.59
5.19
4.66
4.19
3.81
3.73
3.68
3.60
3.30
2.91
2.71
2.32
2.14
1.58
0.84
0.80
0.42
0.01
Parameter
Value
Data File Name / Users/ jordankthompson/ Desktop/ JKT-2-24-1/ PROTON01.fid/ fid
Title PROTON01
Origin Varian
Solvent cdcl3
Temperature 3.0
Pulse Sequence s2pul
Experiment 1D
Number of Scans 8
Receiver Gain 52
Relaxation Delay 1.0000
Pulse Width 5.6500
Acquisition Time 3.0000
Acquisition Date 2022-05-23T10:48:28
Spectrometer Frequency 499.58
Spectral Width 8000.0
Nucleus 1H
Acquired Size 24000
Spectral Size 65536
OH
TBSO
O
Me
H
Me
O
MOM
OMe
94
1.00
1.02
1.03
1.03
2.02
0.96
1.03
3.00
1.03
0.98
2.86
0.94
1.14
1.24
0.91
9.03
3.03
3.01
6.01
f1 (ppm)

Parameter	Value
Data File Name	/ Volumes/ nmrdata-1/ jkthomps/ nmr/ JKT-2-20_pure/ 1/ fid
Title	JKT-2-20_pure.1.fid
Origin	Bruker BioSpin GmbH
Solvent	CDCl3
Temperature	297.2
Pulse Sequence	zg30
Experiment	1D
Number of Scans	16
Receiver Gain	197.4
Relaxation Delay	1.0000
Pulse Width	12.5000
Acquisition Time	4.0894
Acquisition Date	2022-05-18T02:10:22
Spectrometer Frequency	400.13
Spectral Width	8012.8
Nucleus	1H
Acquired Size	32768
Spectral Size	65536

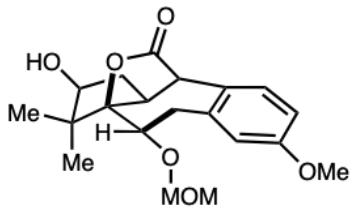

101

f1 (ppm)

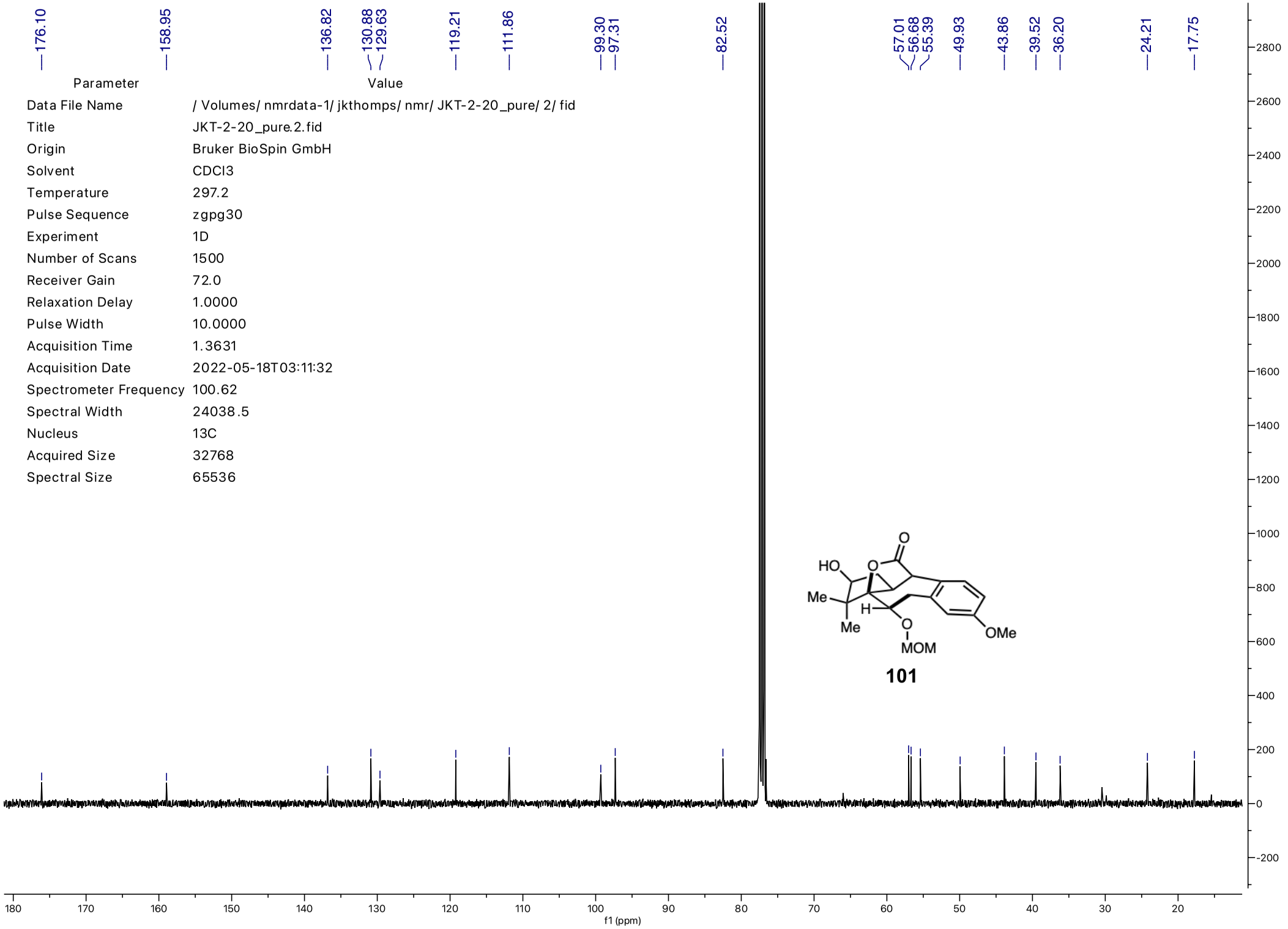
176.10
158.95
136.82
130.88
129.63
119.21
111.86
99.30
97.31
82.52
57.01
56.68
55.39
49.93
43.86
39.52
36.20
24.21
17.75
Parameter
Value
Data File Name / Volumes/ nmrdata-1/ jkthomps/ nmr/ JKT-2-20_pure/ 2/ fid
Title JKT-2-20_pure.2.fid
Origin Bruker BioSpin GmbH
Solvent CDCl3
Temperature 297.2
Pulse Sequence zgpg30
Experiment 1D
Number of Scans 1500
Receiver Gain 72.0
Relaxation Delay 1.0000
Pulse Width 10.0000
Acquisition Time 1.3631
Acquisition Date 2022-05-18T03:11:32
Spectrometer Frequency 100.62
Spectral Width 24038.5
Nucleus 13C
Acquired Size 32768
Spectral Size 65536
HO
O
O
Me
H
Me
O
MOM
OMe
101
2800
2600
2400
2200
2000
1800
1600
1400
1200
1000
800
600
400
200
0
-200
180
170
160
150
140
130
120
110
100
90
80
70
60
50
40
30
20
f1 (ppm)

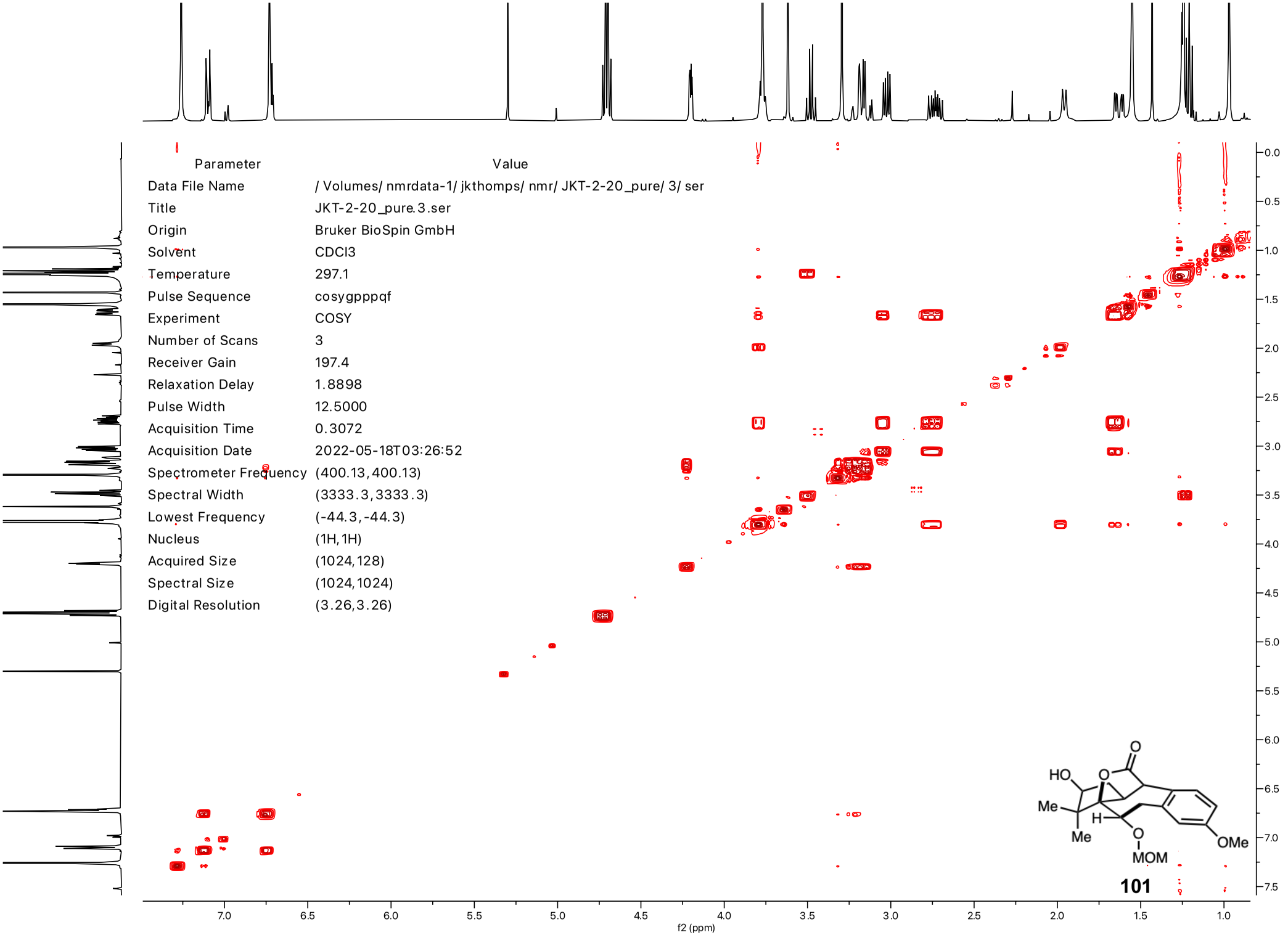
Parameter Value
Data File Name / Volumes/ nmrdata-1/ jkthomps/ nmr/ JKT-2-20_pure/ 3/ ser
Title JKT-2-20_pure.3.ser
Origin Bruker BioSpin GmbH
Solvent CDCl3
Temperature 297.1
Pulse Sequence cosygpppqf
Experiment COSY
Number of Scans 3
Receiver Gain 197.4
Relaxation Delay 1.8898
Pulse Width 12.5000
Acquisition Time 0.3072
Acquisition Date 2022-05-18T03:26:52
Spectrometer Frequency (400.13, 400.13)
Spectral Width (3333.3, 3333.3)
Lowest Frequency (-44.3, -44.3)
Nucleus (1H, 1H)
Acquired Size (1024, 128)
Spectral Size (1024, 1024)
Digital Resolution (3.26, 3.26)
HO
O
O
Me
H
Me
O
MOM
OMe
101
f2 (ppm)
f1 (ppm)

Parameter	Value
Data File Name	/ Volumes/ nmrdata-1/ jkthomps/ nmr/ JKT-2-20_pure/ 4/ ser
Title	JKT-2-20_pure.4.ser
Origin	Bruker BioSpin GmbH
Solvent	CDCl3
Temperature	297.1
Pulse Sequence	hsqcedetgpsisp2.4
Experiment	HSQC-EDITED
Number of Scans	4
Receiver Gain	197.4
Relaxation Delay	1.5000
Pulse Width	12.5000
Acquisition Time	0.2135
Acquisition Date	2022-05-18T03:49:02
Spectrometer Frequency	(400.13,100.62)
Spectral Width	(4795.4,16611.3)
Lowest Frequency	(-524.5,-1262.8)
Nucleus	(1H,13C)
Acquired Size	(1024,180)
Spectral Size	(1024,1024)
Digital Resolution	(4.68,16.22)

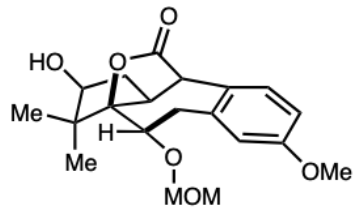

101

f2 (ppm)

f1 (ppm)

Parameter	Value
Data File Name	/ Volumes/ nmrdata/ jkthomps/ nmr/ JKT-2-21-1-2/ 1/ fid
Title	JKT-2-21-1-2.1.fid
Origin	Bruker BioSpin GmbH
Solvent	CDCl3
Temperature	297.2
Pulse Sequence	zg30
Experiment	1D
Number of Scans	16
Receiver Gain	176.8
Relaxation Delay	1.0000
Pulse Width	12.5000
Acquisition Time	4.0894
Acquisition Date	2022-05-21T08:15:05
Spectrometer Frequency	400.13
Spectral Width	8012.8
Nucleus	1H
Acquired Size	32768
Spectral Size	65536

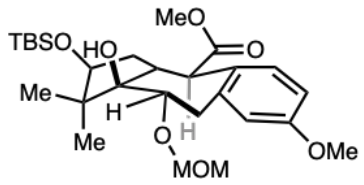

102

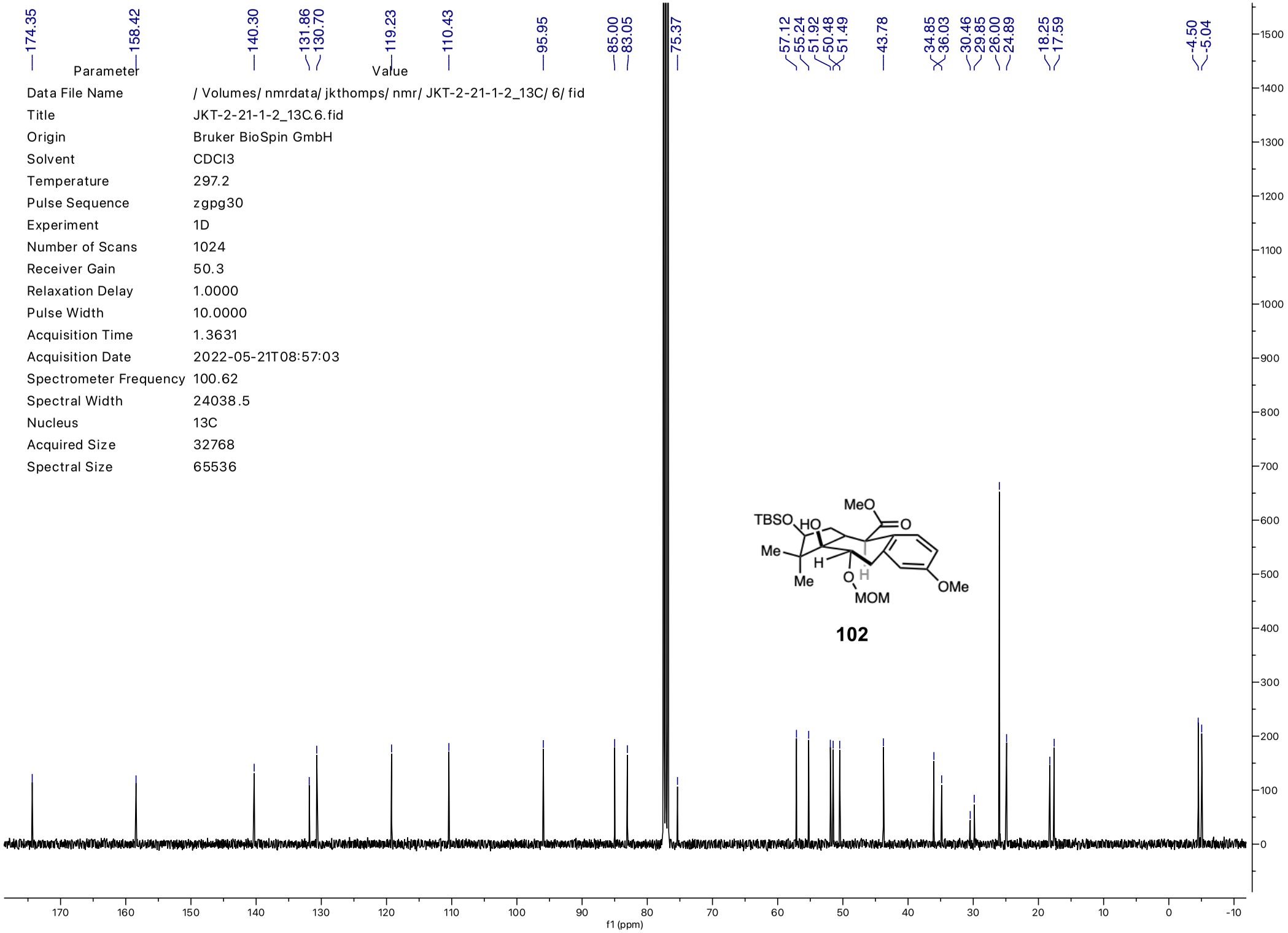
174.35
158.42
140.30
131.86
130.70
119.23
110.43
95.95
85.00
83.05
75.37
57.12
55.24
51.92
50.48
51.49
43.78
34.85
36.03
30.46
29.85
26.00
24.89
18.25
17.59
-4.50
-5.04
Parameter
Value
Data File Name / Volumes/ nmrdata/ jkthomps/ nmr/ JKT-2-21-1-2_13C/ 6/ fid
Title JKT-2-21-1-2_13C.6.fid
Origin Bruker BioSpin GmbH
Solvent CDCl3
Temperature 297.2
Pulse Sequence zgpg30
Experiment 1D
Number of Scans 1024
Receiver Gain 50.3
Relaxation Delay 1.0000
Pulse Width 10.0000
Acquisition Time 1.3631
Acquisition Date 2022-05-21T08:57:03
Spectrometer Frequency 100.62
Spectral Width 24038.5
Nucleus 13C
Acquired Size 32768
Spectral Size 65536
MeO
TBSO
HO
O
Me
H
Me
O
H
MOM
OMe
102
1500
1400
1300
1200
1100
1000
900
800
700
600
500
400
300
200
100
0
170
160
150
140
130
120
110
100
90
80
70
60
50
40
30
20
10
0
-10
f1 (ppm)

Parameter	Value
Data File Name	/ Volumes/ nmrdata/ jkthomps/ nmr/ JKT-2-21-1-2_HSQC/ 7/ ser
Title	JKT-2-21-1-2_HSQC.7.ser
Origin	Bruker BioSpin GmbH
Solvent	CDCl3
Temperature	297.1
Pulse Sequence	hsqcedetgpsisp2.4
Experiment	HSQC-EDITED
Number of Scans	2
Receiver Gain	197.4
Relaxation Delay	1.5000
Pulse Width	12.5000
Acquisition Time	0.1704
Acquisition Date	2022-05-21T09:08:29
Spectrometer Frequency	(400.13,100.62)
Spectral Width	(6009.6,16611.3)
Lowest Frequency	(-1133.0,-1262.8)
Nucleus	(1H,13C)
Acquired Size	(1024,180)
Spectral Size	(1024,1024)
Digital Resolution	(5.87,16.22)

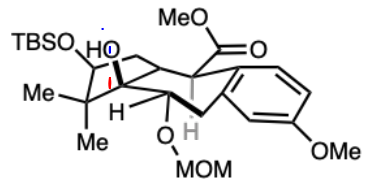

102

f2 (ppm)

f1 (ppm)

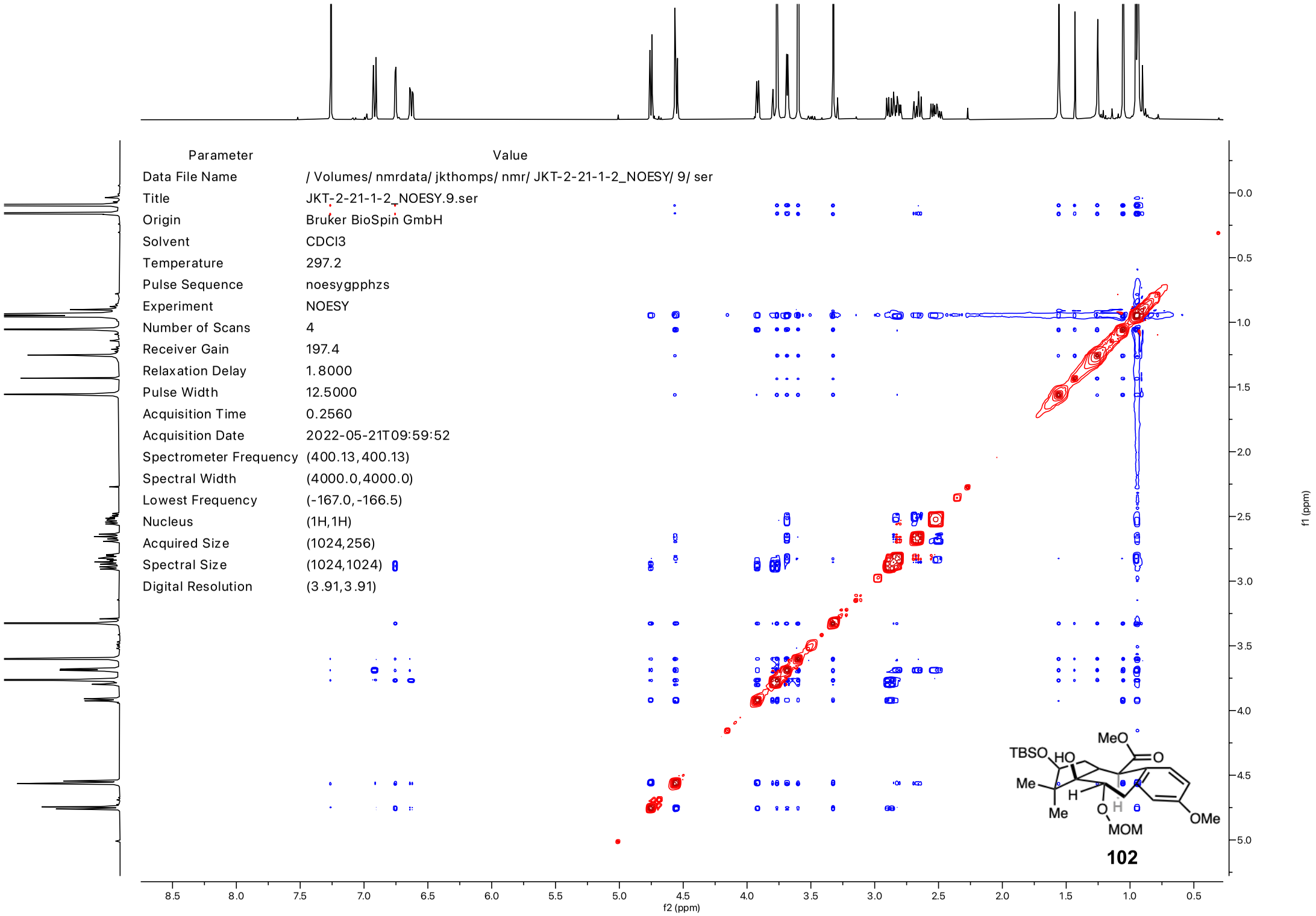
Parameter Value
Data File Name / Volumes/ nmrdata/ jkthomps/ nmr/ JKT-2-21-1-2_NOESY/ 9/ ser
Title JKT-2-21-1-2_NOESY.9.ser
Origin Bruker BioSpin GmbH
Solvent CDCl3
Temperature 297.2
Pulse Sequence noesygpphzs
Experiment NOESY
Number of Scans 4
Receiver Gain 197.4
Relaxation Delay 1.8000
Pulse Width 12.5000
Acquisition Time 0.2560
Acquisition Date 2022-05-21T09:59:52
Spectrometer Frequency (400.13,400.13)
Spectral Width (4000.0,4000.0)
Lowest Frequency (-167.0,-166.5)
Nucleus (1H,1H)
Acquired Size (1024,256)
Spectral Size (1024,1024)
Digital Resolution (3.91,3.91)
f2 (ppm)
f1 (ppm)
TBSO
HO
MeO
O
Me
Me
H
O
H
MOM
OMe
102

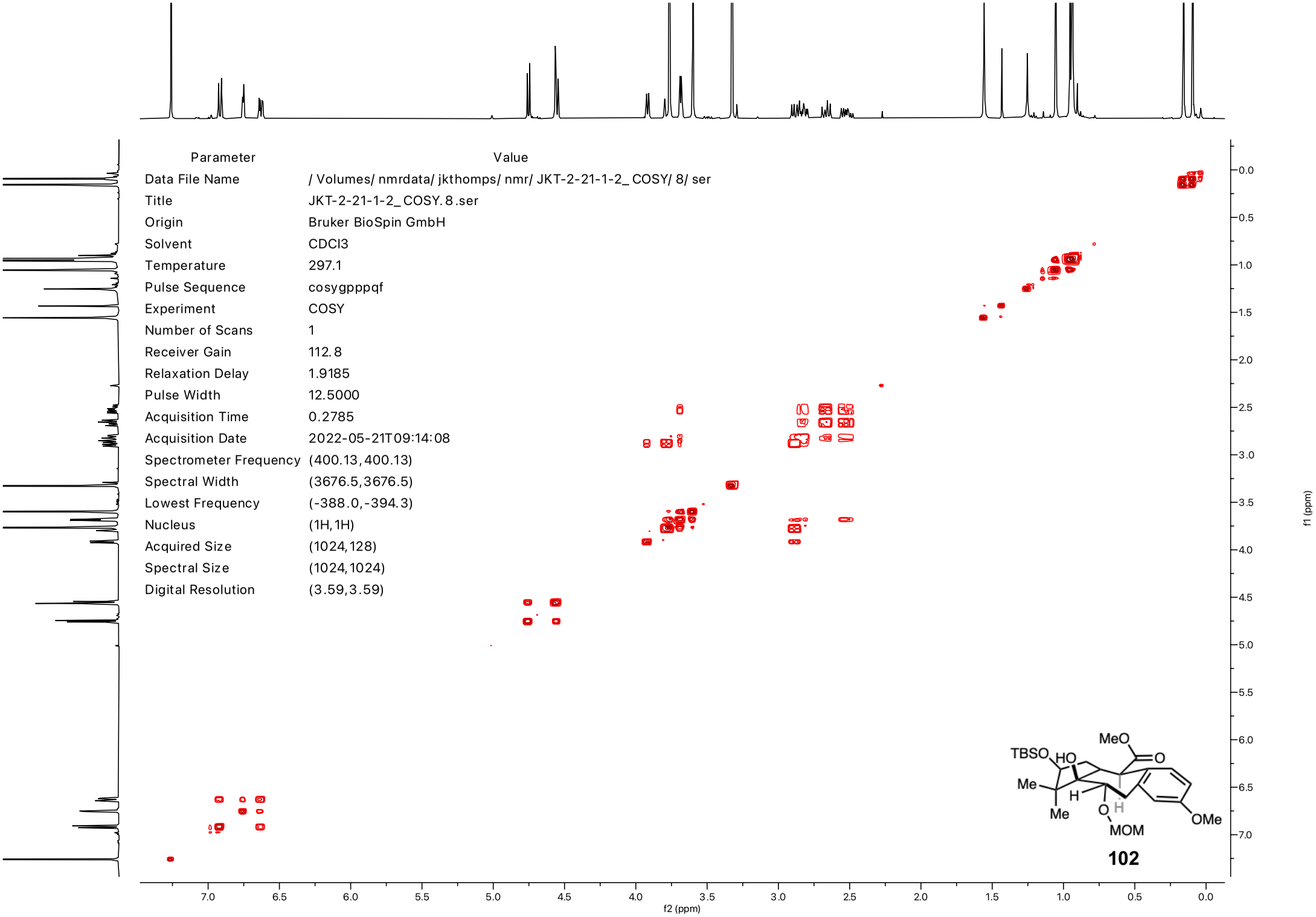
Parameter Value
Data File Name / Volumes/ nmrdata/ jkthomps/ nmr/ JKT-2-21-1-2_ COSY/ 8/ ser
Title JKT-2-21-1-2_ COSY. 8 .ser
Origin Bruker BioSpin GmbH
Solvent CDCl3
Temperature 297.1
Pulse Sequence cosygpppqf
Experiment COSY
Number of Scans 1
Receiver Gain 112. 8
Relaxation Delay 1.9185
Pulse Width 12.5000
Acquisition Time 0.2785
Acquisition Date 2022-05-21T09:14:08
Spectrometer Frequency (400.13, 400.13)
Spectral Width (3676.5, 3676.5)
Lowest Frequency (-388.0, -394.3)
Nucleus (1H, 1H)
Acquired Size (1024, 128)
Spectral Size (1024, 1024)
Digital Resolution (3.59, 3.59)
f2 (ppm)
f1 (ppm)
TBSO
HO
MeO
O
Me
H
Me
O
H
MOM
OMe
102

Parameter	Value
Data File Name	/ Volumes/ nmrdata/ jkthomps/ nmr/ JKT-1-341-6_3D/ 1/ fid
Title	JKT-1-341-6_3D.1.fid
Origin	Bruker BioSpin GmbH
Solvent	CDCl3
Temperature	297.2
Pulse Sequence	zg30
Experiment	1D
Number of Scans	16
Receiver Gain	197.4
Relaxation Delay	1.0000
Pulse Width	12.5000
Acquisition Time	4.0894
Acquisition Date	2022-03-11T10:10:30
Spectrometer Frequency	400.13
Spectral Width	8012.8
Nucleus	1H
Acquired Size	32768
Spectral Size	65536

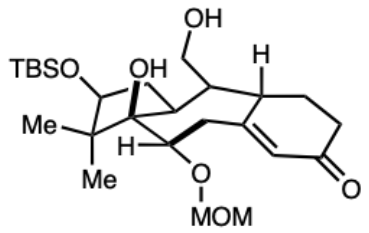

103

198.84
161.70
132.75
107.80
100.02
97.47
85.53
77.22
61.85
57.22
51.17
42.90
40.73
40.30
37.66
37.58
31.00
26.03
25.82
19.31
18.35
-4.74
-5.13

Parameter	Value
Data File Name	/ Volumes/ nmrdata/ jkthomps/ nmr/ JKT-1-331-6_pure/ 2/ fid
Title	JKT-1-331-6_pure.2.fid
Origin	Bruker BioSpin GmbH
Solvent	CDCl3
Temperature	297.1
Pulse Sequence	zgpg30
Experiment	1D
Number of Scans	1000
Receiver Gain	38.0
Relaxation Delay	1.0000
Pulse Width	10.0000
Acquisition Time	1.3631
Acquisition Date	2022-03-10T21:16:30
Spectrometer Frequency	100.62
Spectral Width	24038.5
Nucleus	13C
Acquired Size	32768
Spectral Size	65536

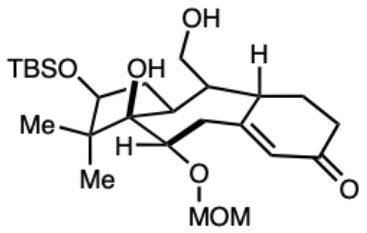

103

f1 (ppm)

Parameter	Value
Data File Name	/ Volumes/ nmrdata/ jkthomps/ nmr/ JKT-1-341-6_3D/ 2/ ser
Title	JKT-1-341-6_3D.2.ser
Origin	Bruker BioSpin GmbH
Solvent	CDCl3
Temperature	297.1
Pulse Sequence	cosygpppqf
Experiment	COSY
Number of Scans	2
Receiver Gain	176.8
Relaxation Delay	1.9205
Pulse Width	12.5000
Acquisition Time	0.2765
Acquisition Date	2022-03-11T10:20:59
Spectrometer Frequency	(400.13,400.13)
Spectral Width	(3703.7,3703.7)
Lowest Frequency	(-399.1,-399.5)
Nucleus	(1H,1H)
Acquired Size	(1024,128)
Spectral Size	(1024,1024)
Digital Resolution	(3.62,3.62)

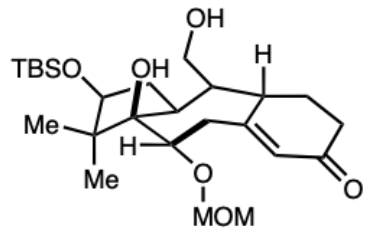

103

f2 (ppm)

f1 (ppm)

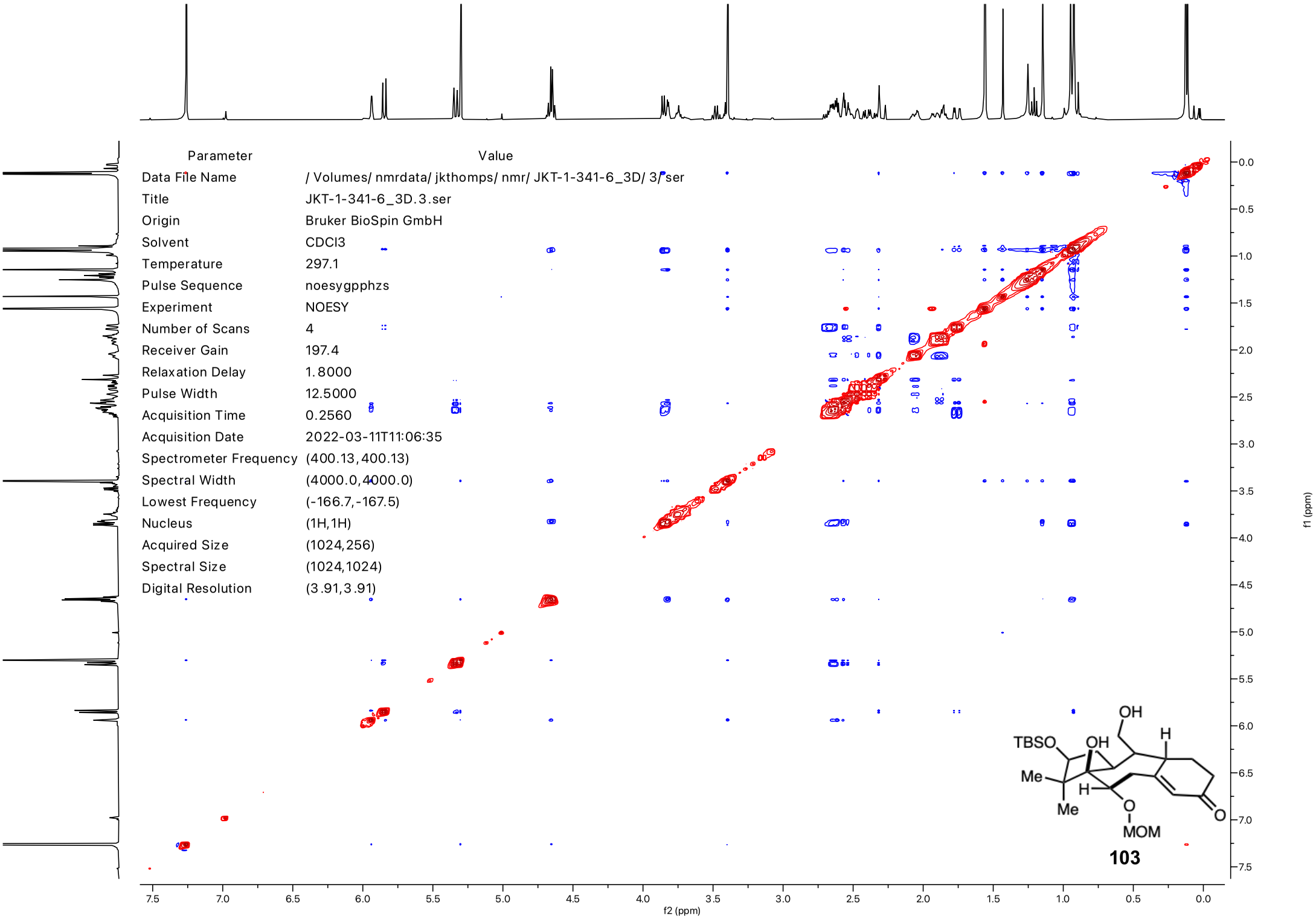
Parameter Value
Data File Name / Volumes/ nmrdata/ jkthomps/ nmr/ JKT-1-341-6_3D/ 3/ ser
Title JKT-1-341-6_3D.3.ser
Origin Bruker BioSpin GmbH
Solvent CDCl3
Temperature 297.1
Pulse Sequence noesygpphzs
Experiment NOESY
Number of Scans 4
Receiver Gain 197.4
Relaxation Delay 1.8000
Pulse Width 12.5000
Acquisition Time 0.2560
Acquisition Date 2022-03-11T11:06:35
Spectrometer Frequency (400.13, 400.13)
Spectral Width (4000.0, 4000.0)
Lowest Frequency (-166.7, -167.5)
Nucleus (1H, 1H)
Acquired Size (1024, 256)
Spectral Size (1024, 1024)
Digital Resolution (3.91, 3.91)
f2 (ppm)
f1 (ppm)
OH
TBSO
OH
H
Me
H
Me
O
MOM
O
103

Parameter	Value
Data File Name	/ Volumes/ nmrdata/ jkthomps/ nmr/ JKT-1-331-6_pure/ 3/ ser
Title	JKT-1-331-6_pure.3.ser
Origin	Bruker BioSpin GmbH
Solvent	CDCl3
Temperature	297.1
Pulse Sequence	hsqcedetgpsisp2.4
Experiment	HSQC-EDITED
Number of Scans	4
Receiver Gain	197.4
Relaxation Delay	1.5000
Pulse Width	12.5000
Acquisition Time	0.2135
Acquisition Date	2022-03-10T21:38:43
Spectrometer Frequency	(400.13,100.62)
Spectral Width	(4795.4,16611.3)
Lowest Frequency	(-574.9,-1262.8)
Nucleus	(1H,13C)
Acquired Size	(1024,180)
Spectral Size	(1024,1024)
Digital Resolution	(4.68,16.22)

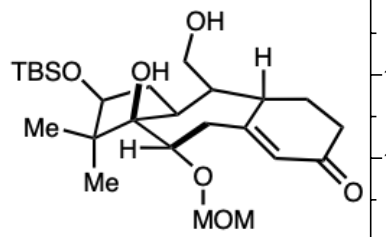

103

f2 (ppm)

f1 (ppm)

Parameter	Value
Data File Name	/ Volumes/ nmrdata/ jkthomps/ nmr/ JKT-1-342_pureflushed/ 1/ fid
Title	JKT-1-342_pureflushed.1.fid
Origin	Bruker BioSpin GmbH
Solvent	CDCl3
Temperature	297.2
Pulse Sequence	zg30
Experiment	1D
Number of Scans	16
Receiver Gain	197.4
Relaxation Delay	1.0000
Pulse Width	12.5000
Acquisition Time	4.0894
Acquisition Date	2022-03-13T13:39:09
Spectrometer Frequency	400.13
Spectral Width	8012.8
Nucleus	1H
Acquired Size	32768
Spectral Size	65536

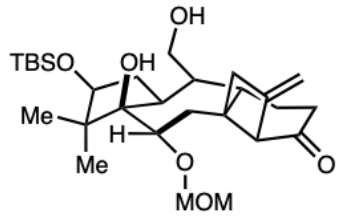

104

Parameter	Value
Data File Name	/ Volumes/ nmrdata/ jkthomps/ nmr/ JKT-1-342_pureflushed/ 2/ fid
Title	JKT-1-342_pureflushed.2.fid
Origin	Bruker BioSpin GmbH
Solvent	CDCl3
Temperature	297.1
Pulse Sequence	zgpg30
Experiment	1D
Number of Scans	750
Receiver Gain	78.7
Relaxation Delay	1.0000
Pulse Width	10.0000
Acquisition Time	1.3631
Acquisition Date	2022-03-13T14:10:00
Spectrometer Frequency	100.62
Spectral Width	24038.5
Nucleus	13C
Acquired Size	32768
Spectral Size	65536

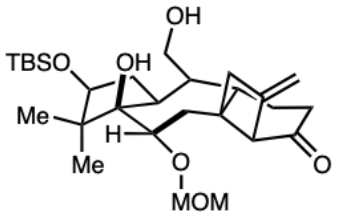

104

209.60
141.99
110.37
109.23
100.24
98.22
85.76
78.78
62.78
58.65
57.11
51.29
47.80
43.52
41.66
39.86
39.66
39.60
33.82
27.74
26.51
25.81
19.51
18.33
-4.75
-5.13

f1 (ppm)

Parameter	Value
Data File Name	/ Volumes/ nmrdata/ jkthomps/ nmr/ JKT-1-342_pureflushed/ 3/ ser
Title	JKT-1-342_pureflushed.3.ser
Origin	Bruker BioSpin GmbH
Solvent	CDCl3
Temperature	297.2
Pulse Sequence	hsqcedetgpsisp2.4
Experiment	HSQC-EDITED
Number of Scans	4
Receiver Gain	197.4
Relaxation Delay	1.5000
Pulse Width	12.5000
Acquisition Time	0.2135
Acquisition Date	2022-03-13T14:32:13
Spectrometer Frequency	(400.13,100.62)
Spectral Width	(4795.4,16611.3)
Lowest Frequency	(-527.1,-1273.3)
Nucleus	(1H,13C)
Acquired Size	(1024,180)
Spectral Size	(1024,1024)
Digital Resolution	(4.68,16.22)

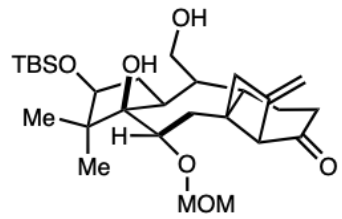

104

f2 (ppm)

f1 (ppm)

Parameter	Value
Data File Name	/ Volumes/ nmrdata/ jkthomps/ nmr/ JKT-1-342_pureflushed/ 4/ ser
Title	JKT-1-342_pureflushed.4.ser
Origin	Bruker BioSpin GmbH
Solvent	CDCl3
Temperature	297.1
Pulse Sequence	cosygpppqf
Experiment	COSY
Number of Scans	2
Receiver Gain	197.4
Relaxation Delay	1.9164
Pulse Width	12.5000
Acquisition Time	0.2806
Acquisition Date	2022-03-13T14:42:40
Spectrometer Frequency	(400.13,400.13)
Spectral Width	(3649.6,3649.6)
Lowest Frequency	(-413.9,-413.9)
Nucleus	(1H,1H)
Acquired Size	(1024,128)
Spectral Size	(1024,1024)
Digital Resolution	(3.56,3.56)

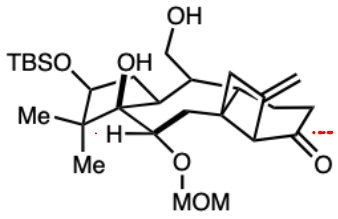

104

f2 (ppm)

f1 (ppm)

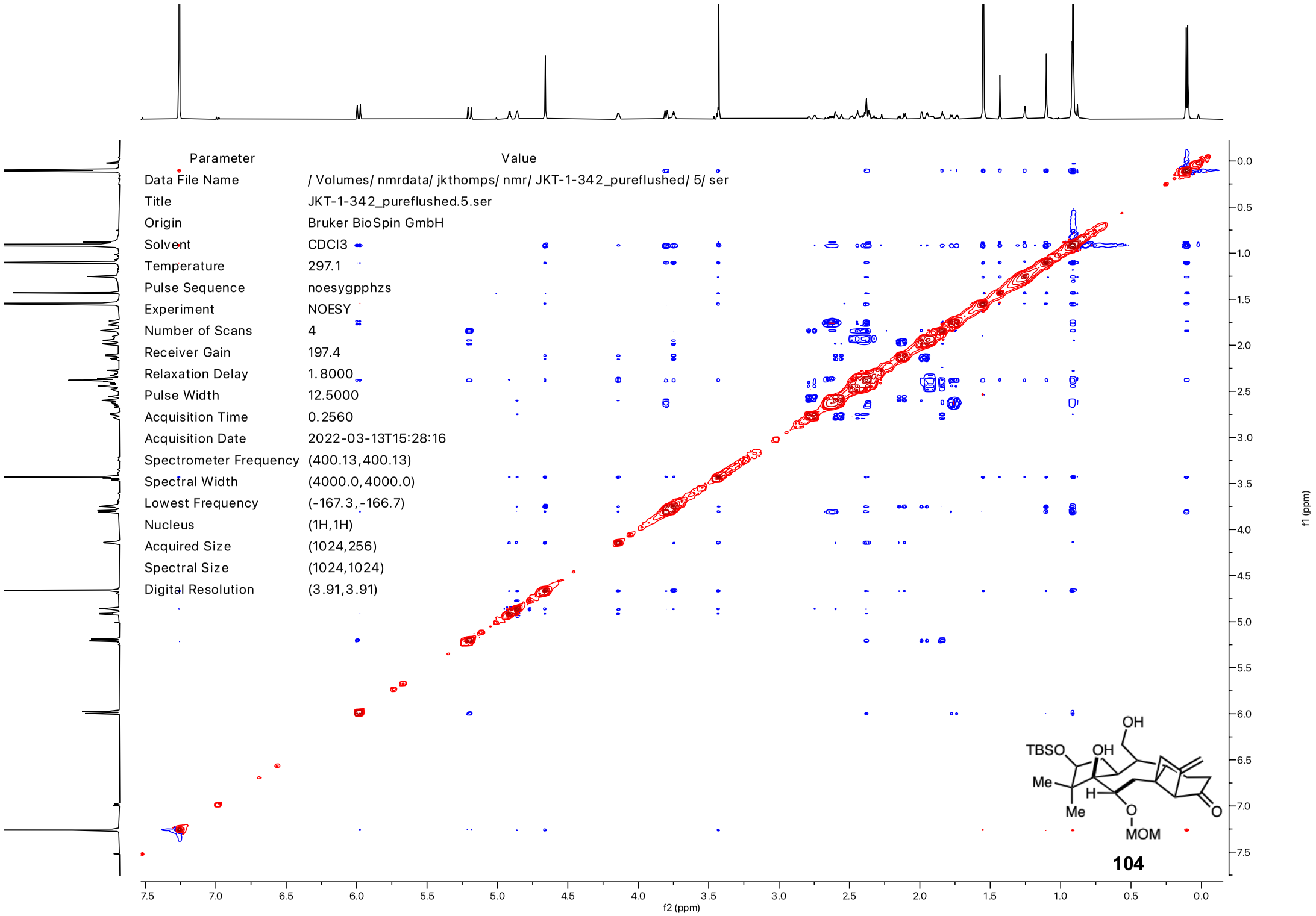
Parameter Value
Data File Name / Volumes/ nmrdata/ jkthomps/ nmr/ JKT-1-342_pureflushed/ 5/ ser
Title JKT-1-342_pureflushed.5.ser
Origin Bruker BioSpin GmbH
Solvent CDCl3
Temperature 297.1
Pulse Sequence noesygpphzs
Experiment NOESY
Number of Scans 4
Receiver Gain 197.4
Relaxation Delay 1.8000
Pulse Width 12.5000
Acquisition Time 0.2560
Acquisition Date 2022-03-13T15:28:16
Spectrometer Frequency (400.13,400.13)
Spectral Width (4000.0,4000.0)
Lowest Frequency (-167.3,-166.7)
Nucleus (1H,1H)
Acquired Size (1024,256)
Spectral Size (1024,1024)
Digital Resolution (3.91,3.91)
CDCl3
OH
TBSO
OH
Me
H
Me
O
O
MOM
104
f2 (ppm)
f1 (ppm)

Chapter 4

3.2.1 bicycle synthesis[†]

4.1 INTRODUCTION

This chapter summarizes efforts to complete 3.2.1 bicycle synthesis in the context of the total synthesis of auriculatol A. Various radical cascade processes, transition metal catalyzed reactions, and annulations are discussed, including a Snider radical cascade, palladium-catalyzed decarboxylative Tsuji-Stoltz allyation, nickel-catalyzed intramolecular carbonyl 1,2-addition, and Michael-Aldol cascade. Several failed routes are discussed in detail. Taken together, these data provide foundational information for

[†] Portions of this chapter were adapted from the following communication: Thompson, J. K.; Youngblood, K. C.; Teh, S. Y. H.; Farley, C. M.; Zhang, Z.; Virgil, S. C.; Reisman, S. E. *J. Am. Chem. Soc.* **2025**, *147*, 42170–42174. Scott C. Virgil is acknowledged for his expertise enabling the preparatory HPLC purification of **107A**. J.K.T. was supported by the NSF GRFP (DGE-1745301). S.E.R. acknowledges fellowship support by the NIH (R35GM118191). The research presented in this chapter was completed in collaboration with Shawn Teh and Kala Youngblood, a former master's student and graduate student in the Reisman group, respectively.

disclosure of a standalone approach for the synthesis of 3.2.1 bicycles through the use of Tsuji-Stoltz allylation and nickel-catalyzed intramolecular carbonyl 1,2-addition. Coupled with work done by other colleagues, Dr. Sven Richter and Dr. Ray Turro, these data may be of particular interest for future publication.

4.2 VERSATILE 3.2.1 BICYCLE SYNTHESIS THROUGH THE SNIDER RADICAL CASCADE

4.2.1 A transform-based approach for 3.2.1 bicyclic aldehyde synthesis: use of the Snider Radical Cascade

As described in the concluding paragraph of Chapter 3.3.3, a new route that could circumvent the use of the Birch reduction was devised. The simplest and perhaps most elegant solution invoked the use of a fragment containing the eastern part of the molecule already intact. The key fragment would need to be synthesized and tested in the vinylogous Mukaiyama aldol coupling reaction.

Scheme 4.1. *Revised, convergent route necessitates the development of 3.2.1 bicyclic aldehyde synthesis.*

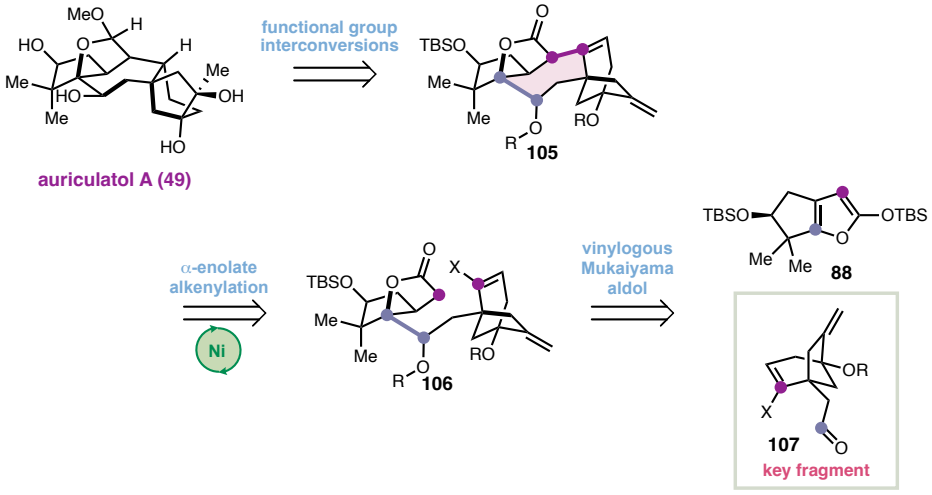

Several strategies were outlined as potentially feasible to the key fragment. Searching the literature, it became clear that 3.2.1 bicycle synthesis is often accomplished through the use of a radical cascade from acyclic α-allylated β-keto esters, colloquially referred to as the Snider radical cascade.[1] This is often accomplished with stoichiometric loadings of $Mn(OAc)_3$. Mn^{III}, following coordination to ketone, oxidizes β-keto esters to the corresponding α-radical, which can cyclize to form an alkyl radical. It has been shown that Mn^{III} has the ability to oxidize tertiary radicals to cations but is not oxidizing enough to oxidize primary and secondary radicals.[2] For this reason, $Cu(OAc)_2$ is often employed as a stoichiometric oxidant under the reaction conditions. Taken together, the Snider radical cascade has been applied to 3.2.1 bicycle synthesis in various contexts. Indeed, compound **110** was identified as a viable substrate that could be applied to the synthesis of the key fragment (Scheme 4.2).[3] Due to the fact that MEM groups are acid-labile, the reaction was conducted in EtOH rather than AcOH. In this report, unique solvent effects were observed and discussed as they apply to various substrates, such as the greater propensity for 5-*exo* and alkene-containing products in EtOH, while alcohols and lactones were generated in AcOH.[3] In our transform-based approach, compound **110** could be accessed in 2 steps from α-allyl methyl acetoacetate (**108**, Scheme 4.2), but it was not known how scalable the reaction to form **109** would be and if the step could support the first step of a total synthesis.

Scheme 4.2. *Important precedent from Snider and coworkers.*

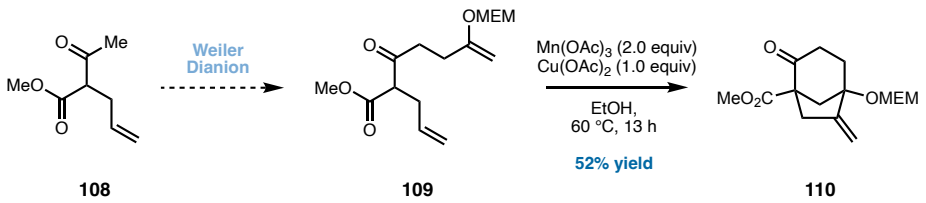

In our retrosynthetic analysis of **107A**, it was believed the product could be formed

from acid-mediated hydrolysis of vinyl methoxy ether **111** (Scheme 4.3). **111** could arise from a Wittig homologation of aldehyde **112**, which could be formed from a 2-step oxidation/reduction protocol from ester **114**. **114** could be formed through ketone triflation of **110**, which was shown to be accessible from the Snider radical cascade of **109** (Scheme 4.3).

Scheme 4.3. *Retrosynthetic analysis of* ***107A***.

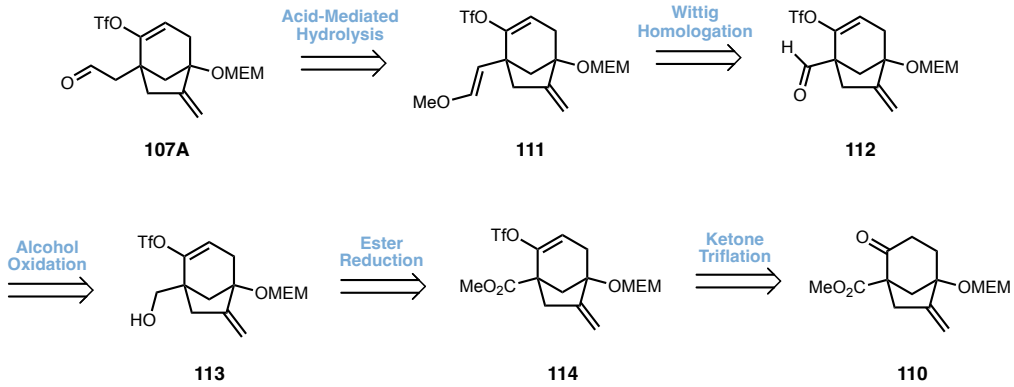

During the early synthetic planning of the fragment synthesis, we were aware that compound **107A** could be prepared as the racemate to test the vinylogous Mukaiyama Aldol but anticipated that it could be resolved through the use of chiral preparatory HPLC. This would enable access to (*R,S*)-**107A** (Scheme 4.4). Furthermore, upon subjection to our triflex methodology[4] to form the alkenyl bromide, fragment **107B** could also be prepared and tested. Depending on the competency of the fragment in the vinylogous Mukaiayama Aldol coupling reaction and the functional group required for the Ni-catalyzed alkenylation, a variety of substrates could be synthesized and tested.

Scheme 4.4. *Elaboration of* ***107A*** *(if necessary).*

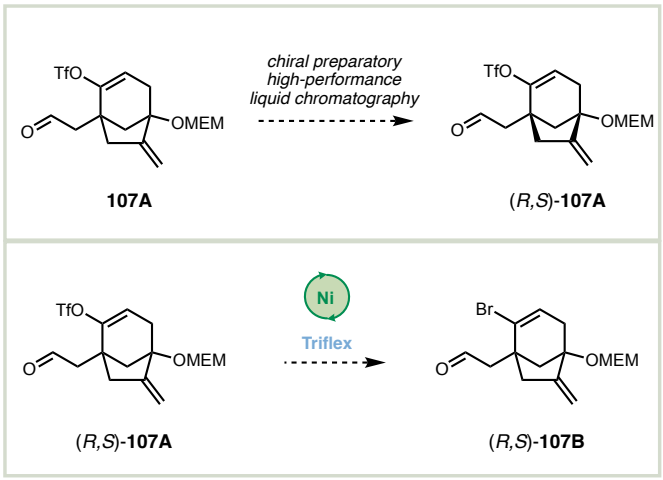

4.2.2 Synthesis of the Snider Radical Cascade substrate

Allylation of methyl acetoacetate could be accomplished using NaH and allyl bromide; however, the yields to form **108** were lower than reported in the literature (see experimental section for preparation details).[5] Literature precedent for the α-alkylation of **108** with α-chloroethers exists through the Weiler dianion;[6] nevertheless, in our hands, only substrates containing the MEM group produced the coupled product when compared to MOM (**116** or **109**). As shown in Scheme 4.5, use of vinyl MOM ethers led to coupling and hydrolysis to compound **117**. HMPA was a necessary additive, but the reaction could be accomplished using 1.1 equiv. of **115**. An essential aspect of the reaction is the use of dry, 90% NaH, which is stored and handled in a nitrogen-filled glovebox. Use of 60% NaH in mineral oil led to diminished yields (< 20%) of the product and messier reaction profiles to several uncharacterized side products. Weiler dianions are reported to be extremely sensitive to moisture. For that reason, and taking the data from Scheme 4.5 into account, a protocol employing 2 equivalents of hexamethylphosphoramide (HMPA) and 90% NaH, used and handled in the glovebox, provided 52% yield of **109**. The yield and scalability of

this reaction up to 20 g scale was tolerated.

Scheme 4.5. *Exploration of Weiler dianion functionalization.*

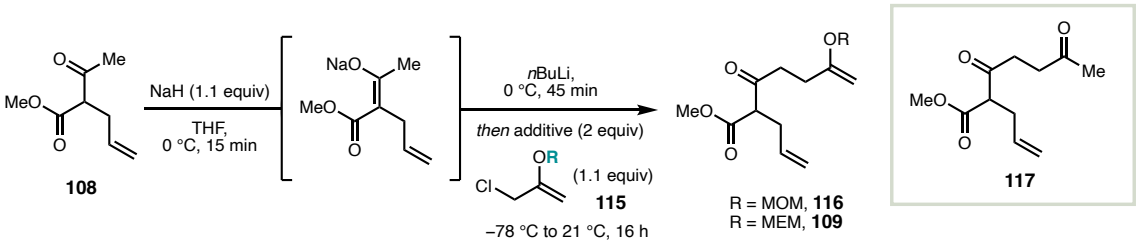

entry	R	additive	equiv. **115**	yield product (%)	yield **117** (%)
1	MOM	-	1.1	-	-
2	MOM	-	1.1	-	-
3	MOM	-	2.0	-	-
4	MOM	HMPA	1.1	-	56
5	MEM	-	1.1	-	-
6	MEM	HMPA	1.1	52	-

4.2.3 Studies to affect the Snider Radical Cascade

With **109** in hand, the Snider Radical Cascade could be tested. Excitingly, the precedent from Snider could be repeated in identical yield, given a couple of considerations that were imperative to the yield of the reaction: the use of homemade $Mn(OAc)_3$ was essential to good yields of the product; use of $Mn(OAc)_3$, as supplied by Combi Blocks, led to diminished formation of the product (< 20% yield, result not shown). Additionally, the yield of the Snider Radical Cascade could be increased to 58% by use of degassed EtOH. While the reaction had yields ranging consistently from 40-58%, it could be conducted on 20 g scale without reduction in yield and with good reproducibility.

Scheme 4.6. *Formation of* ***110***.

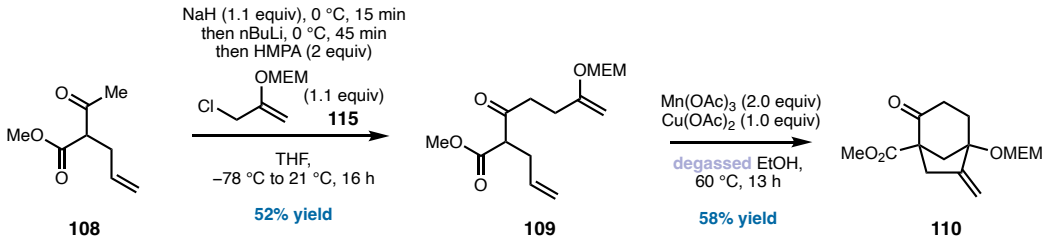

While the route to **110** was amenable to large scale and reliable, the use of expensive, toxic reagents on scale were somewhat prohibitive. The use of superstoichiometric MEMCl to prepare fragment **115** over two steps, followed by stoichiometric *n*BuLi and HMPA to form **109**, followed by super stoichiometric quantities of $Mn(OAc)_3$ (that could not be purchased and had to be made), limited material throughput when trying to exceed 20 g scale. See the experimental section for more details. Nevertheless, for early proof-of-concept studies, the route could suffice.

4.2.4 Advancement to the key fragment (107A)

With **110** in hand, triflation could be accomplished under literature-reported conditions to form **114** (Scheme 4.7).[4] The enol triflate (**114**), containing a bridgehead methyl ester, could be subjected to a four-step homologation sequence to aldehyde **107A** through: 1) exhaustive DIBAL reduction to alcohol **113**, 2) Swern oxidation to aldehyde **112**, 3) Wittig olefination to vinyl methyl ether **111**, and finally 4) hydrolysis to the terminal aldehyde **107A**.

Scheme 4.7. *Initial route to* ***107A***.

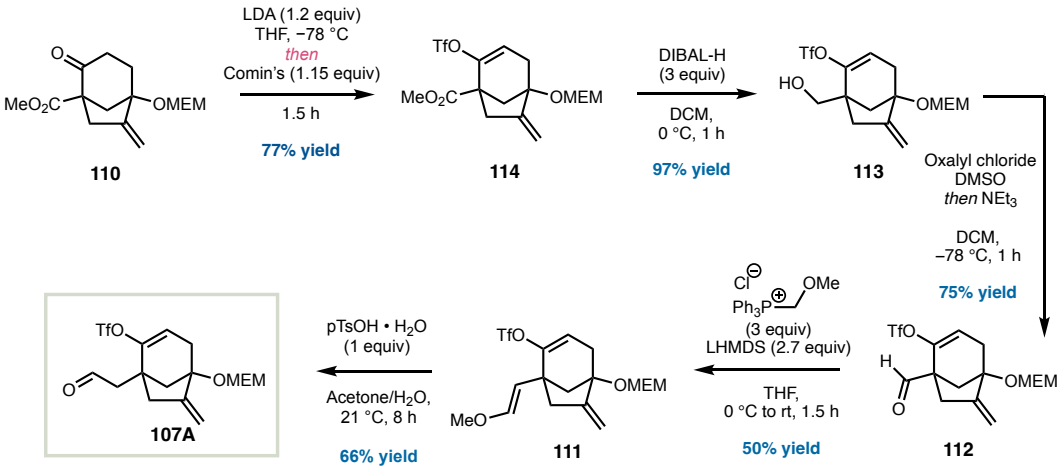

The development of the route depicted in Scheme 4.7 occurred swiftly with only a few challenges. Screening oxidation conditions of **113** to **114** was uneventful; use of Stahl oxidation led to a messy reaction profile and low conversion, likely due to side reactivity with the enol triflate, although this is not confirmed (Scheme 4.8, entry 1). Ley oxidation (TPAP/NMO) led to 56% yield, while Swern oxidation delivered the product in 75% yield (Scheme 4.8, entry 2-3).

Scheme 4.8. *Oxidation of alcohol* ***113***.

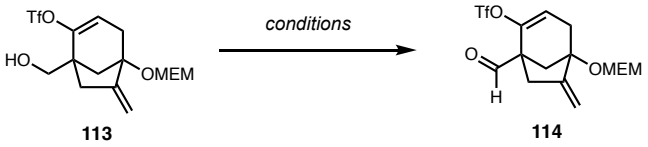

entry	*conditions*	yield **114** (%)
1	$Cu(NCCH_3)_4 \cdot CF_3SO_3$, bpy, ABNO, 1-methylimidazole	27
2	TPAP, NMO • H_2O	57
3	DMSO, oxalyl chloride, NEt_3	75

One challenge that arose was the Wittig olefination step. Surprisingly, use of KO*t*Bu did not lead to the desired product but instead resulted in formation of an unidentified side product (Scheme 4.9, entry 1). However, LHMDS furnished the product

in 50% yield as a 2:1 inconsequential mixture of diastereomers (Scheme 4.9, entry 2). The yield of this reaction was low but was adequate for material throughput. One of the other challenges that arose was the vinyl methyl ether hydrolysis. While use of *p*TsOH • H_2O led to 66% yield, BBr_3 led to substrate decomposition (Scheme 4.9, entry 3-4), and HCl led to primarily cleavage of the MEM protecting group (not shown). More thorough investigation could be conducted to try to optimize the yield, but for the purpose of exploring downstream chemistry, was adequate.

Scheme 4.9. *Wittig Homologation of* ***114*** *followed by acid-mediated hydrolysis.*

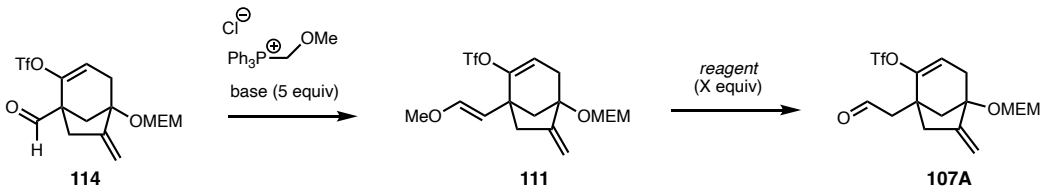

entry	base	*dr*	yield **111** (%)
1	KO*t*Bu	-	-
2	LHMDS	2 : 1	50

entry	*reagent*	yield **107A** (%)
3	BBr_3 (1 equiv)	-
4	*p*TsOH • H_2O (3 equiv)	66

4.2.5 Further derivatization of the key fragment (107A)

As shown in Scheme 4.4, **107A** could be resolved through the use of chiral preparatory HPLC and subjected to adapted conditions from our Triflex methodology to form enantioenriched **107B**. 1.5 g of compound could be separated to afford 500 mg of product; this took a total of 10 h at the instrument, however, with only modest yield overall.

Scheme 4.10. *Access to enantioenriched* ***107B****.*

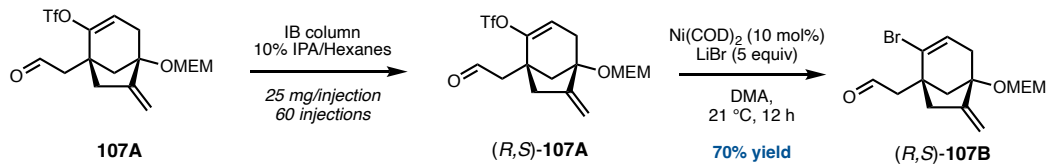

The halide exchange of **107A** to **107B** occurred uneventfully. Use of 10 mol%

Ni(COD) with 1.5 equiv of LiBr for 3 h led to 65% yield and > 90% conversion, while stirring for 12 h led to an increase in conversion and 68% yield (Scheme 4.11).

Scheme 4.11. *Access to enantioenriched* ***107B****.*

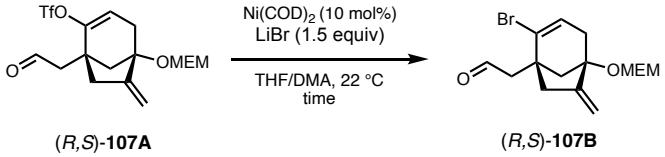

(*R,S*)-**107A** (*R,S*)-**107B**

entry	time (h)	conversion (%)	yield **107B** (%)
1	3	91	65
2	12	95	68

4.2.6 Strategies to shorten the key fragment (107B) synthesis

Several strategies to shorten the fragment synthesis at this stage were brainstormed. One of the least step-economical parts of the fragment synthesis involves the conversion of ester **110** to aldehyde **107A**. As shown in Scheme 4.7, this is accomplished in 5 steps and 18% overall yield. The most thoroughly investigated strategy was the application of a decarboxylative Giese addition in order to install the pendant aldehyde in the key fragment in a more expedient manner (Scheme 4.12). In theory, aldehyde **107A** could arise from alkyl sulfone **118** and be traced back to **119** following ketone triflation. Alkyl sulfone **119** could arise from decarboxylative Giese addition, providing carboxylic acid **120**. In the forward sense, decarboxylation of **120** using photoredox catalysis could deliver a radical intermediate, which could engage in Giese addition with the desired Giese acceptor. The ideal Giese addition unit would add two-carbons that could be converted to the terminal aldehyde. A variety of Giese acceptors were envisioned under these conditions. Perhaps the most exciting was Hwu and Murphree's use of phenyl vinyl sulfone, which is literature-reported to undergo a one-pot oxidation with KHMDS and O_2.[7] Other acceptors were

thought to be plausible for investigation of the reactivity, including methyl vinyl ketone, various acrylates, and 2-propenenitrile. These three-carbon units could form the terminal aldehyde following ozonolytic cleavage of the silyl enol ether or some other internal olefin equivalent (although this route would be less direct than the sulfone). While there is certainly a flurry of papers in the realm of decarboxylative Giese additions, we were drawn to the work of Morita, Liang, Aggarwal, MacMillan, and Pospech.[8-13] A review from Lee and coworkers in this area nicely summarizes the state of the art for this research aim.[14,15]

Scheme 4.12. *Decarboxylative Giese addition.*

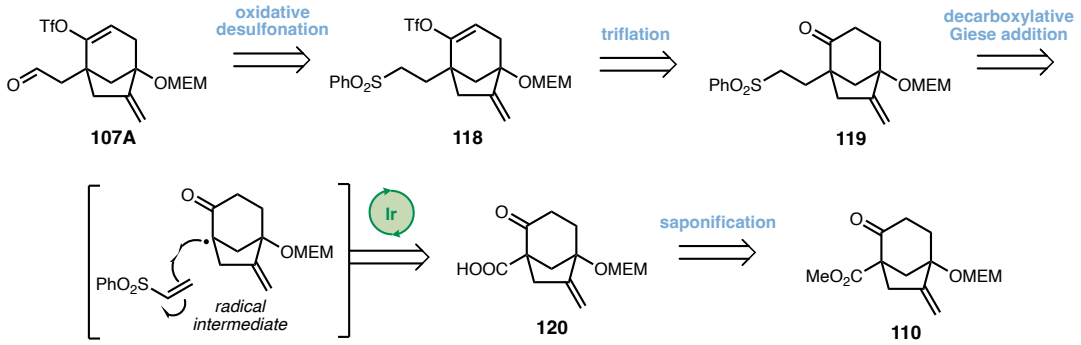

While the operation seemed simple in synthetic planning, it was difficult in practice. Saponification of ester **110** to **120** proved challenging (Scheme 4.13). Upon subjection to LiOH, NaOH, and KOH in THF/H_2O mixtures, no reaction was observed. There are a variety of reasons this could be, likely sterics, but it is also possible that the ketone is deprotonated to an anionic intermediate. Perhaps charge repulsion prevents a second addition of hydroxide in the saponification mechanism. Other reagents such as BBr_3 or trimethyltin hydroxide led to MEM deprotection and no reaction, respectively (not shown).

Scheme 4.13. *Failure to induce saponification on substrate* ***180****.*

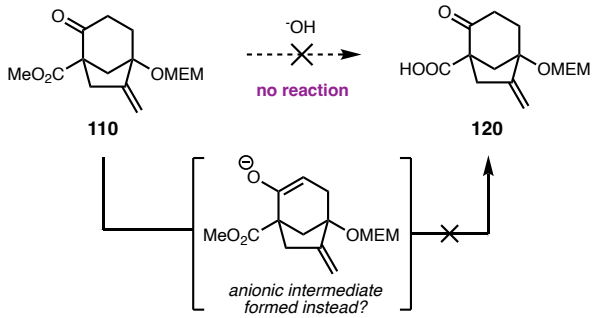

We then turned to the hypothesis that switching the order of the steps could provide a suitable decarboxylative Giese addition substrate. Namely, ketone triflation of **110** could provide **121**, which could act itself as a decarboxylative Giese addition substrate (Scheme 4.14). Alternatively, **114** could be converted to **121** *via* triflate-bromide exchange, which could also undergo saponification to **123** and thus allow investigation of the decarboxylative Giese addition to provide **122**. The same oxidative desulfonation could deliver **107B**.

Scheme 4.14. *Changing the order of the steps could solve saponification issue.*

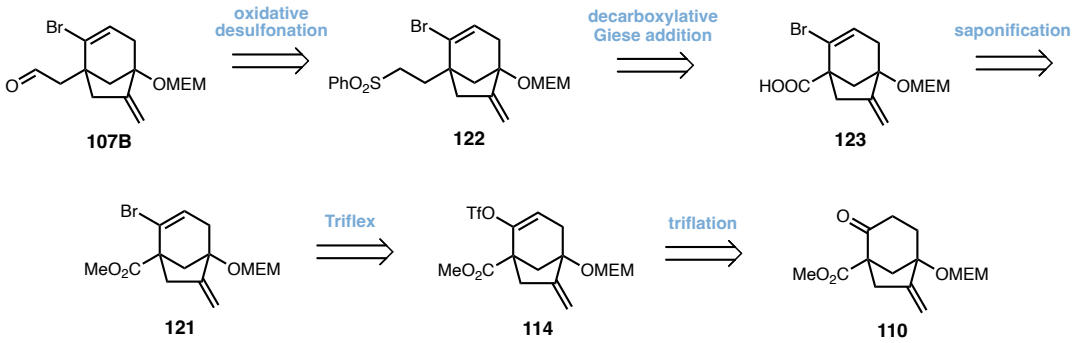

When opting to perform the saponification on enol triflate **114**, less than 10% yield was isolated (Scheme 4.15). Instead, triflate hydrolysis was observed as the primary product. Indeed, triflates are base-labile upon hydroxide addition to form the tetrahedral sulfoxide intermediate.[16] As described in Scheme 4.13, substrate **110** (the product of triflate

hydrolysis) is incompetent under saponification conditions. Turning our attention to screen triflex conditions on substrate **114**, it quickly became clear that protodebromination was an issue. Nevertheless, after some screening, it was revealed that the protodebromination increased with Ni^{II} loading. Keeping the $Ni(OAc)_2 \cdot H_2O$ loading to 5 mol%, 51% of product could be formed (Scheme 4.15, entry 1). Increasing the amounts of nickel, COD, or LiBr led to increased levels of protodebromination (Scheme 4.15, entry 2-5).

Scheme 4.15. *Vinyl halide (**121**) formation.*

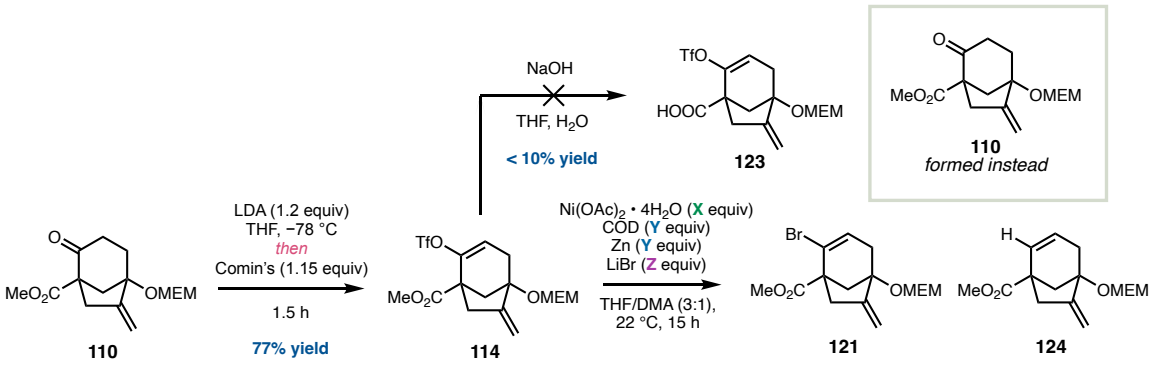

entry	X	Y	Z	ratio **114** : **121** : **124**	yield **121** (%)
1	0.05	0.1	1.5	0.07 : 1 : 0.06	51
2	0.1	0.2	3	0.51 : 1 : 0.2	36
3	0.15	0.3	4.5	0.42 : 1 : 0.42	10
4	0.83	1.7	10	1.09 : 1 : 4.66	10
5	0.15	0.3	6	0.27 : 1 : 0.60	10

Substrate **121** proved competent under saponification reaction conditions, affording **123** in 85% yield after treatment with excess NaOH. These data bolster the hypothesis that enolization of the ketone was the issue in the saponification after all. Finally, with access to a decarboxylative Giese addition substrate, the key photoredox catalysis step could be tested; however, the difficulties of this route did not subside. Additional efforts to engage the carboxylic acid under photoredox catalysis conditions were unfruitful. In almost all cases, no reaction was observed, even at elevated reaction temperatures and times (Scheme 4.16).

Scheme 4.16. *Low conversion of* ***123*** *and* ***120*** *under photoredox conditions.*

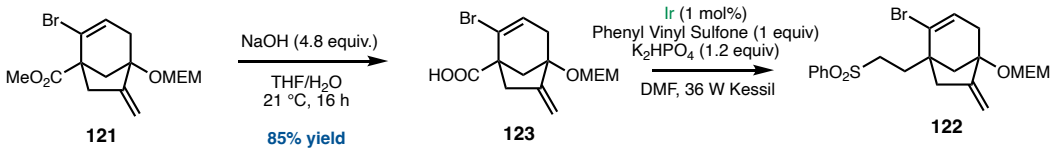

entry	Ir	temp, time	result
1	Ir[dF(CF$_3$)ppy)]$_2$(bpy)PF$_6$ (1 mol%)	21 °C, 12 h	**123**
2	Ir[dF(CF$_3$)ppy)]$_2$(dtbbpy)PF$_6$ (1 mol%)	21 °C, 12 h	**123**
3	Ir[dF(CF$_3$)ppy)]$_2$(bpy)PF$_6$ (1 mol%)	40 °C, 12 h	**123**
4	Ir[dF(CF$_3$)ppy)]$_2$(dtbbpy)PF$_6$ (1 mol%)	40 °C, 12 h	**123**
5	Ir[dF(CF$_3$)ppy)]$_2$(bpy)PF$_6$ (1 mol%)	40 °C, 72 h	**123**
6	Ir[dF(CF$_3$)ppy)]$_2$(dtbbpy)PF$_6$ (1 mol%)	40 °C, 72 h	**123**

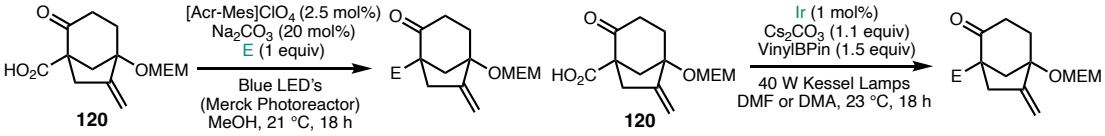

entry	E	result
1	vinyl-SO$_2$Ph	**120**
2	diethyl-ethylidene malonate	**120**

entry	Ir	result
1	[Ir(dtbbpy)(ppy)$_2$]PF$_6$	**120**
2	[Ir(dF(Me)ppy)$_2$(dtbbpy)]PF$_6$	**120**

Given that there was difficulty getting reactivity of the carboxylic acid, we opted to abandon the research goal of applying decarboxylative Giese addition chemistry. However, one area that could be interesting is finding a higher yield to the two-step homologation sequence (**112** to **107A**), which provided **107A** in a modest 33% yield over 2 steps. Nonetheless, finding a one-step, higher-yielding reaction could make the route more efficient. To this end, strategies utilizing ylides were literature searched, but never tried due to time constraints. Use of conditions from Scheidt, for example, offer a mild, selective homologation of esters to aldehydes in a single step and could be potentially useful in applying in this system.[17] Generally, several types of ylides could be synthesized and tested for the homologation chemistry and optimized for yield.

4.3 ASYMMETRIC 3.2.1 BICYCLE SYNTHESIS THROUGH RADICAL INTERMEDIATES

4.3.1 Chiral induction through the use of a chiral auxiliary

With a suitable route to *rac*-**107B** and acknowledging the shortcomings of the preparatory HPLC for material throughput, we wondered if asymmetry could be induced through the use of a chiral auxiliary. Indeed, chiral auxiliary's have been demonstrated in the Snider radical cascade. The chiral auxiliary is usually installed through the ester functionality of the Snider β-keto ester substrate. Most notably, menthol, phenylmenthol, oxazolidinone, sultam, sulfoxide, and pyrrolo groups have been reported previously.[18-23] Substrates could be prepared simply by mixing the starting material with DMAP in refluxing toluene. The substrates provided a wide range of observed diastereoselectivity, from 0 to 92% diastereomeric excess (*de*) (Scheme 4.17). Additionally, the auxiliaries could be cleaved simply by saponification or exhaustive reduction to the primary alcohol (not shown).

Scheme 4.17. *Asymmetric induction in Mn-based oxidative radical cascades.*

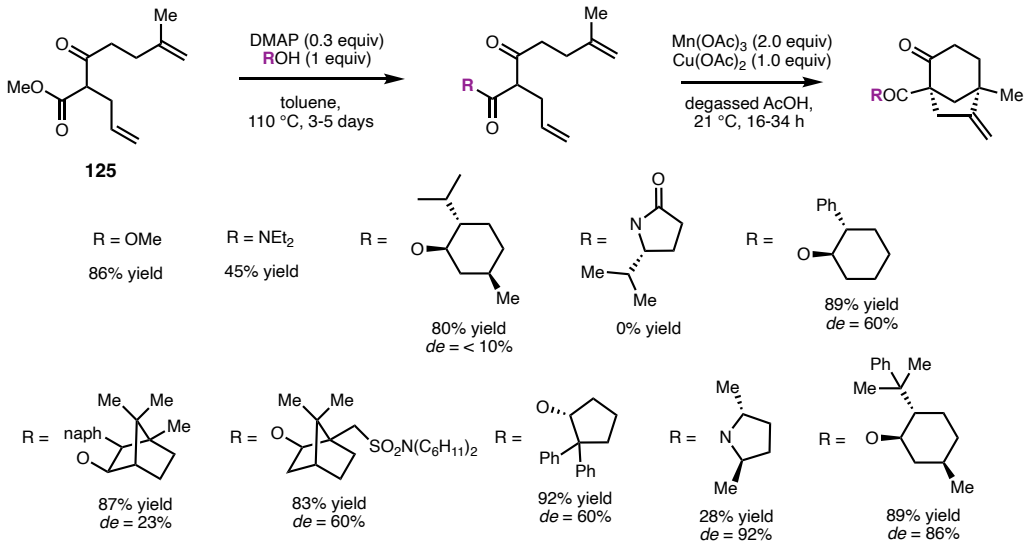

Despite the strong precedent in this area, Snider's substrates never contained oxygen-containing functionalities at the bridgehead system required in auriculatol A. When attempting the derivative bearing 8-phenyl menthol (**127**), unfortunately, only a modest *de* was observed. Furthermore, the yield of both the transesterification and the radical cascade suffered compared to the racemic methyl ester system, providing **128** in 5% yield over 3 steps. Given these results, a new strategy would be necessary to investigate asymmetric 3.2.1 bicycle synthesis; the material throughput of this route was simply too limiting. Trying other chiral auxiliaries did not seem very promising, given the relatively low yields and *de*'s for other substrates shown in Scheme 4.17.

Scheme 4.18. *8-phenyl menthol derivative provides low yield and moderate de.*

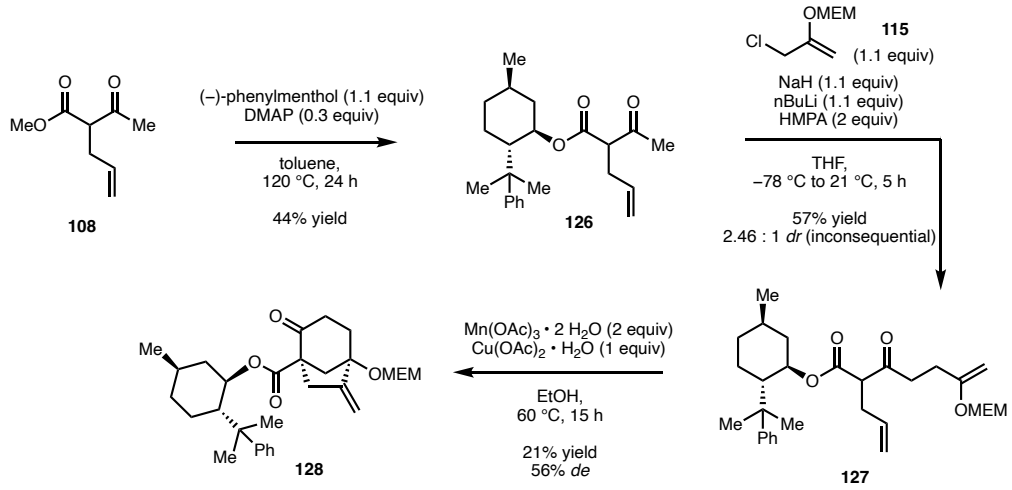

4.3.2 Chiral atom-transfer reactions

Due to the difficulties with the chiral auxiliary strategy, a new approach through the use of a chiral atom-transfer reaction was imagined. In theory, α-bromination of **109** could provide **129**, from which chelation to a chiral ligand, halogen atom abstraction, 6-*endo* cyclization, 5-*exo* cyclization, and bromine atom termination could provide **130** (Scheme 4.19). The primary bromide **130** could undergo elimination to deliver the terminal olefin in **(***R,S***)-110**.

Scheme 4.20. *Access to (R,S)-**110** through chiral atom-transfer strategy*

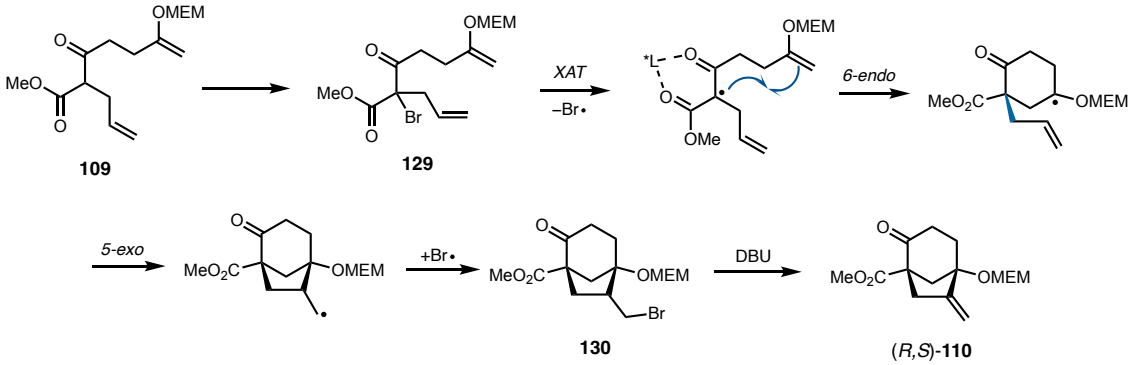

When searching the literature in the realm of chiral atom-transfer reactions, it

became clear that most systems employ bisoxazoline ligands. Lewis acids such as Mg^{2+} that chelate to the ligand. In two seminal reports for the enantioselective atom-transfer radical cyclization catalyzed by chiral Lewis acids, $Mg(ClO_4)_2$ as the Mg^{2+} source and BEt_3/O_2 as the radical generation mode were essential to high yields and *ee* of the reaction (Scheme 4.20).[24,25] Furthermore, specifically the use of (4*R*,4'*R*)-2,2'-(propane-2,2-diyl)bis(4-(tert-butyl)-4,5-dihydrooxazole (**131**) as the ligand led to superior enantioselectivity over other ligands.

Scheme 4.20. *Cheung and Zhu's precedent for chiral atom transfer reactions.*

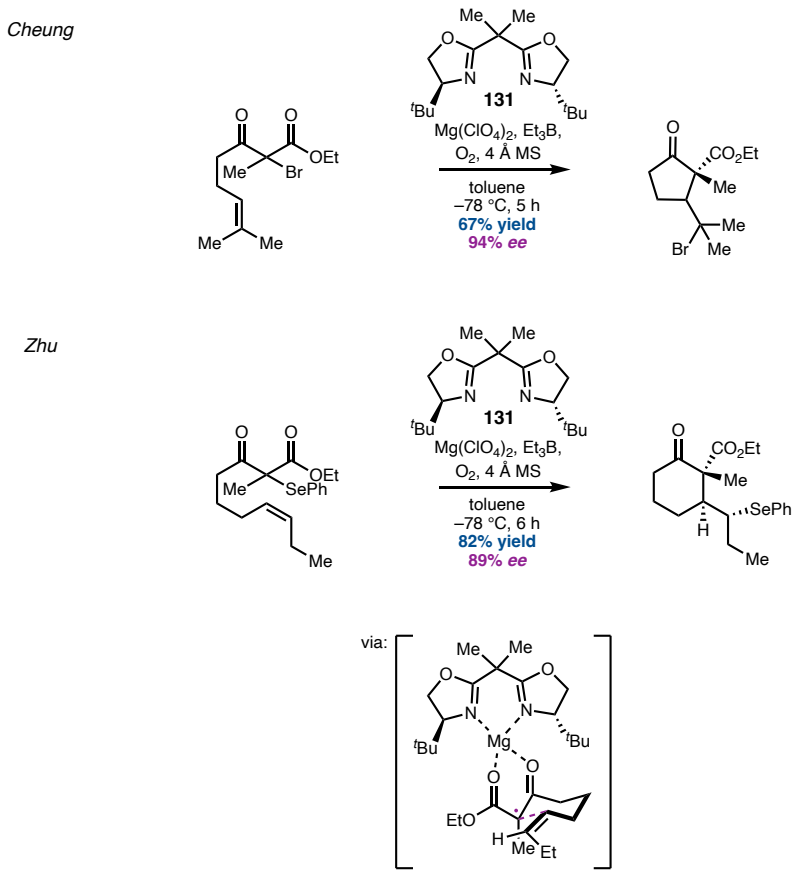

In order to test the reactivity, **125** was envisioned as a model substrate that could be accessed quickly. The model system would also allow sufficient exploration of the key chiral atom transfer reaction, given that compound **109** was unstable and could not be

stored frozen in benzene, for example, for periods of time greater than one week due to the hydrolytic instability of the methyl ether. As a result, the model system allowed for a more stable substrate to explore the chiral atom transfer reaction. The synthesis of the model substrate **132** goes as follows: allylation of α-allyl methylacetoacetate (**108**) delivers **125** in 42% yield, which can be subsequently α-brominated to form **132** in quantitative yield.

Scheme 4.21. *Model system synthesis.*

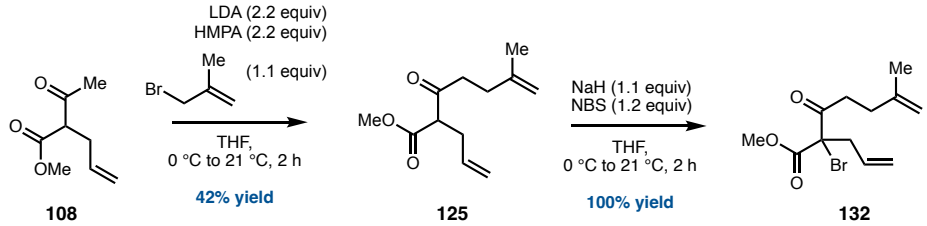

Following the model system substrate synthesis, application of Cheung and Zhu's protocol led to a 14% yield of **130**. In the reaction mixture contained a mix of starting material (22%), monocyclization and bromine radical capture (34%, not shown), and protodebromination (10%, not shown). While the yield was low, indicating that the 5-*exo*-trig product was either thermodynamically uphill or kinetically inaccessible under the reaction conditions, the enantioselectivity following elimination with DBU of the reaction was quite good (79% *ee*). As a result, the model study was concluded and a new route was envisioned that would bear bridgehead oxidation to turn the model system into one that could be relevant for the synthesis.

Scheme 4.22. *Model system delivers 79% ee.*

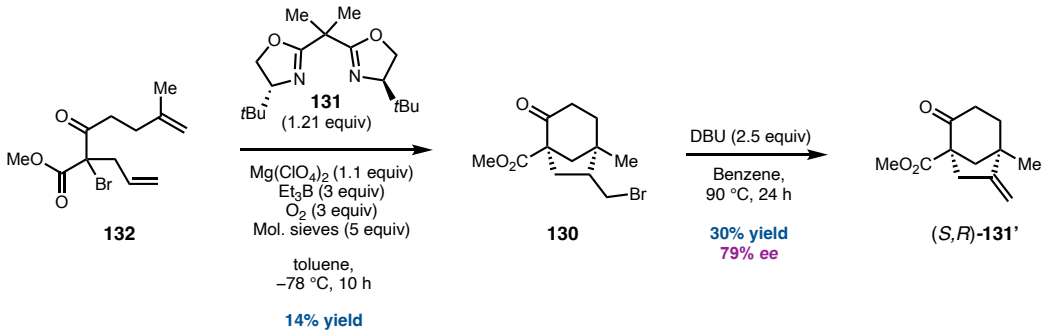

Keeping in mind the degradation of **109** when stored over time, even frozen in benzene and stored at −20 °C, phosphonate ester-protected compound **134** was targeted to alleviate these stability concerns. The electrophile for the Weiler coupling reaction could be formed through a Perkow reaction in 91% yield (Scheme 4.23).[26]

Scheme 4.23. *Phosphonate ester electrophile (**134**) synthesis with Perkow reaction.*

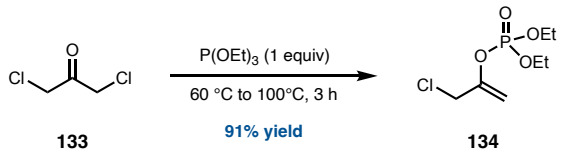

When mining the literature, the phosphonate ester protecting group was identified as a less-labile protecting group that has also displayed competence in Snider radical cascade chemistry.[3] In order to verify these data in our own hands and gain access to a racemic-trace of **214**, substrate **213** was synthesized in the same manner to the OMEM-substrate (**179**) and tested in the Snider radical cascade. Indeed, the product (rac-**214**) was isolated in 79% yield, consistent with the literature-reported yield.[3]

Scheme 4.24. *Racemic phosphonate ester-protected 3.2.1 bicycle (**136**) synthesis.*

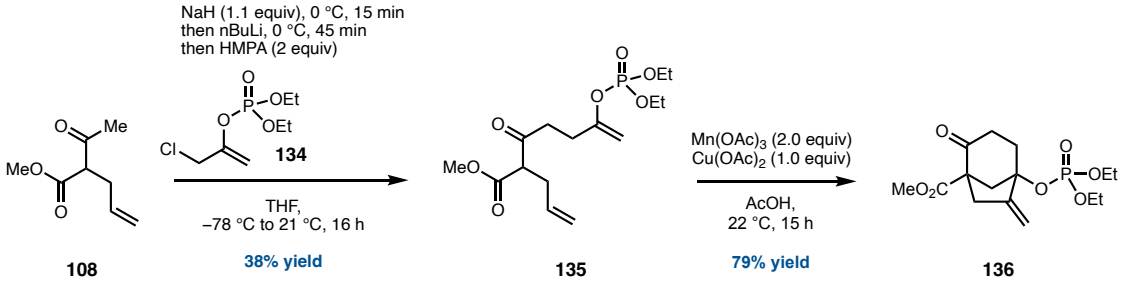

From there, α-bromination of **135** was explored as the final step of the chiral atom-transfer substrate. Unfortunately, however, use of conditions from the model system (NaH & NBS) delivered allyl bromide **137** instead of the desired α-brominated compound **138** (Scheme 4.25). It was thought that the allyl bromide could arise from α-bromination, but the intermediate **137** could undergo elimination to form a diene which could be susceptible to 1,4 nucleophilic addition of bromide.

***Scheme 4.25**. Difficulties with α-bromination of **135**.*

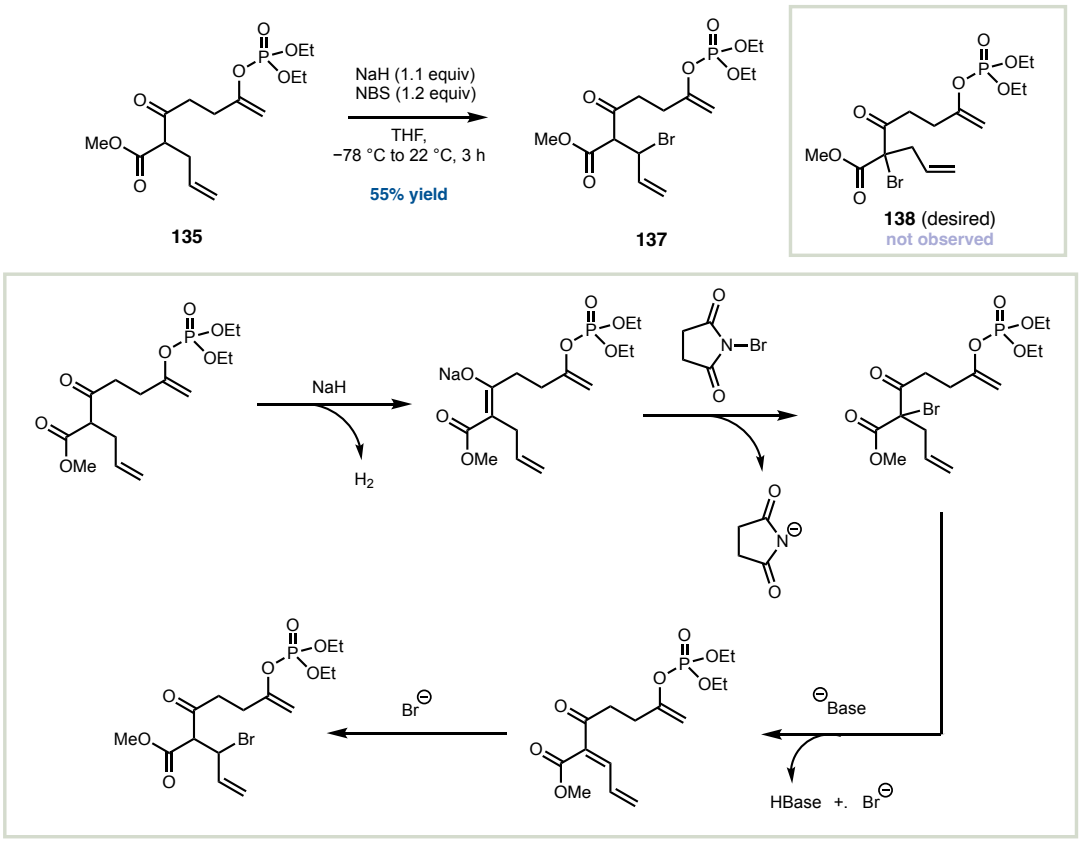

After exhaustive screening and screening other bromination conditions,[27-30] it was revealed that running the reaction at more dilute concentration reduces the amount of allylic bromination and allows for 36% yield of compound **138** (Scheme 4.26). α-selenylation was also accomplished under similar reaction conditions (not shown). With access to **138**, a variety of halogen atom-transfer conditions were explored using the magnesium (4*R*,4'*R*)-2,2'-(propane-2,2-diyl)bis(4-(tert-butyl)-4,5-dihydrooxazole ligand system (**131**) and various radical generation modes.

Scheme 4.26. *A) Preparation of atom-transfer substrates. B) Various radical generation modes do not lead to any observed cyclization products.*

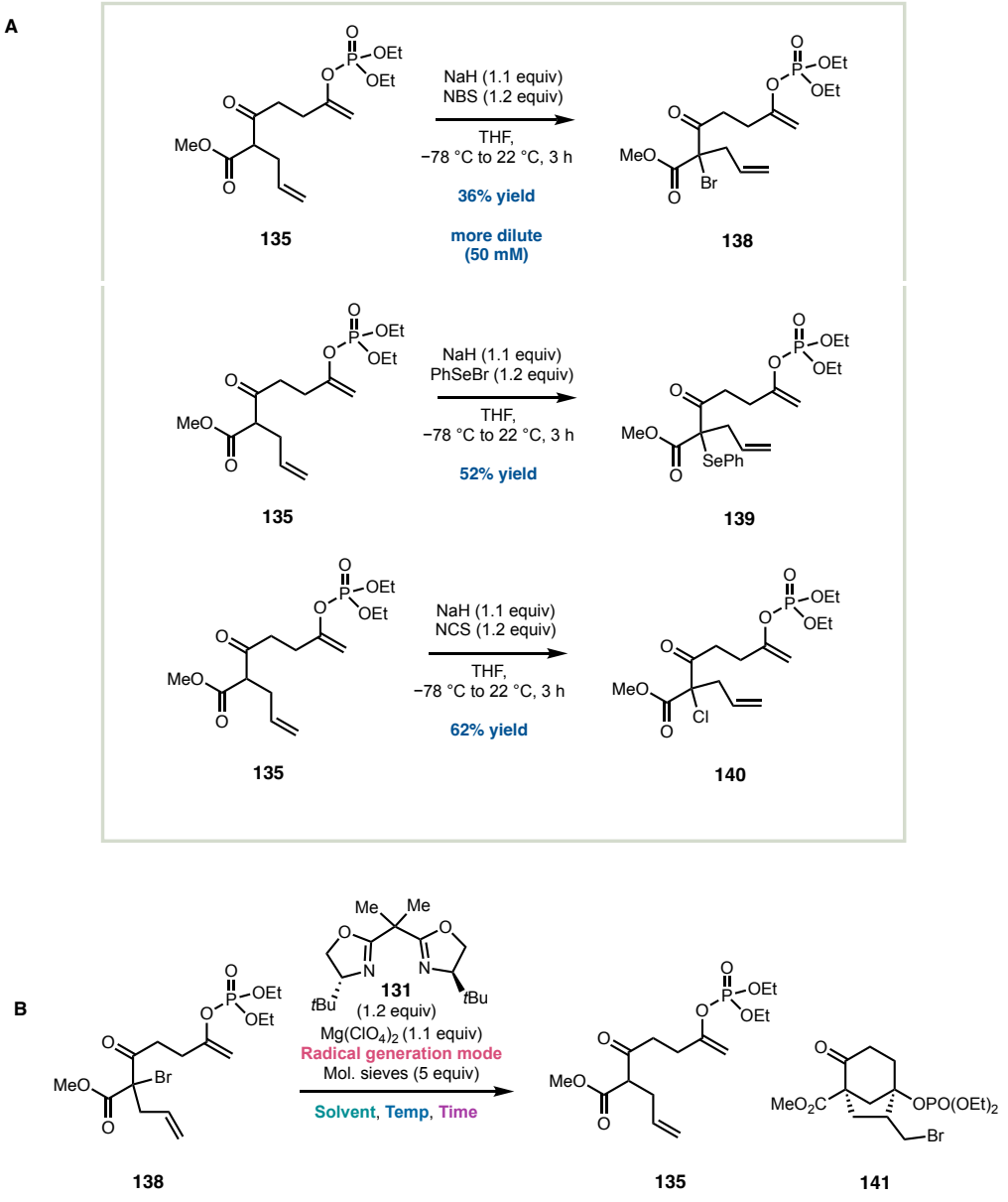

entry	radical generation mode	solvent	temp	time	138 : 135 : 141
1	Et_3B (5 equiv), O_2 (1000 equiv)	Et_2O/DCM	−78 °C	4.5 h	0 : 1
2	$(BzO)_2$ (0.2 equiv)	Toluene	90 °C	12 h	1 : 0.1
3	$(Bu_3Sn)_2$	Toluene	50 °C	2 h	1 : 0.06
4	$(Bu_3Sn)_2$, hv (UVA)	Toluene	25 °C	12 h	1 : 0.85
5	Purple LED's	EtOAc	25 °C	12 h	1 : 0.05
6	hv (UVA)	EtOAc	25 °C	12 h	0 : 1

With difficulty from the bromide, the α-selenylated and α-chloro compound were also explored. Unfortunately, the α-selenylated and α-chloro substrates were also incompetent in the reaction, leading to higher levels of protodeselenation or protodechlorination and no reaction, respectively.

***Scheme 4.27**. Atom-transfer substrate modifications do not promote cyclization.*

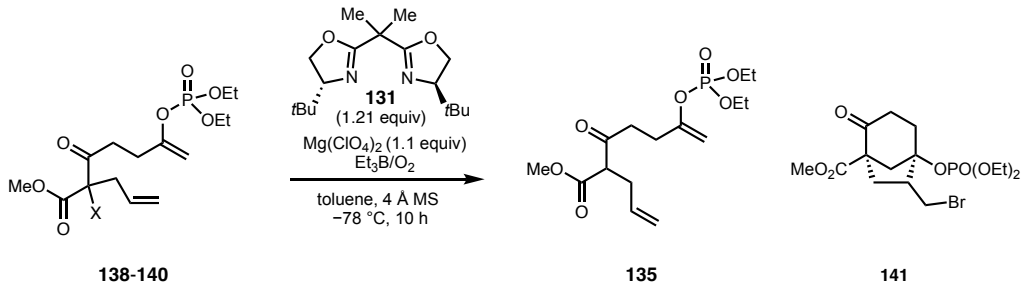

entry	X	sm : 135 : 141
1	Br	1 : 1 : 0
2	SePh	5 : 1 : 0
3	Cl	no reaction

4.3.3 Asymmetric radical cascade from chiral enamine

A final strategy that was explored regarding asymmetric radical cascade chemistry involved the use of chiral enamine catalysis. In theory, starting from substrate **135**, chiral amines could be condensed onto the ketone moiety, providing chiral β-enamino-esters. Recently, α-oxidation of various chiral enamines has been well-documented in the literature, and the redox properties of some chiral enamines has been investigated by Luo, Macmillan, and others.[31-33] Following α-oxidation of the chiral enamines, these α-imino radicals have been demonstrated in several reactions, including alkynylation (Scheme 2.48),[34] amination,[35] hydroxyamination,[36] allylation,[37] oxyamination,[38] and arylation,[39,40] among others.

Scheme 4.28. *Luo's photochemical alkynylation of α-imino radicals.*

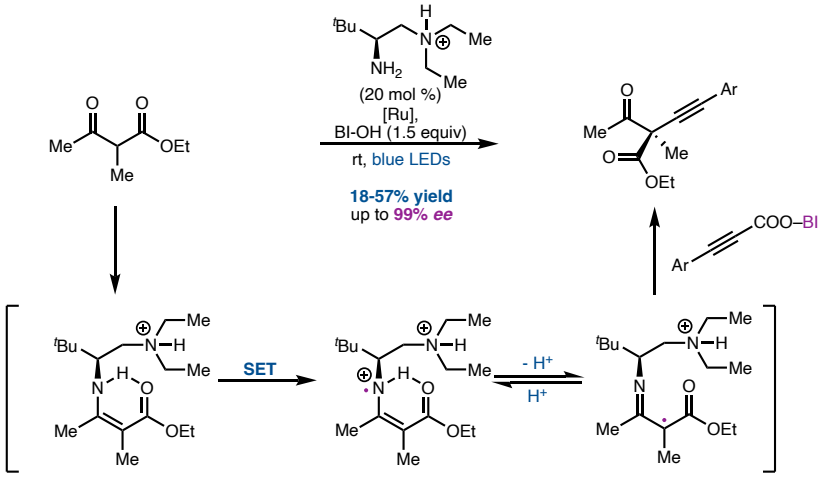

Using various α-oxidation techniques and tuning the redox properties of the oxidant or the enamine employed, we set out to study the possibility of inducing a radical cascade from the α-radical generated from α-oxidation of chiral enamines. Given that the α-imino radical has been implicated before in various contexts, such as the alkynylation from Luo shown in Scheme 4.28, we wondered if it could be applied to systems similar to Snider's studies (Scheme 4.29).

Scheme 4.29. *Use of enamine catalysis for asymmetric 3.2.1 synthesis.*

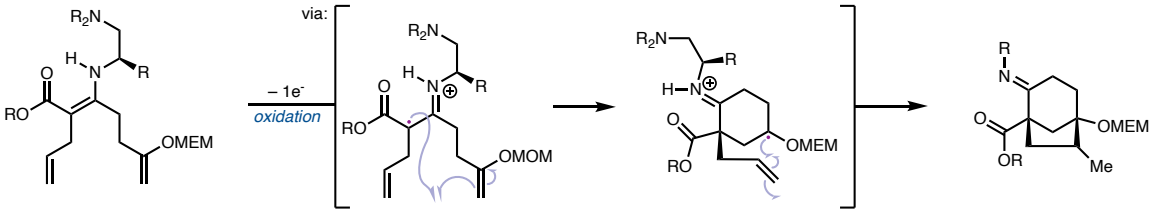

In practice, the condensation of the chiral enamine with the new β-keto ester substrate was challenging. Simply taking the model substrate **125** and screening various conditions[41-44] led to no observed reaction (Scheme 4.30). This was surprising given the precedent in the area for these kinds of reactions, and we hypothesized that the

incorporation of the allyl group could be deactivating for the amine addition.

Scheme 4.30. *Low conversion for canonical enamine formation conditions on model substrate.*

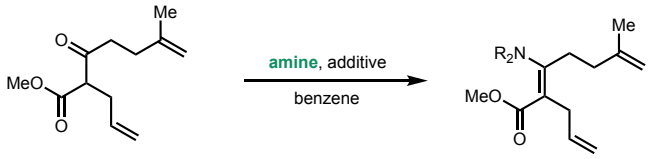

125

entry	amine	condition	conversion	yield (%)
1	pyrrolidine (1.5 equiv)	$FeCl_3$	0	-
2	pyrrolidine (1.5 equiv)	$Zn(OAc)_2$	0	-
3	pyrrolidine (1.5 equiv)	$CeCl_3$	0	-
4	pyrrolidine (1.5 equiv)	$Yb(OTf)_3$	24	-
5	pyrrolidine (1.5 equiv)	L-Proline	28	-
6	aniline (1.5 equiv)	L-Proline (5 mol%)	0	-
7	pyrrolidine (3 equiv)	L-Proline (15 mol%)	11	-
8	L-Proline (2 equiv)	-	0	-
9	L-Proline methyl ester HCl (2 equiv)	-	0	-
10	L-Proline methyl ester HCl (2 equiv)	L-Proline (10 mol%)	0	-
11	$BnNH_2$ (2 equiv)	L-Proline (10 mol%)	0	-
12	$BuNH_2$ (2 equiv)	L-Proline (10 mol%)	0	-
13	iPr_2NH (2 equiv)	L-Proline (10 mol%)	0	-
14	*p*-$MeOPhNH_2$ (2 equiv)	L-Proline (10 mol%)	0	-
15	*p*-$FPhNH_2$ (2 equiv)	L-Proline (10 mol%)	0	-
16	MeBuNH (2 equiv)	L-Proline (10 mol%)	0	-

The results were equally bleak for attempted conditions from substrate **135**. Acid-mediated conditions that had been successful on the model system (not shown) led to trace formation of the desired enamine (Scheme 4.31). Other conditions, such as use of $Fe(OTf)_3$, led to substrate decomposition, and use of HFIP as solvent led to no conversion (not shown).

Scheme 4.31. *Low conversion for canonical enamine formation conditions on phosphonate ester-protected substrate.*

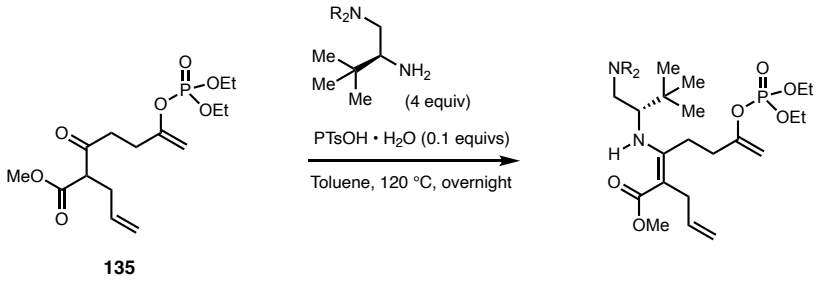

135

entry	NR_2	result
1	NEt_2	< 5% conversion
2	morpholine	< 5% conversion
3	pyrrolidine	< 5% conversion

Difficulties in enamine substrate preparation thwarted attempts to exhaustively explore chiral enamine radical cascade strategies. Although enamine formation was a challenge, in the future exploration of nickel-catalyzed methodologies, specifically through the α-keto substrate bearing an imidazole, could be fruitful. To elaborate, in 2022, Guo and coworkers disclosed the controlled liberation of chiral α-keto radical species from electrogenerated nickel-mediated oxidation toward enantioselective radical capture of alkene partners. The scope of the transformation included a variety of coupling partners in good *ee*.[45]

Scheme 4.32. *Future opportunity within this research aim.*

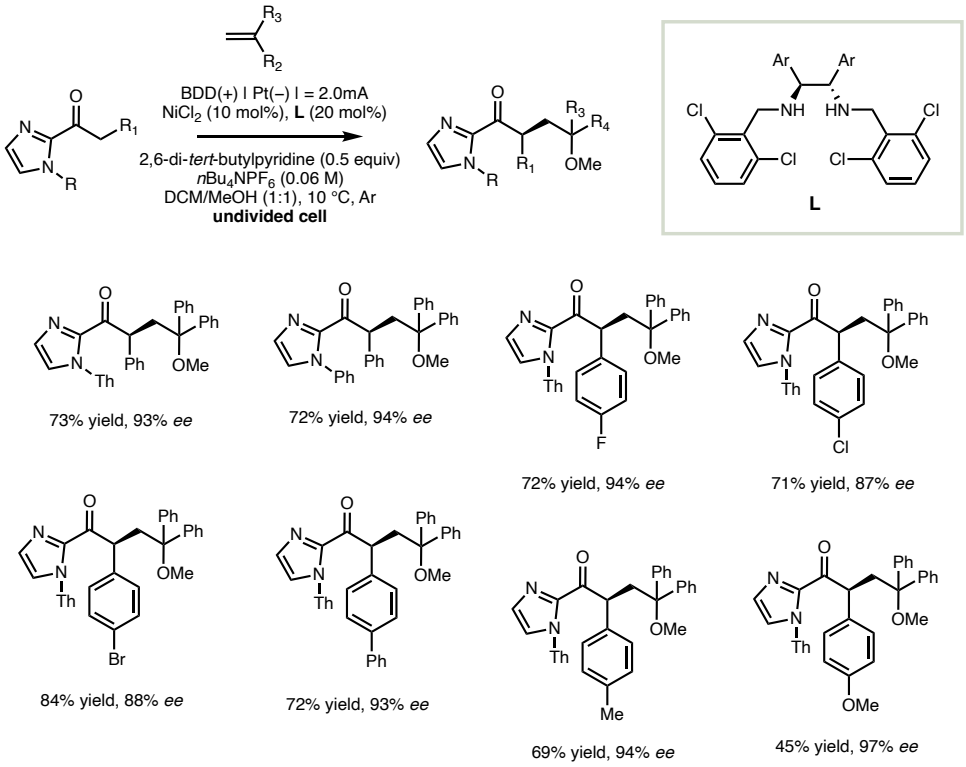

The key intermediate for this process involves ligation of the chiral nickel catalyst to the "enolate equivalent" followed by electrochemical activation to the α-keto radical (Scheme 4.33). Alkene radical coupling and oxidation yield a tertiary carbocation that can be trapped by the nucleophilic solvent. While this strategy is intriguing, due to time constraints, it was not attempted. Future work in this realm could provide an elegant asymmetric 3.2.1 bicycle synthesis through a chiral radical cascade.

Scheme 4.33. *Posited mechanism invokes α-keto radical formation.*

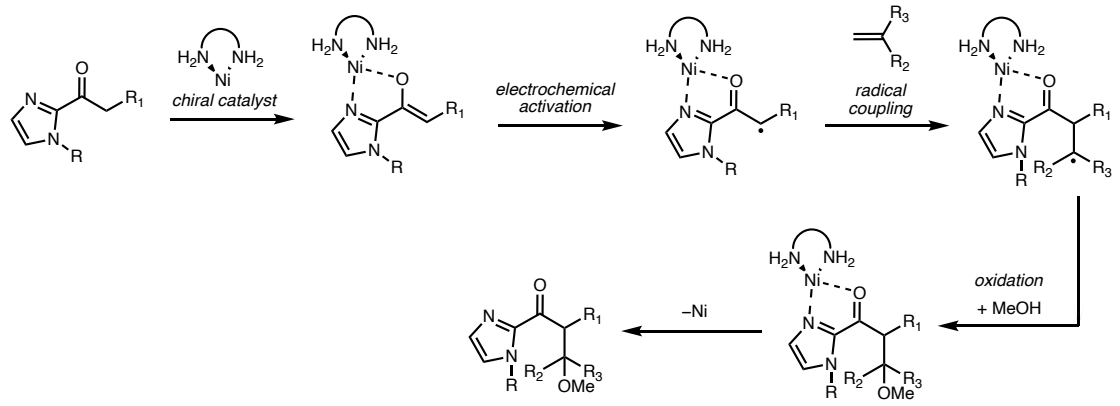

4.4 ASYMMETRIC STRATEGIES THROUGH CYCLOHEXANONE SUBSTRATES

4.4.1 Early studies from cyclohexanone substrates

One way to circumvent the issue of product selectivity for mono versus di-cyclization would be to do the reactions stepwise. Although this can lead to higher step counts, it is possible that the route can be shortened by other means. Furthermore, utilizing symmetry of cyclohexanone starting materials, an expedient synthesis to fragment **107A** may be possible. For this reason, it was envisioned that fragment **107A** could be simplified to allyl compound **142**. From there, following ketone triflation of **143**, the nickel-catalyzed 1,2-addition transform could trace back to diketone **144**. The key quaternary center in **144** could be formed from a palladium-catalyzed decarboxylative allylation of **145**, from which deprotection of the product of that reaction could provide **144**. Racemic **145** could simply be formed from alkylation of **146** with 2,3-dibromo propene or the 2-chloro equivalent.

***Scheme 4.34**. Asymmetric 3.2.1 bicycle retrosynthesis through cyclohexanone intermediates.*

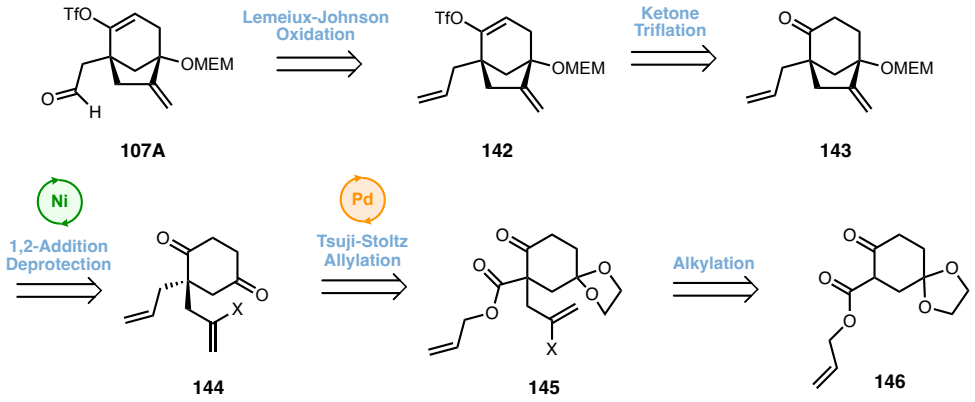

In the forward direction, it was prudent to investigate the acylation of **147** to form **146**. To that end, treatment of **147** with lithium diisopropylamine followed by allyl chloroformate, in our hands, led to 14% yield of the desired product (Scheme 4.35, entry 1). In order to increase the yield under these reaction conditions, further drying and meticulous preparation of allyl chloroformate could increase the yield.[46,47] Use of conditions reported in the literature using NaH and diallylcarbonate were equally ineffective, delivering 10% yield of the product (Scheme 4.35, entry 2); again, however, the literature reports a higher yield for this reaction.[48] Synthesis of allyl 1*H*-imidazole-1-carboxylate (**148**) and use with lithium hexmethyldisilazide (LHMDS) was much more effective, providing 44% yield of the product (Scheme 4.35, entry 3). After some experimentation, it was found that increasing the concentration to 2 M could increase the yield to 73% (Scheme 4.35, entry 4). It is worth noting that compound **146** was found to tautomerize to the enol form. **146** was typically isolated as a 1 : 0.27 ratio of enol : keto tautomers.

Scheme 4.35. *Acylation of* ***147****.*

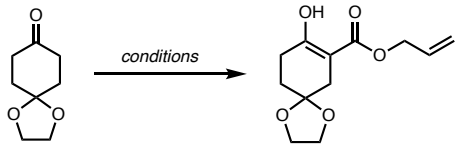

147 **146**

entry	base	reagent	solvent, temp, time	yield (%)
1	LDA	allyl chloroformate	THF, –78 °C to 21 °C, 4 h	14
2	NaH	diallylcarbonate	THF, 21 °C, 18 h	10
3	LHMDS	allyl 1*H*-imidazole-1-carboxylate	THF, –78 °C to 21 °C, 18 h	44
4*	LHMDS	allyl 1*H*-imidazole-1-carboxylate	THF, –78 °C to 21 °C, 18 h	73

*reaction run at higher concentration (2M)

synthesis of allyl 1*H*-imidazole-1-carboxylate

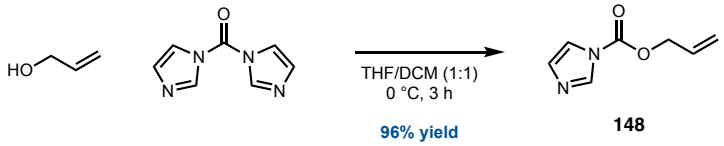

148

From **146**, it was found that alkylation with 2,3-dibromopropene was difficult. Using conditions from Newhouse and Berkowitz,[49,50] only 14% yield was isolated. Use of 2-chloro-3-bromopropene led to no yield of the product. In some reports, hexamethylphosphoramide (HMPA) was used as a superstoichiometric additive to facilitate conversion of the sodium enolate.[51] However, use of HMPA was not desired, especially so early in the synthesis. Instead, use of Cs_2CO_3 and KI in acetone led to 87% yield of the product (Scheme 4.36). We commend Xu for their disclosure of these conditions in their 2024 publication.[52] The analogous reaction also worked for the chloro and iodo variants, providing **145A**, **B**, and **C** in excellent yields.

Scheme 4.36. *Alkylation of* ***146****.*

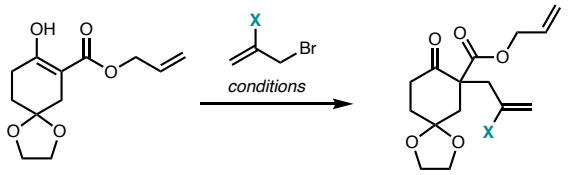

146

145A X = Br
145B X = Cl
145C X = I

entry	base	additive	solvent, temp, time	X	yield (%)
1	NaH	-	DMF, 0 °C to 21 °C, 14 h	Br	14
2	NaH	-	DMF, 0 °C to 21 °C, 14 h	Cl	-
3	Cs_2CO_3	KI	Acetone, 21 °C, 4 h	Br	87
4	Cs_2CO_3	KI	Acetone, 21 °C, 4 h	Cl	89
5	Cs_2CO_3	KI	Acetone, 21 °C, 4 h	I	90

A variety of other Tsuji-Stoltz allylation substrates were prepared. It was found that **147** could be acylated with 2-haloallyl 1*H*-imidazole-1-carboxylates **149A** and **149B** (Scheme 4.37). Both the bromide and chloride could be prepared (**150A** and **150B**).

Scheme 4.37. *Preparation of* ***150A*** *and* ***150B****.*

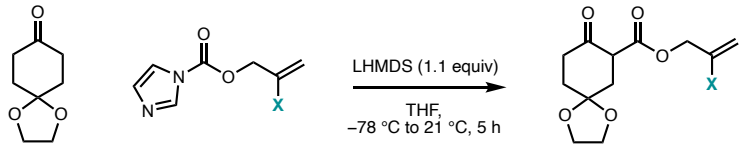

147

149A X = Br
149B X = Cl

150A X = Br, **57% yield**
150B X = Cl, **72% yield**

From **150A** and **150B**, a variety of α-substituted β-keto esters (Stoltz precursors) were synthesized. Specifically, the preparation of alkylated and allylated substrates bearing α-alkoxy (or protected variants), α-cyano, and allyl groups were prepared (a total of at least six Tsuji-Stoltz decarboxylative allylation substrates), which could be tested under the palladium-catalyzed reaction conditions (Scheme 4.38).

Scheme 4.38. *Preparation of a myriad of α-substituted β-keto esters for investigation of the palladium-catalyzed Tsuji-Stoltz allylation.*

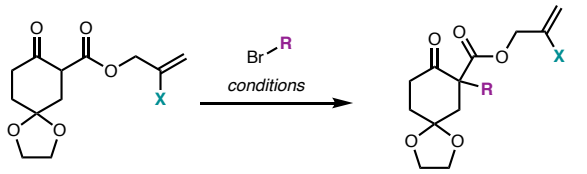

150A/B *see "prod." for compound number*

entry	X	R	base	additive	solvent, temp, time	prod.	yield (%)
1	Br	$-CH_2CN$	NaH	KI	DMF, 21 °C, 18 h	**151**	52
2	Cl	$-CH_2CN$	NaH	KI	DMF, 21 °C, 18 h	**152**	65
3	Br	$-CH_2OH$	$NaHCO_3$	-	THF, 0 °C to 21 °C, 16 h	**153**	78
4	Cl	$-CH_2OH$	$NaHCO_3$	-	THF, 0 °C to 21 °C, 16 h	**154**	55
5	Br	allyl	NaH	KI	THF, 0 °C to 21 °C, 16 h	**155**	71
6	Cl	allyl	NaH	KI	THF, 0 °C to 21 °C, 16 h	**156**	90
7	Br	$-CH_2CH_2OTES$	NaH	-	DMF, 21 °C, 18 h	-	-
8	Cl	$-CH_2CH_2OTES$	NaH	-	DMF, 21 °C, 18 h	-	-
9	Br	$-CH_2CH_2OTES$	NaH	KI	THF, 50 °C, 18 h	-	-

4.4.2 Tsuji-Stoltz Allylation as a method for quaternary stereocenter formation

In addition to substrate **145A**, **145B**, and **145C**, which contained parent allyl compounds, compounds **151** through **156** enabled access to a plethora of Tsuji-Stoltz allylation precursors. Reading the literature and talking to colleagues in the Stoltz group, it became apparent that most successful screening campaigns identify either solvent screening or use of CF_3-*t*Bu-Phox as a ligand compared to *t*Bu-Phox as very impactful to enantioselectivity.[53,54] Ether, 1,4-dioxane, THF, and toluene were identified as some of the most common solvents. Additionally, reactions typically require 12.5 mol% ligand with 5 mol% Pd_2dba_3 and are run between 21-40 °C for extended reaction times.[55,56] Finally, the reactions are most often carried out at dilute concentrations of approximately 30 mM, often requiring more than 36 h to achieve full conversion.[57]

Moving on to test the Tsuji-Stoltz allylation, **145C and 145A** were tested first. Although the vinyl iodide-containing substrate (**145C**) led to no reaction, use of (*S*)-*t*Bu-Phox with the bromide substrate (**145A**) led to 70% isolated yield and 40% *ee*. The iodide substrate did not react likely due to either: 1) coordination to the iodine atom and catalyst deactivation or 2) oxidative addition into the vinyl iodide (~5% palladium oxidative addition complex) which may idle as the resting state.

Scheme 4.39. *Initial studies for the Tsuji-Stoltz decarboxylative allylation on parent-allyl substrates.*

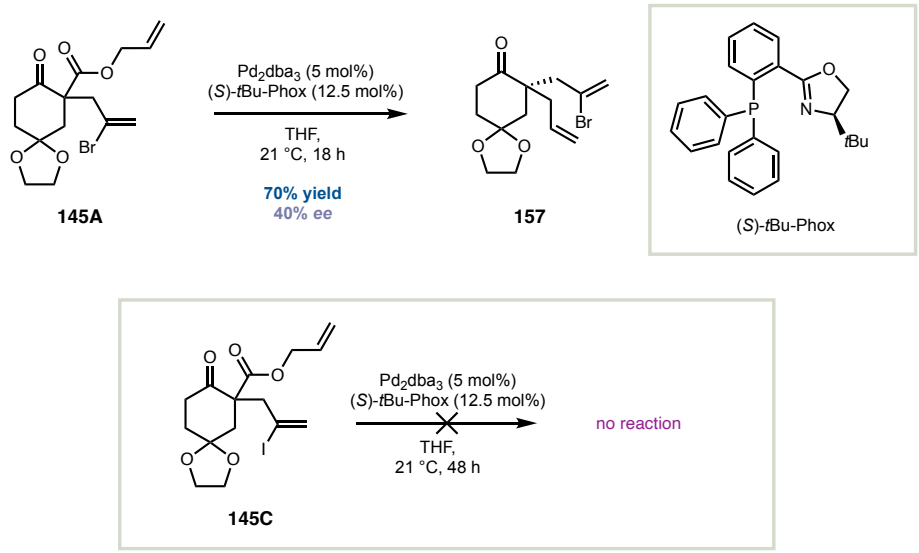

Turning to compounds **151** through **156**, which contained substitution on the migrating allyl group, moderate success was seen. Specifically, for the substrate **156**, which contained chloride substitution on the migrating allyl group and an allyl group as "R", the product **161** was formed in 70% yield and 93% *ee* (Scheme 4.40). Substrate **154'**, which contained an α-OTES group on the R-group formed 52% yield of **160**. While this was exciting, other substrates **151** and **152**, which contained α-cyano substitution on the R-group, did not react. Furthermore, substrate **155**, which contained bromide substitution on

the migrating allyl group, also led to no observed reaction and no observed formation of product **157**. Similar observations on the poor reactivity of the alkenyl bromide substrates have been noted by Stoltz.[55-57]

Scheme 4.40. *Decarboxylative allylation studies on new substrates: promising results on vinyl-Cl containing substrate* ***156***.

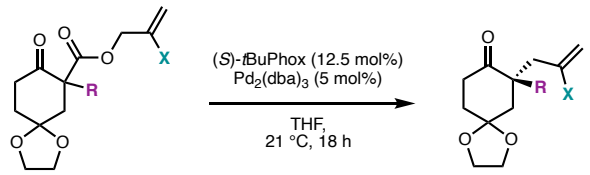

see "starting material" for compound number

see "prod." for compound number

entry	starting material	X	R	prod.	yield (%)
1	**151**	Br	CN	**158**	-
2	**152**	Cl	CN	**159**	-
3	**154'**	Cl	OTES	**160**	52% yield
4	**155**	Br		**157**	-
5	**156**	Cl		**161**	**70% yield**, 93% *ee*

A mechanistic hypothesis for the lack in reactivity of substrate **151** and **152** is depicted in Scheme 4.41.The elucidated active catalyst species is believed to be [Pd((*S*)-*t*BuPhox)(dba))].[58] It is possible that chelating groups, such as larger bromine and iodide heteroatoms or nitriles could inhibit the catalyst through σ-donation or (in the case of the nitrile) π-backdonation from the metal center into the π*-nitrile orbitals.[59] Turning to computational studies from Goddard and coworkers, it is believed the oxidative addition begins with ligand exchange to form an olefin bound active species, from which oxidative addition into the C-O bond of the allyl group can be facilitated. The oxidative addition is believed to lead to anti-displacement in an S_n2-type mechanism to form [Pd((*S*)-*t*BuPhox)(η^3-allyl)$^+$(RCOO)$^-$, from rapid equilibration to the η^1-bound allyl as the resting

state occurs.[60]

Scheme 4.41. *Mechanistic hypothesis for catalyst deactivation.*

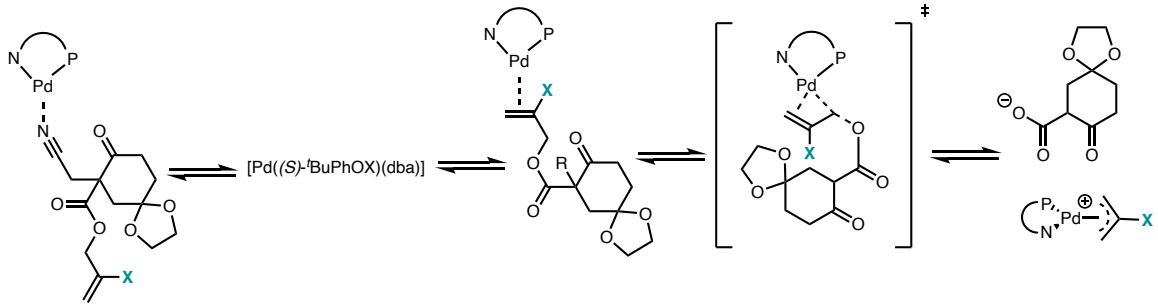

With the chloride substrate **156** showing success in the decarboxylative allylation, forming **161** in 70% yield and 93% *ee*, we turned to optimization of the bromide-containing substrate in order to provide both vinyl chloride and vinyl bromide handles for ring closure to the 3.2.1 bicycle. Attempting to increase the *ee* through ligand modification, the (*R*)-$(CF_3)_3$-*t*Bu-Phox ligand was synthesized. Using keto ester **145A**, a variety of solvents were evaluated, with yields ranging from 50–73% to form **157** (Scheme 4.42). The higher enantioselectivity of the process compared to the parent phenyl-containing ligand is believed to be due to greater charge separation in the transition state between the electron rich palladium catalyst and the electron deficient Phox ligand.[58] Larger charge separation leads to stronger ligand-catalyst interactions, which prevents unligated, racemic palladium background reactivity. On scaling this reaction up, it was found that reducing the palladium-loading to 5 mol% enabled an increase in yield to 70% yield and 85% *ee*.

Scheme 4.42. *Solvent screening with the p-$(CF_3)_3$-tBuPhox ligand on substrate* ***145A****: optimized Tsuji-Stoltz conditions for the vinyl-Br containing substrate.*

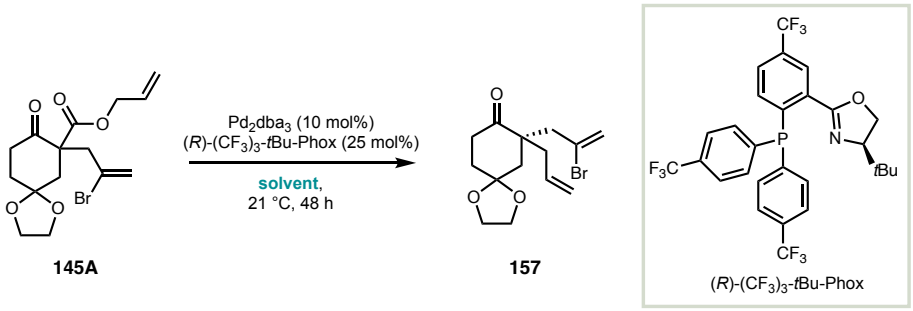

entry	solvent	yield (%)*	*ee* (%)
1	dioxane	49%	86
2	DME	55%	83
3	Et_2O	73%	80
4	EtOAc	64%	78
5	MeCN	52%	5
6	MTBE	38%	85
7	2-MeTHF	55%	84
8	THF	62%	83
9	toluene	50%	88

*all yields are QNMR yields

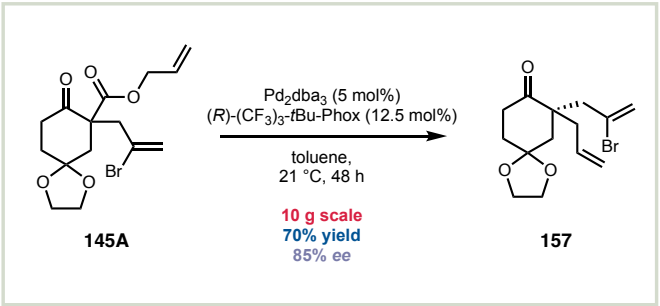

4.4.3 Strategies for ring closure

With the palladium-catalyzed Tsuji-Stoltz allylation delivering good yields and *ee*'s of two substrates, **161** (vinyl-Cl) and **157** (vinyl-Br), efforts to close the 3.2.1 bicycle were pursued. Many strategies were envisioned. Common to all routes involved deprotection of the ethylene glycol moiety, both of which proceeded on each substrate in 91% yield (**144B**) and 99% yield (**144A**), respectively.

Scheme 4.43. *Acetal deprotection to form ring closure substrates* ***144A*** *and* ***144B***.

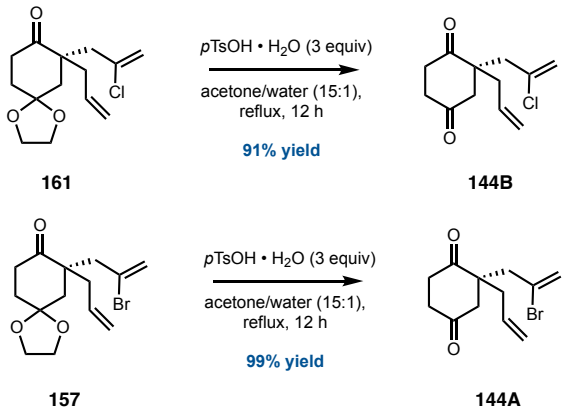

The first strategy explored involved treatment with SmI_2. Reading the literature, it became clear that Barbier addition of vinyl bromides to ketones to form 3.2.1 bicycles is a well-studied process.[61] Furthermore, many reviews for Barbier addition exist in the literature; although, most examples involve alkyl halides, especially alkyl iodides, rather than the corresponding vinyl bromides or chlorides.[62] Nevertheless, we opted to first test HMPA and $Ni(acac)_2$ as additives due to their precedence for Barbier addition.[63] To our surprise, the primary product involved ketyl radical formation and 5-*exo* cyclization with the allyl group, followed by HAT to form an exocyclic methyl group (**162**) in both cases (Scheme 4.44). The reaction proceeded in 70% yield to give **162** as a single diastereomer, while the $Ni(acac)_2$ reaction formed a messier reaction profile with a 1:1 diastereoselectivity. This might indicate that the HMPA-ligated SmI_2 • THF complex is likely much more of a controlled cyclization due to steric bulk of what is presumably the Sm^{III} alkoxide. Indeed, SmI_2-HMPA-induced 5-*exo* trig cyclization with an unactivated allyl group is a documented process.[64,65] What was reassuring by this result was the fact that ketyl radical formation selectively engaged the less-hindered ketone. This was exciting due to the chance of developing a Pinacol coupling of a substrate bearing the methyl ketone

rather than the vinyl bromide. With methods to convert the vinyl bromide to methyl ketone formation being known, it was seen as a high-priority experiment to test substrate **164** in a Pinacol coupling. Due to time constraints, however, this was not pursued further.

Scheme 4.44. *Efforts to induce SmI_2-mediated Barbier addition thwarted by engagement with unactivated olefin followed by keyl radical formation.*

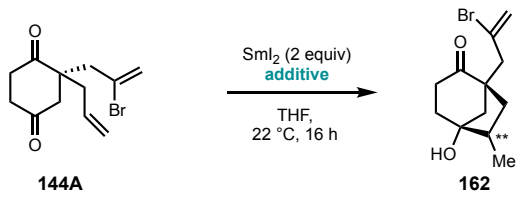

entry	additive	yield (%)	sm	5-*exo*-trig (%)	mass balance (%)
1	HMPA (10.5 equiv)	6	14	70*	90
2	$Ni(acac)_2$ (1 mol%)	3	31	38**	72

*single diastereomer
**1:1 mixture of diastereomers

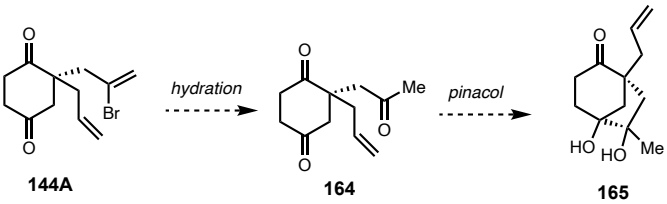

Alternatively, it was thought that the chemoselectivity problem of having two olefins could be avoided by selectively dihydroxylating and protecting the unactivated allyl group. Given that the unactivated allyl group needs to be cleaved to the aldehyde, this strategy seemed strategic for fixing the problem of engagement of the unactivated olefin. Unfortunately, while dihydroxylation of the unactivated allyl group worked, cyclization of the secondary alcohol to compound **166** occurred (Scheme 4.45), which could not be protected or cleaved in subsequently attempted experiments (not shown).

Scheme 4.45. *Efforts to induce selective dihydroxylation of* ***144A***.

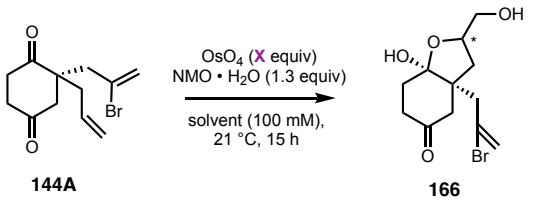

entry	X	solvent	product (%)	*dr**
1	0.05	*t*BuOH/Acetone (1:1)	56	1.2 : 1
2	0.05	*t*BuOH/Water (1:1)	47	1.3 : 1
3	0.10	*t*BuOH/Acetone (5:1)	51	1.5 : 1
4	0.10	*t*BuOH/Water (5:1)	45	1.3 : 1
5	0.10	*t*BuOH	80	1.7: 1

Barbier addition through organocopper-catalyzed reactions,[66,67] organolithiates,[68,69,70] or use in the Nozaki-Hiyama-Kishi (NHK) reaction are reported.[71] Although, organolithiates are not really precedented from the vinyl bromide; the vinyl iodide is typically invoked instead. Additionally, the NHK reaction is typically performed on aldehydes rather than ketones.

When lithiation and cupration chemistry was attempted on both the chloride and bromide substrates, no evidence for 1,2-addition was observed for most reactions (Scheme 4.46). Instead, either no reaction (in the case of the vinyl-Cl substrate) or a messy reaction profile with trace amounts of product (< 5% for the vinyl-Br substrate) was observed. The most promising result involved the use of Bu_2CuLi at lower temperatures, which formed the 1,2-addition product **163** in 25% yield. The primary product corresponded to protodebromination and other unidentified products. Attempts to further optimize the process was not beneficial. The NHK was not attempted but could be undertaken in future studies.

***Scheme 4.46**. Explored lithiation and cupration chemistry.*

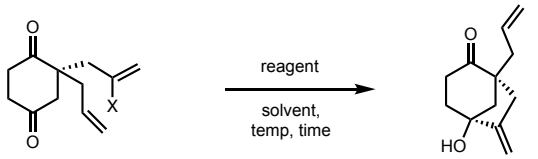

144A/B **163**

entry	X	reagent	solvent	temp (°C)	time (h)	yield **163** (%)
1	Br	*n*BuLi (2.5 equiv)	Et_2O	−78 °C to 21 °C	1	< 5%
2	Cl	*n*BuLi (2.5 equiv)	Et_2O	−78 °C to 21 °C	12	-
3	Br	*t*BuLi (2.5 equiv)	Et_2O	−78 °C to 21 °C	1	< 5%
4	Cl	*t*BuLi (2.5 equiv)	Et_2O	−78 °C to 21 °C	12	-
5	Br	*n*Bu_2CuLi (2 equiv)	Et_2O	−50 °C to 10 °C	1	25
6	Cl	*n*Bu_2CuLi (2 equiv)	Et_2O	−50 °C to 10 °C	12	-
7	Br	*n*Bu_2CuLi (6 equiv)	Et_2O	−50 °C to 10 °C	1	25
8	Cl	*n*Bu_2CuLi (6 equiv)	Et_2O	−50 °C to 10 °C	12	-

Moving forward, it was clear that a separate strategy for 1,2-addition of the vinyl halide was necessary. Mining the literature and through the expertise in the Reisman group, we believed that the Ni-catalyzed 1,2-addition could be developed.

4.4.4 Nickel-catalyzed carbonyl 1,2-addition

In 2000, Cheng and coworkers disclosed the intermolecular nickel-catalyzed 1,2-addition of aryl bromides to aromatic aldehydes accomplished by a Ni(II)/Zn(0)-powder system (Scheme 4.47).[72] In this report, they disclosed the dramatic ligand effects of the reaction, eventually arriving at dppe as optimal, but the reaction could also tolerate use of bisoxazoline. The reaction, however, could not be developed in an asymmetric manner to the extent that they tried. Shortly thereafter, Cheng disclosed the 1,2 addition of aryl iodides to aromatic aldehydes.[73] Interestingly, the reaction used identical conditions to their publication in 2000, except for the fact that it required higher temperatures, and led to the formation of diaryl ketones due to an additional β-hydride elimination step to turn over the catalyst following 1,2-addition.

Scheme 4.47. *Cheng's nickel-catalyzed 1,2-addition of aryl bromides and iodides to aryl aldehydes.*

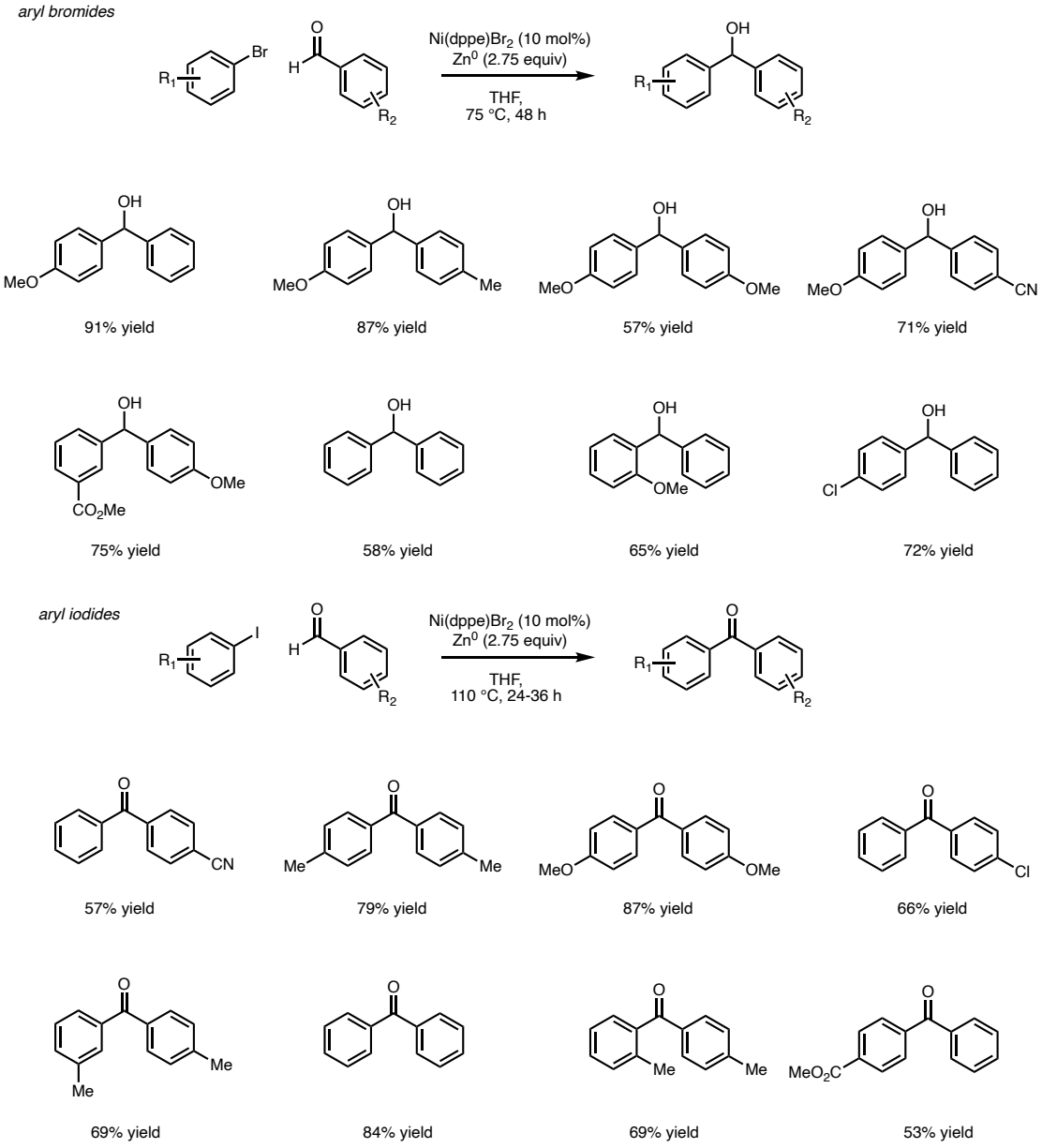

Since these initial discoveries, several nickel-catalyzed carbonyl additions have been developed, both intramolecularly and intermolecularly.[74-79] Turning to our desired transformation, we were drawn to the report from Xu for the nickel-catalyzed intramolecular desymmetrization of aryl halides to 1,3-diketones (Scheme 4.48).[83] Key to

Xu's success was the use of 2,2-bipyridine as a ligand and superstoichiometric quantities of Mn^0 and $MgCl_2$ in dimethylacetamide (DMA) at elevated temperature. The reaction displayed good functional group tolerance for modification on the aryl group, although it is not documented if vinyl bromides were prepared or ever tried. In comparison to our desired transformation (**144** to **163**), the reaction forms a single five-membered ring through an intramolecular process with two possible electrophilic ketones, making it relatively similar to the desired transformation. Perhaps the largest difference between the desired transformation is that the reaction uses aryl bromides rather than vinyl bromides. The Reisman group has a standing interest in nickel-catalyzed reductive cross couplings, specifically utilizing the Ni^{II} oxidative addition complex for radical capture to form Ni^{III} complexes,[80,81] along with the development of a nickel-catalyzed enantioselective acyl coupling of prochiral benzyl chlorides with acid chlorides.[82] Due to our studies, for example, in the mechanism of specifically nickel-catalyzed vinyl bromide reductive cross couplings, we believed that Xu's protocol could extend to the use of vinyl bromides and chlorides in the desired context. Perhaps one of the largest anticipated challenges would be avoiding engagement with the unsubstituted allyl group in **144**. If this were to occur, however, we believed in the potential to tune the ligand on the nickel center to promote carbonyl 1,2-addition.

Scheme 4.48. *Xu's nickel-catalyzed intramolecular desymmetrization addition of aryl halides to 1,3-diketones.*

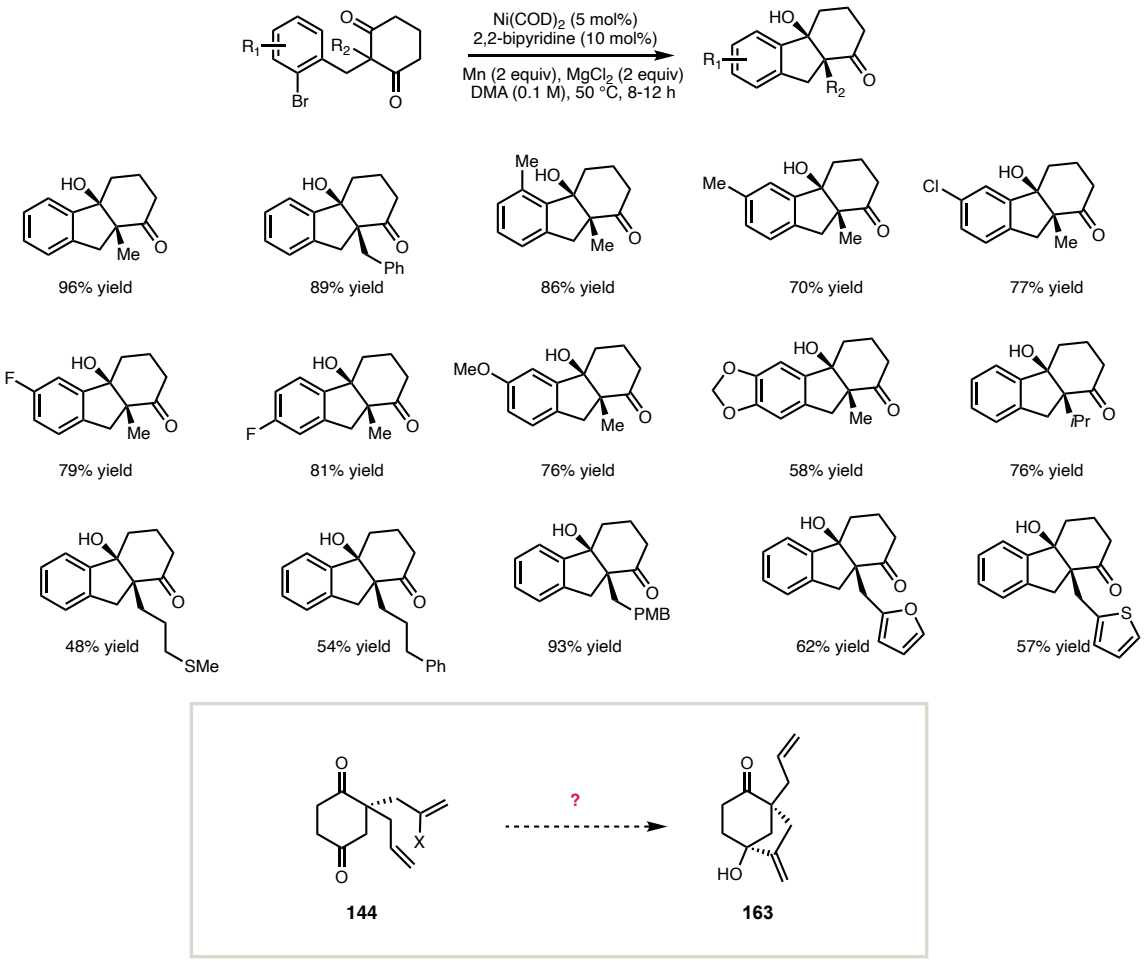

Using Xu's exact conditions, we were excited by the fact that 3% product had been formed starting from both the bromide and chloride substrates **144A** and **144B** (Scheme 4.49, entry 1-2). Nevertheless, and perhaps disappointingly, engagement with the allyl group to form diene **167** and halide exchange from the bromide (**144A**) to the chloride (**144B**) were observed. Switching to di-*t*Bu-bpy as ligand, no reaction was observed (Scheme 4.49, entry 3-4). Interestingly, the yield of the diene side product was increased to 25% and 44% using BPhen (Scheme 4.49, entry 5-6). Use of terpy as ligand from the bromide and chloride led to adequate yield (43% and 33% yield) of the product (Scheme

4.49, entry 7-8). Use of tri-*t*Bu-terpy, however, led to a complex mixture (Scheme 4.49, entry 9). 1-bpp led to halide exchange to the chloride in nearly quantitative yield (Scheme 4.49, entry 10). Without ligand, halide exchange to the chloride from the bromide and recovery of chloride was observed (Scheme 4.49, entry 10-11). It is worth noting that it was later found that the products were volatile, and the yields of this table (with exception of recovery of starting materials, which were not volatile), are likely deflated.

Scheme 4.49. *Ligand screen adopting Xu's protocol.*

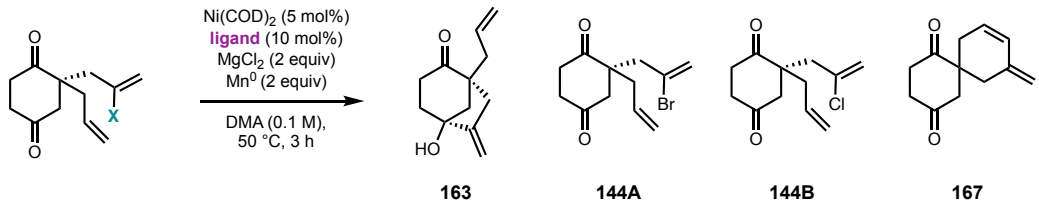

163 **144A** **144B** **167**

entry	X	ligand	**163** (%)*	**144A** (%)	**144B** (%)	**167** (%)	mass balance (%)
1	Br	bpy	< 3%	-	19	17	36
2	Cl	bpy	< 3%	-	38	16	54
3	Br	di-*t*Bu-bpy	-	38	-	-	38
4	Cl	di-*t*Bu-bpy	-	-	74	-	74
5	Br	Bphen	< 3%	-	-	25	25
6	Cl	Bphen	< 3%	-	-	44	44
7	Br	terpy	43	-	-	-	43
8	Cl	terpy	33	-	-	-	33
9	Br	tri-*t*Bu-terpy	5	-	-	-	5
10	Br	1-bpp	-	-	93	-	-
11	Br	-	-	-	72	-	72
12	Cl	-	-	-	86	-	86

*all yields are QNMR yields

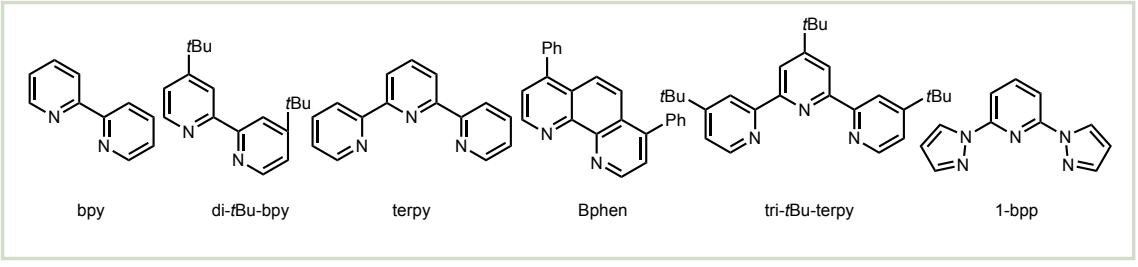

Diene formation was an interesting result. We reasoned that, following oxidative addition, engagement with the terminal allyl group was favored for certain ligands, such as

BPhen, for steric or electronic purposes (Scheme 4.50).

Scheme 4.50. *Mechanistic hypothesis for diene formation (**167**).*

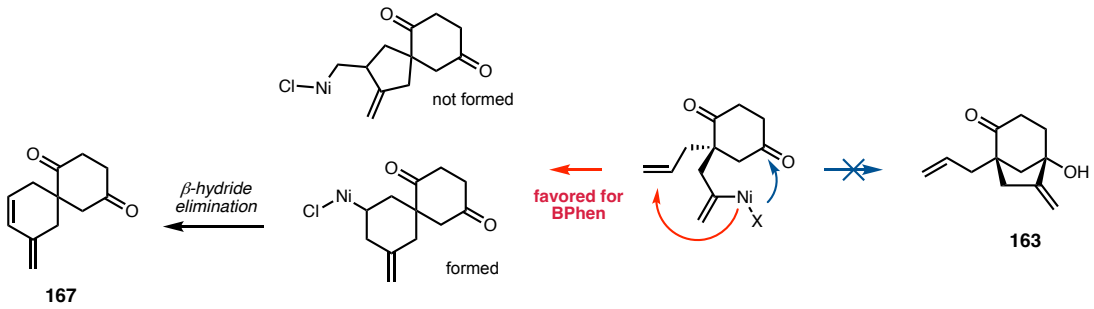

From the preliminary ligand screen, it became clear that oxidative addition into the vinyl chloride and bromide had been occurring. The halide exchange from the bromide to the chloride, for example, is a good indication of this. In general, good conversions for the different ligands was observed. The halide exchange results made us wonder about what would occur if the $MgCl_2$ was switched to other additives, such as $MgBr_2$ or MgI_2, or $Mg(OTf)_2$. We also wondered generally about other Lewis acids used in carbonyl 1,2-addition chemistry, such as $Ti(OiPr)_2$/HFIP disclosed by Zhou and coworkers.[76] Perhaps, following oxidative addition into the alkenyl bromide, the carbonyl 1,2-addition was slow with $MgCl_2$ as an additive, and reductive elimination to form the alkenyl chloride dominates (Scheme 4.51). Indeed, certain reports for halide exchange posit a Ni^I mechanism, whereby either irreversible oxidative addition or irreversible halide transmetallation occurs, rather than a thermodynamically-driven process.[4,84,85] Although the mechanism is unclear, the results of the ligand screen were exciting and drove a much more expansive investigation into Lewis acid additive exploration, reaction setup, and reaction design. Especially due to the fact that the terpy ligand seemed to be relatively effective, delivering adequate yields of the product, we wanted to know if the yield could be further optimized under these conditions.

Scheme 4.51. *Mechanistic hypothesis for halide exchange and diene formation.*

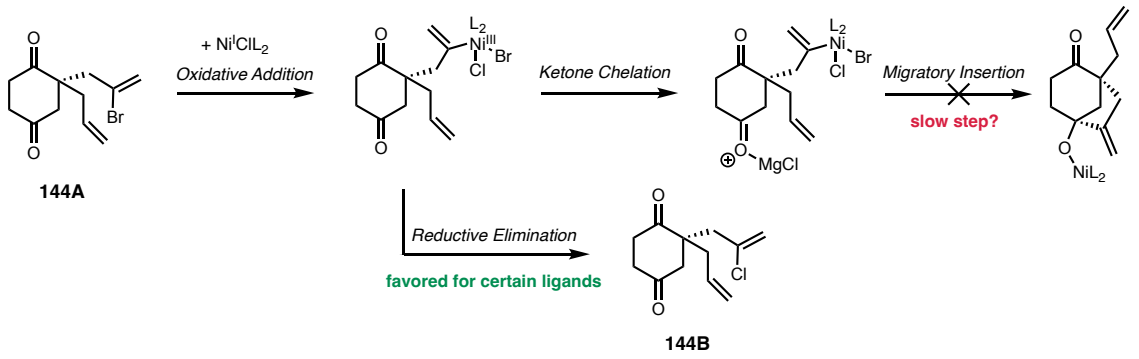

Investigation of different Lewis acids with 1-bpp as ligand did not provide productive results. The most promising Lewis acid seemed to be $ZnBr_2$, which provided an increased yield of 16% compared to other Lewis acids, such as TESBr, $BF_3 \bullet OEt_2$, and Ti(*i*OPr)$_4$/HFIP (Scheme 4.52).

Scheme 4.52. *Lewis acid screen with 1-bpp as ligand.*

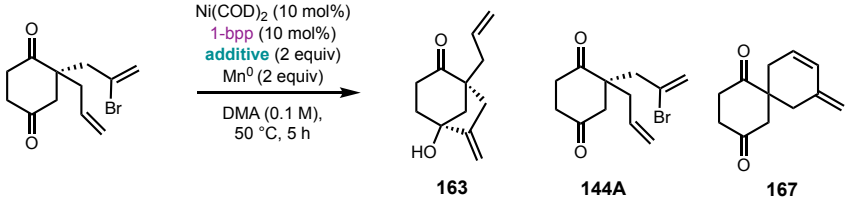

entry	additive	**163** (%)*	**144A** (%)	**167** (%)	mass balance (%)
1	none	-	52	-	52
2	Ti(*i*OPr)$_4$, HFIP	-	-	-	substrate decomposition
3	TESBr	-	5	-	49**
4	BF_3•OEt_2	-	13	10	23
5	$ZnBr_2$	16	74	-	90

*all yields are QNMR yields
** isolated compound contains 2 TES groups, but no cyclization observed

Turning back to terpy as ligand, other Mg^{2+} halide sources were screened. We speculated that the counterion in the magnesium salt could greatly inhibit or enhance the rate and/or product distribution of the reaction. To our delight, it was realized that MgI_2 seemed optimal, delivering 55% yield, while other Mg^{2+} halide salts provided between

43% and 46% yield (Scheme 4.53).

Scheme 4.53. *Lewis acid screen with terpy as ligand.*

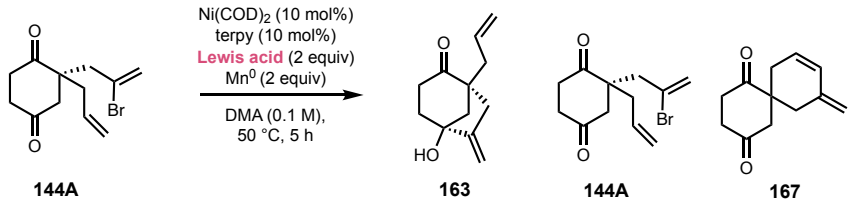

entry	Lewis acid	**163** (%)*	**144A** (%)	**167** (%)	mass balance (%)
1	$MgCl_2$	34	-	-	43
2	$MgBr_2 \bullet OEt_2$	46	-	-	46
3	MgI_2	55	-	-	55
4	$MgOTf_2$	40	6	2	61**

*all yields are QNMR yields
** 13% protodebromination (not shown)

Although $MgCl_2$ seemed to work in moderate yields (Scheme 4.49, entry 7 and Scheme 4.53, entry 1), the result was not scalable even with multiple attempts at different setups (Scheme 4.54).

Scheme 4.54. *Attempts to scale up $MgCl_2$ as a Lewis acid.*

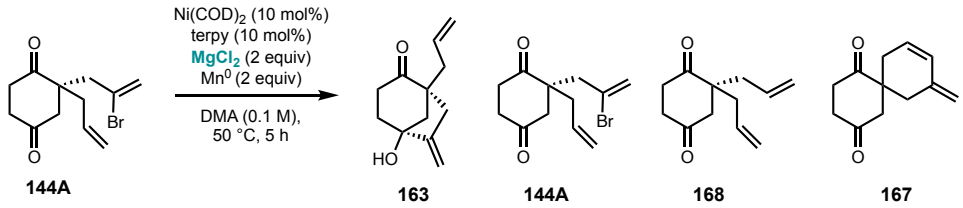

entry	scale	time	setup method	**163** (%)	**144A** (%)	**168** (%)	**167** (%)	mass balance
1	100 mg	15 h	round bottom flask, under N_2, outside gb in oil bath	10	14	10	-	34
2	50 mg	15 h	1-dram vial, large magnetic stir bar, on gb hot plate	7	12	9	-	28
3	30 mg	5 h	vial in the glovebox as normal, larger stir bar	10	45	-	-	55

With MgI_2 providing optimal yield with terpy as the ligand (Scheme 4.53), we next moved on to investigate the catalyst. It is unclear the exact mechanism of the reaction, but it is possible that the reaction proceeds through a Ni^0-Ni^{II} or a Ni^1-Ni^{III} cycle. In either case, we wondered if we could start from a Ni^{II} precatalyst, such as $NiBr_2 \bullet$ dme, rather than

$Ni(COD)_2$. Furthermore, we wanted to investigate the ligand/catalyst loading to see if lower or higher yields of catalyst loading could boost the yield. Indeed, use of $NiBr_2$ • dme with 10 mol% catalyst loading seemed optimal (Scheme 4.55, entry 4), while other entries also provided somewhat promising results. Integral to the increased yields was a new workup procedure. After extensive investigation, it was realized that product **163** is volatile when subjected to *in vacuo* concentration. In order to prevent loss of product during *in vacuo* concentration, solvent was blown off under a stream of nitrogen (see experimental section for further information).

Scheme 4.55. *Catalyst/ligand loading screen.*

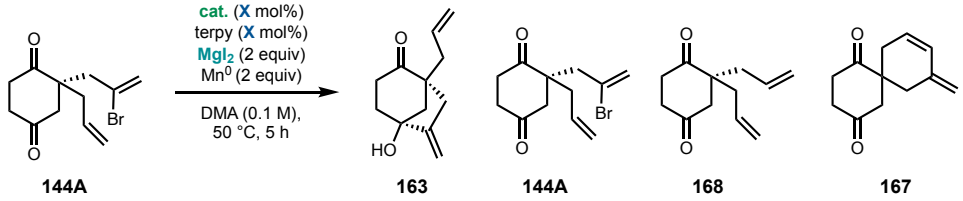

entry	cat.	X	**163** (%)	**144A** (%)	**168** (%)	**167** (%)	mass balance
1	$Ni(COD)_2$	5*	56	-	2	-	58
2	$Ni(COD)_2$	15	61	-	5	-	66
3	$NiBr_2$dme	5*	71	-	9	-	80
4	$NiBr_2$dme	10	76	-	2	-	78
5	$NiBr_2$dme	15	44	2	8	-	54

* stirred overnight (16 h)

The results in Scheme 4.55 were ultimately scalable with one major change: no additive. It was found that MgI_2 introduces impurities on scale (perhaps trace moisture) which is detrimental to reaction yield. A simple leave-out experiment verified that the additive was not necessary. Given the newly found volatility of the product, the data in Scheme 4.53 suggests the identity of the Lewis Acid is relatively agnostic to the reaction yield and may not be implicated in the reaction mechanism.

Using a pressure flask, the reaction could be scaled up to 480 mg scale without any

significant reduction in yield (Scheme 4.56). At much larger scales (8 g scale), the yield of the reaction dropped to 55% yield.

Scheme 4.56. *Successful scale-up of Ni-catalyzed 1,2-addition using additive-free conditions.*

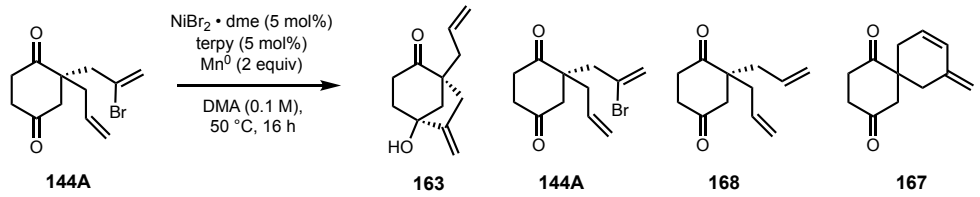

entry	scale	time	purification	vessel size (%)	**163** (%)	**144A** (%)	**168** (%)	**167**. (%)	mass balance
1	36 mg	5 h	none, QNMR	1-dram vial	70	-	4	-	74
2	108 mg	5 h	none, QNMR	15 mL pressure flask	71	-	3	-	74
3	480 mg	5 h	column	75 mL pressure flask	72	-	3	-	75
4	8 g	5 h	column	500 mL RBF	55	-	4	-	59

4.4.5 Advancement to the asymmetric key fragment

From compound **163**, the route to compound **107B** could be accomplished in a relatively straightforward manner (Scheme 4.57). MEM protection could be accomplished to form **143** in 84% yield,[86] followed by triflation with *N*-Ph bistriflimide to form **142**.[87] Notably, Comin's reagent could not be used in this case, leading to partial conversions (see Scheme 4.58 for more information).[88] Selective Lemiux-Johnson oxidation occurred uneventfully in 50% yield to form **107A**.[89,90] Enol triflate to alkenyl bromide exchange occurred in 70%, allowing access to fragment **107B**.

***Scheme 4.57**. Completing the 3.2.1 bicycle synthesis.*

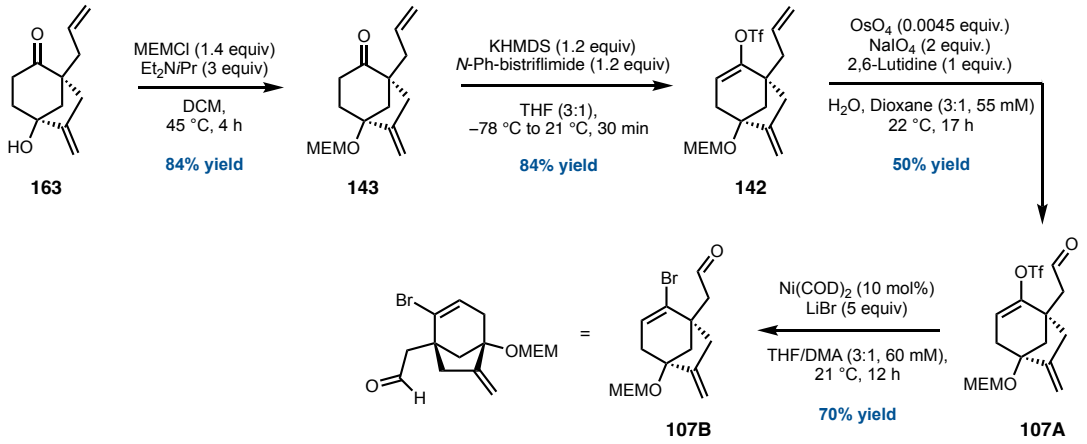

Although it is surprising that triflation could not be accomplished successfully with Comin's reagent, *N*-Ph bistriflimide could be used in 84% yield using KHMDS as base, without the need for 18-crown-6 or other additives (Scheme 4.58).

***Scheme 4.58**. Identification of optimal triflation conditions.*

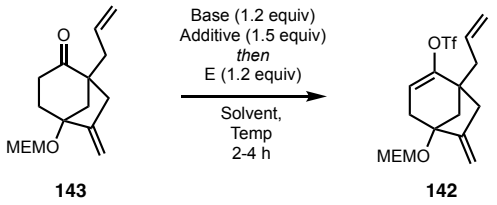

entry	Base	E (source)	Solvent	Temp	Additive	**142** (%)*	recovered **143** (%)	mass balance
1	LDA	Comin's (Jordan's, old bottle)	THF	–78 °C	-	-	97	97
2	LHMDS	Comin's (Jordan's, old bottle)	THF	–78 °C	-	9	88	97
3	NaHMDS	Comin's (Andrea's)	Et_2O	0 °C	-	12	84	96
4	KHMDS	Comin's (Andrea's)	Et_2O	0 °C	-	32	60	92
5	KHMDS	Comin's (Jordan's, new bottle)	Et_2O	–78 °C	-	-	98	98
6	KHMDS	Comin's (Jordan's, new bottle)	Et_2O	–78 °C	-	50	50	100
7	KHMDS	Comin's (Jordan's, new bottle)	Et_2O	–78 °C	-	32	64	96
8	KHMDS	Comin's (Jordan's, new bottle)	Tol/THF	–78 °C	18-crown-6	47	42	89
9	KHMDS	Comin's (Jordan's, new bottle)	Tol/THF	–78 °C	18-crown-6	45	42	87
10	KHMDS	Comin's (Jordan's, new bottle)	THF	–78 °C	18-crown-6	57	39	96
11	KHMDS	N-phenyl-bis-triflimide	THF	–78 °C	18-crown-6	83	-	83
12	KHMDS	N-phenyl-bis-triflimide	THF	–78 °C	none	84	-	84**
13	KHMDS	N-phenyl-bis-triflimide	THF	–78 °C	18-crown-6	84	-	84

*QNMR yields
**reaction conducted for 30 minutes rather than 2-4 hours.

4.4.6 Other avenues for more expedient 3.2.1 bicycle synthesis: use of a Michael-Aldol cascade

While the development of a viable asymmetric route to **107B** was incredibly enabling for the project, allowing access to more than double the quantity of material in a single pass than the Snider/chiral preparatory hplc route, some brainstorming on more direct annulations to access **107B** more efficiently were explored. One of the more exciting approaches involved the use of a Michael-Aldol cascade to forge the 3.2.1 bicycle in a single step (Scheme 4.59). When using a fragment such as phenyl acrylate, Baeyer-Villager oxidation could install the tertiary alcohol required in auriculatol A.

Scheme 4.59. *A Michael-Aldol cascade quickly forges 3.2.1 bicycle.*

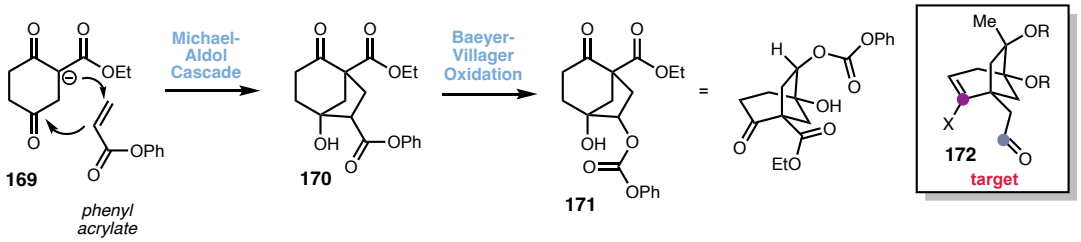

The route was undertaken by studying the acylation of 1,4-dioxaspiro[4.5]decan-8-one (**147**). This could simply be accomplished using HMPA as a stoichiometric additive in 59% yield (Scheme 4.60).[91] Interestingly, use of NaH and diethylcarbonate[92] or LDA and Mander's reagent[93] (without HMPA) led to no observed yield of the product.

Scheme 4.60. *Acylation of **147** with Mander's reagent.*

147 **173**

entry	base	reagent	additive	solvent	temp/time	product (%)
1	NaH	diethylcarbonate	-	-	140 °C, 1 h	-
2	LDA	Mander's	-	THF	–78 °C, 1 h	-
3	LDA	Mander's	HMPA (1 equiv)	THF	0 °C, 1 h	59

With **173** in hand, we were curious about attempting the direct Michael addition before ethylene glycol deprotection rather than the cascade process. Identification of viable Michael addition conditions before moving on to study the more complex cascade process could help with troubleshooting. After a quick base and solvent screen, it was shown that the Michael addition occurred to form **174** in 44% using triethylamine in acetonitrile (Scheme 4.61).[94] Shockingly, switching to other bases, such as K_2CO_3, DBU, or KO*t*Bu, or switching from acetonitrile to ethanol, led to no yield of the product. The reaction was noticeably slow, as monitoring the reaction after 72 h still had leftover starting material.

Scheme 4.61. *Testing the Michael addition with phenyl acrylate.*

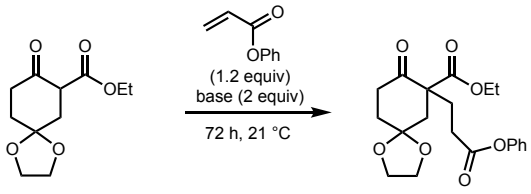

173 **174**

entry	base	solvent	product (%)
1	K_2CO_3	EtOH	-
2	K_2CO_3	ACN	-
3	DBU	EtOH	-
4	DBU	ACN	-
5	TEA	EtOH	-
6	TEA	ACN	44% yield
7	KO*t*Bu	EtOH	-
8	KO*t*Bu	ACN	-

With viable Michael addition conditions identified, moving on to the cascade process seemed fruitful. Deprotection of the ethylene glycol ketal could be accomplished in an ethanol/water mixture with HCl. The cascade process worked in roughly the same yield as the single-step Michael addition (48% yield) to deliver **176**.

Scheme 4.62. *Preparation and testing of a racemic Michael-Aldol cascade substrate.*

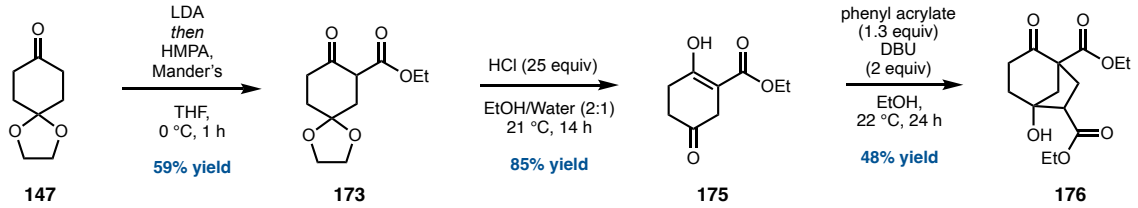

Future studies in this area should center on achieving enantioselectivity. There are several reports in the literature, focused on using chiral copper enolates,[95] lanthanum-BINOL complexes,[96] chiral Michael acceptors (enamines),[97] gallium-BINOL complexes,[98] aluminum-BINOL complexes,[99] and chiral nickel enolates.[100] These ideas, for the most part, have not been extensively explored. Taken together, this approach could provide a more expedient route to the key 3.2.1 bicycle used in the vinylogous Mukaiyama Aldol coupling; although, some major challenges, such as achieving enantioselectivity and the exact route to achieving the synthesis of the target aldehyde (**107B**) remains elusive.

Scheme 4.63. *Future studies: development of an asymmetric Michael-Aldol cascade.*

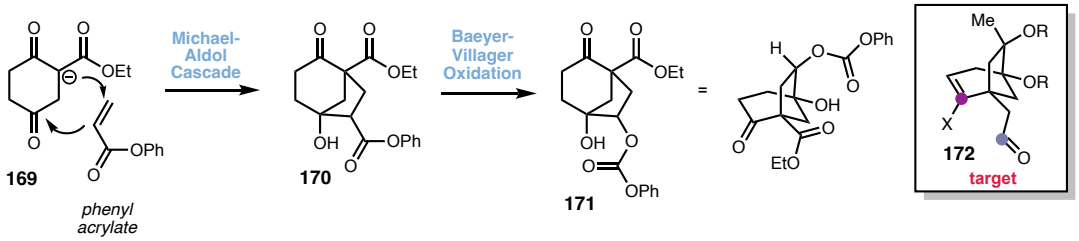

4.5 CONCLUDING REMARKS

Taken together, this chapter provides foundational studies for 3.2.1 bicycle synthesis in the context of the total synthesis of auriculatol A. Several challenging transformations were explored. For example, this chapter describes the synthesis of key aldehyde fragment **107B** originally through the use of the Snider radical cascade. Despite the unsuccessful endeavors toward applying a decarboxylative Giese addition, fragment **107B** was synthesized in 10 steps and resolved through the use of chiral preparatory HPLC. Although the development of the 10-step route had very few challenges, it lacked scalability, and yields were typically quite low (~50% yield) for most steps. Several asymmetric strategies for 3.2.1 bicycle synthesis through chiral radical cascades were attempted, including the development of a chiral radical cascade process through halogen-atom transfer reactions, chiral α-imino catalysis, and use of chiral auxiliaries. Unfortunately, with unproductive results to induce enantioselectivity in this research aim, we opted to pivot strategies.

A palladium-catalyzed decarboxylative Tsuji-Stoltz allylation for enantioselective quaternary center formation provided compelling results on several substrates, the most exciting of which contained a vinyl halide substituent and unsubstituted allyl unit. Coupled with the discovery of a unique nickel-catalyzed intramolecular carbonyl 1,2 addition of vinyl bromides to 1,3-diketones, a new, more efficient route to **107B** was found. Seminal to the success of the route is the optimization of triflation reaction to form compound **142** and development of a chemoselective Lemeuix-Johnson oxidation to furnish **107A**.

Insights into product selectivity (product vs. diene) in the nickel-catalyzed 1,2-addition based on tuning of the ligand are intriguing and could be useful to the community

in the realm of nickel-catalyzed reaction development. Furthermore, it is possible that the methods for the palladium-catalyzed decarboxylative Tsuji-Stoltz allylation and nickel-catalyzed 1,2-addition could be compared more generally; that is, a paper disclosing our group's longstanding interest in 3.2.1 bicycle synthesis could be of interest. Preliminary data investigating a Michael-Aldol cascade are disclosed; nonetheless, this strategy needs considerable development in order to become a viable option for the synthesis.

4.6 EXPERIMENTAL SECTION

Preparation of methyl 2-acetylpent-4-enoate (108):

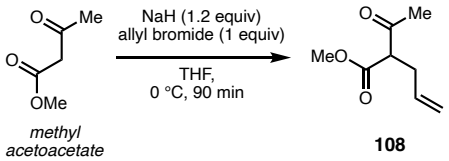

methyl acetoacetate

108

In a flame-dried 500 mL flask with a stir bar was added 13.8 g of NaH (1.2 equiv, 60% mineral oil). The flask was capped with a 250 mL addition funnel (also flame dried) and vacuumed and backfilled with N_2 three times before 150 mL of THF was added via cannula directly from the SPS. The NaH/THF mixture was allowed to stir for 1 min at room temperature to evenly disperse before it was cooled to 0 °C with an ice bath. Methyl acetoacetate (46.5 mL, 1.5 equiv) was measured and poured into addition funnel via a graduated cylinder. The flask was capped with a rubber septum, vacuumed, and backfilled three times with N_2. Then, 150 mL of dry SPS THF was again added, this time into the addition funnel. The methyl acetoacetate solution was added over a 1.5 h period at 0 °C using the addition funnel. CAUTION: This is an exothermic deprotonation that evolves a large quantity of H_2 gas. Be sure that the addition funnel does not add too quickly, as over-

pressurization of the system may occur and cause the addition funnel to pop off and break. Do not have an open flame in the hood during this time to avoid potential explosion hazards from the H_2 that is emitted. Following addition of the methyl acetoacetate solution, the sides of the addition funnel were rinsed with 20 mL of THF, and the system was removed from the ice bath and allowed to warm to room temperature, where it was stirred for 1 h. After 1 h of stirring at room temperature, the system was cooled back to 0 °C before 24.8 mL of allyl bromide (1 equiv) was added via direct injection (not dropwise). The reaction was stirred for 90 min before 200 mL of water was added to the reaction. The mixture was partitioned in a 1 L separatory funnel, the organic phase was collected, and the aqueous phase was extracted 3x with ether. The combined organic phases were washed with brine, dried with Na_2SO_4, and concentrated. Column chromatography using a 4 L column using very minimal silica and 5 to 8% EtOAc/Hex gradient going up by 1% per column volume gave 54% yield (24.0 g).

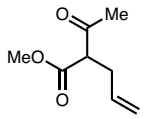

108

TLC (30% EtOAc/Hexanes): R_f 0.66 (p-anis (red/pink), $KMnO_4$).

^{1}H NMR ($CDCl_3$, 400 MHz): δ 5.74 (ddt, J = 17.1, 10.3, 6.9 Hz, 1H), 5.12 – 5.03 (m, 2H), 3.74 (s, 3H), 3.54 (t, J = 7.4 Hz, 1H), 2.59 (tt, J = 7.0, 1.3 Hz, 2H), 2.23 (s, 3H).

^{13}C NMR ($CDCl_3$, 101 MHz): δ 202.55, 169.86, 134.27, 117.70, 59.23, 52.59, 32.35, 29.33.

FTIR (Neat, NaCl, thin film): 2955, 1746, 1643, 1435, 1233, 920 cm^{-1}.

HRMS (ESI): calc'd for $[M+H]^+$ 156.07864, found 156.07796.

Preparation of 1,3-dichloro-2-((2-methoxyethoxy)methoxy)propane:

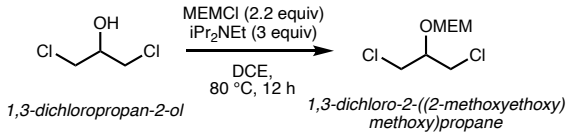

To an oven-dried, 3-neck, 2L flask was added the starting material (60 g, 465 mmol, 1 equiv), dichloroethane (800 mL, 581 mM), and a large, cylindrical magnetic stir bar. The flask was capped with two rubber septa and a reflux condenser, backfilled with N_2 three times, and cooled to 0 °C. Then, one of the rubber septa was removed and freshly distilled diisopropylethylamine (243 mL, 1.4 mol, 3 equiv) was poured into the stirring solution and stirred for 3 min. Methoxyethoxymethyl chloride (117 mL, 1.02 mol, 2.2 equiv) was then added by pouring directly from a clean, glass graduated cylinder. CAUTION: the mixture will smoke up upon addition of MEMCl. While an exotherm has not been observed, it is important to add the reagent at 0 °C and turn on the emergency exhaust to limit exposure. Pour MEMCl in the hood and segregate waste. Following addition of MEMCl, the septa was put back onto the flask and the apparatus was removed from the ice bath and placed into an 80 °C oil bath and stirred for 13 h. After stirring for 13 h, the apparatus was brought out of the oil bath and cooled to room temperature before addition of 800 mL of saturated aqueous ammonium chloride. The solution was added to a 2 L separatory funnel, and the bottom DCE layer was collected. The aqueous layer was then extracted with DCM (3 x 400 mL), and the collected organic fractions were washed with brine, dried with Na_2SO_4, and concentrated *in vacuo*. The crude red/brown oil was loaded directly onto a column and flushed with 30% EtOAc/Hex (2 L). Following the short silica plug, the 2L collected were concentrated, affording a pale-yellow oil that was carried forward to the next step (82 g, 81% yield).

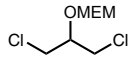

1,3-dichloro-2-((2-methoxyethoxy) methoxy)propane

TLC (30% EtOAc/Hexanes): R_f 0.5 ($KMnO_4$).

^{1}H NMR ($CDCl_3$, 400 MHz): ^{1}H NMR (400 MHz, CDCl3) δ 4.84 (s, 2H), 4.03 (p, *J* = 5.2 Hz, 1H), 3.79 – 3.76 (m, 2H), 3.76 – 3.69 (m, 4H), 3.56 (dd, *J* = 5.7, 3.5 Hz, 2H), 3.39 (s, 3H).

^{13}C NMR ($CDCl_3$, 101 MHz): δ 95.53, 76.81, 71.75, 67.67, 59.22, 43.87.

FTIR (Neat, NaCl, thin film): 2928, 1440, 1114, 753 cm^{-1}.

HRMS (ESI): calc'd for [M+H] 217.0393, found 217.0390.

Preparation of 3-chloro-2-((2-methoxyethoxy)methoxy)prop-1-ene (115):

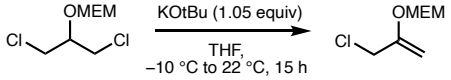

1,3-dichloro-2-((2-methoxyethoxy) methoxy)propane **115**

A 1 L flask fitted with a cylindrical stir bar was added the starting material (47.0 g, 217 mmol, 1 equiv) and 361 mL of anhydrous THF (600 mM). The solution was cooled to -10 °C using a salted ice bath. Solid KOtBu (25.5 g, 227 mmol, 1.05 equiv) was added in slowly, a few chunks at a time. Following completion of the addition, the septum was used to cap the top, and the reaction flask was evacuated and backfilled 3x with nitrogen. The reaction was stirred vigorously overnight. The next day, 175 mL of H_2O was added, and following separation of the aq. and organic phases, the aq. phase was extracted three times with DCM (3 x 200 mL). The combined organics were washed with brine, dried with Na_2SO_4, filtered, and concentrated. The crude oil was loaded onto a silica gel column and eluted with 10-15% EtOAc/Hexanes, going up by 1% each column volume, to provide 38.7

g of product, corresponding to a 99% yield.

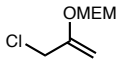

115

TLC (10% EtOAc/Hex): R_f 0.13 ($KMnO_4$).

^{1}H NMR ($CDCl_3$, 400 MHz): δ 5.11 (s, 2H), 4.46 (d, *J* = 2.5 Hz, 1H), 4.41 (d, *J* = 2.5 Hz, 1H), 3.98 (s, 2H), 3.80 – 3.76 (m, 2H), 3.57 (dd, *J* = 5.7, 3.7 Hz, 2H), 3.39 (s, 3H).

^{13}C NMR ($CDCl_3$, 101 MHz): δ 155.87, 93.12, 89.83, 71.70, 68.04, 59.18, 45.21.

FTIR (Neat, NaCl, thin film): 2922, 1638, 1299, 1188, 1022 cm^{-1}.

HRMS (ESI): calc'd for $[M+H]^+$ 180.05532, found 180.05544.

Preparation of methyl 2-allyl-6-((2-methoxyethoxy)methoxy)-3-oxohept-6-enoate (109):

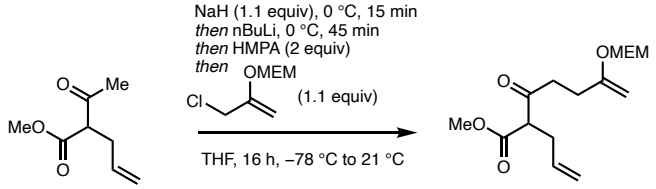

108 **109**

An oven-dried 1L round bottom flask and large magnetic stir bar were pumped into the glovebox and charged with NaH (90% purity, 3.76 g, 141 mmol, 1.1 equiv). The flask was capped, brought out of the glovebox, and put under nitrogen with a 250 mL addition funnel hooked in. Then, 400 mL of anhydrous THF was added via cannulation from the SPS, and the flask was cooled to 0 °C. To the stirring solution at 0 °C was added a 1M solution of methyl-2-allylacetoacetate (20.0 g, 128 mmol, 1 equiv) in anhydrous THF dropwise over 35 min using an addition funnel. The deprotonation was evidently exothermic, as bubbling and melting of the ice in the ice bath was observed. The resulting enolate was stirred for

15 min at 0 °C. Then, to the stirring solution at 0 °C was added *n*BuLi (1.69 M in hexanes, 83.4 mL, 1.1 equiv) dropwise over 5 min. A change in color from grey/pale yellow to a dark orange was observed. The double enolate was stirred for 45 min at 0 °C, after which time HMPA (44.6 mL, 256 mmol, 2 equiv, distilled over CaH_2 and stored in a Schlenk with activated molecular sieves) was added dropwise over 2 min. The ice bath was then replaced by a − 78 °C dry-ice/acetone bath. To the resulting diluted solution at −78 °C was added the electrophile (azeotroped with benzene three times) dropwise over 45 min neat (25.4 g, 141 mmol, 1.1 equiv). The resulting solution was stirred for 16 h and gradually allowed to warm to room temperature from − 78 °C upon which a color change from dark red to bright orange was observed. Following 16 h, 500 mL of water was added. The solution was stirred for 5 min, then transferred over to a separatory funnel and extracted with diethyl ether (3 x 400 mL). The combined organic phases were washed with brine, dried with $NaSO_4$, and filtered. The organic phases were then concentrated on the rotatory evaporator and loaded onto the 8 L column packed 35% full with silica. The crude material was then it was loaded onto a column and purified with 7% EtOAc/Hexanes for one column volume, 9% EtOAc/Hexanes for one column volume, 11% EtOAc/Hexanes for two column volumes, 12% EtOAc/Hexanes for two column volumes, 13% EtOAc/Hexanes for two column volumes, and 15% EtOAc/Hex until all the product had eluted, affording a yellow oil which was determined to be 96% pure (20.3 g, 55% yield) by qNMR with technazene (2.0 mg as compared to 8.6 mg of the crude oil). This compound cannot be stored overnight, as decomposition (MEM group deprotection) will occur, so it was carried forward directly into the next step.

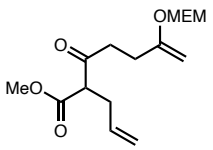

109

TLC (20% Hexanes/EtOAc): R_f 0.13 (*p*-anisaldehyde, stains black/blue).

^{1}H NMR ($CDCl_3$, 400 MHz): δ 5.78 – 5.68 (m, 1H), 5.11 – 4.99 (m, 4H), 4.14 (d, J = 2.2 Hz, 1H), 4.00 (d, J = 2.1 Hz, 1H), 3.74 – 3.70 (m, 5H), 3.57 – 3.55 (m, 2H), 3.39 (s, 3H), 2.78 – 2.68 (m, 2H), 2.59 (ddd, J = 7.4, 6.5, 1.3 Hz, 2H), 2.39 (td, J = 7.3, 0.8 Hz, 2H).

^{13}C NMR ($CDCl_3$, 101 MHz): δ 203.62, 169.75, 159.21, 134.36, 117.69, 92.77, 85.17, 71.76, 68.01, 59.20, 58.47, 52.57, 40.07, 32.37, 28.97.

FTIR (Neat, NaCl, thin film): 3444, 2922, 1758, 1643, 1434, 1267, 1034 cm^{-1}.

HRMS (ESI): calc'd for $[M+H]^+$ 300.15729, found 300.15670.

Preparation of Methyl 5-[(2-methoxyethoxy)methoxy]-6-methylene-2-oxobicyclo[3.2.1]octane-1-carboxylate (110):

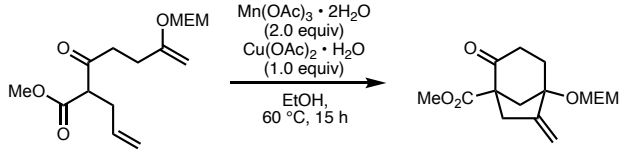

109 **110**

To a two-neck 2 L round bottom flask charged with a large (2 x 1 inch), cylindrical stir bar and the starting material (21.3 g, 70.9 mmol) was added 740 mL of EtOH (degassed, 93.8 mM), and the reaction was stirred for 1 min to ensure complete homogeneity of the solution. Then, to the stirring solution was added $Mn(OAc)_3 • 2H_2O$ (38.0 g, 142.0 mmol, 2 equiv) following immediately by $Cu(OAc)_2 • H_2O$ (14.2 g, 70.9 mmol, 1 equiv). 16 mL of additional EtOH was added to wash any salts that were stuck to the neck of the flask

down. The flask was fitted with a reflux condenser and connected to a nitrogen inlet. The headspace was evacuated and backfilled three times with N_2. The dark brown solution was stirred vigorously at 60 °C using an oil bath for 15 h. After the 2nd hour, it was noted that the dark brown solution had turned a bright turquoise color, likely from change in oxidation state of the added Mn(III)/Cu(II) salts. After the 15th hour, the flask was brought out of the oil and cooled back down to room temperature. The mixture was poured slowly into a 1L separatory funnel that contained 500 mL of water and 50 mL of saturated sodium bisulfite solution (aq). A color change to a dark green was observed, and some bubbling was observed but no exotherm. The aq. phase was extracted with dichloromethane (4 x 300 mL). The collected organic phases were then washed with brine, dried with $NaSO_4$, filtered, and concentrated down *in vacuo*. The crude material was then loaded onto a 2 L column filled 50% with silica and purified with 10% EtOAc/Hexanes to 20% EtOAc/Hexanes and holding at 20% until all product was eluted (took like 4 column volumes of this), affording a yellow oil (11.0 g, 52% yield). The primary impurity is a less-polar impurity that is quite difficult to separate (hence the very moderate gradient from 10-20% EtOAc/Hex). It corresponds to hydrolyzing the MEM group of the product and is usually formed between 20 and 30% yield.

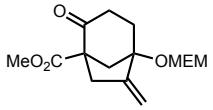

110

TLC (30% Hexanes/EtOAc): R_f 0.16 ($KMnO_4$).

^{1}H NMR ($CDCl_3$, 400 MHz): δ 5.25 (t, *J* = 2.6 Hz, 1H), 5.22 (s, 1H), 4.92 (s, 1H), 4.78 (s, 1H), 3.83 (s, 1H), 3.75 (s, 3H), 3.65 (s, 1H), 3.55 (s, 2H), 3.38 (s, 3H), 2.95 (s, 1H), 2.77 (s, 1H), 2.63 (s, 1H), 2.48 (s, 2H), 2.30 (s, 1H), 2.18 (s, 1H), 1.90 (s, 1H).

^{13}C NMR ($CDCl_3$, 101 MHz): δ 206.17, 171.07, 148.22, 108.61, 91.36, 82.91, 71.87, 67.37, 60.60, 59.16, 52.43, 42.19, 38.19, 37.52, 35.08.

FTIR (Neat, NaCl, thin film): 2921, 1742, 1446, 1265, 1073 cm^{-1}.

HRMS (ESI): calc'd for $[M+H]^+$ 298.14164, found 298.14211.

Preparation of enol triflate bicycle 114:

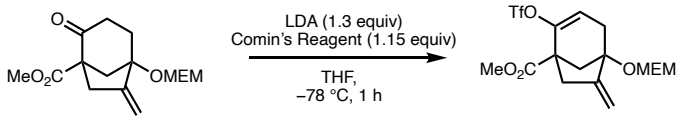

110 **114**

The starting material was azeotroped in benzene (3 x 10 mL). In a flame dried, N_2 filled 500 mL round bottom flask was added 2.87 mL of diisopropylamine (20.5 mmol, 1.3 equiv) and 50 mL of SPS THF. The vessel was cooled to −78 °C before *n*-Butylithium was added dropwise via syringe addition (8.19 mL, 2.5 M, 20.5 mmol). The reaction mixture was stirred for 15 minutes at −78 °C, warmed to 0 °C with an ice bath and stirred for 15 minutes, then cooled back down to −78 °C. Methyl 5-[(2-methoxyethoxy)methoxy]-6-methylene-2-oxobicyclo[3.2.1]octane-1-carboxylate was then added dropwise by syringe addition dropwise to the stirring solution of lithium diisopropylamine as a 1M solution in THF (4.7 g, 15.8 mL, 15.8 mmol) and stirred for 45 minutes at −78 °C. A small amount of THF was used to transfer residual starting material to the reaction flask to ensure quantitative transfer. Comin's reagent (1M in THF, 18.1 mmol, 18.1 mL, 1.15 equiv) was then added via cannula as a steady stream (about 3 min to add all 18 mL), and the reaction was stirred for 90 minutes at −78 °C. Upon addition of Comin's reagent, the mixture turned orange and a small amount of white gas evolved from the solution. After 90 minutes, the reaction was quenched by addition of saturated aq. $NaHCO_3$ (100 mL) at -78 °C and

warmed to room temperature. The crude mixture was diluted with 50 mL of Et_2O, and the organic phase was collected (separating from the aqueous phase) using a 250 mL separatory funnel. The aqueous phase was then extracted with Et_2O (3 x 100 mL) and the combined organic layers were washed with brine, dried over Na_2SO_4, filtered and concentrated. The product was purified by column chromatography (silica, 20% EtOAc/hexanes to 25% to fully elute) to isolate a yellow oil with some residual white solids (Comin's reagent byproduct). To get rid of the solid, a filtration of the starting material was done through a pad of cotton, eluting with hexanes. The yield of the isolated product was 5.2 g (77% yield) as a yellow oil. Starting material was reisolated in the column (if present).

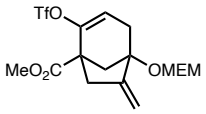

114

TLC (30% EtOAc/Hexanes): R_f 0.35 ($KMnO_4$).

^{1}H NMR ($CDCl_3$, 400 MHz): δ 5.67 (dd, *J* = 5.1, 2.7 Hz, 1H), 5.20 (dt, *J* = 8.7, 2.3 Hz, 2H), 4.92 (d, *J* = 7.6 Hz, 1H), 4.72 (d, *J* = 7.6 Hz, 1H), 3.88 – 3.79 (m, 1H), 3.77 (s, 3H), 3.67 – 3.59 (m, 1H), 3.56 – 3.52 (m, 2H), 3.38 (s, 3H), 3.07 – 2.92 (m, 2H), 2.77 (dd, *J* = 16.9, 2.7 Hz, 1H), 2.58 (dd, *J* = 11.0, 1.8 Hz, 1H), 2.38 – 2.24 (m, 2H).

^{13}C NMR ($CDCl_3$, 101 MHz): δ 170.16, 149.51, 149.02, 116.26, 110.12, 91.26, 82.58, 71.86, 67.41, 59.15, 52.76, 51.88, 44.09, 42.68, 40.62.

FTIR (Neat, NaCl, thin film): 2891, 1734, 1667, 1415, 1300, 1000, 858 cm^{-1}.

HRMS (ESI): calc'd for [M+H] 431.09875, found 431.10053.

Preparation of primary alcohol 113:

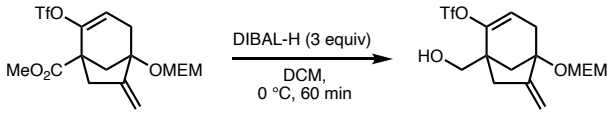

114 **113**

A 500 mL round bottom flask was charged with the starting material (7.14 g, 16.6 mmol) and a magnetic stir bar. 116 mL of dichloromethane were added from a graduated cylinder, and the round bottom was capped with a rubber septum, hooked up to the Schlenk, and vacuumed and backfilled with an N_2 atmosphere three times. The flask was put into an ice bath and cooled to 0 °C. DIBAL-H (7.07 g, 49.8 mmol, 1M, 49.8 mL) was added dropwise as a premade Aldrich solution in dichloromethane via syringe. Following the addition, the mixture was stirred for 10 minutes at 0 °C, TLC'd to ensure completion, and worked up by: 1) dropwise addition of ethyl acetate (4 mL) and 2) addition of saturated aqueous Rochelle's salt (200 mL). The flask was then removed from the ice bath and warmed to room temperature, where it was stirred for 1 h to ensure complete decomposition of Al salts. After an hour of stirring, it was noted that a once cloudy, clumpy mixture (that slightly warmed up upon formation of the Al aggregate) was clear in the dichloromethane layer and a murky white in the aqueous layer. The mixture was poured into a 500 mL separatory funnel, the organic phase was collected, and the aqueous phase was extracted with dichloromethane (3 x 200 mL). The collected organic phases were then washed with brine, dried with Na_2SO_4, filtered and concentrated. The NMR revealed the relatively high purity of the sample (some residual solvent peaks) and so it was carried forward into the Swern Oxidation without further purification. 6.68 g was isolated, corresponding to quantitative yield.

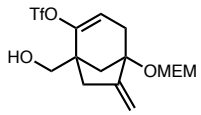

113

TLC (30% EtOAc/Hex): R_f 0.10 (p-anis (blue), $KMnO_4$).

^{1}H NMR ($CDCl_3$, 400 MHz): δ 5.64 (dd, *J* = 4.8, 2.8 Hz, 1H), 5.19 (t, *J* = 2.4 Hz, 1H), 5.13 (t, *J* = 2.0 Hz, 1H), 4.93 (d, *J* = 7.5 Hz, 1H), 4.72 (d, *J* = 7.6 Hz, 1H), 3.92 (d, *J* = 11.3 Hz, 1H), 3.88 – 3.80 (m, 1H), 3.66 – 3.56 (m, 2H), 3.54 (dd, *J* = 5.6, 3.7 Hz, 2H), 3.37 (d, *J* = 0.8 Hz, 3H), 2.75 (q, *J* = 2.4 Hz, 1H), 2.71 (d, *J* = 2.8 Hz, 1H), 2.39 (dt, *J* = 16.0, 3.0 Hz, 1H), 2.34 – 2.24 (m, 2H), 2.15 (dd, *J* = 11.0, 2.7 Hz, 1H), 1.95 (s, 1H).

^{13}C NMR ($CDCl_3$, 101 MHz): δ 152.40, 150.71, 116.65, 109.61, 91.20, 83.06, 71.88, 67.22, 64.27, 59.09, 47.52, 43.37, 42.08, 41.05.

FTIR (Neat, NaCl, thin film): 3464, 2889, 1666, 1409, 1217, 1046, 883 cm^{-1}.

HRMS (ESI): calc'd for [M+H] 403.10383, found 403.10408.

Preparation of aldehyde 112:

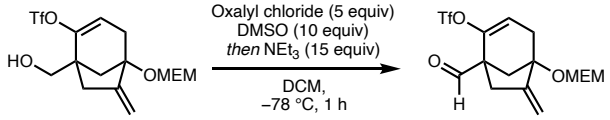

113 **112**

To a solution of oxalyl chloride (3.07 mL, 36.3 mmol) and in CH_2Cl_2 (36 mL) at -78 °C under N_2 is added dropwise a solution of DMSO (5.15 mL, 72.6 mmol). A noticeable exotherm and bubbling was observed. After 15 min a solution of the alcohol (2.92 g, 7.26 mmol) in CH_2Cl_2 (30 mL, 0.24 M) is slowly added dropwise (rxn turned cloudy white), and the reaction was warmed to -40 °C over 30 min. After 30 min, the mixture was cooled back down to -78 °C and Et_3N (15.2 mL, 109 mmol) is added dropwise. The reaction is

stirred 30 min at -78 °C then slowly allowed to warm to rt. In order to work the reaction up, the flask was cooled to 0 ° C and ammonium chloride (60 mL) was added. Separate the phases and extract the aqueous phase with CH_2Cl_2 (60 mL) three times. Wash the combined organic phases with saturated aq. ammonium chloride and brine, dry over Na_2SO_4, and concentrate. The crude reaction mixture was loaded onto a column and purified with a 30 to 35% EtOAc/Hex gradient as a pale yellow oil (2.18 g, 75% yield).

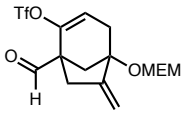

112

TLC (30% EtOAc/Hexanes): R_f 0.20 ($KMnO_4$).

^{1}H NMR ($CDCl_3$, 400 MHz): δ 9.77 (s, 1H), 5.80 (dd, *J* = 5.1, 2.8 Hz, 1H), 5.24 (dd, *J* = 2.6 Hz, 2.2 Hz, 2H), 4.93 (d, *J* = 7.6 Hz, 1H), 4.73 (d, *J* = 7.6 Hz, 1H), 3.87 – 3.79 (m, 1H), 3.66 – 3.59 (m, 1H), 3.57 – 3.52 (m, 2H), 3.37 (s, 3H), 2.93 (p, *J* = 2.4 Hz, 2H), 2.78 (dd, *J* = 17.1, 2.8 Hz, 1H), 2.46 (dt, *J* = 10.9, 1.3 Hz, 1H), 2.35 (ddd, *J* = 17.6, 5.3, 1.8 Hz, 1H), 2.19 (dd, *J* = 11.2, 2.1 Hz, 1H).

^{13}C NMR ($CDCl_3$, 101 MHz): δ 196.52, 148.83, 148.49, 117.90, 110.65, 91.26, 82.79, 71.85, 67.48, 59.18, 55.88, 42.39, 40.99, 40.77.

FTIR (Neat, NaCl, thin film): 2887, 1731, 1415, 1211, 1047, 851 cm^{-1}.

HRMS (ESI/FD$^+$): calc'd for $[M]^+$ 400.08036, found 400.07842.

Preparation of methyl ether 111:

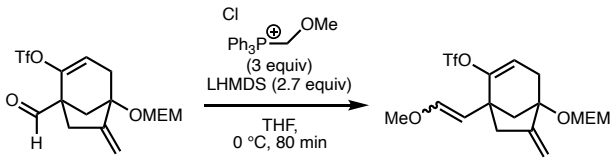

112 **111**

A 500 mL round bottom flask was flame-dried under vacuum and cooled to room temperature. Methoxymethylphosphonium chloride (5.73 g, 16.7 mmol) was added, and the flask was evacuated and backfilled with N_2 3x. THF (100 mL) was added, and the flask was cooled to 0 °C. LHMDS (15 mL, 15.0 mmol, 1 M soln in THF) was added dropwise, which turned the stirring solution turned orange/red. The reaction was then stirred at 0 °C for 45 min. Next, the starting material **193** (2.23 g, 5.57 mmol, 1.0 equiv.) was added as a solution in 1 M THF (5.57 mL). After 30 min the now yellow colored reaction mixture was treated with NH_4Cl and extracted 3x with ether. The organic layer was then dried (Na_2SO_4) and concentrated *in vacuo*. A 2 L column was loaded slightly less than halfway with silica, and the compound was loaded with toluene. A 20% EtOAc/Hexanes isocratic column condition was used. A yellow oil was isolated (1.19 g, 50% yield) as an inconsequential mixture of E/Z diastereomers.

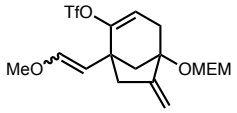

111

TLC (30% EtOAc/Hexanes): R_f 0.44 ($KMnO_4$).

^{1}H NMR ($CDCl_3$, 400 MHz): δ 6.43 (d, *J* = 13.0 Hz, 1H), 5.99 (d, *J* = 6.5 Hz, 1H), 5.57 (dd, *J* = 5.1, 2.7 Hz, 1H), 5.53 (dd, *J* = 5.0, 2.7 Hz, 1H), 5.20 – 5.07 (m, 4H), 4.94 – 4.89 (m, 3H), 4.73 (dd, *J* = 7.6, 1.9 Hz, 2H), 4.31 (d, *J* = 6.5 Hz, 1H), 3.84 (ddd, *J* = 8.4, 6.9, 3.7 Hz, 2H), 3.67 – 3.60 (m, 5H), 3.55 (d, *J* = 5.0 Hz, 7H), 3.39 (d, *J* = 1.0 Hz, 6H), 3.12 – 3.04 (m, 1H), 2.99 – 2.90 (m, 1H), 2.74 (dd, *J* = 16.6, 2.7 Hz, 2H), 2.62 (dt, *J* = 16.3, 3.0 Hz, 1H), 2.52 (dt, *J* = 15.8, 3.0 Hz, 1H), 2.39 (dt, *J* = 11.1, 2.2 Hz, 2H), 2.34 – 2.20 (m, 3H), 2.12 (dd, *J* = 11.0, 2.8 Hz, 1H).

^{13}C NMR ($CDCl_3$, 101 MHz): δ 153.77, 153.71, 151.95, 151.24, 149.62, 149.56, 115.09, 114.27, 109.40, 108.71, 103.01, 101.08, 91.24, 82.87, 82.85, 71.93, 67.28, 67.20, 60.11, 59.17, 59.14, 55.88, 47.06, 46.19, 45.97, 45.83, 44.61, 44.42, 40.96, 40.83.

FTIR (Neat, NaCl, thin film): 2937, 1657, 1416, 1211, 1012 cm^{-1}.

HRMS (ESI/FD$^+$): calc'd for $[M]^+$ 428.11166, found 428.11188.

Preparation of aldehyde 107A:

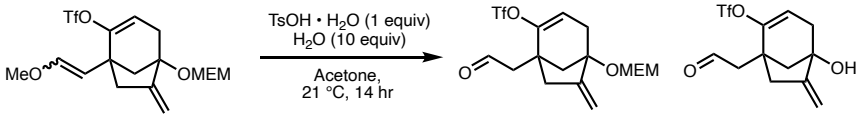

111 **107A** **107A'**

TsOH monohydrate (1.13 g, 5.95 mmol, 1 equiv) was added as a solid at room temperature (23 °C) to a stirring solution of starting material (2.55 g, 5.95 mmol, 1 equiv) in acetone (95.6 mL, 62.2 M) and water (1.07 mL, 59.5 mmol, 10 equiv). The reaction was monitored with TLC. After 8 hours of monitoring by TLC, TLC indicated that the starting material was just about barely present. 100 mL of aqueous sodium bicarbonate solution was added slowly, and the now quenched solution was transferred to a 500 mL separatory funnel, where it was diluted with 100 mL of ether, the organic phase was separated and collected, and the aqueous phase was extracted with ether three times (3 x 200 mL). The organic phase was then washed with brine. The combined organic phases were dried with Na_2SO_4, filtered, and concentrated. The crude material was loaded onto a column and flushed with 20-29% EtOAc/Hex, going up by 1% EtOAc with each 500 mL solvent eluted (see photo attached of column setup and number of fractions). MEM deprotection was carefully separated out from the desired product. The product was stored frozen in benzene under N_2. If the product is not cleanly separated out from any acidic byproducts, it will

decompose in the fridge (MEM deprotection), making the column chromatography step very important.

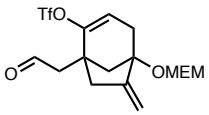

107A

TLC (30% EtOAc/Hexanes): R_f 0.26 ($KMnO_4$).

^{1}H NMR ($CDCl_3$, 400 MHz): δ 9.76 (s, 1H), 5.65 (s, 1H), 5.20 (p, *J* = 1.2 Hz, 1H), 5.16 – 5.13 (m, 1H), 4.92 (s, 1H), 4.71 (s, 1H), 3.84 (s, 1H), 3.61 (s, 1H), 3.53 (s, 2H), 3.37 (s, 3H), 2.95 (s, 2H), 2.77 (s, 1H), 2.52 (s, 1H), 2.40 (s, 2H), 2.28 (s, 2H).

^{13}C NMR ($CDCl_3$, 101 MHz): δ 198.76, 151.49, 149.90, 115.31, 109.70, 91.22, 83.06, 71.86, 67.27, 59.13, 47.66, 46.08, 44.98, 42.26, 41.10.

FTIR (Neat, NaCl, thin film): 2922, 1731, 1416, 1238, 1006, 682 cm^{-1}.

HRMS (ESI): calc'd for [M+H] 415.10383, found 415.10539.

Chiral preparatory HPLC of 107A.

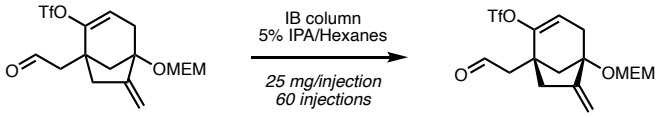

107A (*R,S*)-**107A**

1.46 g was used with 12 mL hexanes for 120 injections (overestimate) but can add more, vial position set to 81. See experimental notes, below.

The procedure began by disconnecting all equipment and refilling the solvents. Solvent A was hexanes, connected to the top tubes, and Solvent B was isopropanol (IPA), connected to the bottom tubes, used at 5%. The method was loaded without overwriting the existing one, and a method such as C18 was selected to start. The flow rate was reduced from 40 to

20, and all flow rates were adjusted to 20 as well. Solvent A was flushed by setting its flow to 0, and all systems, including the multi-wavelength detector (MWD), were turned on. The system was flushed with 5% IPA in hexanes, followed by a flush with pure hexanes. Once the pressure dropped, the IB column was connected at both ends, taking care not to overtighten or misalign the fittings. The system was then unhooked from the fraction collector, and a green line was connected instead. Although the method could have been loaded into the sequence table at this point, it was noted that it might be better to recreate it for next time. A first pass using small injections was recommended to check if the retention times were consistent, using 5% IPA in hexanes at a flow rate of 30 mL per minute. Finally, the sample was loaded into an LCMS vial and placed in position 81, with the wavelength detector set to store data at 210 nm and 280 nm.

Compounds related to **107A** have been enantiomerically resolved by classical resolution. See PhD theses of Jordan Beck and Andrea Stegner for representative examples.

Preparation of vinyl bromide 107B.

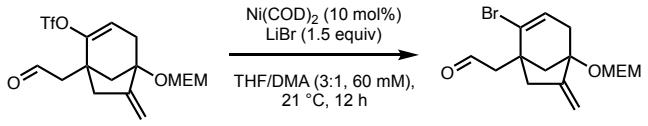

107A **107B**

The starting material was added to an oven-dried 1-dram vial cooled under vacuum and pumped into the glovebox. To a different oven-dried, 2-dram vial was added solid $Ni(COD)_2$ and LiBr. DMA (200 uL) and THF (300 mL, rigorously anhydrous dried over mol. sieves) were added. The vial was capped and stirred for 5 min in the glovebox. Then, the starting material was transferred to the reaction vial in 300 uL of THF. The reaction

was capped with a rubber septum and taped shut, pumped out of the glovebox and stirred for 16 h at room temperature. The color should be a deep aqua blue. Then it should turn kind of a grey/green. Then a bright green. Monitor by TLC under air-free technique, and an NMR aliquot is valuable information in case the conversion stalls. The TLC is best in 20% acetone/hexanes (due to streakiness in EtOAc/Hex). In order to work this reaction up, it was filtered through a silica plug, eluting with 50% EtOAc/Hex. Then, the resulting organics were subjected to 3 saturated aqueous LiCl washes (3 x 0.3 mL). Column chromatography was performed in 3-10% acetone/hexanes.

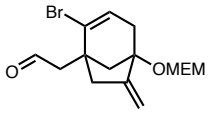

107B

TLC (20% Acetone/Hexanes): R_f 0.29 ($KMnO_4$).

^{1}H NMR ($CDCl_3$, 400 MHz): δ 9.81 (dd, J = 1.9, 1.2 Hz, 1H), 5.94 (dd, J = 5.3, 2.5 Hz, 1H), 5.17 (dd, J = 3.2, 1.8 Hz, 1H), 5.10 (t, J = 2.1 Hz, 1H), 4.92 (d, J = 7.6 Hz, 1H), 4.71 (d, J = 7.6 Hz, 1H), 3.83 (ddd, J = 10.6, 4.8, 3.6 Hz, 1H), 3.64 – 3.57 (m, 1H), 3.56 – 3.48 (m, 2H), 3.37 (s, 3H), 3.10 (dd, J = 17.6, 1.2 Hz, 1H), 2.75 – 2.66 (m, 2H), 2.43 – 2.26 (m, 4H), 2.16 (dddd, J = 16.4, 5.3, 2.1, 0.9 Hz, 1H).

^{13}C NMR ($CDCl_3$, 101 MHz): δ 200.39, 151.00, 128.93, 128.15, 109.33, 91.14, 83.41, 71.86, 67.19, 59.13, 51.41, 46.65, 45.81, 45.31, 45.09.

FTIR (Neat, NaCl, thin film): 2924, 1725, 1453, 1048 cm^{-1}.

HRMS (ESI): calc'd for [M+H] 345.0696, found 345.0701.

$[\alpha]_D^{23}$: +103.8 (c 1.0 in $CHCl_3$).

Preparation of vinyl bromide 121.

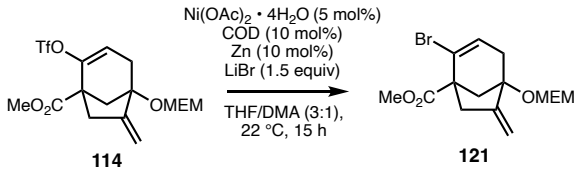

An oven-dried 1-dram vial equipped with a stir bar was brought into an N_2-filled glovebox. The vial was charged with $Ni(OAc)_2 \bullet 4H_2O$ (0.05 equiv), Zn (0.1 equiv), LiBr (1.5 equiv), and COD (0.1 equiv). Anhydrous DMA and THF were added in a 1:3 ratio (0.25 M overall), resulting in a blue color. Enol triflate (50 mg, 116 umol, 1 equiv) was added neat, and the vial was sealed with a Teflon cap, and brought out of the glovebox to stir on the bench (600 rpm) for 24 hours at room temperature. For the workup, 1/2 saturated ammonium chloride (1 mL) was added, and the aqueous residue was extracted three times with ether (2 mL), washed with water (1 mL) four times, washed with brine, dried Na_2SO_4, filtered, and concentrated *in vacuo*. For purification, the crude residue was purified by test tube column (15x150) with a 10-20% EtOAc/Hex gradient, going up by 5% each 25 mL to afford 21.4 mg of product, corresponding to 51% yield. Reaction also contained approximately 3% protodebromination.

Preparation of carboxylic acid 123.

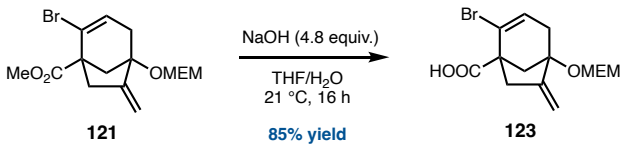

A 2M NaOH stock solution was created. Then, the substrate (20 mg, 55.4 umol, 1 equiv) was dissolved in THF to a total concentration of 200 mM. NaOH (4.8 equiv, 133 uL, 2 M) was added in dropwise. After 16 h, the reaction was diluted with Et_2O (0.5 mL) and acidified with 2M HCl. The organic layer was collected. Then, the aqueous layer was

extracted with Et_2O (3 x 0.5 mL), dried (Na_2SO_4), and concentrated to provide **199** in 85% yield.

Preparation of carboxylic acid 120:

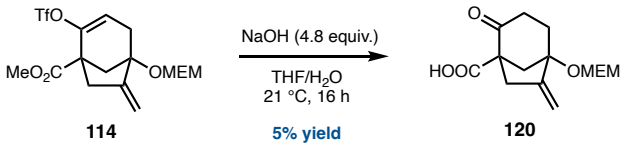

A 2M NaOH stock solution was created. Then, the substrate (20 mg, 55.4 umol, 1 equiv) was dissolved in THF to a total concentration of 200 mM. NaOH (4.8 equiv, 133 uL, 2 M) was added in dropwise. After 16 h, the reaction was diluted with Et_2O (0.5 mL) and acidified with 2M HCl. The organic layer was collected. Then, the aqueous layer was extracted with Et_2O (3 x 0.5 mL), dried (Na_2SO_4), and concentrated to provide **199'** in 5% yield.

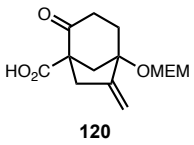

TLC (99% EtOAc/1% AcOH): R_f 0.20 (p-anisaldehyde, blue).

^{1}H NMR (400 MHz, $CDCl_3$): δ 5.28 (dd, *J* = 3.2, 2.1 Hz, 1H), 5.22 (dd, *J* = 3.2, 2.1 Hz, 1H), 4.94 (d, *J* = 7.5 Hz, 1H), 4.80 (d, *J* = 7.5 Hz, 1H), 3.85 – 3.79 (m, 1H), 3.69 – 3.63 (m, 1H), 3.54 (m, 2H), 3.38 (s, 3H), 3.12 (dt, *J* = 17.9, 3.0 Hz, 1H), 2.81 – 2.70 (m, 2H), 2.60 – 2.53 (m, 2H), 2.31 – 2.17 (m, 2H), 2.02 – 1.89 (m, 1H).

^{13}C NMR (101 MHz, $CDCl_3$): δ 209.75, 173.52, 147.71, 108.82, 91.36, 82.88, 71.85, 67.44, 59.18, 58.30, 43.20, 38.54, 38.17, 35.44.

FTIR (MeOH, NaCl, thin film): 2932, 1731, 1415, 1240, 1039 cm^{-1}.

HRMS (ESI): calc'd for $[M+H]^+$ 285.13381, found 285.13265.

Preparation of 8-phenthylmenthol derivative 127.

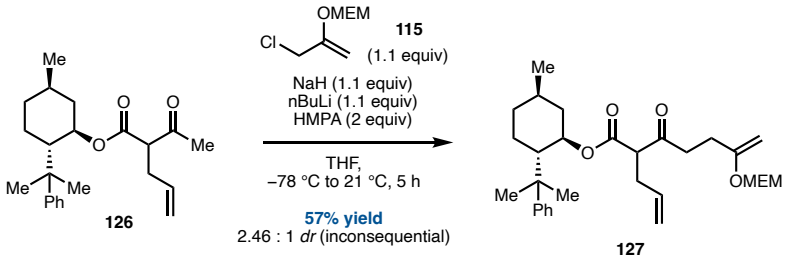

To a stirred solution of NaH (1.15mg, 1.1 equiv) from the glovebox in THF (340 uL) at 0 °C was added phenylmenthyl-2-allylacetoacetate (in 44 uL of a 50uL stock solution of 15.8mg). The mixture was stirred at 0 °C for 15 min at which time nbuli (1.1 equiv) was added dropwise. The resulting yellow solution was stirred for 30 min at 0 °C. HMPA (13.7 uL) was then added, followed by addition of 200uL of THF and the reaction was cooled to -78 °C. At -78 °C, 3-iodo-2-((2-methoxyethoxy)methoxy)propene (43 uL, 1M solution) was added. The mixture was warmed to 21 °C and stirred overnight for 9 h. The reaction was quenched by the addition of water (1 mL). The mixture was acidified with saturated NaH_2PO_4 and extracted with three parts of ether. The combined organic phases were washed with saturated brine solution and dried Na_2SO_4. Removal of the solvent in vacuo gave 333 mg of crude material. Columned 5-7% acetone/hexanes.

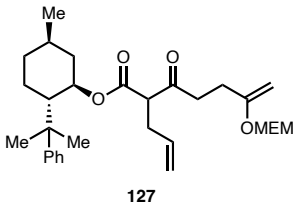

^{1}H NMR ($CDCl_3$, 400 MHz): ^{1}H NMR (500 MHz, $CDCl_3$) δ 7.30 – 7.25 (m, 5H), 7.16 – 7.11 (m, 1H), 5.59 (dddt, *J* = 27.0, 17.1, 10.3, 6.9 Hz, 1H), 5.09 – 4.89 (m, 5H), 4.80 (tt, *J* = 10.8, 4.1 Hz, 1H), 4.14 (dd, *J* = 5.7, 2.2 Hz, 1H), 3.96 – 3.93 (m, 1H), 3.75 – 3.70 (m, 2H), 3.59 – 3.54 (m, 2H), 3.39 (d, *J* = 5.8 Hz, 3H), 2.66 – 2.54 (m, 1H), 2.52 – 2.32 (m,

4H), 2.28 – 2.20 (m, 2H), 2.03 (dddd, *J* = 16.2, 9.6, 6.0, 3.5 Hz, 1H), 1.89 – 1.61 (m, 3H), 1.44 (dt, *J* = 11.7, 3.2 Hz, 1H), 1.29 (d, *J* = 5.4 Hz, 3H), 1.27 – 1.14 (m, 5H), 0.92 – 0.81 (m, 5H).

Preparation of 3.2.1 bicycle 128.

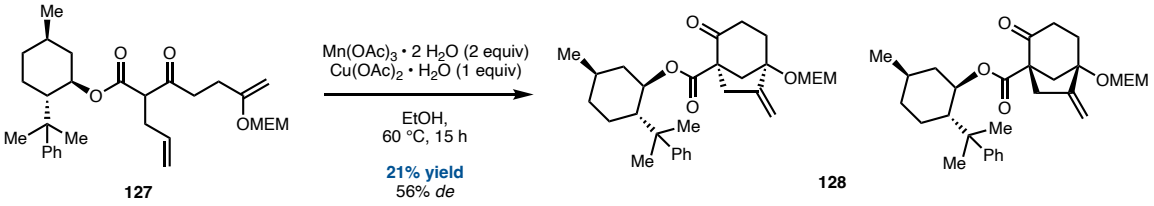

The substrate (100 mg) was dissolved in EtOH. $Mn(OAc)_3$ and $Cu(OAc)_2$ were added, followed by a reflux condenser. The dark brown solution was stirred vigorously at 60 °C using an oil bath for 15 h. The mixture was poured slowly into a 60 mL separatory funnel that contained 1 mL of water and 0.1 mL of saturated sodium bisulfite solution (aq). A color change to a dark green was observed, and some bubbling was observed but no exotherm. The aq. phase was extracted with dichloromethane (4 x 1 mL). The collected organic phases were then washed with brine, dried with $NaSO_4$, filtered, and concentrated down *in vacuo*. The crude material was then loaded onto a column and purified with 20% EtOAc/Hexanes to 20% EtOAc/Hexanes and holding at 25% until all product was eluted (took like 4 column volumes of this), affording the product in 21% yield as a 3.6:1 mixture of diastereomers (~60% *de*).

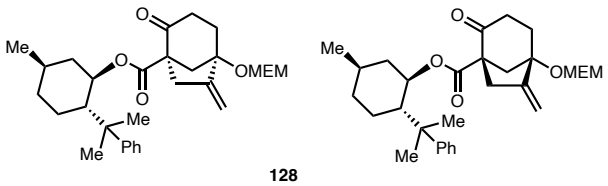

^{1}H NMR ($CDCl_3$, 400 MHz): δ 7.32 – 7.22 (m, 7H), 7.14 (ddd, *J* = 8.8, 4.3, 1.7 Hz, 1H), 5.16 (t, *J* = 2.6 Hz, 1H), 5.05 (t, *J* = 2.2 Hz, 1H), 4.97 – 4.80 (m, 3H), 4.75 (dd, *J* = 7.5, 2.6 Hz, 1H), 3.89 – 3.75 (m, 1H), 3.72 – 3.48 (m, 5H), 3.43 (s, 3H), 3.37 (s, 1H), 2.38 (tdd, *J* = 14.3, 6.6, 3.6 Hz, 3H), 2.32 – 2.23 (m, 2H), 2.22 – 1.98 (m, 6H), 1.84 – 1.59 (m, 6H), 1.33 (d, *J* = 4.8 Hz, 5H), 1.26 (s, 3H), 1.16 (s, 4H), 0.89 (dd, *J* = 6.5, 2.9 Hz, 6H).

^{13}C NMR ($CDCl_3$, 101 MHz): δ 206.11, 206.02, 169.85, 169.77, 152.46, 151.76, 148.64, 148.56, 135.89, 128.06, 127.98, 125.84, 125.76, 125.66, 125.14, 108.13, 108.04, 91.37, 91.19, 82.84, 82.78, 76.62, 76.25, 71.89, 71.84, 67.34, 67.23, 60.62, 60.41, 59.23, 59.17, 50.25, 49.83, 42.02, 41.68, 41.63, 40.87, 40.02, 39.69, 38.12, 37.96, 36.82, 36.53, 35.27, 34.99, 34.79, 34.76, 34.36, 31.45, 31.44, 30.45, 29.84, 29.58, 27.06, 26.76, 26.63, 23.95, 22.83, 21.92, 14.27.

FTIR (Neat, NaCl, thin film): 3131, 3001, 1656, 1555, 1067, 967 cm^{-1}.

HRMS (ESI): calc'd for [M+H^+]: 499.3054, found: 499.3054.

Preparation of β-keto ester 125:

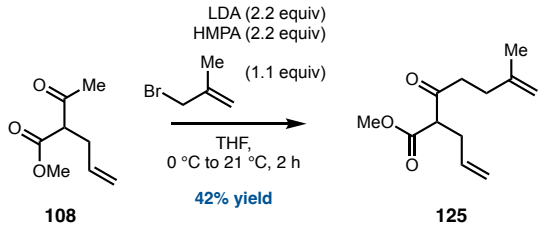

207 was prepared according to the procedure by Xu *et. al.*[101] LDA was prepared conventionally: To a solution of THF (70 mL) in a flame-dried schlenk tube was added a newly distilled *i*Pr_2NH (5.6 mL, 40.3 mmol), and the formed solution was cooled to -78 °C. To this solution was slowly added a solution of *n*BuLi (2.5M, 16.2 mL, 40.3 mmol,

THF), and the mixture was then warmed up to 0 °C, followed by stirring for additional 20 min. To the solution of the above freshly prepared LDA was added the compounds **108** (3 g, 19.2 mmol) at -78 °C in a drop-wise manner, and the formed mixture was then warmed up to 0 °C, and stirred for 30 min. To this solution was sequentially added hexamethylphosphoramide (7.0 mL, 40.3 mmol) and **6** (2.1 mL, 21.1 mmol), and the formed mixture was warmed up to room temperature, and stirred for additional 2 h. The reaction was quenched by addition of a saturated solution of NH_4Cl (50 mL), and the mixture was extracted with Et_2O (3 x 40 mL). The combined extracts were dried over Na_2SO_4. The solvent was removed under vacuum, and the residue was purified by a flash chromatography on silica gel (EtOAc/hexane =1/20) to give compound **125** as colorless oil.

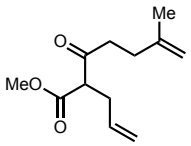

125

TLC (20% EtOAc/Hexanes): R_f = 0.59 (*p*-anisaldehyde).

^{1}H NMR (500 MHz, $CDCl_3$) δ 5.73 (ddt, *J* = 17.1, 10.2, 6.9 Hz, 1H), 5.14 – 5.01 (m, 2H), 4.73 (s, 1H), 4.65 (s, 1H), 3.72 (s, 3H), 3.57 (t, *J* = 7.4 Hz, 1H), 2.70 (t, *J* = 7.6 Hz, 1H), 2.64 (t, *J* = 7.5 Hz, 1H), 2.60 (t, *J* = 7.1 Hz, 2H), 2.28 (t, *J* = 7.5 Hz, 2H), 1.72 (s, 3H).

^{13}C NMR (125 MHz, $CDCl_3$) δ 203.85, 169.78, 144.23, 134.43, 117.58, 110.46, 77.41, 77.16, 76.91, 58.58, 52.44, 40.60, 32.38, 31.15, 22.68.

HRMS (ESI): calc'd for $[M+H^+]$: 211.1334, found: 211.1333.

Preparation of α-brominated β-keto ester 132:

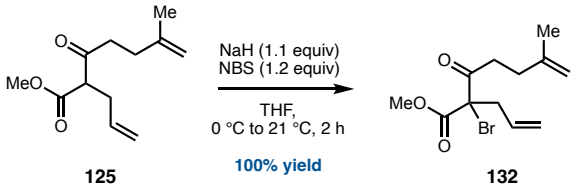

To a suspension of NaH (60% oil dispersion, 1.23 g, 30.8 mmol) in THF (90 mL) was added slowly compound 6a (5.45 g,25.6 mmol) in THF (10 mL) at 0 °C. After 1.0 h, N-bromosuccinimide (5.03 g, 28.2 mmol) was added in one portion at –78 °C. The mixture was stirred for 3 h. After removal of THF, the residue was extracted with ether. The combined extracts were washed with water, dried over $MgSO_4$ and then concentrated. The crude product was purified by filtering through a silica plug, eluting with 10% EA/hexanes to isolate a white solid.

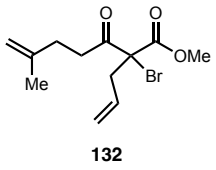

132

TLC (20% EtOAc/Hexanes): R_f 0.71 (UV, p-anisaldehyde).

^{1}H NMR ($CDCl_3$, 400 MHz): δ 5.83 – 5.71 (m, 1H), 5.19 (s, 1H), 5.15 (d, J = 6.4 Hz, 1H), 4.75 (s, 1H), 4.69 (s, 1H), 3.80 (s, 3H), 2.99 (t, J = 6.7 Hz, 2H), 2.92 (t, J = 7.3 Hz, 1H), 2.82 – 2.72 (m, 1H), 2.32 (t, J = 7.6 Hz, 2H), 1.73 (s, 3H).

^{13}C NMR (101 MHz, $CDCl_3$): δ 199.55, 167.89, 144.06, 131.75, 120.42, 110.71, 67.68, 53.86, 41.94, 37.34, 32.16, 22.70.

FTIR (Neat, NaCl, thin film): 3080, 2954, 1737, 1714, 1434, 1233, 926 cm^{-1}.

HRMS (ESI): calc'd for $[M+H]^+$ 289.0433, found 289.0432.

Preparation of bromine atom-transfer product 130:

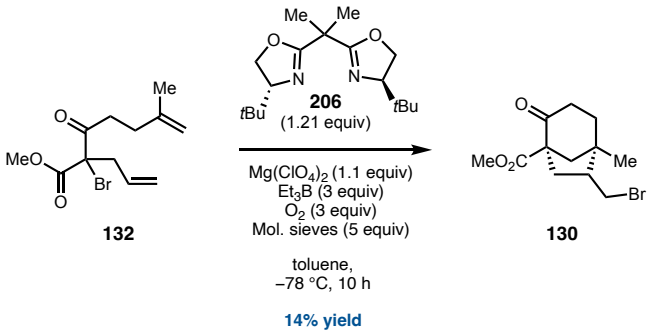

Chiral ligand 2,2'-isopropylidenebis[(4s)-4-tert-butyl-2-oxazoline] (4, 49 mg, 0.23 mmol) and $Mg(ClO_4)_2$ (49 mg, 0.22 mmol) were mixed in dry toluene (10 mL) for 0.5 h at room temperature. Then substrate **132** (60 mg, 0.21 mmol) was added. The mixture was stirred at room temperature for 15 min and cooled to –78 °C. After 30 min, Et_3B (1.0 M in hexane, 0.6 mL, 0.6 mmol) and O_2 gas (4 mL) were added via syringe. When the reaction was completed, the mixture was filtered through a thin pad of silica gel and then concentrated. The crude product was purified by prep plate in 20% EA/hex to afford 14% yield product, along with 22% starting material, 10% protodebromination, 34% monocyclization and bromine radical capture.

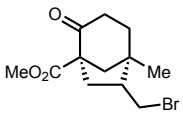

130

TLC (20% EtOAc/Hexanes): R_f 0.62 (p-anisaldehyde, yellow).

^{1}H NMR ($CDCl_3$, 400 MHz): δ 3.75 (s, 3H), 3.63 (ddd, J = 21.4, 9.7, 4.3 Hz, 1H), 3.39 – 3.22 (m, 1H), 2.73 – 2.34 (m, 4H), 2.23 – 2.06 (m, 2H), 1.99 – 1.90 (m, 1H), 1.88 – 1.76 (m, 1H), 1.75 – 1.63 (m, 1H), 1.15 (s, 3H).

^{13}C NMR (101 MHz, $CDCl_3$): δ 207.72, 207.31, 171.99, 171.82, 63.59, 52.36, 49.93, 48.81, 46.29, 45.09, 43.21, 42.84, 40.83, 39.60, 38.30, 38.07, 34.78, 34.62, 33.25, 32.96, 24.81, 21.43.

FTIR (Neat, NaCl, thin film): 3083, 2950, 1637, 1514, 1434, 1223, 947 cm^{-1}.

HRMS (ESI): calc'd for $[M+H]^+$ 289.0433, found 289.0430.

Preparation of 3.2.1 bicycle 131':

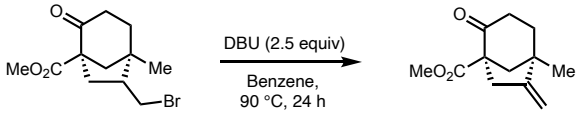

209 **30% yield** **79% *ee*** **131'**

The starting material (5 mg, 1 equiv) was dissolved in benzene and DBU (2.5 equiv) was added. The reaction was heated in a sealed vial at 90 °C overnight for 24 h. Then, to work the reaction up, 0.3 mL of NH_4Cl was added, and the aq. phase was extracted three times with diethyl ether. Drying with sodium sulfate and concentrating, followed by prep TLC with 20% EA/hex provided 2 mg (30% yield) of product 3.2.1 bicycle.

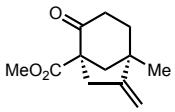

131'

TLC (20% EtOAc/Hexanes): R_f 0.40 ($KMnO_4$).

^{1}H NMR ($CDCl_3$, 400 MHz): δ 5.06 (t, *J* = 2.2 Hz, 1H), 5.00 (t, *J* = 2.6 Hz, 1H), 3.75 (s, 3H), 2.98 – 2.90 (m, 1H), 2.83 (d, *J* = 18.0 Hz, 1H), 2.55 – 2.44 (m, 1H), 2.36 (dd, *J* = 15.6, 5.8 Hz, 1H), 2.09 (s, 2H), 1.79 (td, *J* = 12.4, 6.6 Hz, 1H), 1.72 – 1.64 (m, 1H), 1.24 (s, 3H).

^{13}C NMR (101 MHz, $CDCl_3$): δ 207.76, 171.95, 153.72, 106.54, 62.37, 52.30, 47.19, 44.17, 40.48, 40.11, 35.75, 22.92.

FTIR (Neat, NaCl, thin film): 2954, 2871, 2744, 1714, 1434, 1329, 1240, 1080, 897 cm^{-1}.

HRMS (ESI): calc'd for $[M+H]^+$ 231.0991, found 231.0993.

Preparation of 3-chloro-2-[(diethoxyphosphoryl)oxy]-1-propene (134):

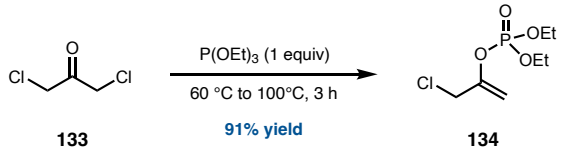

133 134

A 25-mL, single-necked, round-bottomed flask equipped with a thermocouple, a reflux condenser, a nitrogen inlet, and a magnetic stirring bar was charged with 1,3-dichloroacetone (5.93 g, 44.4 mmol). The solid was warmed to 40 °C and the solid melted. Then, it was moved to a water bath and triethyl phosphite (8.01 mL, 46.7 mmol) was syringed into the flask, under vigorous stirring, at such a rate that the temperature was maintained between 40 and 50 °C. To increase the rate at which triethylphosphite could be added, the flask was removed from the oil bath and put into a room temperature water bath. Following addition of triethylphosphite, the reaction mixture was then stirred for 1 h at 60 °C, 1 h at 80 °C,and then 1 h at 100 °C. Bulb-to-bulb distillation (kugelrohr) of the crude product with full high vac (14 mTorr) and 115 °C on the kugelrohr oven with three bulbs (two in the oven, one over ice) gave 9.73 g from the second bulb (91% yield).

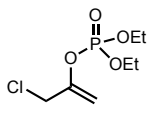

134

TLC (45% EtOAc/Hexanes): R_f 0.28 (*p-anisaldehyde*aldehyde).

^{1}H NMR ($CDCl_3$, 400 MHz): δ 5.10 – 5.08 (m, 1H), 4.91 (t, J = 2.3 Hz, 1H), 4.24 – 4.16 (m, 4H), 4.06 (s, 2H), 1.36 (td, J = 7.1, 1.2 Hz, 6H).

^{31}P NMR (162 MHz, CDCl3): δ -6.94.

^{13}C NMR (101 MHz, $CDCl_3$): δ 150.40, 101.40, 64.88, 44.19, 16.21.

FTIR (Neat, NaCl, thin film): 2984, 1653, 1280, 1163, 1030, 926 cm^{-1}.

HRMS (ESI): calc'd for $[M+H]^+$ 229.0390, found 229.0392.

Preparation of vinyl phosphonate ester 135:

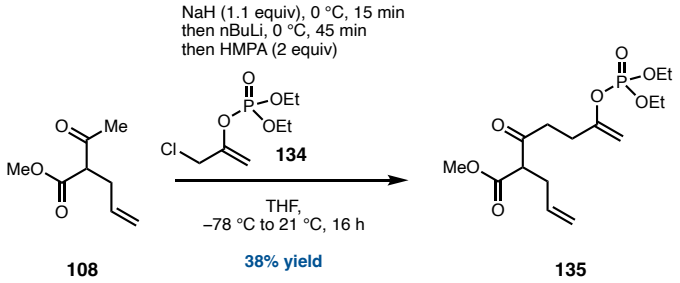

An oven-dried 250 mL round bottom flask and large magnetic stir bar were pumped into the glovebox and charged with NaH (90% purity). Then, anhydrous THF was added, and the flask was capped with a rubber septum, brought out of the glovebox, put under nitrogen, and cooled to 0 °C. To the stirring solution at 0 °C was added a 1M solution of starting material in anhydrous THF dropwise over 2 min. The deprotonation was evidently exothermic, as bubbling and melting of the ice in the ice bath was observed. The resulting enolate was stirred for 15 min at 0 °C. Then, to the stirring solution at 0 °C was added *n*BuLi dropwise over 5 min. A change in color from grey/pale yellow to a orange was observed. The double enolate was stirred for 45 min at 0 °C, after which time HMPA (2 equiv, distilled over CaH_2 and stored in a Schlenk with activated molecular sieves) was

added dropwise over 1 min. The ice bath was then replaced by a −78 °C dry-ice/acetone bath, and to the resulting diluted solution at −78 °C was added the electrophile dropwise over 45 min neat. The resulting orange solution was stirred for 3.5 h and gradually allowed to warm to 0 °C upon which a color change from dark orange to bright yellow was observed. Following 3.5 h, 50 mL of water was added. The solution was stirred for 5 min, then transferred over to a separatory funnel and extracted with diethyl ether (3 x 20 mL). The combined organic phases were washed with brine, dried with $NaSO_4$, and filtered. The organic phases were then concentrated on the rotatory evaporator and loaded onto the 100 mL column packed 70% full with silica. The crude material was loaded onto a column and purified with a 30%, 35%, 40%, 42.5%, 45%, 47.5%, 50% then flushed with 100% EtOAc to afford 38% yield of pure product as a clear or pale-yellow oil.

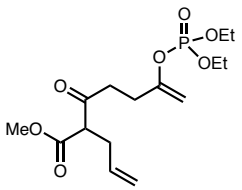

135

TLC (45% EtOAc/Hexanes): R_f 0.20 (*p-anisaldehyde*aldehyde).

^{1}H NMR ($CDCl_3$, 400 MHz): δ 5.72 (ddt, J = 17.1, 10.1, 6.8 Hz, 1H), 5.13 – 5.01 (m, 2H), 4.84 (t, J = 2.1 Hz, 1H), 4.53 (s, 1H), 4.21 – 4.11 (m, 4H), 3.72 (s, 3H), 3.57 (t, J = 7.4 Hz, 1H), 2.87 – 2.66 (m, 2H), 2.59 (t, J = 6.5 Hz, 2H), 2.48 (t, J = 6.8 Hz, 2H), 1.35 (t, J = 7.1 Hz, 6H).

^{13}C NMR (101 MHz, $CDCl_3$): δ 202.97, 169.65, 154.09, 134.22, 117.80, 97.90, 64.49, 58.42, 52.62, 39.24, 32.34, 28.50, 16.26.

FTIR (Neat, NaCl, thin film): 3477, 2983, 1735, 1654, 1438, 1273, 1050, 860 cm^{-1}.

HRMS (ESI): calc'd for $[M+H]^+$ 349.1411, found 349.1444.

Preparation of 3.2.1 bicycle 136:

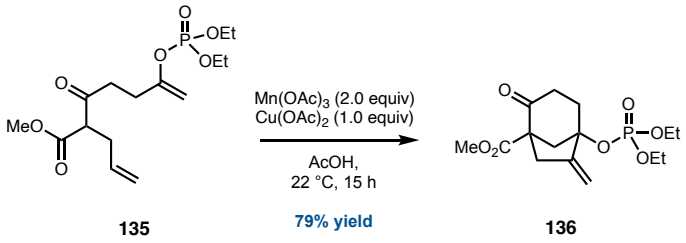

To a stirred solution of $Mn(OAc)_3$ $2H_2O$ (154 mg, 574 umol) and $Cu(OAc)_2$ H_2O (57.3 mg, 574 umol) in 2.5 mL of glacial acetic acid was added the starting material (100 mg, 287 umol) in 0.85 mL of glacial acetic acid. The reaction mixture was stirred at room temperature for 15 h at which time 2 mL of water was added. A solution of 10% $NaHSO_3$ (1 mL) was added dropwise to the mixture to decompose any residual $Mn(OAc)_3$. The resulting solution was extracted with three 3-mL portions of methylene chloride. The combined organic extracts were poured into a 125 mL separatory funnel and saturated $NaHCO_3$ solution was added dropwise slowly (CAUTION: lots of bubbling neutralizing AcOH) and dried over anhydrous Na_2SO_4. Removal of the solvent invacuo gave 70 mg of crude product which was purified by silica gel chromatography (40% EA/hexanes).

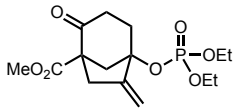

136

TLC (45% EtOAc/Hexanes): R_f 0.17 (*p-anisaldehyde*aldehyde).

^{1}H NMR ($CDCl_3$, 400 MHz): δ 5.43 – 5.40 (m, 1H), 5.22 (t, J = 2.6 Hz, 1H), 4.16 – 4.07 (m, 4H), 3.74 (s, 3H), 3.02 (dt, J = 18.1, 2.9 Hz, 1H), 2.79 – 2.70 (m, 2H), 2.66 (dd, J = 12.0, 2.1 Hz, 1H), 2.56 – 2.44 (m, 3H), 2.14 – 2.05 (m, 1H), 1.34 (tdd, J = 7.1, 2.6, 1.1 Hz, 6H).

^{13}C NMR (101 MHz, $CDCl_3$): δ 204.91, 170.48, 147.73, 109.40, 84.95, 64.08, 60.84, 52.52, 42.78, 37.70, 36.57, 34.91, 16.21.

FTIR (Neat, NaCl, thin film): 2983, 2953, 1744, 1717, 1269, 1246, 1026, 971 cm^{-1}.

HRMS (ESI): calc'd for $[M+H]^+$ 347.1254, found 347.1261.

Preparation of α-brominated β-keto ester 138:

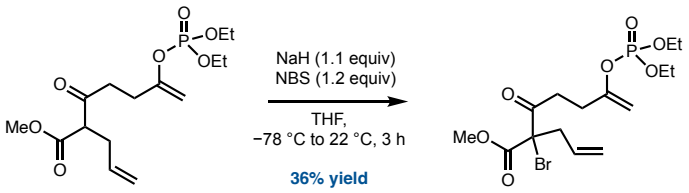

135 138

To a suspension of NaH (5.74 mg, 144 umol, 60% in mineral oil) in 0.4 mL of THF was added the starting material dropwise in a solution of THF (0.1 mL) at 0 °C. After 1 hour stirring at 0 °C, NBS stock solution (1M) was added in. The vial was shielded form light with aluminum foil. The mixture was stirred at −78 °C for 2 h. Following completion by TLC, the mixture was treated with ammonium chloride at −78 °C, allowed to warm to 21 °C, and extracted with ether three times, and concentrated down. The crude resideue was columned 0 to 2.5% to 5% ether in DCM and kept at 5% until all product was eluted to isolate **138** as an orange oil (3 mg, 36% yield).

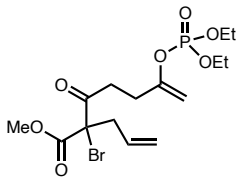

138

TLC (5% ether/DCM): R_f 0.40 (*p-anisaldehyde*aldehyde).

^{1}H NMR (CDCl$_3$, 400 MHz): δ 5.78 (ddt, *J* = 15.9, 11.0, 7.1 Hz, 1H), 5.23 – 5.15 (m, 2H), 4.89 (t, *J* = 2.2 Hz, 1H), 4.58 (td, *J* = 2.1, 1.0 Hz, 1H), 4.19 (tt, *J* = 7.6, 6.6 Hz, 4H), 3.83 (s, 3H), 3.12 – 2.87 (m, 4H), 2.58 – 2.48 (m, 2H), 1.38 (td, *J* = 7.1, 1.1 Hz, 6H).

^{13}C NMR (CDCl3, 101 MHz): δ 198.70, 167.75, 153.83, 153.75, 131.60, 120.55, 98.15, 98.11, 67.28, 64.57, 64.51, 53.94, 41.90, 36.14, 30.45, 29.59, 29.53, 16.27, 16.20.

FTIR (Neat, NaCl, thin film): 2982, 2911, 1727, 1275, 1031 cm^{-1}.

HRMS (ESI): calc'd for $[M+H]^+$ 427.0515, found 427.0531.

Preparation of α-selenylated β-keto ester 139:

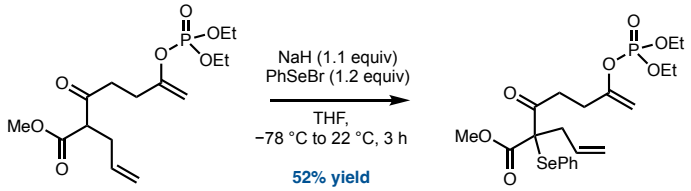

To a suspension of NaH (5.74 mg, 144 umol, 60% in mineral oil) in 0.4 mL of THF was added the starting material dropwise in a solution of THF (0.1 mL) at 0 °C. After 1 hour stirring at 0 °C, PhSeBr stock solution (1M) was added in. The vial was shielded form light with aluminum foil. The mixture was stirred at -78 °C for 2 h. Following completion by TLC, the mixture was treated with ammonium chloride, allowed to warm to rt, and extracted with ether three times, and concentrated down. The crude resideue was columned 0 to 2.5% to 5% ether in DCM and kept at 5% until all product was eluted to isolate **139** as an clear oil (5 mg, 52% yield).

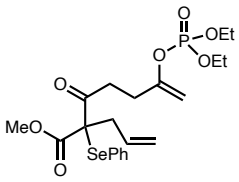

139

^{1}H NMR (300 MHz, $CDCl_3$): δ 7.51 – 7.27 (m, 5H), 5.89 (ddt, *J* = 17.2, 10.3, 6.9 Hz, 1H), 5.19 – 5.05 (m, 2H), 4.87 (t, *J* = 2.2 Hz, 1H), 4.61 – 4.53 (m, 1H), 4.26 – 4.08 (m, 4H), 3.77 (s, 3H), 3.16 (ddd, *J* = 17.0, 9.3, 6.2 Hz, 1H), 2.77 – 2.60 (m, 2H), 2.59 – 2.44 (m, 3H), 1.36 (tt, *J* = 7.1, 1.0 Hz, 6H).

Preparation of α-chloro β-keto ester 140:

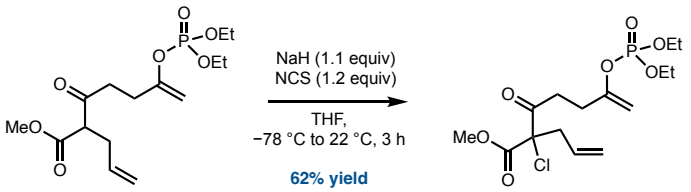

135 **140**

To a suspension of NaH (5.74 mg, 144 umol, 60% in mineral oil) in 0.4 mL of THF was added the starting material dropwise in a solution of THF (0.1 mL) at 0 °C. After 1 hour stirring at 0 °C, NCS stock solution (1M) was added in. The vial was shielded form light with aluminum foil. The mixture was stirred at −78 °C for 2 h. Following completion by TLC, the mixture was treated with ammonium chloride, allowed to warm to room temperature, and extracted with ether three times, and concentrated down. The crude resideue was columned 0 to 2.5% to 5% ether in DCM and kept at 5% until all product was eluted to isolate **140** as an orange oil (3.5 mg, 62% yield).

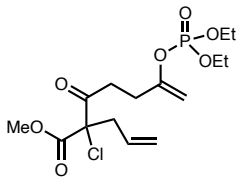

140

^{1}H NMR (300 MHz, $CDCl_3$): δ 5.90 – 5.60 (m, 1H), 5.22 – 5.09 (m, 2H), 4.87 (t, *J* = 2.2 Hz, 1H), 4.56 (tt, *J* = 2.0, 0.9 Hz, 1H), 4.17 (dq, *J* = 8.2, 7.1 Hz, 4H), 3.88 – 3.75 (m, 3H), 3.09 – 2.78 (m, 4H), 2.56 – 2.44 (m, 2H), 1.36 (td, *J* = 7.1, 1.1 Hz, 6H).

Preparation of acyl imidazole 148:

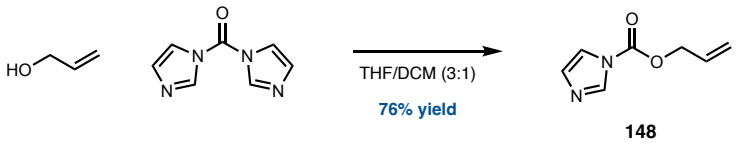

148

A 1L flask with a magnetic stir bar and an addition funnel was flame dried under vacuum. Following cooling, 83.8 g of CDI (1.5 equiv, 517 mmol) was added. The apparatus was evacuated and backfilled and 517 mL of THF was added in. Then, into the addition funnel was added 172 mL of DCM and 23.4 mL of allyl alcohol (344 mmol, 1 equiv). The reaction was cooled to 0 °C. The allyl alcohol mixture was added in dropwise over 30 min. Then, the reaction was stirred for 2 more hours at 0 °C. After completion of 2 hrs. of stirring at 0 °C, the septum was removed, the stir bar was removed, and the solvent was evacuated. The crude oil was loaded onto a column and columned with a 30-50% EA/hex gradient, moving up by 10% each column volume until reaching 50% EA/hex.

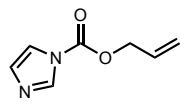

148

TLC (50% EtOAc/Hexanes): R_f 0.25 (*p*-anisaldehyde).

FTIR (Neat, NaCl, thin film): 3129, 1760, 1474, 1394, 1166, 998, 945, 769 cm^{-1}.

HRMS (ESI): calc'd for $[M+H]^+$ 153.0659, found 153.0662.

Preparation of β-keto ester 146:

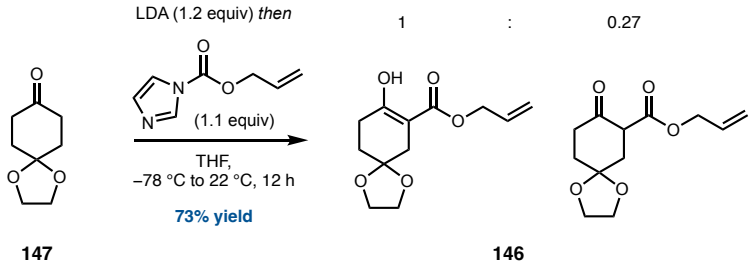

To a flame dried 1L flask with a stir bar under N_2 was added diisopropylamine (50.2 mL, 358 mmol) and THF (100 mL), and it was cooled to −78 °C. *n*BuLi (143 mL, 2.5 M, 358 mmol) was added in dropwise by use of an addition funnel over 10 minutes. After the addition, the LDA was stirred for 15 min at −78 ºC, warmed to 0 °C for 15 min, then cooled back to −78 °C. The starting material in 150 mL of THF (299 mmol, 2 M) was added dropwise over 10 min. The resulting solution was stirred for 30 min before the electrophile (50.0 g, 329 mmol) was added dropwise at −78 ºC neat over 60 min using a syringe pump. Reaction turned orange then brown as carbamate was added. Reaction was kept at −78 °C for a few hours and slowly allowed to warm to room temperature. After 3 hours at −78 °C, TLC shows some conversion, but not a lot. I think extended reaction time and slowly increasing the temperature to room temperature is important. Reaction was quenched with 300 mL $NaHCO_3$. The organic layer was separated out from the aqueous layer. The remaining aqueous layer was extracted three times with DCM (3 x 300 mL). The organics were washed with brine, dried over $MgSO_4$, filtered through celite, then concentrated. The crude was subjected to column chromatography (5 to 12% EtOAc/Hex)

to afford the product as a pale oil (52.3 g, 218 mmol, 73% yield) as a 1:0.27 mixture of enol to keto forms.

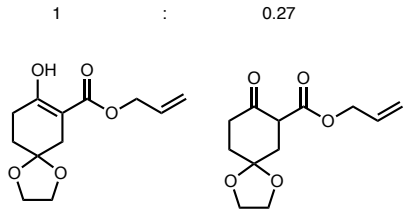

146

TLC (25% EtOAc/Hexanes): R_f 0.48 (*p*-anisaldehyde).

^{1}H NMR ($CDCl_3$, 400 MHz): δ 12.14 (s, 1H), 6.01 – 5.82 (m, 1H), 5.32 (dd, *J* = 17.2, 1.5 Hz, 1H), 5.24 (dd, *J* = 10.5, 1.3 Hz, 1H), 4.64 (dt, *J* = 5.6, 1.4 Hz, 3H), 4.07 – 3.94 (m, 5H), 2.55 – 2.47 (m, 4H), 1.84 (t, *J* = 7.0 Hz, 2H).

^{13}C NMR ($CDCl_3$, 101 MHz) δ 204.73, 171.84, 171.61, 169.14, 132.18, 131.91, 118.71, 118.26, 107.34, 106.75, 95.33, 65.99, 65.06, 64.97, 64.92, 64.72, 54.11, 38.30, 36.67, 34.54, 32.81, 30.41, 28.08.

FTIR (Neat, NaCl, thin film): 2944, 2884, 1744, 1719, 1650, 1421, 1241, 1059, 998, 844 cm^{-1}.

HRMS (ESI): calc'd for $[M+H]^+$ 241.1071, found 241.1078.

Preparation of vinyl bromide 145A:

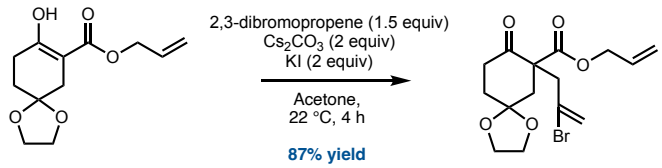

146 **145A**

A 3-neck, round bottom flask with a mechanical stirrer were set up and a N_2 inlet was charged to the flask to allow for a continuous stream of N_2. To the starting material (20.0

g, 83.2 mmol, 1 equiv.) was added 400 mL of acetone. Then, KI (27.6 g, 166 mmol, 2 equiv.) and Cs_2CO_3 (54.2 g, 166 mmol, 2 equiv.) were added in sequentially. 155 mL of acetone were used to rinse all of the salts into the flask to allow for a total reaction concentration of 150 mM. Then, 2,3-dibromopropene (12.7 mL, 104 mmol, 80% technical grade Sigma Aldrich, 1.25 equiv.) was added in dropwise. The reaction was stirred overnight with the mechanical stirrer for 12 h. The reaction was quenched by the addition of H_2O (200 mL) and saturated $NaHCO_3$ aqueous solution (100 mL). The organic layer was separated, and the aqueous layer was extracted with EtOAc (3 x 300 mL), the organic layers were combined, washed with saturated brine (300 mL), dried with anhydrous Na_2SO_4, filtered, and subjected to column chromatography (10 to 20% EA/hex) to afford 26.0 g of pale-yellow product, corresponding to 87% yield.

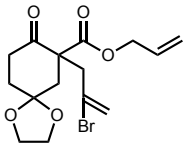

145A

TLC (25% EtOAc/Hexanes): R_f 0.40 (*p*-anisaldehyde).

^{1}H NMR ($CDCl_3$, 400 MHz): δ 5.91 (dd, *J* = 16.9, 10.7 Hz, 1H), 5.66 (s, 1H), 5.57 (d, *J* = 1.4 Hz, 1H), 5.38 – 5.22 (m, 2H), 4.67 – 4.57 (m, 2H), 4.06 – 4.00 (m, 1H), 3.97 (dd, *J* = 5.5, 1.8 Hz, 3H), 3.09 (d, *J* = 15.0 Hz, 1H), 3.03 – 2.92 (m, 2H), 2.74 (dd, *J* = 14.1, 3.1 Hz, 1H), 2.57 – 2.50 (m, 1H), 2.05 – 1.96 (m, 3H).

^{13}C NMR ($CDCl_3$, 101 MHz): δ 204.88, 170.94, 131.58, 127.22, 122.47, 119.09, 106.76, 66.52, 65.00, 64.49, 58.69, 44.85, 40.69, 37.68, 34.93.

FTIR (Neat, NaCl, thin film): 3508, 2957, 2891, 1731, 1429, 1367, 1098, 936 cm^{-1}.

HRMS (ESI): calc'd for $[M+H]^+$ 359.0489, found 359.0490.

Preparation of ligand (*R*)-(CF$_3$)$_3$-tBuPhox:[53]

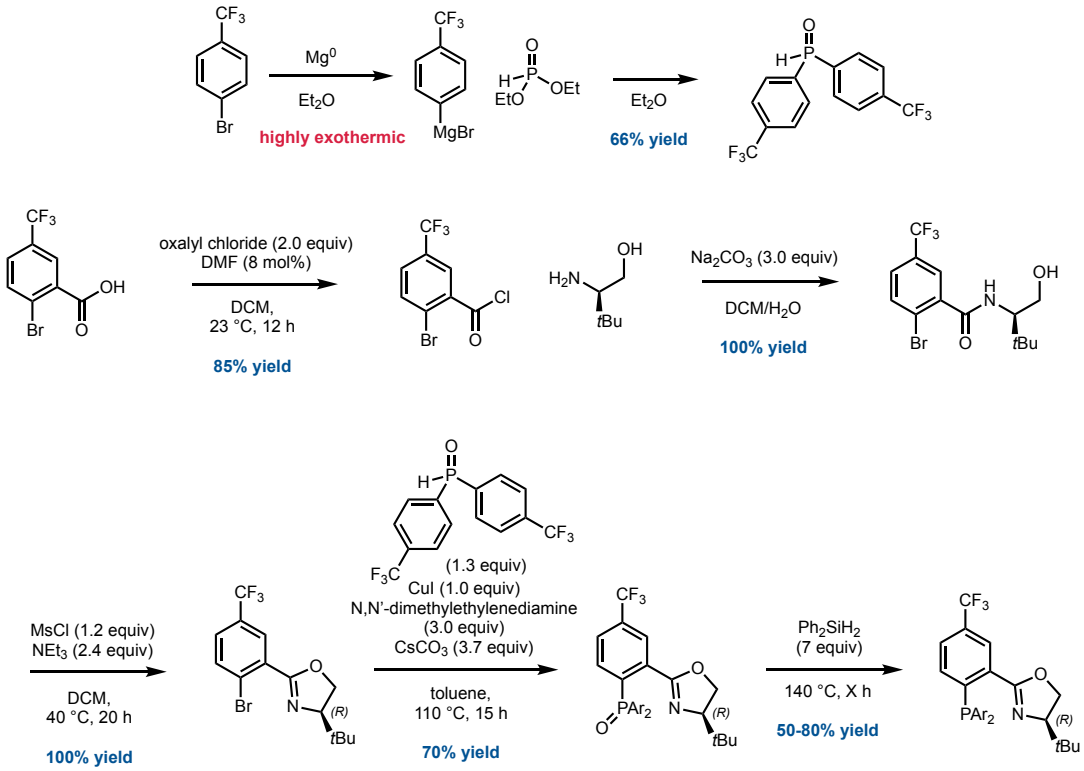

Preparation of diketone 144A:

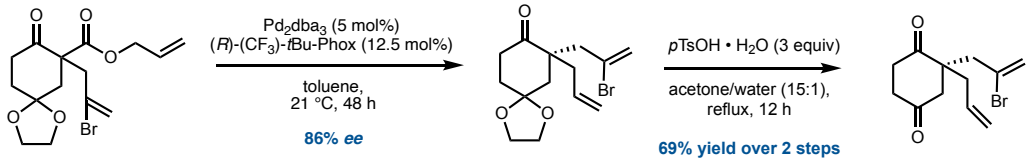

145A **157** **144A**

In the glovebox, (*R*)-(CF$_3$)$_3$-tBuPhox (0.125 equiv) and Pd$_2$dba$_3$ (0.05 equiv) were weighed out in an oven-dried 1000 mL flask equipped with a magnetic stir bar. Toluene was added in (800 mL). The reaction was stirred at room temperature for 30 min before the starting material (10.0 g, 50 mL) was added in. The flask was stirred at room temperature for 3 days. After 1 day, the reaction was completely converted. The crude reaction mixture was hooked up to a rotavap to get off all the toluene. The crude was NMR'd and purified by

silica gel chromatography 10-20% EtOAc/Hex to afford 8.2 g of mixed product with ligand. The mixture was carried forward to the next step. SFC analysis on a pure fraction taken from column shows 86% ee. SFC method: PAPCl_S3C6_10_05min.

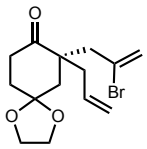

157

TLC (20% EtOAc/Hexanes): R_f 0.48 (*p*-anisaldehyde).

^{1}H NMR ($CDCl_3$, 400 MHz): δ 5.73 – 5.51 (m, 3H), 5.10 (d, *J* = 8.0 Hz, 2H), 4.01 (d, *J* = 2.1 Hz, 4H), 2.93 (d, *J* = 9.1 Hz, 2H), 2.51 (d, *J* = 7.4 Hz, 2H), 2.03 (d, *J* = 12.8 Hz, 4H).

^{13}C NMR ($CDCl_3$, 101 MHz): δ 204.88, 170.94, 131.58, 127.22, 122.47, 119.09, 106.76, 66.52, 65.00, 64.49, 58.69, 44.85, 40.69, 37.68, 34.93.

FTIR (Neat, NaCl, thin film): 3059, 2912, 1660, 1431, 1263, 843, 742 cm^{-1}.

HRMS (ESI): calc'd for $[M+H]^+$ 315.0590, found 315.0594.

$[\alpha]_D^{23}$: +16.0 (c 1.0 in $CHCl_3$).

SFC data for racemic 157:

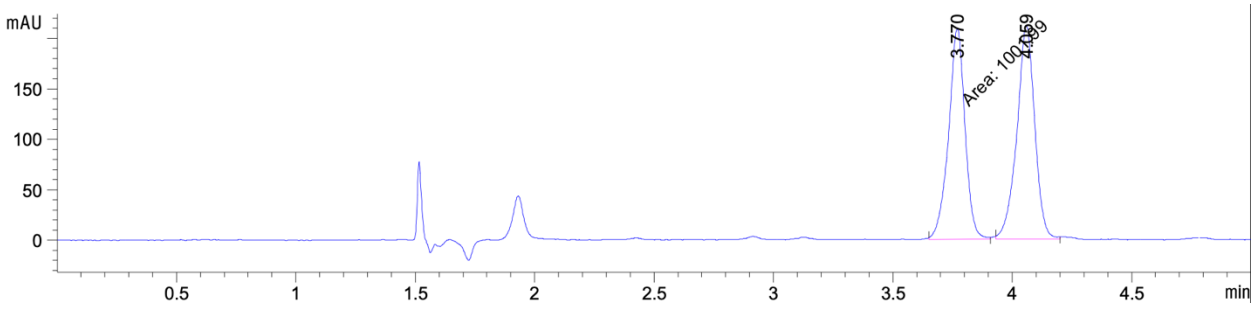

Peak #	RetTime [min]	Type	Width [min]	Area [mAU*s]	Height [mAU]	Area %
1	3.770	MF	0.0800	1001.98859	208.67805	47.5601
2	4.059	BB	0.0779	1104.79578	211.73280	52.4399

SFC data for enantioenriched 157:

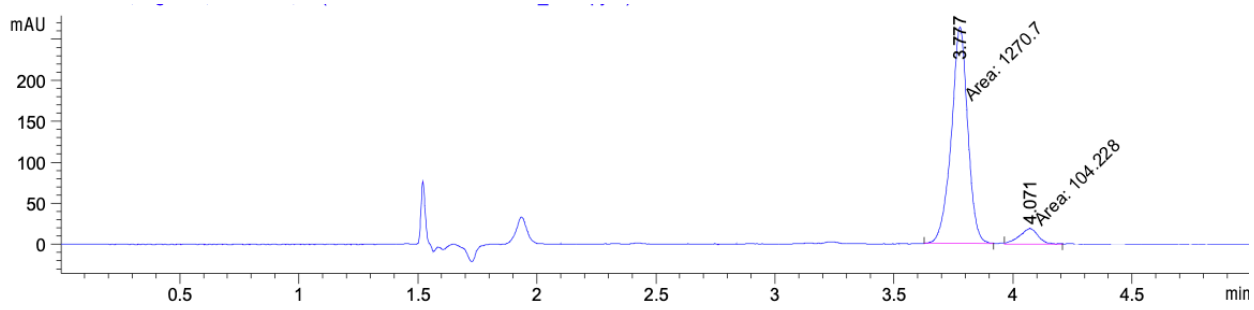

Peak #	RetTime [min]	Type	Width [min]	Area [mAU*s]	Height [mAU]	Area %
1	3.777	FM	0.0801	1270.69678	264.56183	92.4194
2	4.071	MF	0.0913	104.22815	19.02923	7.5806

The deprotection of **157** was telescoped forward with analytically impure material from the Tsuji-Stoltz decarboxylative allylation due to difficulty in separating the substrate from the ligand in the prior purification. Assuming 70% yield from the Tsuji-Stoltz reaction, the starting material (6.10 g, 19.4 mmol, 1 equiv.) was dissolved in acetone. To do this, adding in 10 mL of acetone and sonicating at 40 °C could be performed. The dissolved starting material was added into a 1 L flask equipped with a magnetic stir bar and charged with acetone/H_2O (15 : 1, 914 mL / 61 mL, 20 mM total concentration). *p*TsOH monohydrate (11.0 g, 58.1 mmol, 3.0 equiv.) was added in, and the reaction was fitted with a reflux condenser and heated to reflux for 12 h. After 12 h the reaction was cooled to room temperature and quenched with sat. aq. $NaHCO_3$ (250 mL, pH paper shows neutral pH = 7). The crude mixture was diluted with 400 mL of Et_2O and a white solid (probably *p*TsOH) was filtered off. The phases were separated; the aq. phase was extracted with Et_2O (3 x 100 mL). The combined organic phases were washed with brine twice (2 x 300 mL). The organic phase was dried over anhydrous Na_2SO_4 and reduced *in vacuo*. The

residue was purified by flash column chromatography (10-30% EtOAc in hexanes) to diketone 220A (5.20 g, 19.2 mmol, 69% yield over 2 steps) as a colorless (or slightly pale yellow) oil.

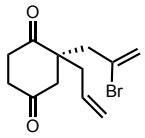

144A

TLC (25% EtOAc/Hexanes): R_f 0.39 (*p*-anisaldehyde).

^{1}H NMR ($CDCl_3$, 400 MHz): δ 5.73 – 5.56 (m, 3H), 5.20 (d, *J* = 10.2 Hz, 1H), 5.13 (d, *J* = 16.9 Hz, 1H), 3.12 (d, *J* = 14.5 Hz, 1H), 3.05 – 2.89 (m, 2H), 2.86 – 2.49 (m, 5H), 2.39 (dd, *J* = 13.9, 7.0 Hz, 1H), 2.17 (dd, *J* = 13.9, 7.9 Hz, 1H).

^{13}C NMR ($CDCl_3$, 101 MHz): δ 210.76, 208.48, 131.27, 127.80, 122.79, 121.24, 50.39, 47.66, 46.59, 42.64, 37.97, 35.94.

FTIR (Neat, NaCl, thin film): 2975, 2912, 1712, 1623, 1429, 1296, 1250, 1164, 989 cm^{-1}.

HRMS (ESI): calc'd for $[M+H]^+$ 271.0328, found 271.0331.

$[\alpha]_D^{23}$: +21.1 (c 1.0 in $CHCl_3$).

Preparation of 3.2.1 bicycle 162:

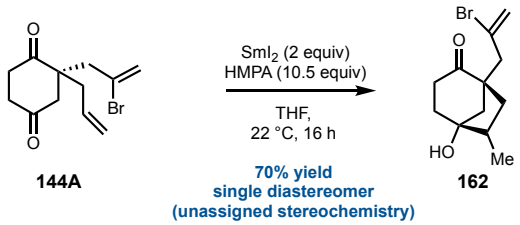

144A

70% yield
single diastereomer
(unassigned stereochemistry)

162

A mixture of starting material in THF (1.2 mL) was added to a solution of SmI_2 in THF (0.10 M) containing HMPA (10.5 equiv). The reaction was stirred at 23°C for 12 h

and then quenched with sat. NH_4Cl and extracted with ether. The organic extracts were washed with water, 3% $Na_2S_2O_3$, and brine and dried over MgSO4. Filtration and concentration gave a crude oil which was purified via prep plate in 50% EA/hexanes to provide 56% isolated yield of the 5-*exo* trig product **162**.

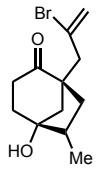

162

TLC (36% EtOAc/Hexanes): R_f 0.30 (*p*-anisaldehyde).

^{1}H NMR (400 MHz, $CDCl_3$): δ 5.51 (d, *J* = 6.9 Hz, 2H), 2.80 (d, *J* = 15.5 Hz, 1H), 2.64 (d, *J* = 15.9 Hz, 1H), 2.59 – 2.47 (m, 1H), 2.43 – 2.22 (m, 4H), 2.13 – 2.03 (m, 1H), 1.85 – 1.74 (m, 2H), 1.30 – 1.23 (m, 1H), 1.09 (d, *J* = 7.0 Hz, 3H).

^{13}C NMR (101 MHz, $CDCl_3$): δ 211.43, 129.55, 121.27, 78.56, 52.94, 48.14, 43.43, 41.95, 38.43, 34.27, 32.26, 14.01.

FTIR (Neat, NaCl, thin film): 3420, 2940, 1614, 1513, 1332, 1112, 919 cm^{-1}.\

HRMS (ESI): calc'd for $[M+H]^+$ 273.0485, found 273.0489.

Preparation of 3.2.1 bicycle 163:

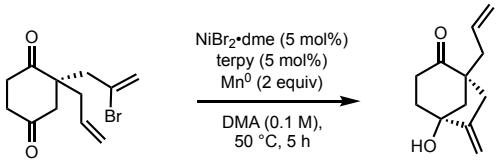

144A **163**

In a nitrogen-filled glovebox, Mn^0 (1.50 g, 27.2 mmol, 2 equiv.) and 2,2':6',2"-terpyridine (159 mg, 680 umol, 0.05 equiv.) and $NiBr_2$•dme (210 mg, 680 umol, 0.05 equiv.) were weighed out into an oven-dried 500 mL round-bottom flask equipped with a large stir bar.

DMA (108 mL) was added. A color change from a turquoise lighter green to a much darker green upon stirring for 30 minutes at room temperature in order to allow ligation of the 2,2':6',2''-terpyridine to the Ni catalyst. Then, the starting material as a stock solution in DMA was added in (3.69 g, 15 mL). The flask was capped, taped, and pumped out of the glovebox. It was heated in an oil bath at 50 °C for 17 h. After 17 h, the reaction was cooled to 0 °C. Then, it was quenched with sat. aq. NH_4Cl (100 mL). Add the NH_4Cl slowly, as reaction with leftover Mn^0 was observed (evolution of H_2 gas), and following the addition, stir vigorously open to air for 5 min. The reaction was filtered to remove Mn salts and washed with water (~100 mL) and 60 mL of Et_2O. The organic phase was collected, and the remaining aqueous layer was three times more (3 x 100 mL). The combined organic extract was washed with 10% LiCl three times (50 mL x 3), brine twice (50 mL x 2), and dried over anhydrous Na_2SO_4, filtered, and the solvent was blown off using a strong stream of N_2 for 120 minutes. This compound is volatile and cannot be concentrated using a rotavap. The crude reaction was loaded onto a column and subject to a very generous gradient of 50 to 75% ether/hexanes to elute the product rather quickly. The product-containing fractions were concentrated again by blowing off the solvent using a strong stream of N_2 to isolate the product **163** as a white solid (1.77 g, 68% yield). Product is volatile but can be left uncapped overnight to fully dry rather than high-vac'd. Only use volatile solvents like hexanes or ether so that they come off easier.

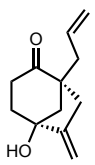

163

TLC (36% EtOAc/Hexanes): R_f 0.36 (*p*-anisaldehyde).

^{1}H NMR ($CDCl_3$, 400 MHz): δ 5.87 – 5.71 (m, 1H), 5.29 (t, *J* = 2.7 Hz, 1H), 5.10 – 5.02 (m, 3H), 2.57 (dt, *J* = 17.9, 2.6 Hz, 1H), 2.47 – 2.36 (m, 3H), 2.29 (dd, *J* = 12.3, 6.9 Hz, 2H), 2.08 (td, *J* = 11.7, 7.6 Hz, 1H), 1.97 – 1.86 (m, 3H), 1.75 (s, 1H).

^{13}C NMR ($CDCl_3$, 101 MHz): δ 211.52, 153.74, 134.55, 118.15, 106.74, 78.95, 51.95, 48.18, 39.24, 38.70, 37.75, 35.65.

FTIR (DCM, NaCl, thin film): 3418, 2933, 1711, 1432, 1332, 1132, 917 cm^{-1}.

HRMS (ESI): calc'd for $[M+H]^+$ 193.1223, found 193.1230.

$[\alpha]_D^{23}$: +15.7 (c 1.0 in $CHCl_3$).

Melting Point: 57-59 °C

Other products in the reaction:

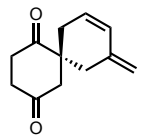

167

TLC (36% EtOAc/Hexanes): R_f 45 (*p*-anisaldehyde).

^{1}H NMR ($CDCl_3$, 400 MHz): δ 6.18 (d, *J* = 9.8 Hz, 1H), 5.69 (t, *J* = 5.0 Hz, 1H), 4.97 (s, 1H), 4.87 (s, 1H), 2.91 – 2.77 (m, 2H), 2.72 – 2.63 (m, 3H), 2.63 – 2.54 (m, 3H), 2.21 (d, *J* = 17.1 Hz, 1H), 1.97 – 1.91 (m, 1H).

^{13}C NMR (101 MHz, $CDCl_3$): δ 211.35, 207.82, 138.57, 128.83, 125.44, 114.98, 47.56, 46.98, 38.34, 37.10, 36.36, 33.24.

FTIR (Neat, NaCl, thin film): 2940, 1717, 1450, 1215, 1146, 990, 918 cm^{-1}.

HRMS (ESI): calc'd for $[M+H]^+$ 191.1067, found 191.1067.

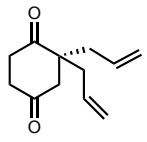

168

TLC (36% EtOAc/Hexanes): R_f 0.59 (*p*-anisaldehyde).

^{1}H NMR (400 MHz, $CDCl_3$) δ 5.72 – 5.57 (m, 2H), 5.16 – 5.06 (m, 4H), 2.72 – 2.65 (m, 6H), 2.48 – 2.41 (m, 2H), 2.14 – 2.08 (m, 2H).

^{13}C NMR (101 MHz, $CDCl_3$) δ 211.57, 209.02, 132.13, 120.42, 50.98, 47.25, 41.93, 37.90, 36.10.

FTIR (Neat, NaCl, thin film): 2932, 1715, 1433, 1253, 1131, 998, 917 cm^{-1}.

HRMS (FD): calc'd for $[M+H]^+$ 193.1223, found 193.1227.

if $MgCl_2$ is used:

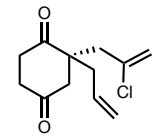

144B

TLC (30% EtOAc in hexanes): R_f 0.31 (*p*-anisaldehyde).

^{1}H NMR ($CDCl_3$, 400 MHz): δ 5.65 (dddd, *J* = 17.1, 10.1, 8.1, 7.1 Hz, 1H), 5.31 (d, *J* = 0.9 Hz, 1H), 5.21 – 5.08 (m, 3H), 3.02 – 2.87 (m, 3H), 2.78 – 2.57 (m, 4H), 2.40 (dd, *J* = 14.0, 7.0 Hz, 2H), 2.16 (dd, *J* = 13.8, 7.9 Hz, 1H).

^{13}C NMR ($CDCl_3$, 101 MHz): δ 210.80, 208.49, 137.67, 131.33, 121.22, 118.03, 50.05, 46.63, 45.98, 42.66, 37.74, 35.94.

FTIR (Neat, NaCl, thin film): 3417, 3078, 2915, 2253, 1711 1422, 1300, 1255, 1169, 986, 906 cm^{-1}.

HRMS (ESI): calc'd for $[M+H]^+$ 227.0833, found 227.0838.

Preparation of MEM-protected compound 143.

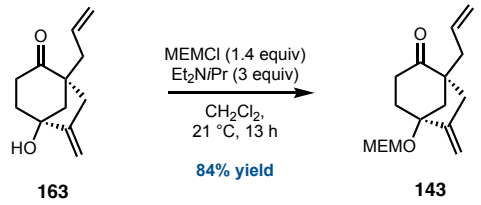

163 **143**

The starting material (1.70 g, 8.84 mmol, 1 equiv.) as a solution in CH_2Cl_2 (20 mL) was dispensed into an flame-dried 250 mL, 3-neck round-bottom flask equipped with a magnetic stir bar and a reflux condenser. CH_2Cl_2 (24 mL) was added in to make a total concentration of 200 mM, and the vessel was cooled to 0 °C. MEMCl (1.41 mL, 12.4 mmol, 1.4 equiv.) was added slowly, dropwise. Then, even slower, Hunig's base (4.62 mL, 26.5 mmol, 3 equiv.) was added in. The reaction was removed from the ice bath and allowed to warm to room temperature, then it was heated to reflux (55 °C) for 12 h. Make sure there is good refluxing throughout the reaction vessel and up into the reflux condenser. After 12 h, to make sure there is full conversion, an NMR aliquot was taken, evacuated, high vac'd, and NMR'd. To workup the reaction, sat. aq. NH_4Cl (50 mL) was added, and the organic phase was collected. The remaining aq. phase was extracted with dichloromethane three times (3 x 50 mL). The organic phase was washed with water and brine, dried with sodium sulfate, filtered, and concentrated. The residue was loaded onto a column and eluted with 10 to 15% EtOAc/Hexanes to afford 2.08 g of pure product (84% yield) as a pale yellow oil after high vac overnight.

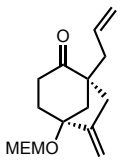

143

TLC (24% EtOAc/Hexanes): R_f 0.23 (*p*-anisaldehyde).

^{1}H NMR ($CDCl_3$, 400 MHz): δ 5.76 (s, 1H), 5.19 (s, 1H), 5.11 (s, 1H), 5.05 (d, *J* = 6.3 Hz, 1H), 5.02 (s, 1H), 4.93 (d, *J* = 7.5 Hz, 1H), 4.77 (d, *J* = 7.5 Hz, 1H), 3.82 (d, *J* = 11.4 Hz, 1H), 3.69 – 3.61 (m, 1H), 3.54 (t, *J* = 4.7 Hz, 2H), 3.38 (s, 3H), 2.52 – 2.25 (m, 7H), 2.12 (d, *J* = 7.4 Hz, 1H), 1.85 (d, *J* = 12.1 Hz, 2H).

^{13}C NMR ($CDCl_3$, 101 MHz): δ 211.68, 150.31, 134.73, 117.93, 107.51, 91.29, 83.63, 71.91, 67.18, 59.16, 52.22, 44.52, 39.78, 38.49, 38.18, 35.79.

FTIR (Neat, NaCl, thin film): 2930, 1715, 1445, 1145, 1045, 913 cm^{-1}.

HRMS (ESI): calc'd for $[M+H]^+$ 281.1747, found 281.1750.

$[\alpha]_D^{23}$: +37.3 (c 1.0 in $CHCl_3$).

Preparation of hemiacetal 166.

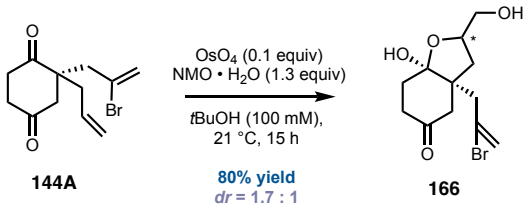

The starting material and stir bar were added to a 10 mL round-bottom flask, and solid NMO monohydrate (1.3 equiv) was added in. Then, a 0.01 M stock solution of OsO_4 was added in (0.1 equiv). The reaction was stirred overnight for 12 h. Following completion of the reaction, 4 mL of acetone was added to the reaction. The reaction was transferred to a separatory funnel containing 25 mL of 10% $NaHSO_3$ and 25 mL of ethyl acetate. The separatory funnel was shaken very vigorously to ensure complete reduction of osmium, then the organic layer was separated. The remaining aq. layer was extracted three times with a 1:2 mixture of acetone/ethyl acetate, and the combined organic layer was washed with brine. All aq. waste was tagged as osmium-containing waste in a separate, labeled

waste container and disposed of properly. The organic layer was dried with sodium sulfate, filtered, and concentrated. The crude oil was filtered through a silica plug, eluting with ethyl acetate, and isolation of a yellow oil (80% yield). Crude NMR reveals pure product, in a 1.7 : 1 mixture of inconsequential diastereomers.

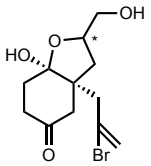

166

Preparation of enol triflate 142.

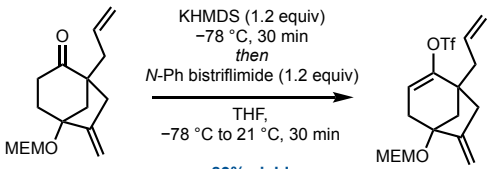

143 **142**

To an oven-dried round-bottom flask (200 mL) was added KHMDS solution (8.13 mL, 1 M in THF, 8.13 mmol, 1.2 equiv.), and it was cooled to -78 °C. The dissolved starting material (1.90 g, 6.78 mmol, 1 equiv.) in 44 mL of THF was added to the KHMDS. The deprotonation was stirred for 30 min at -78 °C. Color change from yellow to orange was observed. The reaction was stirred for 30 more minutes, then a stock solution of *N*-Ph bistriflimide (12.7 mL, 0.64 M in THF, 8.13 mmol, 1.2 equiv) was added in dropwise. The anionic reaction was quenched with NH_4Cl (50 mL). The phases were separated, and the aqueous layer was extracted with diethyl ether (3 x 50 mL). The combined organic layers were washed with brine (1 x 50 mL), dried over sodium sulfate, filtered, and the solvent was removed *in vacuo*. The crude oil obtained was loaded onto a silica gel column and

eluted with 5 to 15% EA/hexanes to afford 2.50 g of product as an orange oil, corresponding to 89% yield.

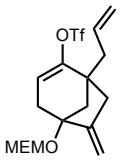

142

TLC (24% EtOAc/Hexanes): R_f 0.38 ($KMnO_4$).

^{1}H NMR ($CDCl_3$, 400 MHz): δ 5.76 (s, 1H), 5.19 (s, 1H), 5.11 (s, 1H), 5.05 (d, *J* = 6.3 Hz, 1H), 5.02 (s, 1H), 4.93 (d, *J* = 7.5 Hz, 1H), 4.77 (d, *J* = 7.5 Hz, 1H), 3.82 (d, *J* = 11.4 Hz, 1H), 3.69 – 3.61 (m, 1H), 3.54 (t, *J* = 4.7 Hz, 2H), 3.38 (s, 3H), 2.52 – 2.25 (m, 7H), 2.12 (d, *J* = 7.4 Hz, 1H), 1.85 (d, *J* = 12.1 Hz, 2H).

^{13}C NMR ($CDCl_3$, 101 MHz): δ 211.63, 150.31, 134.72, 117.91, 107.49, 91.28, 83.61, 71.90, 67.17, 59.15, 52.21, 44.52, 39.77, 38.48, 38.17, 35.78.

FTIR (Neat, NaCl, thin film): 2924, 2891, 1414, 1206, 1168, 1048. 914, 872 cm^{-1}.

HRMS (ESI): calc'd for $[M+H]^+$ 413.1240, found 413.1246.

$[\alpha]_D^{23}$: +103.8 (c 1.0 in $CHCl_3$).

Preparation of aldehyde 107A.

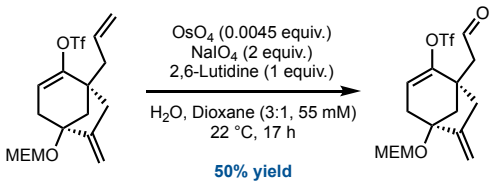

142 **107A**

To the starting material (2.50 g, 6.06 mmol, 1 equiv.) in 1,4-dioxane/H_2O (83 mL dioxane, 28 mL H_2O, 3:1, 55 mM) was added 2,6-lutidine (706 uL, 6.06 mmol, 1 equiv.) and $NaIO_4$ (2.59 g, 12.1 mmol, 2 equiv). OsO_4 as a solution (6.06 mL, 0.01 M in H_2O, 0.01

equiv.). The reaction was capped and stirred for 17 h. TLC analysis is tough to interpret, so an NMR aliquot was taken. NMR aliquot reveals full conversion with ~10-20% diol (dihydroxylation without oxidative cleavage, see attached crude NMR stacked with pure isolated diol). The solution was treated with H_2O (100 mL) and extracted with CH_2Cl_2 (75 mL x 4). The combined organic extracts were washed with H_2O (150 mL), and brine (150 mL). The segregated aqueous waste was tagged as osmium-containing waste. The organic extract was dried over Na_2SO_4 and concentrated under reduced pressure. The residue was purified by column chromatography (10-15% then flushing 20% Acetone/Hex) to afford pure product (1.43 g, 57% yield) as a clear or pale brown oil.

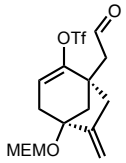

107A

TLC (30% EtOAc/Hexanes): R_f 0.26 ($KMnO_4$).

^{1}H NMR ($CDCl_3$, 400 MHz): δ 9.76 (s, 1H), 5.65 (s, 1H), 5.20 (p, *J* = 1.2 Hz, 1H), 5.16 – 5.13 (m, 1H), 4.92 (s, 1H), 4.71 (s, 1H), 3.84 (s, 1H), 3.61 (s, 1H), 3.53 (s, 2H), 3.37 (s, 3H), 2.95 (s, 2H), 2.77 (s, 1H), 2.52 (s, 1H), 2.40 (s, 2H), 2.28 (s, 2H).

^{13}C NMR ($CDCl_3$, 101 MHz): δ 198.76, 151.49, 149.90, 115.31, 109.70, 91.22, 83.06, 71.86, 67.27, 59.13, 47.66, 46.08, 44.98, 42.26, 41.10.

FTIR (Neat, NaCl, thin film): 2922, 1731, 1416, 1238, 1006, 682 cm^{-1}.

HRMS (ESI): calc'd for $[M+H]^+$ 415.10383, found 415.10539.

$[\alpha]_D^{23}$: +184.4 (c 1.0 in $CHCl_3$).

Preparation of vinyl bromide 150A:

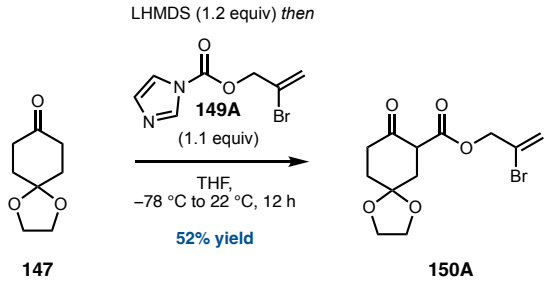

To a cooled solution of 1,4-cyclohexanedione mono-ethylene ketal (**223**, 1.0 equiv.) in THF (661 mM) was added LiHMDS solution in THF (1.06 M, 1.1 equiv.) at −78 °C. The reaction mixture was stirred for 15 min, then a solution of acylimidazole (1.2 equiv.) in THF (685 mM) was dropwise added. The reaction mixture was allowed to warm to 21 °C. After 4 h the reaction was quenched with sat. aq. NH_4Cl and the phases were separated. The aq. phase was extracted with EtOAc (3 x), the combined organic phases were washed with brine and dried over anhydrous Na_2SO_4 and reduced *in vacuo.* The residue was purified by flash column chromatography. The title compound was synthesized according to the general procedure for alkylation with acylimidazole using mono-ethylene ketal (500 mg, 3.2 mmol, 1.0 equiv.) and 2-bromoallyl 1H-imidazole-1-carboxylate (717 mg, 3.8 mmol, 1.2 equiv.). Purification by flash column chromatography (15% EtOAc in hexanes) gave title compound **150A** (52% yield) as a white waxy solid.

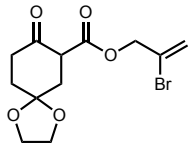

150A

TLC (30% EtOAc in hexanes): R_f 0.71 (*p*-anisaldehyde, UV).

^{1}H NMR (400 MHz, $CDCl_3$): δ 11.96 (s, 1H), 5.91 (q, *J* = 1.6 Hz, 1H), 5.67 – 5.64 (m, 1H), 4.77 (t, *J* = 1.2 Hz, 2H), 4.05 – 3.95 (m, 5H), 2.55 – 2.50 (m, 4H), 2.04 (s, 1H), 1.86 (t, *J* = 7.1 Hz, 2H), 1.26 (t, *J* = 7.1 Hz, 1H).

^{13}C NMR (101 MHz, $CDCl_3$): δ 172.52, 170.99, 126.22, 119.03, 107.25, 95.06, 67.34, 64.75, 32.71, 30.36, 28.17.

Preparation of vinyl chloride 150B:

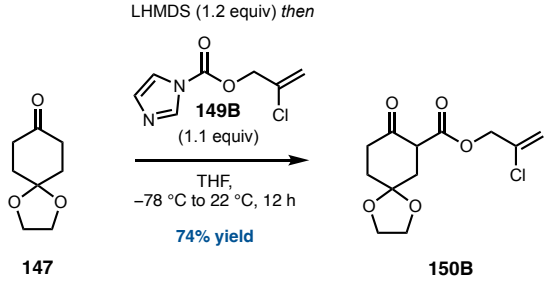

To a cooled solution of 1,4-cyclohexanedione mono-ethylene ketal (**223**, 1.0 equiv.) in THF (661 mM) was added LiHMDS solution in THF (1.06 M, 1.1 equiv.) at −78 °C. The reaction mixture was stirred for 15 min, then a solution of acylimidazole (1.2 equiv.) in THF (685 mM) was dropwise added. The reaction mixture was allowed to warm to 21 °C. After 4 h the reaction was quenched with sat. aq. NH_4Cl and the phases were separated. The aq. phase was extracted with EtOAc (3 x), the combined organic phases were washed with brine and dried over anhydrous Na_2SO_4 and reduced *in vacuo.* The residue was purified by flash column chromatography. The title compound was synthesized according to the general procedure for alkylation with acylimidazole using mono-ethylene ketal (500 mg, 3.2 mmol, 1.0 equiv.) and 2-chloroallyl 1H-imidazole-1-carboxylate (717 mg, 3.8 mmol, 1.2 equiv.). Purification by flash column chromatography (15% EtOAc in hexanes) gave title compound **150B** (637 mg, 2.3 mmol, 72% yield) as a white waxy solid.

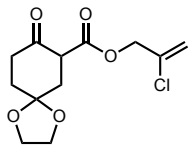

150B

TLC (30% EtOAc in hexanes): R_f 0.73 (*p*-anisaldehyde, UV).

^{1}H NMR ($CDCl_3$, 400 MHz): δ 11.97 (s, 1H), 5.52 – 5.45 (m, 1H), 5.44 – 5.37 (m, 1H), 4.71 (dd, J = 1.2, 0.7 Hz, 2H), 4.09 – 3.94 (m, 5H), 2.55 – 2.50 (m, 4H), 2.04 (s, 1H), 1.85 (tt, J = 6.9, 0.9 Hz, 2H), 1.30 – 1.21 (m, 2H). (mixture of tautomeric form)

^{13}C NMR (101 MHz, $CDCl_3$): δ 172.49, 171.10, 135.84, 114.91, 107.24, 95.05, 69.54, 65.80, 64.75, 60.55, 32.73, 30.36, 28.16, 21.21, 14.35.

FTIR (Neat, NaCl, thin film): 2946, 1751, 1663, 1355, 1285, 1229, 1193, 1060, 1015 cm^{-1}.

HRMS (FD): m/z: calc. for $C_{12}H_{15}O_5Cl$ $[M]^{\cdot+}$ 274.06080, found 274.06135.

Preparation of allylated 155:

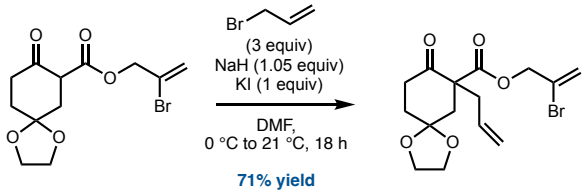

A flame-dried flask was charged with NaH (1.0 equiv.) and a magnetic stir bar. The NaH was suspended in DMF (1 M) at 0 °C. To the cooled suspension was dropwise added a solution of starting material (1.0 equiv.) in DMF (3.2 M) and stirred for 1 h. The the crude reaction mixture was added electrophile in one portion, stirred for 10 min before KI (1.0 equiv.) was added. The reaction was stirred for 18 h, before quenched with sat. aq. NH_4Cl. The crude reaction mixture was extracted with EtOAc (4 x), the combined organic layers

were washed with aq. sat. LiCl twice, dried over anhydrous Na_2SO_4 and reduced *in vacuo*. The residue was purified by flash column chromatography. (5% → 15% EtOAc in hexanes) gave title compound **155** (71% yield) as a colorless oil.

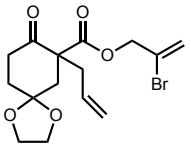

155

TLC (20% EtOAc in hexanes): R_f 0.53 (*p*-anisaldehyde).

^{1}H NMR (600 MHz, $CDCl_3$): δ 5.95 – 5.92 (m, 1H), 5.79 (ddt, *J* = 16.5, 10.7, 7.3 Hz, 1H), 5.66 (d, *J* = 1.9 Hz, 1H), 5.09 – 5.04 (m, 2H), 4.76 (dt, *J* = 13.7, 1.1 Hz, 1H), 4.68 (dt, *J* = 13.9, 1.0 Hz, 1H), 4.03 – 3.96 (m, 4H), 3.05 (ddd, *J* = 14.7, 11.6, 8.6 Hz, 1H), 2.60 – 2.55 (m, 1H), 2.54 – 2.46 (m, 4H), 2.02 – 1.98 (m, 2H).

Preparation of allylated 156:

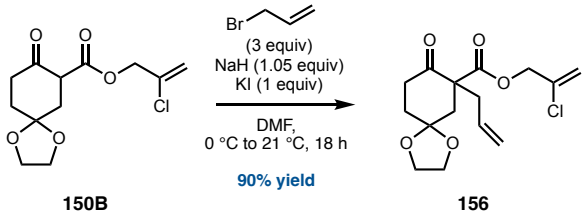

150B **156**

A flame-dried flask was charged with NaH (1.0 equiv.) and a magnetic stir bar. The NaH was suspended in DMF (1 M) at 0 °C. To the cooled suspension was dropwise added a solution of starting material (1.0 equiv.) in DMF (3.2 M) and stirred for 1 h. The the crude reaction mixture was added electrophile in one portion, stirred for 10 min before KI (1.0 equiv.) was added. The reaction was stirred for 18 h, before quenched with sat. aq. NH_4Cl. The crude reaction mixture was extracted with EtOAc (4 x), the combined organic layers were washed with aq. sat. LiCl twice, dried over anhydrous Na_2SO_4 and reduced *in vacuo*.

The residue was purified by flash column chromatography. (5% → 15% EtOAc in hexanes) gave title compound **156** (85 mg, 215 µmol, 90% yield) as a colorless oil.

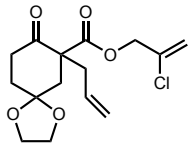

156

TLC (20% EtOAc in hexanes): R_f 0.51 (*p*-anisaldehyde).

^{1}H NMR ($CDCl_3$, 400 MHz): δ 5.88 – 5.65 (m, 1H), 5.49 (d, *J* = 1.6 Hz, 1H), 5.41 (d, *J* = 1.7 Hz, 1H), 5.09 – 5.00 (m, 2H), 4.69 (d, *J* = 13.6 Hz, 1H), 4.61 (d, *J* = 13.5 Hz, 1H), 4.06 – 3.99 (m, 1H), 3.96 (td, *J* = 5.0, 3.0 Hz, 3H), 3.12 – 2.94 (m, 1H), 2.56 (dt, *J* = 14.1, 1.9 Hz, 1H), 2.54 – 2.48 (m, 1H), 2.46 (d, *J* = 7.3 Hz, 2H), 2.04 – 1.96 (m, 2H), 1.85 (d, *J* = 14.1 Hz, 1H).

^{13}C NMR ($CDCl_3$, 101 MHz): δ 206.10, 171.29, 135.43, 133.20, 119.32, 115.83, 106.83, 66.98, 65.08, 64.45, 58.64, 41.41, 39.70, 37.93, 35.22.

FTIR (Neat, NaCl, thin film): 2932, 1719, 1437, 1106, 1043, 924 cm-1.

HRMS (FD): m/z: calc. for $C_{15}H_{19}O_5Cl$ $[M]^{\cdot+}$ 314.09210, found 314.09469.

Preparation of decarboxylative allylic alkylation product 161:

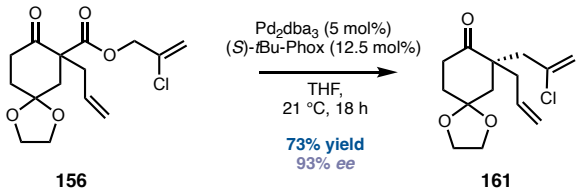

156 **161**

An oven-dried 250 mL round bottom flask was charged with $Pd_2(dba)_3$ (124 mg, 136 µmol, 5 mol%), *(S)*-*t*BuPhOX (131 mg, 339 µmol, 12.5 mol%) and a magnetic stir bar in the glovebox and capped with a rubber septum and sealed with electrical tape. To the solids

was added argon sparged THF (78.2 mL) and the mixture was allowed to stir for 30 min. To the reaction mixture was added diallyl chloro **232** as a solution in argon sparged THF (4 mL) in one portion. After 18 h the reaction was filtered through a celite plug and the filtrate was concentrated *in vacuo*. The residue was purified by flash column chromatography (15% → 20% EtOAc in hexanes) to give chloro diallyl **161** (524 mg, 2.0 mmol, 73% yield, 93% *ee*) as a colorless oil.

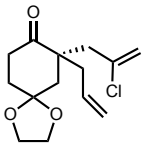

161

TLC (30% EtOAc in hexanes): R_f 0.68 (*p*-anisaldehyde).

^{1}H NMR ($CDCl_3$, 400 MHz): δ 5.73 – 5.55 (m, 1H), 5.27 (s, 1H), 5.17 – 5.02 (m, 3H), 4.00 (d, *J* = 2.0 Hz, 4H), 2.86 (d, *J* = 14.8 Hz, 1H), 2.75 (d, *J* = 14.8 Hz, 1H), 2.72 – 2.55 (m, 2H), 2.51 (d, *J* = 7.7 Hz, 2H), 2.10 – 1.91 (m, 4H).

^{13}C NMR ($CDCl_3$, 101 MHz): δ 211.90, 138.75, 133.37, 119.28, 117.02, 107.73, 64.67, 64.55, 50.68, 44.35, 42.17, 40.26, 36.37, 34.35.

FTIR (Neat, NaCl, thin film): 3077, 2955, 2887, 1712, 1629, 1430, 1365, 1306, 1284, 1114,1042, 994, 947, 913, 740, 644 cm^{-1}.

HRMS (FD): m/z: calc. for $C_{14}H_{19}O_3Cl$ $[M]^{\cdot+}$ 270.10227, found 270.10028.

Preparation of deprotected compound 144B:

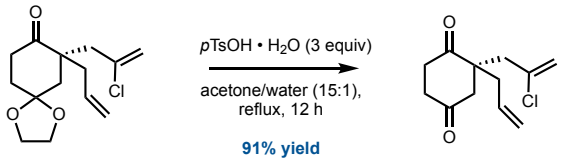

161 **144B**

A 50 mL round bottom flask was charged with chloro diallyl **161** (150 mg, 554 µmol, 1.0 equiv.), *p*-TsOH (316 mg, 1.66 mmol, 3.0 equiv.), acetone (26.2 mL), H_2O (1.75 mL) and magnetic stir bar. To the reaction flask was attached a reflux condenser and the mixture was heated to reflux. After 12 h the reaction was cooled to room temperature and quenched with sat. aq. $NaHCO_3$ (25 mL). The phases were separated, the aq. phase was extracted with Et_2O (3 x 45 mL). The combined organic phases were washed with brine and dried over anhydrous Na_2SO_4 and reduced *in vacuo*. The residue was purified by flash column chromatography (30% EtOAc in hexanes) to diketone **144B** (106 mg, 416 µmol, 91% yield) as a colorless oil.

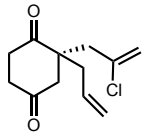

144B

TLC (30% EtOAc in hexanes): R_f 0.31 (*p*-anisaldehyde).

^{1}H NMR ($CDCl_3$, 400 MHz): δ 5.65 (dddd, *J* = 17.1, 10.1, 8.1, 7.1 Hz, 1H), 5.31 (d, *J* = 0.9 Hz, 1H), 5.21 – 5.08 (m, 3H), 3.02 – 2.87 (m, 3H), 2.78 – 2.57 (m, 4H), 2.40 (dd, *J* = 14.0, 7.0 Hz, 2H), 2.16 (dd, *J* = 13.8, 7.9 Hz, 1H).

^{13}C NMR ($CDCl_3$, 101 MHz): δ 210.80, 208.49, 137.67, 131.33, 121.22, 118.03, 50.05, 46.63, 45.98, 42.66, 37.74, 35.94.

FTIR (Neat, NaCl, thin film): 3417, 3078, 2915, 2253, 1711 1422, 1300, 1255, 1169, 986, 906 cm^{-1}.

HRMS (FD): m/z: calc. for $C_{12}H_{15}O_2Cl$ $[M]^{\cdot+}$ 226.07606, found 226.07519.

General Procedure for the Second Alkylation

A flame-dried flask was charged with NaH (1.0 equiv.) and a magnetic stir bar. The NaH was suspended in DMF (1 M) at 0 °C. To the cooled suspension was dropwise added a solution of starting material (1.0 equiv.) in DMF (3.2 M) and stirred for 1 h. The the crude reaction mixture was added electrophile in one portion, stirred for 10 min before KI (1.0 equiv.) was added. The reaction was stirred for 18 h, before quenched with sat. aq. NH_4Cl. The crude reaction mixture was extracted with EtOAc (4 x), the combined organic layers were washed with aq. sat. LiCl twice, dried over anhydrous Na_2SO_4 and reduced *in vacuo*. The residue was purified by flash column chromatography.

2-bromoallyl 7-(cyanomethyl)-8-oxo-1,4-dioxaspiro[4.5]decane-7-carboxylate (158)

The title compound was synthesized according to the general procedure for the second alkylation using bromo allyl carboxylate **151** (150 mg, 470 µmol, 1.0 equiv.) and bromoacetonitrile (98.2 µL, 169 mg, 940 µmol, 3.0 equiv.). Purification by flash column chromatography (50% EtOAc in hexanes) gave title compound **158** (87.5 mg, 244 µmol, 52% yield) as a colorless oil.

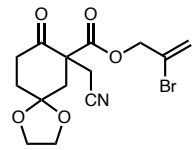

158

TLC (50% EtOAc in hexanes): R_f 0.53 (KMnO4).

^{1}H NMR ($CDCl_3$, 600 MHz): δ = 5.97 (dq, J = 2.2, 0.9 Hz, 1H), 4.04 – 3.92 (m, 3H), 3.18 – 3.07 (m, 1H), 2.93 – 2.85 (m, 1H), 2.76 (dt, J = 14.0, 1.5 Hz, 1H), 2.70 (d, J = 16.4 Hz, 1H), 2.62 (dt, J = 15.2, 4.4 Hz, 1H), 2.11 – 2.05 (m, 3H).

^{13}C NMR (101 MHz, $CDCl_3$): δ 203.22, 169.33, 124.90, 121.10, 116.23, 106.13, 69.52, 65.32, 64.71, 60.54, 56.43, 41.38, 37.19, 34.92, 23.70, 21.20, 14.34.

FTIR (Neat, NaCl, thin film): 2964, 2250, 1743, 1721, 1633, 1433, 1368, 1215, 1116, 1050, 912, 729 cm^{-1}.

HRMS (FD): m/z: calc. for $C_{14}H_{16}NO_5Br$ $[M]^{\cdot+}$ 357.02119, found 357.01888.

2-chloroallyl 7-(cyanomethyl)-8-oxo-1,4-dioxaspiro[4.5]decane-7-carboxylate (159)

The title compound was synthesized according to the general procedure for the second alkylation using chloro allyl carboxylate **152** (129 mg, 470 μmol, 1.0 equiv.) and bromoacetonitrile (98.2 μL, 169 mg, 940 μmol, 3.0 equiv.). Purification by flash column chromatography (50% EtOAc in hexanes) gave title compound **159** (95.8 mg, 306 μmol, 71% yield) as a colorless oil.

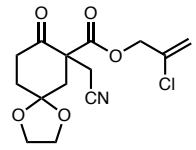

159

TLC (50% EtOAc in hexanes): R_f 0.53 (KMnO4).

^{1}H NMR ($CDCl_3$, 600 MHz): δ = 5.53 (dt, J = 2.0, 1.0 Hz, 1H), 5.46 (d, J = 1.8 Hz, 1H), 4.79 (dd, J = 13.2, 1.1 Hz, 1H), 4.68 (dd, J = 13.2, 1.1 Hz, 1H), 4.03 – 3.93 (m, 4H), 3.10 (dt, J = 15.2, 10.0 Hz, 1H), 2.88 (d, J = 16.6 Hz, 1H), 2.75 (dt, J = 14.0, 1.8 Hz, 1H), 2.68 (d, J = 16.5 Hz, 1H), 2.61 (dt, J = 15.1, 4.4 Hz, 1H), 2.08 – 2.04 (m, 3H).

^{13}C NMR (101 MHz, $CDCl_3$): δ 203.24, 134.80, 116.93, 116.21, 106.13, 68.00, 65.32, 64.71, 56.42, 41.39, 37.15, 34.94, 23.67.

FTIR (Neat, NaCl, thin film): 2957, 1720, 1171, 1100, 1051, 947, 684 cm^{-1}.

HRMS (FD): m/z: calc. for $C_{14}H_{16}NO_5Cl$ $[M]^{\cdot+}$ 313.07170, found 313.06922.

General Procedure for the Formaldehyde Condensation

The starting material was dissolved in THF (0.55 M) and cooled to 0°C. To the cooled solution was added aq. formaldehyde solution (12 M, 7.0 equiv.) and $NaHCO_3$ (3.0 equiv.). The reaction was allowed to warm up to 21 °C over 16 h, the reaction was quenched with water. The crude reaction mixture was extracted with CH_2Cl_2 (3 x) the combined organic phases were washed with brine and dried over anhydrous Na_2SO_4 and reduced *in vacuo.* The residue was purified by flash column chromatography.

Preparation of 2-bromoallyl 7-(hydroxymethyl)-8-oxo-1,4-dioxaspiro[4.5]decane-7-carboxylate (153)

The title compound was synthesized according to the general procedure for the second alkylation using bromo allyl carboxylate **150A** (150 mg, 470 µmol, 1.0 equiv.). Purification by flash column chromatography (10% → 50% EtOAc in hexanes) gave title compound **153** (128 mg, 367 µmol, 78% yield) as a colorless oil.

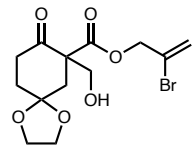

153

TLC (50% EtOAc in hexanes): R_f 0.50 (*p*-anisaldehyde).

^{1}H NMR ($CDCl_3$, 400 MHz): δ = 5.97 (d, J = 1.9 Hz, 1H), 5.67 (d, J = 2.2 Hz, 1H), 4.83 (d, J = 13.9 Hz, 2H), 4.74 (d, J = 13.9 Hz, 1H), 4.06 – 3.94 (m, 5H), 3.85 (dd, J = 11.4, 4.8

Hz, 1H), 3.68 (t, J = 10.7 Hz, 1H), 3.15 (ddd, J = 15.0, 11.4, 9.1 Hz, 1H), 2.93 (dd, J = 10.1, 4.8 Hz, 1H), 2.59 – 2.45 (m, 2H), 2.07 – 1.90 (m, 3H), 1.82 (d, J = 13.9 Hz, 1H).

^{13}C NMR (101 MHz, $CDCl_3$): δ 209.61, 170.36, 125.38, 120.03, 106.50, 68.78, 66.78, 65.23, 64.63, 60.26, 38.71, 38.24, 34.88, 31.09.

FTIR (Neat, NaCl, thin film): 3516, 2888, 1713, 1213, 1123, 1036, 947 cm^{-1}.

HRMS (FD): m/z: calc. for $C_{13}H_{17}O_6Br$ $[M]^{\cdot+}$ 348.02085, found 348.02140.

Preparation of 2-chloroallyl 7-(hydroxymethyl)-8-oxo-1,4-dioxaspiro[4.5]decane-7-carboxylate (154)

The title compound was synthesized according to the general procedure for the second alkylation using chloro allyl carboxylate **150B** (129 mg, 470 µmol, 1.0 equiv.). Purification by flash column chromatography (10% → 50% EtOAc in hexanes) gave title compound **154** (79.1 mg, 259 µmol, 55% yield) as a colorless oil.

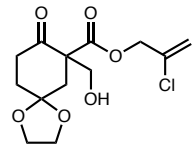

154

TLC (50% EtOAc in hexanes): R_f 0.50 (*p*-anisaldehyde).

^{1}H NMR ($CDCl_3$, 400 MHz): δ = 5.61 – 5.43 (m, 1H), 5.36 (d, J = 1.8 Hz, 1H), 4.79 – 4.59 (m, 3H), 3.99 – 3.87 (m, 5H), 3.80 – 3.75 (m, 1H), 3.61 (dd, J = 11.3, 10.1 Hz, 1H), 3.07 (ddd, J = 15.0, 11.4, 9.3 Hz, 1H), 2.86 (dd, J = 10.2, 4.8 Hz, 1H), 2.52 – 2.38 (m, 3H), 1.97 (d, J = 3.6 Hz, 2H), 1.76 (d, J = 13.9 Hz, 1H).

^{13}C NMR ($CDCl_3$, 101 MHz): δ = 209.50, 170.34, 135.05, 115.78, 106.36, 67.10, 66.63, 65.11, 64.50, 60.12, 38.57, 38.07, 34.77.

FTIR (Neat, NaCl, thin film): 2959, 1713, 1109, 1033 cm^{-1}.

HRMS (FD): m/z: calc. for $C_{13}H_{17}O_6Cl$ $[M]^{\cdot+}$ 304.07137, found 304.07097.

Preparation of acylated compound 173:

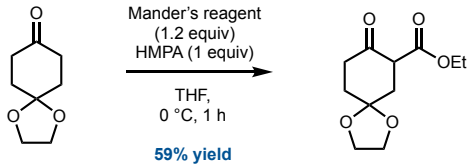

147 173

LDA was prepared. To do this, oven dried flask was cooled under vacuum. 1.2 equiv of diisopropylamine was dissolved in 64 mL of THF. It was cooled to -78 °C. Then, nBuLi was added via cannula addition (1.2 equiv). The reaction was stirred for 15 min at -78 °C, 15 min at 0 °C, and then 15 min at -78 °C again before the substrate was added dropwise as a 2M solution in THF. Then, It was stirred for 30 min at -78 °C before freshly distilled HMPA was added in. It was stirred for 30 min at -78°C before being warmed to 0 °C and freshly distilled ethyl chloroformate (1.25 equiv) was added in dropwise. It was stirred for 1 h at 0 °C. TLC shows full conversion of starting material and the presence of a less polar, purple spot (staining with p-anisaldehyde, see attached photo) that is copolar with a grey spot. These are both product! Just enol and keto forms. LCMS analysis using PES10AX shows mass hit with retention time of about 4 min. Looks like there are some more non-polar impurity spots and a massive more polar spot. Looks like a tough separation by LCMS. Product was purified via column with a 5-10% EA/hex gradient.

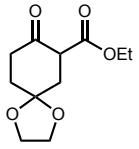

173

TLC (24% EtOAc/Hexanes): R_f 0.54 (UV, *p*-anisaldehyde).

^{1}H NMR (500 MHz, $CDCl_3$): δ 4.26 (q, *J* = 7.1 Hz, 2H), 3.96 (s, 4H), 2.45 – 2.25 (m, 4H), 1.83 (t, *J* = 6.4 Hz, 4H), 1.34 (t, *J* = 7.1 Hz, 3H).

FTIR (Neat, NaCl, thin film): 2959, 2887, 1743, 1718, 1407, 1357, 1124, 849, 832 cm^{-1}.

HRMS (ESI): calc'd for $[M+H]^+$ 229.1071, found 229.1077.

Preparation of Michael adduct 174:

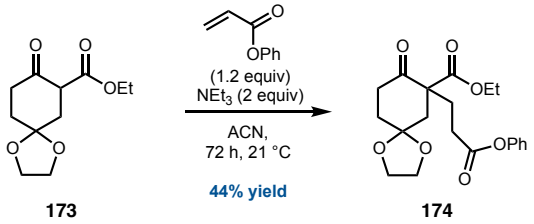

The starting material was dissolved in acetonitrile (200 mM). Then, TEA (2 equiv) was added in, and the reaction was stirred for 3 days at room temperature. After 3 days, ammonium chloride (sat. aq., 3 mL) was added in, and the crude was purified via 5 to 20% EA/hex gradient to afford 44% yield of the desired Michael adduct product (**174**).

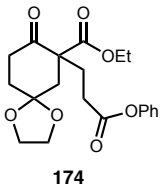

TLC (24% EtOAc/Hexanes): R_f 0.31 (UV, *p*-anisaldehyde).

^{1}H NMR (500 MHz, $CDCl_3$): δ 7.40 – 7.32 (m, 2H), 7.21 (t, *J* = 7.4 Hz, 1H), 7.08 (d, *J* = 8.7 Hz, 2H), 4.29 (dq, *J* = 10.7, 7.1 Hz, 1H), 4.19 (dq, *J* = 10.7, 7.1 Hz, 1H), 4.09 – 4.04 (m, 1H), 4.02 – 3.94 (m, 3H), 3.09 (ddd, *J* = 14.5, 12.1, 8.4 Hz, 1H), 2.90 – 2.79 (m, 1H), 2.66 (dd, *J* = 13.9, 3.9 Hz, 1H), 2.51 (dt, *J* = 14.5, 4.3 Hz, 1H), 2.42 (ddd, *J* = 16.6, 10.9,

5.4 Hz, 1H), 2.23 (ddd, *J* = 13.9, 10.9, 5.2 Hz, 1H), 2.08 – 1.94 (m, 3H), 1.82 (d, *J* = 13.9 Hz, 1H), 1.32 (t, *J* = 7.1 Hz, 3H).

^{13}C NMR (101 MHz, $CDCl_3$): δ 207.06, 172.04, 171.61, 150.83, 129.53, 125.90, 121.70, 106.73, 65.12, 64.45, 61.76, 57.44, 42.50, 37.99, 35.46, 30.36, 29.99, 14.17.

FTIR (Neat, NaCl, thin film): 2965, 2901, 1755, 1710, 1195, 1139, 1033 cm^{-1}.

HRMS (ESI): calc'd for $[M+H]^+$ 377.1595, found 377.1602.

Preparation of deprotected compound 175:

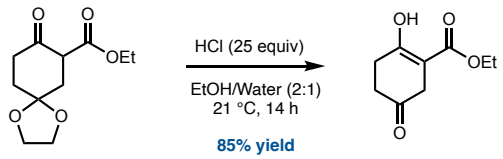

173 **175**

The starting material was dissolved in ethanol in a round bottom flask. No precaution to exclude moisture or air was taken. Then, 25 equiv of HCl were added in, neat. Then, finally, water was added. The reaction was stirred overnight. LCMS shows full conversion. The reaction was worked up by addition SLOW sodium bicarbonate until pH = 9. Watch out for bubbling. At pH = 9, a color change was observed from clear to yellow. Then, the mixture was diluted with 50 mL of EtOAc and the phases were separated, and the aqueous phase was extracted three times with 50 mL of EtOAc. The combined organic extracts were concentrated to afford a crude oil that was NMR'd and loaded onto a column. A 5% to 20% slow gradient was run to afford 85% yield of a clear oil. Stains grey with *p*-anisaldehyde. Looks like starting material by TLC but LCMS shows the mass of the product.

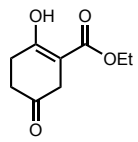

175

TLC (24% EtOAc/Hexanes): R_f 0.50 (UV, *p*-anisaldehyde).

^{1}H NMR (400 MHz, $CDCl_3$): δ 12.28 (s, 1H), 4.24 (q, *J* = 7.1 Hz, 2H), 3.10 (s, 2H), 2.69 (t, *J* = 7.0 Hz, 2H), 2.58 (t, *J* = 6.8 Hz, 2H), 1.30 (t, *J* = 7.1 Hz, 3H).

FTIR (Neat, NaCl, thin film): 3437, 2984, 1728, 1662, 1367, 1245, 1067, 1025 cm^{-1}.

HRMS (ESI): calc'd for $[M+H]^+$ 185.0808, found 185.0817.

Preparation of Michael-Aldol cascade product 251:

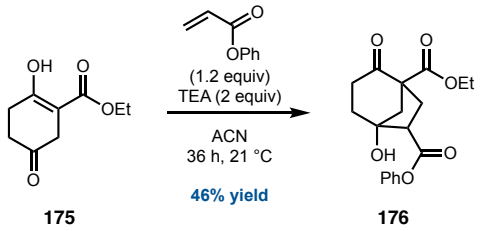

175 **176**

To the two starting materials in EtOH (200 mM) was added TEA (2 equiv). The reaction was stirred for 24 h at room temperature before NH_4Cl was added in. The aq. phase was extracted 3 times with diethyl ether (3 x 0.5 mL) before concentration afforded a crude oil. Purification by preparatory TLC in 50% EA/hexanes afforded 46% yield of the desired Michael-Aldol cascade product as a clear oil.

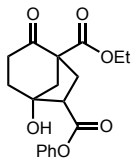

176

TLC (36% EtOAc/Hexanes): R_f 0.27 (UV, *p*-anisaldehyde).

^{1}H NMR (400 MHz, $CDCl_3$): δ 4.23 – 4.18 (m, 4H), 3.14 (s, 1H), 3.04 (dd, *J* = 10.1, 6.3 Hz, 1H), 2.63 – 2.50 (m, 4H), 2.42 – 2.27 (m, 1H), 2.22 (t, *J* = 11.1 Hz, 1H), 2.13 – 2.03 (m, 2H), 1.30 (d, *J* = 7.3 Hz, 8H).

FTIR (Neat, NaCl, thin film): 3420, 2933, 1715, 1332, 1297, 1135, 918 cm^{-1}.

HRMS (ESI): calc'd for $[M+H]^+$ 333.1333, found 333.1338.

4.7 NOTES AND REFERENCES

(1) Snider, B. B. Manganese(III)-Based Oxidative Free-Radical Cyclizations. *Chem. Rev.* **1996**, *96*, 339–363. (b) Dombroski, M. A.; Kates, S. A.; Snider, B. B. Manganese(III)-Based Oxidative Free-Radical Tandem and Triple Cyclizations. *J. Am. Chem. Soc.* **1990**, *112*, 2759–2767.

(2) (a) de Klein, W. J. In *Organic Syntheses by Oxidation with Metal Compounds*; Mijs, W. J.; de Jonge, C. R. H. I., Eds.; Plenum: New York, 1986; Chapter 4. (b) Badanyan, Sh. O.; Melikyan, G. G.; Mkrtchyan, D. A., *Russ. Chem. Rev. (Engl. Transl.)* **1989**, *58*, 286. (c) Snider, B., *Chemtracts–Org. Chem.* **1991**, *4*, 403. (d) Demir, A. S.; Jeganathan, A., *Synthesis* **1992**, 235. (e) Melikyan, G. G., *Synthesis* **1993**, 833.

(3) Snider, B. B.; Merritt, J. E.; Dombroski, M. A.; Buckman, B. O. Solvent Effects on Manganese(III)-Based Oxidative Free-Radical Cyclizations: Ethanol and Acetic Acid. *J. Org. Chem.* **1991**, *56*, 5544–5553.

(4) Hofstra, J. L.; Poremba, K. E.; Shimozono, A. M. Reisman, S. E. Nickel-Catalyzed Conversion of Enol Triflates into Alkenyl Halides. *Angew. Chem. Int. Ed.* **2019**, *58*, 14901–14905.

(5) Welch, S. C.; Assercq, J. M.; Loh, J. P.; Glase, S. A. 3-Chloro-2-

[(diethoxyphosphoryl)oxy]-1-propene: A New Reagent for a "One-Pot" Cyclopentenone Annelation. Syntheses of Desoxyallethrolone, *cis*-Jasmone, and Methylenomycin B. *J. Org. Chem.* **1987**, *52*, 1440–1450.

(6) (a) Sum, P. E.; Weiler, L. Alkylation of β-Keto-ester Dianions with α-Chloroethers. *J.C.S. Chem. Comm.* **1977**, 91–92. (b) Huckin, S. N.; Weiler, L. Alkylation of Dianions of β-Keto-esters. *J. Am. Chem. Soc.* **1974**, *96*, 1082–1087. (c) Weiler, L. Alkylation of Dianions of β-Keto-esters. *J. Am. Chem. Soc.* **1970**, *92*, 6702–6704.

(7) (a) Hwu, J. R. A Novel Oxidative Desulfonylation. Facile Conversion of Sulfones to Aldehydes or Ketones. *J. Org. Chem.* **1983**, *48*, 4432–4433. (b) Bonaparte, A. C.; Betush, M. P.; Panseri, B. M.; Mastarone, D. J.; Murphy, R. K.; Murphree, S. S. Novel Aerobic Oxidation of Primary Sulfones to Carboxylic Acids. *Org. Lett.* **2011**, *13*, 1447–1449.

(8) Yoshimi, Y.; Washida, S.; Okita, Y.; Nishikawa, K.; Maeda, K.; Hayashi, S.; Morita, T. Radical Addition to Acrylonitrile via Catalytic Photochemical Decarboxylation of Aliphatic Carboxylic Acids. *Tetrahedron Lett.* **2013**, *54*, 4324–4326.

(9) Bao, Q. F.; Li, M.; Xia, Y.; Wang, Y. Z.; Zhou, Z. Z.; Liang, Y. M. Visible-Light-Mediated Decarboxylative Radical Addition of Biofunctionalization Cascade for the Production of 1,4-Amino Alcohols. *Org. Lett.* **2021**, *23*, 1107–1112.

(10) Noble, A.; Mega, R. S.; Pflästerer, D.; Myers, E. L.; Aggarwal, V. K. Visible-Light-Mediated Decarboxylative Radical Additions to Vinyl Boronic Esters: Rapid Access to γ-Amino Boronic Esters. *Angew. Chem. Int. Ed.* **2018**, *57*, 2155–2159.

(11) Ramirez, N. P.; Gonzalez-Gomez, J. C. Decarboxylative Giese-Type Reaction of Carboxylic Acids Promoted by Visible Light: A Sustainable and Photoredox-Neutral

Protocol. *Eur. J. Org. Chem.* **2017**, 15, 2154–2163.

(12) Chu, L.; Ohta, C.; Zuo, Z.; MacMillan, D. W. C. Carboxylic Acids as A Traceless Activation Group for Conjugate Additions: A Three-Step Synthesis of (±)-Pregabalin. *J. Am. Chem. Soc.* **2014**, *136*, 10886–10889.

(13) El-Hage, F.; Schöll, C.; Pospech, J. Photo-Mediated Decarboxylative Giese-Type Reaction Using Organic Pyrimidopteridine Photoredox Catalysts. *J. Org. Chem.* **2020**, *85*, 13853–13867.

(14) Minagawa, K.; Kamakura, D.; Hagiwara, K.; Inoue, M. Construction of the ABCDE-Ring Structure of Talatisamine via Decarboxylative Radical Cyclization. *Tetrahedron*, **2020**, 76, 131385–131393.

(15) Kitcatt, D. M.; Nicolle, S.; Lee, A. L. Direct Decarboxylative Giese Reactions. *Chem. Soc. Rev.* **2022**, *51*, 1415–1453.

(16) Watanabe, T.; Oga, K.; Matoba, H.; Nagatomo, M.; Inoue, M. Total Synthesis of Taxol Enabled by Intermolecular Radical Coupling and Pd-Catalyzed Cyclization. *J. Am. Chem. Soc.* **2023**, *145*, 25894–25902.

(17) Nam, Y.; Tam, A. T.; Miller, E. R.; Scheidt, K. A. A Platform for the Synthesis of Corynantheine-Type Alkaloids. *J. Am. Chem. Soc.* **2024**, *146*, 118–124.

(18) Zhang, Q.; Mohan, R. M.; Cook, L.; Kazanis, S.; Peisach, D.; Foxman, B. M.; Snider, B. B. Asymmetric Induction in Mn(III)-Based Oxidative Free-Radical Cyclizations of Phenylmenthyl Acetoacetates and 2,5-Dimethylpyrrolidine Acetoacetamides. *J. Org. Chem.* **1993**, *58*, 7640–7651.

(19) Zoretic, P. A.; Weng, X.; Biggers, C. K.; Biggers, M. S.; Caspar, M. L. *Tetrahedron Lett.* **1992**, *33*, 2637–2640.

(20) Snider, B. B.; Wan, B. Y.; Buckman, B. O.; Foxman, B. M. Manganese(III)-Based Asymmetric Oxidative Free-Radical Cyclizations of Unsaturated β-Keto Sulfoxides. *J. Org. Chem*. **1991**, *56*, 328–334.

(21) Crich, D.; Davies, J. W. Stereoselectivity in Free Radical Reactions. *Tetrahedron Lett.* **1987**, *28*, 4205.

(22) Hamon, D. P. G.; Razzino, P.; Massy-Westropp, R. A. *J. Chem. Soc.* **1991**, *332*. Hamon, D. P. G.; Massy-Westropp, R. Razzino, P. *J. Chem. Soc*. **1991**, 722; *Tetrahedron* **1992**, *48*, 5163; *Tetrahedron Lett.* **1993**, *49*, 6419.

(23) Chen, M.-Y.; Fang, J.-M.; Tsai, Y.-M.; Yeh, R.-L. *J. Am. Chem. Soc.* **1991**, 113, 1603.

(24) Yang, D.; Gu, S.; Yan, Y.-L., Zhu, N.-Y.: Cheung, K.-K. Highly Enantioselective Atom-Transfer Radical Cyclization Reactions Catalyzed by Chiral Lewis Acids. *J. Am. Chem. Soc.* **2001**, *123*, 8612–8613.

(25) Zhu, N. Y., *et al.* Enantioselective PhSe-Group-Transfer Tandem Radical Cyclization Reactions Catalyzed by Chiral Lewis Acid. *Angew. Chem. Int. Ed.* **2006.** *45,* 255–258.

(26) Welch, S. C.; Assercq, J.-M.; Loh, J.-P.; Glase, S. A. 3-Chloro-2-[(diethoxyphosphoryl)oxy]-1-propene: A New Reagent for a "One-Pot" Cyclopentenone Annelation. Syntheses of Desoxyallethrolone, *cis*-Jasmone, and Methylenomycin B. *J. Org. Chem.* **1987**, *52*, 1440–1450.

(27) Marigo, M.; Kumaragurubaran, N.; Jørgensen, K. A. Catalytic Asymmetric Bromination and Chlorination of β-Ketoesters. *Chem. Eur. J.* **2004**, *10*, 2133–2137.

(28) Yang, D.; Yan, Y.-L.; Lui, B. Mild α-Halogenation Reactions of 1,3-Dicarbonyl Compounds Catalyzed by Lewis Acids. *J. Org. Chem.* **2002**, *67*, 7429–7431.

(29) Khan, A. T.; Ali, M. A.; Goswami, P.; Choudhury, L. H. *J. Org. Chem.* **2006**, *71*, 8961–8963.

(30) Aoyama, T.; Takido, T.; Kodomari, M. One-pot Synthesis of α-Bromoesters and Ketones from β-Ketoesters and Diketones using Supported Reagents System. *Tetrahedron Lett.* **2004**, *45*, 1873–1876.

(31) Li, Y.; Wang, D.; Zhang, L.; Luo, S. Redox Property of Enamines. *J. Org. Chem.* **2019**, *84*, 12071–12090.

(32) Beeson, T. D.; Mastracchio, A.; Hong, J.-B.; Ashton, K.; MacMillan, D. W. C. Enantioselective Organocatalysis Using SOMO Activation. *Science.* **2007**, *316*, 582–585.

(33) Mondal, S.; Dumur, F.; Gigmes, D.; Sibi, M. P.; Bertrand, M. P.; Nechab, M. Enantioselective Radical Reactions Using Chiral Catalysts. *Chem. Rev.* **2022**, *122*, 5842–5976.

(34) Wang, D.; Zhang, L.; Luo, S. Enantioselective Decarboxylative a-Alkynylation of β-Ketocarbonyls via a Catalytic α-Imino Radical Intermediate. *Org. Lett.* **2017**, *19*, 4924–4927.

(35) Tang, S.; Wu, X.; Liao, W.; Liu, K.; Liu, C.; Luo, S.; Lei, A. Synergistic Pd/Enamine Catalysis: A Strategy for the C−H/C−H Oxidative Coupling of Allylarenes with Unactivated Ketones. *Org. Lett.* **2014**, *16*, 3584−3587.

(36) (a) Kano, T.; Shirozu, F.; Maruoka, K. Metal-Free Enantioselective Hydroxyamination of Aldehydes with Nitrosocarbonyl Compounds Catalyzed by an

Axially Chiral Amine. *J. Am. Chem. Soc.* **2013**, *135*, 18036−18039. (b) Kano, T.; Shirozu, F.; Maruoka, K. Practical Approach for Asymmetric Hydroxyamination of Aldehydes with in Situ Generated Nitrosocarbonyl Compounds: Application to One-Pot Synthesis of Chiral Allylamines. *Org. Lett.* **2014**, *16*, 1530−1532.

(37) Maji, B.; Yamamoto, H. Proline-Tetrazole-Catalyzed Enantioselective N-Nitroso Aldol Reaction of Aldehydes with *In Situ* Generated Nitrosocarbonyl Compounds. *Angew. Chem., Int. Ed*. **2014**, *53*, 8714− 8717.

(38) Van Humbeck, J. F.; Simonovich, S. P.; Knowles, R. R.; MacMillan, D. W. C. Concerning the Mechanism of the $FeCl_3$- Catalyzed α-Oxyamination of Aldehydes: Evidence for a Non-SOMO Activation Pathway. *J. Am. Chem. Soc*. **2010**, *132*, 10012−10014.

(39) Nicolaou, K. C.; Reingruber, R.; Sarlah, D.; Braše, S. Enantioselective Intramolecular Friedel-Crafts-Type α-Arylation of Aldehydes. *J. Am. Chem. Soc.* **2009**, *131*, 2086−2087.

(40) Conrad, J. C.; Kong, J.; Laforteza, B. N.; MacMillan, D. W. C. Enantioselective α-Arylation of Aldehydes via Organo-SOMO Catalysis. An Ortho-Selective Arylation Reaction Based on an Open-Shell Pathway. *J. Am. Chem. Soc.* **2009**, *131*, 11640−11641.

(41) Feng, C.-L.; Chu, N.-N.; Zhang, S.-G.; Cai, J.; Chen, J.-Q.; Hu, H.-Y.; Ji, M. Solvent-free Synthesis of β-Enamino Ketones and Esters Catalyzed by Recyclable Iron(III) Triflate. Chemical Papers. DOI: 10.2478/s11696-014-0544-8

(42) Kunda, D.; Majee, A.; Hajra, A. *L*-Proline Catalyzed Enamination of b-Dicarbonyl Compounds under Solvent-free Conditions. *Chinese Journal of Chemistry*. **2008**, *26,* 1545–1548.

(43) Kardon, F.; Mörtl, M.; Knausz, D. Reactions of Silylcarbamates with Ketones. *Tetrahedron Lett.* **2000**, *41*, 8937–8939.

(44) Vohra, R. K.; Renaud, J.-L.; Bruneau, C. Tertiary 3-Aminopropenones and 3-Aminopropenoates: Their Preparation, with and without Lewis Acids, from Secondary Amines and 1,3-Diketo Compounds. *Synthesis*. **2007**, *5*, 731–738.

(45) Liang, K.; Zhang, Q.; Guo, C. Nickel-catalyzed Switchable Asymmetric Electrochemical Functionalization of Alkenes. *Sc. Adv.* **2022**, *8*, eadd7134.

(46) Kawamoto, Y.; Yomura, S.; Karube, F.; Kobayashi, T.; Ito, H. Total Synthesis of Leptosperol B through Stereocontrolled Intramolecular 1,4-Addition to Construct the Octahydronaphthalene Framework. *J. Org. Chem.* **2023**, *88*, 3217–3227.

(47) Mohr, J. T.; Behenna, D. C.; Harned, A. M.; Stoltz, B. M. Deracemization of Quaternary Stereocenters by Pd-Catalyzed Enantioconvergent Decarboxylative Allylation of Racemic β-Ketoesters. *Angew. Chem. Int. Ed.* **2005**, *44*, 6924–6927.

(48) Behenna, D. C.; Mohr, J. T.; Sherden, N. H.; Marinescu, S. C.; Harned, A. M.; Tani, K; Seto, M.; Ma, S.; Novák, Z.; Krout, M. R.; McFadden, R. M.; Roizen, J. L.; Enquist Jr., J. A.; White, D. E.; Levine, S. R.; Petrova, K. V.; Iwashita, A.; Virgil, S. C.; Stoltz, B. M. Enantioselective Decarboxylative Alkylation Reactions: Catalyst Development, Substrate Scope, and Mechanistic Studies. *Chem. Eur. J.* **2011**, *17*, 14199–14223.

(49) Berkowitz, W. F.; Wilson, P. J. Vinyl Radical Cycliations: Synthesis of Substituted Bicyclooctanols. *J. Org. Chem.* **1991**, *56*, 3102–3108.

(50) Turlik, A.; Chen, Y.; Scruse, A. C.; Newhouse, T. R. Convergent Total Synthesis of Principinol D, a Rearranged Kaurane Diterpenoid. *J. Am. Chem. Soc.* **2019**, *141*, 8088–8092.

(51) Shi, S.; Lalancette, R.; Szostak, R.; Szostak, M. Highly Chemoselective Synthesis of Indolizidine Lactams by SmI_2-Induced Umpolung of the Amide Bond via Aminoketylradicals: Efficient Entry to Alkaloid Scaffolds. *Chem. Eur. J.* **2016**, *22*, 11949–11953.

(52) Yu, F.; Xu, L. A Concise and Stereoselective Synthesis of the BCDF Tetracyclic Ring System of C_{19}-Diterpenoid Alkaloids. *RSC Adv.* **2024**, *14*, 21102–21106.

(53) McDougal, N. T.; Streuff, J.; Mukherjee, H.; Virgil, S. C.; Stoltz, B. M. Rapid Synthesis of an Electron-Deficient *t*BuPhox Ligand: Cross-Coupling of Aryl Bromides with Secondary Phosphine Oxides. *Tetrahedron Lett.* **2010**, *51*, 5550–5554.

(54) Craig, R. A.; Loskot, S. A.; Mohr, J. T.; Behenna, D. C.; Harned, A. M.; Stoltz, B. M. Palladium-Catalyzed Enantioselective Decarboxylative Allylic Alkylation of Cyclopentanones. *Org. Lett.* **2015**, *17*, 5160–5163.

(55) White, D. E.; Stewart, I. C.; Grubbs, R. H.; Stoltz, B. M. The Catalytic Asymmetric Total Synthesis of Elatol. *J. Am. Chem. Soc.* **2008**, *130*, 810–811.

(56) Duquette, D. C.; Cusumano, A. Q.; Lefoulon, L.; Moore, J. T.; Stoltz, B. M. Probing Trends in Enantioinduction via Substrate Design: Palladium-Catalyzed Decarboxylative Allylic Alkylation of Enaminones. *Org. Lett.* **2020**, *22*, 4966–4969.

(57) Sercel, Z. P.; Sun, A. W.; Stoltz, B. M. Palladium-Catalyzed Decarboxylative Asymmetric Allylic Alkylation of 1,4-Diazepan-5-ones. *Org. Lett.* **2019**, *21*, 9158–9161.

(58) Sherden, N. H.; Behenna, D. C.; Virgil, S. C.; Stoltz, B. M. Unusual Allylpalladium Carboxylate Complexes: Identification of the Resting State of Catalytic Enantioselective Decarboxylative Allylic Alkylation Reactions of Ketones. *Angew. Chem. Int. Ed.* **2009**, *48*, 6840–6843.

(59) Palluccio, T. D.; Germain, M. E.; Marazzi, M.; Temprado, M.; Silvia, J. S.; Müller, P.; Cummins, C. C.; Davis, J. V.; Serafim, L. F.; Captain, B.; Hoff, C. D.; Rybak-Akimova, E. V. Binding of Nitriles and Isonitriles to V(III) and Mo(III) Complexes: Ligand vs Metal Controlled Mechanism. *Inorg. Chem.* **2023**, *62*, 10559–10571.

(60) Cusumano, A. Q.; Stoltz, B. M.; Goddard, W. A. Reaction Mechanism, Origins of Enantioselectivity, and Reactivity Trends in Asymmetric Allylic Alkylation: A Comprehensive Quantum Mechanics Investigation of a $C(Sp^3)$–$C(Sp^3)$ Cross-Coupling. *J. Am. Chem. Soc.* **2020**, *142*, 13917–13933.

(61) Curran, D. P.; Yoo, B. New Reagents for Radical Allylations. *Tetrahedron Lett.* **1992**, *33*, 6931–6934.

(62) Nicolaou, K. C.; Ellery, S. P.; Chen, J. S. Samarium Diiodide Mediated Reactions in Total Synthesis. *Angew. Chem. Int. Ed.* **2009**, *48*, 7140–7165.

(63) Sadasivam, D. V.; Choquotte, K. A.; Flowers, R. A. Preparation and Use of Samarium Diiodide (SmI_2) in Organic Synthesis: The Mechanistic Role of HMPA and Ni(II) Salts in the Samarium Barbier Reaction. DOI:10.3791/4323.

(64) Prasad, E.; Flowers, R. A. Reduction of Ketones and Alkyl Iodides by SmI_2 and Sm(II)-HMPA Complexes. Rate and Mechanistic Studies. *J. Am. Chem. Soc.* **2002**, *124*, 6895–6899.

(65) Molander, G. Reductions with Samarium Iodide. *Organic Reactions.* ***1994****, © by Organic Reactions Inc. Published by John Wiley and Sons, Inc.* https://doi.org/10.1002/0471264180.or046.03.

(66) Corey, E. J.; Munroe, J. E. Total Synthesis of Gibberelic Acid. A Simple Synthesis of a Key Intermediate. *J. Am. Chem. Soc.* **1982**, *104*, 6130–6132.

(67) Lipshutz, B. H.; Sengupta, S. Organocopper Reagents: Substitution, Conjugate Addition, Carbo/Metallocupration, and Other Reactions. *Organic Reactions.* ***1992****, © by Organic Reactions Inc. Published by John Wiley and Sons, Inc.* https://doi.org/10.1002/0471264180.or041.02

(68) Marquesa, F. A.; Ferreirab, J. T. B.; Piers. *J. Braz. Chem. Soc.* **2000**, *11*, DOI: https://doi.org/10.1590/S0103-50532000000500012.

(69) Corey, E. J.; Narisada, M.; Hiraoka, T.; Ellison, R. A. *J. Am. Chem. Soc.* **1970**, *92*, 396–397.

(70) Piers, E.; Marais, P. C. An Annulation Leading to Fused Bicyclic Systems Containing an Allylic Angular Hydroxyl Group. *Tetrahedron Lett.* **1988**, *33*, 4053–4056.

(71) Gil ,A.; Albericio, F.; Álvarez, M. Role of the Nozaki-Hiyama-Kishi Reaction in the Synthesis of Natural Products. *Chem. Rev.* **2017**, *117*, 8420–8446.

(72) Majumdar, K. K.; Cheng, C.-H. Ni(II)/Zn-Mediated Chemoselective Arylation of Aromatic Aldehydes: Facile Synthesis of Diaryl Carbinols. *Org. Lett.* **2000**, *2*, 2295–2298.

(73) Huang, Y.-C.; Majumdar, K. K.; Cheng, C.-H. Nickel-Catalyzed Coupling of Aryl Iodides with Aromatic Aldehydes: Chemoselective Synthesis of Ketones. *J. Org. Chem.* **2002**, *67*, 1682–1684.

(74) Li, Y.; Li, W.; Tian, J.; Huang, G.; Lv, H. Nickel-Catalyzed Asymmetric Addition of Aromatic Halides to Ketones: Highly Enantioselective Synthesis of Chiral 2,3-Dihydrobenzofurans Containing a Tertiary Alcohol. *Org. Lett.* **2020**, *22*, 5353–5357.

(75) Ishida, S.; Suzuki, H.; Uchida, S.; Yamaguchi, E.; Itoh, A. Nickel-Catalyzed Intermolecular Carbonyl Addition of Aryl Halide, *Eur. J. Org. Chem.* **2019**, 7483–7487. DOI: 10.1002/ejoc.201901367.

(76) Huang, S.; Zhou, J. S. Nickel-Catalyzed Enantioselective Reductive Arylation of Common Ketones. *J. Am. Chem. Soc.* **2024**, *146*, 12895–12900.

(77) Nasim, A.; Thomas, G. T.; Ovens, J. S.; Newman, S. G. Reductive 1,2-Arylation of Isatins. *Org. Lett.* **2022**, *24*, 7232–7236.

(78) Garcia, K. J.; Gilbert, M. M.; Weix, D. J. Nickel-Catalyzed Addition of Aryl Bromides to Aldehydes to Form Hindered Secondary Alcohols. *J. Am. Chem. Soc.* **2019**, *141*, 1823–1827.

(79) Moragas, T.; Correa, A.; Martin, R. Metal-Catalyzed Reductive Coupling Reactions of Organic Halides with Carbonyl-Type Compounds. *Chem. Eur. J.* **2014**, *20*, 8242–8258.

(80) Cherney, A.; Reisman, S. E. Nickel-Catalyzed Asymmetric Reductive Cross-Coupling Between Vinyl and Benzyl Electrophiles. *J. Am. Chem. Soc.* **2014**, *136*, 14365–14368.

(81) Turro, R. F.; Wahlman, J. L. H.; Tong, J.; Chen, X.; Yang, M.; Chen, E. P.; Hong, X.; Hadt, R. G.; Houk, K. N.; Yang, Y.-F.; Reisman, S. E. Mechanistic Investigation of Ni-Catalyzed Reductive Cross-Coupling of Alkenyl and Benzyl Electrophiles. *J. Am. Chem. Soc.* **2023**, *145*, 14705–14715.

(82) Cherney, A. H.; Kadunce, N. T.; Reisman, S. E. Catalytic Asymmetric Reductive Acyl Cross-Coupling: Synthesis of Enantioenriched Acyclic α,α-Disubstituted Ketones. *J. Am. Chem. Soc.* **2013**, *135*, 7442–7445.

(83) Xu, T.; Zhou, P. Nickel-Catalyzed Intramolecular Desymmetrization Addition of Aryl Halides to 1,3-Diketones. *Chem. Commun.*, **2020**, *56*, 8194–8197.

(84) Liang, J.-X.; Yang, P.-F.; Shu, W. Synthesis of (Hetero)aryl/Alkenyl Iodides via Ni-Catalyzed Finkelstein Reaction from Bromides or Chlorides. *Organometallics*, **2022**, *41*, 3795–3800.

(85) Tsou, T. T.; Kochi, J. K. Nickel Catalysis in Halogen Exchange with Aryl and Vinylic Halides. *J. Org. Chem.* **1980**, *45*, 1930–1937.

(86) (a) Chen, J.; Yang, Y.; Wu, C.; Huo, L.; Xie, X.; Li, H.; She, X. *De Novo* Diastereoselective Synthesis of 1-Hydroxyl Allogibberic Methyl Ester *en Route* to Diverse Bioactive Molecules. *Org. Lett.* **2022**, *24*, 6402–6406. (b) Barco, A.; Benetti, S.; Casolari, A.; Manfredini, S.; Pollini, G. P.; Polo, E.; Zanirato, V. 3,4-Bismethylenecyclopentanone Ethylene Ketal: A Useful Diene for [6.5]-Ring Systems: Application to a Formal Synthesis of Gibberellic Acid. *Tetrahedron Lett.* **1989**, *45*, 3935–3944.

(87) Xie, J.; Zheng, Z.; Liu, X.; Zhang, N.; Choi, S.; He, C.; Dong, G. Asymmetric Total Synthesis of (+)-Phainanoid A and Biological Evaluation of the Natural Product and Its Synthetic Analogues. *J. Am. Chem. Soc.* **2023**, *145*, 4828–4852.

(88) Tucker, J. K.; Shair, M. D. Catalytic Allylic Oxidation to Generate Vinylogous Acyl Sulfonates from Vinyl Sulfonates. *Org. Lett.* **2019**, *21*, 2473–2476.

(89) Pappo, R.; Allen, D. S.; Lemieux, R. U.; Johnson, W. S. Osmium Tetroxide-Catalyzed Periodate Oxidation of Olefinic Bonds. *J. Org. Chem.* **1956**, *21*, 478–479.

(90) Trost, B. M. In Comprehensive Organic Synthesis*; Elsevier,* **1991**; 541–591.

(91) Suzuki, M.; Koyama, H.; Noyori, R. Effects of HMPA on the Structure and reactivity of the Lithium Enolate of Cyclopentanone in THF: The Dimer is Responsible for Alkylation and Proton Exchange Reactions. *Bull. Chem. Soc. Jpn.* **2004**, *77*, 259–268.

(92) Du, X.; Eksterowicz, J.; Fantin, V. R.; Rew, Y.; Sun, D.; Ye, Q.; Zhou, H.; Kawai, H.; Moore, J. Preparation of substituted benzoindazoles as glucocorticoid receptor modulators. *World Intellectual Property Organization,* WO2020076999 A1 2020-04-26.

(93) Cherney, R. J.; Mo, R.; Meyer, D. T.; Voss, M. M.; Yang, M. G.; Santella III, J. B.; Duncia, J. V.; Lo, Y. C.; Yang, G.; Miller, P. B.; Scherle, P. A.; Zhao, Q.; Mandlekar, S.; Cvijic, M. E.; Barrish, J. C.; Decicco, C. P.; Carter, P. H. g-Lactams as Glycinamide Replacements in Cyclohexane-based CC Chemokine Receptor 2 (CCR2) Antagonists. *Bioorg. Med. Chem. Lett.* **2010**, *20*, 2425–2430.

(94) Muthusamy, S.; Arulananda Babu, S.; Gunanathan, C. 1,8-Diazabicyclo[5.4.0]undec-7-ene (DBU): A Powerful Catalyst for the Michael Addition

Reaction of β-Ketoesters to Acrylates and Enones. *Synthetic Communications*, **2002**, *32*, 3247–3254. https://doi.org/10.1081/SCC-120014028.

(95) Chichowicz, N. R.; Kaplan, W.; Khomutnyk, Y.; Bhattarai, B.; Sun, Z.; Nagorny, P. *J. Am. Chem. Soc*. **2015**, *137*, 45, 14341–14348.

(96) (a) Majima, K.; Takita, R.; Okada, A.; Ohshima, T.; Shibasaki, M. Catalytic Asymmetric Michael Reaction of β-Keto Esters: Effects of the Linker Heteroatom in Linked-BINOL. *J. Am. Chem. Soc.* **2003**, *125*, 15837–15845. (b) Sasai, H.; Emori, E.; Arai, T.; Shibasaki, M. Catalytic asymmetric Michael reactions promoted by the La-Na-BINOL complex (LSB). Enantioface selection on Michael donors. *Tetrahedron Lett.* **1996**, *37*, 5561-5564. https://doi.org/10.1016/0040-4039(96)01156-2. (c) Kim, Y. S.; Matsunaga, S.; Das, J.; Sekine, A.; Ohshima, T.; Shibasaki, M. Stable, Storable, and Reusable Asymmetric Catalyst: A Novel La-linked-BINOL Complex for the Catalytic Asymmetric Michael Reaction. *J. Am. Chem. Soc*. **2000**, *122*, 27, 6506–6507. https://doi.org/10.1021/ja001036u.

(97) (a) Liu, G.; Shirley, M. E.; Van, K. N.; McFarlin, R. L.; Romo, D. Rapid Assembly of Complex Cyclopentanes Employing Chiral α,β-Unsaturated Acylammonium Intermediates. *Nat. Chem.* **2013**, *5*, 1049–1057. (b) Palomo, C., *et. al.* Catalytic Michael Reactions of Ketoesters with a Camphor-Derived Acrylate Equivalent: Stereoselective Access to All Carbon Quaternary centers. **2008**, *Org. Lett. 10*, 2637–2640. https://doi.org/10.1021/ol800564d.

(98) (a) Arai T.; Yamada, Y. M. A.; Yamamoto, N.; Sasai, H.; Shibasaki, M. *Chem. Eur. J.* **1996**, *2*, 1368–1372. (b) Wong, A. R.; Fastuca, N. J.; Mak, V. W.; Kerkovius, J. K.; Stevenson, S. M.; Reisman, S. E. *ACS Cent. Sci.* **2021**, *7*, 1311–1316.

(99) Arai T.; Sasai, H.; Aoe, K.; Okamura, K.; Date, T.; Shibasaki, M. A New Multifunctional Heterobimetallic Asymmetric Catalyst for Michael Additions and Tandem Michael-Aldol Reactions.f *Angew. Chem. Int. Ed.* **1996**, *35,* 104–106.

(100) Christoffers, J.; Roßler, U.; Werner, T. Construction of Quaternary Stereocenters by Nickel-Catalysis of Asymmetric Michael Reactions. *Eur. J. Org. Chem*. **2000**, *5,* 701–705.

(101) Xu, T.; Li, C. C.; Yang, Z. A Concise Approach for the Total Synthesis of Pseudolaric Acid A. *Org. Lett.* **2011,** *13*, 2630–2633.

Appendix 4

Spectra Relevant to Chapter 4:

3.2.1 bicycle synthesis

Parameter	Value
Data File Name	/ Users/ jordankthompson/ Desktop/ JKT-2-allylation_pure/ 1/ fid
Title	JKT-2-allylation_pure.1.fid
Origin	Bruker BioSpin GmbH
Solvent	CDCl3
Temperature	297.2
Pulse Sequence	zg30
Experiment	1D
Number of Scans	16
Receiver Gain	176.8
Relaxation Delay	1.0000
Pulse Width	12.5000
Acquisition Time	4.0894
Acquisition Date	2022-12-23T11:11:38
Spectrometer Frequency	400.13
Spectral Width	8012.8
Nucleus	1H
Acquired Size	32768
Spectral Size	65536

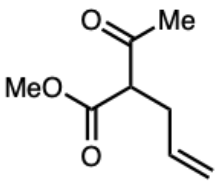

108

202.55 169.86 134.27 117.70 59.23 52.59 32.35 29.33

Parameter	Value
Data File Name	/ Users/ jordankthompson/ Desktop/ JKT-2-allylation_pure/ 2/ fid
Title	JKT-2-allylation_pure.2.fid
Origin	Bruker BioSpin GmbH
Solvent	CDCl3
Temperature	297.1
Pulse Sequence	zgpg30
Experiment	1D
Number of Scans	512
Receiver Gain	72.0
Relaxation Delay	1.0000
Pulse Width	10.0000
Acquisition Time	1.2496
Acquisition Date	2022-12-23T11:32:27
Spectrometer Frequency	100.62
Spectral Width	26223.8
Nucleus	13C
Acquired Size	32768
Spectral Size	65536

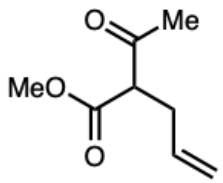

108

f1 (ppm)

Parameter	Value
Data File Name	/ Volumes/ nmrdata/ jkthomps/ nmr/ JKT-2-MEMprotection/ 1/ fid
Title	JKT-2-MEMprotection.1.fid
Origin	Bruker BioSpin GmbH
Solvent	CDCl3
Temperature	298.2
Pulse Sequence	zg30
Experiment	1D
Number of Scans	16
Receiver Gain	101.0
Relaxation Delay	1.0000
Pulse Width	9.8500
Acquisition Time	3.9977
Acquisition Date	2022-08-13T15:39:08
Spectrometer Frequency	400.15
Spectral Width	8196.7
Nucleus	1H
Acquired Size	32768
Spectral Size	65536

1,3-dichloro-2-((2-methoxyethoxy)methoxy)propane

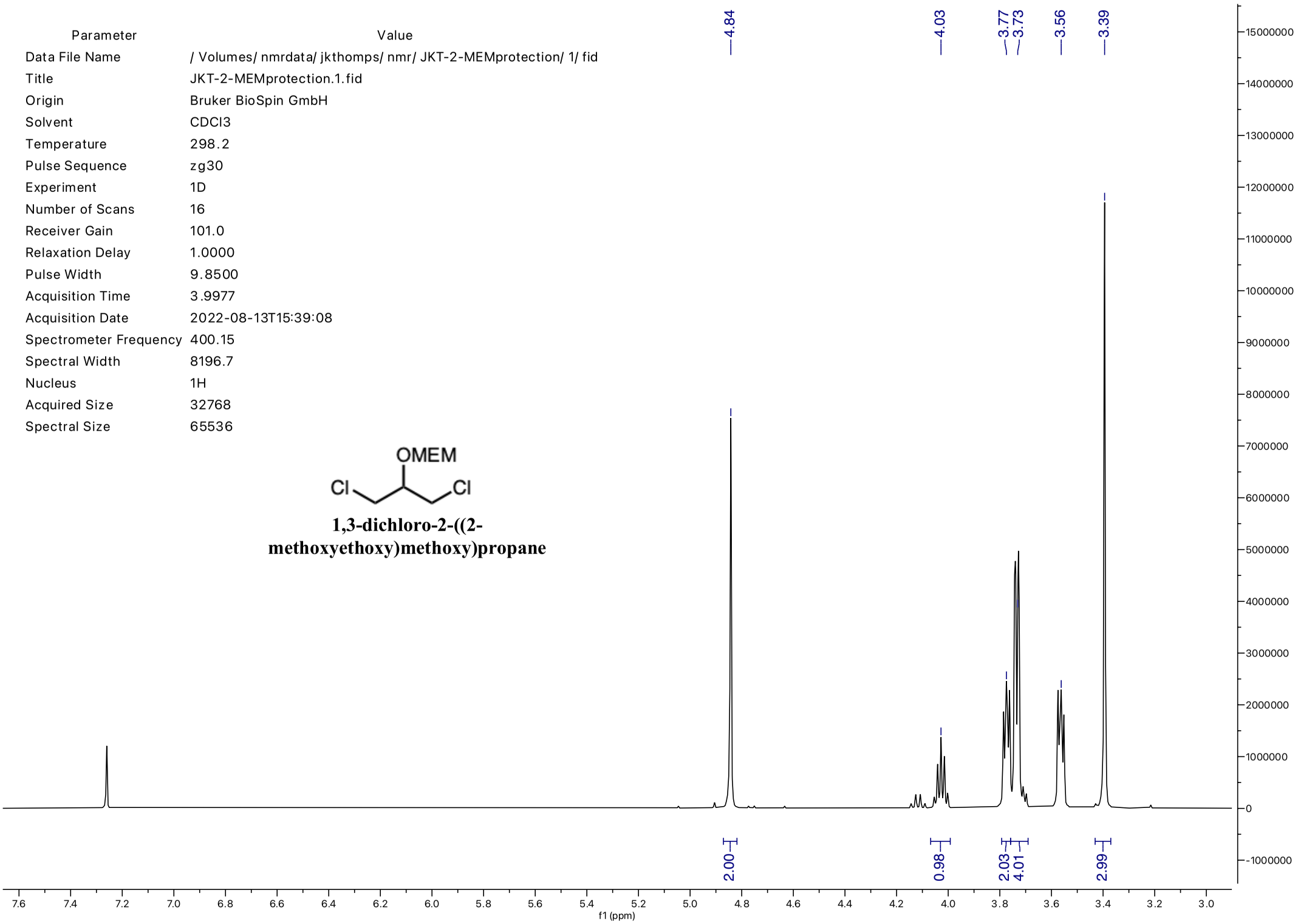

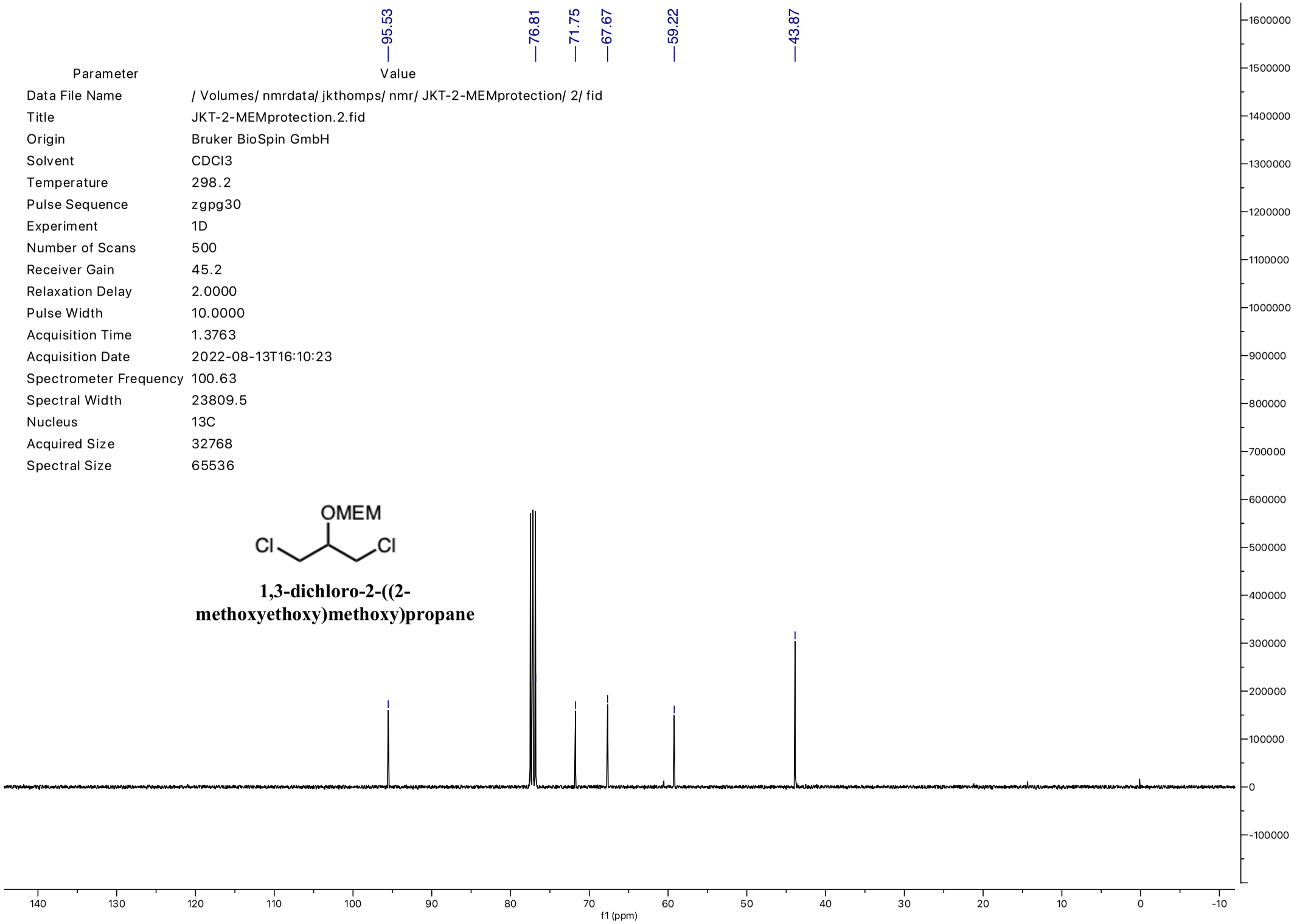
95.53
76.81
71.75
67.67
59.22
43.87
Parameter
Value
Data File Name
/ Volumes/ nmrdata/ jkthomps/ nmr/ JKT-2-MEMprotection/ 2/ fid
Title
JKT-2-MEMprotection.2.fid
Origin
Bruker BioSpin GmbH
Solvent
CDCl3
Temperature
298.2
Pulse Sequence
zgpg30
Experiment
1D
Number of Scans
500
Receiver Gain
45.2
Relaxation Delay
2.0000
Pulse Width
10.0000
Acquisition Time
1.3763
Acquisition Date
2022-08-13T16:10:23
Spectrometer Frequency
100.63
Spectral Width
23809.5
Nucleus
13C
Acquired Size
32768
Spectral Size
65536
OMEM
Cl
Cl
1,3-dichloro-2-((2-methoxyethoxy)methoxy)propane
1600000
1500000
1400000
1300000
1200000
1100000
1000000
900000
800000
700000
600000
500000
400000
300000
200000
100000
0
-100000
140
130
120
110
100
90
80
70
60
50
40
30
20
10
0
-10
f1 (ppm)

Parameter	Value
Data File Name	/ Volumes/ nmrdata/ jkthomps/ nmr/ CHM-1-12_pure_/ 1/ fid
Title	CHM-1-12_pure_.1.fid
Origin	Bruker BioSpin GmbH
Solvent	CDCl3
Temperature	298.2
Pulse Sequence	zg30
Experiment	1D
Number of Scans	16
Receiver Gain	101.0
Relaxation Delay	1.0000
Pulse Width	9.8500
Acquisition Time	3.9977
Acquisition Date	2022-08-01T17:13:14
Spectrometer Frequency	400.15
Spectral Width	8196.7
Nucleus	1H
Acquired Size	32768
Spectral Size	65536

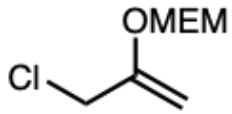

115

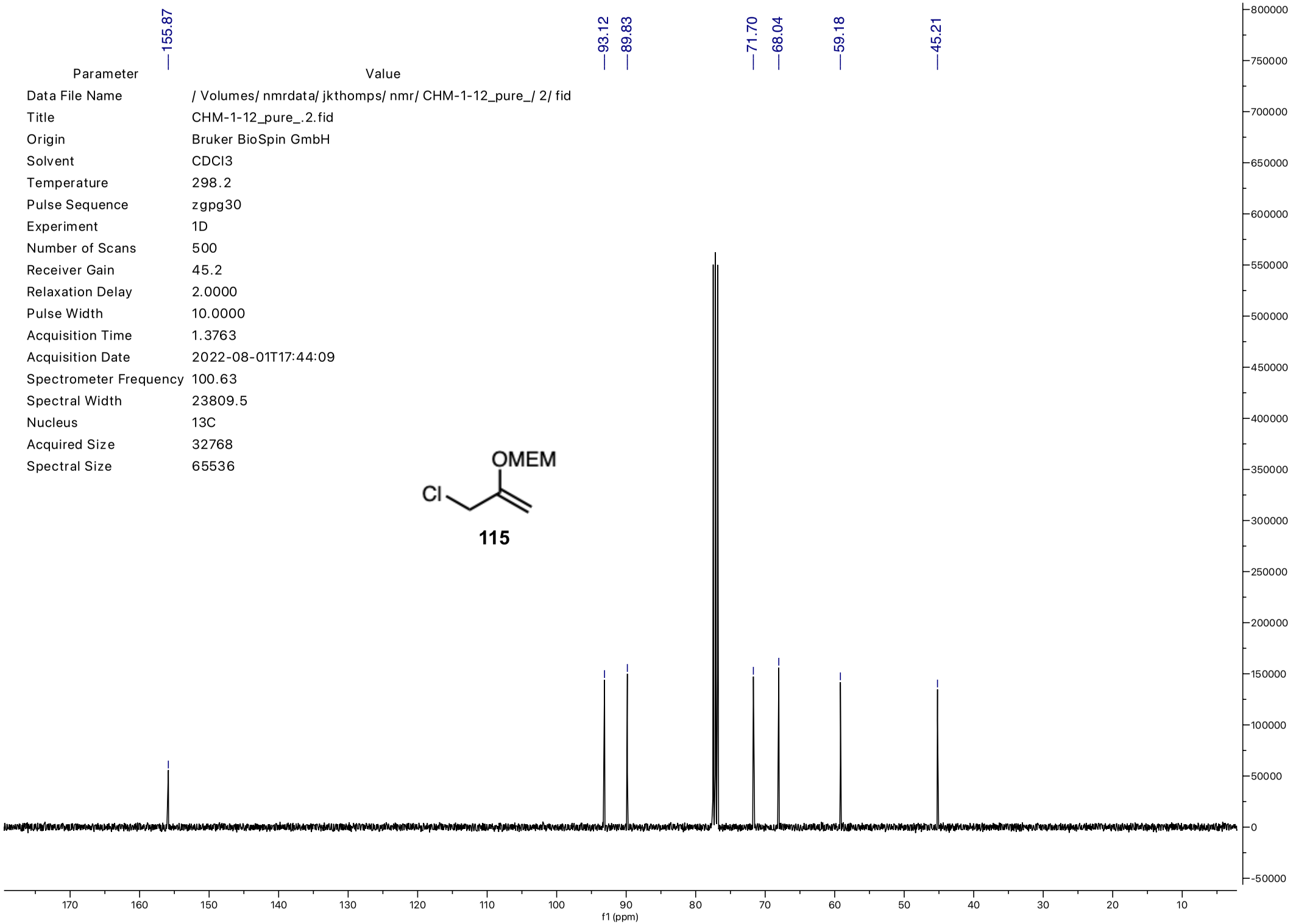
155.87
93.12
89.83
71.70
68.04
59.18
45.21
Parameter
Value
Data File Name
/ Volumes/ nmrdata/ jkthomps/ nmr/ CHM-1-12_pure_/ 2/ fid
Title
CHM-1-12_pure_.2.fid
Origin
Bruker BioSpin GmbH
Solvent
CDCl3
Temperature
298.2
Pulse Sequence
zgpg30
Experiment
1D
Number of Scans
500
Receiver Gain
45.2
Relaxation Delay
2.0000
Pulse Width
10.0000
Acquisition Time
1.3763
Acquisition Date
2022-08-01T17:44:09
Spectrometer Frequency
100.63
Spectral Width
23809.5
Nucleus
13C
Acquired Size
32768
Spectral Size
65536
OMEM
Cl
115
800000
750000
700000
650000
600000
550000
500000
450000
400000
350000
300000
250000
200000
150000
100000
50000
0
-50000
170
160
150
140
130
120
110
100
90
80
70
60
50
40
30
20
10
f1 (ppm)

Parameter	Value
Data File Name	/ Volumes/ nmrdata-1/ jkthomps/ nmr/ snider _sm_RR/ 1/ fid
Title	snider _sm_RR.1.fid
Origin	Bruker BioSpin GmbH
Solvent	CDCl3
Temperature	297.1
Pulse Sequence	zg30
Experiment	1D
Number of Scans	16
Receiver Gain	112.8
Relaxation Delay	1.0000
Pulse Width	12.5000
Acquisition Time	4.0894
Acquisition Date	2024-03-13T14:31:56
Spectrometer Frequency	400.13
Spectral Width	8012.8
Nucleus	1H
Acquired Size	32768
Spectral Size	65536

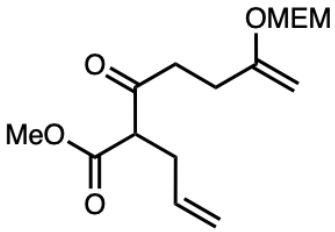

109

Parameter	Value
Data File Name	/ Volumes/ nmrdata-1/ jkthomps/ nmr/ snider _sm_RR/ 2/ fid
Title	snider _sm_RR.2.fid
Origin	Bruker BioSpin GmbH
Solvent	CDCl3
Temperature	297.1
Pulse Sequence	zgpg30
Experiment	1D
Number of Scans	512
Receiver Gain	72.0
Relaxation Delay	1.0000
Pulse Width	10.0000
Acquisition Time	1.3631
Acquisition Date	2024-03-13T14:53:10
Spectrometer Frequency	100.62
Spectral Width	24038.5
Nucleus	13C
Acquired Size	32768
Spectral Size	65536

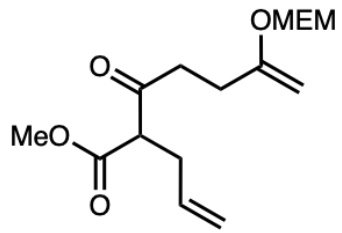

109

Parameter	Value
Data File Name	/ Volumes/ nmrdata-1/ jkthomps/ nmr/ JKT-2-95-4_pure/ 1/ fid
Title	JKT-2-95-4_pure.1.fid
Origin	Bruker BioSpin GmbH
Solvent	CDCl3
Temperature	298.2
Pulse Sequence	zg30
Experiment	1D
Number of Scans	16
Receiver Gain	101.0
Relaxation Delay	1.0000
Pulse Width	9.8500
Acquisition Time	3.9977
Acquisition Date	2022-08-17T13:25:54
Spectrometer Frequency	400.15
Spectral Width	8196.7
Nucleus	1H
Acquired Size	32768
Spectral Size	65536

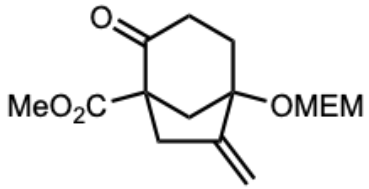

110

206.17
171.07
148.22
108.61
91.36
82.91
71.87
67.37
60.60
59.16
52.43
42.19
38.19
37.52
35.08

Parameter	Value
Data File Name	/ Volumes/ nmrdata-1/ jkthomps/ nmr/ JKT-2-95-4_pure/ 2/ fid
Title	JKT-2-95-4_pure.2.fid
Origin	Bruker BioSpin GmbH
Solvent	CDCl3
Temperature	298.2
Pulse Sequence	zgpg30
Experiment	1D
Number of Scans	500
Receiver Gain	45.2
Relaxation Delay	2.0000
Pulse Width	10.0000
Acquisition Time	1.3763
Acquisition Date	2022-08-17T13:55:18
Spectrometer Frequency	100.63
Spectral Width	23809.5
Nucleus	13C
Acquired Size	32768
Spectral Size	65536

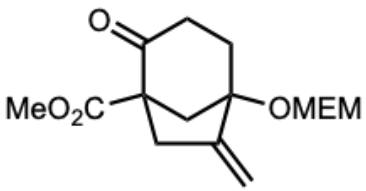

110

850000
800000
750000
700000
650000
600000
550000
500000
450000
400000
350000
300000
250000
200000
150000
100000
50000
0
-50000

210 200 190 180 170 160 150 140 130 120 110 100 90 80 70 60 50 40 30

f1 (ppm)

Parameter	Value
Data File Name	/ Volumes/ nmrdata-1/ jkthomps/ nmr/ JKT-2-76_pure/ 1/ fid
Title	JKT-2-76_pure.1.fid
Origin	Bruker BioSpin GmbH
Solvent	CDCl3
Temperature	298.1
Pulse Sequence	zg30
Experiment	1D
Number of Scans	16
Receiver Gain	101.0
Relaxation Delay	1.0000
Pulse Width	9.8500
Acquisition Time	3.9977
Acquisition Date	2022-07-28T14:18:34
Spectrometer Frequency	400.15
Spectral Width	8196.7
Nucleus	1H
Acquired Size	32768
Spectral Size	65536

114

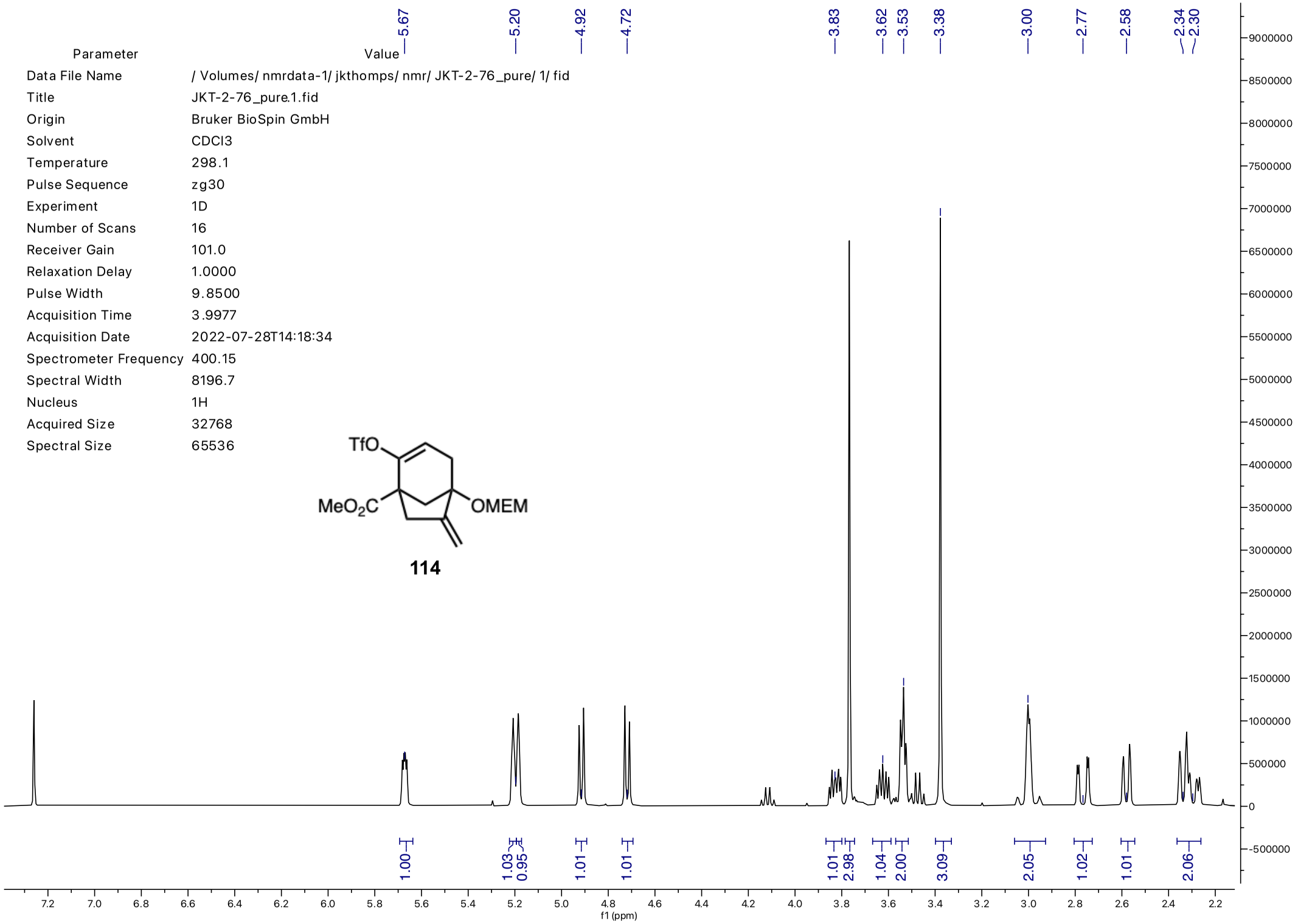

Parameter	Value
Data File Name	/ Volumes/ nmrdata-1/ jkthomps/ nmr/ JKT-2-76_pure/ 2/ fid
Title	JKT-2-76_pure.2.fid
Origin	Bruker BioSpin GmbH
Solvent	CDCl3
Temperature	298.2
Pulse Sequence	zgpg30
Experiment	1D
Number of Scans	520
Receiver Gain	45.2
Relaxation Delay	2.0000
Pulse Width	10.0000
Acquisition Time	1.3763
Acquisition Date	2022-07-28T14:50:44
Spectrometer Frequency	100.63
Spectral Width	23809.5
Nucleus	13C
Acquired Size	32768
Spectral Size	65536

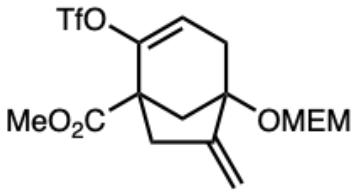

114

Parameter	Value
Data File Name	/ Users/ jordankthompson/ Desktop/ JKT-2-77_crude/ 1/ fid
Title	JKT-2-77_crude.1.fid
Origin	Bruker BioSpin GmbH
Solvent	CDCl3
Temperature	298.1
Pulse Sequence	zg30
Experiment	1D
Number of Scans	16
Receiver Gain	101.0
Relaxation Delay	1.0000
Pulse Width	9.8500
Acquisition Time	3.9977
Acquisition Date	2022-07-28T18:18:45
Spectrometer Frequency	400.15
Spectral Width	8196.7
Nucleus	1H
Acquired Size	32768
Spectral Size	65536

113

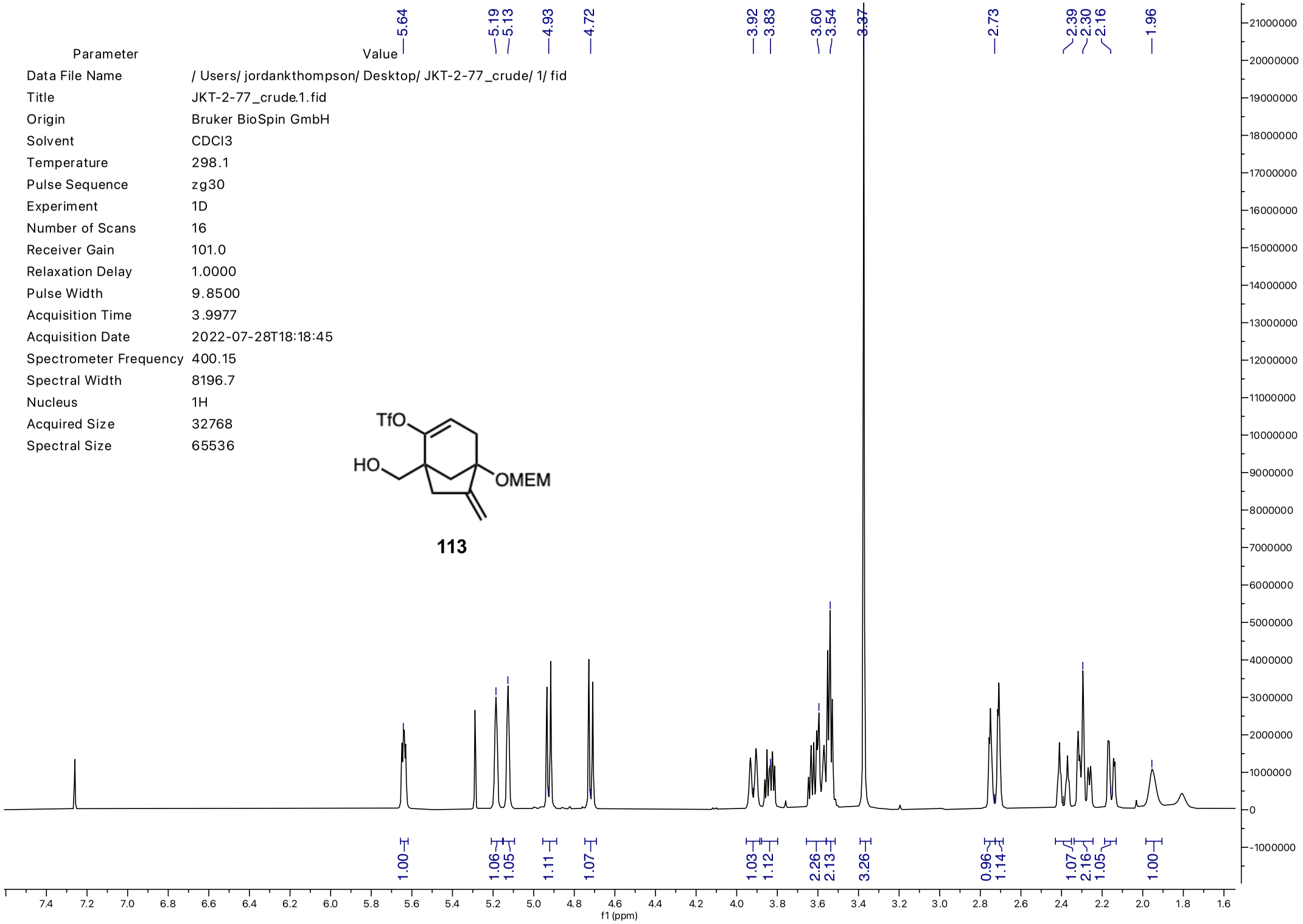

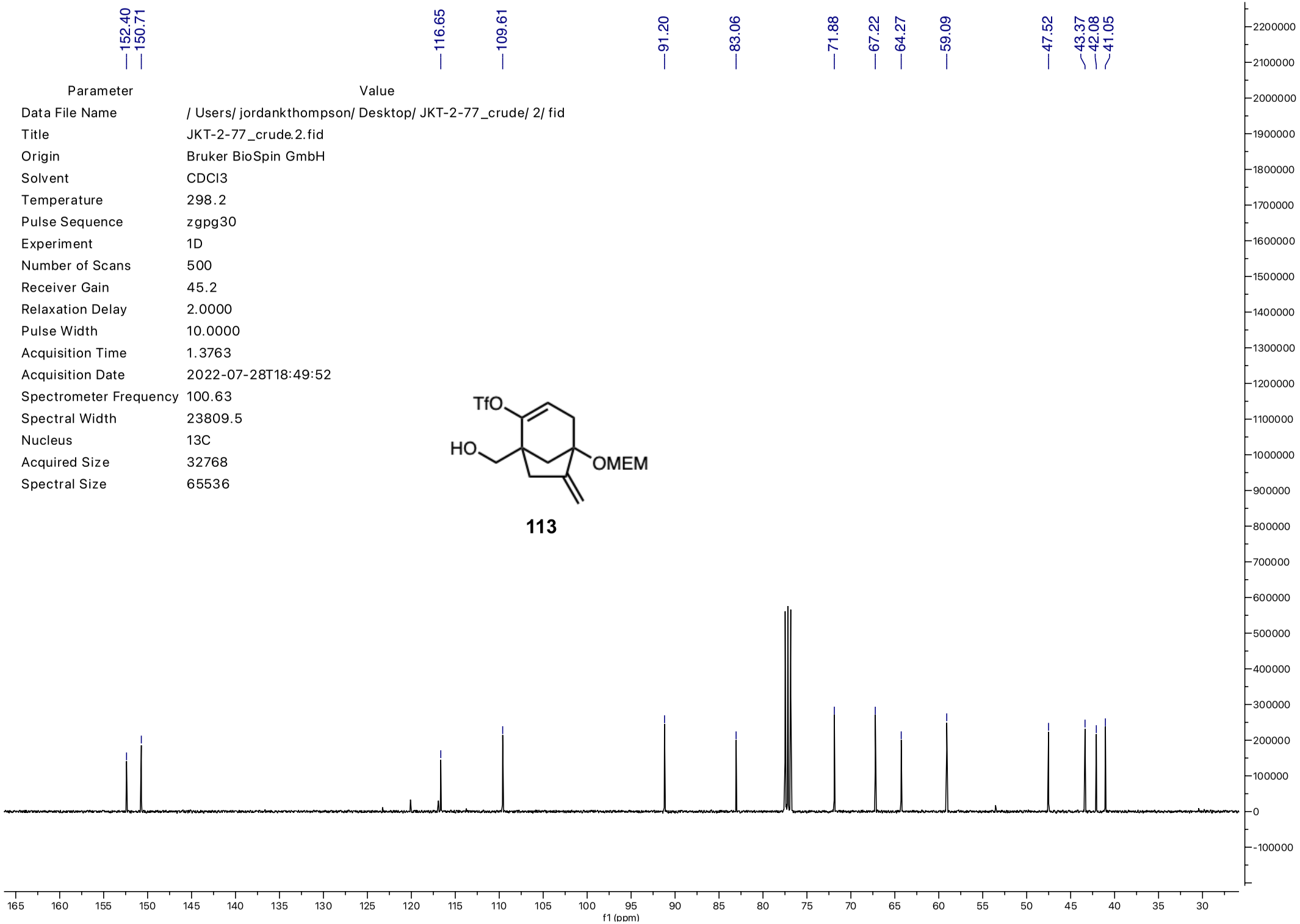

Parameter	Value
Data File Name	/ Users/ jordankthompson/ Desktop/ JKT-2-77_crude/ 2/ fid
Title	JKT-2-77_crude.2.fid
Origin	Bruker BioSpin GmbH
Solvent	CDCl3
Temperature	298.2
Pulse Sequence	zgpg30
Experiment	1D
Number of Scans	500
Receiver Gain	45.2
Relaxation Delay	2.0000
Pulse Width	10.0000
Acquisition Time	1.3763
Acquisition Date	2022-07-28T18:49:52
Spectrometer Frequency	100.63
Spectral Width	23809.5
Nucleus	13C
Acquired Size	32768
Spectral Size	65536

113

Parameter	Value
Data File Name	/ Volumes/ nmrdata-1/ jkthomps/ nmr/ JKT-2-108-2_pure/ 1/ fid
Title	JKT-2-108-2_pure.1.fid
Origin	Bruker BioSpin GmbH
Solvent	CDCl3
Temperature	298.2
Pulse Sequence	zg30
Experiment	1D
Number of Scans	16
Receiver Gain	101.0
Relaxation Delay	1.0000
Pulse Width	9.8500
Acquisition Time	3.9977
Acquisition Date	2022-08-31T15:01:43
Spectrometer Frequency	400.15
Spectral Width	8196.7
Nucleus	1H
Acquired Size	32768
Spectral Size	65536

112

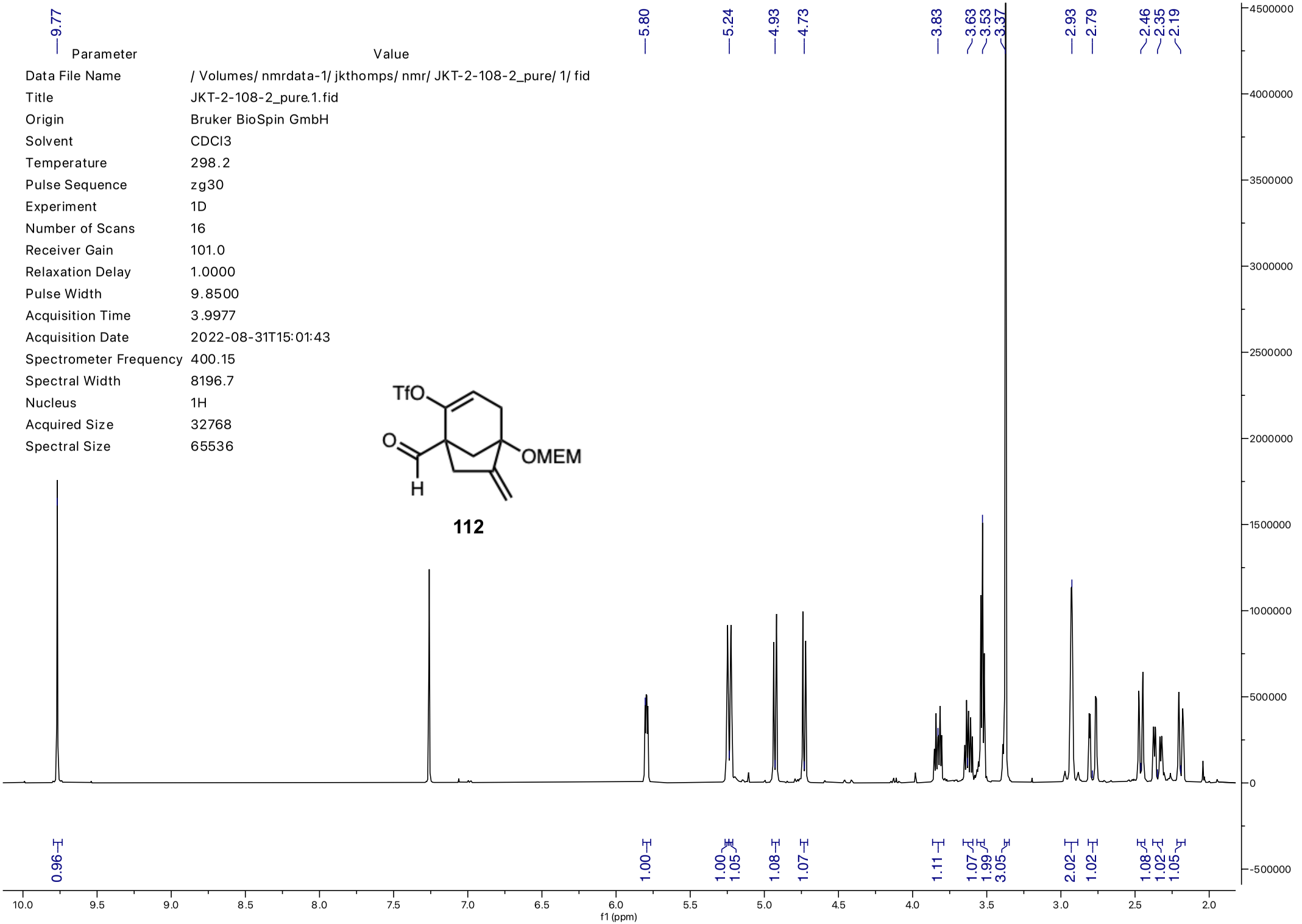

Parameter	Value
Data File Name	/ Volumes/ nmrdata-1/ jkthomps/ nmr/ JKT-2-108-2_pure/ 2/ fid
Title	JKT-2-108-2_pure.2.fid
Origin	Bruker BioSpin GmbH
Solvent	CDCl3
Temperature	298.2
Pulse Sequence	zgpg30
Experiment	1D
Number of Scans	500
Receiver Gain	45.2
Relaxation Delay	2.0000
Pulse Width	10.0000
Acquisition Time	1.3107
Acquisition Date	2022-08-31T15:32:08
Spectrometer Frequency	100.63
Spectral Width	25000.0
Nucleus	13C
Acquired Size	32768
Spectral Size	65536

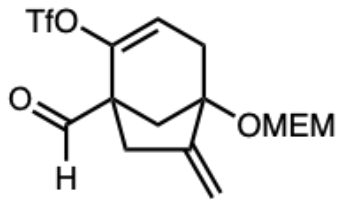

112

Parameter	Value
Data File Name	/ Volumes/ nmrdata/ jkthomps/ nmr/ JKT-2-86_pure/ 1/ fid
Title	JKT-2-86_pure.1.fid
Origin	Bruker BioSpin GmbH
Solvent	CDCl3
Temperature	298.2
Pulse Sequence	zg30
Experiment	1D
Number of Scans	16
Receiver Gain	101.0
Relaxation Delay	1.0000
Pulse Width	9.8500
Acquisition Time	3.9977
Acquisition Date	2022-08-05T18:31:36
Spectrometer Frequency	400.15
Spectral Width	8196.7
Nucleus	1H
Acquired Size	32768
Spectral Size	65536

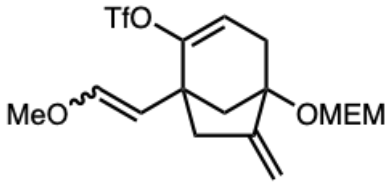

111

153.77
153.71
151.95
151.24
149.62
149.56
115.09
114.27
109.40
108.71
103.01
101.08
91.24
82.87
82.85
71.93
67.28
67.20
60.11
59.17
59.14
55.88
47.06
46.19
45.97
45.83
44.61
44.42
40.96
40.83

Parameter	Value
Data File Name	/ Volumes/ nmrdata/ jkthomps/ nmr/ JKT-2-86_pure/ 2/ fid
Title	JKT-2-86_pure.2.fid
Origin	Bruker BioSpin GmbH
Solvent	CDCl3
Temperature	298.2
Pulse Sequence	zgpg30
Experiment	1D
Number of Scans	500
Receiver Gain	45.2
Relaxation Delay	2.0000
Pulse Width	10.0000
Acquisition Time	1.3763
Acquisition Date	2022-08-05T19:02:21
Spectrometer Frequency	100.63
Spectral Width	23809.5
Nucleus	13C
Acquired Size	32768
Spectral Size	65536

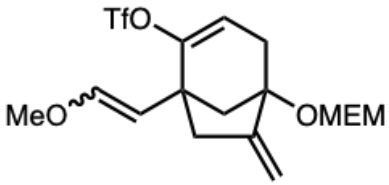

111

360000
340000
320000
300000
280000
260000
240000
220000
200000
180000
160000
140000
120000
100000
80000
60000
40000
20000
0
-20000

160
150
140
130
120
110
100
90
80
70
60
50
40
30
20
f1 (ppm)

Parameter	Value
Data File Name	/ Volumes/ nmrdata/ jkthomps/ nmr/ JKT-2-87_pure/ 1/ fid
Title	JKT-2-87_pure.1.fid
Origin	Bruker BioSpin GmbH
Solvent	CDCl3
Temperature	298.2
Pulse Sequence	zg30
Experiment	1D
Number of Scans	16
Receiver Gain	101.0
Relaxation Delay	1.0000
Pulse Width	9.8500
Acquisition Time	3.9977
Acquisition Date	2022-08-07T14:21:40
Spectrometer Frequency	400.15
Spectral Width	8196.7
Nucleus	1H
Acquired Size	32768
Spectral Size	65536

107A

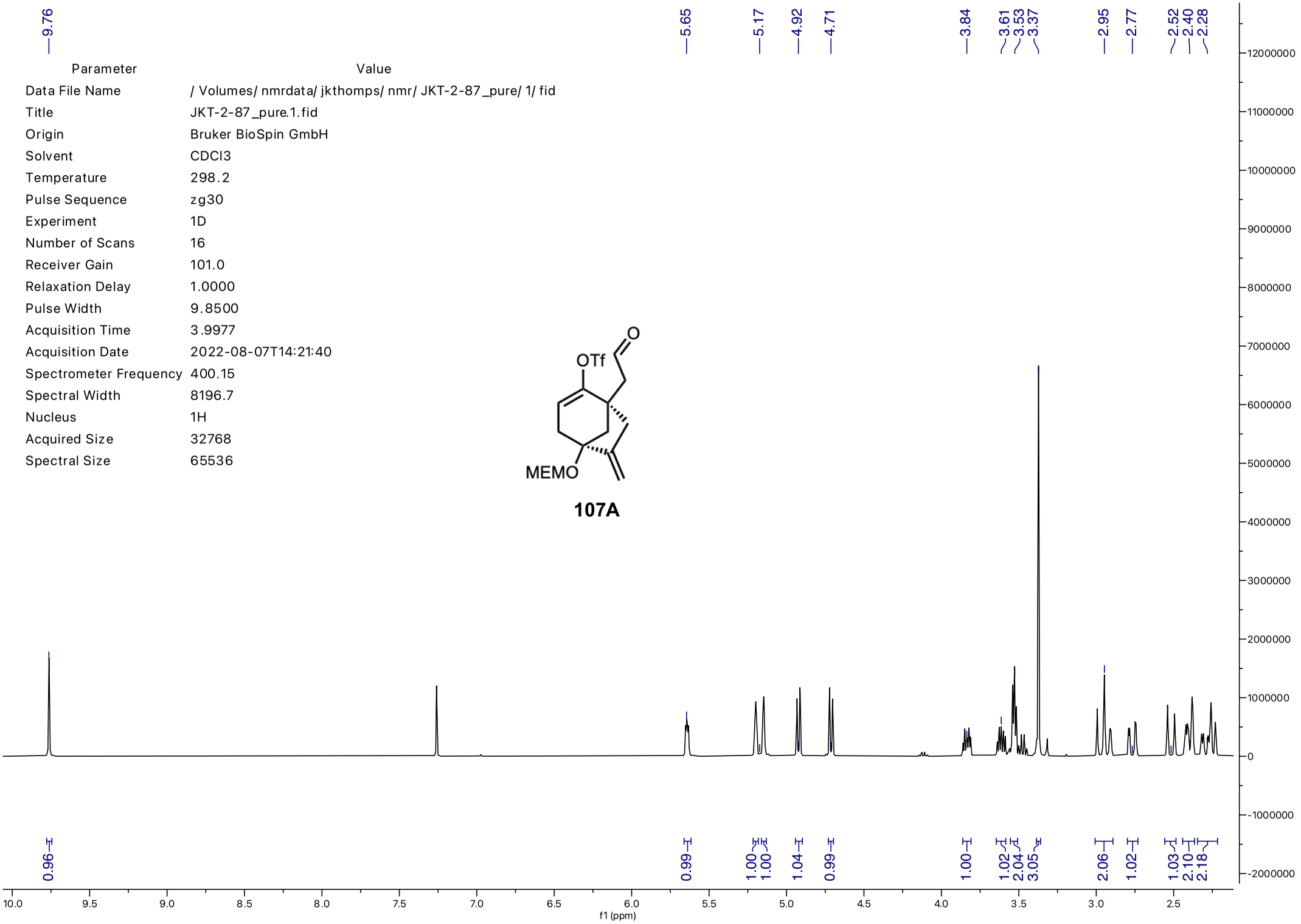

198.76
151.49
149.90
115.31
109.70
91.22
83.06
71.86
67.27
59.13
47.66
46.08
44.98
42.26
41.10

Parameter	Value
Data File Name	/ Volumes/ nmrdata/ jkthomps/ nmr/ JKT-2-87_pure/ 2/ fid
Title	JKT-2-87_pure.2.fid
Origin	Bruker BioSpin GmbH
Solvent	CDCl3
Temperature	298.2
Pulse Sequence	zgpg30
Experiment	1D
Number of Scans	500
Receiver Gain	45.2
Relaxation Delay	2.0000
Pulse Width	10.0000
Acquisition Time	1.3763
Acquisition Date	2022-08-07T14:51:01
Spectrometer Frequency	100.63
Spectral Width	23809.5
Nucleus	13C
Acquired Size	32768
Spectral Size	65536

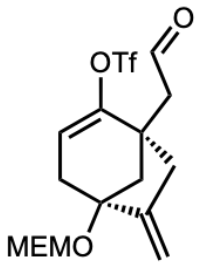

107A

1000000
900000
800000
700000
600000
500000
400000
300000
200000
100000
0
-100000

200 190 180 170 160 150 140 130 120 110 100 90 80 70 60 50 40

f1 (ppm)

Parameter	Value
Data File Name	/ Volumes/ nmrdata-2/ jkthomps/ nmr/ JKT-2-165-1/ 1/ fid
Title	JKT-2-165-1.1.fid
Origin	Bruker BioSpin GmbH
Solvent	CDCl3
Temperature	297.1
Pulse Sequence	zg30
Experiment	1D
Number of Scans	16
Receiver Gain	87.8
Relaxation Delay	1.0000
Pulse Width	12.5000
Acquisition Time	4.0894
Acquisition Date	2022-11-02T15:22:46
Spectrometer Frequency	400.13
Spectral Width	8012.8
Nucleus	1H
Acquired Size	32768
Spectral Size	65536

107B

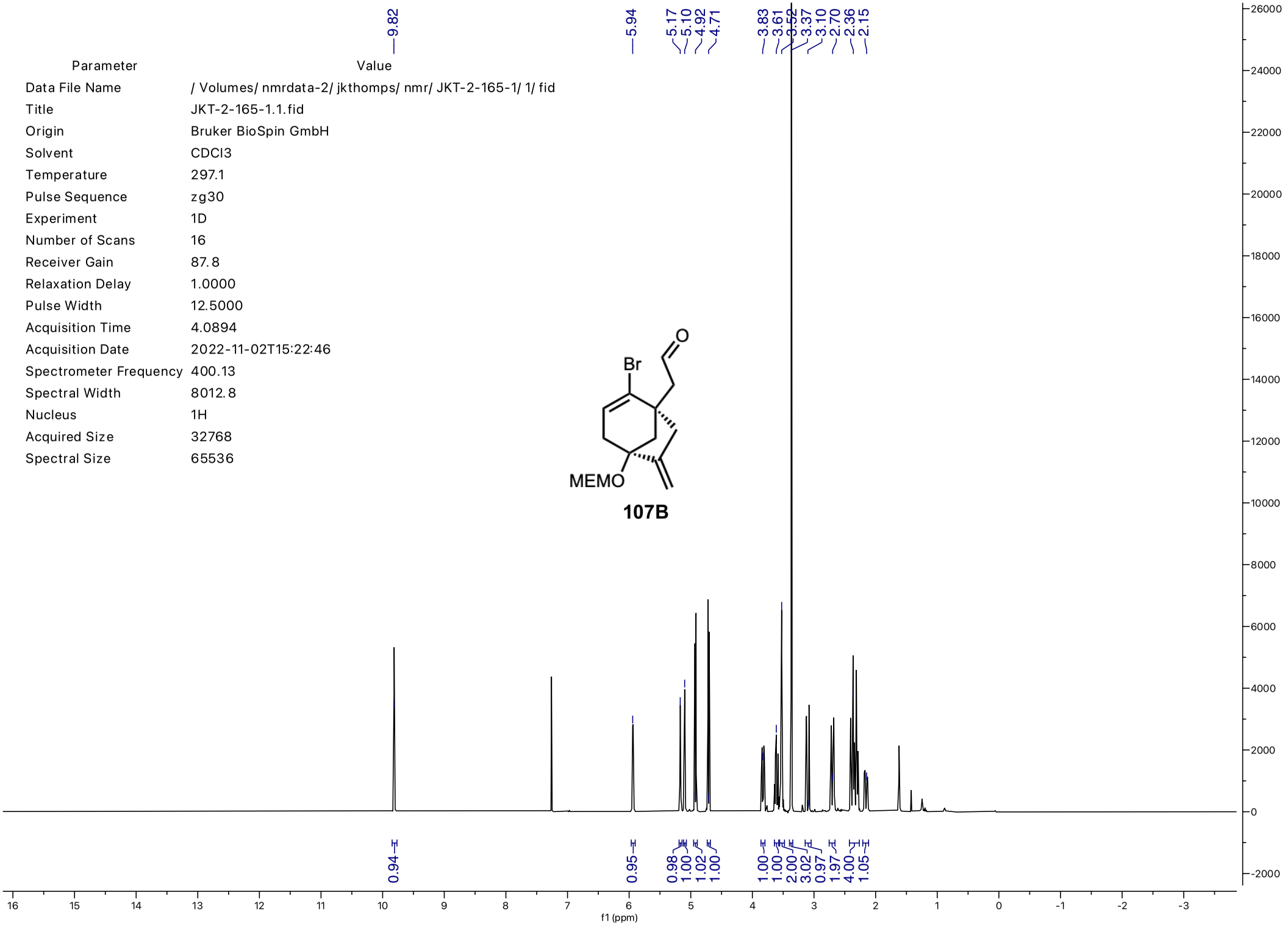

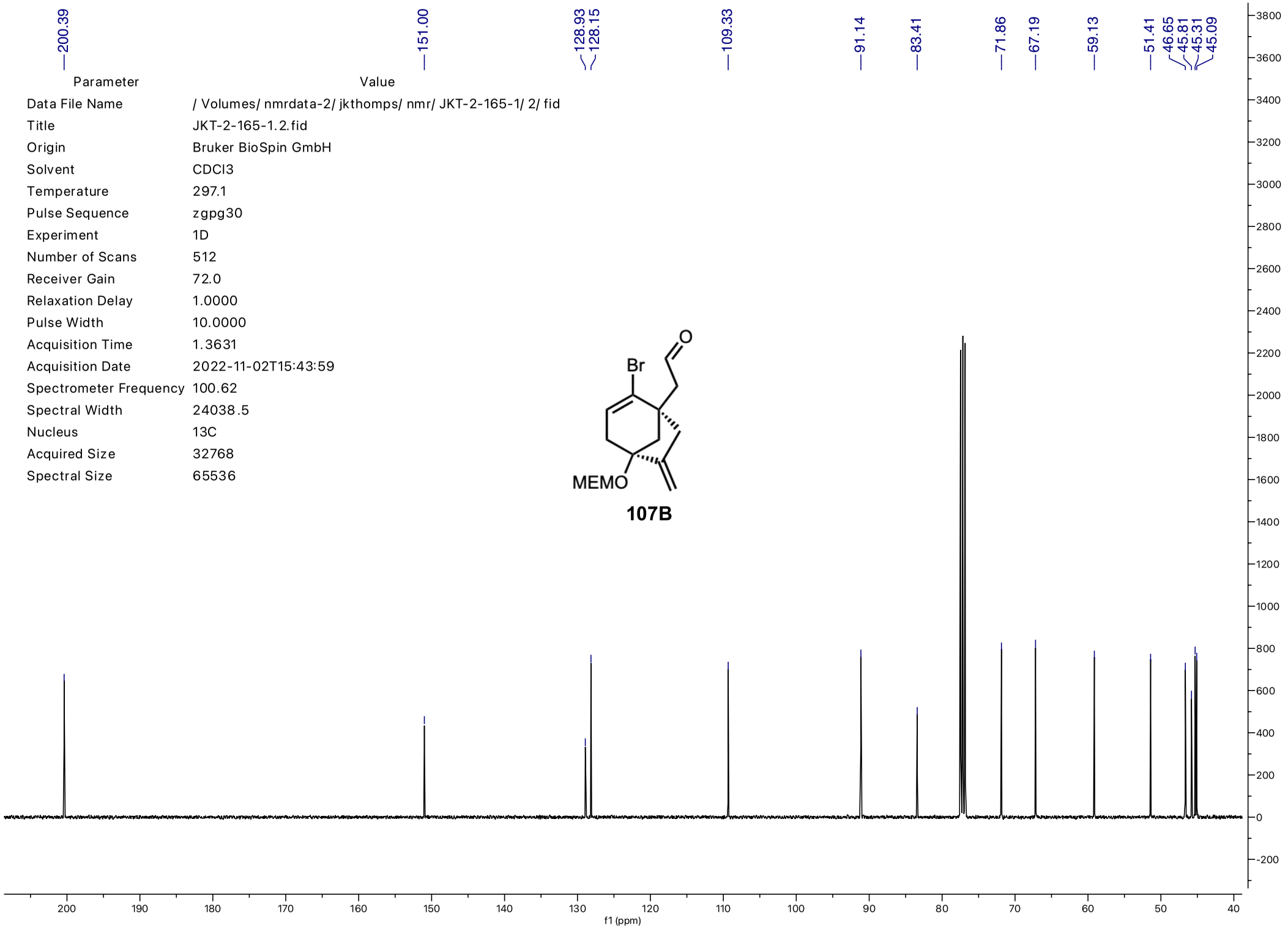
200.39
151.00
128.93
128.15
109.33
91.14
83.41
71.86
67.19
59.13
51.41
46.65
45.81
45.31
45.09
Parameter
Value
Data File Name / Volumes/ nmrdata-2/ jkthomps/ nmr/ JKT-2-165-1/ 2/ fid
Title JKT-2-165-1.2.fid
Origin Bruker BioSpin GmbH
Solvent CDCl3
Temperature 297.1
Pulse Sequence zgpg30
Experiment 1D
Number of Scans 512
Receiver Gain 72.0
Relaxation Delay 1.0000
Pulse Width 10.0000
Acquisition Time 1.3631
Acquisition Date 2022-11-02T15:43:59
Spectrometer Frequency 100.62
Spectral Width 24038.5
Nucleus 13C
Acquired Size 32768
Spectral Size 65536
Br
O
MEMO
107B
f1 (ppm)

Parameter	Value
Data File Name	/ Users/ jordankthompson/ Desktop/ JKT-2-18_pure_char/ 1/ fid
Title	JKT-2-18_pure_char.1.fid
Origin	Bruker BioSpin GmbH
Solvent	CDCl3
Temperature	297.2
Pulse Sequence	zg30
Experiment	1D
Number of Scans	16
Receiver Gain	197.4
Relaxation Delay	1.0000
Pulse Width	12.5000
Acquisition Time	4.0894
Acquisition Date	2023-01-25T05:51:18
Spectrometer Frequency	400.13
Spectral Width	8012.8
Nucleus	1H
Acquired Size	32768
Spectral Size	65536

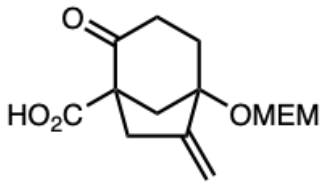

123

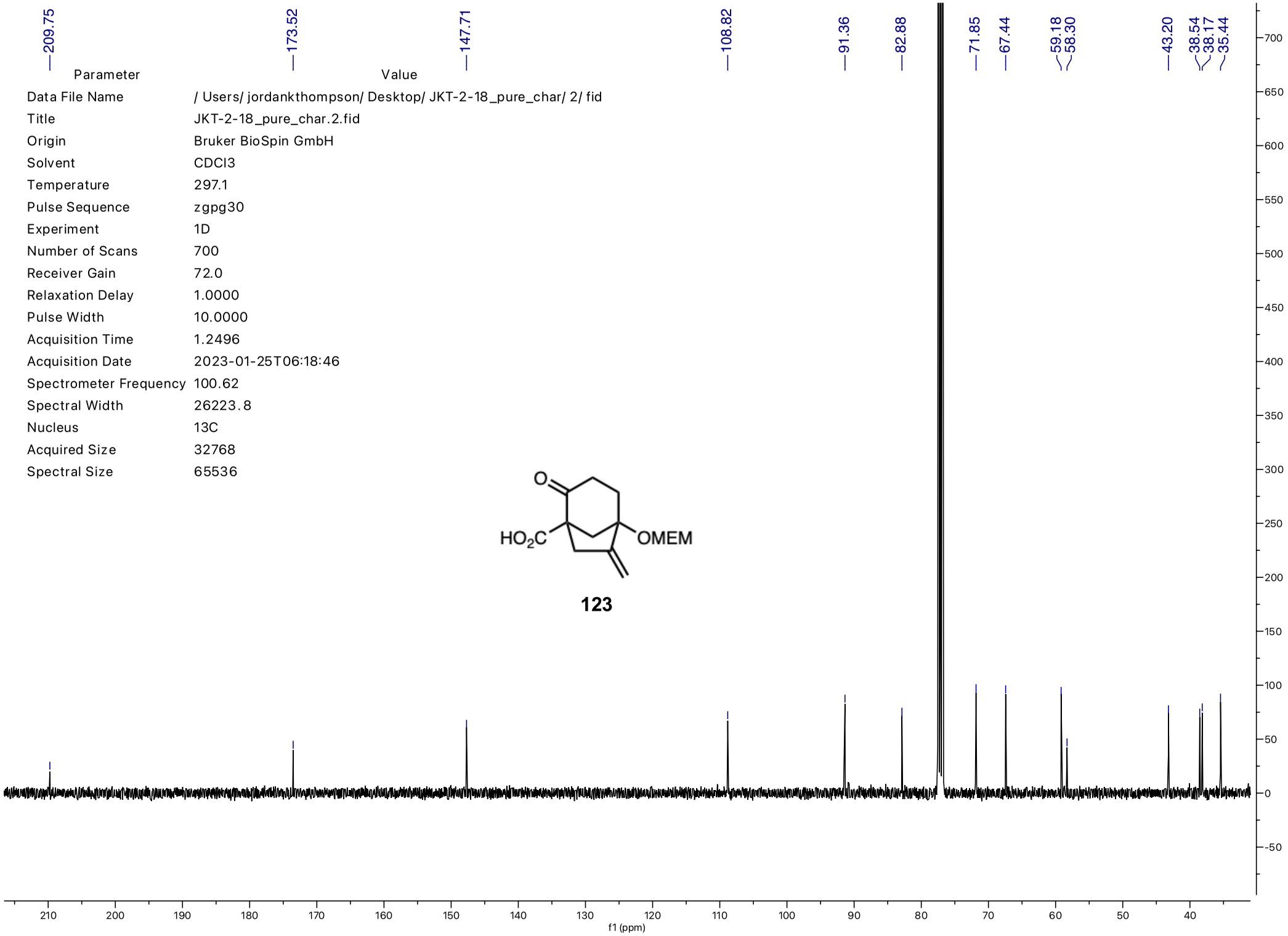
209.75
173.52
147.71
108.82
91.36
82.88
71.85
67.44
59.18
58.30
43.20
38.54
38.17
35.44
Parameter
Value
Data File Name / Users/ jordankthompson/ Desktop/ JKT-2-18_pure_char/ 2/ fid
Title JKT-2-18_pure_char.2.fid
Origin Bruker BioSpin GmbH
Solvent CDCl3
Temperature 297.1
Pulse Sequence zgpg30
Experiment 1D
Number of Scans 700
Receiver Gain 72.0
Relaxation Delay 1.0000
Pulse Width 10.0000
Acquisition Time 1.2496
Acquisition Date 2023-01-25T06:18:46
Spectrometer Frequency 100.62
Spectral Width 26223.8
Nucleus 13C
Acquired Size 32768
Spectral Size 65536
O
HO2C
OMEM
123
f1 (ppm)

Parameter	Value
Data File Name	/ Users/ jordankthompson/ Desktop/ JKT-2-147-2_pure/ PROTON01.fid/ fid
Title	PROTON01
Origin	Varian
Solvent	cdcl3
Temperature	25.0
Pulse Sequence	s2pul
Experiment	1D
Number of Scans	8
Receiver Gain	50
Relaxation Delay	1.0000
Pulse Width	5.6500
Acquisition Time	3.0000
Acquisition Date	2022-10-12T15:47:50
Spectrometer Frequency	499.57
Spectral Width	8000.0
Nucleus	1H
Acquired Size	24000
Spectral Size	65536

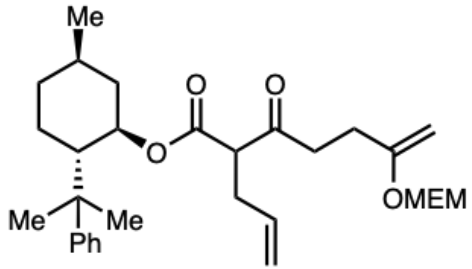

127

Parameter	Value
Data File Name	/ Volumes/ nmrdata-1/ jkthomps/ nmr/ JKT-2-148-2/ 1/ fid
Title	JKT-2-148-2.1.fid
Origin	Bruker BioSpin GmbH
Solvent	CDCl3
Temperature	297.2
Pulse Sequence	zg30
Experiment	1D
Number of Scans	16
Receiver Gain	78.7
Relaxation Delay	1.0000
Pulse Width	12.5000
Acquisition Time	4.0894
Acquisition Date	2022-10-13T14:02:18
Spectrometer Frequency	400.13
Spectral Width	8012.8
Nucleus	1H
Acquired Size	32768
Spectral Size	65536

128

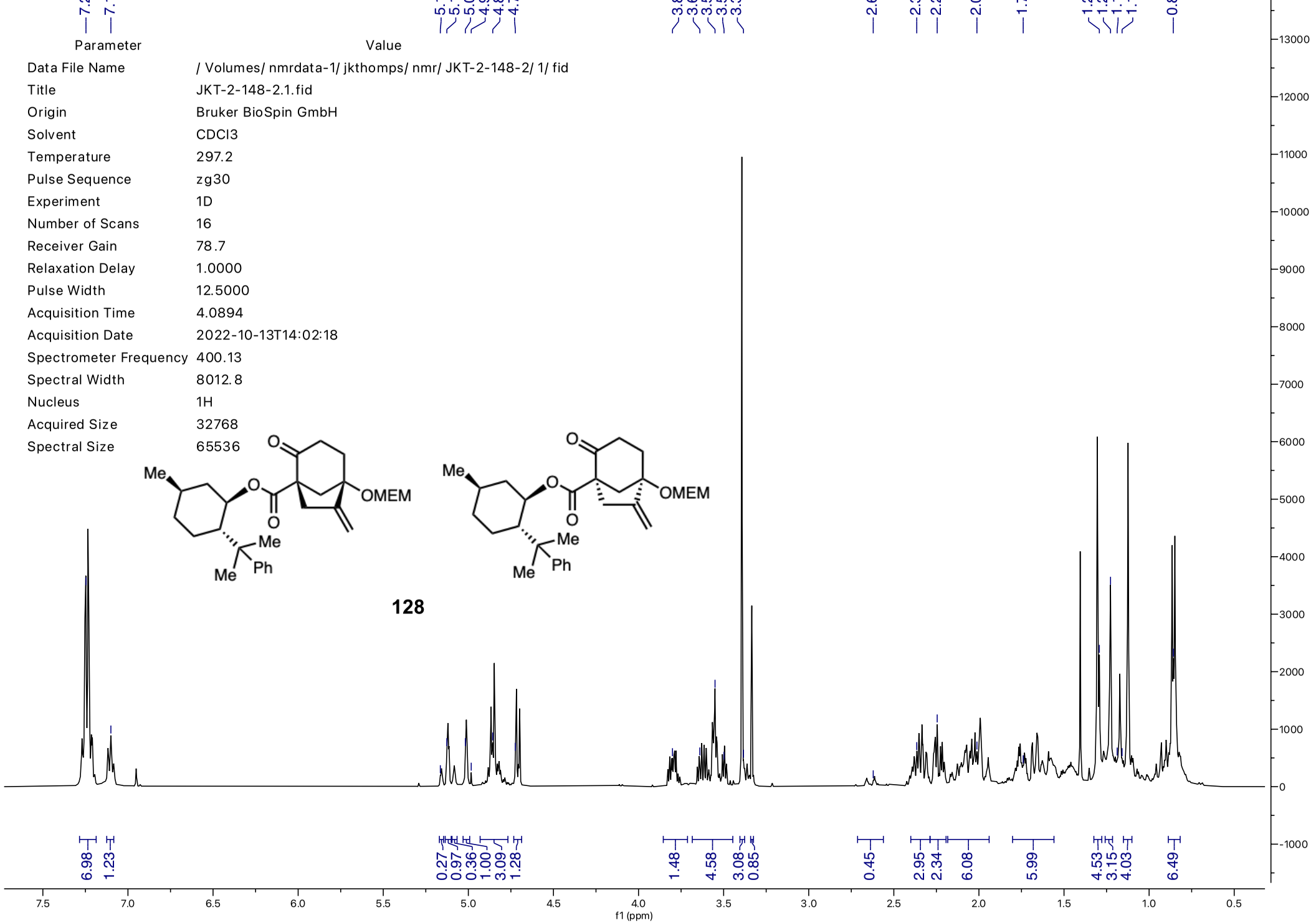

206.11
206.02
169.85
169.77
152.46
151.76
148.64
148.56
135.89
128.06
127.98
125.84
125.76
125.66
125.14
108.13
108.04
91.37
91.19
82.84
82.78
76.62
76.25
71.89
71.84
67.34
67.23
60.62
60.41
59.23
59.17
50.25
49.83
42.02
41.68
41.63
40.87
40.02
39.69
38.12
37.96
36.82
36.53
35.27
34.99
34.79
34.76
34.36
31.45
31.44
30.45
29.84
29.58
27.06
26.76
26.63
23.95
22.83
21.92
14.27

Parameter	Value
Data File Name	/ Volumes/ nmrdata-1/ jkthomps/ nmr/ JKT-2-148-2/ 2/ fid
Title	JKT-2-148-2.2.fid
Origin	Bruker BioSpin GmbH
Solvent	CDCl3
Temperature	297.1
Pulse Sequence	zgpg30
Experiment	1D
Number of Scans	512
Receiver Gain	64.2
Relaxation Delay	1.0000
Pulse Width	10.0000
Acquisition Time	1.3631
Acquisition Date	2022-10-13T14:24:17
Spectrometer Frequency	100.62
Spectral Width	24038.5
Nucleus	13C
Acquired Size	32768
Spectral Size	65536

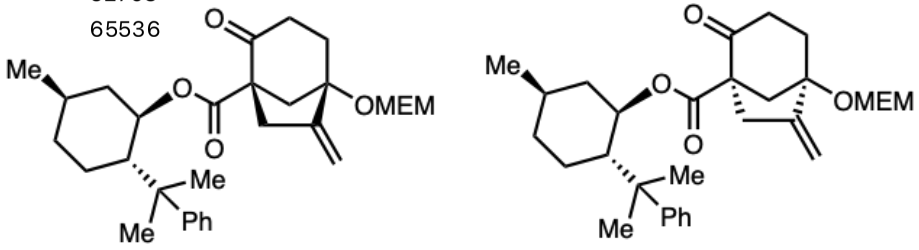

128

2500
2400
2300
2200
2100
2000
1900
1800
1700
1600
1500
1400
1300
1200
1100
1000
900
800
700
600
500
400
300
200
100
0
-100
-200

210
200
190
180
170
160
150
140
130
120
110
100
90
80
70
60
50
40
30
20
f1 (ppm)

Parameter	Value
Data File Name	/ Volumes/ nmrdata/ jkthomps/ nmr/ JKT-4-273_sm/ 1/ fid
Title	JKT-4-273_sm.1.fid
Origin	Bruker BioSpin GmbH
Solvent	CDCl3
Temperature	297.2
Pulse Sequence	zg30
Experiment	1D
Number of Scans	16
Receiver Gain	64.2
Relaxation Delay	1.0000
Pulse Width	12.5000
Acquisition Time	4.0894
Acquisition Date	2023-08-21T13:21:18
Spectrometer Frequency	400.13
Spectral Width	8012.8
Nucleus	1H
Acquired Size	32768
Spectral Size	65536

132

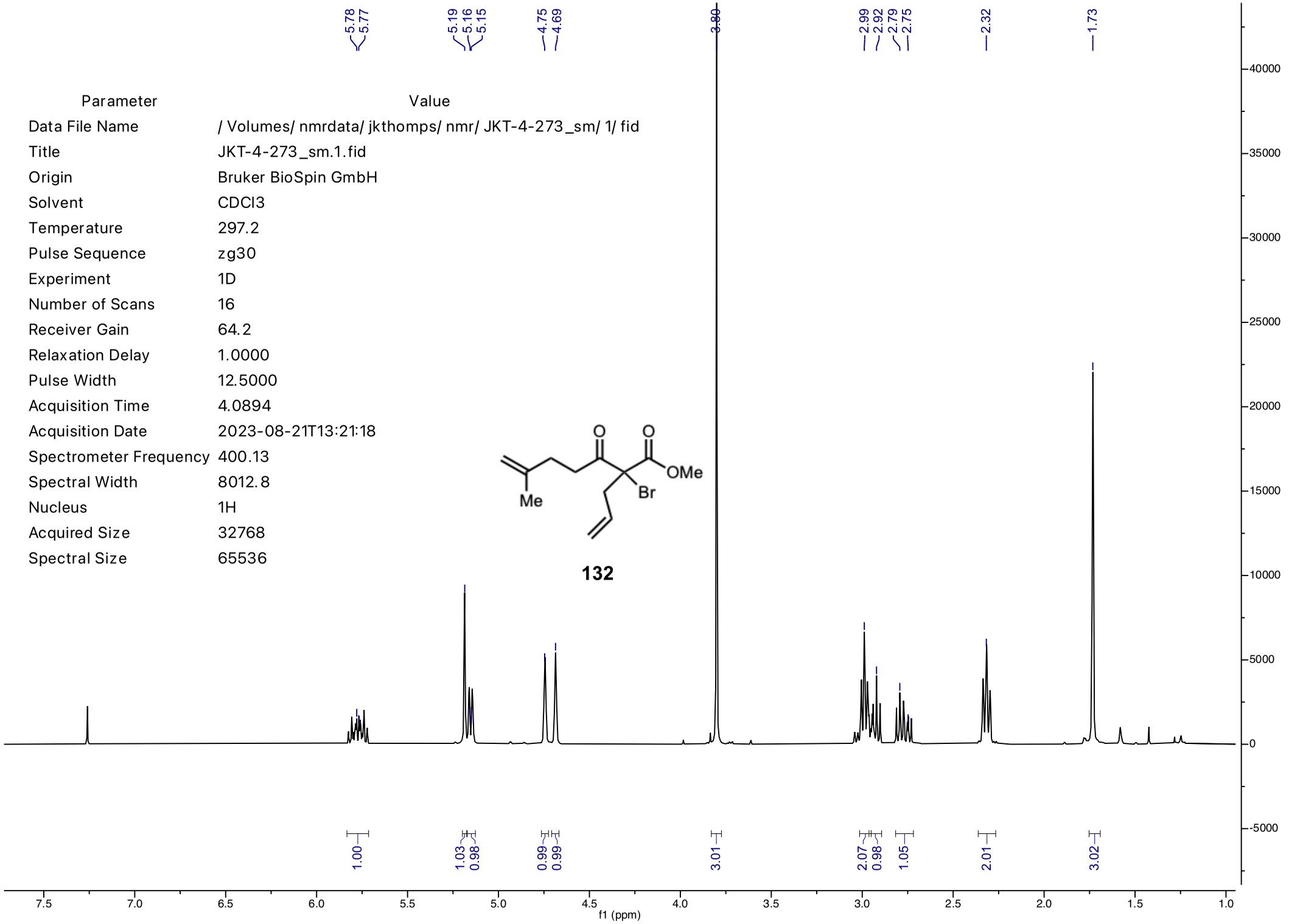

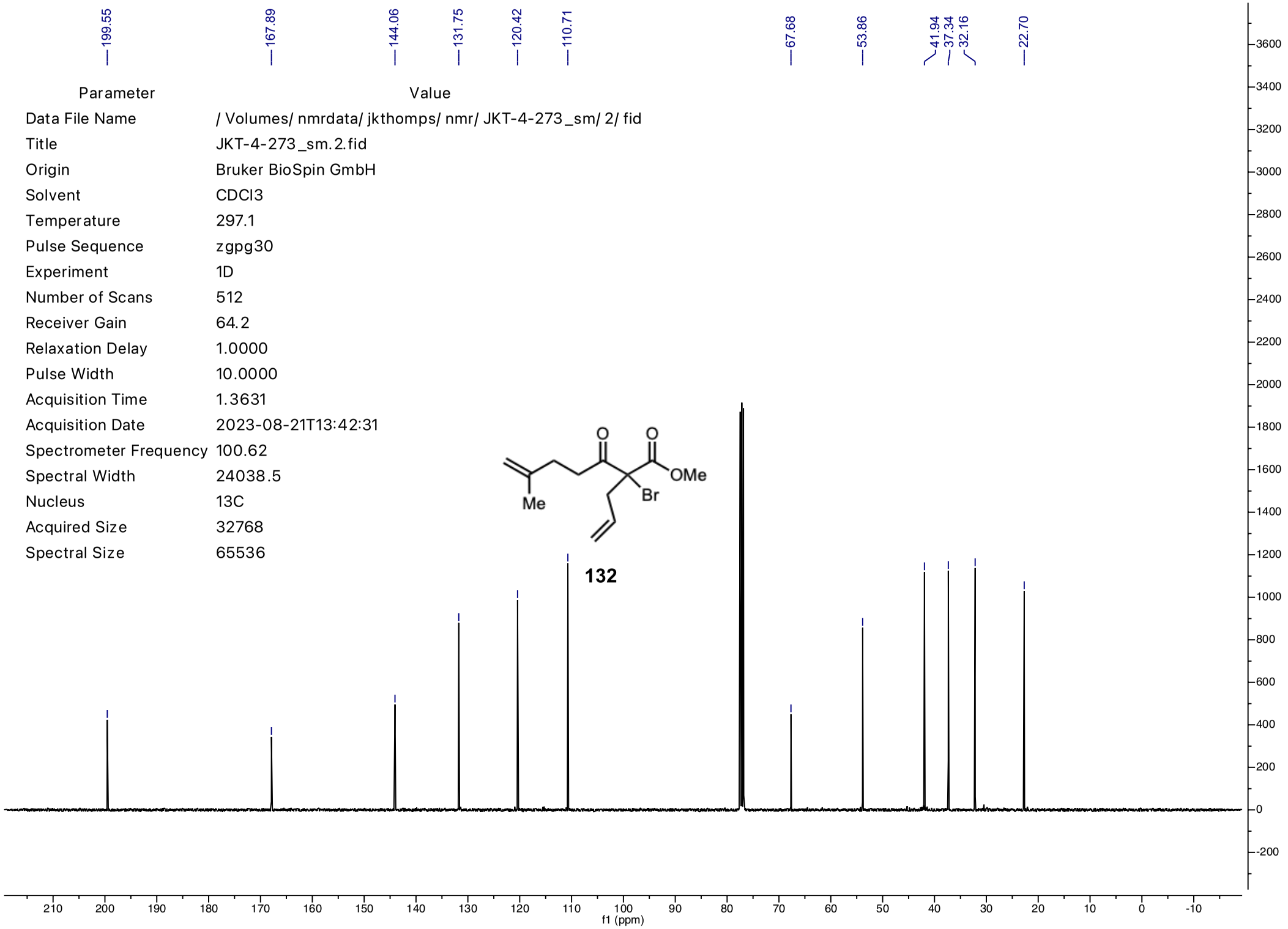
199.55
167.89
144.06
131.75
120.42
110.71
67.68
53.86
41.94
37.34
32.16
22.70
Parameter
Value
Data File Name
/ Volumes/ nmrdata/ jkthomps/ nmr/ JKT-4-273_sm/ 2/ fid
Title
JKT-4-273_sm.2.fid
Origin
Bruker BioSpin GmbH
Solvent
CDCl3
Temperature
297.1
Pulse Sequence
zgpg30
Experiment
1D
Number of Scans
512
Receiver Gain
64.2
Relaxation Delay
1.0000
Pulse Width
10.0000
Acquisition Time
1.3631
Acquisition Date
2023-08-21T13:42:31
Spectrometer Frequency
100.62
Spectral Width
24038.5
Nucleus
13C
Acquired Size
32768
Spectral Size
65536
O
O
OMe
Br
Me
132
f1 (ppm)

Parameter	Value
Data File Name	/ Volumes/ nmrdata/ jkthomps/ nmr/ JKT-4-269-3_pure/ 1/ fid
Title	JKT-4-269-3_pure.1.fid
Origin	Bruker BioSpin GmbH
Solvent	CDCl3
Temperature	297.2
Pulse Sequence	zg30
Experiment	1D
Number of Scans	16
Receiver Gain	197.4
Relaxation Delay	1.0000
Pulse Width	12.5000
Acquisition Time	4.0894
Acquisition Date	2023-08-17T18:51:03
Spectrometer Frequency	400.13
Spectral Width	8012.8
Nucleus	1H
Acquired Size	32768
Spectral Size	65536

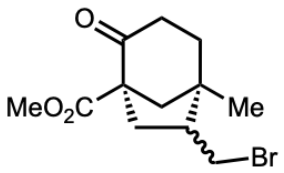

130

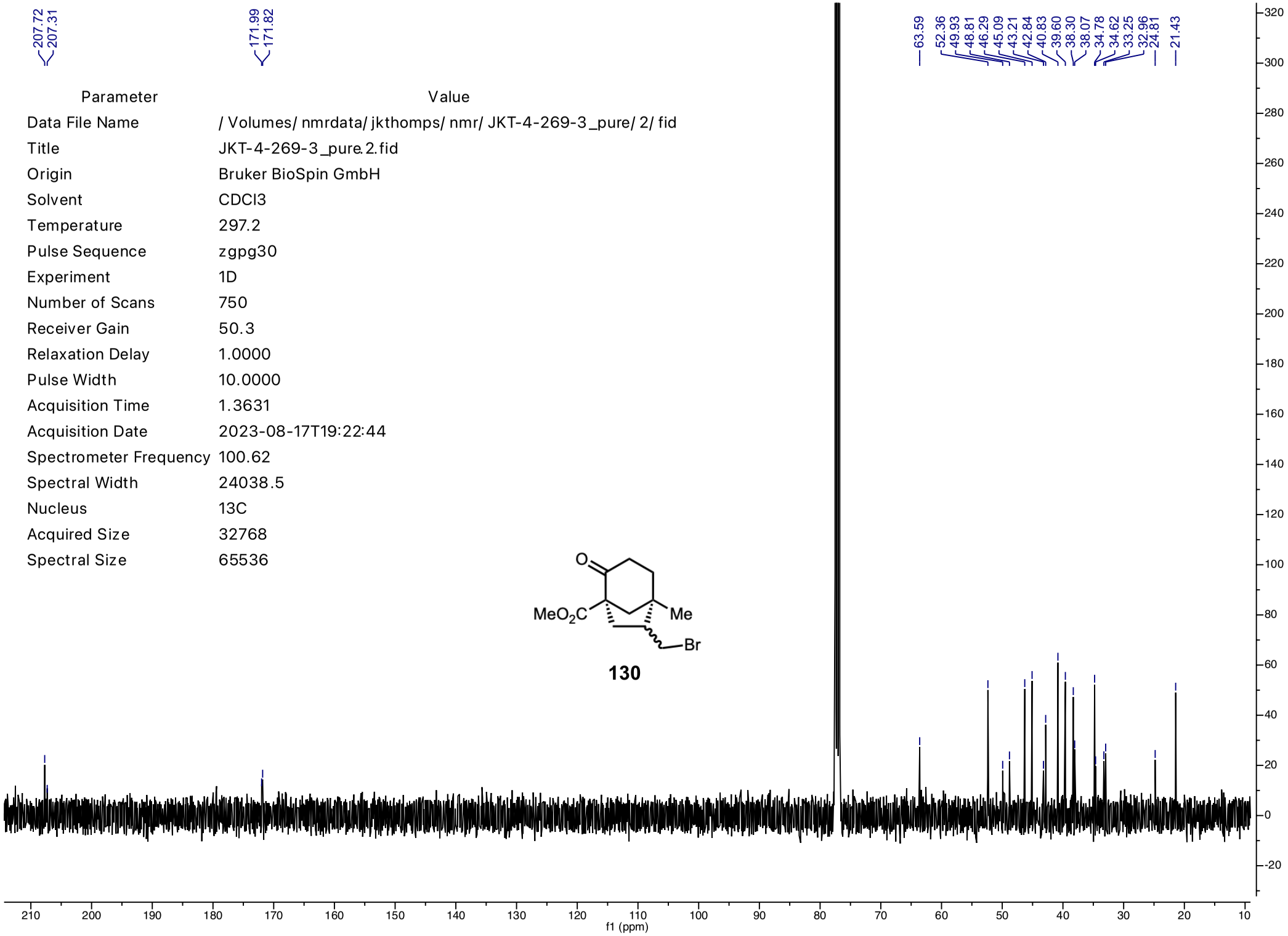
207.72
207.31
171.99
171.82
63.59
52.36
49.93
48.81
46.29
45.09
43.21
42.84
40.83
39.60
38.30
38.07
34.78
34.62
33.25
32.96
24.81
21.43
Parameter
Value
Data File Name
/ Volumes/ nmrdata/ jkthomps/ nmr/ JKT-4-269-3_pure/ 2/ fid
Title
JKT-4-269-3_pure.2.fid
Origin
Bruker BioSpin GmbH
Solvent
CDCl3
Temperature
297.2
Pulse Sequence
zgpg30
Experiment
1D
Number of Scans
750
Receiver Gain
50.3
Relaxation Delay
1.0000
Pulse Width
10.0000
Acquisition Time
1.3631
Acquisition Date
2023-08-17T19:22:44
Spectrometer Frequency
100.62
Spectral Width
24038.5
Nucleus
13C
Acquired Size
32768
Spectral Size
65536
O
MeO2C
Me
Br
130
f1 (ppm)

Parameter	Value
Data File Name	/ Volumes/ nmrdata/ jkthomps/ nmr/ JKT-4-279_pdt_std_char/ 1/ fid
Title	JKT-4-279_pdt_std_char.1.fid
Origin	Bruker BioSpin GmbH
Solvent	CDCl3
Temperature	297.1
Pulse Sequence	zg30
Experiment	1D
Number of Scans	16
Receiver Gain	197.4
Relaxation Delay	1.0000
Pulse Width	12.5000
Acquisition Time	4.0894
Acquisition Date	2023-08-25T14:17:16
Spectrometer Frequency	400.13
Spectral Width	8012.8
Nucleus	1H
Acquired Size	32768
Spectral Size	65536

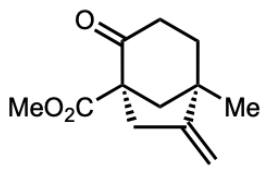

131'

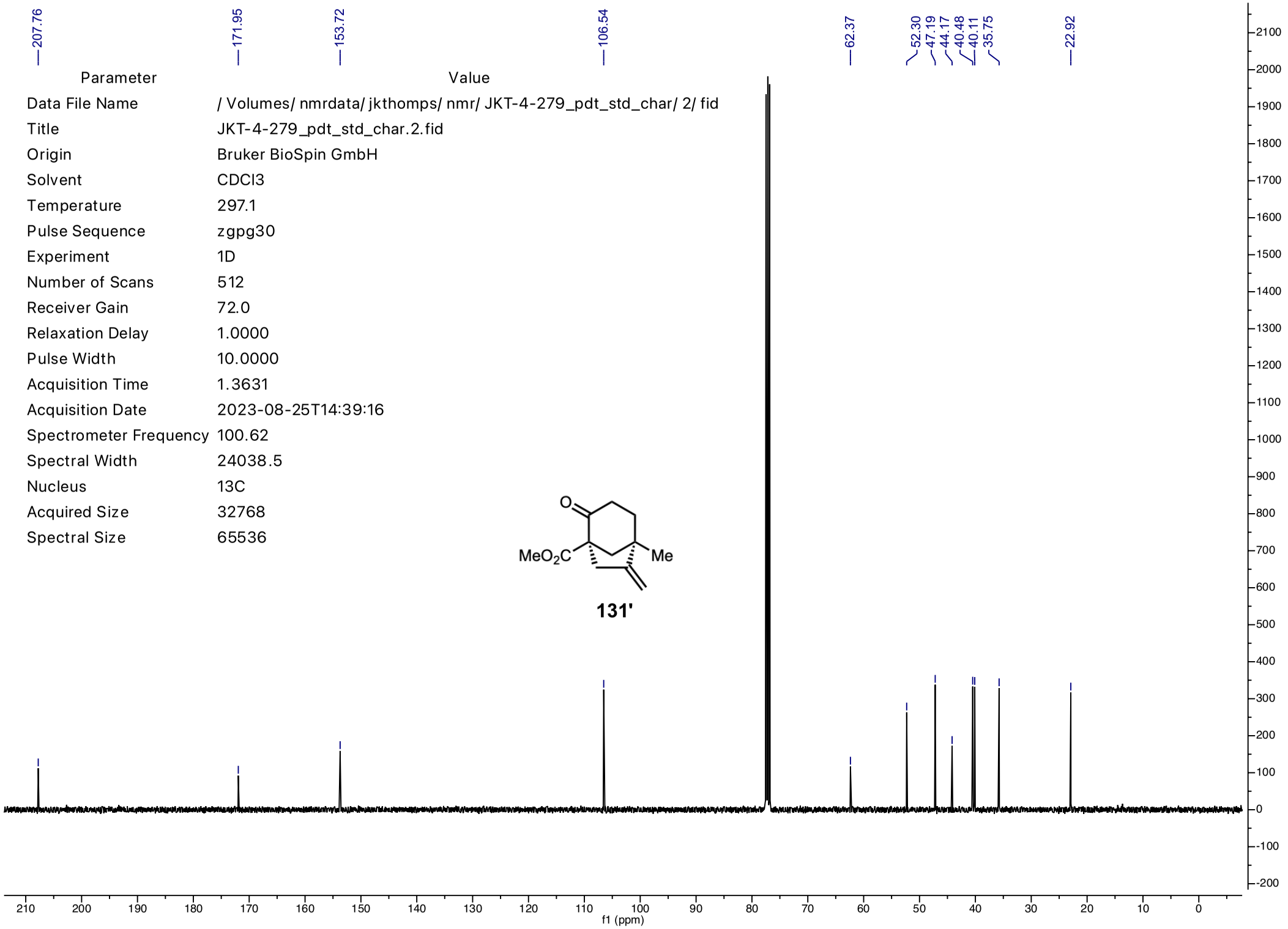
207.76
171.95
153.72
106.54
62.37
52.30
47.19
44.17
40.48
40.11
35.75
22.92
Parameter
Value
Data File Name / Volumes/ nmrdata/ jkthomps/ nmr/ JKT-4-279_pdt_std_char/ 2/ fid
Title JKT-4-279_pdt_std_char.2.fid
Origin Bruker BioSpin GmbH
Solvent CDCl3
Temperature 297.1
Pulse Sequence zgpg30
Experiment 1D
Number of Scans 512
Receiver Gain 72.0
Relaxation Delay 1.0000
Pulse Width 10.0000
Acquisition Time 1.3631
Acquisition Date 2023-08-25T14:39:16
Spectrometer Frequency 100.62
Spectral Width 24038.5
Nucleus 13C
Acquired Size 32768
Spectral Size 65536
O
MeO2C
Me
131'
f1 (ppm)

Parameter	Value
Data File Name	/ Volumes/ nmrdata/ jkthomps/ nmr/ JKT-4-276_distilled/ 1/ fid
Title	JKT-4-276_distilled.1.fid
Origin	Bruker BioSpin GmbH
Solvent	CDCl3
Temperature	297.1
Pulse Sequence	zg30
Experiment	1D
Number of Scans	16
Receiver Gain	87.8
Relaxation Delay	1.0000
Pulse Width	12.5000
Acquisition Time	4.0894
Acquisition Date	2023-08-26T18:50:00
Spectrometer Frequency	400.13
Spectral Width	8012.8
Nucleus	1H
Acquired Size	32768
Spectral Size	65536

134

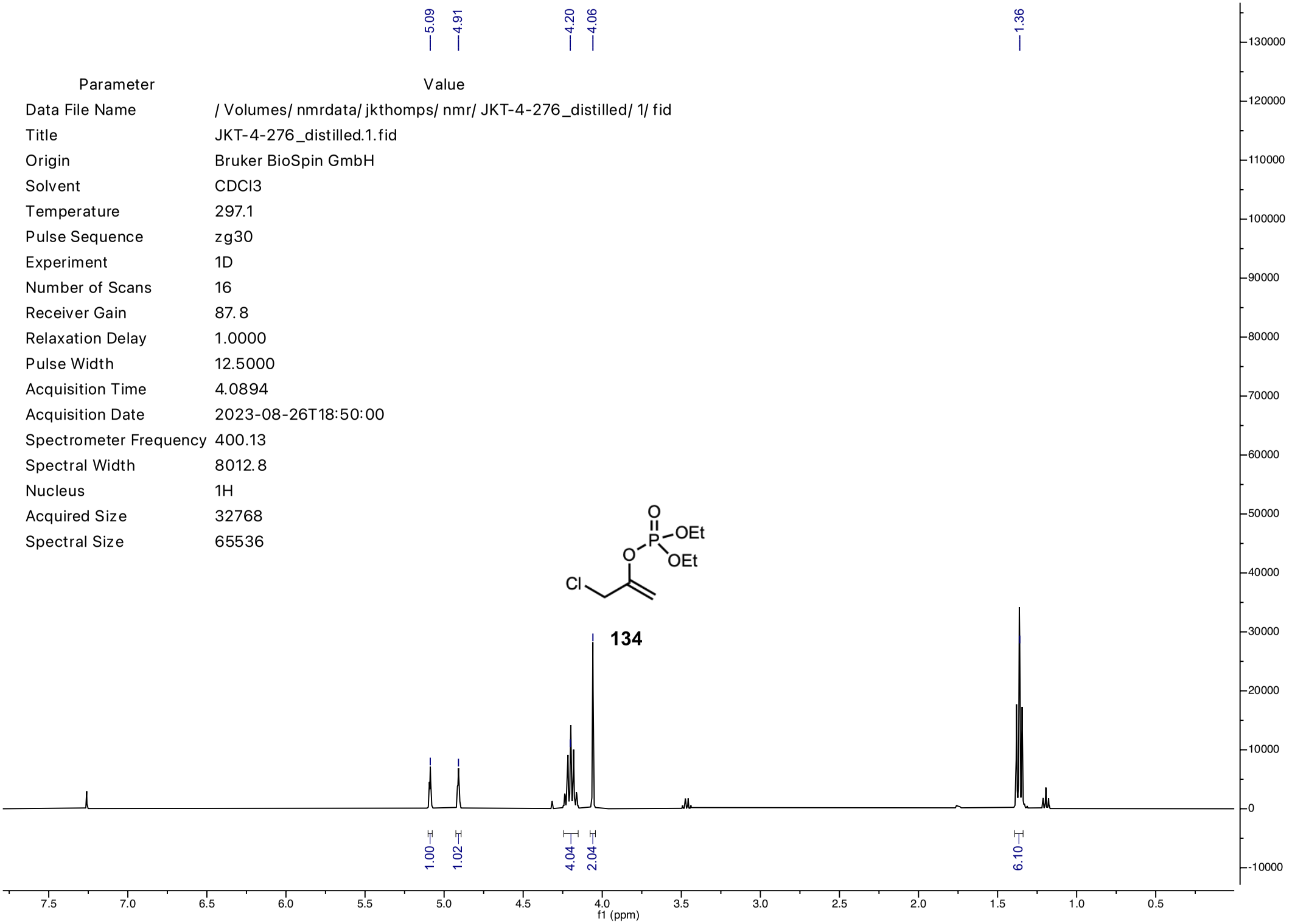

Parameter	Value
Data File Name	/ Volumes/ nmrdata/ jkthomps/ nmr/ JKT-4-276_distilled/ 2/ fid
Title	JKT-4-276_distilled.2.fid
Origin	Bruker BioSpin GmbH
Solvent	CDCl3
Temperature	297.2
Pulse Sequence	zgpg30
Experiment	1D
Number of Scans	16
Receiver Gain	197.4
Relaxation Delay	2.0000
Pulse Width	12.0000
Acquisition Time	0.5112
Acquisition Date	2023-08-26T18:52:01
Spectrometer Frequency	161.97
Spectral Width	64102.6
Nucleus	31P
Acquired Size	32768
Spectral Size	65536

134

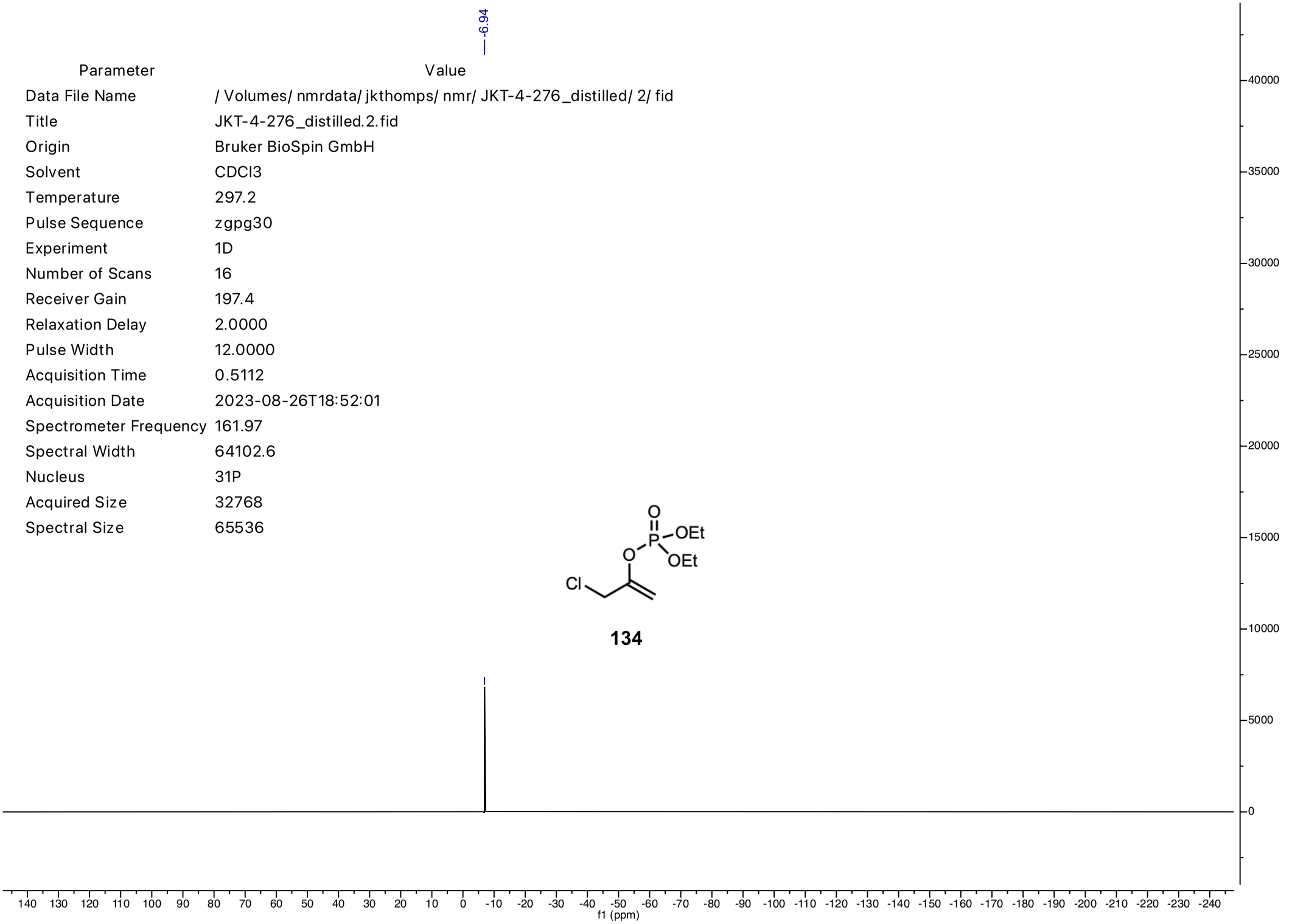

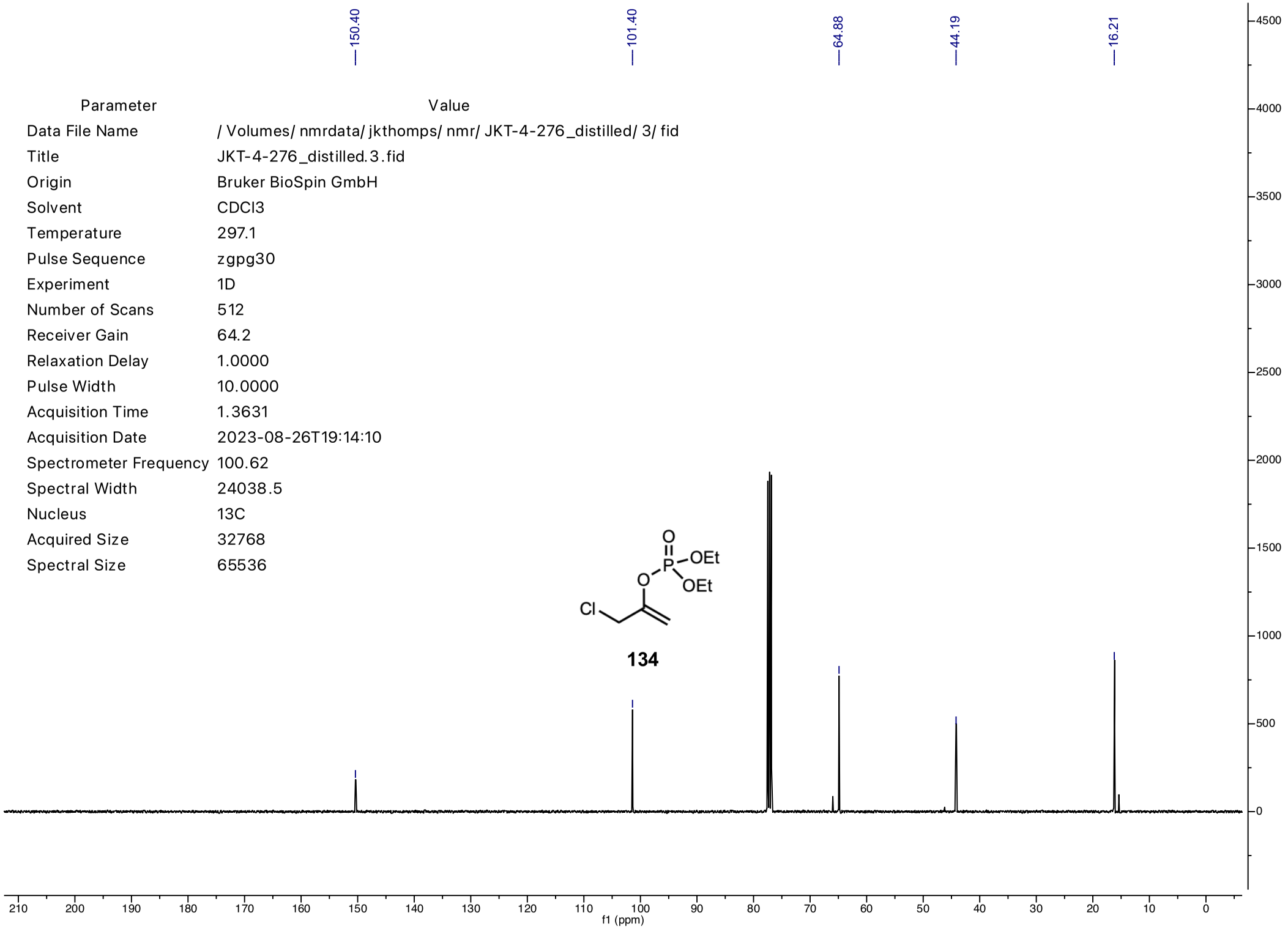

Parameter	Value
Data File Name	/ Volumes/ nmrdata/ jkthomps/ nmr/ JKT-4-276_distilled/ 3/ fid
Title	JKT-4-276_distilled.3.fid
Origin	Bruker BioSpin GmbH
Solvent	CDCl3
Temperature	297.1
Pulse Sequence	zgpg30
Experiment	1D
Number of Scans	512
Receiver Gain	64.2
Relaxation Delay	1.0000
Pulse Width	10.0000
Acquisition Time	1.3631
Acquisition Date	2023-08-26T19:14:10
Spectrometer Frequency	100.62
Spectral Width	24038.5
Nucleus	13C
Acquired Size	32768
Spectral Size	65536

134

Parameter	Value
Data File Name	/ Volumes/ nmrdata/ jkthomps/ nmr/ JKT-4-281_pure/ 1/ fid
Title	JKT-4-281_pure.1.fid
Origin	Bruker BioSpin GmbH
Solvent	CDCl3
Temperature	297.1
Pulse Sequence	zg30
Experiment	1D
Number of Scans	16
Receiver Gain	112.8
Relaxation Delay	1.0000
Pulse Width	12.5000
Acquisition Time	4.0894
Acquisition Date	2023-08-28T13:48:47
Spectrometer Frequency	400.13
Spectral Width	8012.8
Nucleus	1H
Acquired Size	32768
Spectral Size	65536

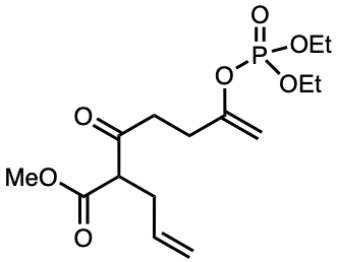

135

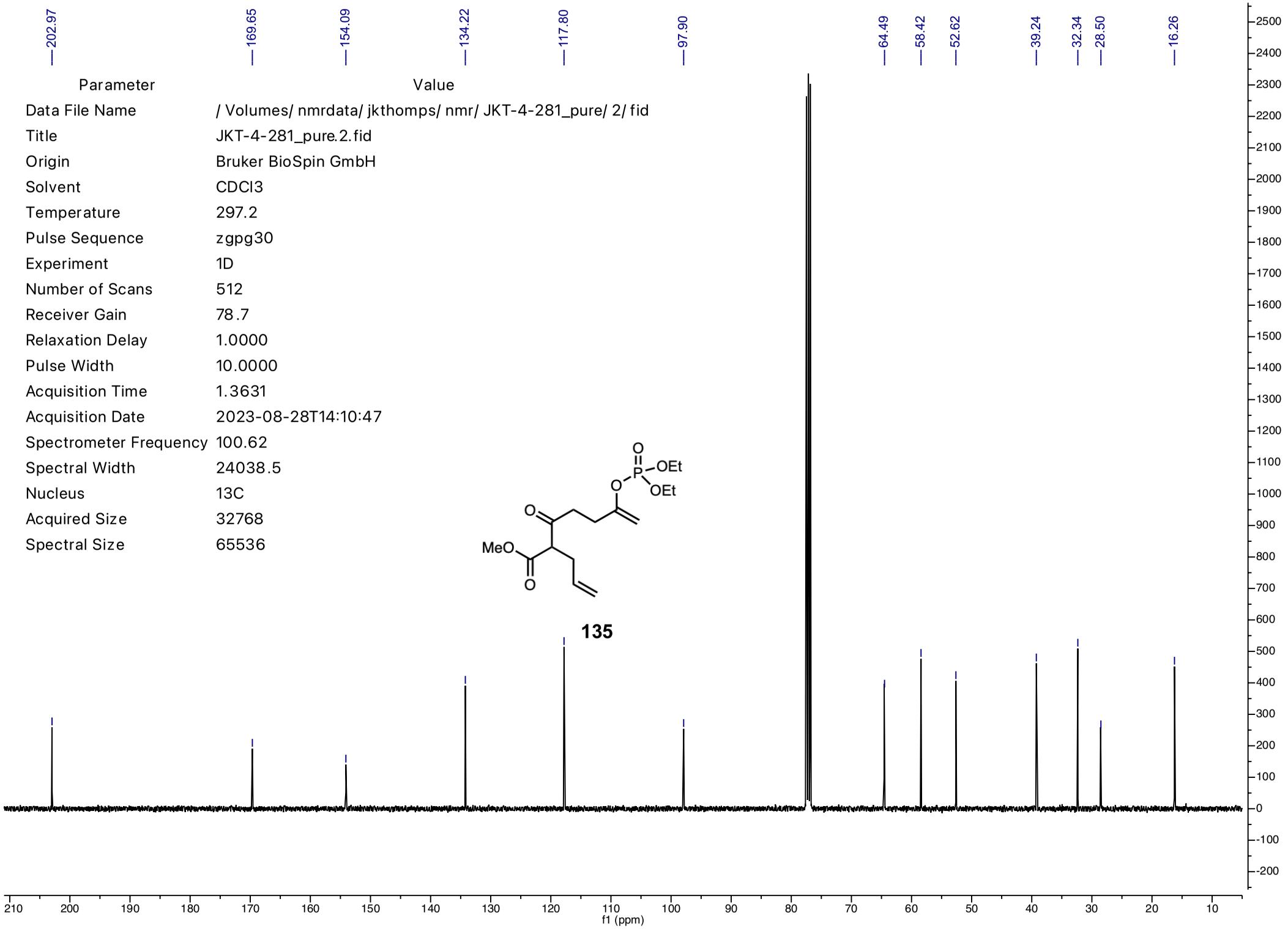
202.97
169.65
154.09
134.22
117.80
97.90
64.49
58.42
52.62
39.24
32.34
28.50
16.26
Parameter
Value
Data File Name
/ Volumes/ nmrdata/ jkthomps/ nmr/ JKT-4-281_pure/ 2/ fid
Title
JKT-4-281_pure.2.fid
Origin
Bruker BioSpin GmbH
Solvent
CDCl3
Temperature
297.2
Pulse Sequence
zgpg30
Experiment
1D
Number of Scans
512
Receiver Gain
78.7
Relaxation Delay
1.0000
Pulse Width
10.0000
Acquisition Time
1.3631
Acquisition Date
2023-08-28T14:10:47
Spectrometer Frequency
100.62
Spectral Width
24038.5
Nucleus
13C
Acquired Size
32768
Spectral Size
65536
O
P
OEt
OEt
O
O
MeO
O
135
f1 (ppm)

Parameter	Value
Data File Name	/ Volumes/ nmrdata-1/ jkthomps/ nmr/ JKT-4-284_pure/ 1/ fid
Title	JKT-4-284_pure.1.fid
Origin	Bruker BioSpin GmbH
Solvent	CDCl3
Temperature	297.2
Pulse Sequence	zg30
Experiment	1D
Number of Scans	16
Receiver Gain	78.7
Relaxation Delay	1.0000
Pulse Width	12.5000
Acquisition Time	4.0894
Acquisition Date	2023-08-30T09:10:22
Spectrometer Frequency	400.13
Spectral Width	8012.8
Nucleus	1H
Acquired Size	32768
Spectral Size	65536

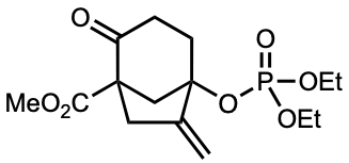

136

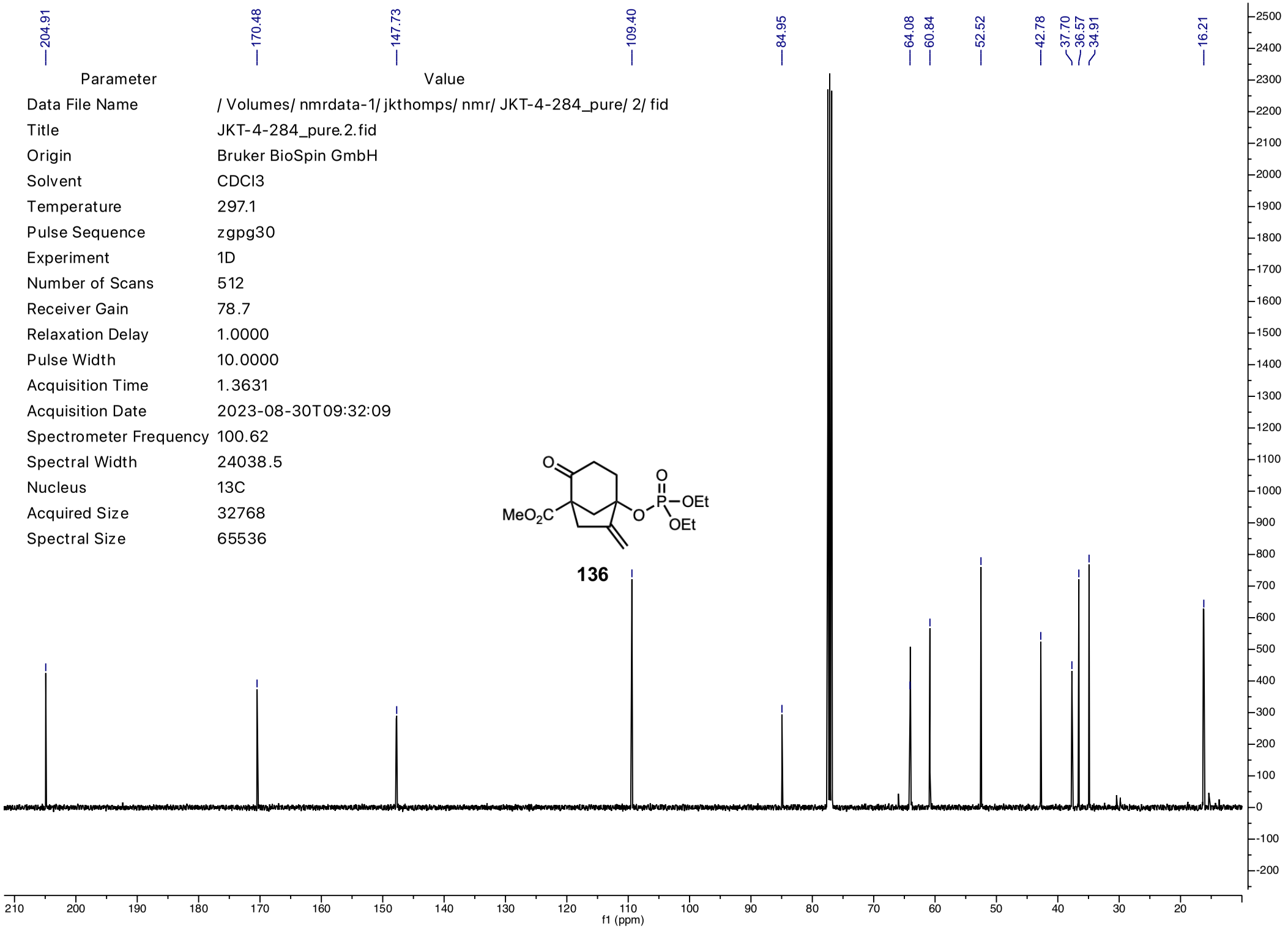

Parameter	Value
Data File Name	/ Volumes/ nmrdata-1/ jkthomps/ nmr/ JKT-4-284_pure/ 2/ fid
Title	JKT-4-284_pure.2.fid
Origin	Bruker BioSpin GmbH
Solvent	CDCl3
Temperature	297.1
Pulse Sequence	zgpg30
Experiment	1D
Number of Scans	512
Receiver Gain	78.7
Relaxation Delay	1.0000
Pulse Width	10.0000
Acquisition Time	1.3631
Acquisition Date	2023-08-30T09:32:09
Spectrometer Frequency	100.62
Spectral Width	24038.5
Nucleus	13C
Acquired Size	32768
Spectral Size	65536

136

Parameter	Value
Data File Name	/ Volumes/ nmrdata/ jkthomps/ nmr/ JKT-4-299_pure/ 1/ fid
Title	JKT-4-299_pure.1.fid
Origin	Bruker BioSpin GmbH
Solvent	CDCl3
Temperature	297.1
Pulse Sequence	zg30
Experiment	1D
Number of Scans	16
Receiver Gain	98.9
Relaxation Delay	1.0000
Pulse Width	12.5000
Acquisition Time	4.0894
Acquisition Date	2023-09-05T00:27:13
Spectrometer Frequency	400.13
Spectral Width	8012.8
Nucleus	1H
Acquired Size	32768
Spectral Size	65536

138

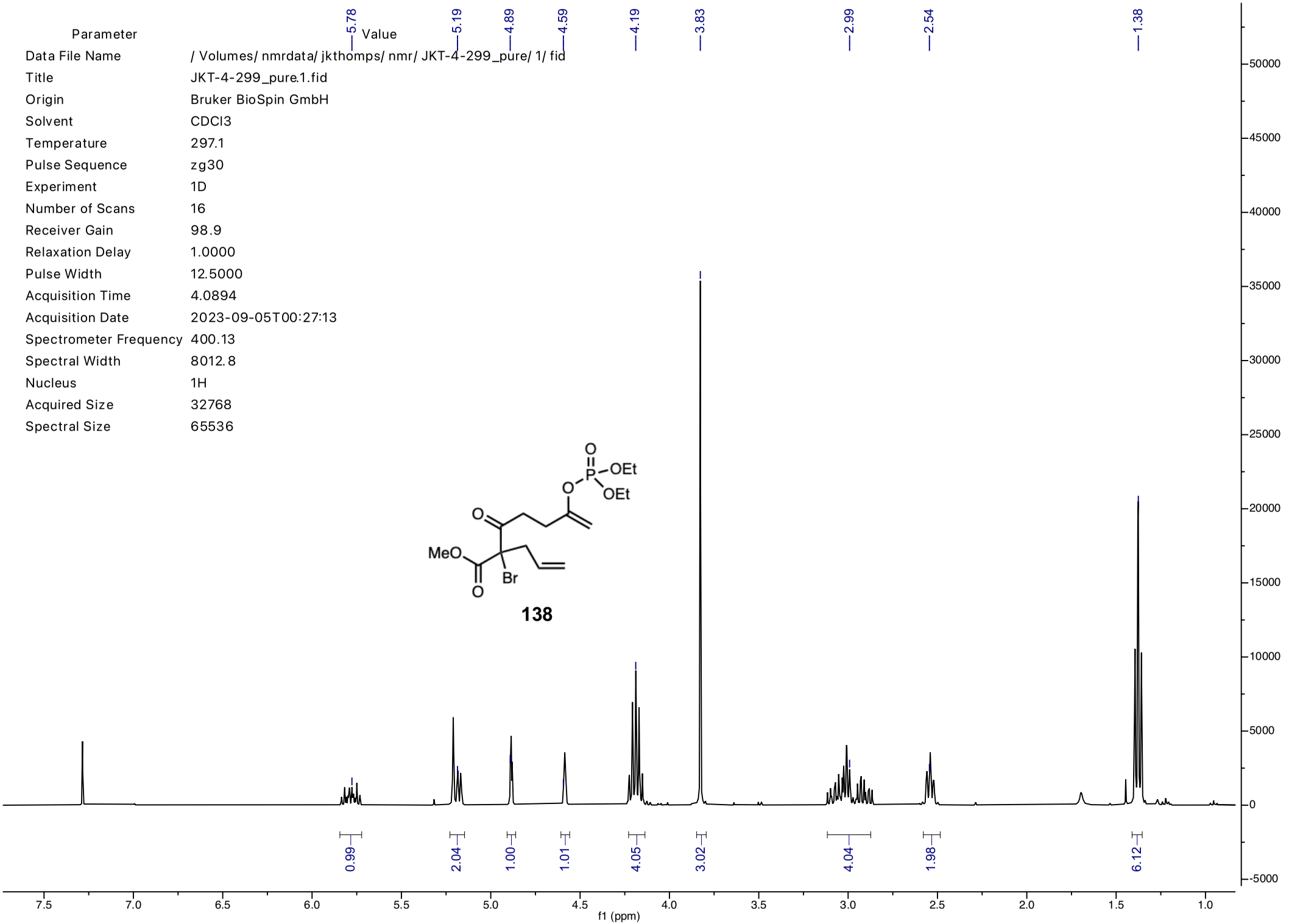

198.70
167.75
153.83
153.75
131.60
120.55
98.15
98.11
67.28
64.57
64.51
53.94
41.90
36.14
29.59
29.53
16.27
16.20

Parameter	Value
Data File Name	/ Volumes/ nmrdata/ jkthomps/ nmr/ JKT-4-299_pure/ 2/ fid
Title	JKT-4-299_pure.2.fid
Origin	Bruker BioSpin GmbH
Solvent	CDCl3
Temperature	297.2
Pulse Sequence	zgpg30
Experiment	1D
Number of Scans	512
Receiver Gain	72.0
Relaxation Delay	1.0000
Pulse Width	10.0000
Acquisition Time	1.3631
Acquisition Date	2023-09-05T00:25:21
Spectrometer Frequency	100.62
Spectral Width	24038.5
Nucleus	13C
Acquired Size	32768
Spectral Size	65536

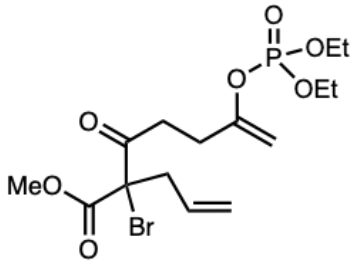

138

f1 (ppm)

Parameter	Value
Data File Name	/ Users/ jordankthompson/ Desktop/ JKT_4_293 _prepped01/ PROTON01.fid/ fid
Title	PROTON01
Origin	Varian
Solvent	cdcl3
Temperature	25.0
Pulse Sequence	s2pul
Experiment	1D
Number of Scans	8
Receiver Gain	30
Relaxation Delay	1.0000
Pulse Width	5.1000
Acquisition Time	1.7089
Acquisition Date	2023-09-02T13:41:14
Spectrometer Frequency	300.09
Spectral Width	4793.9
Nucleus	1H
Acquired Size	8192
Spectral Size	65536

139

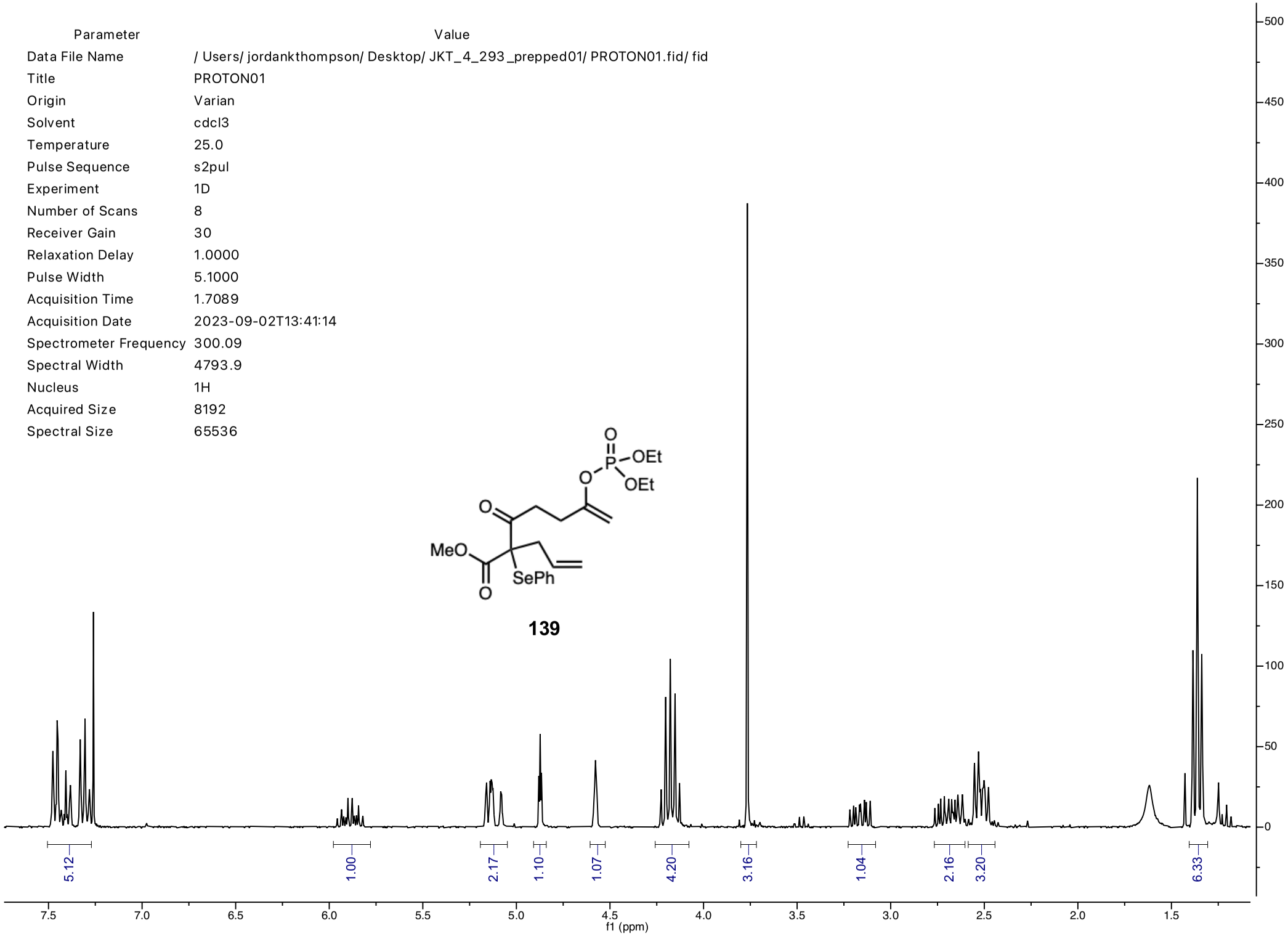

Parameter	Value
Data File Name	/ Users/ jordankthompson/ Desktop/ JKT_4_294_prepped01/ PROTON01.fid/ fid
Title	PROTON01
Origin	Varian
Solvent	cdcl3
Temperature	25.0
Pulse Sequence	s2pul
Experiment	1D
Number of Scans	8
Receiver Gain	34
Relaxation Delay	1.0000
Pulse Width	5.1000
Acquisition Time	1.7089
Acquisition Date	2023-09-02T13:43:46
Spectrometer Frequency	300.09
Spectral Width	4793.9
Nucleus	1H
Acquired Size	8192
Spectral Size	65536

140

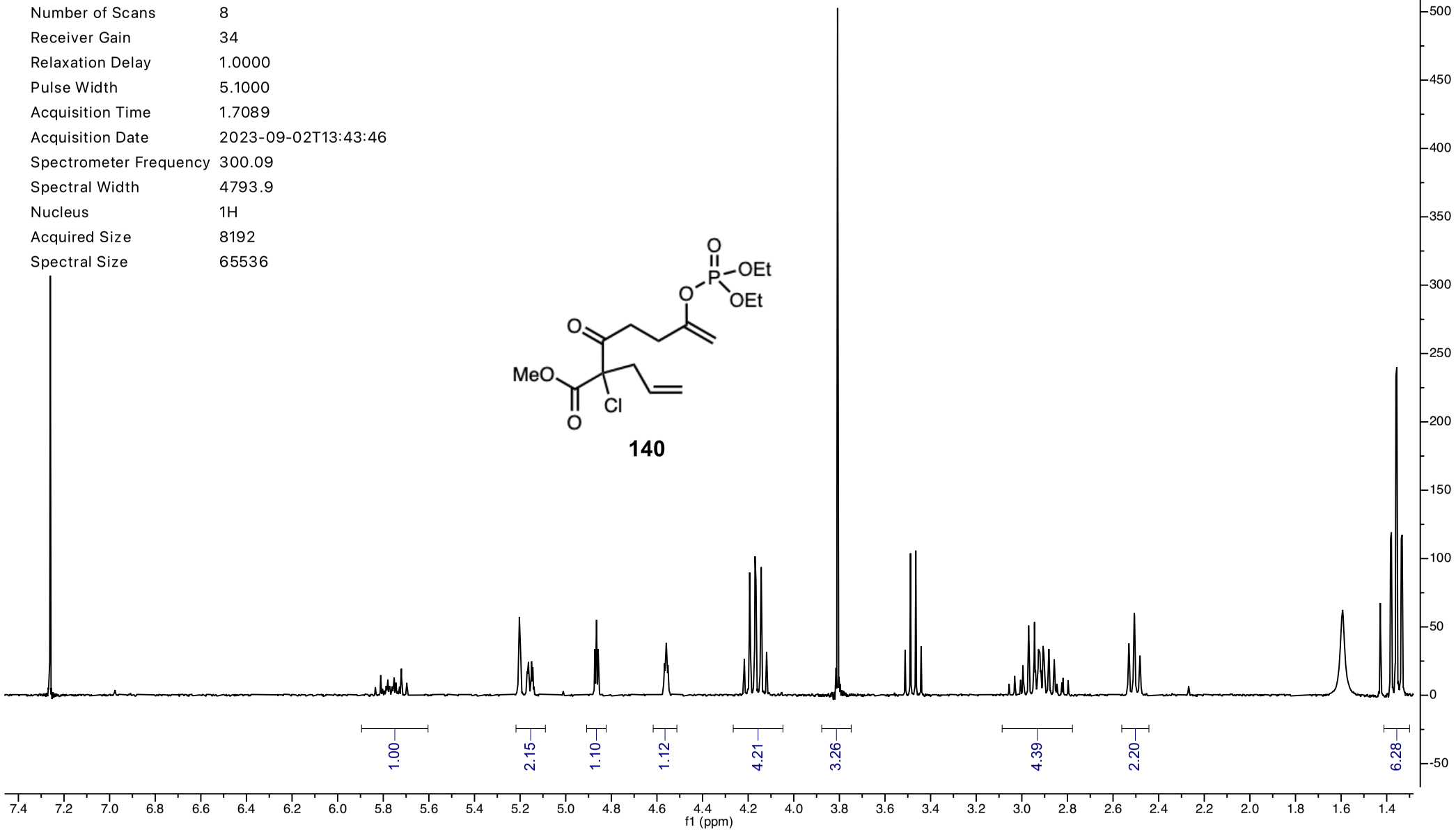

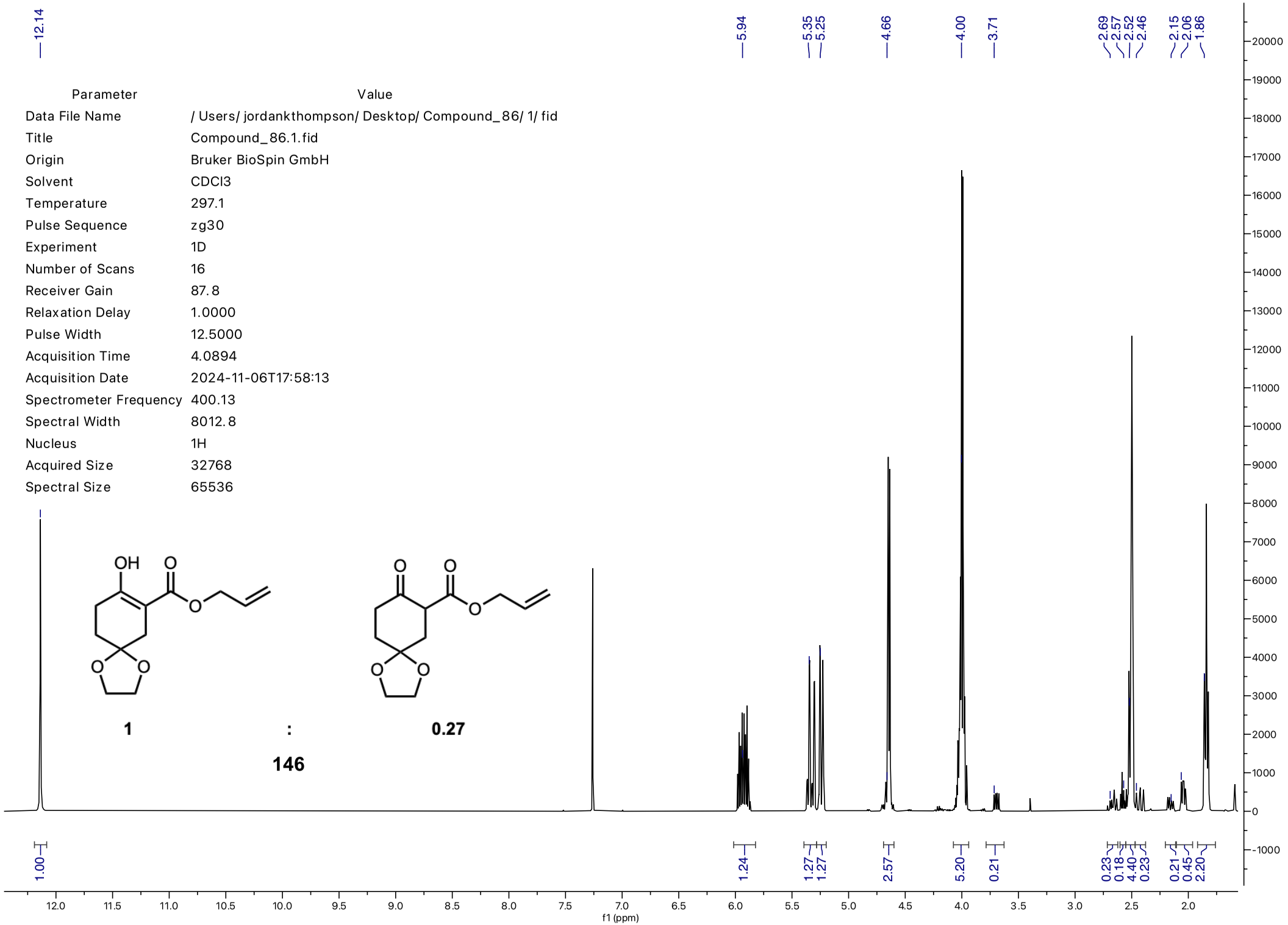
12.14
5.94
5.35
5.25
4.66
4.00
3.71
2.69
2.57
2.52
2.46
2.15
2.06
1.86
Parameter Value
Data File Name / Users/ jordankthompson/ Desktop/ Compound_86/ 1/ fid
Title Compound_86.1.fid
Origin Bruker BioSpin GmbH
Solvent CDCl3
Temperature 297.1
Pulse Sequence zg30
Experiment 1D
Number of Scans 16
Receiver Gain 87.8
Relaxation Delay 1.0000
Pulse Width 12.5000
Acquisition Time 4.0894
Acquisition Date 2024-11-06T17:58:13
Spectrometer Frequency 400.13
Spectral Width 8012.8
Nucleus 1H
Acquired Size 32768
Spectral Size 65536
OH
O
O
O
O
O
O
O
O
1
:
0.27
146
1.00
1.24
1.27
1.27
2.57
5.20
0.21
0.23
0.18
4.40
0.23
0.21
0.45
2.20
20000
19000
18000
17000
16000
15000
14000
13000
12000
11000
10000
9000
8000
7000
6000
5000
4000
3000
2000
1000
0
-1000
12.0
11.5
11.0
10.5
10.0
9.5
9.0
8.5
8.0
7.5
7.0
6.5
6.0
5.5
5.0
4.5
4.0
3.5
3.0
2.5
2.0
f1 (ppm)

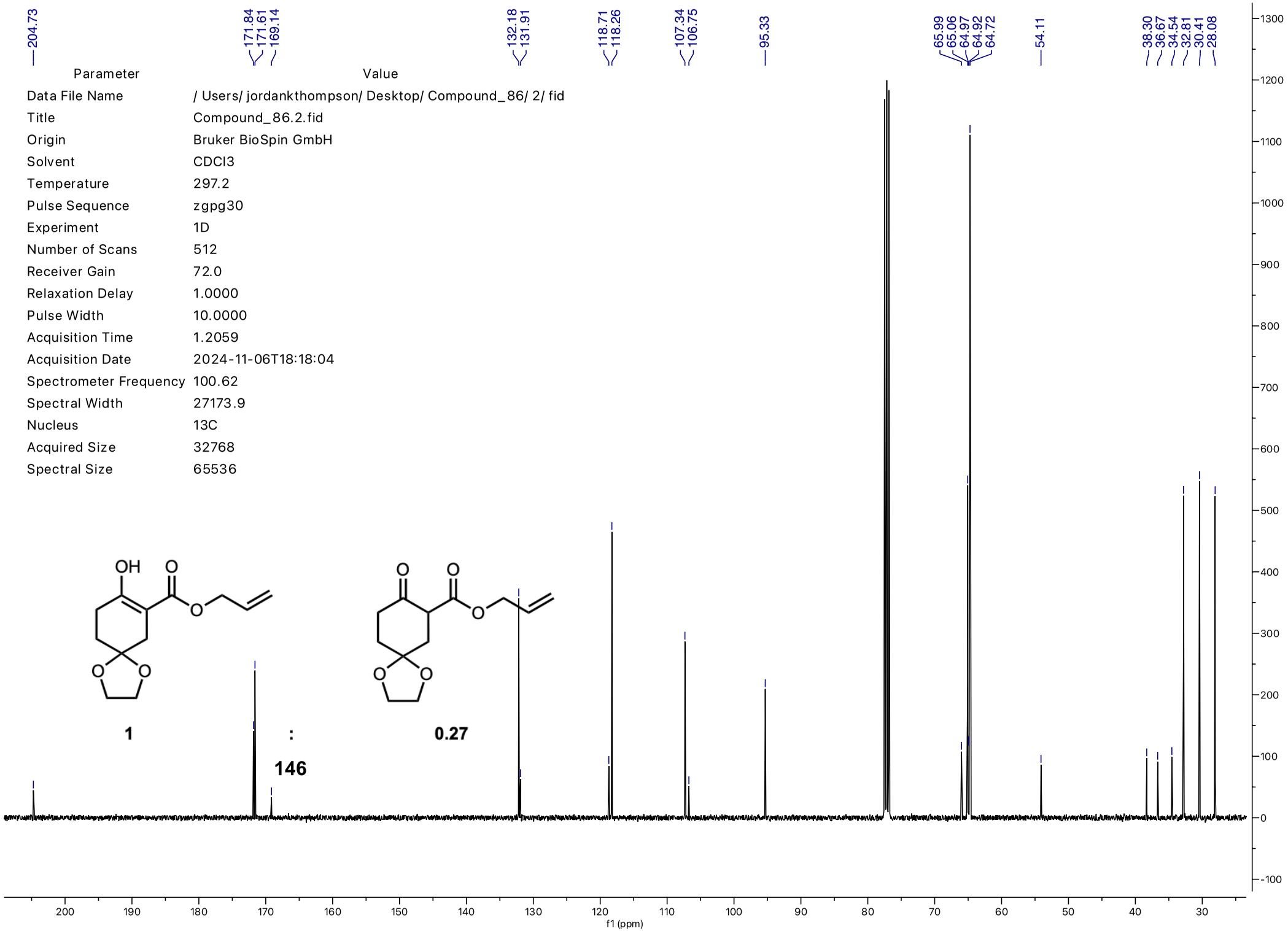
204.73
171.84
171.61
169.14
132.18
131.91
118.71
118.26
107.34
106.75
95.33
65.99
65.06
64.97
64.92
64.72
54.11
38.30
36.67
34.54
32.81
30.41
28.08
Parameter Value
Data File Name / Users/ jordankthompson/ Desktop/ Compound_86/ 2/ fid
Title Compound_86.2.fid
Origin Bruker BioSpin GmbH
Solvent CDCl3
Temperature 297.2
Pulse Sequence zgpg30
Experiment 1D
Number of Scans 512
Receiver Gain 72.0
Relaxation Delay 1.0000
Pulse Width 10.0000
Acquisition Time 1.2059
Acquisition Date 2024-11-06T18:18:04
Spectrometer Frequency 100.62
Spectral Width 27173.9
Nucleus 13C
Acquired Size 32768
Spectral Size 65536
OH
O
O
O
O
O
O
O
O
1
:
0.27
146
f1 (ppm)

Parameter	Value
Data File Name	/ Volumes/ nmrdata-1/ jkthomps/ nmr/ JKT-6-165_pure/ 1/ fid
Title	JKT-6-165_pure.1.fid
Origin	Bruker BioSpin GmbH & Co.KG
Solvent	CDCl3
Temperature	298.1
Pulse Sequence	zg30
Experiment	1D
Number of Scans	16
Receiver Gain	101.0
Relaxation Delay	1.0000
Pulse Width	9.8500
Acquisition Time	3.9977
Acquisition Date	2024-09-11T18:31:29
Spectrometer Frequency	400.15
Spectral Width	8196.7
Nucleus	1H
Acquired Size	32768
Spectral Size	65536

145A

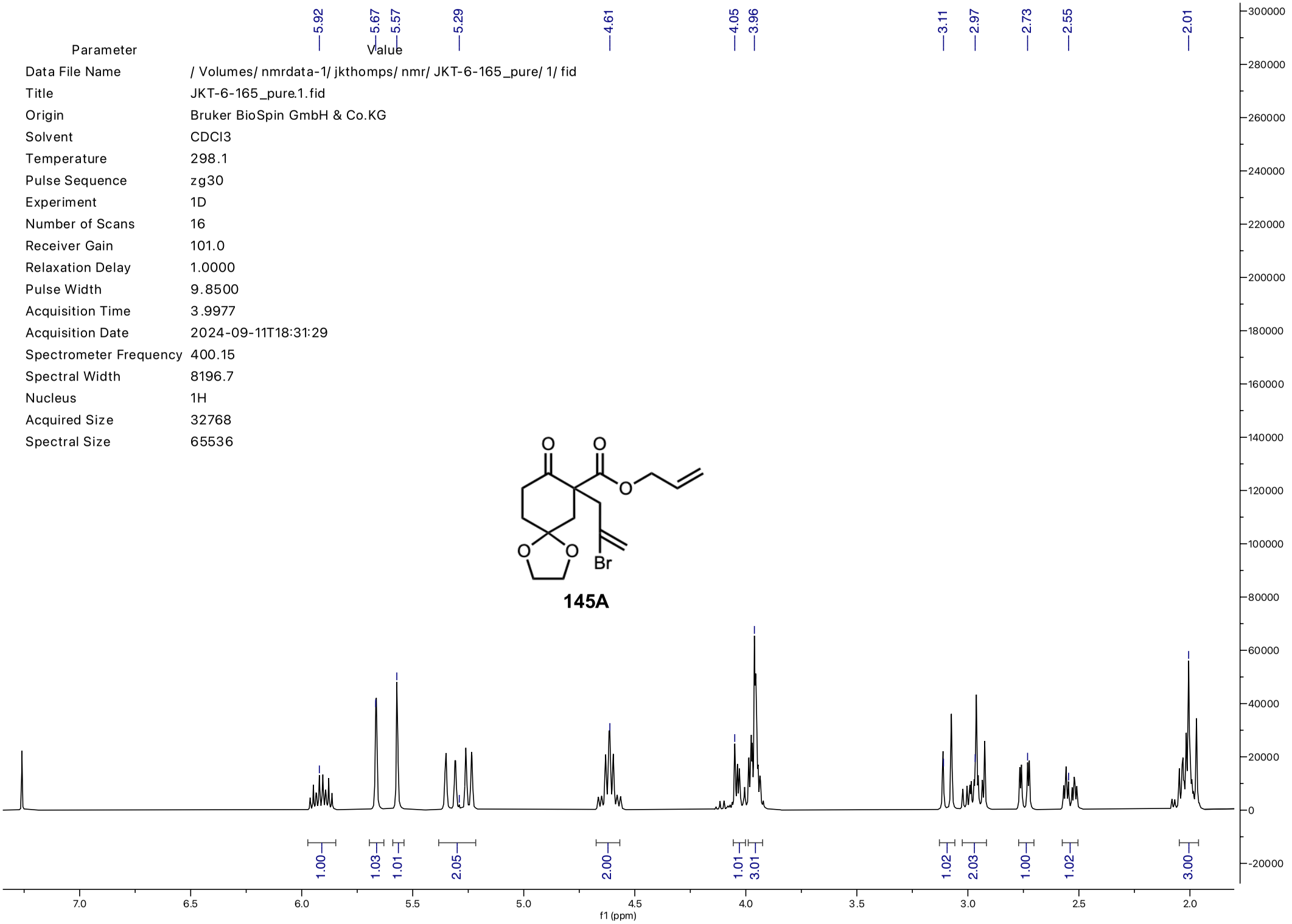

Parameter	Value
Data File Name	/ Volumes/ nmrdata-1/ jkthomps/ nmr/ JKT-6-165_pure/ 2/ fid
Title	JKT-6-165_pure.2.fid
Origin	Bruker BioSpin GmbH & Co.KG
Solvent	CDCl3
Temperature	298.1
Pulse Sequence	zgpg30
Experiment	1D
Number of Scans	512
Receiver Gain	45.2
Relaxation Delay	1.0000
Pulse Width	10.0000
Acquisition Time	1.2190
Acquisition Date	2024-09-11T18:51:21
Spectrometer Frequency	100.63
Spectral Width	26881.7
Nucleus	13C
Acquired Size	32768
Spectral Size	65536

145A

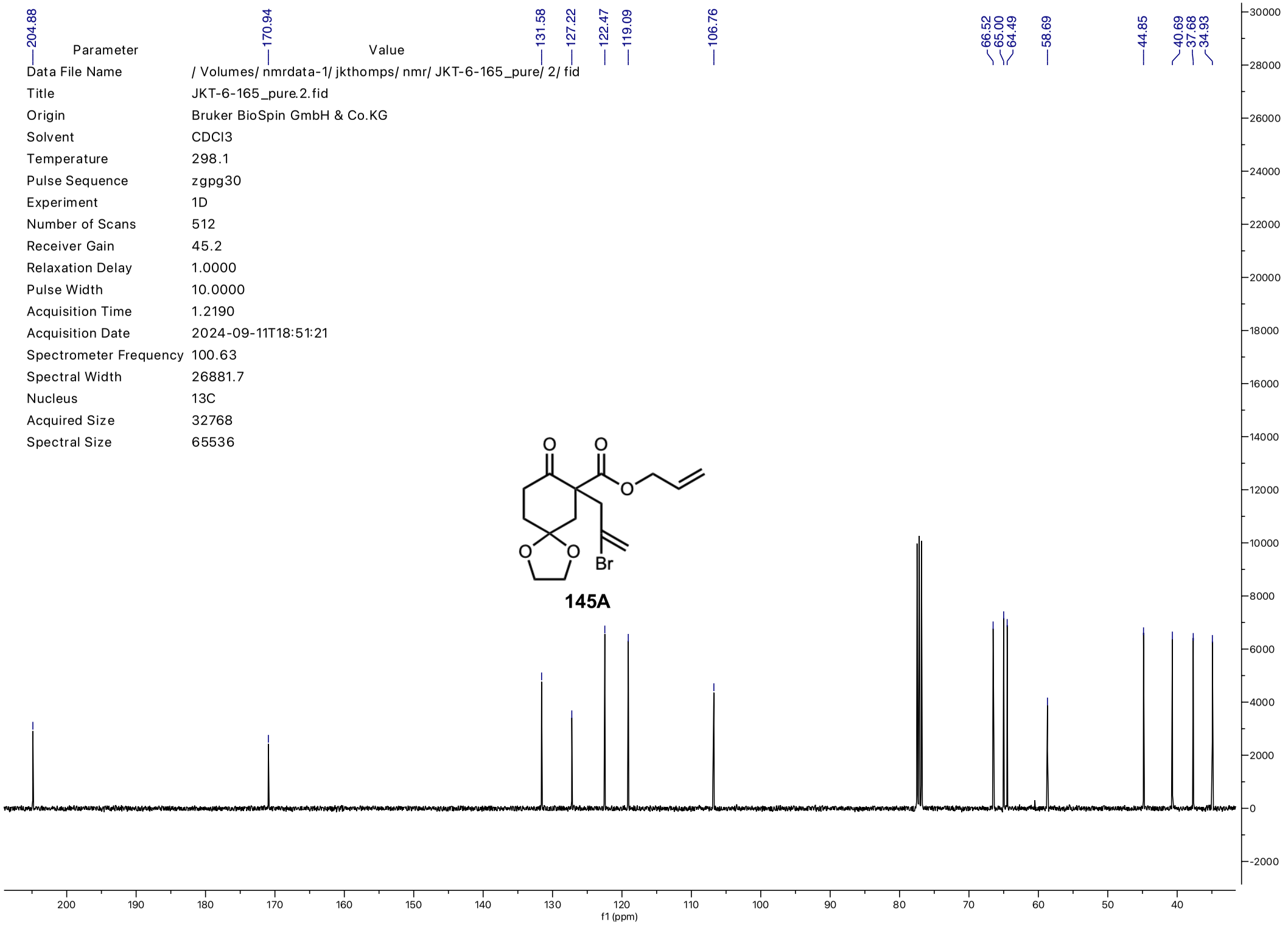

Parameter	Value
Data File Name	/ Volumes/ nmrdata/ jkthomps/ nmr/ JKT-6-167-2/ 1/ fid
Title	JKT-6-167-2.1.fid
Origin	Bruker BioSpin GmbH
Solvent	CDCl3
Temperature	297.2
Pulse Sequence	zg30
Experiment	1D
Number of Scans	16
Receiver Gain	197.4
Relaxation Delay	1.0000
Pulse Width	12.5000
Acquisition Time	4.0894
Acquisition Date	2024-09-13T06:02:43
Spectrometer Frequency	400.13
Spectral Width	8012.8
Nucleus	1H
Acquired Size	32768
Spectral Size	65536

157

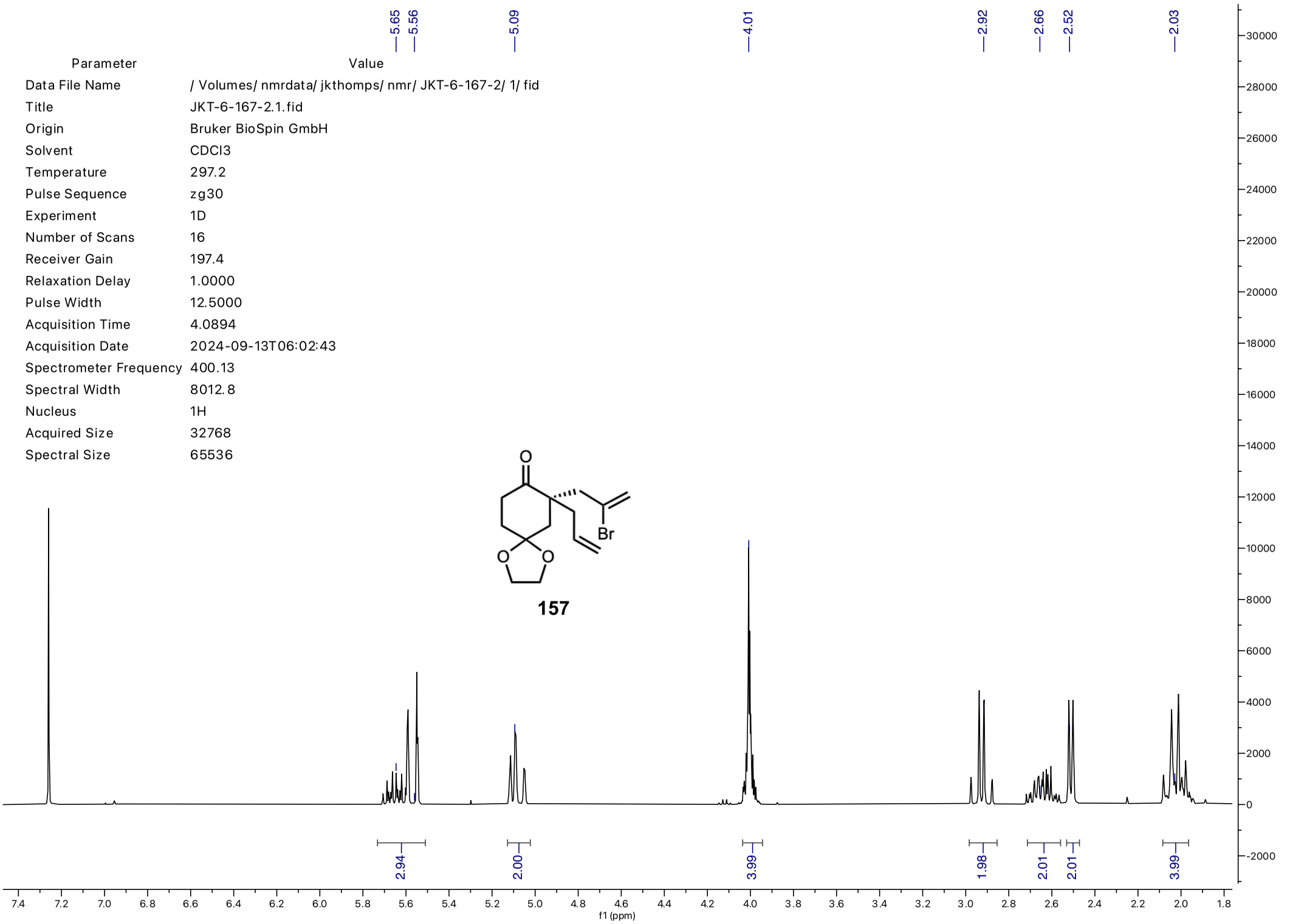

Parameter	Value
Data File Name	/ Users/ jordankthompson/ Desktop/ Compound88/ 2/ fid
Title	Compound88.2.fid
Origin	Bruker BioSpin GmbH
Solvent	CDCl3
Temperature	297.1
Pulse Sequence	zgpg30
Experiment	1D
Number of Scans	2000
Receiver Gain	72.0
Relaxation Delay	1.0000
Pulse Width	10.0000
Acquisition Time	1.1796
Acquisition Date	2024-12-22T22:21:22
Spectrometer Frequency	100.62
Spectral Width	27777.8
Nucleus	13C
Acquired Size	32768
Spectral Size	65536

157

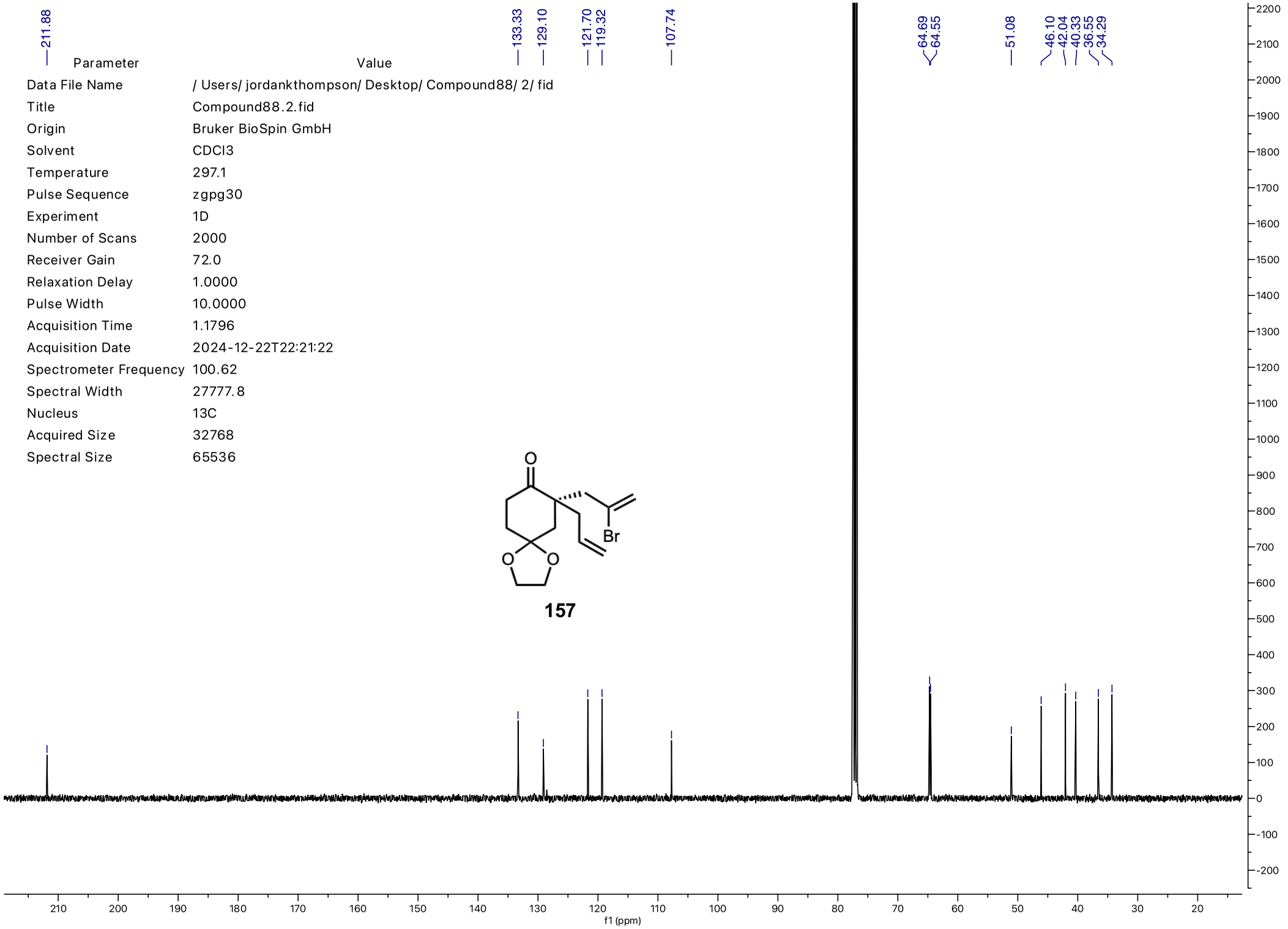

Parameter	Value
Data File Name	/ Volumes/ nmrdata-1/ jkthomps/ nmr/ JKT-6-174_pure/ 1/ fid
Title	JKT-6-174_pure.1.fid
Origin	Bruker BioSpin GmbH
Solvent	CDCl3
Temperature	297.1
Pulse Sequence	zg30
Experiment	1D
Number of Scans	16
Receiver Gain	127.1
Relaxation Delay	1.0000
Pulse Width	12.5000
Acquisition Time	4.0894
Acquisition Date	2024-09-18T14:02:43
Spectrometer Frequency	400.13
Spectral Width	8012.8
Nucleus	1H
Acquired Size	32768
Spectral Size	65536

144A

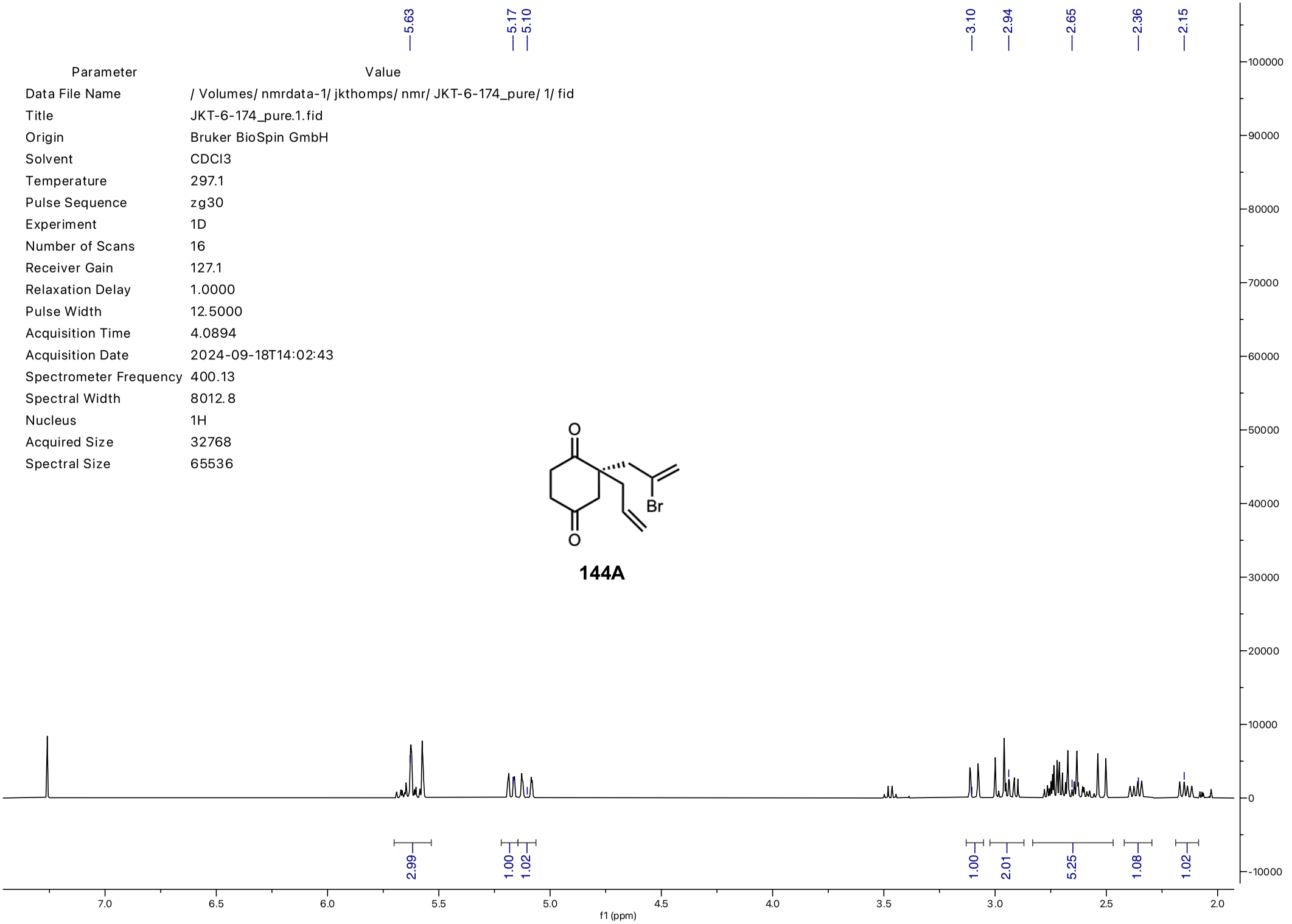

210.76
208.48
131.27
127.80
122.79
121.24
50.39
47.66
46.59
42.64
37.97
35.94

Parameter	Value
Data File Name	/ Volumes/ nmrdata/ jkthomps/ nmr/ JKT-6-174_pure/ 2/ fid
Title	JKT-6-174_pure.2.fid
Origin	Bruker BioSpin GmbH
Solvent	CDCl3
Temperature	297.2
Pulse Sequence	zgpg30
Experiment	1D
Number of Scans	512
Receiver Gain	55.5
Relaxation Delay	1.0000
Pulse Width	10.0000
Acquisition Time	1.2059
Acquisition Date	2024-09-18T14:22:35
Spectrometer Frequency	100.62
Spectral Width	27173.9
Nucleus	13C
Acquired Size	32768
Spectral Size	65536

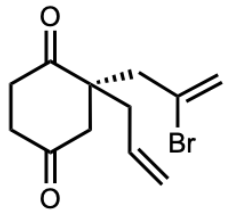

144A

f1 (ppm)

Parameter	Value
Data File Name	/ Volumes/ nmrdata/ jkthomps/ nmr/ JKT-6-203A-1/ 1/ fid
Title	JKT-6-203A-1.1.fid
Origin	Bruker BioSpin GmbH
Solvent	CDCl3
Temperature	297.2
Pulse Sequence	zg30
Experiment	1D
Number of Scans	16
Receiver Gain	197.4
Relaxation Delay	1.0000
Pulse Width	12.5000
Acquisition Time	4.0894
Acquisition Date	2024-10-20T10:52:57
Spectrometer Frequency	400.13
Spectral Width	8012.8
Nucleus	1H
Acquired Size	32768
Spectral Size	65536

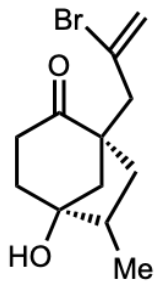

162

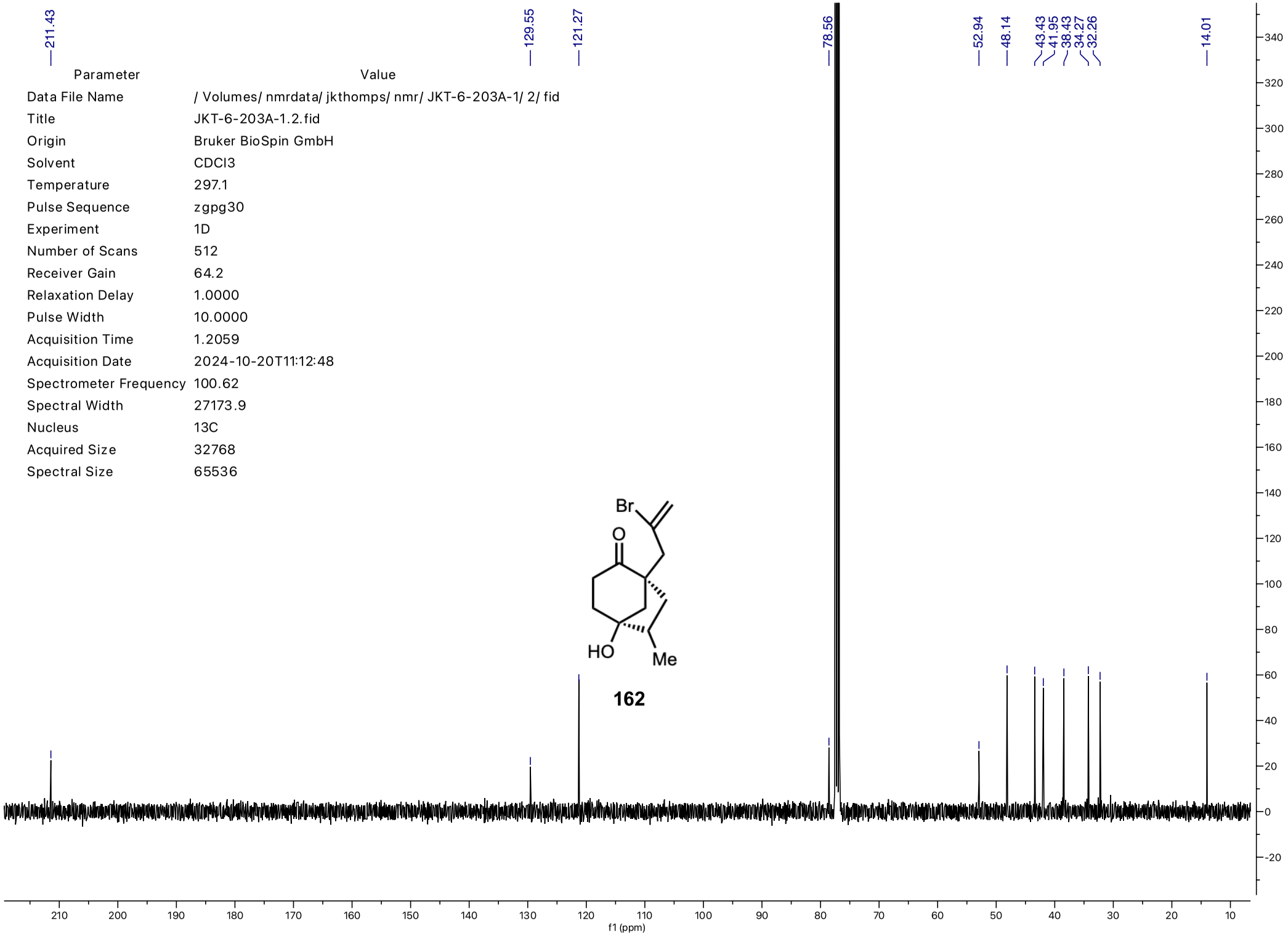
211.43
129.55
121.27
78.56
52.94
48.14
43.43
41.95
38.43
34.27
32.26
14.01
Parameter Value
Data File Name / Volumes/ nmrdata/ jkthomps/ nmr/ JKT-6-203A-1/ 2/ fid
Title JKT-6-203A-1.2.fid
Origin Bruker BioSpin GmbH
Solvent CDCl3
Temperature 297.1
Pulse Sequence zgpg30
Experiment 1D
Number of Scans 512
Receiver Gain 64.2
Relaxation Delay 1.0000
Pulse Width 10.0000
Acquisition Time 1.2059
Acquisition Date 2024-10-20T11:12:48
Spectrometer Frequency 100.62
Spectral Width 27173.9
Nucleus 13C
Acquired Size 32768
Spectral Size 65536
Br
O
HO
Me
162
f1 (ppm)

Parameter	Value
Data File Name	/ Volumes/ nmrdata/ jkthomps/ nmr/ JKT-6-203A-1/ 3/ ser
Title	JKT-6-203A-1.3.ser
Origin	Bruker BioSpin GmbH
Solvent	CDCl3
Temperature	297.1
Pulse Sequence	cosygpppqf
Experiment	COSY
Number of Scans	1
Receiver Gain	197.4
Relaxation Delay	1.7956
Pulse Width	12.5000
Acquisition Time	0.4014
Acquisition Date	2024-10-20T11:18:32
Spectrometer Frequency	(400.13,400.13)
Spectral Width	(2551.0,2551.0)
Lowest Frequency	(19.5,25.1)
Nucleus	(1H,1H)
Acquired Size	(1024,128)
Spectral Size	(1024,1024)
Digital Resolution	(2.49,2.49)

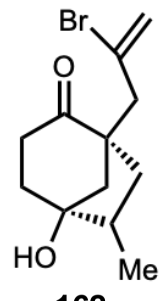

162

f2 (ppm)

f1 (ppm)

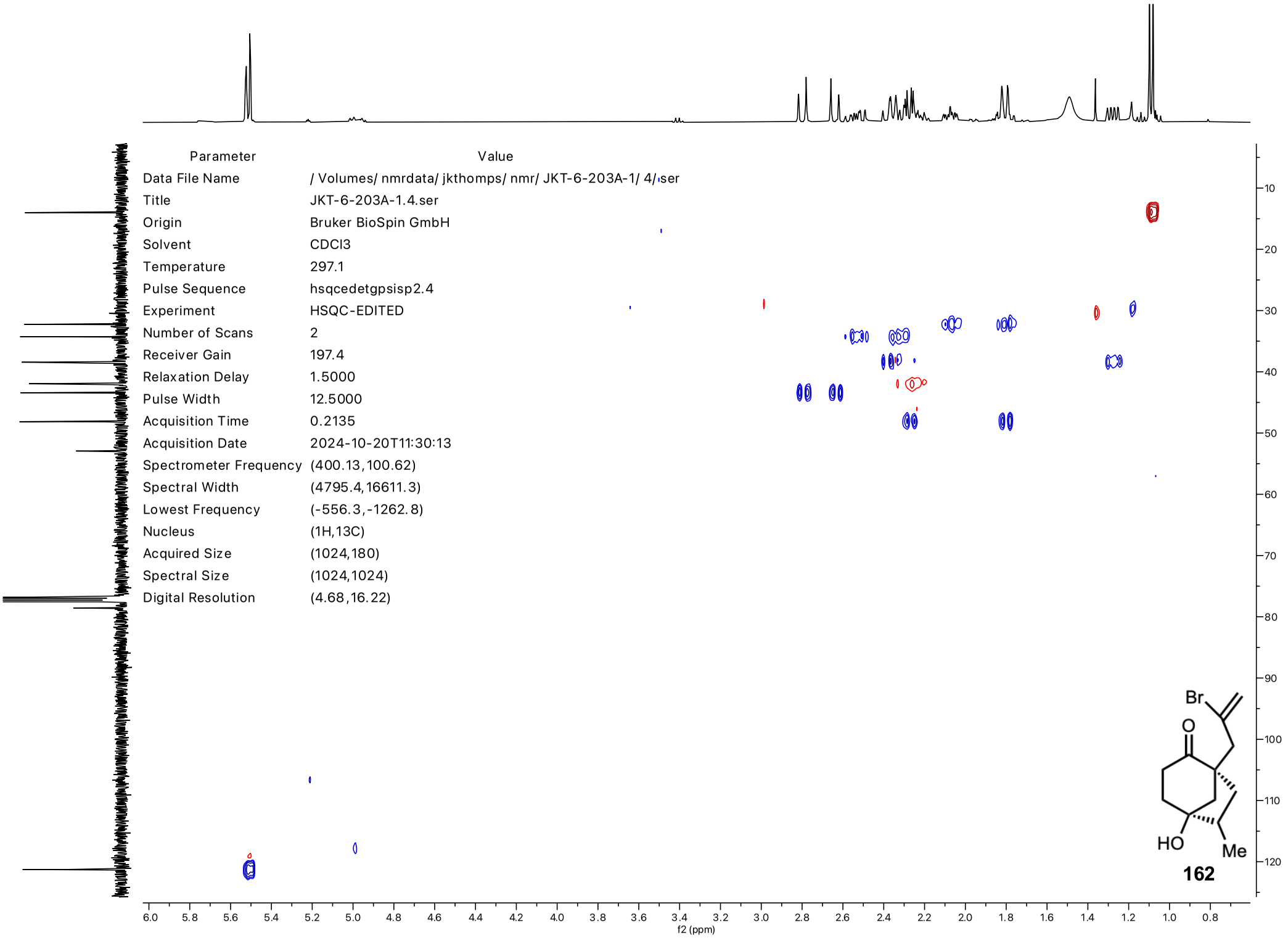
Parameter Value
Data File Name / Volumes/ nmrdata/ jkthomps/ nmr/ JKT-6-203A-1/ 4/ser
Title JKT-6-203A-1.4.ser
Origin Bruker BioSpin GmbH
Solvent CDCl3
Temperature 297.1
Pulse Sequence hsqcedetgpsisp2.4
Experiment HSQC-EDITED
Number of Scans 2
Receiver Gain 197.4
Relaxation Delay 1.5000
Pulse Width 12.5000
Acquisition Time 0.2135
Acquisition Date 2024-10-20T11:30:13
Spectrometer Frequency (400.13,100.62)
Spectral Width (4795.4,16611.3)
Lowest Frequency (-556.3,-1262.8)
Nucleus (1H,13C)
Acquired Size (1024,180)
Spectral Size (1024,1024)
Digital Resolution (4.68,16.22)
Br
O
HO
Me
162
f2 (ppm)
f1 (ppm)

Parameter	Value
Data File Name	/ Volumes/ nmrdata/ jkthomps/ nmr/ JKT-6-203A-1/ 5/ ser
Title	JKT-6-203A-1.5.ser
Origin	Bruker BioSpin GmbH
Solvent	CDCl3
Temperature	297.1
Pulse Sequence	hmbcetgpl3nd
Experiment	HMBC
Number of Scans	4
Receiver Gain	197.4
Relaxation Delay	2.0000
Pulse Width	12.5000
Acquisition Time	0.4260
Acquisition Date	2024-10-20T21:45:56
Spectrometer Frequency	(400.13,100.62)
Spectral Width	(4807.7,22321.4)
Lowest Frequency	(-199.5,-1116.4)
Nucleus	(1H,13C)
Acquired Size	(2048,256)
Spectral Size	(2048,1024)
Digital Resolution	(2.35,21.80)

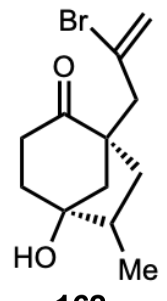

162

f2 (ppm)

f1 (ppm)

Parameter	Value
Data File Name	/ Users/ jordankthompson/ Desktop/ JKT-6-191C-2/ 1/ fid
Title	JKT-6-191C-2.1.fid
Origin	Bruker BioSpin GmbH
Solvent	CDCl3
Temperature	297.1
Pulse Sequence	zg30
Experiment	1D
Number of Scans	16
Receiver Gain	197.4
Relaxation Delay	1.0000
Pulse Width	12.5000
Acquisition Time	4.0894
Acquisition Date	2024-10-10T15:03:25
Spectrometer Frequency	400.13
Spectral Width	8012.8
Nucleus	1H
Acquired Size	32768
Spectral Size	65536

163

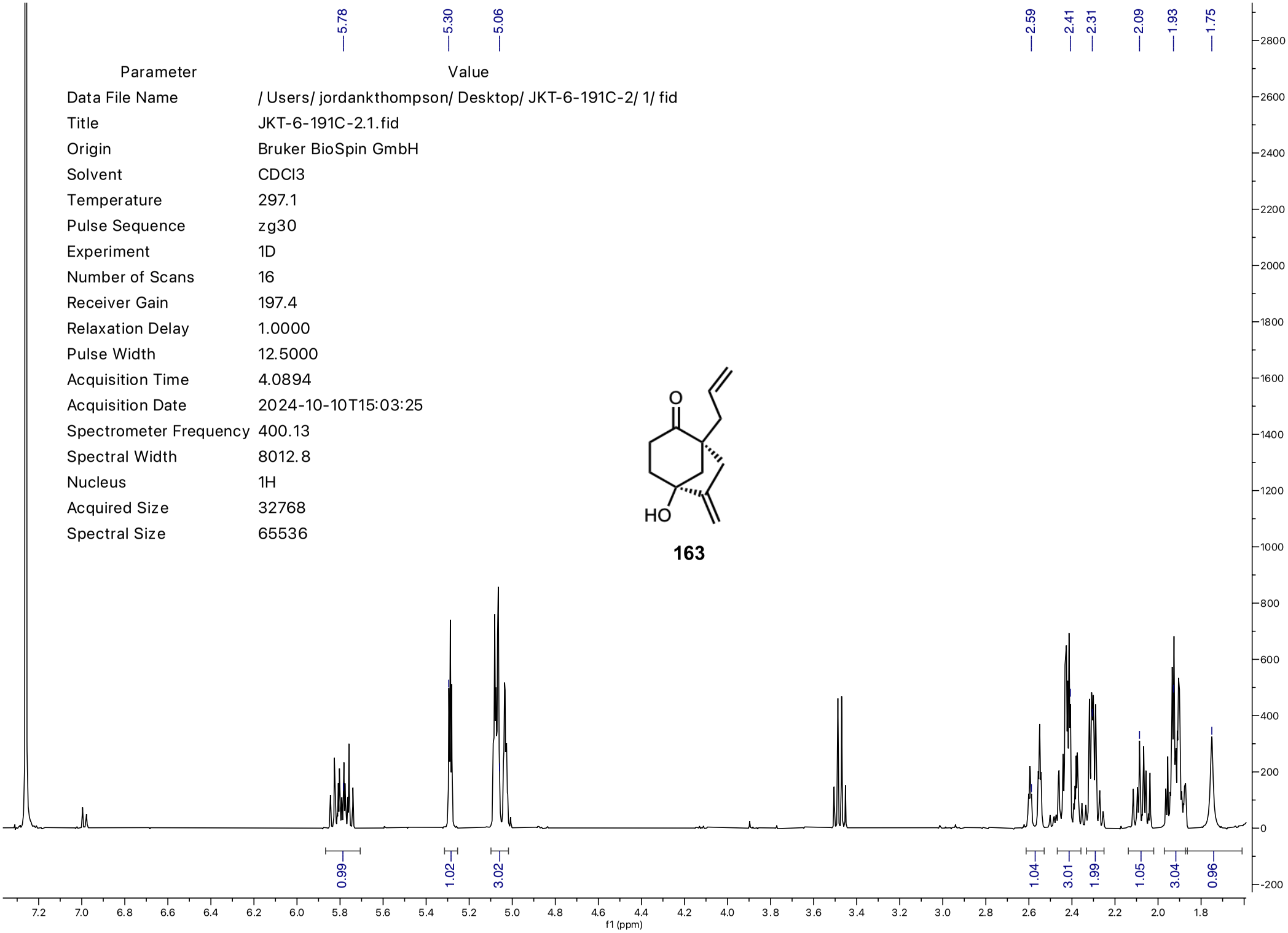

Parameter	Value
Data File Name	/ Users/ jordankthompson/ Desktop/ JKT-6-191C-2/ 2/ fid
Title	JKT-6-191C-2.2.fid
Origin	Bruker BioSpin GmbH
Solvent	CDCl3
Temperature	297.2
Pulse Sequence	zgpg30
Experiment	1D
Number of Scans	700
Receiver Gain	64.2
Relaxation Delay	1.0000
Pulse Width	10.0000
Acquisition Time	1.3631
Acquisition Date	2024-10-10T15:32:15
Spectrometer Frequency	100.62
Spectral Width	24038.5
Nucleus	13C
Acquired Size	32768
Spectral Size	65536

163

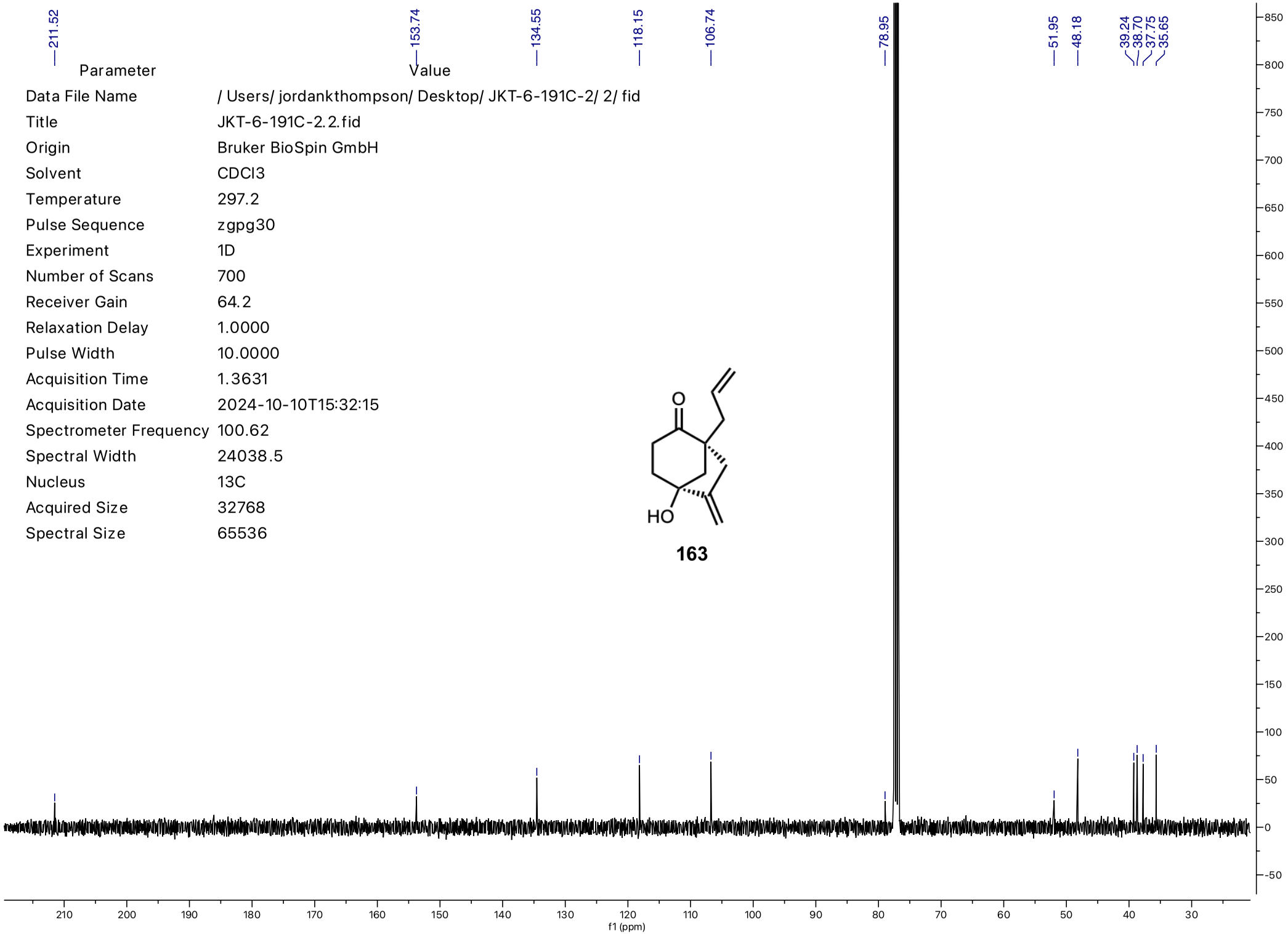

Parameter	Value
Data File Name	/ Users/ jordankthompson/ Desktop/ JKT-6-191C-2/ 3/ ser
Title	JKT-6-191C-2.3.ser
Origin	Bruker BioSpin GmbH
Solvent	CDCl3
Temperature	297.2
Pulse Sequence	cosygpppqf
Experiment	COSY
Number of Scans	1
Receiver Gain	197.4
Relaxation Delay	1.7956
Pulse Width	12.5000
Acquisition Time	0.4014
Acquisition Date	2024-10-10T15:37:58
Spectrometer Frequency	(400.13,400.13)
Spectral Width	(2551.0,2551.0)
Lowest Frequency	(51.5,50.6)
Nucleus	(1H,1H)
Acquired Size	(1024,128)
Spectral Size	(1024,1024)
Digital Resolution	(2.49,2.49)

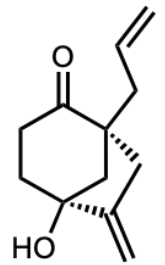

163

f2 (ppm)

f1 (ppm)

Parameter	Value
Data File Name	/ Users/ jordankthompson/ Desktop/ JKT-6-191C-2/ 5/ ser
Title	JKT-6-191C-2.5.ser
Origin	Bruker BioSpin GmbH
Solvent	CDCl3
Temperature	297.1
Pulse Sequence	hsqcedetgpsisp2.4
Experiment	HSQC-EDITED
Number of Scans	2
Receiver Gain	197.4
Relaxation Delay	1.5000
Pulse Width	12.5000
Acquisition Time	0.2135
Acquisition Date	2024-10-10T15:49:38
Spectrometer Frequency	(400.13,100.62)
Spectral Width	(4795.4,16611.3)
Lowest Frequency	(-517.1,-1262.8)
Nucleus	(1H,13C)
Acquired Size	(1024,180)
Spectral Size	(1024,1024)
Digital Resolution	(4.68,16.22)

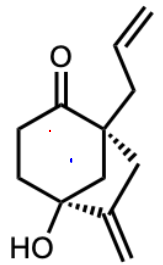

163

f2 (ppm)

f1 (ppm)

Parameter	Value
Data File Name	/ Users/ jordankthompson/ Desktop/ JKT-6-156-2/ PROTON01.fid/ fid
Title	PROTON01
Origin	Varian
Solvent	cdcl3
Temperature	25.0
Pulse Sequence	s2pul
Experiment	1D
Number of Scans	8
Receiver Gain	60
Relaxation Delay	1.0000
Pulse Width	5.6500
Acquisition Time	3.0000
Acquisition Date	2024-09-05T12:46:31
Spectrometer Frequency	499.54
Spectral Width	8000.0
Nucleus	1H
Acquired Size	24000
Spectral Size	65536

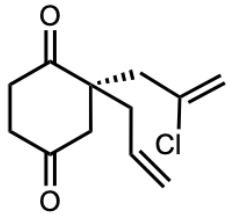

144B

210.80
208.49
137.67
131.33
121.22
118.03
50.05
46.63
45.98
42.66
37.74
35.94

Parameter	Value
Data File Name	/ Users/ jordankthompson/ Desktop/ ST-1-151-prod-c/ 3/ fid
Title	ST-1-151-prod-c.3.fid
Origin	Bruker BioSpin GmbH
Solvent	CDCl3
Temperature	297.1
Pulse Sequence	zgpg30
Experiment	1D
Number of Scans	512
Receiver Gain	78.7
Relaxation Delay	1.0000
Pulse Width	10.0000
Acquisition Time	1.3631
Acquisition Date	2024-05-01T12:05:48
Spectrometer Frequency	100.62
Spectral Width	24038.5
Nucleus	13C
Acquired Size	32768
Spectral Size	65536

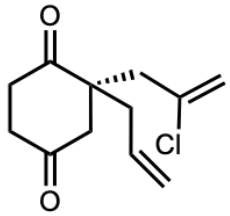

144B

2500
2000
1500
1000
500
0

210 200 190 180 170 160 150 140 130 120 110 100 90 80 70 60 50 40

f1 (ppm)

Parameter	Value
Data File Name	/ Users/ jordankthompson/ Desktop/ JKT-6-191D-2/ 1/ fid
Title	JKT-6-191D-2.1.fid
Origin	Bruker BioSpin GmbH
Solvent	CDCl3
Temperature	297.1
Pulse Sequence	zg30
Experiment	1D
Number of Scans	16
Receiver Gain	197.4
Relaxation Delay	1.0000
Pulse Width	12.5000
Acquisition Time	4.0894
Acquisition Date	2024-10-10T16:19:19
Spectrometer Frequency	400.13
Spectral Width	8012.8
Nucleus	1H
Acquired Size	32768
Spectral Size	65536

167

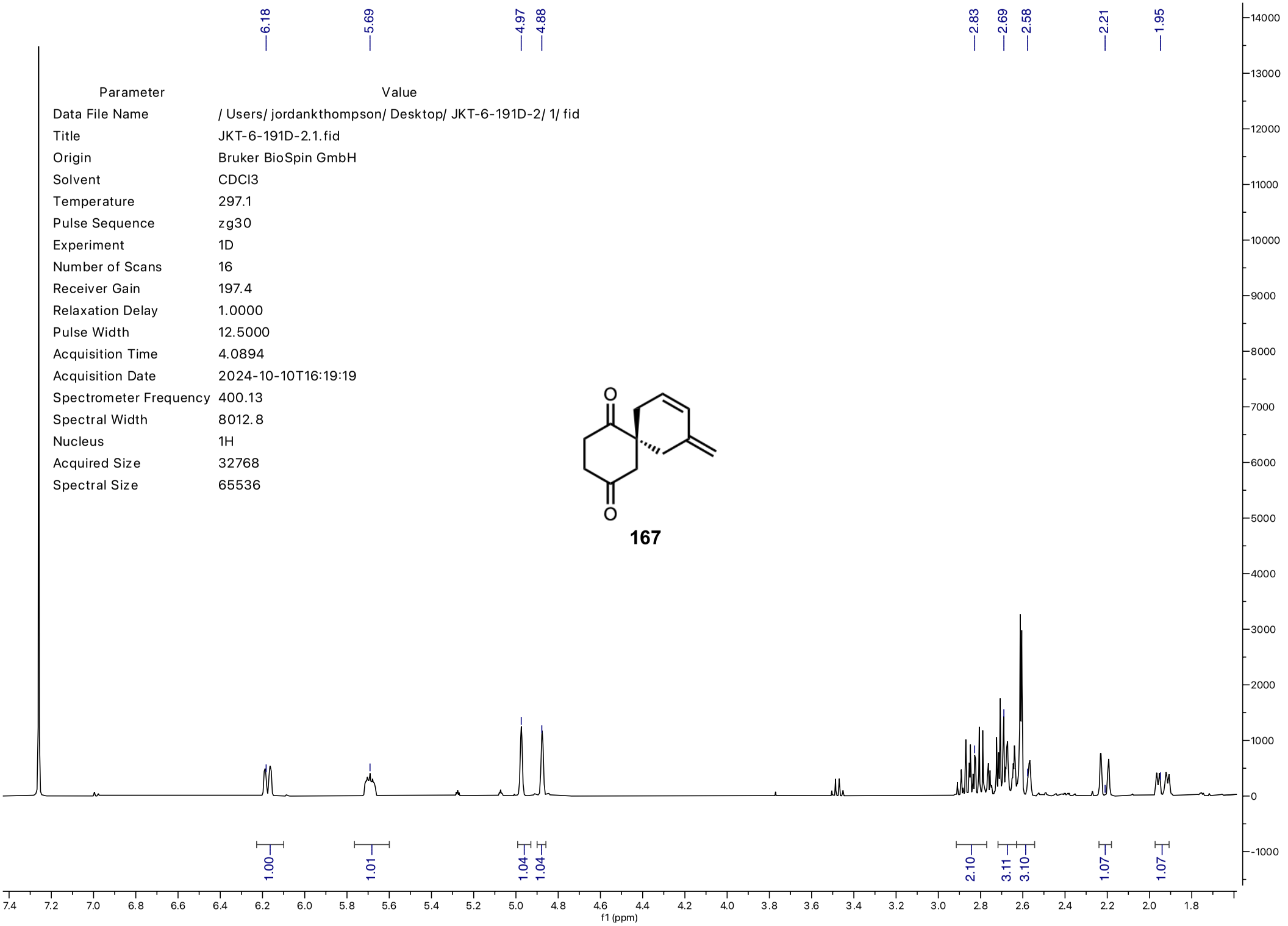

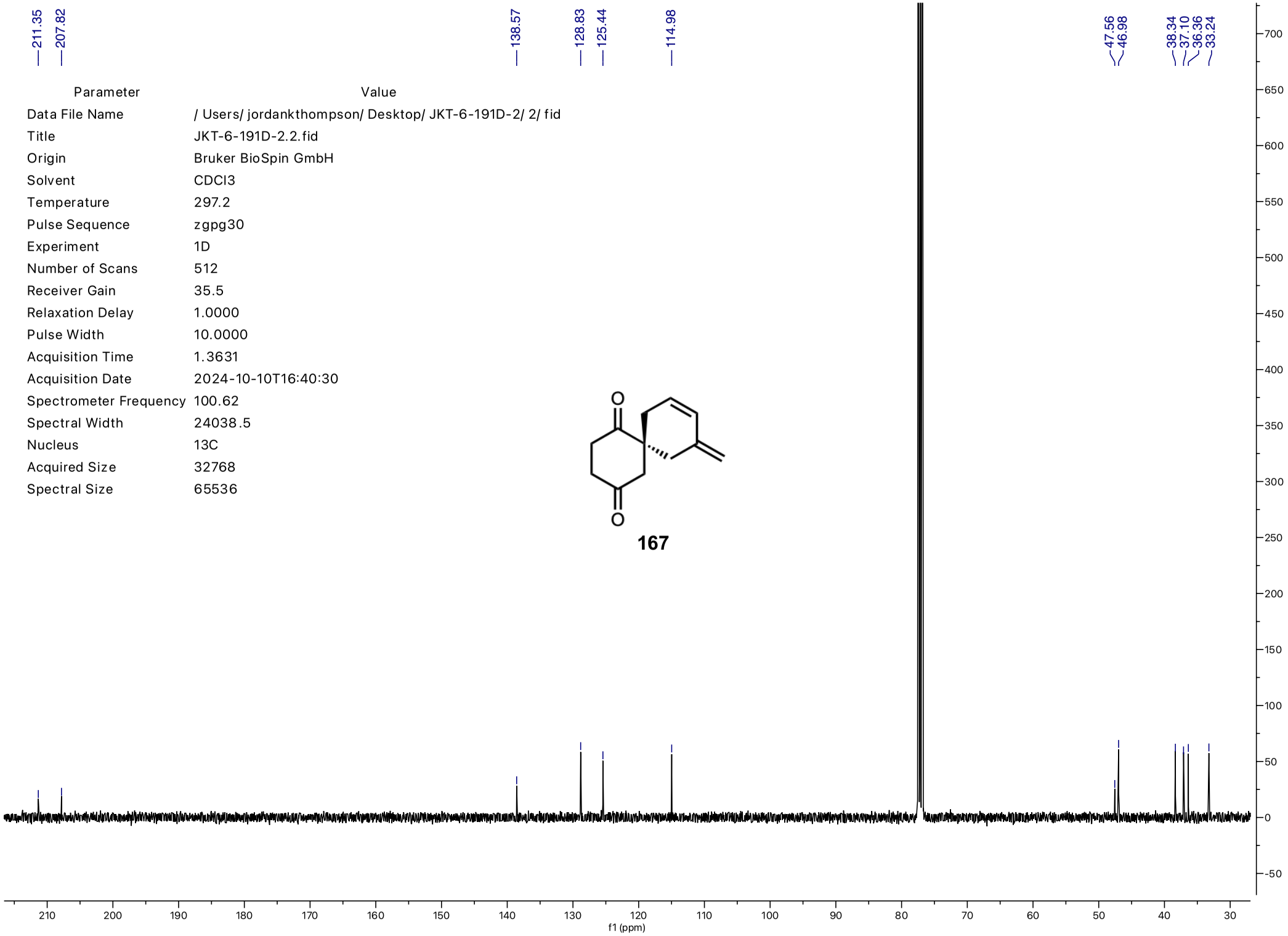

Parameter	Value
Data File Name	/ Users/ jordankthompson/ Desktop/ JKT-6-191D-2/ 2/ fid
Title	JKT-6-191D-2.2.fid
Origin	Bruker BioSpin GmbH
Solvent	CDCl3
Temperature	297.2
Pulse Sequence	zgpg30
Experiment	1D
Number of Scans	512
Receiver Gain	35.5
Relaxation Delay	1.0000
Pulse Width	10.0000
Acquisition Time	1.3631
Acquisition Date	2024-10-10T16:40:30
Spectrometer Frequency	100.62
Spectral Width	24038.5
Nucleus	13C
Acquired Size	32768
Spectral Size	65536

167

Parameter	Value
Data File Name	/ Users/ jordankthompson/ Desktop/ JKT-6-191D-2/ 3/ ser
Title	JKT-6-191D-2.3.ser
Origin	Bruker BioSpin GmbH
Solvent	CDCl3
Temperature	297.2
Pulse Sequence	cosygpppqf
Experiment	COSY
Number of Scans	1
Receiver Gain	197.4
Relaxation Delay	1.8202
Pulse Width	12.5000
Acquisition Time	0.3768
Acquisition Date	2024-10-10T16:46:14
Spectrometer Frequency	(400.13,400.13)
Spectral Width	(2717.4,2717.4)
Lowest Frequency	(46.4,40.4)
Nucleus	(1H,1H)
Acquired Size	(1024,128)
Spectral Size	(1024,1024)
Digital Resolution	(2.65,2.65)

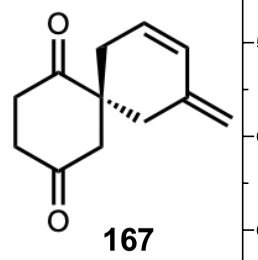

167

f2 (ppm)

f1 (ppm)

Parameter	Value
Data File Name	/ Users/ jordankthompson/ Desktop/ JKT-6-191D-2/ 4/ ser
Title	JKT-6-191D-2.4.ser
Origin	Bruker BioSpin GmbH
Solvent	CDCl3
Temperature	297.1
Pulse Sequence	hsqcedetgpsisp2.4
Experiment	HSQC-EDITED
Number of Scans	2
Receiver Gain	197.4
Relaxation Delay	1.5000
Pulse Width	12.5000
Acquisition Time	0.2135
Acquisition Date	2024-10-10T16:57:54
Spectrometer Frequency	(400.13,100.62)
Spectral Width	(4795.4,16611.3)
Lowest Frequency	(-526.7,-1258.0)
Nucleus	(1H,13C)
Acquired Size	(1024,180)
Spectral Size	(1024,1024)
Digital Resolution	(4.68,16.22)

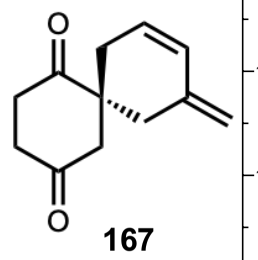

167

f2 (ppm)

f1 (ppm)

Parameter	Value
Data File Name	/ Volumes/ nmrdata/ jkthomps/ nmr/ JKT-6-179-1/ 6/ fid
Title	JKT-6-179-1.6.fid
Origin	Bruker BioSpin GmbH
Solvent	CDCl3
Temperature	297.1
Pulse Sequence	zg30
Experiment	1D
Number of Scans	16
Receiver Gain	197.4
Relaxation Delay	1.0000
Pulse Width	12.5000
Acquisition Time	4.0894
Acquisition Date	2024-10-13T11:59:32
Spectrometer Frequency	400.13
Spectral Width	8012.8
Nucleus	1H
Acquired Size	32768
Spectral Size	65536

168

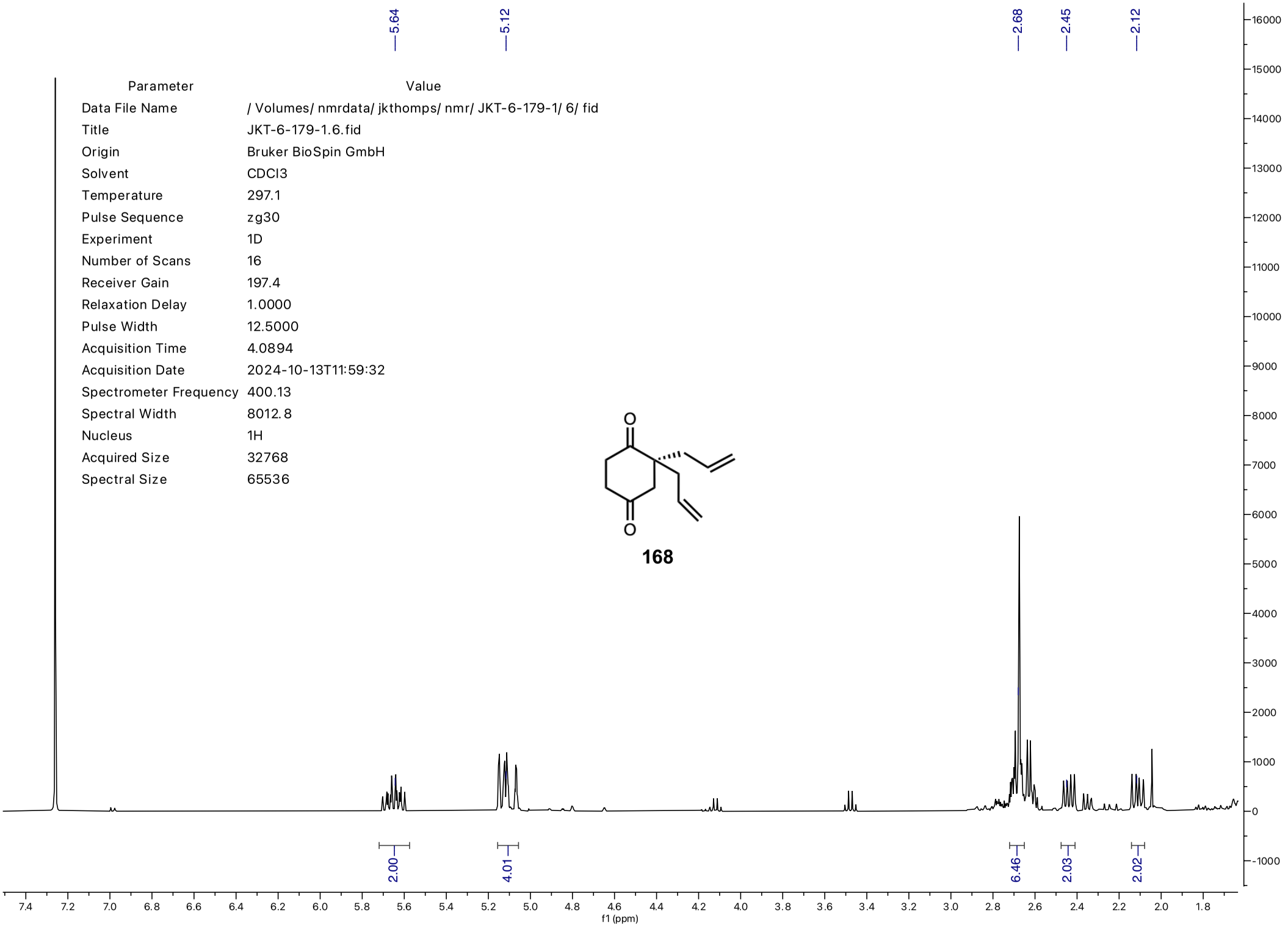

Parameter	Value
Data File Name	/ Volumes/ nmrdata/ jkthomps/ nmr/ JKT-6-179-1/ 7/ fid
Title	JKT-6-179-1.7.fid
Origin	Bruker BioSpin GmbH
Solvent	CDCl3
Temperature	297.1
Pulse Sequence	zgpg30
Experiment	1D
Number of Scans	750
Receiver Gain	50.3
Relaxation Delay	1.0000
Pulse Width	10.0000
Acquisition Time	1.2059
Acquisition Date	2024-10-13T12:28:25
Spectrometer Frequency	100.62
Spectral Width	27173.9
Nucleus	13C
Acquired Size	32768
Spectral Size	65536

168

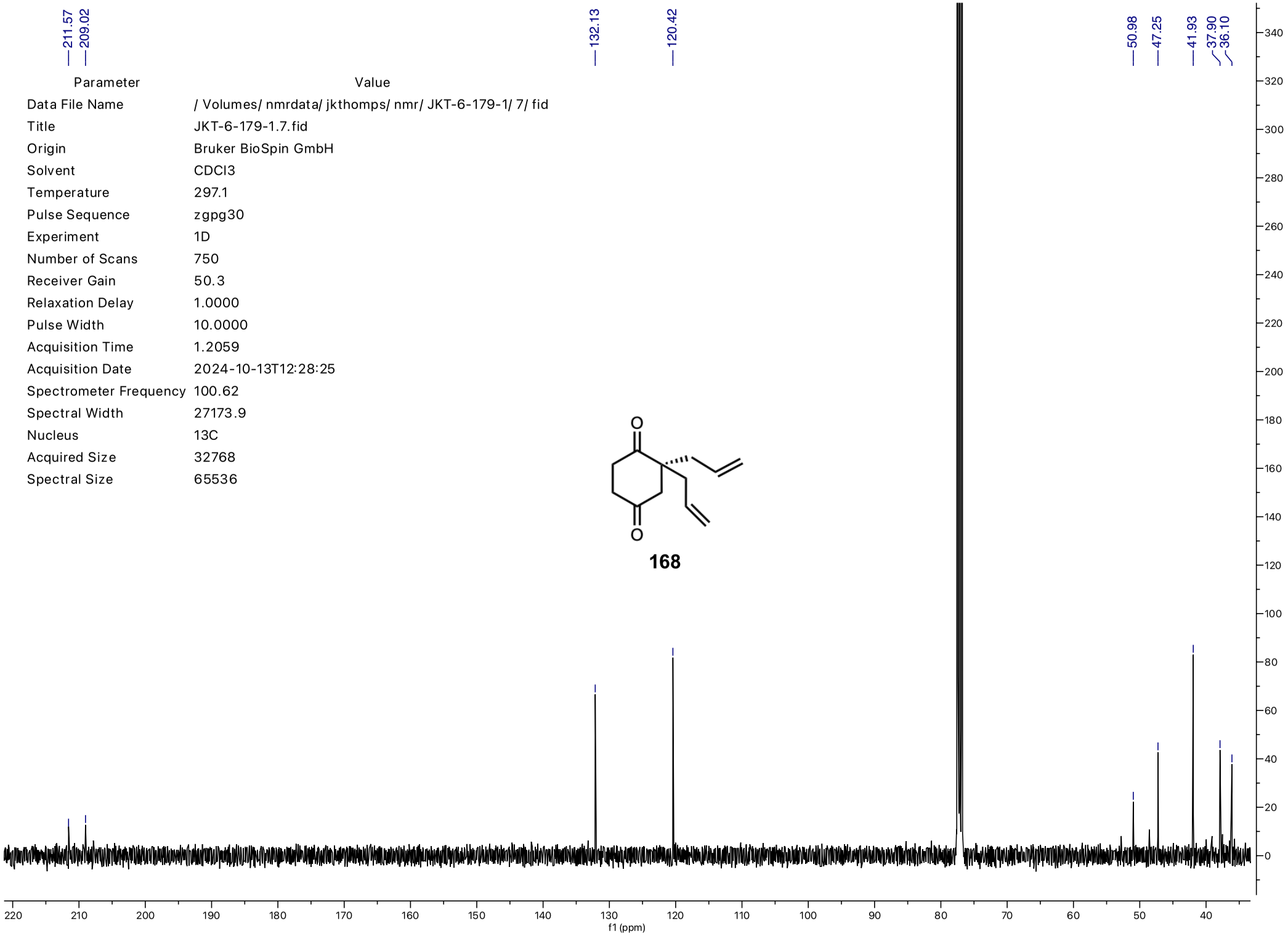

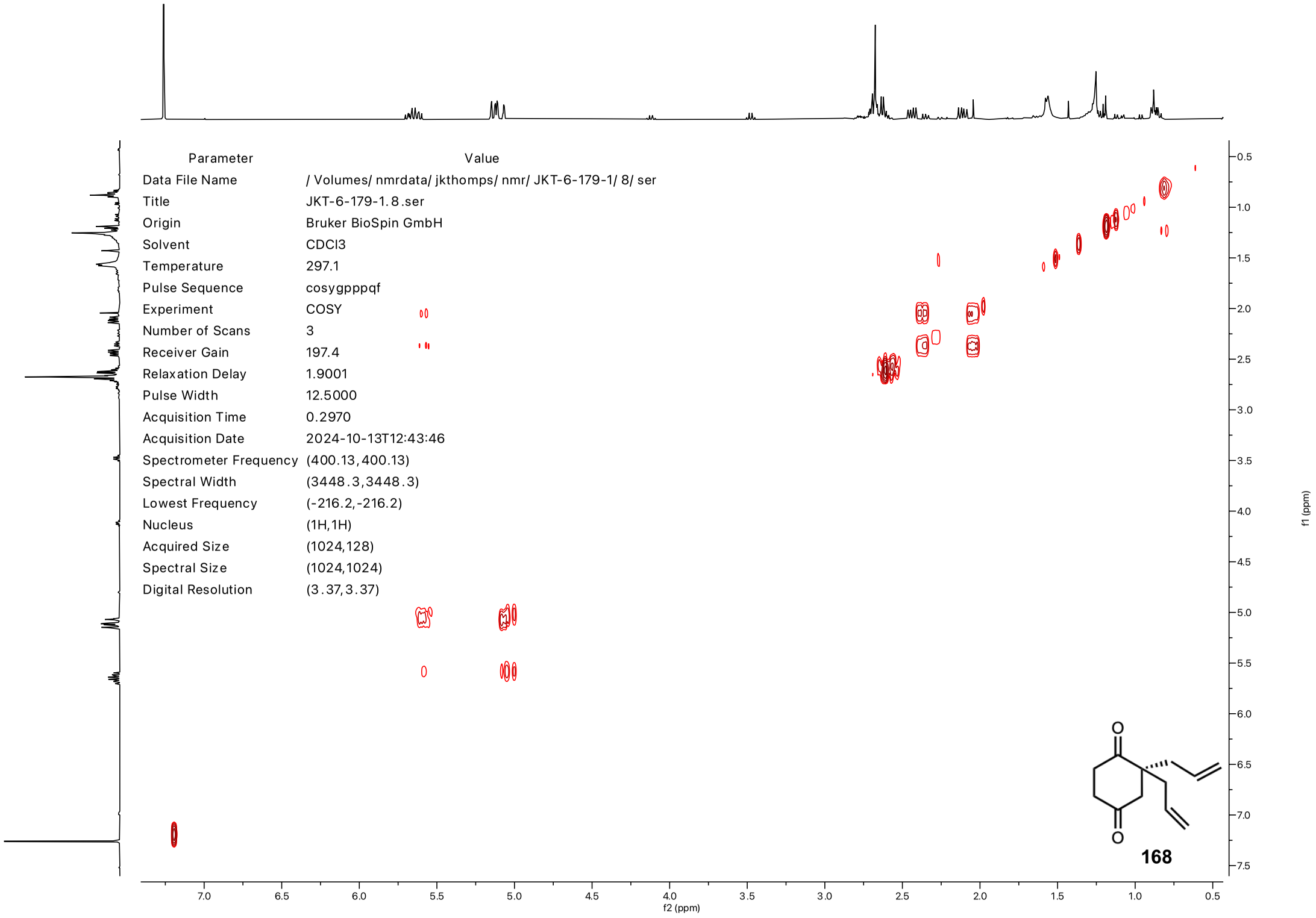
Parameter Value
Data File Name / Volumes/ nmrdata/ jkthomps/ nmr/ JKT-6-179-1/ 8/ ser
Title JKT-6-179-1.8.ser
Origin Bruker BioSpin GmbH
Solvent CDCl3
Temperature 297.1
Pulse Sequence cosygpppqf
Experiment COSY
Number of Scans 3
Receiver Gain 197.4
Relaxation Delay 1.9001
Pulse Width 12.5000
Acquisition Time 0.2970
Acquisition Date 2024-10-13T12:43:46
Spectrometer Frequency (400.13,400.13)
Spectral Width (3448.3,3448.3)
Lowest Frequency (-216.2,-216.2)
Nucleus (1H,1H)
Acquired Size (1024,128)
Spectral Size (1024,1024)
Digital Resolution (3.37,3.37)
7.0
6.5
6.0
5.5
5.0
4.5
4.0
3.5
3.0
2.5
2.0
1.5
1.0
0.5
f2 (ppm)
f1 (ppm)
168

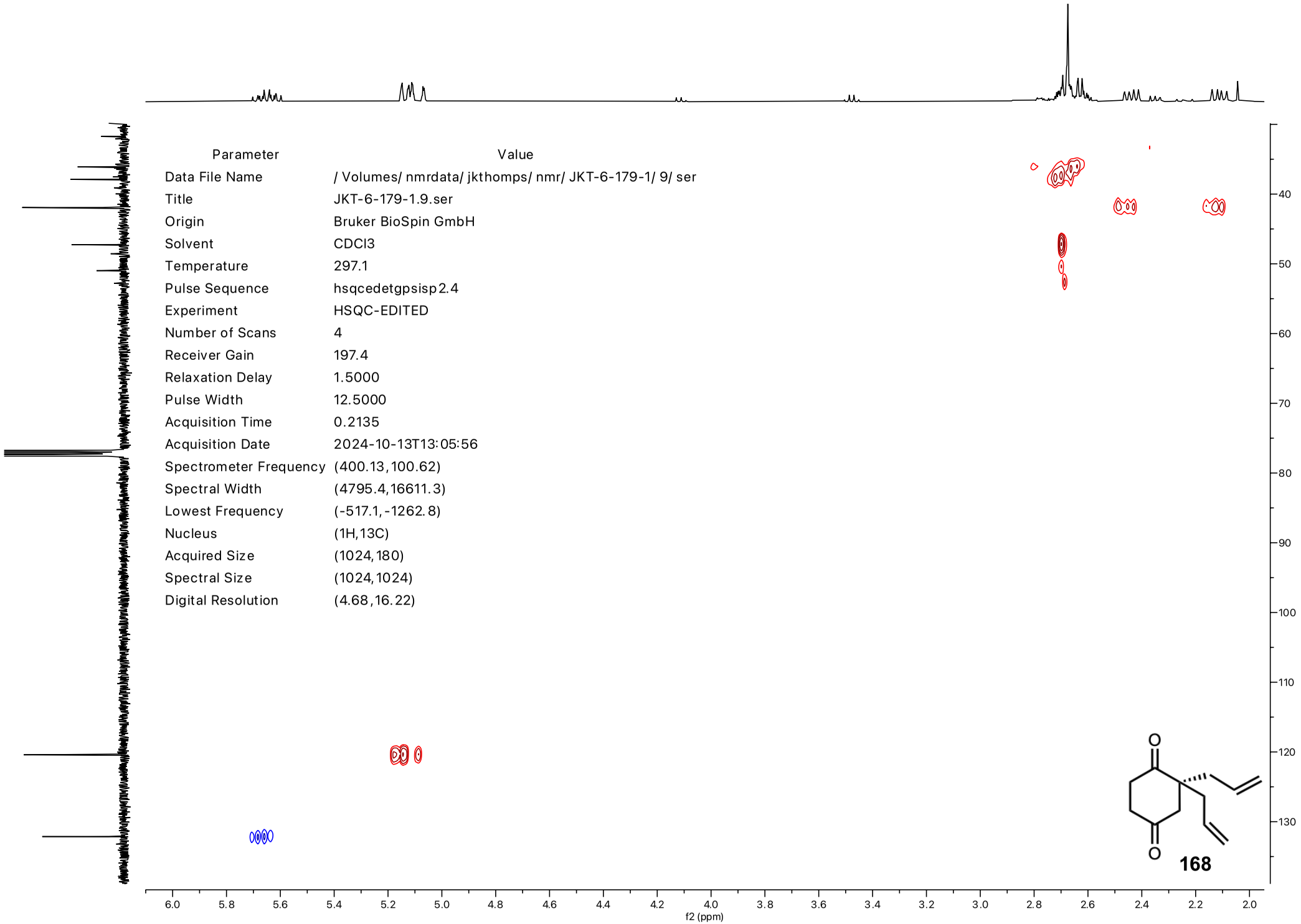
Parameter Value
Data File Name / Volumes/ nmrdata/ jkthomps/ nmr/ JKT-6-179-1/ 9/ ser
Title JKT-6-179-1.9.ser
Origin Bruker BioSpin GmbH
Solvent CDCl3
Temperature 297.1
Pulse Sequence hsqcedetgpsisp2.4
Experiment HSQC-EDITED
Number of Scans 4
Receiver Gain 197.4
Relaxation Delay 1.5000
Pulse Width 12.5000
Acquisition Time 0.2135
Acquisition Date 2024-10-13T13:05:56
Spectrometer Frequency (400.13,100.62)
Spectral Width (4795.4,16611.3)
Lowest Frequency (-517.1,-1262.8)
Nucleus (1H,13C)
Acquired Size (1024,180)
Spectral Size (1024,1024)
Digital Resolution (4.68,16.22)
6.0 5.8 5.6 5.4 5.2 5.0 4.8 4.6 4.4 4.2 4.0 3.8 3.6 3.4 3.2 3.0 2.8 2.6 2.4 2.2 2.0
f2 (ppm)
40 50 60 70 80 90 100 110 120 130
f1 (ppm)
O
O
168

Parameter	Value
Data File Name	/ Volumes/ nmrdata/ jkthomps/ nmr/ JKT-6-201_pure/ 1/ fid
Title	JKT-6-201_pure.1.fid
Origin	Bruker BioSpin GmbH
Solvent	CDCl3
Temperature	297.1
Pulse Sequence	zg30
Experiment	1D
Number of Scans	16
Receiver Gain	156.2
Relaxation Delay	1.0000
Pulse Width	12.5000
Acquisition Time	4.0894
Acquisition Date	2024-10-18T03:47:35
Spectrometer Frequency	400.13
Spectral Width	8012.8
Nucleus	1H
Acquired Size	32768
Spectral Size	65536

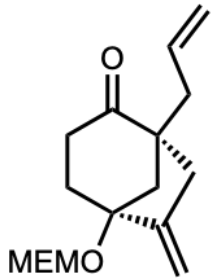

143

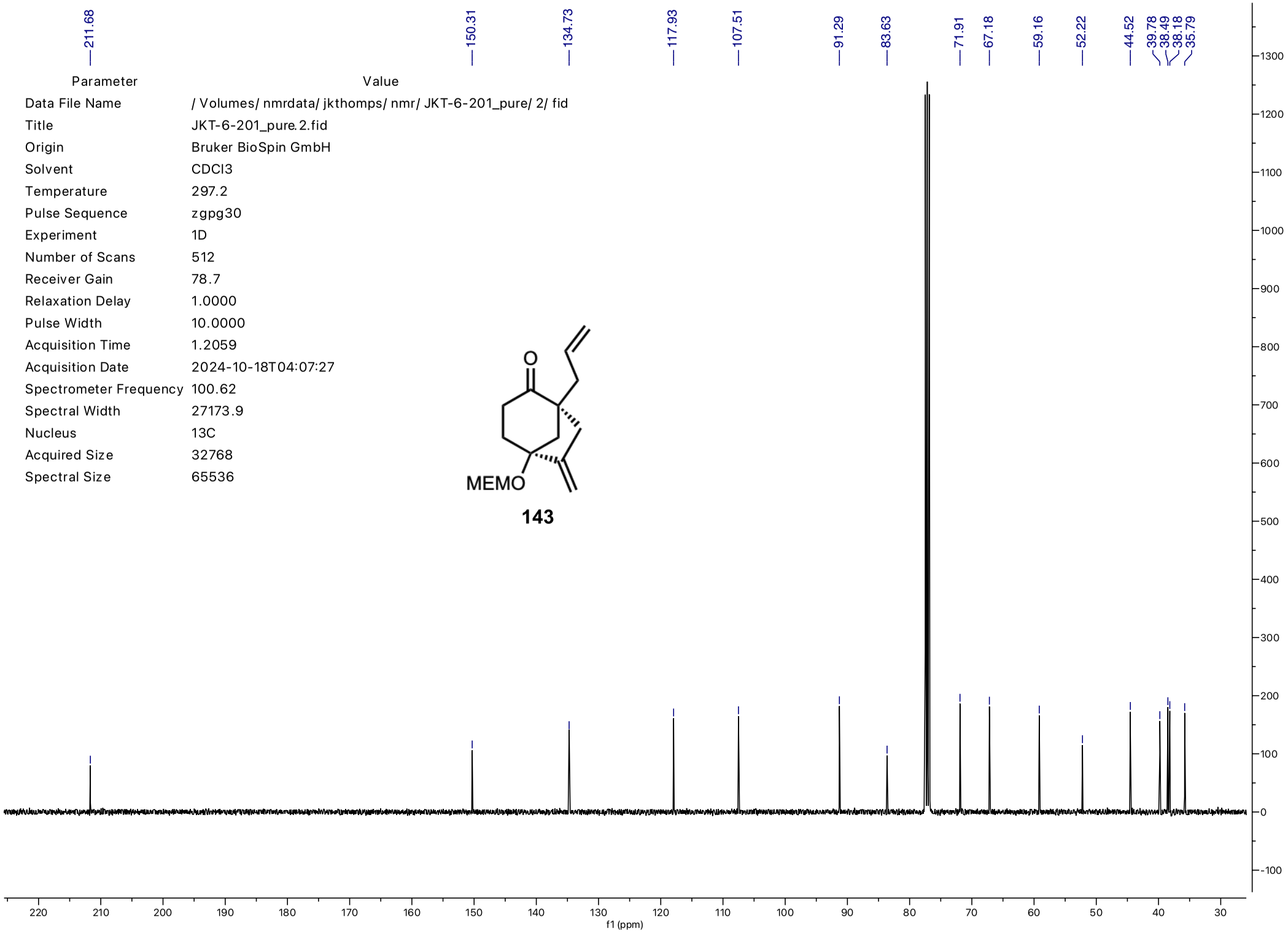
211.68
150.31
134.73
117.93
107.51
91.29
83.63
71.91
67.18
59.16
52.22
44.52
39.78
38.49
38.18
35.79
Parameter
Value
Data File Name
/ Volumes/ nmrdata/ jkthomps/ nmr/ JKT-6-201_pure/ 2/ fid
Title
JKT-6-201_pure.2.fid
Origin
Bruker BioSpin GmbH
Solvent
CDCl3
Temperature
297.2
Pulse Sequence
zgpg30
Experiment
1D
Number of Scans
512
Receiver Gain
78.7
Relaxation Delay
1.0000
Pulse Width
10.0000
Acquisition Time
1.2059
Acquisition Date
2024-10-18T04:07:27
Spectrometer Frequency
100.62
Spectral Width
27173.9
Nucleus
13C
Acquired Size
32768
Spectral Size
65536
O
MEMO
143
f1 (ppm)

Parameter	Value
Data File Name	/ Volumes/ nmrdata-1/ jkthomps/ nmr/ JKT-6-280-1_high_vac/ 3/ ser
Title	JKT-6-280-1_high_vac.3.ser
Origin	Bruker BioSpin GmbH
Solvent	CDCl3
Temperature	297.1
Pulse Sequence	cosygpppqf
Experiment	COSY
Number of Scans	1
Receiver Gain	64.2
Relaxation Delay	1.7977
Pulse Width	12.5000
Acquisition Time	0.3994
Acquisition Date	2024-12-17T07:42:44
Spectrometer Frequency	(400.13,400.13)
Spectral Width	(2564.1,2564.1)
Lowest Frequency	(56.0,56.0)
Nucleus	(1H,1H)
Acquired Size	(1024,128)
Spectral Size	(1024,1024)
Digital Resolution	(2.50,2.50)

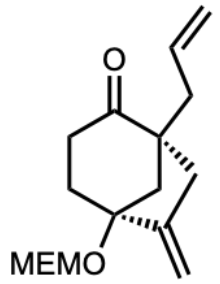

143

f2 (ppm)

f1 (ppm)

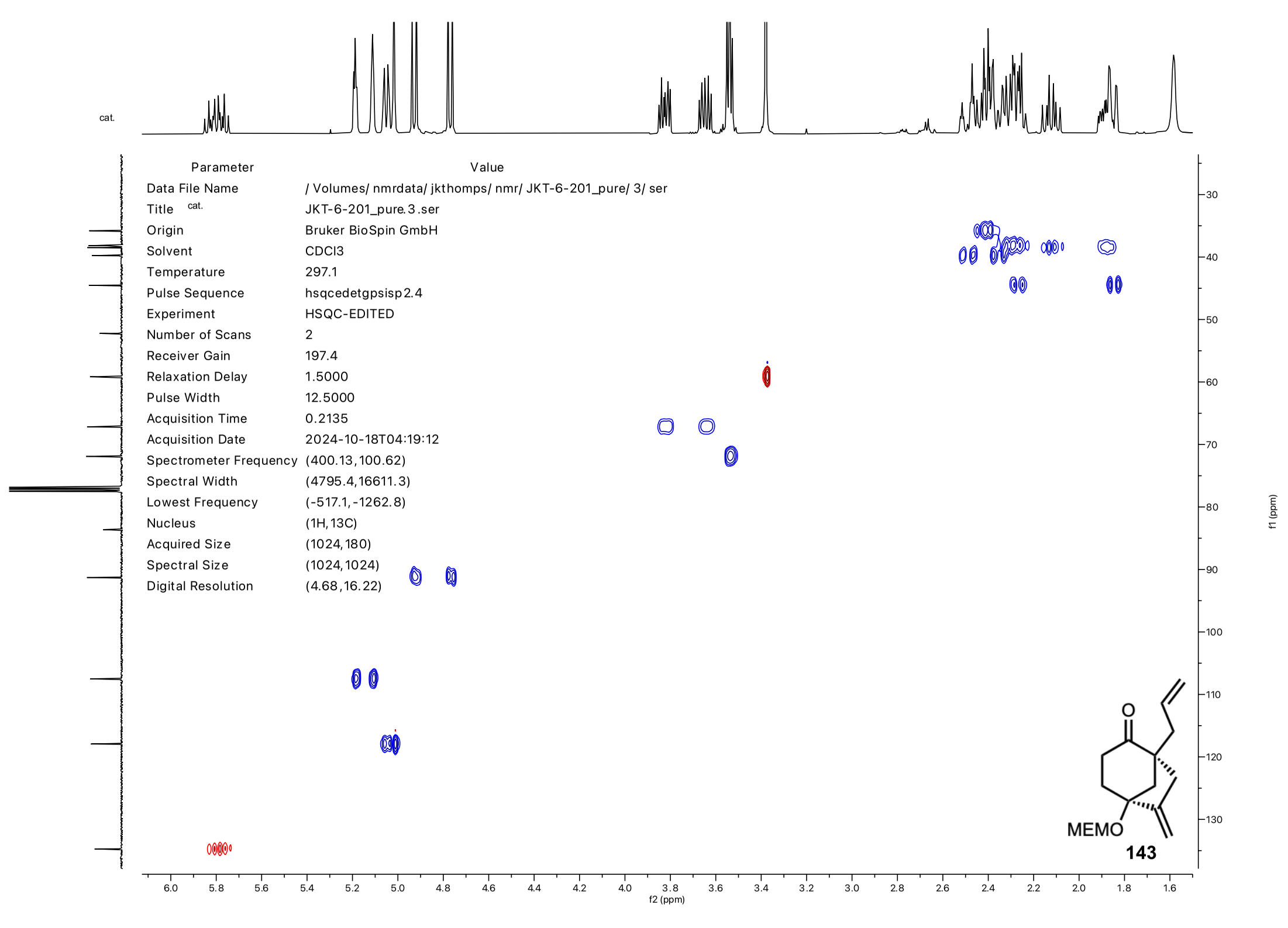
cat.
Parameter Value
Data File Name / Volumes/ nmrdata/ jkthomps/ nmr/ JKT-6-201_pure/ 3/ ser
Title cat.
JKT-6-201_pure.3.ser
Origin Bruker BioSpin GmbH
Solvent CDCl3
Temperature 297.1
Pulse Sequence hsqcedetgpsisp2.4
Experiment HSQC-EDITED
Number of Scans 2
Receiver Gain 197.4
Relaxation Delay 1.5000
Pulse Width 12.5000
Acquisition Time 0.2135
Acquisition Date 2024-10-18T04:19:12
Spectrometer Frequency (400.13,100.62)
Spectral Width (4795.4,16611.3)
Lowest Frequency (-517.1,-1262.8)
Nucleus (1H,13C)
Acquired Size (1024,180)
Spectral Size (1024,1024)
Digital Resolution (4.68,16.22)
f2 (ppm)
f1 (ppm)
MEMO
143

Parameter	Value
Data File Name	/ Volumes/ nmrdata-1/ jkthomps/ nmr/ JKT-6-246_pure/ 1/ fid
Title	JKT-6-246_pure.1.fid
Origin	Bruker BioSpin GmbH
Solvent	CDCl3
Temperature	297.1
Pulse Sequence	zg30
Experiment	1D
Number of Scans	16
Receiver Gain	197.4
Relaxation Delay	1.0000
Pulse Width	12.5000
Acquisition Time	4.0894
Acquisition Date	2024-11-14T13:27:52
Spectrometer Frequency	400.13
Spectral Width	8012.8
Nucleus	1H
Acquired Size	32768
Spectral Size	65536

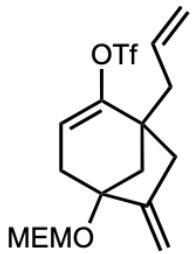

142

Parameter	Value
Data File Name	/ Volumes/ nmrdata-1/ jkthomps/ nmr/ JKT-6-246_pure/ 2/ fid
Title	JKT-6-246_pure.2.fid
Origin	Bruker BioSpin GmbH
Solvent	CDCl3
Temperature	297.1
Pulse Sequence	zgpg30
Experiment	1D
Number of Scans	512
Receiver Gain	64.2
Relaxation Delay	1.0000
Pulse Width	10.0000
Acquisition Time	1.2059
Acquisition Date	2024-11-14T13:47:43
Spectrometer Frequency	100.62
Spectral Width	27173.9
Nucleus	13C
Acquired Size	32768
Spectral Size	65536

153.19
151.44
133.35
118.89
115.76
109.35
91.19
83.03
77.48
77.16
76.84
71.91
67.20
59.17
45.43
45.28
44.71
41.04
37.77

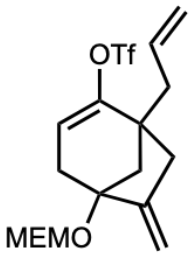

142

f1 (ppm)

Parameter	Value
Data File Name	/ Volumes/ nmrdata/ jkthomps/ nmr/ JKT-2-87_pure/ 1/ fid
Title	JKT-2-87_pure.1.fid
Origin	Bruker BioSpin GmbH
Solvent	CDCl3
Temperature	298.2
Pulse Sequence	zg30
Experiment	1D
Number of Scans	16
Receiver Gain	101.0
Relaxation Delay	1.0000
Pulse Width	9.8500
Acquisition Time	3.9977
Acquisition Date	2022-08-07T14:21:40
Spectrometer Frequency	400.15
Spectral Width	8196.7
Nucleus	1H
Acquired Size	32768
Spectral Size	65536

107A

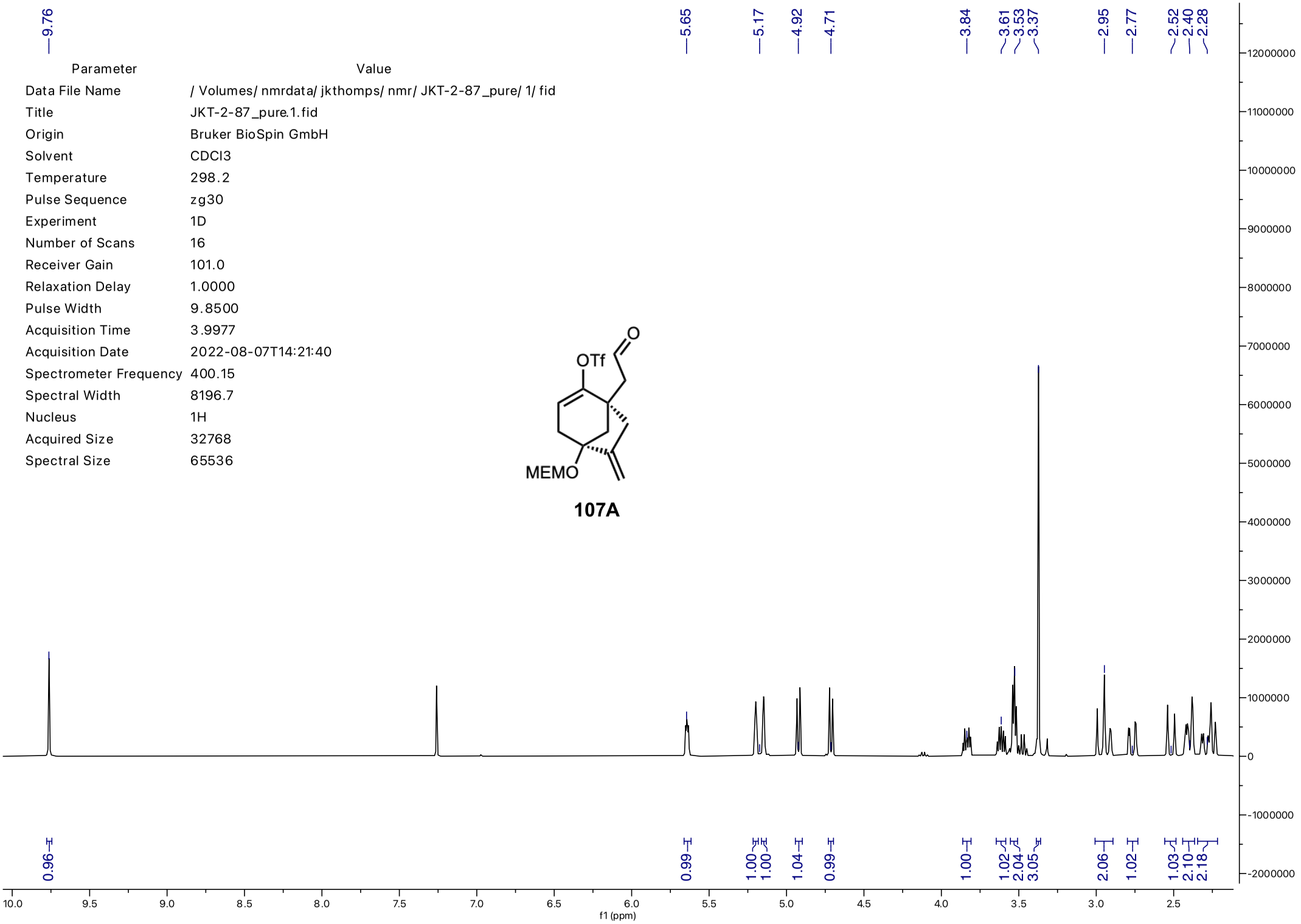

198.76
151.49
149.90
115.31
109.70
91.22
83.06
71.86
67.27
59.13
47.66
46.08
44.98
42.26
41.10

Parameter	Value
Data File Name	/ Volumes/ nmrdata/ jkthomps/ nmr/ JKT-2-87_pure/ 2/ fid
Title	JKT-2-87_pure.2.fid
Origin	Bruker BioSpin GmbH
Solvent	CDCl3
Temperature	298.2
Pulse Sequence	zgpg30
Experiment	1D
Number of Scans	500
Receiver Gain	45.2
Relaxation Delay	2.0000
Pulse Width	10.0000
Acquisition Time	1.3763
Acquisition Date	2022-08-07T14:51:01
Spectrometer Frequency	100.63
Spectral Width	23809.5
Nucleus	13C
Acquired Size	32768
Spectral Size	65536

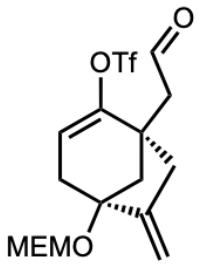

107A

1000000
900000
800000
700000
600000
500000
400000
300000
200000
100000
0
-100000

200 190 180 170 160 150 140 130 120 110 100 90 80 70 60 50 40

f1 (ppm)

Parameter	Value
Data File Name	/ Volumes/ nmrdata-2/ jkthomps/ nmr/ JKT-2-165-1/ 1/ fid
Title	JKT-2-165-1.1.fid
Origin	Bruker BioSpin GmbH
Solvent	CDCl3
Temperature	297.1
Pulse Sequence	zg30
Experiment	1D
Number of Scans	16
Receiver Gain	87.8
Relaxation Delay	1.0000
Pulse Width	12.5000
Acquisition Time	4.0894
Acquisition Date	2022-11-02T15:22:46
Spectrometer Frequency	400.13
Spectral Width	8012.8
Nucleus	1H
Acquired Size	32768
Spectral Size	65536

107B

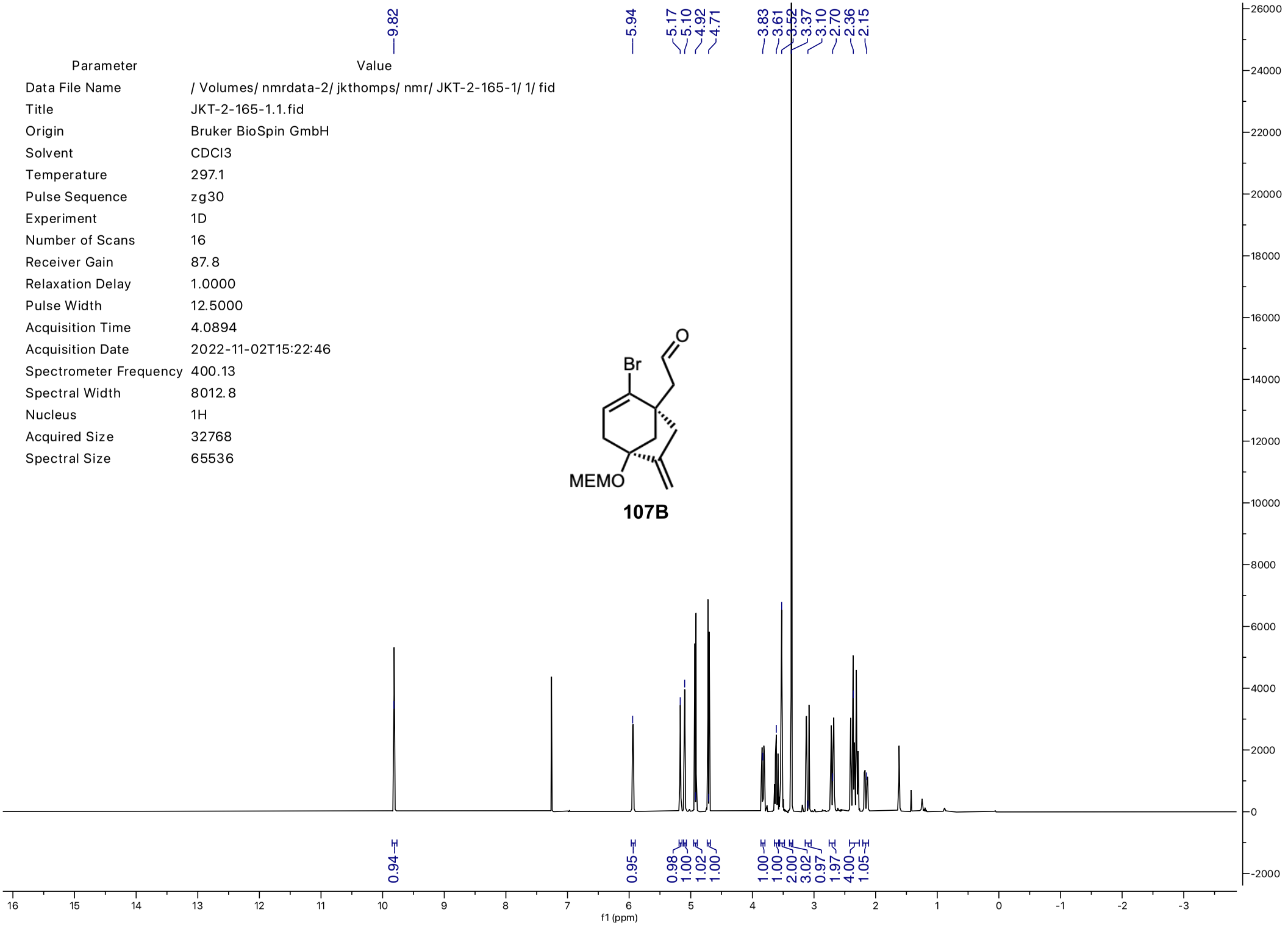

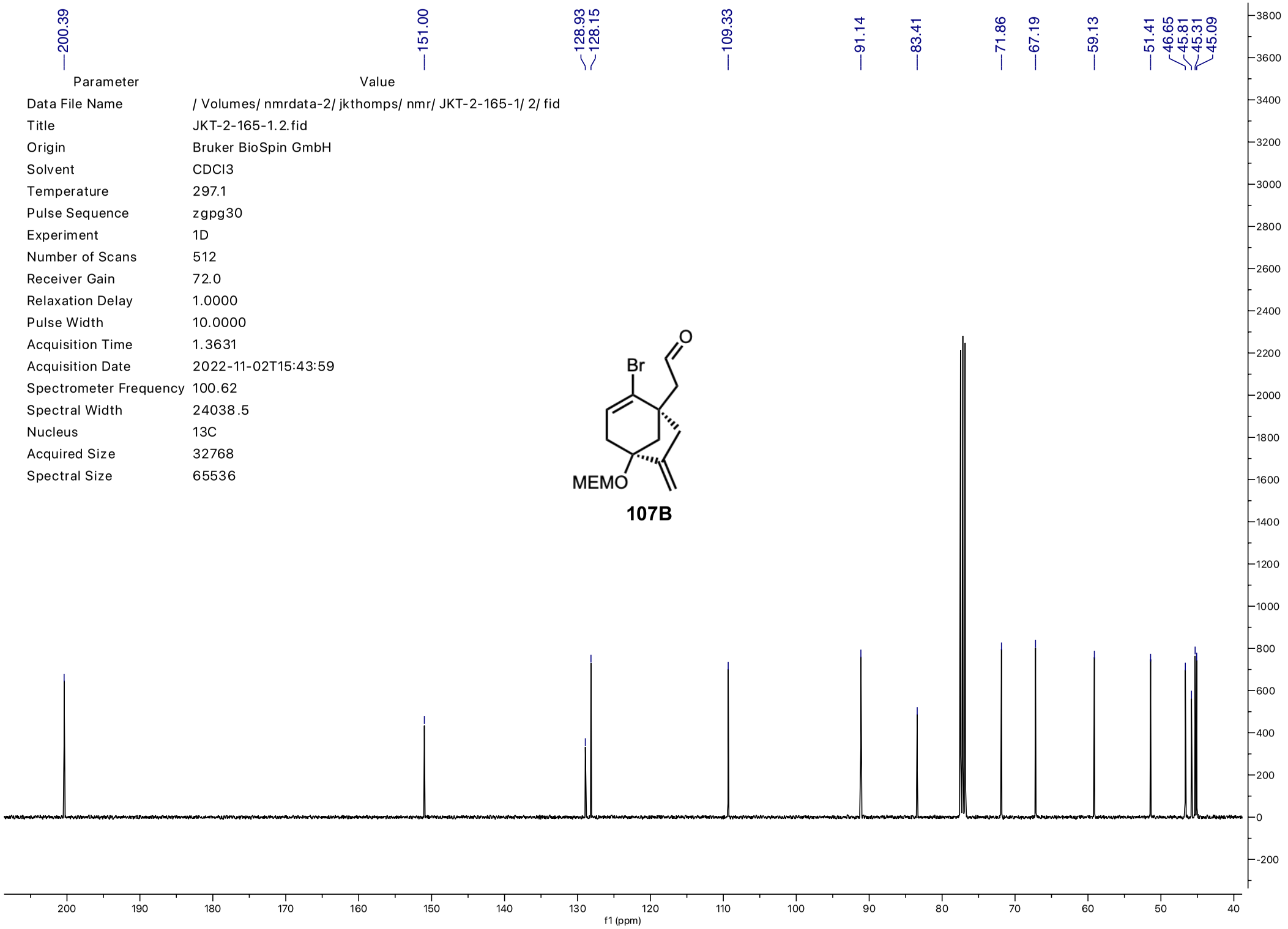
200.39
151.00
128.93
128.15
109.33
91.14
83.41
71.86
67.19
59.13
51.41
46.65
45.81
45.31
45.09
Parameter
Value
Data File Name / Volumes/ nmrdata-2/ jkthomps/ nmr/ JKT-2-165-1/ 2/ fid
Title JKT-2-165-1.2.fid
Origin Bruker BioSpin GmbH
Solvent CDCl3
Temperature 297.1
Pulse Sequence zgpg30
Experiment 1D
Number of Scans 512
Receiver Gain 72.0
Relaxation Delay 1.0000
Pulse Width 10.0000
Acquisition Time 1.3631
Acquisition Date 2022-11-02T15:43:59
Spectrometer Frequency 100.62
Spectral Width 24038.5
Nucleus 13C
Acquired Size 32768
Spectral Size 65536
Br
O
MEMO
107B
f1 (ppm)

Parameter	Value
Data File Name	/ Users/ shawnteh/ Desktop/ Tobesorted/ ST-1-111-prod/ 1/ fid
Title	ST-1-111-prod.1.fid
Origin	Bruker BioSpin GmbH & Co.KG
Solvent	CDCl3
Temperature	298.2
Pulse Sequence	zg30
Experiment	1D
Number of Scans	16
Receiver Gain	101.0
Relaxation Delay	1.0000
Pulse Width	9.8500
Acquisition Time	3.9977
Acquisition Date	2024-04-12T15:50:01
Spectrometer Frequency	400.15
Spectral Width	8196.7
Nucleus	1H
Acquired Size	32768
Spectral Size	65536

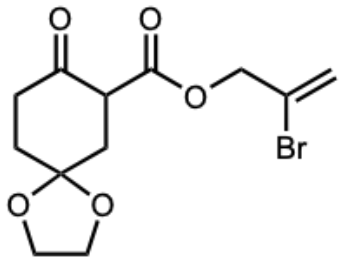

150A

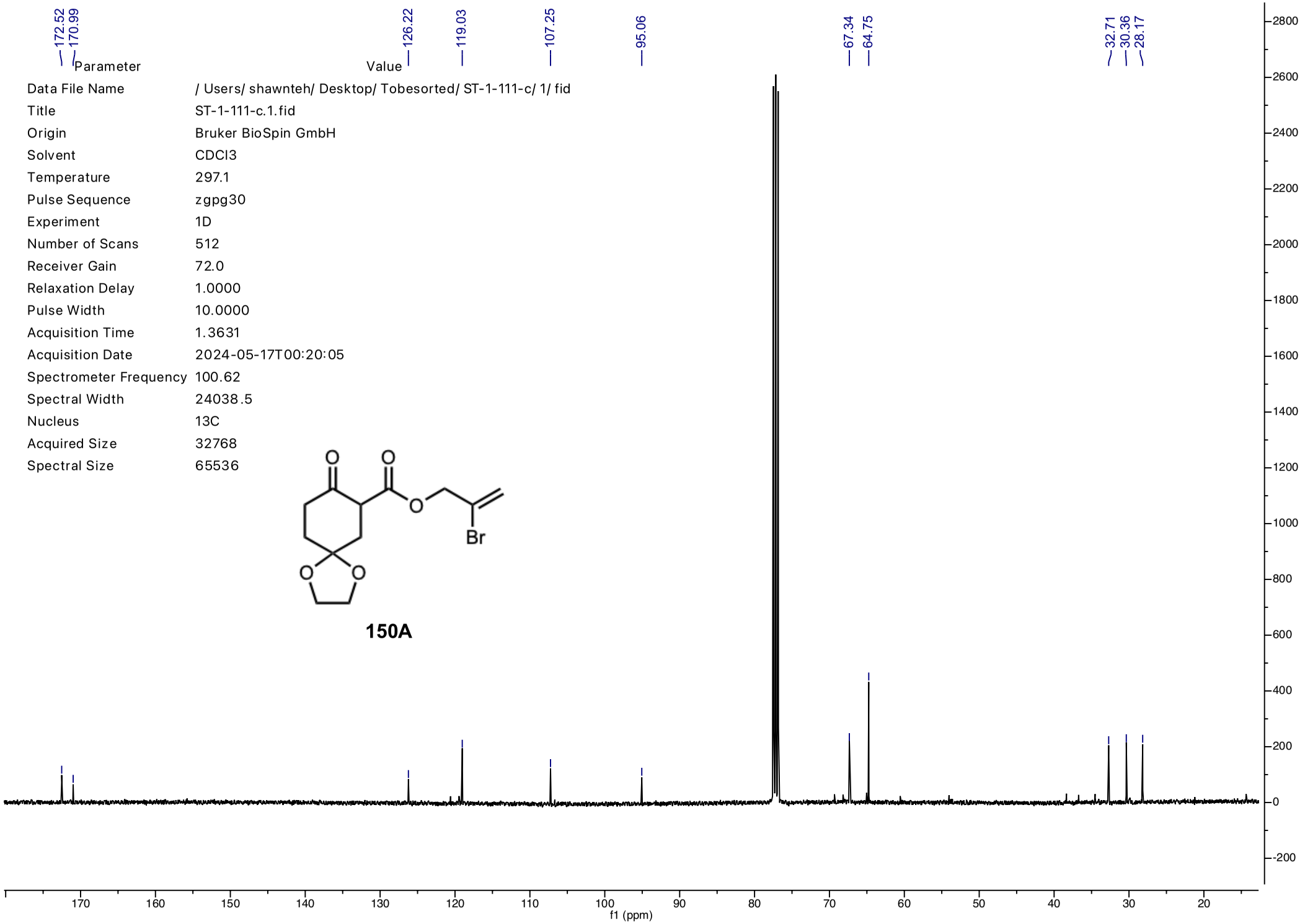
172.52
170.99
126.22
119.03
107.25
95.06
67.34
64.75
32.71
30.36
28.17
Parameter
Value
Data File Name / Users/ shawnteh/ Desktop/ Tobesorted/ ST-1-111-c/ 1/ fid
Title ST-1-111-c.1.fid
Origin Bruker BioSpin GmbH
Solvent CDCl3
Temperature 297.1
Pulse Sequence zgpg30
Experiment 1D
Number of Scans 512
Receiver Gain 72.0
Relaxation Delay 1.0000
Pulse Width 10.0000
Acquisition Time 1.3631
Acquisition Date 2024-05-17T00:20:05
Spectrometer Frequency 100.62
Spectral Width 24038.5
Nucleus 13C
Acquired Size 32768
Spectral Size 65536
O
O
O
O
O
O
Br
150A
2800
2600
2400
2200
2000
1800
1600
1400
1200
1000
800
600
400
200
0
-200
170
160
150
140
130
120
110
100
90
80
70
60
50
40
30
20
f1 (ppm)

Parameter	Value
Data File Name	/ Users/ shawnteh/ Desktop/ ST-chloro-h/ 1/ fid
Title	ST-chloro-h.1.fid
Origin	Bruker BioSpin GmbH
Solvent	CDCl3
Temperature	297.1
Pulse Sequence	zg30
Experiment	1D
Number of Scans	16
Receiver Gain	197.4
Relaxation Delay	1.0000
Pulse Width	12.5000
Acquisition Time	4.0894
Acquisition Date	2024-05-16T18:20:12
Spectrometer Frequency	400.13
Spectral Width	8012.8
Nucleus	1H
Acquired Size	32768
Spectral Size	65536

150B

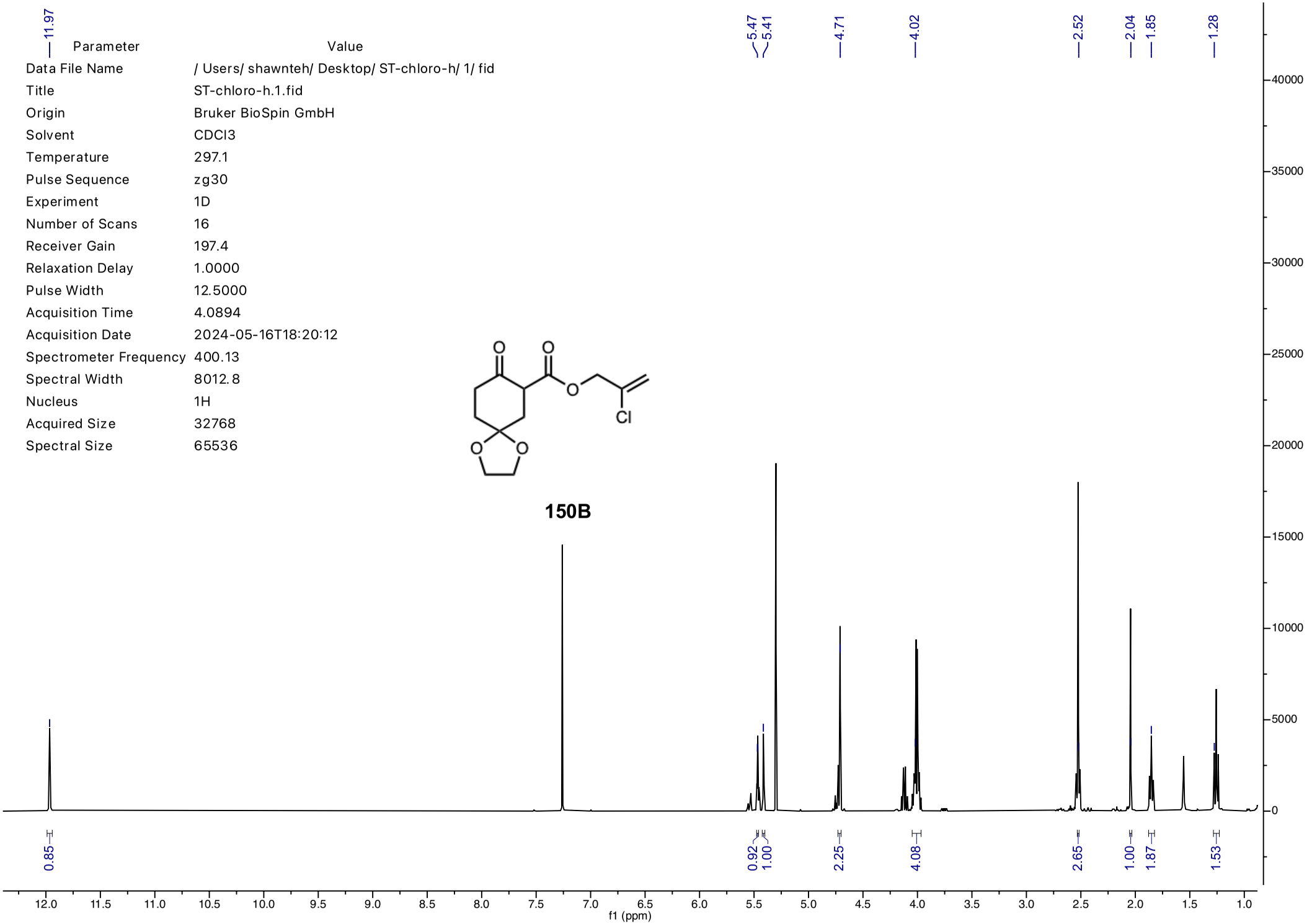

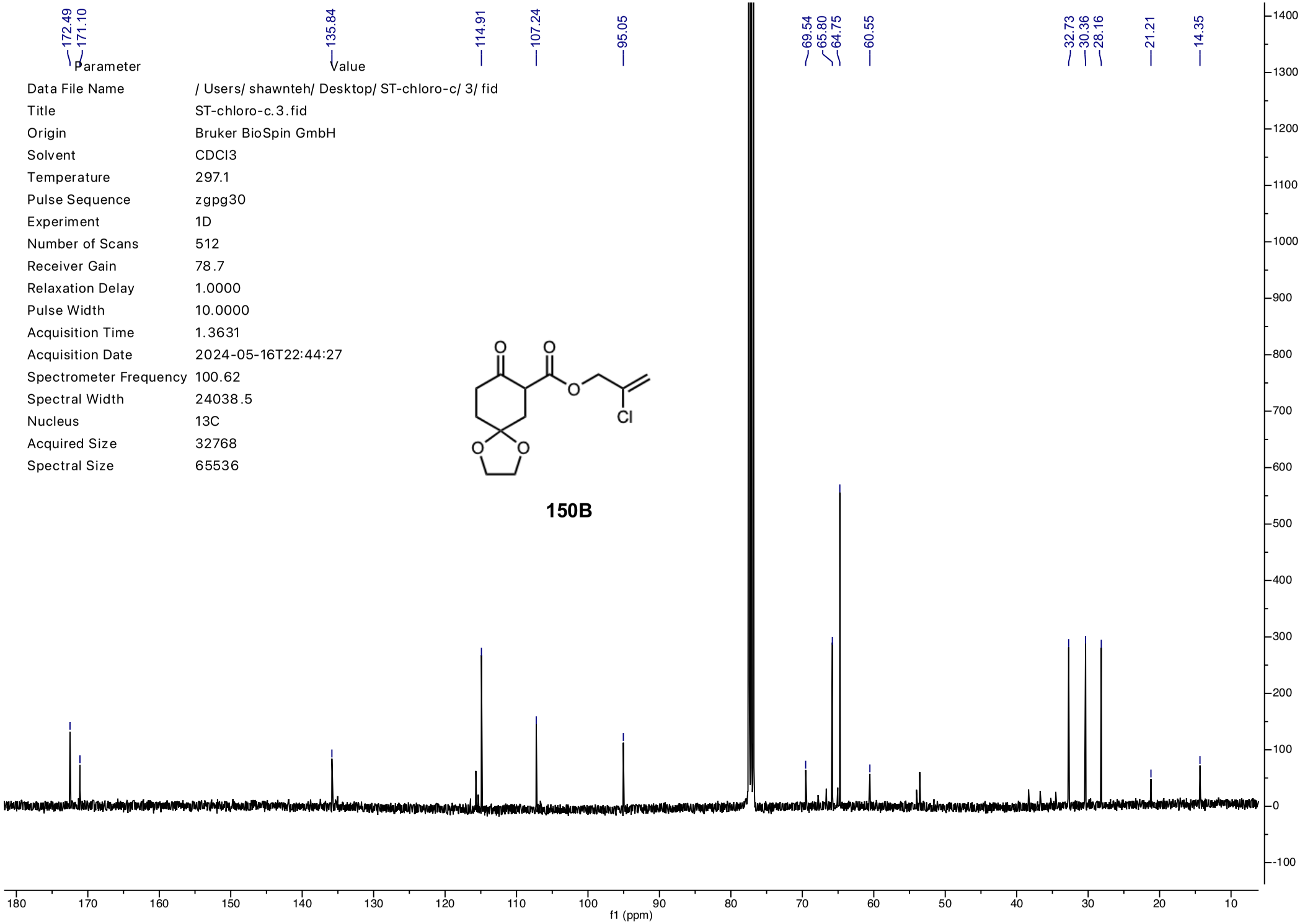
172.49
171.10
135.84
114.91
107.24
95.05
69.54
65.80
64.75
60.55
32.73
30.36
28.16
21.21
14.35
Parameter
Value
Data File Name / Users/ shawnteh/ Desktop/ ST-chloro-c/ 3/ fid
Title ST-chloro-c.3.fid
Origin Bruker BioSpin GmbH
Solvent CDCl3
Temperature 297.1
Pulse Sequence zgpg30
Experiment 1D
Number of Scans 512
Receiver Gain 78.7
Relaxation Delay 1.0000
Pulse Width 10.0000
Acquisition Time 1.3631
Acquisition Date 2024-05-16T22:44:27
Spectrometer Frequency 100.62
Spectral Width 24038.5
Nucleus 13C
Acquired Size 32768
Spectral Size 65536
O
O
O
O
O
Cl
150B
1400
1300
1200
1100
1000
900
800
700
600
500
400
300
200
100
0
-100
180
170
160
150
140
130
120
110
100
90
80
70
60
50
40
30
20
10
f1 (ppm)

Parameter	Value
Data File Name	/ Users/ shawnteh/ Desktop/ Tobesorted/ ST-1-109-prod_20240412_01/ ST-1-109-prod-PROTON_01.fid/ fid
Title	ST-1-109-prod-PROTON_01
Origin	Varian
Solvent	cdcl3
Temperature	25.0
Pulse Sequence	s2pul
Experiment	1D
Number of Scans	16
Receiver Gain	42
Relaxation Delay	1.0000
Pulse Width	2.6500
Acquisition Time	1.7080
Acquisition Date	2024-04-12T20:03:45
Spectrometer Frequency	599.56
Spectral Width	9592.3
Nucleus	1H
Acquired Size	16384
Spectral Size	65536

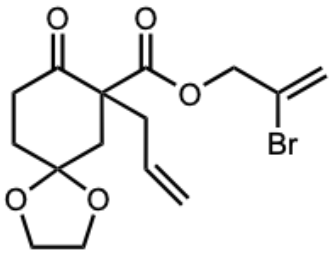

155

Parameter	Value
Data File Name	/ Users/ jordankthompson/ Desktop/ JKT-6-137_pure/ 1/ fid
Title	JKT-6-137_pure.1.fid
Origin	Bruker BioSpin GmbH
Solvent	CDCl3
Temperature	297.1
Pulse Sequence	zg30
Experiment	1D
Number of Scans	16
Receiver Gain	72.0
Relaxation Delay	1.0000
Pulse Width	12.5000
Acquisition Time	4.0894
Acquisition Date	2024-08-21T17:27:28
Spectrometer Frequency	400.13
Spectral Width	8012.8
Nucleus	1H
Acquired Size	32768
Spectral Size	65536

156

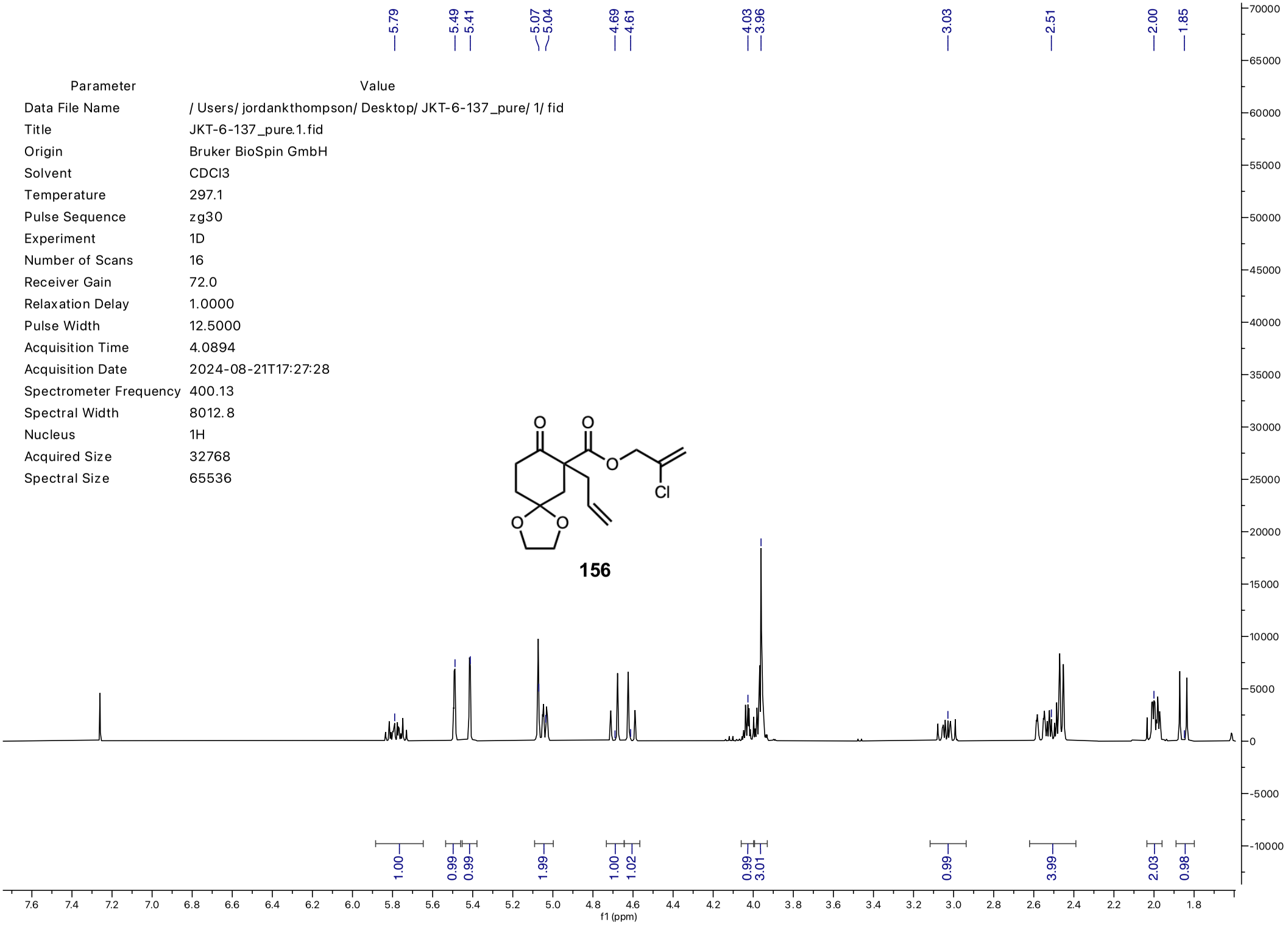

206.10
171.29
135.43
133.20
119.32
115.83
106.83
66.98
65.08
64.45
58.64
41.41
39.70
37.93
35.22

Parameter	Value
Data File Name	/ Volumes/ nmrdata-1/ jkthomps/ nmr/ JKT-6-137_pure/ 2/ fid
Title	JKT-6-137_pure.2.fid
Origin	Bruker BioSpin GmbH
Solvent	CDCl3
Temperature	297.1
Pulse Sequence	zgpg30
Experiment	1D
Number of Scans	512
Receiver Gain	87.8
Relaxation Delay	1.0000
Pulse Width	10.0000
Acquisition Time	1.3631
Acquisition Date	2024-08-21T17:48:42
Spectrometer Frequency	100.62
Spectral Width	24038.5
Nucleus	13C
Acquired Size	32768
Spectral Size	65536

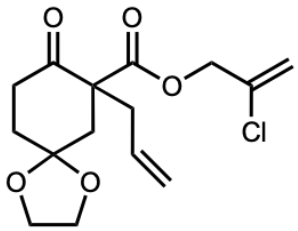

156

4500
4000
3500
3000
2500
2000
1500
1000
500
0

210 200 190 180 170 160 150 140 130 120 110 100 90 80 70 60 50 40 30

f1 (ppm)

Parameter	Value
Data File Name	/ Volumes/ nmrdata/ jkthomps/ nmr/ JKT-6-140_pure/ 1/ fid
Title	JKT-6-140_pure.1.fid
Origin	Bruker BioSpin GmbH
Solvent	CDCl3
Temperature	297.1
Pulse Sequence	zg30
Experiment	1D
Number of Scans	16
Receiver Gain	127.1
Relaxation Delay	1.0000
Pulse Width	12.5000
Acquisition Time	4.0894
Acquisition Date	2024-08-27T06:02:56
Spectrometer Frequency	400.13
Spectral Width	8012.8
Nucleus	1H
Acquired Size	32768
Spectral Size	65536

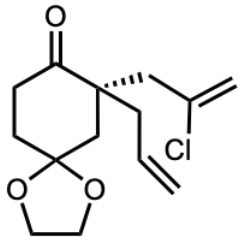

161

Parameter	Value
Data File Name	/ Volumes/ nmrdata/ jkthomps/ nmr/ JKT-6-140_pure/ 2/ fid
Title	JKT-6-140_pure.2.fid
Origin	Bruker BioSpin GmbH
Solvent	CDCl3
Temperature	297.2
Pulse Sequence	zgpg30
Experiment	1D
Number of Scans	512
Receiver Gain	35.5
Relaxation Delay	1.0000
Pulse Width	10.0000
Acquisition Time	1.3631
Acquisition Date	2024-08-27T06:24:07
Spectrometer Frequency	100.62
Spectral Width	24038.5
Nucleus	13C
Acquired Size	32768
Spectral Size	65536

161

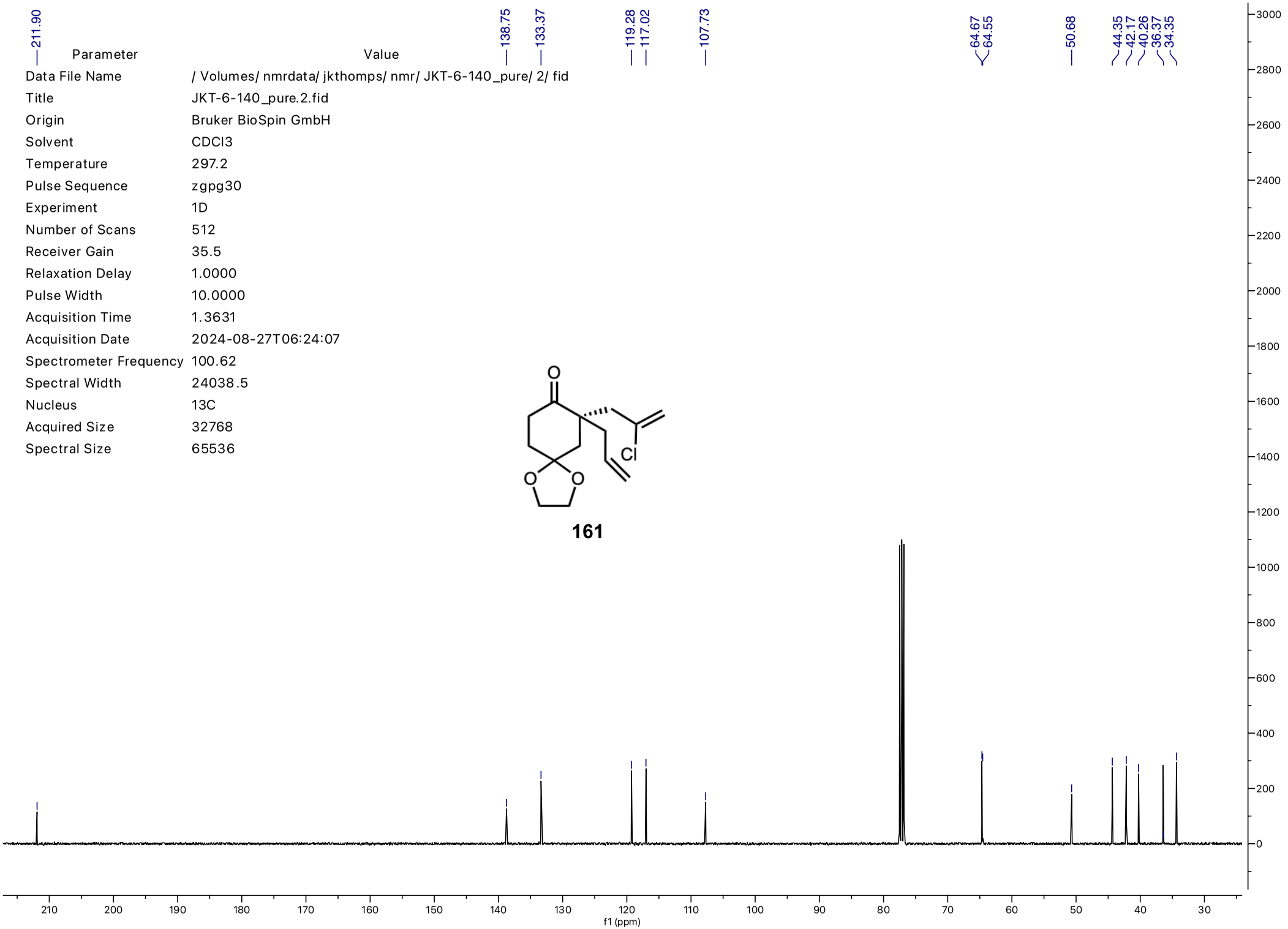

Parameter	Value
Data File Name	/ Users/ jordankthompson/ Desktop/ JKT-6-156-2/ PROTON01.fid/ fid
Title	PROTON01
Origin	Varian
Solvent	cdcl3
Temperature	25.0
Pulse Sequence	s2pul
Experiment	1D
Number of Scans	8
Receiver Gain	60
Relaxation Delay	1.0000
Pulse Width	5.6500
Acquisition Time	3.0000
Acquisition Date	2024-09-05T12:46:31
Spectrometer Frequency	499.54
Spectral Width	8000.0
Nucleus	1H
Acquired Size	24000
Spectral Size	65536

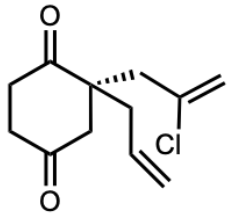

144B

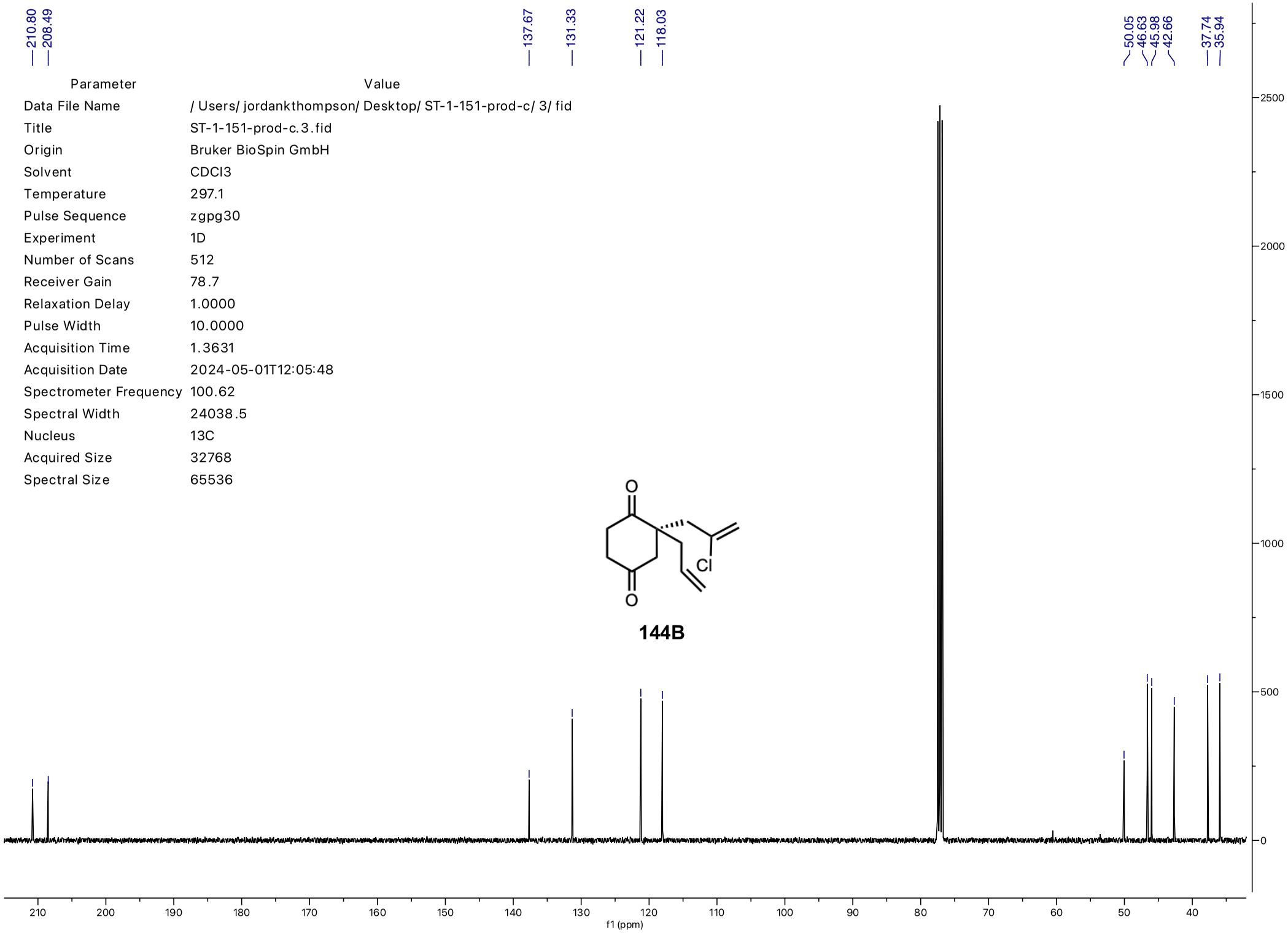

Parameter	Value
Data File Name	/ Users/ jordankthompson/ Desktop/ ST-1-151-prod-c/ 3/ fid
Title	ST-1-151-prod-c.3.fid
Origin	Bruker BioSpin GmbH
Solvent	CDCl3
Temperature	297.1
Pulse Sequence	zgpg30
Experiment	1D
Number of Scans	512
Receiver Gain	78.7
Relaxation Delay	1.0000
Pulse Width	10.0000
Acquisition Time	1.3631
Acquisition Date	2024-05-01T12:05:48
Spectrometer Frequency	100.62
Spectral Width	24038.5
Nucleus	13C
Acquired Size	32768
Spectral Size	65536

144B

Parameter	Value
Data File Name	/ Users/ shawnteh/ Desktop/ Tobesorted/ ST-1-126-prod_20240419_01/ ST-1-126-prod-PROTON_01.fid/ fid
Title	ST-1-126-prod-PROTON_01
Origin	Varian
Solvent	cdcl3
Temperature	25.0
Pulse Sequence	s2pul
Experiment	1D
Number of Scans	8
Receiver Gain	38
Relaxation Delay	1.0000
Pulse Width	2.6500
Acquisition Time	1.7080
Acquisition Date	2024-04-19T15:55:02
Spectrometer Frequency	599.56
Spectral Width	9592.3
Nucleus	1H
Acquired Size	16384
Spectral Size	65536

158

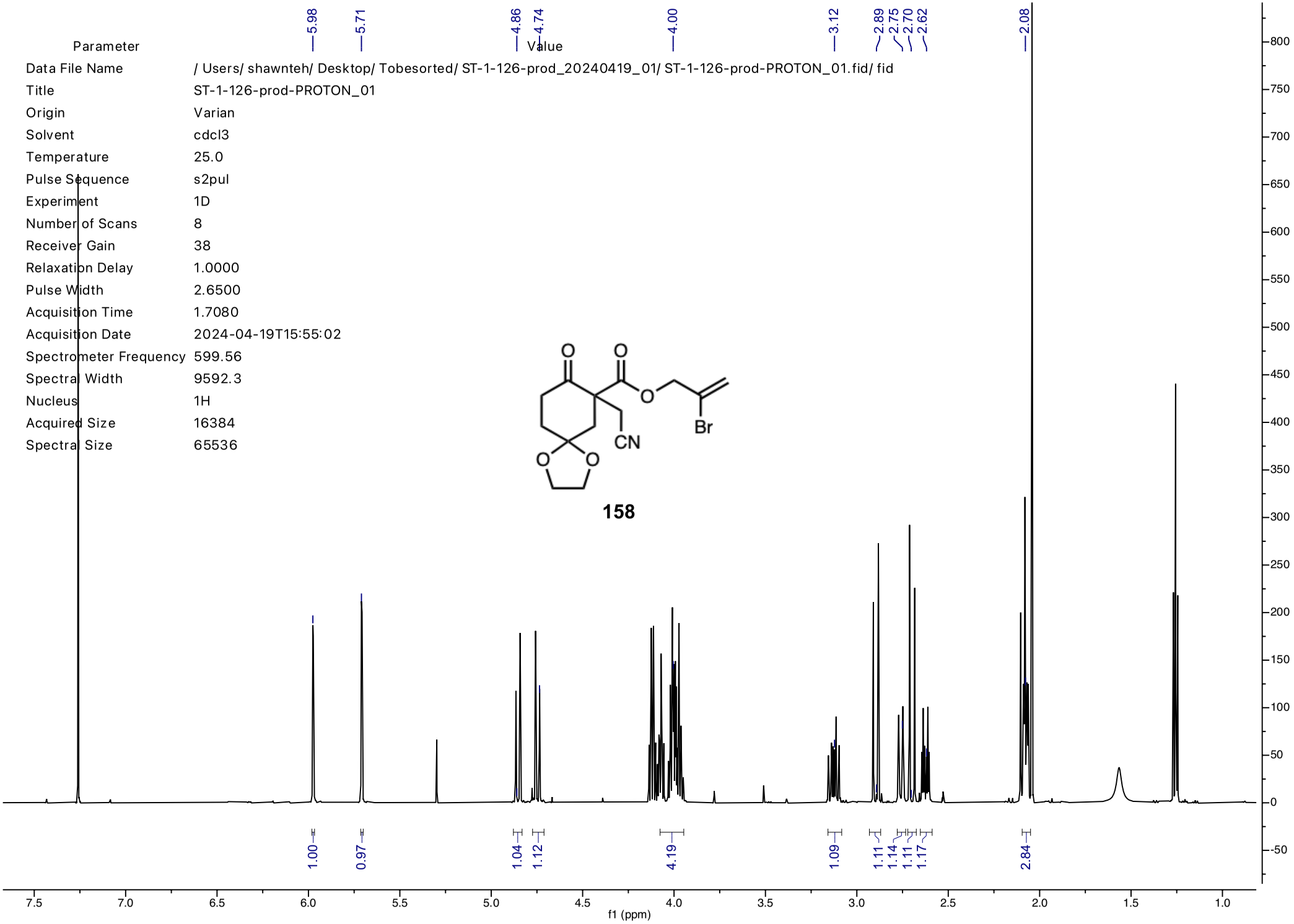

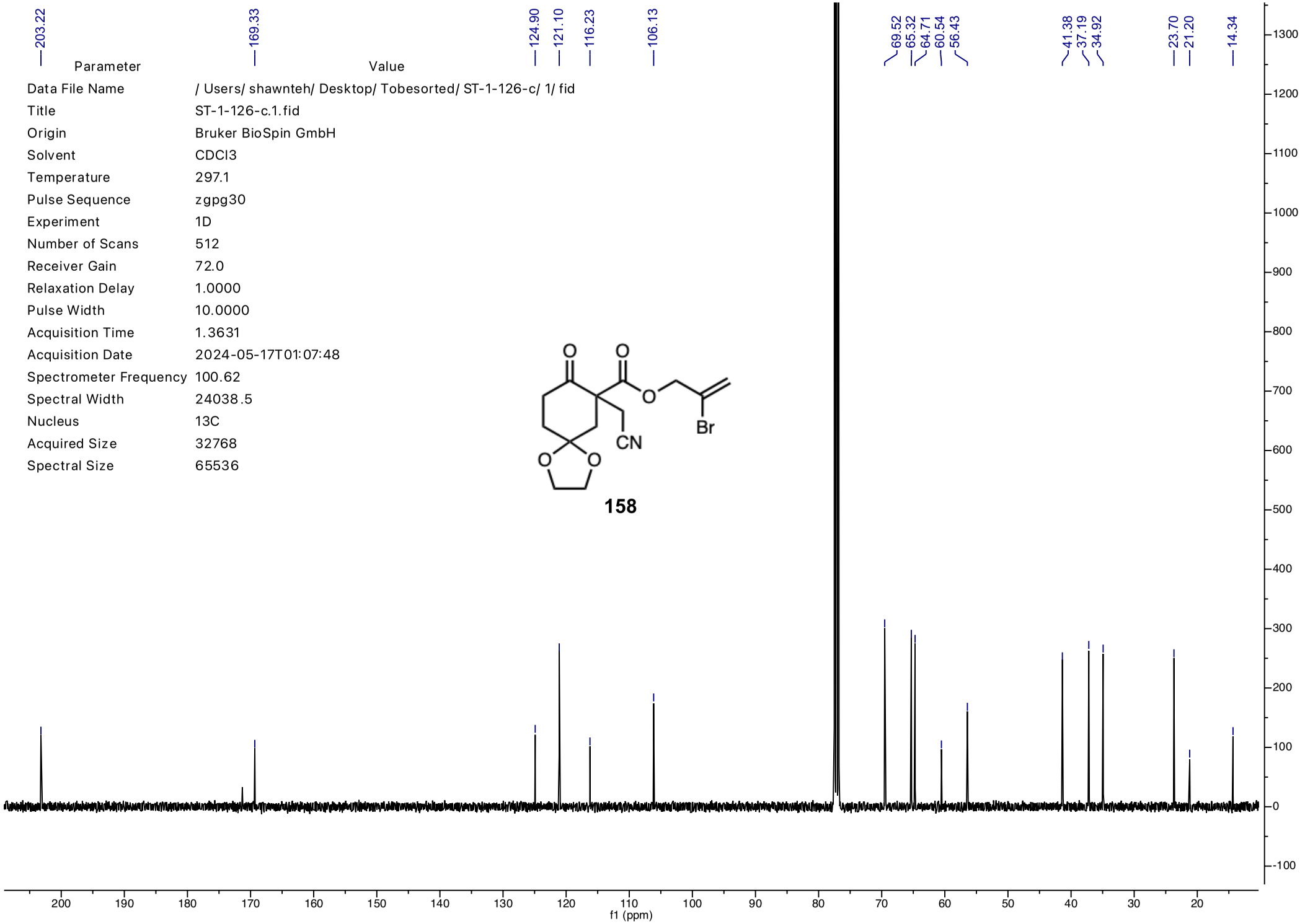
203.22
169.33
124.90
121.10
116.23
106.13
69.52
65.32
64.71
60.54
56.43
41.38
37.19
34.92
23.70
21.20
14.34
Parameter
Value
Data File Name / Users/ shawnteh/ Desktop/ Tobesorted/ ST-1-126-c/ 1/ fid
Title ST-1-126-c.1.fid
Origin Bruker BioSpin GmbH
Solvent CDCl3
Temperature 297.1
Pulse Sequence zgpg30
Experiment 1D
Number of Scans 512
Receiver Gain 72.0
Relaxation Delay 1.0000
Pulse Width 10.0000
Acquisition Time 1.3631
Acquisition Date 2024-05-17T01:07:48
Spectrometer Frequency 100.62
Spectral Width 24038.5
Nucleus 13C
Acquired Size 32768
Spectral Size 65536
O
O
O
O
O
CN
Br
158
f1 (ppm)

Parameter	Value
Data File Name	/ Users/ shawnteh/ Desktop/ Tobesorted/ St-1-127-prod_20240419_01/ St-1-127-prod-PROTON_01.fid/ fid
Title	St-1-127-prod-PROTON_01
Origin	Varian
Solvent	cdcl3
Temperature	25.0
Pulse Sequence	s2pul
Experiment	1D
Number of Scans	8
Receiver Gain	42
Relaxation Delay	1.0000
Pulse Width	2.6500
Acquisition Time	1.7080
Acquisition Date	2024-04-19T17:47:44
Spectrometer Frequency	599.56
Spectral Width	9592.3
Nucleus	1H
Acquired Size	16384
Spectral Size	65536

159

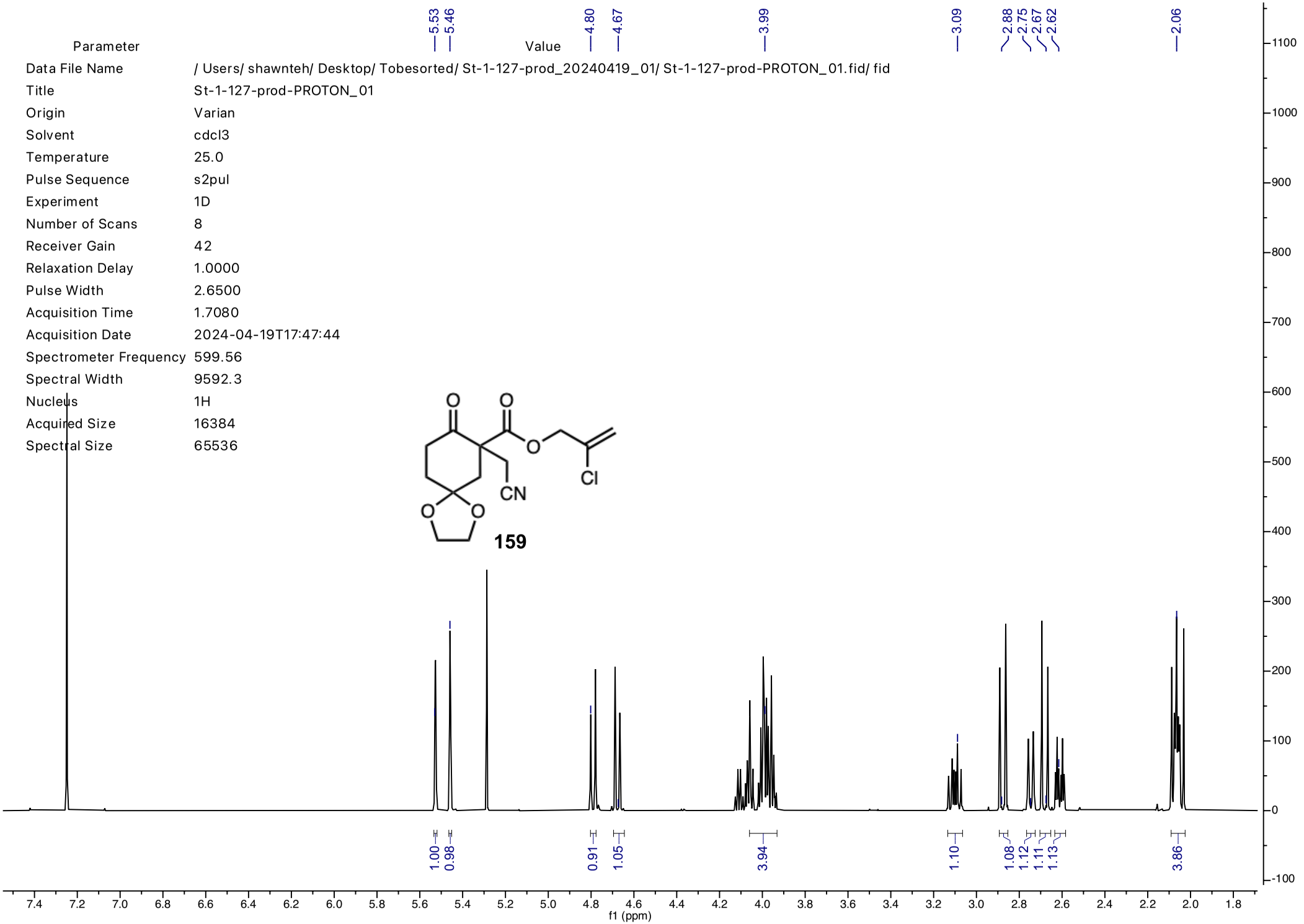

Parameter	Value
Data File Name	/ Users/ shawnteh/ Desktop/ Tobesorted/ ST-1-127-c/ 1/ fid
Title	ST-1-127-c.1.fid
Origin	Bruker BioSpin GmbH
Solvent	CDCl3
Temperature	297.2
Pulse Sequence	zgpg30
Experiment	1D
Number of Scans	512
Receiver Gain	72.0
Relaxation Delay	1.0000
Pulse Width	10.0000
Acquisition Time	1.3631
Acquisition Date	2024-05-17T01:30:53
Spectrometer Frequency	100.62
Spectral Width	24038.5
Nucleus	13C
Acquired Size	32768
Spectral Size	65536

159

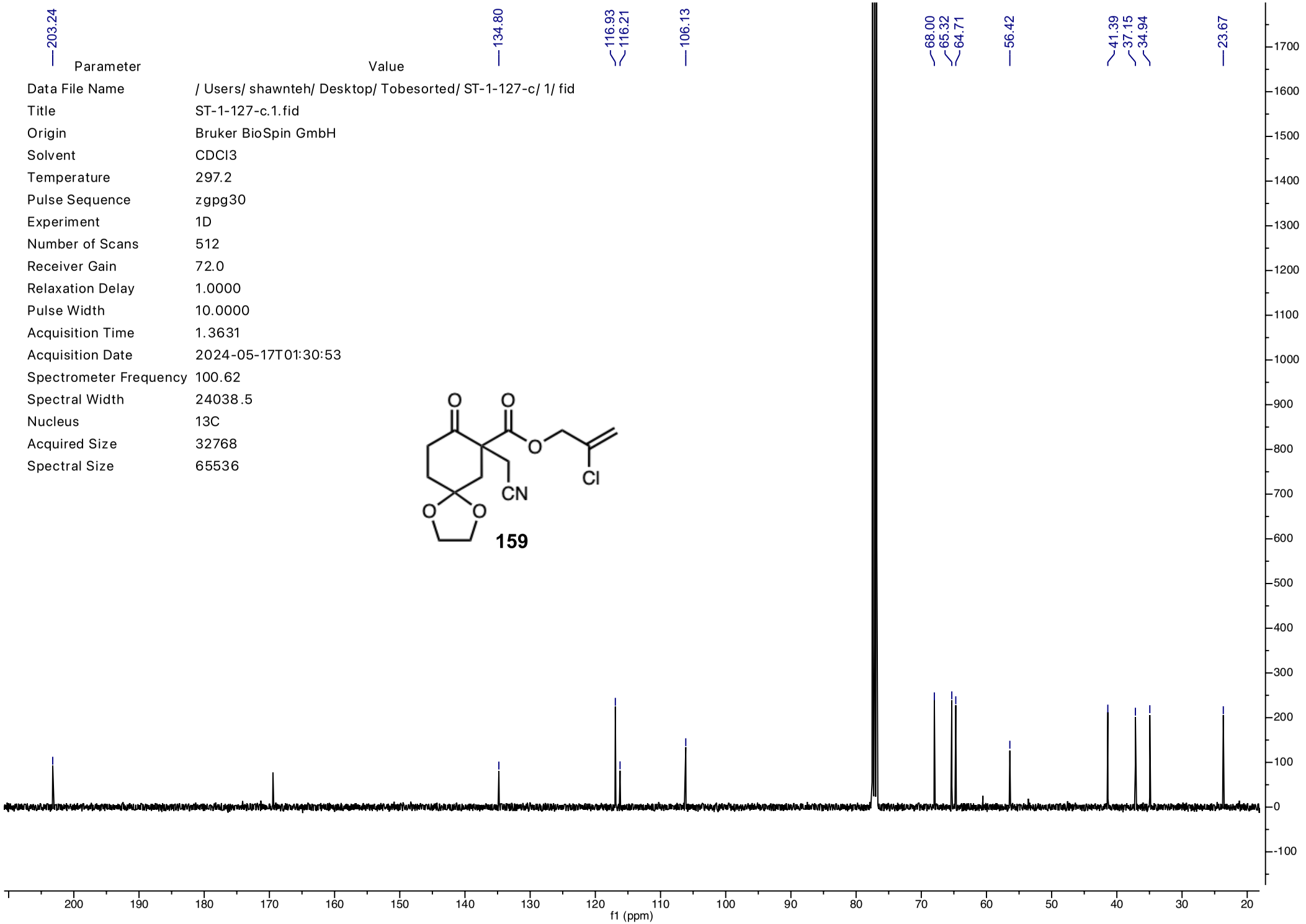

Parameter	Value
Data File Name	/ Users/ shawnteh/ Desktop/ Tobesorted/ ST-1-119-prod/ 1/ fid
Title	ST-1-119-prod.1.fid
Origin	Bruker BioSpin GmbH & Co.KG
Solvent	CDCl3
Temperature	298.2
Pulse Sequence	zg30
Experiment	1D
Number of Scans	16
Receiver Gain	101.0
Relaxation Delay	1.0000
Pulse Width	9.8500
Acquisition Time	3.9977
Acquisition Date	2024-04-18T11:44:50
Spectrometer Frequency	400.15
Spectral Width	8196.7
Nucleus	1H
Acquired Size	32768
Spectral Size	65536

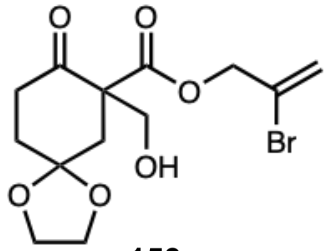

153

Parameter	Value
Data File Name	/ Users/ shawnteh/ Desktop/ Tobesorted/ ST-1-119-c/ 1/ fid
Title	ST-1-119-c.1.fid
Origin	Bruker BioSpin GmbH
Solvent	CDCl3
Temperature	297.1
Pulse Sequence	zgpg30
Experiment	1D
Number of Scans	512
Receiver Gain	72.0
Relaxation Delay	1.0000
Pulse Width	10.0000
Acquisition Time	1.3631
Acquisition Date	2024-05-16T23:56:03
Spectrometer Frequency	100.62
Spectral Width	24038.5
Nucleus	13C
Acquired Size	32768
Spectral Size	65536

153

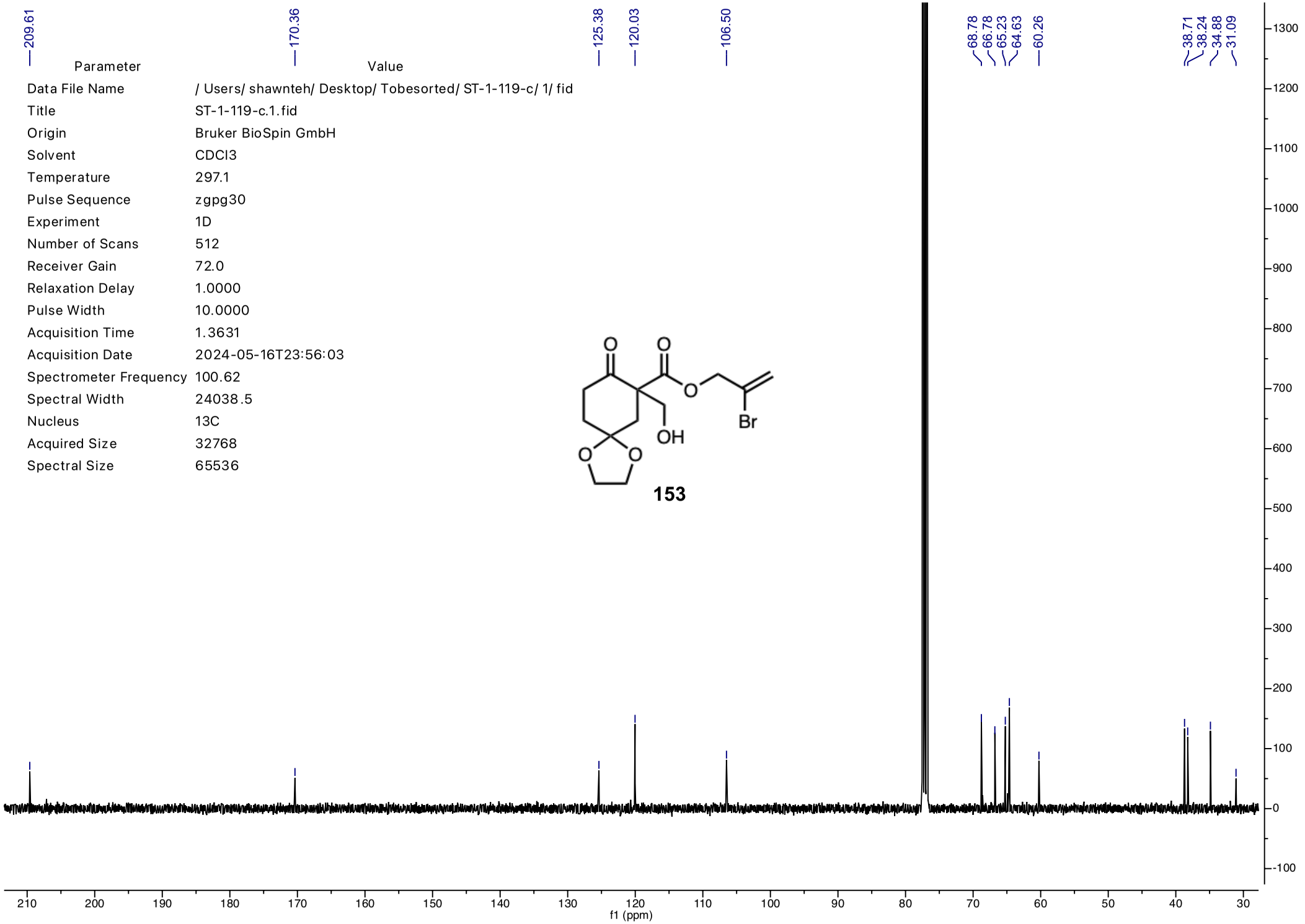

Parameter	Value
Data File Name	/ Users/ shawnteh/ Desktop/ Tobesorted/ ST-1-120-prod/ 1/ fid
Title	ST-1-120-prod.1.fid
Origin	Bruker BioSpin GmbH & Co.KG
Solvent	CDCl3
Temperature	298.2
Pulse Sequence	zg30
Experiment	1D
Number of Scans	16
Receiver Gain	101.0
Relaxation Delay	1.0000
Pulse Width	9.8500
Acquisition Time	3.9977
Acquisition Date	2024-04-18T11:49:39
Spectrometer Frequency	400.15
Spectral Width	8196.7
Nucleus	1H
Acquired Size	32768
Spectral Size	65536

154

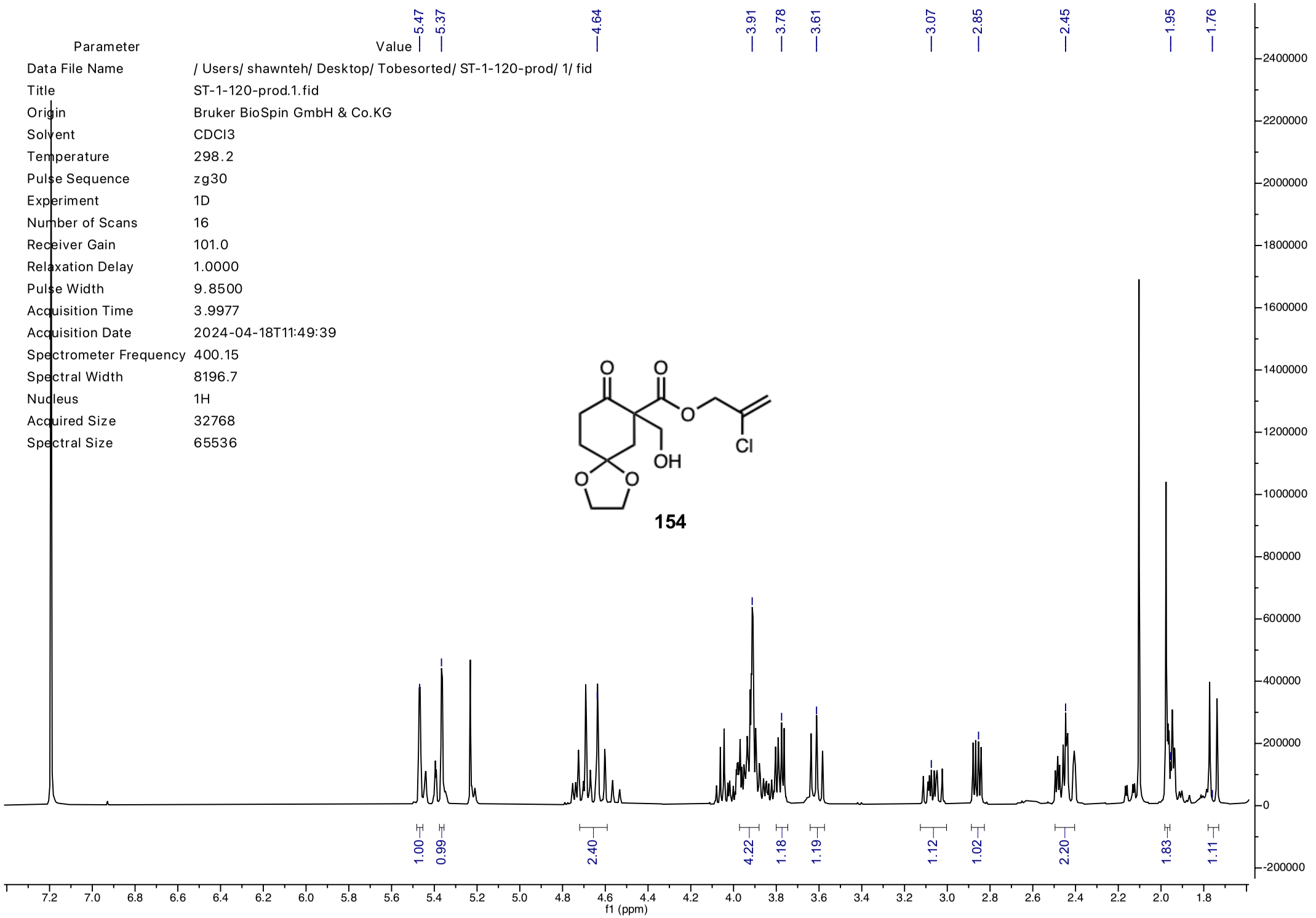

Parameter	Value
Data File Name	/ Users/ shawnteh/ Desktop/ Tobesorted/ ST-1-120-c/ 1/ fid
Title	ST-1-120-c.1.fid
Origin	Bruker BioSpin GmbH
Solvent	CDCl3
Temperature	297.2
Pulse Sequence	zgpg30
Experiment	1D
Number of Scans	512
Receiver Gain	72.0
Relaxation Delay	1.0000
Pulse Width	10.0000
Acquisition Time	1.3631
Acquisition Date	2024-05-17T00:44:13
Spectrometer Frequency	100.62
Spectral Width	24038.5
Nucleus	13C
Acquired Size	32768
Spectral Size	65536

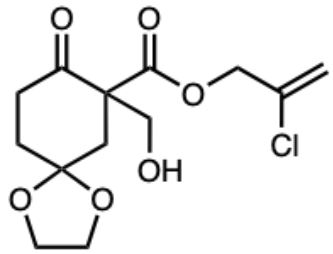

154

Parameter	Value
Data File Name	/ Users/ shawnteh/ Desktop/ Tobesorted/ ST-1-135-2_20240424_01/ ST-1-135-2-PROTON_01.fid/ fid
Title	ST-1-135-2-PROTON_01
Origin	Varian
Solvent	cdcl3
Temperature	25.0
Pulse Sequence	s2pul
Experiment	1D
Number of Scans	8
Receiver Gain	36
Relaxation Delay	1.0000
Pulse Width	2.6500
Acquisition Time	1.7080
Acquisition Date	2024-04-24T15:36:25
Spectrometer Frequency	599.56
Spectral Width	9592.3
Nucleus	1H
Acquired Size	16384
Spectral Size	65536

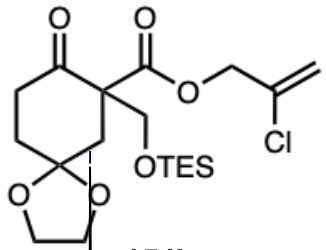

154'

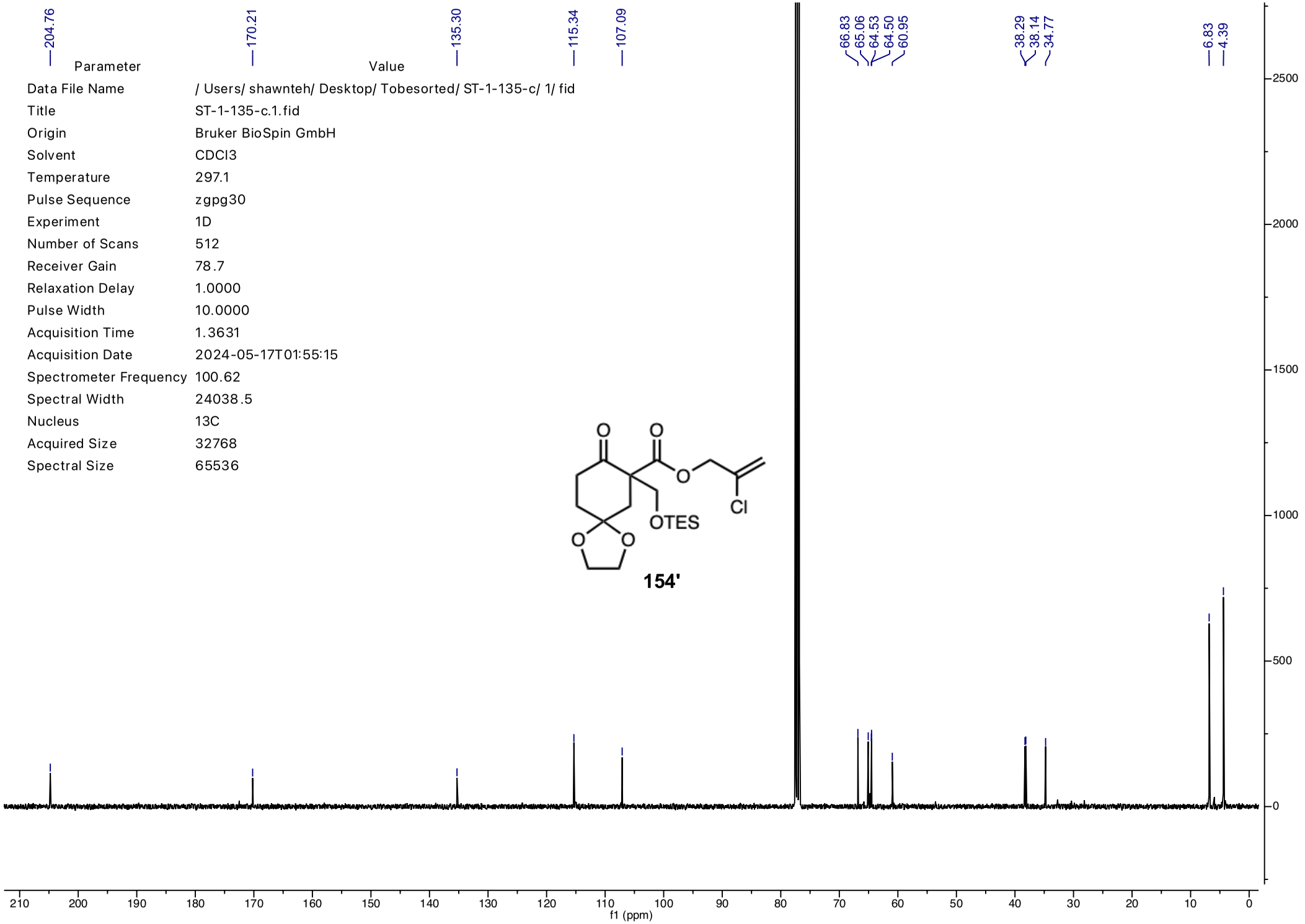
204.76
170.21
135.30
115.34
107.09
66.83
65.06
64.53
64.50
60.95
38.29
38.14
34.77
6.83
4.39
Parameter
Value
Data File Name / Users/ shawnteh/ Desktop/ Tobesorted/ ST-1-135-c/ 1/ fid
Title ST-1-135-c.1.fid
Origin Bruker BioSpin GmbH
Solvent CDCl3
Temperature 297.1
Pulse Sequence zgpg30
Experiment 1D
Number of Scans 512
Receiver Gain 78.7
Relaxation Delay 1.0000
Pulse Width 10.0000
Acquisition Time 1.3631
Acquisition Date 2024-05-17T01:55:15
Spectrometer Frequency 100.62
Spectral Width 24038.5
Nucleus 13C
Acquired Size 32768
Spectral Size 65536
O
O
O
Cl
OTES
O
O
154'
2500
2000
1500
1000
500
0
210
200
190
180
170
160
150
140
130
120
110
100
90
80
70
60
50
40
30
20
10
0
f1 (ppm)

Parameter	Value
Data File Name	/ Users/ jordankthompson/ Desktop/ JKT-6-139-2/ PROTON01.fid/ fid
Title	PROTON01
Origin	Varian
Solvent	cdcl3
Temperature	25.0
Pulse Sequence	s2pul
Experiment	1D
Number of Scans	8
Receiver Gain	48
Relaxation Delay	1.0000
Pulse Width	5.6500
Acquisition Time	3.0000
Acquisition Date	2024-08-21T21:41:52
Spectrometer Frequency	499.54
Spectral Width	8000.0
Nucleus	1H
Acquired Size	24000
Spectral Size	65536

173

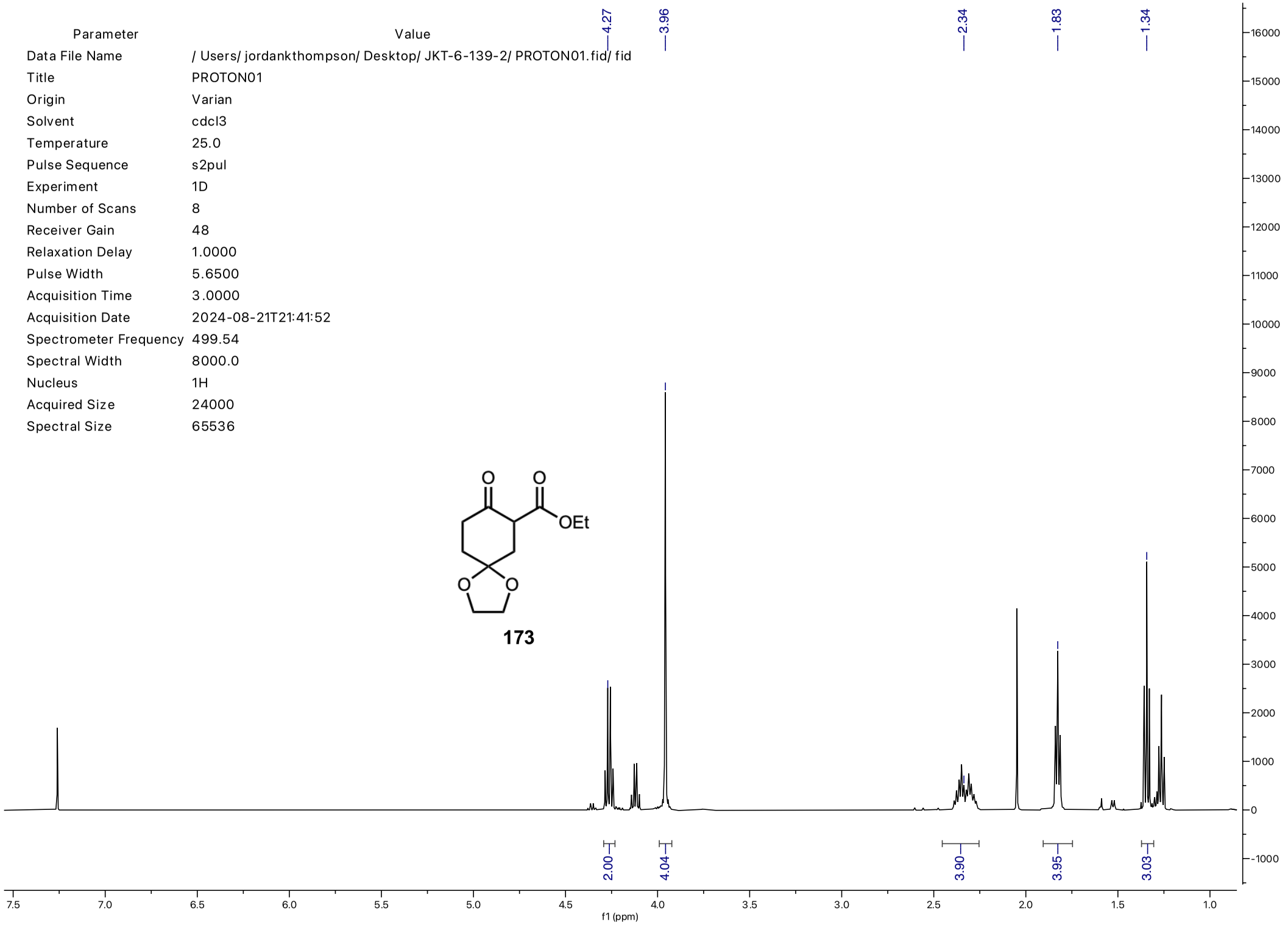

Parameter	Value
Data File Name	/ Users/ jordankthompson/ Desktop/ JKT-6-141-C2-3/ PROTON01.fid/ fid
Title	PROTON01
Origin	Varian
Solvent	cdcl3
Temperature	25.0
Pulse Sequence	s2pul
Experiment	1D
Number of Scans	8
Receiver Gain	42
Relaxation Delay	1.0000
Pulse Width	5.6500
Acquisition Time	3.0000
Acquisition Date	2024-08-26T11:24:30
Spectrometer Frequency	499.54
Spectral Width	8000.0
Nucleus	1H
Acquired Size	24000
Spectral Size	65536

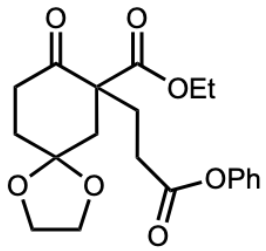

174

Parameter	Value
Data File Name	/ Volumes/ nmrdata-1/ jkthomps/ nmr/ JKT-6-141-C2-3/ 2/ fid
Title	JKT-6-141-C2-3.2.fid
Origin	Bruker BioSpin GmbH
Solvent	CDCl3
Temperature	297.2
Pulse Sequence	zgpg30
Experiment	1D
Number of Scans	700
Receiver Gain	64.2
Relaxation Delay	1.0000
Pulse Width	10.0000
Acquisition Time	1.3631
Acquisition Date	2024-08-26T12:46:39
Spectrometer Frequency	100.62
Spectral Width	24038.5
Nucleus	13C
Acquired Size	32768
Spectral Size	65536

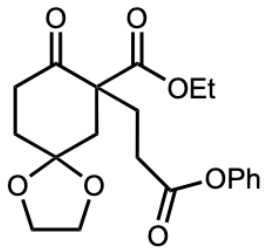

174

Parameter	Value
Data File Name	/ Volumes/ nmrdata-1/ jkthomps/ nmr/ JKT-6-153-1/ 1/ fid
Title	JKT-6-153-1.1.fid
Origin	Bruker BioSpin GmbH
Solvent	CDCl3
Temperature	297.1
Pulse Sequence	zg30
Experiment	1D
Number of Scans	16
Receiver Gain	112.8
Relaxation Delay	1.0000
Pulse Width	12.5000
Acquisition Time	4.0894
Acquisition Date	2024-08-30T14:57:29
Spectrometer Frequency	400.13
Spectral Width	8012.8
Nucleus	1H
Acquired Size	32768
Spectral Size	65536

175

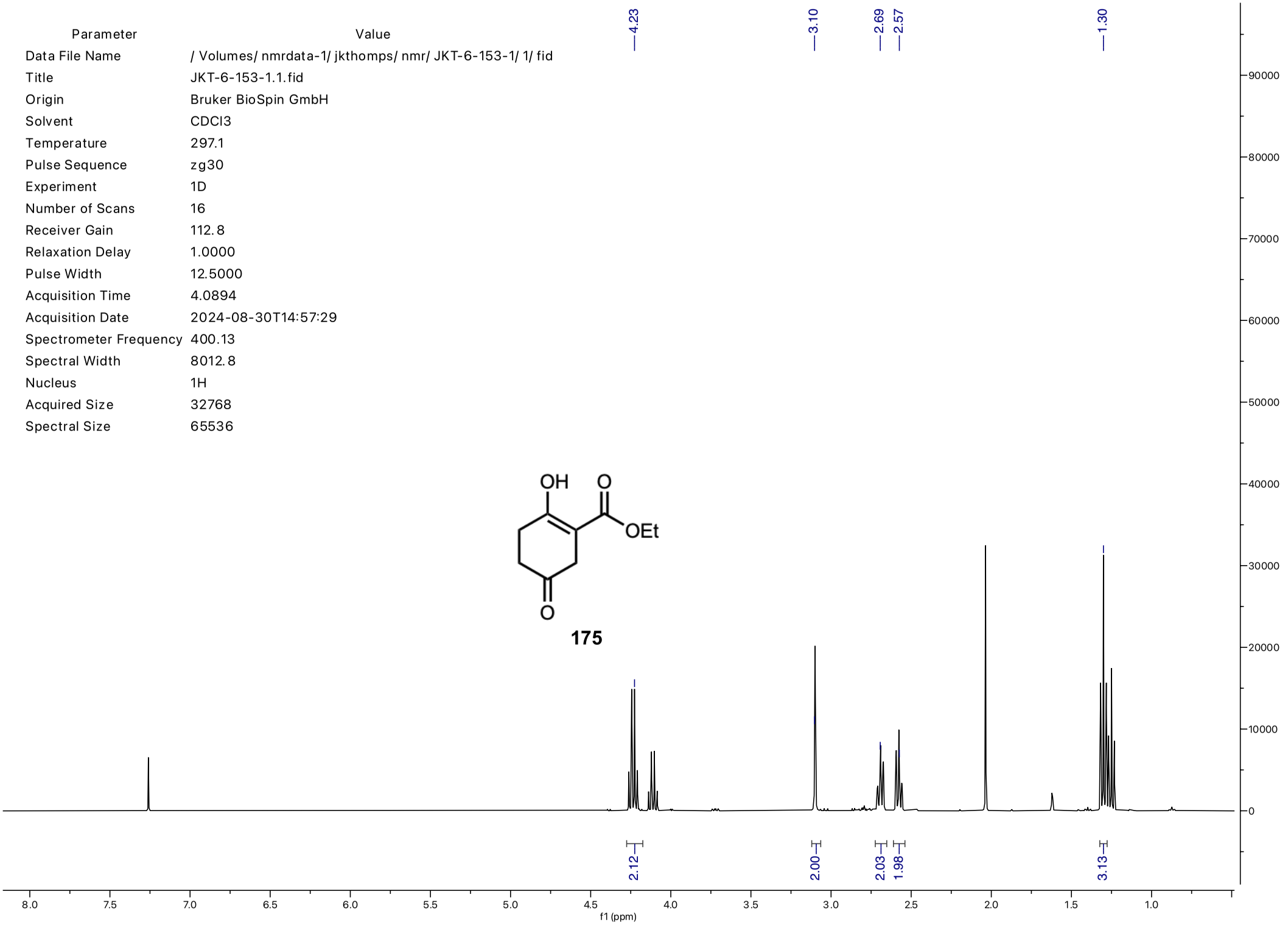

Parameter	Value
Data File Name	/ Volumes/ nmrdata/ jkthomps/ nmr/ JKT-6-155-B3-L/ 1/ pdata/ 1/ 1r
Title	JKT-6-155-B3-L.1.1.1r
Origin	Bruker BioSpin GmbH & Co.KG
Solvent	
Temperature	298.0
Pulse Sequence	zg30
Experiment	1D
Number of Scans	16
Receiver Gain	32.0
Relaxation Delay	1.0000
Pulse Width	10.0000
Acquisition Time	0.0000
Acquisition Date	2024-09-03T14:46:14
Spectrometer Frequency	400.15
Spectral Width	8196.7
Nucleus	1H
Acquired Size	0
Spectral Size	65536

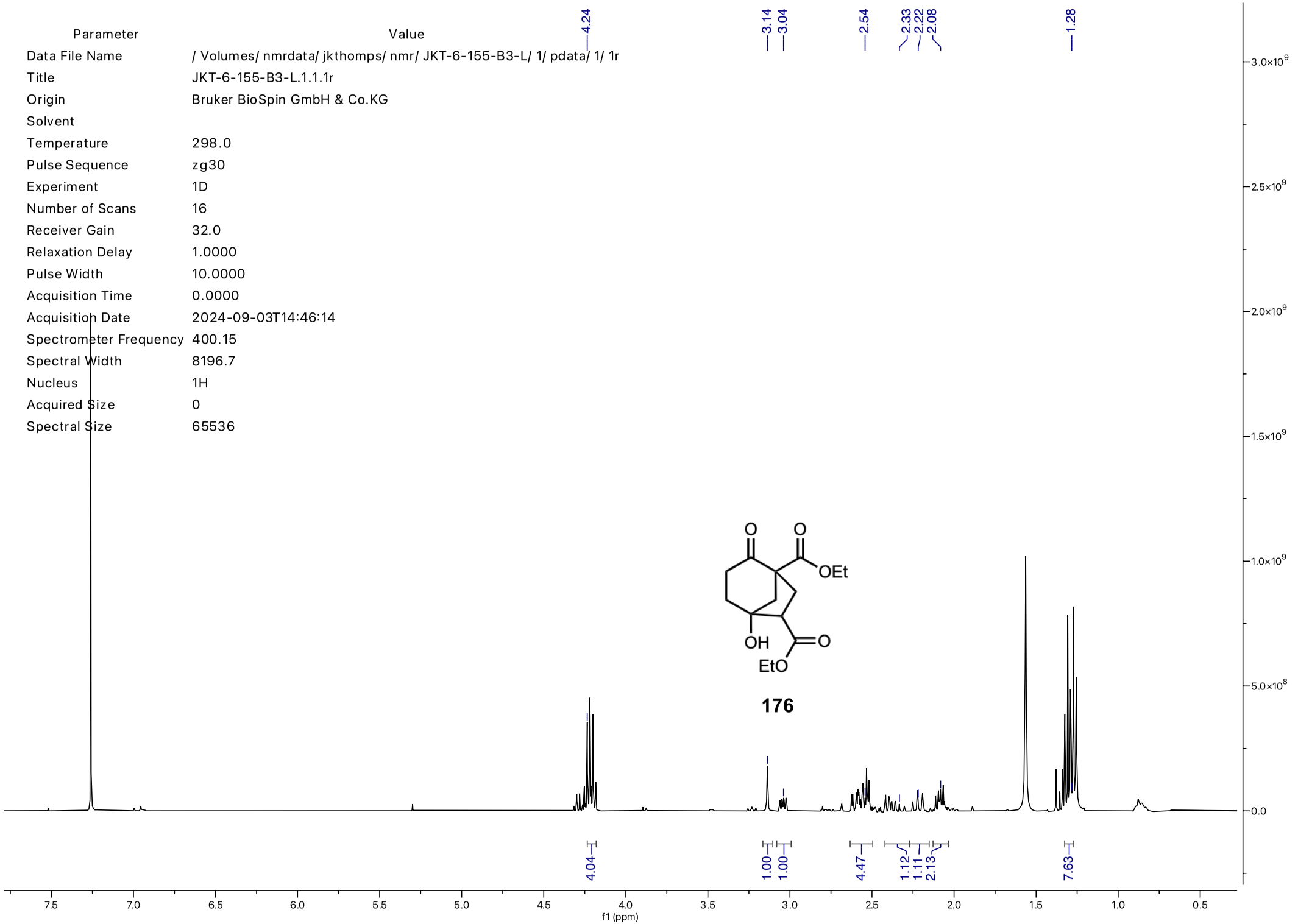

Chapter 5

Development of a vinylogous Mukaiyama Aldol fragment coupling reaction and intramolecular Ni-catalyzed α-enolate alkenylation[†]

5.1 INTRODUCTION

This chapter describes the development of the two most important steps of the synthesis: the vinylogous Mukaiyama aldol reaction and the Ni-catalyzed α-enolate alkenylation. Early hit identification in the vinylogous Mukaiyama aldol reaction along with the subsequent reaction optimization are explored. Synthesis of the α-enolate alkenylation substrate followed by development of Ni-catalyzed α-enolate alkenylation conditions using electron-deficient olefin ligands is presented. Taken together, this chapter

[†] Portions of this chapter were adapted from the following communication: Thompson, J. K.; Youngblood, K. C.; Teh, S. Y. H.; Farley, C. M.; Zhang, Z.; Virgil, S. C.; Reisman, S. E. *J. Am. Chem. Soc.* **2025**, *147*, 42170–42174. Dr. Michael Takase is acknowledged for acquiring the X-ray diffraction data, and Preston Mott is thanked for assistance in solving the X-ray structure of **106A**. J.K.T. was supported by the NSF GRFP (DGE-1745301). S.E.R. acknowledges fellowship support by the NIH (R35GM118191).

reports a rapid fragment coupling assembly to establish the pentacyclic core of auriculatol A.

5.2 CONVERGENT FRAGMENT COUPLING: OPTIMIZATION OF THE VINYLOGOUS MUKAIYAMA ALDOL ADDITION

5.2.1 Early optimization of enol triflate substrate (107A) VMAR

Initially, using conditions optimized on the model aryl aldehyde from Chapter 2 for the vinylogous Mukaiyama aldol reaction (VMAR) on the more complex 3.2.1 bicyclic aldehyde (**107A**) led to 8% yield of **106A** (Scheme 5.1). Clearly, exploration of the reaction conditions and a thorough optimization campaign were required to increase the yield to adequate quantities.

Scheme 5.1. *Initial experimentation in the more advanced VMAR coupling.*

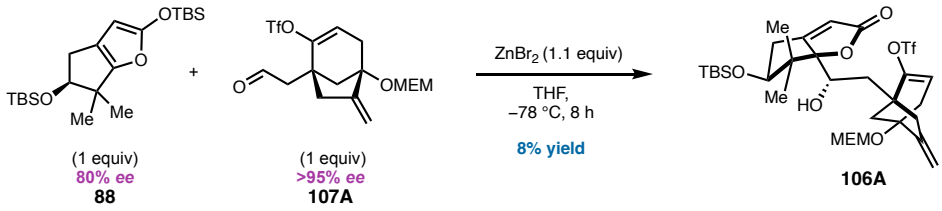

Recrystallization by slow evaporation of toluene overnight enabled isolation of crystals suitable for X-ray diffraction (XRD) analysis. In line with previous results described in Chapter 2, the major diastereomer exhibited α-stereochemistry at the alcohol stereogenic center (Scheme 5.2). While this was undesired for the synthesis of auriculatol A, it was envisioned that epimerization later in the synthesis would be possible. The crystal structure verified γ-functionalization of the silyloxyfuran starting material, establishing the fully-substituted γ-position of the product butenolide in the desired fashion; that is, functionalization of the silyloxyfuran starting material occurred from the less-hindered

face, opposite to that of the TBS group, in line with results from Chapter 2.

Scheme 5.2. *XRD verifies major product (**106A**) structure and stereochemistry.*

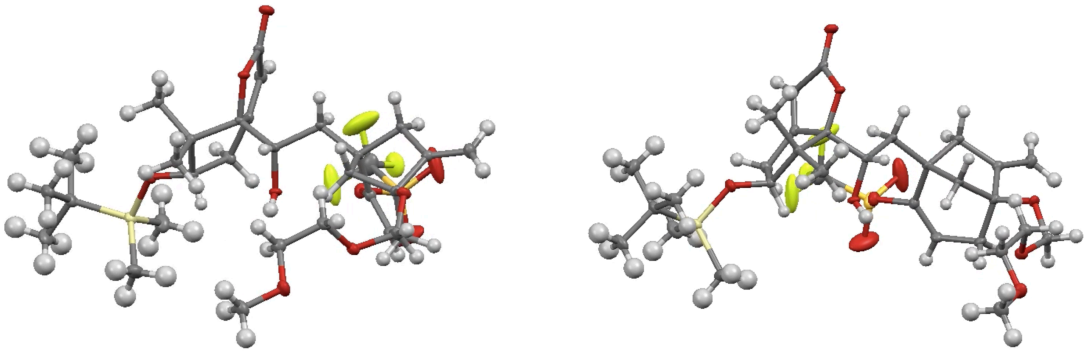

In comparison to the aryl aldehyde **61**, which provided the desired coupled product in 52% yield, the conversion with **107A** was much lower (< 20%, Scheme 5.3). It was hypothesized that the steric bulk of the 3.2.1-bicycle in **107A**, despite being distal to the aldehyde-functionality, disfavors the desired coupling reaction – or any coupling reaction for the matter. It is possible, as well, that the electronic effect of the homobenzylic aldehyde is important in the aryl-aldehyde (**61**) system.

The distribution of recovered butenolide **60** in the model system VMAR was also of interest. Higher levels of butenolide **60** in the reaction with **61** vs. **107A** were observed. Although this product could result from hydrolysis under the work up conditions, it is also possible that the butenolide **60** forms under the reaction conditions from deprotonation of the α-aldehyde protons (Scheme 5.3, protons highlighted in purple). The increased acidity of the benzylic α-aldehyde protons in **61** could explain the higher conversion and formation of **60**.

Scheme 5.3. *Model system VMAR vs. more advanced VMAR conversions and yields.*

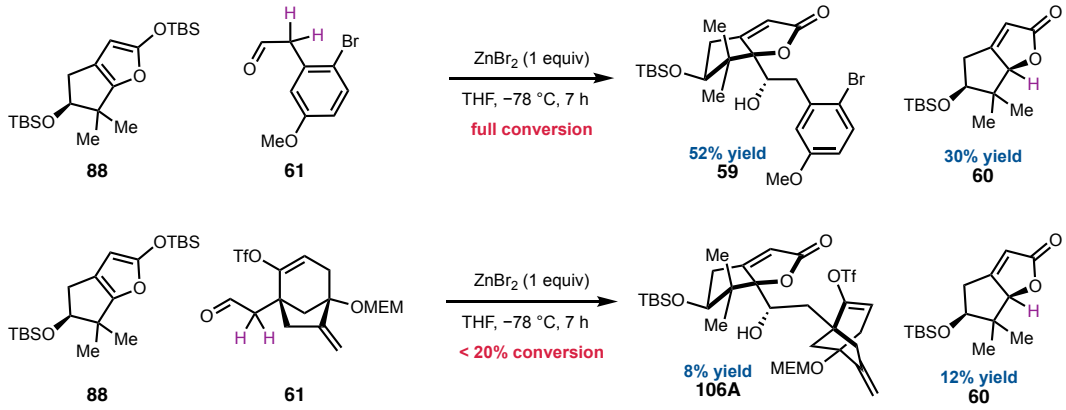

As with the model system, choice of solvent had a dramatic influence on conversion. Preliminary results indicated that the reaction could be conducted at 22 °C and give higher conversion (not shown). For this reason, early studies focused on screening parameters of the reaction at room temperature broadly. No yield was observed across several solvents, including non-polar (toluene), alcohol-containing (TFE), amide-containing (DMA), and nitrile-containing (ACN) solvents (Scheme 5.4). Carbonyl-containing solvents (EtOAc, acetone, and isopropyl acetate) were determined to be better, providing yields ranging from 13-16%. Et_2O was identified as the best solvent, leading to slightly increased yields (25%) when compared to THF (16%).

Scheme 5.4. *Solvent screen in the more advanced key VMAR coupling.*

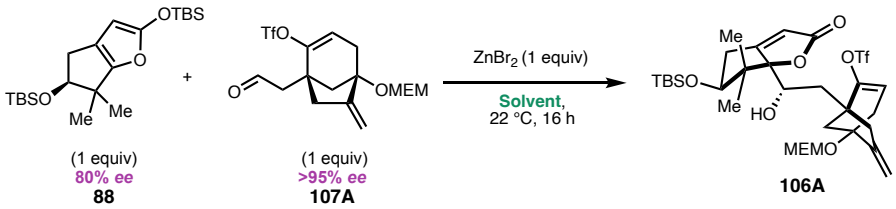

(1 equiv) 80% *ee* **88** | (1 equiv) >95% *ee* **107A** | **106A**

Solvent	Result	Solvent	Result
ACN	no product	THF	16% yield
TFE	no product	THP	7% yield
DMA	no product	EtOAc	13% yield
DMSO	no product	Acetone	13% yield
Dioxane	no product	Isopropyl Acetate	13% yield
2-methyl THF	trace product	Dimethyl Carbonate	16% yield
Toluene	no product	**Et_2O**	**25% yield**

Next, studies investigating different Zn(II) salts were conducted. Preliminary investigations identified that Zn-halide salts were important over pseudo-halide or non-coordinating counterions such as OTf and BF_4 (Scheme 5.6). These data are consistent with a mechanism that relies on a nucleophilic counterion, possibly one that can displace TBS from the silyloxyfuran, generating TBS-X, where X is the halide counterion.

Scheme 5.5. *Zn-salt screen in the more advanced key VMAR coupling.*

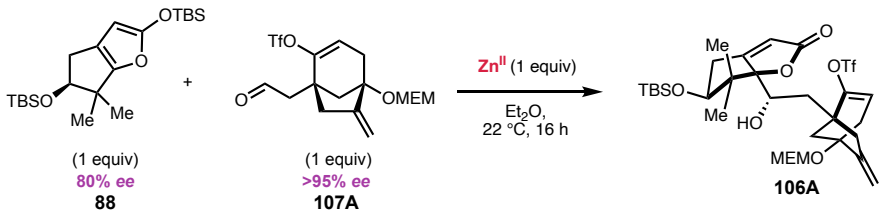

(1 equiv) 80% *ee* **88** | (1 equiv) >95% *ee* **107A** | **106A**

Zn^{II}	Result
$ZnBr_2$	**25% yield**
$ZnCl_2$	17% yield
ZnI_2	27% yield, messier reaction profile
$Zn(OTf)_2$	no product
$Zn(BF_4)_2$	no product

In a brief equivalency screen, 1 equivalent was identified as optimal (Scheme 5.6). Catalytic loading led to reduced yield, while super stoichiometric loading led to lower

yields. One possibility for the lower yield involves competitive MEM-deprotection of **107A** or **106A** under the reaction conditions.

Scheme 5.6. *Zn-salt equivalence screen in the more advanced key VMAR coupling.*

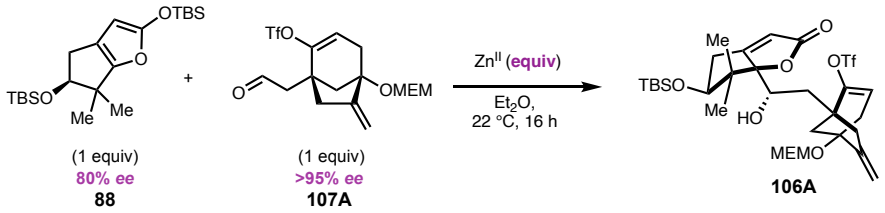

equiv	Result
0.2	12% yield
1	**25% yield**
2	17% yield
5	7% yield
10	7% yield

Scaling up of the reaction confirmed the occurrence of Zn-mediated MEM-deprotection (Scheme 5.7). Turning to the literature, it became clear that deprotection does not occur as readily in non-polar, aromatic solvents like benzene or toluene.[1] While the VMAR did not convert in toluene (Scheme 5.4) a 1:1 cosolvent mixture led to reduction in MEM deprotection and 40% yield of the desired product (Scheme 5.7).

Scheme 5.7. *Et_2O/benzene cosolvent: importance for reduced MEM-deprotection.*

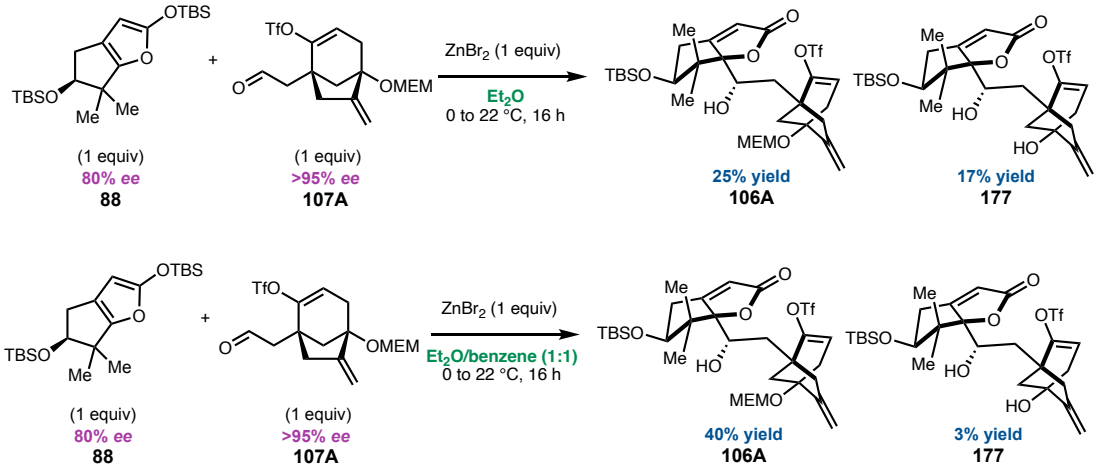

5.2.2 Investigation of Br substrate (107B)

In addition to investigating the VMAR of triflate-containing aldehyde **107A**, the reaction of alkenyl bromide substrate **107B** was pursued. After 2D NMR analysis, it became clear that the product (**106B**) was formed as a mixture of diastereomers at the alcohol (**178**) and fully substituted center (**179**). Additionally, high levels of silyl enol ether product **180** were observed, along with recovered silyloxyfuran (**88**), butenolide (**60**), and aldehyde (**107B**, Scheme 5.8). For these data, yields were back-calculated from the crude reaction mixture, taking into account the isolated yield of analytically pure product **106B**. Therefore, the yields provided in Scheme 5.8 are estimates.

Scheme 5.8. *Characterization of all products on Br-containing substrate.*

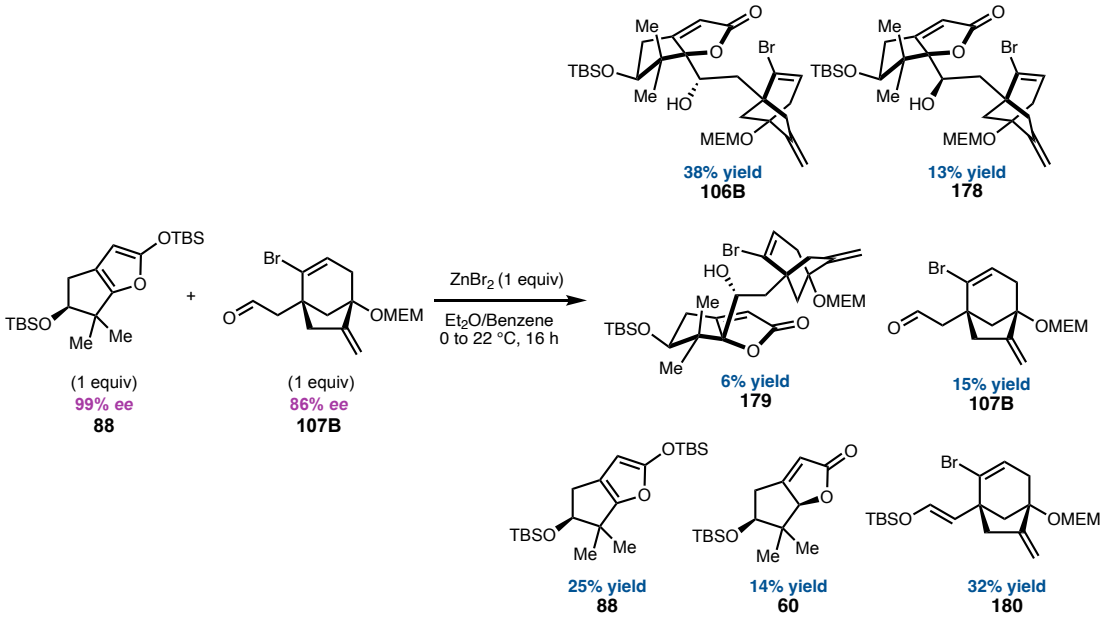

The formation of **180** was surprising and required a closer look at the posited mechanism. Presumably $ZnBr_2$ acts as a Lewis acid, chelating to the aldehyde functionality in **107B** (Scheme 5.9). Following $ZnBr_2$ chelation, **88** could add in to form a silylium intermediate, from which addition of Br^- could generate TBSBr.[2,3] The resulting Zn-

alkoxide intermediate could be subjected to another nucleophilic attack of Br^-, regenerating $ZnBr_2$ and liberating the alkoxide-containing butenolide. Alternatively, the Zn-alkoxide intermediate is protonated upon workup with NH_4Cl to deliver the product **106B**.

Scheme 5.9. *Posited mechanism for silyl enol ether formation involves TBSBr.*

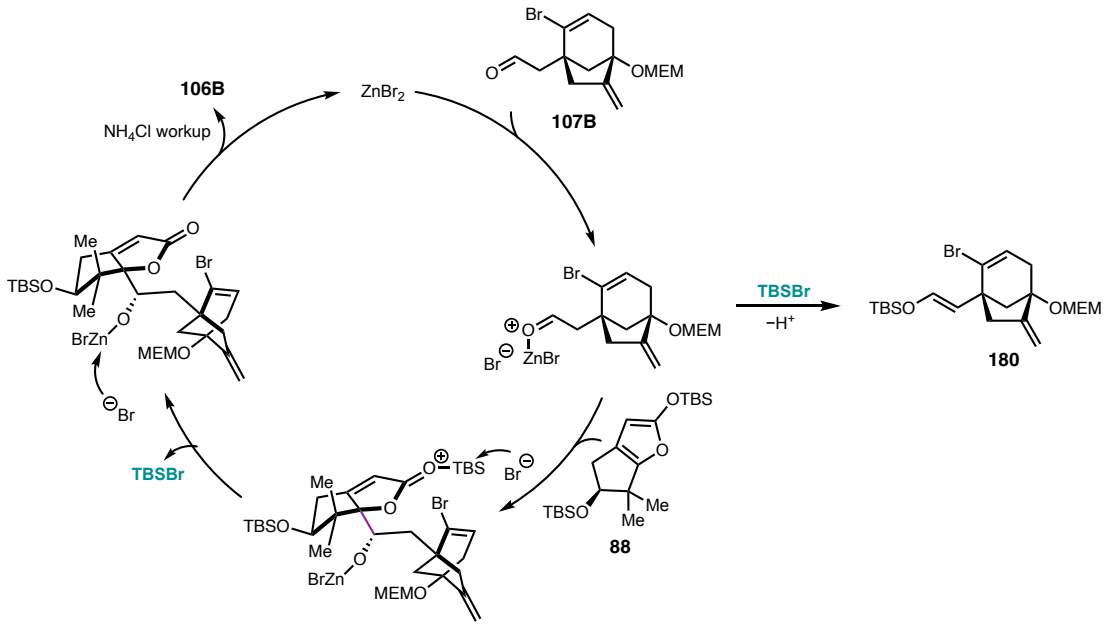

A simple hypothesis was formed from this mechanistic picture: what would happen if the bromide counterion was replaced with chloride? One possibility is that the TBSCl would be less reactive under the reaction conditions, preventing formation of **180**. Indeed, this seemed to be the case. Indeed, replacing $ZnBr_2$ with $ZnCl_2$ led to diminished formation of **180** (Scheme 5.10).

Scheme 5.10. *Use of $ZnCl_2$ prevents silyl-transfer.*

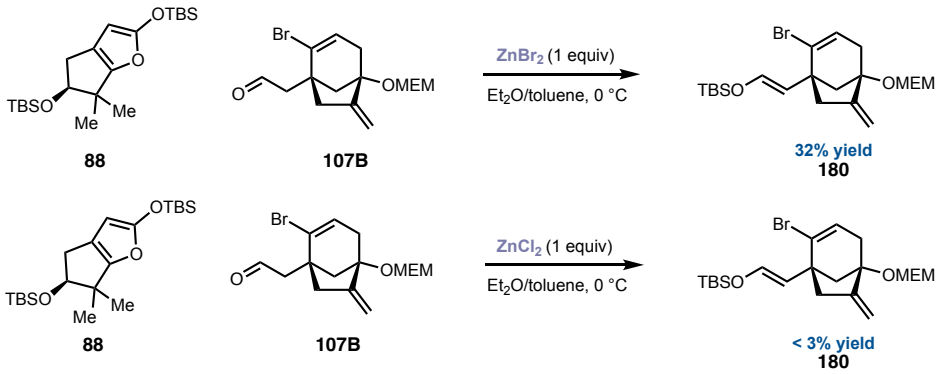

From the observation in Scheme 5.10, a screen of ZnI_2/$ZnBr_2$/$ZnCl_2$ was conducted. While ZnI_2 and $ZnBr_2$ led to low yields (20-24%, Scheme 5.11, entry 1-2), use of $ZnCl_2$ led to 48% yield (Scheme 5.11, entry 3). The increase in yield is attributed to the less reactive *in situ* generated TBSCl the more reactive TBSBr and TBSI in the side reaction to form **180**.

Scheme 5.11. *Optimization of VMAR on Br-containing substrate.*

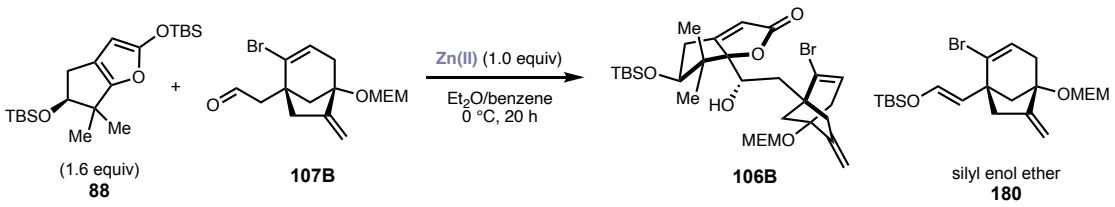

entry	Zn(II)	aldehyde **107B** (%)	product **106B** (%)	silyl enol ether **180** (%)
1	ZnI_2	14	20	37
2	$ZnBr_2$	21	24	32
3	$ZnCl_2$	21	**48**	< 3

Upon scaling up the VMAR, it became clear that the diastereoselectivity of the process dropped significantly, mostly at the formed fully-substituted center at the γ-position of the butenolide. This was surprising, as previously the γ-position was set in good *dr*. It became apparent the diastereoselectivity was not consistent; setting up two of the same reaction in parallel led to 3:1 and 5:1 observed diastereoselectivity (Scheme 5.12,

entry 1-2). In repeating a third time, increasing the equivalents of the furan to 1.4 to try to push the conversion led to observation of a 3:1 *dr* (5.12, entry 3). An important observation was made at this time: crashing out of $ZnCl_2$. It was reasoned that, while addition of benzene in cosolvent mixtures helped reduce MEM-deprotection, it also made the $ZnCl_2$ less-soluble in the reaction media. Switching to a 3:1 mixture of Et_2O:benzene led to complete MEM-deprotection. However, turning the stir rate to 800 rpm and using a large stir bar that exhibited good surface coverage and milling was essential to repeatability of the *dr* on-scale. The reaction was successfully scaled up to 700 mg scale (Scheme 5.12, entry 6). The drop in *dr* with less stirring is of interest and might be due to non-Zn-mediated background reactivity.

Scheme 5.12. *Scale-up optimization of the VMAR.*

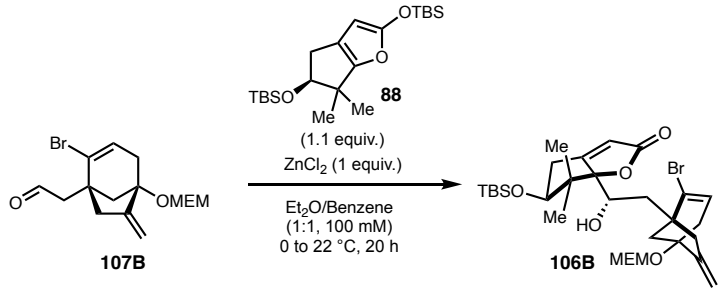

entry	scale	vessel size	deviation	*dr* (%)	product (%)	furan rsm (%)	rsm butenolide	aldehyde rsm
1	30 mg	2-dram	-	3 : 2.3 : 1	51	-	42	48
2	30 mg	2-dram	-	5 : 1.9 : 1	65	-	41	32
3	30 mg	2-dram	1.4 equiv. furan	3 : 1.2 : 1	61	-	54	35
4*	30 mg	2-dram	-	7 : 2.4 : 1	72	-	36	25
5*	180 mg	40 mL vial	-	7 : 2.3 : 1	70	-	34	24
6*	694 mg	40 mL vial	-	7.7 : 1.7 : 1	56	-	31	29

***stirring 800 rpm**

The final reaction conditions are displayed below in Scheme 5.13. The separation of the three diastereomers was tricky. Isolation of the pure, major diastereomer resulted in ~40% yield due to several mixed fractions. Isolation of all product-containing fractions

resulted in 56% yield as a 7.7.1.7:1 mixture of diastereomers.

Scheme 5.13. *Final optimized conditions.*

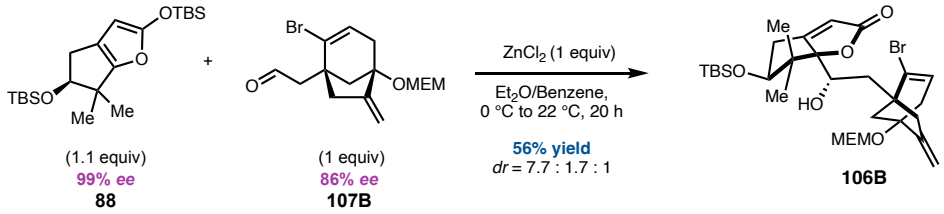

5.3 Ni-CATALYZED A-ENOLATE ALKENYLATION

5.3.1 Synthesis of OTf and Br substrates

From the product of the VMAR (**106A**/**B**), the Ni-catalyzed α-enolate alkenylation substrate synthesis proceeded smoothly (Scheme 5.14). Protection with TMS-imidazole occurred in 74% yield (**181A**/**B**). Importantly, the use of electrophilic reagents for protecting group installation and avoidance of strong base were important to avoid retro-aldol. Use of TBSOTf and other silyl protecting group agents led to no reaction (not shown). Next, Cu-H reduction occurred in good yield (**182A**/**B**).[21-23] Notably, the diastereoselectivity of the reduction is > 20:1 due to the preference for formation of the *cis* lactone. It is believed that the *trans* lactone is kinetically and/or thermodynamically inaccessible under the reaction conditions. From these substrates, investigation to ring closure to key compound **105** could be investigated.

Scheme 5.14. *α-enolate alkenylation substrate synthesis.*

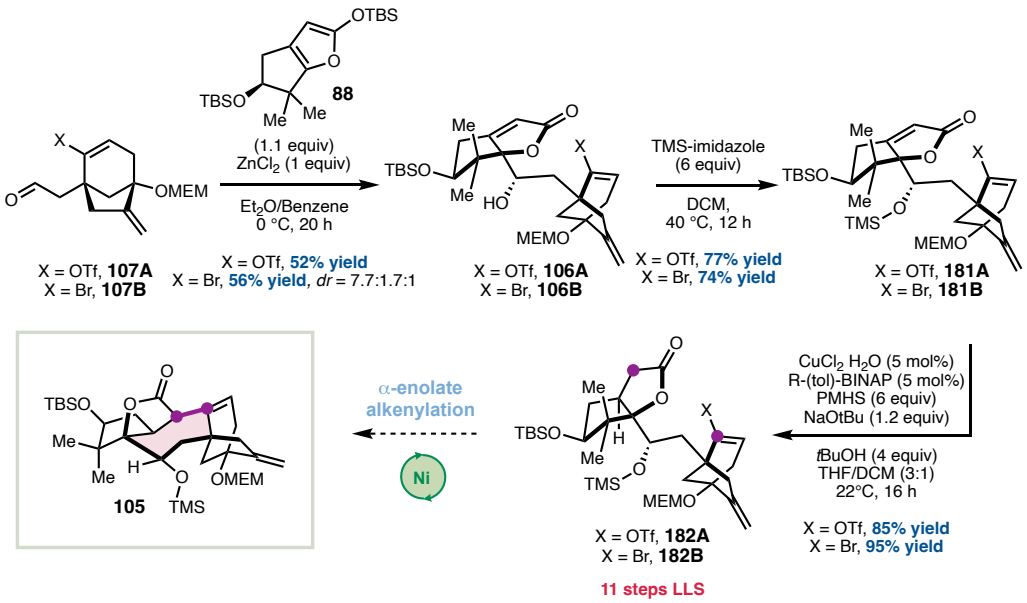

5.3.2 Initial experimentation on the key intramolecular cross-coupling: use of phosphine ligands

Drawing inspiration from the model study involving the α-enolate arylation reaction (Chapter 2), we were eager to try the identical reaction conditions utilizing a variety of bidentate phosphine ligands. Unfortunately, use of Ni(COD)dppp on substrates **182A** resulted in decomposition and recovery of starting material, respectively (Scheme 5.15, entry 1). Alternative conditions, including DavePhos, inverse order of addition, and use of Ni(COD)DQ provided recovered starting material or substrate decomposition for substrate **182A** (Scheme 5.15, entries 2-4). In the cases where substrate decomposition was observed, the presence of trace quantities of product **183** accompanied, formed from hydrolysis of the enol triflate moiety. Upon initial experimentation, substrate **182B**, bearing the vinyl bromide, was unreactive to Ni(COD)dppp (Scheme 5.15, entry 5).

Scheme 5.15. *Discouraging initial studies on substrates **182A/B** using dppp as the ligand.*

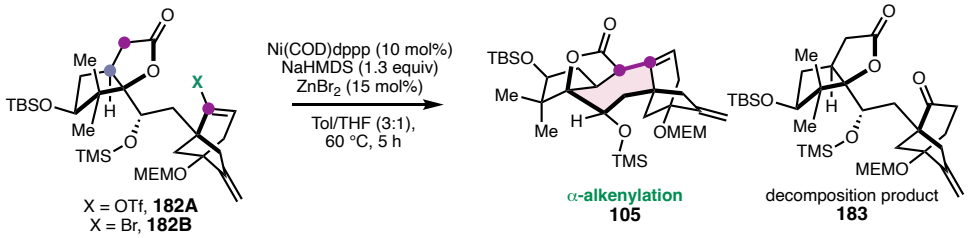

entry	X	deviation	result
1	OTf	none	decomposition, **183**
2	OTf	DavePhos (20 mol%)	decomposition, **183**
3	OTf	inverse order of addition	decomposition, **183**
4	OTf	Ni(COD)DQ	recovered **182A**
5	Br	none	recovered **182B**

Over time, it became clear that the substrate decomposition was likely base-mediated and could be prevented by decreasing the base stoichiometry (Scheme 5.16). Upon a simple base equivalency screen, the decomposition could be reduced (albeit the conversion of the reaction was < 10%). After exhaustive screening on this substrate, it was ultimately concluded that further exploration on the vinyl bromide substrate was required.

Scheme 5.16. *Base and temperature screen on enol triflate substrate **182A** with dppp.*

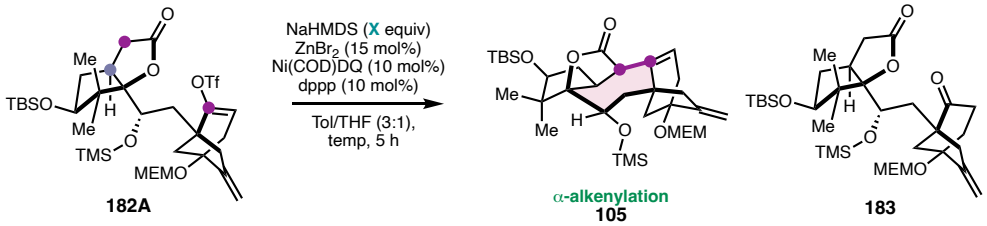

entry	X	inverse addition?	temp. (°C)	starting material (%)	α-alkenylation (%)	**183** (%)	mass balance (%)
1	1.3	-	60	10	-	9	19
2	0.7	-	60	38	-	8	46
3	1.3	yes	60	6	-	16	22
4	0.7	-	21	73	-	7	80
5	1.3	-	21	27	-	7	34
6	2.6	-	60	0	-	7	7

Investigation of the vinyl bromide substrate **182B** proved to be more fruitful. Preliminary investigations on this substrate focused on screening various phosphine ligands. A brief screen identified *t*BuXantPhos and dCypp as potentially fruitful ligands, delivering the product in 30% and 64% yield, respectively (Scheme 5.17). However, in follow up screens, the yields dropped below 10%. The reactions seemed to exhibit on/off reactivity. Additionally, different selectivities between α and β-alkenylation were observed in seemingly "identical" runs. Desperately to repeat the results, several parameters were investigated, including the purity of the starting material/reagents, reaction concentration, catalyst loading, base loading, and setting the reactions up in duplicate. Nevertheless, in about 50 entries experiments, the reaction only worked successfully approximately four times. Clearly, an alternative strategy would need to be explored or the reason for reaction success elucidated. As a result of the base sensitivity of the enol triflate, the Br substrate **182B** was pursued moving forward.

Scheme 5.17. *Use of phosphines: disfavored selectivity and irreproducible results.*

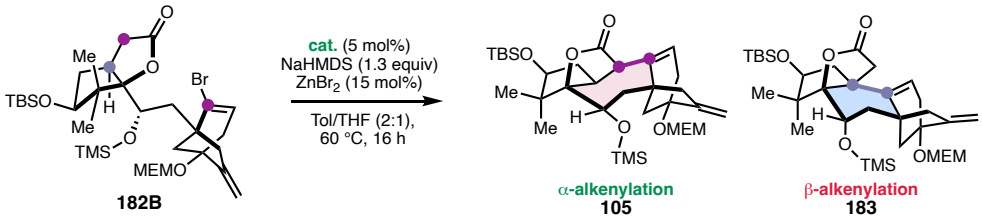

entry	cat.	starting material (%)	α-alkenylation (%)	β-alkenylation (%)
1	(COD)Ni(DPPP)	10	12	37
2	(COD)Ni(DTBPF)	-	13	15
3*	(COD)Ni(XantPhos)	-	34	44
4*	(COD)Ni(*t*BuXantPhos)	-	30	47
5*	(COD)Ni(DCPP)	-	64	6
6	(COD)Ni(*t*BuXantPhos)	15	6	22
7	(COD)Ni(DCPP)	17	3	27

***high yielding results with phosphine ligands were not reproducible**

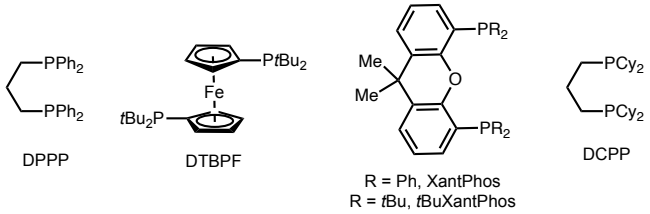

For the case of (COD)Ni(DCPP), efforts to prepare and isolate this catalyst independently were undertaken. It was thought that perhaps some of the reproducibility issues stemmed from irreproducible formation of the active catalyst *in situ*. Following the procedure from Mézailles,[24] the DCPP-ligated Ni complex was prepared. Additionally, the Ni(II) variant that did not contain COD could be prepared in 85% yield for use of *in situ* reduction protocols (use of Mn as a reductant, for example). In the literature, there exist multiple reports attempting α-enolate functionalization starting from Ni^{II} precatalysts; however, these reports claim that there is difficulty in achieving high conversion and high yields under such conditions.[25-28] Testing of complex **185** could possibly provide insight as to whether COD was inhibitory for the α-enolate alkenylation chemistry. In the presence of COD, for example, Mézailles reports oxidative addition with an aryl chloride taking 90

days at 60 °C. In the absence of COD, using phenyl-bound **184**, oxidative addition occurred on the timescale of minutes to hours (Scheme 5.18).[24]

Scheme 5.18. *Precedent for isolation of Ni(COD)DCPP.*

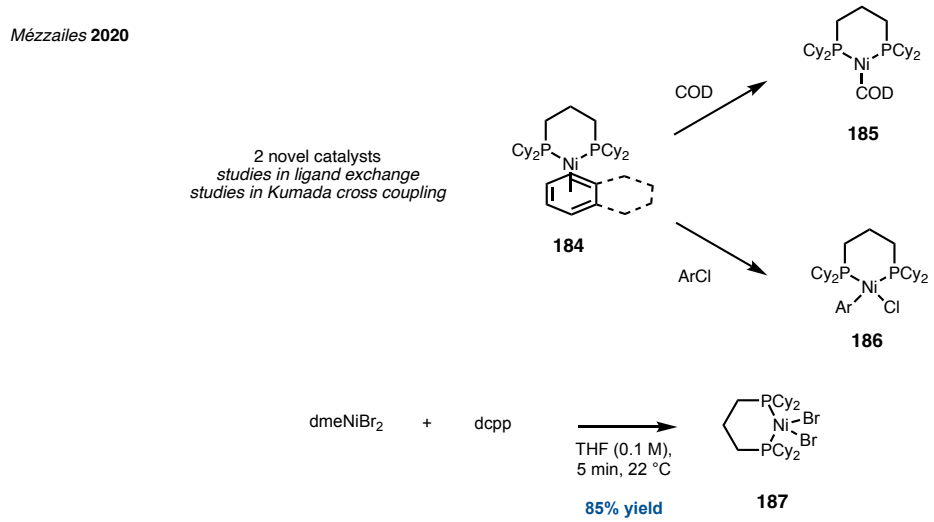

Unfortunately, use of these catalysts in the α-enolate alkenylation chemistry were unfruitful (Scheme 5.19). In both cases, complex mixtures likely resulting from of substrate decomposition were observed. At this point in time, it remained unclear why the reaction had worked so well off-hand but was not reproducible. Nevertheless, these data served as motivation that the reaction *could* work well; promising results using nickel catalysis had been achieved, but the problem needed to be approached from a different angle.

Scheme 5.19. *Use of pure, crystalized Ni catalysts.*

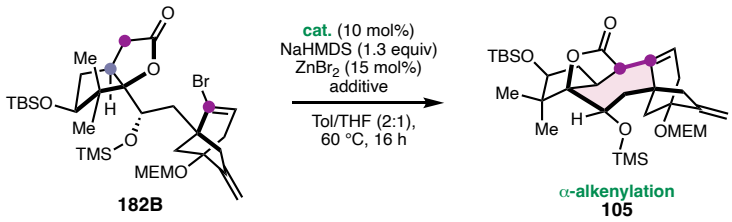

entry	cat.	catalyst source	reductant	result
1	(COD)Ni(DCPP)	prepared *in situ*	-	6% yield **105**
2	(COD)Ni(DCPP)	isolated by crystalization	-	complex mixture
3	Br_2Ni(DCPP)	isolated by crystalization	Mn^0	complex mixture
4	Br_2Ni(DCPP)	isolated by crystalization	Zn^0	complex mixture

In addition to the Ni-catalyzed conditions, palladium-catalyzed reactions were also investigated next. Indeed, there exist some reports for palladium-catalyzed α-enolate alkenylation but very few to form medium sized rings.[29-34] Although the data shown does not describe an exhaustive screen, preliminary investigations did not show significantly more promise compared to the explored Ni-catalyzed methodology (Scheme 5.20). Attempts to further optimize the conditions from entry 3 were not fruitful, providing messy reaction profiles and uncharacterized side products (not shown).

Scheme 5.20. *Palladium-catalyzed methods deliver low yields.*

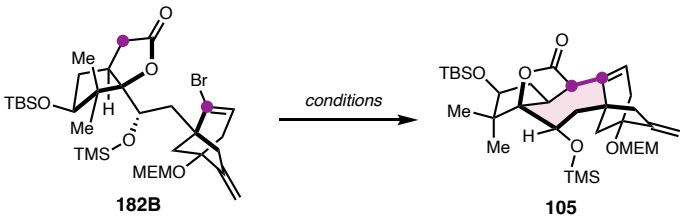

entry	*conditions*	result
1	$[PdBrP(t)Bu_3]_2$ (1.25 mol%), LHMDS (2.5 equiv), Tol, 80 °C, 15 h	decomposition
2	LiTMP (1.3 equiv), $Pd_2(dba)_3$ (5 mol%), dtbpf (5 mol%), $ZnBr_2$ (1.4 equiv), THF, 45 °C, 16 h	22% yield, 36% brsm
3	LiTMP (1.3 equiv), $Pd_2(dba)_3$ (5 mol%), dtbpf (5 mol%), $ZnBr_2$ (1.4 equiv), THF, 60 °C, 16 h	14% yield

Attempts to approach the problem directly from butenolide **106A** were also undertaken (Scheme 5.21). The idea involved Cu-H 1,4-addition to be intercepted by the

Pd catalytic cycle. Transmetalation between a Cu-enolate with Pd, for example, could lead to intermediates *en-route* to the desired coupled product **105** in a single step.[35-40] One challenge that arose, however, was identification of Cu-catalyzed conditions that could reduce the butenolide. In Buchwald's precedent, less-hindered, acyclic alkenes were used as substrates, not butenolides. Indeed, application of Buchwald's conditions led to low conversion in the reduction step of the butenolide.

It was thought then that the Cu-H conditions used in the stepwise approach could be adapted for Cu/Pd synergistic catalysis (not shown). In the conditions from Scheme 5.14, for example, use of superstoichiometric *t*BuOH and NaO*t*Bu are required and encourage rapid proton transfer with the Cu-enolate to turnover the catalyst.[24-27] Employing conditions in the absence of *t*BuOH or NaO*t*Bu and in the presence of Pd^0 precatalysts led to low conversions (not shown). Furthermore, attempts to affect CuH reduction from Cu^I salts were not fruitful on the model system, as Cu^I is often used for these kinds of reactions shown by Buchwald and others.[35-40]

Scheme 5.21. A. *Attempts at Cu-Pd Synergistic catalysis* ***B.*** *Attempts from Cu(I).*

A.

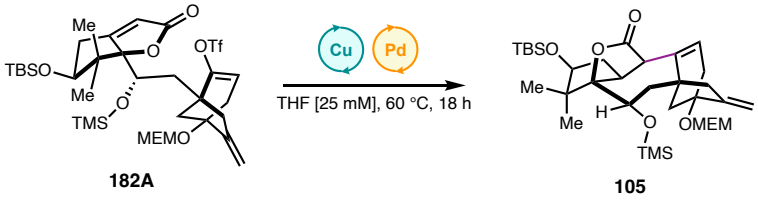

182A **105**

entry	Cu/Ligand(5 mol%)/Silane (2 equiv)	Base (2 equiv)	Pd (4 mol%)	result
1	$CuCl_2$•$2H_2O$/(R)-ptol-BINAP/Me_2PhSiH	NaOTMS	Pd(cinnamyl)(Cl)(dppbz)	no product
2	$CuCl_2$•$2H_2O$/(R)-ptol-BINAP/Me_2PhSiH	NaOTMS	Pd BrettPhos G4	no product
3	$CuCl_2$•$2H_2O$/(R)-ptol-BINAP/Me_2PhSiH	NaOTMS	$Pd(OAc)_2$/dppp	no product

B.

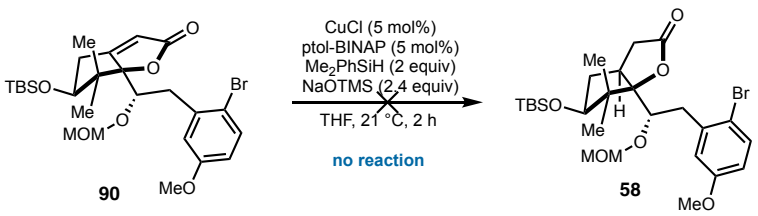

5.3.3 Discovery of electron-deficient olefin (EDO) ligands for the intramolecular α-enolate alkenylation

Other nickel-catalyzed methods for α-enolate alkenylation exist, although they are few and far between. In 2015, Helquist reported the Ni-catalyzed cross coupling of ketone enolates with alkenyl halides (Scheme 5.22A).[41] The intermolecular coupling utilizes lithium enolates of ketones and a unique N-heterocyclic carbene (NHC) ligand, IPrHCl. LiI was found as a successful additive to increase the reaction rate. In their substrate scope, a variety of electron-neutral and electron-rich substrates underwent coupling in high yields, while electron-deficient aryl ketones were somewhat lower yielding. Furthermore, reactions generating α-quaternary centers proceeded in high yield. An attractive feature of the reaction is its mild reaction conditions: just 5 mol% catalyst, 1.05 equiv. of base, short reaction times, and low temperatures were effective at delivering products in proficient yields. Nevertheless, while the Helquist example was attractive, subjection to **182B** led to no observed product (Scheme 5.22B).

Scheme 5.22. A. *Helquist's[41] Ni-catalyzed α-enolate alkenylation* ***B.*** *Failure to apply conditions to substrate* ***182B****.*

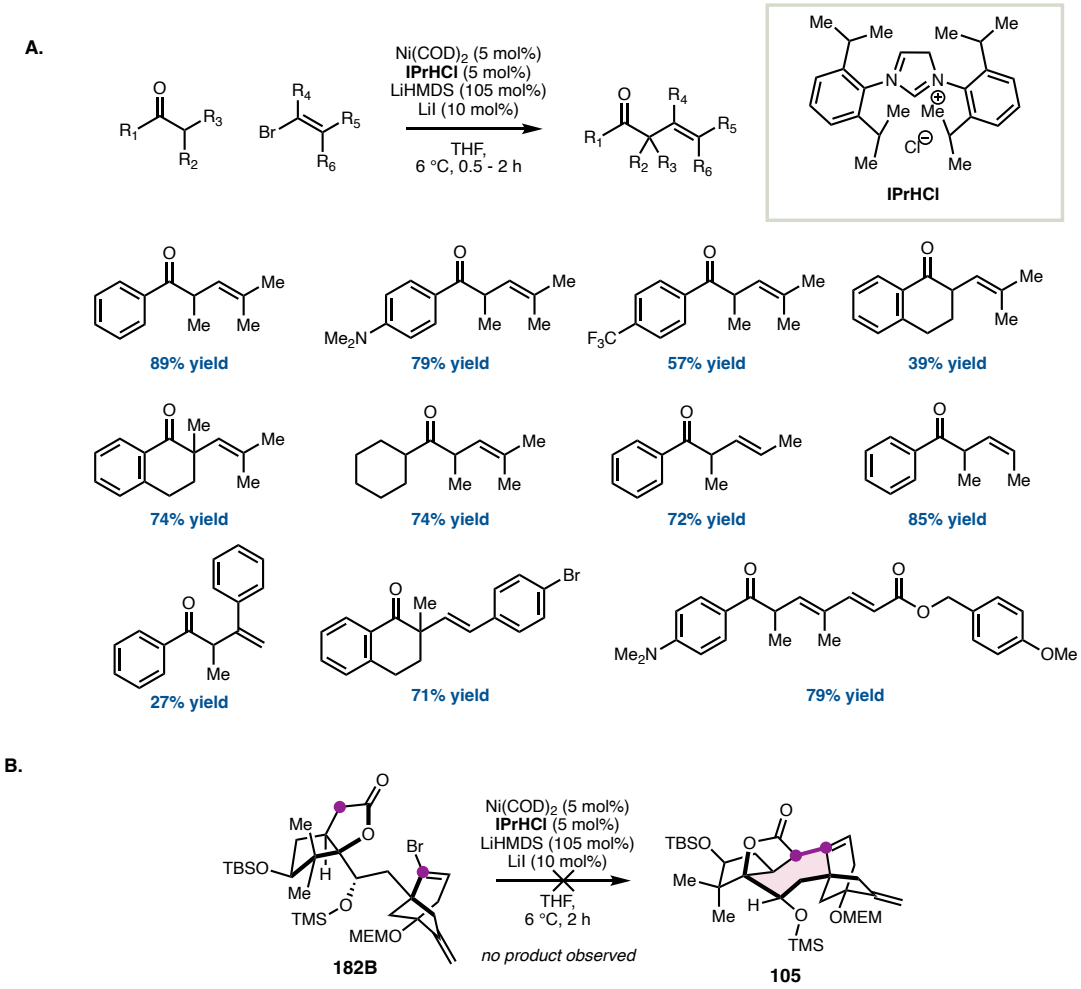

Since Helquist's report in 2015, very few nickel catalyzed α-enolate alkenylations have been disclosed. While Ni-catalyzed α-enolate arylation has been explored to much greater depths (see Chapter 2 for more information on Ni-catalyzed α-enolate arylation),[42-45] the corresponding α-enolate alkenylations literature seemed are rare. Dating back to 1977, Rathke disclosed the stoichiometric Ni-coupling of lithium ester enolates with alkenyl bromides utilizing $NiBr_2$-*n*BuLi.[46-48] Pregenerating the enolate with lithium diisopropylamine (LDA) and adding to a stirring solution of $NiBr_2$-*n*BuLi led to excellent

yields up to 99% (Scheme 5.23A). It is possible that *n*BuLi leads to Ni^{II} reduction via sequential Br^- displacement and β-hydride elimination, which would lead to an olefin-bound active catalyst. Although the reaction employed stoichiometric loadings of Ni, it did not require addition of exogenous ligands.

In 2002, the conditions were applied in the synthesis of terrecyclic acid A in 81% yield (Scheme 5.23B).[49] While this was exciting, unfortunately, these conditions did not yield any desired product in the desired reaction for auriculatol A (Scheme 5.23C). It was thought that either oxidative addition into the more hindered alkenyl bromide or transmetalation with the lithium enolate of the lactone might be challenging in the desired system, leading to recovery of starting material (**182B**).

Scheme 5.23. A. *Rathke's[46-48] Ni-mediated α-enolate alkenylation.* ***B.*** *Application by Wender.[49]* ***C.*** *Failure in the desired reaction providing recovered starting material.*

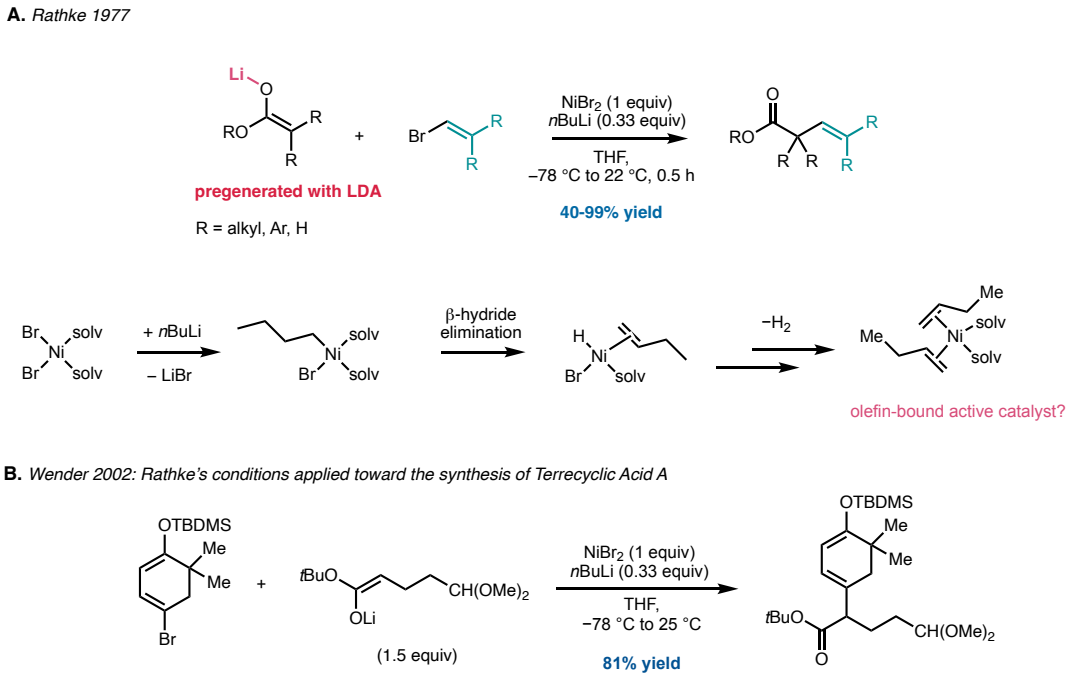

c.

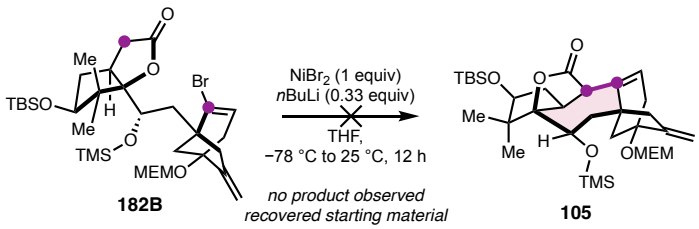

Despite the difficulties adapting the α-enolate arylation conditions from Chapter 2 to the more ambitious α-enolate alkenylation described herein, scrutinizing of literature outside the realm of the alkenylation literature for Ni(0)-catalyzed reactions provided key insights. Among the explored reports, papers disclosing Ni(0)-catalyzed amination,[50-52] carboxylation,[53] desaturation,[54,55] Michael addition,[56,57] and Kumada cross-coupling[58,61] were particularly notable.

Two common themes emerged from reading these papers – first, was the absence of exogeneous ligands. Traditionally, Ni-catalysis often requires phosphine or nitrogen ligands. Presumably, the strongly nucleophilic phosphine or nitrogen ligand can displace COD under the reaction conditions, and it is the ligand-bound catalyst that is active in the reaction. Several reports, however, use Ni(0) precatalysts without the addition of phosphine or nitrogen ligands, meaning that the precatalyst ligands (often olefin-containing ligands) are suitable for catalyst activity. Particularly, we were intrigued by the report from Li and coworkers, in which the precatalyst Ni(COD)(DQ) in the presence of base was able to catalyze the C–N cross-coupling for the synthesis of *N,N*-diarylsulfonamides (Scheme 5.24A).[50] Engle and coworkers have found Ni(COD)DQ to be privileged for the 1,2-difunctionalization of olefins (Scheme 5.24B).[61,] Murphy and coworkers disclosed the synthesis of biaryls from aryl halides and PhH utilizing Ni(COD)DQ and KO*t*Bu.[62]

Scheme 5.24. *Recent reports of Ni-catalyzed reactions using Ni(0) precatalysts in the absence of exogenous ligands.*

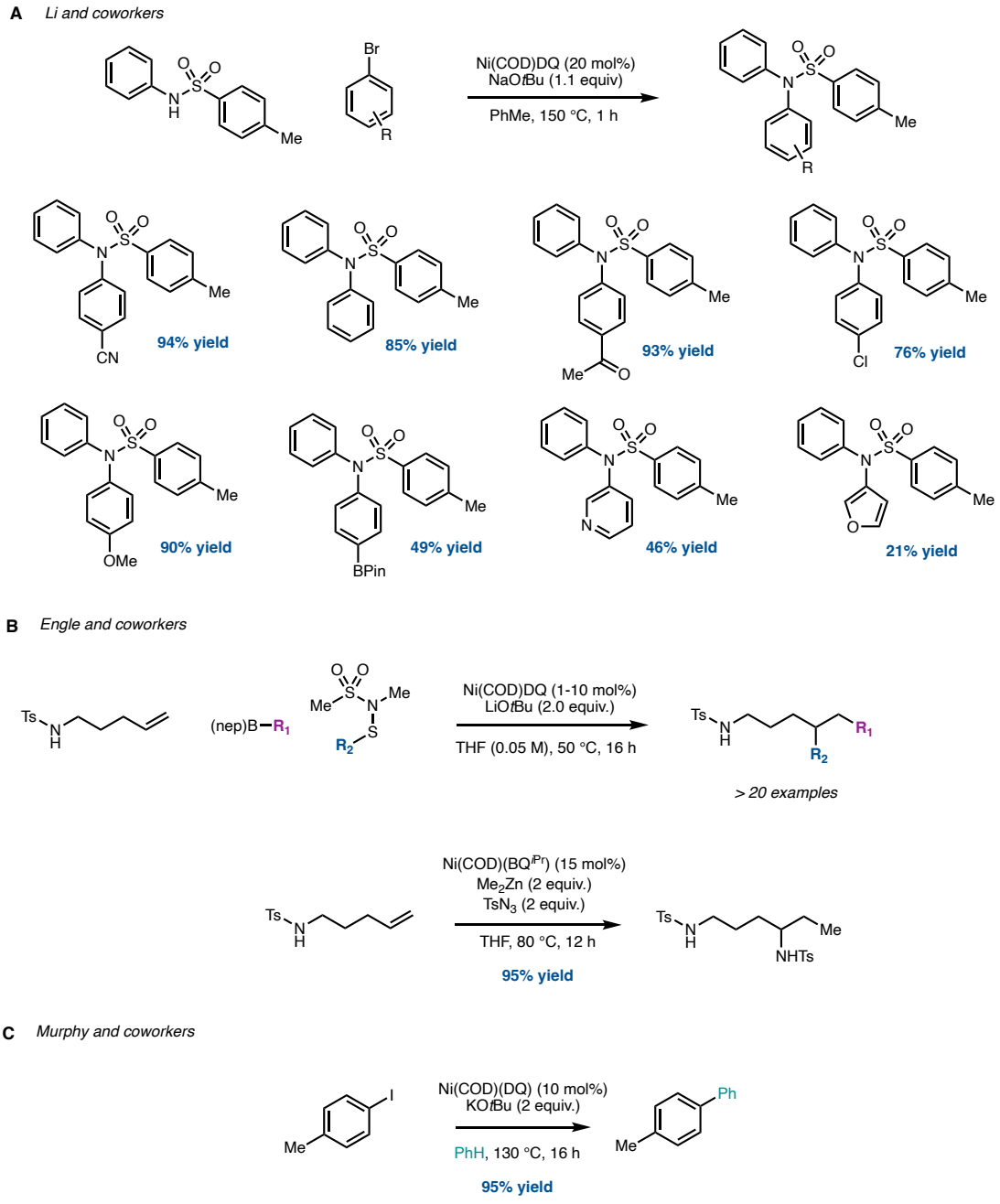

The second observation from the Ni(0)-catalyzed literature is the use of electron-deficient olefins as ligands. We were particularly inspired by the report of benzonitrile as a privileged ligand for the BINAP-ligated Ni-catalyzed amination of aryl and heteroaryl

chlorides (Scheme 5.25A).[52] The (BINAP)Ni(η^2-NC-Ph) catalyst was found to limit the formation of Ni(I) and $(BINAP)_2Ni$ species that were found to be detrimental to the reaction. It was hypothesized that the benzonitrile may act as a stabilizing ligand for the Ni-center through π-backdonation with benzonitrile. Indeed, Rousseux has incorporated a benzonitrile functionality within a single pyrazole ligand scaffold for Ni-catalyzed cross coupling of tertiary nucleophiles,[63] while Doyle has utilized the electron-withdrawing Fro-DO ligand for aziridine cross coupling[64] (Scheme 5.25 B&C).

Scheme 5.25. *Hartwig's amination of aryl and heteroaryl chlorides.*

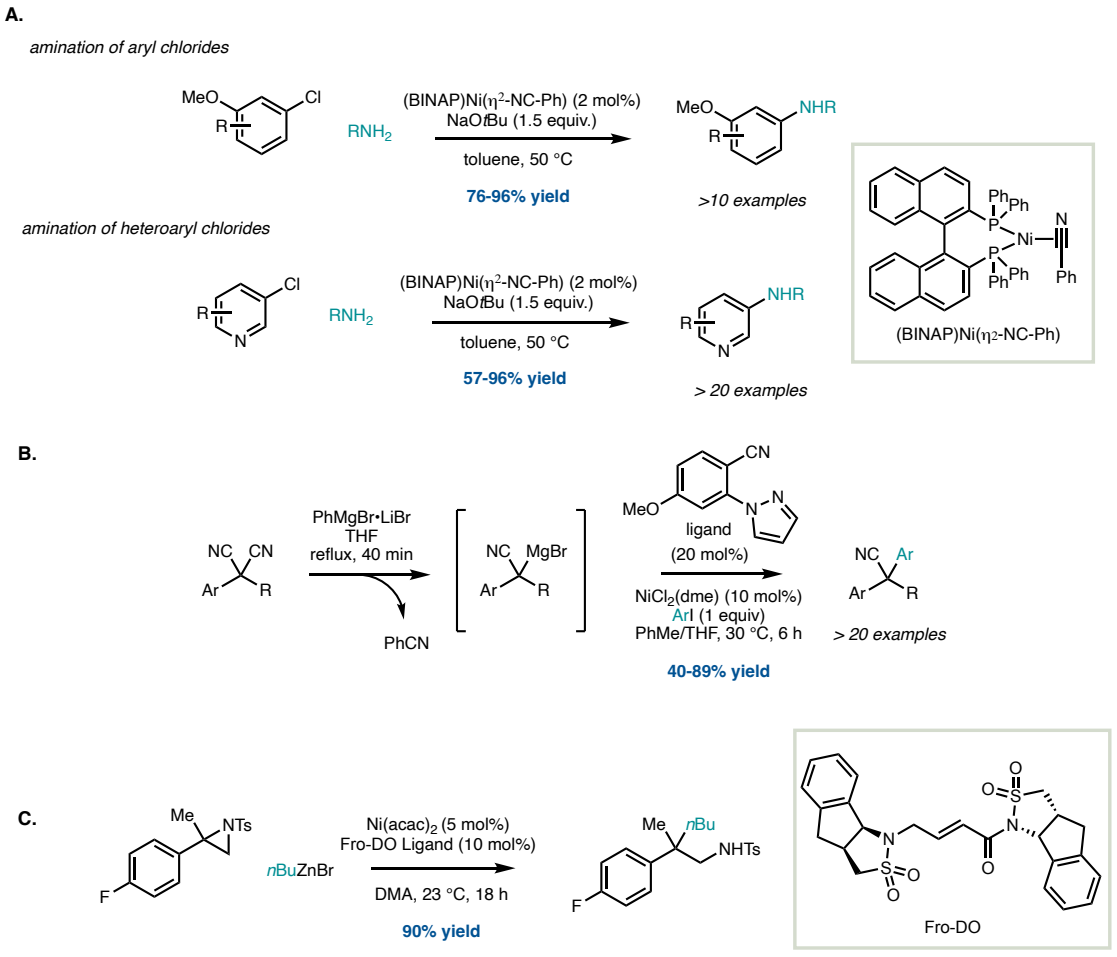

We were also inspired by Cornella's mechanistic study on the Ni-catalyzed Kumada cross-coupling. In this study, investigation into the mechanism of the low

temperature $C(sp^2)$–$C(sp^3)$ Kumada cross-coupling helped uncover olefin-bound 16-electron nickel complexes as privileged catalysts in the reaction.[65] Specifically, a series of NMR experiments revealed that Grignard coordination of hexyl magnesium bromide to the $Ni(nor)_3$ catalyst is required before oxidative addition of 2-bromovinyl benzene (Scheme 5.26). No evidence of oxidative addition in the absence of hexyl magnesium bromide occurred when monitored in an NMR tube. Conversely, in a separate experiment, precomplexation of hexyl magnesium bromide to the Ni-catalyst followed by addition of 2-bromovinyl benzene led to catalyst turnover. In line with their studies, the Cornella group successfully crystallized an analogous olefin-bound Ni-complex coordinated to $(Me)_2Mg(TMEDA)$ and showed it was competent in the reaction (not shown). These studies are consistent with a grignard coordination first mechanism as shown in Scheme 5.26.

While olefin-bound 16 e^- Ni-complexes are extremely reactive and unstable to air,[66,67] they were essential to success of the reaction, as other 18 e^- Ni complexes were ineffective. Furthermore, strongly σ-donating ligands such as phosphines, NHC's, and diamines were incompetent, likely because these ligands destabilize or are too electron rich for Grignard coordination. We wondered if parallels between this study and the α-enolate alkenylation reaction we were working to develop existed and what implications this study has on Ni-catalyzed cross coupling more generally.[68-70]

Scheme 5.26. *Cornella's mechanistic study of the Ni-catalyzed Kumada cross coupling.*

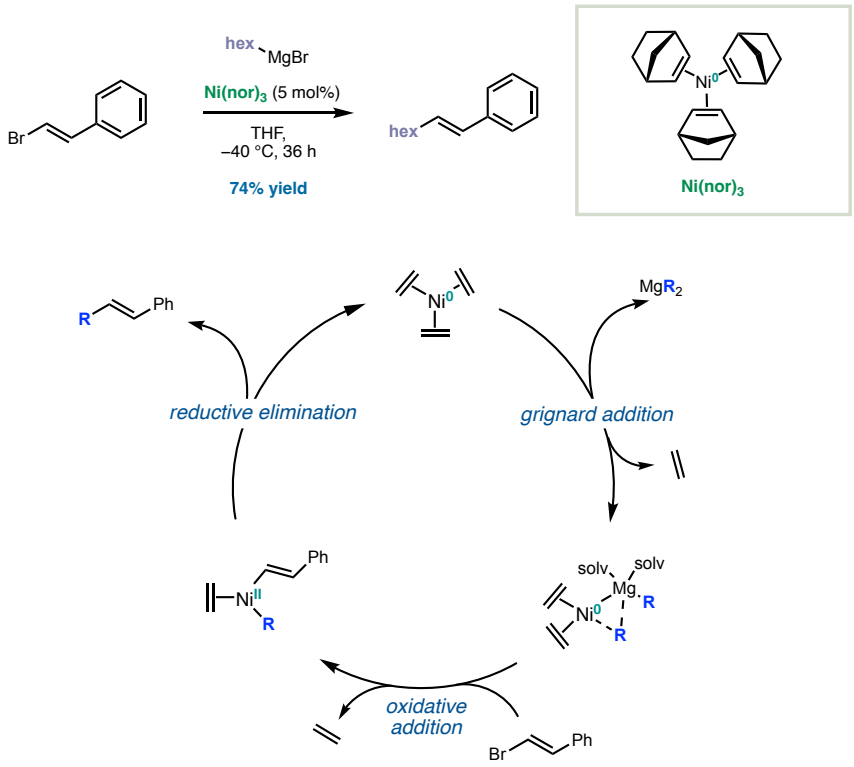

These hypotheses were consistent with model studies in the α-enolate arylation reaction from Chapter 2, which showed it did not require phosphine ligands (Scheme 5.27). Taking just $Ni(COD)_2$, the α-enolate arylation reaction could be achieved in 75% yield, reproducibly, and on larger scales (> 20 mg). Use of Ni(COD)DQ precatalyst led to 80% yield and no observed β-arylation (not shown).

Scheme 5.27. *Use of 16 e⁻ EDO-ligated Ni(COD)DMFU provides promising results.*

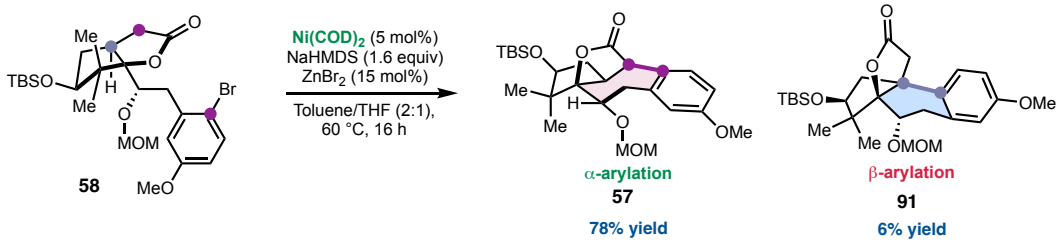

Because of the promising results of olefin ligands from the model study, a series of experiments were designed to test Ni complexes with varying electronic properties (Scheme 5.28). Mongomery reported NHC-ligated Ni(0) catalysts for C–C and C–N bond formation,[71] while Cornella developed Ni(0) stillbene (stb) catalysts, containing 4-F, 4-Me, 3,5-Me, and 4-*t*Bu substitution.[65] Engle has a library of bench-stable, commercially available nickel precatalysts, containing a unique plethora of olefin ligands,[72] and Doyle's air-stable TMEDA-ligated nickel precatalyst was also appealing.[73] In 2016, Jamison reported an air-stable nickel precatalyst for internally selective benzylation of terminal alkenes.[74] Finally, there was a recently disclosed Ni(COD)DMFU catalyst from the Engle group, which was privileged for 1,2-diarylation of alkenes.[75,76]

Scheme 5.28. *Some recently reported Ni(0) precatalysts.*

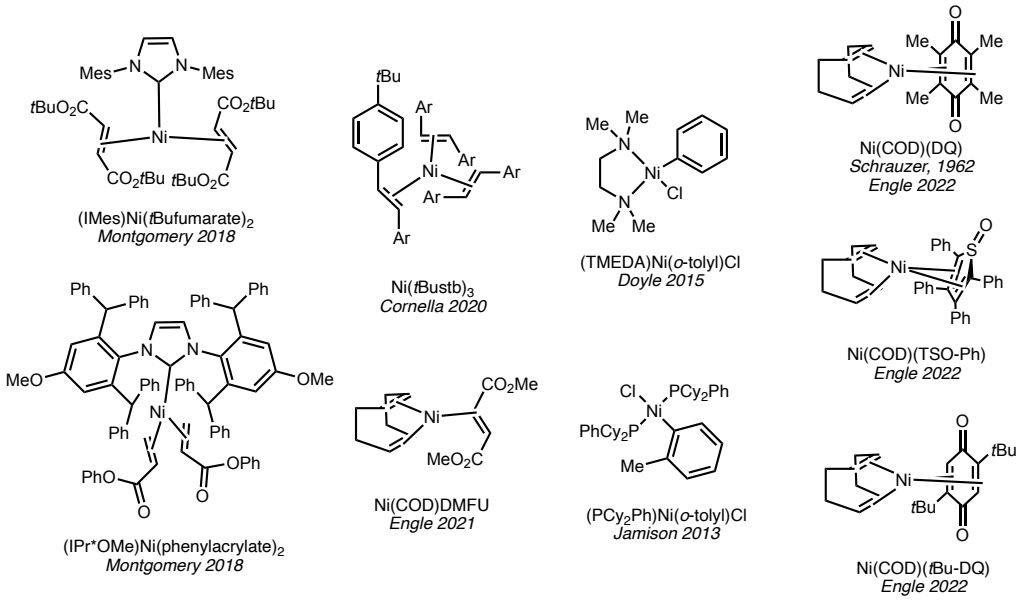

With these precatalysts in mind and adapting conditions tested in the model study (Scheme 5.27), both $Ni(COD)_2$ and Ni(COD)DQ were tested in the absence of exogenous ligands. Unfortunately, trace product with a low mass balance was observed (Scheme 5.29,

entry 1 & 2). Furthermore, in the case of $Ni(COD)_2$, formation of nickel black was observed. Screening other nickel precatalysts revealed that Ni(COD)DMFU and (TMEDA)Ni(*o*-tolyl)Cl delivered moderate yield of the desired product with relatively low selectivity for α-alkenylation over β-alkenylation (Scheme 5.29, entry 3 & 4). Lowering the catalyst loading in the case of Ni(COD)DMFU to 5 mol% led to a rapid change of product selectivity, minimalizing the formation of β-alkenylation to 4% (Scheme 5.29, entry 5). In this case, however, only moderate conversion of the starting material was observed. While it was thought that adding LiCl could increase conversion,[69] the hypothesis turned out to be incorrect (Scheme 5.29, entry 6). The optimal reaction was conducted for 12 h using 5 mol% of Ni(COD)DMFU, allowing for a 59% isolated yield of the product as an inseparable mixture with 6% β-alkenylation (Scheme 5.29).

Scheme 5.29. *Use of 16 e⁻ EDO-ligated Ni(COD)DMFU provides promising results.*

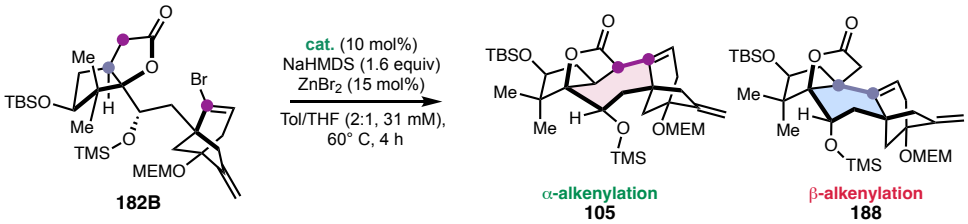

entry	cat.	starting material (%)	α-alkenylation (%)	β-alkenylation (%)
1	$Ni(COD)_2$*	32	4	16
2	Ni(COD)(DQ)	34	7	0
3	Ni(COD)DMFU	7	37	31
4	(TMEDA)Ni(*o*-tolyl)Cl	18	31	27
5	Ni(COD)DMFU (5 mol%)	30	37	4
6	Ni(COD)DMFU, LiCl (2 equiv)	12	3	17
7	Ni(COD)DMFU (5 mol%), 12 h	0	59	6

*formation of nickel black

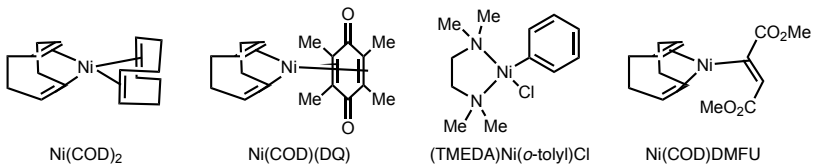

Ni(COD)DMFU works well compared to other metal-ligand systems due to its

unique coordination sphere and electron properties. Ni(COD)DMFU contains an interesting 16 e^- heteroleptic structure and can be stored at low temperature under inert atmosphere. The Engle group has shown that X-ray crystallography and density functional theory calculations are consistent with a zerovalent metal center engaging in high levels of π-backbonding interactions with DMFU.[75,76] The electron deficient olefin ligand is believed to possess valence electrons that more formally reside on the ligand, leading to a more electron-deficient, stable Ni-center (Scheme 5.30).

Scheme 5.30. *Ni(COD)DMFU: a unique Ni^0 catalyst system (figure adapted from Engle and coworkers)*[61].

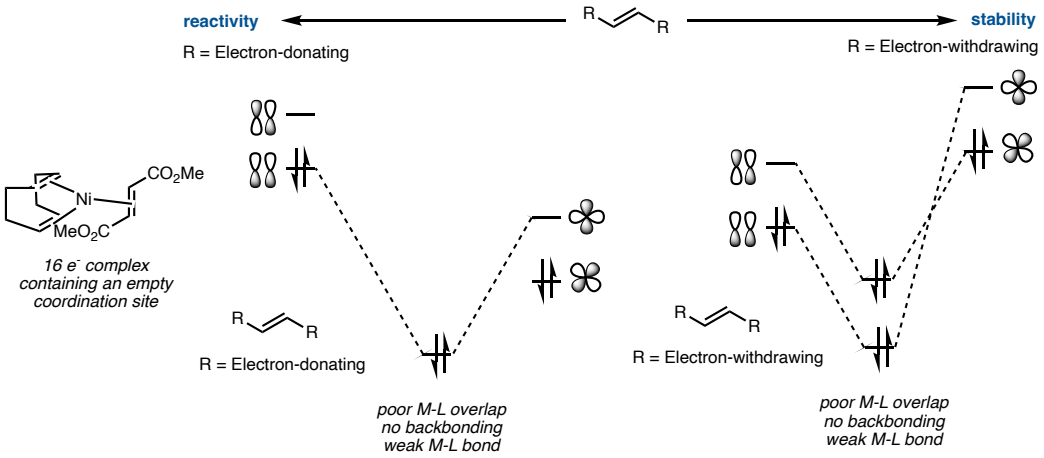

When considering Cornella's mechanistic study on Ni-catalyzed Kumada cross coupling, a possible mechanistic paradigm should be considered: does the α-enolate alkenylation operate *via* a "transmetalation first" mechanism? The requirement for an olefin-bound, 16 e^- metal center provides support for this hypothesis in which enolate coordination to the Ni center is required before oxidative addition. This would perhaps explain why using electron-deficient olefin ligands could aid in the reaction; that is, a more electron deficient metal center would engage the Lewis basic enolate in faster, more rapid

transmetalation, The electron deficient metal center could also undergo faster reductive elimination.[77] Although further mechanistic investigation would be required to definitively prove this hypothesis, the observations from this study combined with Cornella's work provide interesting implications for the design and development of enolate functionalization methods using nickel catalysis more broadly.

Scheme 5.31. *A possible mechanistic paradigm for nickel-catalyzed α-enolate alkenylation.*

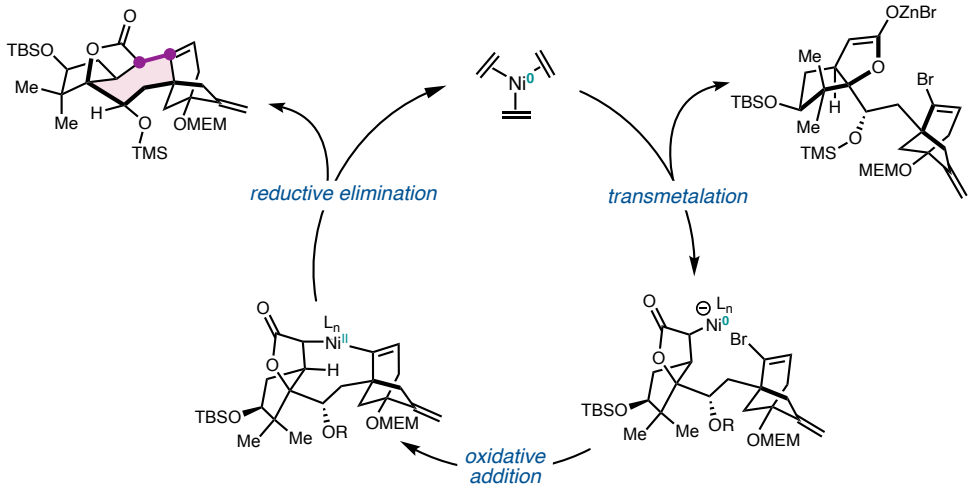

5.3.4 Assessing the necessity of reaction components and scalability of the Ni-catalyzed α-enolate alkenylation

For the purpose of synthetic studies toward auriculatol A, a focused set of controls were conducted in order to determine the necessary aspects of the reaction. First, the standard condition was repeated, verifying the yield and selectivity upon attempting separate runs (Scheme 5.32, entry 1). In some cases, small amounts of recovered starting material are observed, likely attributed to the sensitivity of the reaction to trace moisture or O_2, leading to slightly diminished yields (Scheme 5.32, entry 2). Performing the reaction

without $ZnBr_2$ (Scheme 5.32, entry 3) and heat (Scheme 5.32, entry 4), suggests that both were necessary for the reaction. Finally, the reaction was scaled up to 290 mg scale without a reduction in yield or selectivity (Scheme 5.32, entry 7).

Scheme 5.32. *α-alkenylation controls and scale-up.*

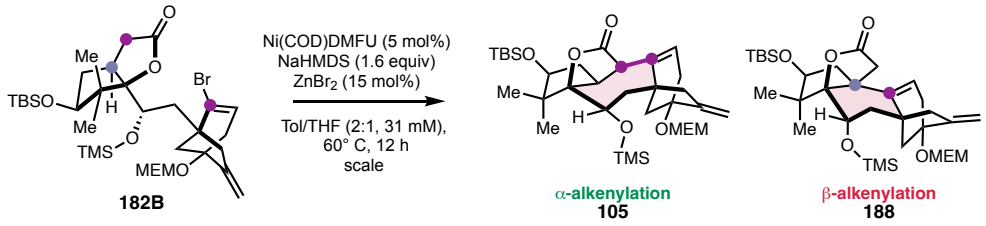

entry	scale	deviation	rsm (%)	product (%)	selectivity (α : β)
1	4 mg	-	-	70	9 : 1
2	4 mg	-	6	58	9 : 1
3	4 mg	no $ZnBr_2$	28	19	9 : 1
4	4 mg	no heat	21	40	> 20 : 1
5	4 mg	DavePhos*	9	42	3 : 1
6	150 mg	-	-	74	9 : 1
7	290 mg	-	-	79	9 : 1

*10 mol%

5.4 CONCLUDING REMARKS

In conclusion, a vinylogous Mukaiyama aldol (VMAR) addition of silyloxyfuran intermediate with 3.2.1 bicyclic aldehyde has been developed on substrates bearing an enol triflate and alkenyl bromide functionality. Central to the development of the reaction was close monitoring of temperature and judicious solvent selection. Additionally, it was important to pay close attention to the purification method used for the silyloxyfuran fragment and the quality of TBSOTf used. Following the intermolecular coupling reaction, strategies to elaborate to an α-enolate alkenylation substrate were undertaken, consisting of TMS protection and CuH reduction. For the CuH reduction, Buchwald's reduction worked uniquely well, delivering the product in high yields and as a single diastereomer. Synthetic methods for ring closure were explored in detail. Originally, conditions from the

model system were attempted to be adapted for the intramolecular cross coupling, both on the enol triflate and the alkenyl bromide. While the reaction worked a few times, it was not reproducible and mainly returned decomposition.

It was not until the reaction was tested with olefin-containing ligands, in the absence of phosphines, that the reaction began to work well. Ultimately, it was found that Ni(COD)DMFU was a privileged catalyst in the reaction, delivering the product in 65% yield in good selectivity. The study of the reaction may have implications in electron-deficient olefins as ligands in nickel catalysis more broadly, perhaps leading to the future development of related nickel catalyzed methods within the group. Taken together, this chapter details the rapid construction of molecular complexity through two powerful C-C bond forming reactions *en-route* to auriculatol A and other grayanane natural products. With the two most difficult key steps of the synthesis developed, efforts focused on the end-game stages of the synthesis were undertaken.

5.5 EXPERIMENTAL SECTION

Preparation of silyloxyfuran (88):

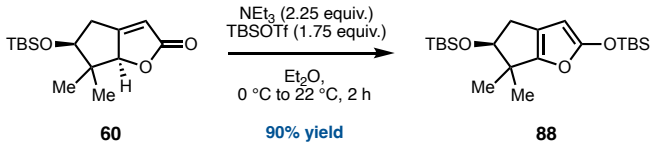

60 **90% yield** **88**

A 100 mL round-bottom flask was flame-dried under vacuum. Upon cooling to room temperature, the cap was removed and the flask was charged with butenolide **60** (625 mg, 2.21 mmol, 1.0 equiv), a magnetic stir bar, and placed under N_2 atmosphere. To the starting material was added dry Et_2O (44 mL) and freshly distilled NEt_3 (700 uL, 5.0 mmol, 2.25 equiv). The reaction was stirred at room temperature until all butenolide starting

material was dissolved, then cooled to 0 °C. At 0 °C, TBSOTf (900 uL, 3.9 umol, 1.75 equiv) was added dropwise. The reaction was vigorously stirred at 0 °C to make sure there is complete mixing of TBSOTf, which in some cases may crash out of solution. After 30 min stirring at. 0 °C, the reaction was warmed to room temperature and stirred for 90 min. After 2 h total, the reaction mixture was poured directly onto a phosphate-buffered silica plug (25 g of buffered silica) pre-packed with hexanes, and the flask was rinsed with Et_2O (~15 mL) to guarantee minimal loss of product. The eluent was collected in a 500 mL receiving flask as it was passed through the buffered silica, and the silica was further rinsed with hexanes (3 x 50 mL) to ensure complete elution of product. The eluent was concentrated under reduced pressure, and the crude residue was redissolved in MeCN (50 mL). The MeCN solution was subjected to sequential pentane extractions (4 x 50 mL). The combined pentane extracts were concentrated under reduced pressure and subjected to high vacuum for 12 h to afford **88** as a yellow oil (790 mg, 90% yield).

Experimental Note: the purity of TBSOTf is important for this step, as it may affect the aldol step depending on the concentration of trace silyl impurities. It is considered best practice to store the TBSOTf cold under a blanket of Ar to ensure the reagent quality is maintained over time. The phosphate buffered silica was prepared according to literature-reported procedures from Newton and coworkers.

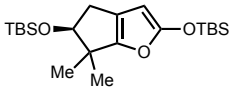

88

TLC: N/A (unstable to silica)

^{1}H NMR ($CDCl_3$, 400 MHz): ^{1}H NMR (400 MHz, $CDCl_3$) δ 4.96 (s, 1H), 4.24 (t, *J* = 6.9 Hz, 1H), 2.72 (dd, *J* = 14.1, 7.1 Hz, 1H), 2.31 (dd, *J* = 14.1, 6.7 Hz, 1H), 1.19 (s, 3H), 1.00 (s, 3H), 0.96 (s, 9H), 0.91 (s, 9H), 0.22 (s, 6H), 0.08 (s, 6H).

^{13}C NMR ($CDCl_3$, 101 MHz): δ 158.1, 151.2, 117.8, 83.6, 82.7, 43.0, 34.1, 26.0, 25.7, 25.2, 20.41, 18.3, 18.2, -4.4, -4.7, -4.1, -4.8.

FTIR (Neat, NaCl, thin film): 2956, 2930, 2859, 1585, 1471, 1361, 1255, 1101, 866, 787 cm^{-1}.

HRMS (ESI-TOF): calc'd for $C_{21}H_{41}O_3Si_2$ $[M+H]^+$ 397.2589, found 396.2597.

$[\alpha]_D^{22}$: +38.4 (c 1.0 in $CHCl_3$).

Preparation of vinyl bromide 107B.

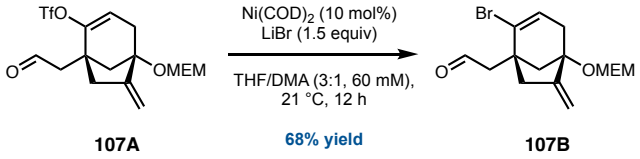

107A **107B**

In an N_2-filled glovebox, an oven-dried 100 mL round-bottom flask containing a magnetic stir bar was charged with $Ni(COD)_2$ (80 mg, 290 umol, 10 mol%) and LiBr (380 mg, 4.3 mmol, 1.5 equiv). DMA (2.90 mL) and THF (7.0 mL) were added in, and the solution was stirred for 5 min or until all the $Ni(COD)_2$ dissolved. Then, aldehyde **107A** (1.20 g, 2.90 mmol, 1 equiv) was added as a solution in THF (1.7 mL). The reaction vessel was capped with a rubber septum, removed from the glovebox, connected to an N_2 inlet, and stirred for 12 h at room temperature. An initial color of deep aqua blue was observed, which turned to a pale-green, then finally a bright green. After 12 h, an NMR aliquot was taken, which confirmed full conversion. The reaction was filtered through a short silica plug, eluting with 50% EtOAc/hexanes (200 mL). The eluent was then washed with sat.

aq. LiCl (3 x 50 mL), and the organic layers were dried with Na_2SO_4, filtered, and concentrated under reduced pressure. The crude residue was purified via flash column chromatography (SiO_2, 3% to 10% acetone/hexanes slow gradient) to afford the vinyl bromide **107B** (683 mg, 68% yield) as a colorless oil.

Experimental note: This reaction is sensitive to air.

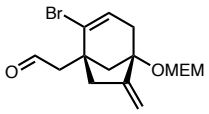

107B

TLC (20% Acetone/Hexanes): R_f 0.29 ($KMnO_4$).

^{1}H NMR ($CDCl_3$, 400 MHz): δ 9.82 (s, 1H), 5.94 (dd, *J* = 5.3, 2.5 Hz, 1H), 5.17 (dd, *J* = 3.2, 1.8 Hz, 1H), 5.10 (s, 1H), 4.92 (d, *J* = 7.6 Hz, 1H), 4.71 (d, *J* = 7.6 Hz, 1H), 3.83 (ddd, *J* = 10.6, 4.8, 3.6 Hz, 1H), 3.64 – 3.57 (m, 1H), 3.56 – 3.48 (m, 2H), 3.37 (s, 3H), 3.10 (dd, *J* = 17.6, 1.2 Hz, 1H), 2.75 – 2.66 (m, 2H), 2.43 – 2.26 (m, 4H), 2.15 (dddd, *J* = 16.4, 5.3, 2.1, 0.9 Hz, 1H).

^{13}C NMR ($CDCl_3$, 101 MHz): δ 200.4, 151.0, 128.3, 128.2, 109.3, 91.1, 83.4, 71.9, 67.2, 59.1, 51.4, 46.7, 45.8, 45.3, 45.1.

FTIR (Neat, NaCl, thin film): 2924, 1725, 1453, 1048, 887 cm^{-1}.

HRMS (ESI-TOF): calc'd for $C_{15}H_{22}BrO_4$ [M+H] 345.0696, found 345.0701.

$[\alpha]_D^{23}$: +103.8 (c 1.0 in $CHCl_3$).

Preparation of aldol product 106A.

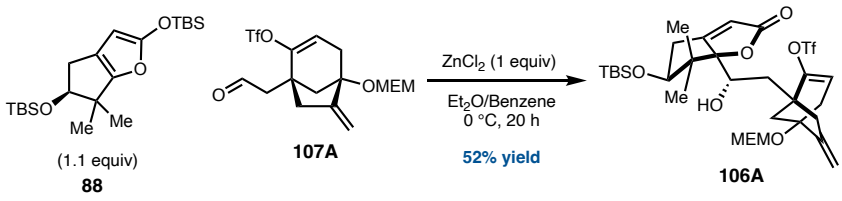

An oven-dried 2 dram vial was charged with aldehyde (44.2 mg, 107 μmol, 1.0 equiv.), silyloxyfuran **88** in benzene and Et_2O and a magnetic stir bar in a glovebox to make a solution of concentration equal to 100 mM. The reaction mixture was cooled to 0 °C and $ZnCl_2$ (1M in Et_2O, 111 uL, 1.04 equiv.) was added dropwise. After the reaction time the reaction was quenched with sat. aq. NH_4Cl at 0 °C, warmed to room temperature, extracted with Et_2O (3 x 1 mL). The combined organic phases were washed with brine and dried over anhydrous Na_2SO_4 and reduced *in vacuo.* The title compound was purified by flash column chromatography (0% to 10% Et_2O in CH_2Cl_2) to give product **106A** (33.7 mg, 56.3 μmol, 52% yield) as a white solid. *XRD analysis for **106A** is provided in Appendix 5.*

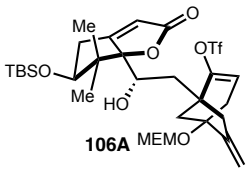

TLC (30% EtOAc/Hexanes): R_f 0.20 ($KMnO_4$).

^{1}H NMR ($CDCl_3$, 400 MHz): δ 5.87 – 5.84 (m, 1H), 5.57 (dd, J = 5.2, 2.5 Hz, 1H), 5.18 (dd, J = 3.2, 1.7 Hz, 1H), 5.13 (t, J = 2.1 Hz, 1H), 4.93 (d, J = 7.5 Hz, 1H), 4.75 (d, J = 7.6 Hz, 1H), 4.61 (dd, J = 9.9, 4.8 Hz, 1H), 4.20 (t, J = 6.9 Hz, 1H), 3.88 – 3.80 (m, 1H), 3.63 (ddd, J = 10.7, 5.4, 3.6 Hz, 1H), 3.60 – 3.54 (m, 2H), 3.39 (s, 3H), 3.06 (ddd, J = 17.9, 10.0, 2.5 Hz, 1H), 2.82 (ddt, J = 16.0, 3.1, 1.6 Hz, 1H), 2.74 (dd, J = 16.5, 2.6 Hz, 1H), 2.39 (dt, J = 16.1, 2.9 Hz, 1H), 2.34 (dd, J = 11.0, 1.9 Hz, 1H), 2.31 – 2.22 (m, 2H), 2.11 (dd, J =

11.0, 2.8 Hz, 1H), 2.01 (d, J = 6.9 Hz, 1H), 1.83 (dd, J = 15.0, 10.1 Hz, 1H), 1.59 (dd, J = 15.1, 2.6 Hz, 1H), 1.23 (s, 3H), 0.89 (s, 9H), 0.74 (s, 3H), 0.05 (s, 6H).

^{13}C NMR (101 MHz, $CDCl_3$): δ 175.53, 173.50, 152.89, 150.58, 120.08, 116.89, 114.94, 109.71, 91.22, 82.98, 79.77, 71.80, 67.37, 59.17, 47.44, 44.02, 43.52, 40.95, 35.04, 30.46, 29.85, 25.83, 21.06, 18.09, 17.24, 1.48, 0.92, -4.51, -5.04.

FTIR (Neat, NaCl, thin film): 3435, 2930, 1731, 1416, 1211, 1049 cm^{-1}.

HRMS (ESI): calc'd for $[M+H]^+$ 697.2684, found 697.2681.

Preparation of TMS-protected 181A.

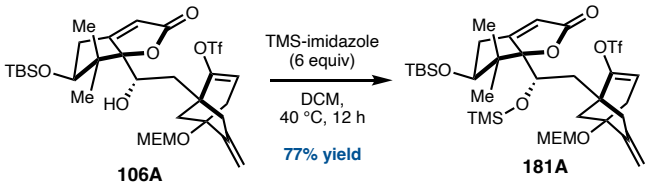

106A (33.7 mg, 48.4 umol, 1 equiv) in an oven-dried round-bottom flask equipped with a magnetic stir bar was dissolved in CH_2Cl_2 (242 uL, 200 mM). TMS-imidazole (43 uL, 6 equiv) was added dropwise at room temperature, and the reaction was heated to reflux for 12 h. After 12 h, TLC showed complete conversion. The reaction was quenched by addition of water (1 mL). The aqueous phase was separated from the organic phase, and it was extracted with CH_2Cl_2 (3 x 1 mL). The combined organic phases were washed with NH_4Cl to remove imidazole (3 x 1 mL), brine, and dried with $MgSO_4$. Following concentration, column chromatography (15% EA/hex) delivered the pure product **181A** (28.6 mg, 77% yield) as a yellow oil.

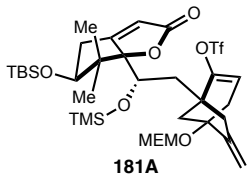

181A

TLC (30% EtOAc/Hexanes): R_f 0.39 ($KMnO_4$).

^{1}H NMR ($CDCl_3$, 400 MHz: δ 5.88 – 5.83 (m, 1H), 5.50 (dd, J = 5.3, 2.4 Hz, 1H), 5.17 (dd, J = 3.1, 1.7 Hz, 1H), 5.14 (t, J = 2.1 Hz, 1H), 4.94 (d, J = 7.7 Hz, 1H), 4.72 (d, J = 7.7 Hz, 1H), 4.46 (dd, J = 9.8, 5.6 Hz, 1H), 3.85 (dt, J = 10.8, 4.2 Hz, 1H), 3.66 – 3.58 (m, 1H), 3.52 (dd, J = 5.3, 4.0 Hz, 2H), 3.36 (s, 3H), 3.02 – 2.93 (m, 1H), 2.85 (d, J = 16.1 Hz, 1H), 2.70 (dd, J = 16.6, 2.6 Hz, 1H), 2.44 – 2.20 (m, 4H), 1.96 (dd, J = 10.7, 2.7 Hz, 1H), 1.25 (s, 3H), 0.89 (s, 9H), 0.72 (s, 3H), 0.19 (s, 9H), 0.07 (d, J = 5.4 Hz, 6H).

^{13}C NMR (101 MHz, $CDCl_3$) δ 175.53, 173.50, 152.89, 150.58, 120.08, 116.89, 114.94, 109.71, 91.22, 82.98, 79.77, 71.80, 67.37, 59.17, 47.44, 44.02, 43.52, 40.95, 35.04, 30.46, 29.85, 25.83, 21.06, 18.09, 17.24, 0.92, -4.51, -5.04.

FTIR (Neat, NaCl, thin film): 3437, 2928, 1729, 1412, 1282, 1070 cm^{-1}.

HRMS (ESI): calc'd for $[M+NH_4]^+$ 786.3344, found 786.3345.

Preparation of lactone 182A.

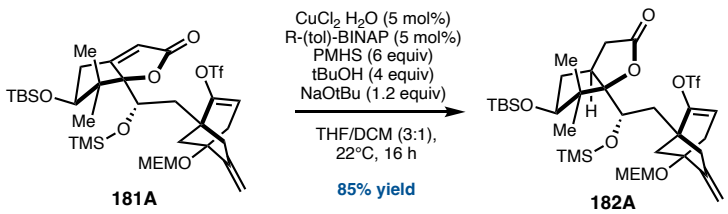

181A **182A**

An oven-dried vial equipped with a Teflon-coated magnetic stir bar was charged with copper (II) chloride dihydrate (0.3 mg, 1.86 umol, 0.05 equiv), (R)-Tol-BINAP (1.3 mg, 1.86 umol, 0.05 equiv.), and sodium tert-butoxide (4.3 mg, 44.6 umol, 1.2 equiv) in the

glovebox. The vial was capped with a rubber septum, taped, and pumped out of the glovebox. SPS THF (0.6 mL) was then added to the vial and the mixture was allowed to stir at room temperature for 5 minutes. PMHS (50 uL, 223 umol, 6 equiv.) was then added dropwise and allowed to stir for 5 minutes. There is a color change to orange and then potentially a darker orange/black following addition of PMHS and 5 min of stirring. After 5 minutes of stirring, the starting material was added as a solution in remaining THF / CH_2Cl_2 / *t*-BuOH (330 uL / 310 uL / 14 uL) and allowed to stir at room temperature 12 h, at which point TLC indicated complete conversion of the starting material. At this point, ammonium chloride (1 mL) was carefully added to the reaction and allowed to stir for 15 minutes. The aq and organic phase were then separated, and the aq phase was extracted with EtOAc (3 x 1 mL). The combined organics were washed with brine, dried over Na_2SO_4, filtered, and concentrated to dryness with the aid of a rotary evaporator. The resulting residue was then purified by flash chromatography (30% EtOAc/hexanes) to provide the product **182A** (24.4 mg, 85% yield) as a white solid.

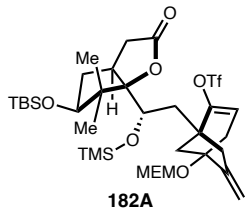

182A

TLC (30% EtOAc/Hexanes): R_f 0.43 (*p*-anisaldehyde, blue, $KMnO_4$).

^{1}H NMR ($CDCl_3$, 400 MHz): δ 5.53 (dd, *J* = 5.2, 2.5 Hz, 1H), 5.19 (dd, *J* = 3.2, 1.7 Hz, 1H), 5.14 (d, *J* = 2.1 Hz, 1H), 4.93 (d, *J* = 7.6 Hz, 1H), 4.74 (d, *J* = 7.6 Hz, 1H), 4.01 – 3.87 (m, 1H), 3.87 – 3.80 (m, 1H), 3.75 (dd, *J* = 5.9, 3.2 Hz, 1H), 3.69 – 3.61 (m, 1H), 3.53 (dd, *J* = 5.4, 4.0 Hz, 2H), 3.36 (s, 3H), 2.89 – 2.79 (m, 2H), 2.72 (dd, *J* = 16.6, 2.6 Hz, 1H),

2.43 – 2.15 (m, 7H), 2.00 (dd, J = 10.8, 2.7 Hz, 1H), 1.63 (dd, J = 15.1, 2.7 Hz, 1H), 1.48 (dt, J = 13.7, 3.7 Hz, 1H), 1.03 (d, J = 5.9 Hz, 6H), 0.88 (s, 9H), 0.18 (s, 9H).

^{13}C NMR (101 MHz, $CDCl_3$): δ 176.67, 152.72, 150.88, 120.05, 116.87, 115.18, 109.68, 99.35, 91.22, 82.95, 67.40, 60.54, 59.14, 49.60, 46.81, 44.10, 43.78, 40.83, 39.82, 39.08, 38.56, 35.82, 25.87, 23.38, 21.20, 20.62, 18.21, 1.31, -4.52, -4.93.

FTIR (Neat, NaCl, thin film): 2929, 1779, 1412, 1213, 1050 cm^{-1}.

HRMS (ESI): calc'd for $[M+NH_4]^+$ 788.3501, found 788.3503.

Preparation of aldol product 106B.

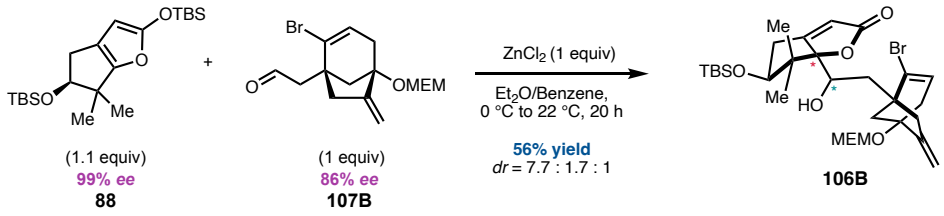

An oven-dried 40 mL vial with a magnetic stir bar was cooled under vacuum. The vial was then charged with aldehyde **107B** (683 mg, 1.98 mmol, 1 equiv) and silyloxyfuran **88** (785 mg, 1.98 mmol, 1 equiv), capped with a rubber septum, and evacuated and backfilled with N_2 three times. To the vial was added dry benzene (9.9 mL) and dry Et_2O (7.9 mL). The reaction vessel was cooled to 0 °C and vigorous stirring (800 rpm) was initiated. A solution of $ZnCl_2$ (1 M in Et_2O, 270 mg, 1.98 mmol, 1.98 mL) was added dropwise to the vial at 0 °C. The reaction was stirred for 9 h maintaining a constant temperature of 0 °C. After 9 h, the reaction was allowed to slowly warm to room temperature and stirred for 11 more h. After stirring for a total of 20 h, the reaction was quenched with sat. aq. NH_4Cl (20 mL). The phases were separated, and the aqueous layer was extracted with Et_2O (3 x 20 mL). The combined organic layers were washed with brine

(50 mL), dried with Na_2SO_4, filtered, and concentrated under reduced pressure. The crude oil was purified via flash column chromatography (SiO_2, slow gradient, 5-10% acetone/hexanes). The volatiles were concentrated under reduced pressure to afford **106B** as a mixture of diastereomers (7.7 : 1.7 : 1.0) obtained as a thick yellow oil (694 mg, 56% yield) Analytically pure samples of the diastereomers were obtained, but on larger scales the mixture was carried forward and the single diastereomer of compound **181B** was separated during the subsequent step.

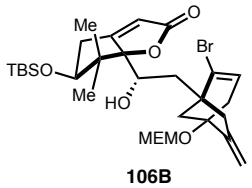

106B

TLC (24% Acetone/Hexanes): R_f 0.32 (*p*-anisaldehyde, brown, UV).

^{1}H NMR ($CDCl_3$, 400 MHz): δ 5.92 (dd, *J* = 5.5, 2.3 Hz, 1H), 5.87 (s, 1H), 5.15 (s, 1H), 5.07 (s, 1H), 4.91 (d, *J* = 7.4 Hz, 1H), 4.74 (d, *J* = 7.4 Hz, 1H), 4.67 (dd, *J* = 10.0, 4.7 Hz, 1H), 4.26 – 4.17 (m, 1H), 3.86 – 2.80 (m, 1H), 3.67 – 3.61 (m, 1H), 3.56 (t, *J* = 4.6 Hz, 2H), 3.39 (s, 3H), 3.10 – 2.97 (m, 1H), 2.70 (dd, *J* = 16.4, 2.4 Hz, 1H), 2.66 – 2.57 (m, 1H), 2.36 – 2.24 (m, 3H), 2.24 – 2.18 (m, 1H), 2.17 – 2.04 (m, 3H), 1.58 (dd, *J* = 15.2, 3.2 Hz, 1H), 1.24 (s, 3H), 0.89 (s, 9H), 0.73 (s, 3H), 0.04 (s, 6H).

^{13}C NMR (101 MHz, $CDCl_3$): δ 175.9, 174.1, 151.7, 131.7, 128.6, 115.5, 109.4, 97.3, 91.2, 83.1, 79.9, 72.0, 70.0, 67.2, 59.2, 48.1, 47.4, 47.3, 44.8, 44.2, 38.3, 35.2, 25.9, 20.5, 18.1, 16.3, -4.5, -4.9.

FTIR (Neat, NaCl, thin film): 3461, 2930, 2888, 1785, 1738, 1253, 1195, 1089, 1045, 836 cm^{-1}.

HRMS (ESI-TOF): calc'd for $C_{30}H_{47}BrO_7SiNa$ $[M+Na]^+$ 649.2166, found 649.2170.

$[\alpha]_D^{22}$: +171.8 (c 1.0 in $CHCl_3$).

Preparation of TMS-protected 181B.

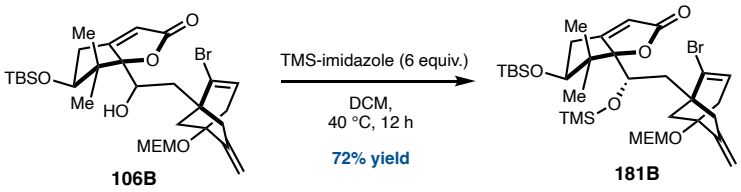

TMS•imidazole was purchased from Millipore Sigma and used as is. An oven-dried two neck 25 mL round-bottom flask was equipped with a magnetic stir bar, and reflux condenser then charged with the alcohol **106B** (694 mg, 1.10 mmol, 1 equiv). The flask was evacuated and backfilled with N_2 three times. DCM (5.5 mL, 200 mM) was added to the vial followed by dropwise addition of TMS-imidazole (970 uL, 6.60 mmol, 6 equiv) at room temperature. The reaction was then lowered into an oil bath and refluxed at 45 °C for 12 h. Upon TLC indicating complete conversion, the reaction was cooled to 0 °C and quenched by slow addition of H_2O (10 mL). The layers were separated, and the aqueous phase was extracted with DCM (3 x 10 mL). The combined organic phases were washed with sat. aq. NH_4Cl (3 x 10 mL), brine (10 mL), dried with $MgSO_4$, filtered, and concentrated under reduced pressure. The crude oil was purified by flash column chromatography (SiO_2, 5% to 30% EtOAc/hexanes gradient) to afford a single diastereomer **181B** (557 mg, 72% yield) as a white solid.

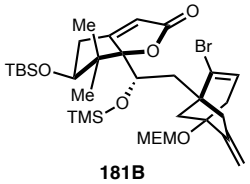

TLC: (20% EtOAc/hexanes): R_f 0.22 (*p*-anisaldehyde, brown, UV).

^{1}H NMR (CDCl$_3$, 400 MHz): δ 5.89 (s, 1H), 5.85 (dd, *J* = 5.4, 2.3 Hz, 1H), 5.15 (t, *J* = 2.3 Hz, 1H), 5.10 (s, 1H), 4.93 (d, *J* = 7.6 Hz, 1H), 4.73 (d, *J* = 7.6 Hz, 1H), 4.50 (dd, *J* = 9.8, 5.4 Hz, 1H), 3.94 (bs, 1H), 3.85 (dt, *J* = 11.0, 4.3 Hz, 1H), 3.64 (dt, *J* = 10.7, 5.1 Hz, 1H), 3.53 (t, *J* = 4.8 Hz, 2H), 3.37 (s, 3H), 3.01 (ddd, *J* = 18.1, 9.9, 2.4 Hz, 1H), 2.69 – 2.54 (m, 2H), 2.45 – 2.22 (m, 3H), 2.20 – 1.60 (m, 4H), 1.27 (s, 3H), 0.90 (s, 9H), 0.72 (s, 3H), 0.21 (s, 9H), 0.07 (d, *J* = 6.1 Hz, 6H).

^{13}C NMR (CDCl3, 101 MHz): δ 176.0, 173.7, 133.0, 127.1, 125.7, 116.8, 109.2, 91.2, 83.2, 79.90, 71.9, 67.4, 66.0, 59.1, 51.4, 47.4, 46.7, 45.0, 39.9, 35.2, 30.5, 25.8, 21.2, 18.1, 17.1, 15.4, 1.1, -4.4, -4.8.

FTIR (Neat, NaCl, thin film): 2930, 1758, 1461, 1249, 1096, 1051, 836 cm^{-1}.

HRMS (ESI-TOF): calc'd for $C_{33}H_{55}BrO_7Si_2Na$ $[M+Na]^+$ 721.2563 found 721.2563.

$[\alpha]_D^{23}$: +95.2 (c 1.0 in $CHCl_3$).

Melting Point: 135-137 °C.

Preparation of lactone 182B.

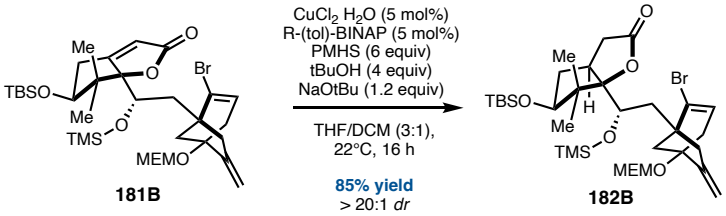

In an N_2-filled glovebox, an oven-dried round-bottom flask was equipped with a magnetic stir bar and charged with $CuCl_2$•$2H_2O$ (7.5 mg, 44 umol, 0.075 equiv), (*rac*)-tol-BINAP (30 mg, 44 umol, 0.075 equiv), and NaO^{t}Bu (67 mg, 700 umol, 1.20 equiv) The vial was sealed with a rubber septum and removed from the glovebox. Anhydrous THF (13

mL) was added to the vial, and the solution was stirred at room temperature (22 °C) for 5 min. After 5 min, poly(methylhydrosiloxane) (390 uL, 940 umol, 3 equiv) was added dropwise, and the reaction was stirred for 5 more min. A color change to bright orange and then brown was observed. Finally, **181B** (408 mg, 583 umol, 1 equiv) was added as a solution in THF/DCM/^{t}BuOH (2 mL/4.9 mL/0.22 mL) and the reaction was allowed to stir at room temperature for 14 h. Upon completion of the reaction as determined by TLC analysis, the reaction was quenched by slow addition of sat. aq. NH_4Cl (20 mL), and the solution was stirred for 15 min or until bubbling ceased. The layers were separated, and the aqueous layer was extracted with EtOAc (3 x 15 mL). The combined organic layers were washed with brine (15 mL), then dried over Na_2SO_4, filtered, and concentrated under reduced pressure. The crude residue was purified via flash column chromatography (5-10% acetone/hexanes) to afford lactone **182B** (348 mg, 85% yield) as a viscous, colorless oil. The reduction occurred in >20:1 *dr*.

Experimental notes: The purification can be difficult to separate the product **182B** from yellow copper or PMHS-derived compounds. It is advised to carefully load the column in a small amount of 5% acetone/hexanes to increase ease of separation. The starting material **181B** and product **182B** have a similar R_f but can be differentiated based on UV activity.

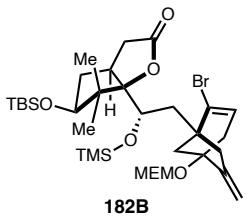

182B

TLC (30% EtOAc/hexanes): R_f 0.57 (*p*-anisaldehyde, blue).

^{1}H NMR (600 MHz, $CDCl_3$): δ 5.83 (dd, *J* = 5.5, 2.3 Hz, 1H), 5.16 (s, 1H), 5.08 (s, 1H), 4.93 (d, *J* = 7.5 Hz, 1H), 4.75 (d, *J* = 7.5 Hz, 1H), 3.96 (s, 1H), 3.84 (dt, *J* = 10.8, 4.4 Hz, 1H), 3.80 – 3.70 (m, 1H), 3.65 (dt, *J* = 10.7, 5.1 Hz, 1H), 3.53 (t, *J* = 4.8 Hz, 2H), 3.37 (s, 3H), 2.91 – 2.83 (m, 1H), 2.77 (s, 1H), 2.41 – 2.20 (m, 2H), 2.41 – 2.27 (m, 4H), 2.24 (m, 1H), 2.14 (dd, *J* = 16.3, 5.5 Hz, 1H), 2.02 (dd, *J* = 10.7, 2.7 Hz, 1H), 1.80 (dd, *J* = 15.4, 3.0 Hz, 1H), 1.49 (dt, *J* = 13.7, 3.4 Hz, 1H), 1.07 (s, 3H), 1.03 (bs, 3H), 0.89 (s, 9H), 0.20 (s, 9H), 0.04 (d, *J* = 6.1 Hz, 6H).

^{13}C NMR ($CDCl_3$, 101 MHz): δ 177.1, 152.3, 132.9, 127.2, 109.1, 99.8, 91.2, 83.3, 71.9, 67.3, 66.0, 59.1, 49.5, 46.8, 44.9, 44.3, 40.5, 39.9, 39.3, 38.8, 30.5, 29.8, 25.9, 23.5, 18.2, 15.4, 1.5, -4.5, -4.9.

FTIR (Neat, NaCl, thin film): 2950, 2853, 1776, 1251, 1047, 840 cm^{-1}.

HRMS (ESI-TOF): calc'd for $C_{33}H_{61}BrNO_7Si_2$ $[M+NH_4]^+$ 718.3164, found 718.3163.

$[\alpha]_D^{23}$: +70.8 (c 1.0 in $CHCl_3$).

Preparation of pentacycle 105:

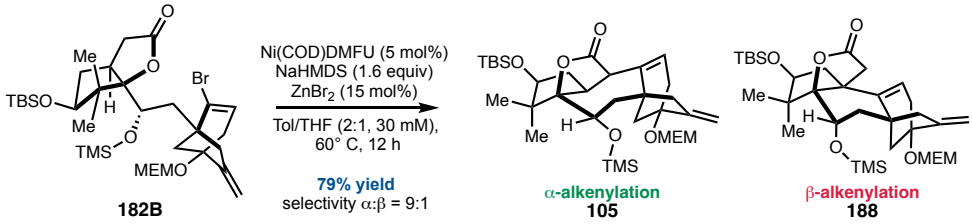

In an N_2-filled glovebox, an oven-dried 50 mL Schlenk flask equipped with a magnetic stir bar was charged with **182B** (290 mg, 413 umol, 1 equiv) in toluene (2 mL). A 5.0 M solution of NaHMDS was prepared by dissolving 150.0 mg in 1.5 mL of toluene along with a 0.02 M solution of Ni(COD)DMFU by dissolving 12.8 mg in 2 mL. Both stock solutions were stirred for 5 minutes to ensure complete dissolution of the solids. The

NaHMDS solution (1.3 mL, 121 mg, 661 umol, 1.6 equiv) was drawn up and dispensed dropwise into the Schlenk flask containing the starting material. $ZnBr_2$ (14.0 mg, 62.0 umol, 0.15 equiv) as a solution in THF (4.6 mL) was added next in one portion. Finally, the Ni(COD)DMFU solution (1.0 mL, 6.4 mg, 20.7 umol, 0.05 equiv) was added slowly dropwise to create a final reaction concentration of 30 mM and a 2:1 ratio of toluene:THF. The Schlenk flask was closed with a tightly-fitted Kontes valve, pumped out of the glovebox, connected to an N_2-inlet, and lowered into an oil bath. The reaction was stirred for 16 h at 60 °C. After 16 h, TLC indicated complete conversion, and the solution was filtered through a silica plug eluting with 50% Et_2O/hexanes (100 mL). The collected volatiles were concentrated under reduced pressure. The crude residue was purified via flash column chromatography (10% to 30% Et_2O/hexanes gradient) to afford the product **105** (203 mg, 79% yield) as a 9:1 mixture of isomers (α:β).

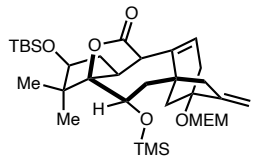

105

TLC (50% Et_2O/hexanes): R_f 0.71 (*p*-anisaldehyde, light blue).

^{1}H NMR ($CDCl_3$, 400 MHz): δ 5.36 (dd, *J* = 4.3, 2.8 Hz, 1H), 5.02 (s, 1H), 4.92 (d, *J* = 7.5 Hz, 2H), 4.71 (d, *J* = 7.5 Hz, 1H), 4.30 – 4.27 (m, 1H), 3.83 (dt, *J* = 10.9, 4.0 Hz, 1H), 3.68 – 3.62 (m, 2H), 3.53 (t, *J* = 5.0 Hz, 2H), 3.37 (s, 3H), 3.10 (s, 1H), 2.98 (dd, *J* = 11.1, 4.7 Hz, 1H), 2.68 (d, *J* = 13.8 Hz, 1H), 2.60 – 2.46 (m, 2H), 2.29 (dd, *J* = 16.0, 2.1 Hz, 1H), 2.23 – 2.13 (m, 3H), 1.98 (d, *J* = 12.2 Hz, 1H), 1.70 (dd, *J* = 16.0, 5.5 Hz, 1H), 1.39 (ddd, *J* = 14.7, 4.7, 2.0 Hz, 1H), 1.07 (s, 3H), 0.92 (s, 3H), 0.87 (s, 9H), 0.19 (s, 9H), 0.00 (d, *J* = 5.0 Hz, 6H).

^{13}C NMR ($CDCl_3$, 101 MHz): δ 177.1, 152.3, 143.2, 123.9, 107.0, 98.9, 91.2, 85.0, 83.0, 71.9, 71.0, 67.2, 59.1, 57.8, 51.2, 50.8, 49.9, 44.9, 43.5, 42.4, 42.3, 39.7, 25.8, 24.4, 18.5, 18.1, 1.3, -4.6, -5.00.

FTIR (Neat, NaCl, thin film): 2951, 2929, 1768, 1265, 1046, 840, 736 cm^{-1}.

HRMS (ESI-TOF): calc'd for $C_{33}H_{57}O_7Si_2$ $[M+H]^+$ 621. 3638, found 621.3670.

$[\alpha]_D^{24}$: +74.8 (c 0.2 in $CHCl_3$).

Melting Point: 104-106 °C

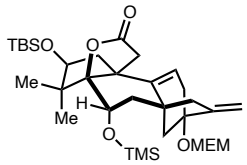

188

TLC (50% Et_2O/hexanes): R_f 0.68 (*p*-anisaldehyde, pink).

^{1}H NMR ($CDCl_3$, 400 MHz): δ 5.36 (dd, *J* = 4.6, 2.6 Hz, 1H), 5.10 (s, 1H), 5.02 (s, 1H), 4.95 (d, *J* = 7.5 Hz, 1H), 4.73 (d, *J* = 7.5 Hz, 1H), 4.08 (dd, *J* = 11.8, 4.1 Hz, 1H), 3.87 – 3.82 (m, 1H), 3.62 (m, 2H), 3.54 (m, 2H), 3.38 (s, 3H), 2.76 (dd, *J* = 16.3, 9.6 Hz, 3H), 2.63 (dd, *J* = 16.6, 2.6 Hz, 1H), 2.47 (dd, *J* = 14.0, 4.6 Hz, 1H), 2.30 (d, *J* = 15.5 Hz, 1H), 2.26 – 1.93 (m, 4H), 1.81 (bs, 1H), 1.64 – 1.57 (m, 1H), 1.23 (s, 3H), 1.08 (s, 3H), 0.88 (s, 9H), 0.15 (s, 9H), 0.03 (d, *J* = 4.9 Hz, 6H).

^{13}C NMR ($CDCl_3$, 101 MHz): δ 175.4, 152.6, 142.7, 124.2, 108.2, 108.1, 98.3, 91.1, 83.5, 83.3, 72.0, 67.1, 59.2, 52.4, 50.6, 48.5, 48.1, 43.9, 42.2, 30.5, 29.9, 25.9, 25.8, 24.4, 21.3, 18.4, 0.4, -4.7, -4.9.

FTIR (Neat, NaCl, thin film): 2951, 2929, 1768, 1265, 1046, 840, 736 cm^{-1}.

HRMS (ESI-TOF): calc'd for $C_{33}H_{56}O_7Si_2Na$ $[M+Na]^+$ 643.3457, found 643.3461.

$[\alpha]_D^{23}$: +97.6 (c 0.2 in $CHCl_3$).

5.6 NOTES AND REFERENCES

(1) Ribes, C.; Falomir, E.; Murga, J. Selective Cleavage of Acetals with $ZnBr_2$ in Dichloromethane. *Tetrahedron,* **2006**, *62*, 1239–1244.

(2) Casiraghi, G.; Zanardi, F. The Vinylogous Aldol Reaction: A Valuable, Yet Understated Carbon–Carbon Bond-Forming Maneuver. *Chem. Rev.* **2000**, *100*, 1929–1972.

(3) Casiraghi, G.; Battistini, L.; Claudio, C.; Rassu, G.; Zanardi, F. The Vinylogous Aldol and Related Addition Reactions: Ten Years of Progress. *Chem. Rev.* **2011**, *111*, 3076–3154.

(4) Gilman, H.; Calloway, N. O. Super-Aromatic Properties of Furan. II. The Friedel–Crafts Reaction. *J. Am. Chem. Soc.* **1933**, *55*, 4197–4205.

(5) Finan, P. A.; Fothergill, G. A. 506. Furans. Part II. Friedel–Crafts Acylation of Furan, 2-methylfuran, and 3-methylfuran. *J. Chem. Soc.* **1963**, *0*, 2723–2727.

(6) Schlessinger, R. H.; Wu, X.-H.; Pettus, T. R. R. Diastereoselective Diels-Alder Reactions of Furan Substituted with a Proline Derived Auxiliary. *Synlett.* **1995**, 536–538.

(7) Schlessinger, R. H.; Pettus, T. R. R. Diastereoselective Diels-Alder Reactions Using Furan Substituted with a Nonracemic Amine. *J. Org. Chem.* **1994**, *59*, 3246–3247.

(8) Schlessinger, R. H.; Bergstrom, C. P. Enantioselective Synthesis of (+)-Cyclophellitol. *J. Org. Chem.* **1995**, *60*, 16–17.

(9) Franey, A. M.; Serratore, N. D.; Setterholm, N. A.; Bur, S. K. Dynamics of Diels-Alder Reactions involving 2-Trialkylsilyloxyufrans. *Tetrahedron Lett.* **2012**, *53*, 179–181.

(10) Gravel, D.; Deziel, R. Diels-Alder Adducts of 2-Acetoxyfuran as a Route to 2,3-Functionalized 4-Hydroxycyclohexanones. Application of X-ray Diffraction to the

Problem of Regio- and Stereochemistry. *Can. J. Chem.* **1981**, *59*, 2997–3006.

(11) Bur, S.; Padwa, A. [4+2] Cycloaddition Chemistry of Substituted Furans. *Methods and Applications of Cycloaddition Reactions in Organic Syntheses,* First Edition. Edited by Nagatoshi Nishiwaki. **2014**, John Wiley & Sons, Inc. 355–406.

(12) Salavati-fard, T.; Caratzoulas, S.; Lobo, R. F.; Doren, D. J. Catalysis of the Diels-Alder Reaction of Furan and Methyl Acrylate in Lewis Acidic Zeolites. *ACS Catal.* **2017**, *7*, 2240–2246.

(13) Dissanayake, I.; Hart, J. D.; Becroft, E. C.; Sumby, C. J.; Newton, C. J. Bisketene Equivalents as Diels-Alder Dienes. *J. Am. Chem. Soc.* **2020**, *142*, 13328–13333.

(14) Wang, Z.; Wu, J.; Lamine, W; Li, B.; Sotiropoulos, J.-M. Chrostowska, A.; Miqueu, K.; Liu, S.-Y. C–Boron Enolates Enable Palladium Catalyzed Carboboration of Internal 1,3-Enynes. *Angew. Chem. Int. Ed.* **2021**, *60,* 21231–21236.

(15) Ng, E. W. H.; L, K.-H.; Chiu, P. Synthesis and Applications of Unquaternized C-Bound Boron Enolates. *J. Am. Chem. Soc.* **2018**, *140*, 3537–3541.

(16) Abiko, A. The Chemistry of Boron Enolate: Synthesis and Reactivity. *PATAI's Chemistry of Functional Groups*, **2020**, John Wiley & Sons. Ltd. 10.1002/9780470682531.pat0977

(17) Doucet, H. Suzuki-Miyaura Cross-Coupling Reactions of Alkylboronic Acid Derivatives or Alkyltrifluoroborates with Aryl, Alkenyl, or Alkyl Halides and Triflates. *Eur. J. Org. Chem.* **2008**, 2013–2030.

(18) Deng, J. Z.; Paone, D. V.; Ginnetti, A. T.; Kurihara, H.; Dreher, S. D.; Seissman, S. A.; Stauffer, S. R.; Burgey, C. S. Copper-Facilitated Suzuki Reactions: Application of 2-Heterocyclic Boronates. *Org. Lett.* **2009**, *11*, 345–347.

(19) Crudden, C. M.; Glasspoole, B. W.; Lata, C. J. Expanding the Scope of Transformations of Organoboron Species: Carbon-Carbon Bond Formation with Retention of Configuration. *Chem. Commun.* **2009**, 6704–6716.

(20) Zapf, A.; Ehrentraut, A.; Beller, M. A New Highly Efficient Catalyst System for Coupling of Nonactivated and Deactivated Aryl Chlorides with Arylboronic Acids. *Angew. Chem. Int. Ed.* **2000**, *39*, 4153–4155.

(21) Rainka, M. P.; Milne, J. E.; Buchwald, S. L. Dynamic Kinetic Resolution of α,β-Unsaturated Lactones through Asymmetric Copper-Catalyzed Conjugate Reduction: Application to the Total Synthesis of Eupomatilone-3. *Angew. Chem. Int. Ed.* **2005**, *44*, 6177–6180.

(22) Hughes, G.; Kimura, M.; Buchwald, S. L. Catalytic Enantioselective Conjugate Reduction of Lactones and Lactams. *J. Am. Chem. Soc.* **2003**, *125*, 11253–11258.

(23) Lee, S.; Ryu, D. H.; Yun, J. Kinetic Resolution and Dynamic Kinetic Resolution of γ-Aryl-Substituted Butenolides via Copper-Catalyzed 1,4-Hydroboration. *Adv. Synth. Catal.* **2021**, *363*, 2377–2381.

(24) D'Accriscio, F.; Ohleier, A.; Nocolas, E.; Demange, M.; Du Boullay, O. T.; Saffon-Merceron, N.; Fustier-Boutignon, M.; Rezabal, E.; Frison, G.; Nebra, N.; Mézailles. [(dcpp)Ni(η^2-Arene)] Precursors: Synthesis, Reactivity, and Catalytic Application to the Suzuki-Miyaura Reaction. *Organometallics*, **2020**, *39*, 1688–1699.

(25) Cristau, H. J.; Vogel, R.; Taillefer, M.; Gadras, A. A Novel and Efficient Arylation of Malonitrile Catalyzed by Nickel(0) Complexes. *Tetrahedron Lett.* **2000**, *41*, 8457–8460.

(26) Mills, L. R.; Edjoc, R. K.; Rousseaux, S. A. L. Design of an Electron-Withdrawing Benzonitrile Ligand for Ni-Catalyzed Cross-Coupling Involving Tertiary Nucleophiles. *J.*

Am. Chem. Soc. **2021**, *143*, 10422–10428.

(27) Spielvogel, D. J.; Davis, W. M.; Buchwald, S. L. Preparation, Crystal Structure Analysis, and Catalytic Application of [(*S*)-BINAP]Ni(COD) and [(*S*)-BINAP]$NiBr_2$. *Organometallics*, **2002**, *21*, 3833–3836.

(28) Yamamoto, T.; Yamakawa, T. Nickel-Catalyzed Vinylation of Aryl Chlorides and Bromides with Vinyl ZnBr•MgBrCl. *J. Org. Chem.* **2009**, *74*, 3603–3605.

(29) Anker, T.; Cosner, C. C.; Helquist, P. Palladium- and Nickel-Catalyzed Alkenylation of Enolates. *Chem. Eur. J.* **2013**, *19*, 1858–1871.

(30) Huang, J.; Bunel, E.; Faul, M. M. Palladium-Catalyzed α-Vinylation of Carbonyl Compounds. *Org. Lett.* **2007**, *9*, 4343–4346.

(31) Grigalunas, M.; Anker, T.; Norrby, P.-O.; Wiest, O.; Helquist, P. Palladium-Catalyzed Alkenylation of Ketone Enolates under Mild Conditions. *Org. Lett.* **2014**, *16*, 3970–3973.

(32) Johansson, C. C. C.; Colacot, T. J. Metal-Catalyzed α-Arylation of Carbonyl and Related Molecules: Novel Trends in C-C Bond Formation by C-H Bond Functionalization. *Angew. Chem. Int. Ed.* **2010**, *49*, 676–707.

(33) Jiang, L.; Weist, S.; Jansat, S. Diastereoselective Room-Temperature Pd-Catalyzed α-Arylation and Vinylation of Arylmandelic Acid Derivatives. *Org. Lett.* **2009**, *11*, 1543–1546.

(34) Cosner, C. C.; Helquist, P. Concise, Convergent Syntheses of (±)-Trichostatin A Utilizing a Pd-Catalyzed Ketone Enolate α-Alkenylation Reaction. *Org. Lett.* **2011**, *13*, 3564–3567.

(35) Deutsch, C.; Krause, N.; Lipshutz, B. H. CuH-Catalyzed Reactions. *Chem. Rev.*

2008, *108*, 2916–2927.

(36) Friis, S.; Pirnot, M. T.; Buchwald, S. L. Asymmetric Hydroarylation of Vinylarenes Using a Synergistic Combination of CuH and Pd Catalysis. *J. Am. Chem. Soc.* **2016**, *138*, 8372–8375.

(37) Knippel, J. L.; Ni, A. Z.; Schuppe, A. W.; Buchwald, S. L. Dual Strategy for the Asymmetric Preparation of α-Stereogenic Silanes, Germanes, and Boronate Esters via Dual Copper Hydride- and Palladium-Catalysis. *Angew. Chem. Int. Ed.* **2022**, *61*, e202212630.

(38) Schuppe, A. W.; Borrajo-Calleja, G. M.; Buchwald, S. L. Enantioselective Olefin Hydrocyanation without Cyanide. *J. Am. Chem. Soc.* **2019**, *141*, 18668–18672.

(39) Schuppe, A. W.; Knippel, J. L.; Borrajo-Calleja, G. M.; Buchwald, S. L. Enantioselective Hydroalkenylation of Olefins with Enol Sulfonates Enabled by Dual Copper Hydride and Palladium Catalysis. *J. Am. Chem. Soc.* **2021**, *143*, 5330–5335.

(40) Chae, J.; Yun, J.; Buchwald, S. L. One-Pot Sequential Cu-Catalyzed Reduction and Pd-Catalyzed Arylation of Silyl Enol Ethers. *Org. Lett.* **2004**, *6*, 4809–4812.

(41) Grigalunas, M.; Anker, T.; Norrby, P.-O.; Wiest, O.; Helquist, P. Ni-Catalyzed Alkenylation of Ketone Enolates under Mild Conditions: Catalyst Identification and Optimization. *J. Am. Chem. Soc.* **2015**, *137*, 7019–7022.

(42) Li, M.; Wang, J. Nickel-Catalyzed Enantioselective C(sp^3)-H Arylation of Ketones with Aryl Ethers via Selective C_{Ar}-O Cleavage to Construct All-Carbon Quaternary Stereocenters. *CCS Chem.* **2022**, *4*, 2921–2929.

(43) Ge, S.; Hartwig, J. F. Nickel-Catalyzed Asymmetric α-Arylation and Heteroarylation of Ketones with Chloroarenes: Effect of Halide on Selectivity, Oxidation

State, and Room-Temperature Reactions. *J. Am. Chem. Soc.* **2011**, *133*, 41, 16330–16333.

(44) Spielvogel, D. J.; Buchwald, S. L. Nickel-BINAP Catalyzed Enantioselective α-Arylation of α-Substituted γ-Butyrolactones. *J. Am. Chem. Soc.* **2002**, *124*, 3500–3501.

(45) Yu, D.; Wang, C.-S.; Yao, C.; Shen, Q.; Lu, L. Nickel-Catalyzed α-Arylation of Zinc Enolates with Polyfluoroarenes via C–F Bond Activation under Neutral Conditions. *Org. Lett.* **2014**, *16*, 5544–5547.

(46) Millar, A. A.; Rathke, M. W. A Nickel Catalyst for the Arylation and Vinylation of Lithium Ester Enolates. *J. Am. Chem. Soc.* **1977**, *99*, 4833–4835.

(47) Semmelhack, M. F.; Stauffer, R. D.; Rogerson, T. D. Nucleophilic Aromatic Substitution via a New Nickel-Catalyzed Process and via the $S_{RN}1$ Reaction, Improved Synthesis of Cephalotaxinone. *Tetrahedron Lett.* **1973**, *45*, 4519–4522.

(48) Semmelhack, M. F.; Chong, B. P.; Stauffer, R. D.; Rogerson, T. D.; Chong, A.; Jones, L. D. Total Synthesis of the *Cephalotaxus* Alkaloids. A Problem in Nucleophilic Aromatic Substitution. *J. Am. Chem. Soc.* **1975**, *97*, 2507–2516.

(49) Wender, P. A.; Wolanin, D. J. Total Synthesis of Quadrone and Terrecyclic Acid A. *J. Am. Chem. Soc.* **1985**, *50*, 4418–4420.

(50) You, T.; Li, J. Ni(COD)(Duroquinone)-Catalyzed C-N Cross-Coupling for the Synthesis of *N,N*-Diarylsulfonamides. *Org. Lett.* **2022**, *24*, 6642–6646.

(51) Bismuto, A.; Delcaillau, T.; Müller, P.; Morandi, B. Nickel-Catalyzed Amination of Aryl Thioethers: A Combined Synthetic and Mechanistic Study. *ACS Catal.* **2020**, *10*, 4630.

(52) Ge, S.; Green, R. A.; Hartwig, J. F. Controlling First-Row Catalysts: Amination of Aryl and Heteroaryl Chlorides and Bromides with Primary Aliphatic Amines Catalyzed by

a BINAP-Ligated Single-Component Ni(0) Complex. *J. Am. Chem. Soc.* **2014**, *136*, 1617–1627.

(53) Fujihara, T.; Nogi, K.; Xu, T.; Terao, J.; Tsuji, Y. Nickel-Catalyzed Carboxylation of Aryl and Vinyl Chlorides Employing Carbon Dioxide. *J. Am. Chem. Soc.* **2012**, *134*, 9106–9109.

(54) Huang, D.; Szewczyk, S. M.; Zhang, P.; Newhouse, T. R. Allyl-Nickel Catalysis Enables Carbonyl Dehydrogation and Oxidative Cycloalkenylation of Ketones. *J. Am. Chem. Soc.* **2019**, *141*, 5669.

(55) Bodnar, A. K.; Szewczyk, S. M.; Sun, Y.; Chen, Y.; Huang, A. X.; Newhouse, T. R. Comprehensive Mechanistic Analysis of Palladium- and Nickel-Catalyzed α,β-Dehydrogenation of Carbonyls via Organozinc Intermediates. *J. Org. Chem.* **2024**, *89*, 3123.

(56) Zhang, L.; Zhao, M.; Pu, M.; Ma, Z.; Zhou, J.; Chen, C.; Wu, Y.-D.; Chi, Y. R.; Zhou, J. S. Nickel-Catalyzed Enantioselective Reductive Conjugate Arylation and Heteroarylation via an Elementary Mechanism of 1,4-Addition. *J. Am. Chem. Soc.* **2022**, *144*, 20249.

(57) Zhang, X.; Tutkowski, B.; Oliver, A.; Helquist, P.; Wiest, O. Mechanistic Study of the Nickel-Catalyzed α,β-Coupling of Saturated Ketones. *ACS Catal.* **2018**, *8*, 1740–1747.

(58) Lutz, S.; Nattmann, L.; Nöthling, N.; Cornella, J. 16-Electron Nickel(0)-Olefin Complexes in Low-Temperature $C(sp^2)$-$C(sp^3)$ Kumada Cross-Couplings. *Organometallics*, **2021**, *40*, 2220–2230.

(59) Poisson, P.-A.; Tran, G.; Besnard, C.; Mazet, C. Nickel-Catalyzed Kumada Vinylation of Enol Phosphates: A Comparative Mechanistic Study. *ACS Catal.* **2021**, *11*,

15041–15050.

(60) Li, Z.-Q.; Cao, Y.; Kang, T.; Engle, K. M. Electrophilic Sulfur Reagent Design Enables Directed *syn*-Carbosulfenylation of Unactivated Alkenes. *J. Am. Chem. Soc.* **2022**, *144*, 7189–7197.

(61) Rubel, C. Z.; He, W.-J.; Wisniewski, S. R.; Engle, K. E. Benchtop Nickel Catalysis Invigorated by Electron-Deficient Diene Ligands. *Acc. Chem. Res.* **2024***,* 57*,* 312–326.

(62) Tyerman, S.; Robertson, C.; Murphy, J. Radical Coupling of Aryl Halides to Arenes Facilitated by Ni(COD)(DQ) and Other Nickel Sources. *Org. Biomol. Chem.* **2024**, *22*, 1023–1026.

(63) Estrada, J. G.; Williams, W. L.; Ting, S. I.; Doyl, A. G. Role of Electron-Deficient Olefin Ligands in a Ni-Catalyzed Aziridine Cross-Coupling to Generate Quaternary Carbons. *J. Am. Chem. Soc.* **2020**, *142*, 8928–8937.

(64) Mills, L. R.; Edjoc, R. K.; Rousseaux, S. A. L. Design of an Electron-Withdrawing Benzonitrile Ligand for Ni-Catalyzed Cross-Coupling Involving Tertiary Nucleophiles. *J. Am. Chem. Soc.* **2021**, *143*, 10422–10428.

(65) Nattmann, L.; Cornella, J. Ni($^{4\text{-}t\text{Bu}}$stb)$_3$: A Robust 16-Electron Ni(0) Olefin Complex for Catalysis. *Organometallics*, **2020**, *39*, 3295–3300.

(66) Fischer, K.; Jonas, K.; Wilke, G. Tris(ethylene)nickel(0). *Angew. Chem. Int. Ed. Engl.* **1973**, *12*, 565–566.

(67) Blum, K.; Chernyshova, E. S.; Goddard, R.; Jonas, K.; Pörschke, K.-R. 4,9-Diazododeca-1,trans-6,11-trienes as Ligands for Nickel(0), Palladium(0), and Platinum(0). *Organometallics,* **2007**, *26*, 5174–5178.

(68) Guard, L. M.; Beromi, M.; Brudvig, G. W.; Hazari, N.; Vinyard. D. J. Comparison

of dppf-Supported Nickel Precatalysts for the Suzuki-Miyaura Reaction: The Observation and Activity of Nickel(I). *Angew. Chem. Int. Ed.* **2015**, *54*, 13352–13356.

(69) Liang, H.; Borys, A.; Hevia, E.; Perrin, M.-E.; Payard, P.-A. Shedding Light on the Hidden Roles of Lithium in the Nickel-Catalyzed Cross-Coupling of Aryl Ethers. *J. Am. Chem. Soc.* **2023**, *145*, 19989–19999.

(70) Chen, G.; Kwong, F. Y.; Chan, H. O.; Yu, W.-Y.; Chan, A. S. C. Nickel-Catalyzed Asymmetric α-Arylation of Ketone Enolates. *Chem. Commun.* **2006**, 1413–1415.

(71) Nett, A. J.; Cańellas, S.; Higuchi, Y.; Robo, M. T.; Kochkodan, J. M.; Haynes, II, M. T.; Kampf, J. W.; Montgomery, J. Stable, Well-Defined Nickel(0) Catalysts for Catalytic C-C and C-N Bond Formation. *ACS Catal.* **2018**, *8*, 6606–6611.

(72) Tran, V. T.; Kim, N.; Rubel, C. Z.; Wu, X.; Kang, T.; Jankins, T. C.; Li, Z.-Q.; Joannou, M. V.; Ayers, S.; Gembicky, M.; Bailey, J.; Sturgell, E. J.; Sanchez, B. B.; Chen, J. S.; Lin, S.; Eastgate, M. D.; Wisniewski, S. R.; Engle, K. M. Structurally Diverse Bench-Stable Nickel(0) Pre-Catalysts: A Practical Toolkit for In Situ Ligation Protocols. *Angew. Chem. Int. Ed.* **2023**, *62*, e202211794.

(73) Shields, J. D.; Gray, E. E.; Doyle, A. G. A Modular, Air-Stable Nickel Precatalyst. *Org. Lett.* **2015**, *17*, 2166–2169.

(74) Standley, E. A.; Jamison, T. F. Simplifying Nickel(0) Catalysis: An Air-Stable Nickel Precatalyst for the Internally Selective Benzylation of Terminal Alkenes. *J. Am. Chem. Soc.* **2013**, *135*, 1585–1592.

(75) Kim, N.; Tran, V. T.; Apolinar, O.; Wisniewski, S. R.; Eastegate, M. D.; Engle, K. M. Ni(COD)(DMFU): A Heteroleptic 16-Electron Precatalyst for 1,2-Diarylation of Alkenes. *Synlett.* **2021**, *62*, e202211794.

(76) Derosa, J.; Kleinmans, R.; Tran, V. T.; Karunananda, M. K.; Wisniewski, S. R.; Eastgate, M. D.; Engle, K. M. Nickel-Catalyzed 1,2-Diarylation of Simple Alkenyl Amides. *J. Am. Chem. Soc.* **2018**, *140*, 17878–17883.

(77) Hartwig, J. F. (2010). *Organotransition Metal Chemistry: From Bonding to Catalysis*. University Science Books.

Appendix 5

Supporting Information Relevant to Chapter 5:

Development of a vinylogous Mukaiyama Aldol fragment coupling reaction and Intramolecular Ni-catalyzed α-enolate alkenylation

X-Ray Crystallography Data

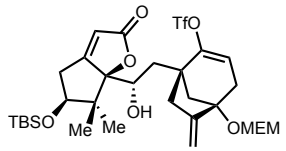

106A

Table A5.1. Crystal data and structure refinement for 106A (V22432).

Identification code	V22432	
Empirical formula	C31 H47 F3 O10 S Si	
Formula weight	696.83	
Temperature	100(2) K	
Wavelength	1.54178 Å	
Crystal system	Orthorhombic	
Space group	$P2_12_12_1$	
Unit cell dimensions	a = 7.5072(7) Å	a= 90°.
	b = 17.6749(18) Å	b= 90°.
	c = 26.655(3) Å	g = 90°.
Volume	3536.8(6) $Å^3$	
Z	4	
Density (calculated)	1.309 Mg/m^3	
Absorption coefficient	1.729 mm^{-1}	
F(000)	1480	
Crystal size	0.400 x 0.200 x 0.100 mm^3	
Theta range for data collection	3.000 to 74.561°.	
Index ranges	-9<=h<=9, -22<=k<=22, -33<=l<=33	
Reflections collected	48096	
Independent reflections	7212 [R(int) = 0.0467]	
Completeness to theta = 67.679°	100.0 %	
Absorption correction	Semi-empirical from equivalents	
Max. and min. transmission	0.7538 and 0.4186	
Refinement method	Full-matrix least-squares on F^2	
Data / restraints / parameters	7212 / 1 / 426	
Goodness-of-fit on F^2	1.023	
Final R indices [I>2sigma(I)]	R1 = 0.0303, wR2 = 0.0837	
R indices (all data)	R1 = 0.0305, wR2 = 0.0839	

Absolute structure parameter	0.007(6)
Extinction coefficient	n/a
Largest diff. peak and hole	0.578 and -0.302 e.Å^{-3}

Table A5.2. Atomic coordinates (x 10^4) and equivalent isotropic displacement parameters (Å^{2}x 10^3) for V22432. U(eq) is defined as one third of the trace of the orthogonalized U^{ij} tensor.

	x	y	z	U(eq)
C(1)	9557(4)	8019(1)	4588(1)	34(1)
F(1)	10162(2)	8594(1)	4856(1)	39(1)
F(2)	10882(3)	7716(2)	4340(1)	79(1)
F(3)	8882(4)	7516(1)	4885(1)	75(1)
S(1)	7885(1)	8378(1)	4151(1)	25(1)
O(1)	6534(3)	8689(2)	4449(1)	66(1)
O(2)	8748(4)	8822(1)	3792(1)	62(1)
O(3)	7343(2)	7588(1)	3942(1)	18(1)
C(2)	6448(3)	7535(1)	3465(1)	15(1)
C(3)	4918(3)	7891(1)	3394(1)	18(1)
C(4)	4008(3)	7867(1)	2888(1)	18(1)
C(5)	5258(3)	7531(1)	2490(1)	14(1)
O(4)	4460(2)	7448(1)	2006(1)	17(1)
C(11)	2606(3)	7346(1)	1972(1)	18(1)
O(5)	1980(2)	6677(1)	2194(1)	17(1)
C(12)	2414(3)	6013(1)	1913(1)	20(1)
C(13)	1485(3)	5344(1)	2141(1)	20(1)
O(6)	-390(2)	5435(1)	2092(1)	23(1)
C(14)	-1316(3)	4779(1)	2248(1)	25(1)
C(6)	6050(3)	6791(1)	2699(1)	12(1)
C(7)	7455(2)	7095(1)	3070(1)	12(1)
C(15)	8760(3)	6503(1)	3274(1)	13(1)

C(16)	7863(2)	5813(1)	3514(1)	12(1)
O(7)	6529(2)	6034(1)	3864(1)	15(1)
C(17)	9224(2)	5305(1)	3792(1)	11(1)
O(8)	10667(2)	5179(1)	3441(1)	12(1)
C(18)	12169(3)	5508(1)	3625(1)	14(1)
O(9)	13540(2)	5503(1)	3386(1)	20(1)
C(19)	11813(3)	5800(1)	4132(1)	16(1)
C(20)	10106(3)	5664(1)	4236(1)	13(1)
C(21)	8992(3)	5571(1)	4692(1)	17(1)
C(22)	7806(3)	4873(1)	4558(1)	14(1)
O(10)	7950(2)	4291(1)	4920(1)	18(1)
Si(1)	6887(1)	4231(1)	5463(1)	16(1)
C(24)	4432(3)	4301(2)	5353(1)	30(1)
C(25)	7591(4)	5000(1)	5898(1)	30(1)
C(26)	7594(3)	3275(1)	5702(1)	19(1)
C(27)	7163(3)	2669(1)	5308(1)	23(1)
C(28)	6594(4)	3083(1)	6191(1)	30(1)
C(29)	9610(3)	3277(1)	5801(1)	28(1)
C(23)	8453(3)	4571(1)	4036(1)	12(1)
C(30)	6931(3)	4196(1)	3746(1)	17(1)
C(31)	9960(3)	3993(1)	4107(1)	17(1)
C(8)	8418(3)	7686(1)	2733(1)	15(1)
C(9)	6918(3)	8029(1)	2430(1)	14(1)
C(10)	6987(3)	8645(1)	2146(1)	20(1)

Table A5.3. Bond lengths [Å] and angles [°] for V22432.

C(1)-F(3)	1.295(3)
C(1)-F(2)	1.309(4)
C(1)-F(1)	1.323(3)
C(1)-S(1)	1.825(3)
S(1)-O(2)	1.398(2)
S(1)-O(1)	1.400(2)
S(1)-O(3)	1.5576(15)
O(3)-C(2)	1.442(2)
C(2)-C(3)	1.323(3)
C(2)-C(7)	1.511(3)
C(3)-C(4)	1.513(3)
C(3)-H(3)	0.9500
C(4)-C(5)	1.536(3)
C(4)-H(4A)	0.9900
C(4)-H(4B)	0.9900
C(5)-O(4)	1.431(2)
C(5)-C(9)	1.535(3)
C(5)-C(6)	1.540(3)
O(4)-C(11)	1.407(2)
C(11)-O(5)	1.403(2)
C(11)-H(11A)	0.9900
C(11)-H(11B)	0.9900
O(5)-C(12)	1.431(3)
C(12)-C(13)	1.501(3)
C(12)-H(12A)	0.9900
C(12)-H(12B)	0.9900
C(13)-O(6)	1.423(3)
C(13)-H(13A)	0.9900
C(13)-H(13B)	0.9900
O(6)-C(14)	1.415(3)
C(14)-H(14A)	0.9800
C(14)-H(14B)	0.9800

C(14)-H(14C)	0.9800
C(6)-C(7)	1.544(3)
C(6)-H(6A)	0.9900
C(6)-H(6B)	0.9900
C(7)-C(15)	1.532(3)
C(7)-C(8)	1.556(3)
C(15)-C(16)	1.533(3)
C(15)-H(15A)	0.9900
C(15)-H(15B)	0.9900
C(16)-O(7)	1.423(2)
C(16)-C(17)	1.549(2)
C(16)-H(16)	1.0000
O(7)-H(7O)	0.82(2)
C(17)-O(8)	1.449(2)
C(17)-C(20)	1.498(3)
C(17)-C(23)	1.563(2)
O(8)-C(18)	1.361(2)
C(18)-O(9)	1.210(3)
C(18)-C(19)	1.472(3)
C(19)-C(20)	1.333(3)
C(19)-H(19)	0.9500
C(20)-C(21)	1.483(3)
C(21)-C(22)	1.563(3)
C(21)-H(21A)	0.9900
C(21)-H(21B)	0.9900
C(22)-O(10)	1.415(2)
C(22)-C(23)	1.569(3)
C(22)-H(22)	1.0000
O(10)-Si(1)	1.6542(14)
Si(1)-C(25)	1.864(2)
Si(1)-C(24)	1.870(2)
Si(1)-C(26)	1.883(2)
C(24)-H(24A)	0.9800
C(24)-H(24B)	0.9800

C(24)-H(24C)	0.9800
C(25)-H(25A)	0.9800
C(25)-H(25B)	0.9800
C(25)-H(25C)	0.9800
C(26)-C(27)	1.533(3)
C(26)-C(29)	1.536(3)
C(26)-C(28)	1.542(3)
C(27)-H(27A)	0.9800
C(27)-H(27B)	0.9800
C(27)-H(27C)	0.9800
C(28)-H(28A)	0.9800
C(28)-H(28B)	0.9800
C(28)-H(28C)	0.9800
C(29)-H(29A)	0.9800
C(29)-H(29B)	0.9800
C(29)-H(29C)	0.9800
C(23)-C(30)	1.530(3)
C(23)-C(31)	1.536(3)
C(30)-H(30A)	0.9800
C(30)-H(30B)	0.9800
C(30)-H(30C)	0.9800
C(31)-H(31A)	0.9800
C(31)-H(31B)	0.9800
C(31)-H(31C)	0.9800
C(8)-C(9)	1.513(3)
C(8)-H(8A)	0.9900
C(8)-H(8B)	0.9900
C(9)-C(10)	1.326(3)
C(10)-H(10A)	0.9500
C(10)-H(10B)	0.9500

F(3)-C(1)-F(2)	109.0(3)
F(3)-C(1)-F(1)	109.4(2)
F(2)-C(1)-F(1)	109.0(2)

F(3)-C(1)-S(1)	111.1(2)
F(2)-C(1)-S(1)	110.1(2)
F(1)-C(1)-S(1)	108.25(18)
O(2)-S(1)-O(1)	120.23(19)
O(2)-S(1)-O(3)	112.30(11)
O(1)-S(1)-O(3)	111.47(13)
O(2)-S(1)-C(1)	108.23(16)
O(1)-S(1)-C(1)	105.87(15)
O(3)-S(1)-C(1)	95.51(10)
C(2)-O(3)-S(1)	119.66(13)
C(3)-C(2)-O(3)	119.98(18)
C(3)-C(2)-C(7)	125.46(18)
O(3)-C(2)-C(7)	114.46(16)
C(2)-C(3)-C(4)	120.38(18)
C(2)-C(3)-H(3)	119.8
C(4)-C(3)-H(3)	119.8
C(3)-C(4)-C(5)	110.55(16)
C(3)-C(4)-H(4A)	109.5
C(5)-C(4)-H(4A)	109.5
C(3)-C(4)-H(4B)	109.5
C(5)-C(4)-H(4B)	109.5
H(4A)-C(4)-H(4B)	108.1
O(4)-C(5)-C(9)	107.68(15)
O(4)-C(5)-C(4)	114.05(16)
C(9)-C(5)-C(4)	110.25(16)
O(4)-C(5)-C(6)	113.63(16)
C(9)-C(5)-C(6)	102.20(15)
C(4)-C(5)-C(6)	108.37(16)
C(11)-O(4)-C(5)	118.96(15)
O(5)-C(11)-O(4)	114.38(17)
O(5)-C(11)-H(11A)	108.7
O(4)-C(11)-H(11A)	108.7
O(5)-C(11)-H(11B)	108.7
O(4)-C(11)-H(11B)	108.7

H(11A)-C(11)-H(11B)	107.6
C(11)-O(5)-C(12)	113.18(15)
O(5)-C(12)-C(13)	109.14(16)
O(5)-C(12)-H(12A)	109.9
C(13)-C(12)-H(12A)	109.9
O(5)-C(12)-H(12B)	109.9
C(13)-C(12)-H(12B)	109.9
H(12A)-C(12)-H(12B)	108.3
O(6)-C(13)-C(12)	109.43(17)
O(6)-C(13)-H(13A)	109.8
C(12)-C(13)-H(13A)	109.8
O(6)-C(13)-H(13B)	109.8
C(12)-C(13)-H(13B)	109.8
H(13A)-C(13)-H(13B)	108.2
C(14)-O(6)-C(13)	111.42(18)
O(6)-C(14)-H(14A)	109.5
O(6)-C(14)-H(14B)	109.5
H(14A)-C(14)-H(14B)	109.5
O(6)-C(14)-H(14C)	109.5
H(14A)-C(14)-H(14C)	109.5
H(14B)-C(14)-H(14C)	109.5
C(5)-C(6)-C(7)	101.54(15)
C(5)-C(6)-H(6A)	111.5
C(7)-C(6)-H(6A)	111.5
C(5)-C(6)-H(6B)	111.5
C(7)-C(6)-H(6B)	111.5
H(6A)-C(6)-H(6B)	109.3
C(2)-C(7)-C(15)	115.13(16)
C(2)-C(7)-C(6)	106.48(15)
C(15)-C(7)-C(6)	115.20(16)
C(2)-C(7)-C(8)	106.83(16)
C(15)-C(7)-C(8)	111.46(15)
C(6)-C(7)-C(8)	100.43(14)
C(7)-C(15)-C(16)	114.21(16)

C(7)-C(15)-H(15A)	108.7
C(16)-C(15)-H(15A)	108.7
C(7)-C(15)-H(15B)	108.7
C(16)-C(15)-H(15B)	108.7
H(15A)-C(15)-H(15B)	107.6
O(7)-C(16)-C(15)	111.35(15)
O(7)-C(16)-C(17)	108.01(14)
C(15)-C(16)-C(17)	111.78(15)
O(7)-C(16)-H(16)	108.5
C(15)-C(16)-H(16)	108.5
C(17)-C(16)-H(16)	108.5
C(16)-O(7)-H(7O)	109(2)
O(8)-C(17)-C(20)	104.19(14)
O(8)-C(17)-C(16)	105.86(14)
C(20)-C(17)-C(16)	115.12(15)
O(8)-C(17)-C(23)	114.69(14)
C(20)-C(17)-C(23)	100.74(15)
C(16)-C(17)-C(23)	115.88(15)
C(18)-O(8)-C(17)	108.73(14)
O(9)-C(18)-O(8)	120.77(18)
O(9)-C(18)-C(19)	129.84(19)
O(8)-C(18)-C(19)	109.32(16)
C(20)-C(19)-C(18)	107.61(17)
C(20)-C(19)-H(19)	126.2
C(18)-C(19)-H(19)	126.2
C(19)-C(20)-C(21)	137.07(19)
C(19)-C(20)-C(17)	109.68(17)
C(21)-C(20)-C(17)	110.57(16)
C(20)-C(21)-C(22)	102.81(15)
C(20)-C(21)-H(21A)	111.2
C(22)-C(21)-H(21A)	111.2
C(20)-C(21)-H(21B)	111.2
C(22)-C(21)-H(21B)	111.2
H(21A)-C(21)-H(21B)	109.1

O(10)-C(22)-C(21)	112.03(16)
O(10)-C(22)-C(23)	109.50(15)
C(21)-C(22)-C(23)	107.17(15)
O(10)-C(22)-H(22)	109.4
C(21)-C(22)-H(22)	109.4
C(23)-C(22)-H(22)	109.4
C(22)-O(10)-Si(1)	127.29(13)
O(10)-Si(1)-C(25)	111.11(10)
O(10)-Si(1)-C(24)	109.56(10)
C(25)-Si(1)-C(24)	109.20(13)
O(10)-Si(1)-C(26)	102.55(9)
C(25)-Si(1)-C(26)	111.34(11)
C(24)-Si(1)-C(26)	112.95(11)
Si(1)-C(24)-H(24A)	109.5
Si(1)-C(24)-H(24B)	109.5
H(24A)-C(24)-H(24B)	109.5
Si(1)-C(24)-H(24C)	109.5
H(24A)-C(24)-H(24C)	109.5
H(24B)-C(24)-H(24C)	109.5
Si(1)-C(25)-H(25A)	109.5
Si(1)-C(25)-H(25B)	109.5
H(25A)-C(25)-H(25B)	109.5
Si(1)-C(25)-H(25C)	109.5
H(25A)-C(25)-H(25C)	109.5
H(25B)-C(25)-H(25C)	109.5
C(27)-C(26)-C(29)	109.07(19)
C(27)-C(26)-C(28)	108.78(19)
C(29)-C(26)-C(28)	109.53(19)
C(27)-C(26)-Si(1)	109.67(15)
C(29)-C(26)-Si(1)	109.51(16)
C(28)-C(26)-Si(1)	110.26(15)
C(26)-C(27)-H(27A)	109.5
C(26)-C(27)-H(27B)	109.5
H(27A)-C(27)-H(27B)	109.5

C(26)-C(27)-H(27C)	109.5
H(27A)-C(27)-H(27C)	109.5
H(27B)-C(27)-H(27C)	109.5
C(26)-C(28)-H(28A)	109.5
C(26)-C(28)-H(28B)	109.5
H(28A)-C(28)-H(28B)	109.5
C(26)-C(28)-H(28C)	109.5
H(28A)-C(28)-H(28C)	109.5
H(28B)-C(28)-H(28C)	109.5
C(26)-C(29)-H(29A)	109.5
C(26)-C(29)-H(29B)	109.5
H(29A)-C(29)-H(29B)	109.5
C(26)-C(29)-H(29C)	109.5
H(29A)-C(29)-H(29C)	109.5
H(29B)-C(29)-H(29C)	109.5
C(30)-C(23)-C(31)	108.91(16)
C(30)-C(23)-C(17)	115.24(15)
C(31)-C(23)-C(17)	109.34(15)
C(30)-C(23)-C(22)	111.37(16)
C(31)-C(23)-C(22)	110.21(15)
C(17)-C(23)-C(22)	101.57(14)
C(23)-C(30)-H(30A)	109.5
C(23)-C(30)-H(30B)	109.5
H(30A)-C(30)-H(30B)	109.5
C(23)-C(30)-H(30C)	109.5
H(30A)-C(30)-H(30C)	109.5
H(30B)-C(30)-H(30C)	109.5
C(23)-C(31)-H(31A)	109.5
C(23)-C(31)-H(31B)	109.5
H(31A)-C(31)-H(31B)	109.5
C(23)-C(31)-H(31C)	109.5
H(31A)-C(31)-H(31C)	109.5
H(31B)-C(31)-H(31C)	109.5
C(9)-C(8)-C(7)	103.39(15)

C(9)-C(8)-H(8A)	111.1
C(7)-C(8)-H(8A)	111.1
C(9)-C(8)-H(8B)	111.1
C(7)-C(8)-H(8B)	111.1
H(8A)-C(8)-H(8B)	109.0
C(10)-C(9)-C(8)	127.2(2)
C(10)-C(9)-C(5)	124.21(19)
C(8)-C(9)-C(5)	108.60(16)
C(9)-C(10)-H(10A)	120.0
C(9)-C(10)-H(10B)	120.0
H(10A)-C(10)-H(10B)	120.0

Symmetry transformations used to generate equivalent atoms:

Table A5.4. Anisotropic displacement parameters ($Å^2 x\ 10^3$) for V22432. The anisotropic displacement factor exponent takes the form: $-2p^2[\ h^2\ a^{*2}U^{11} + ...\ + 2\ h\ k\ a^*\ b^*\ U^{12}\ ]$

	U^{11}	U^{22}	U^{33}	U^{23}	U^{13}	U^{12}
C(1)	39(1)	26(1)	36(1)	-5(1)	-18(1)	-3(1)
F(1)	49(1)	34(1)	35(1)	-7(1)	-18(1)	-14(1)
F(2)	39(1)	90(2)	110(2)	-59(2)	-37(1)	31(1)
F(3)	128(2)	46(1)	50(1)	25(1)	-54(1)	-44(1)
S(1)	32(1)	18(1)	25(1)	-5(1)	-8(1)	2(1)
O(1)	45(1)	71(2)	82(2)	-55(2)	-11(1)	21(1)
O(2)	113(2)	38(1)	33(1)	12(1)	-24(1)	-43(1)
O(3)	22(1)	18(1)	16(1)	-2(1)	-4(1)	0(1)
C(2)	14(1)	16(1)	14(1)	1(1)	-1(1)	-1(1)
C(3)	16(1)	20(1)	18(1)	-1(1)	3(1)	4(1)
C(4)	11(1)	22(1)	20(1)	1(1)	-1(1)	4(1)
C(5)	10(1)	15(1)	15(1)	1(1)	-2(1)	1(1)
O(4)	11(1)	23(1)	16(1)	4(1)	-2(1)	-2(1)
C(11)	13(1)	19(1)	22(1)	6(1)	-3(1)	-2(1)
O(5)	15(1)	17(1)	20(1)	1(1)	2(1)	-3(1)
C(12)	19(1)	22(1)	18(1)	-2(1)	3(1)	-2(1)
C(13)	21(1)	20(1)	19(1)	0(1)	-2(1)	0(1)
O(6)	20(1)	20(1)	28(1)	4(1)	-3(1)	-6(1)
C(14)	26(1)	23(1)	25(1)	0(1)	1(1)	-9(1)
C(6)	10(1)	13(1)	14(1)	1(1)	0(1)	0(1)
C(7)	7(1)	13(1)	16(1)	1(1)	1(1)	-1(1)
C(15)	8(1)	15(1)	17(1)	4(1)	0(1)	0(1)
C(16)	8(1)	14(1)	13(1)	1(1)	0(1)	0(1)
O(7)	7(1)	18(1)	20(1)	1(1)	3(1)	2(1)
C(17)	7(1)	12(1)	13(1)	0(1)	1(1)	0(1)

O(8)	7(1)	15(1)	14(1)	0(1)	1(1)	1(1)
C(18)	10(1)	15(1)	18(1)	4(1)	-2(1)	1(1)
O(9)	10(1)	27(1)	24(1)	4(1)	2(1)	0(1)
C(19)	14(1)	18(1)	17(1)	1(1)	-5(1)	-3(1)
C(20)	14(1)	12(1)	14(1)	1(1)	-2(1)	1(1)
C(21)	19(1)	19(1)	14(1)	-2(1)	1(1)	-5(1)
C(22)	13(1)	15(1)	12(1)	2(1)	2(1)	0(1)
O(10)	20(1)	20(1)	14(1)	5(1)	3(1)	0(1)
Si(1)	16(1)	18(1)	14(1)	2(1)	3(1)	-1(1)
C(24)	17(1)	37(1)	37(1)	9(1)	3(1)	2(1)
C(25)	43(1)	25(1)	21(1)	-3(1)	6(1)	-3(1)
C(26)	21(1)	20(1)	16(1)	3(1)	2(1)	-2(1)
C(27)	22(1)	20(1)	28(1)	-1(1)	4(1)	-4(1)
C(28)	41(2)	27(1)	23(1)	9(1)	13(1)	2(1)
C(29)	26(1)	31(1)	26(1)	3(1)	-7(1)	1(1)
C(23)	11(1)	12(1)	13(1)	1(1)	0(1)	-2(1)
C(30)	16(1)	15(1)	19(1)	0(1)	-1(1)	-4(1)
C(31)	17(1)	16(1)	19(1)	4(1)	2(1)	3(1)
C(8)	10(1)	15(1)	19(1)	3(1)	0(1)	-2(1)
C(9)	13(1)	15(1)	15(1)	-1(1)	-1(1)	0(1)
C(10)	20(1)	19(1)	22(1)	5(1)	-3(1)	-3(1)

Table A5.5. Hydrogen coordinates (x 10^4) and isotropic displacement parameters ($Å^2$x 10^3) for V22432.

	x	y	z	U(eq)
H(3)	4388	8162	3663	21
H(4A)	3659	8386	2788	21
H(4B)	2914	7557	2911	21
H(11A)	2010	7781	2134	22
H(11B)	2261	7346	1614	22
H(12A)	3718	5931	1917	24
H(12B)	2031	6076	1560	24
H(13A)	1866	4874	1970	24
H(13B)	1806	5301	2500	24
H(14A)	-1004	4355	2028	37
H(14B)	-2601	4871	2231	37
H(14C)	-982	4656	2594	37
H(6A)	6606	6485	2430	15
H(6B)	5135	6484	2872	15
H(15A)	9537	6747	3527	16
H(15B)	9529	6328	2995	16
H(16)	7287	5508	3243	14
H(7O)	5550(30)	5908(16)	3756(10)	23
H(19)	12648	6042	4347	20
H(21A)	8256	6027	4754	21
H(21B)	9736	5470	4991	21
H(22)	6534	5037	4532	16
H(24A)	4166	4771	5173	45
H(24B)	3809	4300	5676	45
H(24C)	4036	3868	5152	45

H(25A)	8889	4987	5938	44
H(25B)	7022	4926	6225	44
H(25C)	7234	5491	5760	44
H(27A)	7542	2172	5432	35
H(27B)	7795	2784	4996	35
H(27C)	5877	2662	5245	35
H(28A)	5313	3053	6123	46
H(28B)	6819	3479	6440	46
H(28C)	7015	2595	6320	46
H(29A)	9985	2772	5911	41
H(29B)	9888	3648	6062	41
H(29C)	10242	3410	5491	41
H(30A)	7357	4041	3414	25
H(30B)	5948	4556	3709	25
H(30C)	6515	3750	3931	25
H(31A)	9493	3542	4276	26
H(31B)	10908	4218	4311	26
H(31C)	10441	3849	3779	26
H(8A)	9024	8076	2939	18
H(8B)	9306	7439	2513	18
H(10A)	8067	8921	2118	25
H(10B)	5955	8809	1971	25

Parameter	Value
Data File Name	/ Volumes/ nmrdata/ jkthomps/ nmr/ JKT-2-215_pure/ 1/ fid
Title	JKT-2-215_pure.1.fid
Origin	Bruker BioSpin GmbH
Solvent	CDCl3
Temperature	297.2
Pulse Sequence	zg30
Experiment	1D
Number of Scans	16
Receiver Gain	98.9
Relaxation Delay	1.0000
Pulse Width	12.5000
Acquisition Time	4.0894
Acquisition Date	2022-12-05T03:39:47
Spectrometer Frequency	400.13
Spectral Width	8012.8
Nucleus	1H
Acquired Size	32768
Spectral Size	65536

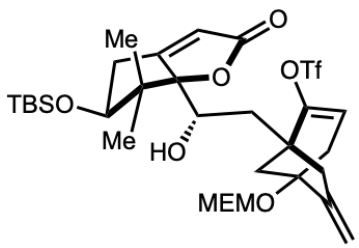

106A

Parameter	Value
Data File Name	/ Volumes/ nmrdata/ jkthomps/ nmr/ JKT-2-215_pure/ 2/ fid
Title	JKT-2-215_pure.2.fid
Origin	Bruker BioSpin GmbH
Solvent	CDCl3
Temperature	297.2
Pulse Sequence	zgpg30
Experiment	1D
Number of Scans	512
Receiver Gain	64.2
Relaxation Delay	1.0000
Pulse Width	10.0000
Acquisition Time	1.3631
Acquisition Date	2022-12-05T04:01:00
Spectrometer Frequency	100.62
Spectral Width	24038.5
Nucleus	13C
Acquired Size	32768
Spectral Size	65536

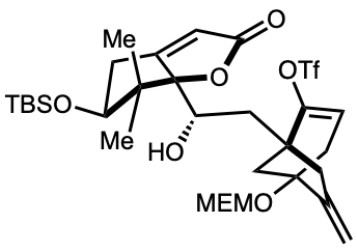

106A

175.53
173.50
152.89
150.58
120.08
116.89
114.94
109.71
91.22
82.98
79.77
71.80
67.37
59.17
47.44
44.02
43.52
40.95
35.04
30.46
29.85
25.83
21.06
18.09
17.24
1.48
0.92
-4.51

f1 (ppm)

Parameter	Value
Data File Name	/ Volumes/ nmrdata/ jkthomps/ nmr/ JKT-2-215_pure/ 3/ ser
Title	JKT-2-215_pure.3.ser
Origin	Bruker BioSpin GmbH
Solvent	CDCl3
Temperature	297.1
Pulse Sequence	cosygpppqf
Experiment	COSY
Number of Scans	1
Receiver Gain	64.2
Relaxation Delay	1.9492
Pulse Width	12.5000
Acquisition Time	0.2478
Acquisition Date	2022-12-05T04:06:39
Spectrometer Frequency	(400.13, 400.13)
Spectral Width	(4132.2, 4132.2)
Lowest Frequency	(-789.7, -799.4)
Nucleus	(1H, 1H)
Acquired Size	(1024, 128)
Spectral Size	(1024, 1024)
Digital Resolution	(4.04, 4.04)

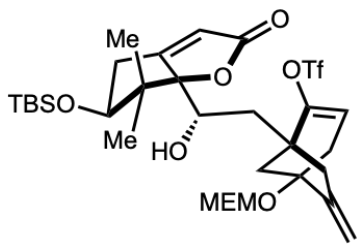

106A

f2 (ppm)

f1 (ppm)

Parameter	Value
Data File Name	/ Volumes/ nmrdata/ jkthomps/ nmr/ JKT-2-215_pure/ 4/ ser
Title	JKT-2-215_pure.4.ser
Origin	Bruker BioSpin GmbH
Solvent	CDCl3
Temperature	297.1
Pulse Sequence	hsqcedetgpsisp2.4
Experiment	HSQC-EDITED
Number of Scans	2
Receiver Gain	197.4
Relaxation Delay	1.5000
Pulse Width	12.5000
Acquisition Time	0.2135
Acquisition Date	2022-12-05T04:18:21
Spectrometer Frequency	(400.13,100.62)
Spectral Width	(4795.4,16611.3)
Lowest Frequency	(-527.8,-1359.6)
Nucleus	(1H,13C)
Acquired Size	(1024,180)
Spectral Size	(1024,1024)
Digital Resolution	(4.68,16.22)

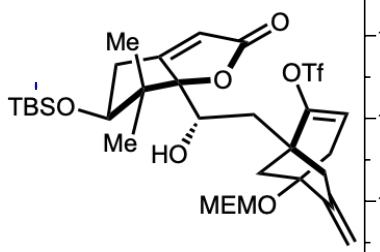

106A

f2 (ppm)

f1 (ppm)

Parameter	Value
Data File Name	/ Users/ jordankthompson/ Desktop/ JKT-7-57_pure/ 1/ fid
Title	JKT-7-57_pure.1.fid
Origin	Bruker BioSpin GmbH
Solvent	CDCl3
Temperature	297.2
Pulse Sequence	zg30
Experiment	1D
Number of Scans	16
Receiver Gain	72.0
Relaxation Delay	1.0000
Pulse Width	12.5000
Acquisition Time	4.0894
Acquisition Date	2025-02-11T13:00:19
Spectrometer Frequency	400.13
Spectral Width	8012.8
Nucleus	1H
Acquired Size	32768
Spectral Size	65536

106B

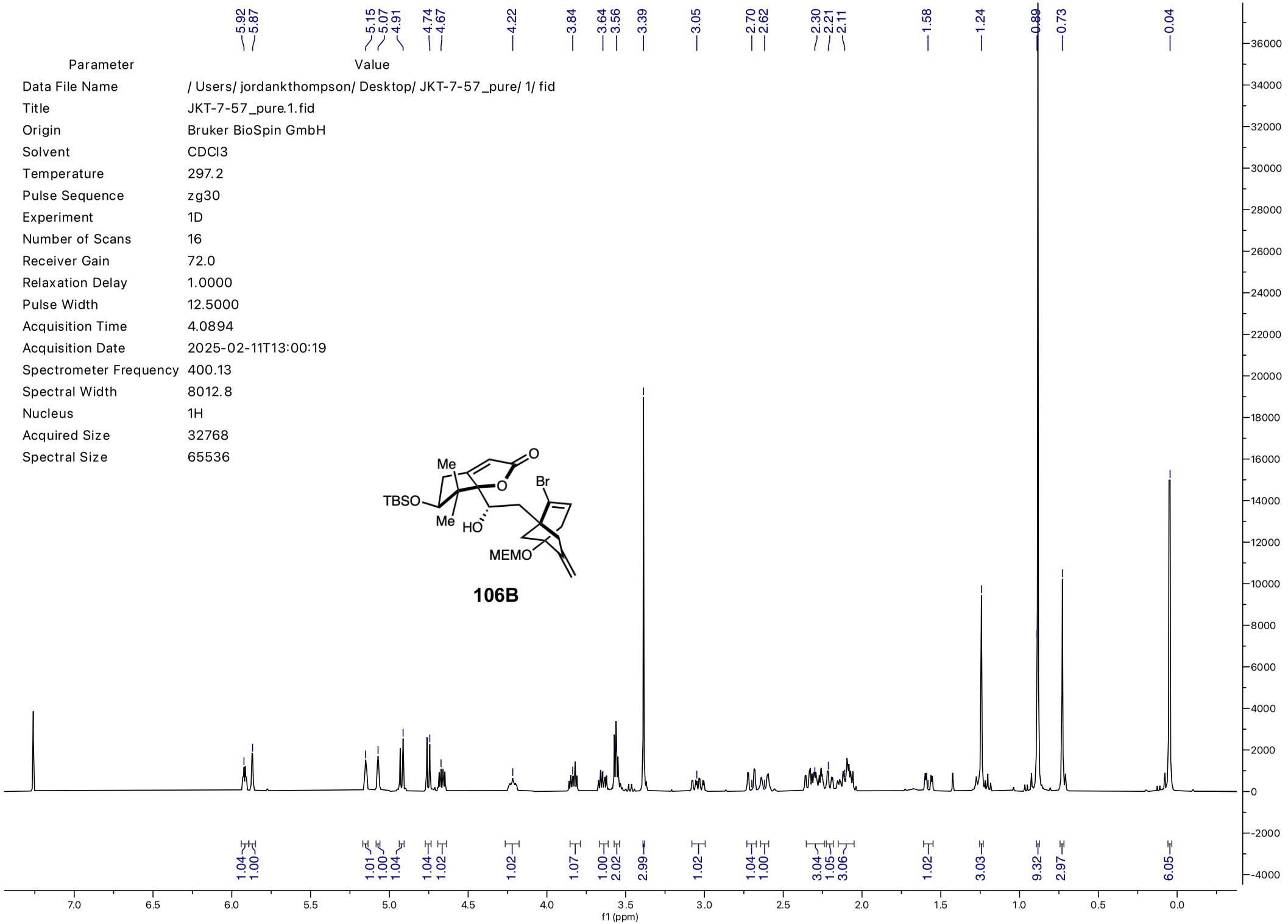

Parameter	Value
Data File Name	/ Volumes/ nmrdata-1/ jkthomps/ nmr/ JKT-7-57_pure/ 2/ fid
Title	JKT-7-57_pure.2.fid
Origin	Bruker BioSpin GmbH
Solvent	CDCl3
Temperature	297.2
Pulse Sequence	zgpg30
Experiment	1D
Number of Scans	512
Receiver Gain	72.0
Relaxation Delay	1.0000
Pulse Width	10.0000
Acquisition Time	1.1796
Acquisition Date	2025-02-11T13:19:58
Spectrometer Frequency	100.62
Spectral Width	27777.8
Nucleus	13C
Acquired Size	32768
Spectral Size	65536

106B

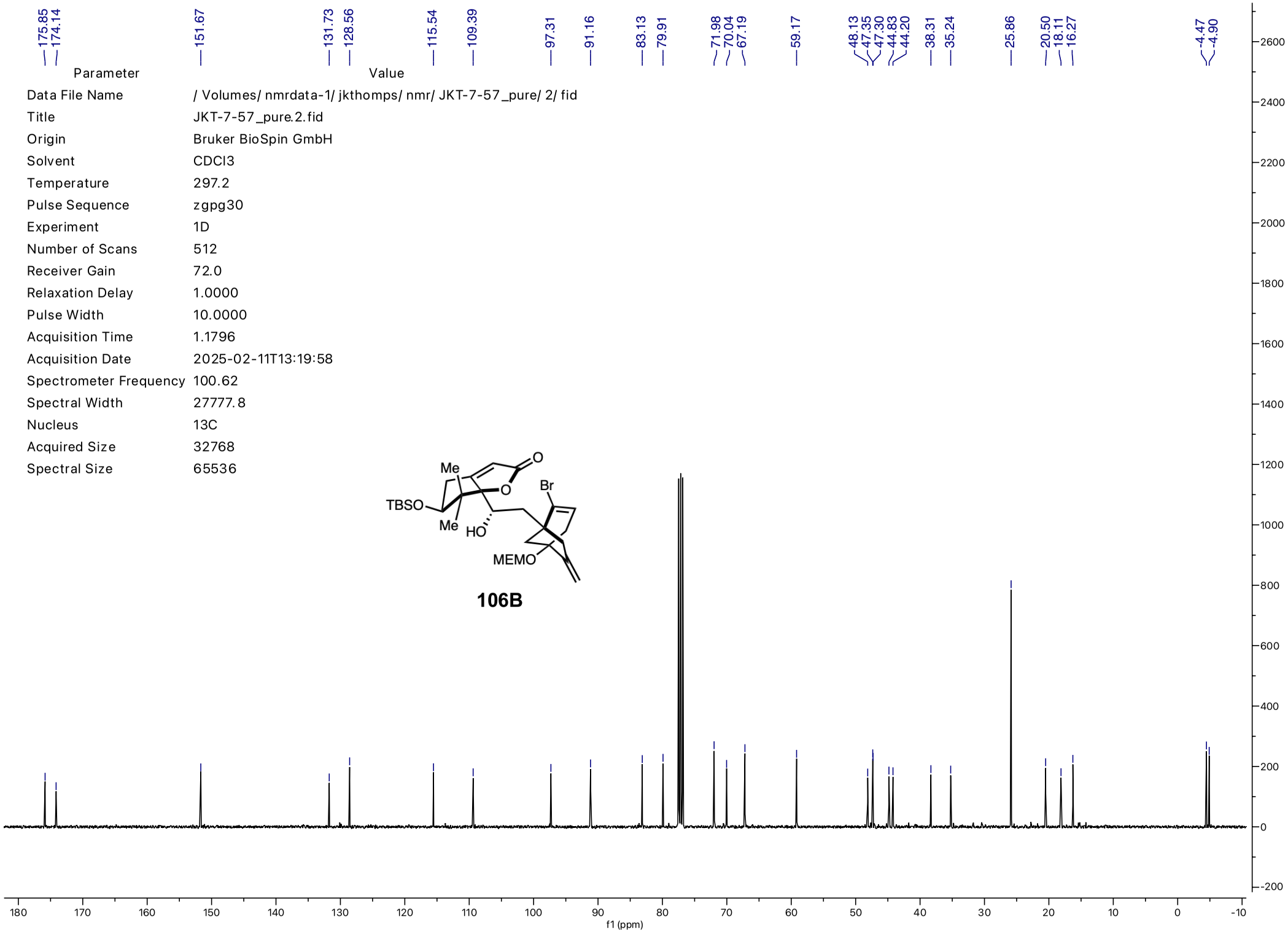

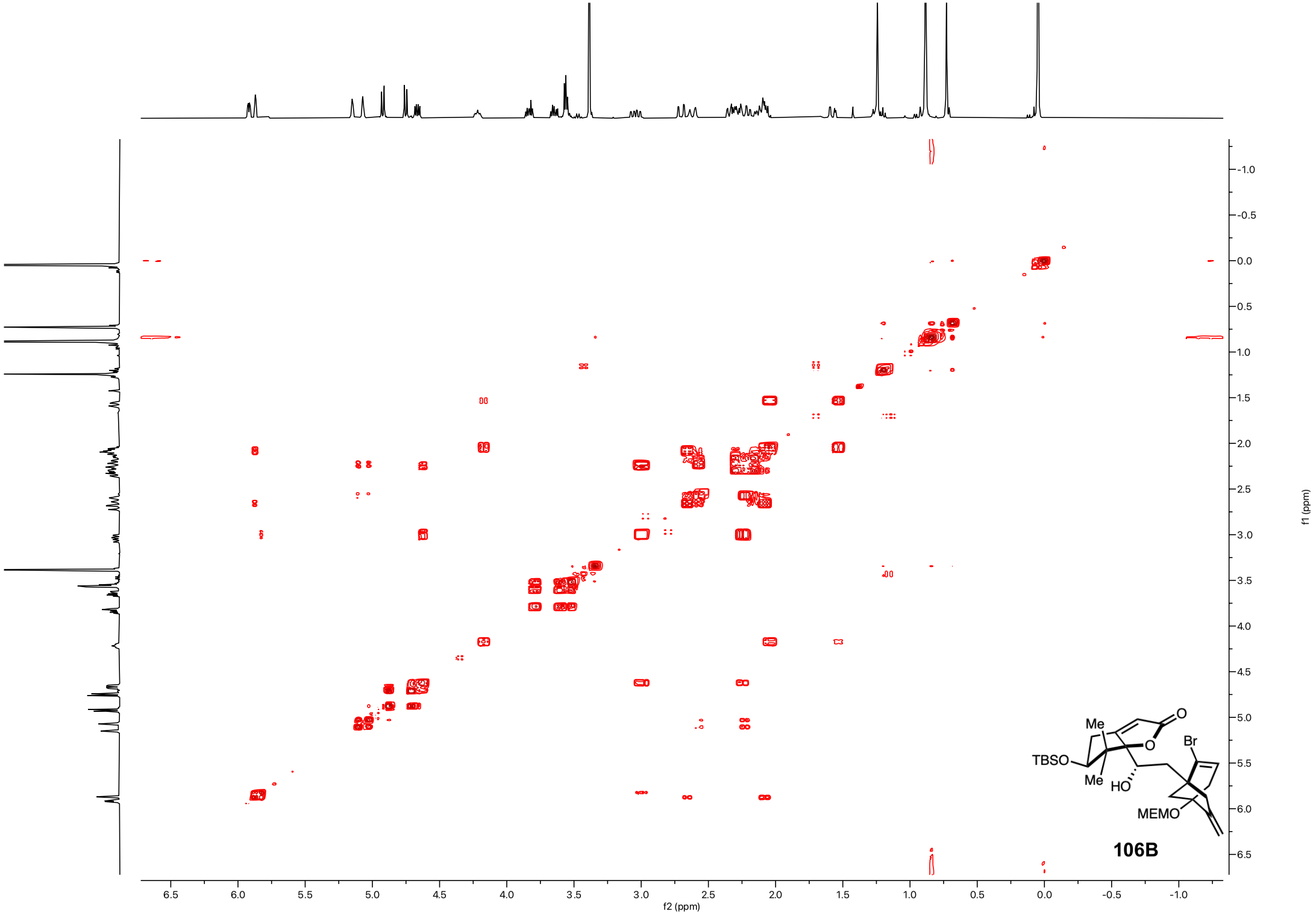
f2 (ppm)
f1 (ppm)
Me
TBSO
Me
HO
O
O
Br
MEMO
106B

Parameter	Value
Data File Name	/ Volumes/ nmrdata-1/ jkthomps/ nmr/ JKT-7-57_pure/ 4/ ser
Title	JKT-7-57_pure.4.ser
Origin	Bruker BioSpin GmbH
Solvent	CDCl3
Temperature	297.1
Pulse Sequence	hsqcedetgpsisp2.4
Experiment	HSQC-EDITED
Number of Scans	2
Receiver Gain	197.4
Relaxation Delay	1.5000
Pulse Width	12.5000
Acquisition Time	0.2135
Acquisition Date	2025-02-11T13:37:25
Spectrometer Frequency	(400.13,100.62)
Spectral Width	(4795.4,16611.3)
Lowest Frequency	(-517.1,-1262.8)
Nucleus	(1H,13C)
Acquired Size	(1024,180)
Spectral Size	(1024,1024)
Digital Resolution	(4.68,16.22)

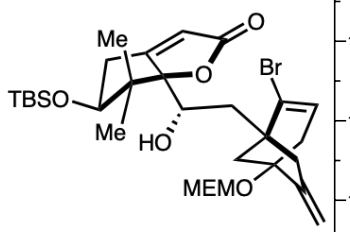

106B

f2 (ppm)

f1 (ppm)

Parameter	Value
Data File Name	/ Volumes/ nmrdata-1/ jkthomps/ nmr/ JKT-7-57_pure/ 5/ ser
Title	JKT-7-57_pure.5.ser
Origin	Bruker BioSpin GmbH
Solvent	CDCl3
Temperature	297.1
Pulse Sequence	hmbcetgpl3nd
Experiment	HMBC
Number of Scans	4
Receiver Gain	197.4
Relaxation Delay	2.0000
Pulse Width	12.5000
Acquisition Time	0.4260
Acquisition Date	2025-02-11T14:21:10
Spectrometer Frequency	(400.13,100.62)
Spectral Width	(4807.7,22321.4)
Lowest Frequency	(-163.1,-1116.4)
Nucleus	(1H,13C)
Acquired Size	(2048,256)
Spectral Size	(2048,1024)
Digital Resolution	(2.35,21.80)

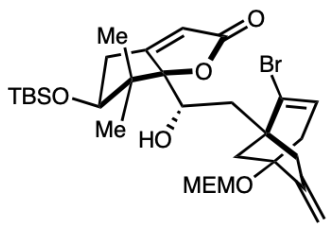

106B

f2 (ppm)

f1 (ppm)

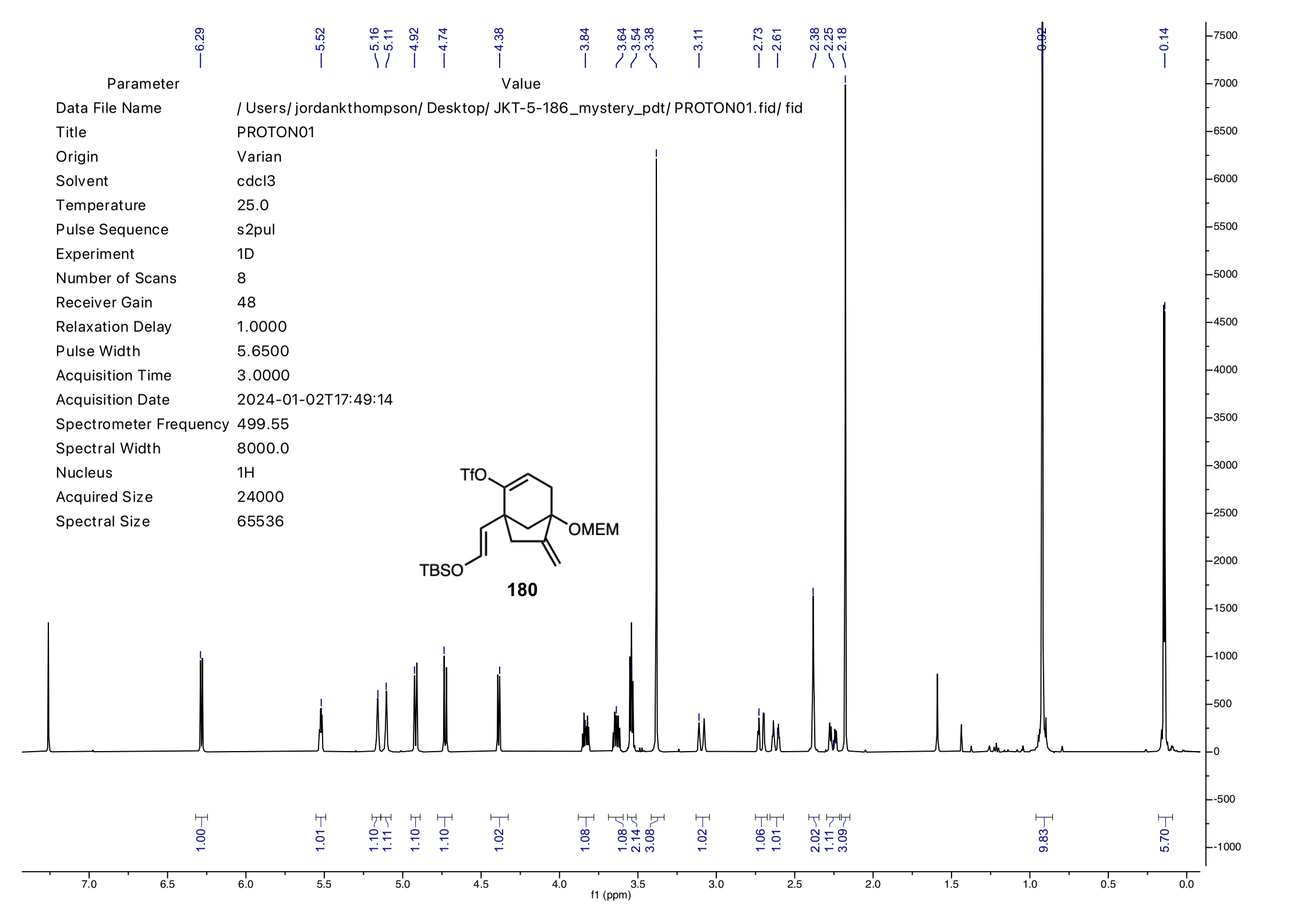
6.29
5.52
5.16
5.11
4.92
4.74
4.38
3.84
3.64
3.54
3.38
3.11
2.73
2.61
2.38
2.25
2.18
0.92
0.14
Parameter
Value
Data File Name
/ Users/ jordankthompson/ Desktop/ JKT-5-186_mystery_pdt/ PROTON01.fid/ fid
Title
PROTON01
Origin
Varian
Solvent
cdcl3
Temperature
25.0
Pulse Sequence
s2pul
Experiment
1D
Number of Scans
8
Receiver Gain
48
Relaxation Delay
1.0000
Pulse Width
5.6500
Acquisition Time
3.0000
Acquisition Date
2024-01-02T17:49:14
Spectrometer Frequency
499.55
Spectral Width
8000.0
Nucleus
1H
Acquired Size
24000
Spectral Size
65536
TfO
OMEM
TBSO
180
1.00
1.01
1.10
1.11
1.10
1.10
1.02
1.08
1.08
2.14
3.08
1.02
1.06
1.01
2.02
1.11
3.09
9.83
5.70
f1 (ppm)

Parameter	Value
Data File Name	/ Volumes/ nmrdata-1/ jkthomps/ nmr/ JKT-5-186_mystery/ 2/ fid
Title	JKT-5-186_mystery.2.fid
Origin	Bruker BioSpin GmbH
Solvent	CDCl3
Temperature	297.1
Pulse Sequence	zgpg30
Experiment	1D
Number of Scans	512
Receiver Gain	64.2
Relaxation Delay	1.0000
Pulse Width	10.0000
Acquisition Time	1.3631
Acquisition Date	2024-01-02T19:26:22
Spectrometer Frequency	100.62
Spectral Width	24038.5
Nucleus	13C
Acquired Size	32768
Spectral Size	65536

180

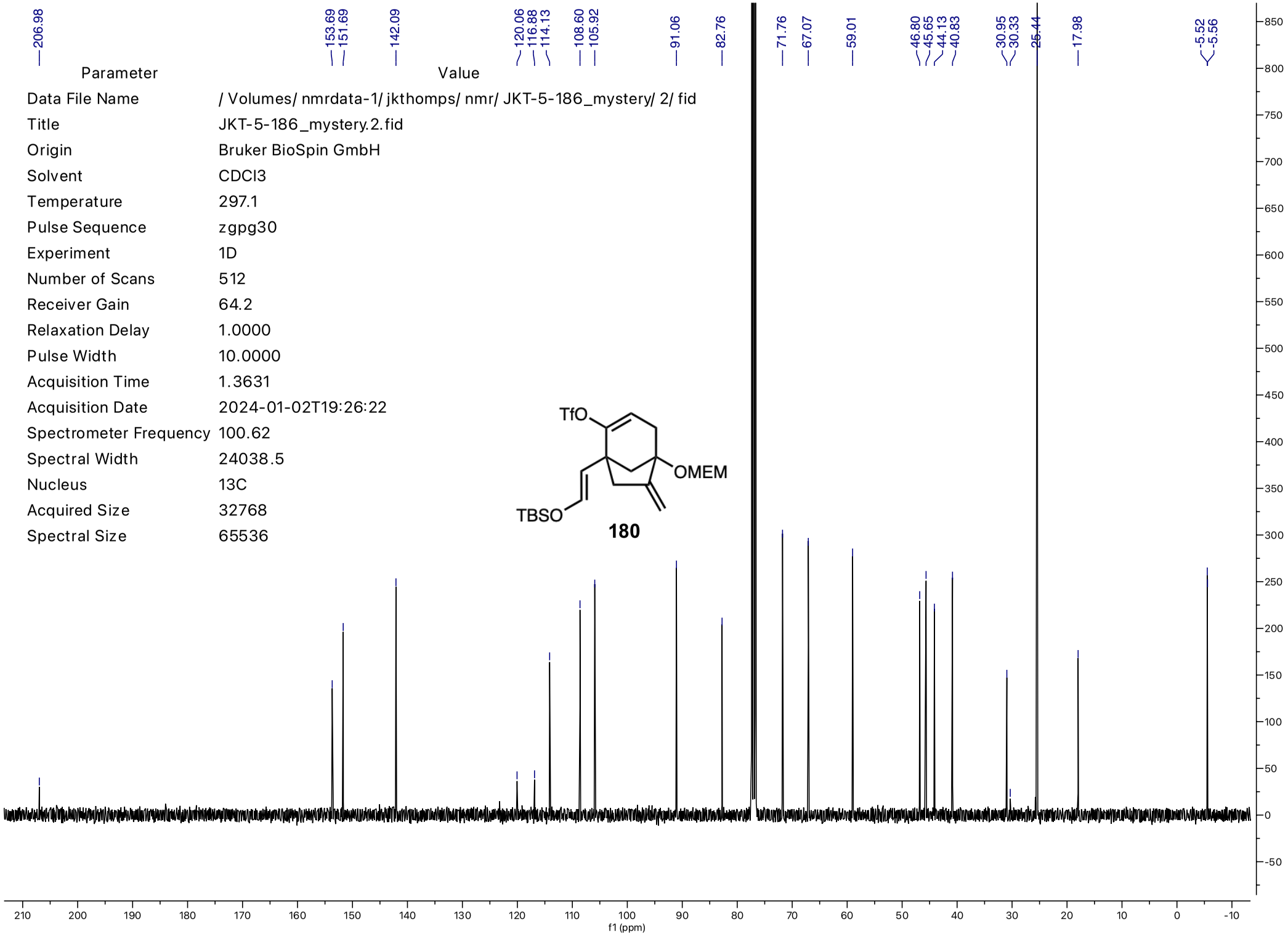

Parameter	Value
Data File Name	/ Volumes/ nmrdata/ jkthomps/ nmr/ JKT-2-215_pure/ 1/ fid
Title	JKT-2-215_pure.1.fid
Origin	Bruker BioSpin GmbH
Solvent	CDCl3
Temperature	297.2
Pulse Sequence	zg30
Experiment	1D
Number of Scans	16
Receiver Gain	98.9
Relaxation Delay	1.0000
Pulse Width	12.5000
Acquisition Time	4.0894
Acquisition Date	2022-12-05T03:39:47
Spectrometer Frequency	400.13
Spectral Width	8012.8
Nucleus	1H
Acquired Size	32768
Spectral Size	65536

181A

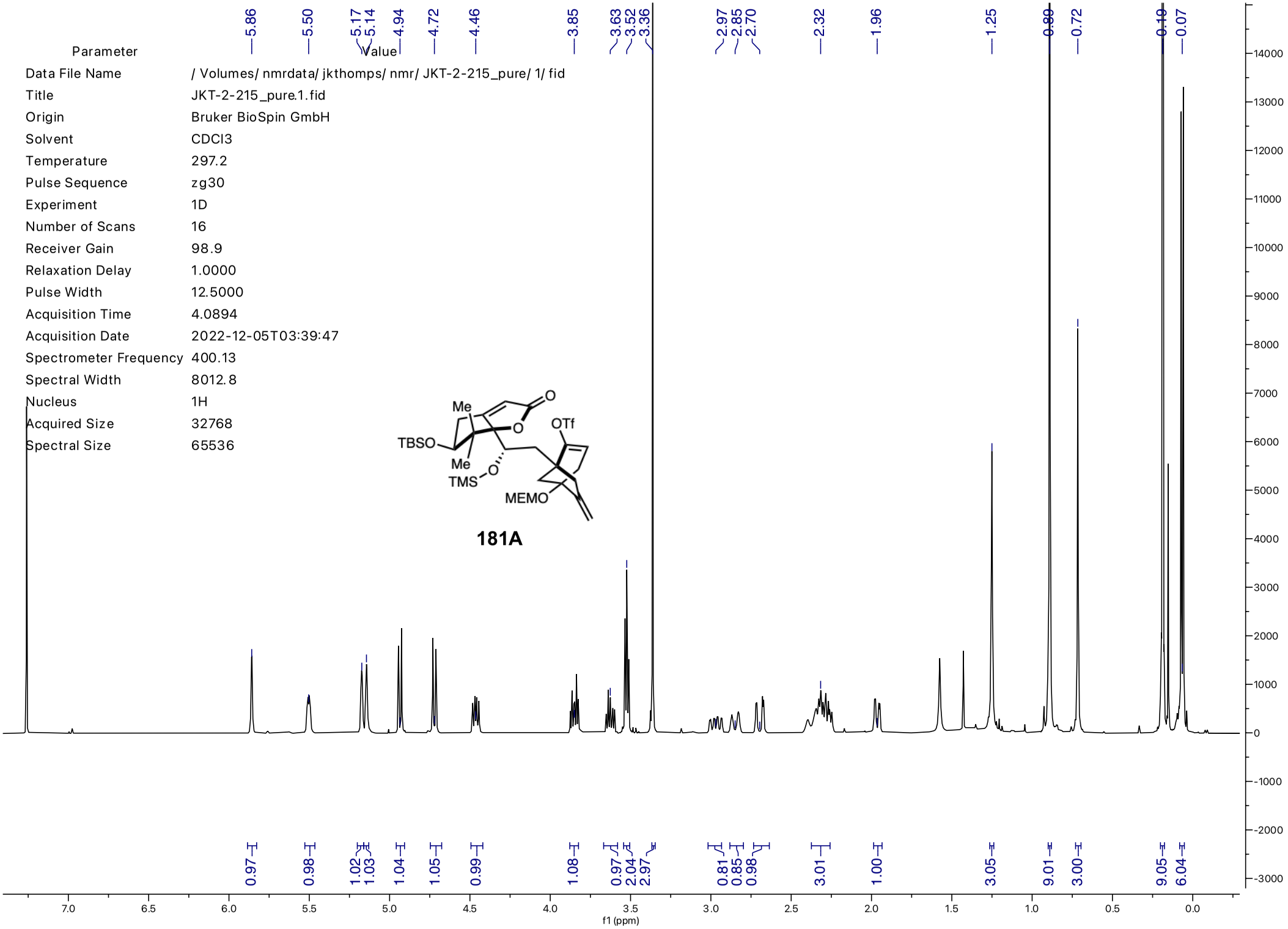

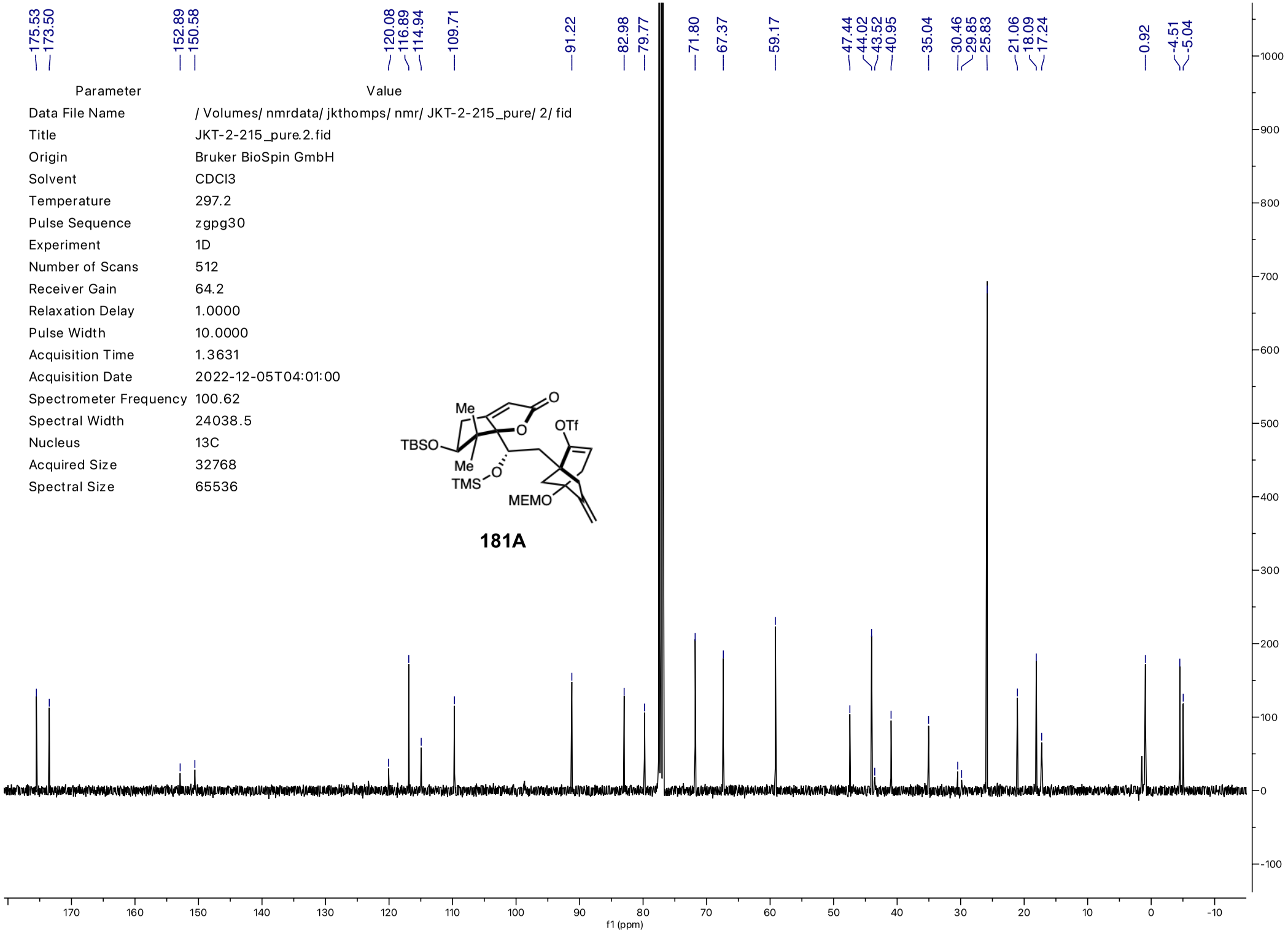
175.53
173.50
152.89
150.58
120.08
116.89
114.94
109.71
91.22
82.98
79.77
71.80
67.37
59.17
47.44
44.02
43.52
40.95
35.04
30.46
29.85
25.83
21.06
18.09
17.24
0.92
-4.51
-5.04
Parameter Value
Data File Name / Volumes/ nmrdata/ jkthomps/ nmr/ JKT-2-215_pure/ 2/ fid
Title JKT-2-215_pure.2.fid
Origin Bruker BioSpin GmbH
Solvent CDCl3
Temperature 297.2
Pulse Sequence zgpg30
Experiment 1D
Number of Scans 512
Receiver Gain 64.2
Relaxation Delay 1.0000
Pulse Width 10.0000
Acquisition Time 1.3631
Acquisition Date 2022-12-05T04:01:00
Spectrometer Frequency 100.62
Spectral Width 24038.5
Nucleus 13C
Acquired Size 32768
Spectral Size 65536
Me
O
O
OTf
TBSO
Me
TMS
O
MEMO
181A
1000
900
800
700
600
500
400
300
200
100
0
-100
170
160
150
140
130
120
110
100
90
80
70
60
50
40
30
20
10
0
-10
f1 (ppm)

Parameter	Value
Data File Name	/ Volumes/ nmrdata-1/ jkthomps/ nmr/ compound81/ 1/ fid
Title	compound81.1.fid
Origin	Bruker BioSpin GmbH
Solvent	CDCl3
Temperature	297.1
Pulse Sequence	zg30
Experiment	1D
Number of Scans	16
Receiver Gain	197.4
Relaxation Delay	1.0000
Pulse Width	12.5000
Acquisition Time	4.0894
Acquisition Date	2024-04-20T22:33:13
Spectrometer Frequency	400.13
Spectral Width	8012.8
Nucleus	1H
Acquired Size	32768
Spectral Size	65536

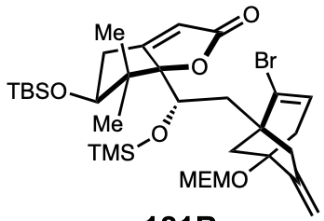

181B

Parameter	Value
Data File Name	/ Volumes/ nmrdata/ jkthomps/ nmr/ compound81_RR/ 2/ fid
Title	compound81_RR.2.fid
Origin	Bruker BioSpin GmbH
Solvent	CDCl3
Temperature	297.2
Pulse Sequence	zgpg30
Experiment	1D
Number of Scans	512
Receiver Gain	50.3
Relaxation Delay	1.0000
Pulse Width	10.0000
Acquisition Time	1.1796
Acquisition Date	2024-04-21T00:57:33
Spectrometer Frequency	100.62
Spectral Width	27777.8
Nucleus	13C
Acquired Size	32768
Spectral Size	65536

175.95, 173.73, 133.00, 127.06, 125.66, 116.80, 109.20, 91.17, 83.21, 79.90, 71.88, 67.35, 66.00, 59.13, 51.43, 47.37, 46.70, 44.95, 39.86, 35.24, 30.45, 25.84, 21.20, 18.11, 17.12, 15.42, 1.12, -4.37, -4.80

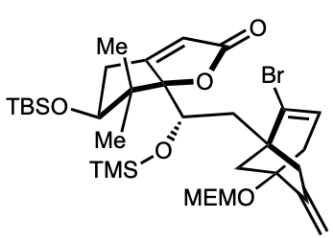

181B

f1 (ppm)

Parameter	Value
Data File Name	/ Volumes/ nmrdata-1/ jkthomps/ nmr/ JKT-2-227_pure/ 1/ fid
Title	JKT-2-227_pure.1.fid
Origin	Bruker BioSpin GmbH
Solvent	CDCl3
Temperature	297.1
Pulse Sequence	zg30
Experiment	1D
Number of Scans	16
Receiver Gain	72.0
Relaxation Delay	1.0000
Pulse Width	12.5000
Acquisition Time	4.0894
Acquisition Date	2022-12-15T20:18:20
Spectrometer Frequency	400.13
Spectral Width	8012.8
Nucleus	1H
Acquired Size	32768
Spectral Size	65536

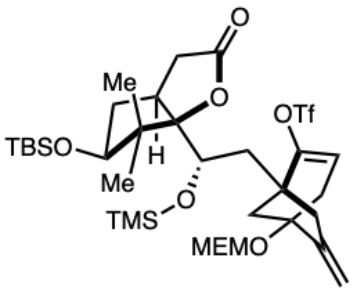

182A

Parameter	Value
Data File Name	/ Volumes/ nmrdata-1/ jkthomps/ nmr/ JKT-2-227_pure/ 2/ fid
Title	JKT-2-227_pure.2.fid
Origin	Bruker BioSpin GmbH
Solvent	CDCl3
Temperature	297.2
Pulse Sequence	zgpg30
Experiment	1D
Number of Scans	512
Receiver Gain	98.9
Relaxation Delay	1.0000
Pulse Width	10.0000
Acquisition Time	1.3631
Acquisition Date	2022-12-15T20:39:34
Spectrometer Frequency	100.62
Spectral Width	24038.5
Nucleus	13C
Acquired Size	32768
Spectral Size	65536

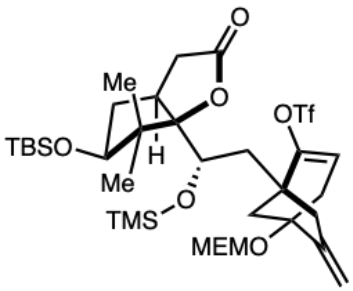

182A

176.67 152.72 150.88 120.05 116.87 115.18 109.68 99.35 91.22 82.95 67.40 60.54 59.14 49.60 46.81 44.10 43.78 40.83 39.82 39.08 38.56 35.82 25.87 23.38 21.20 20.62 18.21 1.31 -4.52 -4.93

f1 (ppm)

Parameter	Value
Data File Name	/ Volumes/ nmrdata-1/ jkthomps/ nmr/ JKT-2-227_pure/ 3/ ser
Title	JKT-2-227_pure.3.ser
Origin	Bruker BioSpin GmbH
Solvent	CDCl3
Temperature	297.2
Pulse Sequence	cosygpppqf
Experiment	COSY
Number of Scans	1
Receiver Gain	38.0
Relaxation Delay	1.9410
Pulse Width	12.5000
Acquisition Time	0.2560
Acquisition Date	2022-12-15T20:45:21
Spectrometer Frequency	(400.13, 400.13)
Spectral Width	(4000.0, 4000.0)
Lowest Frequency	(-618.2, -627.1)
Nucleus	(1H, 1H)
Acquired Size	(1024, 128)
Spectral Size	(1024, 1024)
Digital Resolution	(3.91, 3.91)

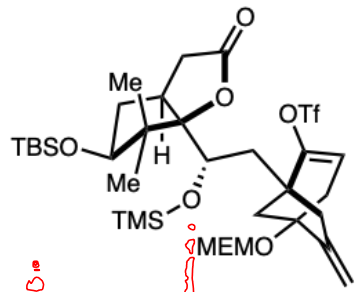

182A

f2 (ppm)

f1 (ppm)

Parameter	Value
Data File Name	/ Volumes/ nmrdata-1/ jkthomps/ nmr/ JKT-2-227_pure/ 4/ ser
Title	JKT-2-227_pure.4.ser
Origin	Bruker BioSpin GmbH
Solvent	CDCl3
Temperature	297.1
Pulse Sequence	hsqcedetgpsisp2.4
Experiment	HSQC-EDITED
Number of Scans	2
Receiver Gain	197.4
Relaxation Delay	1.5000
Pulse Width	12.5000
Acquisition Time	0.2135
Acquisition Date	2022-12-15T20:57:02
Spectrometer Frequency	(400.13,100.62)
Spectral Width	(4795.4,16611.3)
Lowest Frequency	(-528.9,-1385.6)
Nucleus	(1H,13C)
Acquired Size	(1024,180)
Spectral Size	(1024,1024)
Digital Resolution	(4.68,16.22)

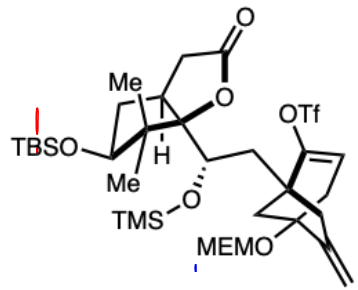

182A

f2 (ppm)

f1 (ppm)

Parameter	Value
Data File Name	/ Users/ jordankthompson/ Desktop/ JKT-2-333_pure_20221222_01/ JKT-2-333_pure-PROTON_01.fid/ fid
Title	JKT-2-333_pure-PROTON_01
Origin	Varian
Solvent	cdcl3
Temperature	25.0
Pulse Sequence	s2pul
Experiment	1D
Number of Scans	8
Receiver Gain	26
Relaxation Delay	1.0000
Pulse Width	2.6500
Acquisition Time	1.7046
Acquisition Date	2022-12-22T12:06:14
Spectrometer Frequency	599.56
Spectral Width	9611.9
Nucleus	1H
Acquired Size	16384
Spectral Size	65536

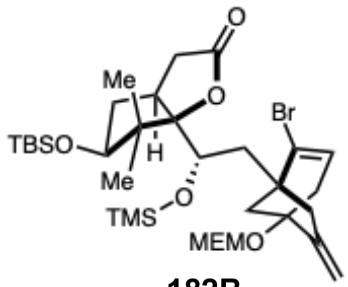

182B

5.84 5.16 5.08 4.93 4.75 3.96 3.84 3.76 3.65 3.53 3.37 2.87 2.78 2.64 2.33 2.24 2.14 2.02 1.80 1.49 1.07 1.03 0.89 0.20 0.04

1.00 1.04 1.05 1.05 1.04 0.96 1.00 1.01 1.06 2.06 3.04 1.05 1.05 2.03 4.01 1.04 1.02 0.98 0.87 1.00 3.09 2.61 9.32 8.94 5.87

f1 (ppm)

Parameter	Value
Data File Name	/ Volumes/ nmrdata-2/ jkthomps/ nmr/ JKT-4-185_pure/ 2/ fid
Title	JKT-4-185_pure.2.fid
Origin	Bruker BioSpin GmbH
Solvent	CDCl3
Temperature	297.2
Pulse Sequence	zgpg30
Experiment	1D
Number of Scans	750
Receiver Gain	64.2
Relaxation Delay	1.0000
Pulse Width	10.0000
Acquisition Time	1.3631
Acquisition Date	2023-06-15T13:47:33
Spectrometer Frequency	100.62
Spectral Width	24038.5
Nucleus	13C
Acquired Size	32768
Spectral Size	65536

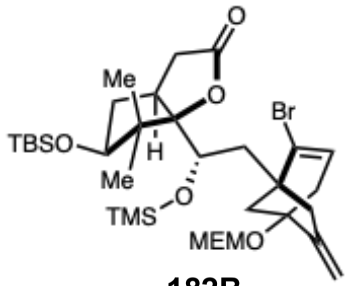

182B

Parameter	Value
Data File Name	/ Users/ jordankthompson/ Desktop/ JKT-2-235_rsm/ 3/ ser
Title	JKT-2-235_rsm.3.ser
Origin	Bruker BioSpin GmbH
Solvent	CDCl3
Temperature	297.2
Pulse Sequence	cosygpppqf
Experiment	COSY
Number of Scans	1
Receiver Gain	112.8
Relaxation Delay	1.9226
Pulse Width	12.5000
Acquisition Time	0.2744
Acquisition Date	2022-12-23T13:07:52
Spectrometer Frequency	(400.13,400.13)
Spectral Width	(3731.3,3731.3)
Lowest Frequency	(-495.4,-494.3)
Nucleus	(1H,1H)
Acquired Size	(1024,128)
Spectral Size	(1024,1024)
Digital Resolution	(3.64,3.64)

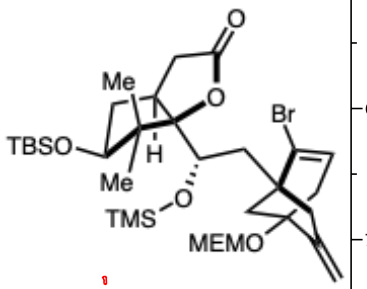

182B

f2 (ppm)

f1 (ppm)

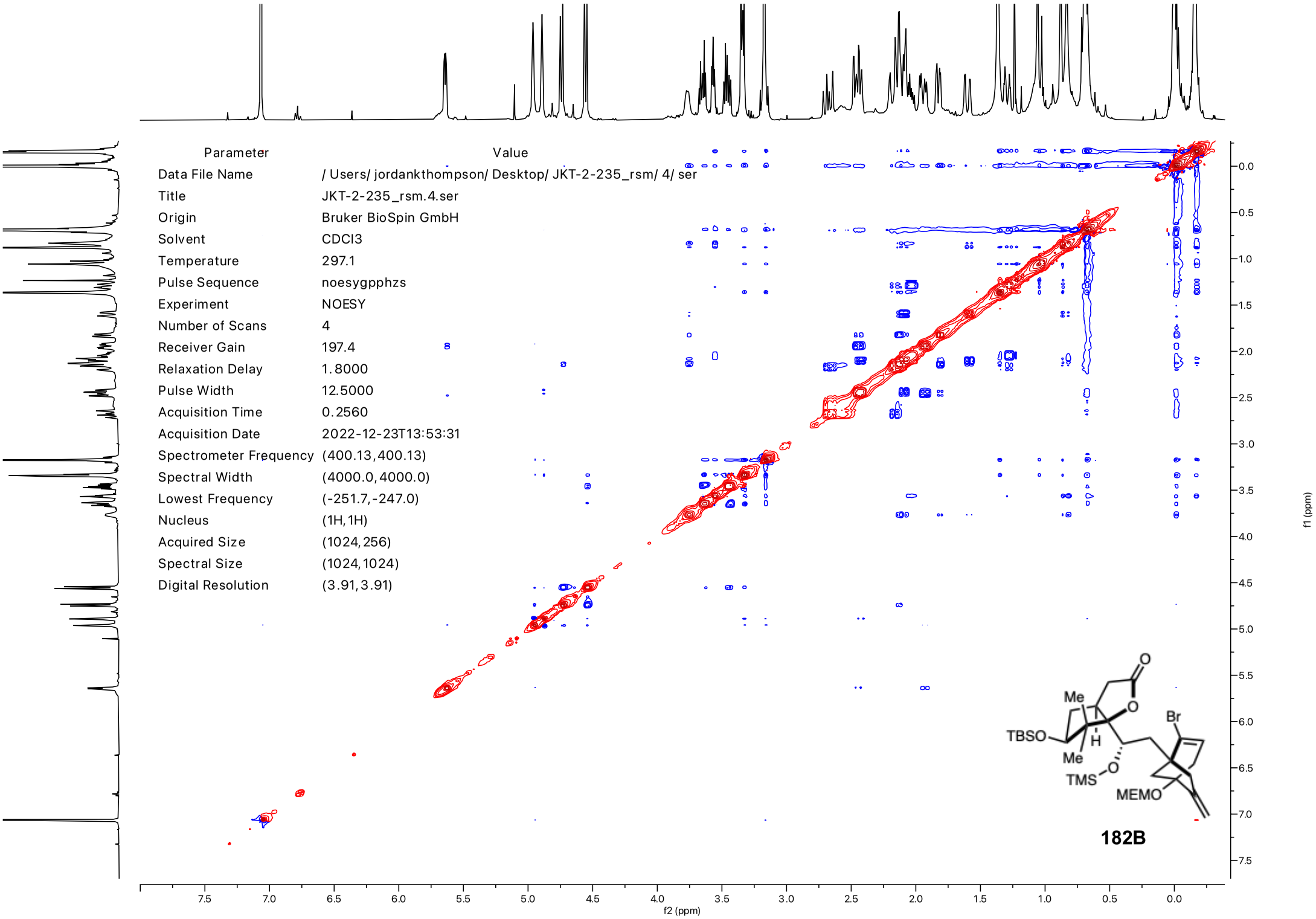
Parameter Value
Data File Name / Users/ jordankthompson/ Desktop/ JKT-2-235_rsm/ 4/ ser
Title JKT-2-235_rsm.4.ser
Origin Bruker BioSpin GmbH
Solvent CDCl3
Temperature 297.1
Pulse Sequence noesygpphzs
Experiment NOESY
Number of Scans 4
Receiver Gain 197.4
Relaxation Delay 1.8000
Pulse Width 12.5000
Acquisition Time 0.2560
Acquisition Date 2022-12-23T13:53:31
Spectrometer Frequency (400.13,400.13)
Spectral Width (4000.0,4000.0)
Lowest Frequency (-251.7,-247.0)
Nucleus (1H,1H)
Acquired Size (1024,256)
Spectral Size (1024,1024)
Digital Resolution (3.91,3.91)
TBSO
Me
H
Me
O
TMS
O
O
Br
MEMO
182B
f2 (ppm)
f1 (ppm)

Parameter	Value
Data File Name	/ Volumes/ nmrdata-1/ jkthomps/ nmr/ JKT-4-enolate_vinylation/ 1/ fid
Title	JKT-4-enolate_vinylation.1.fid
Origin	Bruker BioSpin GmbH
Solvent	CDCl3
Temperature	297.2
Pulse Sequence	zg30
Experiment	1D
Number of Scans	16
Receiver Gain	176.8
Relaxation Delay	1.0000
Pulse Width	12.5000
Acquisition Time	4.0894
Acquisition Date	2023-07-25T18:49:53
Spectrometer Frequency	400.13
Spectral Width	8012.8
Nucleus	1H
Acquired Size	32768
Spectral Size	65536

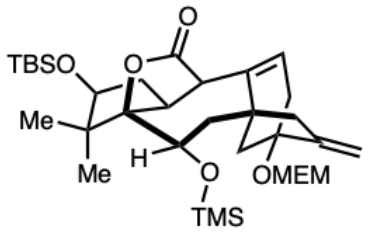

105

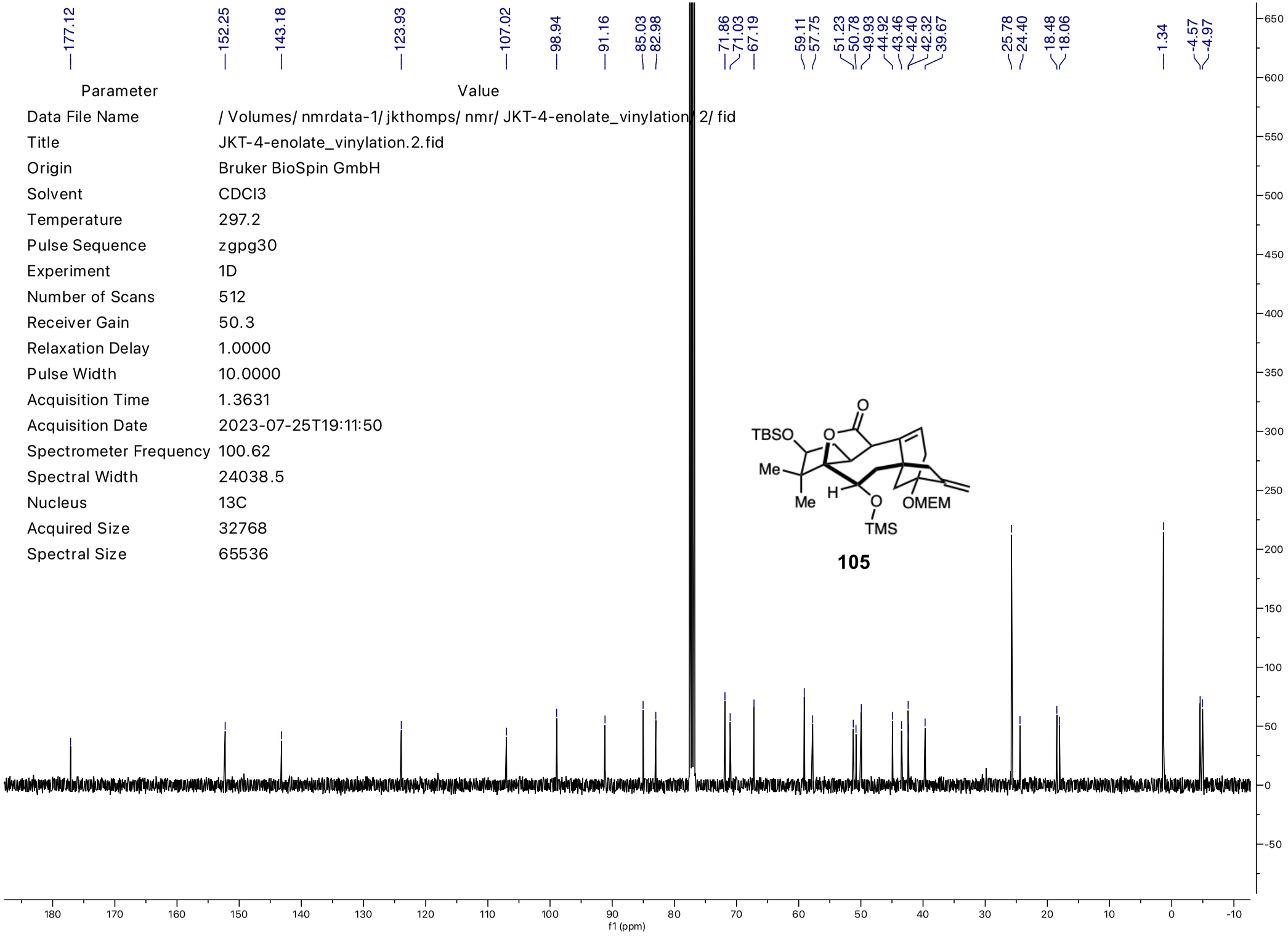
177.12
152.25
143.18
123.93
107.02
98.94
91.16
85.03
82.98
71.86
71.03
67.19
59.11
57.75
51.23
50.78
49.93
44.92
43.46
42.40
42.32
39.67
25.78
24.40
18.48
18.06
1.34
-4.57
-4.97
Parameter
Value
Data File Name / Volumes/ nmrdata-1/ jkthomps/ nmr/ JKT-4-enolate_vinylation/ 2/ fid
Title JKT-4-enolate_vinylation.2.fid
Origin Bruker BioSpin GmbH
Solvent CDCl3
Temperature 297.2
Pulse Sequence zgpg30
Experiment 1D
Number of Scans 512
Receiver Gain 50.3
Relaxation Delay 1.0000
Pulse Width 10.0000
Acquisition Time 1.3631
Acquisition Date 2023-07-25T19:11:50
Spectrometer Frequency 100.62
Spectral Width 24038.5
Nucleus 13C
Acquired Size 32768
Spectral Size 65536
TBSO
O
Me
Me
H
O
TMS
OMEM
105
650
600
550
500
450
400
350
300
250
200
150
100
50
0
-50
180
170
160
150
140
130
120
110
100
90
80
70
60
50
40
30
20
10
0
-10
f1 (ppm)

Parameter	Value
Data File Name	/ Volumes/ nmrdata-1/ jkthomps/ nmr/ JKT-4-enolate_vinylation/ 3/ ser
Title	JKT-4-enolate_vinylation.3.ser
Origin	Bruker BioSpin GmbH
Solvent	CDCl3
Temperature	297.1
Pulse Sequence	cosygpppqf
Experiment	COSY
Number of Scans	1
Receiver Gain	98.9
Relaxation Delay	1.9205
Pulse Width	12.5000
Acquisition Time	0.2765
Acquisition Date	2020-07-25T19:17:33
Spectrometer Frequency	(400.13,400.13)
Spectral Width	(3703.7,3703.7)
Lowest Frequency	(-423.0,-414.8)
Nucleus	(1H,1H)
Acquired Size	(1024,128)
Spectral Size	(1024,1024)
Digital Resolution	(3.62,3.62)

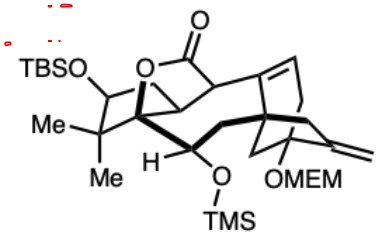

105

f1 (ppm)

Parameter	Value
Data File Name	/ Volumes/ nmrdata-1/ jkthomps/ nmr/ JKT-4-enolate_vinylation/ 4/ ser
Title	JKT-4-enolate_vinylation.4.ser
Origin	Bruker BioSpin GmbH
Solvent	CDCl3
Temperature	297.1
Pulse Sequence	hsqcedetgpsisp2.4
Experiment	HSQC-EDITED
Number of Scans	2
Receiver Gain	197.4
Relaxation Delay	1.5000
Pulse Width	12.5000
Acquisition Time	0.2135
Acquisition Date	2023-07-25T19:29:15
Spectrometer Frequency	(400.13,100.62)
Spectral Width	(4795.4,16611.3)
Lowest Frequency	(-535.3,-1262.8)
Nucleus	(1H,13C)
Acquired Size	(1024,180)
Spectral Size	(1024,1024)
Digital Resolution	(4.68,16.22)

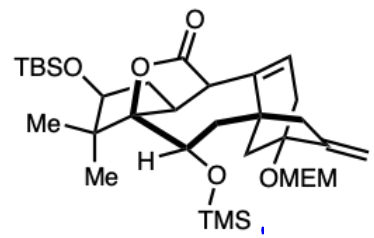

105

f1 (ppm)

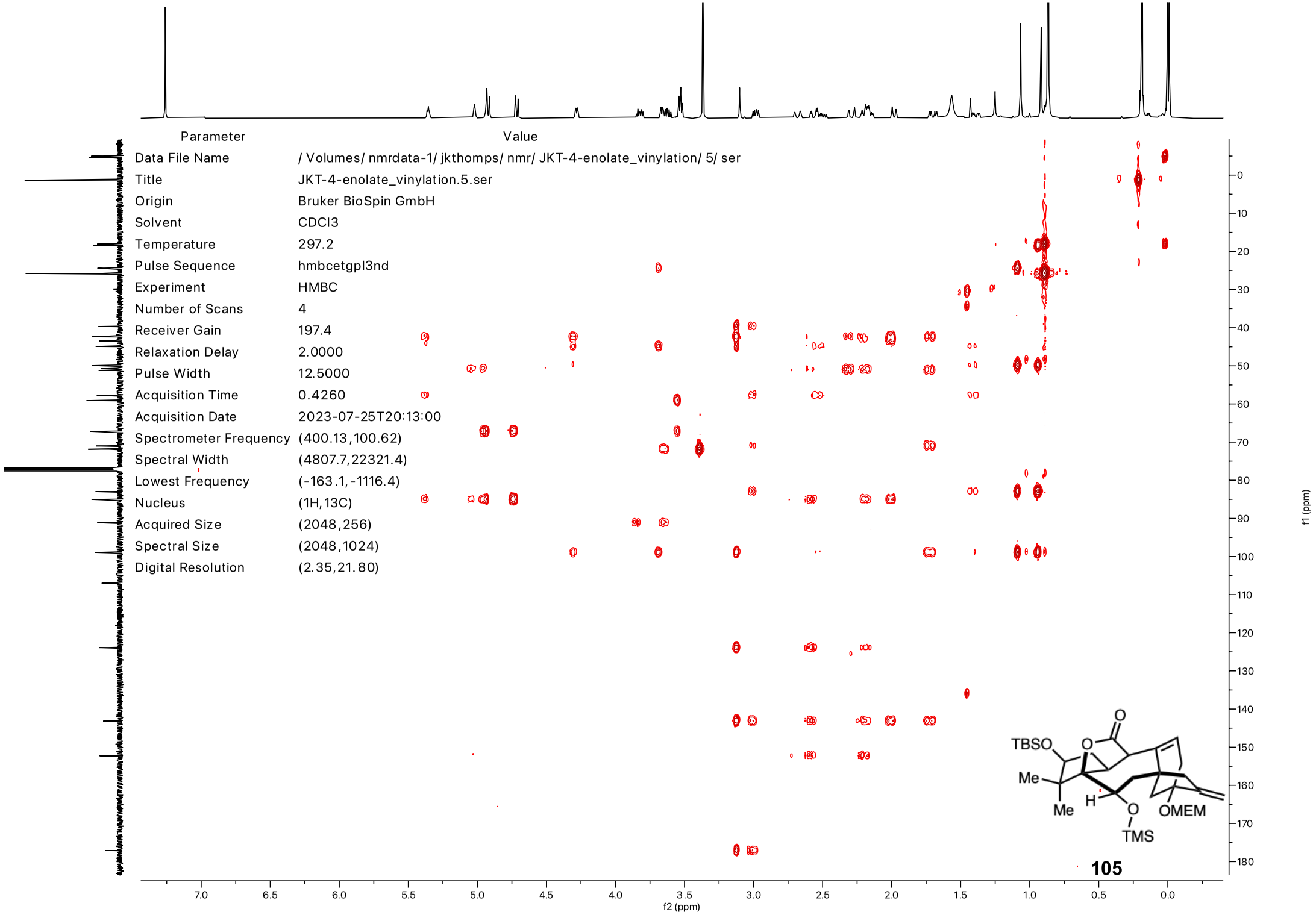
Parameter
Value
Data File Name / Volumes/ nmrdata-1/ jkthomps/ nmr/ JKT-4-enolate_vinylation/ 5/ ser
Title JKT-4-enolate_vinylation.5.ser
Origin Bruker BioSpin GmbH
Solvent CDCl3
Temperature 297.2
Pulse Sequence hmbcetgpl3nd
Experiment HMBC
Number of Scans 4
Receiver Gain 197.4
Relaxation Delay 2.0000
Pulse Width 12.5000
Acquisition Time 0.4260
Acquisition Date 2023-07-25T20:13:00
Spectrometer Frequency (400.13,100.62)
Spectral Width (4807.7,22321.4)
Lowest Frequency (-163.1,-1116.4)
Nucleus (1H,13C)
Acquired Size (2048,256)
Spectral Size (2048,1024)
Digital Resolution (2.35,21.80)
f2 (ppm)
f1 (ppm)
TBSO
Me
Me
H
O
TMS
O
O
OMEM
105

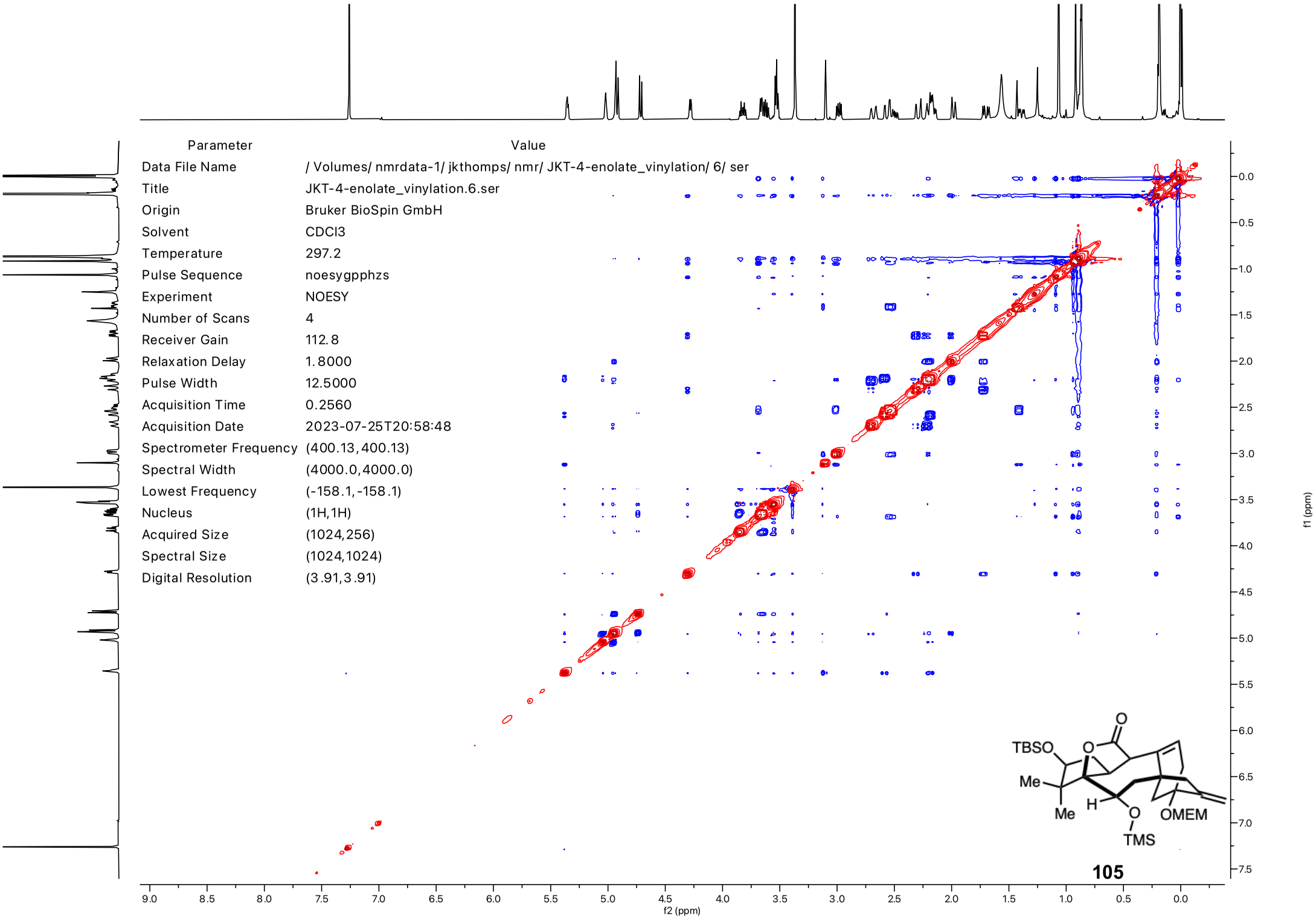
Parameter Value
Data File Name / Volumes/ nmrdata-1/ jkthomps/ nmr/ JKT-4-enolate_vinylation/ 6/ ser
Title JKT-4-enolate_vinylation.6.ser
Origin Bruker BioSpin GmbH
Solvent CDCl3
Temperature 297.2
Pulse Sequence noesygpphzs
Experiment NOESY
Number of Scans 4
Receiver Gain 112.8
Relaxation Delay 1.8000
Pulse Width 12.5000
Acquisition Time 0.2560
Acquisition Date 2023-07-25T20:58:48
Spectrometer Frequency (400.13,400.13)
Spectral Width (4000.0,4000.0)
Lowest Frequency (-158.1,-158.1)
Nucleus (1H,1H)
Acquired Size (1024,256)
Spectral Size (1024,1024)
Digital Resolution (3.91,3.91)
TBSO
O
Me
Me
H
O
OMEM
TMS
105
f2 (ppm)
f1 (ppm)

Parameter	Value
Data File Name	/ Volumes/ nmrdata/ jkthomps/ nmr/ JKT-7-284-2/ 1/ fid
Title	JKT-7-284-2.1.fid
Origin	Bruker BioSpin GmbH
Solvent	CDCl3
Temperature	297.2
Pulse Sequence	zg30
Experiment	1D
Number of Scans	16
Receiver Gain	197.4
Relaxation Delay	1.0000
Pulse Width	12.5000
Acquisition Time	4.0894
Acquisition Date	2025-07-15T08:30:46
Spectrometer Frequency	400.13
Spectral Width	8012.8
Nucleus	1H
Acquired Size	32768
Spectral Size	65536

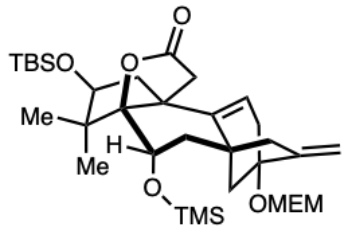

188

Parameter	Value
Data File Name	/ Volumes/ nmrdata/ jkthomps/ nmr/ JKT-7-284-2/ 2/ fid
Title	JKT-7-284-2.2.fid
Origin	Bruker BioSpin GmbH
Solvent	CDCl3
Temperature	297.1
Pulse Sequence	zgpg30
Experiment	1D
Number of Scans	2750
Receiver Gain	64.2
Relaxation Delay	1.0000
Pulse Width	10.0000
Acquisition Time	1.1796
Acquisition Date	2025-07-15T22:49:38
Spectrometer Frequency	100.62
Spectral Width	27777.8
Nucleus	13C
Acquired Size	32768
Spectral Size	65536

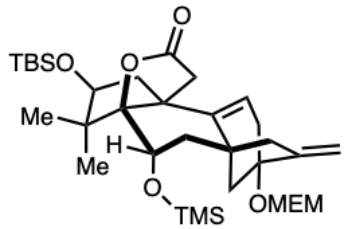

188

Parameter	Value
Data File Name	/ Volumes/ nmrdata/ jkthomps/ nmr/ JKT-7-284-2/ 7/ ser
Title	JKT-7-284-2.7.ser
Origin	Bruker BioSpin GmbH
Solvent	CDCl3
Temperature	297.1
Pulse Sequence	hsqcedetgpsisp2.4
Experiment	HSQC-EDITED
Number of Scans	10
Receiver Gain	197.4
Relaxation Delay	1.5000
Pulse Width	12.5000
Acquisition Time	0.2135
Acquisition Date	2025-07-16T01:18:23
Spectrometer Frequency	(400.13,100.62)
Spectral Width	(4795.4,16611.3)
Lowest Frequency	(-525.5,-1262.8)
Nucleus	(1H,13C)
Acquired Size	(1024,180)
Spectral Size	(1024,1024)
Digital Resolution	(4.68,16.22)

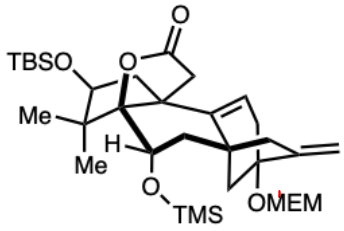

188

f2 (ppm)

f1 (ppm)

Parameter	Value
Data File Name	/ Volumes/ nmrdata/ jkthomps/ nmr/ JKT-7-284-2/ 3/ ser
Title	JKT-7-284-2.3.ser
Origin	Bruker BioSpin GmbH
Solvent	CDCl3
Temperature	297.1
Pulse Sequence	cosygpppqf
Experiment	COSY
Number of Scans	1
Receiver Gain	176.8
Relaxation Delay	1.9164
Pulse Width	12.5000
Acquisition Time	0.2806
Acquisition Date	2025-07-15T22:55:21
Spectrometer Frequency	(400.13,400.13)
Spectral Width	(3649.6,3649.6)
Lowest Frequency	(-446.2,-446.2)
Nucleus	(1H,1H)
Acquired Size	(1024,128)
Spectral Size	(1024,1024)
Digital Resolution	(3.56,3.56)

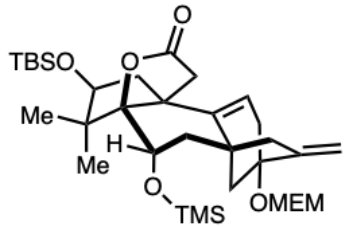

188

f2 (ppm)

f1 (ppm)

Parameter	Value
Data File Name	/ Volumes/ nmrdata/ jkthomps/ nmr/ JKT-7-284-2/ 5/ ser
Title	JKT-7-284-2.5.ser
Origin	Bruker BioSpin GmbH
Solvent	CDCl3
Temperature	297.1
Pulse Sequence	hmbcetgpl3nd
Experiment	HMBC
Number of Scans	4
Receiver Gain	197.4
Relaxation Delay	2.0000
Pulse Width	12.5000
Acquisition Time	0.4260
Acquisition Date	2025-07-15T23:39:07
Spectrometer Frequency	(400.13,100.62)
Spectral Width	(4807.7,22321.4)
Lowest Frequency	(-163.1,-1116.4)
Nucleus	(1H,13C)
Acquired Size	(2048,256)
Spectral Size	(2048,1024)
Digital Resolution	(2.35,21.80)

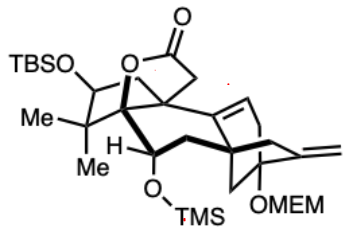

188

f2 (ppm)

f1 (ppm)

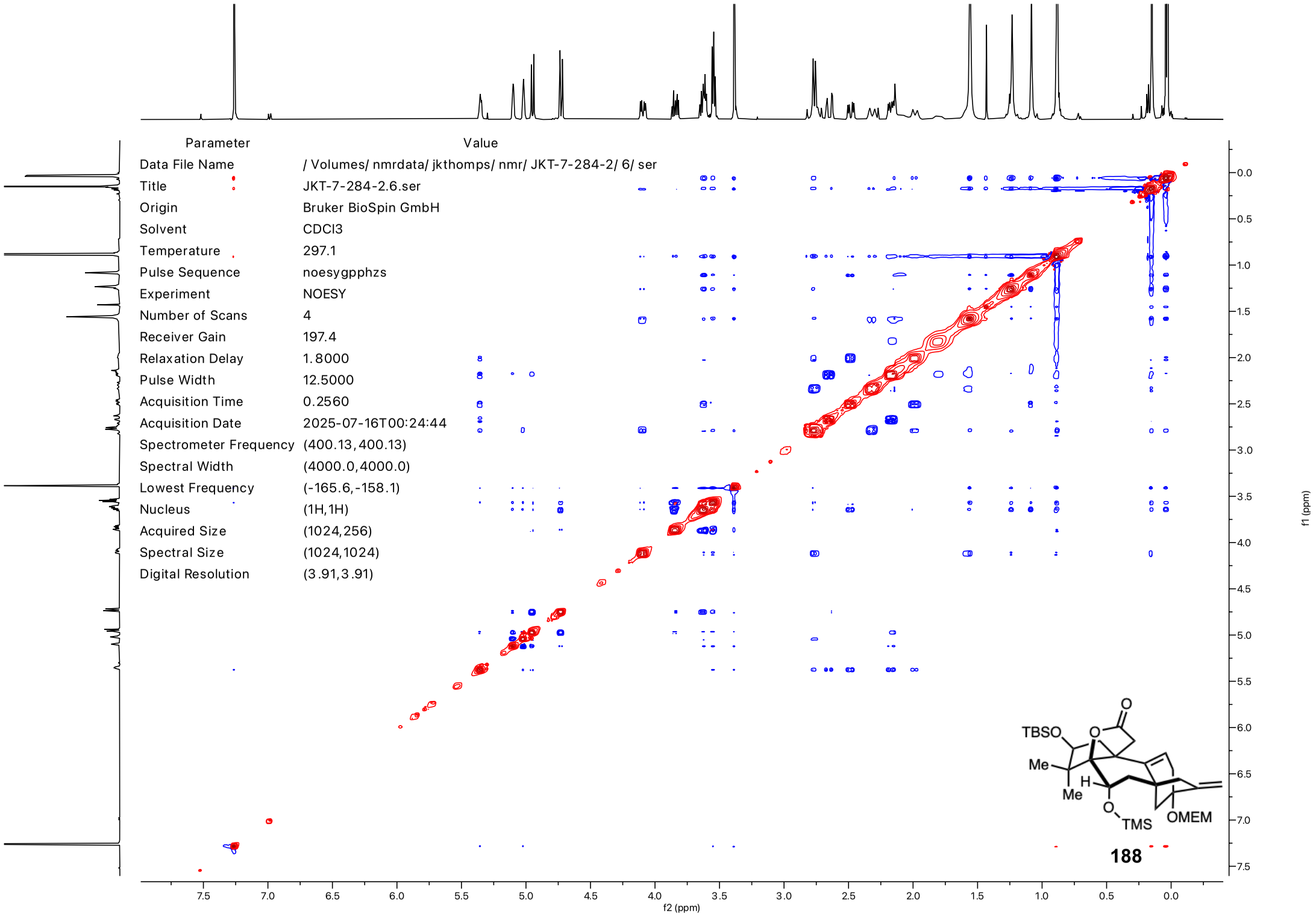
Parameter Value
Data File Name / Volumes/ nmrdata/ jkthomps/ nmr/ JKT-7-284-2/ 6/ ser
Title JKT-7-284-2.6.ser
Origin Bruker BioSpin GmbH
Solvent CDCl3
Temperature 297.1
Pulse Sequence noesygpphzs
Experiment NOESY
Number of Scans 4
Receiver Gain 197.4
Relaxation Delay 1.8000
Pulse Width 12.5000
Acquisition Time 0.2560
Acquisition Date 2025-07-16T00:24:44
Spectrometer Frequency (400.13,400.13)
Spectral Width (4000.0,4000.0)
Lowest Frequency (-165.6,-158.1)
Nucleus (1H,1H)
Acquired Size (1024,256)
Spectral Size (1024,1024)
Digital Resolution (3.91,3.91)
TBSO
O
Me
H
Me
O
TMS
OMEM
188
f2 (ppm)
f1 (ppm)

Chapter 6

End Game[†]

6.1 INTRODUCTION

This chapter describes the completion of the first enantioselective synthesis of (+)-auriculatol A from the key pentacyclic intermediate (**105**) accessed in Chapter 5. Various olefin functionalization strategies, lactone reduction, and hydrogenation strategies were investigated. Although many routes were explored, the successful route overcame challenges in the diastereoselective C9-C11 double bond reduction, culminating in the first synthesis of (+)-auriculatol A (**49**) and (+)-9-*epi*-auriculatol A (**219**) in 19 steps from 1,4-dioxaspiro[4.5]decan-8-one. The studies captured in this chapter could provide a synthetic

---

[†] Portions of this chapter were adapted from the following communication: Thompson, J. K.; Youngblood, K. C.; Teh, S. Y. H.; Farley, C. M.; Zhang, Z.; Virgil, S. C.; Reisman, S. E. *J. Am. Chem. Soc.* **2025**, *147*, 42170–42174. Scott C. Virgil is acknowledged for his analytical chemistry expertise, especially in completing the separation of the natural product from its C9-epimer. J.K.T. was supported by the NSF GRFP (DGE-1745301). S.E.R. acknowledges fellowship support by the NIH (R35GM118191).

blueprint for the future end-game of related grayanane natural products.

6.2 PREFUNCTIONALIZED *EXO*-OLEFIN STRATEGIES

6.2.1 Mukaiyama hydration of the exo-olefin

With a fragment coupling and intramolecular cyclization strategy established, efforts were centered around the end-game stages of the synthesis. One of the strategies that emerged as potentially fruitful became Mukaiyama hydration of the *exo*-olefin. Preliminary studies on the 3.2.1 bicycle drew inspiration from the reaction development of Shenvi and coworkers, among others.[1-6] We were particularly inspired by Carreira and coworker's use of Shenvi's conditions toward (±)-indoxamycin B, which formed 49% yield of product in the presence of other olefins (Scheme 6.1).[7]

Scheme 6.1. *Precedent for Mukaiyama hydration of exo-olefins.*[7]

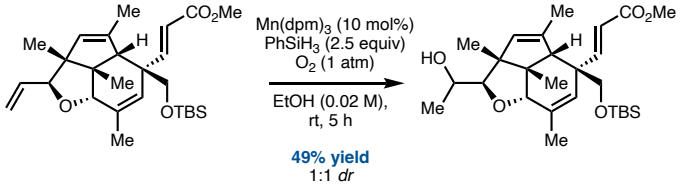

It was thought that Mukaiayma hydration early in the 3.2.1 bicycle synthesis could provide a fragment that could be leveraged in the vinylogous Mukaiyama aldol addition. Indeed, both substrates **107B** and **141** were competent using Shenvi's protocol, but the reaction proceeded in low diastereoselectivity (Scheme 6.2 and Scheme 6.3). Performing a temperature screen on substrate **107B**, the highest *dr* and yield at −20 °C (Scheme 6.2). Warming to room temperature led to lower observed diastereoselectivity (~1.1:1, not shown).

Scheme 6.2. *Preliminary results in the Mukaiyama hydration of exo-olefins: Temperature screen on substrate* ***107B***.

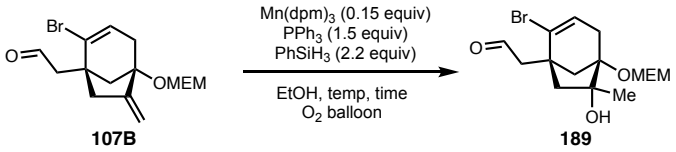

107B **189**

entry	temp	time	conversion	*dr*	yield (%)
1	0 °C	1 h	>99	2.1 : 1	48
2	–20 °C	3.5 h	>99	3.5 : 1	50
3	–40 °C	12 h	58	2.3 : 1	21
4	–78 °C to 21 °C	12 h	90	2.3 : 1	< 10

Later studies on substrate **141** revealed the effect of catalyst loading on the diastereoselectivity, with higher catalyst loadings giving higher *dr* (Scheme 6.3). It was hypothesized that the higher catalyst loading would increase the presence of inner-sphere manganese intermediates that could undergo inner-sphere oxygen-atom transfer and result in higher *dr*. Nevertheless, the improvement in *dr* was moderate at best, and scaling up of the reaction led to lower *dr* (not shown).

Scheme 6.3. *Preliminary results in the Mukaiyama hydration of exo-olefins: Catalyst loading screen on substrate* ***141***.

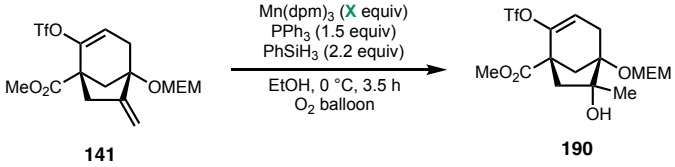

141 **190**

entry	X	conversion	*dr*	yield (%)
1	0.15	90	2.4 : 1	52
2	0.3	>99	2.6 : 1	49
3	1	>99	3.3 : 1	47

While not extensively tested, the vinylogous Mukaiyama aldol addition containing the hydrated *exo*-olefin did not proceed very effectively. Preliminary data showed low

yields (19%) and lower conversions than the optimized substrates containing the *exo*-olefin (Scheme 6.3).

Scheme 6.3. *Preliminary results on the tertiary alcohol substrate* ***189*** *in the VMAR.*

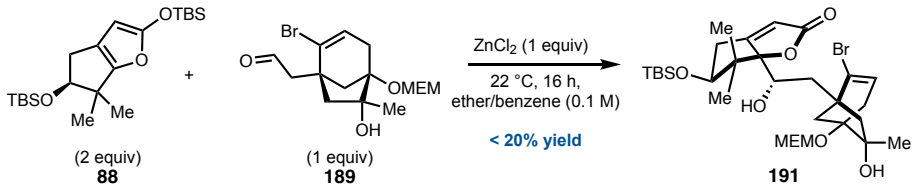

As a result of the shortcomings of the pre-hydrated olefin tactic, it was envisioned that Mukaiyama hydration of the *exo*-alkene could be accomplished prior to Ni-catalyzed α-enolate alkenylation but after the VMAR. To this end, a brief screen of conditions identified $Mn(dpm)_3$ as the best catalyst when compared to $Co(dpm)_3$, $Co(acac)_3$, and $Mn(acac)_3$ (not shown). After a brief optimization effort, the two diastereomers (**192**) could be isolated in 64% yield and 2.7:1 *dr* (Scheme 6.4A). While the yield of the reaction was considered adequate, the *dr* of the reaction was still only moderate. Our attention turned to Studer's Fe-mediated oxygenation conditions, which employ an organic oxidant and are reported to provide higher *dr*;[8] however, the presence of the alkenyl bromide in substrate **282B** likely thwarted the attempt. A complex reaction mixture with no detectible product was formed (Scheme 6.4B).

Scheme 6.4. *Mukaiyama hydration prior to Ni-alkenylation*

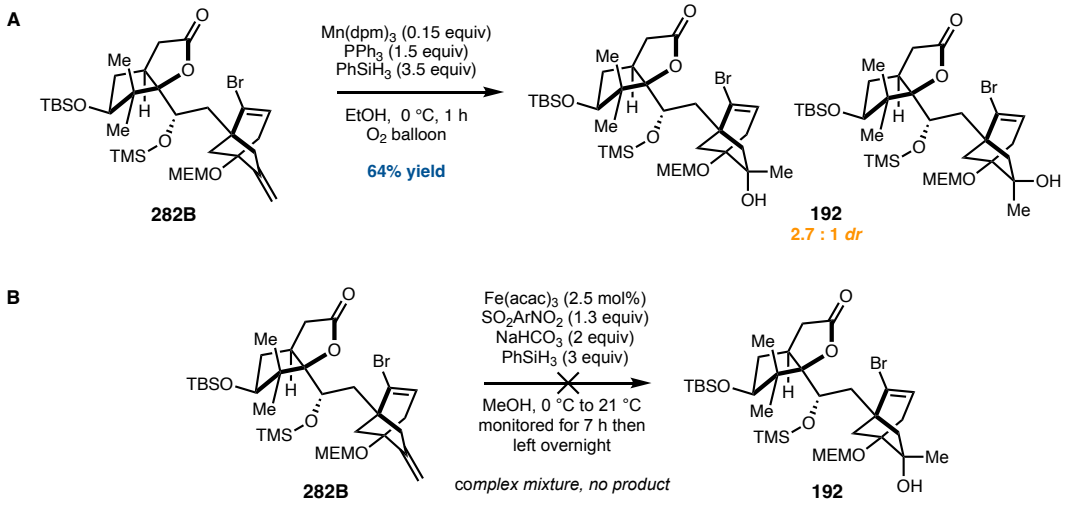

Protection of the tertiary alcohol prior to the Ni-catalyzed alkenylation reaction was necessary. The alkenylation reaction was very sensitive to polar functionalities, including alcohols or other chelating groups. Additionally, traces of $CDCl_3$, MeOH, O_2, H_2O, and other alcohol-containing impurities were found to be detrimental to the reaction. As a result, a protection sequence was pursued. In general, the yield of the Mukaiyama hydration and the protection were reported in the two-step protocol, yielding **193** and **194** from a common starting material (**192**). Separation of both the MOM ether product (**193**) and the TMS ether (**194**) were effectively completed by preparatory TLC or pipet column, although the yield of the process was relatively low due to the difficulty of achieving separation of the diastereomers.

6.2.2 Elaboration of hydrated products

Scheme 6.5. *Protection of tertiary alcohol in* ***192****.*

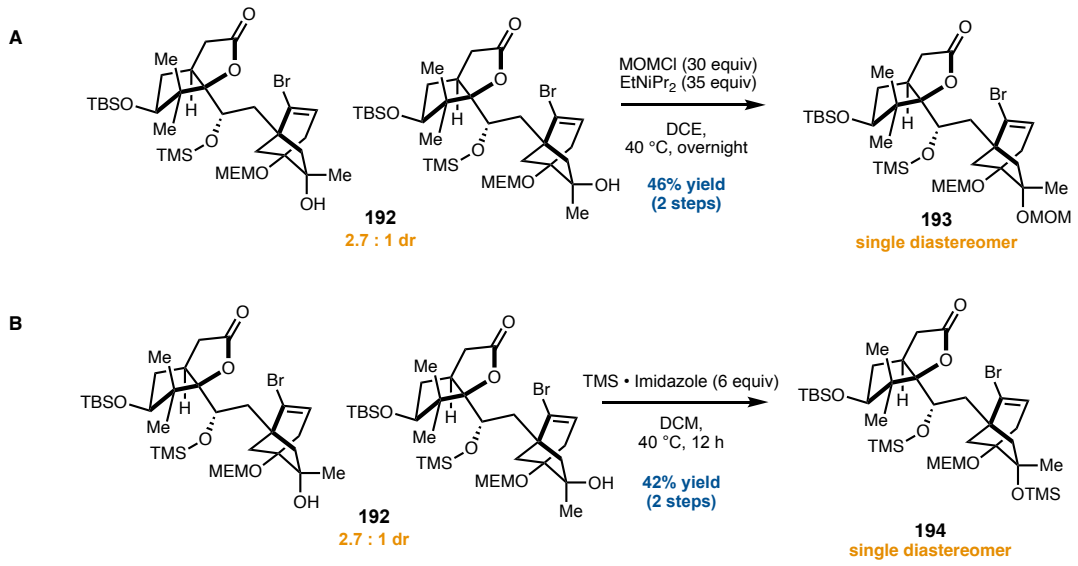

When both substrates were attempted in the Ni-catalyzed α-enolate alkenylation reaction, to our surprise, only substrate **194** provided high yields of the respective product (**196**, Scheme 6.6B). It was hypothesized that the chelating nature of the MOM and MEM group – and the additive effect that the Ni-center experienced due to their proximity – could have inhibited the reaction with substrate **193** (Scheme 6.6A).

Scheme 6.6. *Ni-catalyzed α-enolate alkenylation on substrates* ***193*** *and* ***194****.*

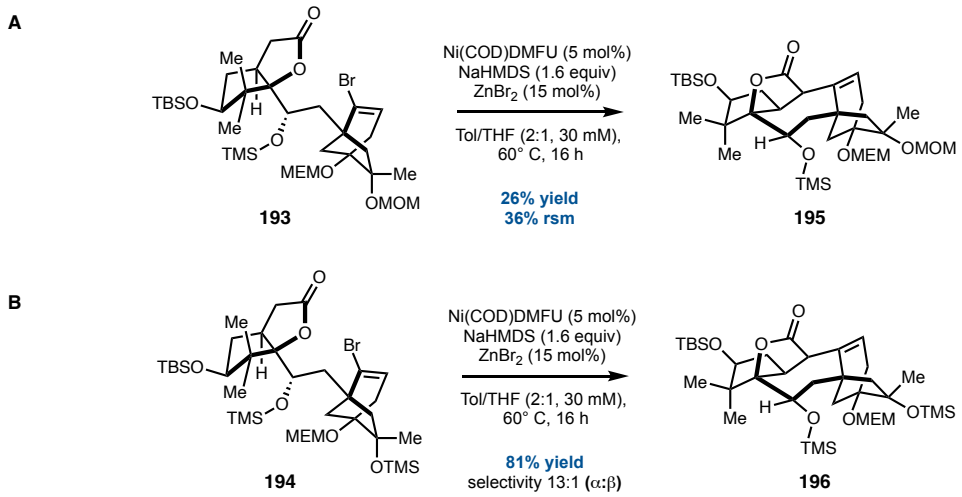

With access to pentacyclic product **196**, subsequent steps focused on the reduction of the trisubstituted olefin. Very quickly, it became clear that the trisubstituted olefin was quite hindered and resistant to hydrogenation. Both Pd/C and Crabtree's catalyst were incompetent at 1 atm in MeOH and DCM, respectively (Scheme 6.7A); however, the literature precedent for similar types of bicyclic systems indicated that much higher pressures of hydrogen would be needed.[9-12] In contrast, under metal hydrogen atom transfer (MHAT) conditions, a single diastereomer of **198** was isolated in 71% yield (Scheme 6.7B). NOESY analysis determined that the product possessed the undesired stereochemistry at C9. A correlation between C1 and C9 in the NOESY was observed. The MHAT literature confirmed that hydrogen atom transfer (HAT) likely involves a complex mechanism, involving both inner-sphere and cage escaped intermediates.[2] Nevertheless, the product formed may be referred to as the *thermodynamic* product, owing to the *trans* nature of the substituents when the reaction forms a ring fusion stereocenter and the mechanism by which the product forms from the radical intermediate.[13] On the other hand, homogeneous or heterogeneous olefin hydrogenation may exhibit complimentary

selectivity to MHAT olefin hydrogenation, due to the different mechanism these reactions operate.[13] For the simple case of Pd/C, the hydrogenation is most often depicted to hydrogenate the face of the molecule that is the most accessible and least hindered by the large heterogeneous palladium catalyst and may provide different selectivity than the MHAT method. Due to the interplay of these mechanistic heuristics, high-pressure hydrogenation was pursued as a strategy to overturn the C9-C11 hydrogenation diastereoselectivity.

Scheme 6.7. *MHAT reduction of* ***196***.

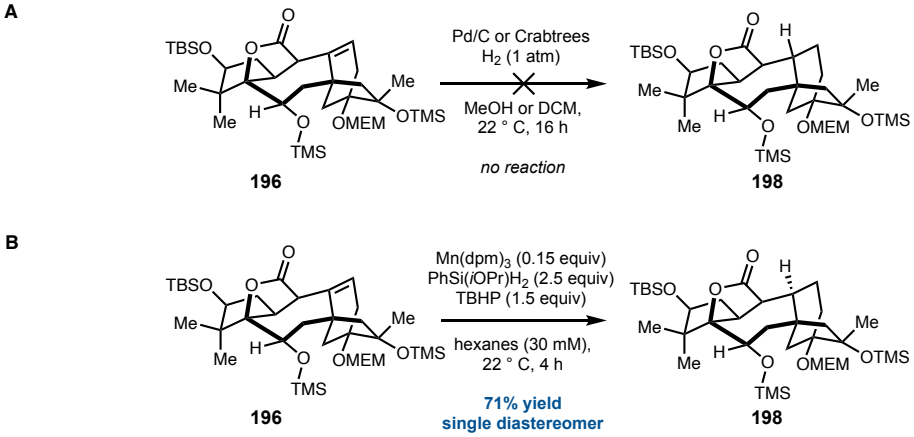

A survey of homogeneous and heterogeneous catalysts were tested to induce the hydrogenation of **196**. Unfortunately, the alkene proved unreactive to the attempts, and only protecting group cleavage was observed. It is likely that the olefin is hindered and would require higher pressures (80-100 bar).

Scheme 6.8. *Hydrogenation screen on substrate* ***196***.

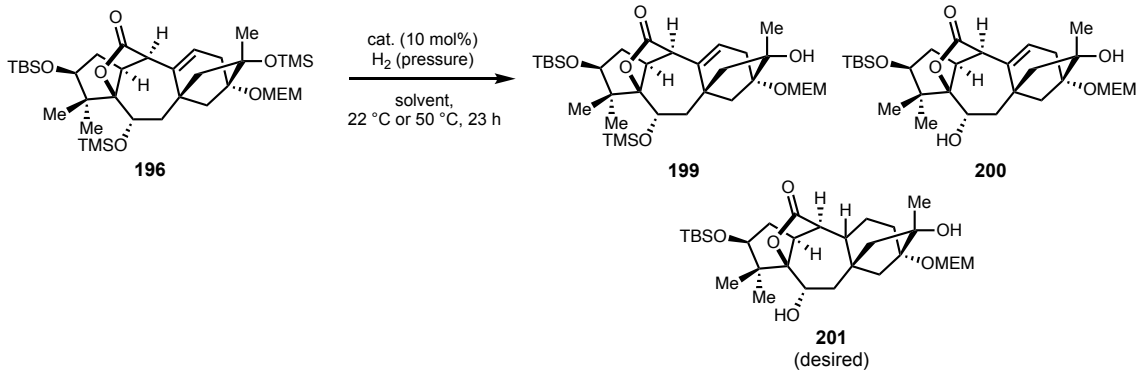

entry	scale	cat.	pressure (bar)	solvent	**199**	**200**	**201**
1	1.8 mg	Pd/C	67	MeOH	19	56	-
2	1.8 mg	PtO_2	65	MeOH	5	70	-
3	1.8 mg	Crabtrees	65	DCM	84	-	-
4	1.8 mg	Pd/C	65	EtOAc	31	43	-
5	1.8 mg	PtO_2	65	EtOAc	29	43	-
6	1.8 mg	Crabtrees	67	IPA	-	65	-
7	1.8 mg	Crabtrees	67	THF	55	-	-

6.2.3 Synthesis of new hydrogenation substrates

In order to more easily test the hydrogenation, substrate **202** was pursued for several reasons: 1) it was hypothesized that the Me group in **196** may be sterically blocking the desired face of the alkene 2) substrate **202** does not contain the labile tertiary OTMS group that was cleaved under hydrogenation and 3) substrate **202** circumvents the Mukaiyama hydration and the low *dr* of the step, allowing for better material throughput. Substrate **202** was formed from **105** using canonical Lemieux-Johnson oxidation conditions.[18-20] The optimization of the reaction went smoothly. Use of 2,6-lutidine as an additive was detrimental to the conversion of the reaction (Scheme 6.10, entry 1).[21] Increasing the catalyst loading led to better conversions rather than stirring the reaction for longer periods of time (Scheme 6.10, entries 1-2). Close monitoring of the reaction by TLC was required.

Scheme 6.10. *Synthesis of hydrogenation substrate* ***202***.

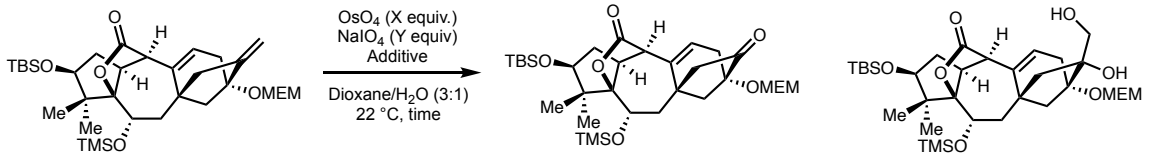

105 **202** **203**

entry	X	Y	Additive	time	ketone	diol	starting material
1	0.01	2	2,6-lutidine	4 h	-	-	91
2	0.05	6	-	48 h	27	20	-
3	0.10	6	More $NaIO_4$ (6 equiv)	16 h then 5 h	57	3	10
4	0.10	6	More $NaIO_4$ (6 equiv)	16 h then 8 h	40	13	-

Hydrogenation of substrate **202** proceeded in full conversion in the presence of both Pd/C and PtO_2 but not Crabtree's catalyst to form **204** (Scheme 6.11). NOESY analysis of **204** again revealed a correlation between C1 and C9, indicating the α-orientation of both hydrogens, which was confirmed upon deprotection of **204** in a separate step (not shown).

Scheme 6.11. A. *Hydrogenation of substrate* ***202***.

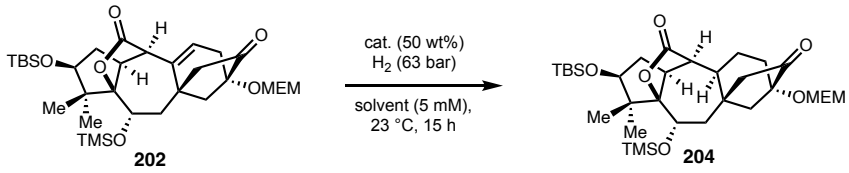

202 **204**

entry	cat.	solvent	*dr*	yield (%)
1	Pd/C	EtOAc	> 20 : 1	89
2	PtO_2	EtOAc	5 : 1	83
3	Crabtree's	DCM	-	no reaction

As a result of the difficulty of both MHAT reduction and high-pressure hydrogenation, goals to induce selective Mukaiyama hydration were prioritized in order to allow for better material throughput to intermediates closer to the end.

6.3 SELECTIVE FUNCTIONALIZATION STRATEGIES

6.3.1 Elaboration of substrate 105

Due to the difficulty of achieving diastereoselective hydrogenation of the C9-C11 double bond, strategies to induce epimerization of the C6 secondary alcohol were pursued directly following the Ni-catalyzed α-enolate alkenylation reaction. The TMS silyl ether could be cleaved utilizing PPTS in MeOH, affording **205** in 89% yield (Scheme 6.12). Then, the secondary alcohol could be oxidized using IBX in DMSO, providing **206** in 74% yield. Notably for this reaction, use of DMP or Swern oxidation led to incomplete conversions and diminished yields.

Scheme 6.12. *Deprotection/oxidation sequence on pentacycle* ***105***.

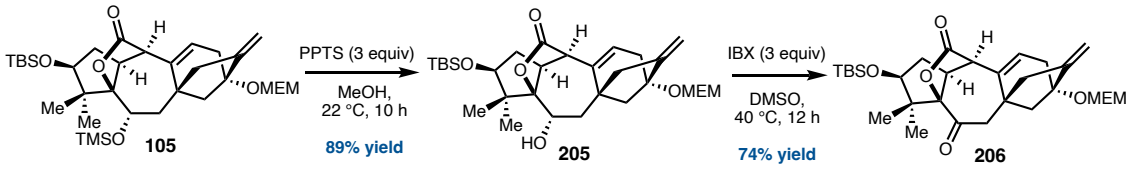

Both the substrates **205** and **206** were tested in the Mukaiyama hydration conditions from Scheme 6.4A. Unfortunately, in both cases, <10% yield of the product was isolated.

Scheme 6.13. *Failed Mukaiyama hydration of substrates* ***205*** *and* ***206***.

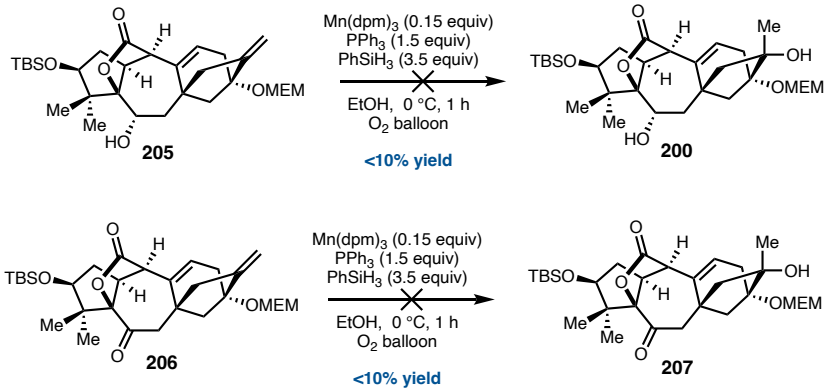

Acid mediated hydration was also attempted using 3M HCl. Unfortunately, under these conditions, a Semi-Pinacol rearrangement to form **306** in 87% yield was observed (Scheme 6.14A).[28] While the result was interesting, it was not useful for the auriculatol A synthesis. Nevertheless, searching the literature, it became apparent that a different natural product, micranthanone A, could be mapped on to this scaffold. While studies toward micranthanone were not thoroughly explored, the rearrangement of [3.2.1]-bicyclic compounds containing the bridgehead hydroxyl to the bicyclic scaffold of micranthanone could present future avenues for exploration.

Scheme 6.14. A. *Acid-mediated rearrangement of* ***105****.* ***B.*** *Micranthanone A: a future avenue for exploration.*

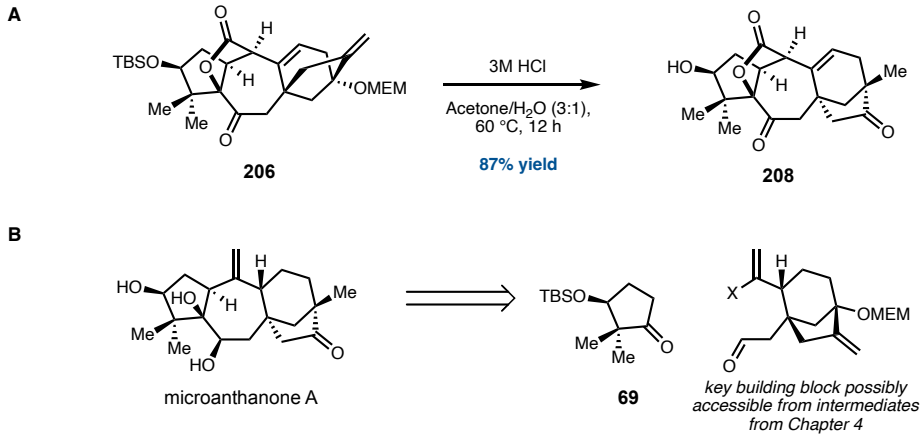

Pivoting away from the Mukaiyama hydration, a double reduction protocol to target **210** was pursued. Upon treatment with excess DIBAL, 40% yield of **210** was obtained utilizing CH_2Cl_2 as solvent (Scheme 6.15, entry 1). Unfortunately, in ethereal solvents, **209** was almost exclusively formed (Scheme 6.14, entry 2-3). Switching back to CH_2Cl_2, it was found that the yield could be slightly increased when the reaction was warmed to 0 °C. Importantly, warming of the reaction higher than 0 °C leads to unselective deprotection of the TBS or MEM either, or both, creating mixtures that are difficult to characterize. The

final yield of **210** may vary slightly but typically ranges from 45-52% yield (Scheme 6.14, entry 4-5). Reproducibility of this reaction may be a concern, likely due to the temperature dependence of the reaction, which could be affected by the rate of warming of the reaction, the rate of addition of DIBAL, and the quality of the reagent. Unfortunately, attempts to manipulate **210** for selective olefin functionalization to progress this compound failed.

Scheme 6.15. *DIBAL reduction of ketone* ***206****.*

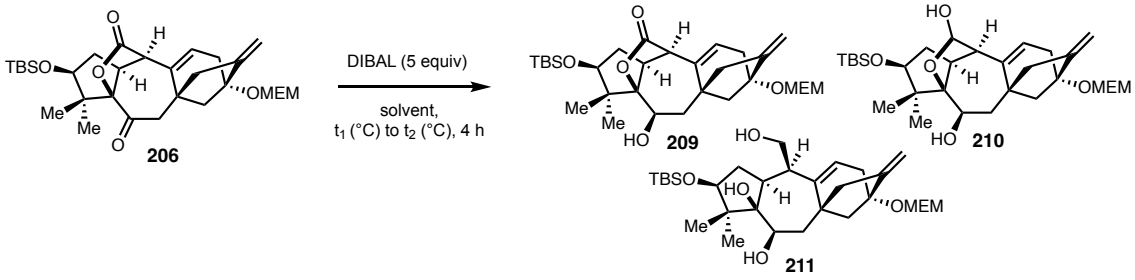

entry	scale	t_1 (°C)	t_2 (°C)	solvent	starting material (%)	**209** (%)	**210** (%)	**211** (%)
1	1.5 mg	–78 °C	–78 °C	DCM	16	17	40	22
2	3.0 mg	–78 °C	0 °C	THF	-	73	< 10	< 10
3	1.5 mg	–78 °C	0 °C	Et_2O	-	69	< 10	< 10
4	1.5 mg	–78 °C	0 °C	DCM	-	12	45	23
5	1.5 mg	–78 °C	0 °C	DCM	-	11	52	23

* caution: allowing the reaction to warm higher than 0 °C will lead to silyl ether cleavage or MEM reduction to the methyl ether.

Other functionalization strategies were envisioned on substrate **105** to provide more viable synthetic routes to intermediates that could help overturn the selectivity of the C9-C11 hydrogenation. One potential strategy includes hydroboration of the *exo*-olefin.[16-17] Upon treatment with 9-BBN, no reaction was observed (Scheme 6.16A). A series of dihydroxylation conditions were tested to no avail (Scheme 6.16B).[22]

Scheme 6.16. A. *Attempted hydroboration of* ***105****.* ***B.*** *Attempted dihydroxylation of* ***105****.*

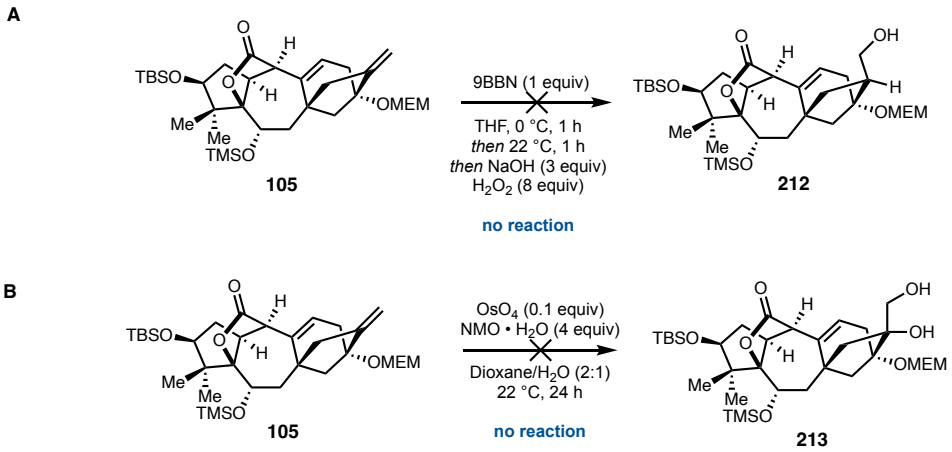

Turning to reductive lactone opening, diol **215** was targeted as a substrate that could direct the hydrogenation of the C9-C11 double bond. To our surprise, the lactone proved resistant to opening, even upon treatment with 3 equiv. of LAH (Scheme 6.17A). The reaction could be optimized to form **214** in 80% yield upon treatment with DIBAL (Scheme 6.17B). Excitingly, installation of the methyl acetal (**216**) occurred smoothly and forming the correct diastereomer with regard to auriculatol A (Scheme 6.17C). The NOESY assignment of this compound is largely based on correlations between the methyl acetal hydrogen and other methylene hydrogens on nearby rings. Modeling of this compound, either in Avogadro or through use of a plastic model, suggests that in most conformations of this structure, the hydrogens highlighted in blue should be in close proximity. DFT computations in order to sample the lowest energy conformations of this and related structures were performed.

Scheme 6.17. A. *Reductive lactone opening attempt with LAH* ***B.*** *Yield of DIBAL reduction to access* ***214****.* ***C.*** *Methyl acetal installation on substrate* ***216****.*

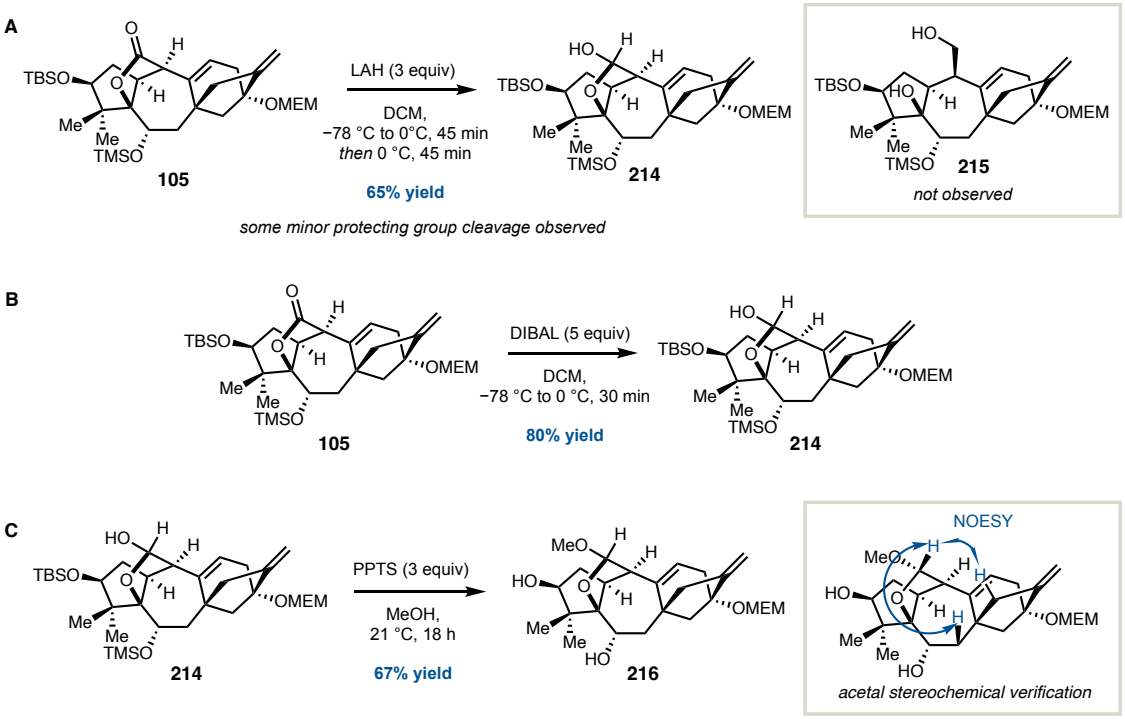

6.3.2 Completion of the synthesis of (+)-auriculatol A

Substrate **105** was more exhaustively investigated with respect to Mukaiyama hydration of the *exo*-olefin. While $Mn(dpm)_3$ and $Fe(acac)_3$ were ineffective in the transformation, use of $Co(acac)_2$ uniquely delivered the product in 80% yield as a single diastereomer (**199**, Scheme 6.18B).[23-25] For more information on Co-mediated MHAT catalysis, see the following recent references.[26,27]

Scheme 6.18. *Successful Mukaiyama hydration of* ***105****.*

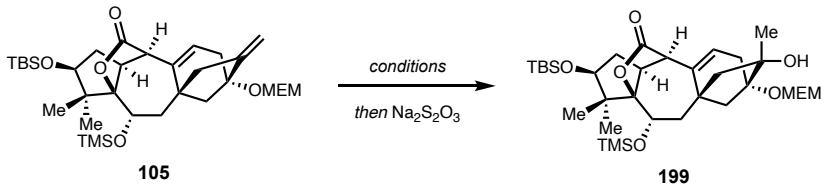

105 **199**

entry	*conditions*	*dr*	yield (%)
1	$Mn(dpm)_3$ (0.15 equiv), $PhSiH_3$ (2.2 equiv), O_2	-	< 10
2	$Fe(acac)_3$ (2.5 mol%), SO_2ArNO_2 (1.3 equiv) $NaHCO_3$ (2 equiv), $PhSiH_3$ (3 equiv)	> 20 : 1	19
3	$Co(acac)_2$ (0.2 equiv.), $PhSiH_3$ (2 equiv), O_2	> 20 : 1	80

Substrate **199** can be advanced in a 2-step protocol to **200** through TMS-deprotection and to **206** through IBX-oxidation (Scheme 6.19). With access to **206**, DIBAL reduction occurred in 61% yield to form **217** along with 24% 6-*epi*-**217** (see experimental procedures for more information). Treatment with acidic methanol converted **218** to C9-C11-dehydro-auriculatol A by way of acetal exchange and global deprotection. Using MHAT conditions developed by Shenvi and coworkers[30], the reduction to (+)-auriculatol A occurred in 43% yield along with 41% yield (+)-9-*epi*-auriculatol A (**219**). The NMR data for **49** is consistent with that reported by Yao and coworkers (see the Experimental Section for more information).[31]

Scheme 6.19. *The successful end-game strategy: elaboration to the natural product.*

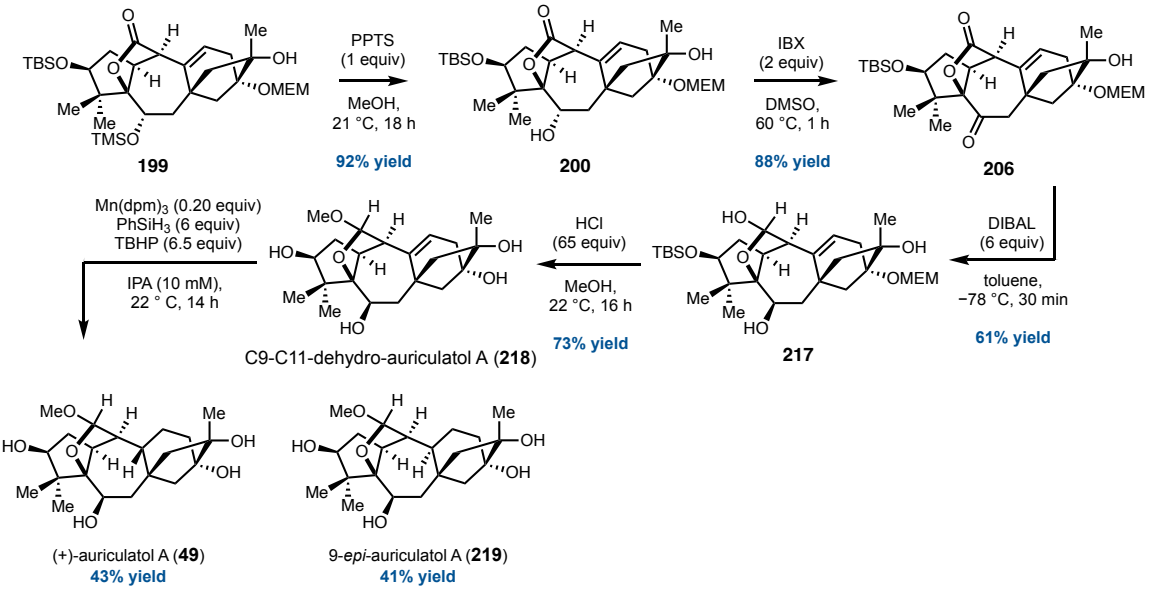

6.4 CONCLUDING REMARKS

This chapter describes early efforts in selective Mukaiyama hydration of the *exo*-olefin on several substrates, both before and after the VMAR. While Mukaiyama hydration prior to the VMAR was challenging, conducting the reaction after the VMAR but before the Ni-catalyzed α-enolate alkenylation was possible. Although the *dr* of the Mukaiyama hydration was low, a protection sequence allowed for separation of diastereomers. The MOM-protected tertiary alcohol was not a competent substrate in the α-enolate alkenylation, but the TMS-protected tertiary alcohol was.

With access to a cyclized product bearing the hydrated alkene, hydrogenation of the C9-C11 bond was pursued. While resistant to hydrogenation, the compound could be subjected to radical based MHAT hydrogenation conditions to produce the α-stereochemistry at the newly formed ring fusion stereocenter. This was unfortunate, as the

β-stereochemistry is what is required in the natural product.

Various hydrogenation substrates and strategies were investigated to overturn the selectivity. A Lemeiux-Johnson was developed to selectively cleave the *exo*-olefin of the Ni-catalyzed α-enolate alkenylation product; however, these substrates were also not competent at delivering the correct C9-stereochemistry. Ultimately, a synthesis of C9-C11-dehydro-auriculatol A was devised after optimization of the DIBAL reduction to deliver direduced compound. Testing the hydrogenation on this new substrate provided a ~1.1:1.0 mixture of the natural product and 9-*epi*-auriculatol A, which could be separated using preparatory HPLC.

6.5 EXPERIMENTAL SECTION

Preparation of hydrated product 189.

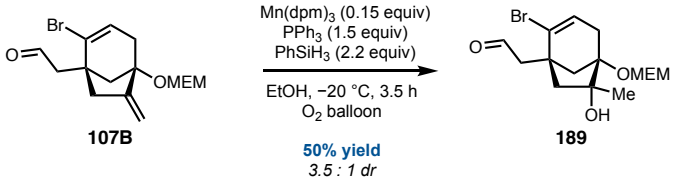

$Mn(dpm)_3$ (0.15 equiv) and PPh_3 (1.50 equiv) were weighed out outside the glovebox and added to a vial containing the starting material (1 equiv). EtOH (1.2 mL, 77.0 mM) was added in at once and it was stirred until all PPh_3 dissolved (5 min). The vial was cooled to −20 °C. An O_2 balloon with a thick, purple needle was added on. After the dropwise addition of $PhSiH_3$ (3.5 equiv), the reaction mixture was then stirred under an oxygen atmosphere at −20 °C for 3.5 hrs. To quench the reaction, sat. aq. $Na_2S_2O_3$ was added. The reaction was stirred for 1 h before the aq. phase was extracted with EtOAc (4x). Then, it was concentrated *in vacuo* and eluted through a short pipette plug of silica gel with

pure ether (5 column volumes) to remove the Mn in solution. Upon crude NMR, a 3.5 : 1 *dr* and full conversion with no peroxide adduct was observed. The crude mixture was purified via column, eluting with 50% EtOAc/Hex to isolate the product **189** (50% yield).

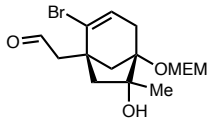

189

TLC (75% EtOAc/Hexanes): R_f 0.5 ($KMnO_4$).

^{1}H NMR ($CDCl_3$, 400 MHz): δ 9.79 (dd, *J* = 1.9, 1.1 Hz, 1H), 5.92 (dd, *J* = 5.0, 2.8 Hz, 1H), 4.94 – 4.84 (m, 2H), 3.78 (dt, *J* = 11.0, 4.7 Hz, 1H), 3.75 – 3.68 (m, 1H), 3.54 (t, *J* = 4.6 Hz, 2H), 3.38 (s, 3H), 3.25 (s, 1H), 3.06 (dd, *J* = 17.7, 1.2 Hz, 1H), 2.72 (dd, *J* = 17.7, 2.8 Hz, 1H), 2.46 – 2.22 (m, 4H), 2.08 (dd, *J* = 13.5, 2.3 Hz, 1H), 1.85 (d, *J* = 13.5 Hz, 1H), 1.27 (s, 3H).

^{13}C NMR ($CDCl_3$, 101 MHz): δ 200.50, 130.76, 126.78, 91.78, 84.28, 78.36, 71.84, 67.89, 59.22, 54.39, 52.12, 45.33, 42.84, 36.98, 25.16.

FTIR (Neat, NaCl, thin film): 2930, 1667, 1145, 1011, 996, 756 cm^{-1}.

HRMS (ESI): calc'd for $[M+H]^+$ 363.0802, found 363.0802.

Preparation of tertiary alcohol 192.

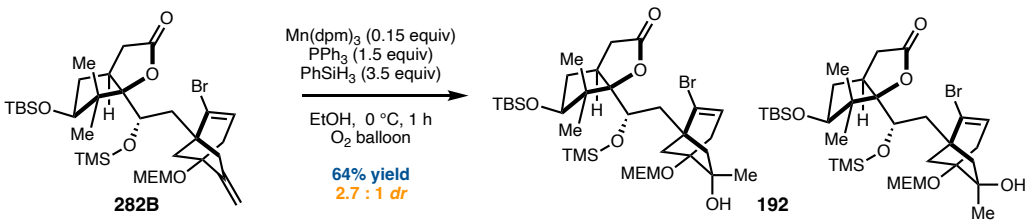

$Mn(dpm)_3$ (8.3 mg, 13.7 umol, 0.15 equiv) and PPh_3 (33.5 mg, 128 umol, 1.40 equiv) were weighed out outside the glovebox and added to a vial containing the starting material (64.0

mg, 91.2 umol, 1 equiv). EtOH (1.2 mL, 77.0 mM) was added in at once and it was stirred until all PPh_3 dissolved (5 min). The vial was cooled to 0 °C. An O_2 balloon with a thick, purple needle was added on. After the dropwise addition of $PhSiH_3$ (40 µL, 319 umol, 3.5 equiv), the reaction mixture was then stirred under an oxygen atmosphere at 0 °C for 1.5 hrs. To quench the reaction, 1.20 mL sat. aq. $Na_2S_2O_3$ was added. The reaction was stirred for 1 h before the aq. phase was extracted with EtOAc (4 x 2 mL). Then, it was concentrated *in vacuo* and eluted through a short pipette plug of silica gel with pure ether (5 column volumes) to remove the Mn in solution. Upon crude NMR, a 2.7 : 1 *dr* and full conversion with no peroxide adduct was observed. The peroxide could be observed by TLC throughout the course of the reaction as a less-polar, pink spot staining with *p*-anisaldehyde. The crude mixture was purified via column, eluting with 30% EA to isolate the products as a thick, clear oil that can puff up into a white solid under high vac (50.0 mg, 76% yield). Notably, the diastereomers were inseparable at this stage and were isolated together.

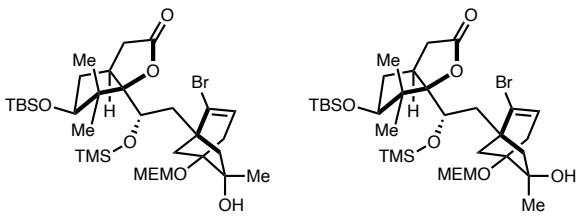

192

TLC (50% EtOAc/Hexanes): R_f 0.40 (*p*-anisaldehyde, grey/blue).

^{1}H NMR (400 MHz, $CDCl_3$): δ 5.81 (dd, *J* = 5.4, 2.6 Hz, 1H), 4.94 (d, *J* = 7.4 Hz, 1H), 4.86 (d, *J* = 7.4 Hz, 1H), 3.92 – 3.62 (m, 4H), 3.54 (q, *J* = 3.9 Hz, 2H), 3.38 (d, *J* = 3.8 Hz, 3H), 2.84 (ddd, *J* = 18.3, 11.3, 7.3 Hz, 1H), 2.76 – 2.47 (m, 2H), 2.38 – 2.11 (m, 5H), 2.12 – 1.88 (m, 3H), 1.87 – 1.59 (m, 3H), 1.48 (dt, *J* = 13.7, 2.9 Hz, 1H), 1.25 (d, *J* = 2.6 Hz, 3H), 1.09 (d, *J* = 4.2 Hz, 3H), 0.88 (s, 9H), 0.19 (s, 9H).

^{13}C NMR (101 MHz, $CDCl_3$): δ 175.43, 175.42, 134.38, 133.19, 131.82, 126.87, 125.39, 124.14, 124.10, 98.77, 98.57, 90.21, 89.85, 83.93, 82.79, 79.38, 77.37, 70.32, 66.35, 65.53, 64.48, 57.67, 57.63, 48.08, 44.57, 43.81, 42.95, 40.40, 39.49, 39.27, 38.28, 38.24, 37.73, 35.41, 34.02, 32.85, 28.94, 28.32, 27.04, 24.38, 23.76, 22.20, 19.33, 19.31, 16.71, 13.90, 12.82, 12.75, 0.00, -0.01, -6.01, -6.03, -6.43.

FTIR (DCM, NaCl, thin film): 3477, 2951, 2929, 1771, 1469, 1302, 1098, 1040, 889, 839 cm^{-1}.

HRMS (ESI): calc'd for $[M+NH_4]^+$ 741.2824, found 741.2854.

$[\alpha]_D^{23}$: +22.3 (c 1.0 in $CHCl_3$).

Preparation of MOM-protected 193.

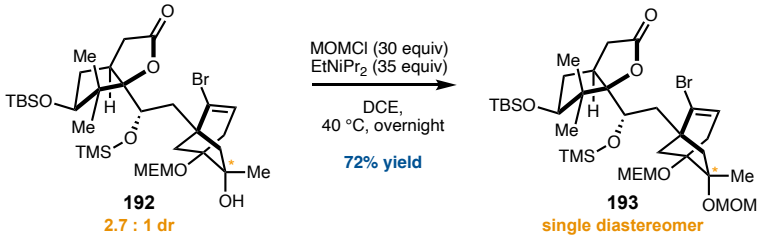

To a 2-dram vial was added the starting material (29.0 mg, 40.3 umol, 1 equiv.) and a magnetic stir bar. Dichloroethane (1.61 mL, 25.0 mM) was added, and the vial was agitated to ensure that the starting material is dissolved. Hunig's base (246 uL, 1.41 mmol, 35 equiv.) and MOMCl (92 uL, 1.21 mmol, 30 equiv.) were added sequentially, and the vial was capped and taped shut. The reaction was stirred at 40 °C. After 12 h, the reaction was worked up by filtration through silica (eluting with pure ether) then concentration down. Column chromatography with a gradient 10-20% EA/hex affords the product **193** as a single diastereomer as a pale yellow oil (22.2 mg, 72% yield).

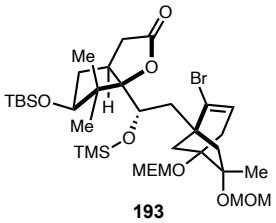

193

TLC (50% EtOAc/Hexanes): R_f 0.64 (*p*-anisaldehyde, blue).

^{1}H NMR (400 MHz, $CDCl_3$): δ 5.78 (dd, *J* = 5.2, 2.6 Hz, 1H), 5.08 (d, *J* = 7.5 Hz, 1H), 4.93 – 4.86 (m, 2H), 4.82 (d, *J* = 7.5 Hz, 1H), 4.63 (d, *J* = 7.3 Hz, 1H), 3.94 (s, 1H), 3.82 – 3.76 (m, 1H), 3.74 (dd, *J* = 4.3, 1.3 Hz, 1H), 3.67 (dt, *J* = 10.7, 4.9 Hz, 1H), 3.53 (t, *J* = 4.7 Hz, 2H), 3.37 (s, 3H), 3.34 (s, 3H), 2.87 (dd, *J* = 18.1, 11.3 Hz, 2H), 2.53 (dd, *J* = 17.9, 2.7 Hz, 1H), 2.44 (d, *J* = 10.7 Hz, 1H), 2.40 – 2.18 (m, 5H), 2.07 (d, *J* = 10.6 Hz, 1H), 2.01 – 1.89 (m, 2H), 1.72 (d, *J* = 15.0 Hz, 1H), 1.51 – 1.48 (m, 1H), 1.10 (s, 3H), 1.03 (s, 3H), 0.88 (s, 11H), 0.20 (s, 9H), 0.04 (d, *J* = 4.0 Hz, 6H).

^{13}C NMR (101 MHz, $CDCl_3$): δ 177.04, 134.33, 125.85, 100.15, 92.10, 91.76, 85.18, 84.15, 71.92, 71.85, 67.19, 59.17, 55.37, 49.61, 45.39, 41.92, 41.21, 39.86, 39.21, 38.87, 30.46, 29.84, 25.89, 23.69, 22.83, 21.84, 18.23, 14.27, 1.44, -4.51, -4.56, -4.91.

FTIR (Neat, NaCl, thin film): 2928, 2860, 1780, 1715, 1562, 1212, 1093, 1048, 1030, 840 cm^{-1}.

HRMS (ESI): calc'd for $[M+NH_4]^+$ 780.3532, found 780.3563.

Preparation of TMS-protected 194.

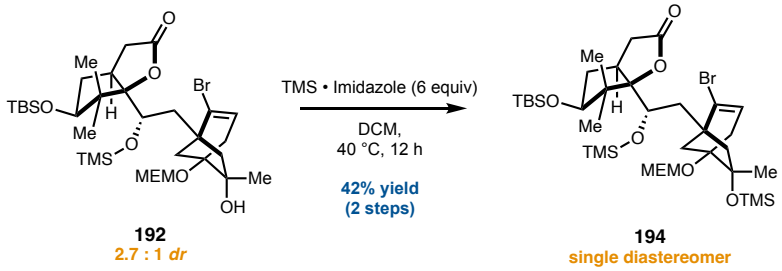

The starting material (50.0 mg, 69.5 umol, 1 equiv.) as a 2.7:1 mixture of diastereomers was added to a 2-dram vial with a magnetic stir bar, and DCM (347 uL, 200 mM) was added in. The solution was treated with TMS-imidazole (102 uL, 695 umol, 10 equiv.) and the reaction was capped and heated to 40 °C overnight. Following completion of the reaction, as indicated by TLC analysis in 50% EtOAc/Hex, the reaction was quenched by addition of H_2O (1 mL). The resulting solution was extracted with DCM (3 x 1 mL), washed with saturated aq. NH_4Cl (3 x 1 mL), brine, and dried with sodium sulfate. Upon filtration and concentration, the mixture of diastereomers were carefully subjected to column chromatography, eluting with 10% EtOAc/Hex in order to isolate the major product **194** as a single diastereomer (36.3 mg, 66% yield) as a pale yellow oil. Notably, the desired diastereomer is the less-polar spot on the TLC plate.

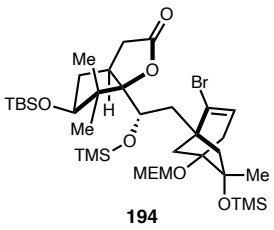

TLC (25% EtOAc/Hexanes): R_f 0.40 (*p*-anisaldehyde, dark blue).

^{1}H NMR (400 MHz, $CDCl_3$): δ 5.77 (dd, J = 5.2, 2.6 Hz, 1H), 5.20 (d, J = 7.5 Hz, 1H), 4.76 (d, J = 7.5 Hz, 1H), 3.94 (broad s, 1H), 3.82 – 3.74 (m, 2H), 3.66 – 3.61 (m, 1H), 3.53

(dd, J = 5.3, 4.2 Hz, 2H), 3.37 (s, 3H), 2.85 (dd, J = 18.1, 11.2 Hz, 1H), 2.78 (broad s, 1H), 2.49 – 2.42 (m, 2H), 2.32 – 2.20 (m, 3H), 2.04 – 1.97 (m, 2H), 1.81 (d, J = 13.7 Hz, 1H), 1.72 (dd, J = 15.2, 2.8 Hz, 1H), 1.48 (dd, J = 13.5, 3.3 Hz, 1H), 1.32 (s, 3H), 1.08 (s, 3H), 0.88 (s, 9H), 0.20 (s, 9H), 0.12 (s, 9H).

^{13}C NMR (101 MHz, $CDCl_3$): δ 176.98, 134.40, 125.92, 99.88, 91.83, 83.37, 82.91, 71.95, 66.97, 59.13, 49.53, 45.25, 41.67, 41.31, 39.89, 39.46, 39.25, 38.80, 30.45, 29.83, 25.88, 25.62, 23.54, 20.62, 18.21, 2.77, 1.46, -4.50, -4.90.

FTIR (Neat, NaCl, thin film): 2953, 2929, 1779, 1251, 1163, 1101, 1046, 889, 838, 773, 753 cm^{-1}.

HRMS (ESI): calc'd for $[M+H]^+$ 791.3400, found 791.3402.

$[\alpha]_D^{23}$: +14.5 (c 1.0 in $CHCl_3$).

Preparation of pentacycle 196.

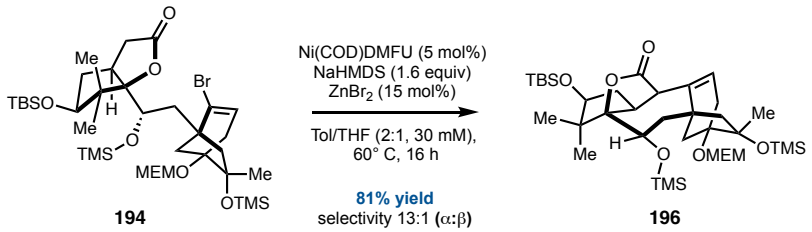

0.5 M solution of NaHMDS was prepared by dissolving 55 mg (0.3 mmol) in 0.6 mL. A 10x stock solution of Ni(COD)DMFU (2.4 mg, 7.58 umol) was prepared in toluene (1 mL). To a 2-dram vial of the starting material (12.0 mg, 15.2 umol, 1 equiv.) was added a 2-dram stir bar and 180 uL of toluene. 5.1 mg of $ZnBr_2$ was dissolved in 1.30 mL of THF, and 130 uL of $ZnBr_2$ as a stock solution in THF was added followed by NaHMDS (100 uL, 24.2 umol, 0.5 M, 1.6 equiv.) and Ni(COD)DMFU (100 uL, 0.76 umol). The final

concentration of the reaction mixture was 30 mM, with a 2:1 ratio of toluene:THF. The vial was stirred at 60 °C for 16 h using an oil bath in the hood, After 16 h, the reaction was TLC'd, and worked up by filtration through a silica plug. The product was purified via pipet column in 10-30% diethyl ether/hexanes to provide a product **196** (8.7 mg, 81% yield) as a mixture of diastereomers (13:1 α:β).

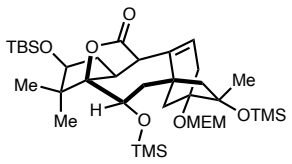

196

TLC (25% EtOAc/Hexanes): R_f 0.40 (*p*-anisaldehyde, light blue).

^{1}H NMR (400 MHz, $CDCl_3$): δ 5.18 (t, *J* = 3.6 Hz, 1H), 5.06 (d, *J* = 7.3 Hz, 1H), 4.65 (d, *J* = 7.3 Hz, 1H), 4.17 – 4.12 (m, 1H), 3.71 – 3.66 (m, 1H), 3.57 – 3.52 (m, 2H), 3.44 (d, *J* = 4.4 Hz, 2H), 3.28 (s, 3H), 2.97 (s, 1H), 2.86 (dd, *J* = 11.1, 4.4 Hz, 1H), 2.41 (ddd, *J* = 14.5, 10.9, 5.8 Hz, 1H), 2.32 – 2.19 (m, 2H), 2.15 – 2.07 (m, 2H), 2.03 – 1.94 (m, 2H), 1.68 – 1.53 (m, 2H), 1.31 – 1.25 (m, 1H), 1.15 (s, 3H), 0.97 (s, 3H), 0.82 (s, 3H), 0.77 (s, 9H), 0.09 (s, 9H), -0.02 (s, 9H), -0.10 (d, *J* = 5.5 Hz, 6H).

^{13}C NMR (101 MHz, $CDCl_3$): δ 177.34, 145.97, 123.07, 99.05, 91.80, 84.94, 83.08, 82.21, 72.02, 71.09, 66.77, 61.38, 59.14, 57.82, 49.98, 47.85, 44.42, 43.38, 41.44, 39.77, 37.53, 29.86, 25.78, 24.56, 24.35, 18.47, 18.06, 2.72, 1.31, -4.57, -4.97.

FTIR (Neat, NaCl, thin film): 2930, 1775, 1252, 1096, 1022, 883, 838 cm^{-1}.

HRMS (ESI): calc'd for $[M+H]^+$ 711.4138, found 711.4144.

$[\alpha]_D^{23}$: −14.1 (c 1.0 in $CHCl_3$).

Preparation of C9-C11-hydrogenated 201.

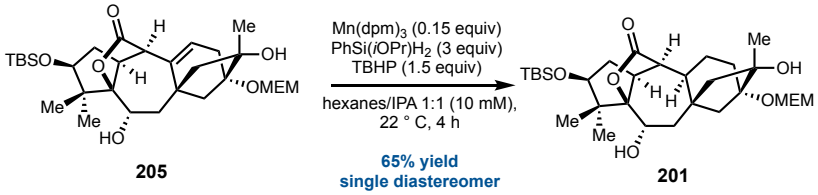

A stirring solution of starting material (7.0 mg, 12.4 umol, 1 equiv.) and $Mn(dpm)_3$ (1.1 mg, 1.85 umol, 0.15 equiv.) in IPA (400 uL, 36 mM) was degassed by bubbling with Ar for 5 min. Although 400 uL of IPA was added, after degassing, only ~300 uL remained. A stock solution of Ph(i-PrO)SiH_2 (20x in hexanes) and TBHP (20x in hexanes) were created. Sequentially at room temperature were added Ph(i-PrO)SiH_2 (133 uL, 3 equiv., 20x stock solution in hexanes) and TBHP (67 uL, 20x stock solution in hexanes, 1.5 equiv.) to the reaction vial containing the starting material and $Mn(dpm)_3$. The reaction mixture was stirred for 12 h before TLC indicated complete conversion. The solution was evaporated with aid from rotatory evaporator and loaded directly onto silica gel pipet column for purification 36-100% EtOAc/Hexanes to afford the product **201** as a clear oil (4.6 mg, 65% yield).

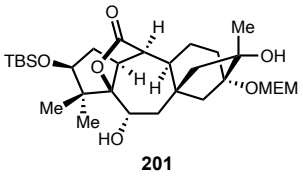

TLC (100% EtOAc): R_f 0.30 (*p*-anisaldehyde, purple)

^{1}H NMR (400 MHz, $CDCl_3$): δ 4.90 – 4.73 (m, 2H), 4.11 (dd, *J* = 10.5, 5.0 Hz, 1H), 3.77 – 3.62 (m, 3H), 3.54 (t, *J* = 4.6 Hz, 2H), 3.38 (s, 3H), 2.75 (dd, *J* = 10.9, 2.7 Hz, 1H), 2.55 (ddd, *J* = 14.7, 10.9, 5.5 Hz, 1H), 2.32 – 2.21 (m, 2H), 2.05 – 1.79 (m, 4H), 1.76 – 1.60 (m,

3H), 1.46 (d, *J* = 10.6 Hz, 1H), 1.30 (dd, *J* = 14.7, 2.6 Hz, 2H), 1.23 (s, 4H), 1.16 (s, 3H), 1.10 (s, 3H), 0.88 (s, 9H), 0.01 (d, *J* = 14.2 Hz, 6H).

^{13}C NMR (101 MHz, $CDCl_3$): δ 176.29, 100.70, 91.62, 85.01, 84.63, 79.36, 71.97, 71.87, 67.40, 59.18, 55.07, 51.67, 51.23, 50.37, 49.48, 43.45, 42.36, 42.22, 40.65, 31.16, 29.86, 25.89, 24.81, 20.94, 18.49, 18.22, -4.69, -4.90.

FTIR (Neat, NaCl, thin film): 3458, 2928, 1763, 1412, 1169, 1010, 840 cm^{-1}.

HRMS (ESI): calc'd for $[M+Na]^+$ 591.3323, found 591.3329.

$[\alpha]_D^{23}$: +112.4 (c 0.2 in $CHCl_3$).

Preparation of ketone 197.

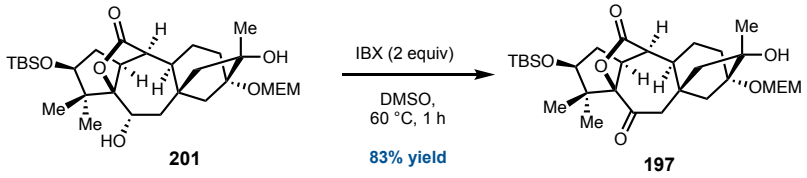

The starting secondary alcohol (5.0 mg, 8.79 umol, 1 equiv) was dissolved in solvent (440 uL, 20 mM). Then, a 1-dram stir bar was added in, followed by IBX (4.9 mg, 17.6 umol, 2.0 equiv.). The reaction was capped, taped, and heated at 60 °C for 1 h. The reaction was worked up by addition of ½ sat. $NaHCO_3$ by slow, dropwise addition at room temperature. The remaining solution was extracted with EtOAc (4 x 0.5 mL). The combined organic extract was washed with H_2O (5 x 1 mL, or as many washes as it takes to get rid of DMSO), brine (1 x 2 mL), dried with sodium sulfate, filtered, and concentrated to afford analytically pure product **197** as a clear oil (3.8 mg, 83% yield).

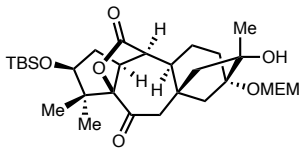

197

TLC (100% EtOAc): R_f 0.42 (*p*-anisaldehyde, brown)

^{1}H NMR (400 MHz, $CDCl_3$): δ 4.83 (q, J = 7.6 Hz, 2H), 3.76 – 3.65 (m, 3H), 3.53 (t, J = 4.6 Hz, 2H), 3.38 (s, 3H), 3.07 (d, J = 14.3 Hz, 1H), 2.99 – 2.92 (m, 1H), 2.65 – 2.58 (m, 1H), 2.54 (d, J = 2.6 Hz, 1H), 2.43 (d, J = 14.4 Hz, 1H), 2.26 (dd, J = 10.7, 2.9 Hz, 1H), 2.03 – 1.88 (m, 3H), 1.85 – 1.78 (m, 2H), 1.68 (d, J = 11.5 Hz, 2H), 1.49 (dd, J = 10.7, 1.9 Hz, 1H), 1.44 – 1.39 (m, 1H), 1.33 (s, 3H), 1.15 (s, 3H), 0.87 (s, 9H), 0.84 (s, 3H), 0.00 (d, J = 12.0 Hz, 6H).

^{13}C NMR (101 MHz, $CDCl_3$): δ 202.33, 176.22, 96.97, 91.59, 84.50, 82.78, 79.42, 71.83, 67.44, 59.18, 56.70, 54.47, 50.96, 50.12, 49.70, 46.50, 43.27, 42.44, 40.23, 30.82, 25.78, 25.77, 22.32, 20.84, 18.51, 18.06, -4.65, -4.98.

FTIR (Neat, NaCl, thin film): 3473, 2930, 1775, 1703, 1267, 848, 776 cm^{-1}.

HRMS (ESI): calc'd for $[M+Na]^+$ 589.3167, found 589.3161.

$[\alpha]_D^{23}$: +87.8 (c 0.2 in $CHCl_3$).

Preparation of reduction product 198.

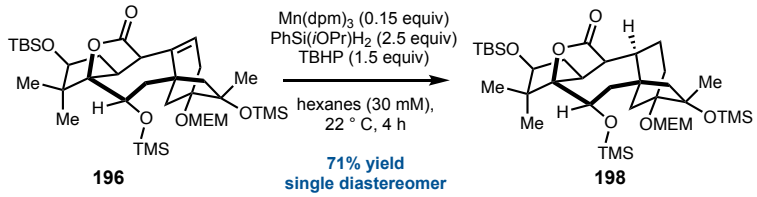

196 **198**

A stirring solution of $Mn(dpm)_3$ (0.15 equiv) in hexanes (180 uL, 36 mM) was degassed by bubbling with Ar for 5 min. Some extra hexanes may be necessary to add to prevent

complete evaporation of solvent. Regardless, the final amount of hexanes should amount to 180 uL (36 mM). Sequentially at room temperature were added Ph(i-PrO)SiH_2 (3.6 uL, 3 equiv) and TBHP (1.80 uL, 5.5-6.5 M in pentane, 1.5 equiv). The reaction mixture was stirred for 4 h before TLC indicated complete conversion. The solution was evaporated with aid from rotatory evaporator and loaded directly onto silica gel pipet column for purification 5-15% EtOAc/Hexanes to afford the product **198** as a yellow oil (3 mg, 71% yield).

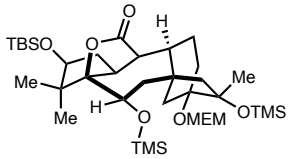

198

TLC (25% EtOAc/Hexanes): R_f 0.38 (*p*-anisaldehyde, purple).

^{1}H NMR (400 MHz, $CDCl_3$): δ 5.19 (d, *J* = 7.5 Hz, 1H), 4.64 (d, *J* = 7.5 Hz, 1H), 4.08 (dd, *J* = 10.7, 4.7 Hz, 1H), 3.85 – 3.76 (m, 1H), 3.63 – 3.52 (m, 4H), 3.39 (s, 3H), 2.79 (dd, *J* = 11.0, 2.6 Hz, 1H), 2.53 (ddd, *J* = 14.6, 10.9, 5.4 Hz, 1H), 2.41 (dd, *J* = 10.9, 2.6 Hz, 1H), 2.24 (d, *J* = 2.7 Hz, 1H), 2.10 – 2.00 (m, 1H), 1.93 – 1.76 (m, 2H), 1.76 – 1.56 (m, 6H), 1.43 (d, *J* = 10.7 Hz, 1H), 1.28 (d, *J* = 2.6 Hz, 1H), 1.19 (s, 3H), 1.17 (s, 3H), 1.03 (s, 3H), 0.87 (s, 10H), 0.16 (s, 10H), 0.08 (s, 9H), -0.00 (d, *J* = 13.7 Hz, 6H).

^{13}C NMR (101 MHz, $CDCl_3$): δ 176.55, 101.52, 91.71, 85.16, 83.82, 83.57, 73.08, 72.06, 66.47, 59.13, 55.19, 51.62, 51.15, 51.05, 49.51, 45.10, 43.77, 41.33, 40.72, 33.51, 29.85, 25.90, 25.82, 24.65, 20.50, 18.21, 2.74, 0.79, -4.70, -4.90.

FTIR (Neat, NaCl, thin film): 2930, 1787, 1262, 1074, 1042, 875, 776 cm^{-1}.

HRMS (ESI): calc'd for $[M+H]^+$ 713.4295, found 713.4297.

$[\alpha]_D^{23}$: +12.1 (c 1.0 in $CHCl_3$).

Preparation of ketone 202.

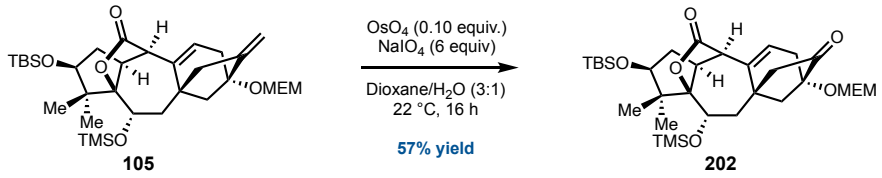

The starting material (8 mg, 12.9 umol, 1 equiv.) was dissolved in 1,4 dioxane and H_2O (3 : 1, 690 uL : 230 uL, 14 mM). OsO_4 (129 uL, 0.01 M in H_2O, 0.10 equiv.) was added in, and the reaction was stirred at room temperature for 5 min. Then, $NaIO_4$ (16.5 mg, 77.3 umol, 6 equiv) was added in, and the reaction was stirred at room temperature for 15 h. Monitor this reaction closely. Stirring too long will result in over-oxidation products that show up near the baseline of the TLC! Just look for enough conversion to get full conversion. May need to add more $NaIO_4$. After 15 h, H_2O (500 uL) was added. The resulting solution was extracted with EtOAc (4 x 1 mL), washed with brine (1 mL), dried with sodium sulfate, filtered, and concentrated. Preparatory TLC (50% EtOAc/Hex) affords the product **202** (4.6 mg, 57% yield) as a white solid.

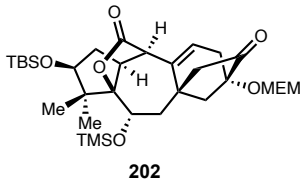

TLC (50% EtOAc/hexanes): R_f 0.60 (*p*-anisaldehyde, blue).

^{1}H NMR (400 MHz, $CDCl_3$): δ 5.44 (t, J = 3.5 Hz, 1H), 4.94 (d, J = 7.6 Hz, 1H), 4.77 (d, J = 7.7 Hz, 1H), 4.35 (d, J = 3.5 Hz, 1H), 3.78 – 3.67 (m, 3H), 3.49 (dt, J = 5.9, 3.7 Hz, 2H), 3.36 (s, 3H), 3.18 (s, 1H), 3.05 (dd, J = 11.0, 4.5 Hz, 1H), 2.64 – 2.41 (m, 5H), 2.28 (d, J = 12.6 Hz, 2H), 2.06 (d, J = 11.3 Hz, 1H), 1.80 (dd, J = 16.0, 5.2 Hz, 1H), 1.47 – 1.37 (m, 1H), 1.09 (s, 3H), 0.93 (s, 3H), 0.88 (s, 9H), 0.22 (s, 9H), 0.08 (s, 6H).

^{13}C NMR (101 MHz, $CDCl_3$): δ 214.95, 176.54, 143.90, 123.44, 98.88, 91.49, 83.72, 82.85, 71.75, 70.92, 67.60, 59.10, 57.47, 55.29, 50.01, 48.70, 44.85, 42.32, 39.72, 39.68, 37.03, 25.76, 24.38, 18.45, 18.04, 1.38, -4.56, -4.98.

FTIR (Neat, NaCl, thin film): 2934, 1776, 1754, 1064, 1042, 834 cm^{-1}.

HRMS (ESI): calc'd for $[M+H]^+$ 623.3430, found 623.3441.

$[\alpha]_D^{23}$: −195.9 (c 0.2 in $CHCl_3$).

Melting Point: 146-148 °C

Preparation of hydrogenation product 204.

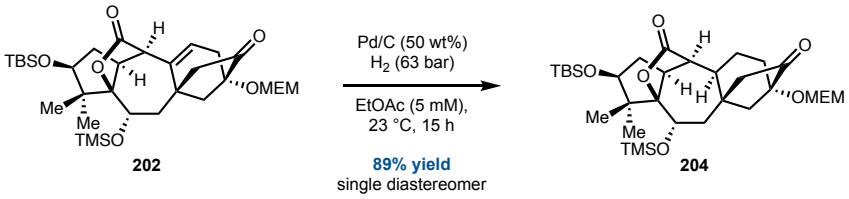

The starting material (3.8 mg, 6.10 umol, 1 equiv.) was dissolved in EtOAc (1 mL, 5 mM) in a 1-dram vial equipped with a. magnetic stir bar. 10% Pd/C was added in (1.9 mg, 50 wt%) was added in, and a rubber septum was added on top. A pink 20 gage needle was pierced through the septum, and the vial was loaded in a bomb hydrogenator apparatus. After equilibrating the bomb hydrogenator vessel with H_2 (3 times), the pressure was increased to 63 bar. The reaction was left to stir at that pressure of H_2 overnight. After stirring for 15 h, the reaction was filtered through a pad of Celite to remove the Pd/C and rinsed with EtOAc. The resultant plug was disposed by separately rinsing with H_2O (3 x 0.3 mL) and tagged as activated Pd/C waste. The resultant EtOAc solution was concentrated to afford the product **204** (3.4 mg, 89% yield) as a white solid.

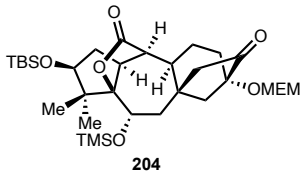

204

TLC (50% EtOAc/hexanes): R_f 0.51 (*p*-anisaldehyde, purple).

^{1}H NMR (400 MHz, $CDCl_3$): δ 4.89 (d, J = 7.7 Hz, 1H), 4.73 (d, J = 7.7 Hz, 1H), 4.10 (dd, J = 10.3, 4.9 Hz, 1H), 3.77 – 3.66 (m, 2H), 3.63 (d, J = 5.2 Hz, 1H), 3.53 – 3.46 (m, 2H), 3.37 (d, J = 0.7 Hz, 3H), 2.83 (dd, J = 10.9, 2.7 Hz, 1H), 2.64 – 2.49 (m, 2H), 2.34 (d, J = 1.9 Hz, 1H), 2.14 – 2.04 (m, 2H), 1.98 – 1.65 (m, 8H), 1.33 – 1.29 (m, 1H), 1.16 (s, 3H), 1.04 (s, 3H), 0.87 (s, 9H), 0.16 (d, J = 0.7 Hz, 9H).

^{13}C NMR (101 MHz, $CDCl_3$): δ 214.56, 175.59, 101.03, 91.28, 84.90, 83.57, 72.45, 71.81, 67.34, 59.11, 55.03, 51.83, 51.01, 50.76, 48.40, 43.52, 43.03, 40.54, 39.25, 33.61, 25.85, 25.64, 24.72, 18.28, 18.21, 0.85, -4.67, -4.93.

FTIR (Neat, NaCl, thin film): 2930, 1776, 1752, 1112, 1057, 834 cm^{-1}.

HRMS (ESI): calc'd for $[M+H]^+$ 625.3586, found 625.3596.

$[\alpha]_D^{23}$: −42.9 (c 0.2 in $CHCl_3$).

Preparation of secondary alcohol 205.

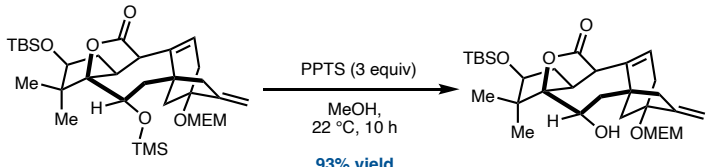

105 **205**

A solution of trimethylsilylated alcohol (23.0 mg, 37 umol, 1 equiv.) in methanol (740 uL, 50 mM) was treated with pyridinium p-toluenesulfonate (27.9 mg, 111 umol, 3 equiv) at room temperature and stirred for 19 hours. No care to exclude air or moisture was taken,

and the PPTS was just added in as the solid, capped, and taped. TLC in 50% ether/hexanes reveals full conversion after 19 h. The reaction was worked up by addition of NH_4Cl (750 uL) and the resulting solution was extracted with diethyl ether (3 x 1 mL). The combined organic extracts were dried with sodium sulfate, filtered, and concentrated. A pipet column with 10-30% EA/hexanes afforded the product as a foamy, clear oil (18.9 mg, 93% yield).

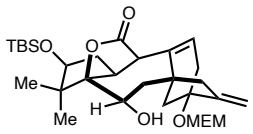

205

TLC: (50% EtOAc/Hexanes): R_f 0.52 (*p*-anisaldehyde, blue).

^{1}H NMR ($CDCl_3$, 400 MHz): δ 5.41 – 5.34 (m, 1H), 5.03 (s, 1H), 4.97 – 4.90 (m, 2H), 4.72 (d, J = 7.5 Hz, 1H), 4.31 (d, J = 3.8 Hz, 1H), 3.87 – 3.80 (m, 1H), 3.73 (dd, J = 6.2, 3.2 Hz, 1H), 3.65 – 3.59 (m, 1H), 3.57 – 3.52 (m, 2H), 3.38 (s, 3H), 3.14 (s, 1H), 2.95 (dd, J = 10.5, 6.4 Hz, 1H), 2.69 (d, J = 13.7 Hz, 1H), 2.59 – 2.45 (m, 2H), 2.38 (d, J = 16.3 Hz, 1H), 2.32 – 2.14 (m, 3H), 2.04 (d, J = 10.8 Hz, 1H), 1.74 (dd, J = 16.3, 5.6 Hz, 1H), 1.41 (ddd, J = 14.4, 6.5, 3.3 Hz, 1H), 1.05 (s, 3H), 1.00 (s, 3H), 0.87 (s, 9H), 0.00 (d, J = 4.5 Hz, 6H).

^{13}C NMR (101 MHz, $CDCl_3$) δ 177.07, 152.12, 143.03, 124.39, 106.91, 98.22, 91.09, 85.03, 82.19, 71.98, 69.95, 66.99, 59.11, 56.68, 50.67, 50.45, 49.27, 45.12, 43.65, 42.22, 41.71, 39.16, 29.85, 25.82, 24.08, 18.59, 18.07, -4.50, -4.93.

FTIR (Neat, NaCl, thin film): 3459, 2928, 1751, 1464, 1249, 1098, 1042, 1019, 883, 837, 773 cm^{-1}.

HRMS (ESI): calc'd for $[M+H]^+$ 549.3242 found 549.3271.

$[\alpha]_D^{23}$: +30.3 (c 0.2 in $CHCl_3$).

Preparation of ketone 206.

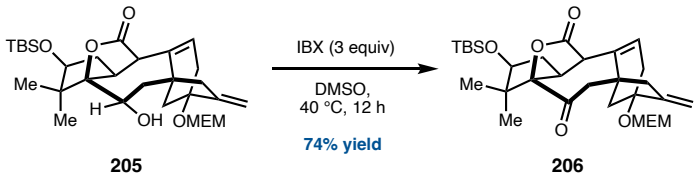

205 **206**

The starting secondary alcohol (18.0 mg, 32.8 umol, 1 equiv) was dissolved in DMSO (164 uL, 200 mM). Then, a 1/2-dram stir bar was added in, followed by IBX (11.9 mg, 42.6 umol, 1.3 equiv.). The reaction was capped, taped, and heated at 50 °C for 1 h. Despite the identical polarity of the two products, TLC analysis was effective at monitoring conversion due to the difference in *p*-anisaldehyde staining (blue for the starting material and brown for the product). The reaction was worked up by addition of 1/2 saturated $NaHCO_3$ (1 mL), and the aqueous phase was extracted with EtOAc (3 x 1 mL). A pipet column 10-30% EtOAc/Hex provides the product as a pale yellow oil (13.3 mg, 74% yield).

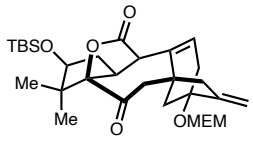

206

TLC: (50% EtOAc/Hexanes): R_f 0.52 (*p*-anisaldehyde, brown).

^{1}H NMR ($CDCl_3$, 400 MHz): δ 5.65 (dd, *J* = 5.0, 2.4 Hz, 1H), 5.07 (s, 1H), 5.00 (s, 1H), 4.90 (d, *J* = 7.6 Hz, 1H), 4.71 (d, *J* = 7.6 Hz, 1H), 3.86 – 3.78 (m, 1H), 3.74 (d, *J* = 5.8 Hz, 1H), 3.66 – 3.58 (m, 1H), 3.53 (t, *J* = 4.8 Hz, 2H), 3.38 (s, 3H), 3.29 (s, 1H), 3.21 (d, *J* = 14.1 Hz, 1H), 3.12 (dd, *J* = 11.0, 4.4 Hz, 1H), 2.74 – 2.51 (m, 3H), 2.44 (d, *J* = 14.2 Hz, 1H), 2.34 (dt, *J* = 16.0, 3.0 Hz, 1H), 2.24 – 2.16 (m, 1H), 2.11 (dd, *J* = 10.8, 2.0 Hz, 1H), 1.94 (dd, *J* = 10.8, 2.8 Hz, 1H), 1.43 (s, 1H), 1.34 (s, 3H), 0.90 (s, 5H), 0.88 (d, *J* = 3.2 Hz, 14H), 0.86 (s, 4H), 0.01 (d, *J* = 10.1 Hz, 6H).

^{13}C NMR (CDCl3, 101 MHz): δ 203.21, 175.89, 151.81, 139.28, 127.78, 109.24, 97.45, 91.15, 82.95, 82.61, 71.93, 67.19, 66.01, 59.15, 53.42, 49.71, 47.49, 44.67, 44.58, 43.04, 39.84, 34.27, 25.76, 22.49, 18.52, 18.06, 15.43, 14.21, 1.17, -4.63, -4.96.

FTIR (Neat, NaCl, thin film): 2926, 2856, 1779, 1714, 1461, 1259, 1093, 1048, 1032, 837 cm^{-1}.

HRMS (ESI): calc'd for $[M+H]^+$ 547.3086 found 547.3090.

$[\alpha]_D^{23}$: +37.6 (c 0.2 in $CHCl_3$).

Preparation of rearranged product 208.

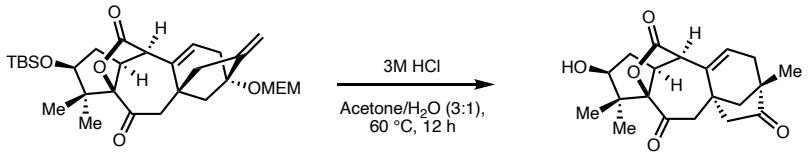

206 208

To the starting material (5 mg, 9.1 umol, 1 equiv.) was added acetone (300 uL). Then, 3 M aqueous HCl (670 uL, 219 equiv.) was added in, and the reaction was stirred overnight for 12 h at 60 °C. To workup the reaction, the reaction was neutralized with sat. aq. $NaHCO_3$. The aqueous phase was extracted with EtOAc (3 x 0.5 mL), and the combined organic extracts were dried with $NaSO_4$, filtered, and concentrated. Prep plate in 50% EtOAc/Hex affords the product **208** (2.7 mg, 87% yield) as a white solid.

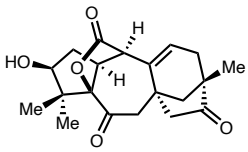

208

TLC (50% EtOAc/Hexanes): R_f 0.22 (*p*-anisaldehyde, brown).

^{1}H NMR (500 MHz, $CDCl_3$): δ 5.67 (t, *J* = 3.4 Hz, 1H), 3.78 – 3.71 (m, 1H), 3.52 – 3.46 (m, 2H), 3.38 (s, 1H), 2.86 – 2.74 (m, 2H), 2.41 (dd, *J* = 17.5, 3.5 Hz, 1H), 2.32 (d, *J* = 17.5 Hz, 1H), 2.22 – 2.09 (m, 4H), 1.71 (dd, *J* = 11.4, 1.1 Hz, 1H), 1.62 – 1.58 (m, 1H), 1.28 – 1.23 (m, 6H), 1.14 (s, 3H).

^{13}C NMR (101 MHz, $CDCl_3$): δ 218.65, 205.21, 177.18, 139.20, 128.15, 100.11, 82.82, 58.13, 54.56, 50.55, 50.28, 48.94, 48.09, 44.69, 40.96, 40.29, 38.88, 23.20, 20.35, 16.97.

FTIR (Neat, NaCl, thin film): 3463, 2925, 1775, 1740, 1457, 1086 cm^{-1}.

HRMS (ESI): calc'd for $[M+H]^+$ 345.1696, found 345.1693.

$[\alpha]_D^{23}$: +127.1 (c 0.2 in MeOH).

Preparation of DIBAL products 209, 210, and 211.

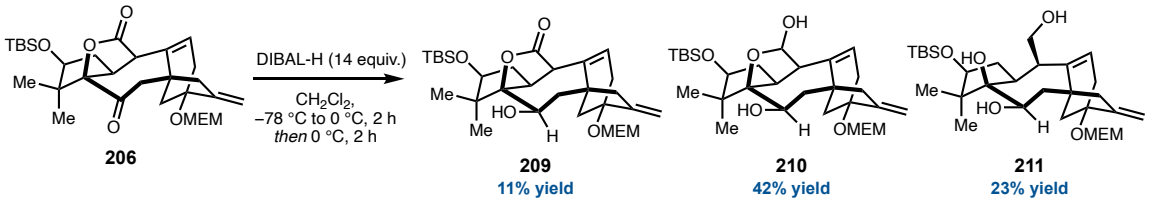

The starting material (3 mg, 5.3 umol, 1 equiv.) was dissolved in DCM (230 uL, 20 uM). Then, it was cooled to −78 °C and DIBAL solution (32 uL, 1M in hexanes, 6 equiv.) was added slowly dropwise. The mixture was immediately warmed to 0 °C by replacing the dry ice/acetone bath with an ice bath and the reaction was stirred for 30 min at that temperature. Following complete conversion by TLC (30 min at 0 °C), the reaction was quenched by addition of sat. aq. Rochelle's salt (250 uL). The reaction was slowly warmed to room temperature and vigorously stirred for 1 h until complete decomposition of aluminum aggregates. The remaining solution was extracted with EtOAc (3 x 0.5 mL), and the combined organics were washed with brine (1 mL), dried with sodium sulfate, filtered, and

concentrated. The lactol was isolated by careful preparatory TLC in 75% EtOAc/Hex to afford **210** as a clear oil (1.4 mg, 42% yield).

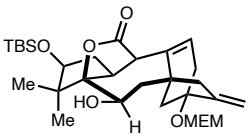

209

TLC: (50% EtOAc/Hexanes): R_f 0.55 (*p*-anisaldehyde, light blue).

^{1}H NMR (CDCl$_3$, 400 MHz): δ 5.31 (q, *J* = 3.0 Hz, 1H), 5.04 (s, 1H), 4.96 – 4.90 (m, 2H), 4.73 (d, *J* = 7.5 Hz, 1H), 4.14 (d, *J* = 5.1 Hz, 1H), 3.90 – 3.80 (m, 2H), 3.67 – 3.59 (m, 1H), 3.54 (dd, *J* = 5.7, 3.7 Hz, 2H), 3.38 (d, *J* = 2.5 Hz, 3H), 3.04 (s, 1H), 2.79 (dd, *J* = 12.2, 4.0 Hz, 1H), 2.70 – 2.61 (m, 1H), 2.61 – 2.51 (m, 2H), 2.44 (d, *J* = 15.6 Hz, 1H), 2.33 – 2.24 (m, 2H), 2.18 (dd, *J* = 16.2, 4.1 Hz, 1H), 2.01 (d, *J* = 10.4 Hz, 1H), 1.87 (dd, *J* = 15.3, 4.0 Hz, 1H), 1.11 (s, 3H), 0.95 (s, 3H), 0.92 (d, *J* = 1.6 Hz, 9H), 0.20 – 0.00 (m, 6H).

^{13}C NMR (151 MHz, CDCl$_3$): δ 177.95, 152.62, 146.15, 121.89, 106.12, 102.66, 99.66, 90.89, 85.11, 84.82, 71.81, 70.31, 66.78, 64.66, 58.93, 51.56, 50.79, 46.01, 43.53, 42.48, 39.28, 25.84, 25.19, 18.51, -4.79, -5.08.

FTIR (Neat, NaCl, thin film): 3457, 2928, 1754, 1267, 1157, 1098, 1042, 869, cm^{-1}.

HRMS (ESI): calc'd for $[M+H]^+$ 549.3242 found 549.3277.

$[\alpha]_D^{23}$: +43.3 (c 0.2 in $CHCl_3$).

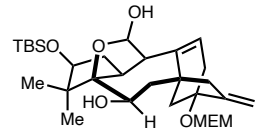

210

TLC: (50% EtOAc/Hexanes): R_f 0.52 (*p*-anisaldehyde, dark blue).

^{1}H NMR (CDCl$_3$, 400 MHz): δ 6.20 (d, *J* = 9.3 Hz, 1H), 5.39 (dd, *J* = 4.6, 2.5 Hz, 1H), 5.26 (d, *J* = 9.2 Hz, 1H), 5.04 (s, 1H), 4.96 (s, 1H), 4.89 (d, *J* = 7.4 Hz, 1H), 4.72 (d, *J* =

7.4 Hz, 1H), 4.08 (s, 1H), 3.91 (d, *J* = 6.6 Hz, 1H), 3.84 – 3.79 (m, 1H), 3.65 – 3.60 (m, 1H), 3.57 – 3.53 (m, 2H), 3.38 (s, 3H), 3.05 (s, 1H), 2.70 – 2.50 (m, 5H), 2.15 – 2.04 (m, 1H), 2.03 – 1.95 (m, 2H), 1.86 – 1.76 (m, 3H), 1.24 (s, 3H), 0.98 (s, 3H), 0.92 (s, 9H), 0.11 (d, *J* = 7.2 Hz, 6H).

^{13}C NMR (101 MHz, CDCl3) δ 154.13, 144.18, 123.65, 107.51, 106.62, 100.42, 91.00, 85.42, 82.82, 71.84, 69.61, 66.95, 66.19, 59.00, 51.60, 50.72, 47.89, 46.27, 44.27, 43.60, 43.29, 39.45, 29.71, 26.61, 25.80, 19.25, 18.29, -4.76, -5.09.

FTIR (Neat, NaCl, thin film): 3461, 2928, 1750, 1222, 1042, 948, 898, cm^{-1}.

HRMS (ESI): calc'd for $[M-OH]^+$ 532.3215, found 532.3215.

$[\alpha]_D^{23}$: +57.0 (c 0.2 in $CHCl_3$).

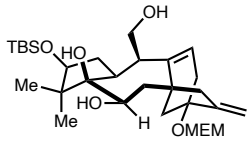

211

TLC: (50% EtOAc/Hexanes): R_f 0.50 (*p*-anisaldehyde, dark blue).

^{1}H NMR ($CDCl_3$, 400 MHz): δ 5.33 (s, 1H), 5.08 (s, 1H), 5.01 – 4.93 (m, 2H), 4.77 (d, J = 7.4 Hz, 1H), 4.11 – 4.01 (m, 1H), 3.84 (d, J = 10.6 Hz, 2H), 3.72 – 3.52 (m, 6H), 3.40 (d, J = 8.7 Hz, 3H), 2.94 – 2.82 (m, 1H), 2.60 (d, J = 16.5 Hz, 2H), 2.44 – 2.30 (m, 3H), 2.22 – 2.02 (m, 4H), 1.40 (d, J = 14.4 Hz, 1H), 1.14 (s, 3H), 0.98 (s, 3H), 0.91 (s, 12H), 0.08 (d, J = 3.6 Hz, 6H).

Preparation of lactol 214.

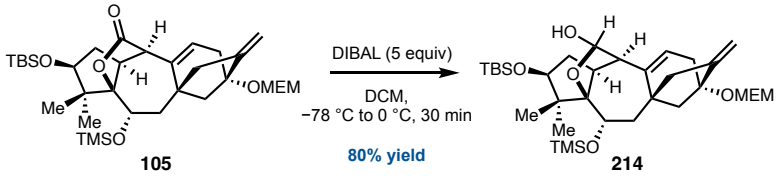

The starting material (5 mg, 8.05 umol, 1 equiv.) in an oven-dried, 1-dram vial equipped with a magnetic stir bar was evacuated and backfilled with N_2 three times. CH_2Cl_2 (810 uL, 10 mM) was added, and the vial was stirred for 2 minutes to ensure complete dissolution of the starting material. Then, the vial was cooled to −78 °C using a dry ice/acetone bath, and DIBAL (40 uL, 40.3 umol, 1 M in hexanes, 5 equiv.) was added in slowly dropwise. The reaction was immediately warmed to 0 °C by replacing the dry ice/acetone bath with an ice bath. At 0 °C, the reaction was TLC'd, indicating complete conversion to a slightly less polar, darker blue spot, and the reaction was quenched by careful addition of sat. aq. Rochelle's salt (500 uL). The ice bath was replaced and the reaction was warmed to room temperature, where it was stirred for 20 minutes to ensure complete decomposition of the aluminum aggregates. The organic phase of the resulting solution was collected, and the remaining aqueous phase was extracted with CH_2Cl_2 (3 x 0.5 mL). The combined organics were washed with brine (1 mL), dried with sodium sulfate, filtered, and concentrated. Preparatory TLC in 50% Ether/Hexanes affords the product **214** (4 mg, 80% yield) as a clear oil.

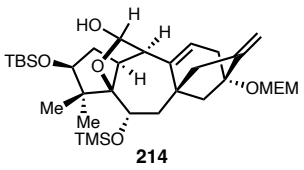

TLC (50% Ether/Hexanes): R_f 0.75 (p-anisaldehyde, dark-blue).

^{1}H NMR (CDCl$_3$, 400 MHz): δ 5.32 (d, *J* = 8.7 Hz, 1H), 5.28 – 5.22 (m, 2H), 5.03 (t, *J* = 2.6 Hz, 1H), 4.92 (d, *J* = 7.5 Hz, 2H), 4.72 (d, *J* = 7.5 Hz, 1H), 4.11 (dd, *J* = 5.1, 1.8 Hz, 1H), 3.86 – 3.77 (m, 2H), 3.66 – 3.59 (m, 1H), 3.55 – 3.50 (m, 2H), 3.37 (s, 3H), 2.99 (s, 1H), 2.78 (dd, *J* = 12.2, 3.6 Hz, 1H), 2.64 (ddd, *J* = 15.3, 12.2, 6.7 Hz, 1H), 2.55 (dt, *J* = 16.3, 2.4 Hz, 2H), 2.37 (dd, *J* = 15.5, 1.9 Hz, 1H), 2.27 (dt, *J* = 16.3, 2.9 Hz, 1H), 2.21 – 2.10 (m, 2H), 1.93 (dd, *J* = 10.6, 1.4 Hz, 1H), 1.81 (dd, *J* = 15.3, 3.7 Hz, 1H), 1.54 – 1.49 (m, 1H), 1.08 (s, 3H), 0.91 (s, 9H), 0.88 (s, 3H), 0.15 (s, 9H), 0.09 (d, *J* = 3.9 Hz, 6H).

^{13}C NMR (101 MHz, CDCl$_3$): δ 152.99, 146.43, 121.39, 106.27, 103.00, 100.23, 91.14, 85.58, 85.37, 71.86, 71.35, 67.19, 65.36, 59.11, 52.13, 51.33, 51.25, 46.26, 43.51, 42.57, 41.91, 39.69, 26.31, 26.00, 18.77, 18.44, 1.43, -4.60, -4.94.

FTIR (Neat, NaCl, thin film): 3412, 2887, 1701, 1414, 1210, 898, 840 cm^{-1}.

HRMS (ESI): calc'd for [M+Na]$^{+}$ 645.3613 found 645.3615.

Preparation of methyl acetal 216.

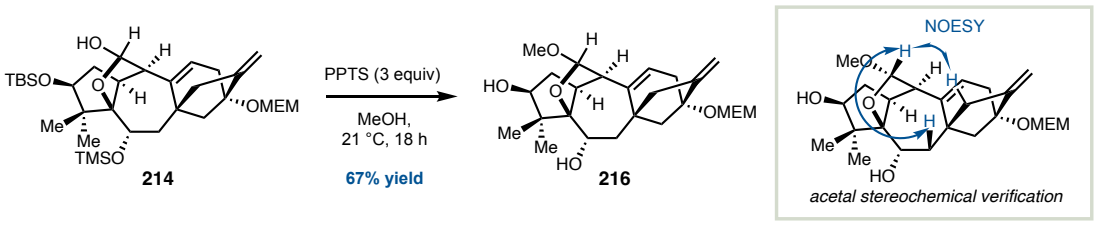

The starting material (4 mg, 6.44 umol, 1 equiv.) was dissolved in MeOH (130 uL, 50 mM). PPTS (4.9 mg, 19.3 umol, 3 equiv.) was added. The vial was capped and stirred overnight for 18 h. Monitoring by TLC for the first 3 hours indicates complete conversion to two polar spots that should be TLC'd in 75% EtOAc/hexanes. The bottom spot was larger, indicating that it was likely formed in short reaction periods in higher quantites. After stirring overnight for 18 h, the top spot became the major spot, corresponding to

structure **216**. The reaction was worked up by addition of sat. aq. $NaHCO_3$ (300 uL). The solution was extracted with EtOAc (4 x 0.5 mL), washed with brine, dried with sodium sulfate, filtered, and concentrated. Preparatory TLC in 75% EtOAc/hexanes affords the product (2.4 mg, 67% yield) as a clear oil.

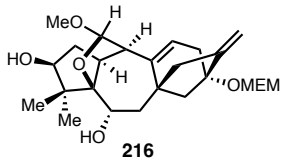

216

TLC (100% EtOAc/Hexanes): R_f 0.40 (p-anisaldehyde, light-blue).

^{1}H NMR ($CDCl_3$, 400 MHz): δ 5.36 (t, *J* = 3.6 Hz, 1H), 5.07 (t, *J* = 2.6 Hz, 1H), 4.97 (s, 1H), 4.95 (s, 1H), 4.93 (d, *J* = 7.5 Hz, 1H), 4.73 (d, *J* = 7.5 Hz, 1H), 4.17 (dd, *J* = 5.5, 1.5 Hz, 1H), 3.87 – 3.79 (m, 1H), 3.66 – 3.58 (m, 2H), 3.56 – 3.51 (m, 2H), 3.41 (s, 3H), 3.38 (s, 3H), 3.01 (s, 1H), 2.73 (dd, *J* = 12.0, 3.8 Hz, 1H), 2.69 – 2.61 (m, 1H), 2.58 (ddd, *J* = 16.4, 5.5, 2.3 Hz, 2H), 2.39 – 2.27 (m, 3H), 2.21 – 2.12 (m, 1H), 2.04 – 2.00 (m, 1H), 1.78 (dd, *J* = 14.9, 3.8 Hz, 1H), 1.67 (dd, *J* = 15.8, 5.5 Hz, 1H), 1.16 (s, 3H), 0.94 (s, 3H).

^{13}C NMR (101 MHz, $CDCl_3$): δ 152.68, 145.43, 122.55, 109.45, 106.55, 101.46, 91.07, 85.15, 83.81, 71.97, 70.07, 66.98, 61.96, 59.13, 56.52, 51.82, 50.75, 50.39, 46.42, 43.72, 42.31, 41.85, 38.78, 25.29, 18.00.

FTIR (Neat, NaCl, thin film): 3430, 2919, 1763, 1420, 1364, 1067, 955 cm^{-1}.

HRMS (ESI): calc'd for $[M+Na]^+$ 473.2510 found 473.2521.

Preparation of hydrated product 199.

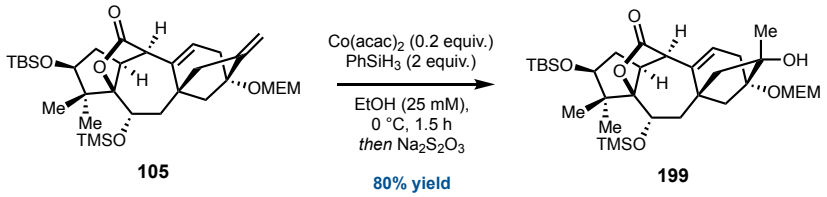

A 10x stock solution of $Co(acac)_2$ was made by dissolving 3.0 mg of the solid in 1 mL of EtOH in a 1-dram vial. Then, the vial was capped with a rubber septum and a vent needle was attached. An O_2 balloon with a long needle was inserted into the $Co(acac)_2$/EtOH solution to sparge the solution with O_2, while, at the same time, the vial was sonicated for 30 seconds or until all $Co(acac)_2$ was dissolved. Once the stock solution was prepared, the vent needle was removed, and it was left under O_2 and used within 10 minutes.

The starting material (18 mg, 29.0 umol, 1 equiv.) in a 1-dram vial was dissolved in EtOH (560 uL) and a magnetic stir bar was added in. Then, $Co(acac)_2$ was added in (500 uL, 5.80 umol, 0.2 equiv.), and the stirring solution was cooled to 0 °C and an O_2 balloon with a purple (thick) needle was added on. $PhSiH_3$ as a 10x stock solution was added in slowly, dropwise (100 uL, 58.0 umol, 2 equiv.) at 0 °C, and the reaction was stirred at 0 °C for 3 h. After 15 min, a color change from pink to yellow/green was observed. After 45 min to 1 h, the color was a deeper green. Following completion (3 h), as determined by TLC, the reaction was quenched by addition of sat. aq. $Na_2S_2O_3$ (250 uL) at 0 °C, warmed to room temperature, and stirred at room temperature for 20 minutes to ensure complete degradation of the peroxide intermediate. The resulting solution was extracted with EtOAc (4 x 0.5 mL), washed with brine, dried with Na_2SO_4, filtered, and concentrated. The crude oil was purified by pipet column (12-24% EtOAc/hexanes) to afford the product **199** as a clear oil (14.8 mg, 80% yield).

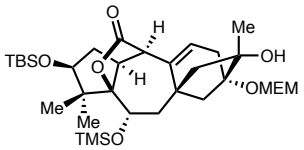

199

TLC (36% EtOAc/hexanes): R_f 0.35 (*p*-anisaldehyde, blue).

^{1}H NMR (400 MHz, $CDCl_3$): δ 5.31 (t, *J* = 3.6 Hz, 1H), 4.91 – 4.83 (m, 2H), 4.25 (td, *J* = 4.5, 2.0 Hz, 1H), 3.83 – 3.75 (m, 1H), 3.73 – 3.64 (m, 2H), 3.54 (q, *J* = 4.7 Hz, 2H), 3.38 (s, 3H), 3.09 (s, 1H), 2.95 (dd, *J* = 11.0, 4.5 Hz, 1H), 2.59 – 2.44 (m, 2H), 2.28 (dt, *J* = 11.2, 4.6 Hz, 2H), 2.18 (dd, *J* = 10.2, 2.0 Hz, 1H), 2.10 – 2.04 (m, 2H), 1.75 – 1.69 (m, 2H), 1.42 – 1.37 (m, 1H), 1.19 (s, 3H), 1.06 (s, 3H), 0.91 (s, 3H), 0.87 (s, 9H), 0.17 (s, 9H), -0.01 (d, *J* = 5.2 Hz, 6H).

^{13}C NMR (101 MHz, $CDCl_3$): δ 177.12, 145.98, 122.85, 98.92, 91.69, 85.82, 82.99, 78.03, 71.86, 71.04, 67.63, 66.01, 59.18, 58.82, 57.70, 49.94, 44.57, 42.22, 39.71, 35.25, 25.77, 24.41, 18.49, 18.05, 15.42, 1.35, -4.58, -4.98.

FTIR (Neat, NaCl, thin film): 3411, 2932, 1772, 1462, 1252, 1129, 1098, 1025, 840 cm^{-1}.

HRMS (ESI): calc'd for $[M+Na]^+$ 661.3562, found 661.3570.

$[\alpha]_D^{23}$: +25.6 (c 0.8 in $CHCl_3$).

Preparation of alcohol 200.

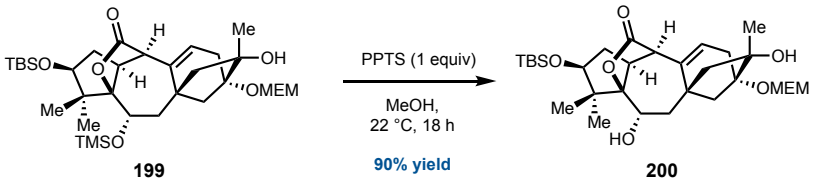

A solution of trimethylsilylated alcohol (10.0 mg, 14.1 umol, 1 equiv.) in methanol (560 uL, 25 mM) was treated with pyridinium *p*-toluenesulfonate (7.1 mg, 28.1 umol, 1 equiv) at room temperature and stirred for 18 hour. No care to exclude air or moisture was taken, and the PPTS was just added in as the solid, capped, and taped. TLC in 75% EtOAc/hexanes reveals full conversion to a more polar spot after 18 h. The reaction was worked up by addition of NH_4Cl (500 uL) and the resulting solution was extracted with EtOAc (3 x 0.5 mL). The combined organic extracts were dried with sodium sulfate, filtered, and concentrated. A pipet column with 50-75% EA/hexanes afforded the product **200** as a white solid (7.2 mg, 90% yield).

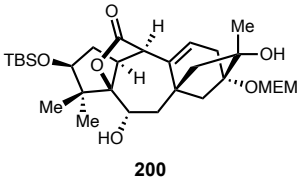

TLC (75% EtOAc/hexanes): R_f 0.38 (*p*-anisaldehyde, blue).

^{1}H NMR (400 MHz, $CDCl_3$): δ 5.33 (t, J = 3.6 Hz, 1H), 4.91 – 4.81 (m, 2H), 4.28 (dd, J = 5.5, 1.6 Hz, 1H), 3.79 – 3.67 (m, 3H), 3.54 (t, J = 4.6 Hz, 2H), 3.38 (s, 3H), 3.12 (s, 1H), 2.92 (dd, J = 10.5, 6.2 Hz, 1H), 2.60 – 2.37 (m, 2H), 2.39 – 2.27 (m, 3H), 2.17 – 2.02 (m, 2H), 1.78 – 1.70 (m, 2H), 1.44 – 1.37 (m, 1H), 1.21 (s, 3H), 1.05 (s, 3H), 0.99 (s, 3H), 0.87 (s, 9H).

^{13}C NMR (101 MHz, $CDCl_3$): δ 177.07, 146.01, 123.32, 98.20, 91.61, 85.86, 82.21, 78.02, 71.89, 69.89, 67.60, 59.17, 58.50, 56.65, 49.30, 47.70, 44.66, 42.24, 42.07, 39.18, 35.45, 25.79, 24.34, 24.03, 18.61, 18.05, -4.52, -4.94.

FTIR (Neat, NaCl, thin film): 3458, 2930, 2857, 1768, 1469, 1255, 1098, 1020, 839, 775 cm^{-1}.

HRMS (ESI): calc'd for $[M+Na]^+$ 589.3167, found 589.3170.

$[\alpha]_D^{23}$: −35.1 (c 0.8 in $CHCl_3$).

Melting Point: 142-144 °C

Preparation of ketone 206

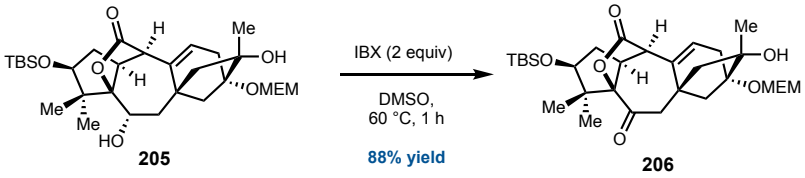

The starting secondary alcohol (8.0 mg, 14.1 umol, 1 equiv) was dissolved in solvent (700 uL, 20 mM). Then, a 1-dram stir bar was added in, followed by IBX (7.9 mg, 28.2 umol, 2.0 equiv.). The reaction was capped, taped, and heated at 60 °C for 1 h. The reaction was worked up by addition of ½ sat. $NaHCO_3$ by slow, dropwise addition at room temperature. The remaining solution was extracted with EtOAc (4 x 0.5 mL). The combined organic extract was washed with H_2O (5 x 1 mL, or as many washes as it takes to get rid of DMSO), brine (1 x 2 mL), dried with sodium sulfate, filtered, and concentrated. A pipet column 50-75% EtOAc/hexanes afforded analytically pure product **206** as a pale yellow oil (7.0 mg, 88% yield).

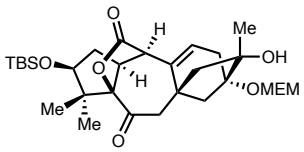

206

TLC (75% EtOAc/Hexanes): R_f 0.42 (*p*-anisaldehyde, brown).

^{1}H NMR (400 MHz, $CDCl_3$): δ 5.63 (dd, J = 4.7, 2.6 Hz, 1H), 4.94 – 4.82 (m, 2H), 3.82 – 3.75 (m, 1H), 3.74 – 3.67 (m, 2H), 3.54 (t, J = 4.4 Hz, 2H), 3.38 (d, J = 1.0 Hz, 3H), 3.30 (s, 1H), 3.20 – 2.96 (m, 3H), 2.72 – 2.58 (m, 2H), 2.47 (d, J = 14.1 Hz, 1H), 2.31 (ddd, J = 18.1, 4.9, 1.7 Hz, 1H), 2.16 (dd, J = 10.2, 1.8 Hz, 1H), 2.01 – 1.85 (m, 3H), 1.45 – 1.40 (m, 1H), 1.33 (s, 3H), 1.18 (s, 3H), 0.89 (s, 3H), 0.87 (d, J = 1.0 Hz, 9H).

^{13}C NMR (101 MHz, $CDCl_3$): δ 176.01, 141.19, 126.49, 97.66, 91.56, 83.65, 82.63, 79.78, 71.83, 67.70, 59.19, 58.88, 54.72, 53.78, 49.82, 47.42, 44.61, 44.09, 39.84, 35.14, 29.85, 25.75, 25.21, 22.45, 18.52, 18.04, -4.63, -4.98.

FTIR (Neat, NaCl, thin film): 3503, 2928, 2856, 1778, 1713, 1458, 1255, 1168, 1094, 1031, 832, 776 cm^{-1}.

HRMS (ESI): calc'd for $[M+Na]^+$ 587.3010, found 587.3013.

$[\alpha]_D^{23}$: +12.6 (c 0.3 in $CHCl_3$).

Preparation of lactol 217.

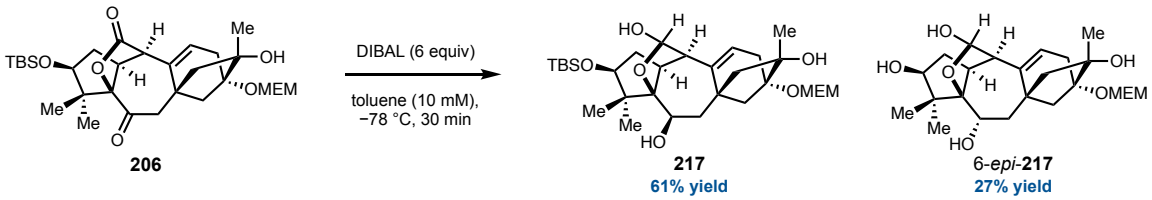

206 **217** 61% yield 6-*epi*-**217** 27% yield

The starting material (13 mg, 23.0 umol, 1 equiv.) was dissolved in toluene (2.1 mL, 10 mM). The solution was stirred for 3 min to ensure complete dissolution into toluene. Then,

it was cooled to −78 °C and DIBAL solution (130 uL, 1 M in hexanes, 5.65 equiv.) was added slowly dropwise. The mixture was stirred for 30 minutes at −78 °C. Following complete conversion by TLC (30 min at −78 °C), the reaction was quenched by slow addition of EtOAc (xs, 100 uL). Then, the vial was removed from the dry ice/acetone bath and allowed to warm to 0 °C. Once at 0 °C, sat. aq. Rochelle's salt (2 mL) was added. The reaction was slowly warmed to room temperature and vigorously stirred for 1 h until complete decomposition of aluminum aggregates. The remaining solution was extracted with EtOAc (3 x 0.5 mL), and the combined organics were washed with brine (2 x 1 mL), dried with sodium sulfate, filtered, and concentrated. The lactol was isolated by careful preparatory TLC in 100% EtOAc to afford **217** as a clear oil (8.0 mg, 61% yield) and 6-*epi*-**217** as a clear oil (3.4 mg, 27% yield).

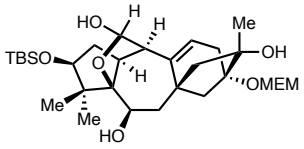

217

TLC (75% EtOAc/Hexanes): R_f 0.28 (*p*-anisaldehyde, dark blue)

TLC (10% MeOH/DCM): R_f 0.48 (*p*-anisaldehyde, blue).

^{1}H NMR (400 MHz, $CDCl_3$): δ 5.92 (d, *J* = 9.2 Hz, 1H), 5.28 – 5.19 (m, 2H), 4.81 – 4.71 (m, 2H), 3.88 (s, 1H), 3.78 (d, *J* = 6.7 Hz, 1H), 3.70 – 3.59 (m, 2H), 3.45 (t, *J* = 4.6 Hz, 2H), 3.28 (s, 3H), 2.93 (s, 1H), 2.59 – 2.51 (m, 1H), 2.44 (dd, *J* = 17.8, 3.0 Hz, 1H), 2.31 (dd, *J* = 12.2, 3.7 Hz, 1H), 2.17 – 2.10 (m, 1H), 2.00 – 1.87 (m, 3H), 1.80 – 1.67 (m, 4H), 1.14 (s, 3H), 1.10 (s, 3H), 0.88 (s, 3H), 0.82 (s, 9H).

^{13}C NMR (101 MHz, $CDCl_3$) δ 146.92, 122.36, 106.18, 100.51, 91.55, 85.67, 84.11, 79.48, 71.87, 70.94, 67.58, 65.90, 59.18, 55.99, 51.92, 47.95, 47.44, 45.30, 42.74, 39.82, 35.39, 26.04, 25.93, 25.25, 19.56, 18.41, -4.63, -4.96.

FTIR (Neat, NaCl, thin film): 3430, 2930, 1461, 1244, 1029, 861 cm^{-1}.

HRMS (ESI): calc'd for $[M+Na]^+$ 591.3323, found 591.3330.

$[\alpha]_D^{23}$: +61.0 (c 0.2 in MeOH).

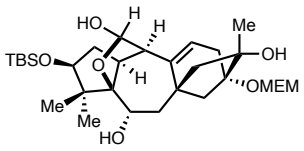

6-*epi*-**217**

TLC (75% EtOAc/Hexanes): R_f 0.34 (*p*-anisaldehyde, light blue).

^{1}H NMR (400 MHz, $CDCl_3$): δ 5.30 (t, *J* = 4.0 Hz, 1H), 5.25 (t, *J* = 3.6 Hz, 1H), 5.07 (d, *J* = 8.5 Hz, 1H), 4.91 – 4.83 (m, 2H), 4.10 (dd, *J* = 5.3, 1.6 Hz, 1H), 3.85 (d, *J* = 6.5 Hz, 1H), 3.79 – 3.70 (m, 2H), 3.55 (d, *J* = 4.6 Hz, 2H), 3.38 (d, *J* = 2.0 Hz, 3H), 3.00 (s, 1H), 2.76 (dd, *J* = 12.2, 3.7 Hz, 1H), 2.64 (ddd, *J* = 15.2, 12.2, 6.7 Hz, 1H), 2.51 (dd, *J* = 17.8, 3.3 Hz, 1H), 2.38 (dd, *J* = 15.7, 1.6 Hz, 1H), 2.32 – 2.24 (m, 2H), 2.11 – 2.06 (m, 1H), 1.96 (dd, *J* = 13.5, 2.0 Hz, 1H), 1.82 (td, *J* = 14.4, 4.6 Hz, 2H), 1.61 (d, *J* = 10.4 Hz, 1H), 1.20 (s, 3H), 1.10 (s, 3H), 0.92 (d, *J* = 7.6 Hz, 12H), 0.09 (d, *J* = 3.6 Hz, 6H).

^{13}C NMR (101 MHz, $CDCl_3$): δ 149.19, 121.09, 102.86, 99.90, 91.56, 86.07, 85.04, 78.04, 71.90, 70.41, 67.58, 64.72, 59.80, 59.18, 51.07, 48.09, 45.68, 43.16, 41.61, 39.49, 35.42, 25.98, 25.37, 24.46, 18.70, 18.41, -4.62, -4.94.

FTIR (Neat, NaCl, thin film): 3410, 2935, 1401, 1207, 1111, 1013 cm^{-1}.

HRMS (ESI): calc'd for $[M+Na]^+$ 591.3323, found 591.3320.

$[\alpha]_D^{23}$: +2.2 (c 0.2 in MeOH).

Preparation of C9-C11 dehydro auriculatol A (218).

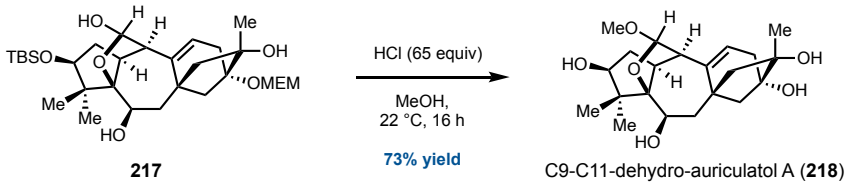

The starting material (3.5 mg, 6.15 umol, 1 equiv.) was dissolved in MeOH (200 uL). Then, a 1.25 M solution of HCl in MeOH (300 uL, 65 equiv.) was added dropwise at room temperature. The reaction was stirred overnight for 16 h. Upon completion, as determined by TLC, which showed complete conversion to a slightly more polar spot, the reaction was treated with $NaHCO_3$ (300 uL). The solution was extracted with EtOAc (0.3 mL x 5), washed with brine (1 x 1 mL), dried with $MgSO_4$, filtered, and concentrated. Careful preparatory TLC, loading the TLC plate with 10% MeOH/DCM and running the plate in 60% acetone/hexanes enabled isolation of the product **218** (1.7 mg, 73% yield) as a clear oil.

TLC (60% acetone/hexanes): R_f 0.50 (*p*-anisaldehyde, dark blue)

^{1}H NMR (400 MHz, CD_3OD): δ 5.28 (t, *J* = 3.6 Hz, 1H), 5.07 (s, 1H), 3.78 (dd, *J* = 10.9, 3.1 Hz, 1H), 3.49 (d, *J* = 6.7 Hz, 1H), 3.43 (s, 3H), 2.92 (s, 1H), 2.71 (ddd, *J* = 15.5, 11.8, 7.0 Hz, 1H), 2.37 – 2.17 (m, 3H), 2.11 – 1.97 (m, 3H), 1.85 – 1.78 (m, 2H), 1.70 (dd, *J* = 15.5, 4.2 Hz, 1H), 1.58 (dd, *J* = 14.7, 3.2 Hz, 1H), 1.30 (s, 3H), 1.18 (s, 3H), 1.02 (s, 3H).

^{13}C NMR (101 MHz, CD_3OD): δ 150.03, 122.52, 112.02, 103.30, 85.87, 80.77, 78.90, 74.36, 63.18, 60.81, 56.57, 52.75, 52.73, 50.02, 46.82, 41.04, 40.47, 38.54, 24.14, 23.79, 20.08.

FTIR (Neat, NaCl, thin film): 3413, 2928, 2854, 1444, 1382, 1172, 1078 cm^{-1}.

HRMS (ESI): calc'd for $[M+Na]^+$ 403.2091, found 403.2091.

$[\alpha]_D^{23}$: +113.9 (c 0.2 in MeOH).

Preparation of auriculatol A (49) and 9-*epi*-auriculatol A (219).

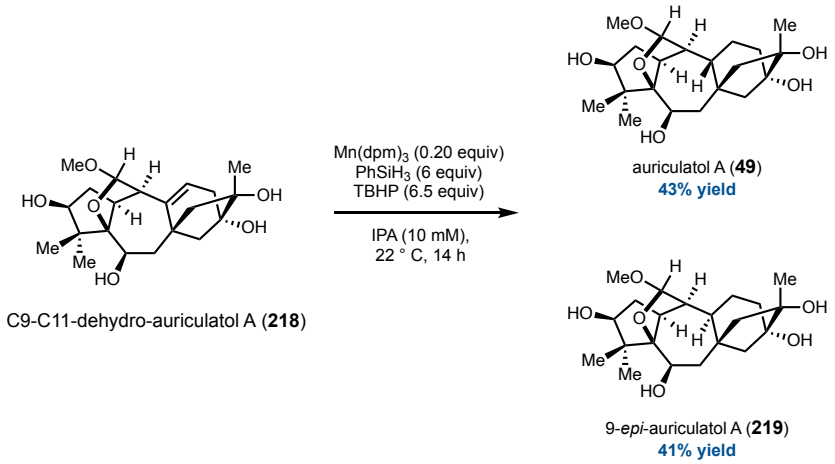

The pentacycle **218** (10.5 mg, 27.6 umol, 1 equiv) was dissolved in isopropanol (1 mL) in a 2-dram vial, and the solution was charged with a magnetic stir bar. Phenylsilane (20 uL, 6 equiv) and TBHP (33 uL, 5.5 M solution in decane, 6.5 equiv) were added to the vial. A separate 2-dram vial was equipped with a magnetic stir bar and charged with $Mn(dpm)_3$ (6.7 mg, 11.0 umol) isopropanol (1 mL), then stirred at room temperature for 5 minutes until the solids dissolved. Both vials were capped with a rubber septum, evacuated and backfilled with N_2 three times, and freeze-pump-thawed three times to remove any trace O_2. After freeze-pump-thaw, both vials were warmed to room temperature and stirred for 5 minutes to ensure complete dissolution of all components. Then, $Mn(dpm)_3$ stock solution (0.5 mL, 5.5 umol) was dispensed into the vial containing the starting material, phenylsilane, and TBHP. The reaction was left to stir at room temperature overnight for 14 h, upon which TLC in 60% acetone/hexanes indicated complete conversion to a slightly more polar spot. The reaction was worked up by removal of the stir bar, rinsing with

isopropanol, and rotatory evaporation. The crude residue was initially purified by preparatory TLC in 60% acetone/hexanes, isolating the major band (9 mg, 90% yield) that contained a 1.1:1 mixture of auriculatol A and 9-*epi*-auriculatol A. The separation of auriculatol A and 9-*epi*-auriculatol A was carried out via HPLC-TOF reverse phase chromatography (Eclipse XDB-C18 – 9.4 mm x 250 mm column, 30% ACN/70% H_2O, flow rate: 0.6 mL/min, t_R (auriculatol A = 6.4 min) t_R (9-*epi*-auriculatol A) = 7.1 min, to yield auriculatol A as a colorless oil (4.5 mg, 43% yield) and 9-*epi*-auriculatol A as a colorless oil (4.3 mg, 41% yield). NMR data of the mixture and analytically pure samples have been provided.

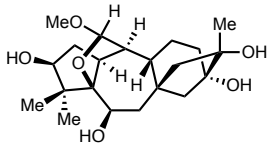

auriculatol A (**49**)

TLC (60% acetone/hexanes): R_f 0.42 (*p*-anisaldehyde, blue).

^{1}H NMR (600 MHz, MeOD): δ 4.98 (s, 1H), 3.71 (dd, *J* = 11.0, 3.7 Hz, 1H), 3.48 (d, *J* = 6.7 Hz, 1H), 3.41 (s, 3H), 2.75 – 2.70 (m, 1H), 2.62 (dd, *J* = 12.0, 3.6 Hz, 1H), 2.08 (s, 1H), 1.97 (dd, *J* = 14.0, 11.0 Hz, 1H), 1.90 (d, *J* = 11.3, 1H), 1.88 – 1.75 (m, 3H), 1.75 – 1.59 (m, 5H), 1.58 – 1.48 (m, 2H), 1.30 (s, 3H), 1.22 (s, 3H), 1.03 (s, 3H).

^{13}C NMR (101 MHz, MeOD): δ 117.80, 103.91, 85.93, 80.99, 78.73, 74.01, 61.49, 61.48, 56.37, 52.82, 49.21, 48.13, 42.96, 41.30, 41.27, 39.91, 32.57, 29.22, 24.72, 21.50, 20.45.

FTIR (DCM, NaCl, thin film): 3413, 2935, 1446, 1192, 1087, 946, 735 cm^{-1}.

HRMS (ESI): calc'd for $C_{21}H_{34}O_6Na$ $[M+Na]^+$ 405.2247, found 405.2248.

$[\alpha]_D^{23}$: +158.0 (c 0.4 in MeOH).

Comparison of synthetic and natural product auriculatol A (49)

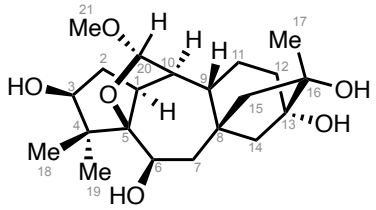

(+)-auriculatol A (49)

Table 6.1: Comparison of synthetic and natural auriculatol A (**1**) by ^{1}H NMR in MeOD

No.	This Report Auriculatol A (MeOD, 600 MHz)	Sun et al.[31] Auriculatol A (MeOD, 400 MHz)
1*α*	2.62, dd (12.0, 3.6)	2.61, dd (12.0, 3.5)
2*α*	2.71, ddd (14.8, 12.0, 6.9)	2.71, ddd (14.8, 12.0, 6.7)
2β	1.56, dd (14.7, 3.4)	1.55, dd (14.8, 3.5)
3*α*	3.48, d (6.5)	3.48, d (6.7)
6*α*	3.71, dd (11.0, 3.8)	3.70, dd (11.0, 3.6)
7*α*	1.51, dd (14.0, 3.6)	1.52, dd (14.0, 3.6)
7β	1.97, dd, (13.9, 11.0)	1.97, dd (14.0, 11.0)
9β	1.69, m	1.69, m
10	2.08, s	2.08, s
11*α*	1.61, m	1.60, m
11β	1.69, m	1.69, m
12*α*	1.66, m	1.67, m
12β	1.86, m	1.85, m
14*α*	1.77, d (11.5)	1.77, d (11.6)
14β	1.90, d, (11.0)	1.90, d (11.6)
15*α*	1.68, d (14.4)	1.68, d (14.5)
15β	1.80, d (14.7)	1.80, d (14.5)
17	1.22, s	1.22, s
18	1.30, s	1.30, s
19	1.03, s	1.03, s
20	4.98, s	4.98, s
21	3.41, s	3.41, s

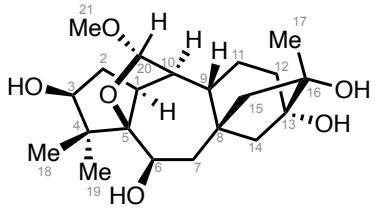

(+)-auriculatol A (49)

Table 6.2: Comparison of synthetic and natural auriculatol A (**1**) by ^{13}C NMR in MeOD

No.	This Report Auriculatol A (MeOD, 101 MHz)	Sun et al.[31] Auriculatol A (MeOD, 100 MHz)	Difference (ppm)
1	42.8	43.0	0.2
2	41.2	41.3	0.1
3	85.8	85.9	0.1
4	52.7	52.8	0.1
5	103.8	103.9	0.1
6	73.9	74.0	0.1
7	48.0	48.1	0.1
8	39.8	39.9	0.1
9	49.1 (overlap with MeOD)	49.2	0.1
10	61.4 (overlap)	61.5	0.1
11	29.1	29.2	0.1
12	32.5	32.6	0.1
13	78.6	78.8	0.2
14	41.1	41.3	0.2
15	61.4 (overlap)	61.5	0.1
16	80.9	81.0	0.1
17	21.4	21.5	0.1
18	20.3	20.5	0.2
19	24.6	24.8	0.2
20	117.7	117.8	0.1
21	56.2	56.4	0.2

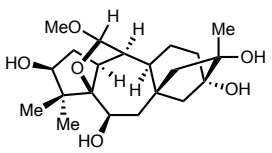

C9-*epi*-auriculatol A (**219**)

TLC (60% acetone/hexanes): R_f 0.43 (*p*-anisaldehyde, blue).

^{1}H NMR (400 MHz, MeOD): δ 5.23 (s, 1H), 4.11 (dd, *J* = 4.5, 2.7 Hz, 1H), 3.56 (dd, *J* = 6.6, 2.9 Hz, 1H), 3.42 (s, 3H), 2.56 – 2.45 (m, 2H), 2.32 (d, *J* = 2.3 Hz, 1H), 2.12 – 2.00 (m, 3H), 1.86 (dd, *J* = 15.4, 2.2 Hz, 1H), 1.73 – 1.66 (m, 4H), 1.63 – 1.55 (m, 3H), 1.25 (m), 1.21 (s, 3H), 1.17 (s, 3H), 0.99 (s, 3H).

^{13}C NMR (101 MHz, MeOD): δ 108.87, 101.12, 84.79, 79.63, 79.20, 71.07, 59.73, 56.68, 56.12, 51.42, 48.86, 48.67, 48.04, 46.07, 42.95, 39.21, 34.55, 28.12, 26.83, 20.73, 19.58.

FTIR (Neat, NaCl, thin film): 3436, 2925, 1456, 1083, 998, 735 cm^{-1}.

HRMS (ESI): calc'd for $C_{21}H_{34}O_6Na$ $[M+Na]^+$ 405.2247, found 405.2249.

$[\alpha]_D^{23}$: +27.5 (c 0.4 in MeOH).

6.6 NOTES AND REFERENCES

(1) Crossley, S. W. M.; Martinez, R. M.; Obradors, C.; Shenvi, R. A. Mn, Fe, and Co-Catalyzed Radical Hydrofunctionalizations of Olefins. *Chem. Rev.* **2016**, *116*, 8912-9000.

(2) Shevick, S. L.; Wilson, C. V.; Kotesova, S.; Kim, D.; Holland, P. L.; Shenvi, R. A. Catalytic hydrogen atom transfer to alkenes: a roadmap for metal hydrides and radicals. *Chem. Sci.* **2020**, 11, 12401–12422.

(3) Wu, J.; Ma, Z. Metal-Hydride Hydrogen Atom Transfer (MHAT) Reactions in Natural Product Synthesis. *Org. Chem. Front.* **2021**, *8*, 7050–7076.

(4) Matos, J. L. M.; Green, S. A.; Shenvi, R. A. Chapter 7. Markovnikov Functionalization by Hydrogen Atom Transfer, Organic Reactions, **2019**, *100*, 383–470.

(5) Green, S.A.; Crossley, S.W.M.; Matos, J.L.M.; Vásquez-Céspedes, S.; Shevick, S. L.; Shenvi, R. A. The High Chemofidelity of Metal-Catalyzed Hydrogen Atom Transfer *Acc. Chem. Res.,* **2018**, *51*, 2628–2640.

(6) Obradors, C. L.; Martinez, R.; Shenvi, R. A. Ph(i-PrO)SiH_2: An Exceptional Reductant for Metal-Catalyzed Hydrogen Atom Transfers. *J. Am. Chem. Soc.* **2016**, *138*, 4962-4971.

(7) Jeker, O. F.; Carreira, E. M. Total Synthesis and Stereochemical Reassignment of (±)-Indoxamycin B. *Angew. Chem., Int. Ed.* **2012**, *51*, 3474−3477.

(8) Bhunia, A.; Bergander, K.; Daniliuc, C. G.; Studer, A. Fe-Catalyzed Anaerobic Mukaiyama-Type Hydration of Alkenes using Nitroarenes. *Angew. Chem. Int. Ed.* **2021**, *60*, 8313–8320.

(9) Ali, G.; Cuny, G. D. Syntheses of Gymnothespirolignans B and C and Non-Isomer 9-Epi-gymnothespirolignan B. *J. Org. Chem.* **2021**, *86*, 10517–10525.

(10) Huang, S.-H.; Liang, K.-H.; Lu, J.-S.; Chang, W.-S.; Su, M.-D.; Yang, T.-F. Total Synthesis of (+)-Antrocin and Its Diastereomer and Clarification of the Absolute Stereochemistry of (−)-Antrocin. *J. Org. Chem.* **2017**, *82*, 9576–9584.

(11) Zhao, Y.; Hu, J.; Chen, R.; Xiong, F.; Xie. H.; Ding, H. Divergent Total Syntheses of (−)-Crinipellins Facilitated by a HAT-Initiated Dowd–Beckwith Rearrangement. *J. Am. Chem. Soc.* **2022**, *144*, 2495–2500.

(12) Nishiyama, Y.; Yokoshima, S.; Fukuyama, T. Total Synthesis of (−)-Cardiopetaline. *Org. Lett.* **2016**, *18*, 2359–2362.

(13) Iwasaki, K.; Wan, K. K.; Oppedisano, A.; Crossley, S. W. M.; Shenvi, R. A. Simple, Chemoselective Hydrogenation with Thermodynamic Stereocontrol. *J. Am. Chem. Soc.* **2014**, *136*, 1300–1303.

(14) Garrett, C. E.; Fu, G. C. Hydroboration of Olefins with Catecholborane at Room Temperature in the Presence of N,N-Dimethylacetamide. *J. Org. Chem.* **1996**, *61*, 3224–3225.

(15) Pozzi, D.; Scanlan, E. M.; Renaud, P. A Mild Radical Procedure for the Reduction of B-Alkylcatecholborane to Alkanes. *J. Am. Chem. Soc.* **2005**, *127*, 14204–14205.

(16) Dhillon, R. S. Hydroboration and Organic Synthesis. *Springer,* © 2007, ISBN 978-3-540-49075-3 Springer-Verlag Berlin Hedelberg.

(17) Wang, J.; Ma, D. 6-Methylenebicyclo[3.2.1]oct-1-en-3-one: A Twisted Olefin as Diels-Alder Dienophile for Expedited Syntheses of Four Kaurane Diterpenoids. *Angew. Chem. Int. Ed.* **2019**, *58*, 15731–15735.

(18) Takahashi, K.; Watanabe, M.; Honda, T. Highly Efficient Stereocontrolled Total Synthesis of (+)-Upial. *Angew. Chem. Int. Ed.* **2007**, *47*, 131–133.

(19) Pappo, R.; Allen, D. S.; Lemieux, R. U.; Johnson, W. S. Osmium Tetroxide-Catalyzed Periodate Oxidation of Olefinic Bonds. *J. Am. Chem. Soc.* **1956**, *21*, 478–479.

(20) Morrison, E.; Chandler, P. M.; Thomson, R. J.; Mander, L. N. Synthesis and Bioactivity of the Gibberellin, 18-hydroxy-GA_1 (GA_{132}). *Org. Biomol. Chem.* **2008**, *6*, 1416–1424.

(21) Yu, W.; Mei, Y.; Kang, Y.; Hua, Z.; Jin, Z. Improved Procedure for the Oxidative Cleavage of Olefin by OsO_4-$NaIO_4$. *Org. Lett.* **2004**, *6*, 3217–3219.

(22) Schröder, M. Osmium Tetoxide Cis Hydroxylation of Unsaturated Substrates. *Chem. Rev.* **1980**, *80*, 187–213.

(23) Shen, Y.; Li, L.; Xiao, X.; Yang, S.; Hua, Y.; Wang, Y.; Zhang, Y.-W.; Zhang, Y. Site-Specific Photochemical Desaturation Enables Divergent Syntheses of *Illicium* Sesquiterpenes. *J. Am. Chem. Soc.* **2021**, *143*, 3256–3263.

(24) Yu, K.; Yang, Z.-N.; Liu, C.-H.; Wu, S.-Q.; Hong, X.; Zhao, X.-L.; Ding, H. Total Syntheses of Rhodomolleins XX and XXII: A Reductive Epoxide-Opening/Beckwith-Dowd Approach. *Angew. Chem. Int. Ed.* **2019**, *58*, 8556–8560.

(25) Hu, X.; Musacchio, A. J.; Shen X.; Yao, Y.; Maimone, T. J. Allylative Approaches to the Synthesis of Complex Guaianolide Sesquiterpenes from Apiaceae and Asteraceae. *J. Am. Chem. Soc.* **2019**, *141*, 14904–14915.

(26) Xiao, S.; Ai, L.; Liu, Q.; Yang, B.; Huang, J.; Xue, W.; Chen, Y. Total Synthesis of Natural Terpenoids Enabled by Cobalt Catalysis. *Frontiers in Chemistry*. **2022**, *10*, 1–7.

(27) Li, Y.; Fu, Y. Recent Advances in the Cobalt-Catalyzed Regio- or Stereoselective Hydrofunctionalization of Alkenes and Alkynes. *CCS. Chem.* **2024**, *6*, 1130–1156.

(28) Eggert, A.; Schuppe, K. T.; Fuchs, H. L. S.; Brönstrup, M.; Kalesse, M. Total Synthesis of Acanthodoral Using a Rearrangement Strategy. *Org. Lett.* **2024**, *26*, 2893–2896.

(29) Zhang, M.; Zhu, Y.; Zhan, G.; Shu, P.; Sa, R.; Lei, L.; Xiang, M.; Xue, Y.; Luo, Z.; Wan, Q.; Yao, G.; Zhang, Y. Micranthanone A, a New Diterpene with an Unprecedented Carbon Skeleton from *Rhododendrum micranthum. Org. Lett.* **2013**, *15*, 3094–3097.

(30) (a) Iwasaki, K.; Wan, K.; Oppedisano, A.; Crossley, S. W. M.; Shenvi, R. A. Simple, Chemoselective Hydrogenation with Thermodynamic Stereocontrol. *J. Am. Chem. Soc.* **2014**, *136*, 1300−1303. (b) Pan, L.; Schneider, F.; Ottenbruch, M.; Wiechert, R.; List, T.; Schoch, P.; Mertes, B.; Gaich, T. A General Strategy for the Synthesis of Taxane Diterpenes. *Nature* **2024**, 632, 543−549.

(31) Sun, N.; Zheng, G.; He, M.; Feng, Y.; Liu, J.; Wang, M.; Zhang, H.; Zhou, J.; Yao, G. Grayanane diterpenoids from the leaves of *Rhododendron auriculatum* and their analgesic activities. *J. Nat. Prod.* **2019**, *82*, 1849−1860.

Appendix 6

Spectra Relevant to Chapter 6:

End Game

Parameter	Value
Data File Name	/ Volumes/ nmrdata-2/ jkthomps/ nmr/ JKT-5-244_pure/ 1/ fid
Title	JKT-5-244_pure.1.fid
Origin	Bruker BioSpin GmbH
Solvent	CDCl3
Temperature	297.1
Pulse Sequence	zg30
Experiment	1D
Number of Scans	16
Receiver Gain	197.4
Relaxation Delay	1.0000
Pulse Width	12.5000
Acquisition Time	4.0894
Acquisition Date	2024-02-06T02:28:23
Spectrometer Frequency	400.13
Spectral Width	8012.8
Nucleus	1H
Acquired Size	32768
Spectral Size	65536

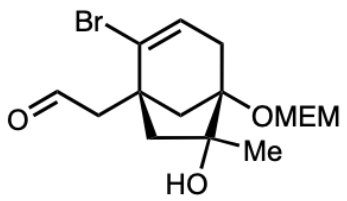

189

Parameter	Value
Data File Name	/ Volumes/ nmrdata-2/ jkthomps/ nmr/ JKT-5-244_pure/ 2/ fid
Title	JKT-5-244_pure.2.fid
Origin	Bruker BioSpin GmbH
Solvent	CDCl3
Temperature	297.2
Pulse Sequence	zgpg30
Experiment	1D
Number of Scans	1024
Receiver Gain	78.7
Relaxation Delay	1.0000
Pulse Width	10.0000
Acquisition Time	1.3631
Acquisition Date	2024-02-06T03:10:46
Spectrometer Frequency	100.62
Spectral Width	24038.5
Nucleus	13C
Acquired Size	32768
Spectral Size	65536

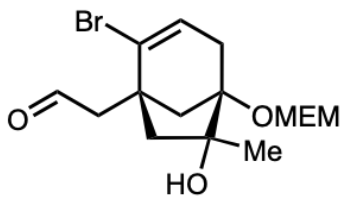

189

Parameter	Value
Data File Name	/ Users/ jordankthompson/ Desktop/ JKT-5-238_pure/ PROTON01.fid/ fid
Title	PROTON01
Origin	Varian
Solvent	cdcl3
Temperature	25.0
Pulse Sequence	s2pul
Experiment	1D
Number of Scans	32
Receiver Gain	58
Relaxation Delay	1.0000
Pulse Width	5.6500
Acquisition Time	3.0000
Acquisition Date	2024-01-31T16:44:53
Spectrometer Frequency	499.55
Spectral Width	8000.0
Nucleus	1H
Acquired Size	24000
Spectral Size	65536

192

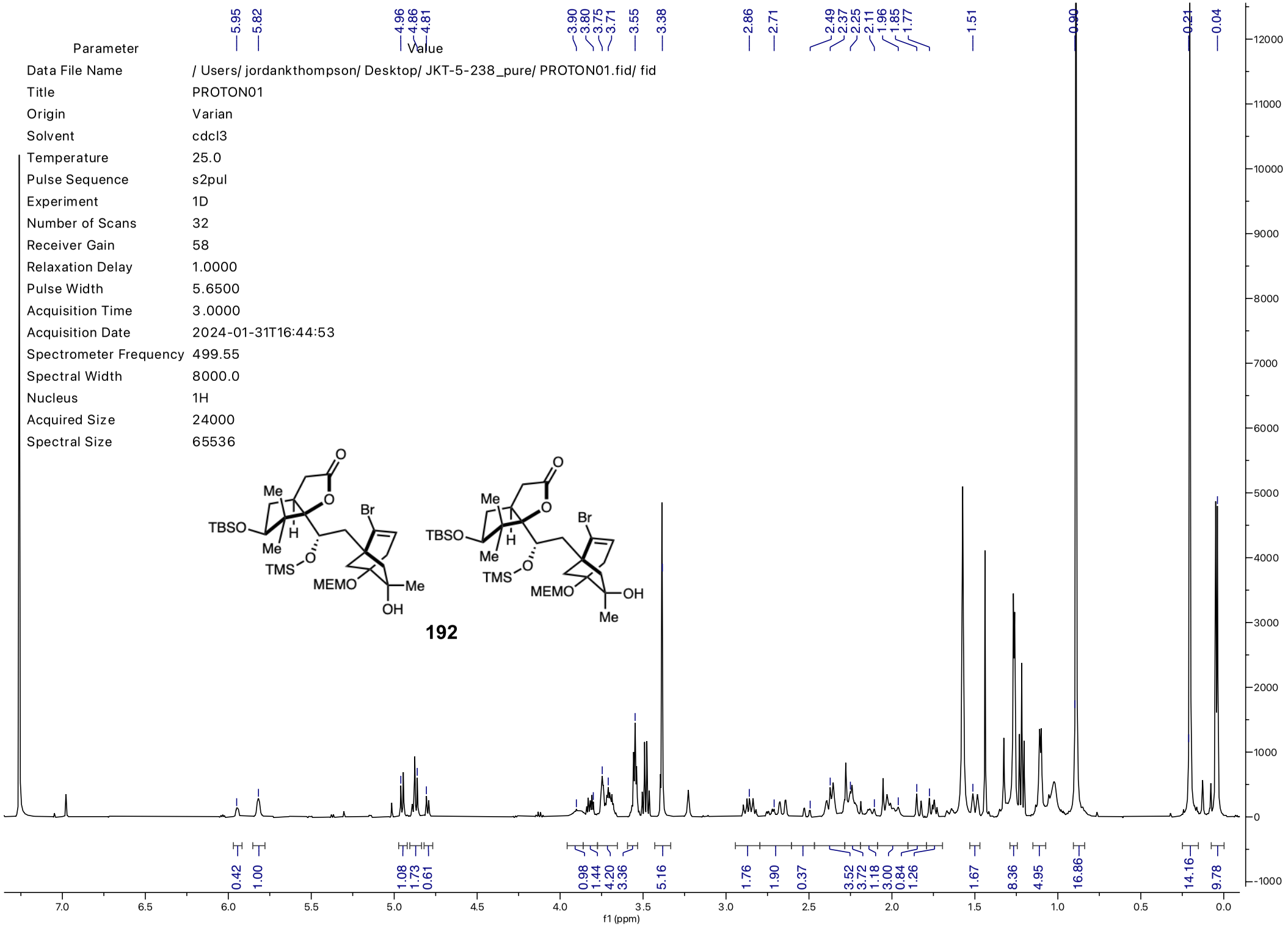

Parameter	Value
Data File Name	/ Volumes/ nmrdata-3/ jkthomps/ nmr/ JKT-6-130_pure/ 2/ fid
Title	JKT-6-130_pure.2.fid
Origin	Bruker BioSpin GmbH
Solvent	CDCl3
Temperature	297.1
Pulse Sequence	zgpg30
Experiment	1D
Number of Scans	512
Receiver Gain	64.2
Relaxation Delay	1.0000
Pulse Width	10.0000
Acquisition Time	1.3631
Acquisition Date	2024-05-22T18:39:43
Spectrometer Frequency	100.62
Spectral Width	24038.5
Nucleus	13C
Acquired Size	32768
Spectral Size	65536

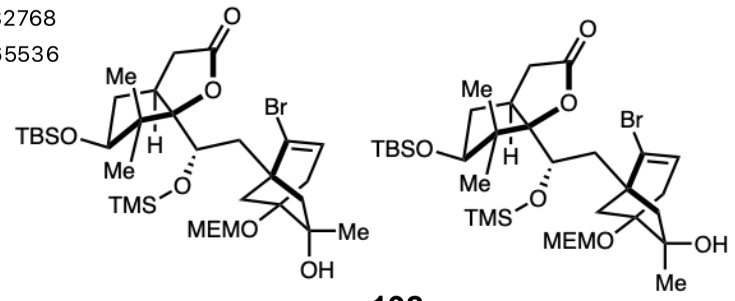

192

Parameter	Value
Data File Name	/ Users/ jordankthompson/ Desktop/ JKT-5-240_pure/ 1/ fid
Title	JKT-5-240_pure.1.fid
Origin	Bruker BioSpin GmbH
Solvent	CDCl3
Temperature	297.1
Pulse Sequence	zg30
Experiment	1D
Number of Scans	64
Receiver Gain	197.4
Relaxation Delay	1.0000
Pulse Width	12.5000
Acquisition Time	4.0894
Acquisition Date	2024-02-01T12:01:08
Spectrometer Frequency	400.13
Spectral Width	8012.8
Nucleus	1H
Acquired Size	32768
Spectral Size	65536

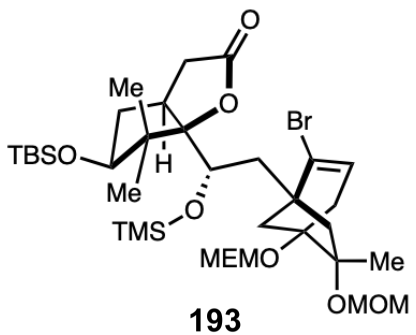

193

Parameter	Value
Data File Name	/ Volumes/ nmrdata-1/ jkthomps/ nmr/ JKT-6-138_sm/ 2/ fid
Title	JKT-6-138_sm.2.fid
Origin	Bruker BioSpin GmbH
Solvent	CDCl3
Temperature	297.2
Pulse Sequence	zgpg30
Experiment	1D
Number of Scans	512
Receiver Gain	87.8
Relaxation Delay	1.0000
Pulse Width	10.0000
Acquisition Time	1.3631
Acquisition Date	2024-08-20T13:27:29
Spectrometer Frequency	100.62
Spectral Width	24038.5
Nucleus	13C
Acquired Size	32768
Spectral Size	65536

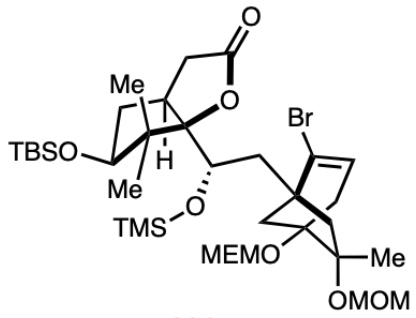

193

Parameter	Value
Data File Name	/ Volumes/ nmrdata/ jkthomps/ nmr/ JKT-7-188_pure3/ 1/ fid
Title	JKT-7-188_pure3.1.fid
Origin	Bruker BioSpin GmbH & Co.KG
Solvent	CDCl3
Temperature	298.1
Pulse Sequence	zg30
Experiment	1D
Number of Scans	16
Receiver Gain	90.5
Relaxation Delay	1.0000
Pulse Width	9.8500
Acquisition Time	3.9977
Acquisition Date	2025-05-07T23:28:12
Spectrometer Frequency	400.15
Spectral Width	8196.7
Nucleus	1H
Acquired Size	32768
Spectral Size	65536

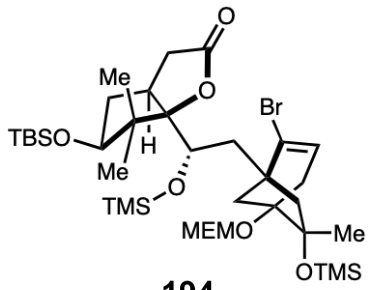

194

Parameter	Value
Data File Name	/ Volumes/ nmrdata/ jkthomps/ nmr/ JKT-7-188_pure3/ 2/ fid
Title	JKT-7-188_pure3.2.fid
Origin	Bruker BioSpin GmbH & Co.KG
Solvent	CDCl3
Temperature	298.2
Pulse Sequence	zgpg30
Experiment	1D
Number of Scans	700
Receiver Gain	101.0
Relaxation Delay	1.0000
Pulse Width	10.0000
Acquisition Time	1.1796
Acquisition Date	2025-05-07T23:54:38
Spectrometer Frequency	100.63
Spectral Width	27777.8
Nucleus	13C
Acquired Size	32768
Spectral Size	65536

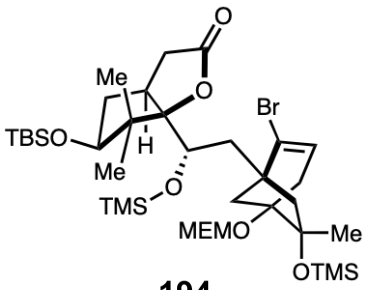

194

Parameter	Value
Data File Name	/ Volumes/ nmrdata/ jkthomps/ nmr/ JKT-7-188_pure3/ 3/ ser
Title	JKT-7-188_pure3.3.ser
Origin	Bruker BioSpin GmbH & Co.KG
Solvent	CDCl3
Temperature	298.1
Pulse Sequence	cosygpppqf
Experiment	COSY
Number of Scans	1
Receiver Gain	101.0
Relaxation Delay	2.0000
Pulse Width	9.8500
Acquisition Time	0.1946
Acquisition Date	2025-05-08T00:00:12
Spectrometer Frequency	(400.15,400.15)
Spectral Width	(5263.2,5263.2)
Lowest Frequency	(-230.7,-230.7)
Nucleus	(1H,1H)
Acquired Size	(1024,128)
Spectral Size	(1024,1024)
Digital Resolution	(5.14,5.14)

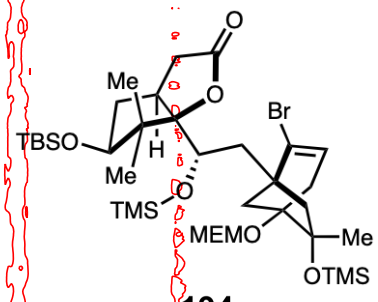

194

f2 (ppm)

f1 (ppm)

Parameter	Value
Data File Name	/ Volumes/ nmrdata/ jkthomps/ nmr/ JKT-7-188_pure3/ 4/ ser
Title	JKT-7-188_pure3.4.ser
Origin	Bruker BioSpin GmbH & Co.KG
Solvent	CDCl3
Temperature	298.2
Pulse Sequence	hmbcgplpndqf
Experiment	HMBC
Number of Scans	4
Receiver Gain	101.0
Relaxation Delay	1.5000
Pulse Width	9.8500
Acquisition Time	0.5980
Acquisition Date	2025-05-08T00:19:26
Spectrometer Frequency	(400.16,100.63)
Spectral Width	(3424.7,22138.1)
Lowest Frequency	(-245.1,-1007.3)
Nucleus	(1H,13C)
Acquired Size	(2048,128)
Spectral Size	(2048,512)
Digital Resolution	(1.67,43.24)

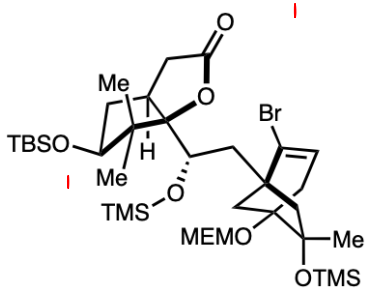

194

f2 (ppm)

f1 (ppm)

Parameter	Value
Data File Name	/ Volumes/ nmrdata/ jkthomps/ nmr/ JKT-7-188_pure3/ 5/ ser
Title	JKT-7-188_pure3.5.ser
Origin	Bruker BioSpin GmbH & Co.KG
Solvent	CDCl3
Temperature	298.2
Pulse Sequence	hsqcedetgpsisp2.3
Experiment	HSQC-EDITED
Number of Scans	2
Receiver Gain	32.0
Relaxation Delay	1.5000
Pulse Width	9.8500
Acquisition Time	0.1946
Acquisition Date	2025-05-08T00:30:47
Spectrometer Frequency	(400.15,100.63)
Spectral Width	(5263.2,16603.2)
Lowest Frequency	(-750.9,-755.3)
Nucleus	(1H,13C)
Acquired Size	(1024,180)
Spectral Size	(1024,1024)
Digital Resolution	(5.14,16.21)

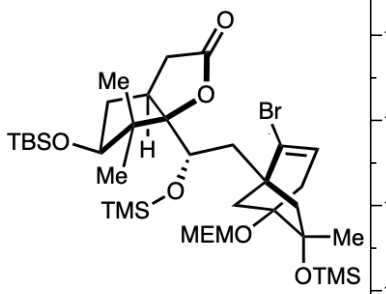

194

f2 (ppm)

f1 (ppm)

Parameter	Value
Data File Name	/ Volumes/ nmrdata/ jkthomps/ nmr/ JKT-7-188_pure3/ 6/ ser
Title	JKT-7-188_pure3.6.ser
Origin	Bruker BioSpin GmbH & Co.KG
Solvent	CDCl3
Temperature	298.1
Pulse Sequence	noesygpphzs
Experiment	NOESY
Number of Scans	4
Receiver Gain	64.0
Relaxation Delay	1.5000
Pulse Width	9.8500
Acquisition Time	0.2580
Acquisition Date	2025-05-08T01:10:58
Spectrometer Frequency	(400.15,400.15)
Spectral Width	(3968.3,3968.3)
Lowest Frequency	(-103.4,-103.4)
Nucleus	(1H,1H)
Acquired Size	(1024,256)
Spectral Size	(1024,1024)
Digital Resolution	(3.88,3.88)

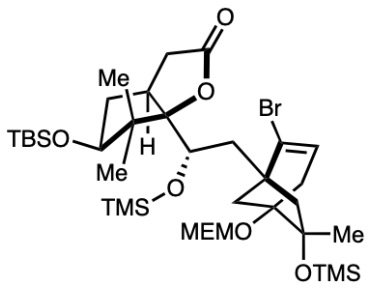

194

f2 (ppm)

f1 (ppm)

Parameter	Value
Data File Name	/ Volumes/ nmrdata/ jkthomps/ nmr/ JKT-3-7_crude/ 1/ fid
Title	JKT-3-7_crude.1.fid
Origin	Bruker BioSpin GmbH
Solvent	CDCl3
Temperature	298.1
Pulse Sequence	zg30
Experiment	1D
Number of Scans	16
Receiver Gain	127.1
Relaxation Delay	1.0000
Pulse Width	8.7000
Acquisition Time	4.0894
Acquisition Date	2025-03-28T09:00:57
Spectrometer Frequency	400.13
Spectral Width	8012.8
Nucleus	1H
Acquired Size	32768
Spectral Size	65536

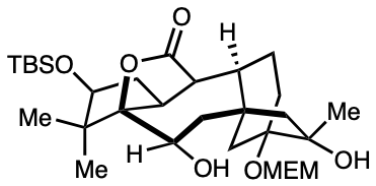

197

Parameter	Value
Data File Name	/ Volumes/ nmrdata/ jkthomps/ nmr/ JKT-3-7_crude/ 6/ fid
Title	JKT-3-7_crude.6.fid
Origin	Bruker BioSpin GmbH
Solvent	CDCl3
Temperature	298.1
Pulse Sequence	zgpg30
Experiment	1D
Number of Scans	3500
Receiver Gain	197.4
Relaxation Delay	1.0000
Pulse Width	10.0000
Acquisition Time	1.1796
Acquisition Date	2025-03-29T00:03:06
Spectrometer Frequency	100.62
Spectral Width	27777.8
Nucleus	13C
Acquired Size	32768
Spectral Size	65536

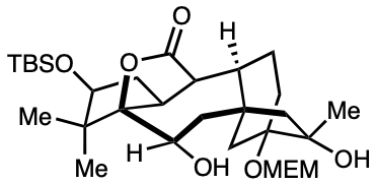

197

Parameter	Value
Data File Name	/ Volumes/ nmrdata/ jkthomps/ nmr/ JKT-3-7_crude/ 3/ ser
Title	JKT-3-7_crude.3.ser
Origin	Bruker BioSpin GmbH
Solvent	CDCl3
Temperature	298.1
Pulse Sequence	cosygpppqf
Experiment	COSY
Number of Scans	3
Receiver Gain	64.2
Relaxation Delay	1.9205
Pulse Width	8.7000
Acquisition Time	0.2765
Acquisition Date	2025-03-28T09:40:42
Spectrometer Frequency	(400.13,400.13)
Spectral Width	(3703.7,3703.7)
Lowest Frequency	(-426.9,-428.0)
Nucleus	(1H,1H)
Acquired Size	(1024,128)
Spectral Size	(1024,1024)
Digital Resolution	(3.62,3.62)

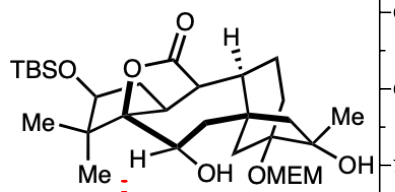

197

f2 (ppm)

f1 (ppm)

Parameter	Value
Data File Name	/ Volumes/ nmrdata/ jkthomps/ nmr/ JKT-3-7_crude/ 4/ ser
Title	JKT-3-7_crude.4.ser
Origin	Bruker BioSpin GmbH
Solvent	CDCl3
Temperature	298.2
Pulse Sequence	hsqcedetgpsisp2.4
Experiment	HSQC-EDITED
Number of Scans	4
Receiver Gain	197.4
Relaxation Delay	1.5000
Pulse Width	8.7000
Acquisition Time	0.2135
Acquisition Date	2025-03-28T10:03:17
Spectrometer Frequency	(400.13,100.62)
Spectral Width	(4795.4,16611.3)
Lowest Frequency	(-517.1,-1262.8)
Nucleus	(1H,13C)
Acquired Size	(1024,180)
Spectral Size	(1024,1024)
Digital Resolution	(4.68,16.22)

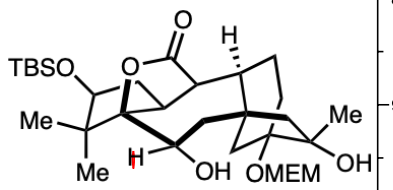

197

f2 (ppm)

f1 (ppm)

Parameter	Value
Data File Name	/ Volumes/ nmrdata/ jkthomps/ nmr/ JKT-3-7_crude/ 5/ ser
Title	JKT-3-7_crude.5.ser
Origin	Bruker BioSpin GmbH
Solvent	CDCl3
Temperature	298.1
Pulse Sequence	noesygpphzs
Experiment	NOESY
Number of Scans	4
Receiver Gain	98.9
Relaxation Delay	1.8000
Pulse Width	8.7000
Acquisition Time	0.2560
Acquisition Date	2025-03-28T14:51:18
Spectrometer Frequency	(400.13,400.13)
Spectral Width	(4000.0,4000.0)
Lowest Frequency	(-158.1,-158.1)
Nucleus	(1H,1H)
Acquired Size	(1024,256)
Spectral Size	(1024,1024)
Digital Resolution	(3.91,3.91)

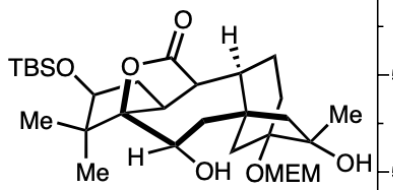

197

f2 (ppm)

f1 (ppm)

Parameter	Value
Data File Name	/ Volumes/ nmrdata/ jkthomps/ nmr/ JKT-7-107_pure/ 1/ fid
Title	JKT-7-107_pure.1.fid
Origin	Bruker BioSpin GmbH
Solvent	CDCl3
Temperature	298.1
Pulse Sequence	zg30
Experiment	1D
Number of Scans	16
Receiver Gain	112.8
Relaxation Delay	1.0000
Pulse Width	8.7000
Acquisition Time	4.0894
Acquisition Date	2025-03-21T21:05:11
Spectrometer Frequency	400.13
Spectral Width	8012.8
Nucleus	1H
Acquired Size	32768
Spectral Size	65536

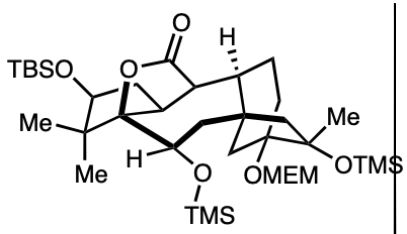

198

5.19 4.65 4.07 3.81 3.58 3.39 2.80 2.53 2.40 2.24 2.06 1.85 1.65 1.43 1.28 1.19 1.17 1.03 0.87 0.16 0.08 0.01 -0.02

1.00 1.00 1.06 1.00 4.15 3.22 1.03 1.01 0.99 1.00 1.01 1.96 6.06 0.95 1.17 3.04 3.00 3.04 9.69 9.79 9.03 6.33

f1 (ppm)

Parameter	Value
Data File Name	/ Volumes/ nmrdata/ jkthomps/ nmr/ JKT-7-107_pure/ 2/ fid
Title	JKT-7-107_pure.2.fid
Origin	Bruker BioSpin GmbH
Solvent	CDCl3
Temperature	298.2
Pulse Sequence	zgpg30
Experiment	1D
Number of Scans	3000
Receiver Gain	197.4
Relaxation Delay	1.0000
Pulse Width	10.0000
Acquisition Time	1.1796
Acquisition Date	2025-03-21T22:58:33
Spectrometer Frequency	100.62
Spectral Width	27777.8
Nucleus	13C
Acquired Size	32768
Spectral Size	65536

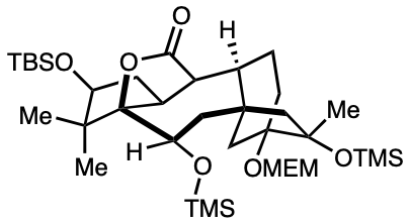

198

Parameter	Value
Data File Name	/ Volumes/ nmrdata/ jkthomps/ nmr/ JKT-7-107_pure/ 3/ ser
Title	JKT-7-107_pure.3.ser
Origin	Bruker BioSpin GmbH
Solvent	CDCl3
Temperature	298.1
Pulse Sequence	cosygpppqf
Experiment	COSY
Number of Scans	1
Receiver Gain	64.2
Relaxation Delay	1.9226
Pulse Width	8.7000
Acquisition Time	0.2744
Acquisition Date	2025-03-21T23:04:12
Spectrometer Frequency	(400.13,400.13)
Spectral Width	(3731.3,3731.3)
Lowest Frequency	(-523.1,-523.1)
Nucleus	(1H,1H)
Acquired Size	(1024,128)
Spectral Size	(1024,1024)
Digital Resolution	(3.64,3.64)

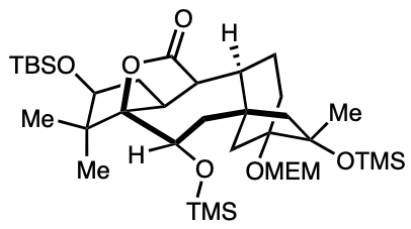

198

f2 (ppm)

f1 (ppm)

Parameter	Value
Data File Name	/ Volumes/ nmrdata/ jkthomps/ nmr/ JKT-7-107_pure/ 4/ ser
Title	JKT-7-107_pure.4.ser
Origin	Bruker BioSpin GmbH
Solvent	CDCl3
Temperature	298.2
Pulse Sequence	hsqcedetgpsisp2.4
Experiment	HSQC-EDITED
Number of Scans	4
Receiver Gain	197.4
Relaxation Delay	1.5000
Pulse Width	8.7000
Acquisition Time	0.2135
Acquisition Date	2025-03-21T23:26:22
Spectrometer Frequency	(400.13,100.62)
Spectral Width	(4795.4,16611.3)
Lowest Frequency	(-590.2,-1243.7)
Nucleus	(1H,13C)
Acquired Size	(1024,180)
Spectral Size	(1024,1024)
Digital Resolution	(4.68,16.22)

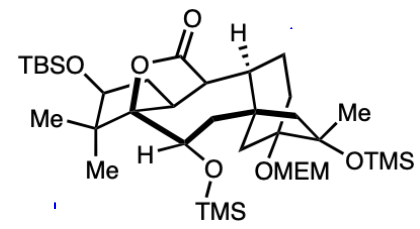

198

f2 (ppm)

f1 (ppm)

Parameter	Value
Data File Name	/ Volumes/ nmrdata/ jkthomps/ nmr/ JKT-7-107_pure/ 5/ ser
Title	JKT-7-107_pure.5.ser
Origin	Bruker BioSpin GmbH
Solvent	CDCl3
Temperature	298.1
Pulse Sequence	hmbcetgpl3nd
Experiment	HMBC
Number of Scans	5
Receiver Gain	197.4
Relaxation Delay	2.0000
Pulse Width	8.7000
Acquisition Time	0.4260
Acquisition Date	2025-03-22T00:20:49
Spectrometer Frequency	(400.13,100.62)
Spectral Width	(4807.7,22321.4)
Lowest Frequency	(-237.8,-1110.0)
Nucleus	(1H,13C)
Acquired Size	(2048,256)
Spectral Size	(2048,1024)
Digital Resolution	(2.35,21.80)

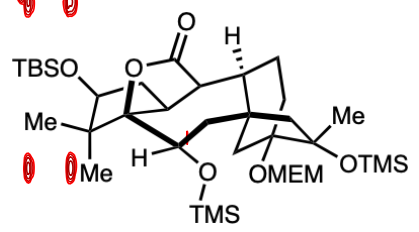

198

f2 (ppm)

f1 (ppm)

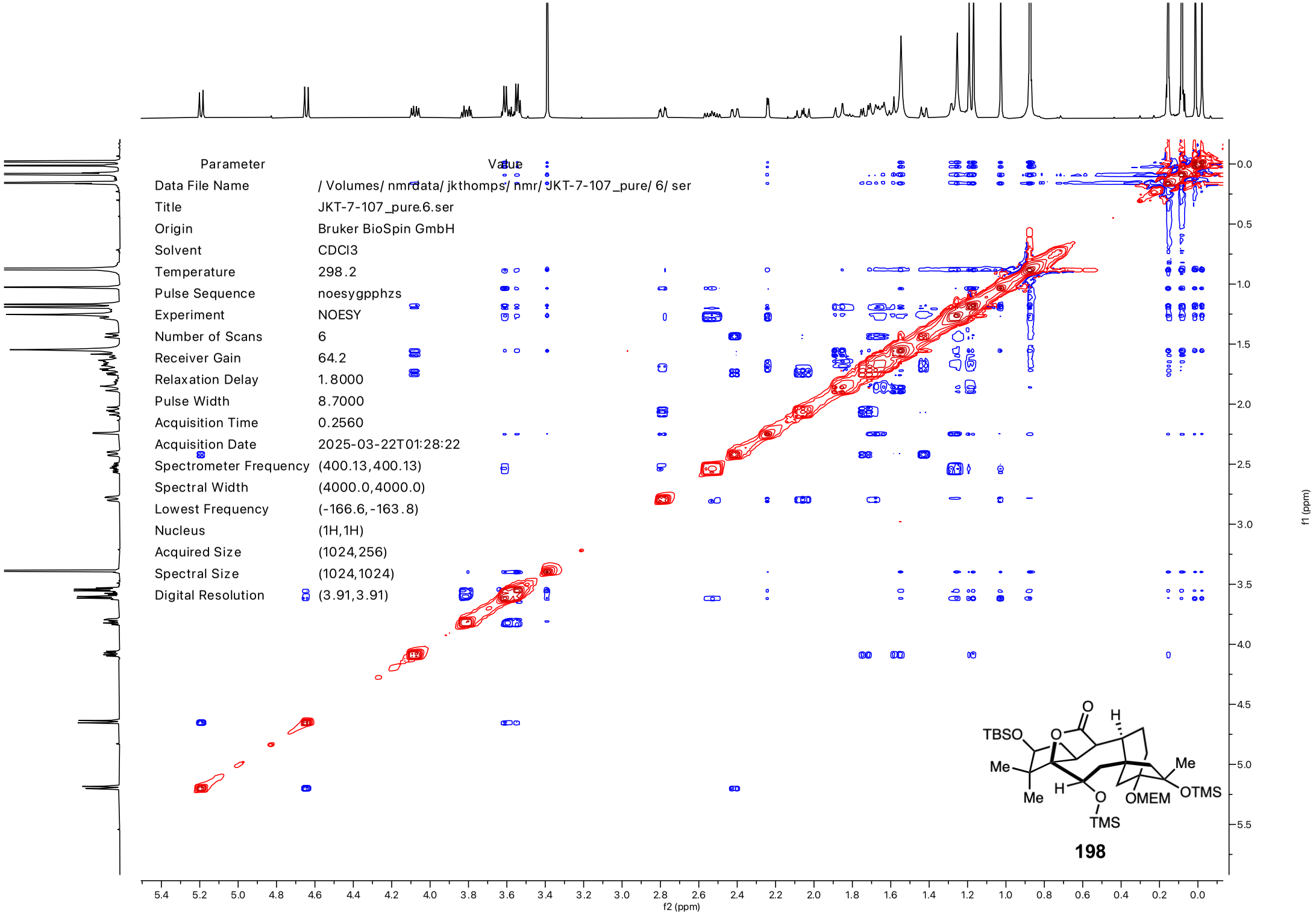
Parameter Value
Data File Name / Volumes/ nmrdata/ jkthomps/ nmr/ JKT-7-107_pure/ 6/ ser
Title JKT-7-107_pure.6.ser
Origin Bruker BioSpin GmbH
Solvent CDCl3
Temperature 298.2
Pulse Sequence noesygpphzs
Experiment NOESY
Number of Scans 6
Receiver Gain 64.2
Relaxation Delay 1.8000
Pulse Width 8.7000
Acquisition Time 0.2560
Acquisition Date 2025-03-22T01:28:22
Spectrometer Frequency (400.13,400.13)
Spectral Width (4000.0,4000.0)
Lowest Frequency (-166.6,-163.8)
Nucleus (1H,1H)
Acquired Size (1024,256)
Spectral Size (1024,1024)
Digital Resolution (3.91,3.91)
TBSO
Me
Me
H
O
TMS
O
O
H
OMEM
Me
OTMS
198
f2 (ppm)
f1 (ppm)

Parameter	Value
Data File Name	/ Volumes/ nmrdata/ jkthomps/ nmr/ JKT-7-107_HMBC/ 2/ ser
Title	JKT-7-107_HMBC.2.ser
Origin	Bruker BioSpin GmbH
Solvent	CDCl3
Temperature	298.1
Pulse Sequence	hmbcetgpl3nd
Experiment	HMBC
Number of Scans	12
Receiver Gain	197.4
Relaxation Delay	2.0000
Pulse Width	8.7000
Acquisition Time	0.4260
Acquisition Date	2025-03-22T12:52:28
Spectrometer Frequency	(400.13,100.62)
Spectral Width	(4807.7,22321.4)
Lowest Frequency	(-234.7,-1116.4)
Nucleus	(1H,13C)
Acquired Size	(2048,256)
Spectral Size	(2048,1024)
Digital Resolution	(2.35,21.80)

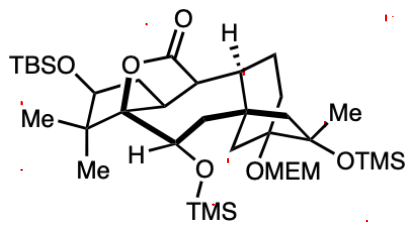

198

f2 (ppm)

f1 (ppm)

Parameter	Value
Data File Name	/ Volumes/ nmrdata/ jkthomps/ nmr/ JKT-7-269_pure/ 1/ fid
Title	JKT-7-269_pure.1.fid
Origin	Bruker BioSpin GmbH
Solvent	CDCl3
Temperature	297.2
Pulse Sequence	zg30
Experiment	1D
Number of Scans	16
Receiver Gain	112.8
Relaxation Delay	1.0000
Pulse Width	12.5000
Acquisition Time	4.0894
Acquisition Date	2025-07-09T04:33:02
Spectrometer Frequency	400.13
Spectral Width	8012.8
Nucleus	1H
Acquired Size	32768
Spectral Size	65536

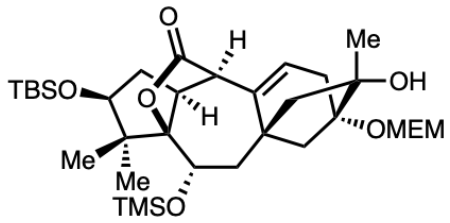

199

Parameter	Value
Data File Name	/ Volumes/ nmrdata/ jkthomps/ nmr/ JKT-7-269_pure/ 2/ fid
Title	JKT-7-269_pure.2.fid
Origin	Bruker BioSpin GmbH
Solvent	CDCl3
Temperature	297.1
Pulse Sequence	zgpg30
Experiment	1D
Number of Scans	750
Receiver Gain	64.2
Relaxation Delay	1.0000
Pulse Width	10.0000
Acquisition Time	1.1796
Acquisition Date	2025-07-09T05:01:33
Spectrometer Frequency	100.62
Spectral Width	27777.8
Nucleus	13C
Acquired Size	32768
Spectral Size	65536

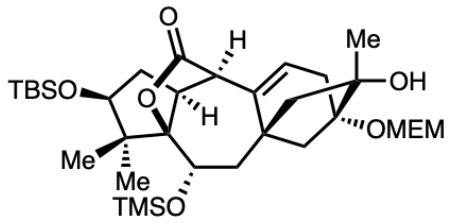

199

Parameter	Value
Data File Name	/ Volumes/ nmrdata/ jkthomps/ nmr/ JKT-7-269_pure/ 3/ ser
Title	JKT-7-269_pure.3.ser
Origin	Bruker BioSpin GmbH
Solvent	CDCl3
Temperature	297.2
Pulse Sequence	cosygpppqf
Experiment	COSY
Number of Scans	3
Receiver Gain	64.2
Relaxation Delay	1.9554
Pulse Width	12.5000
Acquisition Time	0.2417
Acquisition Date	2025-07-09T05:16:49
Spectrometer Frequency	(400.13,400.13)
Spectral Width	(4237.3,4237.3)
Lowest Frequency	(-654.9,-658.7)
Nucleus	(1H,1H)
Acquired Size	(1024,128)
Spectral Size	(1024,1024)
Digital Resolution	(4.14,4.14)

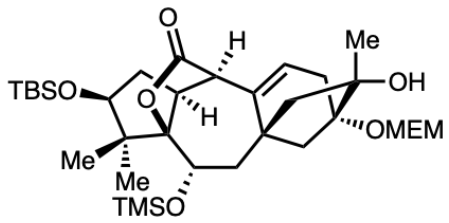

199

f2 (ppm)

f1 (ppm)

Parameter	Value
Data File Name	/ Volumes/ nmrdata/ jkthomps/ nmr/ JKT-7-269_pure/ 4/ ser
Title	JKT-7-269_pure.4.ser
Origin	Bruker BioSpin GmbH
Solvent	CDCl3
Temperature	297.1
Pulse Sequence	hsqcedetgpsisp2.4
Experiment	HSQC-EDITED
Number of Scans	6
Receiver Gain	197.4
Relaxation Delay	1.5000
Pulse Width	12.5000
Acquisition Time	0.2135
Acquisition Date	2025-07-09T05:49:29
Spectrometer Frequency	(400.13,100.62)
Spectral Width	(4795.4,16611.3)
Lowest Frequency	(-594.5,-1262.8)
Nucleus	(1H,13C)
Acquired Size	(1024,180)
Spectral Size	(1024,1024)
Digital Resolution	(4.68,16.22)

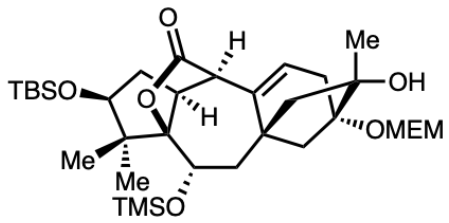

199

f2 (ppm)

f1 (ppm)

Parameter	Value
Data File Name	/ Volumes/ nmrdata/ jkthomps/ nmr/ JKT-7-243_pure/ 1/ fid
Title	JKT-7-243_pure.1.fid
Origin	Bruker BioSpin GmbH & Co.KG
Solvent	CDCl3
Temperature	298.2
Pulse Sequence	zg30
Experiment	1D
Number of Scans	16
Receiver Gain	101.0
Relaxation Delay	1.0000
Pulse Width	9.8500
Acquisition Time	3.9977
Acquisition Date	2025-06-04T16:05:12
Spectrometer Frequency	400.15
Spectral Width	8196.7
Nucleus	1H
Acquired Size	32768
Spectral Size	65536

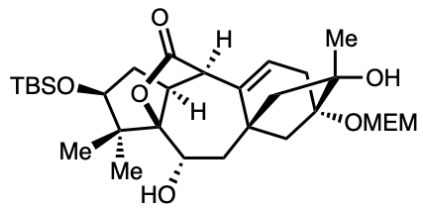

200

Parameter	Value
Data File Name	/ Volumes/ nmrdata/ jkthomps/ nmr/ JKT-7-243_pure/ 2/ fid
Title	JKT-7-243_pure.2.fid
Origin	Bruker BioSpin GmbH & Co.KG
Solvent	CDCl3
Temperature	298.1
Pulse Sequence	zgpg30
Experiment	1D
Number of Scans	750
Receiver Gain	101.0
Relaxation Delay	2.0000
Pulse Width	10.0000
Acquisition Time	1.1796
Acquisition Date	2025-06-04T16:47:36
Spectrometer Frequency	100.63
Spectral Width	27777.8
Nucleus	13C
Acquired Size	32768
Spectral Size	65536

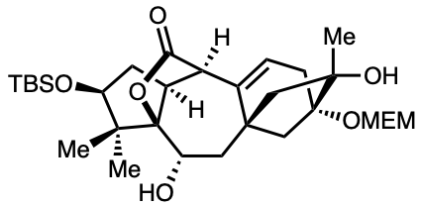

200

Parameter	Value
Data File Name	/ Volumes/ nmrdata/ jkthomps/ nmr/ JKT-7-243_pure/ 3/ ser
Title	JKT-7-243_pure.3.ser
Origin	Bruker BioSpin GmbH & Co.KG
Solvent	CDCl3
Temperature	298.2
Pulse Sequence	cosygpppqf
Experiment	COSY
Number of Scans	1
Receiver Gain	101.0
Relaxation Delay	2.0000
Pulse Width	9.8500
Acquisition Time	0.1946
Acquisition Date	2025-06-04T20:24:21
Spectrometer Frequency	(400.15,400.15)
Spectral Width	(5263.2,5263.2)
Lowest Frequency	(-230.7,-230.7)
Nucleus	(1H,1H)
Acquired Size	(1024,128)
Spectral Size	(1024,1024)
Digital Resolution	(5.14,5.14)

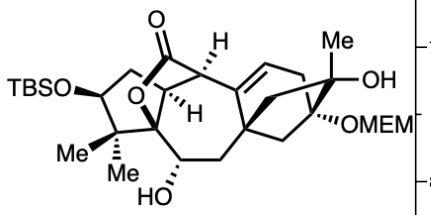

200

f2 (ppm)

f1 (ppm)

Parameter	Value
Data File Name	/ Volumes/ nmrdata/ jkthomps/ nmr/ JKT-7-243_pure/ 4/ ser
Title	JKT-7-243_pure.4.ser
Origin	Bruker BioSpin GmbH & Co.KG
Solvent	CDCl3
Temperature	298.2
Pulse Sequence	hmbcgplpndqf
Experiment	HMBC
Number of Scans	4
Receiver Gain	101.0
Relaxation Delay	1.5000
Pulse Width	9.8500
Acquisition Time	0.5980
Acquisition Date	2025-06-04T20:44:10
Spectrometer Frequency	(400.15,100.63)
Spectral Width	(3424.7,22138.1)
Lowest Frequency	(-263.4,-1007.3)
Nucleus	(1H,13C)
Acquired Size	(2048,128)
Spectral Size	(2048,512)
Digital Resolution	(1.67,43.24)

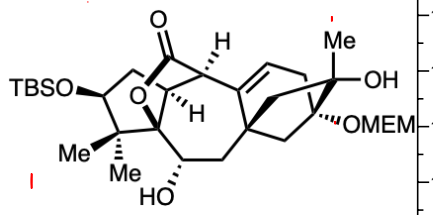

200

f2 (ppm)

f1 (ppm)

Parameter	Value
Data File Name	/ Volumes/ nmrdata/ jkthomps/ nmr/ JKT-7-243_pure/ 5/ ser
Title	JKT-7-243_pure.5.ser
Origin	Bruker BioSpin GmbH & Co.KG
Solvent	CDCl3
Temperature	298.2
Pulse Sequence	hsqcedetgpsisp2.3
Experiment	HSQC-EDITED
Number of Scans	4
Receiver Gain	101.0
Relaxation Delay	1.5000
Pulse Width	9.8500
Acquisition Time	0.1946
Acquisition Date	2025-06-04T21:14:39
Spectrometer Frequency	(400.15,100.63)
Spectral Width	(5263.2,16603.2)
Lowest Frequency	(-750.9,-755.3)
Nucleus	(1H,13C)
Acquired Size	(1024,256)
Spectral Size	(1024,1024)
Digital Resolution	(5.14,16.21)

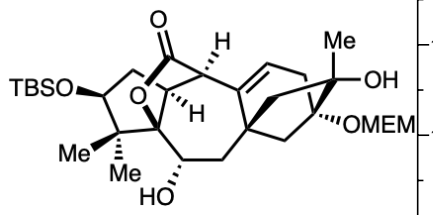

200

f2 (ppm)

f1 (ppm)

Parameter	Value
Data File Name	/ Volumes/ nmrdata/ jkthomps/ nmr/ JKT-7-243_pure/ 6/ ser
Title	JKT-7-243_pure.6.ser
Origin	Bruker BioSpin GmbH & Co. KG
Solvent	CDCl3
Temperature	298.1
Pulse Sequence	noesygpphpp
Experiment	NOESY
Number of Scans	4
Receiver Gain	101.0
Relaxation Delay	1.8239
Pulse Width	9.8500
Acquisition Time	0.4301
Acquisition Date	2025-06-04T22:00:56
Spectrometer Frequency	(400.15, 400.15)
Spectral Width	(2381.0, 2381.0)
Lowest Frequency	(23.5, 23.5)
Nucleus	(1H, 1H)
Acquired Size	(1024, 256)
Spectral Size	(1024, 1024)
Digital Resolution	(2.33, 2.33)

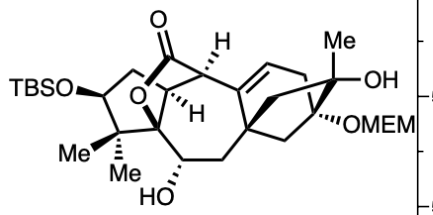

200

f2 (ppm)

f1 (ppm)

Parameter	Value
Data File Name	/ Volumes/ nmrdata/ jkthomps/ nmr/ JKT-7-287_pure/ 1/ fid
Title	JKT-7-287_pure.1.fid
Origin	Bruker BioSpin GmbH
Solvent	CDCl3
Temperature	297.1
Pulse Sequence	zg30
Experiment	1D
Number of Scans	16
Receiver Gain	197.4
Relaxation Delay	1.0000
Pulse Width	12.5000
Acquisition Time	4.0894
Acquisition Date	2025-07-16T06:29:08
Spectrometer Frequency	400.13
Spectral Width	8012.8
Nucleus	1H
Acquired Size	32768
Spectral Size	65536

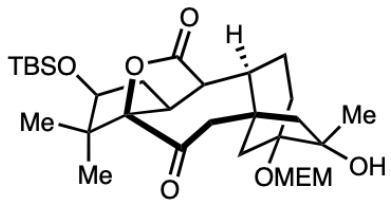

201

Parameter	Value
Data File Name	/ Volumes/ nmrdata/ jkthomps/ nmr/ JKT-7-287_pure/ 2/ fid
Title	JKT-7-287_pure.2.fid
Origin	Bruker BioSpin GmbH
Solvent	CDCl3
Temperature	297.2
Pulse Sequence	zgpg30
Experiment	1D
Number of Scans	4000
Receiver Gain	64.2
Relaxation Delay	0.3000
Pulse Width	10.0000
Acquisition Time	1.1796
Acquisition Date	2025-07-16T22:45:33
Spectrometer Frequency	100.62
Spectral Width	27777.8
Nucleus	13C
Acquired Size	32768
Spectral Size	65536

201

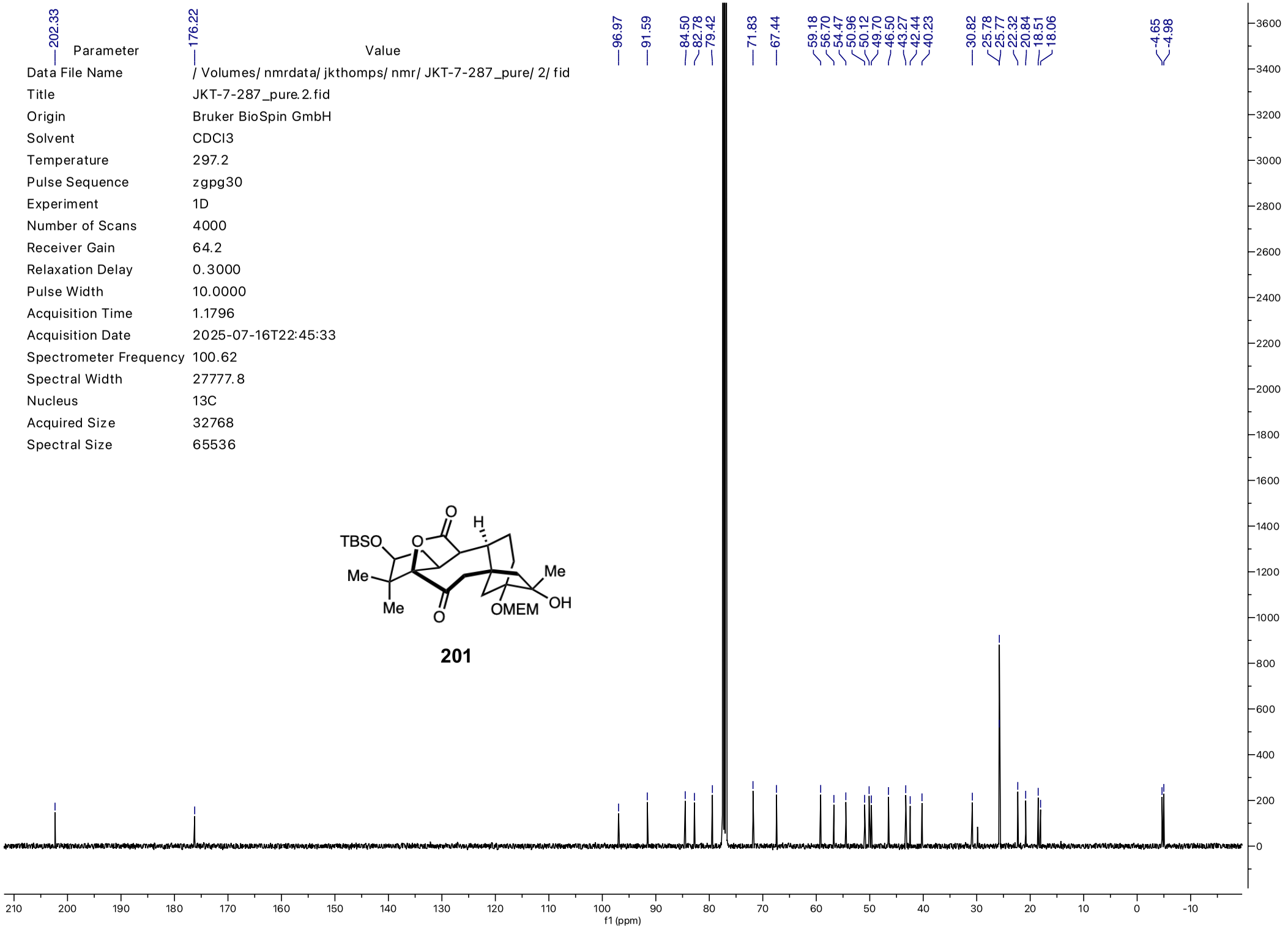

Parameter	Value
Data File Name	/ Volumes/ nmrdata/ jkthomps/ nmr/ JKT-7-287_pure/ 3/ ser
Title	JKT-7-287_pure.3.ser
Origin	Bruker BioSpin GmbH
Solvent	CDCl3
Temperature	297.1
Pulse Sequence	hsqcedetgpsisp2.4
Experiment	HSQC-EDITED
Number of Scans	8
Receiver Gain	197.4
Relaxation Delay	1.5000
Pulse Width	12.5000
Acquisition Time	0.2135
Acquisition Date	2025-07-16T07:12:20
Spectrometer Frequency	(400.13,100.62)
Spectral Width	(4795.4,16611.3)
Lowest Frequency	(-527.2,-1262.8)
Nucleus	(1H,13C)
Acquired Size	(1024,180)
Spectral Size	(1024,1024)
Digital Resolution	(4.68,16.22)

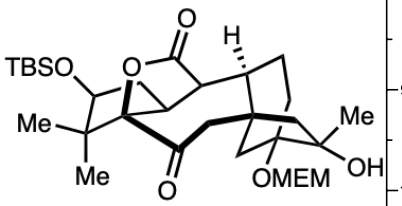

201

f2 (ppm)

f1 (ppm)

Parameter	Value
Data File Name	/ Volumes/ nmrdata/ jkthomps/ nmr/ JKT-7-287_pure/ 6/ ser
Title	JKT-7-287_pure.6.ser
Origin	Bruker BioSpin GmbH
Solvent	CDCl3
Temperature	297.1
Pulse Sequence	cosygpppqf
Experiment	COSY
Number of Scans	2
Receiver Gain	156.2
Relaxation Delay	2.0000
Pulse Width	12.5000
Acquisition Time	0.1970
Acquisition Date	2025-07-17T00:25:24
Spectrometer Frequency	(400.13,400.13)
Spectral Width	(5197.5,5197.5)
Lowest Frequency	(-211.2,-216.7)
Nucleus	(1H,1H)
Acquired Size	(1024,128)
Spectral Size	(1024,1024)
Digital Resolution	(5.08,5.08)

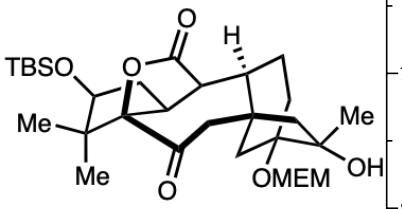

201

f2 (ppm)

f1 (ppm)

Parameter	Value
Data File Name	/ Volumes/ nmrdata/ jkthomps/ nmr/ JKT-7-287_pure/ 4/ ser
Title	JKT-7-287_pure.4.ser
Origin	Bruker BioSpin GmbH
Solvent	CDCl3
Temperature	297.2
Pulse Sequence	hmbcetgpl3nd
Experiment	HMBC
Number of Scans	4
Receiver Gain	197.4
Relaxation Delay	2.0000
Pulse Width	12.5000
Acquisition Time	0.4260
Acquisition Date	2025-07-16T23:29:23
Spectrometer Frequency	(400.13,100.62)
Spectral Width	(4807.7,22321.4)
Lowest Frequency	(-173.7,-1116.4)
Nucleus	(1H,13C)
Acquired Size	(2048,256)
Spectral Size	(2048,1024)
Digital Resolution	(2.35,21.80)

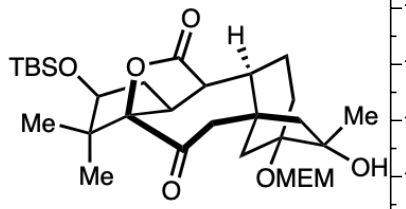

201

f2 (ppm)

f1 (ppm)

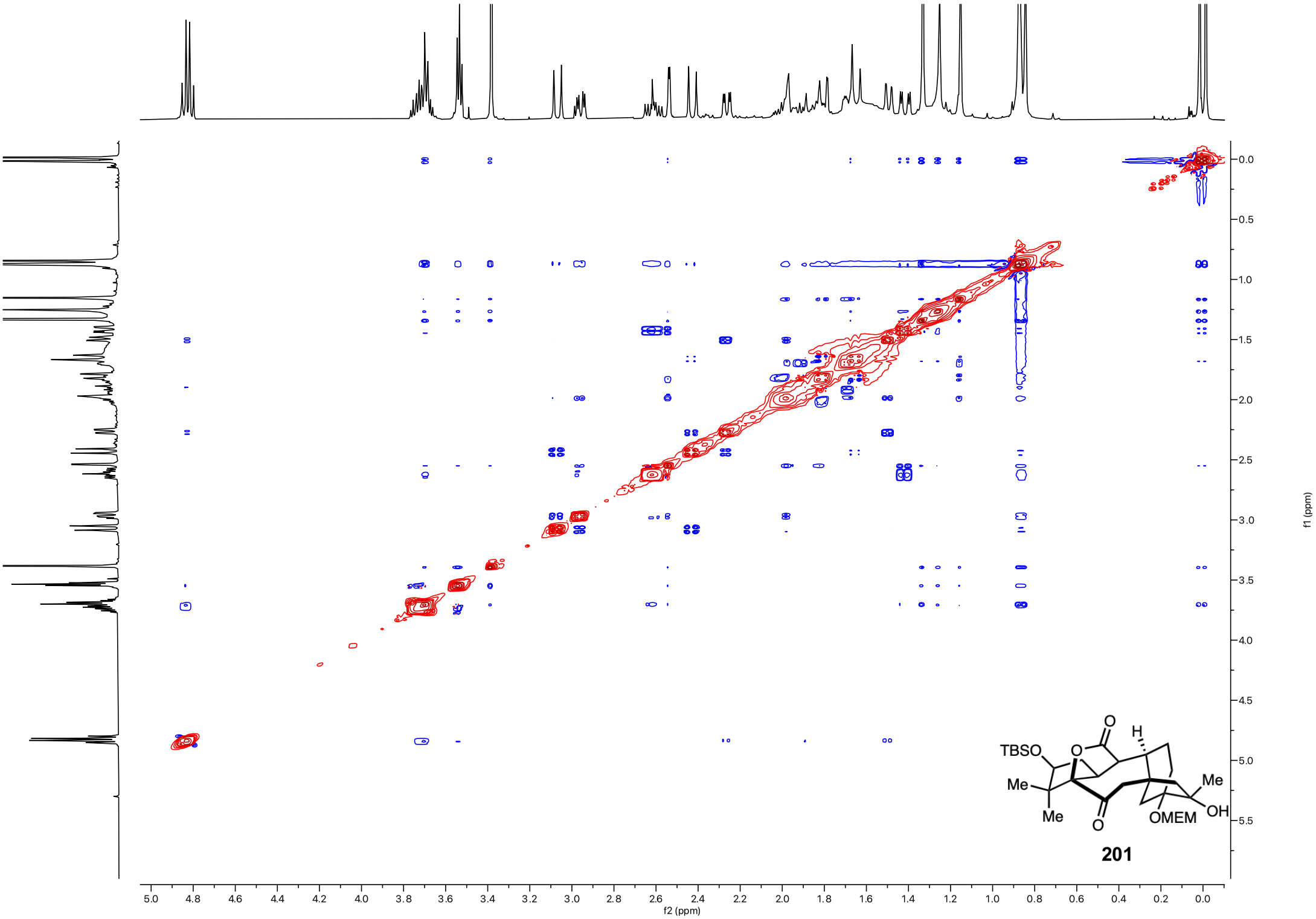
f2 (ppm)
f1 (ppm)
TBSO
Me
Me
Me
OMEM
OH
O
O
O
H
201

Parameter	Value
Data File Name	/ Users/ jordankthompson/ Desktop/ JKT-7-199-1/ PROTON01.fid/ fid
Title	PROTON01
Origin	Varian
Solvent	cdcl3
Temperature	25.0
Pulse Sequence	s2pul
Experiment	1D
Number of Scans	8
Receiver Gain	60
Relaxation Delay	1.0000
Pulse Width	3.3500
Acquisition Time	3.0000
Acquisition Date	2025-05-15T11:21:14
Spectrometer Frequency	499.54
Spectral Width	8000.0
Nucleus	1H
Acquired Size	24000
Spectral Size	65536

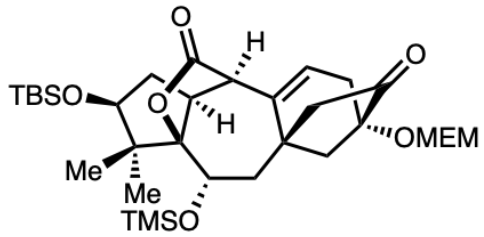

202

214.95 176.54 143.90 123.44 98.88 91.49 83.72 82.85 71.75 70.92 67.60 59.10 57.47 55.29 50.01 48.70 44.85 42.32 39.72 39.68 37.03 25.76 24.38 18.45 18.04 1.38 -4.56 -4.98

Parameter	Value
Data File Name	/ Volumes/ nmrdata/ jkthomps/ nmr/ JKT-7-206_pure/ 2/ fid
Title	JKT-7-206_pure.2.fid
Origin	Bruker BioSpin GmbH
Solvent	CDCl3
Temperature	297.1
Pulse Sequence	zgpg30
Experiment	1D
Number of Scans	750
Receiver Gain	72.0
Relaxation Delay	1.0000
Pulse Width	10.0000
Acquisition Time	1.1796
Acquisition Date	2025-05-16T21:25:14
Spectrometer Frequency	100.62
Spectral Width	27777.8
Nucleus	13C
Acquired Size	32768
Spectral Size	65536

202

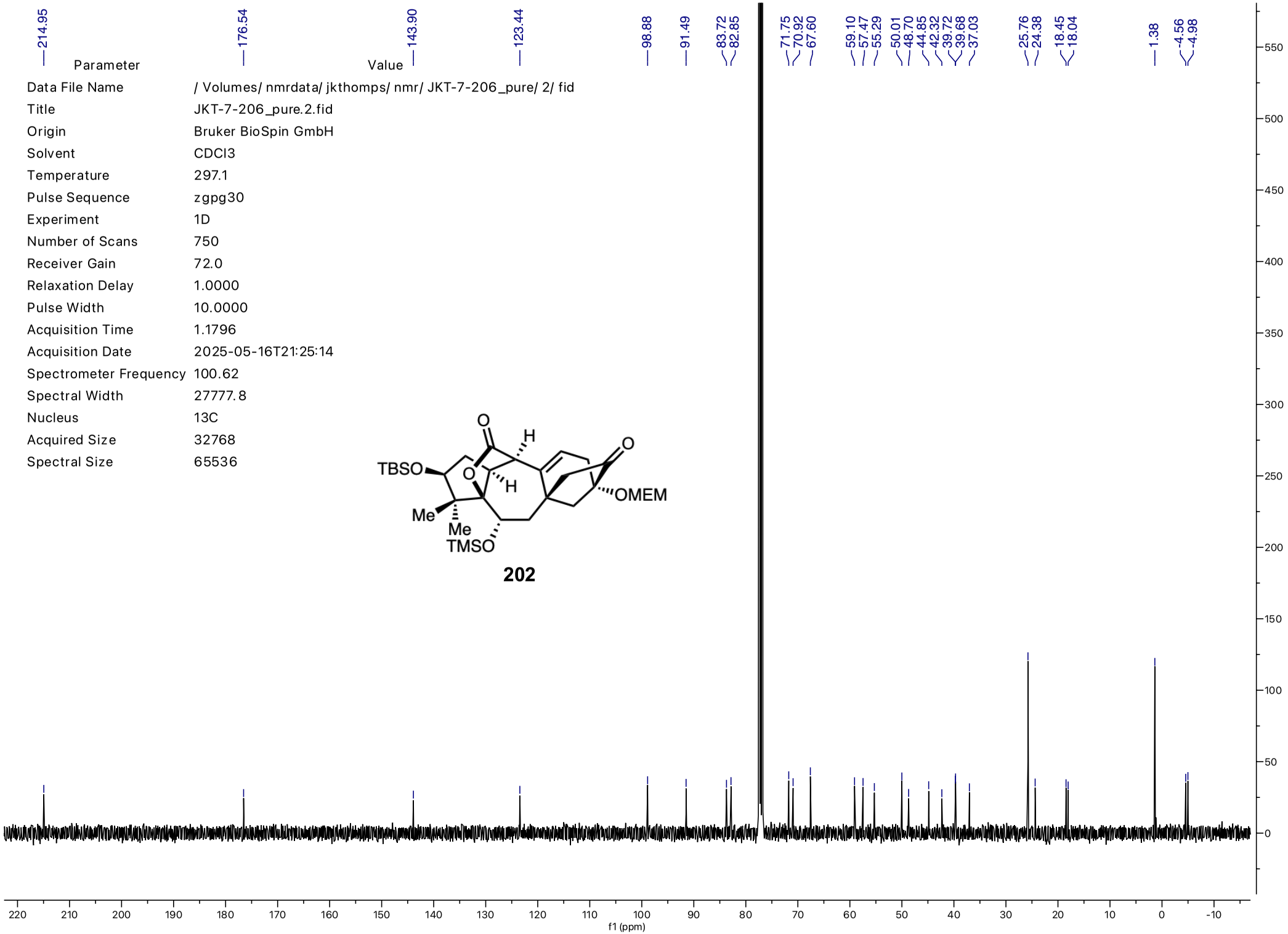

Parameter	Value
Data File Name	/ Volumes/ nmrdata/ jkthomps/ nmr/ JKT-7-206_pure/ 3/ ser
Title	JKT-7-206_pure.3.ser
Origin	Bruker BioSpin GmbH
Solvent	CDCl3
Temperature	297.2
Pulse Sequence	hsqcedetgpsisp2.4
Experiment	HSQC-EDITED
Number of Scans	4
Receiver Gain	197.4
Relaxation Delay	1.5000
Pulse Width	12.5000
Acquisition Time	0.2135
Acquisition Date	2025-05-17T06:26:55
Spectrometer Frequency	(400.13,100.62)
Spectral Width	(4795.4,16611.3)
Lowest Frequency	(-531.0,-1262.8)
Nucleus	(1H,13C)
Acquired Size	(1024,180)
Spectral Size	(1024,1024)
Digital Resolution	(4.68,16.22)

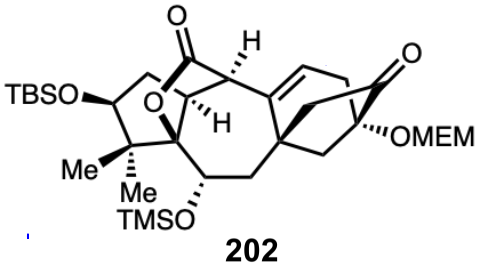

202

f2 (ppm)

f1 (ppm)

Parameter	Value
Data File Name	/ Volumes/ nmrdata/ jkthomps/ nmr/ JKT-7-209-2/ 1/ fid
Title	JKT-7-209-2.1.fid
Origin	Bruker BioSpin GmbH
Solvent	CDCl3
Temperature	297.1
Pulse Sequence	zg30
Experiment	1D
Number of Scans	16
Receiver Gain	197.4
Relaxation Delay	1.0000
Pulse Width	12.5000
Acquisition Time	4.0894
Acquisition Date	2025-05-18T16:55:00
Spectrometer Frequency	400.13
Spectral Width	8012.8
Nucleus	1H
Acquired Size	32768
Spectral Size	65536

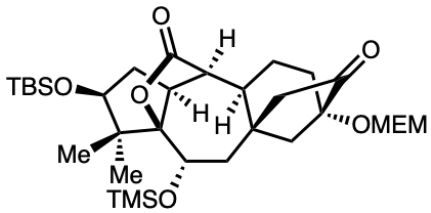

204

Parameter	Value
Data File Name	/ Volumes/ nmrdata/ jkthomps/ nmr/ JKT-7-209-2/ 2/ fid
Title	JKT-7-209-2.2.fid
Origin	Bruker BioSpin GmbH
Solvent	CDCl3
Temperature	297.2
Pulse Sequence	zgpg30
Experiment	1D
Number of Scans	1000
Receiver Gain	72.0
Relaxation Delay	1.0000
Pulse Width	10.0000
Acquisition Time	1.1796
Acquisition Date	2025-05-18T17:32:51
Spectrometer Frequency	100.62
Spectral Width	27777.8
Nucleus	13C
Acquired Size	32768
Spectral Size	65536

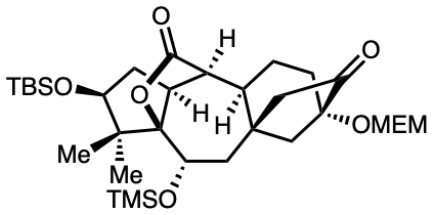

204

214.56 175.59 101.03 91.28 84.90 83.57 72.45 71.81 67.34 59.11 55.03 51.83 51.01 50.76 48.40 43.52 43.03 40.54 39.25 33.61 25.85 25.64 24.72 18.28 18.21 0.85 -4.67 -4.93

f1 (ppm)

Parameter	Value
Data File Name	/ Volumes/ nmrdata/ jkthomps/ nmr/ JKT-7-209-2/ 3/ ser
Title	JKT-7-209-2.3.ser
Origin	Bruker BioSpin GmbH
Solvent	CDCl3
Temperature	297.2
Pulse Sequence	hsqcedetgpsisp2.4
Experiment	HSQC-EDITED
Number of Scans	4
Receiver Gain	197.4
Relaxation Delay	1.5000
Pulse Width	12.5000
Acquisition Time	0.2135
Acquisition Date	2025-05-18T17:55:04
Spectrometer Frequency	(400.13,100.62)
Spectral Width	(4795.4,16611.3)
Lowest Frequency	(-527.7,-1250.8)
Nucleus	(1H,13C)
Acquired Size	(1024,180)
Spectral Size	(1024,1024)
Digital Resolution	(4.68,16.22)

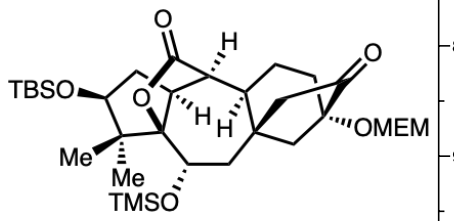

204

f2 (ppm)

f1 (ppm)

Parameter	Value
Data File Name	/ Volumes/ nmrdata/ jkthomps/ nmr/ JKT-7-209-2/ 4/ ser
Title	JKT-7-209-2.4.ser
Origin	Bruker BioSpin GmbH
Solvent	CDCl3
Temperature	297.1
Pulse Sequence	noesygpphzs
Experiment	NOESY
Number of Scans	4
Receiver Gain	197.4
Relaxation Delay	1.8000
Pulse Width	12.5000
Acquisition Time	0.2560
Acquisition Date	2025-05-18T21:48:01
Spectrometer Frequency	(400.13,400.13)
Spectral Width	(4000.0,4000.0)
Lowest Frequency	(-168.0,-168.3)
Nucleus	(1H,1H)
Acquired Size	(1024,256)
Spectral Size	(1024,1024)
Digital Resolution	(3.91,3.91)

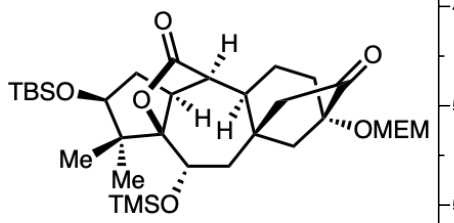

204

f2 (ppm)

f1 (ppm)

Parameter	Value
Data File Name	/ Volumes/ nmrdata/ jkthomps/ nmr/ JKT-7-209-2/ 5/ ser
Title	JKT-7-209-2.5.ser
Origin	Bruker BioSpin GmbH
Solvent	CDCl3
Temperature	297.2
Pulse Sequence	cosygpppqf
Experiment	COSY
Number of Scans	1
Receiver Gain	197.4
Relaxation Delay	1.9205
Pulse Width	12.5000
Acquisition Time	0.2765
Acquisition Date	2025-05-18T21:53:38
Spectrometer Frequency	(400.13,400.13)
Spectral Width	(3703.7,3703.7)
Lowest Frequency	(-428.3,-428.7)
Nucleus	(1H,1H)
Acquired Size	(1024,128)
Spectral Size	(1024,1024)
Digital Resolution	(3.62,3.62)

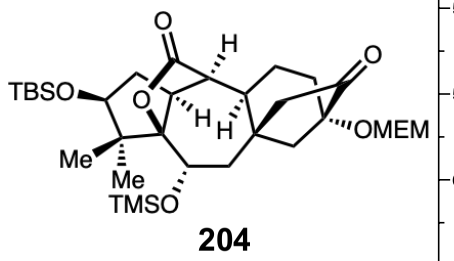

204

f2 (ppm)

f1 (ppm)

Parameter	Value
Data File Name	/ Volumes/ nmrdata/ jkthomps/ nmr/ JKT-7-209-2/ 6/ ser
Title	JKT-7-209-2.6.ser
Origin	Bruker BioSpin GmbH
Solvent	CDCl3
Temperature	297.1
Pulse Sequence	hmbcetgpl3nd
Experiment	HMBC
Number of Scans	4
Receiver Gain	197.4
Relaxation Delay	2.0000
Pulse Width	12.5000
Acquisition Time	0.4260
Acquisition Date	2025-05-18T22:37:24
Spectrometer Frequency	(400.13,100.62)
Spectral Width	(4807.7,22321.4)
Lowest Frequency	(-175.3,-1116.4)
Nucleus	(1H,13C)
Acquired Size	(2048,256)
Spectral Size	(2048,1024)
Digital Resolution	(2.35,21.80)

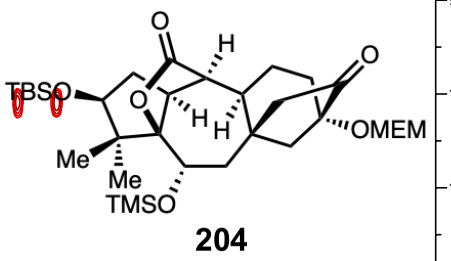

204

f2 (ppm)

f1 (ppm)

Parameter	Value
Data File Name	/ Volumes/ nmrdata-1/ jkthomps/ nmr/ JKT-7-213-1/ 1/ fid
Title	JKT-7-213-1.1.fid
Origin	Bruker BioSpin GmbH
Solvent	MeOD
Temperature	297.2
Pulse Sequence	zg30
Experiment	1D
Number of Scans	16
Receiver Gain	197.4
Relaxation Delay	1.0000
Pulse Width	12.5000
Acquisition Time	4.0894
Acquisition Date	2025-05-21T14:55:08
Spectrometer Frequency	400.13
Spectral Width	8012.8
Nucleus	1H
Acquired Size	32768
Spectral Size	65536

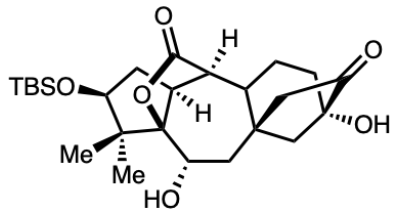

204'

Parameter	Value
Data File Name	/ Volumes/ nmrdata/ jkthomps/ nmr/ JKT-7-213-1/ 7/ fid
Title	JKT-7-213-1.7.fid
Origin	Bruker BioSpin GmbH
Solvent	MeOD
Temperature	297.2
Pulse Sequence	zgpg30
Experiment	1D
Number of Scans	3000
Receiver Gain	87.8
Relaxation Delay	1.0000
Pulse Width	10.0000
Acquisition Time	1.1796
Acquisition Date	2025-05-22T01:11:07
Spectrometer Frequency	100.62
Spectral Width	27777.8
Nucleus	13C
Acquired Size	32768
Spectral Size	65536

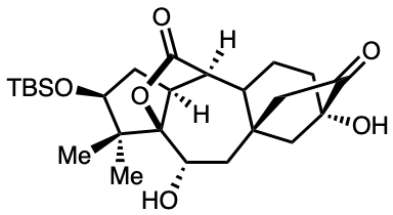

204'

Parameter	Value
Data File Name	/ Volumes/ nmrdata/ jkthomps/ nmr/ JKT-7-213-1/ 8/ ser
Title	JKT-7-213-1.8.ser
Origin	Bruker BioSpin GmbH
Solvent	MeOD
Temperature	297.1
Pulse Sequence	hsqcedetgpsisp2.4
Experiment	HSQC-EDITED
Number of Scans	8
Receiver Gain	197.4
Relaxation Delay	1.5000
Pulse Width	12.5000
Acquisition Time	0.2135
Acquisition Date	2025-05-22T01:54:23
Spectrometer Frequency	(400.13,100.62)
Spectral Width	(4795.4,16611.3)
Lowest Frequency	(-529.2,-1155.4)
Nucleus	(1H,13C)
Acquired Size	(1024,180)
Spectral Size	(1024,1024)
Digital Resolution	(4.68,16.22)

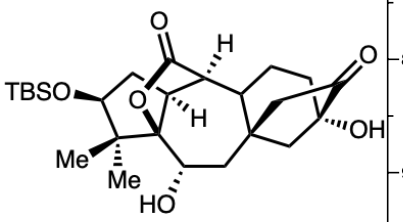

204'

f2 (ppm)

f1 (ppm)

Parameter	Value
Data File Name	/ Volumes/ nmrdata/ jkthomps/ nmr/ JKT-7-213-1/ 3/ ser
Title	JKT-7-213-1.3.ser
Origin	Bruker BioSpin GmbH
Solvent	MeOD
Temperature	297.1
Pulse Sequence	cosygpppqf
Experiment	COSY
Number of Scans	1
Receiver Gain	156.2
Relaxation Delay	1.7874
Pulse Width	12.5000
Acquisition Time	0.4096
Acquisition Date	2025-05-21T22:32:22
Spectrometer Frequency	(400.13,400.13)
Spectral Width	(2500.0,2500.0)
Lowest Frequency	(-276.8,-276.8)
Nucleus	(1H,1H)
Acquired Size	(1024,128)
Spectral Size	(1024,1024)
Digital Resolution	(2.44,2.44)

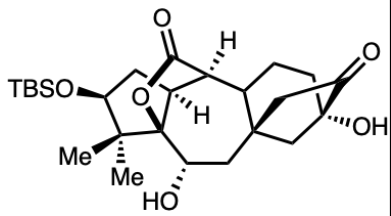

204'

f2 (ppm)

f1 (ppm)

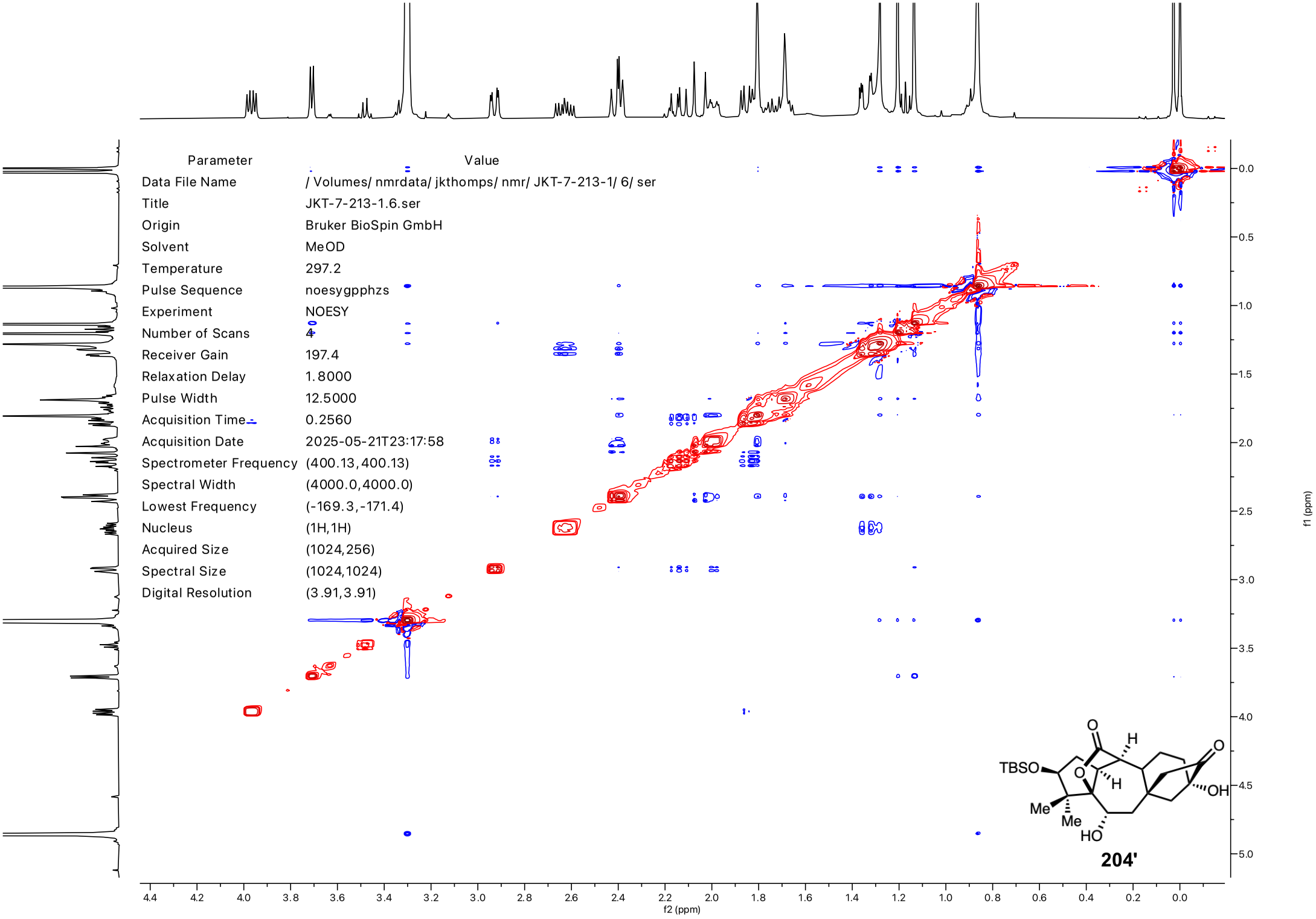
Parameter Value
Data File Name / Volumes/ nmrdata/ jkthomps/ nmr/ JKT-7-213-1/ 6/ ser
Title JKT-7-213-1.6.ser
Origin Bruker BioSpin GmbH
Solvent MeOD
Temperature 297.2
Pulse Sequence noesygpphzs
Experiment NOESY
Number of Scans 4
Receiver Gain 197.4
Relaxation Delay 1.8000
Pulse Width 12.5000
Acquisition Time 0.2560
Acquisition Date 2025-05-21T23:17:58
Spectrometer Frequency (400.13,400.13)
Spectral Width (4000.0,4000.0)
Lowest Frequency (-169.3,-171.4)
Nucleus (1H,1H)
Acquired Size (1024,256)
Spectral Size (1024,1024)
Digital Resolution (3.91,3.91)
f2 (ppm)
f1 (ppm)
TBSO
OH
Me
Me
HO
204'

Parameter	Value
Data File Name	/ Volumes/ nmrdata/ jkthomps/ nmr/ JKT-7-213-1/ 9/ ser
Title	JKT-7-213-1.9.ser
Origin	Bruker BioSpin GmbH
Solvent	MeOD
Temperature	297.2
Pulse Sequence	hmbcetgpl3nd
Experiment	HMBC
Number of Scans	8
Receiver Gain	197.4
Relaxation Delay	2.0000
Pulse Width	12.5000
Acquisition Time	0.4260
Acquisition Date	2025-05-22T03:20:57
Spectrometer Frequency	(400.13,100.62)
Spectral Width	(4807.7,22321.4)
Lowest Frequency	(-175.7,-1116.4)
Nucleus	(1H,13C)
Acquired Size	(2048,256)
Spectral Size	(2048,1024)
Digital Resolution	(2.35,21.80)

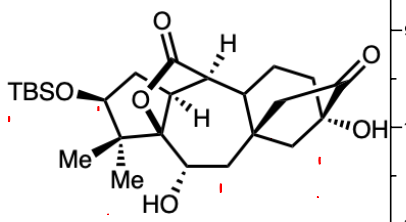

204'

f2 (ppm)

f1 (ppm)

Parameter	Value
Data File Name	/ Users/ jordankthompson/ Desktop/ JKT-7-73_pure/ 1/ fid
Title	JKT-7-73_pure.1.fid
Origin	Bruker BioSpin GmbH
Solvent	CDCl3
Temperature	297.1
Pulse Sequence	zg30
Experiment	1D
Number of Scans	16
Receiver Gain	197.4
Relaxation Delay	1.0000
Pulse Width	12.5000
Acquisition Time	4.0894
Acquisition Date	2025-03-01T10:04:06
Spectrometer Frequency	400.13
Spectral Width	8012.8
Nucleus	1H
Acquired Size	32768
Spectral Size	65536

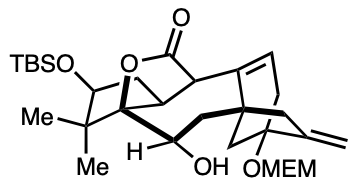

205

Parameter	Value
Data File Name	/ Volumes/ nmrdata/ jkthomps/ nmr/ JKT-7-73_pure/ 2/ fid
Title	JKT-7-73_pure.2.fid
Origin	Bruker BioSpin GmbH
Solvent	CDCl3
Temperature	297.2
Pulse Sequence	zgpg30
Experiment	1D
Number of Scans	1200
Receiver Gain	72.0
Relaxation Delay	1.0000
Pulse Width	10.0000
Acquisition Time	1.1796
Acquisition Date	2025-03-01T10:50:57
Spectrometer Frequency	100.62
Spectral Width	27777.8
Nucleus	13C
Acquired Size	32768
Spectral Size	65536

205

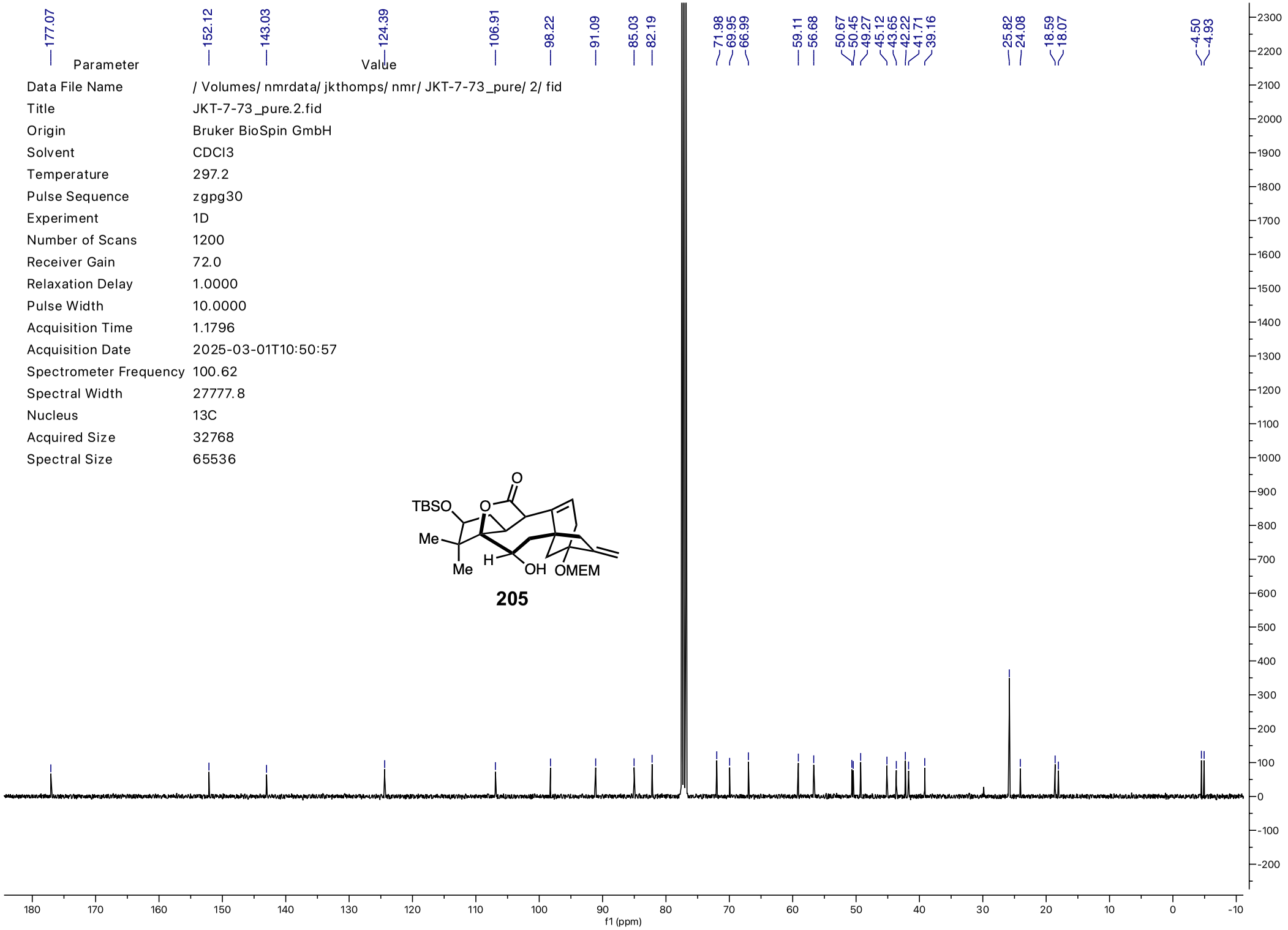

Parameter	Value
Data File Name	/ Users/ jordankthompson/ Desktop/ JKT-7-134_pure_RR_20250404_01/ JKT-7-134_pure_RR-PROTON_01.fid/ fid
Title	JKT-7-134_pure_RR-PROTON_01
Origin	Varian
Solvent	cdcl3
Temperature	25.0
Pulse Sequence	s2pul
Experiment	1D
Number of Scans	8
Receiver Gain	34
Relaxation Delay	1.0000
Pulse Width	5.4000
Acquisition Time	1.7080
Acquisition Date	2025-04-04T08:46:47
Spectrometer Frequency	599.55
Spectral Width	9592.3
Nucleus	1H
Acquired Size	16384
Spectral Size	65536

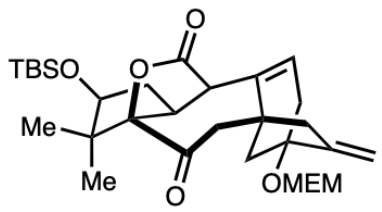

206

Parameter	Value
Data File Name	/ Users/ jordankthompson/ Desktop/ JKT-7-134_pure_20250403_01/ JKT-7-134_pure-CARBON_01.fid/ fid
Title	JKT-7-134_pure-CARBON_01
Origin	Varian
Solvent	cdcl3
Temperature	25.0
Pulse Sequence	s2pul
Experiment	1D
Number of Scans	256
Receiver Gain	30
Relaxation Delay	1.0000
Pulse Width	4.7250
Acquisition Time	0.7627
Acquisition Date	2025-04-03T17:09:05
Spectrometer Frequency	150.77
Spectral Width	42964.6
Nucleus	13C
Acquired Size	32768
Spectral Size	65536

203.20 175.87 151.83 139.29 127.78 109.21 97.45 91.15 82.95 82.62 71.94 67.19 59.15 59.14 53.42 49.76 49.71 47.49 44.68 44.58 43.05 39.85 25.76 22.53 18.52 18.06 -4.63 -4.96

206

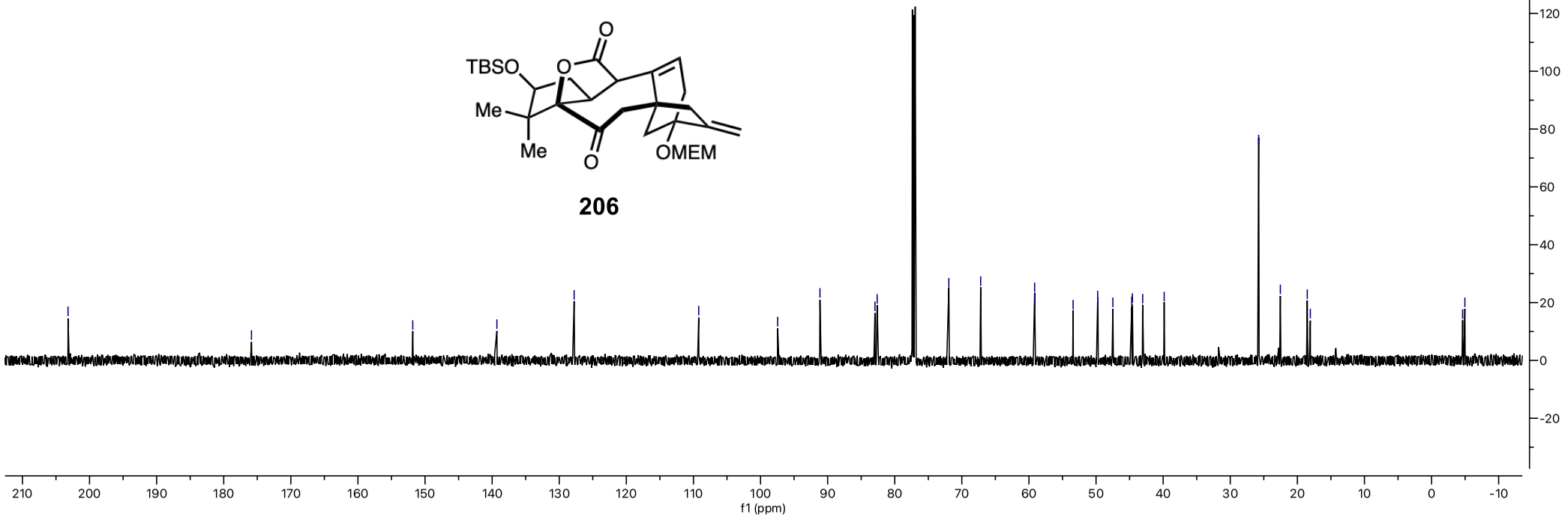

Parameter	Value
Data File Name	/ Volumes/ nmrdata/ jkthomps/ nmr/ JKT-7-92_pure/ 1/ fid
Title	JKT-7-92_pure.1.fid
Origin	Bruker BioSpin GmbH
Solvent	CDCl3
Temperature	297.1
Pulse Sequence	zg30
Experiment	1D
Number of Scans	16
Receiver Gain	197.4
Relaxation Delay	1.0000
Pulse Width	12.5000
Acquisition Time	4.0894
Acquisition Date	2025-03-07T03:28:43
Spectrometer Frequency	400.13
Spectral Width	8012.8
Nucleus	1H
Acquired Size	32768
Spectral Size	65536

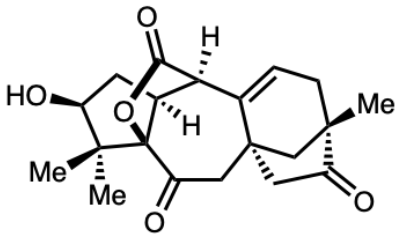

208

Parameter	Value
Data File Name	/ Volumes/ nmrdata/ jkthomps/ nmr/ JKT-7-92_pure/ 2/ fid
Title	JKT-7-92_pure.2.fid
Origin	Bruker BioSpin GmbH
Solvent	CDCl3
Temperature	297.1
Pulse Sequence	zgpg30
Experiment	1D
Number of Scans	3000
Receiver Gain	72.0
Relaxation Delay	1.0000
Pulse Width	10.0000
Acquisition Time	1.1796
Acquisition Date	2025-03-07T05:22:53
Spectrometer Frequency	100.62
Spectral Width	27777.8
Nucleus	13C
Acquired Size	32768
Spectral Size	65536

208

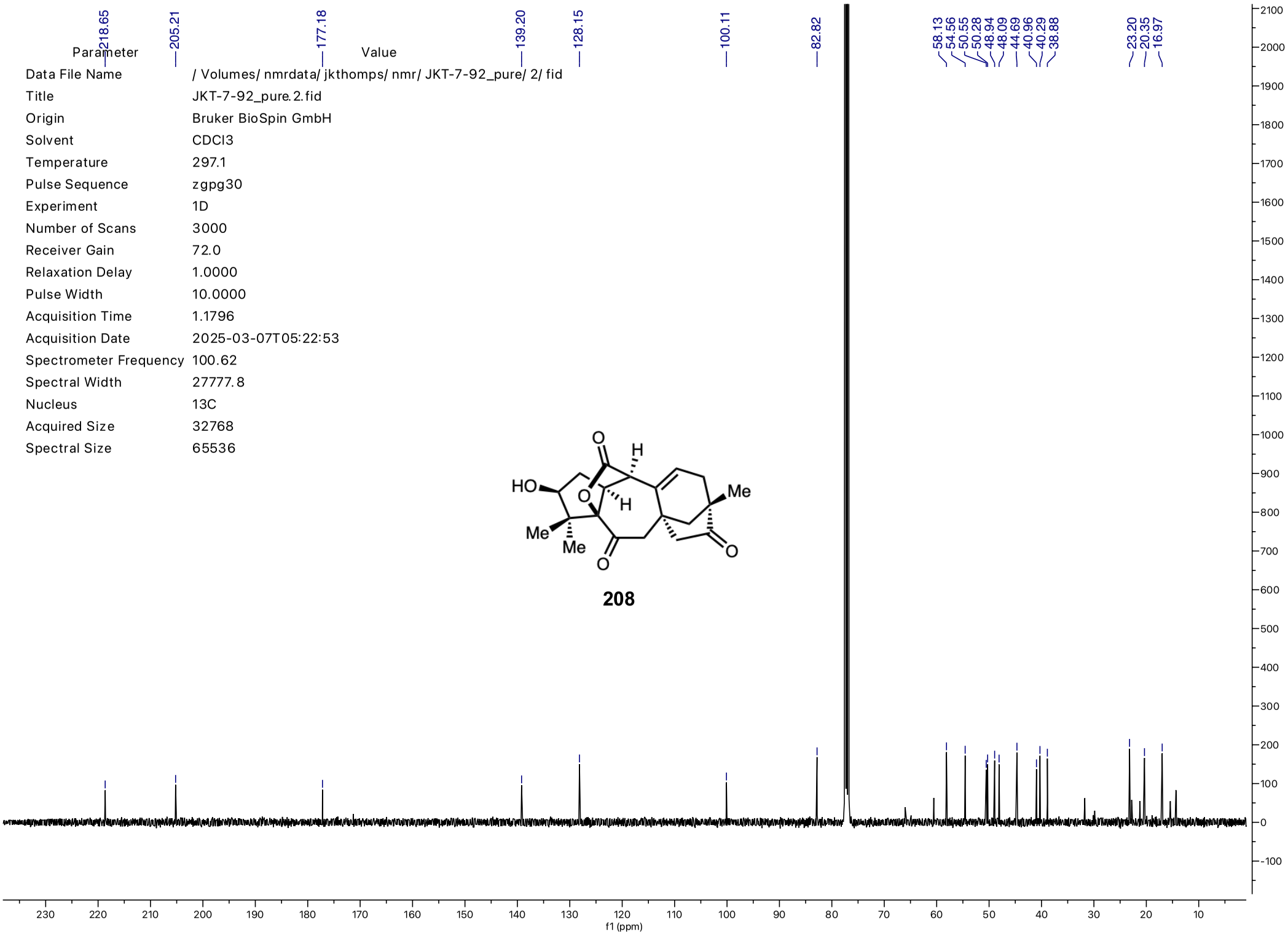

Parameter	Value
Data File Name	/ Volumes/ nmrdata/ jkthomps/ nmr/ JKT-7-92_pure/ 4/ ser
Title	JKT-7-92_pure.4.ser
Origin	Bruker BioSpin GmbH
Solvent	CDCl3
Temperature	297.1
Pulse Sequence	hsqcedetgpsisp2.4
Experiment	HSQC-EDITED
Number of Scans	4
Receiver Gain	197.4
Relaxation Delay	1.5000
Pulse Width	12.5000
Acquisition Time	0.2135
Acquisition Date	2025-03-07T06:00:25
Spectrometer Frequency	(400.13,100.62)
Spectral Width	(4795.4,16611.3)
Lowest Frequency	(-528.1,-1262.8)
Nucleus	(1H,13C)
Acquired Size	(1024,180)
Spectral Size	(1024,1024)
Digital Resolution	(4.68,16.22)

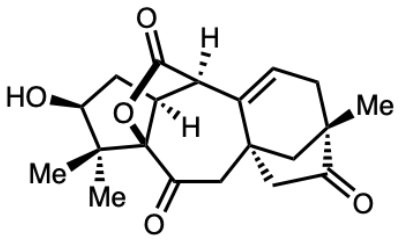

208

f2 (ppm)

f1 (ppm)

Parameter	Value
Data File Name	/ Volumes/ nmrdata/ jkthomps/ nmr/ JKT-7-92_pure/ 3/ ser
Title	JKT-7-92_pure.3.ser
Origin	Bruker BioSpin GmbH
Solvent	CDCl3
Temperature	297.2
Pulse Sequence	cosygpppqf
Experiment	COSY
Number of Scans	3
Receiver Gain	197.4
Relaxation Delay	1.8980
Pulse Width	12.5000
Acquisition Time	0.2990
Acquisition Date	2025-03-07T05:38:15
Spectrometer Frequency	(400.13,400.13)
Spectral Width	(3424.7,3424.7)
Lowest Frequency	(-112.8,-113.4)
Nucleus	(1H,1H)
Acquired Size	(1024,128)
Spectral Size	(1024,1024)
Digital Resolution	(3.34,3.34)

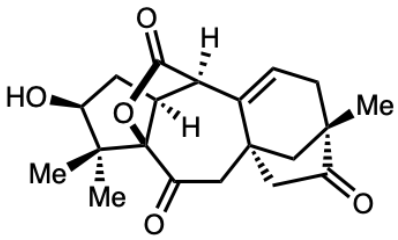

208

f2 (ppm)

f1 (ppm)

Parameter	Value
Data File Name	/ Volumes/ nmrdata/ jkthomps/ nmr/ JKT-7-92_pure/ 5/ ser
Title	JKT-7-92_pure.5.ser
Origin	Bruker BioSpin GmbH
Solvent	CDCl3
Temperature	297.2
Pulse Sequence	hmbcetgpl3nd
Experiment	HMBC
Number of Scans	6
Receiver Gain	197.4
Relaxation Delay	2.0000
Pulse Width	12.5000
Acquisition Time	0.4260
Acquisition Date	2025-03-07T07:05:34
Spectrometer Frequency	(400.13,100.62)
Spectral Width	(4807.7,22321.4)
Lowest Frequency	(-174.5,-1116.4)
Nucleus	(1H,13C)
Acquired Size	(2048,256)
Spectral Size	(2048,1024)
Digital Resolution	(2.35,21.80)

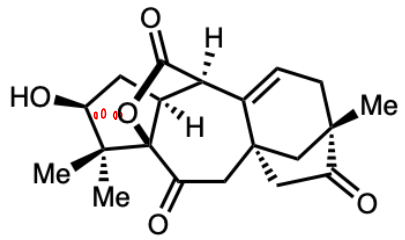

208

f2 (ppm)

f1 (ppm)

Parameter	Value
Data File Name	/ Volumes/ nmrdata/ jkthomps/ nmr/ JKT-7-92_pure/ 6/ ser
Title	JKT-7-92_pure.6.ser
Origin	Bruker BioSpin GmbH
Solvent	CDCl3
Temperature	297.1
Pulse Sequence	noesygpphzs
Experiment	NOESY
Number of Scans	6
Receiver Gain	197.4
Relaxation Delay	1.8000
Pulse Width	12.5000
Acquisition Time	0.2560
Acquisition Date	2025-03-07T08:13:09
Spectrometer Frequency	(400.13,400.13)
Spectral Width	(4000.0,4000.0)
Lowest Frequency	(-168.3,-168.5)
Nucleus	(1H,1H)
Acquired Size	(1024,256)
Spectral Size	(1024,1024)
Digital Resolution	(3.91,3.91)

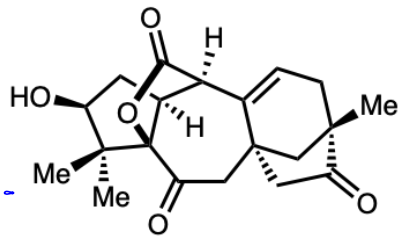

208

f2 (ppm)

f1 (ppm)

Parameter	Value
Data File Name	/ Users/ jordankthompson/ Desktop/ JKT-3-11-1_pure/ PROTON01.fid/ fid
Title	PROTON01
Origin	Varian
Solvent	cdcl3
Temperature	25.0
Pulse Sequence	s2pul
Experiment	1D
Number of Scans	8
Receiver Gain	58
Relaxation Delay	1.0000
Pulse Width	3.3500
Acquisition Time	3.0000
Acquisition Date	2025-04-04T09:47:41
Spectrometer Frequency	499.54
Spectral Width	8000.0
Nucleus	1H
Acquired Size	24000
Spectral Size	65536

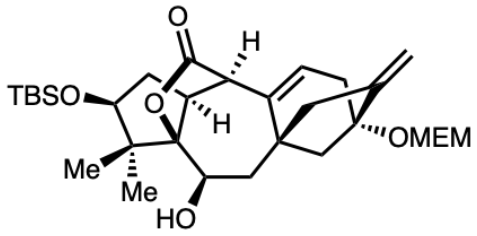

209

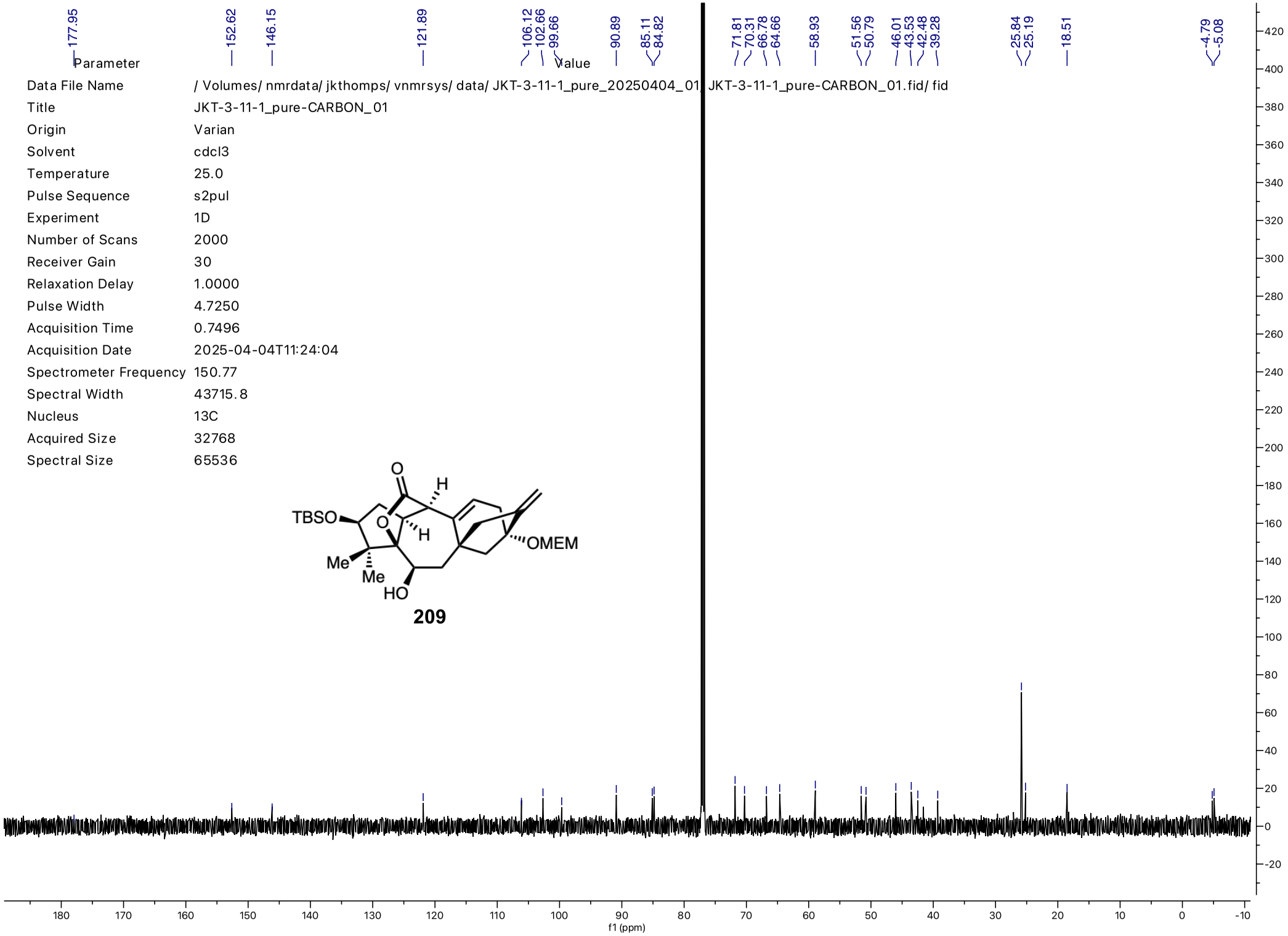
177.95
152.62
146.15
121.89
106.12
102.66
99.66
90.89
85.11
84.82
71.81
70.31
66.78
64.66
58.93
51.56
50.79
46.01
43.53
42.48
39.28
25.84
25.19
18.51
-4.79
-5.08
Parameter
Value
Data File Name / Volumes/ nmrdata/ jkthomps/ vnmrsys/ data/ JKT-3-11-1_pure_20250404_01/ JKT-3-11-1_pure-CARBON_01.fid/ fid
Title JKT-3-11-1_pure-CARBON_01
Origin Varian
Solvent cdcl3
Temperature 25.0
Pulse Sequence s2pul
Experiment 1D
Number of Scans 2000
Receiver Gain 30
Relaxation Delay 1.0000
Pulse Width 4.7250
Acquisition Time 0.7496
Acquisition Date 2025-04-04T11:24:04
Spectrometer Frequency 150.77
Spectral Width 43715.8
Nucleus 13C
Acquired Size 32768
Spectral Size 65536
O
H
TBSO
O
H
OMEM
Me
Me
HO
209
420
400
380
360
340
320
300
280
260
240
220
200
180
160
140
120
100
80
60
40
20
0
-20
180
170
160
150
140
130
120
110
100
90
80
70
60
50
40
30
20
10
0
-10
f1 (ppm)

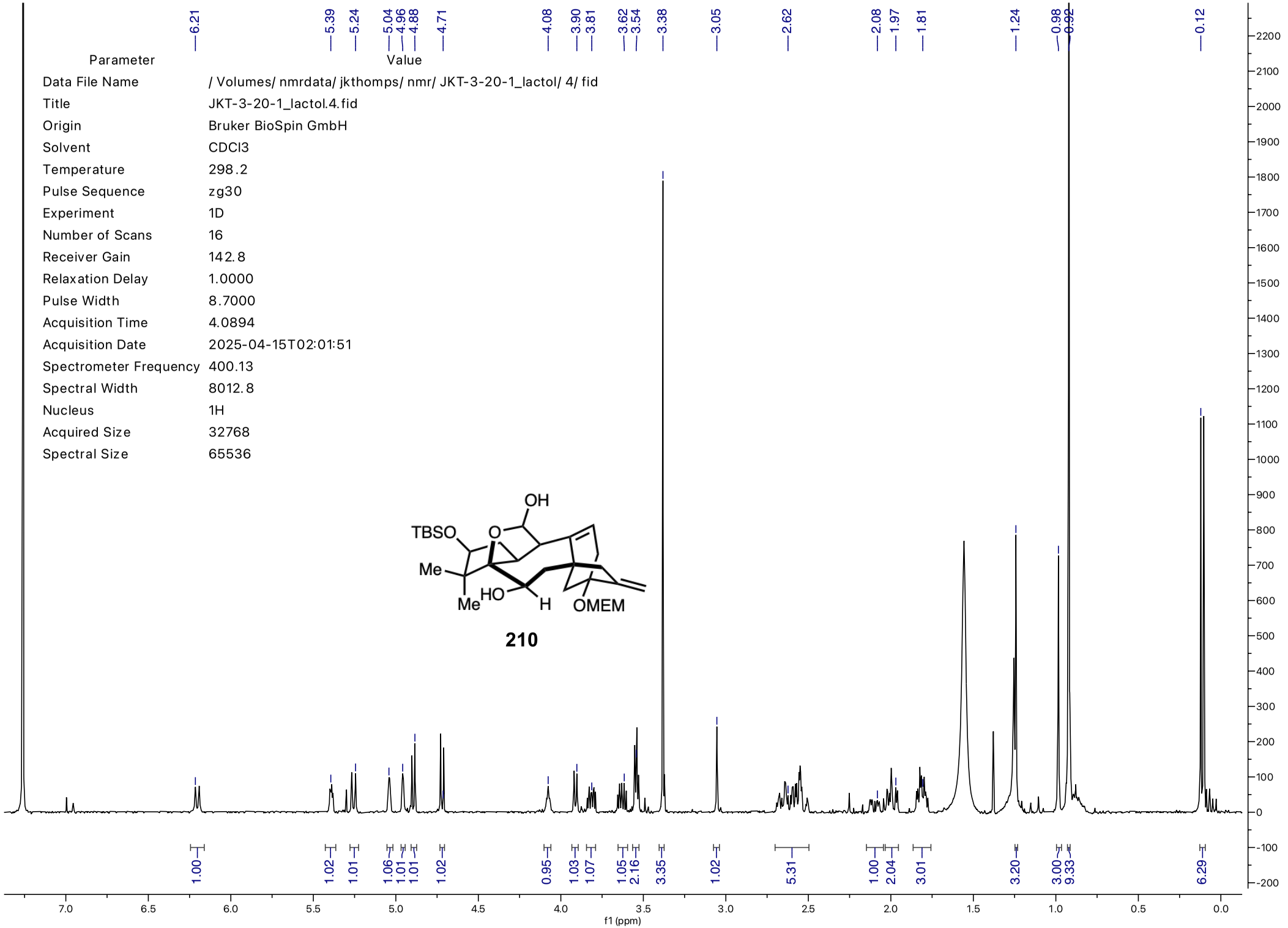
6.21
5.39
5.24
5.04
4.96
4.88
4.71
4.08
3.90
3.81
3.62
3.54
3.38
3.05
2.62
2.08
1.97
1.81
1.24
0.98
0.92
0.12
Parameter
Value
Data File Name / Volumes/ nmrdata/ jkthomps/ nmr/ JKT-3-20-1_lactol/ 4/ fid
Title JKT-3-20-1_lactol.4.fid
Origin Bruker BioSpin GmbH
Solvent CDCl3
Temperature 298.2
Pulse Sequence zg30
Experiment 1D
Number of Scans 16
Receiver Gain 142.8
Relaxation Delay 1.0000
Pulse Width 8.7000
Acquisition Time 4.0894
Acquisition Date 2025-04-15T02:01:51
Spectrometer Frequency 400.13
Spectral Width 8012.8
Nucleus 1H
Acquired Size 32768
Spectral Size 65536
OH
TBSO
O
Me
HO
Me
H
OMEM
210
1.00
1.02
1.01
1.06
1.01
1.01
1.02
0.95
1.03
1.07
1.05
2.16
3.35
1.02
5.31
1.00
2.04
3.01
3.20
3.00
9.33
6.29
f1 (ppm)

Parameter	Value
Data File Name	/ Volumes/ nmrdata/ jkthomps/ nmr/ JKT-3-20-1_lactol/ 3/ fid
Title	JKT-3-20-1_lactol.3.fid
Origin	Bruker BioSpin GmbH
Solvent	CDCl3
Temperature	298.2
Pulse Sequence	zgpg30
Experiment	1D
Number of Scans	5500
Receiver Gain	197.4
Relaxation Delay	1.0000
Pulse Width	10.0000
Acquisition Time	1.3631
Acquisition Date	2025-04-15T05:44:40
Spectrometer Frequency	100.62
Spectral Width	24038.5
Nucleus	13C
Acquired Size	32768
Spectral Size	65536

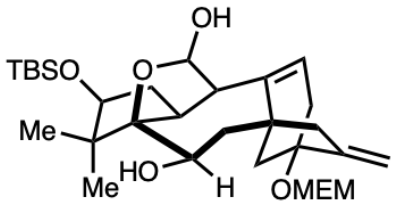

210

Parameter	Value
Data File Name	/ Volumes/ nmrdata/ jkthomps/ nmr/ JKT-3-20-1_lactol_/ 5/ ser
Title	JKT-3-20-1_lactol_.5.ser
Origin	Bruker BioSpin GmbH
Solvent	CDCl3
Temperature	298.2
Pulse Sequence	hsqcedetgpsisp2.4
Experiment	HSQC-EDITED
Number of Scans	10
Receiver Gain	197.4
Relaxation Delay	1.5000
Pulse Width	8.7000
Acquisition Time	0.2135
Acquisition Date	2025-04-15T06:38:22
Spectrometer Frequency	(400.13,100.62)
Spectral Width	(4795.4,16611.3)
Lowest Frequency	(-521.8,-1300.8)
Nucleus	(1H,13C)
Acquired Size	(1024,180)
Spectral Size	(1024,1024)
Digital Resolution	(4.68,16.22)

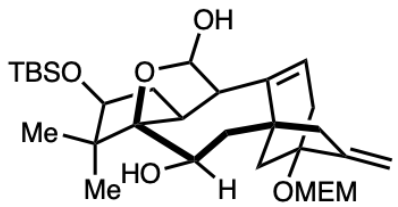

210

f2 (ppm)

f1 (ppm)

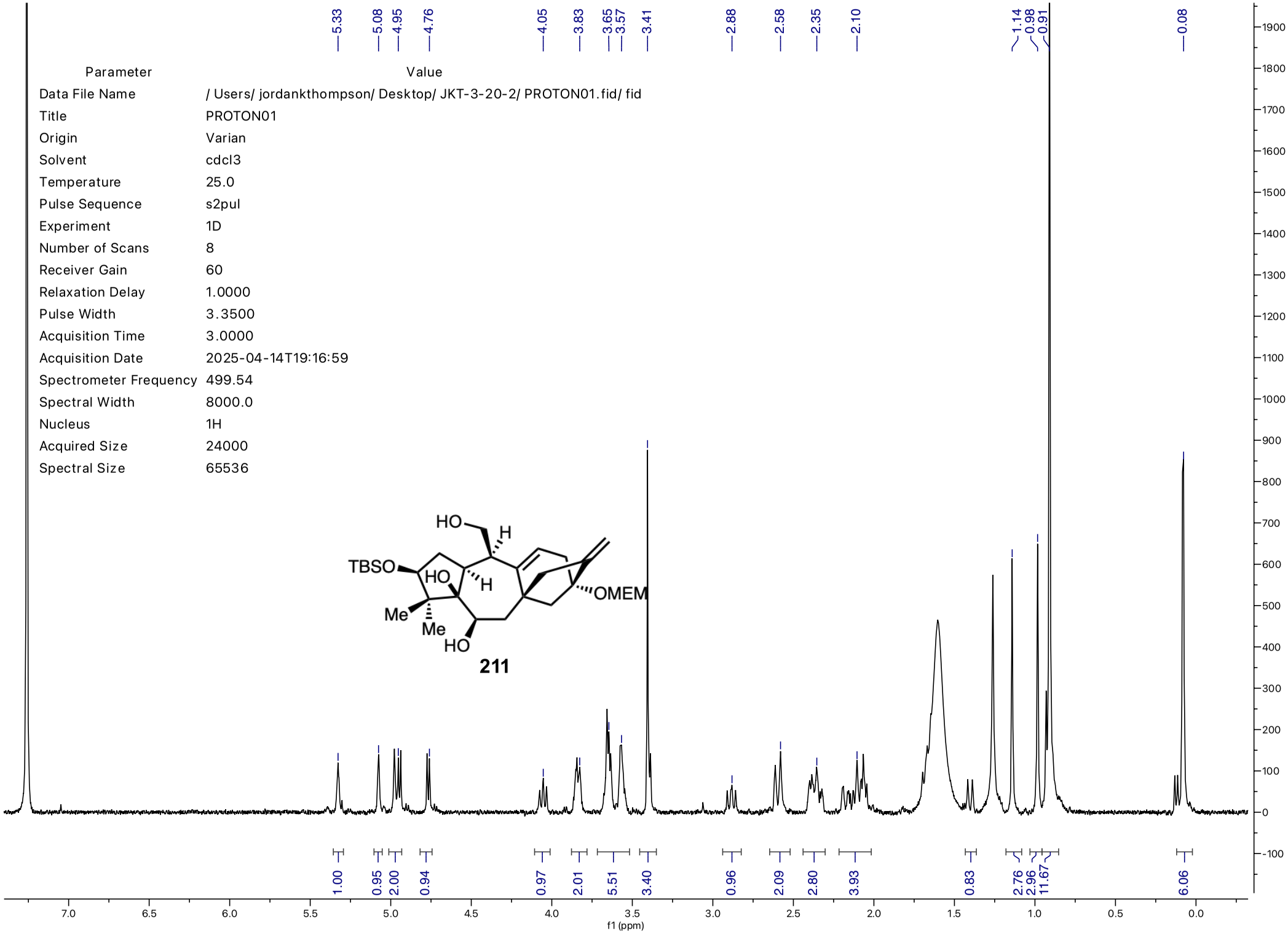
5.33
5.08
4.95
4.76
4.05
3.83
3.65
3.57
3.41
2.88
2.58
2.35
2.10
1.14
0.98
0.91
0.08
Parameter Value
Data File Name / Users/ jordankthompson/ Desktop/ JKT-3-20-2/ PROTON01.fid/ fid
Title PROTON01
Origin Varian
Solvent cdcl3
Temperature 25.0
Pulse Sequence s2pul
Experiment 1D
Number of Scans 8
Receiver Gain 60
Relaxation Delay 1.0000
Pulse Width 3.3500
Acquisition Time 3.0000
Acquisition Date 2025-04-14T19:16:59
Spectrometer Frequency 499.54
Spectral Width 8000.0
Nucleus 1H
Acquired Size 24000
Spectral Size 65536
HO
H
TBSO
HO
H
OMEM
Me
Me
HO
211
1.00
0.95
2.00
0.94
0.97
2.01
5.51
3.40
0.96
2.09
2.80
3.93
0.83
2.76
2.96
11.67
6.06
f1 (ppm)

Parameter	Value
Data File Name	/ Volumes/ nmrdata/ jkthomps/ nmr/ JKT-7-221_pure/ 1/ fid
Title	JKT-7-221_pure.1.fid
Origin	Bruker BioSpin GmbH
Solvent	CDCl3
Temperature	297.1
Pulse Sequence	zg30
Experiment	1D
Number of Scans	16
Receiver Gain	197.4
Relaxation Delay	1.0000
Pulse Width	12.5000
Acquisition Time	4.0894
Acquisition Date	2025-05-23T19:58:54
Spectrometer Frequency	400.13
Spectral Width	8012.8
Nucleus	1H
Acquired Size	32768
Spectral Size	65536

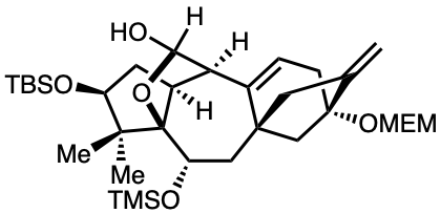

214

Parameter	Value
Data File Name	/ Volumes/ nmrdata/ jkthomps/ nmr/ JKT-7-221_pure/ 2/ fid
Title	JKT-7-221_pure.2.fid
Origin	Bruker BioSpin GmbH
Solvent	CDCl3
Temperature	297.1
Pulse Sequence	zgpg30
Experiment	1D
Number of Scans	1000
Receiver Gain	72.0
Relaxation Delay	1.0000
Pulse Width	10.0000
Acquisition Time	1.1796
Acquisition Date	2025-05-23T20:37:39
Spectrometer Frequency	100.62
Spectral Width	27777.8
Nucleus	13C
Acquired Size	32768
Spectral Size	65536

214

152.99 146.43 121.39 106.27 103.00 100.23 91.14 85.58 85.37 71.86 71.35 67.19 65.36 59.11 52.13 51.33 51.25 46.26 43.51 42.57 41.91 39.69 26.31 26.00 18.77 18.44 1.43 -4.60 -4.94

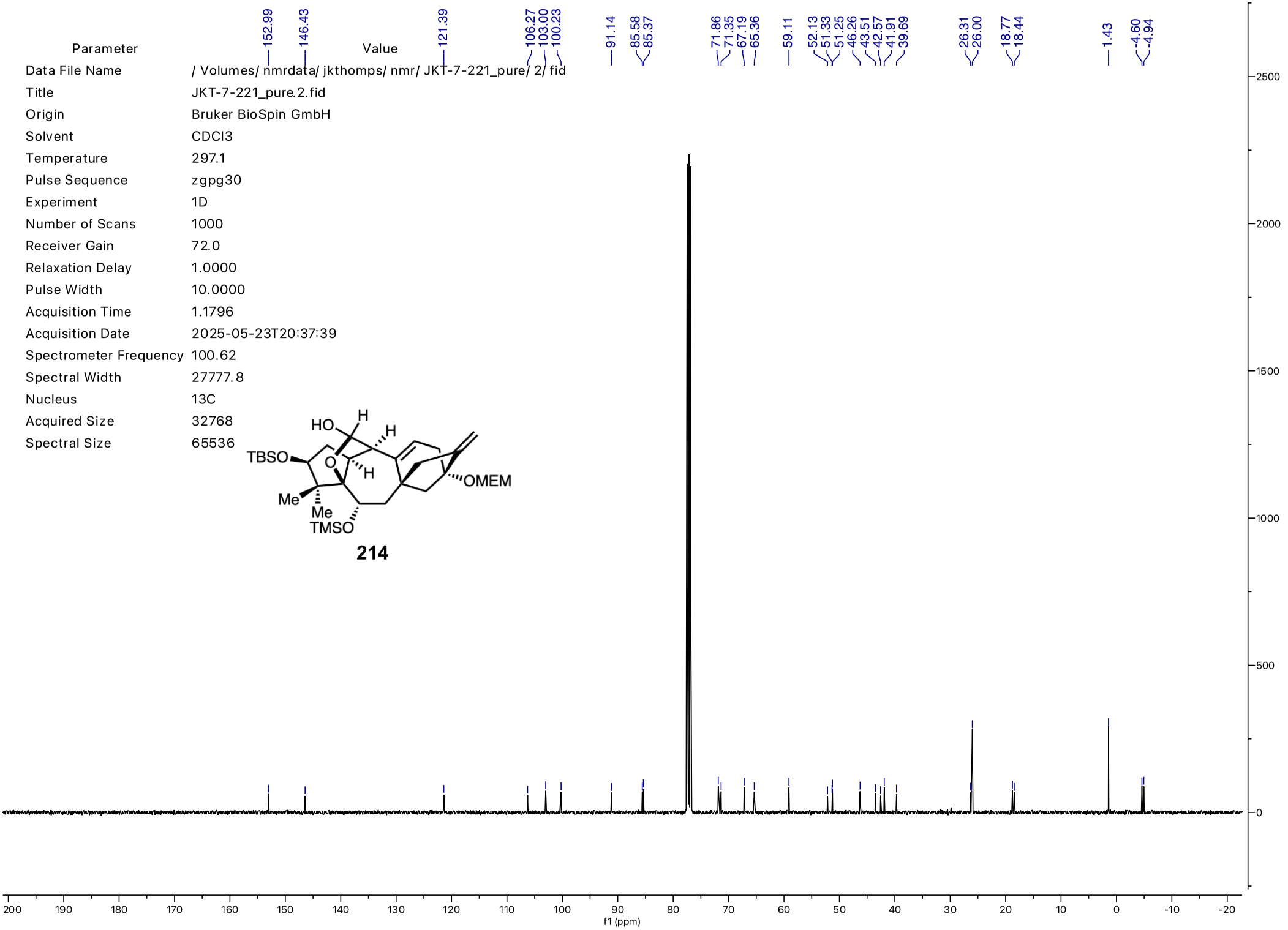

Parameter	Value
Data File Name	/ Volumes/ nmrdata/ jkthomps/ nmr/ JKT-7-221_pure/ 3/ ser
Title	JKT-7-221_pure.3.ser
Origin	Bruker BioSpin GmbH
Solvent	CDCl3
Temperature	297.2
Pulse Sequence	hsqcedetgpsisp2.4
Experiment	HSQC-EDITED
Number of Scans	6
Receiver Gain	197.4
Relaxation Delay	1.5000
Pulse Width	12.5000
Acquisition Time	0.2135
Acquisition Date	2025-05-23T21:06:29
Spectrometer Frequency	(400.13,100.62)
Spectral Width	(4795.4,16611.3)
Lowest Frequency	(-525.8,-1262.8)
Nucleus	(1H,13C)
Acquired Size	(1024,158)
Spectral Size	(1024,1024)
Digital Resolution	(4.68,16.22)

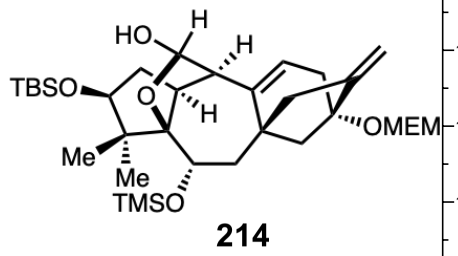

214

f2 (ppm)

f1 (ppm)

Parameter	Value
Data File Name	/ Volumes/ nmrdata/ jkthomps/ nmr/ JKT-7-221_pure/ 4/ ser
Title	JKT-7-221_pure.4.ser
Origin	Bruker BioSpin GmbH
Solvent	CDCl3
Temperature	297.2
Pulse Sequence	cosygpppqf
Experiment	COSY
Number of Scans	1
Receiver Gain	127.1
Relaxation Delay	1.9164
Pulse Width	12.5000
Acquisition Time	0.2806
Acquisition Date	2025-05-23T21:16:00
Spectrometer Frequency	(400.13,400.13)
Spectral Width	(3649.6,3649.6)
Lowest Frequency	(-376.1,-380.0)
Nucleus	(1H,1H)
Acquired Size	(1024,128)
Spectral Size	(1024,1024)
Digital Resolution	(3.56,3.56)

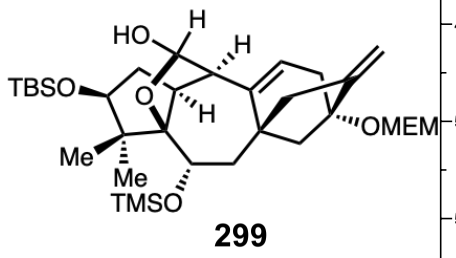

299

f2 (ppm)

f1 (ppm)

Parameter	Value
Data File Name	/ Volumes/ nmrdata/ jkthomps/ nmr/ JKT-7-221_pure/ 5/ ser
Title	JKT-7-221_pure.5.ser
Origin	Bruker BioSpin GmbH
Solvent	CDCl3
Temperature	297.1
Pulse Sequence	hmbcetgpl3nd
Experiment	HMBC
Number of Scans	7
Receiver Gain	197.4
Relaxation Delay	2.0000
Pulse Width	12.5000
Acquisition Time	0.4260
Acquisition Date	2025-05-23T22:31:53
Spectrometer Frequency	(400.13,100.62)
Spectral Width	(4807.7,22621.4)
Lowest Frequency	(-163.1,-1116.4)
Nucleus	(1H,13C)
Acquired Size	(2048,256)
Spectral Size	(2048,1024)
Digital Resolution	(2.35,21.80)

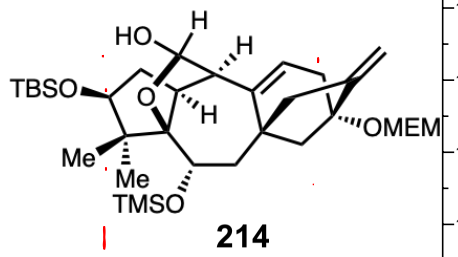

214

f2 (ppm)

f1 (ppm)

Parameter	Value
Data File Name	/ Volumes/ nmrdata/ jkthomps/ nmr/ JKT-7-221_pure/ 6/ ser
Title	JKT-7-221_pure.6.ser
Origin	Bruker BioSpin GmbH
Solvent	CDCl3
Temperature	297.2
Pulse Sequence	noesygpphzs
Experiment	NOESY
Number of Scans	4
Receiver Gain	197.4
Relaxation Delay	1.8000
Pulse Width	12.5000
Acquisition Time	0.2560
Acquisition Date	2025-05-23T23:17:33
Spectrometer Frequency	(400.13,400.13)
Spectral Width	(4000.0,4000.0)
Lowest Frequency	(-167.4,-168.1)
Nucleus	(1H,1H)
Acquired Size	(1024,256)
Spectral Size	(1024,1024)
Digital Resolution	(3.91,3.91)

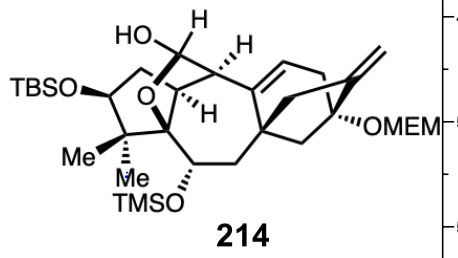

214

f2 (ppm)

f1 (ppm)

Parameter	Value
Data File Name	/ Volumes/ nmrdata/ jkthomps/ nmr/ JKT-7-234_pure/ 1/ fid
Title	JKT-7-234_pure.1.fid
Origin	Bruker BioSpin GmbH
Solvent	CDCl3
Temperature	297.1
Pulse Sequence	zg30
Experiment	1D
Number of Scans	16
Receiver Gain	197.4
Relaxation Delay	1.0000
Pulse Width	12.5000
Acquisition Time	4.0894
Acquisition Date	2025-06-01T16:32:25
Spectrometer Frequency	400.13
Spectral Width	8012.8
Nucleus	1H
Acquired Size	32768
Spectral Size	65536

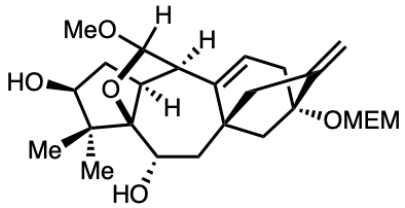

216

Parameter	Value
Data File Name	/ Volumes/ nmrdata/ jkthomps/ nmr/ JKT-7-234_pure/ 2/ fid
Title	JKT-7-234_pure.2.fid
Origin	Bruker BioSpin GmbH
Solvent	CDCl3
Temperature	297.1
Pulse Sequence	zgpg30
Experiment	1D
Number of Scans	1500
Receiver Gain	38.0
Relaxation Delay	1.0000
Pulse Width	10.0000
Acquisition Time	1.1796
Acquisition Date	2025-06-02T00:44:04
Spectrometer Frequency	100.62
Spectral Width	27777.8
Nucleus	13C
Acquired Size	32768
Spectral Size	65536

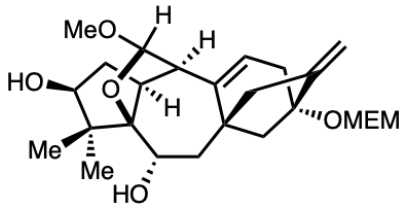

216

Parameter	Value
Data File Name	/ Volumes/ nmrdata/ jkthomps/ nmr/ JKT-7-234_pure/ 3/ ser
Title	JKT-7-234_pure.3.ser
Origin	Bruker BioSpin GmbH
Solvent	CDCl3
Temperature	297.1
Pulse Sequence	cosygpppqf
Experiment	COSY
Number of Scans	3
Receiver Gain	197.4
Relaxation Delay	1.8878
Pulse Width	12.5000
Acquisition Time	0.3092
Acquisition Date	2025-06-02T00:59:23
Spectrometer Frequency	(400.13,400.13)
Spectral Width	(3311.3,3311.3)
Lowest Frequency	(-82.2,-82.2)
Nucleus	(1H,1H)
Acquired Size	(1024,128)
Spectral Size	(1024,1024)
Digital Resolution	(3.23,3.23)

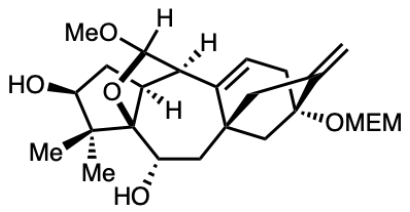

216

f2 (ppm)

f1 (ppm)

Parameter	Value
Data File Name	/ Volumes/ nmrdata/ jkthomps/ nmr/ JKT-7-234_pure/ 4/ ser
Title	JKT-7-234_pure.4.ser
Origin	Bruker BioSpin GmbH
Solvent	CDCl3
Temperature	297.1
Pulse Sequence	hsqcedetgpsisp2.4
Experiment	HSQC-EDITED
Number of Scans	6
Receiver Gain	197.4
Relaxation Delay	1.5000
Pulse Width	12.5000
Acquisition Time	0.2135
Acquisition Date	2025-06-02T01:32:03
Spectrometer Frequency	(400.13,100.62)
Spectral Width	(4795.4,16611.3)
Lowest Frequency	(-552.5,-1262.8)
Nucleus	(1H,13C)
Acquired Size	(1024,180)
Spectral Size	(1024,1024)
Digital Resolution	(4.68,16.22)

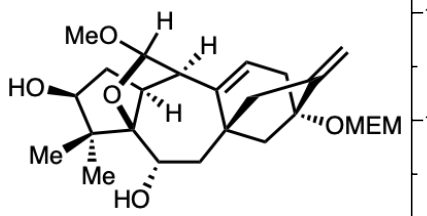

216

f2 (ppm)

f1 (ppm)

Parameter	Value
Data File Name	/ Volumes/ nmrdata/ jkthomps/ nmr/ JKT-7-234_pure/ 5/ ser
Title	JKT-7-234_pure.5.ser
Origin	Bruker BioSpin GmbH
Solvent	CDCl3
Temperature	297.2
Pulse Sequence	hmbcetgpl3nd
Experiment	HMBC
Number of Scans	8
Receiver Gain	197.4
Relaxation Delay	2.0000
Pulse Width	12.5000
Acquisition Time	0.4260
Acquisition Date	2025-06-02T02:58:37
Spectrometer Frequency	(400.13,100.62)
Spectral Width	(4807.7,22321.4)
Lowest Frequency	(-163.1,-1116.4)
Nucleus	(1H,13C)
Acquired Size	(2048,256)
Spectral Size	(2048,1024)
Digital Resolution	(2.35,21.80)

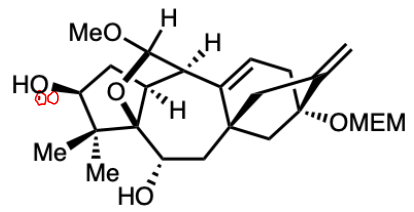

216

f2 (ppm)

f1 (ppm)

Parameter	Value
Data File Name	/ Volumes/ nmrdata/ jkthomps/ nmr/ JKT-7-234_pure/ 6/ ser
Title	JKT-7-234_pure.6.ser
Origin	Bruker BioSpin GmbH
Solvent	CDCl3
Temperature	297.1
Pulse Sequence	noesygpphzs
Experiment	NOESY
Number of Scans	7
Receiver Gain	197.4
Relaxation Delay	1.8000
Pulse Width	12.5000
Acquisition Time	0.2560
Acquisition Date	2025-06-02T04:17:11
Spectrometer Frequency	(400.13,400.13)
Spectral Width	(4000.0,4000.0)
Lowest Frequency	(-194.9,-195.1)
Nucleus	(1H,1H)
Acquired Size	(1024,256)
Spectral Size	(1024,1024)
Digital Resolution	(3.91,3.91)

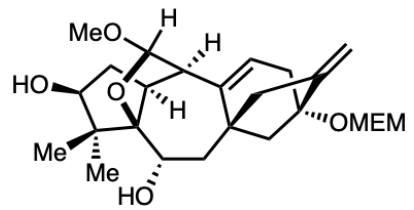

216

f2 (ppm)

f1 (ppm)

Parameter	Value
Data File Name	/ Volumes/ nmrdata/ jkthomps/ nmr/ JKT-8-17_pure/ 1/ fid
Title	JKT-8-17_pure.1.fid
Origin	Bruker BioSpin GmbH & Co.KG
Solvent	CDCl3
Temperature	298.1
Pulse Sequence	zg30
Experiment	1D
Number of Scans	16
Receiver Gain	101.0
Relaxation Delay	1.0000
Pulse Width	9.8500
Acquisition Time	3.9977
Acquisition Date	2025-07-27T22:18:19
Spectrometer Frequency	400.15
Spectral Width	8196.7
Nucleus	1H
Acquired Size	32768
Spectral Size	65536

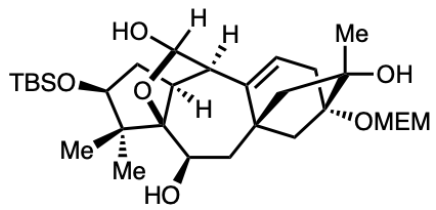

217

Parameter	Value
Data File Name	/ Volumes/ nmrdata/ jkthomps/ nmr/ JKT-8-17_pure/ 2/ fid
Title	JKT-8-17_pure.2.fid
Origin	Bruker BioSpin GmbH & Co.KG
Solvent	CDCl3
Temperature	298.1
Pulse Sequence	zgpg30
Experiment	1D
Number of Scans	3500
Receiver Gain	45.2
Relaxation Delay	2.0000
Pulse Width	10.0000
Acquisition Time	1.1796
Acquisition Date	2025-07-28T01:29:24
Spectrometer Frequency	100.63
Spectral Width	27777.8
Nucleus	13C
Acquired Size	32768
Spectral Size	65536

146.92, 122.36, 106.18, 100.51, 91.55, 85.67, 84.11, 79.48, 71.87, 70.94, 67.58, 65.90, 59.18, 55.99, 51.92, 47.95, 47.44, 45.30, 42.74, 39.82, 35.39, 26.04, 25.93, 25.25, 19.56, 18.41, -4.63, -4.96

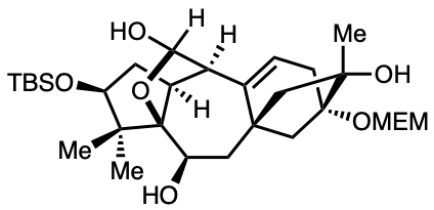

217

70000, 65000, 60000, 55000, 50000, 45000, 40000, 35000, 30000, 25000, 20000, 15000, 10000, 5000, 0, -5000

150, 140, 130, 120, 110, 100, 90, 80, 70, 60, 50, 40, 30, 20, 10, 0

f1 (ppm)

Parameter	Value
Data File Name	/ Volumes/ nmrdata/ jkthomps/ nmr/ JKT-8-17_pure/ 3/ ser
Title	JKT-8-17_pure.3.ser
Origin	Bruker BioSpin GmbH & Co.KG
Solvent	CDCl3
Temperature	298.1
Pulse Sequence	cosygpppqf
Experiment	COSY
Number of Scans	2
Receiver Gain	101.0
Relaxation Delay	2.0000
Pulse Width	9.8500
Acquisition Time	0.1946
Acquisition Date	2025-07-28T01:39:45
Spectrometer Frequency	(400.15,400.15)
Spectral Width	(5263.2,5263.2)
Lowest Frequency	(-283.6,-230.7)
Nucleus	(1H,1H)
Acquired Size	(1024,128)
Spectral Size	(1024,1024)
Digital Resolution	(5.14,5.14)

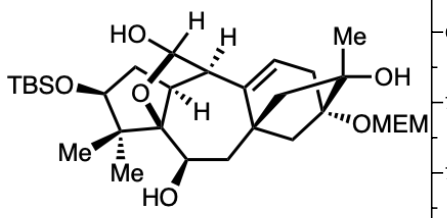

217

f2 (ppm)

f1 (ppm)

Parameter	Value
Data File Name	/ Volumes/ nmrdata/ jkthomps/ nmr/ JKT-8-17_pure/ 4/ ser
Title	JKT-8-17_pure.4.ser
Origin	Bruker BioSpin GmbH & Co.KG
Solvent	CDCl3
Temperature	298.2
Pulse Sequence	hmbcgplpndqf
Experiment	HMBC
Number of Scans	10
Receiver Gain	101.0
Relaxation Delay	1.5000
Pulse Width	9.8500
Acquisition Time	0.5980
Acquisition Date	2025-07-28T02:26:35
Spectrometer Frequency	(400.15,100.63)
Spectral Width	(3424.7,22138.1)
Lowest Frequency	(-286.7,-1007.3)
Nucleus	(1H,13C)
Acquired Size	(2048,128)
Spectral Size	(2048,512)
Digital Resolution	(1.67,43.24)

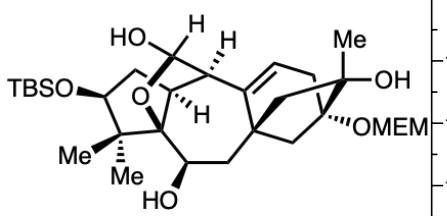

217

f2 (ppm)

f1 (ppm)

Parameter	Value
Data File Name	/ Volumes/ nmrdata/ jkthomps/ nmr/ JKT-8-17_pure/ 5/ ser
Title	JKT-8-17_pure.5.ser
Origin	Bruker BioSpin GmbH & Co.KG
Solvent	CDCl3
Temperature	298.2
Pulse Sequence	hsqcedetgpsisp2.3
Experiment	HSQC-EDITED
Number of Scans	10
Receiver Gain	32.0
Relaxation Delay	1.5000
Pulse Width	9.8500
Acquisition Time	0.1946
Acquisition Date	2025-07-28T03:41:09
Spectrometer Frequency	(400.15,100.63)
Spectral Width	(5263.2,16603.2)
Lowest Frequency	(-798.0,-755.3)
Nucleus	(1H,13C)
Acquired Size	(1024,256)
Spectral Size	(1024,1024)
Digital Resolution	(5.14,16.21)

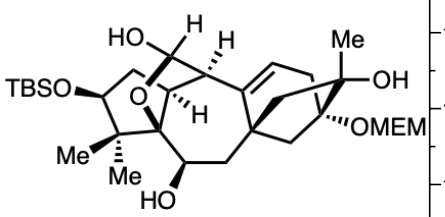

217

f2 (ppm)

f1 (ppm)

Parameter	Value
Data File Name	/ Volumes/ nmrdata/ jkthomps/ nmr/ JKT-8-17_pure/ 6/ ser
Title	JKT-8-17_pure.6.ser
Origin	Bruker BioSpin GmbH & Co.KG
Solvent	CDCl3
Temperature	298.1
Pulse Sequence	noesygpphpp
Experiment	NOESY
Number of Scans	5
Receiver Gain	101.0
Relaxation Delay	1.8730
Pulse Width	9.8500
Acquisition Time	0.3809
Acquisition Date	2025-07-28T04:38:29
Spectrometer Frequency	(400.15,400.15)
Spectral Width	(2688.2,2688.2)
Lowest Frequency	(-23.6,-23.6)
Nucleus	(1H,1H)
Acquired Size	(1024,256)
Spectral Size	(1024,1024)
Digital Resolution	(2.63,2.63)

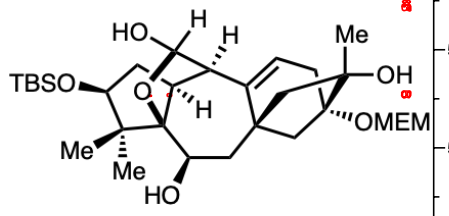

217

f2 (ppm)

f1 (ppm)

Parameter	Value
Data File Name	/ Volumes/ nmrdata/ jkthomps/ nmr/ JKT-8-15-1/ 1/ fid
Title	JKT-8-15-1.1.fid
Origin	Bruker BioSpin GmbH
Solvent	CDCl3
Temperature	297.1
Pulse Sequence	zg30
Experiment	1D
Number of Scans	16
Receiver Gain	197.4
Relaxation Delay	1.0000
Pulse Width	12.5000
Acquisition Time	4.0894
Acquisition Date	2025-07-27T04:33:21
Spectrometer Frequency	400.13
Spectral Width	8012.8
Nucleus	1H
Acquired Size	32768
Spectral Size	65536

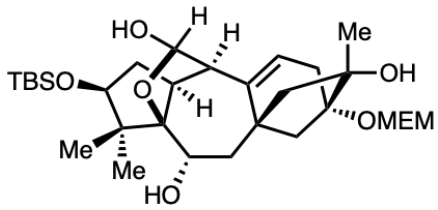

C6-*epi*-**217**

Parameter	Value
Data File Name	/ Volumes/ nmrdata/ jkthomps/ nmr/ JKT-8-15-1/ 5/ fid
Title	JKT-8-15-1.5.fid
Origin	Bruker BioSpin GmbH
Solvent	CDCl3
Temperature	297.1
Pulse Sequence	zgpg30
Experiment	1D
Number of Scans	500
Receiver Gain	98.9
Relaxation Delay	1.0000
Pulse Width	10.0000
Acquisition Time	1.1796
Acquisition Date	2025-07-27T05:10:08
Spectrometer Frequency	100.62
Spectral Width	27777.8
Nucleus	13C
Acquired Size	32768
Spectral Size	65536

149.19 121.09 102.86 99.90 91.56 86.07 85.04 78.04 71.90 70.41 67.58 64.72 59.80 59.18 51.07 48.09 45.68 43.16 41.61 39.49 35.42 25.98 25.37 24.46 18.70 18.41 -4.62 -4.94

C6-*epi*-**217**

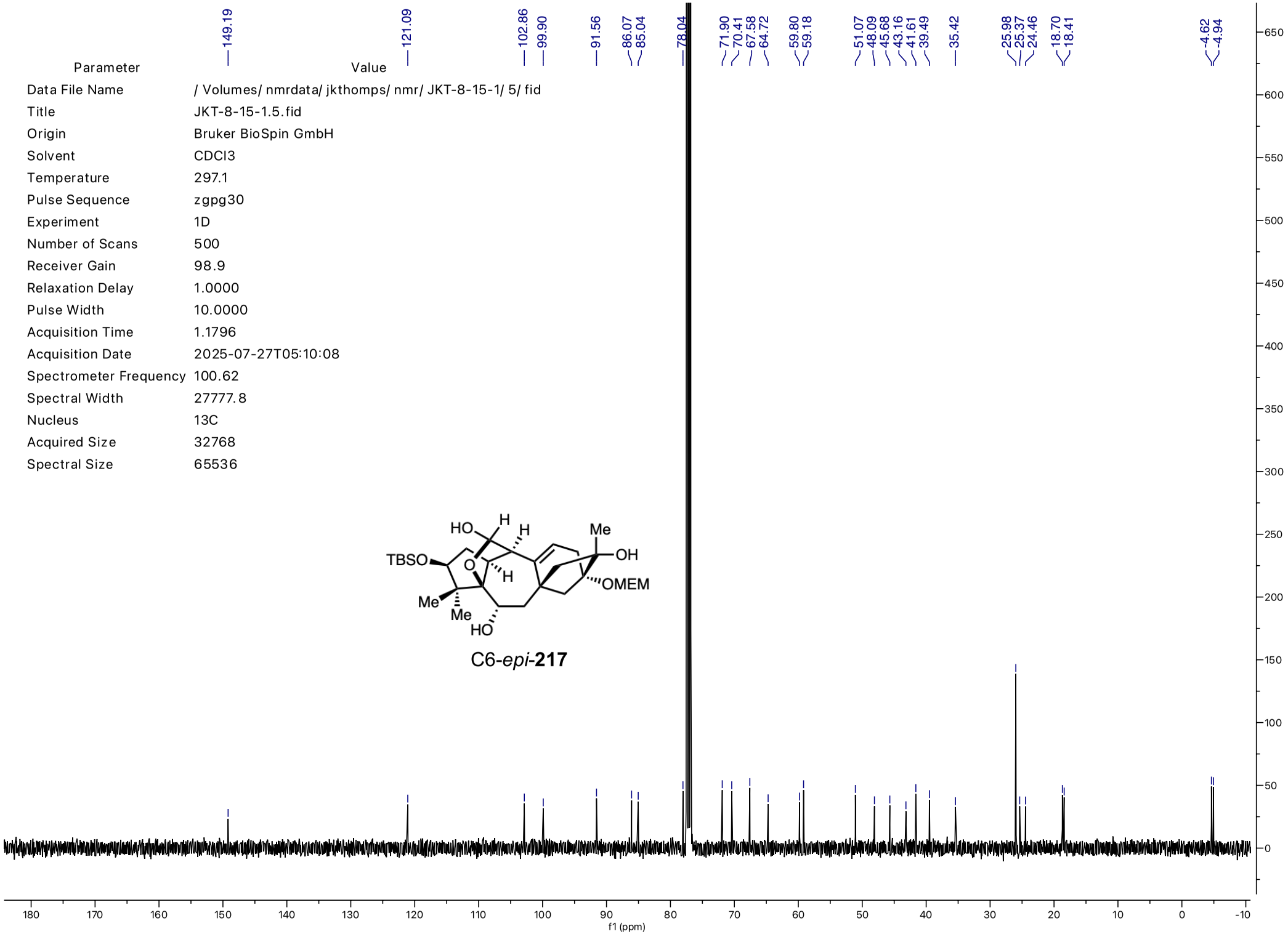

Parameter	Value
Data File Name	/ Volumes/ nmrdata/ jkthomps/ nmr/ JKT-8-15-1/ 4/ ser
Title	JKT-8-15-1.4.ser
Origin	Bruker BioSpin GmbH
Solvent	CDCl3
Temperature	297.1
Pulse Sequence	hsqcedetgpsisp2.4
Experiment	HSQC-EDITED
Number of Scans	2
Receiver Gain	197.4
Relaxation Delay	1.5000
Pulse Width	12.5000
Acquisition Time	0.2135
Acquisition Date	2025-07-27T04:50:43
Spectrometer Frequency	(400.13,100.62)
Spectral Width	(4795.4,16611.3)
Lowest Frequency	(-524.1,-1262.8)
Nucleus	(1H,13C)
Acquired Size	(1024,180)
Spectral Size	(1024,1024)
Digital Resolution	(4.68,16.22)

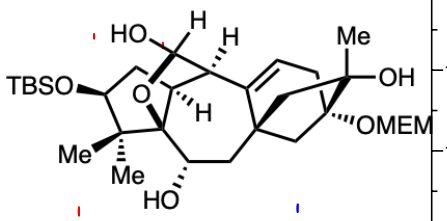

C6-*epi*-**217**

f2 (ppm)

f1 (ppm)

Parameter	Value
Data File Name	/ Volumes/ nmrdata/ jkthomps/ nmr/ JKT-8-15-1/ 3/ ser
Title	JKT-8-15-1.3.ser
Origin	Bruker BioSpin GmbH
Solvent	CDCl3
Temperature	297.1
Pulse Sequence	cosygpppqf
Experiment	COSY
Number of Scans	1
Receiver Gain	156.2
Relaxation Delay	1.9185
Pulse Width	12.5000
Acquisition Time	0.2785
Acquisition Date	2025-07-27T04:39:03
Spectrometer Frequency	(400.13,400.13)
Spectral Width	(3676.5,3676.5)
Lowest Frequency	(-445.3,-445.3)
Nucleus	(1H,1H)
Acquired Size	(1024,128)
Spectral Size	(1024,1024)
Digital Resolution	(3.59,3.59)

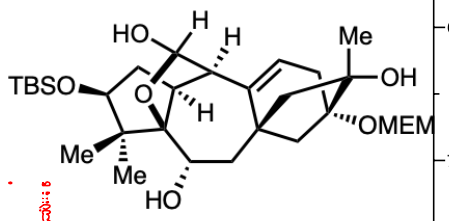

C6-*epi*-**217**

f2 (ppm)

f1 (ppm)

Parameter	Value
Data File Name	/ Volumes/ nmrdata/ jkthomps/ nmr/ JKT-8-15-1_/ 2/ ser
Title	JKT-8-15-1_.2.ser
Origin	Bruker BioSpin GmbH
Solvent	CDCl3
Temperature	297.1
Pulse Sequence	noesygpphzs
Experiment	NOESY
Number of Scans	4
Receiver Gain	197.4
Relaxation Delay	1.8000
Pulse Width	12.5000
Acquisition Time	0.2560
Acquisition Date	2025-07-27T17:17:45
Spectrometer Frequency	(400.13,400.13)
Spectral Width	(4000.0,4000.0)
Lowest Frequency	(-198.7,-204.1)
Nucleus	(1H,1H)
Acquired Size	(1024,256)
Spectral Size	(1024,1024)
Digital Resolution	(3.91,3.91)

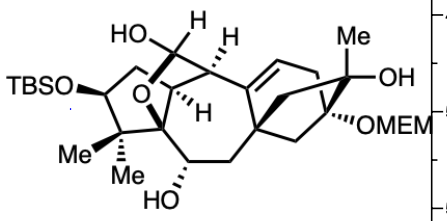

C6-*epi*-**217**

f2 (ppm)

f1 (ppm)

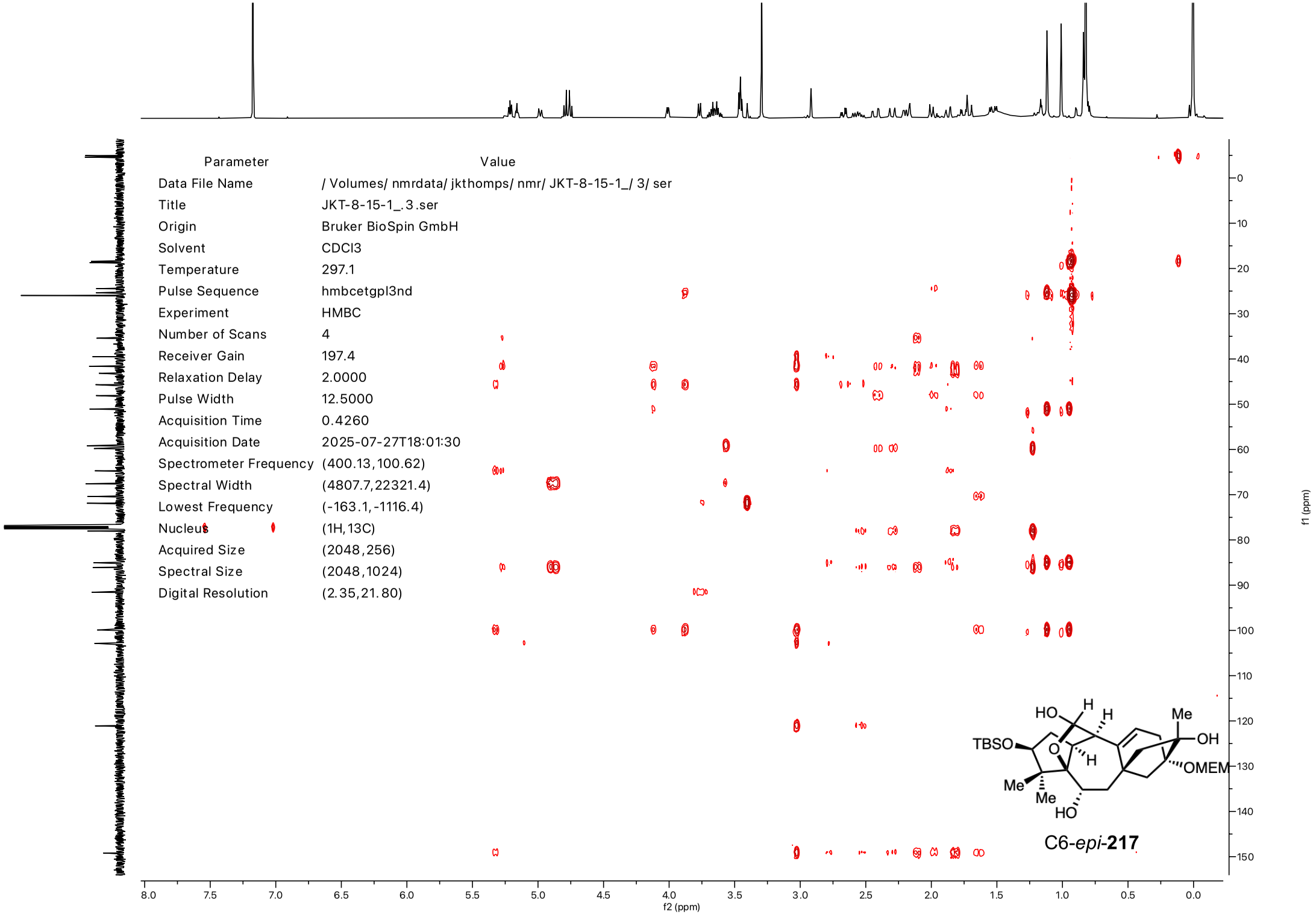
Parameter Value
Data File Name / Volumes/ nmrdata/ jkthomps/ nmr/ JKT-8-15-1_/ 3/ ser
Title JKT-8-15-1_.3.ser
Origin Bruker BioSpin GmbH
Solvent CDCl3
Temperature 297.1
Pulse Sequence hmbcetgpl3nd
Experiment HMBC
Number of Scans 4
Receiver Gain 197.4
Relaxation Delay 2.0000
Pulse Width 12.5000
Acquisition Time 0.4260
Acquisition Date 2025-07-27T18:01:30
Spectrometer Frequency (400.13,100.62)
Spectral Width (4807.7,22321.4)
Lowest Frequency (-163.1,-1116.4)
Nucleus (1H,13C)
Acquired Size (2048,256)
Spectral Size (2048,1024)
Digital Resolution (2.35,21.80)
f2 (ppm)
f1 (ppm)
HO
H
H
Me
OH
TBSO
O
H
OMEM
Me
Me
HO
C6-epi-217

Parameter	Value
Data File Name	/ Volumes/ nmrdata/ jkthomps/ nmr/ JKT-8-22_pure_dehydro/ 1/ fid
Title	JKT-8-22_pure_dehydro.1.fid
Origin	Bruker BioSpin GmbH
Solvent	MeOD
Temperature	297.2
Pulse Sequence	zg30
Experiment	1D
Number of Scans	16
Receiver Gain	142.8
Relaxation Delay	1.0000
Pulse Width	12.5000
Acquisition Time	4.0894
Acquisition Date	2025-07-29T09:27:53
Spectrometer Frequency	400.13
Spectral Width	8012.8
Nucleus	1H
Acquired Size	32768
Spectral Size	65536

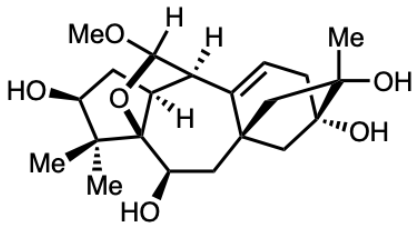

218

5.28 5.07 4.87 3.77 3.49 3.43 2.92 2.71 2.26 2.05 1.81 1.68 1.57 1.30 1.18 1.02

1.00 1.01 1.00 1.05 3.01 1.00 1.00 3.01 3.06 2.01 1.01 1.01 3.02 3.00 3.00

f1 (ppm)

150.03 122.52 112.02 103.30 85.87 80.77 78.90 74.36 63.18 60.81 56.57 52.75 52.73 50.02 46.82 41.04 40.47 38.54 24.14 23.79 20.08

Parameter	Value
Data File Name	/ Volumes/ nmrdata/ jkthomps/ nmr/ JKT-8-22_pure_dehydro/ 2/ fid
Title	JKT-8-22_pure_dehydro.2.fid
Origin	Bruker BioSpin GmbH
Solvent	MeOD
Temperature	297.1
Pulse Sequence	zgpg30
Experiment	1D
Number of Scans	1000
Receiver Gain	38.0
Relaxation Delay	1.0000
Pulse Width	10.0000
Acquisition Time	1.1796
Acquisition Date	2025-07-29T10:06:27
Spectrometer Frequency	100.62
Spectral Width	27777.8
Nucleus	13C
Acquired Size	32768
Spectral Size	65536

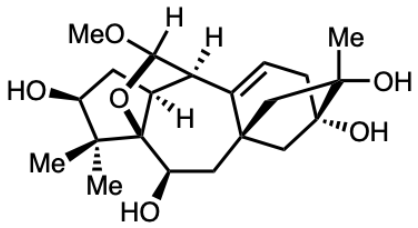

218

650 600 550 500 450 400 350 300 250 200 150 100 50 0

150 140 130 120 110 100 90 80 70 60 50 40 30 20

f1 (ppm)

Parameter	Value
Data File Name	/ Volumes/ nmrdata/ jkthomps/ nmr/ JKT-8-22_pure_dehydro/ 3/ ser
Title	JKT-8-22_pure_dehydro.3.ser
Origin	Bruker BioSpin GmbH
Solvent	MeOD
Temperature	297.1
Pulse Sequence	cosygpppqf
Experiment	COSY
Number of Scans	1
Receiver Gain	64.2
Relaxation Delay	1.7567
Pulse Width	12.5000
Acquisition Time	0.4403
Acquisition Date	2025-07-29T11:47:43
Spectrometer Frequency	(400.13, 400.13)
Spectral Width	(2325.6, 2325.6)
Lowest Frequency	(59.2, 56.9)
Nucleus	(1H, 1H)
Acquired Size	(1024, 128)
Spectral Size	(1024, 1024)
Digital Resolution	(2.27, 2.27)

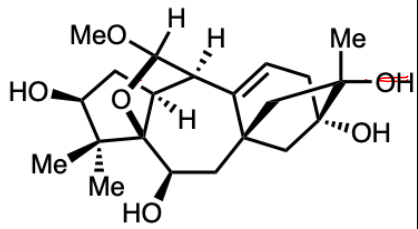

218

f2 (ppm)

f1 (ppm)

Parameter	Value
Data File Name	/ Volumes/ nmrdata/ jkthomps/ nmr/ JKT-8-22_pure_dehydro/ 4/ ser
Title	JKT-8-22_pure_dehydro.4.ser
Origin	Bruker BioSpin GmbH
Solvent	MeOD
Temperature	297.2
Pulse Sequence	hsqcedetgpsisp2.4
Experiment	HSQC-EDITED
Number of Scans	2
Receiver Gain	197.4
Relaxation Delay	1.5000
Pulse Width	12.5000
Acquisition Time	0.2135
Acquisition Date	2025-07-29T12:00:30
Spectrometer Frequency	(400.13,100.62)
Spectral Width	(4795.4,16611.3)
Lowest Frequency	(-526.6,-1137.9)
Nucleus	(1H,13C)
Acquired Size	(1024,180)
Spectral Size	(1024,1024)
Digital Resolution	(4.68,16.22)

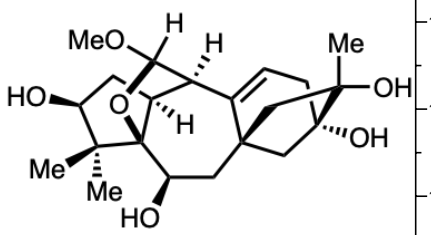

218

f2 (ppm)

f1 (ppm)

Parameter	Value
Data File Name	/ Volumes/ nmrdata/ jkthomps/ nmr/ JKT-8-22_pure_dehydro/ 5/ ser
Title	JKT-8-22_pure_dehydro.5.ser
Origin	Bruker BioSpin GmbH
Solvent	MeOD
Temperature	297.1
Pulse Sequence	hmbcetgpl3nd
Experiment	HMBC
Number of Scans	4
Receiver Gain	197.4
Relaxation Delay	2.0000
Pulse Width	12.5000
Acquisition Time	0.4260
Acquisition Date	2025-07-29T12:44:15
Spectrometer Frequency	(400.13,100.62)
Spectral Width	(4807.7,22321.4)
Lowest Frequency	(-172.9,-976.8)
Nucleus	(1H,13C)
Acquired Size	(2048,256)
Spectral Size	(2048,1024)
Digital Resolution	(2.35,21.80)

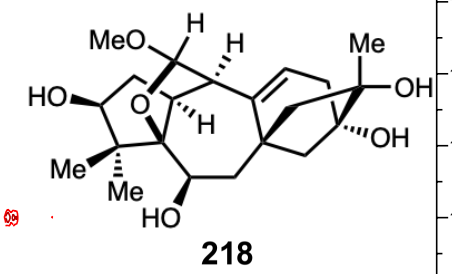

218

f2 (ppm)

f1 (ppm)

Parameter	Value
Data File Name	/ Volumes/ nmrdata/ jkthomps/ nmr/ JKT-8-22_pure_dehydro/ 6/ ser
Title	JKT-8-22_pure_dehydro.6.ser
Origin	Bruker BioSpin GmbH
Solvent	MeOD
Temperature	297.2
Pulse Sequence	noesygpphzs
Experiment	NOESY
Number of Scans	4
Receiver Gain	197.4
Relaxation Delay	1.8000
Pulse Width	12.5000
Acquisition Time	0.2560
Acquisition Date	2025-07-29T13:30:00
Spectrometer Frequency	(400.13,400.13)
Spectral Width	(4000.0,4000.0)
Lowest Frequency	(-161.5,-167.2)
Nucleus	(1H,1H)
Acquired Size	(1024,256)
Spectral Size	(1024,1024)
Digital Resolution	(3.91,3.91)

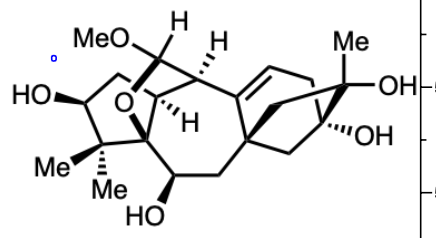

218

f2 (ppm)

f1 (ppm)

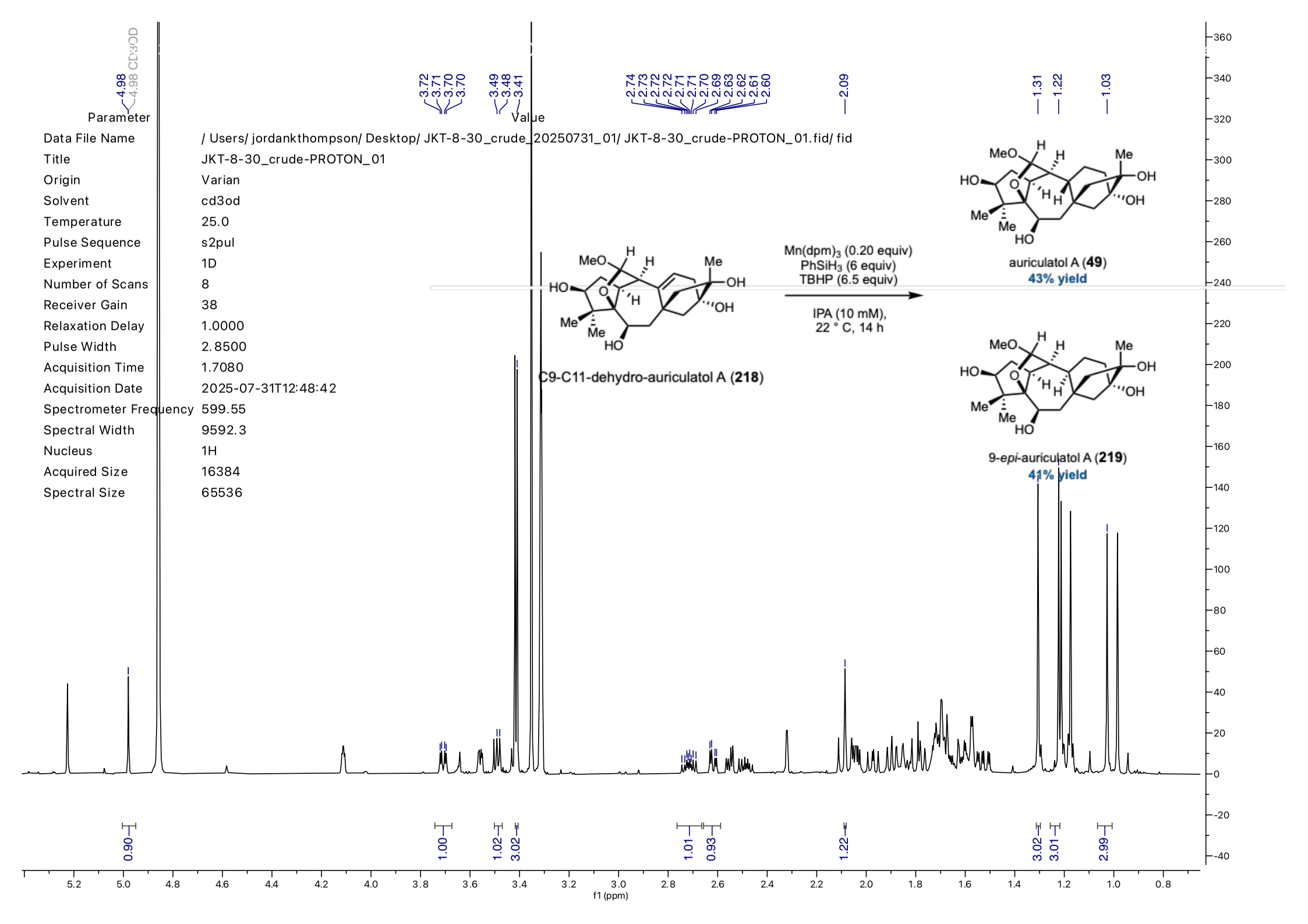
4.98
4.98 CD3OD
3.72
3.71
3.70
3.70
3.49
3.48
3.41
2.74
2.73
2.72
2.72
2.71
2.71
2.70
2.69
2.63
2.62
2.61
2.60
2.09
1.31
1.22
1.03
Parameter
Value
Data File Name / Users/ jordankthompson/ Desktop/ JKT-8-30_crude_20250731_01/ JKT-8-30_crude-PROTON_01.fid/ fid
Title JKT-8-30_crude-PROTON_01
Origin Varian
Solvent cd3od
Temperature 25.0
Pulse Sequence s2pul
Experiment 1D
Number of Scans 8
Receiver Gain 38
Relaxation Delay 1.0000
Pulse Width 2.8500
Acquisition Time 1.7080
Acquisition Date 2025-07-31T12:48:42
Spectrometer Frequency 599.55
Spectral Width 9592.3
Nucleus 1H
Acquired Size 16384
Spectral Size 65536
C9-C11-dehydro-auriculatol A (218)
Mn(dpm)3 (0.20 equiv)
PhSiH3 (6 equiv)
TBHP (6.5 equiv)
IPA (10 mM),
22 ° C, 14 h
auriculatol A (49)
43% yield
9-epi-auriculatol A (219)
41% yield
0.90
1.00
1.02
3.02
1.01
0.93
1.22
3.02
3.01
2.99
f1 (ppm)

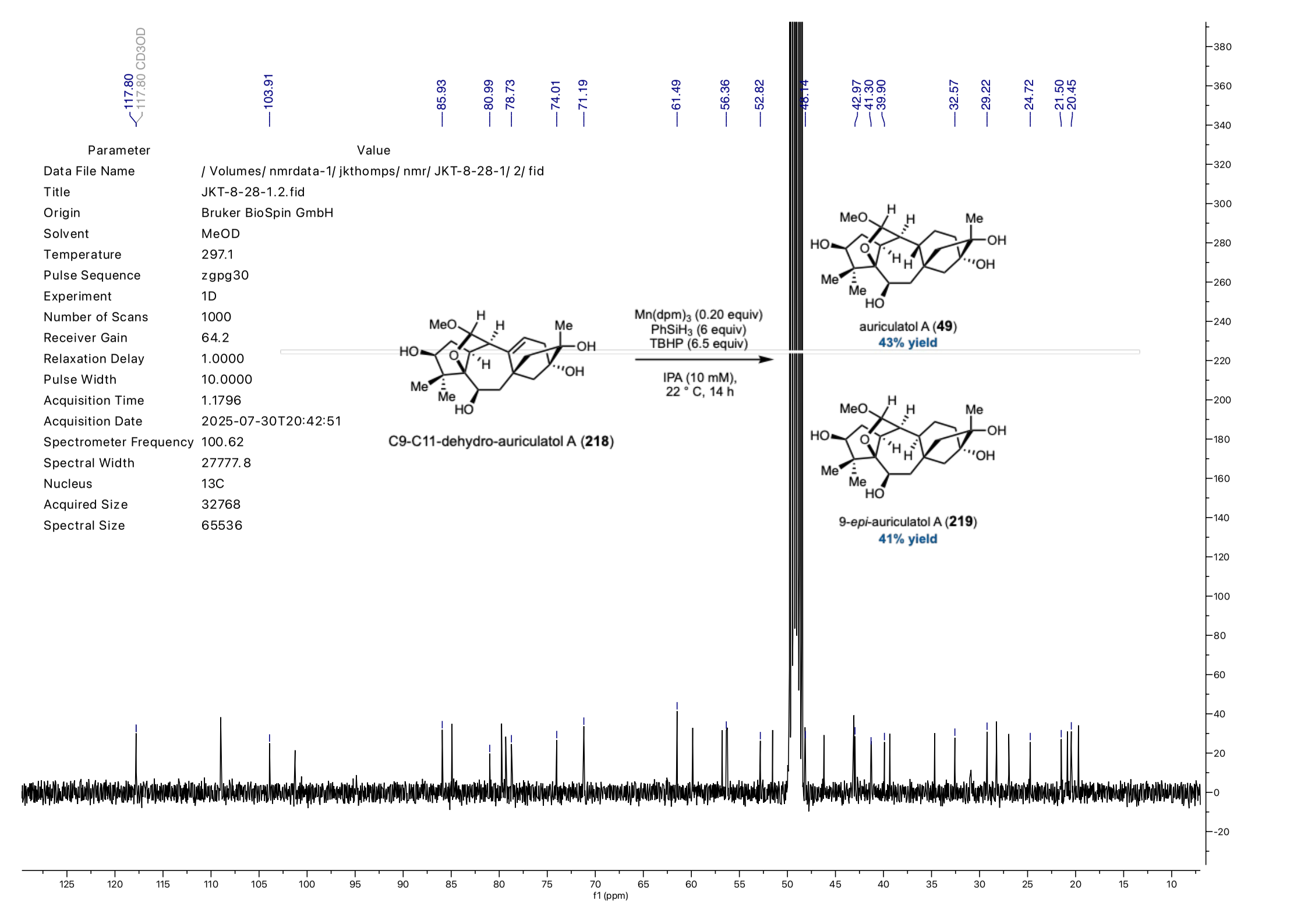
117.80
117.80 CD3OD
103.91
85.93
80.99
78.73
74.01
71.19
61.49
56.36
52.82
48.14
42.97
41.30
39.90
32.57
29.22
24.72
21.50
20.45
Parameter
Value
Data File Name
/ Volumes/ nmrdata-1/ jkthomps/ nmr/ JKT-8-28-1/ 2/ fid
Title
JKT-8-28-1.2.fid
Origin
Bruker BioSpin GmbH
Solvent
MeOD
Temperature
297.1
Pulse Sequence
zgpg30
Experiment
1D
Number of Scans
1000
Receiver Gain
64.2
Relaxation Delay
1.0000
Pulse Width
10.0000
Acquisition Time
1.1796
Acquisition Date
2025-07-30T20:42:51
Spectrometer Frequency
100.62
Spectral Width
27777.8
Nucleus
13C
Acquired Size
32768
Spectral Size
65536
C9-C11-dehydro-auriculatol A (218)
Mn(dpm)3 (0.20 equiv)
PhSiH3 (6 equiv)
TBHP (6.5 equiv)
IPA (10 mM),
22 ° C, 14 h
auriculatol A (49)
43% yield
9-epi-auriculatol A (219)
41% yield
f1 (ppm)

Parameter	Value
Data File Name	/ Volumes/ nmrdata/ jkthomps/ nmr/ JKT-8-30-F1-RR2/ 14/ fid
Title	JKT-8-30-F1-RR2.14.fid
Origin	Bruker BioSpin GmbH
Solvent	MeOD
Temperature	297.1
Pulse Sequence	zg30
Experiment	1D
Number of Scans	16
Receiver Gain	127.1
Relaxation Delay	1.0000
Pulse Width	12.5000
Acquisition Time	4.0894
Acquisition Date	2025-08-02T07:27:39
Spectrometer Frequency	400.13
Spectral Width	8012.8
Nucleus	1H
Acquired Size	32768
Spectral Size	65536

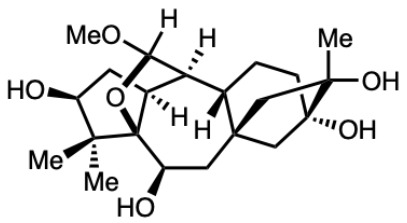

auriculatol A (**49**)

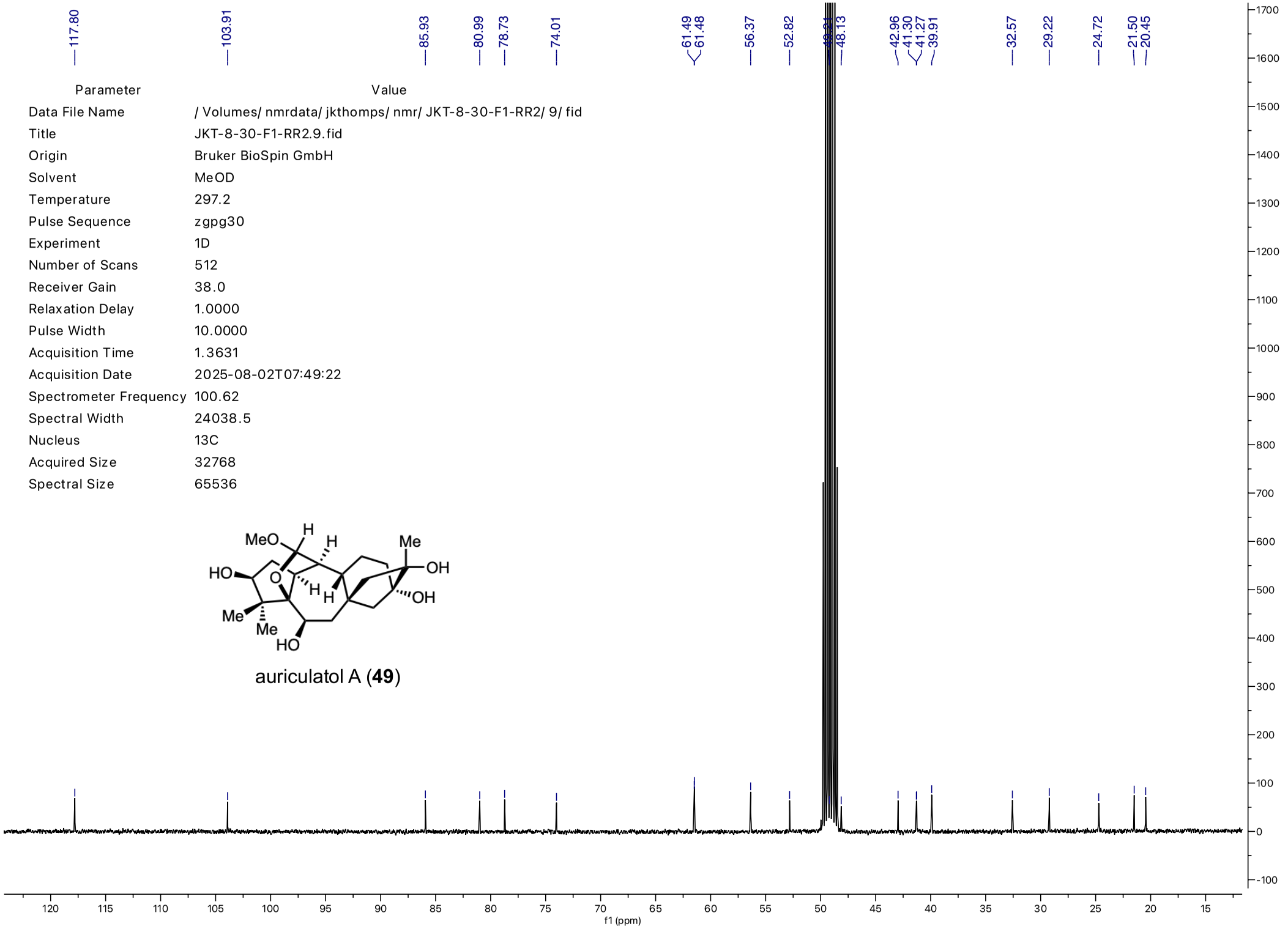

Parameter	Value
Data File Name	/ Volumes/ nmrdata/ jkthomps/ nmr/ JKT-8-30-F1-RR2/ 9/ fid
Title	JKT-8-30-F1-RR2.9.fid
Origin	Bruker BioSpin GmbH
Solvent	MeOD
Temperature	297.2
Pulse Sequence	zgpg30
Experiment	1D
Number of Scans	512
Receiver Gain	38.0
Relaxation Delay	1.0000
Pulse Width	10.0000
Acquisition Time	1.3631
Acquisition Date	2025-08-02T07:49:22
Spectrometer Frequency	100.62
Spectral Width	24038.5
Nucleus	13C
Acquired Size	32768
Spectral Size	65536

auriculatol A (**49**)

Parameter	Value
Data File Name	/ Volumes/ nmrdata/ jkthomps/ nmr/ JKT-8-30-F1-RR2/ 11/ ser
Title	JKT-8-30-F1-RR2.11.ser
Origin	Bruker BioSpin GmbH
Solvent	MeOD
Temperature	297.1
Pulse Sequence	hsqcedetgpsisp2.4
Experiment	HSQC-EDITED
Number of Scans	2
Receiver Gain	197.4
Relaxation Delay	1.5000
Pulse Width	12.5000
Acquisition Time	0.2135
Acquisition Date	2025-08-02T08:06:46
Spectrometer Frequency	(400.13,100.62)
Spectral Width	(4795.4,16611.3)
Lowest Frequency	(-517.1,-1262.8)
Nucleus	(1H,13C)
Acquired Size	(1024,180)
Spectral Size	(1024,1024)
Digital Resolution	(4.68,16.22)

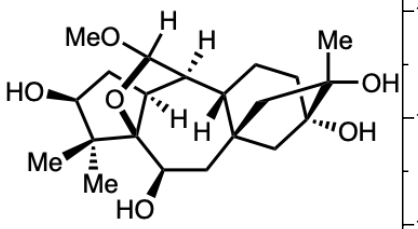

auriculatol A (**49**)

f2 (ppm)

f1 (ppm)

Parameter	Value
Data File Name	/ Volumes/ nmrdata/ jkthomps/ nmr/ JKT-8-30-F1-RR2/ 10/ ser
Title	JKT-8-30-F1-RR2.10.ser
Origin	Bruker BioSpin GmbH
Solvent	MeOD
Temperature	297.2
Pulse Sequence	cosygpppqf
Experiment	COSY
Number of Scans	1
Receiver Gain	64.2
Relaxation Delay	1.7198
Pulse Width	12.5000
Acquisition Time	0.4772
Acquisition Date	2025-08-02T07:55:06
Spectrometer Frequency	(400.13, 400.13)
Spectral Width	(2145.9, 2145.9)
Lowest Frequency	(108.7, 108.7)
Nucleus	(1H, 1H)
Acquired Size	(1024, 128)
Spectral Size	(1024, 1024)
Digital Resolution	(2.10, 2.10)

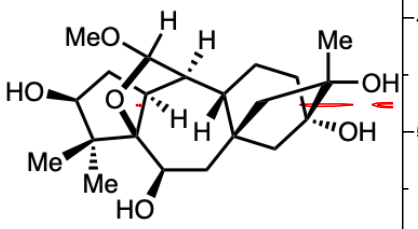

auriculatol A (**49**)

f2 (ppm)

f1 (ppm)

Parameter	Value
Data File Name	/ Volumes/ nmrdata/ jkthomps/ nmr/ JKT-8-30-F1-RR2/ 12/ ser
Title	JKT-8-30-F1-RR2.12.ser
Origin	Bruker BioSpin GmbH
Solvent	MeOD
Temperature	297.1
Pulse Sequence	hmbcetgpl3nd
Experiment	HMBC
Number of Scans	4
Receiver Gain	197.4
Relaxation Delay	2.0000
Pulse Width	12.5000
Acquisition Time	0.4260
Acquisition Date	2025-08-02T08:50:31
Spectrometer Frequency	(400.13,100.62)
Spectral Width	(4807.7,22321.4)
Lowest Frequency	(-168.0,-978.5)
Nucleus	(1H,13C)
Acquired Size	(2048,256)
Spectral Size	(2048,1024)
Digital Resolution	(2.35,21.80)

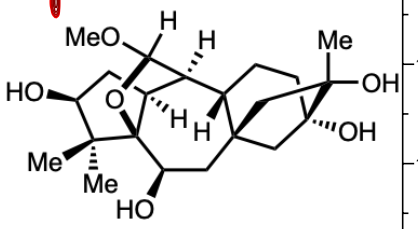

auriculatol A (**49**)

f2 (ppm)

f1 (ppm)

Parameter	Value
Data File Name	/ Volumes/ nmrdata/ jkthomps/ nmr/ JKT-8-30-F1-RR2/ 13/ ser
Title	JKT-8-30-F1-RR2.13.ser
Origin	Bruker BioSpin GmbH
Solvent	MeOD
Temperature	297.1
Pulse Sequence	noesygpphzs
Experiment	NOESY
Number of Scans	4
Receiver Gain	64.2
Relaxation Delay	1.8000
Pulse Width	12.5000
Acquisition Time	0.2560
Acquisition Date	2025-08-02T09:36:06
Spectrometer Frequency	(400.13,400.13)
Spectral Width	(4000.0,4000.0)
Lowest Frequency	(-160.1,-158.1)
Nucleus	(1H,1H)
Acquired Size	(1024,256)
Spectral Size	(1024,1024)
Digital Resolution	(3.91,3.91)

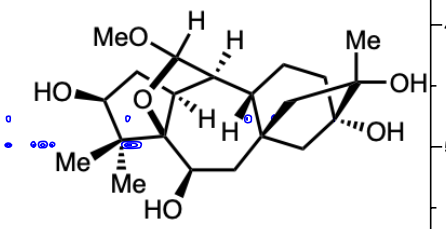

auriculatol A (**49**)

f2 (ppm)

f1 (ppm)

Parameter	Value
Data File Name	/ Volumes/ nmrdata/ jkthomps/ nmr/ JKT-8-30-F2-RR-2/ 1/ fid
Title	JKT-8-30-F2-RR-2.1.fid
Origin	Bruker BioSpin GmbH
Solvent	MeOD
Temperature	297.2
Pulse Sequence	zg30
Experiment	1D
Number of Scans	16
Receiver Gain	176.8
Relaxation Delay	1.0000
Pulse Width	12.5000
Acquisition Time	4.0894
Acquisition Date	2025-08-04T23:33:14
Spectrometer Frequency	400.13
Spectral Width	8012.8
Nucleus	1H
Acquired Size	32768
Spectral Size	65536

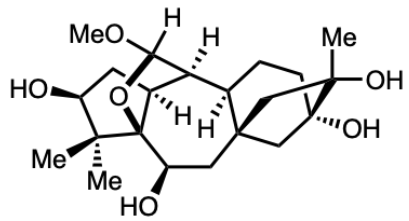

9-*epi*-auriculatol A (**219**)

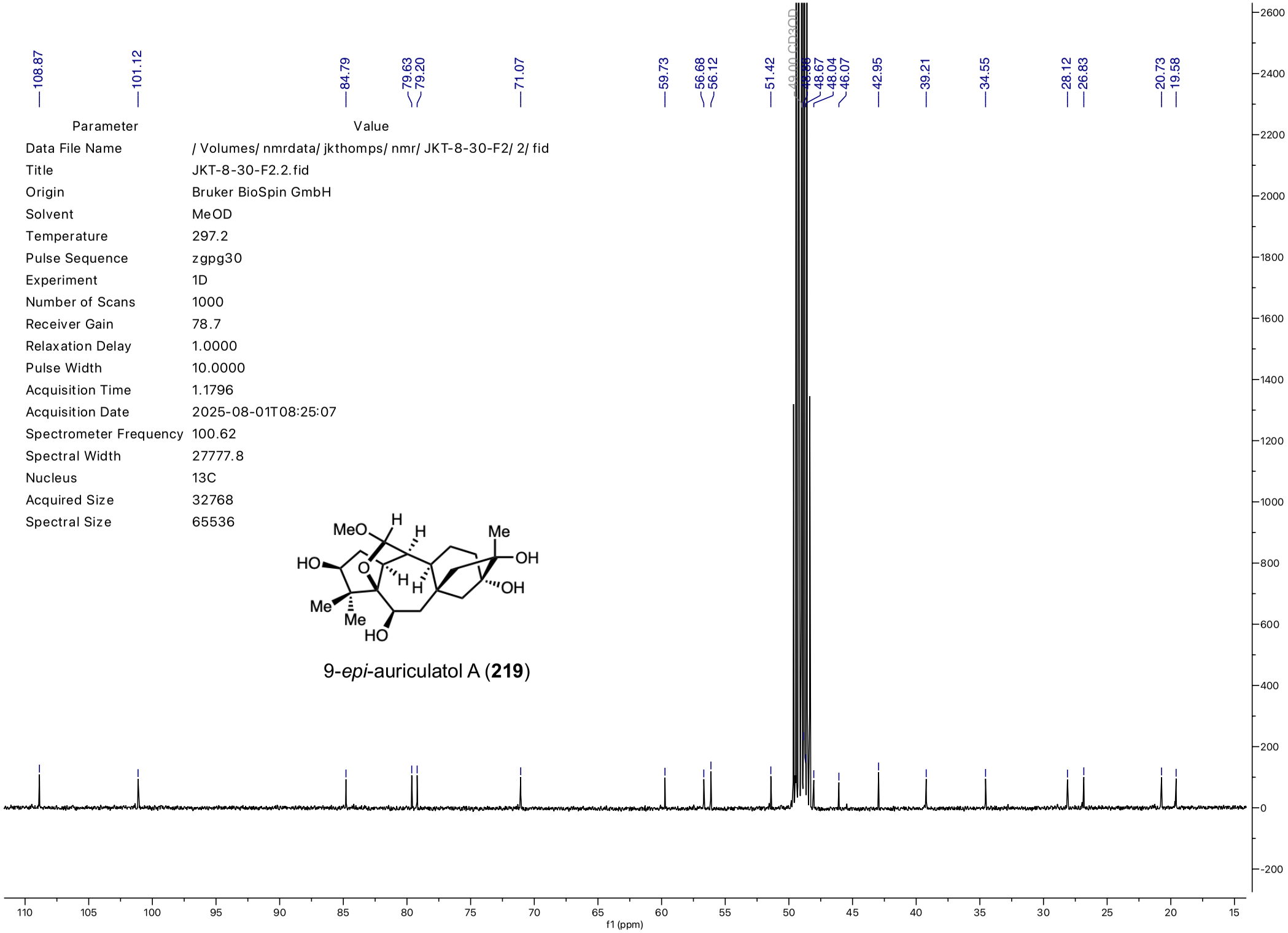

Parameter	Value
Data File Name	/ Volumes/ nmrdata/ jkthomps/ nmr/ JKT-8-30-F2/ 2/ fid
Title	JKT-8-30-F2.2.fid
Origin	Bruker BioSpin GmbH
Solvent	MeOD
Temperature	297.2
Pulse Sequence	zgpg30
Experiment	1D
Number of Scans	1000
Receiver Gain	78.7
Relaxation Delay	1.0000
Pulse Width	10.0000
Acquisition Time	1.1796
Acquisition Date	2025-08-01T08:25:07
Spectrometer Frequency	100.62
Spectral Width	27777.8
Nucleus	13C
Acquired Size	32768
Spectral Size	65536

9-*epi*-auriculatol A (**219**)

Parameter	Value
Data File Name	/ Volumes/ nmrdata/ jkthomps/ nmr/ JKT-8-30-F2/ 3/ ser
Title	JKT-8-30-F2.3.ser
Origin	Bruker BioSpin GmbH
Solvent	MeOD
Temperature	297.1
Pulse Sequence	cosygpppqf
Experiment	COSY
Number of Scans	1
Receiver Gain	127.1
Relaxation Delay	1.7424
Pulse Width	12.5000
Acquisition Time	0.4547
Acquisition Date	2025-08-01T08:30:53
Spectrometer Frequency	(400.13,400.13)
Spectral Width	(2252.3,2252.3)
Lowest Frequency	(99.8,99.8)
Nucleus	(1H,1H)
Acquired Size	(1024,128)
Spectral Size	(1024,1024)
Digital Resolution	(2.20,2.20)

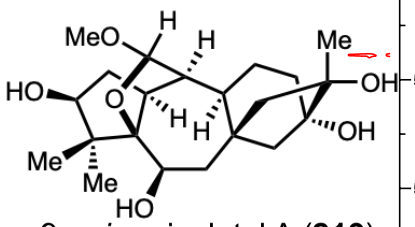

9-*epi*-auriculatol A (**219**)

f2 (ppm)

f1 (ppm)

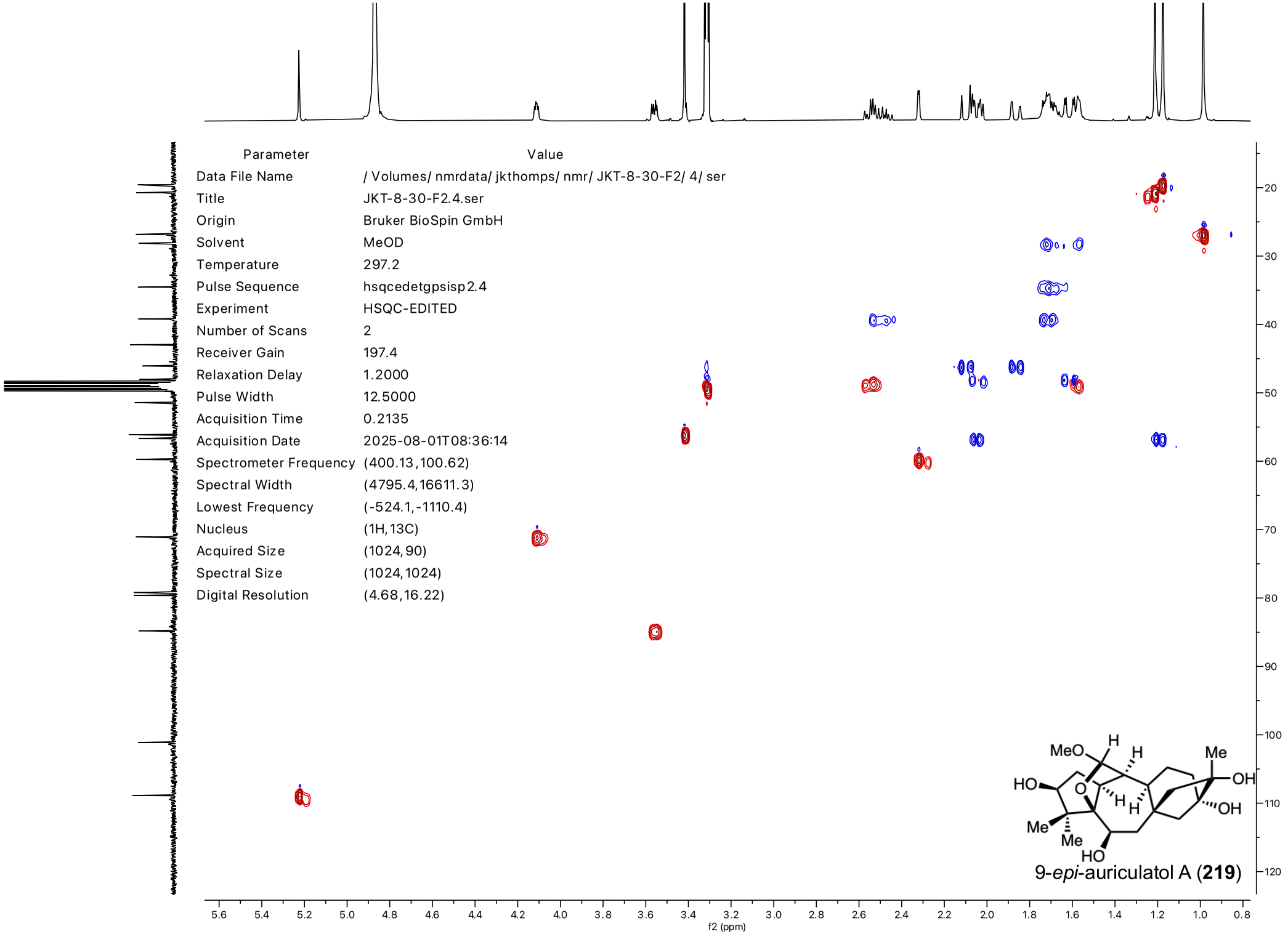
Parameter Value
Data File Name / Volumes/ nmrdata/ jkthomps/ nmr/ JKT-8-30-F2/ 4/ ser
Title JKT-8-30-F2.4.ser
Origin Bruker BioSpin GmbH
Solvent MeOD
Temperature 297.2
Pulse Sequence hsqcedetgpsisp2.4
Experiment HSQC-EDITED
Number of Scans 2
Receiver Gain 197.4
Relaxation Delay 1.2000
Pulse Width 12.5000
Acquisition Time 0.2135
Acquisition Date 2025-08-01T08:36:14
Spectrometer Frequency (400.13,100.62)
Spectral Width (4795.4,16611.3)
Lowest Frequency (-524.1,-1110.4)
Nucleus (1H,13C)
Acquired Size (1024,90)
Spectral Size (1024,1024)
Digital Resolution (4.68,16.22)
f2 (ppm)
f1 (ppm)
MeO
H
H
Me
HO
O
OH
H
H
OH
Me
Me
HO
9-epi-auriculatol A (219)

Parameter	Value
Data File Name	/ Volumes/ nmrdata/ jkthomps/ nmr/ JKT-8-30-F2/ 5/ ser
Title	JKT-8-30-F2.5.ser
Origin	Bruker BioSpin GmbH
Solvent	MeOD
Temperature	297.1
Pulse Sequence	hmbcetgpl3nd
Experiment	HMBC
Number of Scans	4
Receiver Gain	197.4
Relaxation Delay	2.0000
Pulse Width	12.5000
Acquisition Time	0.4260
Acquisition Date	2025-08-02T10:22:17
Spectrometer Frequency	(400.13,100.62)
Spectral Width	(4807.7,22321.4)
Lowest Frequency	(-166.9,-975.7)
Nucleus	(1H,13C)
Acquired Size	(2048,256)
Spectral Size	(2048,1024)
Digital Resolution	(2.35,21.80)

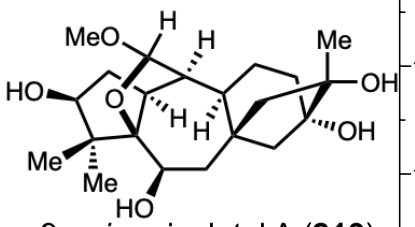

9-*epi*-auriculatol A (**219**)

f2 (ppm)

f1 (ppm)

Parameter	Value
Data File Name	/ Volumes/ nmrdata/ jkthomps/ nmr/ JKT-8-30-F2/ 6/ ser
Title	JKT-8-30-F2.6.ser
Origin	Bruker BioSpin GmbH
Solvent	MeOD
Temperature	297.1
Pulse Sequence	noesygpphzs
Experiment	NOESY
Number of Scans	4
Receiver Gain	197.4
Relaxation Delay	1.8000
Pulse Width	12.5000
Acquisition Time	0.2560
Acquisition Date	2025-08-02T11:07:56
Spectrometer Frequency	(400.13,400.13)
Spectral Width	(4000.0,4000.0)
Lowest Frequency	(-164.7,-158.1)
Nucleus	(1H,1H)
Acquired Size	(1024,256)
Spectral Size	(1024,1024)
Digital Resolution	(3.91,3.91)

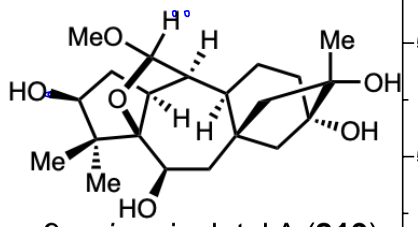

9-*epi*-auriculatol A (**219**)

f2 (ppm)

f1 (ppm)

ABOUT THE AUTHOR

Jordan Kenji Thompson was born on November 2nd, 1998 in Tarzana, CA to Michele H. and Jim J. Thompson. In 2003, the family moved to Calgary, AB, where he grew up in the rural outskirts of Springbank, one of the last suburban communities of Calgary. He spent his childhood being ushered around the city to compete in community hockey alongside his two brothers, Justin and Jack. From a young age, he took an interest in math and the sciences, and in high school primarily enjoyed his chemistry courses.

In 2016, Jordan moved to Berkeley, CA, matriculating at the College of Chemistry of UC Berkeley as a chemistry major. There, he began research in Professor Tom Maimone's lab, where he learned the craft of total synthesis and was a part of the team that completed the synthesis of (+)-6-*epi*-ophiobolin A. After graduating in 2020, he moved to Pasadena, CA and began his graduate studies in Professor Sarah Reisman's lab, continuing his work in natural product total synthesis. In Sarah's lab, he has largely undertaken the auriculatol A project but has also been involved in a collaborative project with Professor Diane Newman's lab and the checking of two OrgSyn procedures. In 2024, he conducted a 10-week internship in the Merck Discovery-Process group in Boston, MA.

Following completion of his Ph.D., Jordan will move to Cambridge, MA, where he will join the medicinal chemistry team at Bristol Myers Squibb.